كلية الطب والصيدلة وطب الأسنان
ⵜⴰⵖⵍⵓⵏⵜ ⵏ ⵜⵙⵏⵉⵏⵜ ⴷ ⵜⵙⴰⵡⴰⵔⵜ ⴷ ⵜⵙⵏⵉⵏⵜ ⵏ ⵜⵣⴰⵎⵜ
FACULTÉ DE MÉDECINE, DE PHARMACIE ET DE MÉDECINE DENTAIRE

جامعة سيدي محمد بن عبد الله - فاس
ⵜⴰⵙⴷⴰⵡⵉⵜ ⵙⵉⴷⵉ ⵎⵓⵃⴰⵎⵎⴷ ⵏ ⵄⴰⴱⴷⵍⵍⴰⵀ - ⴼⴰⵙ
UNIVERSITÉ SIDI MOHAMED BEN ABDELLAH DE FES

YEAR 2021

Thesis N° 338/21

STUDY OF BRAIN CONNECTIVITY IN CHRONIC AND HEAVY CANNABIS USERS: DTI ASSESSMENT AND CLINICAL FEATURES.

THESIS

SUPPORTED AND PRESENTED PUBLICLY ON 31/12/2021

By

Mr. BENMASSAOUD Mahmoud

Born on August 6th, 1995 in Fez

TO OBTAIN MEDICAL DOCTORATE

KEYWORDS:

THC – Structural Connectivity – ATLAS – ROI – Tractography – Brain Networks – CUD – Impulsivity – Correlations

JURY

Mr.	RAMMOUZ ISMAIL……. Professor of Psychiatry	PRESIDENT
Mr.	BOUJRAF SAID……. Professor of Biophysics and Clinical MRI Method	PROTRACTOR
Mr.	AALOUANE RACHID……. Professor of Psychiatry	JUDGES
Mr.	MAAROUFI MUSTAPHA……. Professor of Radiology	
Mr.	BENZAGMOUT MOHAMMED……. Professor of Neurosurgery	
Mr.	ALAMI BADRE EDDINE……. Professor of Biophysics	
Mr.	BOUT AMINE……. Assistant Professor of Psychiatry	ASSOCIATED MEMBER

LIST OF ABBREVIATIONS

2-AG	2-arachidonoyl glycerol
ACC	anterior cingulate cortex
AD	Axial Diffusivity
ADC	apparent diffusion coefficient
AEA	arachidonylethanolamine
ANOVA	Analysis of Variance
BIS-11	Barratt Impulsiveness Scale-11
BLA	Basolateral amygdala
BNST	Bed nucleus of the stria terminalis
CB1R	cannabinoid-1receptor
CB2R	cannabinoid-2 receptor
CBD	cannabidiol
CeA	Central nucleus of the amygdala
CN	Caudate nucleus
CNS	central nervous system
CRF	corticotropin-releasing factor
CSF	cerebrospinal fluid
CUD	Cannabis use disorder
CUDIT-R	The Cannabis Use Disorder Identification Test-Revised
DA	Dopamine
DEC	direction-encoding color
dlPFC	Dorsolateral prefrontal cortex
DLSTr	Dorsolateral striatum
dmPFC	Dorsomedial prefrontal cortex
DSM	Diagnostic and Statistical Manual of Mental Disorders
DTI	Diffusion tensor imaging
DWI	diffusion-weighted image
ECS	Endocannabinoid System
FA	Fractional anisotropy
FAAH	Fatty acid amide hydrolase
FE:	first eigenvector
fMRI	Functional magnetic resonance imaging
GCC	Genu of the Corpus Callosum

GLU	Glutamate
GP	Globus pallidus
GPCR	G protein-coupled receptors
GPE	globus pallidus extern
GPI	globus pallidus interne
HIPP	Hippocampus
HYVs	High yielding varieties
ILF	inferior longitudinal fasciculus
MAP	mitogen-activated protein
MD	Mean diffusivity
MLF	middle longitudinal fascicle
Nac	nucleus accumbens
NADA	N-arachidonoyl dopamine
OFC	Orbital frontal cortex.
PET	positron emission tomography
PFC	Prefrontal cortex
PSS	Perceived Stress Scale
Put	Putamen
RD	Radial Diffusivity
RF	Radio Frequency
ROI	Region of interest
rTMS	Transcranial magnetic stimulation
SLF	superior longitudinal fascicule
SNc	substantia nigra pars compacta ().
SNr	substantia nigra pars reticulata
STN	Subthalamic nucleus
Tdcs	Transcranial direct-current stimulation
THC	Ttetrahydrocannabinol
TPV1	transient receptor potential vanilloid 1
UF	Uncinate fasciculus
vlPFC	Ventrolateral prefrontal cortex
vmPFC	Ventromedial prefrontal cortex
VP	Ventral Pallidum
VTA	ventral tegmental region
WHO	World Health Organization

TABLE OF CONTENTS

General Introduction

Cannabis is the most widely used drug around the world, according to the "World Drug Report 2020," with 192 million users in 2018, accounting for 3.9 per cent of the global population aged 15–64[1]. In its latest survey, the National Observatory for Drugs and Alcohol stated that cannabis was Moroccan teenagers' most popular illicit substance used in 2013[2].

Δ 9 -tetrahydrocannabinol is the major psychoactive substance in cannabis[3]. For this purpose, studies on the potency (concentration of Δ9-tetrahydrocannabinol) of cannabis resin revealed that cannabis potency had increased worldwide lately[45]. In line with those studies, the Δ 9-THC content in Morocco's cannabis resin is shown to be higher than those in the United States and Europe[678].

On the other hand, the main cannabis receptors are CB1 and CB2[9]. They can be activated by endogenous endocannabinoids, phytocannabinoids, or synthetic cannabinoids[10]. CB1-receptors are now known to be abundant throughout the brain, and they are expressed with a significant density in areas considered to be involved in reward, addiction, and cognitive function, such as the amygdala, cingulate cortex, prefrontal cortex, ventral pallidum, caudate, putamen, nucleus accumbens, ventral tegmental region, and lateral hypothalamus [11] [12]. CB1Rs are also found in significant concentrations in other brain areas: the basal ganglia, substantia nigra, globus pallidus, cerebellum, and hippocampus [11] [13]. CB2Rs receptors are also found in all CNS cells, particularly microglial cells [14] [15] [16] [17] [18]. Dopamine neurons in the midbrain ventral tegmental area express CB2 receptors, where THC receptor effects could modulate addiction-related behaviors like drug reinforcement [19].

In terms of pathological impairment, there is a distinction between high-CBR density regions and low-density regions. Thus the most captivating causes of neuroanatomic changes in areas with a high cannabinoid receptor density are the THC mediated neurotoxicity[20] (consequence of THC and its metabolites accumulation in neurons), the downregulation, adaptation, and molecular and signaling modifications downstream of cannabinoid receptors[21] [22] [23]. Regarding regions with a low density of cannabinoid receptors that are functionally and structurally related to the areas with high density, changes are due to the spread of the changes in synaptic oscillations in the latter regions, resulting in neuroanatomic alterations[24].

Another piece of evidence that goes along with the goals of our study is that: In studies of neurodegenerative diseases, there was a strong correlation between changes in intrinsic connectivity between functionally and structurally related regions and changes in grey matter volumes in the same areas[25].

Studies on acute and chronic effects of cannabis show that cannabis use is related to impairments in a broad range of cognitive functions: learning and memory, working memory, attention, decision-making, and cognitive flexibility[26]. In addition, several neuroimaging studies reveal the long-term effects of chronic cannabis use on several different brain systems, including the reward and stress systems and brain areas involved in emotion processing and decision making[27].

The diffusion tensor imaging (DTI) technique is a non-invasive MRI method that contributes to assessing brain tissue (grey and white matter) macrostructure, microstructure, and connectivity, and the segmentation of white matter fibre bundles using tractography. Therefore researchers can investigate these structural changes occurring in grey and white matter by analyzing the diffusibility of water in these tissues.

However, there is no study on the connectivity alteration induced by chronic and heavy cannabis use in Africa and the Middle East. Furthermore, no study has evaluated the grey matter structuring of cannabis users using the DTI Region Of Interest (ROI) technique of a whole anatomical brain region.

Therefore, the fundamental purpose of our research is to evaluate the major brain structures and functions among cannabis users.

This goal is reached through a series of steps:

-All participants undergo the same Diffusion Tensor MRI protocol.

-All participants undergo the same series of psychometric tests.

- Examination of the impact of chronic and heavy cannabis use on brain functions that are part of the reward, cognition, and emotional regulation circuits, using a series of tests on the two groups of cannabis users (heavy and light users) as well as healthy controls.

-Structural evaluation of 36 x 2(Bilaterality) cerebral regions using the Region Of interest Technic (ROI). The integrity of anatomical structures is assessed using fractional anisotropy (FA) and mean diffusivity (MD) markers, and the outcomes of cannabis users (heavy and light) and healthy non-user controls are compared descriptively and statistically.

-Evaluation of white matter structure integrity, using the graph theory and from a network viewpoint, by individualizing first the white matter bundles associated with each anatomical region of interest. Afterwar calculating and recording the diffusion markers (FA and MD) associated with the extracted white matter tracts and comparing the outcomes of the three groups studied.

-Correlation of the clinical (Psychometric tests: CUDIT-R, BIS-11, and PSS) and DTI findings (diffusion markers: FA and MD) in tracts related to several regions.

In our study, the grey matter and white matter analyzed are related to the regions that are known to have a high density of CB1 and CB2 receptors, as well as regions that are involved in cognitive functions: learning and memory, working memory, attention, decision-making, and cognitive flexibility[26].

The population of this study is Moroccan addicts of cannabis compared to healthy non-users control that consented to participate.

Bibliographical context

Chapter I: Cannabis the plant and the drug

I. History of cannabis in the world and Morocco

1. Generalities and geography

The magic plant Cannabis sativa is certainly one of the earliest plants cultivated by man. Despite all the controversies around the plant's history, explorers of the two last centuries attest that the geographic origin of cannabis is in Central Asia or "Eurasia" [28] near the Altai Mountains, and it was present 11700 to 12000 years ago[29,30].

One of the first use of the cannabis Sativa plant reverted to the stems' characteristic of high fibre content, and it is referenced that it's the oldest cultivated fibre plant[31]. The plant had significant roles in Chinese manufacturing (ropes, textiles, paper) and cordage with this characteristic. [30,32]

The introduction of cannabis cultivation to Europe, western Asia and Egypt is linked to the period between 1000 and 2000 BC, and the cultivation in Europe became widespread after 500 AD .[33,34]

On another side, Clake and Merlin claimed that the euphoriant properties of C.Sativa may be considered as an unintentional event and also maintained that the accidental burning of the plants has revealed its psychotropic nature. [34]

The cannabis Sativa plants have also been used about 5000 years ago in the medical field. Shennong the "Divine Farmer" and mythological Chinese ruler[8] wrote the world's oldest pharmacopoeia, and it was prescribed for malaria, rheumatic pain, intestinal constipation, disorders of the female reproductive system and fatigue [9,10]

Medical cannabis use is extensively reported in different other civilisations, Indians, Egyptians [11] and Roman [12]. Hence Cannabis or Hemp has been, from the earliest times, a malleable material from which man has drawn from it, according to his needs, technical products, food or spiritual nourishment.

2. Cannabis in The Maghreb and Morocco

The Maghreb was one of the lands of hemp election, in its two varieties, fibre hemp and resin hemp. In this part, we will individualise the two types of cannabis, the fibre and resin ones by cannabis Sativa and cannabis Indica respectively and this last one we will remake as the variety which contains the most important concentration of the psychoactive drug.

a. The arrival of cannabis in Maghreb and Morocco

First of all, we should know that the first plants acclimatised in the Maghreb and Andalusia from Antiquity belonged to the Sativa variety. According to the proposal of Doctor Jamal Bellakhdar, Ethnobotany researcher , in his publication "Les voies suivies par le chanvre dans sa conquête du Maghreb" cannabis would have arrived in the Maghreb by three different routes : the Mediterranean route, through Egypt and the Sahelian route[35] [36].

The Mediterranean route was the route of introduction of cannabis to the Maghreb, in a period before the 10th century, by the Phoenicians civilisation and not by the Arabs as is usually admitted but rather the Arabs only developed these cultures which they had found on their arrival in the Maghreb and Spain. Like the Cretans and the Egyptians, the Phoenicians used this material to make their rigging of boats and their fishing nets[36].

The Egyptian route was the entry route for the Indica variety, which is much stronger in its capacity, indeed psychotropic. And that was in the 12-13 centuries and spread in the north of Africa [36].

For the Sahelian way, at a later time (XVIIth or XVIIIth century), which brought African strains of cannabis to the Saharan oases[36].

b. The development of cannabis cultivation in Morocco

The first official authorisation for the use of the cannabis plant in its two varieties cited below would have emerged during the reign of Sultan Moulay Hassan I. The latter authorised the cultivation of the plant for local consumption in five villages which are: Tribes des Ketama, Béni Seddate and Beni Khaled and this to contribute to the pacification of the region.[37] [38] [39]

Cannabis cultivation has undergone several changes from 1912 to 1956, which is the period of the French and Spanish protectorate in Morocco.

In the north of Morocco: from 1912 to 1956

- From the arrival of the Spanish protectorate to 1923: Spain, the latter, whose protectorate includes the Rif – One of the historical regions of cannabis cultivation in Morocco given its geographical characteristics and given that it is one of the regions of Morocco less suitable for agriculture due to its rugged relief, steep slopes, poor and eroded soils, and low recourse to irrigation –[40] [41], authorises the cultivation of cannabis to a few tribes.
- During the Rif war from 1923 to 1926, the cultivation of cannabis was banned
- From 1926, a new cannabis tolerance zone extended north of Fez, around Ketama; this area was immediately reduced and eventually officially abolished in 1929. [42][39]

In the rest of the country: from 1912 to 1956

In 1932, the cultivation of cannabis was therefore officially banned by a Dahir (royal decree). Only the undertaken cultivation for the "Régie des Tabacs et du kif" around Kenitra in Gharb, and Marrakech, in Haouz, were authorised. [39]

After 1956:

After the independence and During the reign of King Mohammed V, there was a tolerance of the cultivation of cannabis in the five historic douars of Ketama, Beni Seddate and Beni Khaled.[38] Under traditional cultivation, mainly on small plots, for local consumption.

At the beginning of the 1980s:

Moroccan and foreign intermediaries probably introduced new varieties of cannabis originating from the Near East and requiring little water, with a significant extension of the cultivated areas.[43] And this is in response to the accelerated increase in European demand for hashish since the 1960s.[44] And in 1988, according to Robert C. Clarke, the qualities of traditional kif had already been lost by modern farmers.

II. The Cannabis Sativa

1. General facts

Cannabis sativa L, given the botanical Sativa by Linnaeus in 1753, is an annual, mainly dioecious (male and female flowers occur on separate plants) - sometimes monoecious or maphrodite- a flowering plant that produces geniculate achenes as fruits.[45][46] The reproduction occurs through wind-dispersed pollen released from stamina (male) flowers.[45]

At the higher family level, cannabis is now recognised as the only genus in the Cannabaceae family.[47] At lower taxonomic levels, though, the number of species in the cannabis genus appears to be a subject of controversy[48] with some studies indicating a multi-typical (multiple-species) genus[49] [34], whilst other reports suggest that cannabis is one species system with different varieties.[33]

2. Cannabis drug production

Cannabis sativa generates active ingredients (mostly phytocannabinoids, terpenoids, phenols) within the glandular heads of epidermal multiseriate stalk trichomes[5048] (tiny glands which produce resinous sap that concentrates a large part of the cannabinoids) [51] when the plant is flowering.

Trichomes are where most cannabinoids and terpenes of the plant are concentrated, responsible for potency and flavour, respectively.[5253]

In essence, the female flowers are sessile. Each female flower is subtended by a perigonal bract and grows to surround the fruit. For cannabis drug production, female plants have been chosen to manufacture flowering heads with rich flowers in tight heads.[33] Female plants, proposed for drug production, have 20 times the THC level as the corresponding males.[34]

Cannabis with the highest THC level consists solely of female flower heads which remain unfertilised throughout maturity and, consequently, do not contain seeds (sinsemilla) .[33]

Therefore, according to the UNODC report 2009, sinsemilla production requires identifying the female plants and ensuring they are not exposed to pollen.[54]

3. The Moroccan cultivation and the specificity of the Moroccan cannabis plant and drug

As we mentioned in the previous part, "The development of cannabis cultivation in Morocco ", changes in the cultivation of cannabis began in the 1980s. Following the introduction of feminised seed varieties in the late 1990s and the advent of a newer variety between 1990 and 2000, Morocco's cannabis industry was once again transformed, so these modern high yielding varieties (HYVs) with significantly higher resin yields and potency were eventually replaced by the 1980s cultivated variety [55].

An investigation conducted by Pierre-Arnaud Chouvy and his team in 2017 reported the adoption of modern techniques in cultivation besides the hashish production[53].

The adoption of high-yielding cannabis varieties, modern agricultural practices, and the modern cultivation of hashish began in the 2000s and rapidly accelerated after 2010. Thus the continued implementation of modern agricultural techniques has made it possible to manufacture high-quality hashish and strong modern extracts[53] [38].

These changes had, as a direct effect, a continuous and very dramatic increase in THC levels. These increases have been proven by the analysis of cannabis resin samples seized in Morocco and Europe[78].

A study undertaken by the Royal Gendarmerie Laboratory for Technical and Scientific Research and Analysis, Rabat-Instituts, studied the evolution of the Δ 9-THC content in Morocco's cannabis resin seizures from 2005 to 2014.

This report retained as a result: an upward trend relative to the average of 8% declared in the UNODC study in 2004[56], as the content ranged from 0.6 % - 16.8% in 2005-2006 to 0.5% - 25% in 2014. The increase was felt very significantly in 2007, for the category of resins dosed between 10% and 20% in Δ9-THC (frequency of 40% in 2007 against 17% in 2005-2006), and the appearance in 2009 new resins with a high dosage of more than 20% (5% of seizures).[7] And according to an other European study its shows that the Moroccan Hashish seized in 2014 avreagedd 20.7%[6].

In line with Moroccan trends, other studies on the potency (concentration of Δ9-tetrahydrocannabinol) of cannabis resin in Europe and the United States show that cannabis potency has increased in those regions as well.

In the United States, a study of changes in cannabis potency over the last decade (2008 to 2017) found that the mean Δ9 -THC concentration in confiscated hashish samples rose dramatically to 30,3% from 2008 to 2014, then declined to 17,6% in 2015, and finally to just 15,5% in 2016[5].

A study about changes in the potency, of cannabis resin in Europe found that the resin potency increased from a mean of 8.14% THC (6.89, 9.49) in 2006 to 17.22 (15.23, 19.25) in 2016[4].

These results in Morocco, the USA and Europe show that the increase in cannabis three regions is very significant.

The primary purpose of this section is to state that research on cannabis consumers, particularly heavy cannabis users, will be more and more significant, especially in Morocco, given that Moroccan trends are clearly higher than those in the United States and Europe.

III. Chemical description

1. Introduction

The phytochemistry of chemicals generated by the cannabis Sativa plant is very complicated. Approximately 568 chemicals, including 120 active phytocannabinoids, have been detected in the cannabis plant to the present [57] [58] [59].

These 568 chemicals belong to two different classes: primary metabolism (e.g. amino acids, steroids and fatty acids) and secondary metabolism (cannabinoids, flavonoids, stilbenoids, terpenoids, lignans and alkaloids) [60] [52].

2. Phytocannabinoids

Phytocannabinoids are the isolated natural Cannabinoids [61]. Cannabinoids are C21 Trepenophenolic compounds, and they are the most particular compound category of the cannabis Sativa plant[62]. The most interesting cannabinoid – because of psychoactivity– was discovered in 1964 by Y. Gaoni And R. Mechoulam[63,] and it s the tetrahydrocannabinol (Δ 9-THC).

Δ 9 -tetrahydrocannabinol is the major psychoactive substance in cannabis[3]. THC was originally identified as an agonist of CB1 receptors, but there was considerable evidence of partial agonists at this site[64].
THC alters the signalisation of endocannabinoid transmitters such as anandamide an d 2-arachidonoylglycerol[65]. THC also shows partial agonist properties in the CB2 receptor with less effectiveness than in CB1R[66].

Finally, THC's acute effects are dose-dependent and can be offset by CBD[64]. Later on, we'll talk more about THC's effects and brain chemicals that imitate THC's effects.

Because of its activity as an antiepileptic agent, Cannabidiol is the second most important compound after THC [67]. It was discovered in the late 1930s, but it wasn't until 1963 that its structure was revealed[68].

Unlike THC, CBD is non-psychotropic psychoactive, and some animal experiments show that in animal models, CBD prevents drug-seeking and self-administration[6970].

3. Non-Cannabinoid Constituents:

Cannabis also produces other organic agents, such as flavonoids and terpenoids, which may contribute to the cannabis chemical activity and essentially due to "the entourage effect": when metabolites of active and inactive cannabis combine to affect the receptor potential of active components. Therefore the entourage effect is predicted to affect the subjective or therapeutic interpretation with cannabinoids by non-cannabinoid compounds[71 72].

Flavonoids impart cannabis colour, while terpenes are responsible for the odour and flavour of the different Cannabis plants. Thus, terpenes have considerably contributed to the selection of cannabis narcotic strains .[33]

IV. National and international prevalence of cannabis use

Cannabis is the most widely used drug in the world, according to the "World Drug Report 2020," with an estimated 192 million users in 2018, accounting for 3.9 percent of the global population aged 15–64[1]. The percentage of people who use cannabis, by region and subregion, is 5% in the North African region, including Morocco[1].

Few data are available in Morocco on cannabis epidemiology. In its latest survey, the National Observatory for Drugs and Alcohol stated that cannabis was Moroccan teenagers' most popular illicit drug in 2013[2].

Drug use disorders are one of the most dangerous effects of drug use, and 35.6 million people are estimated to suffer from them among the estimated 269 million people who used drugs in 2018[1]; this equates to a worldwide prevalence of drug use disorders of 0.7 percent in the population aged 15–64[1].

For cannabis use and cannabis use disorder, it has been predicted that nearly 10% of individuals who have ever used cannabis will ultimately become addicted 59. It has also been stated that 9 % of people who consume cannabis present with characteristic symptoms of dependency according to DSM-IV guidelines[73]. It is also stated that progress to regular use has a 50% risk of becoming addicted[74].

Chapter II: Cannabis and brain

I. Endocannabinoid signalling system

For years researchers have been trying to identify and characterise the structure of active cannabis components. In the 1960s, the active component Δ9-tetrahydrocannabinol (THC) was isolated and identified by Gaoni and Mechoulam [63].

For several years, the absence of a determined cell receptor for these compounds has also impaired researchers' interest in how THC and other cannabinoids function in the brain. And it was supposed to work by a non-specific membrane-associated mechanism because of its lipid chemistry.

The St. Louis study group of Allyn Howlett in the 1980s searched for a particular cannabinoid receptor in the rat brain. After they discovered it, they named it a cannabinoid-1 (CB1) receptor [75].

1. Endocannabinoid receptors:

The main cannabis receptors are CB1 and CB2 and belong to the family of G protein-coupled receptors (GPCR) to adenylyl cyclase and mitogen-activated protein kinase. They show an identity of 48% amino acid sequence[9].

They can be activated by endogenous endocannabinoids, phytocannabinoids or synthetic cannabinoids[10]. CB1 is centrally and peripherally located, while CB2, mainly in the periphery but also centrally located [76].

Other receptor proteins, such as CPR55, GPR119, and transient receptor potential vanilloid 1 (TRPV1), have been identified as potential targets for the endocannabinoid system[10].

a. The CB1 Receptor:

History of the receptors:

The CB1 receptor was initially thought to be mainly expressed in the CNS and thus was classified as a brain cannabinoid receptor. We presently recognise that it's present in various peripheral organs, and they are widely distributed in several brain regions and the eye and lower concentrations all over the body[77] [78]. Other receptor proteins, such as CPR55, GPR119, and transient receptor potential vanilloid 1 (TRPV1), have been identified as potential targets for the endocannabinoid system[79].

Density of the receptors:

In the brain, CB1 receptors are expressed in the higher cognitive function cortical areas, midbrain areas associated with motor regulation and hindbrain regions that take part in the autonomous nervous system motor and sensory functions control and regions associated with reward and emotion (Figure 1)[11].

We will focus here on a system that our study will be particularly interested in: The reward system. CB1Rs express a significant density in areas considered to be involved in reward, addiction, and cognitive function, such as the amygdala, cingulate cortex, prefrontal cortex (PFC), ventral pallidum, caudate, putamen, nucleus accumbens (NAc), ventral tegmental region (VTA), and lateral hypothalamus [11] [12]. CB1Rs are also densely present in other brain regions: the basal ganglia, substantia nigra, globus pallidus, cerebellum, and hippocampus [11] [13].

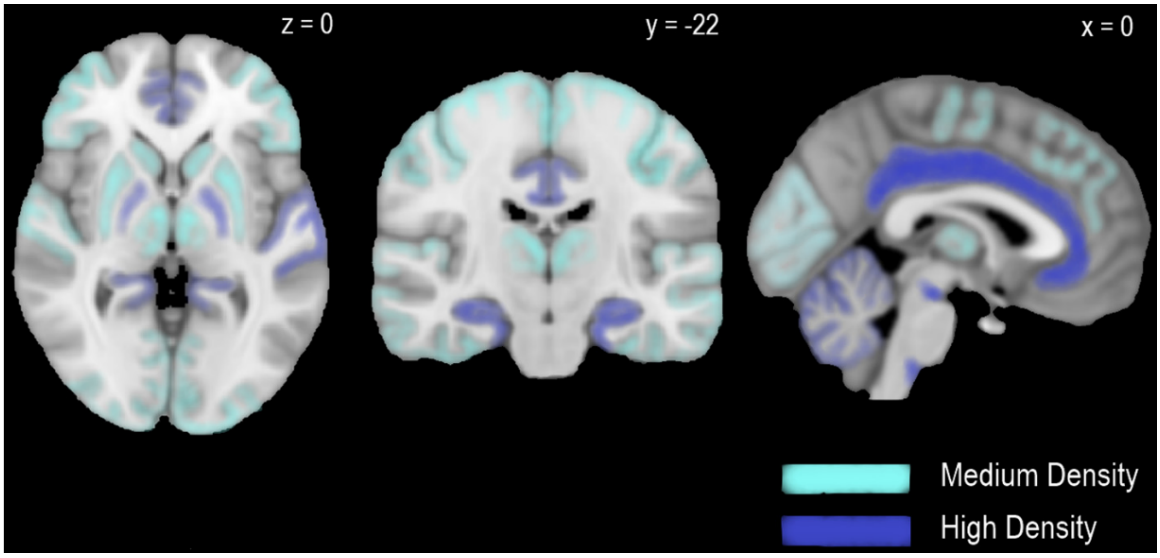

Figure 1: The distribution of CB1Rs across the human brain.

These axial (left), coronal (middle) and sagittal (right) views schematically depict regions of medium and high endocannabinoid type 1 receptor (CB1R) concentration.

Regions with high CB1R concentration are the amygdala (not in view), cerebellum, cingulate gyrus, the dorsal motor nucleus of the vagus, entorhinal cortex, globus pallidus, hippocampal formation, middle frontal gyrus, substantia nigra, and Wernicke's area.

Regions with medium CB1R concentration are the auditory cortex (right), caudate nucleus, mediodorsal nucleus of the thalamus, motor cortex, occipitotemporal gyrus, putamen, somatosensory cortex, and visual cortex.

Montreal Neurological Institute coordinates (x,y,z) are shown above.

A modified figure, from (Bloomfield MAP. 2019) [139]

The development of the receptors:

The density and distribution of the receptors are also significantly different depending on the age and stage of brain development. In white matter regions, the distribution of CB1 receptors at an early age is abundant but much lower later[80].

The distribution of the receptors:

The CB1 receptors are mainly located in the pre-synapse of central and peripheral neurons. They are mostly located in neurons and also in glia[81]. These locations facilitate the realisation of an effect that represents one of the major functions of the endocannabinoid system, which is to inhibit neurotransmitter release[13] (Figure 2).

Activation of the CB1 receptor also stimulates the activity of kinase mitogen-activated protein (MAP). This process affects the synaptic plasticity, cell migration, and probably neuronal development of cannabinoids[9].

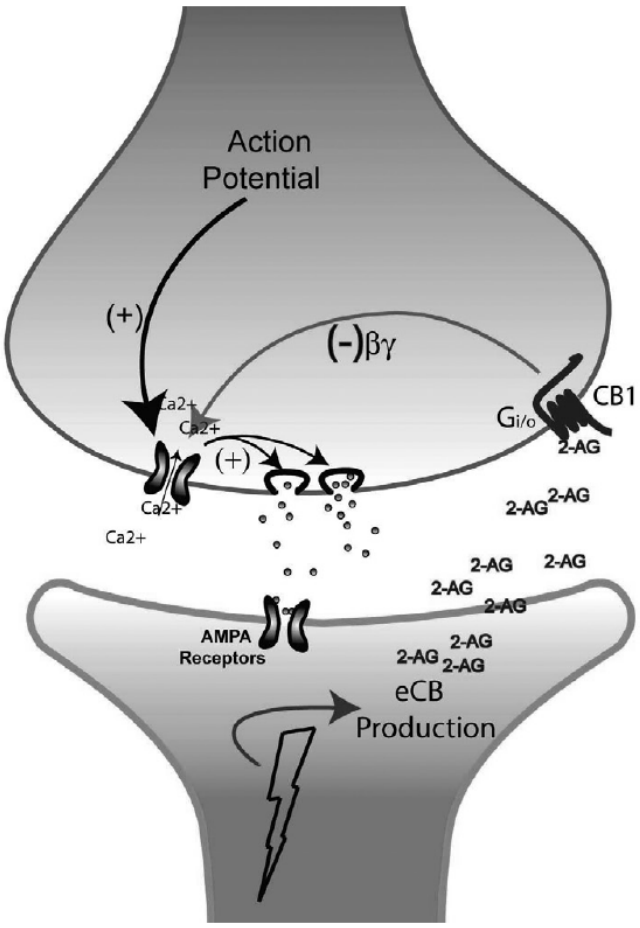

Figure 2: A synaptic junction where CB1 receptors are located and that shows the mechanism by which CB1 repceptor is activated and the consequences of activation.

❶Glutamate is released into the synapse when an action potential reaches the presynaptic terminal end.
❷Glutamate acts on the adjacent dendrite's AMPA receptors, leading the post-synaptic membrane to be depolarized.
❸The subsequent Ca++ influx to a 2-AG production.
This last one is released and acts as retrograde messenger into the synapse. It works on the glutamate containing neuron inhibitory pre-synaptic CB1 receptors to -❹- turn off subsequent release of glutamate.
❺The activity of 2-AG is ended by the degrading enzyme of the pre-synaptic neuron, monoacylglycerol lipase (MAGL).

A modified figure, from (Linda A. Parker 2017) [413]

b. The CB2 Receptor:

The subtype CB2 is present in peripheral organs with immune functions: spleen, tonsils, thymus, macrophages and leukocytes, as well as cells. CB2 appears to suppress immune cell migration activities following stimulation [82].

The CB2 receptors originally were thought to be found only in immune system cells; however, they are now identified in all CNS cells, particularly those of the microglial cells [14] [15] [16] [17] [18]. CB2 receptors are also expressed in the pulmonary, testes and central nervous system [83].

Dopamine neurons in the midbrain ventral tegmental area express CB2 receptors, where THC receptor effects could modulate addiction-related behaviours like drug reinforcement [19]. This localisation corresponds to critical roles in reward, reinforcement, and addiction.

Concerning the immune system's relationship with CB2 receptors, "The mammalian body has a highly developed immune system that guards against continuous invading protein attacks and aims at preventing, attenuating, or repairing the inflicted damage," Pacher & Mechoulam theorised in a review published in 2011. There is emerging evidence that lipid endocannabinoid signalling via CB2 receptors may represent an example/part of such a protective system," they added[84].

2. The endogenous cannabinoid agonists

The recognition of cannabinoid receptors meant the involvement of endogenous molecules that could activate (or inhibit) these receptors. As a result of considerable research, a series of arachidonic acid derivatives with potent effects on cannabinoid receptors were discovered.

First, we separated and classified two compounds: one from the brain, which we named arachidonylethanolamine (anandamide or AEA), and the other from peripheral tissues, which we called 2-arachidonoyl glycerol (2-AG)[85] [86] [87] [9]. Secondly, additional endogenous lipid cannabinoid ligands have been discovered, 2-arachidonyl glyceryl ether (noladin ether)[88], N-arachidonoyl dopamine (NADA) [89], and virodhamine[90].

Anandamide and 2-AG, unlike most neurotransmitters (such as acetylcholine, dopamine, and serotonin), are not retained in vesicles and are instead synthesised when and where they are required [13]. They act as fast retrograde synaptic messengers because their activity is more presynaptic rather than postsynaptic[9].

Endocannabinoids' synthesis and degradation are controlled by enzymes[91] (Blankman and Cravatt 2013). Endocannabinoids are quickly eliminated by a membrane transport method [92].

Fatty acid amide hydrolase (FAAH) hydrolyses anandamide in the cell to produce arachidonic acid and ethanolamine. Both FAAH and monoacyl hydrolases hydrolyse 2-AG enzymatically. The endocannabinoids' function is extended when these enzymes are suppressed[93].

3. Physiological roles of the endocannabinoid system

Scientists have used a variety of methods to determine the physiological function of the endocannabinoid system. With the emergence of advanced technology of electron microscopy and super-resolution microscopy enabled access to revolutionary information about the anatomical distribution of the CB1 receptors on the central nervous system and also enabled the revelation of molecular mechanisms that had the effect of THC and of synthetic CB1 agonists notably on: locomotion, perception, emotion, and cognition in the animal and human model[94] [95].

a. Through CB1 receptors signalling

Without first knowing the synaptic location of the receptors and the neurophysiological mechanisms of signalling through these receptors, it would have been nearly impossible to characterise the exact functions of the endocannabinoid system receptors.

The discovery in 2001 that endocannabinoids mediate retrograde synaptic signaling at central synapses was a significant development and a major milestone in cannabinoid study [96] [97] [98].

Two significant findings were sufficient to argue that endocannabinoids are inhibitory retrograde neuromodulators [99] :

- The discovery of CB1 receptors in presynaptically excitatory and inhibitory neurons was the first step [100] [101].`
- Second, the discovery of certain endocannabinoid synthesising enzymes' postsyna ptic localisation and the observation that postsynaptic activity increases endocannab inoid output[100].

As a result, these two main findings strongly indicate that endocannabinoids are retrograde neuromodulators messengers [99] [102].

CB1 receptors are also present postsynaptically in astrocytes and adult progenitor stem cells.

The physiological function of the endogenous cannabinoid system is still not clear. Endocannabinoids have additionally been shown to play a significant role in hunger, eating behavior, and energy metabolism: It has been demonstrated that postsynaptic CB1 receptors affect the expression of precursors of appetite-controlling peptides in the hypothalamic arcuate nucleus[103] [104].

Furthermore, some studies demonstrated that: CB1 receptor antagonists consistently minimise food consumption in both animal subjects and human study participants, and other research suggests that endocannabinoid activity in the hypothalamus, the mesolimbic dopamine pathway, and the olfactory system together to improve the desire to eat, the hedonic properties of food, and food-mediated reward [105] [106].

Concerning energy metabolism, some evidence suggests that through its receptor CB1, the endocannabinoid system influences brain metabolism and memory function[107] through the CB1's location in the external membrane of mitochondria, where it inhibits electron transport and the respiratory chain[108].

A significant number of studies of rodents have supported the hypothesis that the endocannabinoid system regulates fear, anxiety, and stress reactions based on the fact that acute cannabis use in human beings induces a feeling of rest, decreased anxiety, and an increased mood[109].

CB1 also regulates synaptic plasticity in astrocytes on the hippocampus and in hypothalamus Leptin signaling [110] [111].

Another function of the endocannabinoids is related to the existence of CB1 receptors in adult progenitor stem cells. The activation of the CB1 receptor at this level stimulates the proliferation of the stem cells and their differentiation into neurons or astrocytes [112], a role that could be relevant to neurodegenerative disorders.

b. Through CB2 receptors signalling

From studies on neurobiological disease, immune modulation was related to the CB2 receptors as its primary role[113]. Several other studies assumed that CB2 alters neuronal function[114]; however, the mechanism by which it does so remains unknown.

In addition, the mechanism by which CB2 alters neuronal function is still undefined. According to a study, activation of postsynaptic CB2 decreases neuronal excitability in the hippocampus's CA3 and CA2 regions through functional coupling with the sodium-bicarbonate transporter[115].

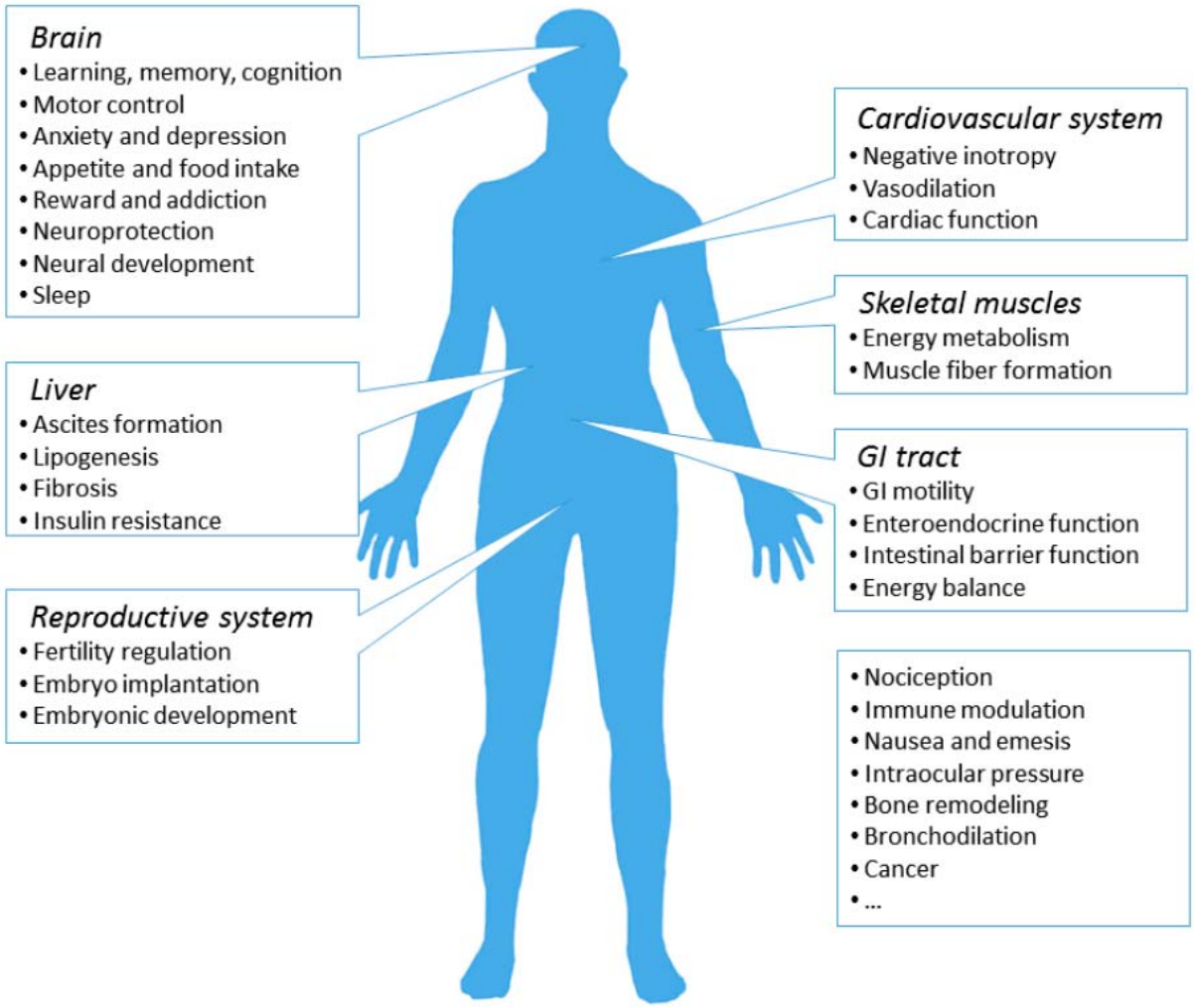

Figure 3: Major localization sites and associated functions of the CB1R in the human body.

The majority of CB1Rs expressed in the human body are found in the brain, which is involved in various neurological activities. CB1Rs on the peripheral sites, although to a lesser extent, participate in regulating local tissue functions. (Zou, S., & Kumar, U. 2018)[414]

II. Neurobiology of the reward and the endocannabinoid system contribution

The reward has a critical role in survival and is essential for positive and negative feedback. This section reviewed the neurobiology of reward and its intersection with cannabinoids and the endocannabinoid pathway (Figure 4).

A largely complex interconnected structure network, including VTA, NAc, ventral pallidum, CeA, BNST, and PFC, mediates reward processing. The dopamine (DA) pathways derived from the VTA midbrain play a crucial role in rewards mediation[116].

In addition to dopamine, many other mechanisms, such as the cholinergic, opioid peptide, glutamatergic (excitatory), and GABAergic (inhibitory) systems, play a role in reward delivery[116 117]. Each of these circuits then innervates the NAc, allowing sensory and emotional input to be translated into motivating behavior via extrapyramidal motor systems[116]. VTA DA neurons also innervate limbic system components such as the amygdala, hippocampus, orbitofrontal cortex, and portions of the PFC [116].

In a simplified manner, amygdala-circuits help create association-related rewards and fear-referenced memories, hippocampal-circuits play a vital role in declarative memory functions[116].

CB1Rs are found in all integrated reward systems[11 12 118], where they modulate excitatory and inhibitory signaling, influencing reward processing[119 120].

The VTA DA projection to the NAc has a prominent role in positive and negative reinforcement.

Positive reinforcement is the appreciation of rewards, and it is the pleasant sensations that provide the motivating results that motivate the individual to do the probability of future participation in the behavior that is providing these effects[116].

Natural rewards and psychostimulants, including cannabinoids, raise NAc DA levels in the brain, which leads to subjective reward and positive reinforcement. [121].

Negative reinforcement refers to attitudes that promote avoiding or alleviating undesirable states. In the negative reinforcement model, undesired factors such as unwanted discomfort, chronic pain, certain negative habits, and abstinence from addictive substances reduce NAc DA levels, and the resulting increased activation of medium spiny output neurons leads to undesired states [117] [122].

Endocannabinoids play a pivotal part in completing the improvement of the activity of the VTA-NAc DA projection and their effect on the approach and avoidance behaviors that govern the acquisition of rewards[116].

Endocannabinoid DA control occurs in NAc as projected Glutamate (GLU) from limbic prefrontal cortex regions, and amygdala stimulates endocannabinoid output, which decreases more releases. This decrease of glutamate release decreases the release of NAc GABA from VTA and therefore (increases) the release of DA from the VTA to NAc[123].

CB1R activation on axon GABAergic neuron terminals in the VTA prevents GABA propagation and eliminates this inhibition in DA neurons leading to a rise in the firing of these cells[123].

Figure 4 resumes the brain reward circuits with corresponding levels of CB1R in each brain region composing the pathways.

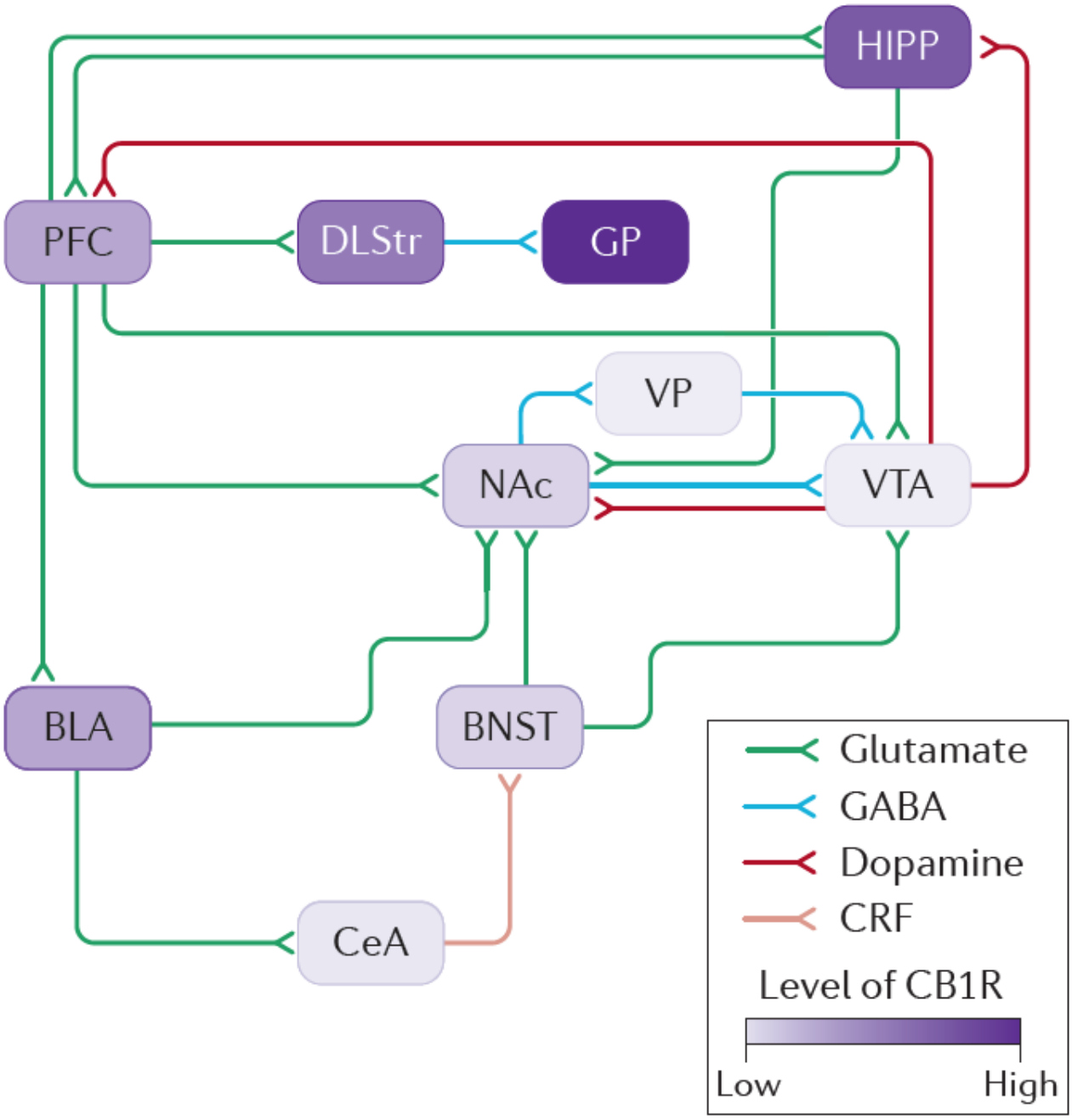

Figure 4: The brain reward circuits and the endocannabinoids system.

BLA: Basolateral amygdala – PFC: Prefrontal cortex – HIPP: Hippocampus – VP: Ventral pallidum – GP: Globus pallidus – DLSTr: Dorsolateral striatum – NAc: Nucleus accumbens – VTA: Ventral tegmental area – BNST: Bed nucleus of the stria terminalis – CeA: Central nucleus of the amygdala.
(Parsons, L. H., & Hurd, Y. L. 2015) [116].

III. The effect of cannabis on the brain

1. Introduction

Cannabinoids have varying effects on the human brain depending on the dose, frequency of use, and intake route. These effects are categorised primarily as cognitive and neurophysiological.

2. Effects on brain development

Many studies have shown that neonatal and immature CNs are more vulnerable to phytocannabinoid harm and suggest that cannabinoids can impair new synapse growth and affect neural cell maturation, particularly at critical neurodevelopmental stages mainly adolescence and neonatal periods [124][125].

Two studies of Smith and his team in 2006 and 2016 confluence that cannabis prenatal exposure can lead to permanent effects on adult working and executive functions [126] [127].

Since adolescence is a crucial step in the brain's development[128] and brain development continues until the age of about 25[129], heavy use of cannabis at this period may be susceptible to cause changes in brain function.

The adolescent period is the transitional period from childhood to adulthood. The World Health Organization (WHO) defined it as an individual between the ages of 10 and 19; however, the exact age period of puberty is not well defined, ages up to 25 years have been suggested as late adolescence by some researchers[130].

Adolescence is characterised by typical adolescent behaviors such as high risk-taking, high exploration, novelty and sensation seeking, social interaction, and increased activity; these behaviors are likely to promote the acquisition of required skills for maturation and independence [131].

In the adolescent period, significant neurodevelopmental phenomena contributing to behavioural changes and cognitive maturation are also observed[132]. Besides that, the PFC, which is associated with higher cognitive function and emotional regulation, is the last region to mature, and the eCB system is an essential mediator of appropriate PFC maturation[133].

Nevertheless, a recent review of neuroimaging findings in adolescent cannabis users concluded that, while there is evidence that frontoparietal development and function are impaired in adolescent cannabis users, it is unknown whether the reported consequences are directly related to the adolescent onset of use or general cannabis use-related conditions[134].

3. Acute effects

a. Rewarding and reinforcing effects of cannabinoids

Because of its psychoactive mechanisms and related impacts on brain dopaminergic activity, THC appears to be responsible for cannabinoids' addictive capacity. As previously explained, the cannabinoid pathway interferes directly and indirectly in the reward circuits and the limbic system.

A recent review on Cannabis Addiction and the brain, supported by the findings of preclinical and clinical studies, summarised the impact of THC. THC has been reported to have reinforcing properties that change salience perception through enhanced dopaminergic signaling, similar to the effect of other drugs of abuse[27].

b. The state of intoxication

Iversen summarised the behavioral effects of cannabis use in his book "The Science of Marijuana "[135]. He has described four distinct stages, each of which is dose and time-dependent: "buzz" - "high" - "stoned" stage, and the "come-down."

● Buzz: A short period of initial response during which the user may feel dizzy or light-headed.

● High: Characterised by euphoria and exhilaration and a sense of disinhibition, which is often expressed as enhanced laughter. In self-report surveys, euphoria has been identified as a primary factor in maintaining cannabis use[136].

● Stoned: The consumer is usually quiet and peaceful and may even be in a dreamlike state. According to the same self-report surveys, relaxation is the most often reported result among cannabis users[136].

● Come-down: A progressive cessation of these symptoms, which ranges in duration based on the THC dosage and the degree of THC metabolism of the user's organism.

Cannabis smoking may also induce temporarily psychotic symptoms such as depersonalisation, derealisation, agitation, and even paranoia[137].

c. Effect of cannabis on cognition, memory, and emotions

As mentioned in part about CB1R density in the brain, the hippocampus and PFC have a high density of CB1Rs. Consequently, learning and memory impairments are some of the acute effects of cannabis most widely replicated[26].

A study on the acute effects of THC inhalation found that THC administration increased activity for low working memory loads and reduced the linear relationship between working memory load and activity in a network of working memory-related brain regions.

Those regions are specifically the left DLPFC, inferior temporal gyrus, inferior parietal gyrus, and cerebellum, while in the placebo condition, brain activity increased linearly with rising working memory load[138].

Based on these studies and other findings, we can say that THC impacts cerebral activity related to memory and learning. One common interpretation of these findings is that THC reduces neuronal efficacy in learning and memory processes[139].

Cannabinoid receptors are abundant in essential brain regions involved in emotional regulation, such as the amygdala and ACC[118].

The first human research investigating the impact of various cannabinoids on emotional treatment gave a partially obvious sign that different pharmacological agents that influence the endocannabinoid system can boost and degrade emotional recognition[140].

The research results were as follows:

*The combination of THC+CBD did not cause any deterioration; however, acute inhalation of THC (8mg) impaired emotional face recognition at the behavioral level.

*CBD enhances knowledge of emotional effects and attenuates THC disability.

In a cognitive revaluation study that examined the impact of THC on the frontolimbic activation and functional communication of a healthy adult population, THC increased amygdala activation and decreased functional coupling of amygdala and dorsolateral prefrontal cortex (dlPFC) during a cognitive re-evaluation of negative emotional pictures[141].

And that may ultimately indicate that the differentiation between subjective and behavioral responses is based on a THC-induced hypoconnectivity between amygdala et cortex[64].

4. Chronic effects

a. Cannabis use disorder and cannabis' long-term effects on emotion and cognitive functioning

i. Cannabis use disorder

A single term has replaced substance abuse and substance dependence, substance use disorder, in the fifth edition of the Diagnostic and Statistical Manual of Mental Disorders (DSM-5). Chronic cannabis use has been linked to a higher risk of substance abuse disorders[142].

According to researchers, about 10% of people who have ever used cannabis will become addicted, with the risk increasing exponentially in proportion to the frequency of use[143].

The (DSM-5) defines diagnostic criteria for cannabis intoxication, withdrawal, and use disorder. "DSM-5 extends the overall list of criteria for a drug use disorder to cannabis users for cannabis use disorder. These criteria imply significant impairment and/or stress in various functional areas, including[144] :

- Problematic habits as a result of long-term cannabis use
- Failed efforts to regulate or reduce cannabis use.
- Excessive time spent purchasing the drug
- The negative effect of cannabis use on work, education, or social roles.
- Consistent cannabis use in potentially dangerous situations.
- The creation of tolerance; and the occurrence of withdrawal symptoms upon cessation of use

Cannabis withdrawal symptoms tend to manifest in the same time frame and manner as withdrawal from other drugs[145]; they usually occur 1-2 days after stoppage of intensive use and can last 7-14 days. [146].

Irritability, fatigue, decreased appetite, restlessness, and sleep disorders are the most common clinical signs of cannabis withdrawal[27]. Anger or aggression, a depressed mood, and physical symptoms such as shakiness or tremors, sweating, fever, chills, and severe headaches are also present[27 145].

It s also known that the withdrawal stage of cannabis addiction is marked by an increase in negative affect[147] and with a greater negative impact on normal daily activities like withdrawal in other drugs of abuse[146 148]

Reduced DA cell firing in the VTA and reduced DA release in the nucleus accumbens, increased corticotropin-releasing factor (CRF) release in the central nucleus of the amygdala, increased secretion of stress hormones such as corticosterone, and various changes in the endocannabinoid system are some of the main findings of the neurochemical mechanisms behind the marijuana abstinence syndrome[149 150].

PET imaging studies have shown widespread reductions in brain CB1 receptor binding in daily marijuana smokers[151 152 153], and there is a strong association with a much larger number of other imaging animal and human studies, indicating that changes in brain CB1 receptors due to heavy marijuana use are linked to the production of cannabis dependency[74].

ii. Long-term use effects on emotion, cognitive functions

Depending on the duration and intensity of use, THC has two contrasting effects on emotions. As previously described in the chapter dedicated to the acute effects of THC on emotions, low doses decrease anxiety and elevate mood. High amounts of chronic exposure, on the other hand, have been linked to affecting dysregulation by increasing anxiety and leading to depressive symptoms[154].

Like emotions, areas of executive function are affected particularly in verbal learning, memory, and attention domains, differently by acute administration or chronic exposure to cannabis. A comprehensive systematic review has outlined and integrated acute and chronic cognitive effects of cannabis[26]; all of these reported effects are summarised in Table 1.

Table 1: Key Findings for Cognitive Impairment in Cannabis Users.

(Broyd SJ et al. 2016)[26]

Acute effects
Impaired verbal learning and memory
Impaired working memory
Impaired attention (task and dose-dependent)
Impaired inhibitory control and (to a lesser extent) other executive functions
Impaired psychomotor function
Chronic Effects
Impaired verbal learning and memory
Impaired attention and attentional bias
Possible impaired psychomotor function
Possibly impaired executive function (depending on the frequency of use and age of onset)
Recovery of function with abstinence
Likely persistent effects on attention and psychomotor function
Possibly persistent effects on verbal learning and memory (insufficient and mixed evidence)

Despite these consistent findings, THC should no longer be regarded as a toxic substance to memory uncritically. This is due to new research showing that THC stimulates neurogenesis, restores memory, and inhibits neurodegenerative mechanisms and cognitive processes decline in animal models with Alzheimer's disease[155] [156] [157].

Among the studies that have reported these findings is one that used intracerebroventricular administration of the synthetic cannabinoid WIN55,212-2 to rats. As a result, it has been concluded that cannabinoid receptors are critical in the pathology of "Alzheimer's disease" and that cannabinoids effectively prevent the disease's neurodegenerative phase[155].

To clarify these apparently conflicting findings, it has been proposed from a review about THC effects that THC modulates memory and cognition in an age- and dose-dependent manner: in old animals, low concentrations enhance memory and cognition while high concentrations impair these functions; in young animals, even a low concentration is toxic[157]. These results are consistent with what has been observed in humans: undeniable proof that marijuana use has an impact on memory and cognition, especially in young people[157][158].

b. Heavy and chronic cannabis usage alters neurobiological systems

The neurophysiological changes due to chronic cannabis use have been well summarised in a recent review[27] . According to this review, the chronic relapsing nature of addiction appears to be associated with underlying neurophysiological abnormalities in the reward, stress, and executive function circuits[27].

i. Reward circuit

Alterations in reward-related circuitry following long-term cannabis use may be linked to changes in the endocannabinoid system. Since CB1 receptors are highly expressed in reward processing and conditioning regions, the eCS has been linked to reward-processing and reward-seeking behavior [116] [159].

Chronic THC exposure has also been found to downregulate CB1Rs, implying a neurobiological basis for tolerance and desensitisation to THC's pleasurable effects[160]. It has also been observed that early-life THC exposure blunts dopaminergic responsiveness to naturally pleasurable stimuli that stimulate DA release later in life[65]. It was also observed that adolescent THC exposure resulted in greater self-administration and a decreased striatal DA response to CB1R agonists in adulthood[161].

ii. Stress circuit

Through its impact on the amygdala and the hypothalamic-pituitary-adrenal axis, the endocannabinoid system appears to be implicated in stress response regulation[159] [133]. In addition, the eCS regulates interactions between the PFC, amygdala, and hippocampus, all of which are connected to emotional memory, anxiety, and drug-related craving in substance use disorder[162].

In animal studies, exogenous cannabis appears to cause stress and anxiety-related behavioral dysfunction[133]. Furthermore, chronic cannabis usage is linked to a disruption in stress response in humans[163].

Chronic cannabis use has been linked to both blunted and hyperactive stress responses in cannabis users, according to studies[164] [165].

iii. Executive function circuits

Neurophysiological changes in executive circuits have a tight connection with adolescence, as eCS is quite active in adolescent brain development, especially within the PFC, an area where executive functions occur[133].

Exogenous cannabis may thereby impair the formation of GABAergic interneurons in the PFC and desynchronise PFC circuits throughout development [166].

Consequently, adolescent cannabis use may cause long-term changes in the GABA/glutamate balance in the PFC[167].

5. Hypotheses of the neuropathology impairment

The main physio-pathological mechanisms for neuroanatomic alteration have been summarised in an excellent literature review entitled: “The Role of Cannabinoids in Neuroanatomic Alterations in Cannabis Users” by Valentina Lorenzetti and her team[24]. The review distinguished between high-CBRs density regions and low-density regions.

Thus in areas with a high cannabinoid receptor density, two of the most captivating causes of neuroanatomic changes are[24]:

- THC and its metabolites accumulation in neurons, which results in THC mediated neurotoxicity[20].
- There is downregulation, adaptation, and molecular and signaling modifications downstream of cannabinoid receptors[21] [22] [23].

In terms of pathology, neurotoxicity is manifested by shrinkage of neuronal cell nuclei and bodies, decreased synapse number, and decreased pyramidal cell density, according to the literature [168] [169] [170] [171].

According to the same review, a relevant conclusion has been made about regions with a low density of cannabinoid receptors. Chronic cannabinoids can

induce changes in synaptic oscillations in areas with a high density of cannabinoid receptors (hippocampus and amygdala), which can then spread to functionally and structurally related regions with low CBR (parietal cortex and orbitofrontal cortex), resulting in neuroanatomic changes in the latter.

Another piece of evidence that goes along with these findings and will support the hypothesis of our study is that: In studies of neurodegenerative diseases, there was a strong correlation between changes in intrinsic connectivity between functionally and structurally related regions and changes in gray matter volumes in the same areas[25].

It has also been shown that cannabis users show alteration in both regions with high and low density of cannabinoid receptors[24].

Chapter III: Diffusion MRI and tensor imaging

I. General theories, concepts, and laws about diffusion

The purpose of diffusion imaging is to highlight water's microscopic motions in the tissues. In fact, water molecules are not immobile in a biological environment: they are subjected to a permanent agitation called "Brownian motion.".

The Brownian motion takes its name from the botanist Robert Brown, who studied in 1826 the seemingly random pattern of movement shown by pollen grains while suspended by his microscope in water. He attributed this phenomenon to the pollen grains at first, but he dismissed this theory, finding the same action with inanimate and inorganic compounds, and it soon became apparent that the motion he observed was due to the shaking of the pollen grains by the water molecules that accompanied them.

Subsequently, this principle was developed, well defined, and elaborated by other physicians, notably Adolf Fick and Albert Einstein [172173174]. Thus, Dr.Fick has developed a very relevant rule and proposed a groundbreaking new coefficient. The law of Fick, which embodies the idea that particles flow from high-concentration regions to low-concentration ones, is:

$$J = -DVC$$

With:

-J is the **diffusion flux**.

- C is the particle concentration

- D is the diffusion coefficient or diffusivity.

This law is analogous to the heat equation introduced by Joseph Fourier in 1822[175]. The diffusion coefficient is an intrinsic environmental property. The magnitude of the diffusion coefficient is defined by:

- The size of the molecules that diffuse
- Temperature
- And the environmental microstructural features.

As we describe above, Fick's law relates diffusion to temperature and concentration. According to the law of Fick, The net flux decreases systematically as the concentration decreases, and so when the concentration gradient becomes null, the net flux fades away, unlike Brownian motion described by Robert Brown in 1828, which report that, on a molecular level, particles move uniformly and with no clear cause. [176]

Einstein well reconciled these two very useful but somewhat contradictory notions in 1905. This reconciliation, which we have just mentioned, is clearly shown in the "displacement distribution," which calculates the probability that a given molecule will travel a certain distance (x) over a given period of time (t):

$$P(x_n, t) = \frac{1}{\sqrt{(4\pi Dt)^n}} \exp\left(-\frac{\mathbf{x}\cdot\mathbf{x}}{4Dt}\right).$$

As a result, the function of the displacement distribution in free diffusion is a Gaussian function, the width of which is defined by the diffusion coefficient.

From the theory of displacement distribution, Einstein draws an explicit relationship between the mean-square displacement of the ensemble, which characterises its Brownian motion, and the classical diffusion coefficient, D, which occurs in Fick's law.

Indeed, the mean square displacement during the time Δ is defined by:

$$\left\langle x^2 \right\rangle = 2D\Delta,$$

II. Introduction to diffusion and MRI

Magnetic resonance imaging depends on the association of the applied magnetic field with the nucleus in the sample. Thus, a standard nuclear magnetic resonance scan begins with the excitation of the nucleus with a 90° radiofrequency (RF) pulse, which inclines the magnetising vector to the plane, whose normal is along the main magnetic field[177].

Spin (cinematic moment) is a quantum mechanical property of a nucleus, and it gives rise to a net magnetisation over a vast number of nuclei when positioned in a magnetic field. The spins then begin to precess around the magnetic field; the net magnetisation of spins precesses with a frequency proportional to the magnetic field's local power[178]. This latter is considered the Larmor precession, and this precession's angular frequency is given by:+u ¼ gB[178]

$$\omega = \gamma B$$

With:

-**B**: the magnetic field that the spin is exposed to.

-**γ**: the gyromagnetic ratio, which is a constant specific to the examined nucleus.

One of the significant applications and contributions of the Larmor precession equation in MRI imaging is acquiring a magnetic resonance image and applying diffusion weighting by exploiting this relationship.

The bulk of the signal for biological tissue comes from the hydrogen nuclei in the water molecule. Seen – as we describe in the paragraph on the diffusion phenomenon – the water molecules are not immobile; the purpose of diffusion imaging would be to highlight water's microscopic motions in the tissues. And since the geometrical environment composition determines diffusion, MR can be used for non-invasive analysis of the structural environment[179] [180] [181].

Molecular movements are spontaneous and vary in amplitude following the environment's structure. On the other hand, the rate of diffusion depends on the free flow of the water in the area, therefore:

- Diffusion is said in a given region to be high when water is free and molecular agitation is consequently important.
- In contrast, the diffusion is stated to have been reduced when molecular agitation is diminished due to the barriers opposing those movements.

By adopting these concepts on the signal acquisition pathways in MRI:

- Hydrogen proton motions induce phase shifts that reduce the signal.
- Such changes in the process are more important if the proton moves faster.

➔ As a consequence, the agitation of the water molecules has a strong effect on the signal[182]

III. Demonstrating and detecting molecular motion

In order to illustrate molecular microscope motions, the signal loss induced by moving protons must be detected, which is not possible with standard sequences, necessitating the employment of a particular sequence capable of collecting diffusion-weighted images.

Hahn was the first to formulate diffusion effects on spin-echo NMR experiments at a constant magnetic field gradient[183]. Since Hahn did not recommend a straightforward approach for calculating the diffusion factor [184], four years later, for such a calculation, Carr and Purcell suggested a complete mathematical and physical structure using Hahn's NMR spin-echo sequence[184].

In 1965 Stejskal and Tanner developed many innovations which allow modern measuring diffusion through MRI [185]. So to obtain "diffusion-weighted" images, additional gradients are added in an EPI-SE type sequence. Stejskal- Tanner sequence and equation are still widely used.

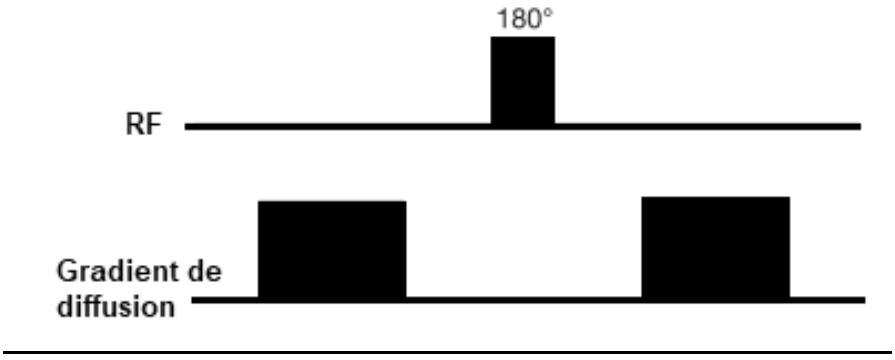

Figure 5: Principle of diffusion gradients.
In an EPI-SE like sequence, diffusion gradients are applied on each side of the 180-degree RF pulse.

And PGSE is arguably the most frequently used method of sensitising the MRI signal to molecular diffusion.

The Stejskal et Tanner 's sequences affect the motion of moving and stationary protons [182] (Figure 6):

● **For immobile protons:** the dephasing caused by the first gradient is perfectly compensated by the second. Therefore the signal of immobile water molecules is not attenuated.

● **For moving protons:** Dephase faster when applying the first gradient, and the second gradient does not compensate for this phase shifting. As a result, the signal is attenuated.

➔ Signal decrease is even more significant when molecular movements are fast; leading to a more elevated phase shifting of the protons, which is even less compensated by the second gradient.

Briefly, diffusion images show a hyper-signal in regions with reduced molecular diffusion and a weaker signal when the explored area contains molecules with high diffusion.

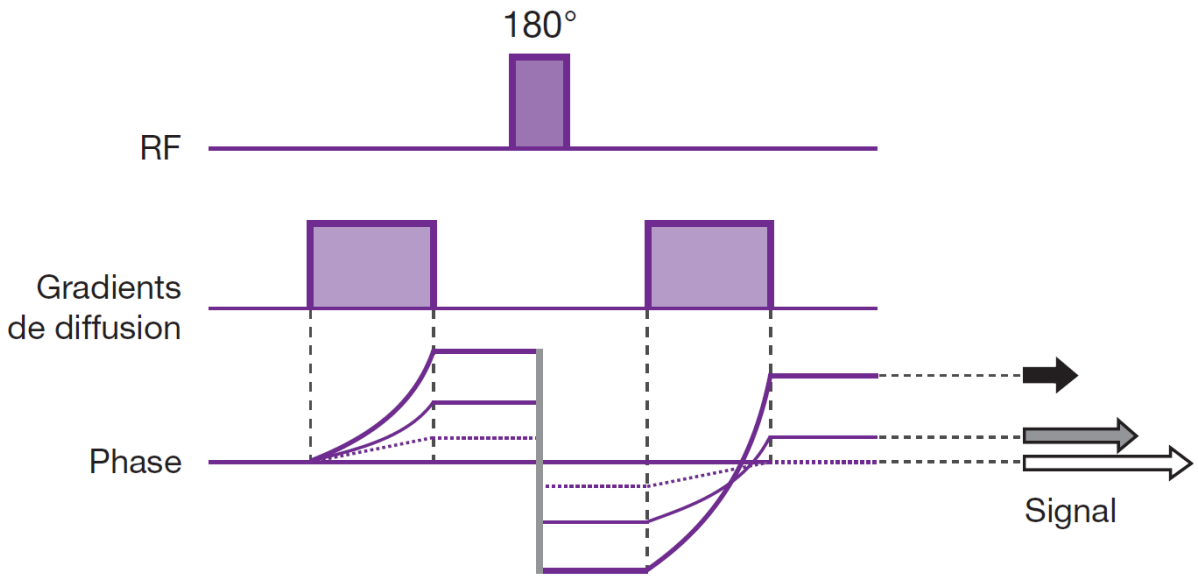

Figure 6: EPI-SE sequence with diffusion gradients and dephasing based on molecular mobility.

RF = Radiofrequency
-White arrow = high signal = unattenuated signal from immobile water molecules.
-Gray arrow = signal attenuation = fast molecule signal = phase shift not compensated by the second gradient.
-Black arrow = even greater attenuation of the signal = faster molecules signal = higher proton phase shift which is even less compensated by the second gradient. (Vetter D, Kastler B, Patay Z. 2011)[182].

IV. Quantifying the diffusion weighting

As previously shown, the diffusion effect depends on the gradients used. These gradients are characterised by a factor which is "b-value.".

Therefore, the "b-value" measures the degree of diffusion weighting applied. It's characterised by the following relationship[186] [182] [187] [181] (Figure 7):

$$b = (\gamma G \tau)^2 (T - \tau/3)$$

With:

ɣ = gyromagnetic ratio

G = amplitude of the gradient

π = duration of application of the gradient

T = time between the application of the two diffusion gradients

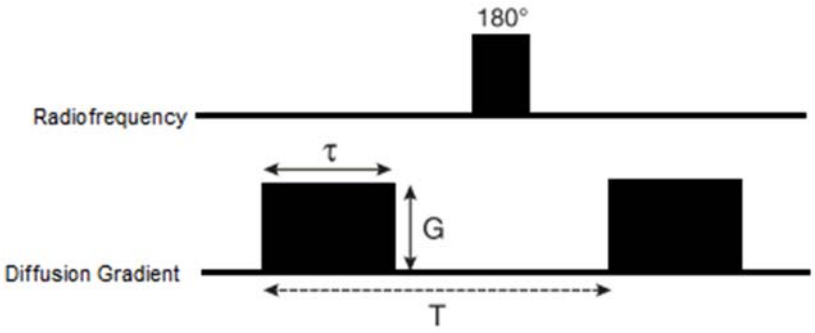

Figure 7: Determination of the "b-value"

V. Relationship between the b-value and the signal

The "b-value" is a robust measure of how far the image signal is impacted by the tissue water diffusion [181] [182]:

-A low b-value scanning has more signal than a high B-value scanning; however, a higher b-value scanning has more signal attenuation in the presence of diffusion than a low B-value scan.

-When b-value = zero: We have no diffusion weighting in the image.

It's worth noting that weighted diffusion acquisitions typically require one or two zero-b-value normalisation scans.

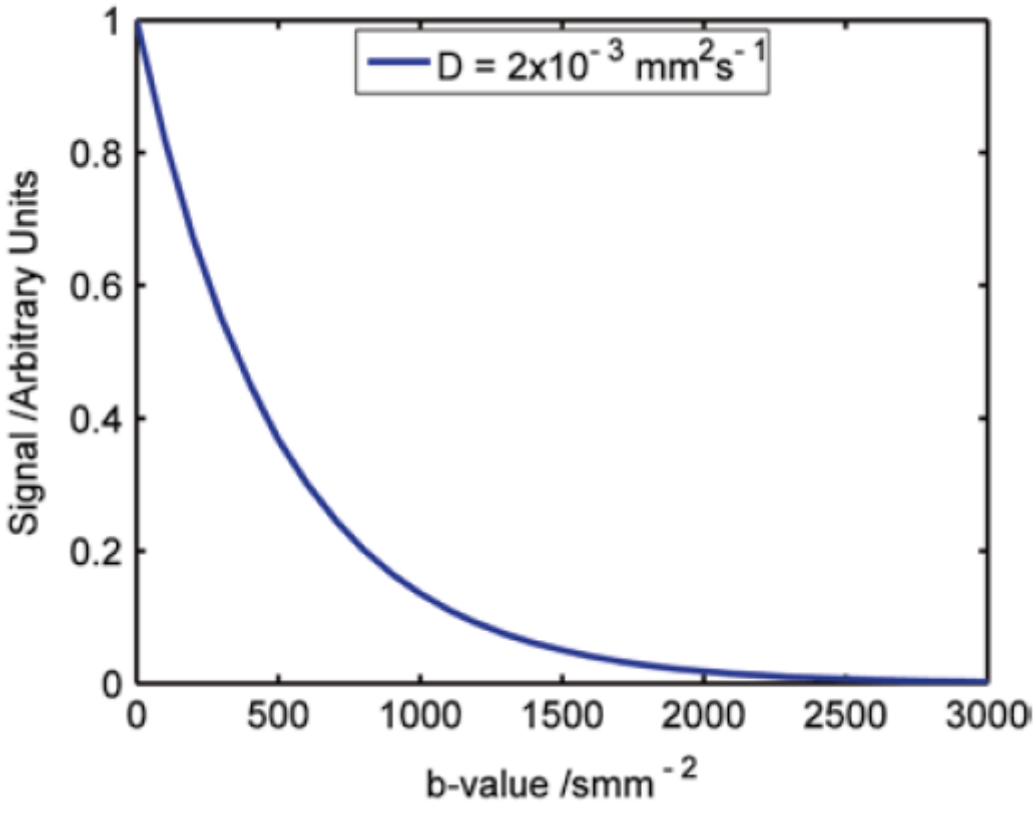

Figure 8: Weighted diffusion of the MRI signal by b-value.
(Rowe M, Siow B, Alexander DC, Ferizi U, Richardson S. 2016)[181]

As a practical interpretation [188]:

-When we set a very small "b-value," the signal loss through the diffusion process will be too small. Therefore we cannot reliably calculate the decay of the signal.

-In another hand, when we set a "b-value" that is too large, we can observe a substantial decrease in the signal, and the signal intensity may reach the noise level.

➔ Clearly, there is an ideal range for the "b-value," which depends on the diffusion constants of the sample and the SNR.

VI. The diffusion constant from signal decay

1. Extraction of the diffusion coefficient

Given that diffusion MRI aims to characterise the diffusion of protons in tissues, we have to extract the liquid diffusion parameter, principally Diffusion coefficient, D.

Using MRI scanner measurements and the Stejskal-Tanner equation[189]: the diffusion D coefficient of free water can be calculated.

The Stejskal-Tanner equation is $S = S_0 \bullet e^{-b \bullet D}$ (1)

With:

S: is the intensity of the diffusion-weighted image

S0: The non-diffusion-weighted, T2-weighted image's intensity

b: The b-value

D: Diffusion coefficient

So, With this equation, we will be able to extract the diffusion coefficient.

From (1), we can rewrite the equation as $-\ln(\frac{S}{S_0}) = b \bullet D$ (2)

And from (2), we have : $D = \frac{-\ln(\frac{S}{S_0})}{b}$ (3)

The value of D is reported in mm2/s.

The diffusion coefficient of pure water is about 2.2×10−3 mm2 /s at 25°[190].

2. The apparent diffusion coefficient (ADC)

For diffusion coefficient "D," the Stejskal-Tanner equation can provide a credible calculation only if nothing disturbs the experiment.

However, cell membranes are present throughout almost all the places in tissues, such as brain tissue. These structures hinder the water molecules, and inside the cells may even be restricted to a confined space.

And therefore, it is apparent that our D calculation will decrease, which is why we call it the ADC, which is different from the diffusion coefficient of free water molecule instead of D.

By measuring the ADC, we have efficient access to a probe that tells us much about these cells that hinder or restrict diffusion and provide interesting information about the microstructure of the studied tissue[190 191 192 193 187 194].

From equation (3), we conclude that: $$\mathrm{ADC} = \frac{-\ln(\frac{S}{S_0})}{b}$$

VII. Characterisation of the apparent diffusion coefficient

The images weighted by diffusion depend on the direction in which the applied diffusion gradient is taken so that diffusion sensitising gradients are applied in a specific direction, and measures are only sensitive to diffusion in that direction[190 191 195 196 197 198 194 199 200].

We define the brain in three axes: x goes from left to right, y from back to front and z from below to top. In these three axes, x, y and z, the diffusion gradients are applied and integrated with an EPI-SE sequence [2].

Suppose we use for instance the diffusion gradient in the direction of x. In that case, the measurements are susceptible to diffusion along x but progressively less sensitive to diffusion along with directions that deviate more and more from x until they are entirely insensitive to diffusion along with directions perpendicular to x. (the YZ-plane)[192].

Practically, a diffusion sequence involves the repeated use of three EPI sequenc es, each with diffusion gradients in the axis of the slice selection, phase coding and frequency coding: three images are generated per slice, diffusion-weighted in each corresponding axis [182].

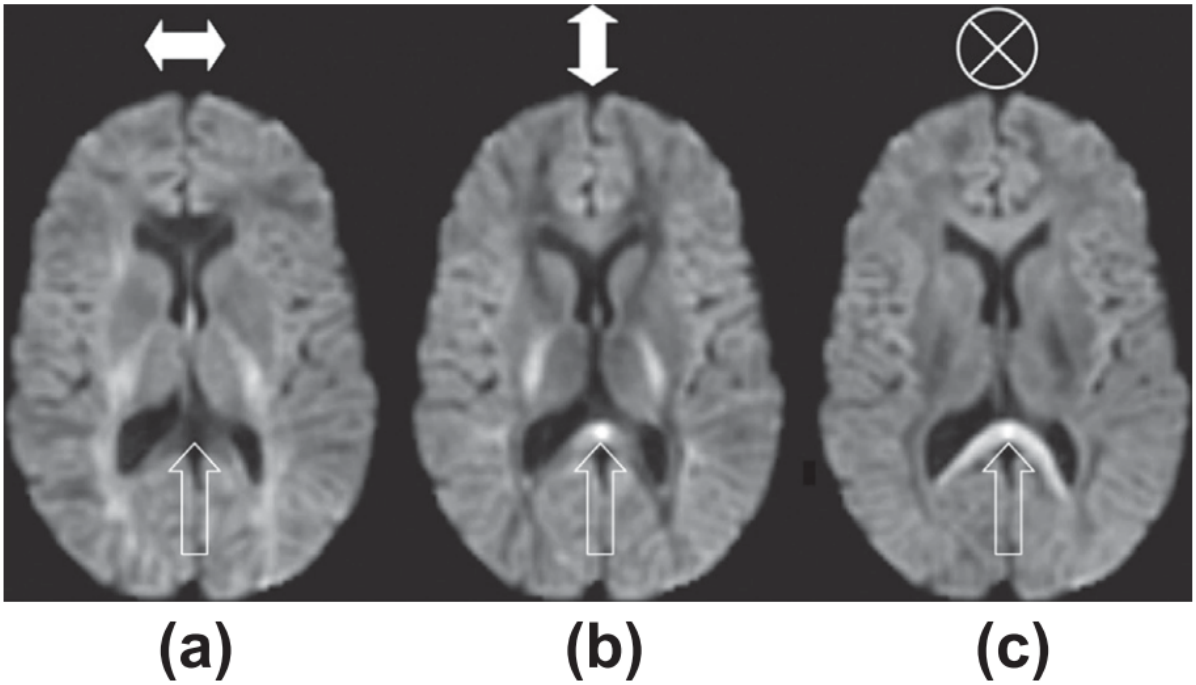

Figure 9: Effect of changing the axis of the diffusion-encoding gradients on the diffusion-weighted signal intensity.

The arrows at the top of the figure show the orientation of the encoding axis.
-(C): The orientation is perpendicular to the viewing plane.
-Dark areas: have high apparent diffusivity.
-Light areas: represent lower apparent diffusivity.
-The area highlighted by the lower arrows, forms the midsagittal portion of the splenium of the corpus callosum, the apparent diffusivity is high along the left-right axis, but low in the two orthogonal directions.
(Jones DK. 2016) [202]

VIII. diffusion tensor imaging

1. Introduction

MRI can help the radiologist and clinicians differentiate and evaluate the general and macroscopic status of an anatomical area. And this is generally based on the -so-called conventionally -: "anatomical" T1 sequence (where the white matter appears white and the grey matter appears grey) and "anti-anatomic" T2 sequence (it is precisely the reverse; therefore, white matter is grey and grey is white).

However, these traditional scans are not sensitive to tissue microstructure architecture and are unaware of the effect of tissue orientation. And here resides the added value of the DTI technique: It makes it possible to reach the microstructural properties difference and changes, particularly in the brain tissue, and to segment: White Matter Fibers in a wide variety of neurological and psychological conditions by tractography[179]. In addition to that, DTI has a significant contribution to ischemic brain injury.[201]

When our image volume comprises ordered tissue, we can no longer accurately describe the water molecules' behaviour with one ADC. Consequently, we should reach a much more complex model for characterising diffusion. And this complex model will be the diffusion tensor, a complicated model for Gaussians diffusion in which the displacements per unit time are not uniform in all directions [190] [191] [194] [202] [203].

In 1846, William Rowan Hamilton invented the term "tensor," which was used to describe something diffrent than what is now known as tensor[204]. Gregorio Ricci-Curbastro formed tensor calculus around 1890, and it was first presented in 1892[205]. And the publication of Ricci-Curbastro and Tullio Levi-in Civita's in 1900 made it available to mathematicians[206].

As a result, the tensors offer a natural and coherent mathematical basis for expressing and solving problems in physics fields like elasticity, fluid dynamics, and general relativity[191 203 207].

In maths: an algebraic tensor is an entity that represents the relationship between several algebraic objects associated with an area of the vector. Between vectors, scalars, and even other tensors, objects may be mapped.

Scalar generalisations, vectors (which have precisely one index), and matrices (which have exactly two indexes) are tensor generalisations of arbitrary numbers of indices [208].

2. Diffusion tensor theory:

To recap, to explain the mobility of molecules in all directions, we need to use the mathematical definition of tensor, which allows one to represent the properties of a three-dimensional ellipse. The components of this tensor are defined by a three-dimensional (3 x 3) matrix containing diffusion coefficient measurements in nine directions[209]:

$$\mathbf{D} = \begin{bmatrix} D_{xx} & D_{xy} & D_{xz} \\ D_{xy} & D_{yy} & D_{yz} \\ D_{xz} & D_{yz} & D_{zz} \end{bmatrix}.$$

There are three equivalences in this matrix: Dyx = Dxy, Dzx = Dxz, Dzy =Dyz To define a diffusion anisotropy, all that is necessary is to acquire images with diffusion gradients in six different directions (xx, yy, zz, xy, xz, yz) instead of the nine original directions, as well as an image without a diffuser gradient[182].

These measurements allow us to quantify three "eigenvectors " for an ellipse, which are the three "eigenvectors " of diffusion (λ1, λ2, and λ3) that describe diffusion in three orthogonal directions (Figure 10). As a consequence, the main diffusion direction can be determined for each ellipse and, as a result, for each voxel: Three "eigenvectors" (e1, e2, e3) associated with these three "eigenvalues" of diffusion are then obtained for an ellipse, allowing us to characterize diffusion in three orthogonal directions (Figure 10) [187 194 195].

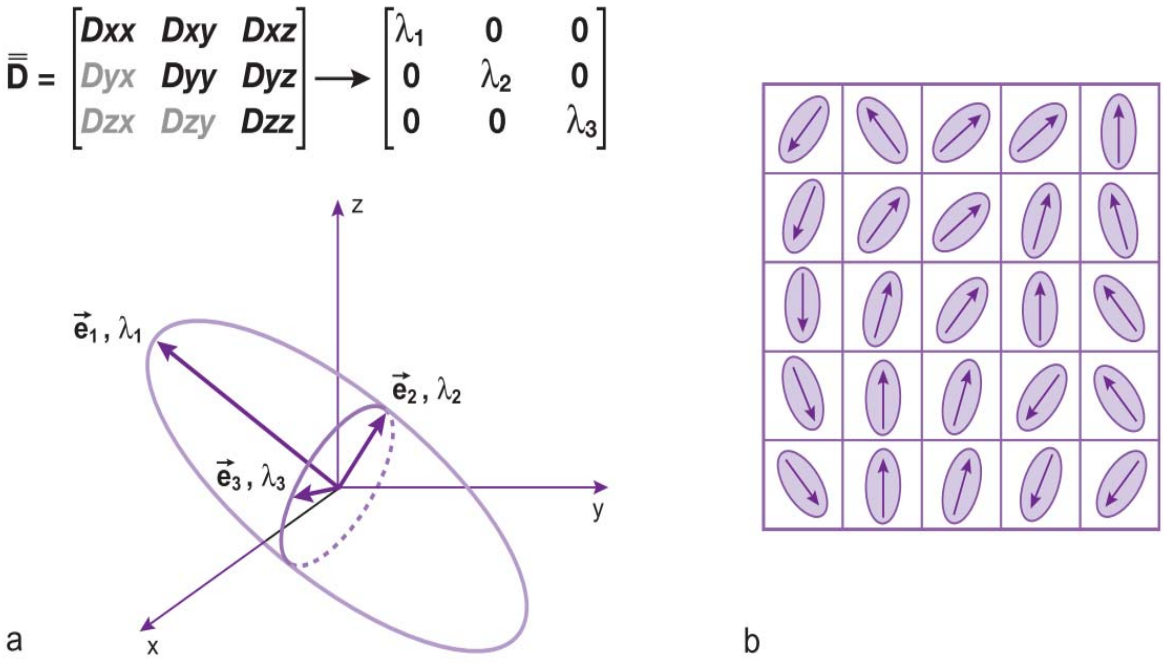

Figure 10: Theoretical and mathematical principles of diffusion tensor imaging.

(a) : A three-dimensional ellipse that represents schematically anisotropic diffusion

(b) : Determining for each ellipse and, therefore, for each voxel, the main diffusion direction. (Vetter D, Kastler B, Patay Z. 2011)[182].

3. The tensor as a practical tool

Using three figures (Figure 11, 12, 13) with corresponding interpretations, we briefly summarise how tensors can provide a practical and valuable brain approach. In figure 11, we show the diagonal diffusion tensor element; then, in figure 12, maps of the off-diagonal tensor elements. Finally, in figure 13, we depict the ADC values represented by the fitted diffusion tensors in a spherical polar plot, shown for the Genu of the Corpus Callosum (GCC) region. Figure 13 also provides evidence that the nearby CSF in the ventricles exhibits an isotropic pattern of diffusion.

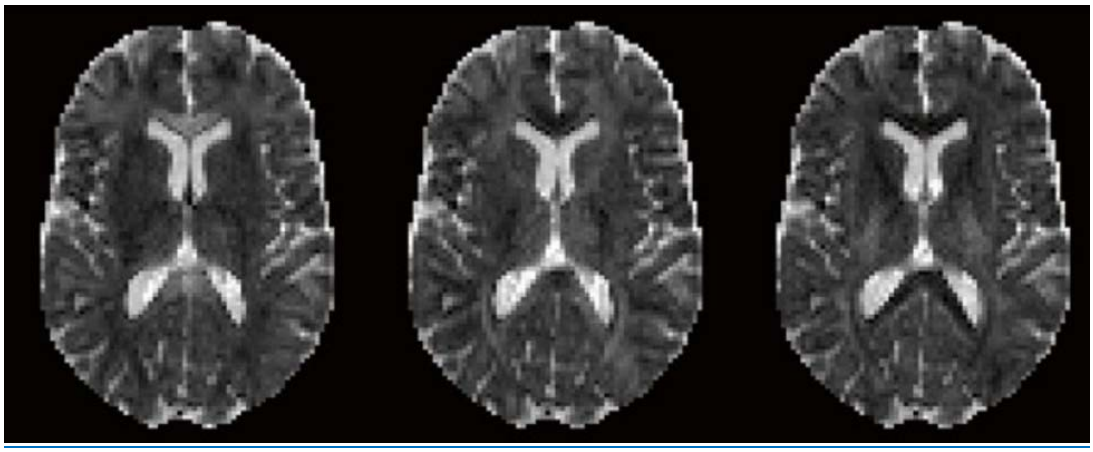

Figure 11: Maps of the diagonal diffusion tensor elements (Dxx, Dyy, Dzz)

Interpretation:

- The background grey level equals zero
- The background darker/brighter levels represent negative/positive values.

(Dhollander T. 2016)[192].

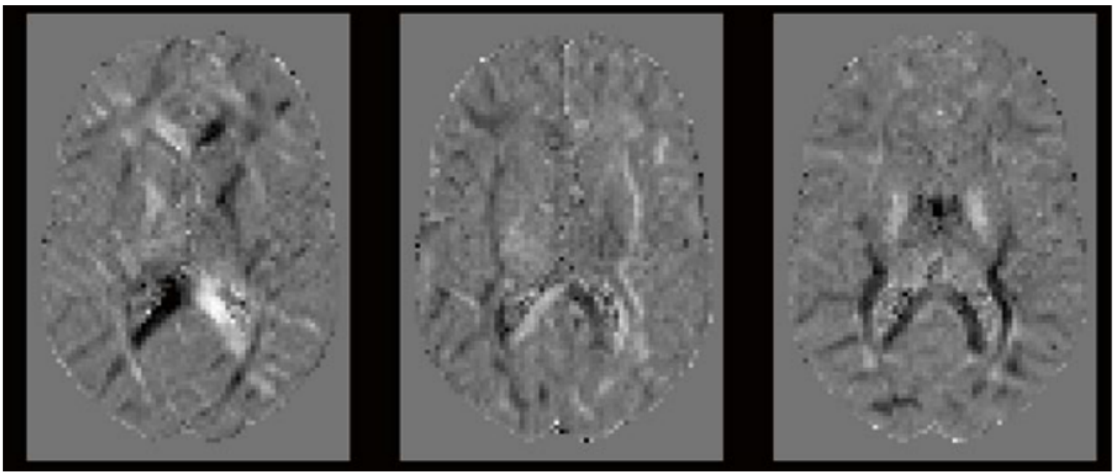

Figure 12: Maps of the off-diagonal diffusion tensor elements (Dxy,Dxz,Dyz)

Interpretation:

●The background grey level equals zero

●The background darker/brighter levels represent negative/positive values.

●The voxels in the center of the GCC, where the main paths of the tensors are neatly matched to the x-axis, have a value of zero on the map of the off-diagonal components, Dxy. (Dhollander T. 2016)[192].

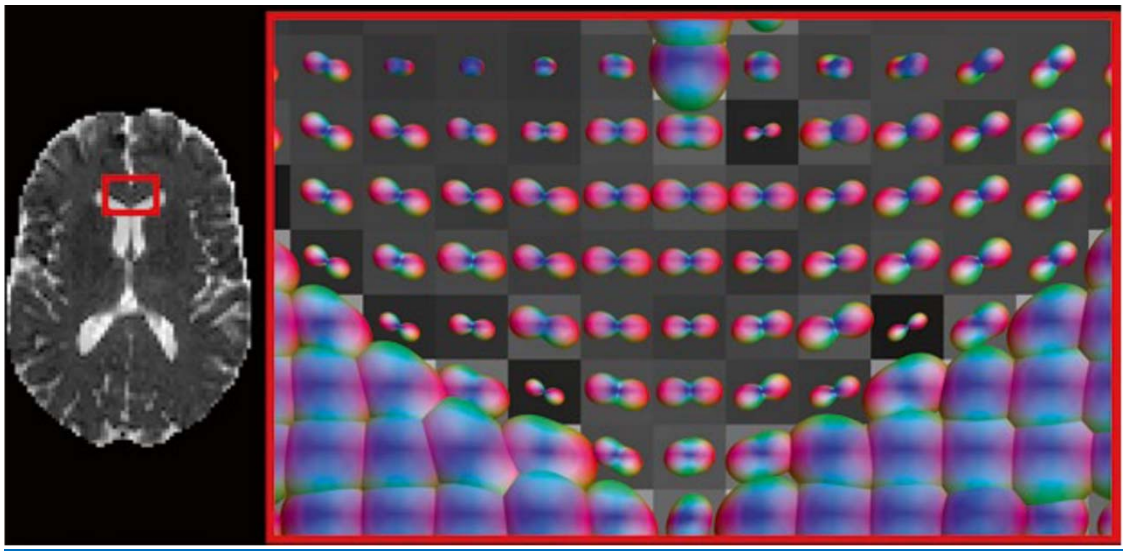

Figure 13: Spherical polar plots of the ADC values provided by the diffusion tensor model in a region of the GCC, overlap on a map of the average ADC value. Note the characteristic peanut shapes that appear in the GCC.

Interpretation:

●The plots usually take the form of peanuts in regions with a single bundle of axons, such as the GCC.

●From the region shown in the figure, it is now also more evident that the nearby CSF in the ventricles exhibits an isotropic pattern of diffusion. (Dhollander T. 2016)[192].

4. Diffusion tensor and diffusion-weighted signal

Calculating the coupling between the signal attenuation and the elements of the diffusion tensor for a given gradient, amplitude, length, and separation is an essential part of the tensor estimation process.[202]

Since the tensor is a 3 x 3 matrix, this scaling is also a 3 x 3 matrix. And from the equation estimating the scalar ADC: [185186]

$$S = S_0 \bullet e^{-b \bullet D}$$

With:

S: is the intensity of the diffusion-weighted image

S0: The non-diffusion-weighted, T2-weighted image's intensity

b: The b-value

D: Diffusion coefficient

So, With this equation, we will be able to extract the diffusion coefficient. Then as an effect, for anisotropic media, this equation is rewritten as:

$$\frac{S}{S_0} = \exp\begin{pmatrix} -b_{xx}D_{xx} - b_{yy}D_{yy} - b_{zz}D_{zz} \\ -2b_{xy}D_{xy} - 2b_{xz}D_{xz} - 2b_{yz}D_{yz} \end{pmatrix}$$

There will be only six unknown elements to decide since the tensor is symmetric (Dyx=Dxy, Dzx=Dxz, Dzy=Dyz). Here are determined from a collection of diffusion-weighted images obtained with non-collinear and non-coplanar gradients[194 198].

And for estimating the elements of the tensor, a minimum of six diffusion-encoding images plus one non-diffusion-weighted image will be needed.

5. DTI data acquisition

Manipulation of fundamental parameters in standard imaging will weigh the sequence to a specific tissue characteristic, change the contrast and signal to noise ratio (SNR), and change the spatial resolution of the image. These same concepts apply to DTI; however, acquiring both non-diffusion and multiple diffusion-weighted images adds another degree of complexity[187].

As a result, data quality and analysis are influenced by DTI acquisition factors such as the[210]:

- Number of diffusion directions
- Image resolution
- b-Value
- Number of b -values
- Number of averages

a. b-value

The involvement of numerous variables complicates the calculation of the ideal b-value[211 212 213 214] :

-SNR: the higher the SNR, the more accurately signal attenuation can be measured with higher b-values.

-Echo-time: the smaller the b-value, the shorter the achievable echo time.

-And other factors such: eddy current and motion artifacts

b. The number of diffusion directions:

While only six directions are necessary for typical DTI[215], obtaining more will enhance the estimate of the diffusion tensor and allow the application of more sophisticated reconstruction methods that may overcome sophisticated fiber architecture[214 216].

Some investigations found that increasing the number of orientations up to 30 enhanced fractional anisotropy (FA) estimates, implying that as many DW gradient orientations as time permits should be used [217] [218]. As a result, the number of directions chosen during acquisition impacts the estimation of fractional anisotropy[214].

6. Quantitative measures calculated from a DTI dataset and their contribution to neurobiology

a. Trace

It is calculated as the sum of the three eigenvalues λ1, λ2, and λ3 or the sum of the diagonal elements of D (Dxx, Dyy, Dzz)[219]:

$$\mathrm{Tr}(D) = \lambda_1 + \lambda_2 + \lambda_3 = D_{xx} + D_{yy} + D_{zz}$$

In terms of neurobiology, the trace can aid in the examination and diagnosis of stroke[201].

b. Mean Diffusivity

It's a measurement of a voxel's total diffusivity, independent of orientation. It's a proportioned version of trace[219]:

$$D = \frac{Tr(D)}{3} = \frac{\lambda_1 + \lambda_2 + \lambda_3}{3} = \frac{D_{xx} + D_{yy} + D_{zz}}{3}$$

MD, like Trace, is low in white matter but high in regions like the ventricles, where water molecules can move freely. As the trace, when evaluating the progression of a stroke, MD is an essential metric to consider.

Water molecule movement becomes more constrained as the brain matures, as cell and axonal membranes become more densely packed. Due to the vast extracellular gaps found in unmyelinated white matter, the MD of white matter in the immature brain is approximately double that of the fully myelinated brain [219].

c. Axial Diffusivity

Axial diffusivity is the diffusivity along the diffusion ellipsoid's main axis, indicated by λ1[219]:

$$AD = \lambda 1$$

It has been linked to axonal injury, namely fragmentation[220221].

d. Radial Diffusivity

It's a measure used to express the diffusivity perpendicular to the principal direction of diffusion[219]:

$$\lambda_{\perp} = \frac{\lambda_2 + \lambda_3}{2}$$

Axonal density, myelin integrity, axonal diameter, and fibre coherence have all been linked to radial diffusivity parameter[220221].

Despite the advantages of axial- and radial diffusivity parameters, it is not advisable to compare the eigenvalues of diffusion tensors, especially by comparing patients to healthy controls, without confirming the alignment of related eigenvectors to the underlying tissue structures[222].

e. Fractional Anisotropy

FA may be used to calculate the ratio of the anisotropic component of D to the total magnitude of D. FA values vary from 0 to 1, and they may be computed in each voxel using the following equation based on the diffusion tensor's eigenvalues or mean Diffusivity value[219]:

$$FA = \sqrt{\frac{3}{2}} \sqrt{\frac{(\lambda_1 - \lambda)^2 + (\lambda_2 - \lambda)^2 + (\lambda_3 - \lambda)^2}{\sqrt{\lambda_1^2 + \lambda_2^2 + \lambda_3^2}}} = \sqrt{\frac{(\lambda_1 - MD)^2 + (\lambda_2 - MD)^2 + (\lambda_3 - MD)^2}{2(\lambda_1^2 + \lambda_2^2 + \lambda_3^2)}}$$

Table 2: Things that describe, influence the FA and relation of the FA with neurobiology.

What does influence the FA parameter[223]?	What does FA describe[219]?	What is the relation of the FA with neurobiology?
-Large macromolecules that are orientated in a specific way. -Organelles and membranes. -Myelination level. -Axon packing. -Water permeability of the membrane. -Internal axonal structure. -The amount of water in the tissue.	-Directional consistency of water diffusion in tissue → very beneficial in the interpretation of **White matter integrity**	-A decrease in FA is linked to neurodegenerative processes[219 224 225]. -FA levels rise during childhood and adolescence[219 226 227]. -A higher FA is linked to a higher IQ or better performance in cognitive domains[219 228 229 230].

As a summary in table 3 below, the interpretation of diffusion indices regarding the brain microstructure changes, and with figure 14, we show some of the important parameters maps derived from diffusion imaging.

Table 3: Contribution of diffusion indices in the analysis of Brain microstructure by DTI. (Alexander AL, Hurley SA, Samsonov AA, et al. 2011) [231]

	FA	MD	AD	RD
Grey matter	↓	—	↓	↑
White mater	↑	—	↑	↓
Cerebrospinal fluid	↓	↑	↑	↑
High Myelination	↑	↓	—	↓
Axonal density	↑	↓	—	↓
Maturation of SB	↑	↓	↑	↓
Axonal degeneration	↓	↑	↓	↑
Demyelination	↓	↑	—	↑

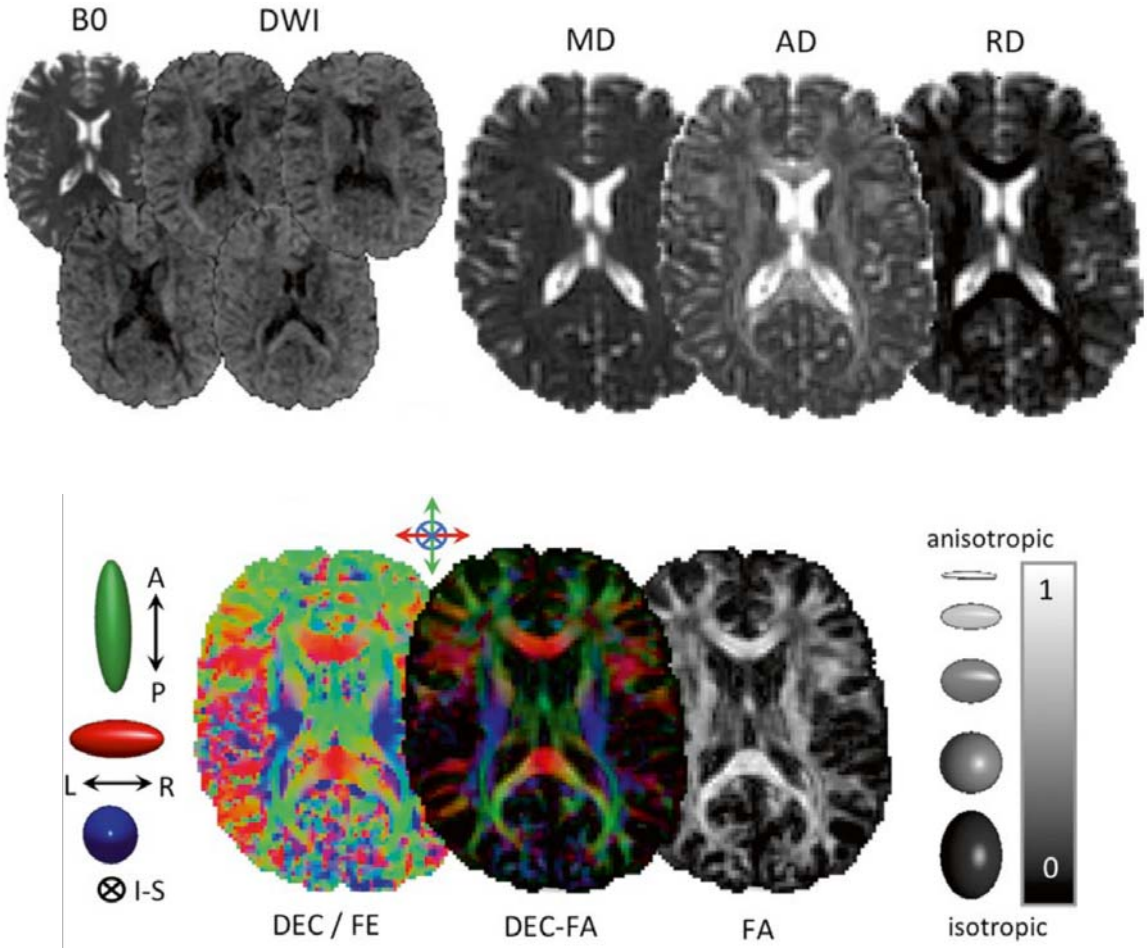

Figure 14: Some parameters maps derived from diffusion imaging.

With:

- B0: non-diffusion-weighted image.
- DWI: diffusion-weighted image.
- MD: mean diffusivity.
- AD: axial diffusivity.
- RD: radial diffusivity.
- DEC: direction-encoding color.
- FE: first eigenvector.
- FA: fractional anisotropy.
- Orientation: A-P: anterior-posterior - L-R: left-right - I-S: inferior-superior.

7. Types of data analysis

After the data has been acquired and pre-processed, the next step is to determine how to extract meaningful information from it.

Comprehensively, using a figure, the many DTI analysis techniques are presented in this section (figure 15).

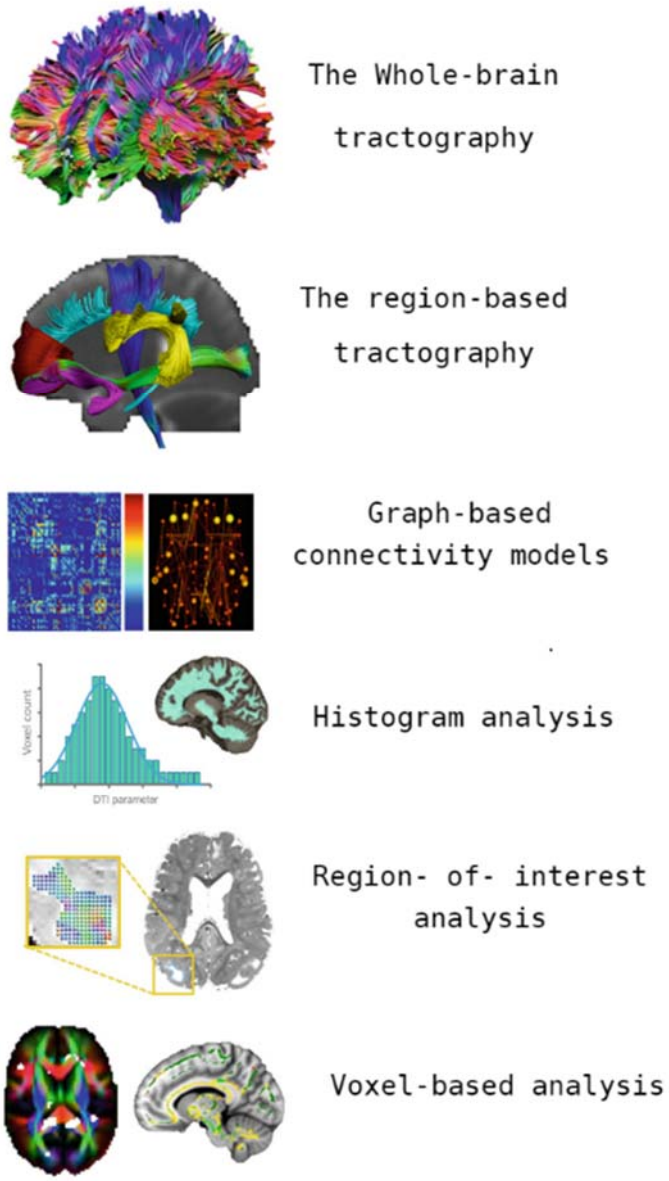

Figure 15: Overview of the different DTI analysis methods.
(Emsell L, Van Hecke W, Tournier JD. 2016) [187]

Material and methods

Chapter I: The overview of the study

I. Study design

All subjects were recruited in the Addiction centre, Department of Psychiatry, University Hospital of Fez; Fez, Morocco. They gave written consent to participate in a clinical and MRI study conducted by Clinical Neuroscience Laboratory, Faculty of Medicine, Pharmacy and Dental Medicine of Fez; the University of Fez in collaboration with the Addiction centre affiliated to the Psychiatry Department, and Radiology and Clinical Imaging Department, University Hospital of Fez.

All patients underwent the same psychological and biological evaluation before launching an identical brain structural MRI, DWI and DTI protocol.

Consequently, using the Mini International Neuropsychiatric Interview (MINI), all cannabis users and non-users were evaluated for any possible clinical comorbidity.

II. Subject's characteristics

13 chronic substance user's (cannabis) volunteers never treated for were recruited for this study. Their duration of cannabis use ranged from 0.5 to 21 years. According to the national regulation, all cannabis substance users were volunteering and consented to participate in the study according to the national regulation complying with most international regulations and ethical standards. Moreover, they were not among the care seekers of our centre.

While the primary criteria of selection are being cannabis substance users during at least the last six months before recruitment independently of the cannabis dose used, the inclusive selection criteria are to be free of any traumatic, neurological and chronic disease and free of any psychiatric disorder except minor depression.

Besides, cannabis user's volunteers are not known to be alcohol drinkers, even light types. Only occasional alcohol drinking is accepted provided that it does not exceed three drinks (glasses) per week, including all kinds of wine and beer. Another critical point in our volunteer groups: There is no comorbid drug use besides cannabis.

The global characteristics of cannabis users were a young average of 26 years old, ranging from 20 years old to 38 years old.

All cannabis users were convened in 2 user's groups. The first cannabis users group (Group I) included seven cannabis users using an average of 16 joints per day and 109 joints per week, with a minimum of 6 joins per day and a maximum of 25 joints per day.

The second cannabis user group (Group II) included 6 cannabis users who are smoking an average of 1\3 joints per day and an average of 4,5 joints per week with a minimum of 1 joint per week and a maximum of 7 joints per week. Detailed data of cannabis users' volunteers are reported in Table 1.

Besides, a healthy non-user control group (Group III) consisting of 6 volunteers were recruited. The average age was 32 years old with a minimum age of 28 years old and a maximum of 48 years old.

Table 4: Average profile of cannabis substance users groups (I and II) and non-users group (Group III).

	Group I	Group II	Group III
Number of subjects	7	6	6
Minimal age (Years-Old)	20	21	28
Maximal age (Years-Old)	38	28	48
Average age (Years-old)	28,5	26,5	32
Average at the first substance use	17,5	20,5	NA
Average number of substance use	16,3/day	4,5/Week	NA
The average number of joints in the lifetime of use	64257	259	NA
Range of number of Joints "J" used per day	6 ≤ J ≤25	1\3≤ J ≤1	NA
Minimal cannabis duration from the first use	4 Years	6 Months	NA
Maximal cannabis duration from the first use	21 Years	8 Years	NA
Average cannabis duration from the first use	11 Years	4 Years	NA
Minimal Tobacco duration from the first use	6 Years	6 months	NA
Maximal Tobacco duration from the first use	21 Years	12 Years	NA
Average Tobacco duration from the first use	10,5 Years	4,25 Years	NA
Average number of cigarettes use per day	16,42	6,66	NA
Range of number of cigarettes used per dafy	0 ≤ J ≤30	0 ≤ J ≤20	NA

III. The type and method of the used cannabis

The literature review section of our thesis contains all necessary information about cannabis as a plant and drug, whether harvesting or producing methods internationally and in Morocco.

All of the cannabis used by our volunteers was grown and cultivated in Morocco's northwestern region. Following that, the stages of preparation are all illustrated in figure 16 below.

As a matter of fact, Moroccan cannabis users mostly use joints and Moroccan pipes. The reported cannabis users in our sample were all smoking joints consisting of cannabis past mixed with tobacco. Cannabis consumers can, on rare occasions, drop one to a few droplets of prepared cannabis oil extract on tobacco cigarettes.

Figure 16: Figure illustrating the stages of cannabis cultivation and production, as well as the stages of preparation of cannabis for consumption and the different forms in which cannabis is consumed.

With:

(a) : The Cannabis herb is harvested at the end of the adulthood of the tree.

(b) : Dried Cannabis in the shadow

(c) ; Crush of the dried plant.

(d) Pipes with which crushed plant is smocked to be directly smoked in pipes (d).

(e) , (f) and (g): The "Past" which is the result of the second processing step of production.

(h) and (i): Some of the steps of preparing a join.

(j) A join smoked as cigarette.

(k) Cannabis essential: extracted from the past and it's the result of the third further processing step. Where a drop of it could be let to be adsorbed by tobacco cigarette that will be consumed and smoked.

Figure taken and modified from the article: Boujraf et al. Heavy and Chronic Cannabis Addiction do not Impact the Motor Function: BOLD-fMRI Study. In press

Chapter II: Clinical and psychological evaluation

Given that one of our goals is to examine the impact of chronic and heavy cannabis use on brain regions that are part of the reward, cognition, and emotional regulation circuits, we used a series of tests on the two groups of cannabis users as well as healthy controls to:

-Identify and assess "the cannabis use disorder" using The Cannabis-Use Disorders Identification Test-R[232], considering that it has a strong sensitivity and specificity for cannabis-use disorders as diagnosed by the DSM. The CUDIT-R is a test that accurately screens for cannabis abuse or dependence scores ranging from 0 to 26 of a possible total score of 40.

-Evaluate impulsivity as a personality trait using the Barratt Impulsiveness Scale-11229, a 30-item measure, rated on a 4-point Likert scale(total score range: 30-120).

-Measure how stressful consumers perceive their life by applying a 5-point Likert scale test (total score range: 0-40), The Perceived Stress Scale (PSS)[233].

Data of participants' psychometrics tests and evaluations are reported in the result section.

Chapter III: DTI material and methods

I. Protocol used in the acquisition of diffusion-weighted images (DWI)

The same brain DTI protocol was applied to all patients. The image data was acquired in the MRI Unit of Radiology and Clinical Imaging Department of the University Hospital of Fez; Fez, Morocco.

We used A 1.5 Tesla MRI system (Sigma, General Electric; Milwaukee, Wisconsin, United States).

Before launching an identical brain MRI and DTI protocol, all patients underwent a StructuralMRI scans with a slice thickness of 1 mm in the coronal and axial plane and 5 mm in the sagittal plane (FOV=256mm, matrix=128 X 128) and include a pair of T1-weighted (T1w) and a pair of T2-weighted (T2w) images.

All measurements were performed using a head coil provided for the clinical routine head examinations by the manufacturer. The DWI was done in accordance with the Stejskal-Tanner technique with a single-shot DW echoplanar imaging sequence (DW-EPI)[209].

The sequence is an"Echo Planer Imaging"(EPI) with an Echo time (TE) of 101ms, repetition time (TR) of 6000, and NEX=1. The field of view is 256 mm, with an acquisition matrix of 128 × 128 and a slice thickness of 1 mm in the coronal and axial plane and 5 mm in the sagittal plane.

A total of 26 images were acquired at each of the 23 slice locations. One image is obtained with no diffusion-weighting gradients applied b = 0 (S/mm2), and 25 diffusion-weighted images are acquired at a b-value of 1,000 s/mm2. The diffusion-weighted images were acquired with encoding gradients applied along 25 non-collinear directions.

II. ExploreDTI, the MR diffusion, and DTI analysis toolbox

The "ExploreDTI" Toolbox was used to collect all of our quantitative diffusion data. ExploreDTI is a software pack that integrates all of the most important MR diffusion analysis techniques. It is written in MATLAB (© 1994-2021 The MathWorks, Inc) and works on various platforms: Windows, Unix, Mac[234].

ExploreDTI focuses on interactive data visualization and manipulation. Figure 17 summarizes interactive display and data manipulation that ExploreDTI allows and focuses on.

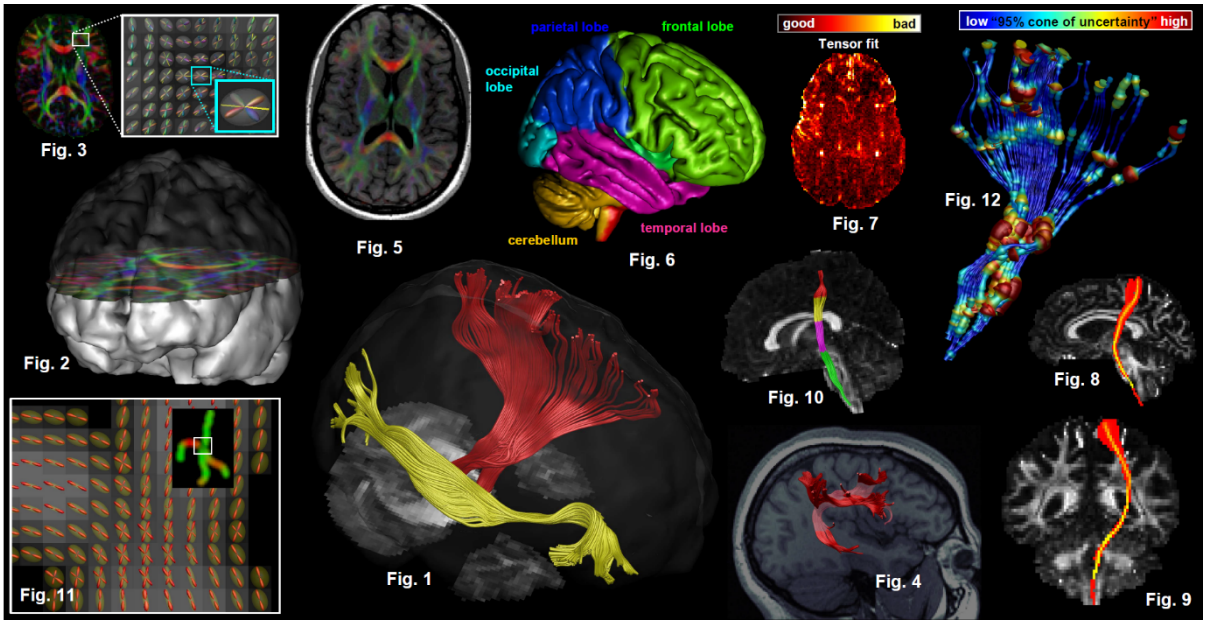

Figure 17: The characteristics that ExploreDTI allows and focuses on (Interactive display and data manipulation).

With:

Fig. 1: WM fibre tracts - Fig. 2:Image of brain surfaces - Fig. 3:Diffusion glyphs - Fig. 4:T1 structural data - Fig. 5:T1 structural data - Fig. 6:Atlas labels - Fig. 7:Analyses of residuals and outliers of the diffusion tensor fit. - Fig. 8:Wild bootstrap streamline tracking - Fig. 9:Wild bootstrap streamline tracking - Fig. 10:Fibre tracts of interest - Fig. 11:Synthetic MR diffusion fibre phantoms - Fig. 12:Stream- tubes with variable width.(Leemans A, Jeurissen B, Sijbers J, DK. J. 2009)[234]

III. Data preprocessing: Acquisition of DTI data for ExploreDTI toolbox

1. Converting the DWI's to the "ExploreDTI file."

After acquiring the participants' data, each participant's result folder and subfolders are DICOM files. This type of format is not practical, so it is usually converted to more manageable formats where all slices/volumes are put in a single file, which is a nii(.gz) (NIFTI) in our case.

All DWIs (including the b0 images) are assumed to be included in the 4D *.nii file with the b0 images at the beginning.

a. Step 1: Visualizing our DTI DICOM files

We used the "RadiAnt DICOM Viewer [Software] along all the study to visualise our files. Version 2020.2. Jul 19, 2020"[235].

Figure 18: Sequence of one of the participants on "RadiAnt DICOM Viewer"

b. Step 2: Converting data DICOM to NIFTI and bval\bvec files (*.nii)

The conversion of DICOM files to NIFTI files (a 4D data set) was done by the "dcm2nii" tool from MRIcroGL.

https://www.nitrc.org/projects/dcm2nii/ – https://www.nitrc.org/projects/mricrogl/

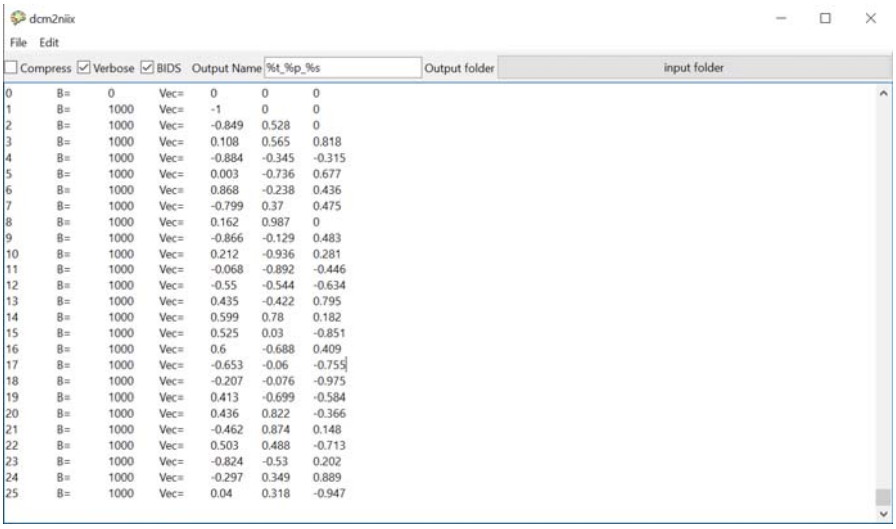

Figure 19: "dcm2nii" Toolbox interface

c. Step 3: Obtaining the "B-Matrix"

Another step must be completed before creating the "*.mat file": obtaining the "B-matrix," which contains the gradient directions and the b-value.

The B-matrix *.txt file is calculated using the files *.bval" and *.bvec".

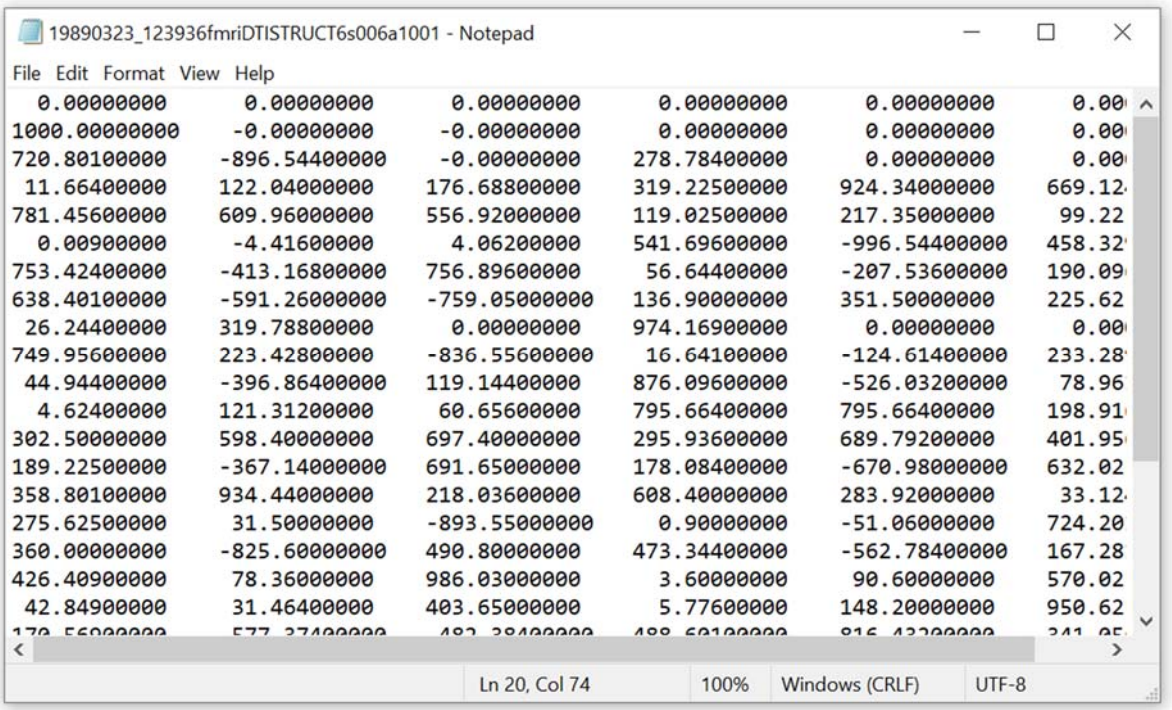

Figure 20: B-matrix *.txt file interface

d. Step 4: Making the nifti files ExploreDTI compatible

Two critical processes have been implemented and followed to ensure the right-left orientation is preserved; the first will be briefly discussed here, while the second will be detailed below in the section " Assuring that the left-right orientation is not flipped."

Before generating the mat.file, we used the ExploreDTI plugging “Flip/permute dimensions in 3D/4D *.nii file(s)” to make all the nifti files ExploreDTI compliant to avoid unexpected axis flips and permutations in any further analysis.

e. Step 5: Finally making the ExploreDTI *.mat format

Now we are about to complete the critical expected step: ‘Convert raw data into DTI *.mat’ to create a file of DTI *.mat that can then be loaded into ExploreDTI

For that, our 4D *.nii file and its corresponding B-matrix -gradient-*.txt file are needed. The figure below explains the steps we took.

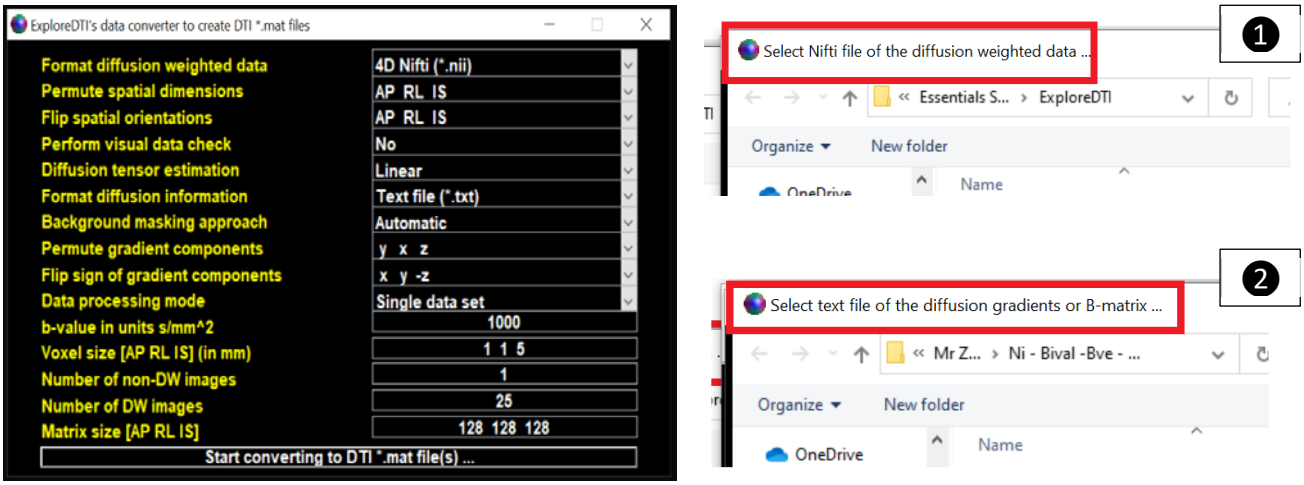

Figure 21: Steps of making the ExploreDTI.mat format.

On the left: ExploreDTI data’s converter (which can create DTI .mat files). On the right: the two steps that we followed to convert the Nifti file + its corresponding Text file to .mat file

2. Assuring that the left-right orientation is not flipped

After the "Flip/permute dimensions in 3D/4D *.nii file(s)" step, we wanted to be even more sure of our Left-Right orientation of the mat.files. For that, we have compared "RAW" data against "Mat.file" data for each volunteer, using :

- "RadiAnt DICOM Viewer [Software]. Version 2020.2. Jul 19, 2020"[235] for RAW data
- "ExploreDTI: A graphical toolbox for processing, analysing, and visualising diffusion MR data" [234] for the Mat.file.

3. Visualization of the First Eigenvector Fractional Anisotropy (FEFA) Cartography.

This step is critical since it ensures that the orientation is correct.

In our series of cases, we have used the widely used colour convention for our data: left-right: red, top-bottom: blue, and front-back: green.

The correct orientation was checked by analysing the colour of the anatomical structures whose architecture is universally known: the pyramidal tracts in blue, the corpus callosum in red, and the longitudinal tracts in green, for the data of each participant (Figure 22).

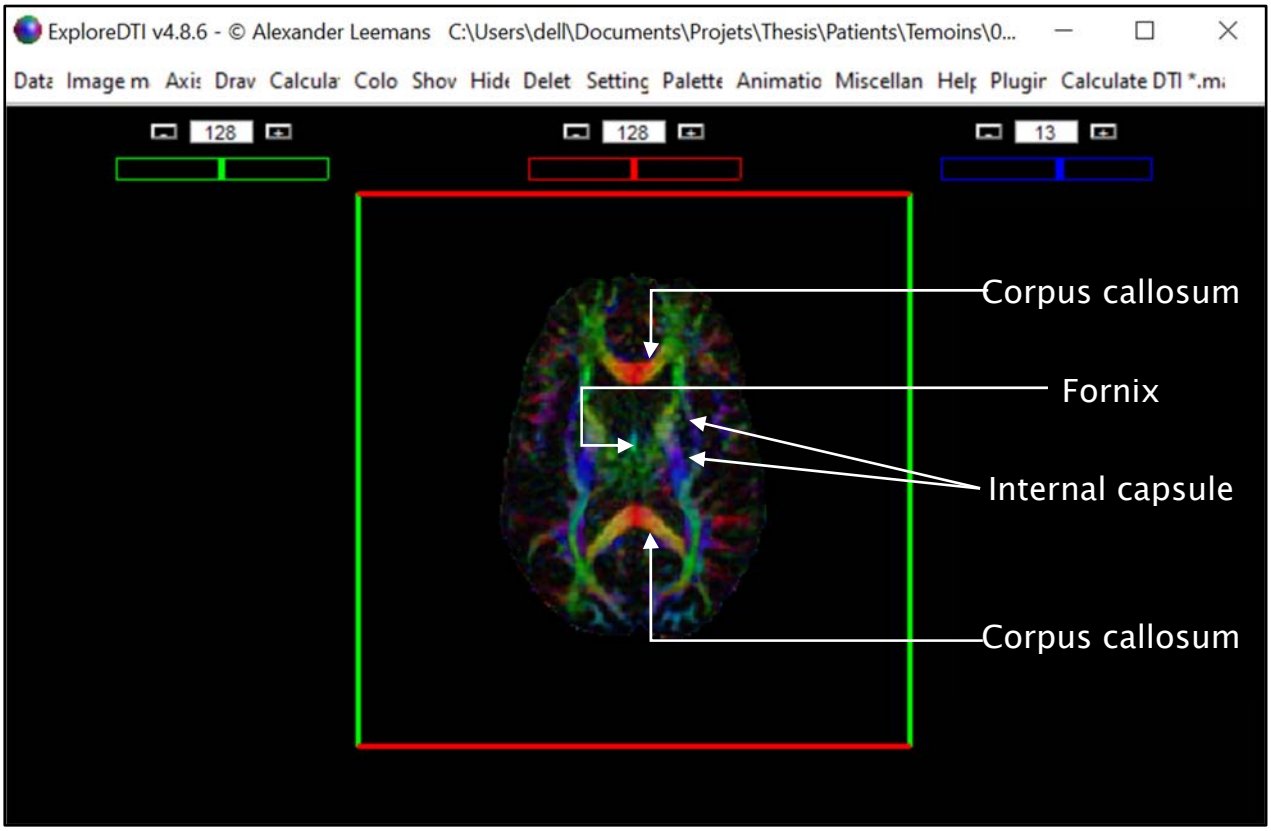

Figure 22: Visualisation of DTI .mat files. FEFA cartography of one of our series participants + location of some anatomical regions on the FEFA cartography.

4. Correcting for subject motion & eddy current-induced geometric distortions

Correcting for motion artefacts increases the precision of DTI, a method of realigning images that refocuses the B-matrix to preserve orientational information[236].

First, in our study, all the diffusion images were checked visually on the three planes for artefacts secondary to the spontaneous movements of the subjects during the scan or geometric distortions linked to the acquisition techniques.

Subsequently, the DTI data were processed using "ExploreDTI" through the "Correct for subject motion & EC / EPI distortions" tool, and this step allows the correction of other artefacts and deformations invisible to the initial inspection.

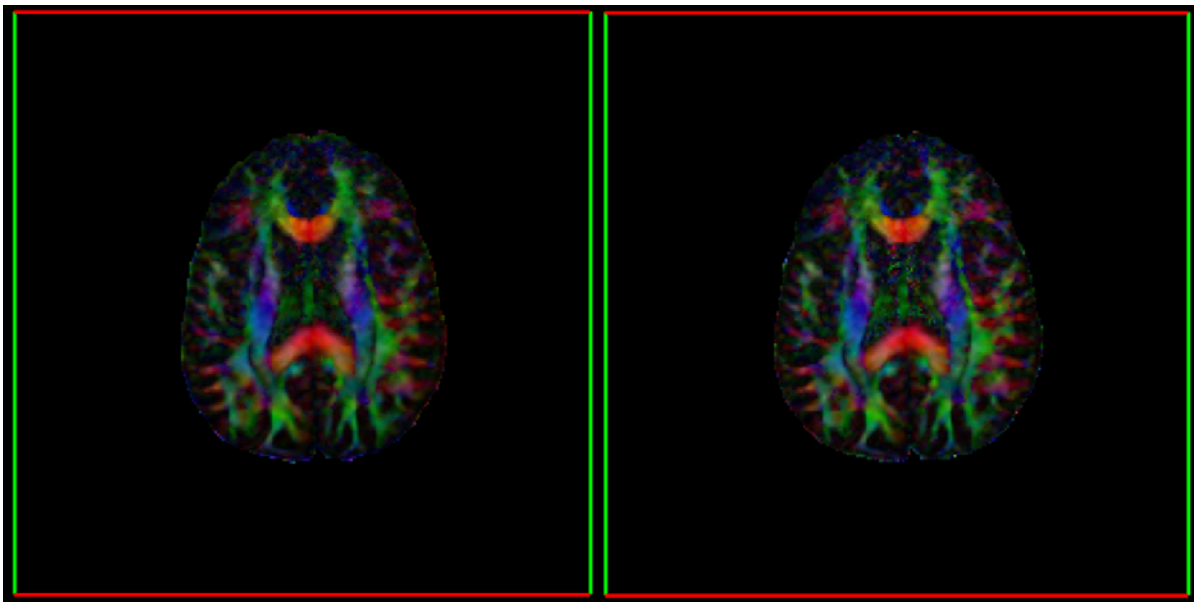

Figure 23: Comparison of the FEFA card of one of our series participants.

On the left before and on the right after correction using the tool "Correct for subject motion & EC/EPI distortions.

IV. Regions of Interest selection and analysis

The region of interest (ROI) technique of analysis relies on defining specific image regions. Therefore, the ROI is a region of an image from which a further analysis may be done by extracting individual or average pixel values. It is a usual method used to analyse data from diffusion tensor imaging quantitatively[237]. ROI should usually be drawn manually, while in some cases (semi-)automatic segmenting may be used.

Generally, the ROI analysis approach may be relatively easily used, and most DTI software supports It[238]. The ROI analysis requires much time and strong hypotheses about lesion localisation [210]. The decision scheme depicted in figure 24 below helps in the decision to select the DTI analysis method based on the DTI study's purpose[210]. In our case, the strategy we adopted has been carefully considered and reviewed, and it is based on various recommendations from anatomical-structural studies and other research in this field.

Since we are studying the anatomic-structural variations between three groups, and we have a clear and well-established hypothesis, we have chosen "Regions of Interest Analysis". But given a large number of regions to analyse: (36x2)/participant — which will require a very long time of drawing and analysis —, and given the intra- and/or inter-variation of surfaces and volumes of the ROIs, we finally decided to use an automated segmentation of the brains of the participants.

Several pre-defined ATLASs are available. Our study employed Automated Anatomical Labeling[239] (AAL) adapted for "ExploreDTI" by Alexander Leemans[234].

AAL is a software application and a human brain digital atlas. It is usually used for neuroanatomical labelling at three-dimensional space locations where measurements have been taken on specific aspects of brain activity. Instead, it projects the brain atlas divisions into brain-formed functional data volumes[239]. The relevant AAL atlas information is represented in three files (figure 25).

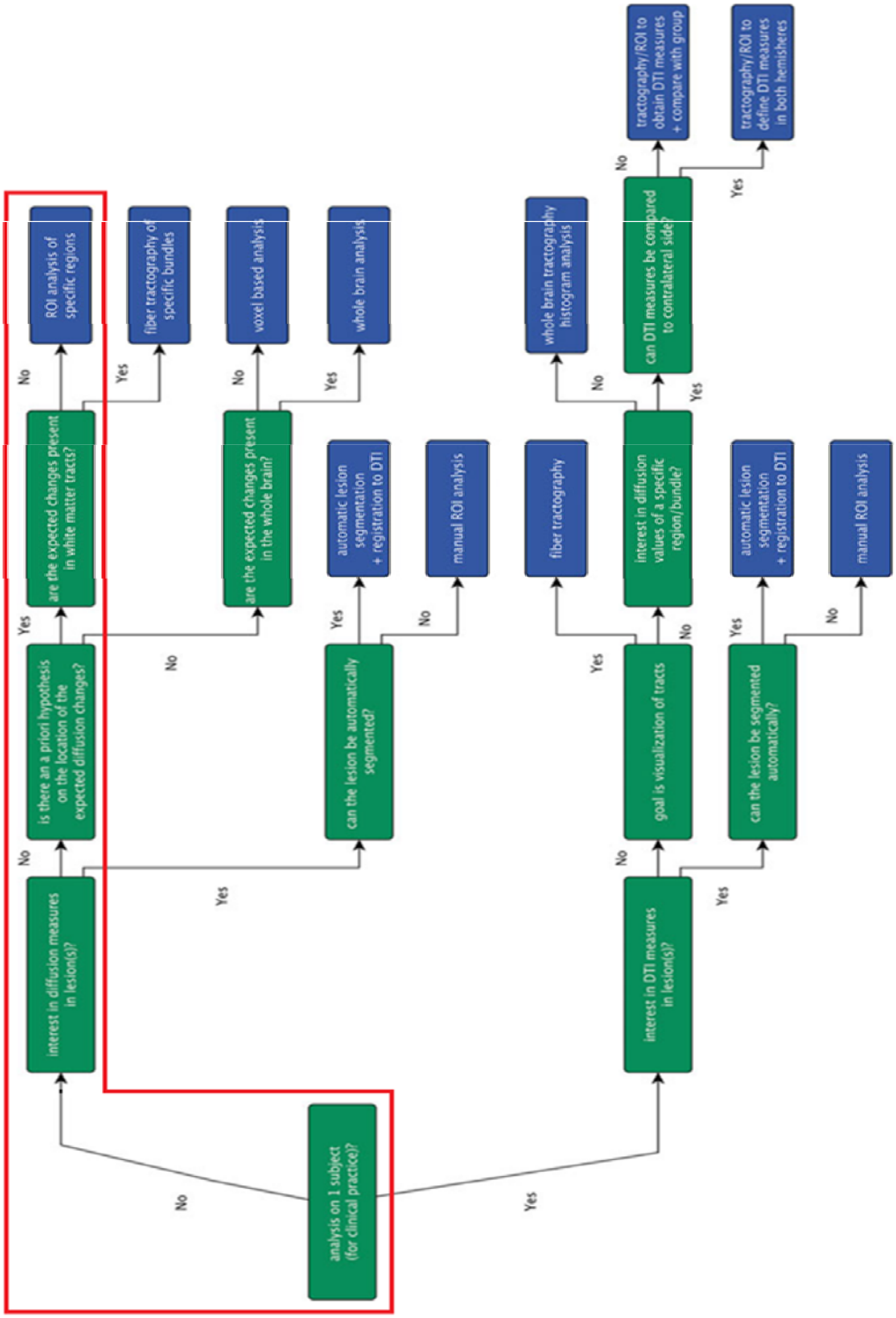

Figure: A decision scheme to assist with DTI analysis method selection based on the aim of the DTI study. (Van Hecke W, Emsell L. 2016) [210]

Name	Type	Size
AAL_Label_Names	Text Document	2 KB
AAL_Labels	NII File	6,943 KB
AAL_Template	NII File	27,771 KB

Figure 25: The three files that contain AAL atlas information,

The Atlas file's labelled regions show the segmentation scheme, which includes a total of 90 cerebral regions (figure 26).

1 Precentral L	1 Frontal Med Orb L	1 Occipital Sup L	1 Putamen L	0 Cerebelum 4 5 L
1 Precentral R	1 Frontal Med Orb R	1 Occipital Sup R	1 Putamen R	0 Cerebelum 4 5 R
1 Frontal Sup L	1 Rectus L	1 Occipital Mid L	1 Pallidum L	0 Cerebelum 6 L
1 Frontal Sup R	1 Rectus R	1 Occipital Mid R	1 Pallidum R	0 Cerebelum 6 R
1 Frontal Sup Orb L	1 Insula L	1 Occipital Inf L	1 Thalamus L	0 Cerebelum 7b L
1 Frontal Sup Orb R	1 Insula R	1 Occipital Inf R	1 Thalamus R	0 Cerebelum 7b R
1 Frontal Mid L	1 Cingulum Ant L	1 Fusiform L	1 Heschl L	0 Cerebelum 8 L
1 Frontal Mid R	1 Cingulum Ant R	1 Fusiform R	1 Heschl R	0 Cerebelum 8 R
1 Frontal Mid Orb L	1 Cingulum Mid L	1 Postcentral L	1 Temporal Sup L	0 Cerebelum 9 L
1 Frontal Mid Orb R	1 Cingulum Mid R	1 Postcentral R	1 Temporal Sup R	0 Cerebelum 9 R
1 Frontal Inf Oper L	1 Cingulum Post L	1 Parietal Sup L	1 Temporal Pole Sup L	0 Cerebelum 10 L
1 Frontal Inf Oper R	1 Cingulum Post R	1 Parietal Sup R	1 Temporal Pole Sup R	0 Cerebelum 10 R
1 Frontal Inf Tri L	1 Hippocampus L	1 Parietal Inf L	1 Temporal Mid L	0 Vermis 1 2
1 Frontal Inf Tri R	1 Hippocampus R	1 Parietal Inf R	1 Temporal Mid R	0 Vermis 3
1 Frontal Inf Orb L	1 ParaHippocampal L	1 SupraMarginal L	1 Temporal Pole Mid L	0 Vermis 4 5
1 Frontal Inf Orb R	1 ParaHippocampal R	1 SupraMarginal R	1 Temporal Pole Mid R	0 Vermis 6
1 Rolandic Oper L	1 Amygdala L	1 Angular L	1 Temporal Inf L	0 Vermis 7
1 Rolandic Oper R	1 Amygdala R	1 Angular R	1 Temporal Inf R	0 Vermis 8
1 Supp Motor Area L	1 Calcarine L	1 Precuneus L	0 Cerebelum Crus1 L	0 Vermis 9
1 Supp Motor Area R	1 Calcarine R	1 Precuneus R	0 Cerebelum Crus1 R	0 Vermis 10
1 Olfactory L	1 Cuneus L	1 Paracentral Lobule L	0 Cerebelum Crus2 L	
1 Olfactory R	1 Cuneus R	1 Paracentral Lobule R	0 Cerebelum Crus2 R	
1 Frontal Sup Medial L	1 Lingual L	1 Caudate L	0 Cerebelum 3 L	
1 Frontal Sup Medial R	1 Lingual R	1 Caudate R	0 Cerebelum 3 R	

Figure 26: List of anatomical label regions from the Atlas file used in the segmentation of volunteers' brains.

The digital Atlas model allows users to automatically extract anatomically labeled regions as well as their diffusion indices using "ExploreDTI."

Automated segmentation is thus a reproducible, efficient, and economical method that ensures a unified ROI analysis across the entire sample to be studied.

Based on our hypothesis, a total of 36 x 2(Bilaterality) cerebral regions have been identified, of which 35 have been subtracted using an atlas file and an automated method. Meanwhile, a single region, the nucleus accumbens, was manually selected due to the unavailability of such parcellation in the AAL file.

Table 5: Regions and structures of anatomical interest and their correspondents on the Atlas file.

Anatomical regions	The Anatomic Structure		ROI correspondence in The Atlas file of anatomical label regions
Orbitofrontal cortex	Medial Orbitofrontal cortex		Frontal Med Orb R/L Frontal Sup Orb R/L
	Lateral orbitofrontal cortex		Frontal Mid Orb R/L Frontal Inf Orb R /L
Orbital surface of the frontal lobe	Gyrus rectus		Rectus R/L
	The piriform (Or primary olfactory)		Olfactory R/L
The prefrontal cortex	Ventromedial prefrontal cortex		Frontal Sup Medial R/L
	Dorsomedial prefrontal cortex		Frontal Sup R/L
	Dorsolateral prefrontal cortex		Frontal Mid R/L
The prefrontal cortex (Broca's area)	Ventrolateral prefrontal cortex		Frontal Inf Oper R/L Frontal Inf Tri R/L
The Parietal lobe	The postcentral gyrus		Postcentral R/L
	The superior parietal lobule		Parietal Sup R/L
	The inferior parietal lobule	Supramarginal gyrus	SupraMarginal R/L
		Angular gyrus	Angular R/L
		Supramarginal and angular gyri.	Parietal Inf R/ NB: It's the part of the parietal cortex above the supramarginalis gyrus and between the supramarginal and angular gyri that doesn't belong to the supramarginal and angular cortex.
	The precuneus		-Precuneus R/L

The temporal lobe - except regions belonging to the limbic system-	The superior temporal gyrus	Temporal Sup R/L
		Temporal Pole Sup R/L
		Heschl R/L -isolated within the superior temporal gyrus-
	The middle temporal gyrus	Temporal Mid R/L
		Temporal Pole Mid R/L
	The inferior temporal gyrus	Temporal Inf R/L
	The occipitotemporal (fusiform) gyrus.	Fusiform R/L
Limbic system	Cingulate gyrus	Cingulum Ant R/L
		Cingulum Mid R/L
		Cingulum Post R/L
	Parahippocampal gyrus	ParaHippocampal R/L
	Hippocampus	Hippocampus R/L
	Insula	Insula R/L
	Amygdala	Amygdala R/L
	Thalamus	Thalamus R/L
The Basal Ganglia	Caudate nucleus	Caudate R/L
	Putamen	Putamen R/L
	Pallidum	Pallidum R/L
	Nucleus Accumbens	N/A

V. Tractography selection and analysis with corresponding extracted tractograms

Our study aims to evaluate the integrity of anatomical brain structures in cannabis users compared to healthy controls. We conducted this by also examining the white matter of each of the regions of interest.

Diffusion tensor imaging (DTI) research has recently made it achievable to analyze the human brain's large-scale connectivity structure from a network viewpoint[240241242]. White matter fibres connecting different parts of the brain may be reconstituted and evaluated using DTI-based fibre tractography[243].

A network, according to graphs theory[244], is made up of nodes that are connected by edges. The network transports information between nodes through the edges that connect them.

In the brain, nodes correspond to cortical or subcortical GM regions that communicate through edges made up of WM fibres.
Therefore, using theoretical graph analysis, the efficiency and robustness of these structural networks may be assessed[242].

We generated a structural network of all participants (cannabis users and healthy controls) in this project. We evaluated the structural integrity of tracts associated with each area in cannabis users by assessing diffusion (Markers FA and MD) and comparing their results to healthy controls.

We used "ExploreDTI" to individualize the white matter bundles associated with each anatomical region of interest (Table 5). "ExploreDTI" was also used to calculate and record the diffusion markers (FA and MD) associated with the extracted white matter tracts.

Unfortunately, we were unable to extract and study connection fibres relating to the nucleus accumbens as this region is not included in the Atlas of automated anatomical segmentation used to acquire ROIs and connections. Given the small volume of this formation, manual extraction of the fibres was unrealistic and imprecise[245].

Afterward, we extracted the existing tractograms between all network components (Plate 1, 2, and 3). The tractograms demonstrate all the connections between the regions studied.

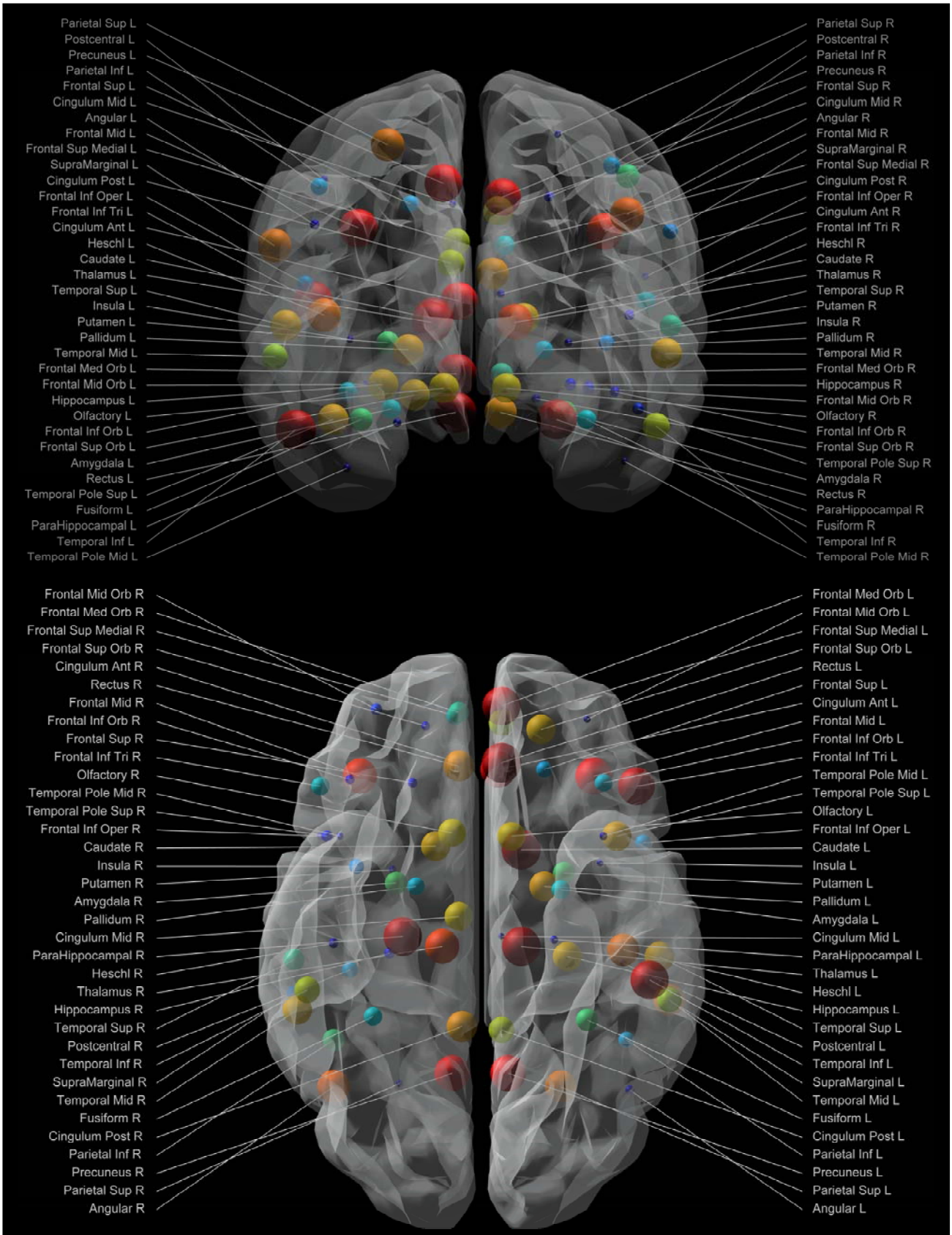

Plate 1: Anterior (A) and inferior (B) views of the brain, with nodes representing the different regions of interest.

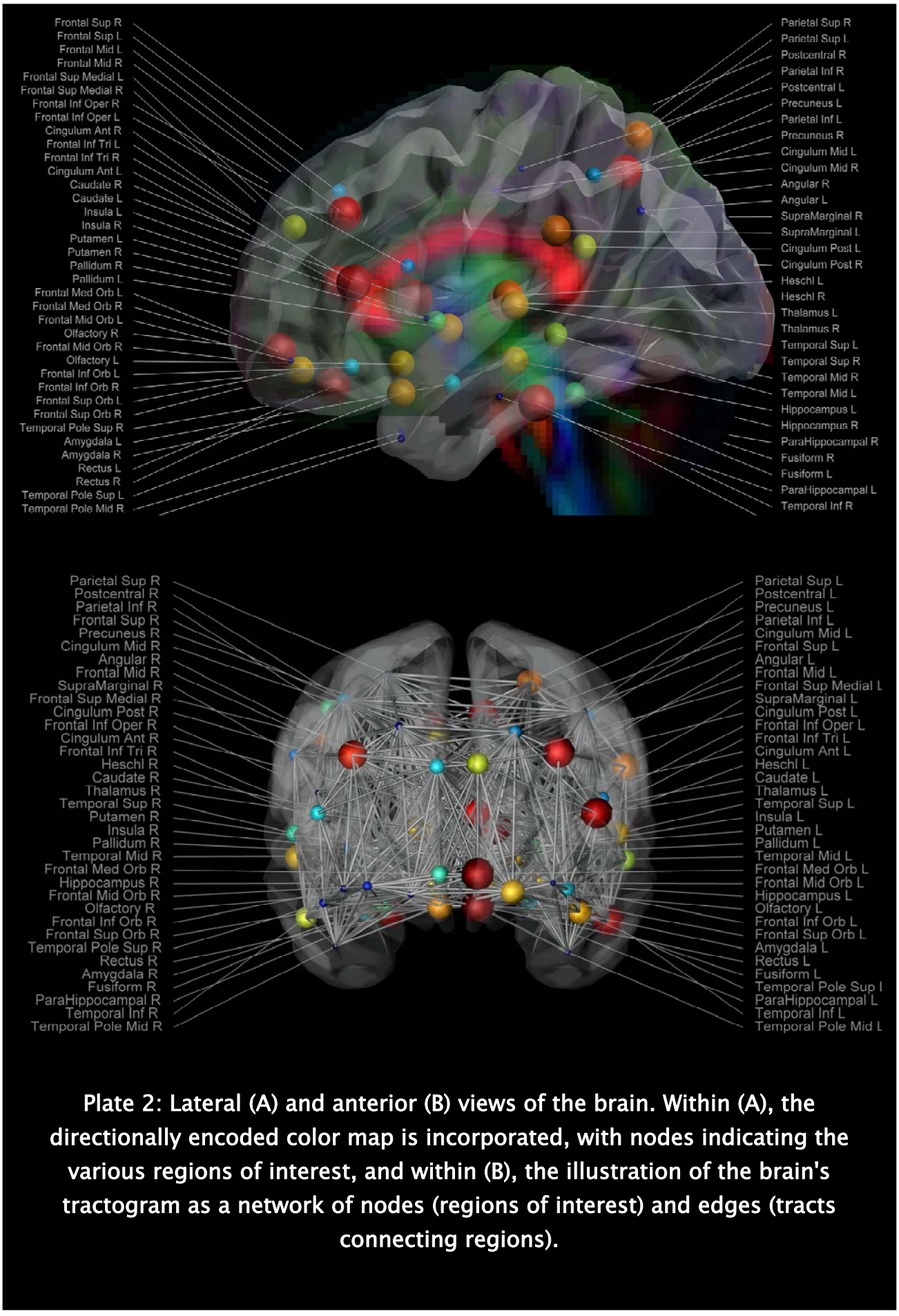

Plate 2: Lateral (A) and anterior (B) views of the brain. Within (A), the directionally encoded color map is incorporated, with nodes indicating the various regions of interest, and within (B), the illustration of the brain's tractogram as a network of nodes (regions of interest) and edges (tracts connecting regions).

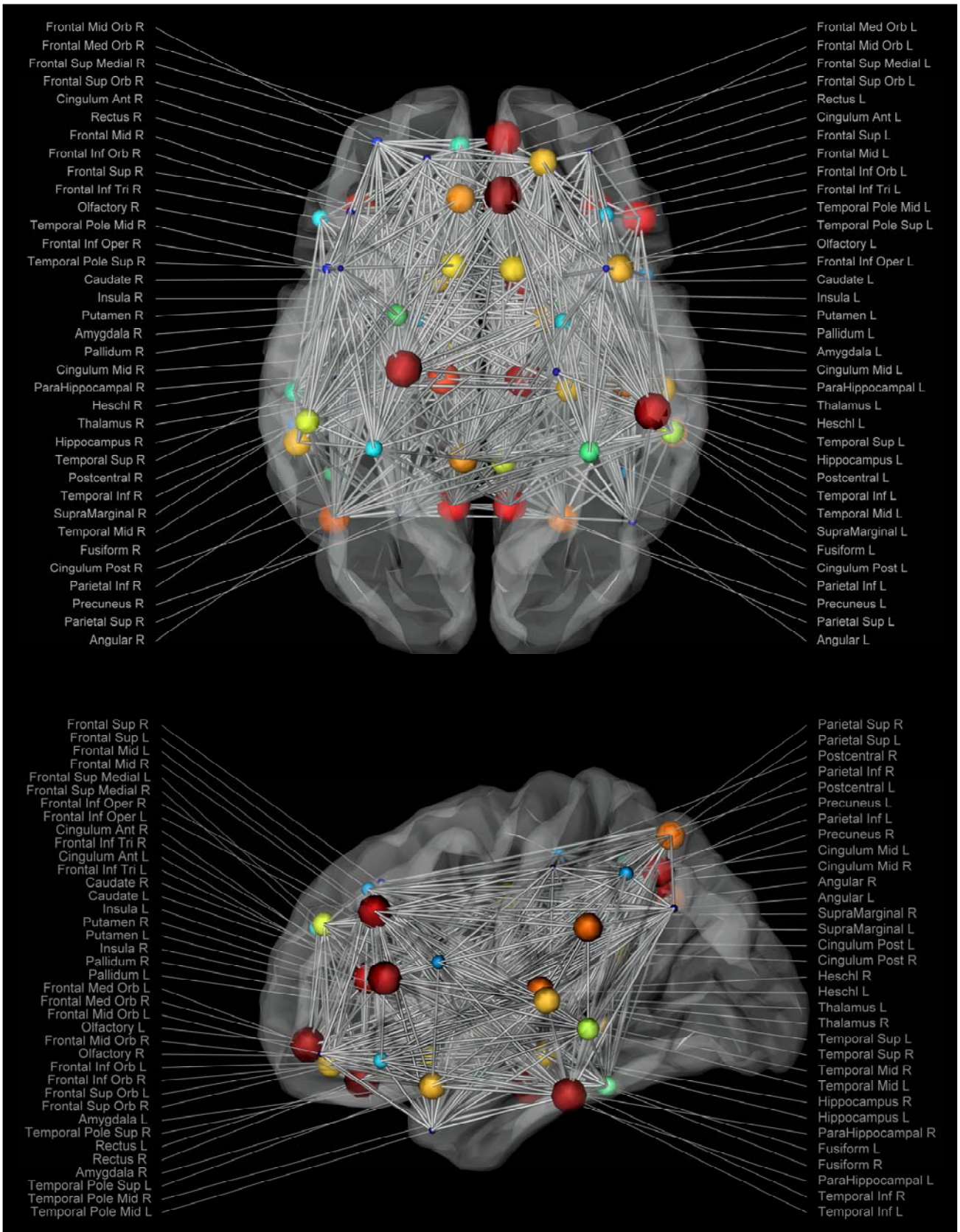

Plate 3: Inferior (A) and lateral (B) images of the brain, illustrating the brain's tractogram as a network of nodes (regions of interest) and edges (tracts connecting regions).

Chapter IV: Statistical analysis

All data were collected and organized in MS Excel® (2019) for windows spreadsheets before being uploaded to and analyzed using GraphPad Prism 8.0.0 for Windows, GraphPad Software, San Diego, California USA, www.graphpad.com.

We considered a p-value < 0.05 to be statistically significant for all statistical analyses performed.

I. The statistical analysis of psychological assessments: psychometric tests results

The individual group results were compared and analyzed statistically using the ANOVA test (Analysis Of Variance). The four groups underwent ANOVA, comparison of pairs of groups was performed, namely (Group I versus Group II), (Group I versus Group III), and (Group II versus Group III).

To determine and compare statistically the diagnostic performance of the screening test used (CUDIT-R), and thus as a quality criterion of screening test used in the protocol (in establishing a distinction between the two groups based on the criteria of cannabis use disorder), we performed the ROC curve.

The test implicates two groups: the heavy group as patients' group or the tested group and light users as the control group for the test.

Additionally, we examined the association between cannabis use disorder, impulsivity, and perceived stress on the one hand and certain consumption-related parameters (age of onset, duration of use, degree of consumption) on the other. Pearson correlation was used to determine these associations.

II. The statistical analysis of DTI results: ROI and Tractography analyses.

As we did with psychometric test results, the individual group results of fractional anisotropy (FA) and mean diffusivity (MD) in each region and each related white matter (in the tractography part) were compared and analyzed statistically using the ANOVA test (Analysis Of Variance).

The four groups underwent ANOVA, comparison of pairs of groups was conducted, respectively (Group I versus Group II), (Group I versus Group III), and (Group II versus Group III) for FA and MD results in both hemispheres, separately.

III. The correlation analysis: Tractography versus psychometric test results in groups.

We statistically correlated the clinical (Psychometric tests: CUDIT-R, BIS-11, and PSS) and tractography findings (diffusion markers: FA and MD) in several regions.
The regions chosen are those reported in the literature and summarized in our Atlas and bibliography as physiologically associated with the function researched by CUDIT-R, BIS-11, and PSS.

The Pearson correlation was used to determine the association between these two functional and structural indicators.

The FA and MD values of the tracts in each selected region were associated with the individual test values for each participant in the three groups, including the group control.

Chapter V: Atlas of anatomical regions of interest

I. Introduction

Our Atlas is valuable for anatomically demonstrating the regions of interest that we identified and studied in our work and exhibiting the quality of our region selection. Since our thesis has an anatomical aspect, with accompanying bibliographic material, it also provides helpful information to the reader.

All the anatomical images and sections presented in this atlas originate from the same scans of one volunteer from our study series.

II. The data and Image processing

The subjects were recruited in the Addiction centre, Department of Psychiatry, University Hospital of Fez; Fez, Morocco. He gave written consent to participate in a clinical and MRI study conducted by Clinical Neuroscience Laboratory, Faculty of Medicine, Pharmacy and Dental Medicine of Fez; the University of Fez in collaboration with the Addiction centre affiliated to the Psychiatry Department, and Radiology and Clinical Imaging Department, University Hospital of Fez.

To obtain the template of the whole brain and the anatomically labelled regions of our volunteer, we followed the steps mentioned above in the parts:

- “Data preprocessing: Acquisition of DTI data for ExploreDTI toolbox.”
- “Regions of Interest selection and analysis”

III. Structures individualization and the Atlas generation

All plates in this section were created using the "MRIcroGL" application.

The template of the whole brain and the anatomically labelled region are obtained from the file generated by ExploreDTI software using the automated segmentation method.

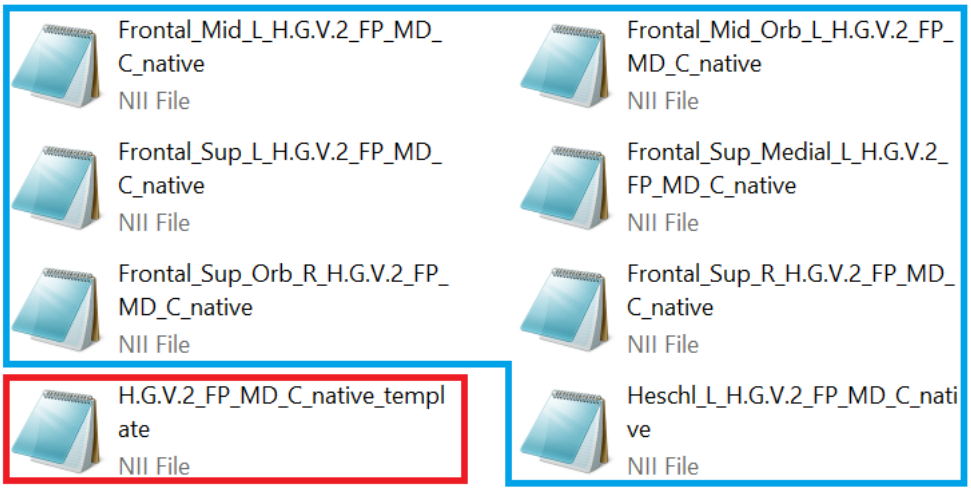

Figure 27: NII Files of the whole brain template (boxed in red) and some of regions of interest (boxed in blue).

Finally, using the MRIcroGL software, we obtained an anatomical plate of each region of interest by overlaying the region of interest on the file of the whole brain template already opened on the software. It's crucial to remember that the nii files are the results of our automated extraction using AAL software and our technique of anatomical extraction.

IV. The regions of interest

1. Orbitofrontal cortex

a. Introduction and functional physiology of the orbitofrontal cortex

In humans, the orbitofrontal cortex is a critical brain region for emotion, reward value representation, and non-reward[246]. It assists in the evaluation and selection of objects as objectives for future actions[247]. This means that the cortical treatment before the orbitofrontal cortex is associated with the identification of stimuli rather than the value of recompense.

The OFC is connected to olfactory, visceral, somatosensory and visual regions, which provide a rich and high-dimensional perception of particular outcomes by combining different inputs[247]. The OFC has important connections with the amygdala, which adjusts the valuation of these outcomes in terms of present biological needs[247].

Two different patterns of neuronal activity have been suggested by a review on human orbitofrontal cortex functional neuroanatomy. The reviews' findings were based on a meta-analysis of neuroimaging studies[248].

These two functional distinctions are going to be essential in the structuring of the regions that will be selected and treated in our studied volunteers.

The distinctions suggested are:

-A mediolateral distinction in which medial orbitofrontal brain activity is related to assessing the reward value of various reinforcers, while activity in the lateral orbitofrontal cortex is linked to the evaluation of punishers, which might lead to a change in current behavior.

- The second differentiation, which is a posterior-anterior difference, with more sophisticated or abstract reinforcers represented more forward in the orbitofrontal cortex than simple reinforcers such as taste or pain (figure 2).

In terms of functionality, table 6 depicts the functions of the two major areas that make up the lobe in considerable detail.

Table 6: Major functions of the two major areas that compose the orbitofrontal lobe.

Medial Orbitofrontal cortex	● The anticipation of rewards and the incorporation of the hedonistic value of stimuli, particularly appetizing stimuli. ● Prediction of errors during decision-making[249].
Lateral orbitofrontal cortex	● It plays a role in associative learning by interacting with the medial orbitofrontal cortex[249]. ●Encodes the most appropriate behaviour to adapt to achieve the best result, such as aversion behaviours in response to unpleasant stimuli[249]. ●It plays a part in emotion regulation[249].

b. The components and neuroanatomy of the OFC

On the ventral side of the frontal lobes, the OFC comprises a wide swath of cortex; however, the exact location of its limits is unknown[247]. The gyrus rectus cortex, for example, is variably classified as part of OFC proper, part of the ventromedial prefrontal cortex (vmPFC), or part of a separate area known as medial OFC[247].

Based on its architectonics*, OFC is divided into two distinguished regions: medial and lateral[246]. For the connectivity-based parcellations, this division is useful since there are differences in the connectivity of these parts[250 251]. Neuroanatomists also demonstrated that OFC has several subregions (Figure 28), distinguished by variances in how neurons are arranged into cortical layers (Figure 29) [247].

*Architectonics : The art of recognising areas is called Architectonics when features such as stained cell bodies (cytoarchitectonics) and the pattern of myelinated fibers (myeloarchitectonics) are involved. [415]

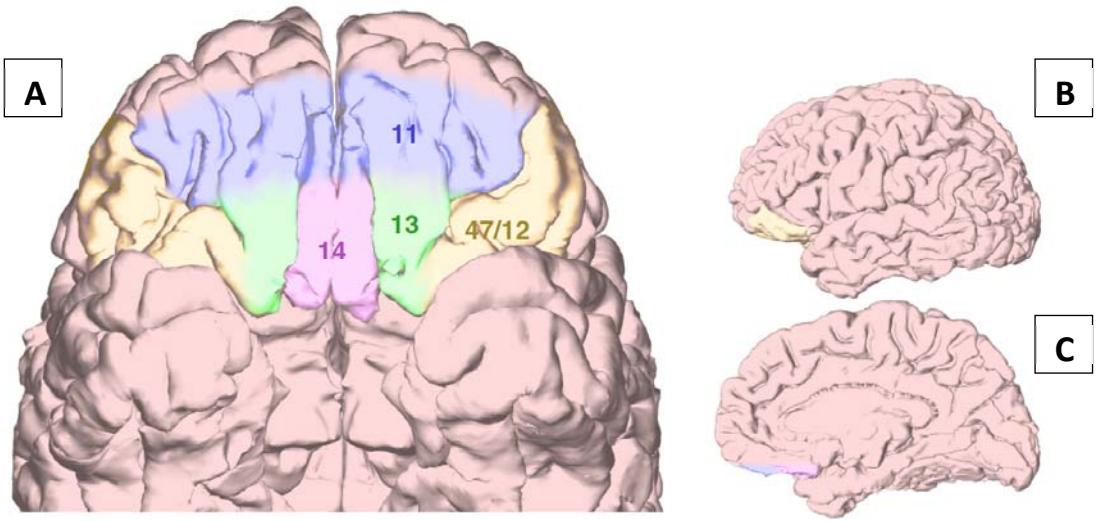

Figure 28: Subregions of the human OFC.

With:

A: Ventral brain view with OFC regions highlighted.

B: Lateral brain view with OFC regions highlighted.

C: Medial brain view with OFC regions highlighted.

While parcellations of OFC into areas 11, 13, 14, and 47/12. (Rudebeck PH, Rich EL. 2018)[247].

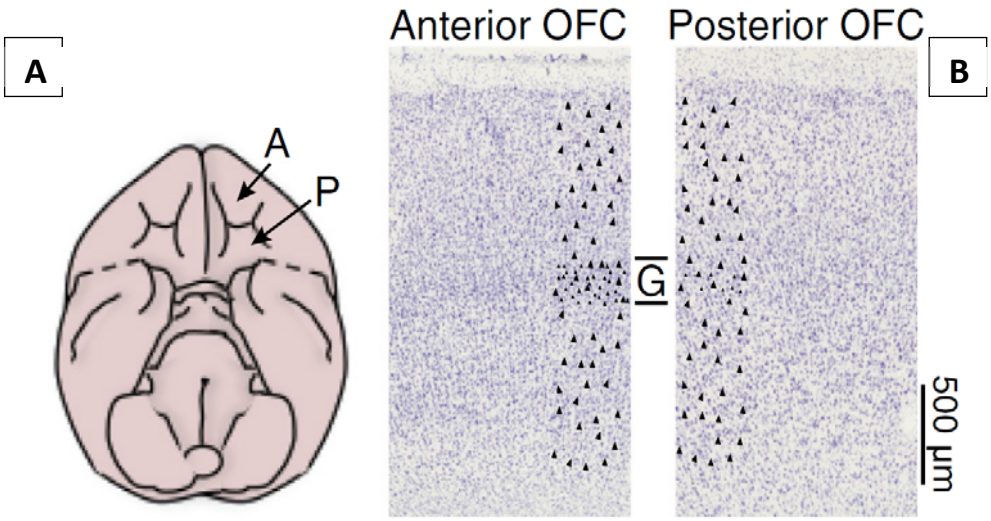

Figure 29: The posterior-anterior differentiation.

With:

A: A ventral view of the monkey brain with anterior temporal lobes removed to show OFC. "A" for anterior and "P" for posterior.

B: Two thionin-stained sections of monkey OFC, oriented with the cortical surface at the top. There are higher densities of granule cells in the middle layer (G) of the anterior section. (Rudebeck PH, Rich EL. 2018)[247].

c. Connectivity of the OFC

The OFC differs from the rest of the prefrontal cortex sections in terms of connections since it gets projections from the magnocellular, medial nucleus of the mediodorsal thalamus. Unlike other areas of the prefrontal cortex that receive projections from the mediodorsal thalamus [247].

The OFC connections are formed so that OFC neurons can encode connections between the external sensory input and internal states associated with emotionally significant events[247].

These signals can subsequently be incorporated in other sections of PFC and beyond into continuous cognitive operational activities. And so, the major outputs are connected to the medium striatum, the intermediate thalamus, and other prefrontal cortex components[247] (Figure 30).

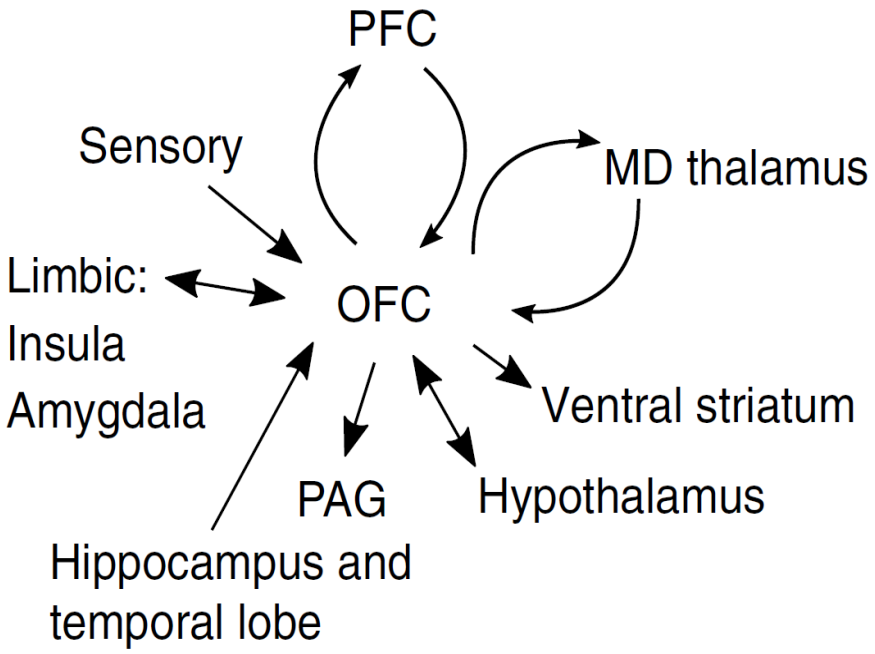

Figure 30: The major cortical and subcortical connections with OFC.
Where: PFC, prefrontal cortex; MD, mediodorsal; PAG, periaqueductal gray.
(Rudebeck PH, Rich EL. 2018)[247].

d. Atlas 1

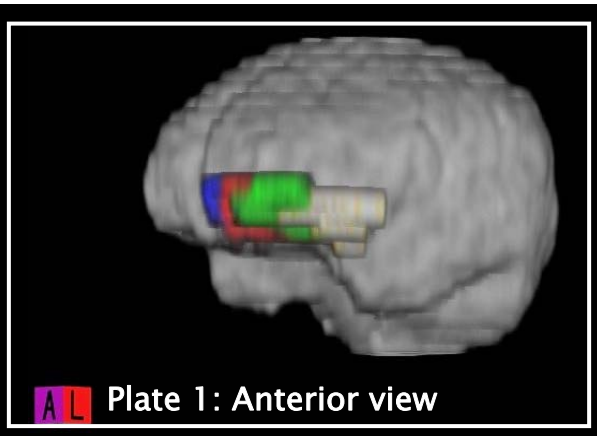

Plate 1: Anterior view

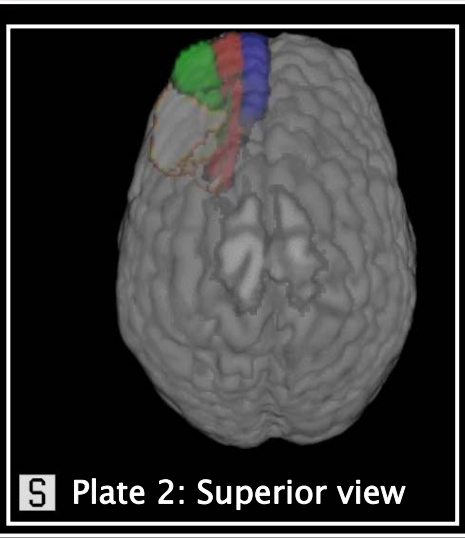

Plate 2: Superior view

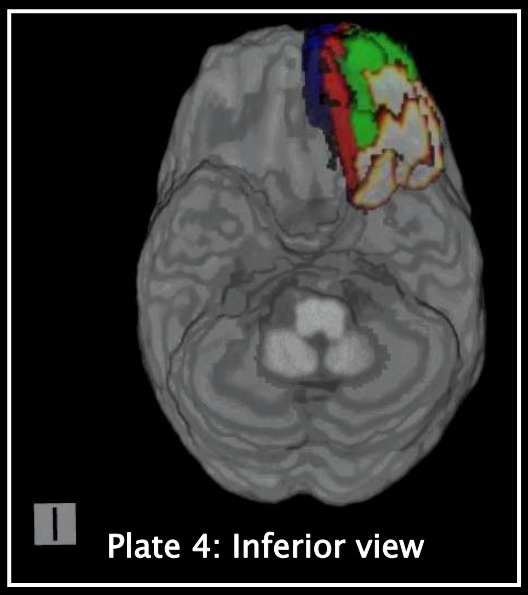

Plate 4: Inferior view

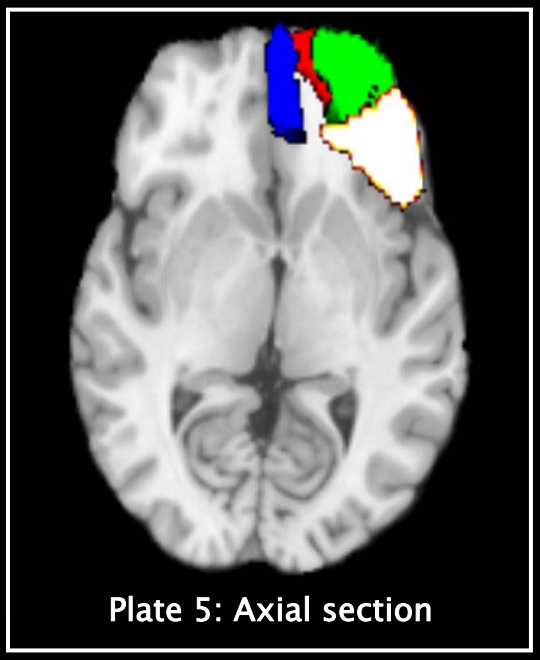

Plate 5: Axial section

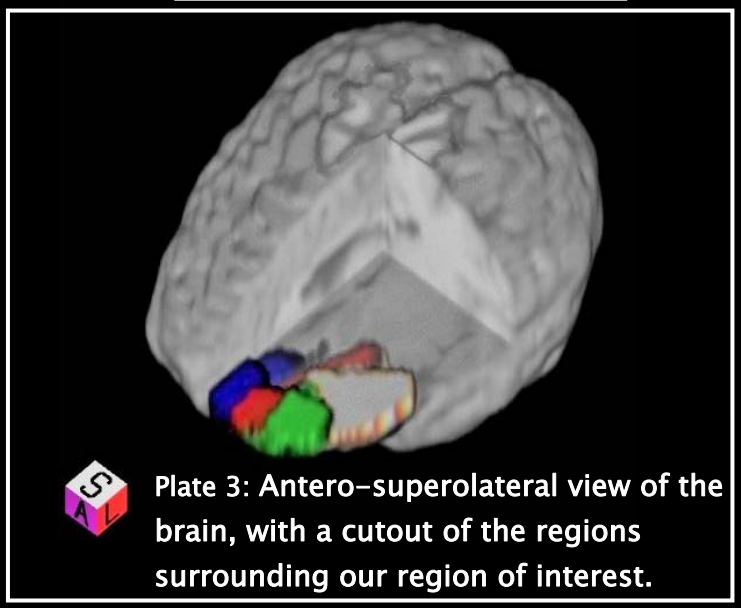

Plate 3: Antero-superolateral view of the brain, with a cutout of the regions surrounding our region of interest.

Atlas 1: Different views and sections of the brain with overlaying of the orbitofrontal region (Medial and Lateral).

*Orientation: A: Anterior – L: Lateral – S: Superior – I: Inferior

*Region colors: The Left Frontal Med Orb. The Left Frontal Sup Orb. The Left Frontal Inf Orb. The Left Frontal Mid Orb.

2. Orbital surface of the frontal lobe

a. Overview of gyrus on the orbital part of the frontal lobe

i. Gyrus rectus

The anterior cranial fossa floor limits the gyrus rectus anteriorly, the olfactory sulcus laterally, and the superior rostral sulcus superiorly. The gyrus rectus and the carrefour olfactif (subcallosal gyrus) are separated by a transverse rostral sulcus[252].

The functions and connections of the rectus gyrus are hypothesized to be related to those of the orbitofrontal lobe.

ii. The piriform (or primary olfactory)

The piriform cortex passes from the anterior olfactory regions to the caudal boundary of the cerebral hemispheres, where it joins the cortical amygdala and entorhinal cortex[253]. The cortex's role appears to be complex and poorly understood, although primarily engaged in olfaction[254].

The following functions have been related to the piriform cortex[255]:

- Learning and memory of odors
- Encoding representations of odor: quality, identity, familiarity, and hedonics.
- Multisensory integration: visual stimuli stimulate brain activity when combined with a pleasant food odor.

The primary olfactory sites (piriform cortex) transmit olfactory information to[254]:

- The hypothalamus,
- The thalamus.
- Limbic structures such as the hippocampus and the rest of the amygdala.

b. Atlas 2

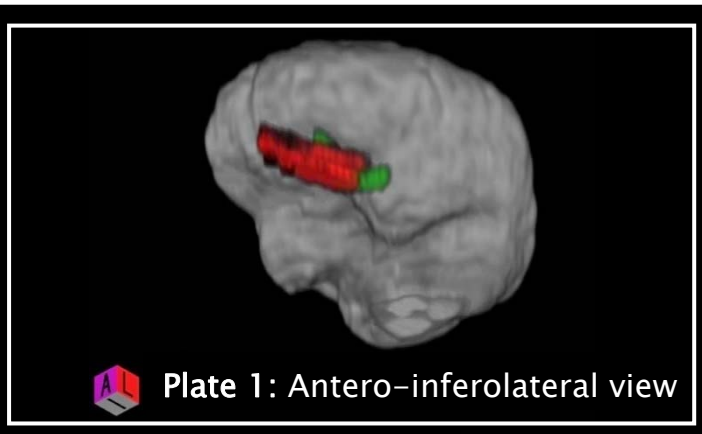

Plate 1: Antero-inferolateral view

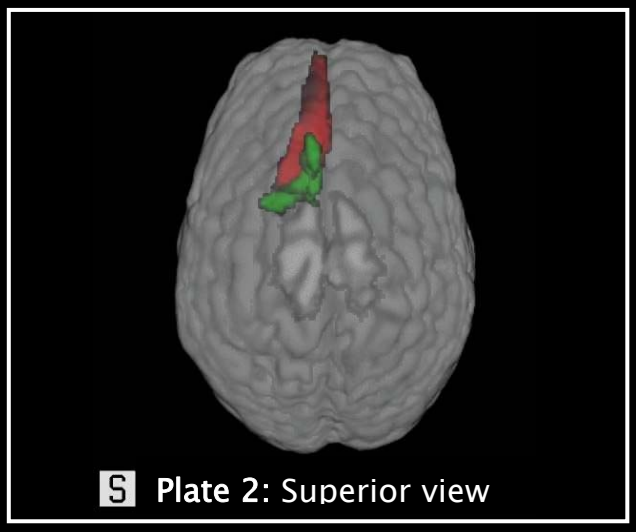

Plate 2: Superior view

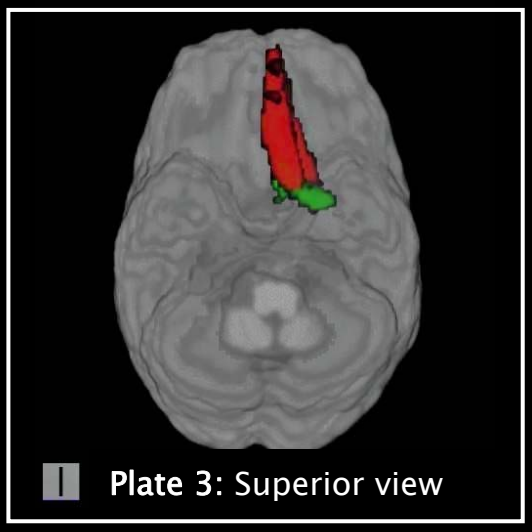

Plate 3: Superior view

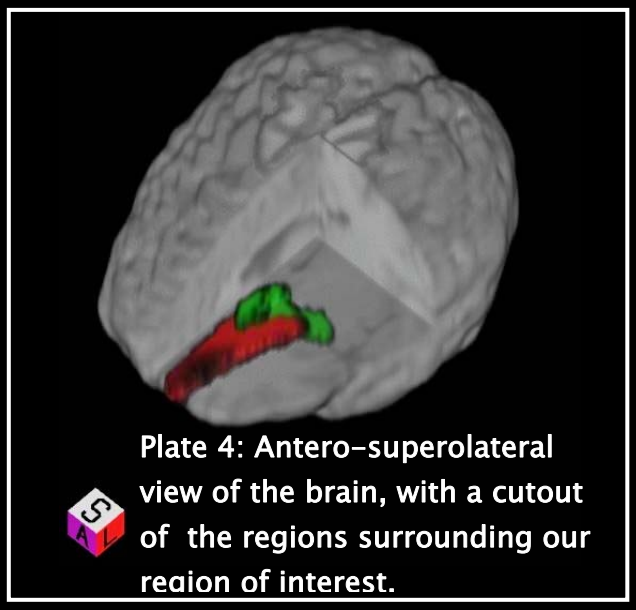

Plate 4: Antero-superolateral view of the brain, with a cutout of the regions surrounding our region of interest.

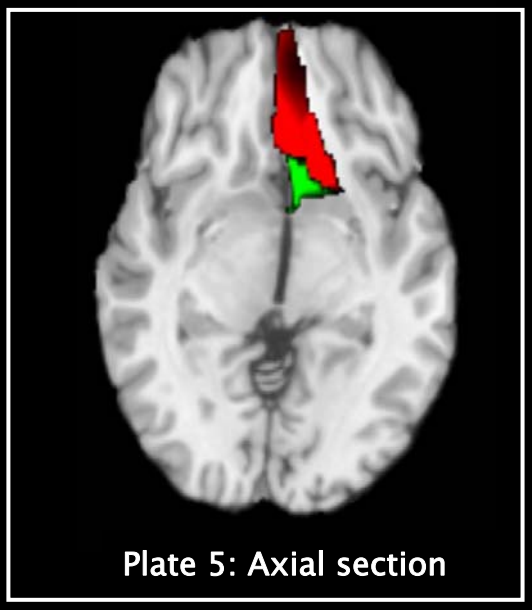

Plate 5: Axial section

Atlas 2: Different views and sections of the brain with overlaying of the orbital surface of the frontal lobe (Rectus and the olfactory gyrus.).

*Orientation: A: Anterior – L: Lateral – S: Superior – I: Inferior
*Region colors: The Left **gyrus rectus.** The Left Olfactory gyrus.

3. The prefrontal lobe

a. Introduction and functional physiology of the region: the Prefrontal Cortex as an Executive, Emotional, and Social Brain

The prefrontal cortex (PFC) is the most developed phylogenetic region in humans, accounting for around one-third of the cerebral cortex[256].

For ages, the PFC remained uncharted and filled with mysteries. Many efforts have been made to map PFC areas, and numerous puzzles appear to have been answered due to the emergence of neuroimaging methods like PET, fMRI, DTI, and noninvasive brain stimulation methods like rTMS, tDCS[256].

Nonetheless, if compared to other brain regions, the PFC is the most mysterious. And there are still heated debates about whether the PFC has a unitary function or is functionally partitioned, and if it is functionally partitioned, how it is divided[256].

The PFC is generally known to perform the most critical function in executive control[257]. The PFC is also recognized to be critical for emotional and motivational behavior[258]. Recent studies also indicate that the PFC is actively involved in social cognition and social behavior[259]. However, the exact partitioning of these functions within the PFC remained unclear.

Even though there is agreement that the lateral region of the PFC is more concerned with executive control, the orbital region with motivation/emotion, and the medial region with self and social cognition/behavior, the functional segregation is hardly absolute, and only a kind of gradient in functional differentiation is observed across the PFC[256]. Likewise, it suggests that the more abstract the representation, the more anterior the active PFC area is[256].

Table 7: A summary of the frontal lobe functions

Functions	Role's explanations
Prospective memory	A sort of memory that involves remembering the plans that have been established, starting from basic daily plans to long-term goals[260].
Speech and language	Broca's area is the part of the brain involved in speech production. Broca's area has recently been linked to the coordination of information translation across large-scale cortical networks involved in spoken word creation and the creation of a suitable articulatory code to be applied by the motor cortex[261].
Personality	Phineas Gage's case is considered as the reference case for personality changes caused by frontal lobe damage[262]. Phineas Gage was a nice, pleasant, and friendly young man until a huge iron rod pierced his eye, injuring his prefrontal cortex. Because of the injury, he became emotionally hypersensitive, engaged in socially inappropriate actions, and was unable to make sensible decisions[263]. According to a study that used two alternative cluster analysis methodologies to ratings on the Iowa Scales of Personality Change in 194 adults with chronic, stable, focal lesions located at various regions of the prefrontal lobes and elsewhere in the brain, there are four sub-types of personality alterations that occur when the prefrontal cortex is damage[264]: ●Executive disturbances in association with generalized disturbance ●Dysregulation of emotions and behavior, ●Hypo-emotionality and de-energization, ●Distress or anxiety [264].

Decision making	The ability to make a decision involves a combination of reasoning, learning, and creativity[265]. A group of researchers presented the PROBE model to clarify how the frontal lobe process in decision making. According to the PROBE model, the brain can only assess three to four behavioral strategies before deciding on the appropriate approach for the circumstances[266]. As a result, there are usually three options for adjusting to a situation: ●Choosing a previously learned method that is perfectly applicable to the current circumstances ●Adjusting a previously taught strategy ●Development of a novel behavioral strategy

b. The components and neuroanatomy of the OFC:

The prefrontal cortex is the cortex of the brain's anterior pole, located in front of the motor cortex on the lateral side of the hemisphere and the limbic cortex on the orbital and medial surfaces.

Many neuroimaging studies have been conducted to investigate the functional location and division of the human prefrontal cortex.

Despite the fact that the size of the subdivisions varies, the dorsolateral, dorsomedial, ventromedial, and orbitofrontal cortical divisions are the most important functional divisions[267].

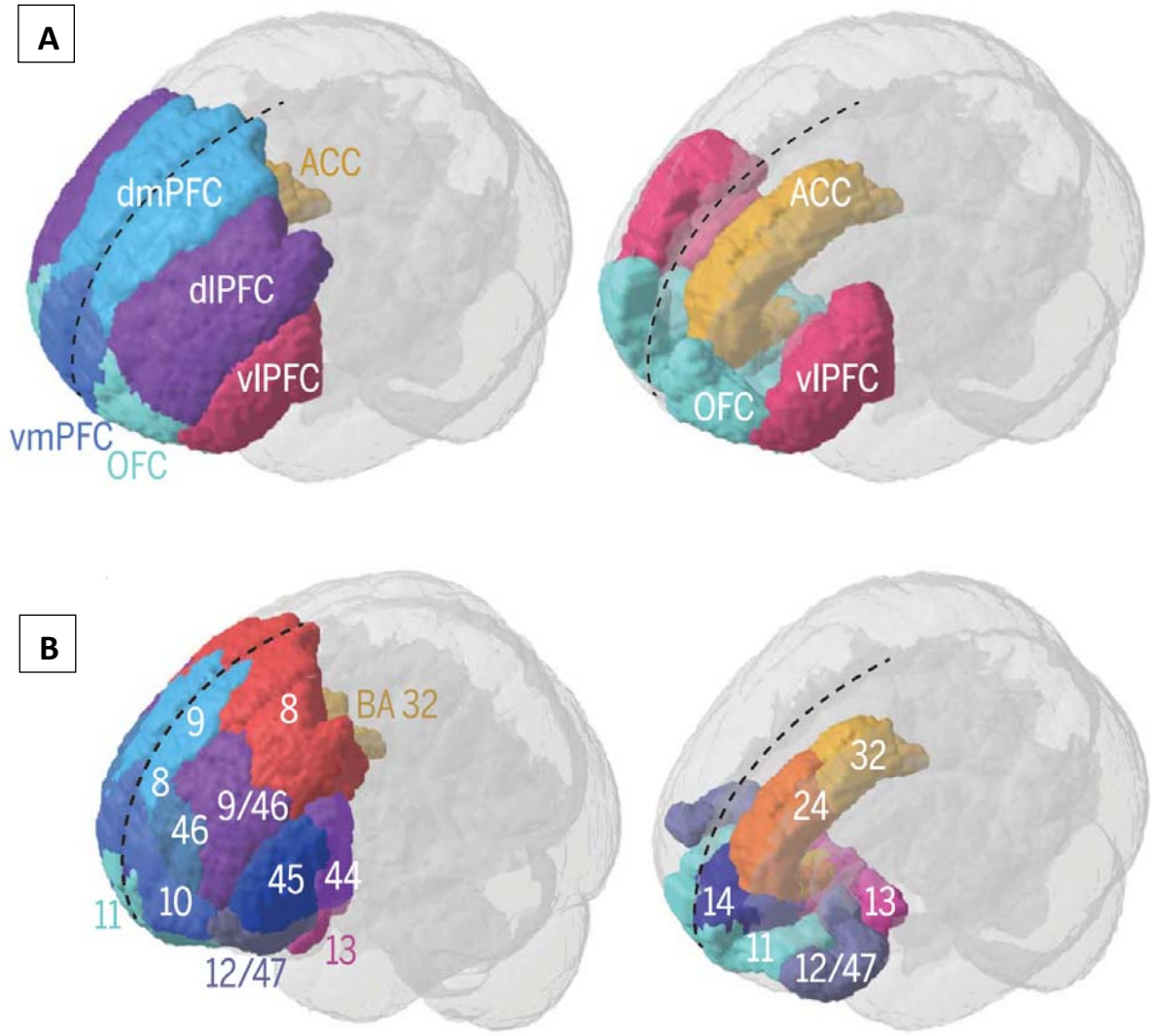

Figure 31: Left frontal-side view of the human brain. Showing in:

(A) : the functional division of the human prefrontal cortex – including anterior cingulate cortex (ACC)–.

(B) : Brodmann areas of the human prefrontal cortex. – including anterior cingulate cortex (ACC)–.

With:

dlPFC: Dorsolateral prefrontal cortex

dmPFC: Dorsomedial prefrontal cortex

vmPFC: Ventromedial prefrontal cortex

vlPFC: Ventrolateral prefrontal cortex

OFC: Orbital frontal cortex.

The dashed black line represents the sagittal midline.

Figure modified taken from: (Marie Carlén. 2017) [267]

The human architectonics included in this figure were taken from:

(Fan L, Li H, Zhuo J, et al. 2021) [416] (Wise SP. 2008) [417].

c. Connectivity of the prefrontal cortex:

This section is based mainly on the works of neuroscientist Joaquin Fuster, one of the world's leading neuroscientists. His book "The prefrontal cortex, fifth edition"264 contributed significantly to our understanding of brain structures that underlie cognition and behavior.

The prefrontal cortex is supplied with afferent fibers by multiple diencephalon, mesencephalon, and limbic regions. Fibers from numerous neocortical locations involved in sensory activities also converge on the prefrontal cortex's lateral and orbital-medial parts[268].

Almost all prefrontal connections are bidirectional, meaning that areas that send fibers to the prefrontal cortex also receive fibers from it. The basal ganglia and pontine nuclei, to which the prefrontal cortex transmits some unidirectional direct projections, are exceptional in this regard[268].

Various parts of the prefrontal cortex have different sets of bidirectional connections[268] (Figure 32):

●The orbital and medial prefrontal cortex is largely associated with the medial thalamus, hypothalamus, amygdala, limbic, medial temporal cortex, and hippocampus. This intricate system is the anatomical substratum for emotional, instinctual, and affect-modulated behavior.

●On the other hand, the lateral prefrontal cortex is predominantly linked to the lateral thalamus, the dorsal caudate nucleus, and the neocortex. Regarding phylogenetic evolution, those connections are regarded as a relatively recent system of linked structures that serve as the foundation for executive cognitive functions and behavior.

Remarque: It is intentional that we focus on connections implied in emotion, cognition, and higher brain functions rather than motor connections of the prefrontal cortex with motor function structures, since emotion, cognition, executive function, and associative function are by far the highest priorities of our study.

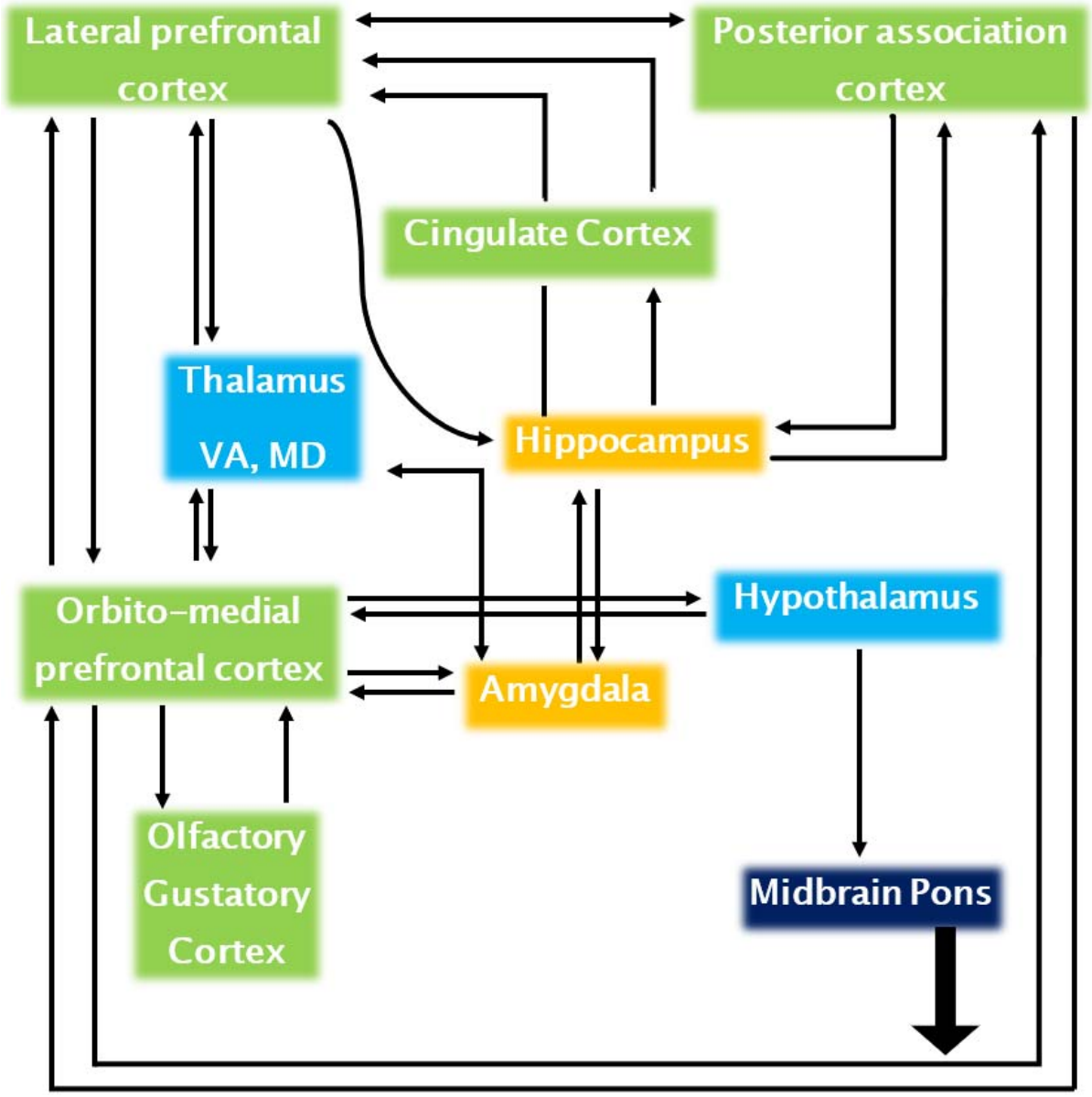

Figure 32: Connectivity of the prefrontal cortex with structures involved in emotion.

With:
VA: anteroventral nucleus – MD: mediodorsal nucleus.
Connectivity data sets from: (Fuster JM. 2015)[281].

d. Atlas 3 and 4

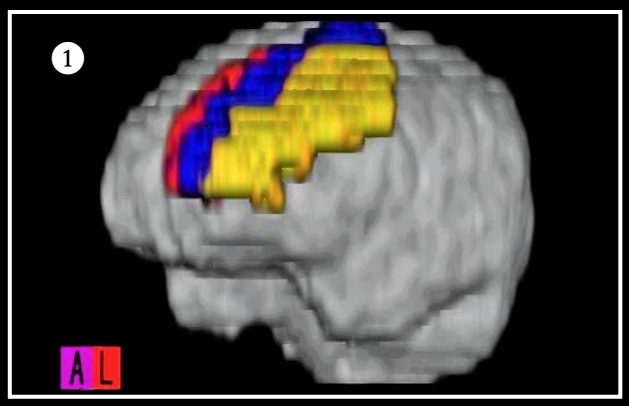

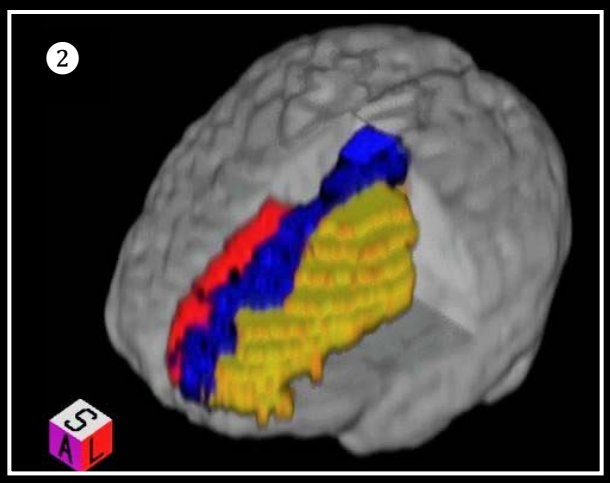

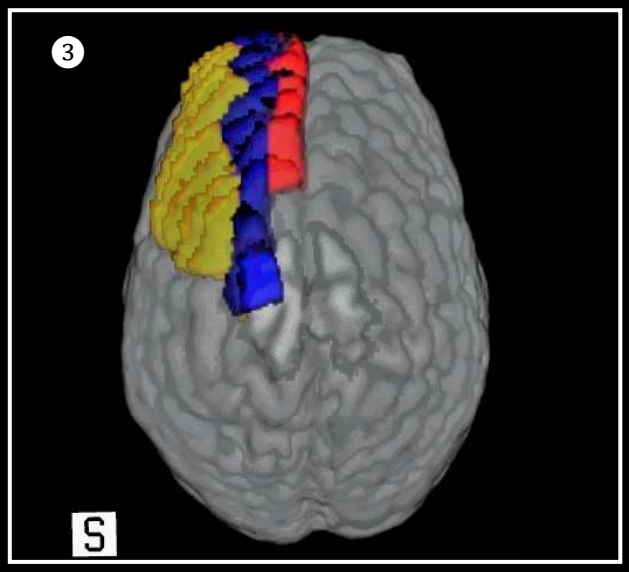

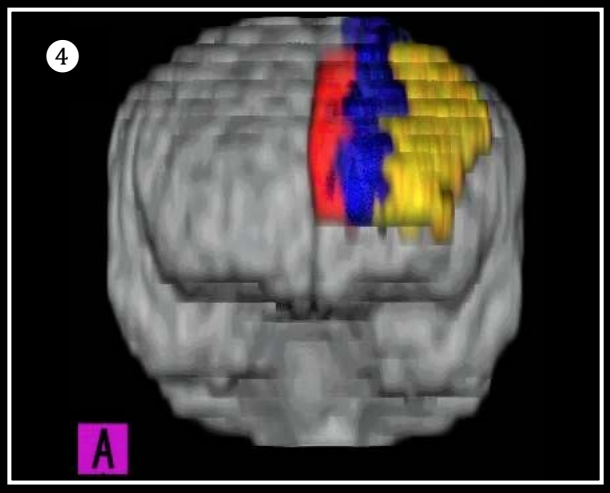

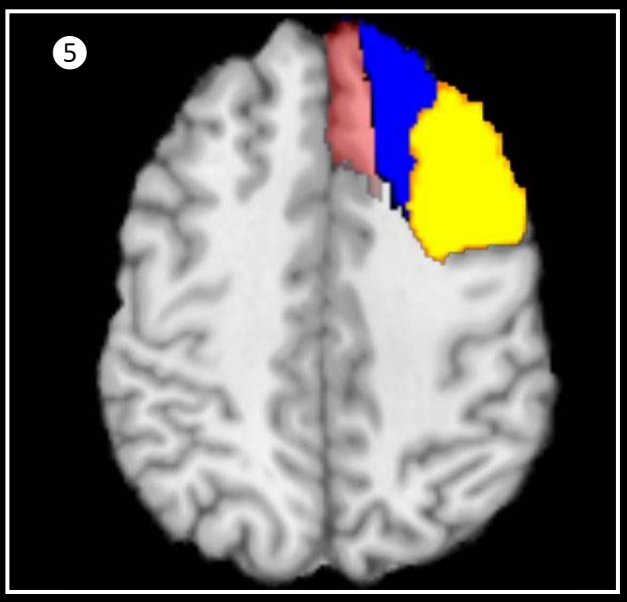

Plate N°1: Antero-lateral view

Plate N°2: Antero-superolateral view of the brain, with a cutout of the regions surrounding our region of interest.

Plate N°3: Superior view

Plate N°4: Anterior view

Plate N°5: Axial section

Atlas 3: Different views and sections of the brain with overlaying of the prefrontal lobe -Except the Broca's area-.

*Orientation: A: Anterior - L: Lateral - S: Superior - I: Inferior

*Region colors: The Left Frontal Sup Medial region.
The Left Frontal Sup region. The Left Frontal Mid region.

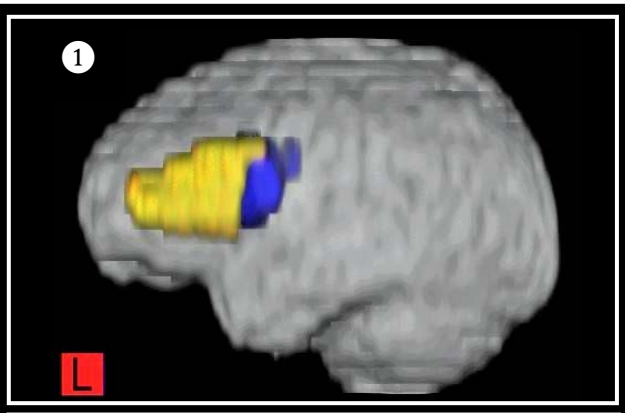

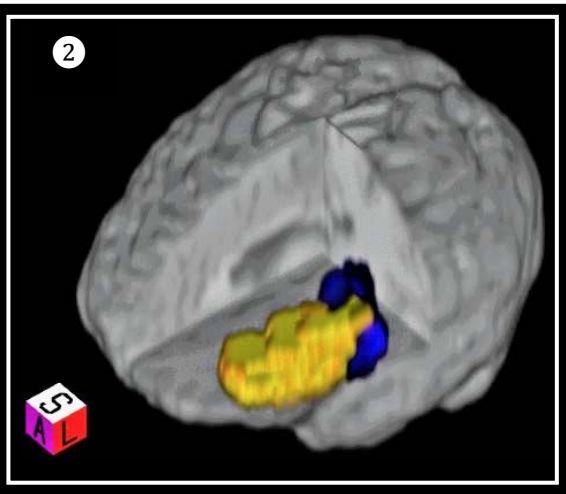

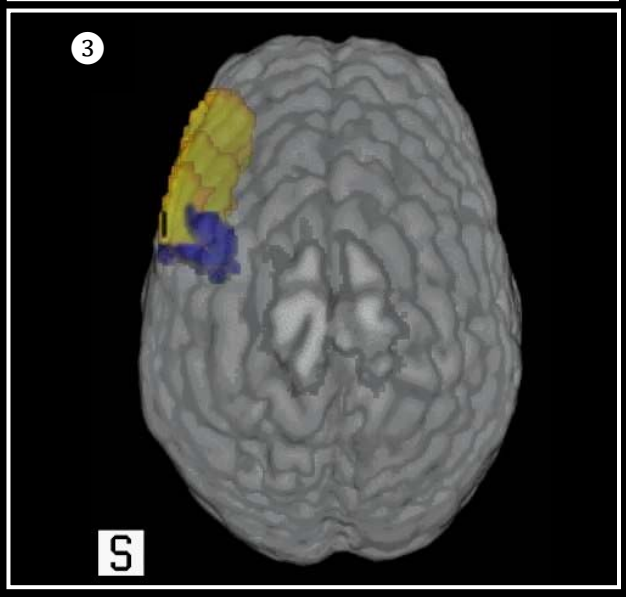

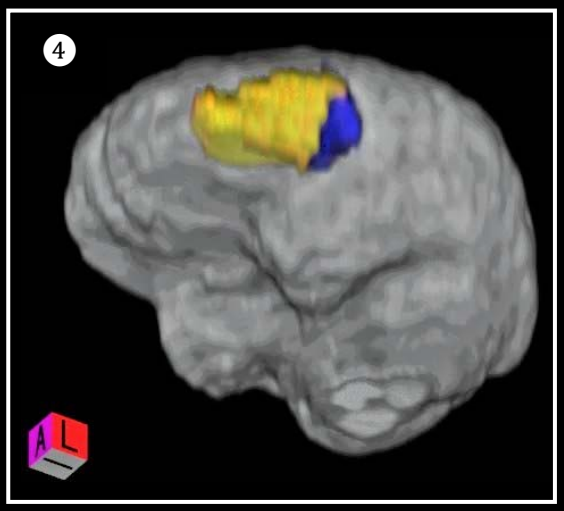

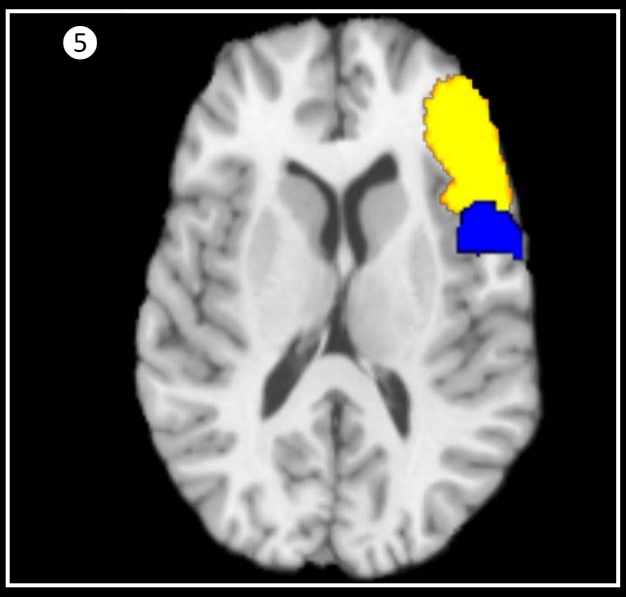

Plate N°1: Lateral view

Plate N°2: Antero-superolateral view of the brain, with a cutout of the regions surrounding our region of interest.

Plate N°3: Superior view

Plate N°4: Antero-inferolateral view

Plate N°5: Axial section.

Atlas 4: Different views and sections of the brain with overlaying of the Broca's area.

*Orientation: A: Anterior – L: Lateral – S: Superior – I: Inferior

*The overlaying: The Left Frontal Inf Tri region.
The Left Frontal Inf Oper region.

4. The parietal lobe

a. Introduction and functional physiology of the parietal lobe

The parietal lobe is the cerebral cortex area above the lateral sulcus and the temporal lobe and posterior to the central sulcus and, therefore, between occipital and frontal lobe[252].

The parietal lobe is classified into two main functional regions in its lateral surface[269]:

-The anterior parietal lobe: The postcentral gyrus.

-The posterior parietal lobe, which contains two regions:

*The superior parietal lobule

*The inferior parietal lobule.

The lobe is completed in the media by the precuneus region, which is limited by the sub-parietal and parietooccipital sulci[269].

In a basic form, three functions are associated with the parietal cortex[265]:

-The post-centred gyrus is the primary cortex somatosensory; it concerns the initial cortical processing of tactile and proprioceptive information (sensory positioning); especially of sensory location.

-The superior parietal lobule is well recognized for participating in higher-order tasks like motor planning.

-A secondary somatosensory cortex is the inferior parietal lobule (supramarginal gyrus and angular gyrus) which receives somatosensory inputs from the thalamus and the controlateral secondary somatosensory cortex, which are integrated with other major modes (visual inputs, auditory Inputs) in order to create a high-order input:

- Sensorimotor planing
- Learning

- Language
- Spatial recognition
- The capacity to distinguish between objects in terms of size, shape, weight and any other differences, what we name stereognosis.

For the precuneus lobule, discoveries of functional imagery suggest a central role for the lobule in a broad range of highly integrated tasks, including [270]:

- Visual-spatial imaging,
- Episodic memory recovery and
- Self-processing operations, i.e., taking the perspective to the first person and an agency experience.

It has also been suggested that precuneus is involved in the intertwined network of neural correlates of self-awareness, engaged in self-related mental representations during rest[270].

b. The components and neuroanatomy of the parietal lobe

The parietal lobe may be divided into two surfaces: the medial and the lateral (Figure 33).

The parietal lobe's lateral surface is subdivided into the post-central gyrus and the superior and inferior parietal lobules[269 252].

-The postcentral gyrus, also known as the ascending postcentral gyrus, is posterior to and parallel to the central sulcus, extending to the postcentral sulcus. It connects to the inferior precentral gyrus at its lower end.

-The superior parietal lobule: Intraparietal sulcus, which extends behind the postcentral sulcus towards the occipital lobe divides the superior from the inferior parietal lobules.

-The inferior parietal lobule consists of the supramarginal gyrus, which covers the inverted end of the lateral sulcus, and the angular gyrus, which covers the superior temporal sulcus in the same way. The angular gyrus is generally divided into tiny sulci, which overlaps the supramarginal gyrus.

The parietal lobe's medial surface contains the media extension of the post-central gyrus and is completed by the precuneus region.

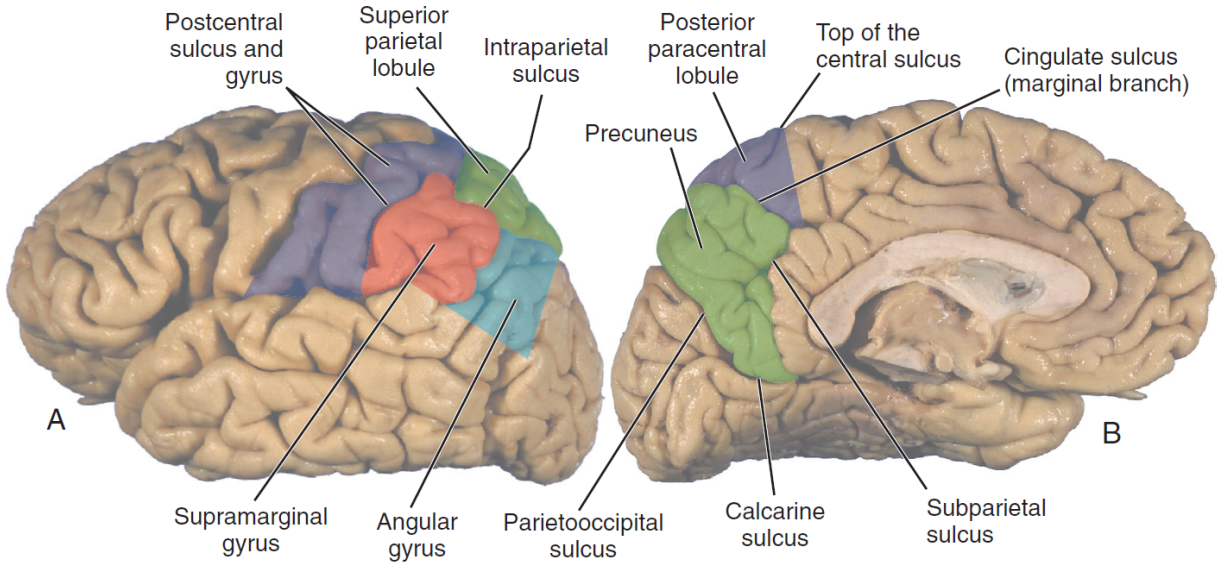

Figure 33: Lateral (A) and medial (B) views of the parietal lobe showing boundaries of the lobe, positions of major sulci and gyri. (Vanderah TW, Gould. 2015)[269]

c. Connectivity of the parietal lobe

➢ **Corticocortical connectivity (Figure 34):**

The parietal lobe's corticocortical connectivity is particularly strong in the posterior parietal cortex areas (PPC)[271]. The PPC is associated with the prefrontal, temporal, and occipital brain regions by the following association fibre bundles:

-The superior longitudinal fascicule (SLF) comprises three separate segments and connects all PPC's components to the frontal cortex[271].

- The superior fronto-occipital fascicle, a large bundle that overlaps the SLF, may represent a caudal extension of the SLF into parieto-occipital cortex[272].

- The arcuate fascicle is another bundle that runs parallel to the SLF and connects the inferior frontal gyrus to the superior temporal cortex through the inferior parietal lobule[273]. Whereas a long direct segment circumvents the inferior parietal lobule, two short components provide connections between the inferior frontal gyrus and the anterior inferior parietal lobule and the caudal inferior parietal lobule and the superior temporal cortex (posterior segment)[274].

- The middle longitudinal fascicle is another large fibre bundle that provides connections of the parietal cortex. This bundle runs from the superior and inferior parietal lobules regions to reach the temporal pole towards the temporal lobe[275][276].

➢ **Cortico-subcortical connectivity:**

Apart from corticocortical connection, the parietal lobe is closely linked to subcortical nuclei. The basal ganglia system[277], which is highly connected to all cortex areas, is a prime target for reciprocal connections.

The thalamus is another significant target for parietal cortex cortico-subcortical connection. In vivo, it is demonstrated that the most crucial target for posterior parietal regions within the thalamus is a zone corresponding to the lateral posterior nucleus and the anterior and lateral pulvinar[278][279].

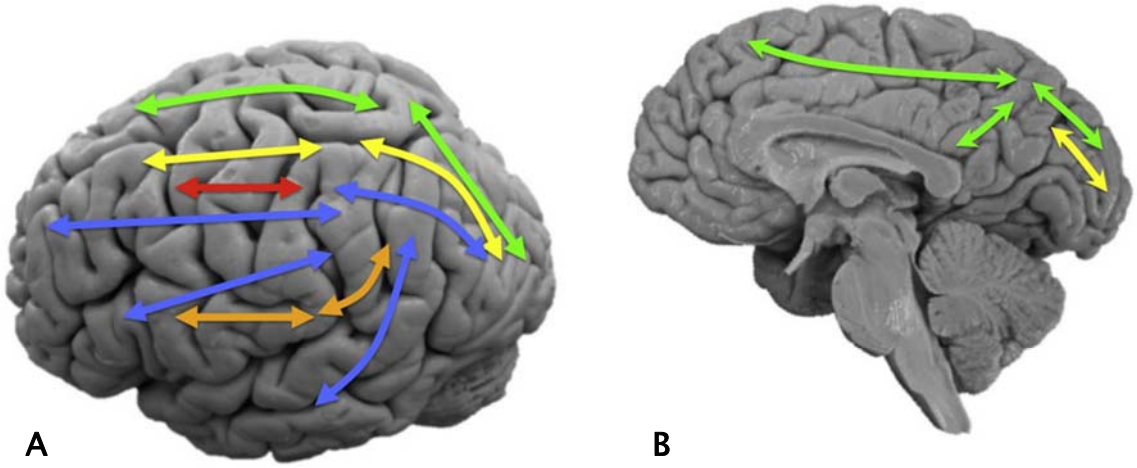

Figure 34: Overview of the overall corticocortical connectivity patterns of human parietal cortex, from lateral (A) and midsagittal (B) view. Connections (depicted by colored arrows) are schematically drawn along the major fiber pathways connecting parietal cortex with other brain regions.

Color coding of the arrows:

*Red: Connections with primary somatosensory cortex),

*Orange: Secondary somatosensory cortex

*Blue: Inferior parietal lobule

*Green: Superior parietal lobule

*Yellow: intraparietal sulcus.

(Caspers S, Zilles K. 2018)[271]

d. Atlas 5 and 6

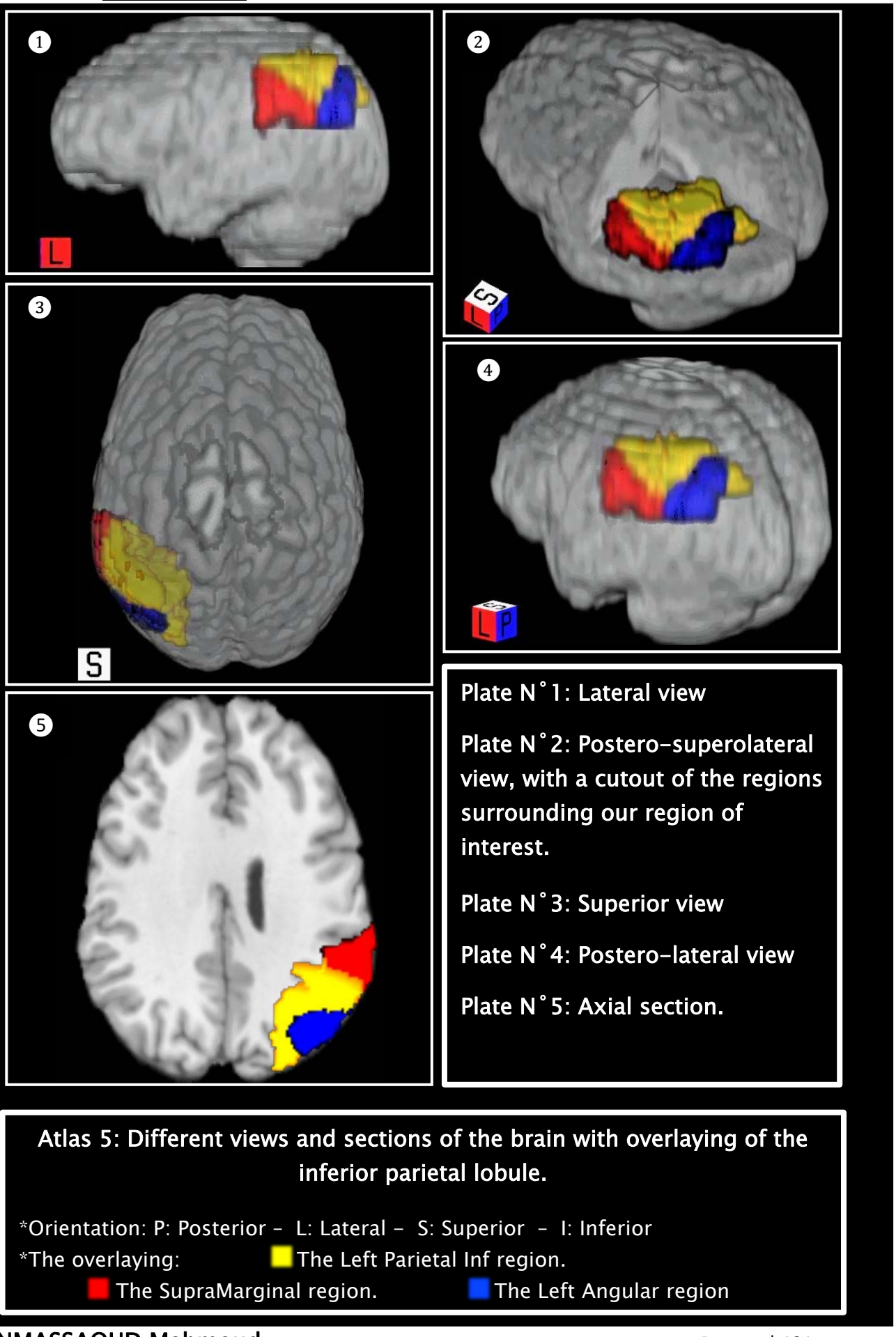

Plate N°1: Lateral view

Plate N°2: Postero-superolateral view, with a cutout of the regions surrounding our region of interest.

Plate N°3: Superior view

Plate N°4: Postero-lateral view

Plate N°5: Axial section.

Atlas 5: Different views and sections of the brain with overlaying of the inferior parietal lobule.

*Orientation: P: Posterior - L: Lateral - S: Superior - I: Inferior

*The overlaying: The Left Parietal Inf region.

The SupraMarginal region. The Left Angular region

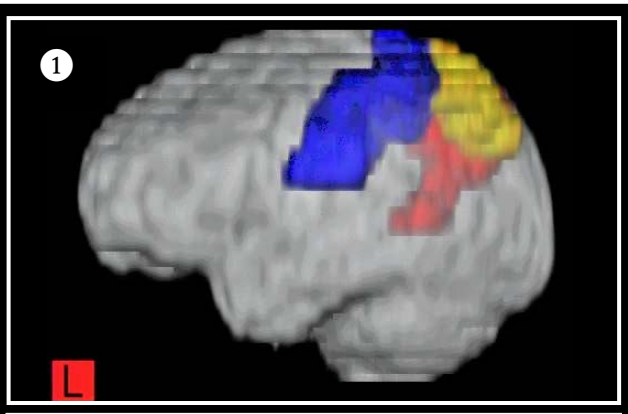

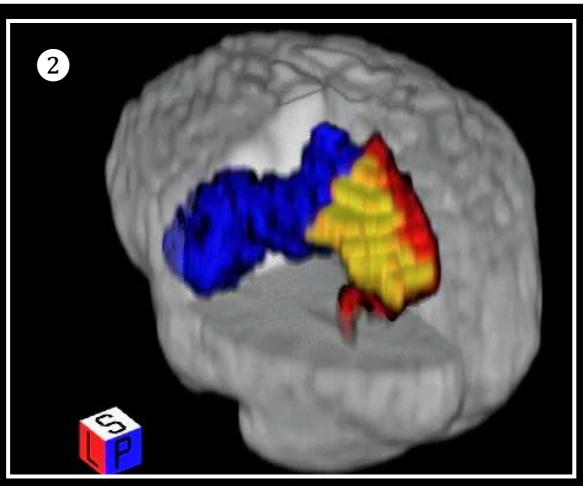

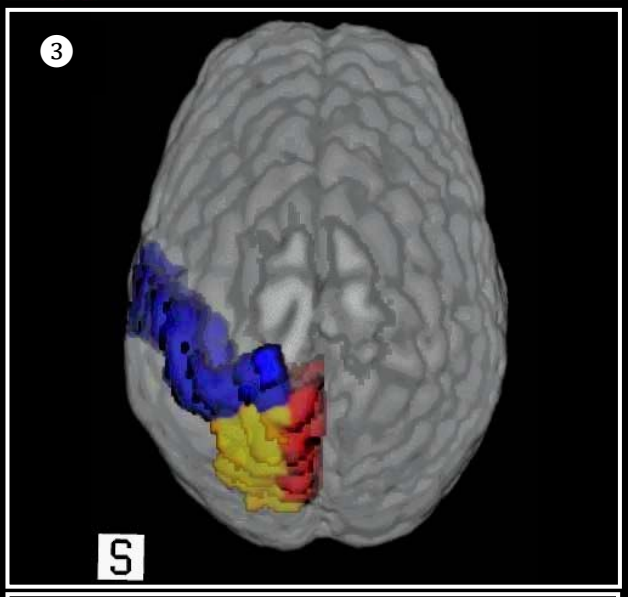

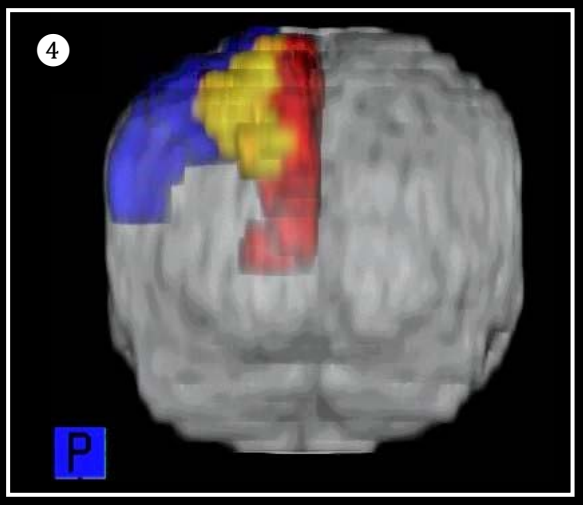

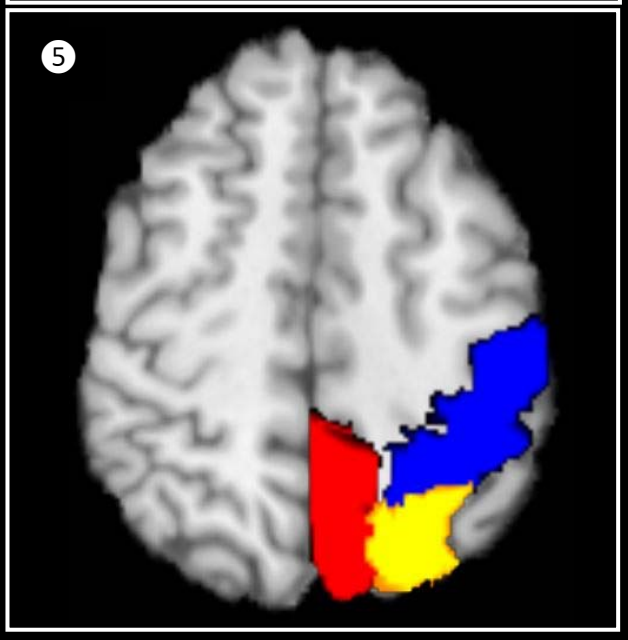

Plate N°1: Lateral view

Plate N°2: Postero-superolateral view, with a cutout of the regions surrounding our region of interest.

Plate N°3: Superior view of the brain.

Plate N°4: Posterior view

Plate N°5: Axial section

Atlas 6: Different views and sections of the brain with overlaying of the Postcentral, Parietal sup and the Precuneus gyrus.

*Orientation: P: Posterior – L: Lateral – S: Superior – I: Inferior

*The overlaying: The Left Postcentral region.

The Left Parietal sup region. The Left Precuneus region

5. The temporal lobe

a. Introduction and functional physiology of the temporal lobe

The temporal cortex, which occupies the middle cranial fossa and lies posterior to the frontal lobe and inferior to the parietal lobe, is the second main portion of the cerebral cortex, accounting for 17% of the volume of the human cerebral cortex (16% in the right and 17% in the left hemisphere) [280] [281].

The temporal lobe is divided into two surfaces: lateral and medial. These surfaces include regions involved in auditory, olfactory, vestibular, and visual perception, as well as spoken and written language perception[281]. The region converts sensory information into deduced interpretations to retain emotions, visual memory, and language understanding[282].

In general, four functions are associated with the lobe [269]:

-**The primary auditory cortex**, commonly known as the Heschl gyri, is a part of the superior area of the temporal lobe.

- Wernicke's region, the posterior portion of the left hemisphere's superior temporal gyrus, this area was previously considered to play a key role in **speech perception and comprehension**. However, recent studies found that it helps **regenerate phonological forms** essential **for speech production and short-term memory** [283].

- Some of the temporal lobe, especially the lower surface, is involved in **visual information processing**.

- The temporal lobe, particularly its medial region, is involved in various complicated aspects of **learning and memory**. And the fusiform gyrus is commonly considered an essential structure of **face perception**, **object recognition, and reading**[284].

b. The components and neuroanatomy of the temporal lobe

The temporal lobe is quite pyramidal in form and has lateral, basal, dorsal, and an anterior pole. Like the other lobes of the cerebral hemisphere, the temporal lobe is demarcated by cortical landmarks and has anatomical contacts on its different sides with the neighbouring lobes. The stem and posterior ramus of the lateral sulcus mark the temporal lobe's separation from the frontal and parietal lobes on the lateral surface [281] [252] (Figure 35).

The temporal lobe interacts superiorly with the inferior parietal lobe and inferiorly with the occipital lobe. The temporal lobe continues ventrally to the collateral sulcus at the hemisphere's base, where it is separated from the limbic lobe. The temporal lobe is continuous in its caudal area, with the inferior parietal lobe at the top, and the occipital lobe, inferiorly. The temporal lobe extends to the collateral sulcus at the base of the hemisphere, separating it from the limbic lobe[252].

The superior temporal sulcus and the lateral temporal sulcus divide the lateral surface into three gyri: superior temporal gyrus, middle temporal gyrus, and inferior temporal gyrus[281].

The large occipitotemporal (fusiform) gyrus, isolated from the limbic lobe by the collateral sulcus, makes up the remainder of the inferior surface. The occipitotemporal sulcus divides the lateral border of the fusiform or medial occipitotemporal gyrus from the medial border of the inferior temporal gyrus[269] [281].

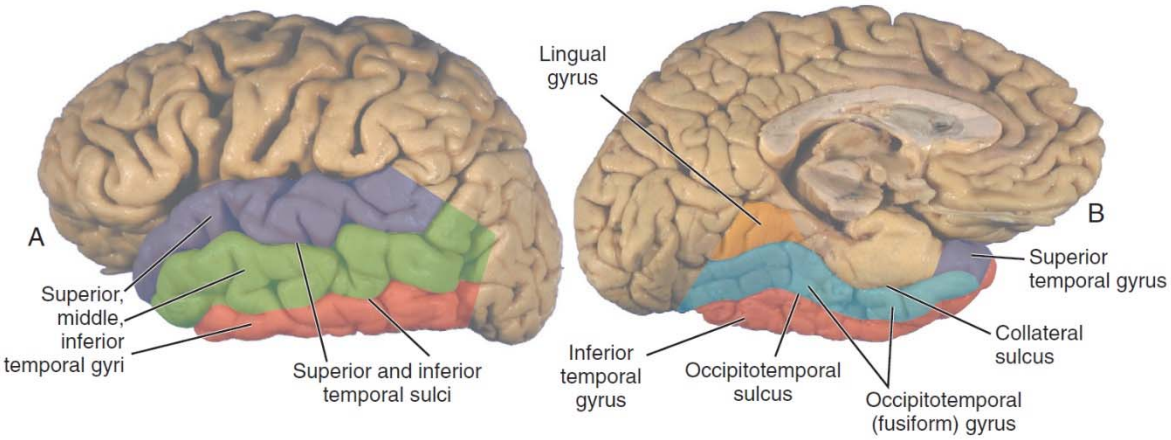

Figure 35: Lateral (A) and medial (B) views of the temporal lobe showing boundaries of the lobe, positions of major sulci and gyri.
(Vanderah TW, Gould. 2015)[269]

c. Connectivity of the temporal lobe

In the sections on each brain region or system in our study, we explain functional relationships with the temporal lobe (when there are any, of course). And in this section on temporal lobe connectivity, we'll go over the main connections based on the three distinct types of subcortical white matter connections and axons:

- Association fibres.
- Commissural fibres.
- Projection fibres.

The following are definitions of the various types of brain fibres and connections[281]:

-Cortical regions within the same brain hemisphere are connected by **association fibres.**

- **Commissural fibres** primarily but not exclusively link symmetrical cortical regions.

- Projection fibres connect cortical regions with grey matter subcortical nuclei.

i. Association fibres of the temporal lobe:

The temporal lobe is linked with all the other lobes of the forebrain through association fibres. In figure 36, we schematise the three principal association fibres related to the temporal lobe[281].

Three major fibre bundles connect the temporal lobe to the other lobes: The arcuate fasciculus tract, the uncinate fasciculus tract, and The inferior longitudinal fasciculus tract.

- **The arcuate fasciculus tract (or superior longitudinal fasciculus) :**

The arcuate fasciculus is a white matter bundle that connects the frontal, parietal, and temporal lobes. It's a large anterior–posterior bundle made up of long and short fibers[273285].

It is a pathway that communicates Wernicke's temporal lobe area to Broca's in the frontal lobe[273]. The arcuate plays a crucial role in language processing in the left hemisphere and visuospatial processing and some language processing elements, such as prosody and semantics, in the right hemisphere[273].

- **The uncinate fasciculus :**

The uncinate fasciculus is a tract that runs around the stem of the lateral sulcus and links the temporal pole cortex with the orbitofrontal cortex[281].

It originates in the orbitofrontal cortex and consists of two components, one from the medial and one from the lateral regions, which combine to create a bundle that extends posteriorly and arches downward to reach the anterior temporal lobe. [286].

Damage to this tract has been related to a deficiency in object identification, decreased verbal fluency, and anomia. Therefore, it has been hypothesized that it plays a function in language[287].

➢ **The inferior longitudinal fasciculus:**

This fibre links the anterior and the medial temporal lobe with the occipital lobe. It connects these visual regions as well as the temporal polar cortex, a major source of afferent fibres to the amygdala. The tract runs ventrally along the inferior wall of the lateral ventricle's temporal horn [281] [286].

The inferior longitudinal fasciculus pathway is involved in the processing of emotions generated by visual stimuli, as well as a minimal involvement in language and facial recognition[286].

ii. Commissural fibres: The corpus callosum

According to some studies, axons from the middle and posterior sections of the temporal cortex cross the midline in the central part of the corpus callosum's body. The anterior commissure fibres are supposed to link the temporal poles, transverse temporal gyri, and amygdala[281].

iii. Projection fibres:

The sources of thalamic afferents have not been discovered for most of the temporal cortex. However, we do know that reciprocal corticothalamic fibres accompany all thalamocortical projections[281].

Projection fibres from the medial geniculate body to the primary auditory region of the transverse temporal gyri are afferent to the temporal cortex. These fibres go via the internal capsule's sublenticular limb, where they are likely joined by fibres from the medioventral thalamic nucleus, which connects the amygdala, hypothalamus, hippocampal formation, and parahippocampal gyrus[281].

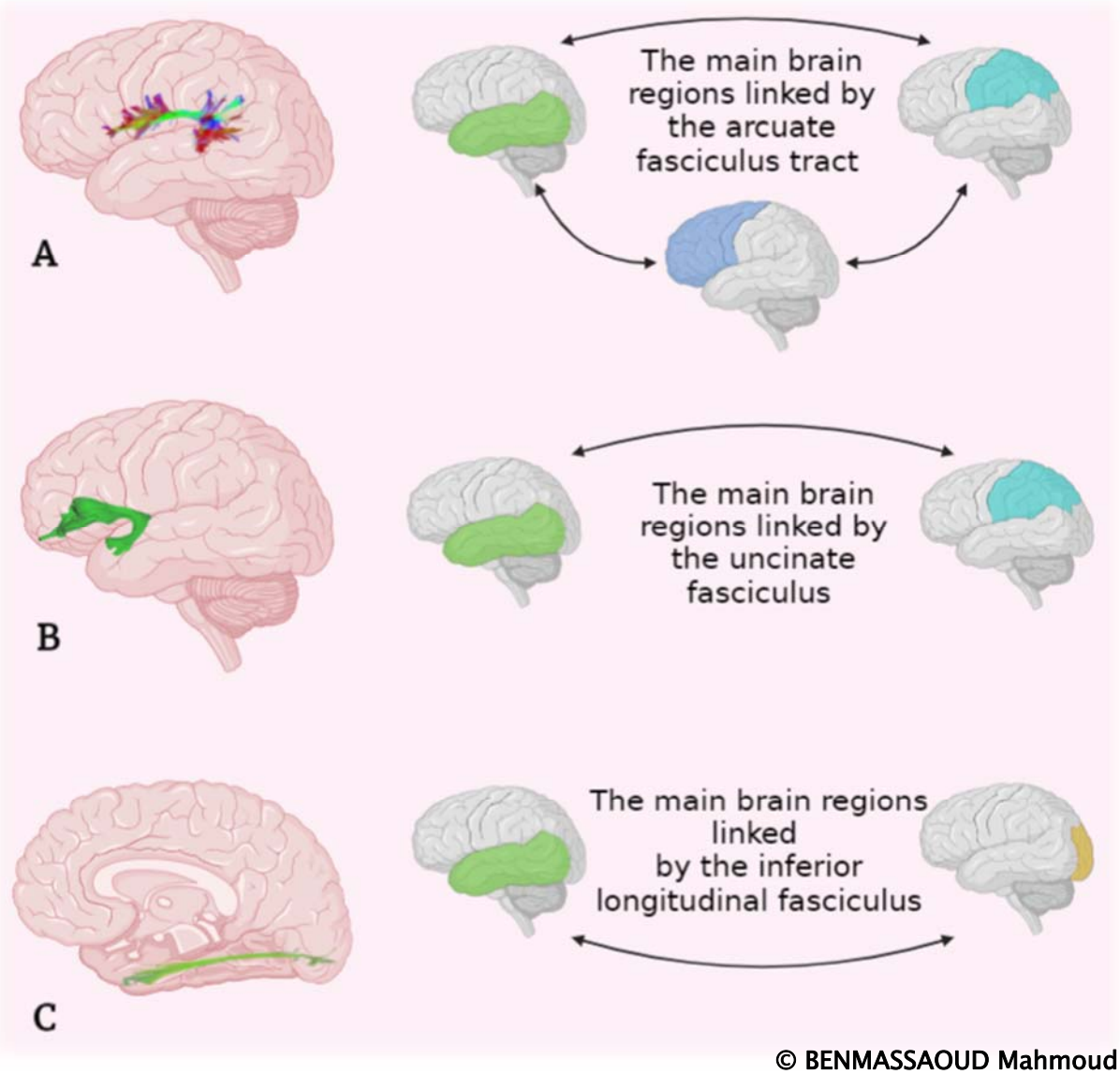

Figure 36: Schematic presentation of temporal connectivity through the main three associative bundles.

With:

A: Illustration of the arcuate fasciculus tract and regions connected by it.

B: Illustration of the uncinate fasciculus tract and regions connected by it.

C: Illustration of the inferior longitudinal fasciculus and regions connected by it.

d. Atlas 7, 8 and 9

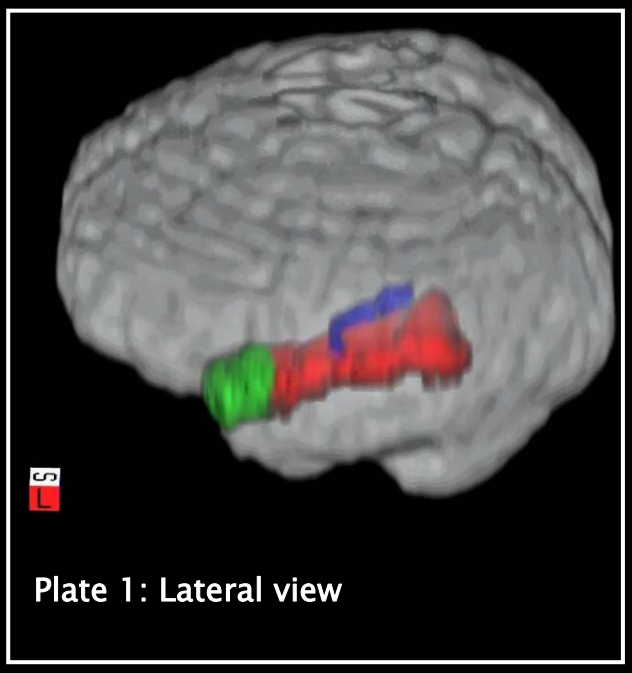

Plate 1: Lateral view

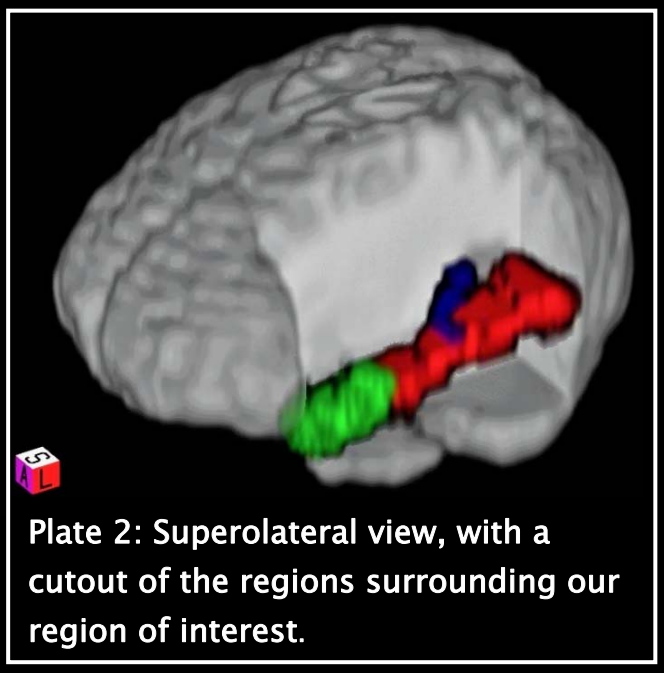

Plate 2: Superolateral view, with a cutout of the regions surrounding our region of interest.

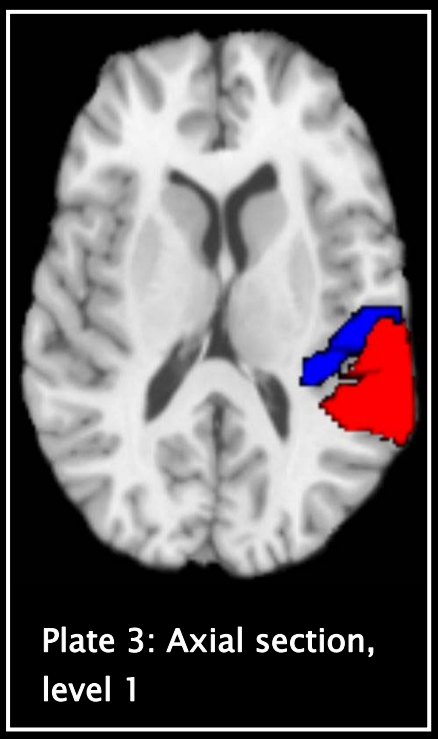

Plate 3: Axial section, level 1

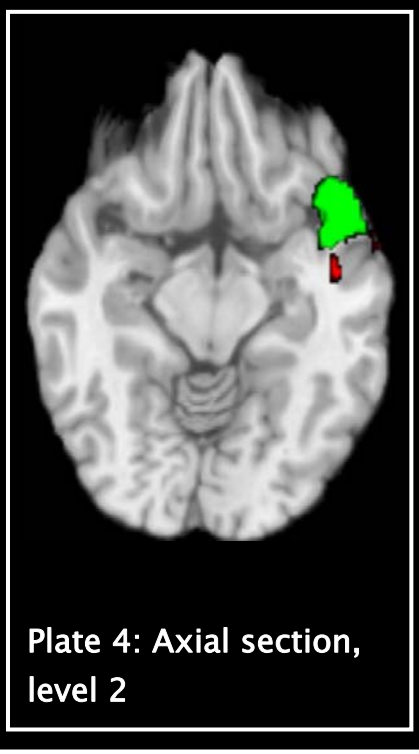

Plate 4: Axial section, level 2

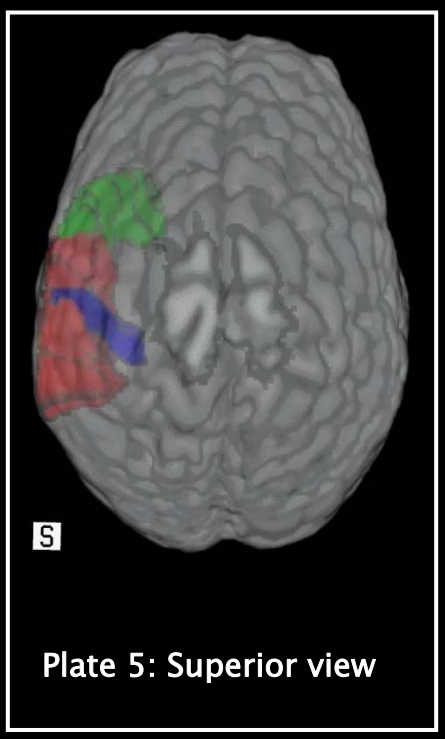

Plate 5: Superior view

Atlas 7: Different views and sections of the brain with overlaying of the superior temporal gyrus.

*Orientation: A: Anterior – L: Lateral – S: Superior – I: Inferior

*The overlaying: The Left Temporal Sup region.

The Left Temporal Pole Sup region. The Left Heschl region

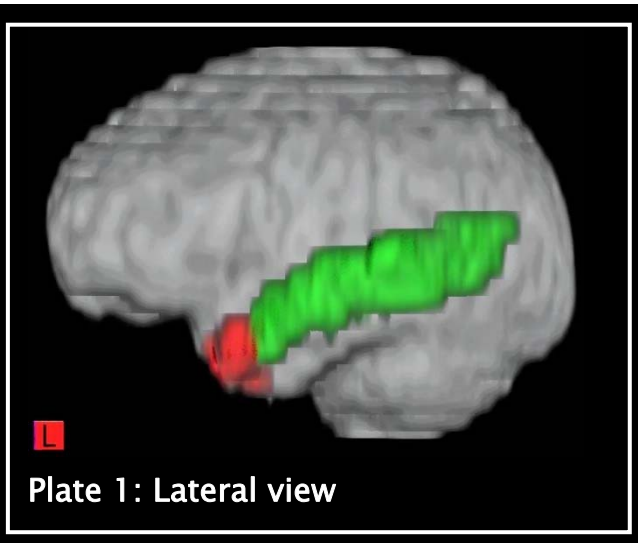

Plate 1: Lateral view

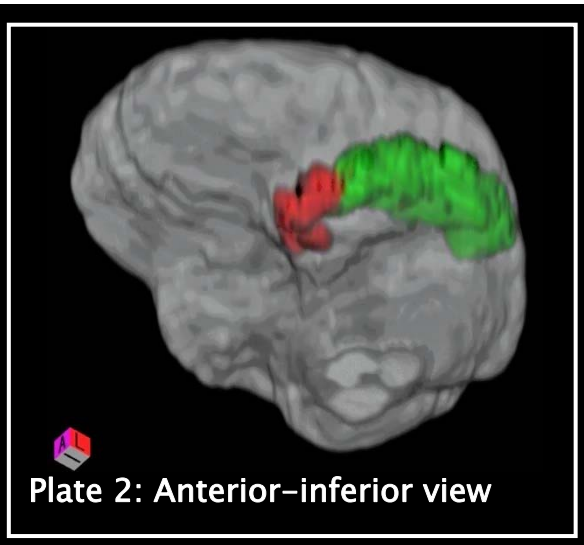

Plate 2: Anterior–inferior view

Plate 3: Axial section, level 1

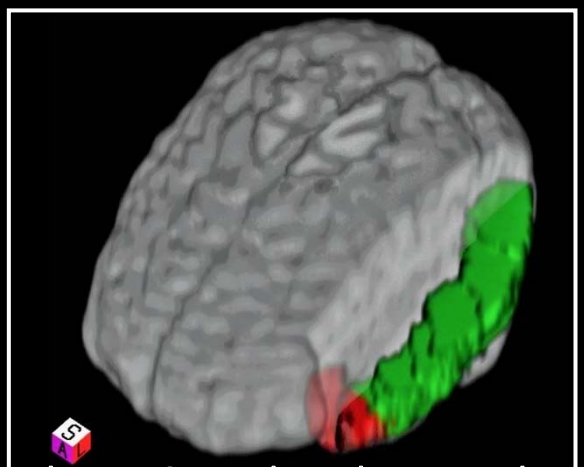

Plate 4: Superolateral view, with a cutout of the regions surrounding our region of interest.

Plate 5: Axial section, level 2

Atlas 8: Different views and sections of the brain with overlaying of the middle temporal gyrus.

*Orientation: A: Anterior – L: Lateral – S: Superior – I: Inferior

*The overlaying:

The Left Temporal Mid region. The Left Temporal Pole Mid region

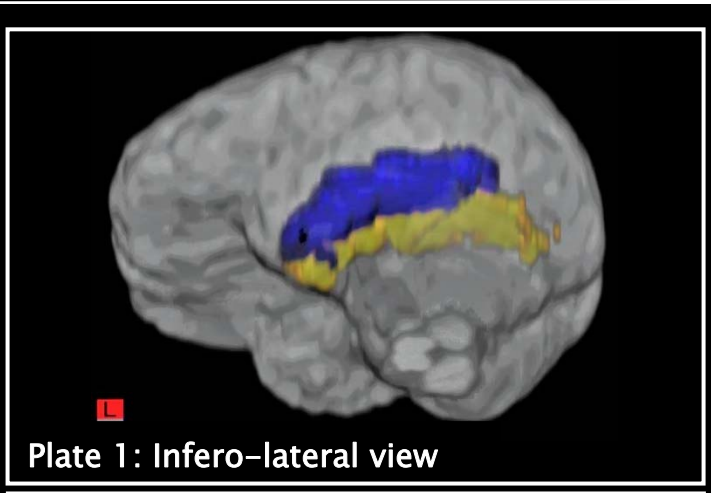

Plate 1: Infero-lateral view

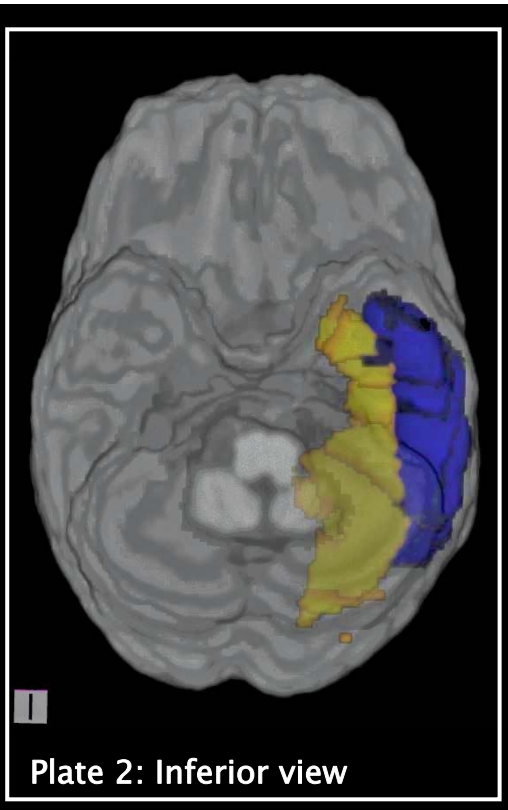

Plate 2: Inferior view

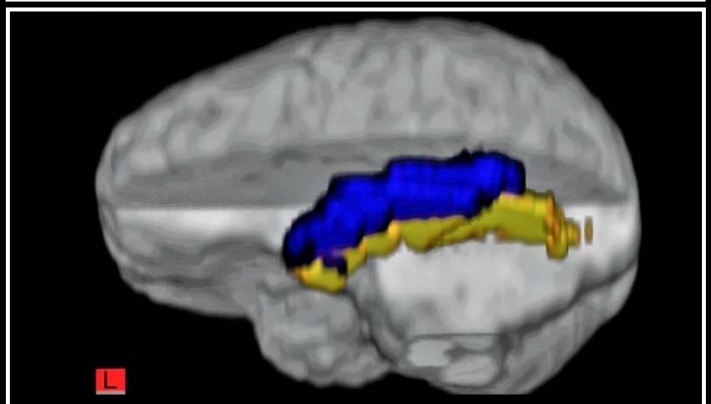

Plate 3: Inferolateral view, with a cutout of the regions surrounding our region of interest.

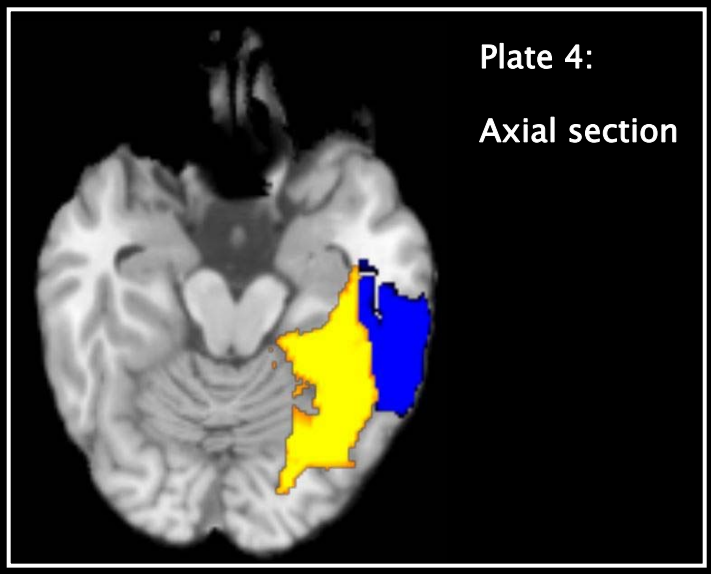

Plate 4:

Axial section

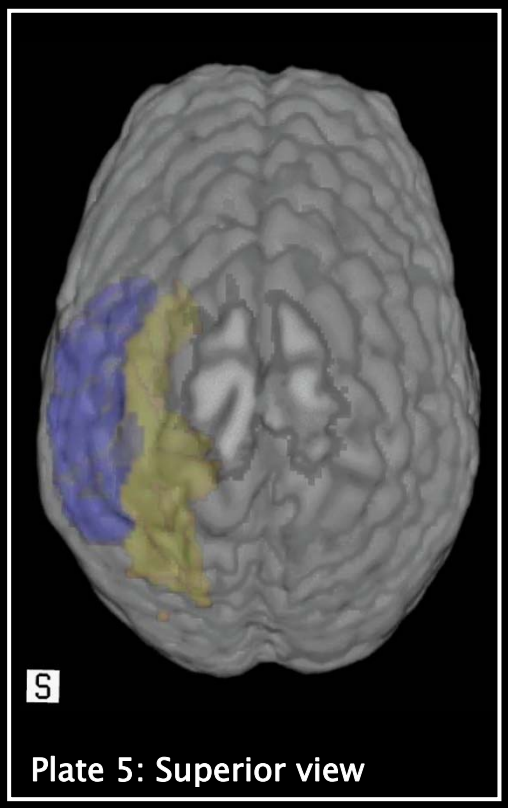

Plate 5: Superior view

Atlas 9: Different views and sections of the brain with overlaying of the inferior temporal and the occipitotemporal (fusiform) gyri.

*Orientation: A: Anterior – L: Lateral – S: Superior – I: Inferior

*The overlaying:

The Left Temporal Inf region. The Left Fusiform region

6. The limbic system

a. Introduction and functional physiology of the limbic system

The limbic system is a network of interconnected cortical and subcortical structures on the thalamus's lateral side, just below the cerebral cortex and above the brainstem. This network connects visceral feelings and emotions with cognition and behaviour [288] [289] [290].

Paul Broca was the first to identify "le grand lobe limbique" in 1878, and he assumed that this region is similar to all mammalian brains and was primarily an olfactory structure, but he maintained that its activities were not restricted to olfaction. Paul Broca has given the term "limbique" to the cortex's curved edge, including the parahippocampus and cingular regions[291].

After all, in 1937, James Papez offered his theory on the limbic's potential function in emotion: "the Papez circuit" [292].

In 1948, Yakovlev posited the orbitofrontal, insular, anterior temporal lobe cortex, the amygdala, and the dorsomedial nucleus of the thalamus in emotion regulation: "The Yakovlev's circuit "[293].

The term "limbic system" was introduced in 1952 by Paul D. MacLean to characterize Broca's limbic lobe and associated subcortical nuclei as the collective neuronal foundation for emotion[294].

The limbic system is now recognized to contribute to different cognitive functions, including spatial memory, learning, motivation, emotional and social processing. The limbic system was also first considered as the only emotional neurology system and is now only one component of the brain that can control visceral autonomous functions [290] (Table 8).

Table 8: A summary of the functions of regions composing the limbic system

Regions	Subregions	Functions
Cingulate gyrus	Cingulate Ant	It is involved in the control of painful and unpleasant sensations. Certain harmful avoidance behaviours, such as drug addiction, eating disorders, and autolysis, emerge through the anterior cingulate via adaptive mechanisms[295].
	Cingulate Mid	A cingulate system component allows reward information from the orbitofrontal cortex to be linked to action information from the posterior cingulate cortex, with the output directed to premotor cortical areas[296].
	Cingulate Post	The posterior cingulate cortex is involved in various forms of decision-making in that it responds when risky, unclear decisions are made or when a huge reward is expected but not received, with a fring of signals until the next trial[296].
Parahippocampal gyrus		The structure plays a role in complicated emotional processes[297]. Part of a highly specialized network for processing many sorts of emotional inputs, and strongly involved in negative and not positive emotive responses[297].
Hippocampus		It is involved in learning and memory storage, spatial navigation, mood, pleasure and unpleasure, motivation, hunger, and sexual desire[298].
Insula		Emotion, empathy, olfaction, taste, interoception, pain, somatosensation, motion, attention, language, speech, memory,

	and work memory are all functions related to this area[299 300 301].
Amygdala[302]	-Learning and representation of valence[302]. - Strongly linked to emotions, selective attention, information processing, and ambiguity resolution[302]. -Assist in determining the value (appetizer/repulsive) of external stimuli and, as a result, in decision-making[302]. -The autonomic vegetative system's operation, as well as physiological neuroendocrine responses and behaviour coordination[302].
Thalamus[303]	-Pain perception psychophysiological activation -Control of sensory regions other than olfaction -Locomotion and language control -Modulation of cognitive functions: mood and motivation control

b. Our concept for anatomy and connectivity of the limbic system

This section will present the anatomical areas and their interconnections using a different concept than the concepts employed in the previous sections of this work.

Since there is no universal agreement on the total list of structures that should be included in the term "Limbic system," and consequently no consensus on how this network of brain structures is connected, our study will be based on a recent and updated model proposed by Catani and his team in 2013[304].

c. The components and neuroanatomy of the limbic system

Firstly, below are the regions that all authors would include as regions of the limbic system - independent of paralimbic regions-:

1. Limbic cortex
    i. Cingulate gyrus
    ii. Parahippocampal gyrus
2. Hippocampal formation
    i. The dentate gyrus
    ii. Hippocampus
    iii. Subicular Complex
3. Amygdala
4. Septal area
5. Hypothalamus

Secondly, in this part, we'll list the limbic and paralimbic areas on which the majority of writers agree, as well as those on which Catani and his colleagues based their identification of the three networks presented in their updated model on the limbic system[304]. The limbic system's subcortical and cortical sections will be presented separately.

- **Subcortical Limbic structures:**

The limbic structures of the subcortical cortex include the following[304]:

-The amygdala,

-Mammillary bodies,

-Hypothalamus,

-Some thalamic nuclei

-The ventral striatum: nucleus accumbens.

➢ **The cortical components:**

The limbic system's cortical components are divided into limbic and paralimbic zones[288]. The cortical regions are:

-The primary olfactory piriform cortex

-Insular cortex

-The orbitofrontal regions

*Medial orbitofrontal cortex

*Lateral orbitofrontal cortex

-The Temporal regions:

*Temporal pole,

*Ventral temporal cortex

*Posterior lateral temporal cortex

-Cingulate

*Subcallosal cingulate

*Anterior

-Occipital regions: Inferior and Dorsal occipital

-The hippocampus

-The parahippocampal gyrus.

-The prefrontal cortex

-Anterior frontal eye fields

-Precuneus

-Posterior parietal cortex

Finally, in figure 37, we present the functional-anatomical division of the limbic system into olfactocentric and hippocampocentric groups as presented by Mega. Michael S[305] and Marsel. Mesulam[288] in their works and adopted by Catani and all.[304] in his revised model on the limbic system.

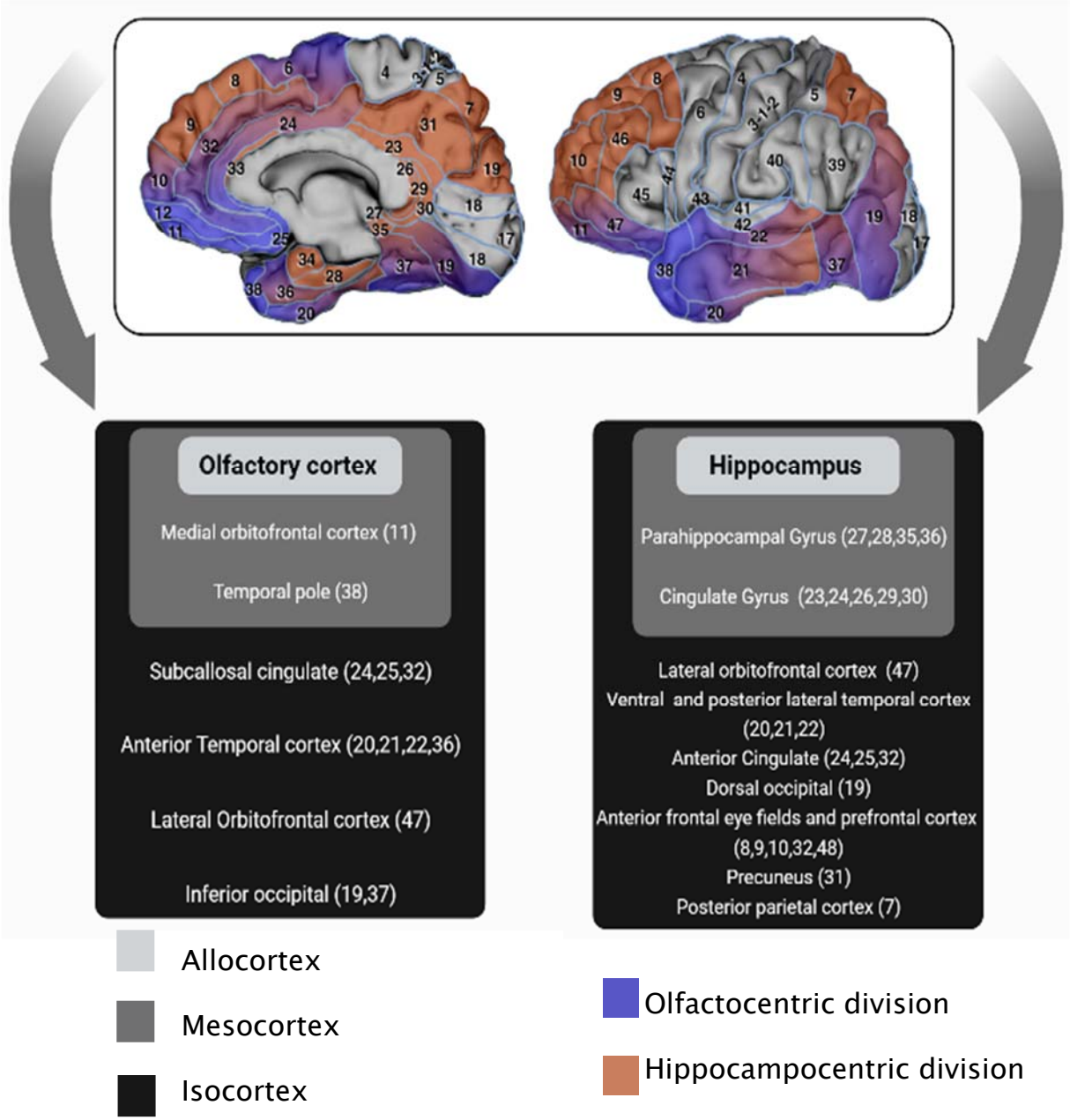

Figure 37: Limbic system division into olfactocentric and hippocampocentric groups. (Some regions are connected to both divisions.)

Data sets and images of the brain divisions were taken from: (Catani M, Dell'Acqua F, Thiebaut de Schotten M. 2013)[304].

Each division is organized around a central core of the allocortex, as seen in figure 37. Subcortical limbic structures and adjacent isocortical areas have reciprocal connections with both divisions. In the anterior cingulate cortex, the two divisions converge[304].

d. Connectivity of the limbic system

The following part presents the diagram of the main pathways of the limbic system previously presented by Catani and all, based on evidence from animal research and human tractography findings (figure 38).

We'll also illustrate the three differentiated but somewhat overlapping networks that have been identified, as well as the roles that each network serves (figure 39 and table 9):

-The Hippocampal-diencephalic and parahippocampal-retrosplenial network.

-The temporal-amygdala-orbitofrontal network.

-The default-mode network.

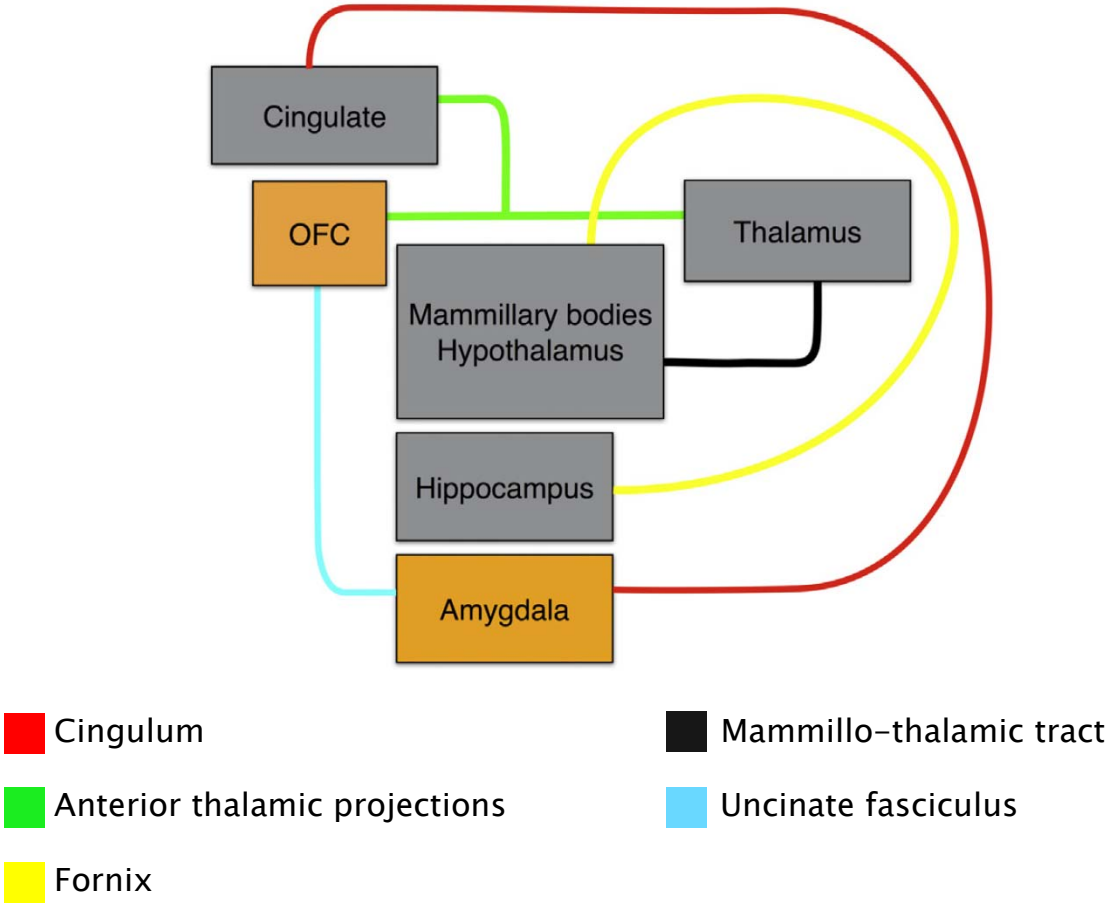

Figure 38: The main pathways of the limbic system.

(Catani M, Dell'Acqua F, Thiebaut de Schotten M. 2013)[304]

Table 9: The three differentiated networks that have been identified, their main connections, and the roles that each network serves.
(Catani M, Dell'Acqua F, Thiebaut de Schotten M. 2013)[304]

Network	Function	Main connections
Hippocampal-diencephalic and parahippocampal retrosplenial	-Memory -Spatial orientation	-Ventral cingulum -Fornix -Mamillo-thalamic tract
Temporo-amygdala-orbitofrontal	-Behavioural inhibition -Memory for temporally complex visual information. -Olfactory-gustatory-visceral functions -Multimodal sensory integration -Object-reward association learning -Outcome monitoring	-Uncinate fasciculus
Dorsomedial default network	-Pain perception -Self-knowledge -Attention -Mentalizing -Empathy -Response selection and action monitoring -Autobiographical memory -Person perception	-Dorsal cingulum

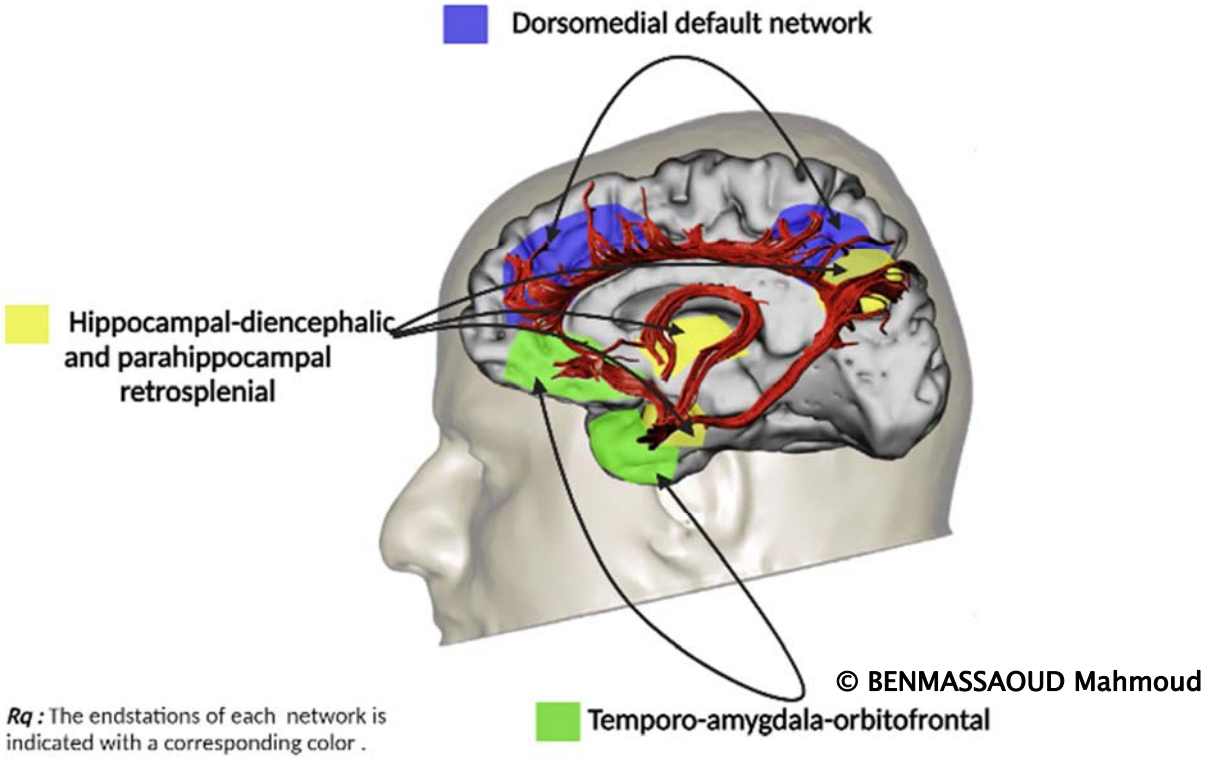

Figure 39: The three differentiated networks that have been identified.

Data sets and images of the brain divisions were taken from: (Catani M, Dell'Acqua F, Thiebaut de Schotten M. 2013)[304].

e. Atlas 10, 11, 12 and 13

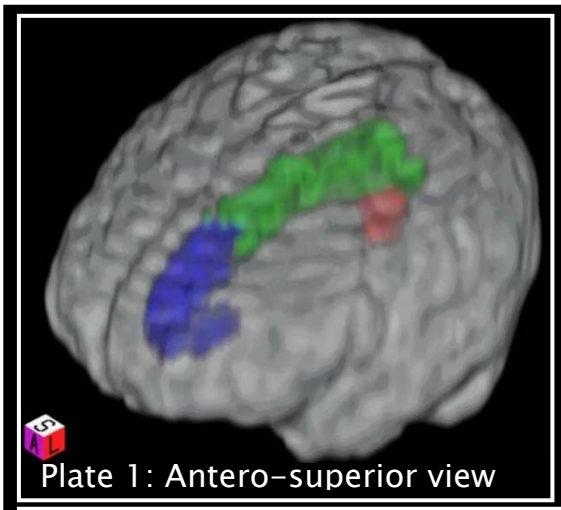
Plate 1: Antero-superior view

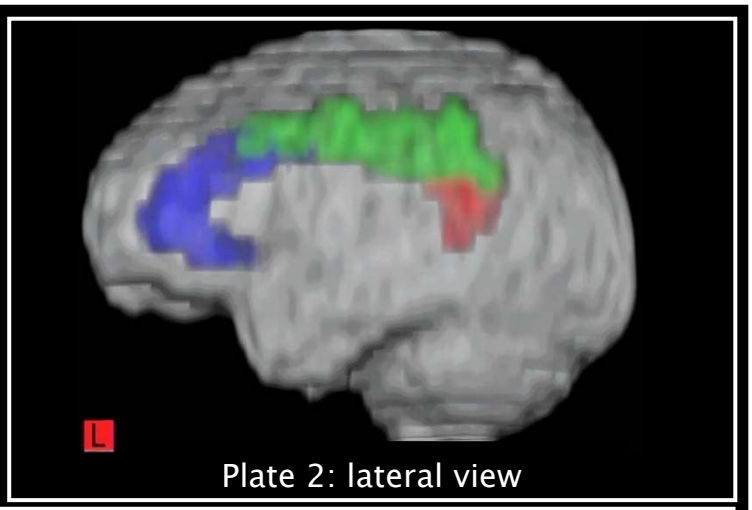
Plate 2: lateral view

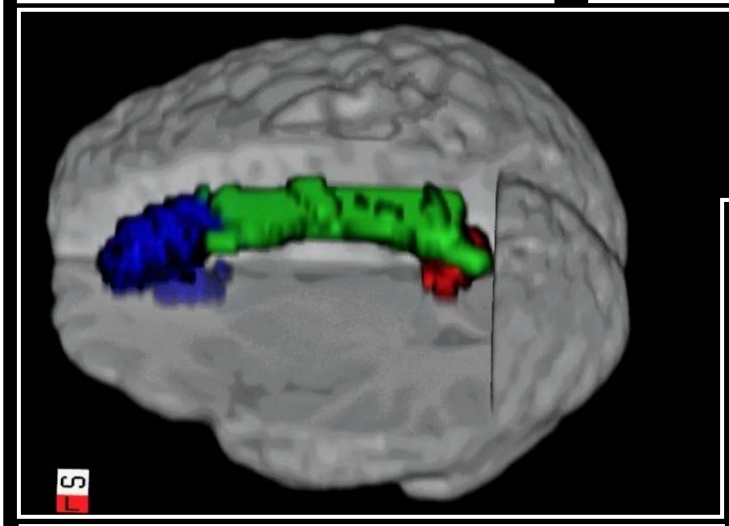
Plate 3: **Superolateral view, with a cutout of the regions surrounding our region of interest.**

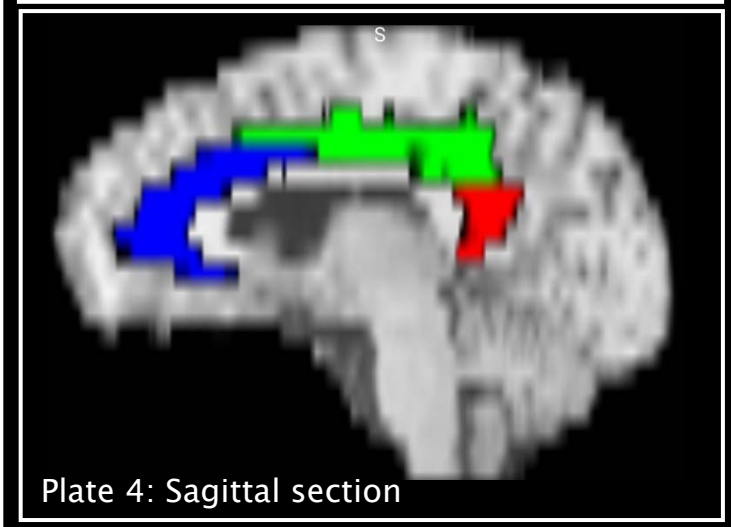
Plate 4: Sagittal section

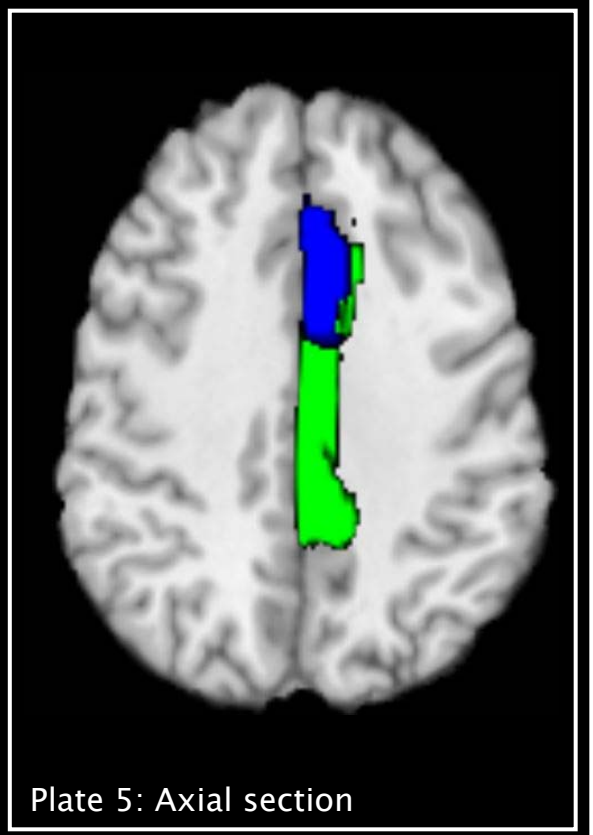
Plate 5: Axial section

Atlas 10: Different views and sections of the brain with overlaying of the cingulate gyrus.

*Orientation: A: Anterior - L: Lateral - S: Superior - I: Inferior

*The overlaying: The Left Cingulum Ant region.
The Left Cingulum Mid region. The Left Cingulum Post region

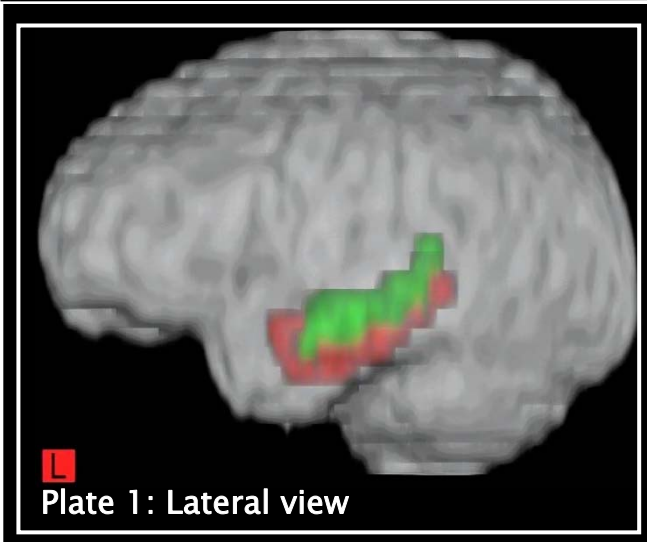

Plate 1: Lateral view

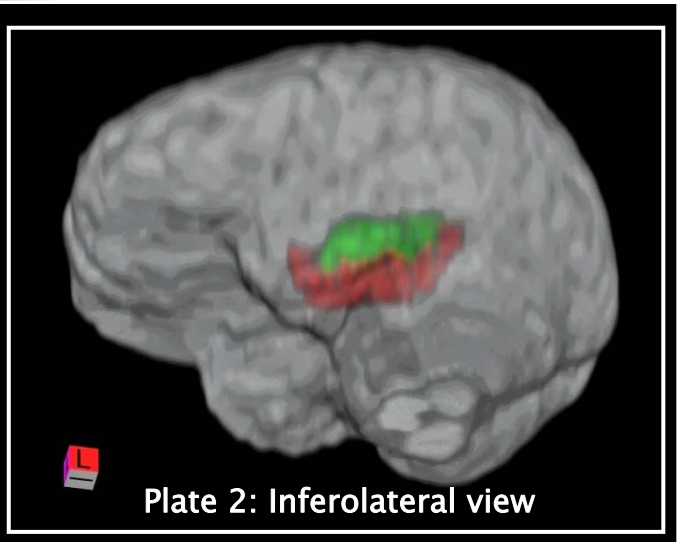

Plate 2: Inferolateral view

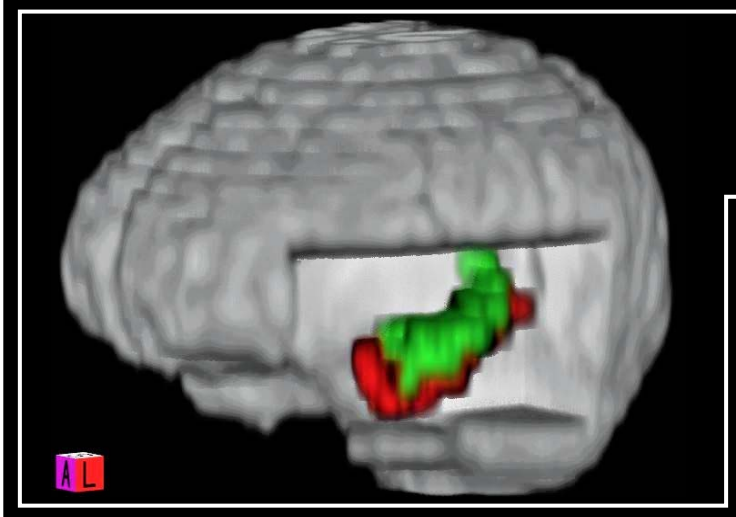

Plate 3: Anterolateral view, with a cutout of the regions surrounding our region of interest.

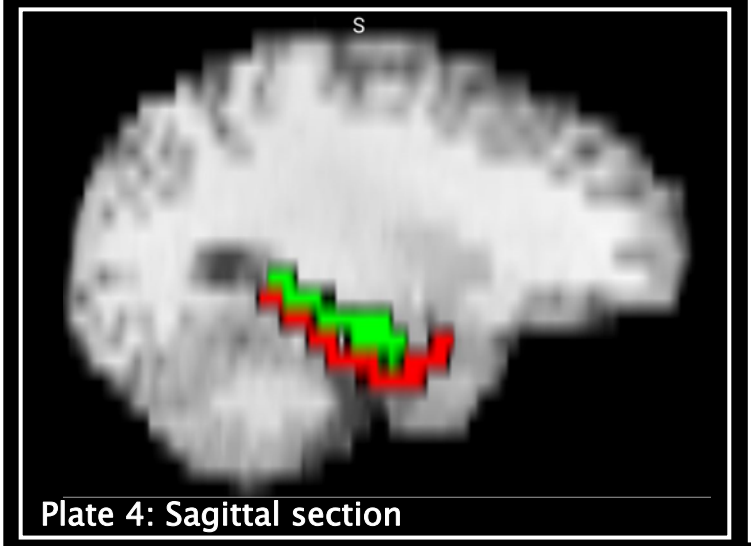

Plate 4: Sagittal section

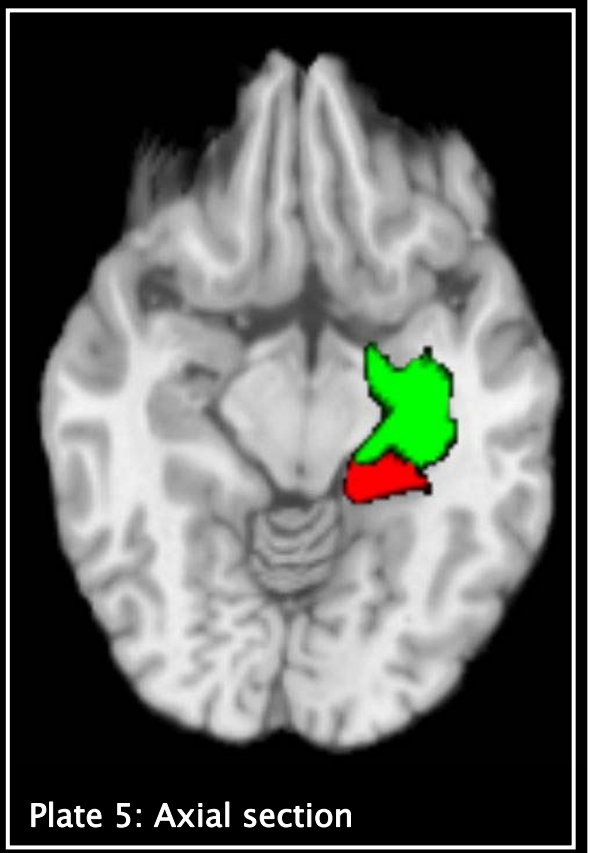

Plate 5: Axial section

Atlas 11: Different views and sections of the brain with overlaying of the ParaHippocampal and Hippocampus regions.

*Orientation: A: Anterior – L: Lateral – S: Superior – I: Inferior

*The overlaying: The Left ParaHippocampal region. The Left Hippocampus

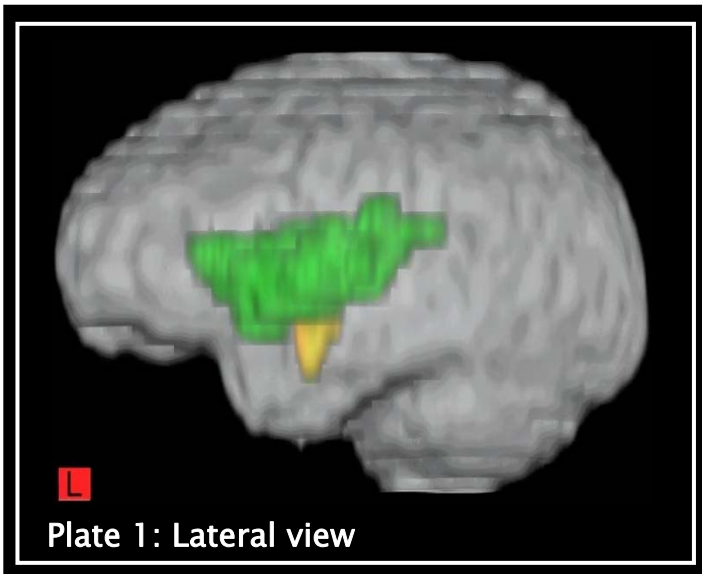

Plate 1: Lateral view

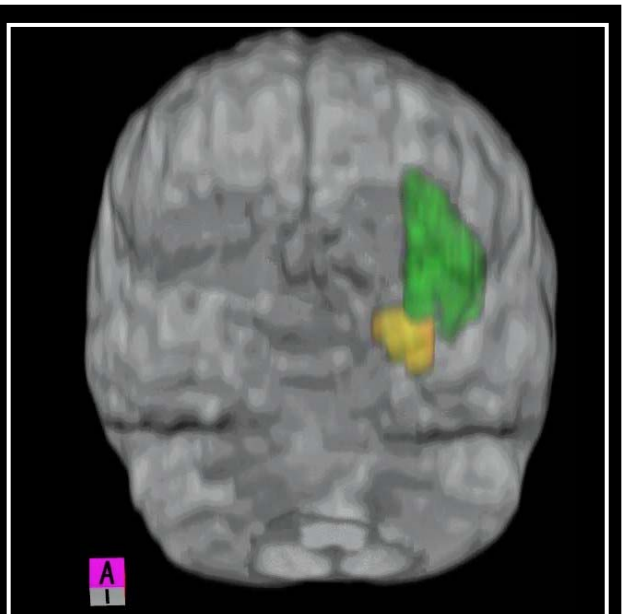

Plate 2: Anteroinferior view

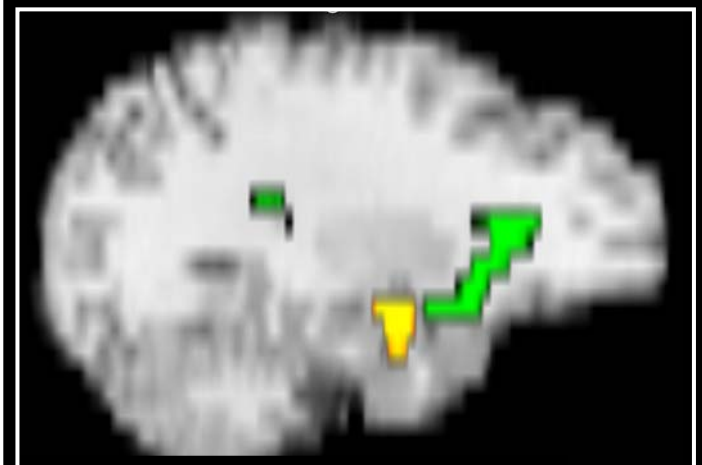

Plate 3: Sagittal section 1

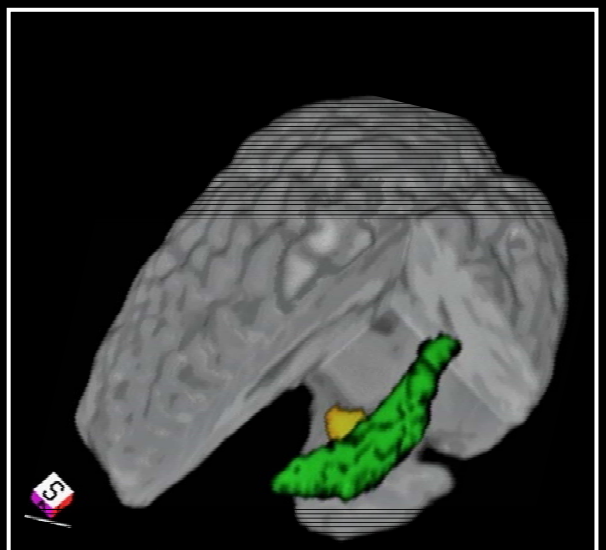

Plate 3: Superolateral view, with a cutout of the regions surrounding our region of interest.

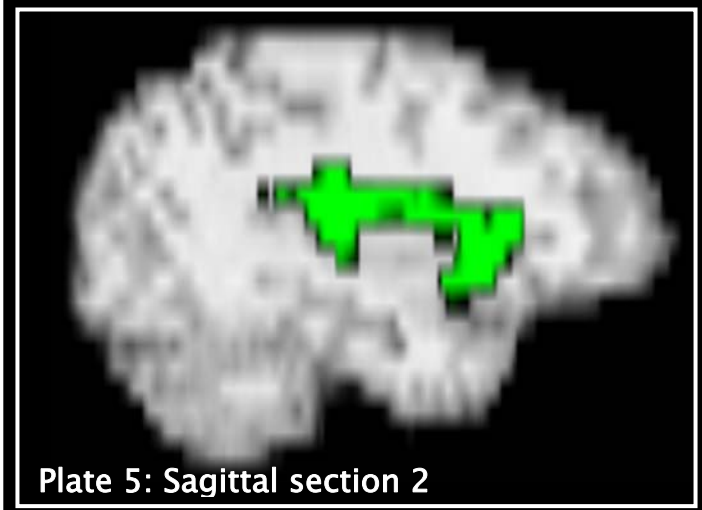

Plate 5: Sagittal section 2

Atlas 12: Different views and sections of the brain with overlaying of the Insula and Amygdala regions.

*Orientation: A: Anterior – L: Lateral – S: Superior – I: Inferior – P: Posterior

*The overlaying: The Left Insula. The Left Amygdala.

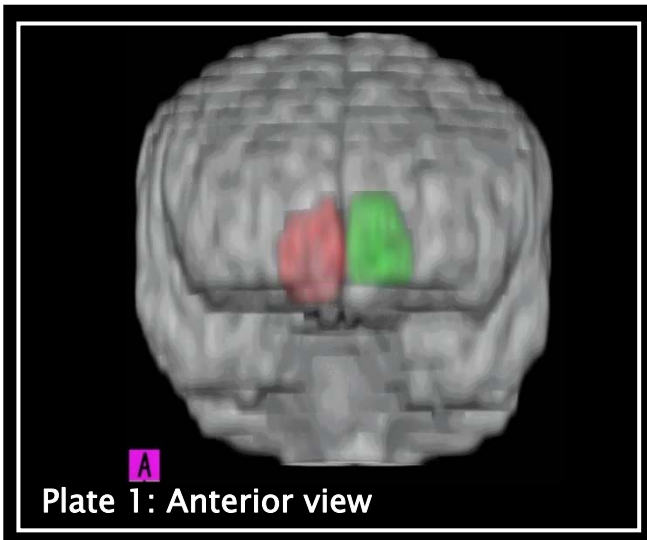

Plate 1: Anterior view

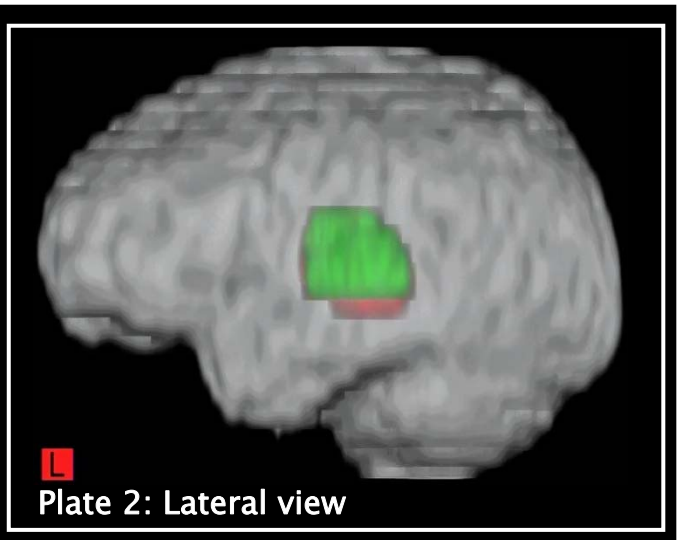

Plate 2: Lateral view

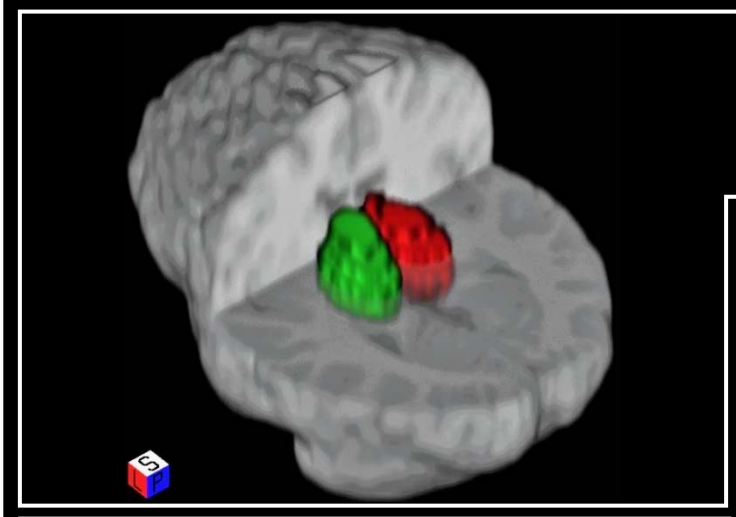

Plate 3: Posterosuperior view, with a cutout of the regions surrounding our region of interest.

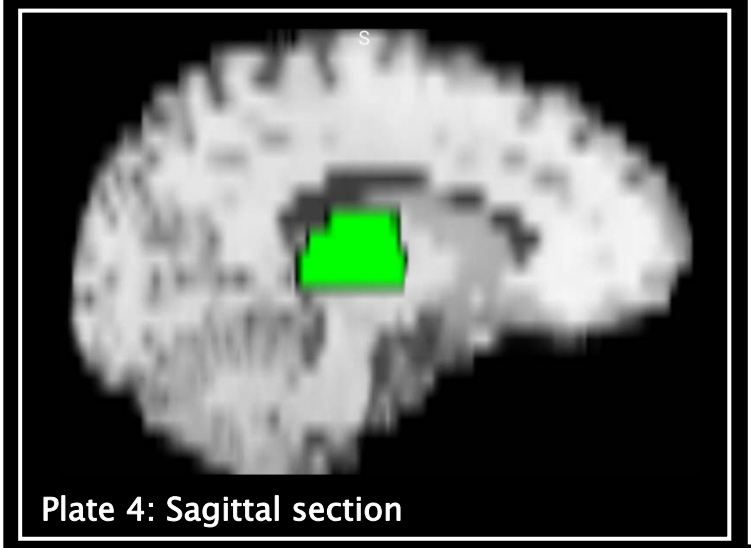

Plate 4: Sagittal section

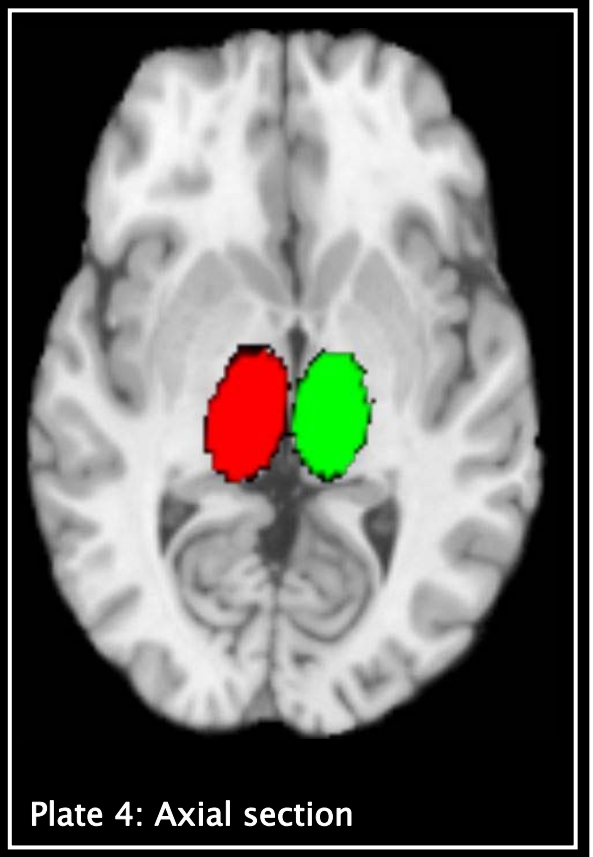

Plate 4: Axial section

Atlas 13: Different views and sections of the brain with overlaying of the left and right thalami.

*Orientation: A: Anterior – L: Left – S: Superior – I: Inferior

*The overlaying: The Left Thalamus The Right Thalamus

7. The basal ganglia

a. Introduction and functional physiology the basal ganglia

The Basal ganglia and related nuclei are made up of a variety of subcortical cell groups involved in motor control and a larger range of other activities such as motor learning, management functions, behaviour, and emotions[306307]. These highly specialized regions operate synergistically due to a high connection that is ensured across the brain by complex networks[306308].

The basal ganglia network may be seen as multifaceted loops and circuits of reentering, wherein motor, associative and limbic regions are primarily engaged in controlling movement, behaviour and emotions[306].

This functional and architectural organization will presumably be used differentially, for[306]:

-Goal-directed system: Selection and acceleration during execution and acquisition of new activities and tasks of prefrontal-striatal-pallidal activity.

-Habit system: Strengthened learning to automatically construct the usual motor circuit responses.

- Stopping the continuous activity and, if required, transitioning to a new one, largely controlled by the lower cortex / STNcortical network.

Consequently, anomalies in these areas' circuits lead to the development of parkinsonism and dyskinesia, obsessive-compulsive disorders and mood changes[306].

Detailed roles of each of the basal nuclei explored in our work are listed in the table 10.

Table 10: Roles of each of the basal nuclei explored in our work.

Subcortical nuclei	Functions
Caudate nucleus (CN).	-Cognitive control : memory regulation and other executive functions, as well as emotional regulation[309]. -The processing of visual-spatial informations and the coordination of movements[309]. -Associative learning, cognitive flexibility, and the execution of complex and oriented behaviors[310].
Putamen (Put).	Learning, motor control, language and speech articulation, motivation, the development of addictive behaviors, and cognition are all linked to putamen[311].
Accumbens nucleus (Acb).	Plays a role in motivation, aversion, reward processing, and the formation of impulsive behaviors which is why it's linked to addiction and dependence[312 313 314 315 316]. It also has a role in the development of pleasant emotions, as opposed to negative emotions, which are mediated by the amygdala[317].
Globus pallidus	Conscious and proprioceptive movement control via thalamic activity regulation[318]. The management and optimization of motivation as well as the processing of salient stimuli, performed by selecting and precisely encoding stimuli with incentive and/or hedonic value[319].

b. The components and neuroanatomy of the basal ganglia

The basal ganglia and related nuclei are commonly classified anatomo-functionally as follows[306] (Table 11):

-**Input nuclei**: Structures that receive information from several sources, primarily cortical, thalamic, and nigral in origin.

-**Output nuclei**: Structures that relay information from the basal ganglia to the thalamus.

-**Intrinsic nuclei**: Structures in the relay of information between the input and output nuclei.

Table 11: Categorization of the basal ganglia into input, output and intrinsic nuclei.

Input nuclei	Output nuclei	Intrinsic nuclei
-Striatum : *Caudate nucleus (CN). *Putamen (Put). *Accumbens nucleus (Acb).	-The internal segment of the globus pallidus (GPi) -The substantia nigra pars reticulata (SNr).	-The external segment of the globus pallidus (GPe). -The subthalamic nucleus (STN). -The substantia nigra pars compacta (SNc).

c. Connectivity of the basal ganglia

In the '80s, the first concept of basal ganglia functional organization and connectivity was drawn up based on the concept that neural signals from cortex flow to the striatum via the global pallidus and the substatia Nigra pars reticulata, project back to the cortex via the thalamus, generating parallel cortico-basal ganglia-thalamocortical loops[320 308].

Below, in figure 9, a synthesis of the initial basal ganglia model.

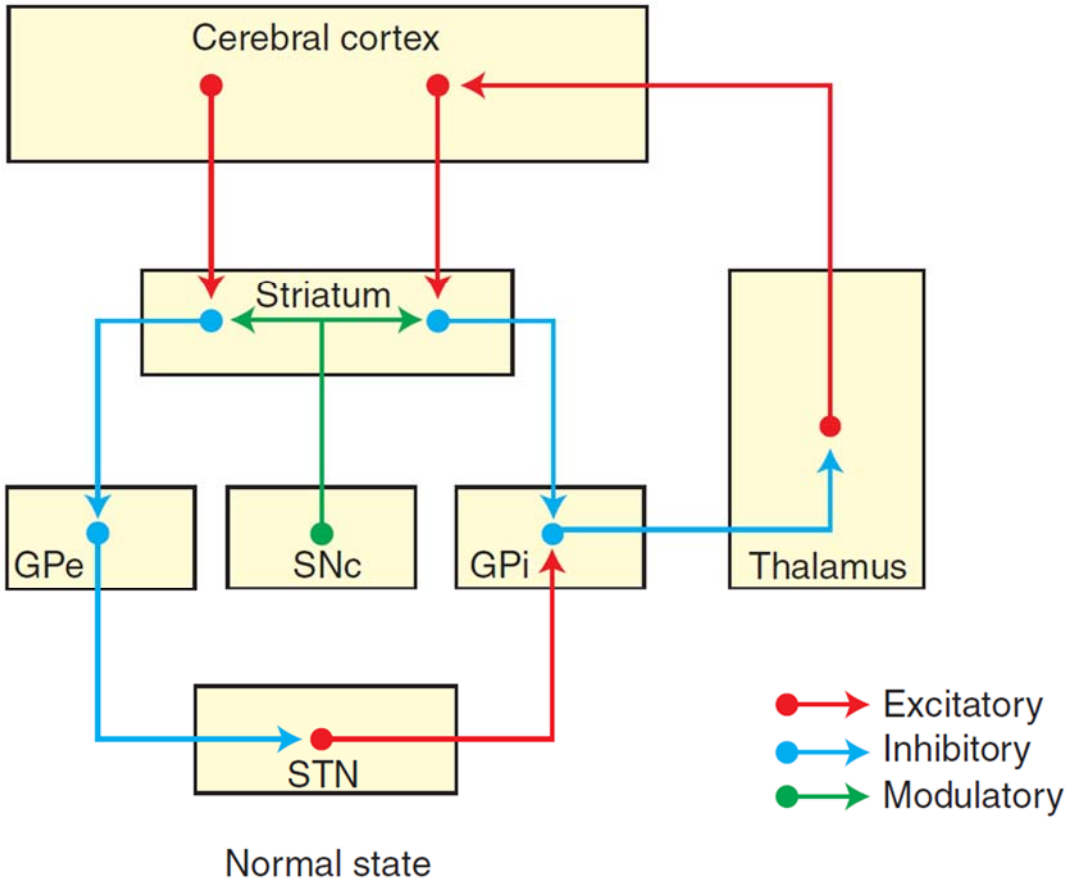

Figure 40: Schematic summary of the first basal ganglia model.

(Du J, Rolls ET, Cheng W, et al. 2020)[250]

In Figure 40, we can see how the motors circuit consists of a corticostriatal (putaminal) projection, two main striatofugal, resulting in direct and indirect pathways, and the effectual pallido-thalamic-cortical projections to complete the motor loop.

As a result, of the original functional organization, basal ganglia was included as a "go on" station inside the motor loop.

This functional model has been modified by current understanding on various fronts and in significant ways. The basal ganglia are now recognized to include multiple loops where cortical and subcortical projections interact with internal reentry loops (Figure 41), producing a complex network, perfectly adapted for choosing and suppressing concurrently occurring events and signals[306].

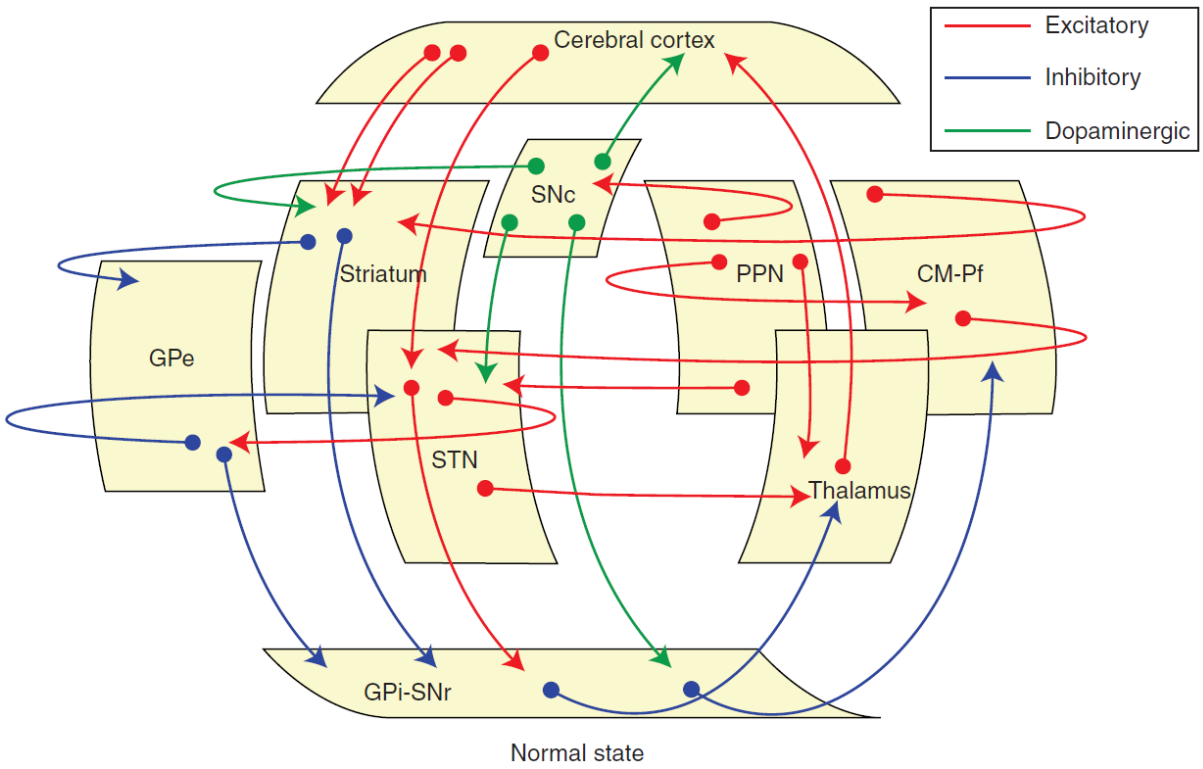

Figure 41: Updated Basal ganglia circuits.

(Du J, Rolls ET, Cheng W, et al. 2020)[250]

Figure 10 shows several transverse loops that have been identified in recent years, the majority of which have a potential modulatory effect.

Therefore, the role of the basal ganglia is to engage in complex circuits with strong connections to various parts of the cerebral cortex, from which they gather information and re-send through the output nuclei, Thalamus and Substantia Nigra, following local processing.

- **Functional summary**

The role of the basal ganglia is to engage in complex circuits with strong connections to various parts of the cerebral cortex, from which they gather information and re-send through the output nuclei, Thalamus and Substantia Nigra, following local processing[308].

This role is ensured by controlling the balance of inhibitory and excitatory effects by suppressing signals that do not serve in the reference or interfere, resulting in an efficient and powerful final result[308]. This concept applies to the motor function and can be adapted to cognitive, relational and emotional processes. The fundamental purpose of the BG is to adjust the equilibrium to attain a harmonic and smooth behavior[308].

Before projecting back to their cerebral origins, highly-segregated circuits process input from distinct cortical areas; as a result, each loop seems to perform different behavioural roles[321].

e. Atlas 14 and 15

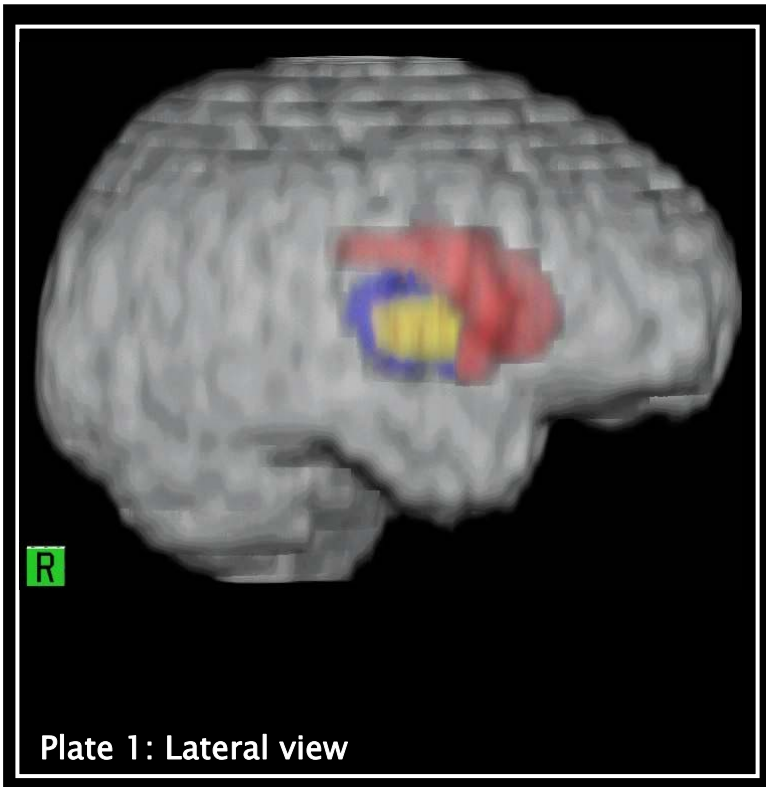

Plate 1: Lateral view

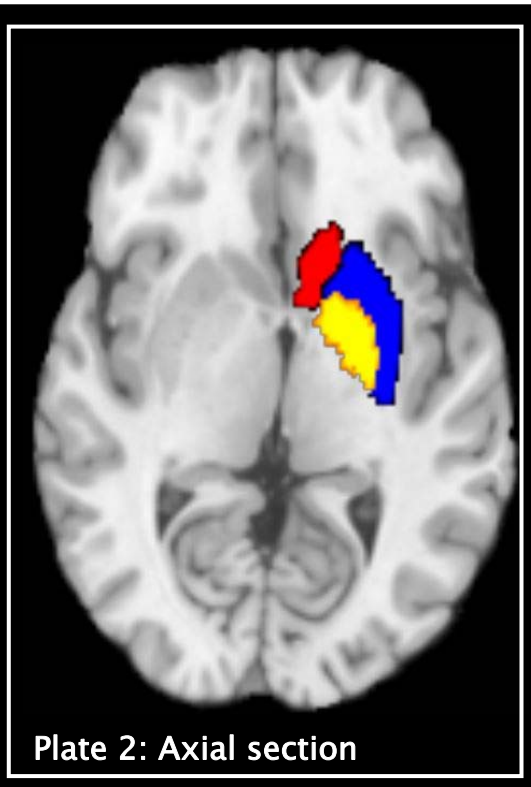

Plate 2: Axial section

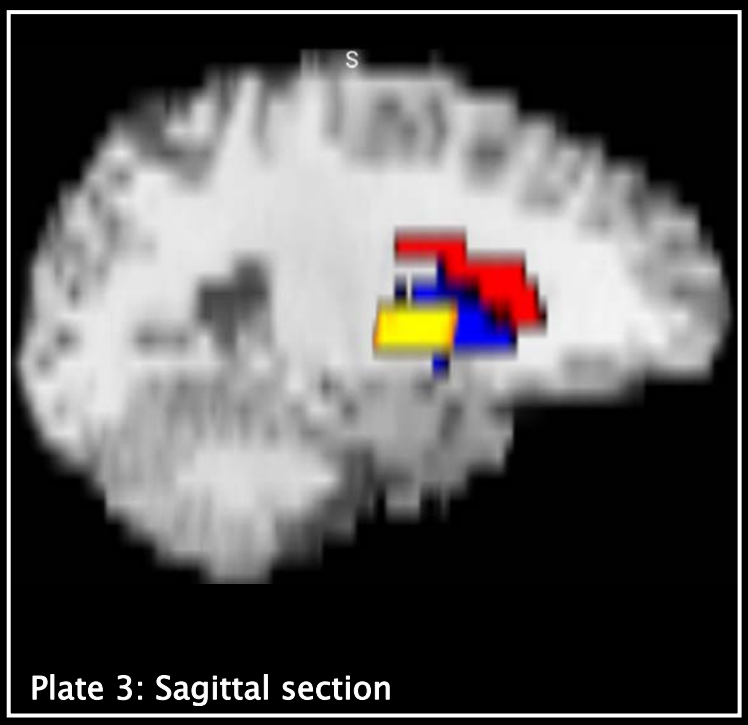

Plate 3: Sagittal section

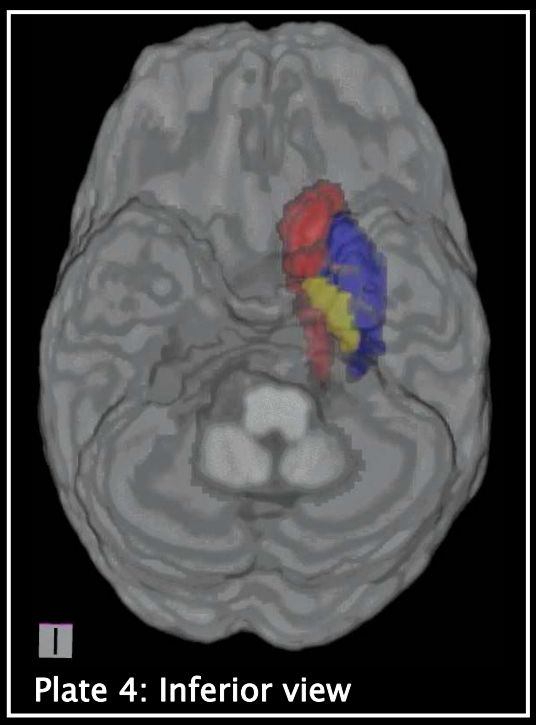

Plate 4: Inferior view

Atlas 14: Different views and sections of the brain with overlaying of the caudate, putamen and pallidum nuclei.

*Orientation: A: Anterior – L: Left – S: Superior – I: Inferior

*The overlaying: The Left caudate nucleus, The Left Putamen nucleus, The left pallidum nucleus .

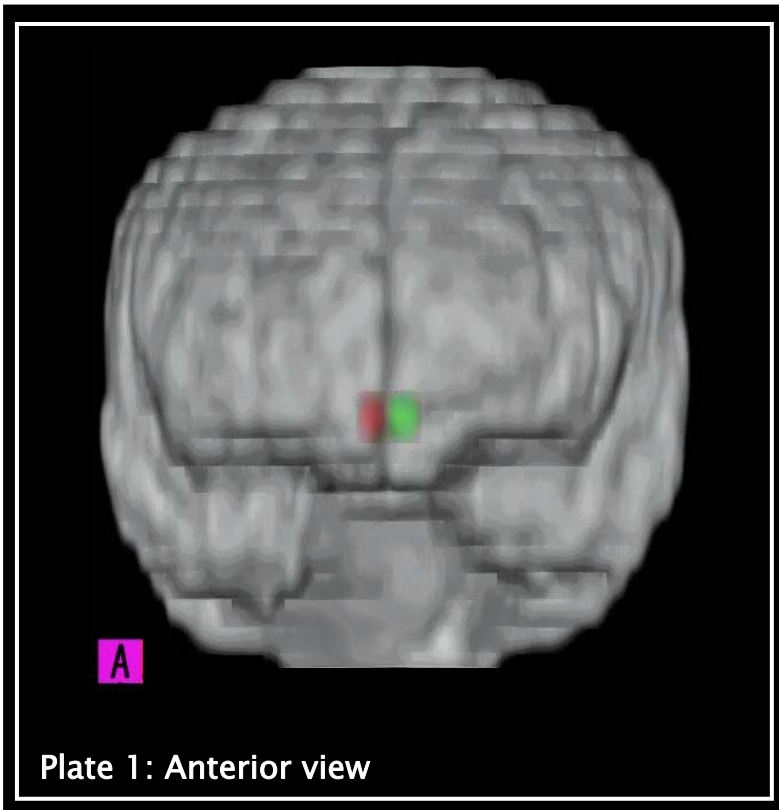

Plate 1: Anterior view

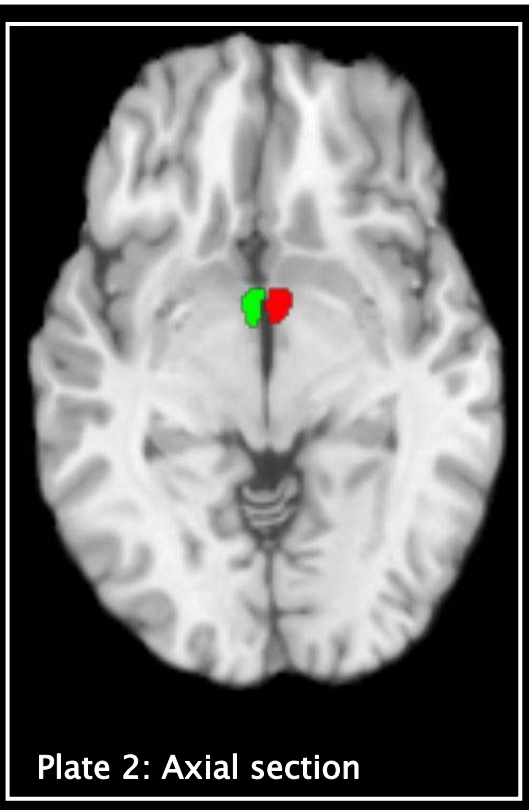

Plate 2: Axial section

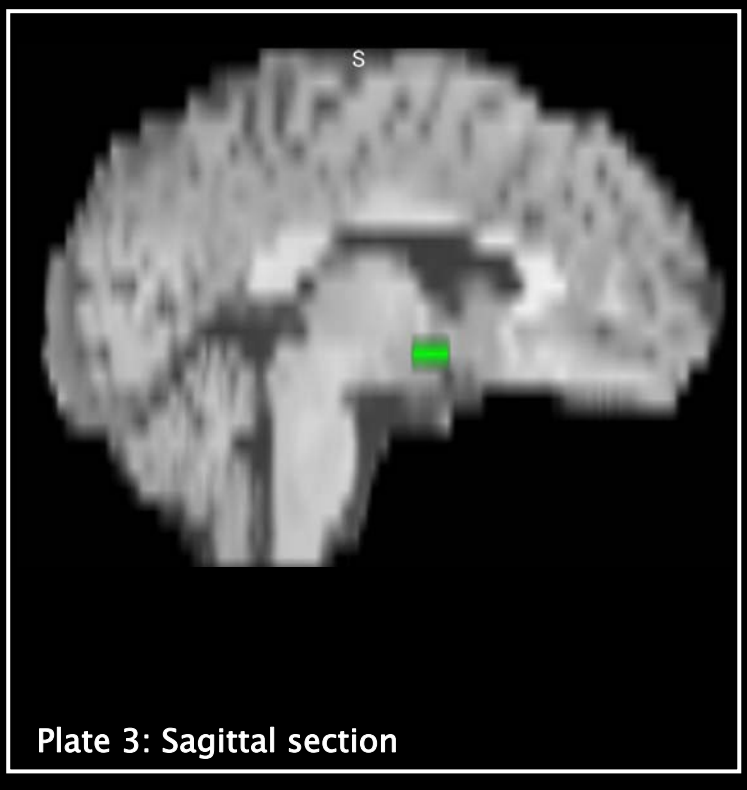

Plate 3: Sagittal section

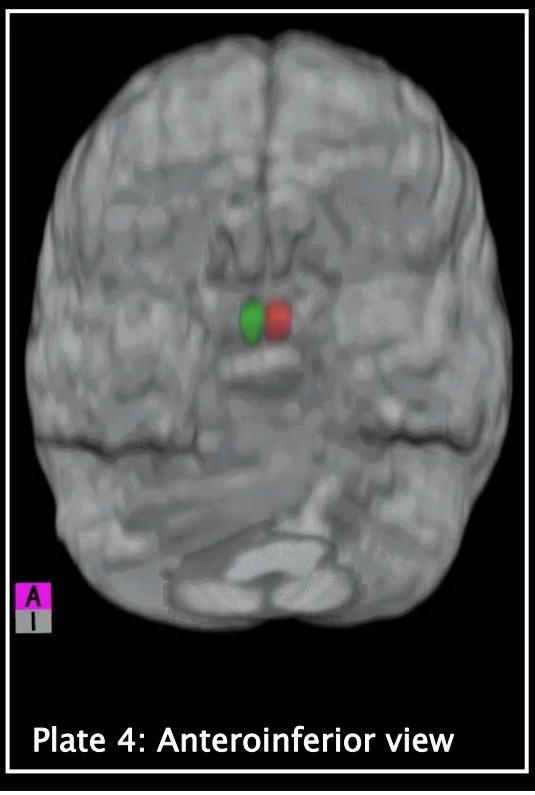

Plate 4: Anteroinferior view

Atlas 15: Different views and sections of the brain with overlaying of the left and right Accumbens nuclei.

*Orientation: A: Anterior – L: Left – S: Superior – I: Inferior

*The overlaying: Left Nucleus Accumbens. Right Nucleus Accumbens.

Results

In the results section, we will present results of:

-Cannabis use disorder levels and psychological functioning stats.

-Qualitative data of the diffusion tensor imaging.

-Diffusion tensor imaging findings (FA and MD) in the grey matter -ROI-.

-Diffusion tensor imaging findings (FA and MD) in white matter -Tractography-.

-Correlations results between cannabis use disorder, psychological functioning findings, and tractography findings.

Reminding that we have the same groups distribution throughout all the study:

- Group I: Heavy cannabis users.
- Group II: Light cannabis users.
- Group III: Healthy controls.

We note that each chapter of II, III, and IV regroup its descriptive and analytic statistics.

Chapter I: Results of Cannabis use disorder and psychological functioning assessment

I. Descriptive statistics

The results of cannabis use disorder levels, impulsivity trait and perceived stress states assessment will be presented with individual value graph and boxplot illustration for each test. In addition to that, following the two illustrations, our findings will be, each time, more detailed in a paragraph.

As we hypothesised, our assessment results showed higher CUD levels in heavy consumers than light smokers. Heavy users scored higher than light and healthy controls in the BIS-11 and PSS also.

Regarding light users, they differ from healthy controls in CUDIT-R scoring (since our healthy controls are naïve individuals) and the perceived stress scale. Conversely, light users and healthy controls had an equivalent range on the Barratt Impulsiveness Scale scores.

ANOVA is used to determine the statistical significance of these findings. Our analytic results will be presented in the next section of this part.

1. The Cannabis Use Disorder Identification Test-Revised (CUDIT-R)

Results of the CUDIT-R test in cannabis users (heavy and light groups) and healthy controls are summarised in the figures below, which contains two types of graphs (individual values and boxplot illustration).

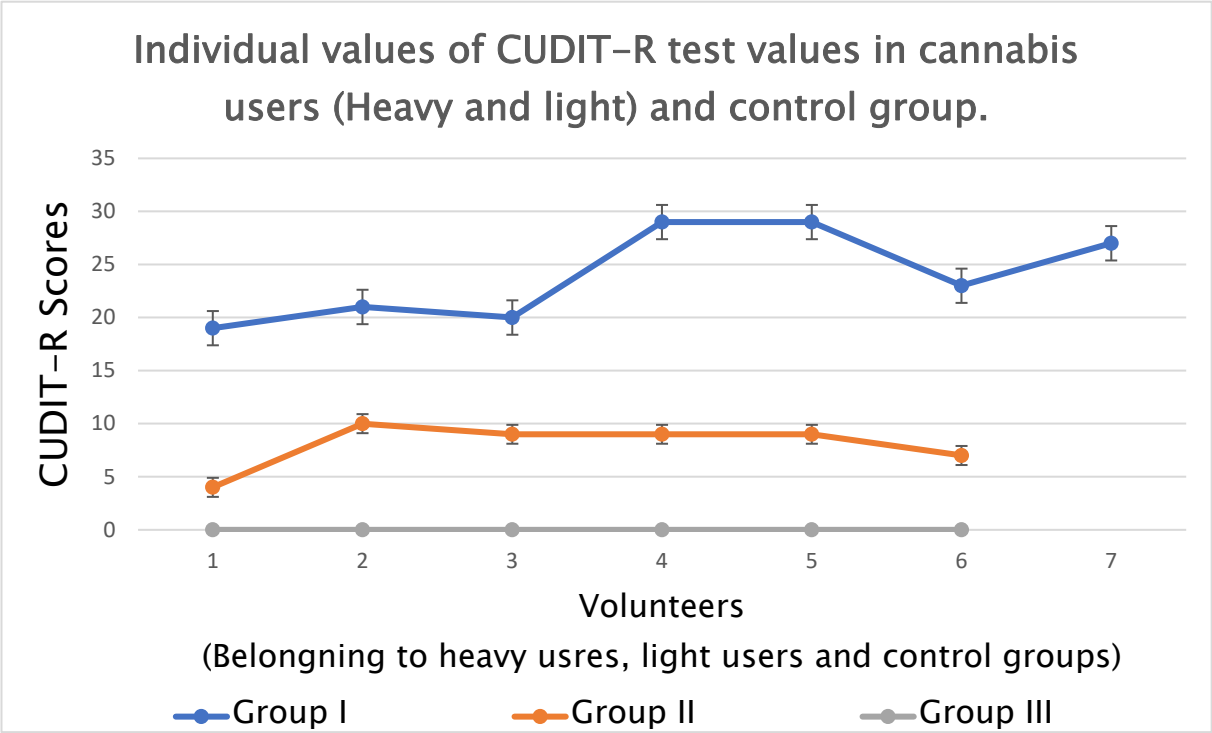

Figure 42: This figure shows individual values of the Cannabis Use Disorder Identification Test-Revised (CUDIT-R) in heavy cannabis users (Group I), light cannabis users (Group II), and healthy controls (Group III). Scores of CUDIT-R are sorted in graph individual (X, Y) points and lines in heavy cannabis users (Group I), light cannabis users (Groupe II), and healthy controls group (Group III). In the "X" horizontal line, we have the numbers of voluntary participants, and in the "Y" vertical line, we have scores of the CUDIT-R test.

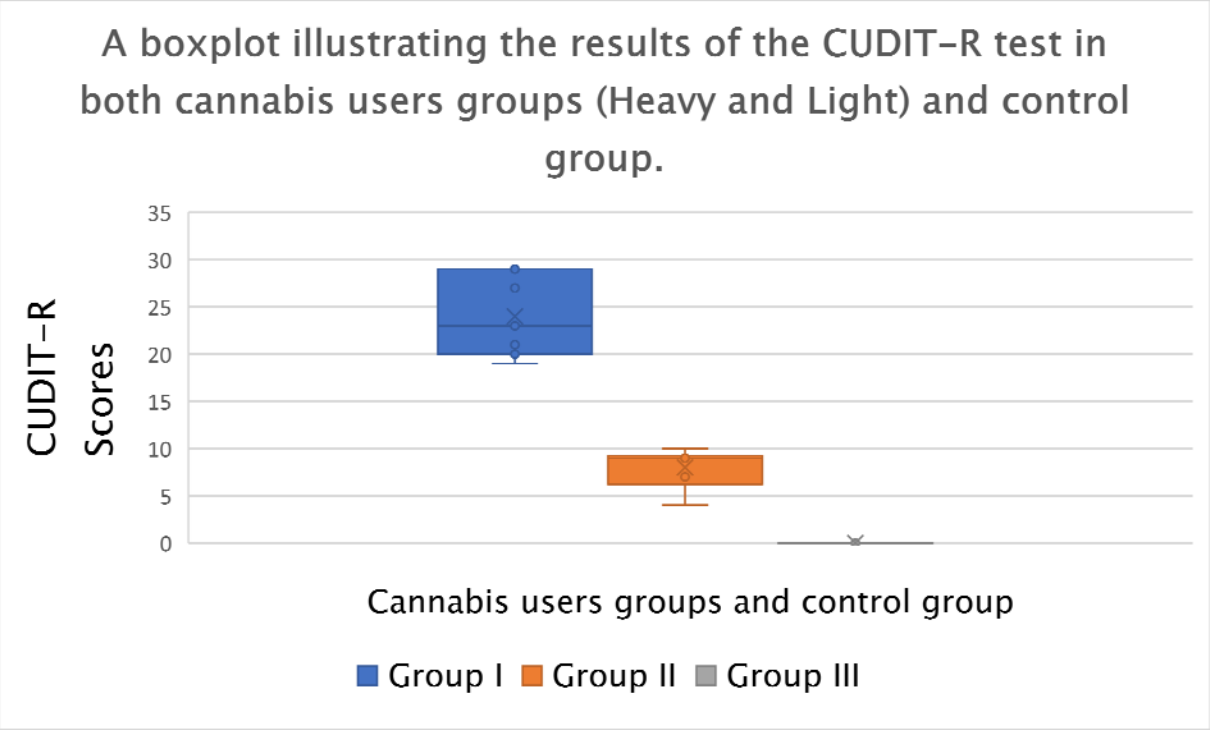

Figure 43: A boxplot that represents, in the cannabis users (heavy cannabis users and light cannabis users) groups and healthy controls group the degree of dispersion, the average, and the standard deviation of the Cannabis Use Disorder Identification Test-Revised (CUDIT-R) results.

From the results presented in the figures above, we can easily deduce that heavy cannabis users have much higher CUDIT-R test scores than light cannabis users. The standard deviations of heavy and light users groups are also very far apart. Concerning healthy controls participants, since none of our healthy controls volunteers has ever used cannabis or any of its derivatives, they all get a score of 0.

2. The Barratt Impulsiveness Scale (BIS):

Results of the BIS-11 test in cannabis users (heavy and light groups) and healthy controls are summarised in the figures below, which contains two types of graphs (individual values and boxplot illustration).

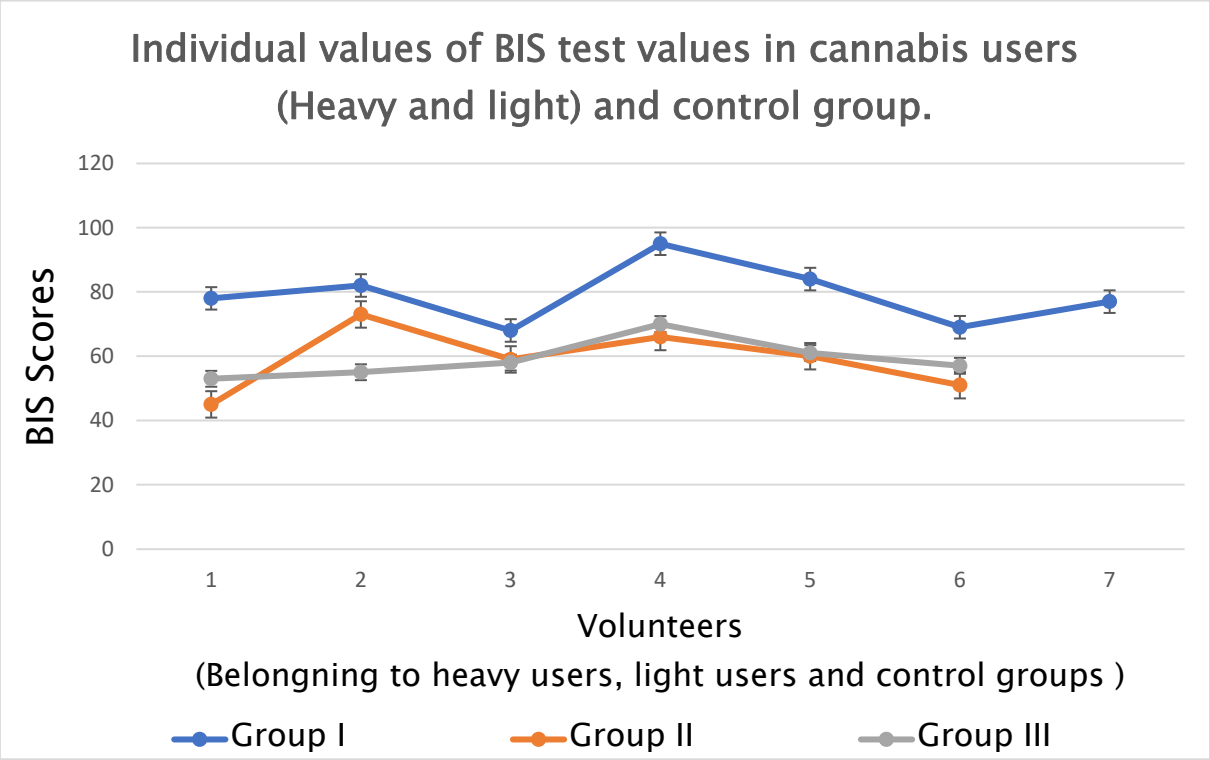

Figure 44: This figure shows individual values of the total score of the Barratt Impulsiveness Scale (BIS-11) in heavy cannabis users (Group I), light cannabis users (Group II), and healthy controls. The total scores of BIS-11 are sorted in graph individual (X, Y) points and lines in heavy cannabis users (Group I), light cannabis users (Group II), and healthy control (Group III). In the "X" horizontal line, we have the numbers of voluntary participants, and in the "Y" vertical line, we have scores of the BIS-11 test.

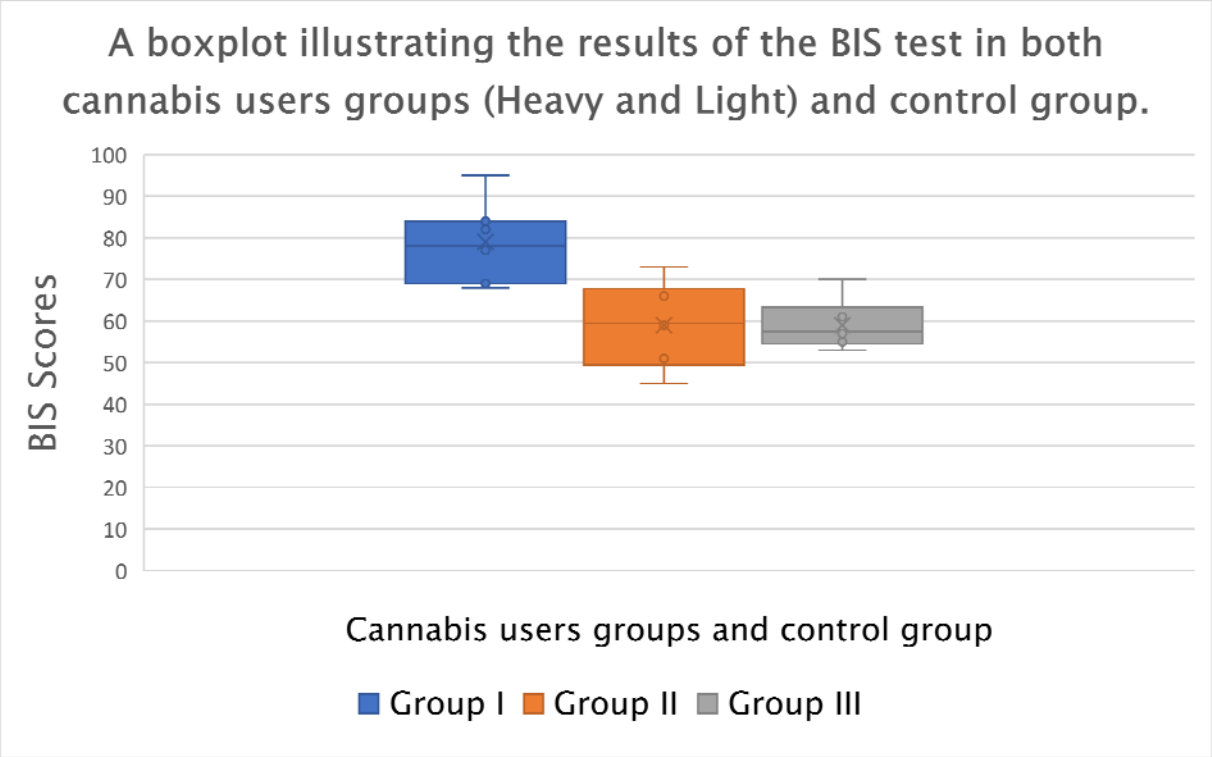

Figure 45: A boxplot that represents, in the cannabis users (heavy cannabis users and light cannabis users) groups and healthy controls group the degree of dispersion, the average, and the standard deviation of the Barratt Impulsiveness Scale (BIS-11) results.

The results presented in the figures above show that heavy cannabis users have a much higher average of the total score of BIS-11 than the light users group and healthy control group. However, the averages of both groups (light users group and healthy controls group) are pretty close, and the healthy control group's standard deviation is within the standard deviation of the light cannabis users group.

3. The Perceived Stress Scale (PSS)

Results of the PSS test in cannabis users (heavy and light groups) and healthy controls are summarised in the figures below, which contains two types of graphs (individual values and boxplot illustration).

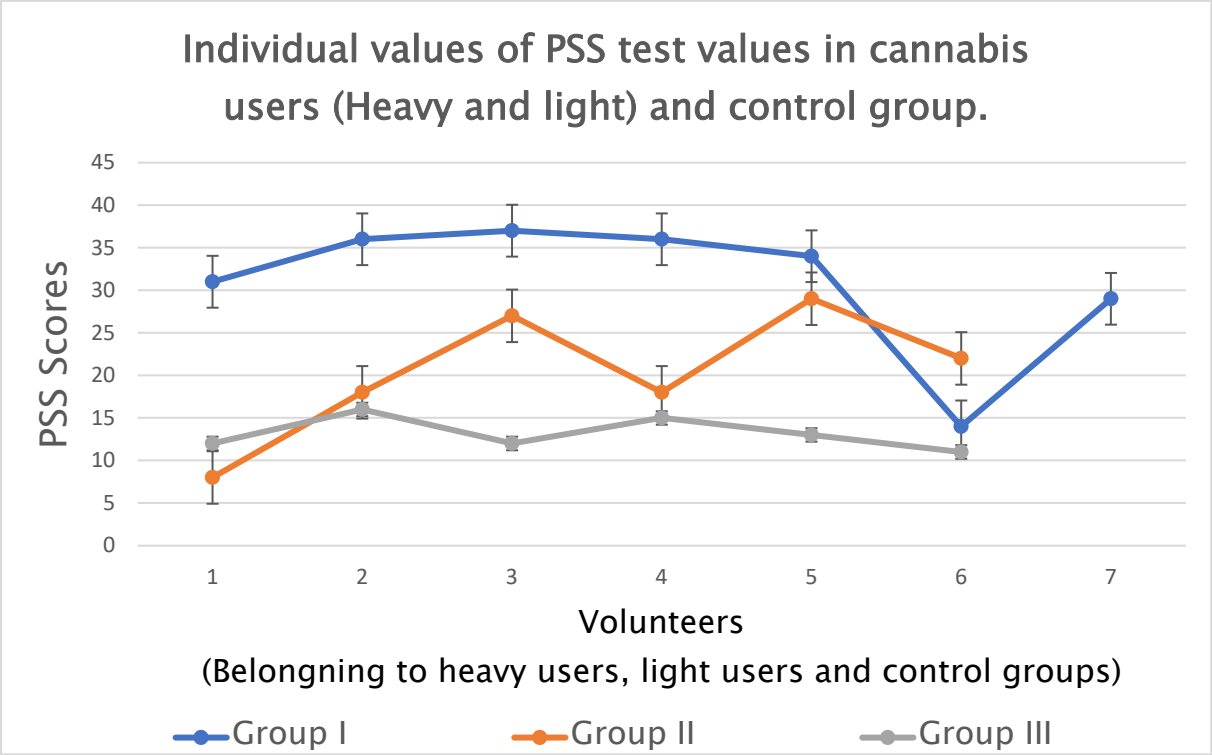

Figure 46: This figure shows individual values The Perceived Stress Scale (PSS) in heavy cannabis users (Group I), light cannabis users (Group II), and healthy controls (Group III). Scores of PSS are sorted in graph individual (X, Y) points and lines in heavy cannabis users (Group I), light cannabis users (Groupe II), and healthy controls group (Group III). In the "X" horizontal line, we have the numbers of voluntary participants, and in the "Y" vertical line, we have scores of the PSS test.

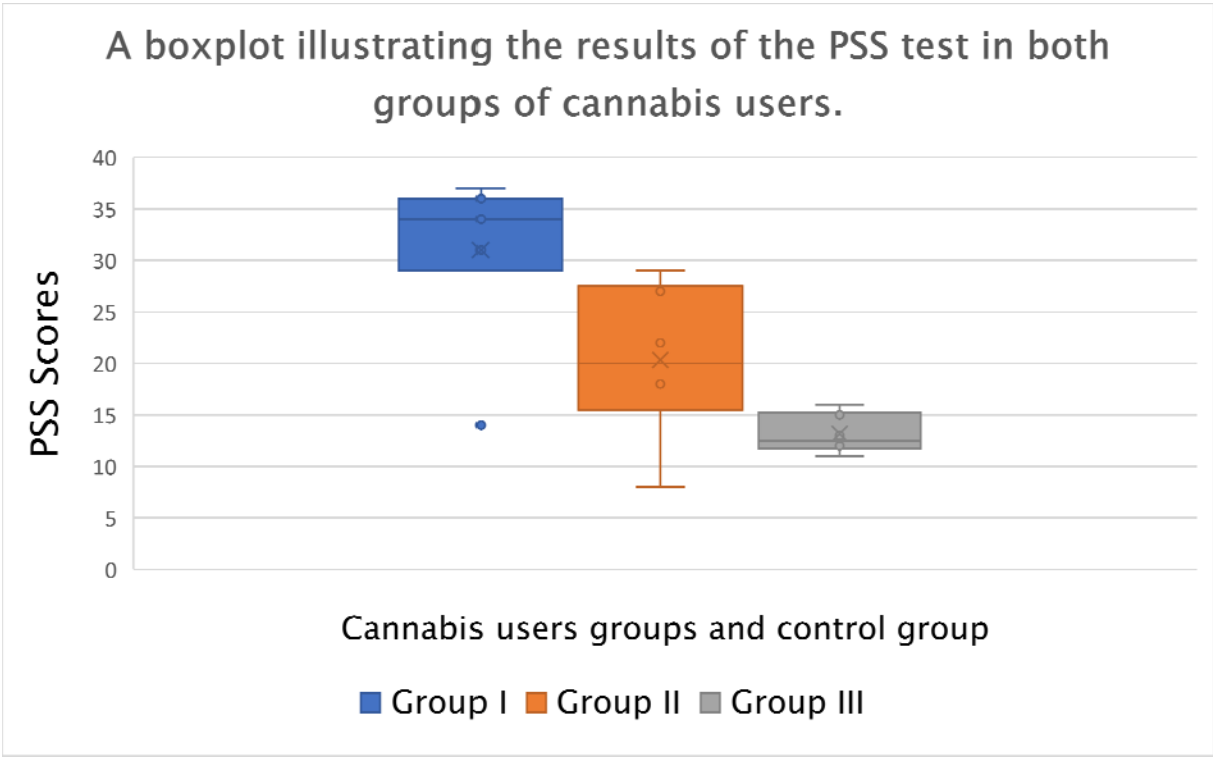

Figure 47: A boxplot that represents, in the cannabis users (heavy cannabis users and light cannabis users) groups and healthy controls group the degree of dispersion, the average, and the standard deviation of The Perceived Stress Scale (PSS) results.

The results presented in the figures above show that heavy cannabis users have a much higher average of PSS scores than the light users group and healthy control group, except one participant that has a score within the standard deviation of light users and healthy control groups. Scores of the light users and healthy control groups are also different in terms of average, which is much lower in healthy controls than light users. Regarding standard deviation, it is larger in the light users' group since one (and only one) volunteer belonging to this group has a score lower than the healthy control group.

II. Analytical results

1. Analysis of Variance (ANOVA)

➢ **The Cannabis Use Disorder Identification Test-Revised (CUDIT-R)**

The ANOVA statistical analysis consists of multiple comparisons of CUDIT-R scores of users groups and non-users groups (I, II, and III), namely pairs of groups (Group I versus Group II), (Group I versus Group III), (Group II versus Group III). The found P-values are reported in the table () below.

	CUDIT-R's P-Value of the analysis of variance (ANOVA) between heavy (Group I) and light (Group II) users' groups		
	Heavy users (Group I)	Light users (Group II)	Non-users (Group III)
Heavy users (Group I)	○	**	**
Light users (Group II)	4.9274 E-06	○	**
Non-users (Group III)	3.0823 E-08	4.3755 E-06	○

Table 12: The statistical analysis results of the Cannabis Use Disorder Identification Test-Revised (CUDIT-R) of heavy cannabis users, light users, and non-users.

ANOVA was conducted in the quantitative analysis to evaluate the levels of significance. Hence with a P-value lower than 0.05, the ANOVA analysis revealed significant differences between all the three groups.

➢ **The Barratt Impulsiveness Scale (BIS-11):**

The ANOVA statistical analysis consists of multiple comparisons of BIS-11 scores of users and non-users groups (I, II, and III), namely pairs of groups (Group I versus Group II), (Group I versus Group III), (Group II versus Group III). The found P-values are reported in the table () below.

	BIS-11's P-Value of the analysis of variance (ANOVA) between heavy (Group I) and light (Group II) users' groups		
	Heavy users (Group I)	Light users (Group II)	Non-users (Group III)
Heavy users (Group I)	○	**	**
Light users (Group II)	0.00332	○	**
Non-users (Group III)	0.000882	1	○

Table 13: The statistical analysis results of the Barratt Impulsiveness Scale (BIS-11) of heavy cannabis users, light users, and non-users. ANOVA was conducted in the quantitative analysis to evaluate the levels of significance. Thus with a P-value lower than 0.05, the ANOVA analysis revealed significant differences of heavy users with non-users and light users groups.

➢ **The Perceived Stress Scale (PSS) :**

The ANOVA statistical analysis consists of multiple comparisons of PSS scores of users and non-users groups (I, II, and III), namely pairs of groups (Group I versus Group II), (Group I versus Group III), (Group II versus Group III). The found P-values are reported in the table () below.

	PSS's P-Value of the analysis of variance (ANOVA) between heavy (Group I) and light (Group II) users' groups		
	Heavy users (Group I)	Light users (Group II)	Non-users (Group III)
Heavy users (Group I)	○	**	**
Light users (Group II)	0.032215	○	**
Non users (Group III)	0.000264	0.048121	○

Table 14: The statistical analysis of the Perceived Stress Scale (PSS) results of heavy cannabis users, light users, and non-users. ANOVA was conducted in the quantitative analysis to evaluate the levels of significance. Hence with a P-value lower than 0.05, the ANOVA analysis revealed significant differences between all the three groups.

2. Sensitivity/specificity: ROC curve (receiver operating characteristic)

The ROC curve was used to statistically determine and compare the screening test's performance (CUDIT-R) in establishing a distinction between the two groups (heavy and light consumers) based on the criteria of cannabis use disorder.

The results reported in the figure below shows that the test has high sensitivity and specificity since the curve is located at the top and left and has the highest effectiveness with AUC =1 and P <0.0027.

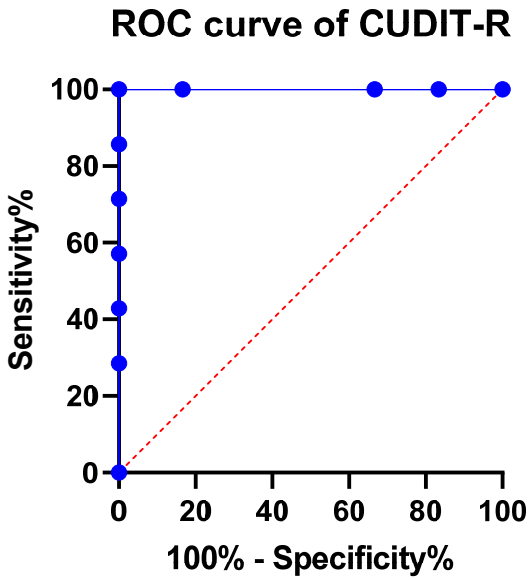

The area under the ROC curve	
Area	1,000
Std. Error	0,000
95% confidence interval	1,000 to 1,000
P value	0,0027
Data	
Controls (Light users)	6
Patients (Heavy users)	7
Missing Controls	0
Missing Patients	0

Figure 48: illustrates the ROC curve of CUDIT-R with AUC = 1 and P <0.0027.

3. Correlation analysis of tests values with the age of onset, duration of use, and degree of consumption (Pearson's correlation coefficient)

Correlations are the concept of a link between two entities that conflict with their independence. Our study correlates psychometric tests outcomes with several consumption parameters: age of onset, duration of use (in years), and degree of consumption (number of joints smoked per week) of our cannabis users volunteers.

Using correlation analysis, we tested the hypothesis that neuropathological alteration varies depending on many consumption parameters (dosage, frequency, duration of exposure, age of onset.)[322].

We have successfully tested the validity of this hypothesis. Our correlation results revealed:

-A solid positive and significant association of the duration of consumption with the three psychometric tests. This association was more solid with cannabis use disorder levels (56.52% of the variation in the duration of consumption values varies depending on the CUDIT-R values and vice versa).

-The number of joints smoked per week was positively and strongly associated (60.47%) with impulsivity trait (BIS-11). The perceived stress was also correlated positively with this parameter; however, without a statistical significance (p-value=0.0619).

-Concerning the age of onset, which is a debated critical parameter, our analyses revealed a significant and robust association, at this point negatively, with the level of cannabis use disorder and the degree of impulsivity trait. On the other hand, the perceived stress was correlated negatively as well but without a statistical significance.

The results of each analysed correlation will be displayed in a distinct scatterplot below with an accompanying table grouping the statistical data.

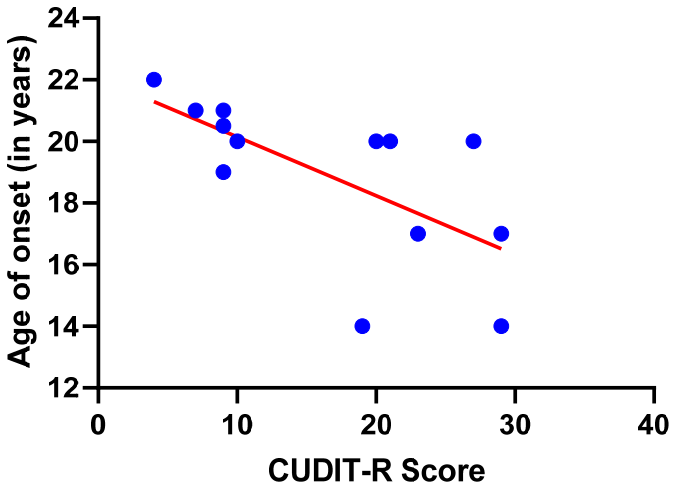

Age of onset Vs CUDIT-R	
Pearson r	
r	-0,6576
R squared	0,4325
P-value	
P (two-tailed)	0,0146
Significant? (alpha = 0.05)	Yes
Number of XY Pairs	13

Figure 49: Correlation scatterplots for CUD and age of onset.

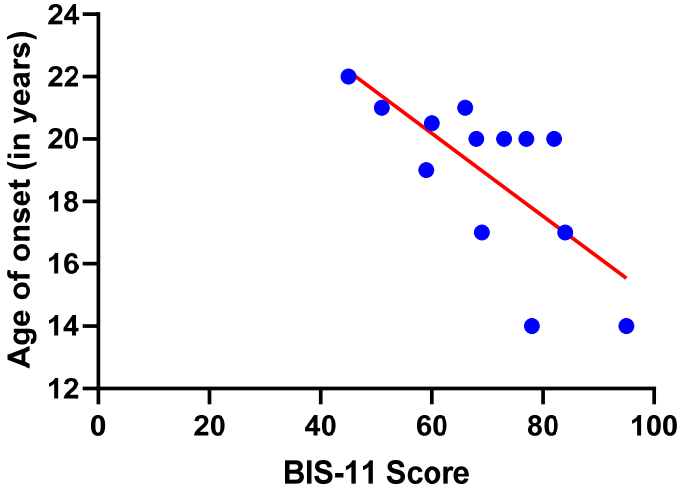

Age of onset Vs BIS-11	
Pearson r	
r	-0,7095
R squared	0,5034
P-value	
P (two-tailed)	0,0066
Significant? (alpha = 0.05)	Yes
Number of XY Pairs	13

Figure 50: Correlation scatterplots for impulsivity and age of onset.

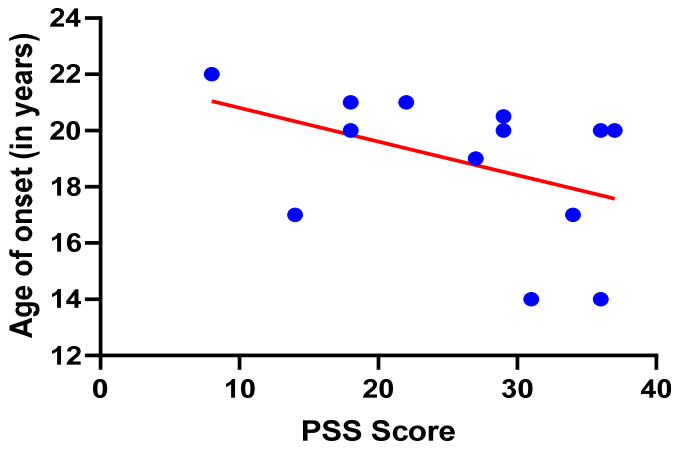

Age of onset Vs PSS	
Pearson r	
r	-0,4282
R squared	0,1833
P-value	
P (two-tailed)	0,1444
Significant? (alpha = 0.05)	No
Number of XY Pairs	13

Figure 51: Correlation scatterplots for perceived stress and age of onset.

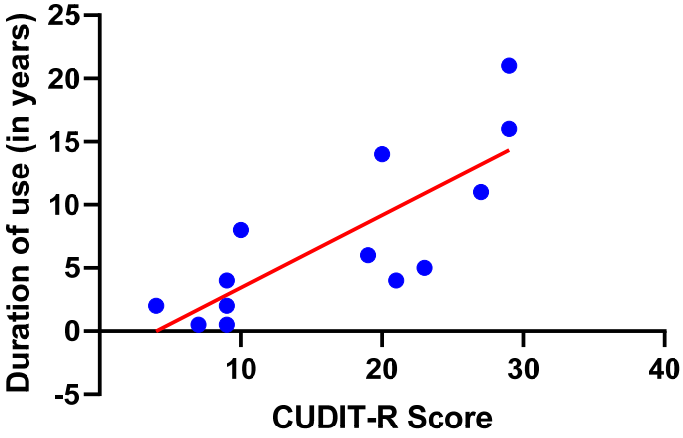

Duration of use Vs CUDIT-R	
Pearson r	
r	0.7952
R squared	0,6324
P-value	
P (two-tailed)	0,0012
Significant? (alpha = 0.05)	Yes
Number of XY Pairs	13

Figure 52: Correlation scatterplots for CUD and age of onset.

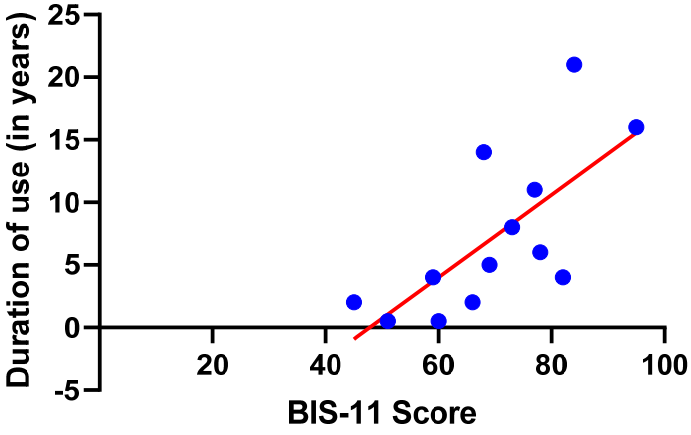

Duration of use Vs BIS-11	
Pearson r	
r	0.7952
R squared	0,6324
P-value	
P (two-tailed)	0,0012
Significant? (alpha = 0.05)	Yes
Number of XY Pairs	13

Figure 53: Correlation scatterplots for impulsivity and duration of use.

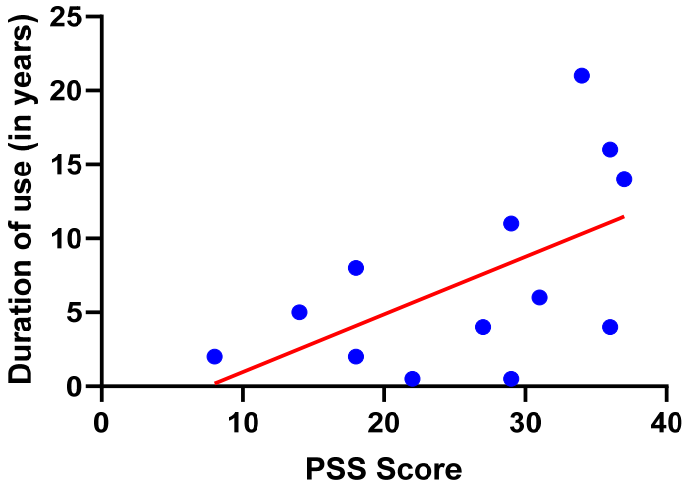

Duration of use Vs PSS	
Pearson r	
r	0.5619
R squared	0,3157
P-value	
P (two-tailed)	0,0457
Significant? (alpha = 0.05)	Yes
Number of XY Pairs	13

Figure 54: Correlation scatterplots for perceived stress and duration of use.

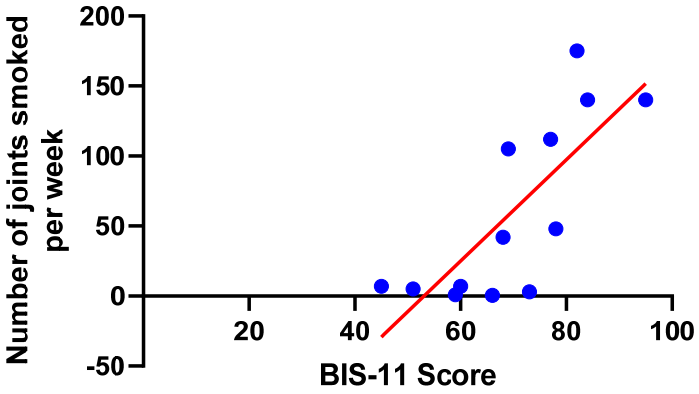

Number of joints per week Vs BIS-11	
Pearson r	
r	0.7776
R squared	0,6047
P-value	
P (two-tailed)	0,0018
Significant? (alpha = 0.05)	Yes
Number of XY Pairs	13

Figure 55: Correlation scatterplots for impulsivity and degree of consumption.

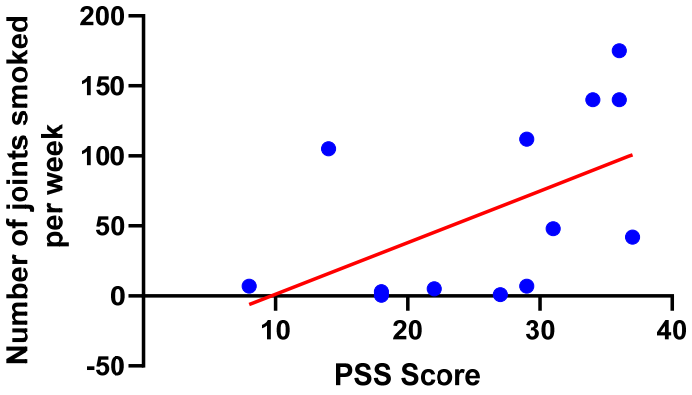

Number of joints per week Vs PSS	
Pearson r	
r	0.5310
R squared	0,2819
P-value	
P (two-tailed)	0,0619
Significant? (alpha = 0.05)	No
Number of XY Pairs	13

Figure 56: Correlation scatterplots for stress and degree of consumption.

Chapter II: Qualitative results of the diffusion tensor imaging (DTI)

I. Qualitative DTI results

The processing of the diffusion images through the "ExploreDTI" toolbox allowed us first to construct the qualitative data of the diffusion tensor in the form of a matrix of the maps of all the sections of the brain scan for each of our participants. The mappings were carried out in three different indices: Directionally encoded colour (Plate 4), fractional anisotropy (Plate 5), and mean diffusion (Plate 6).

Since the hypothesised alterations of the nervous tissue that we seek to objectify are microstructural and are not expressed on a macroscopic scale, the visual observation of descriptive comparison of the qualitative results for the three indices does not allow objective noticeable significant differences between the three groups.

II. Qualitative results of the regions of interest selection

The accuracy and quality of our selection of regions of interest (ROI) were assessed using the same procedures used to create our Atlas.

The ROI selection was evaluated on an individual basis for each participant to confirm that all areas were selected correctly (the 35 regions by AAL and the nucleus acquired by the purely manual technique).

Our Atlases (1–15) reflect the high quality of our region of interest selection across all the 36 evaluated regions.

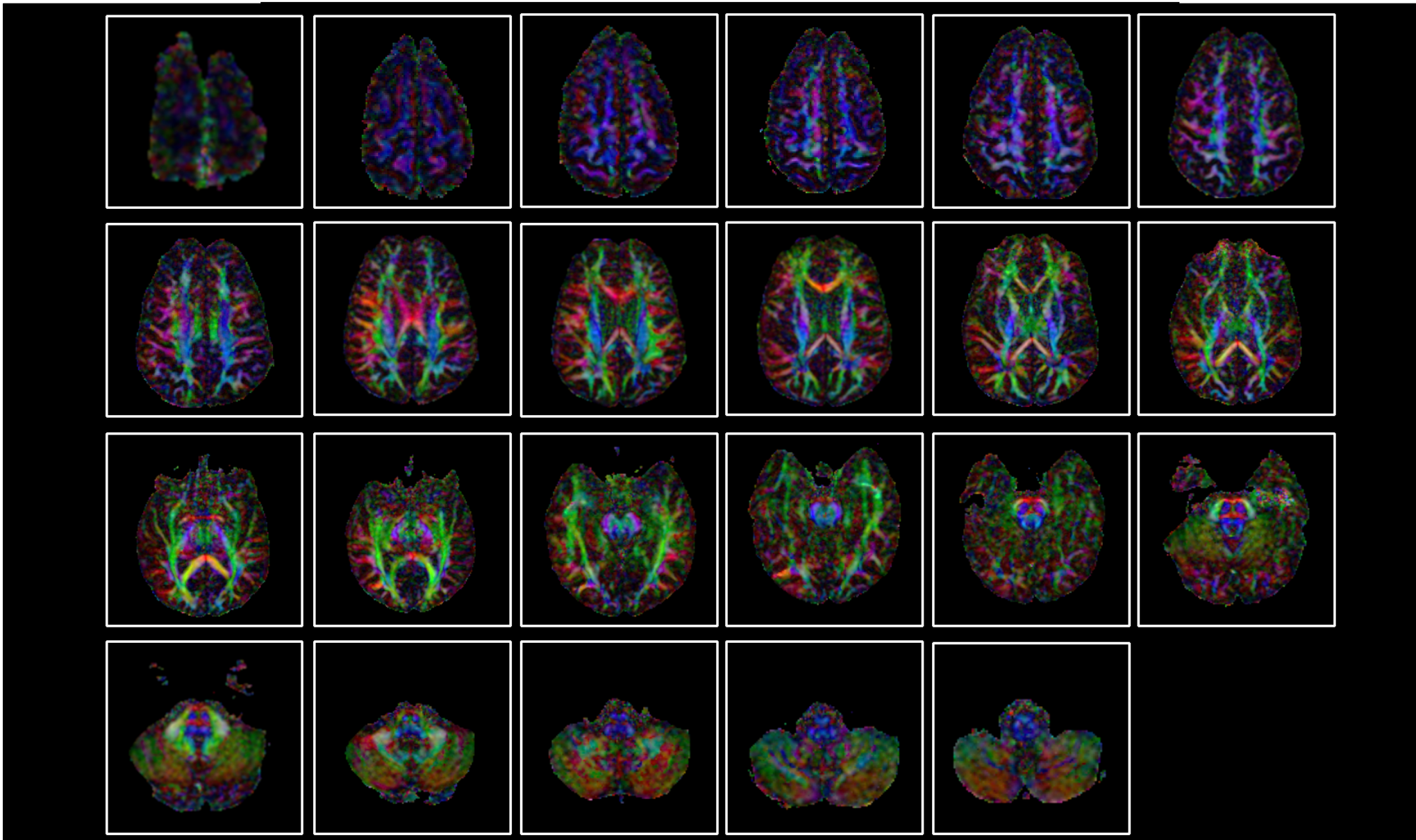

Plate 4: The matrix of First Eigenvector Fractional Anisotropy (FEFA) mappings of all sections of one of our participants' brains.
The interpretation of directionality according to color is as follows: Upper-Lower Right-Left Anterior-Posterior

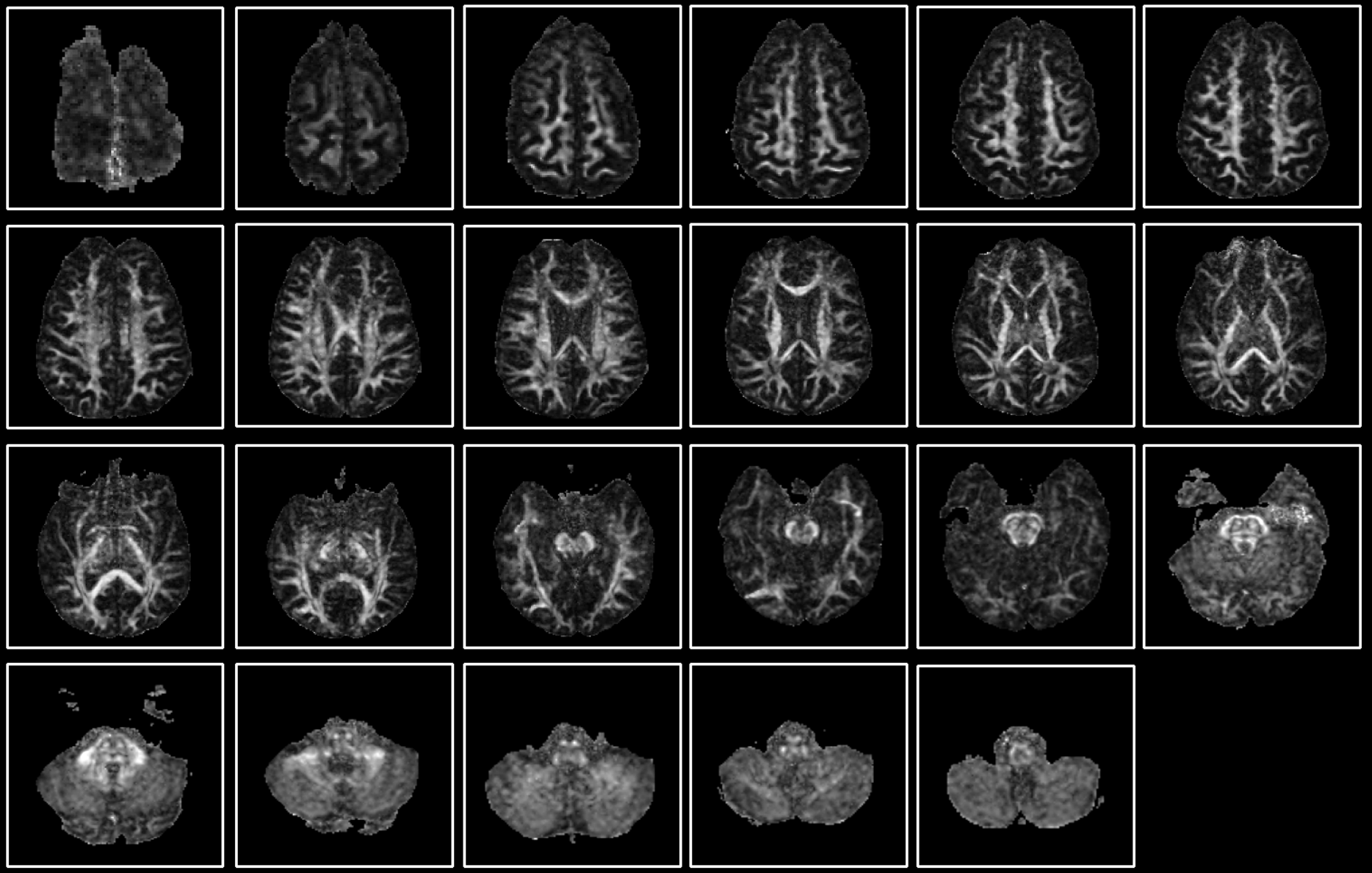

Plate 5: The FA's matrix maps of all sections of the brain of one of our participants.
The signal strength is proportional to the fractional anisotropy.

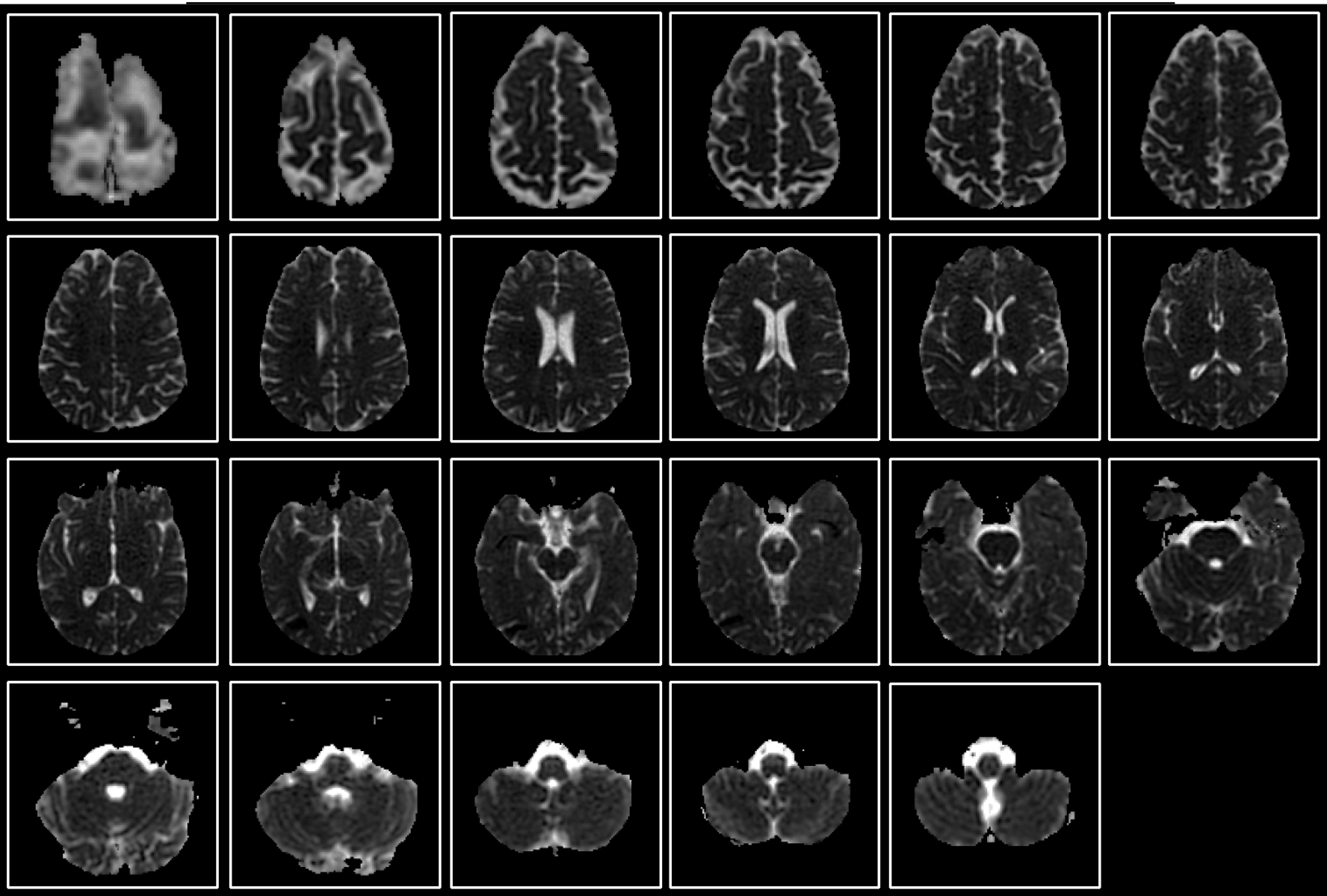

Plate 6: The MD's matrix maps of all sections of the brain of one of our participants.
The signal strength is proportional to the magnitude of diffusivity.

III. Qualitative results of the white matter tractography

Our analysis toolbox, « ExploreDTI, » allowed us to extract the complete tractograms from the brains of each of the participants of the three series included in the study.

Using the toolbox "ExploreDTI," we visually examined and compared all the individuals' tractograms.

Since we are reaching microstructural alterations, all participants' white matter density and structural organization disparities cannot lead to any objective conclusion.

In plates 7, 8 and 9, and 10, we present, respectively, the anterior, posterior, lateral, and superior complete tractography of all white matter bundles of a volunteers' brain.

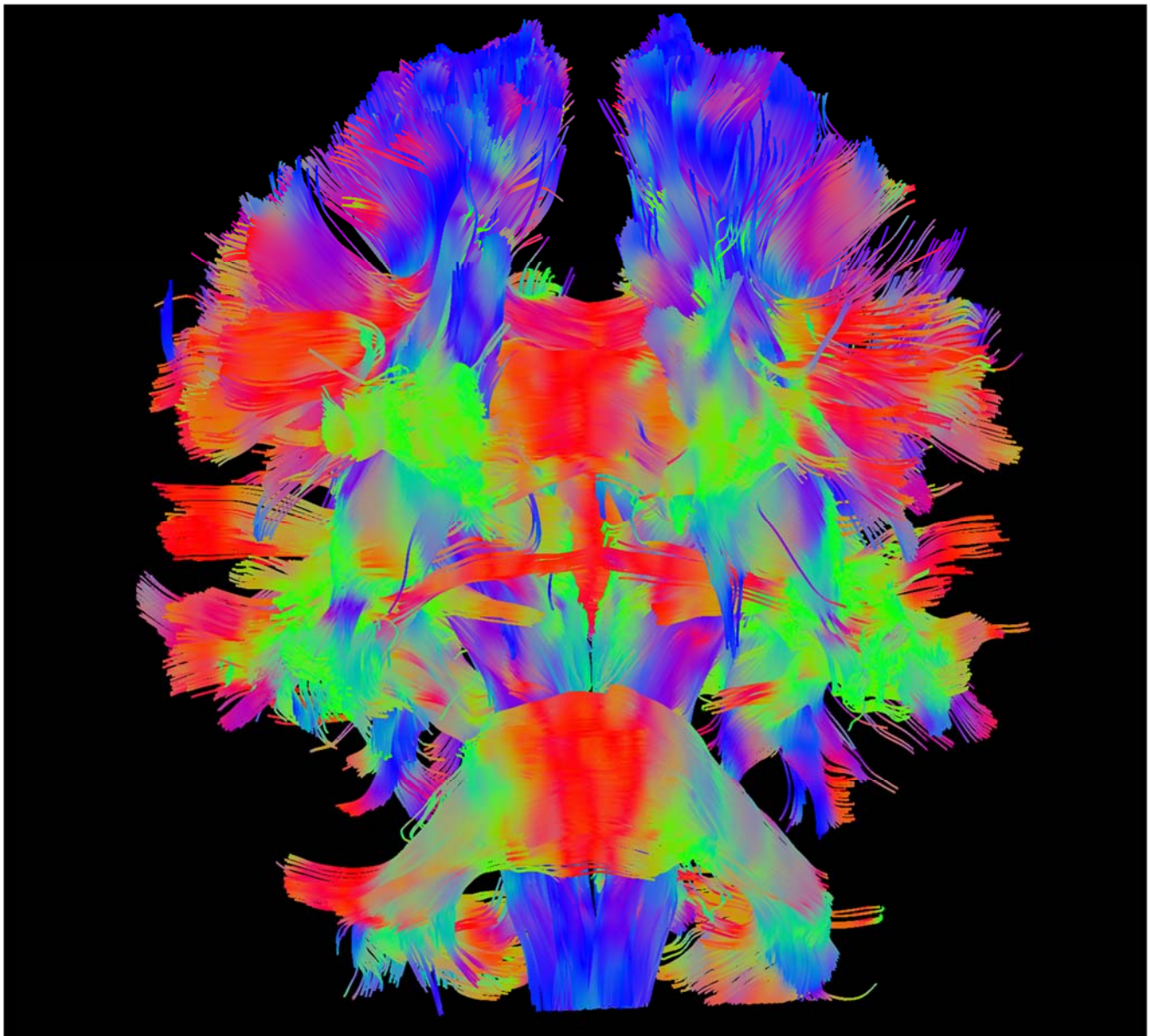

Plate 7: An anterior view of the complete tractography of all white matter bundles of a volunteers' brain.

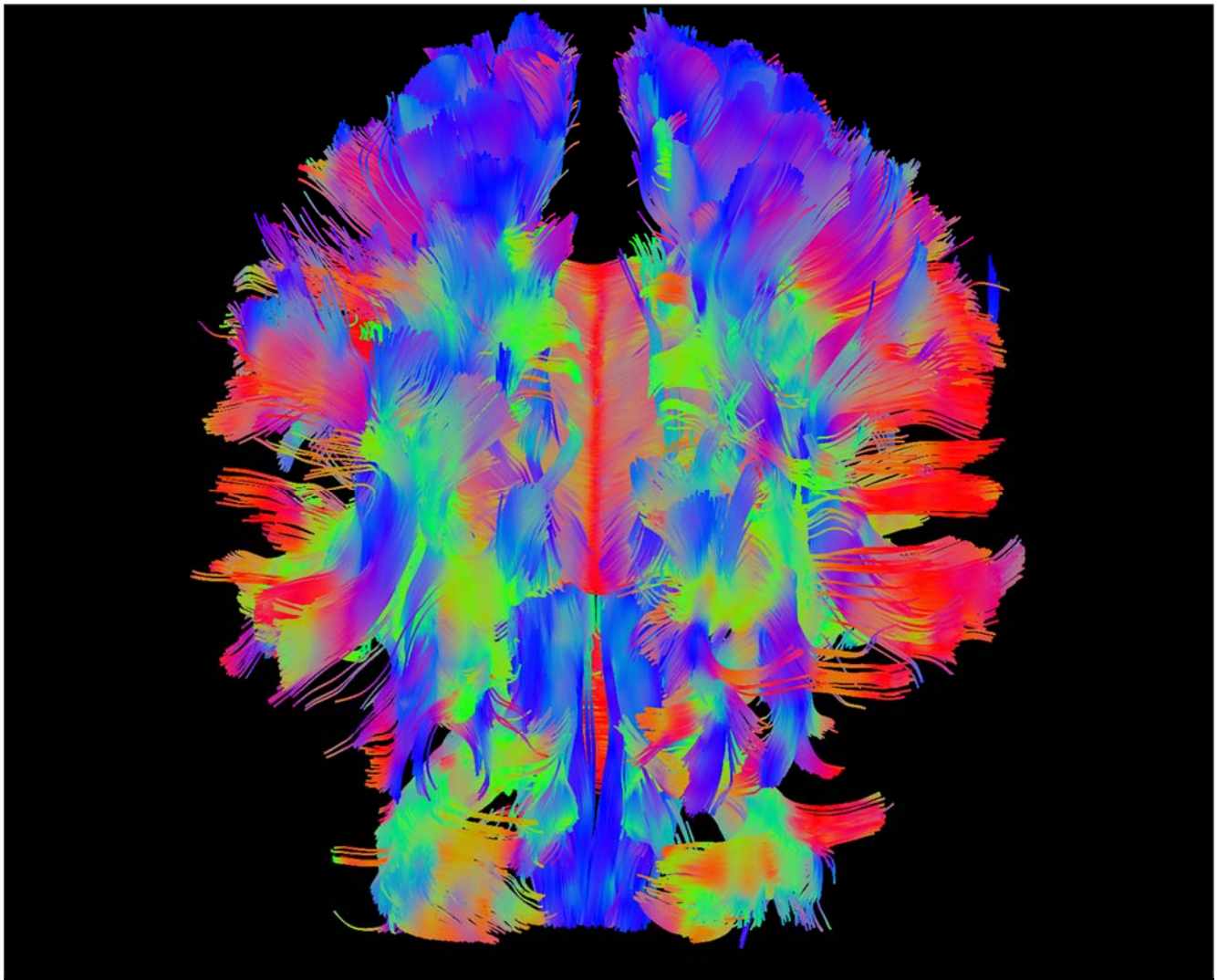

Plate 8: A posterior view of the complete tractography of all white matter bundles of a volunteers' brain.

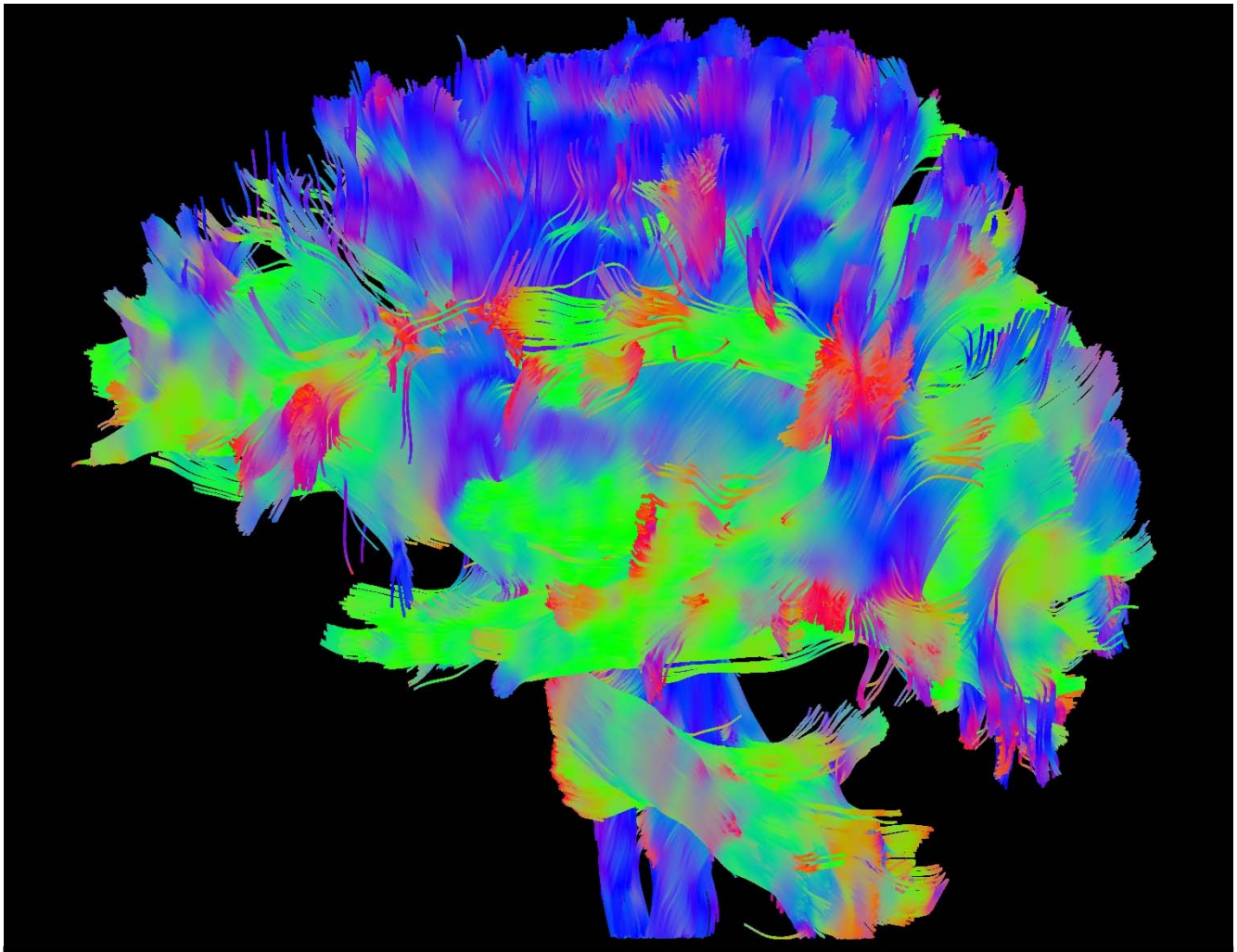

Plate 9: A lateral view of the complete tractography of all white matter bundles of a volunteers' brain.

Plate 10: A superior view of the complete tractography of all white matter bundles of a volunteers' brain.

Chapter III: Diffusion tensor imaging results in grey matter (ROI)

I. Descriptive statistics

Firstly, we will report our descriptive results of the overall quantitative comparisons of the diffusion markers (FA and MD) in tables containing a column indicating the type of noted comparison, another column with corresponding regions, and the third column of commentary for each comparison type. We mentioned that the data is displayed in this table to assist in understanding the results of grey matter structuring of cannabis users compared to healthy controls on a broad and global scale.

Secondly, in the pages following the tables, with graphical curves, we will present compared FA and MD, each separately, by region of interest, and in each hemisphere individual by individual between the three groups.

Using column graph, we also compared in the same way in each region of interest of each hemisphere the averages of FA and MD between the three groups.

Finally, with a table, we summarise for each ROI the averages and standard deviations (SD) values for the groups studied, along with intergroup comparisons.

1. Fractional anisotropy (FA) quantitative results

a. Summary of all the quantitative findings

Table 15: Descriptive results of the overall quantitative comparisons of fractional anisotropy diffusion marker in ROIs.

Intergroup comparison	Regions	Comments
G.III > G. II ≈ G. I	-Frontal Med Orb. Left -Frontal Mid. Left & Right -Frontal Sup. Right -SupraMarginal. Left & Right -Angular. Right -Parietal Inf. Right -Precuneus. Left -Temporal Sup. Left -Frontal Sup Medial. Left & Right -Frontal Inf Tri. Left & Right -Postcentral. Left & Right -Parietal Sup. Right -Heschl. Left -Temporal Mid. Left -Temporal Pole Mid. Left -Temporal Inf. Left -Cingulum Mid. Left -Insula. Left	This intergroup comparison arrangement was objective: * At 23 regions out of 72 (bilaterally), which represents 32% of the total of the regions studied. * In terms of laterality, the two hemispheres were so far equivalent. * The regions with this intergroup comparison belong to the cerebral cortex.
G.III >G. II > G. I	-Frontal Med Orb. Right -Olfactory. Right -Parietal Sup. Left -Angular. Left -Precuneus. Right -Temporal Pole Sup. Left -Cingulum Ant. Left & Right -Cingulum Mid. Right -Pallidum. Right -Nucleus Accumbens. Right	This intergroup comparison arrangement was objective: * At 11 regions out of 72 (bilaterally), which represents 15.27% of the total of the regions studied. * Two-thirds of regions are located in the right hemisphere. * The regions with this intergroup comparison belong to the cerebral cortex, mostly beside basal ganglia.

G.III > G. I > G. II	-Frontal Sup Orb. Left -Frontal Mid Orb. Left & Right -Frontal Inf Orb. Left & Right -Olfactory. Left -Frontal Sup. Left -Frontal Inf Oper. Left -Parietal Inf. Left -Temporal Sup. Right -Heschl. Right -Temporal Mid. Right -Temporal Pole Mid. Right -Temporal Inf. Right -Fusiform. Left -Cingulum Post. Left -ParaHippocampal. Left -Thalamus. Left -Pallidum.Left	This intergroup comparison arrangement was objective: * At 19 regions out of 72 (bilaterally), which represents 25% of the total of the regions studied. * Two-thirds of regions are located in the left hemisphere. * The regions with this intergroup comparison belong to the cerebral cortex, basal ganglia, and diencephalon (Thalamus).
G.III ≈ G. I > G. II	-Frontal Inf Oper. Right -Temporal Pole Sup. Right -Fusiform. Right -ParaHippocamppal. Right -Hippocampus. Left -Amygdala. Left -Thalamus. Right -Putamen. Left & Right	This intergroup comparison arrangement was objective: * At nine regions out of 72 (bilaterally), which represents 12.5% of the total of the regions studied. * Two-thirds of regions are located in the right hemisphere. * The regions with this intergroup comparison belong mostly to the limbic system, basal ganglia, and cerebral cortex.
G. I > G.III > G. II	-Frontal Sup Orb. Right -Rectus. Left & Right	Only three regions show this type of intergroup comparison. All three regions belong to the orbital part of the cerebral cortex.

G. II ≈ G.III > G. I	-Cingulum Post. Right -Insula. Right	Only two regions show this type of intergroup comparison. These regions belong to the limbic system or are known to participate in limbic system functioning.
G. I > G.III ≈ G. II	-Hippocampus. Right	The remaining four categories of intergroup comparisons account for less than 7% of the total. Regions are split between the basal ganglia and the limbic system. The regions are almost equally distributed between the left and the right hemispheres.
G. I > G. II > G.III	-Amygdala. Right	
G. II > G.III ≈ G. I	-Caudate. Left	
G. II > G. I > G.III	-Caudate. Right	
G.III ≈ G. I ≈ G. II	-Nucleus Accumbens. Left	

b. The quantitative findings in each region of interest

For each region of interest and in both hemispheres, we present our mean fractional anisotropy (FA) findings by two separated figures. The first figure depicts the mean FA values of individuals in each group using a line chart.

In the line charts:

- Each participant is denoted numerically, and this nomination is applied throughout all our work.

-The mean fractional anisotropy is sorted in graph individual (X, Y) points and lines in heavy cannabis users (Group I), light cannabis users (Group II), and non-users (Group III). In the "X" horizontal line, we have the nominative numbers of voluntary participants, and in the "Y" vertical line, we have mean fractional anisotropy values.

In the second figure, we compared the groups' FA averages between the three groups.

A table containing every group's FA averages and standard deviations (SD) will be presented for a more specific summary.

➢ Frontal Med Orb region

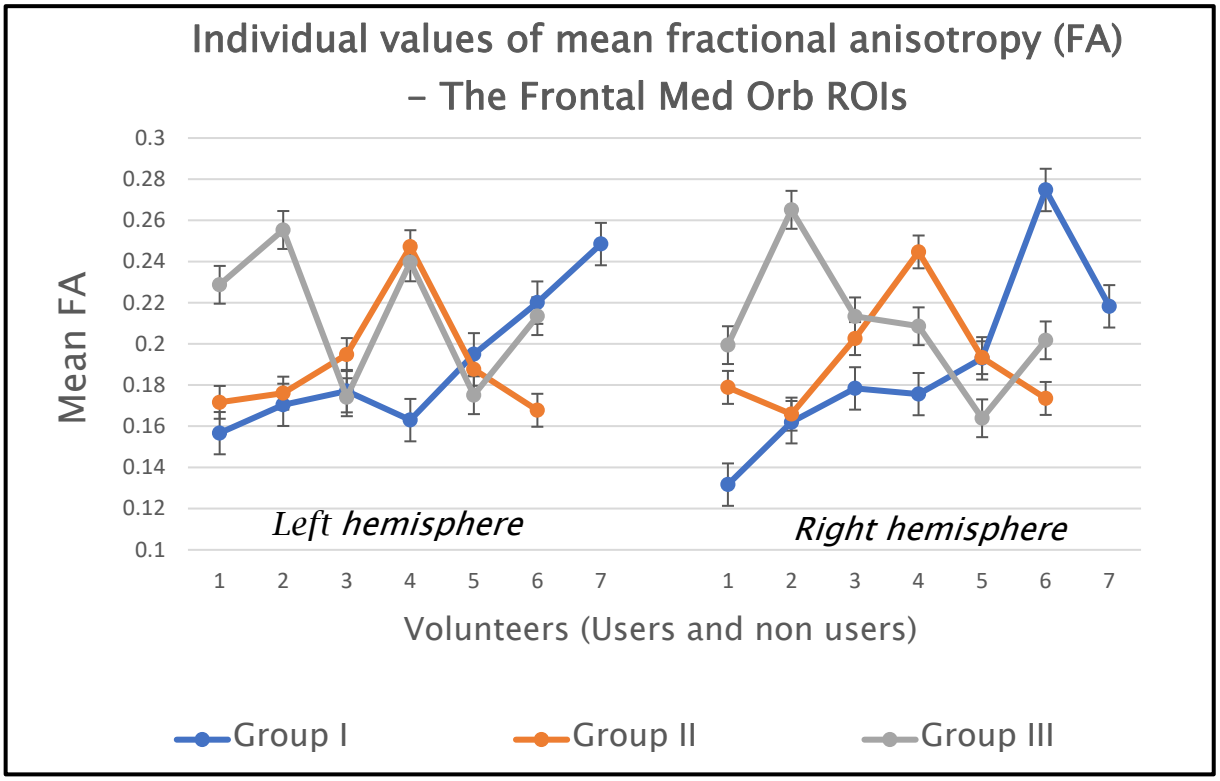

Figure 57: Individual values of mean fractional anisotropy (FA) in both hemispheres' Frontal Med Orb ROIs. This figure depicts the FA values of all the participants belonging to each of the three groups (Heavy and light users and healthy controls).

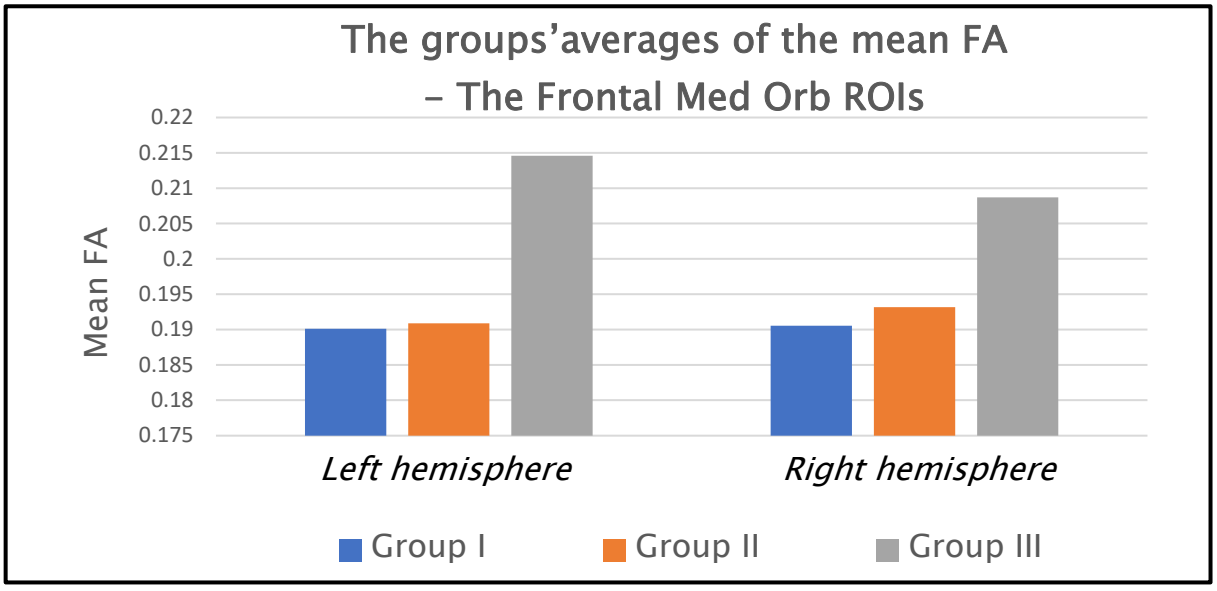

Figure 58: The mean fractional anisotropy (FA) averages of each group in the Frontal Med Orb ROIs in the left and the right hemispheres.

Table 16: The mean fractional anisotropy (FA) averages and standard deviations (SD) values for the groups studied in the Frontal Med Orb ROIs, along with intergroup comparisons.

	Left Hemisphere	Right Hemisphere
Heavy users' group (G. I)	(0,1901±0,0335)	(0,1905±0,0456)
Light users' group (G. II)	(0,1908±0,0294)	(0,193±0,0285)
Non-users' group (G.III)	(0,214±0,0337)	(0,2087±0,0327)
Intergroup comparison	G.III > G. II ≈ G. I	G.III > G. II > G. I

➢ **Frontal Sup Orb**

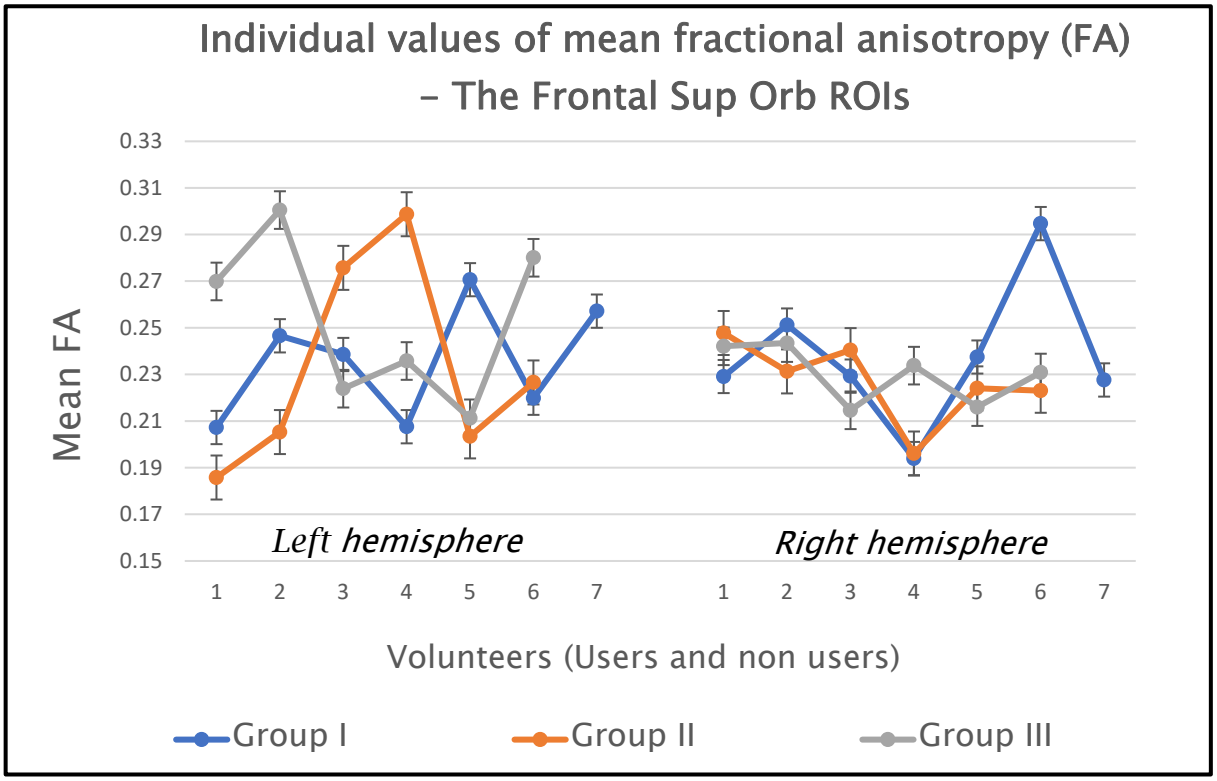

Figure 59: Individual values of mean fractional anisotropy (FA) in both hemispheres' Frontal Sup Orb ROIs. This figure depicts the FA values of all the participants belonging to each of the three groups (Heavy and light users and healthy controls).

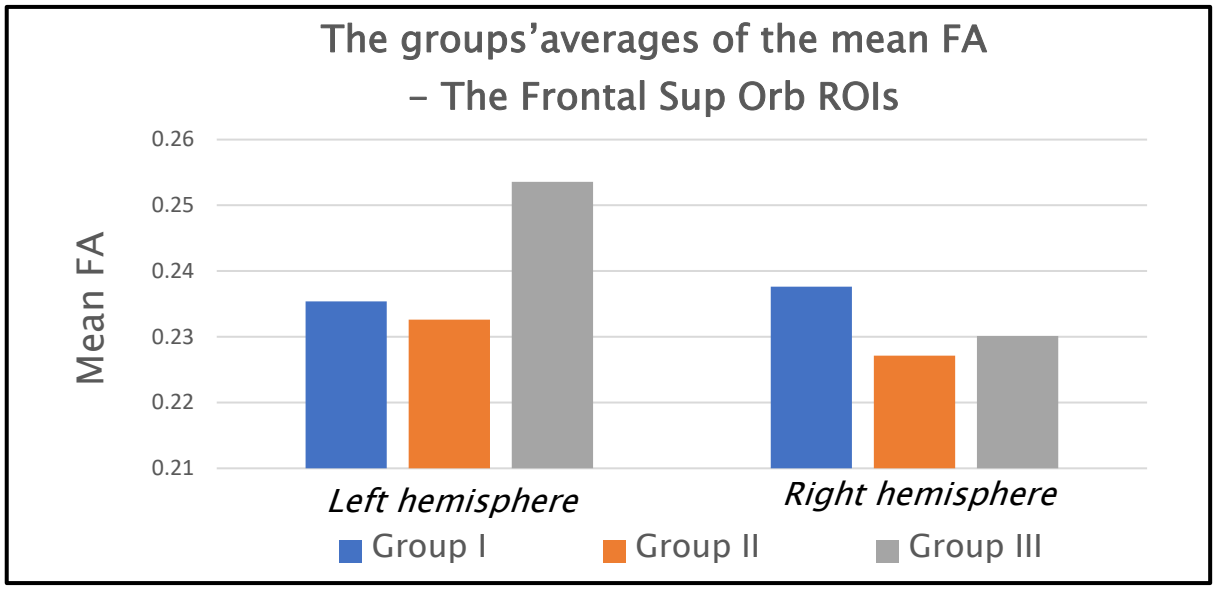

Figure 60: The mean fractional anisotropy (FA) averages of each group in the Frontal Sup Orb ROIs in the left and the right hemispheres.

Table 17: The mean fractional anisotropy (FA) averages and standard deviations (SD) values for the groups studied in the Frontal Sup Orb ROIs, along with intergroup comparisons.

	Left Hemisphere	Right Hemisphere
Heavy users' group (G. I)	(0,235±0,0246)	(0,237±0,03051)
Light users' group (G. II)	(0,232±0,0448)	(0,227±0,0179)
Non-users' group (G.III)	(0,253±0,03509)	(0,2301±0,0124)
Intergroup comparison	G.III > G. I > G. II	G. I > G.III > G. II

➢ Frontal Mid Orb

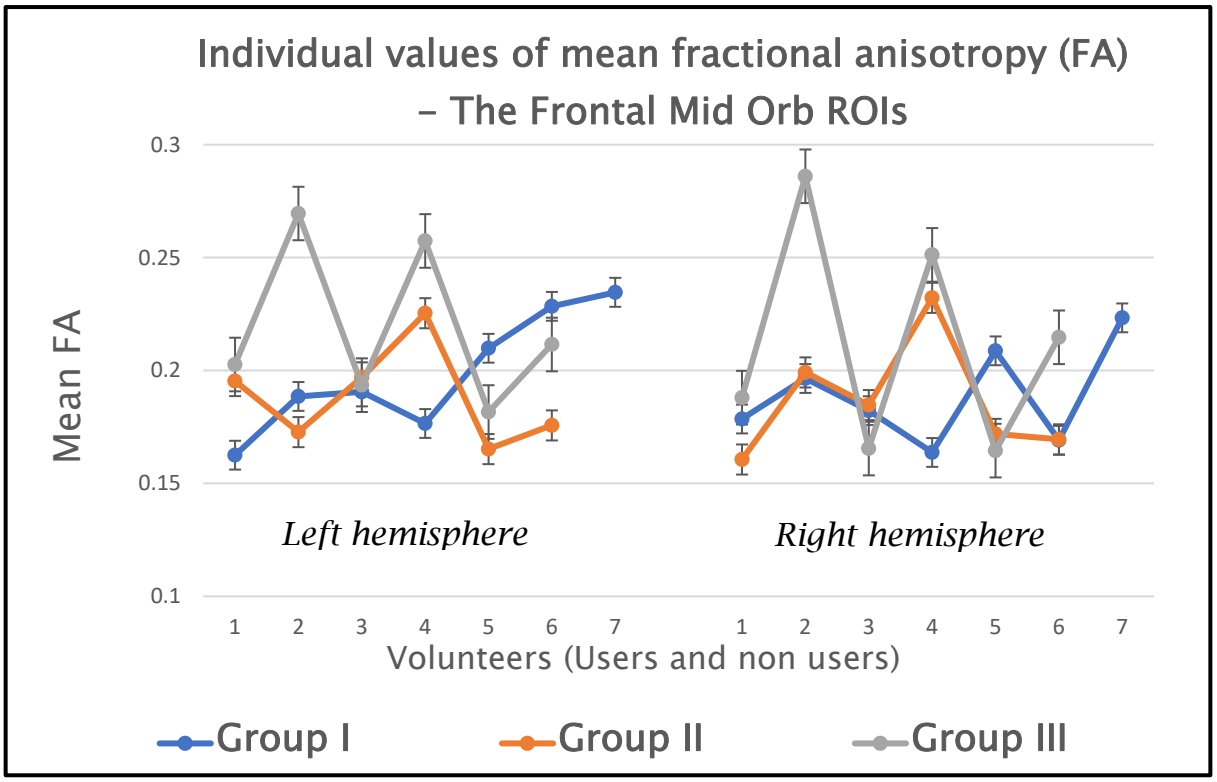

Figure 61: Individual values of mean fractional anisotropy (FA) in both hemispheres' Frontal Mid Orb ROIs. This figure depicts the FA values of all the participants belonging to each of the three groups (Heavy and light users and healthy controls).

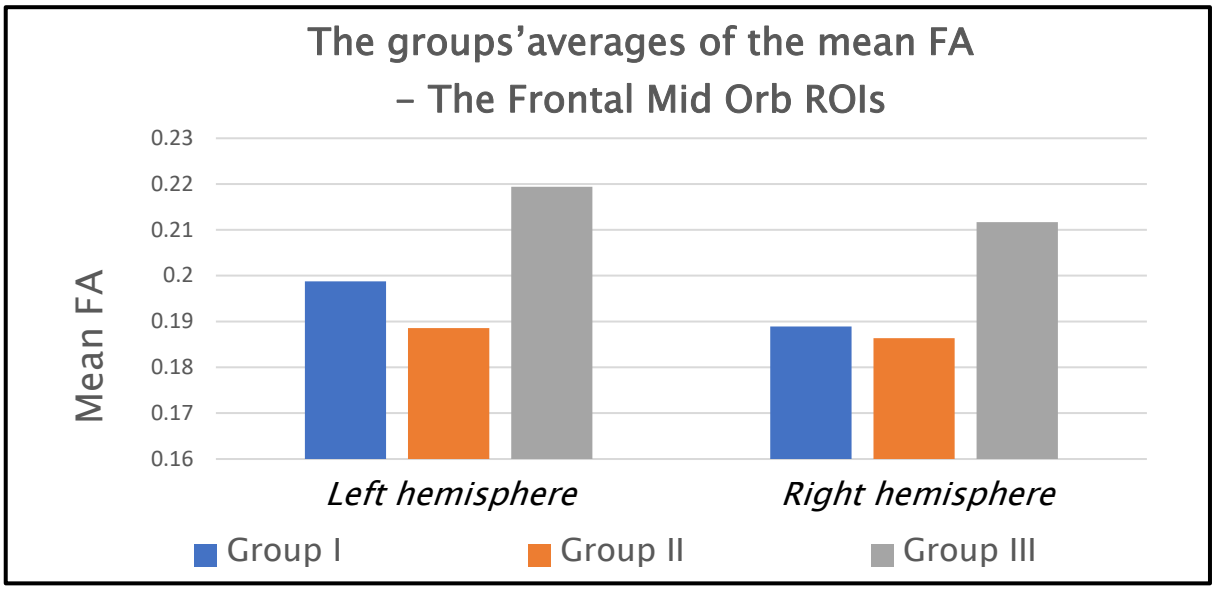

Figure 62: The mean fractional anisotropy (FA) averages of each group in the Frontal Mid ROIs in the left and the right hemispheres.

Table 18: The mean fractional anisotropy (FA) averages and standard deviations (SD) values for the groups studied in the Frontal Mid Orb ROIs, along with intergroup comparisons.

	Left Hemisphere	Right Hemisphere
Heavy users' group (G. I)	(0,198±0,0266)	(0,188±0,0216)
Light users' group (G. II)	(0,188±0,02203)	(0,186±0,0261)
Non-users' group (G.III)	(0,219±0,0357)	(0,211±0,04902)
Intergroup comparison	G.III > G. I > G. II	G.III > G. I > G. II

➢ **Frontal Inf Orb**

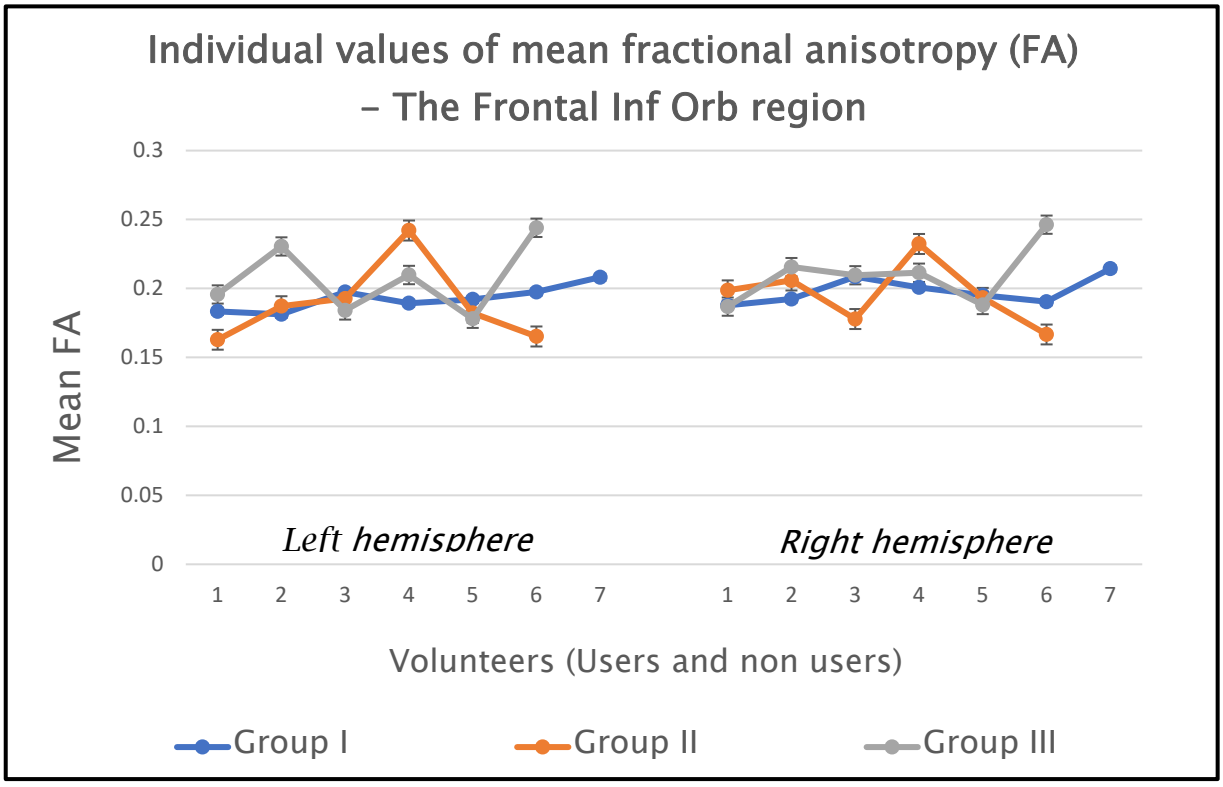

Figure 63: Individual values of mean fractional anisotropy (FA) in both hemispheres' Frontal Inf Orb ROIs. This figure depicts the FA values of all the participants belonging to each of the three groups (Heavy and light users and healthy controls).

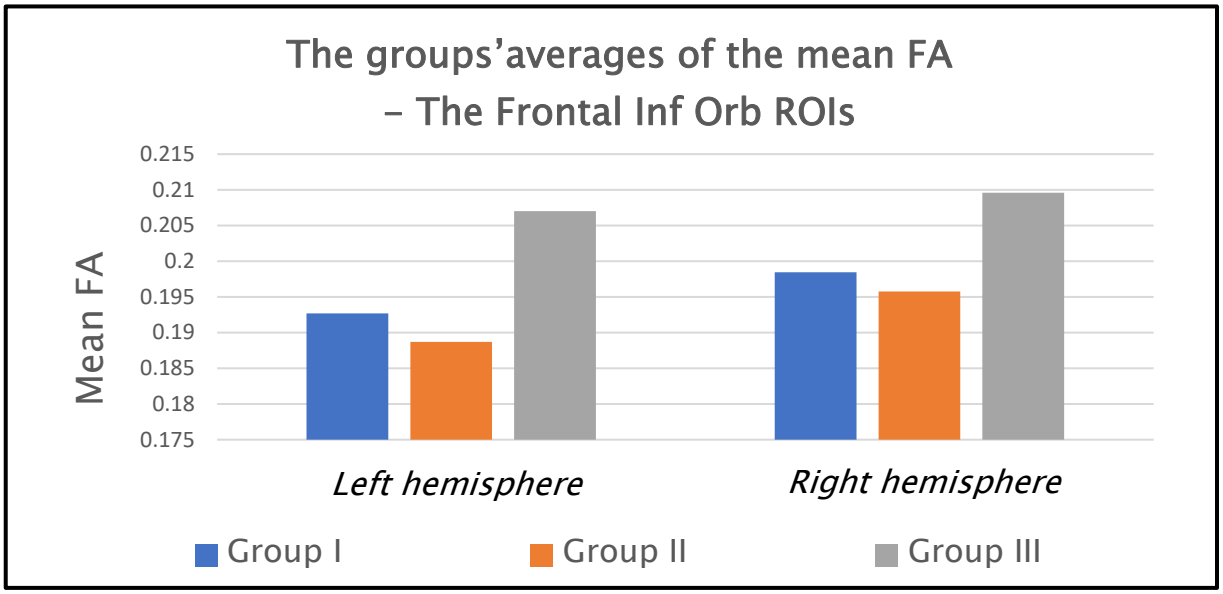

Figure 64: The mean fractional anisotropy (FA) averages of each group in the Frontal Inf Orb ROIs in the left and the right hemispheres.

Table 19: The mean fractional anisotropy (FA) averages and standard deviations (SD) values for the groups studied in the Frontal Inf Orb ROIs, along with intergroup comparisons.

	Left Hemisphere	Right Hemisphere
Heavy users' group (G. I)	(0,192±0,00925)	(0,198±0,009902)
Light users' group (G. II)	(0,188±0,0287)	(0,195±0,0228)
Non-users' group (G.III)	(0,20702±0,0261)	(0,2096±0,0217)
Intergroup comparison	G.III > G. I > G. II	G.III > G. I > G. II

➢ **Rectus**

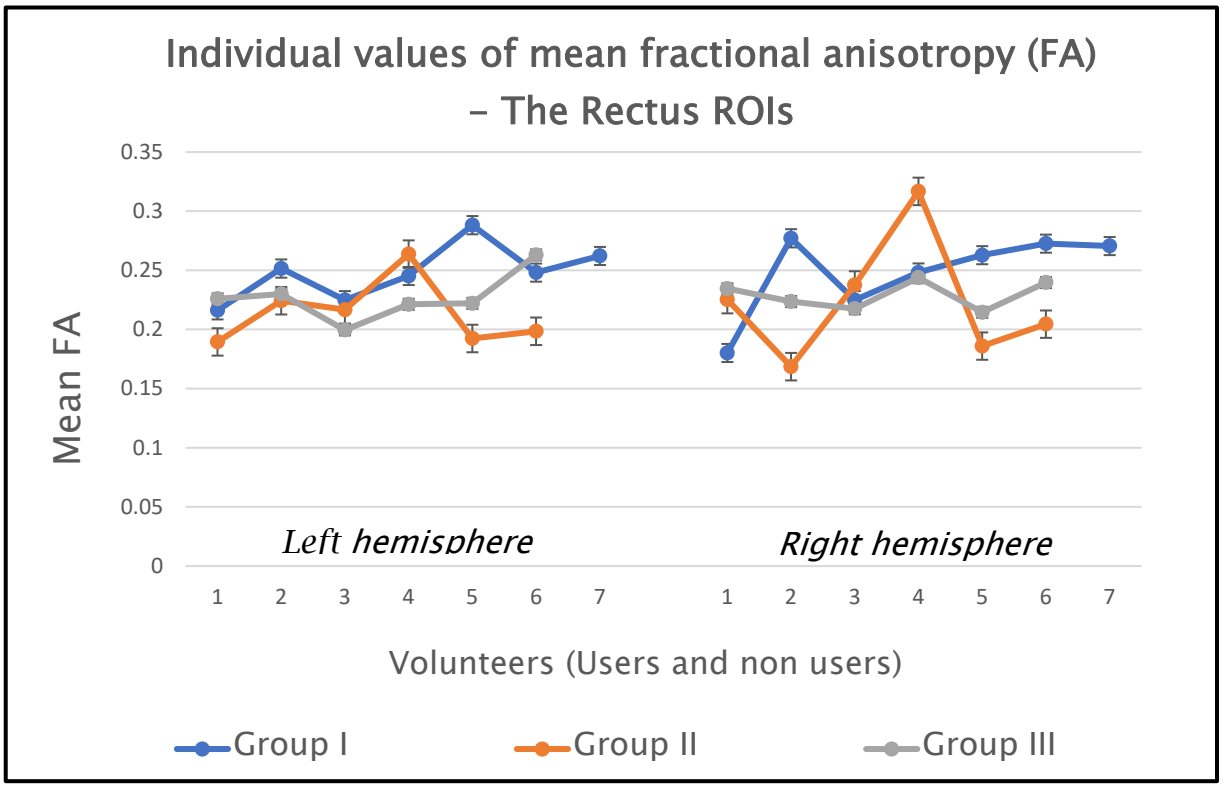

Figure 65: Individual values of mean fractional anisotropy (FA) in both hemispheres' Rectus ROIs. This figure depicts the FA values of all the participants belonging to each of the three groups (Heavy and light users and healthy controls).

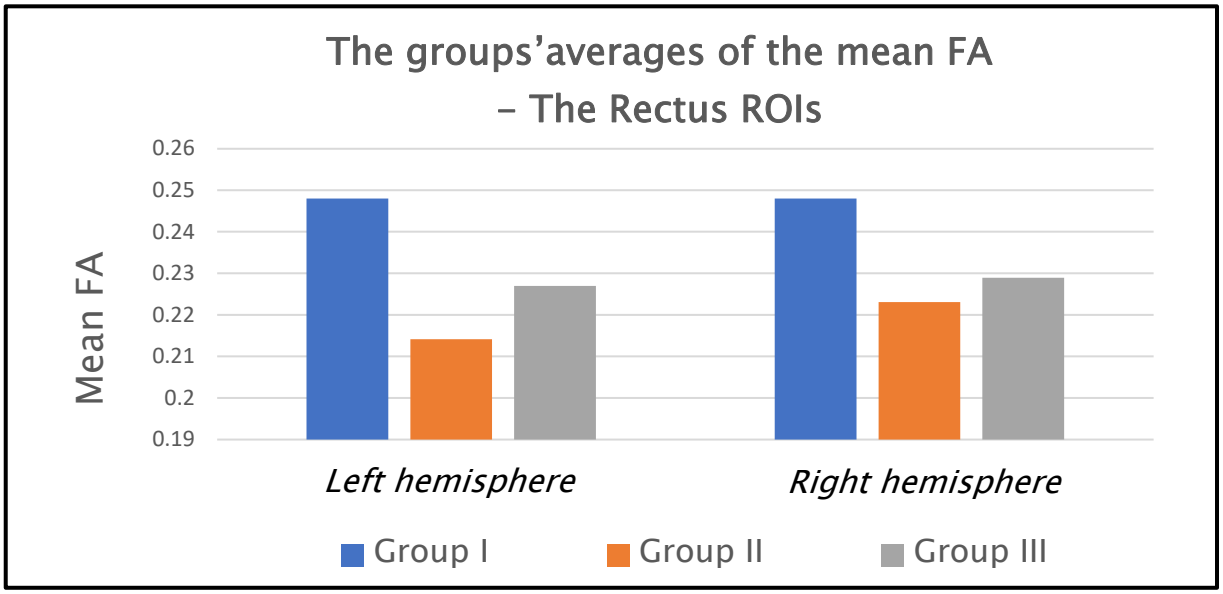

Figure 66: The mean fractional anisotropy (FA) averages of each group in the Rectus ROIs in the left and the right hemispheres.

Table 20: The mean fractional anisotropy (FA) averages and standard deviations (SD) values for the groups studied in the Rectus ROIs, along with intergroup comparisons.

	Left Hemisphere	Right Hemisphere
Heavy users' group (G. I)	(0,247±0,0237)	(0,247±0,0349)
Light users' group (G. II)	(0,214±0,0278)	(0,223±0,0522)
Non-users' group (G.III)	(0,226±0,02056)	(0,228±0,0121)
Intergroup comparison	G. I > G.III > G. II	G. I > G.III > G. II

➢ **Olfactory**

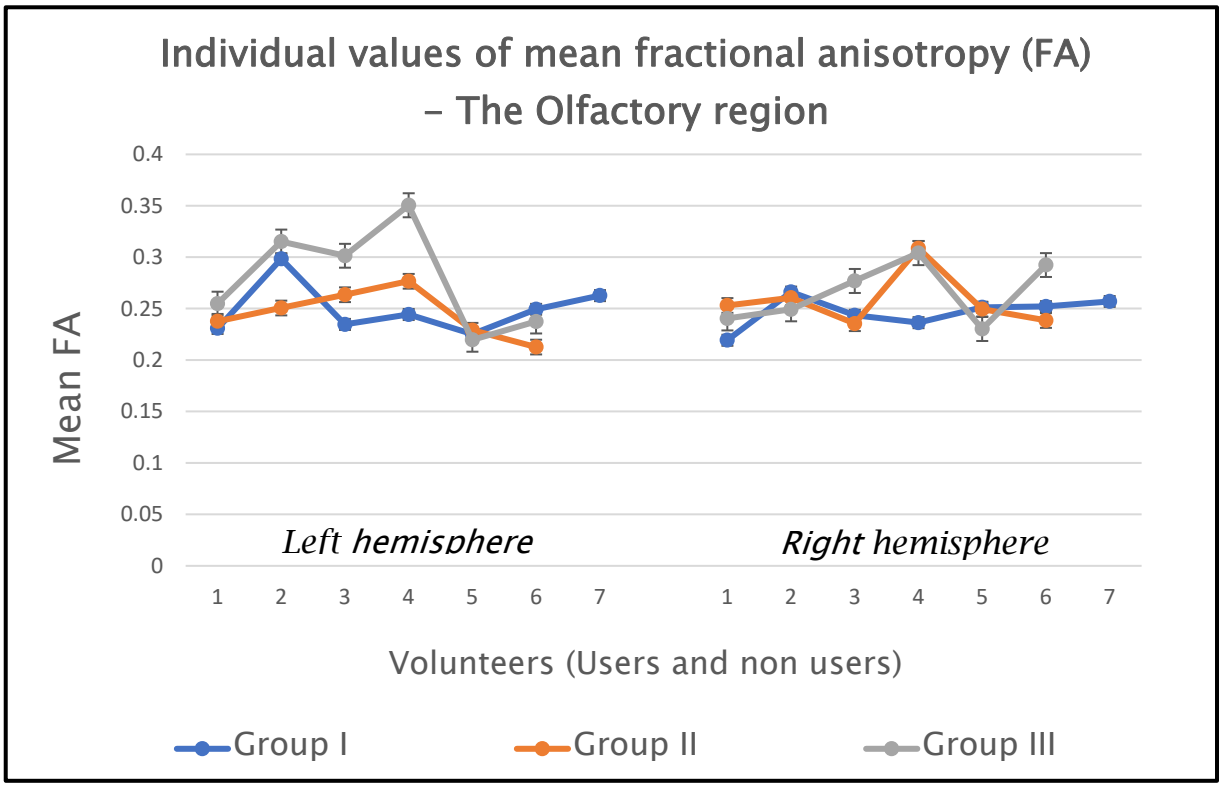

Figure 67: Individual values of mean fractional anisotropy (FA) in both hemispheres' Olfactory ROIs. This figure depicts the FA values of all the participants belonging to each of the three groups (Heavy and light users and healthy controls).

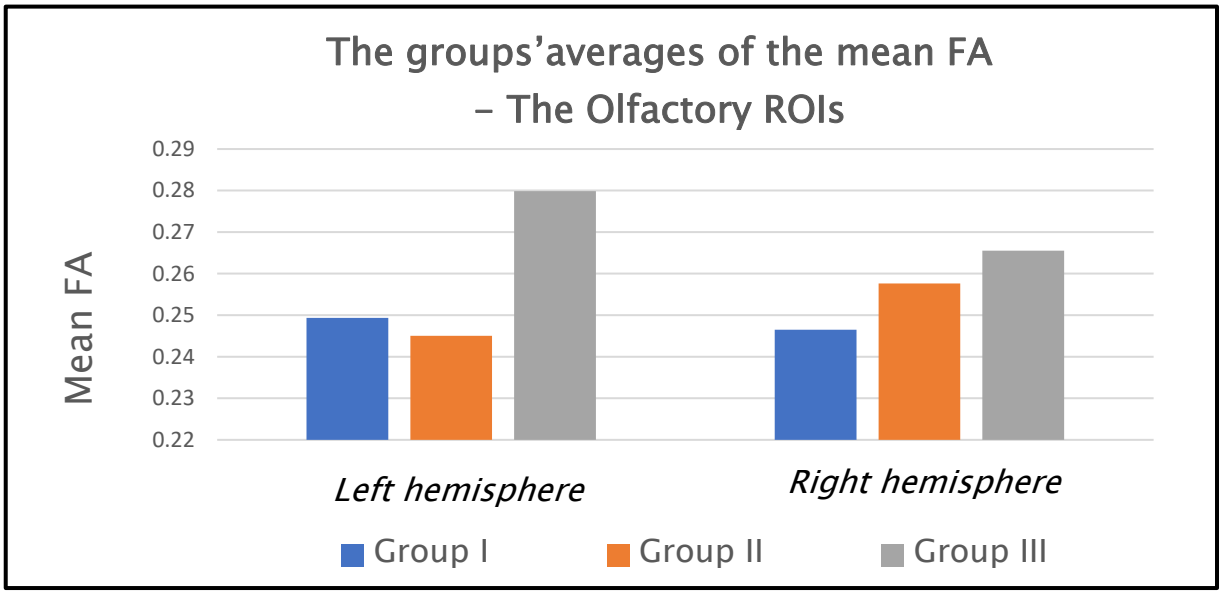

Figure 68: The mean fractional anisotropy (FA) averages of each group in the Olfactory ROIs in the left and the right hemispheres.

Table 21: The mean fractional anisotropy (FA) averages and standard deviations (SD) values for the groups studied in the Olfactory ROIs, along with intergroup comparisons.

	Left Hemisphere	Right Hemisphere
Heavy users' group (G. I)	(0,249±0,02503)	(0,246±0,0152)
Light users' group (G. II)	(0,245±0,0233)	(0,257±0,0266)
Non-users' group (G.III)	(0,279±0,05048)	(0,265±0,0299)
Intergroup comparison	G.III > G. I > G. II	G.III > G. II > G. I

➢ Frontal Sup Medial

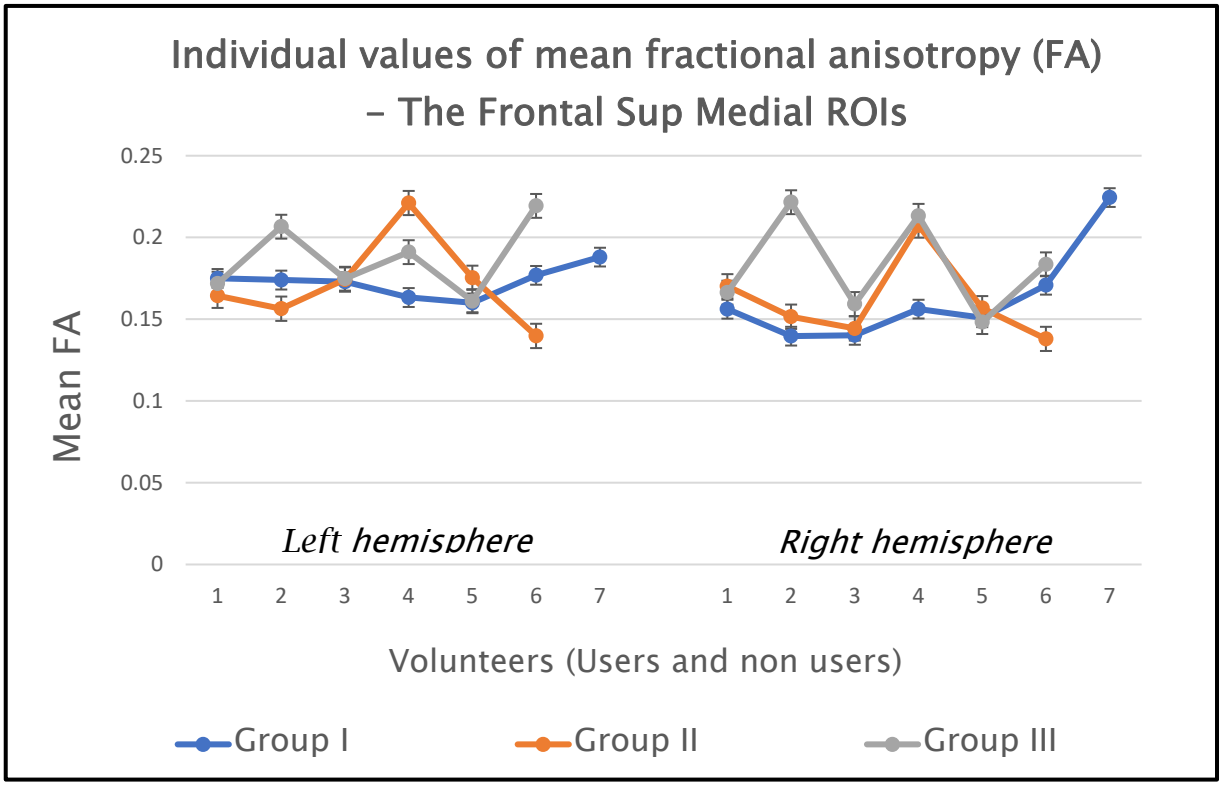

Figure 69: Individual values of mean fractional anisotropy (FA) in both hemispheres' Frontal Sup Medial ROIs. This figure depicts the FA values of all the participants belonging to each of the three groups (Heavy and light users and healthy controls).

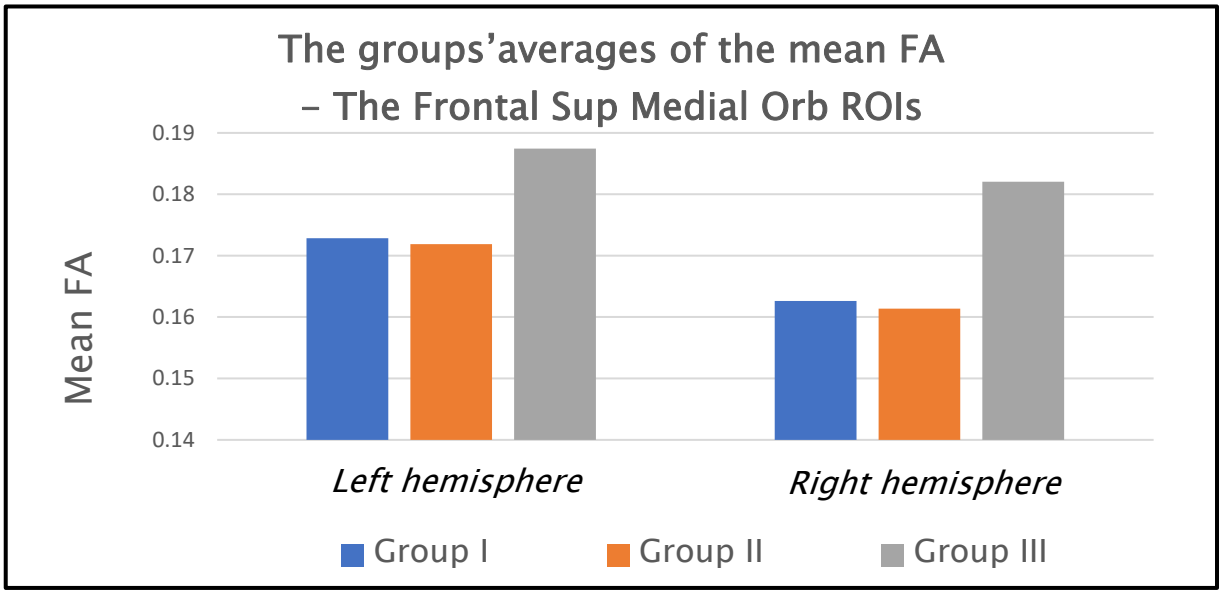

Figure 70: The mean fractional anisotropy (FA) averages of each group in the Frontal Sup Medial Orb ROIs in the left and the right hemispheres.

Table 22: The mean fractional anisotropy (FA) averages and standard deviations (SD) values for the groups studied in the Frontal Sup Medial Orb ROIs, along with intergroup comparisons.

	Left Hemisphere	Right Hemisphere
Heavy users' group (G. I)	(0,172±0,00919)	(0,162±0,0292)
Light users' group (G. II)	(0,171±0,0274)	(0,161±0,02508)
Non-users' group (G.III)	(0,187±0,0223)	(0,182±0,0298)
Intergroup comparison	G.III > G. I ≈ G. II	G.III > G. I ≈ G. II

➢ **Frontal Sup**

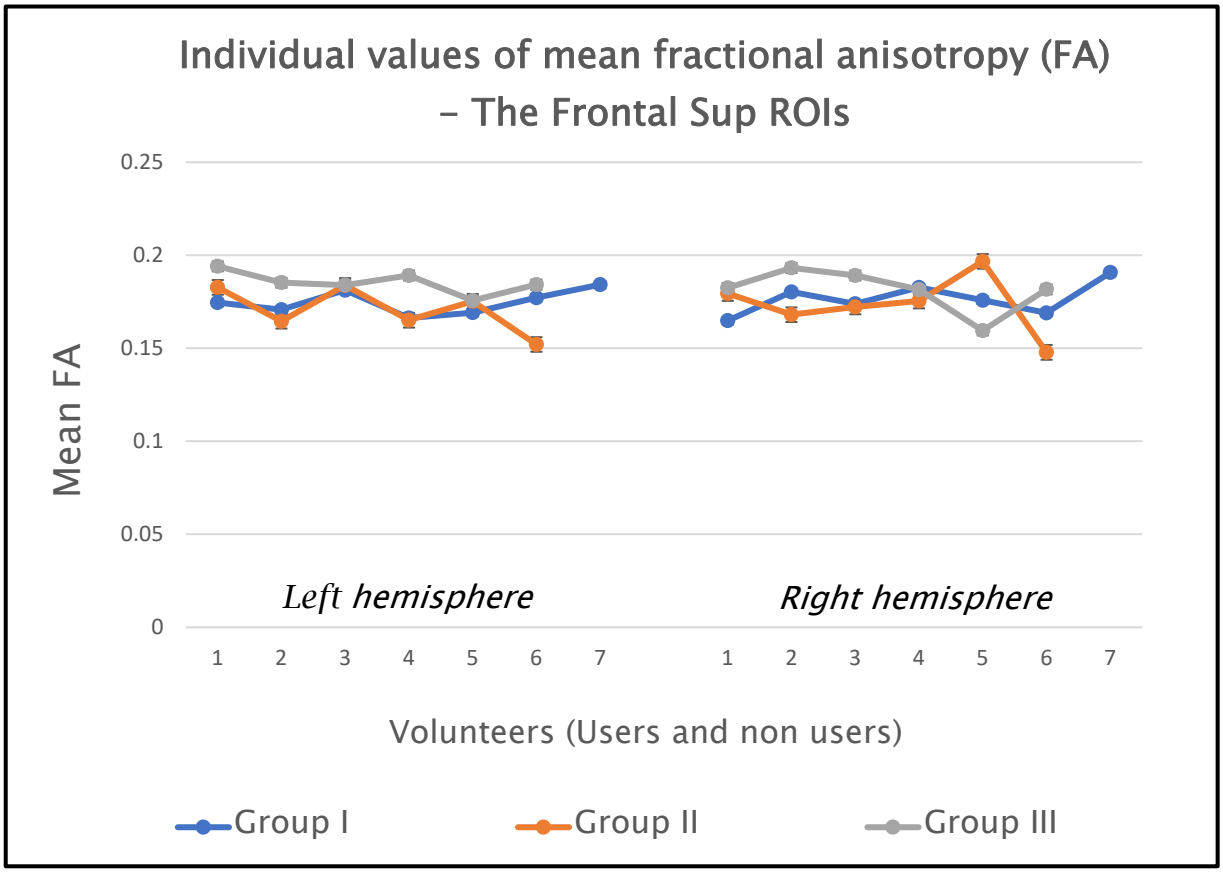

Figure 71: Individual values of mean fractional anisotropy (FA) in both hemispheres' Frontal Sup ROIs. This figure depicts the FA values of all the participants belonging to each of the three groups (Heavy and light users and healthy controls).

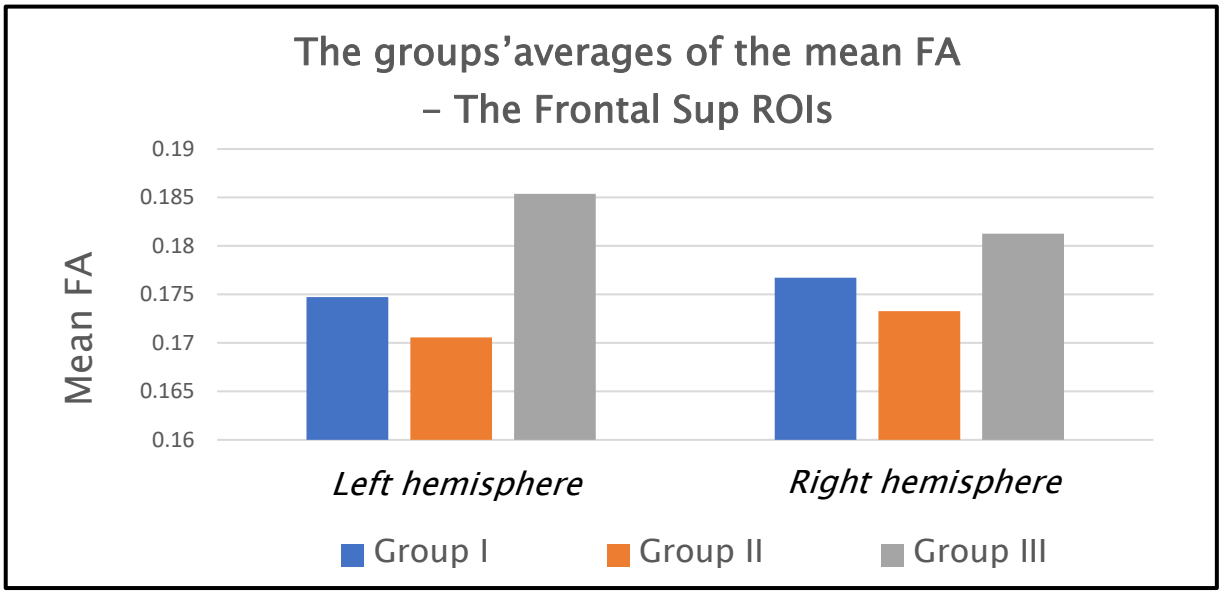

Figure 72: The mean fractional anisotropy (FA) averages of each group in the Frontal Sup ROIs in the left and the right hemispheres.

Table 23: The mean fractional anisotropy (FA) averages and standard deviations (SD) values for the groups studied in the Frontal Sup ROIs, along with intergroup comparisons.

	Left Hemisphere	Right Hemisphere
Heavy users' group (G. I)	(0.174±0.00654)	(0,176±0,00872)
Light users' group (G. II)	(0,1705±0,0122)	(0,173±0,0159)
Non-users' group (G.III)	(0,185±0,00613)	(0,181±0,0116)
Intergroup comparison	G.III > G. I > G. II	G.III > G. I ≈ G. II

➢ **Frontal Mid**

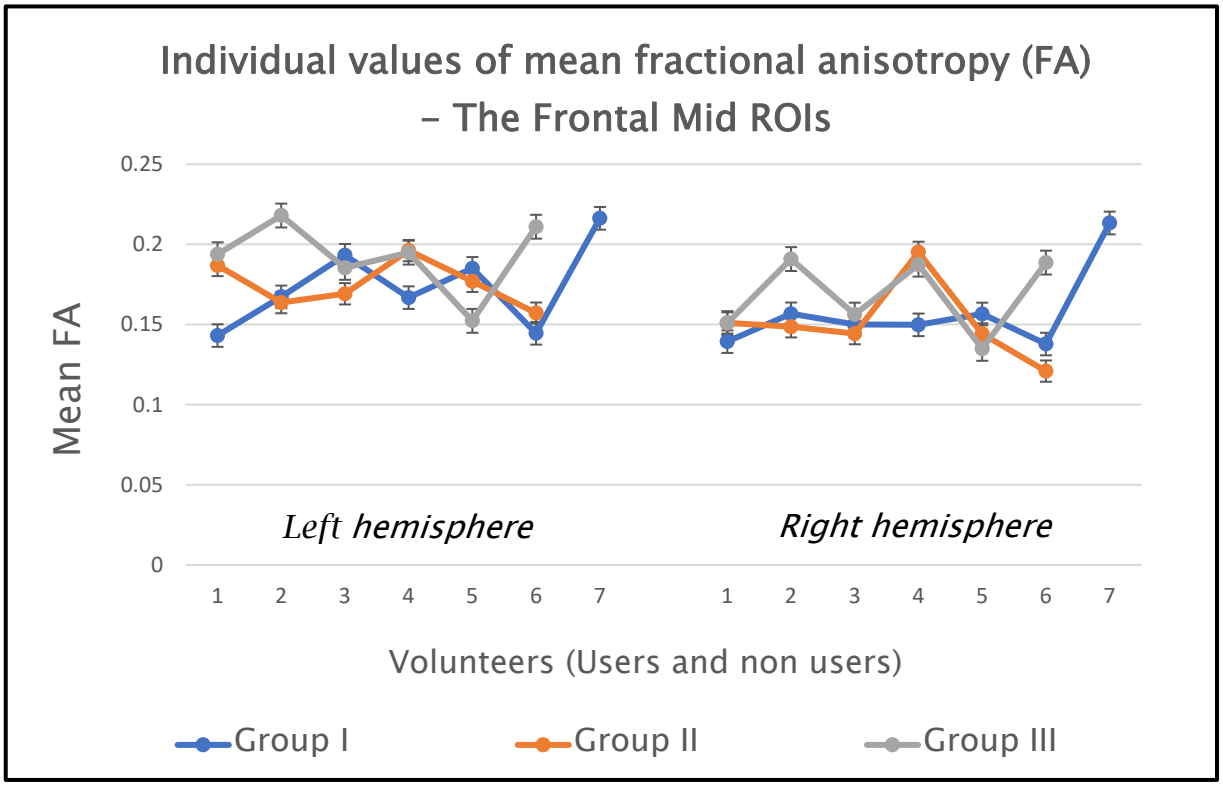

Figure 73: Individual values of mean fractional anisotropy (FA) in both hemispheres' Frontal Mid ROIs. This figure depicts the FA values of all the participants belonging to each of the three groups (Heavy and light users and healthy controls).

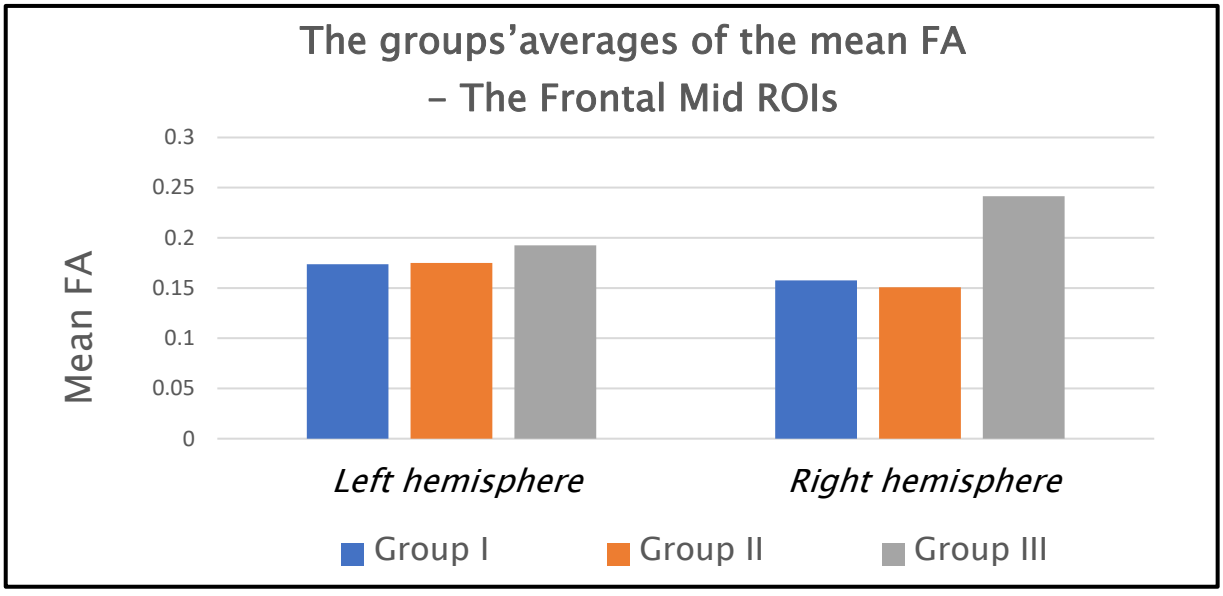

Figure 74: The mean fractional anisotropy (FA) averages of each group in the Frontal Mid ROIs in the left and the right hemispheres.

Table 24: The mean fractional anisotropy (FA) averages and standard deviations (SD) values for the groups studied in the Frontal Mid ROIs, along with intergroup comparisons.

	Left Hemisphere	Right Hemisphere
Heavy users' group (G. I)	(0,173±0,0264)	(0,157±0,0256)
Light users' group (G. II)	(0,174±0,0146)	(0,1506±0,0242)
Non-users' group (G.III)	(0,192±0,02308)	(0,241±0,133)
Intergroup comparison	G.III > G. II ≈ G. I	G.III > G. I ≈ G. II

➢ **Frontal Inf Oper**

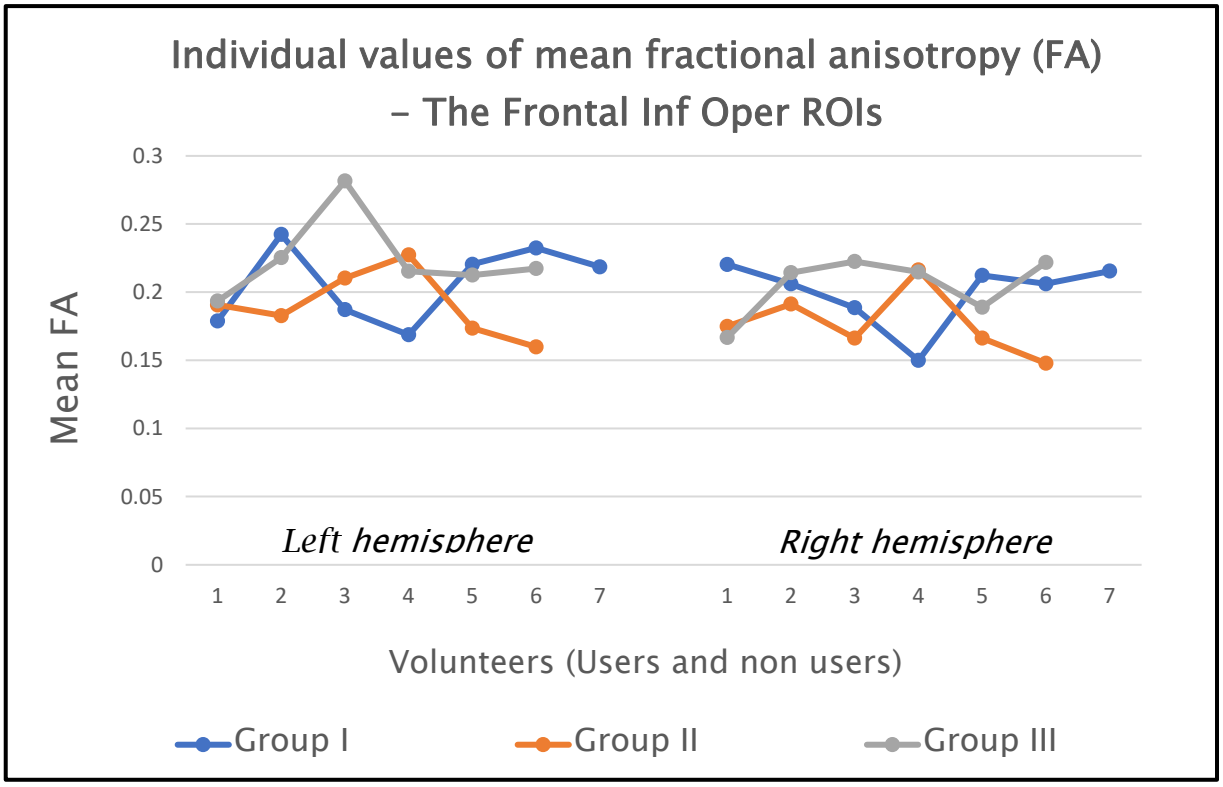

Figure 75: Individual values of mean fractional anisotropy (FA) in both hemispheres' Frontal Inf Oper ROIs. This figure depicts the FA values of all the participants belonging to each of the three groups (Heavy and light users and healthy controls).

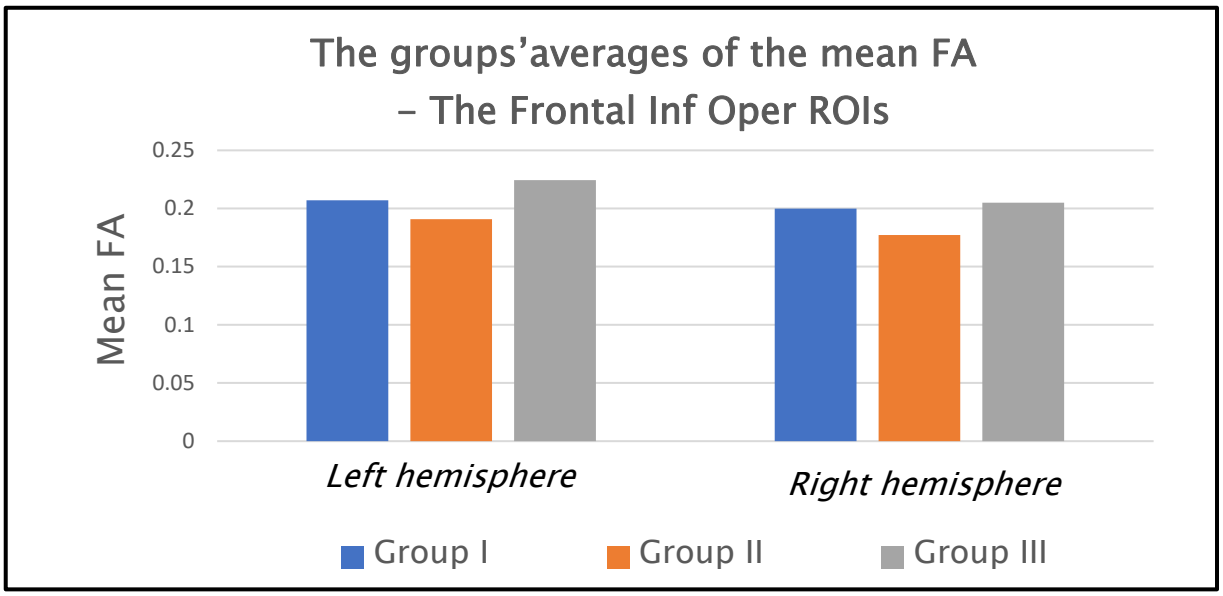

Figure 76: The mean fractional anisotropy (FA) averages of each group in the Frontal Inf Oper ROIs in the left and the right hemispheres.

Table 25: The mean fractional anisotropy (FA) averages and standard deviations (SD) values for the groups studied in the Frontal Inf Oper ROIs, along with intergroup comparisons.

	Left Hemisphere	Right Hemisphere
Heavy users' group (G. I)	(0,2069±0,0284)	(0,199±0,0241)
Light users' group (G. II)	(0,1907±0,0246)	(0,177±0,0238)
Non-users' group (G.III)	(0,224±0,030017)	(0,2048±0,0223)
Intergroup comparison	G.III > G. I > G. II	G.III ≈ G. I > G. II

➢ **Frontal Inf Tri**

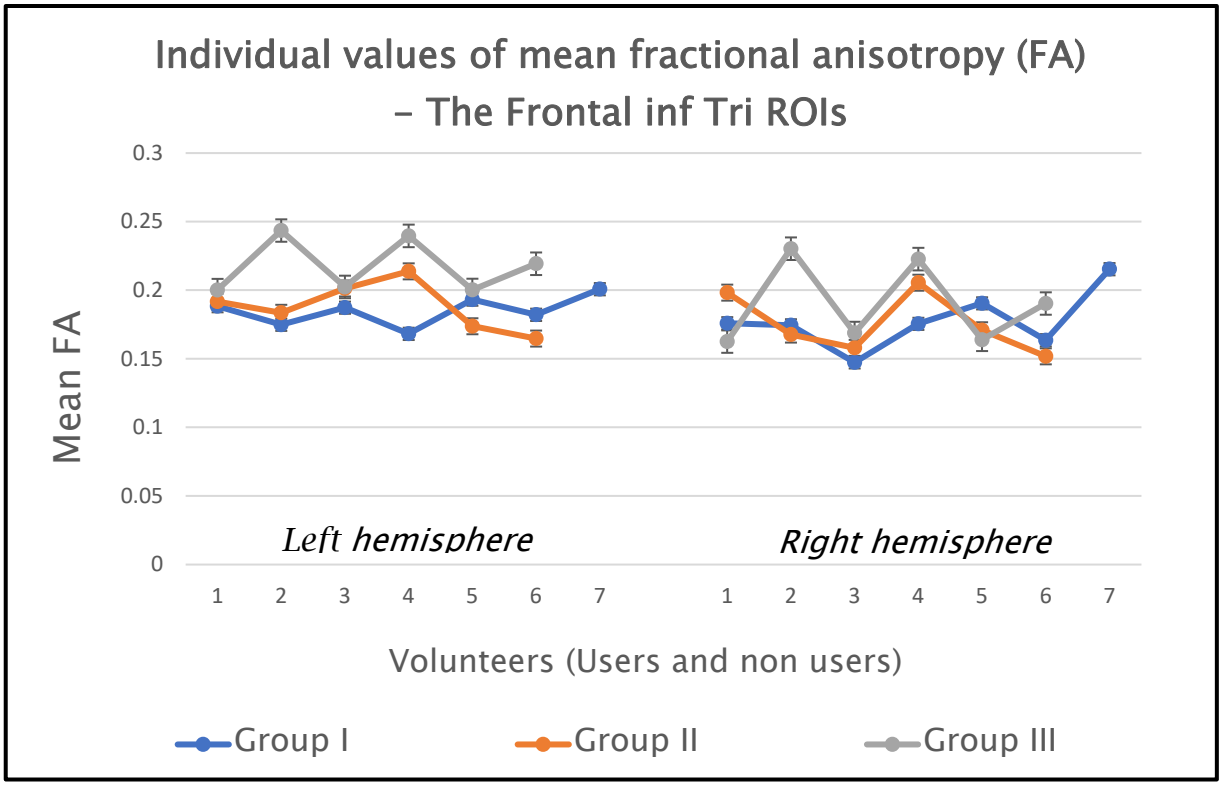

Figure 77: Individual values of mean fractional anisotropy (FA) in both hemispheres' Frontal Inf tri ROIs. This figure depicts the FA values of all the participants belonging to each of the three groups (Heavy and light users and healthy controls).

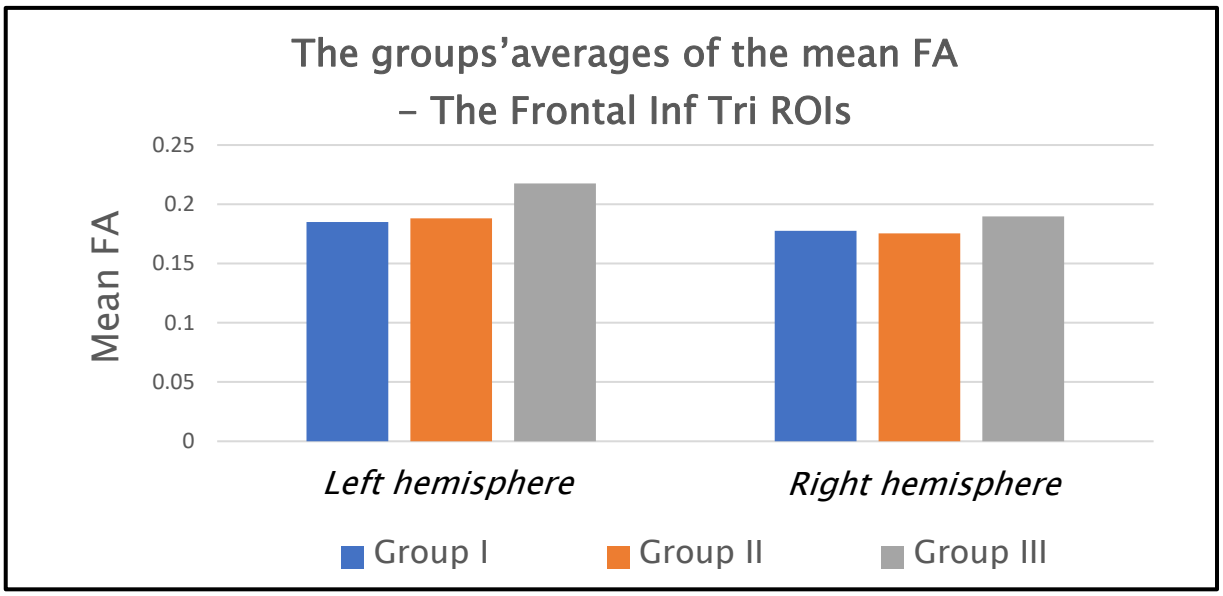

Figure 78: The mean fractional anisotropy (FA) averages of each group in the Frontal Inf Tri ROIs in the left and the right hemispheres.

Table 26: The mean fractional anisotropy (FA) averages and standard deviations (SD) values for the groups studied in the Frontal Inf Tri ROIs, along with intergroup comparisons.

	Left Hemisphere	Right Hemisphere
Heavy users' group (G. I)	(0,184±0,01099)	(0,177±0,0212)
Light users' group (G. II)	(0,188±0,0179)	(0,175±0,0217)
Non-users' group (G.III)	(0,217±0,0199)	(0,189±0,03023)
Intergroup comparison	G.III > G. I ≈ G. II	G.III > G. I ≈ G. II

➢ **Postcentral**

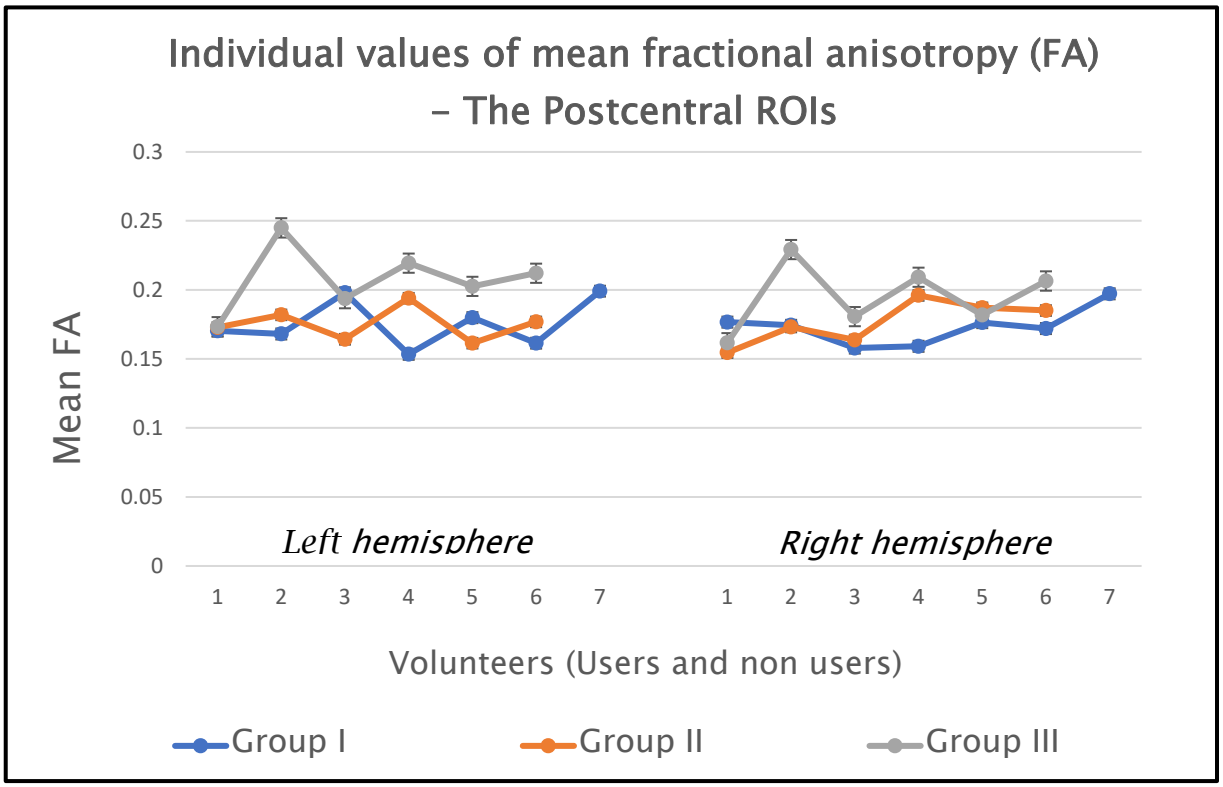

Figure 79: Individual values of mean fractional anisotropy (FA) in both hemispheres' Postcentral ROIs. This figure depicts the FA values of all the participants belonging to each of the three groups (Heavy and light users and healthy controls).

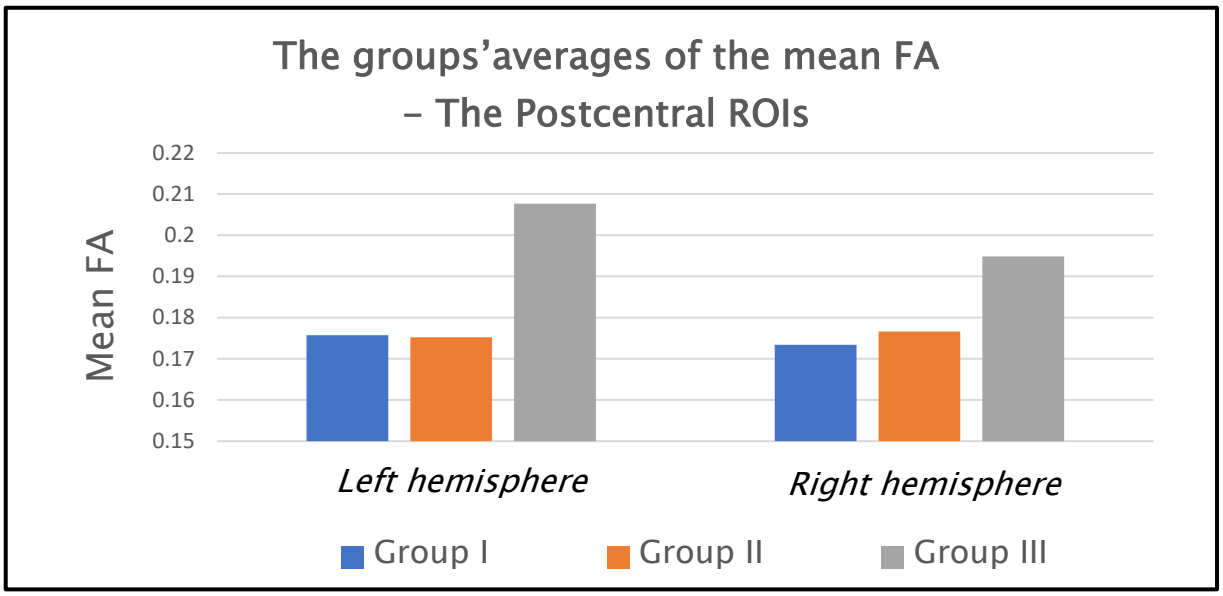

Figure 80: The mean fractional anisotropy (FA) averages of each group in the Postcentral ROIs in the left and the right hemispheres.

Table 27: The mean fractional anisotropy (FA) averages and standard deviations (SD) values for the groups studied in the Postcentral ROIs, along with intergroup comparisons.

	Left Hemisphere	Right Hemisphere
Heavy users' group (G. I)	(0,175±0,0175)	(0,173±0,0131)
Light users' group (G. II)	(0,175±0,0119)	(0,176±0,0156)
Non-users' group (G.III)	(0,2076±0,0242)	(0,194±0,0244)
Intergroup comparison	G.III > G. I ≈ G. II	G.III > G. I ≈ G. II

➢ **Parietal Sup:**

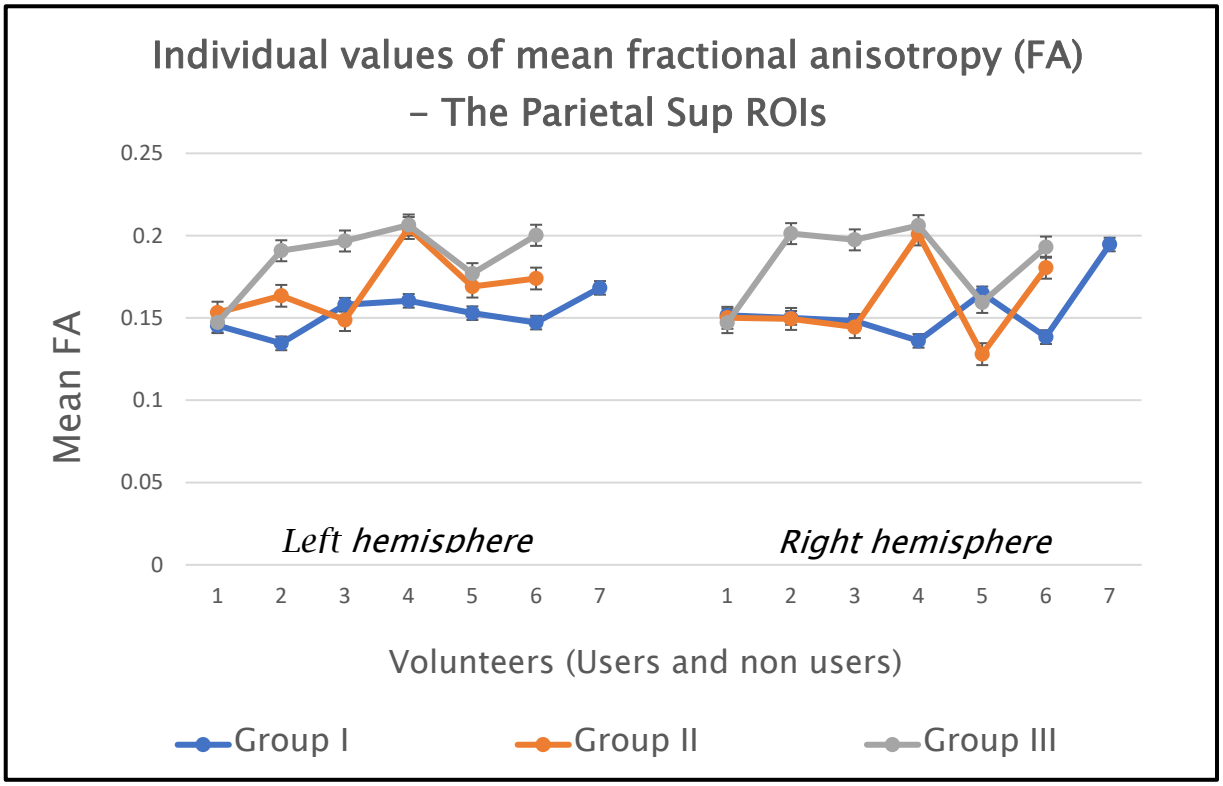

Figure 81: Individual values of mean fractional anisotropy (FA) in both hemispheres' Parietal Sup ROIs. This figure depicts the FA values of all the participants belonging to each of the three groups (Heavy and light users and healthy controls).

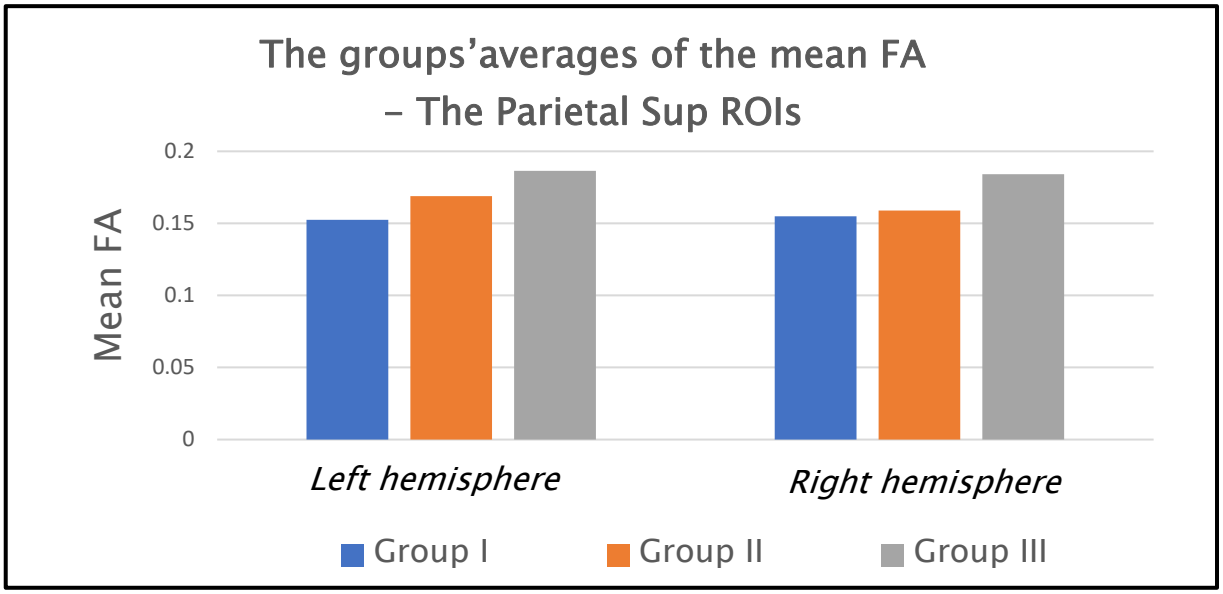

Figure 82: The mean fractional anisotropy (FA) averages of each group in the Parietal Sup ROIs in the left and the right hemispheres.

Table 28: The mean fractional anisotropy (FA) averages and standard deviations (SD) values for the groups studied in the Parietal Sup ROIs, along with intergroup comparisons.

	Left Hemisphere	Right Hemisphere
Heavy users' group (G. I)	(0,152±0,0111)	(0,154±0,0199)
Light users' group (G. II)	(0,168±0,0199)	(0,158±0,0266)
Non-users' group (G.III)	(0,186±0,0216)	(0,184±0,0245)
Intergroup comparison	G.III > G. II > G. I	G.III > G. I ≈ G. II

➢ **SupraMarginal**

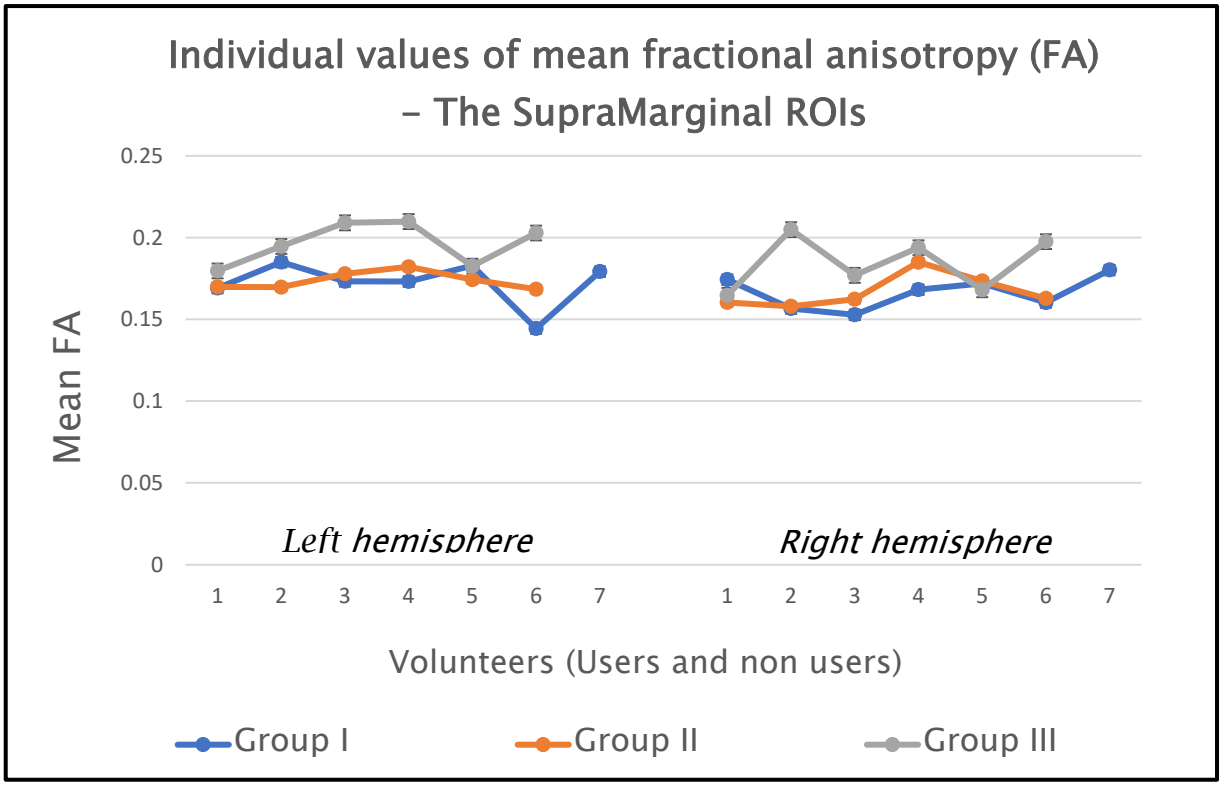

Figure 83: Individual values of mean fractional anisotropy (FA) in both hemispheres' SupraMarginal ROIs. This figure depicts the FA values of all the participants belonging to each of the three groups (Heavy and light users and healthy controls).

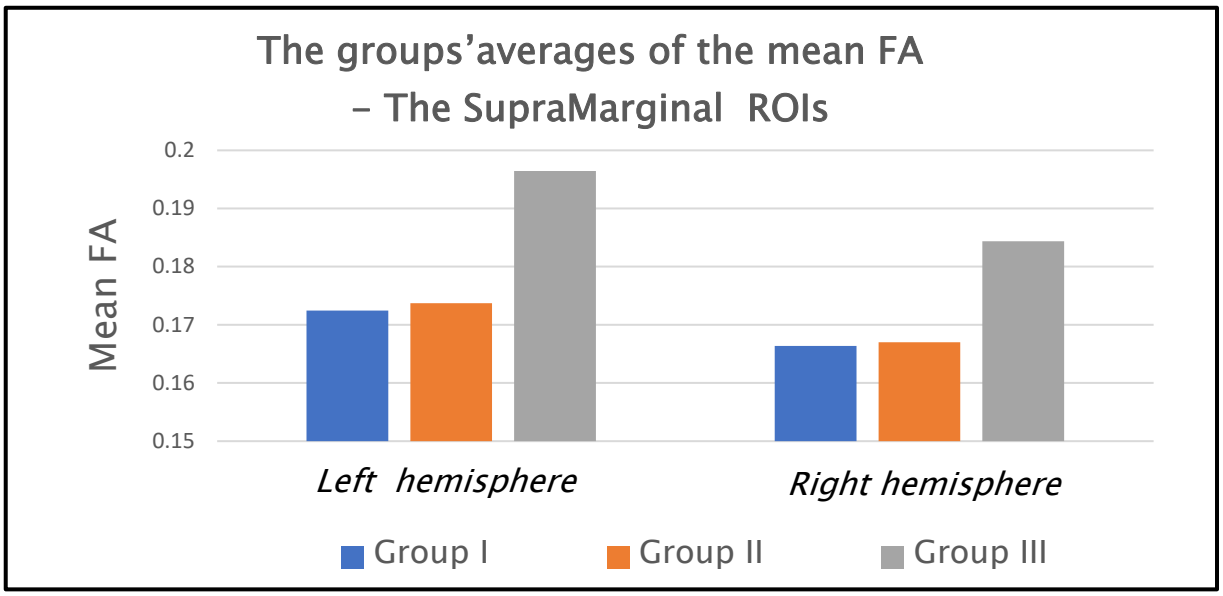

Figure 84: The mean fractional anisotropy (FA) averages of each group in the SupraMarginal ROIs in the left and the right hemispheres.

Table 29: The mean fractional anisotropy (FA) averages and standard deviations (SD) values for the groups studied in the SupraMarginal ROIs, along with intergroup comparisons.

	Left Hemisphere	Right Hemisphere
Heavy users' group (G. I)	(0,172±0,0136)	(0,166±0,0100401)
Light users' group (G. II)	(0,173±0,00543)	(0,166±0,01029)
Non-users' group (G.III)	(0,196±0,01309)	(0,184±0,0166)
Intergroup comparison	G.III > G. II ≈ G. I	G.III > G. I ≈ G. II

➢ Angular

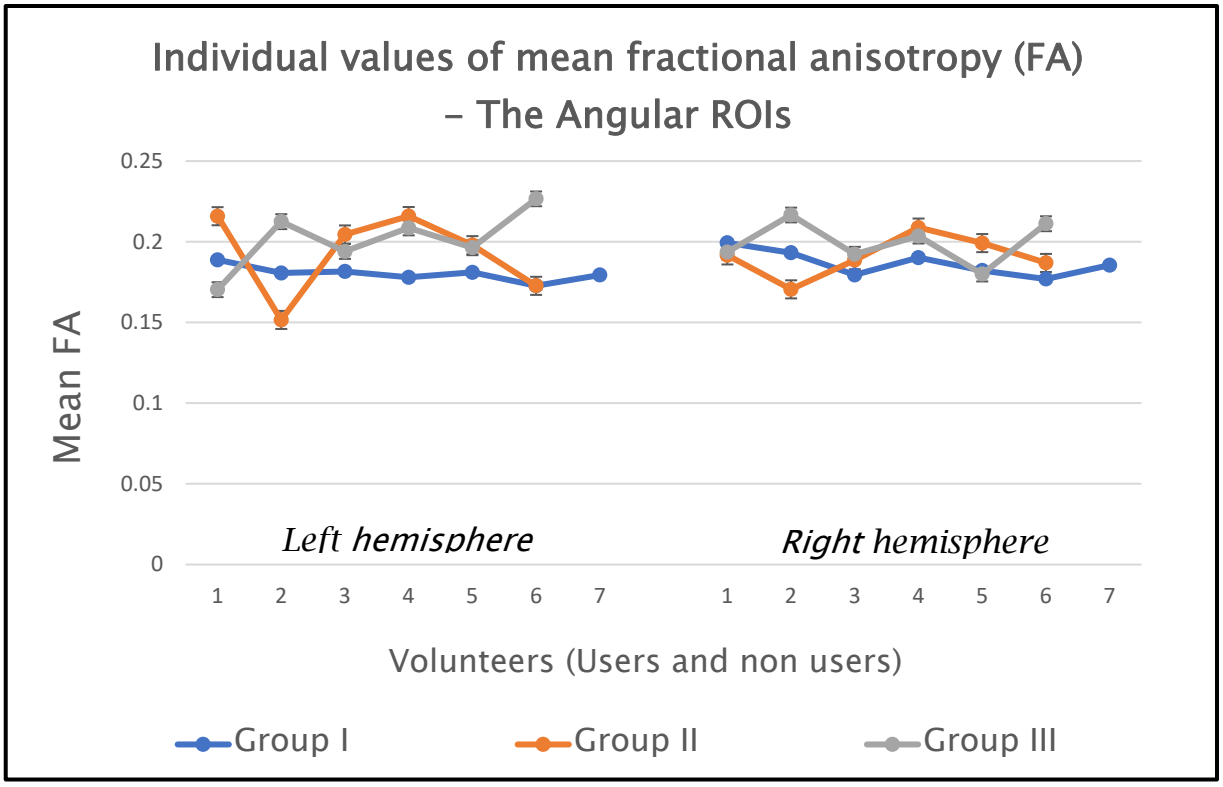

Figure 85: Individual values of mean fractional anisotropy (FA) in both hemispheres' Angular ROIs. This figure depicts the FA values of all the participants belonging to each of the three groups (Heavy and light users and healthy controls).

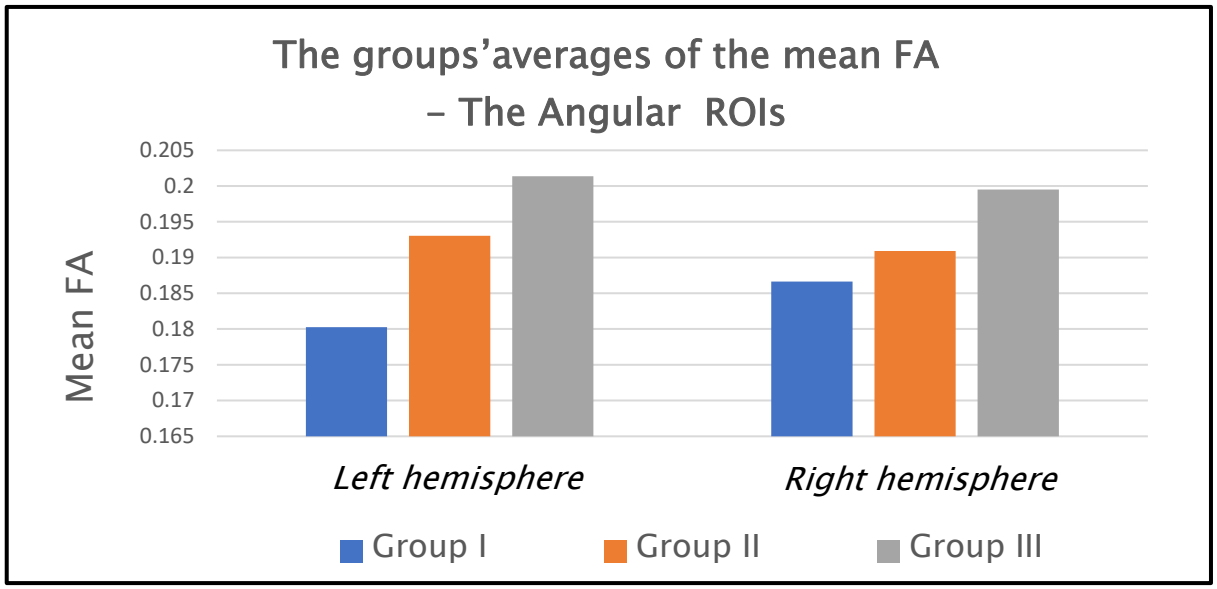

Figure 86: The mean fractional anisotropy (FA) averages of each group in the Angular ROIs in the left and the right hemispheres.

Table 30: The mean fractional anisotropy (FA) averages and standard deviations (SD) values for the groups studied in the Angular ROIs, along with intergroup comparisons.

	Left Hemisphere	Right Hemisphere
Heavy users' group (G. I)	(0,1802±0,00477)	(0,186±0,008019)
Light users' group (G. II)	(0,193±0,0257)	(0,1909±0,0128)
Non-users' group (G.III)	(0,2013±0,0192)	(0,242±0,114)
Intergroup comparison	G.III > G. II > G. I	G.III > G. I ≈ G. II

➢ **Parietal Inf**

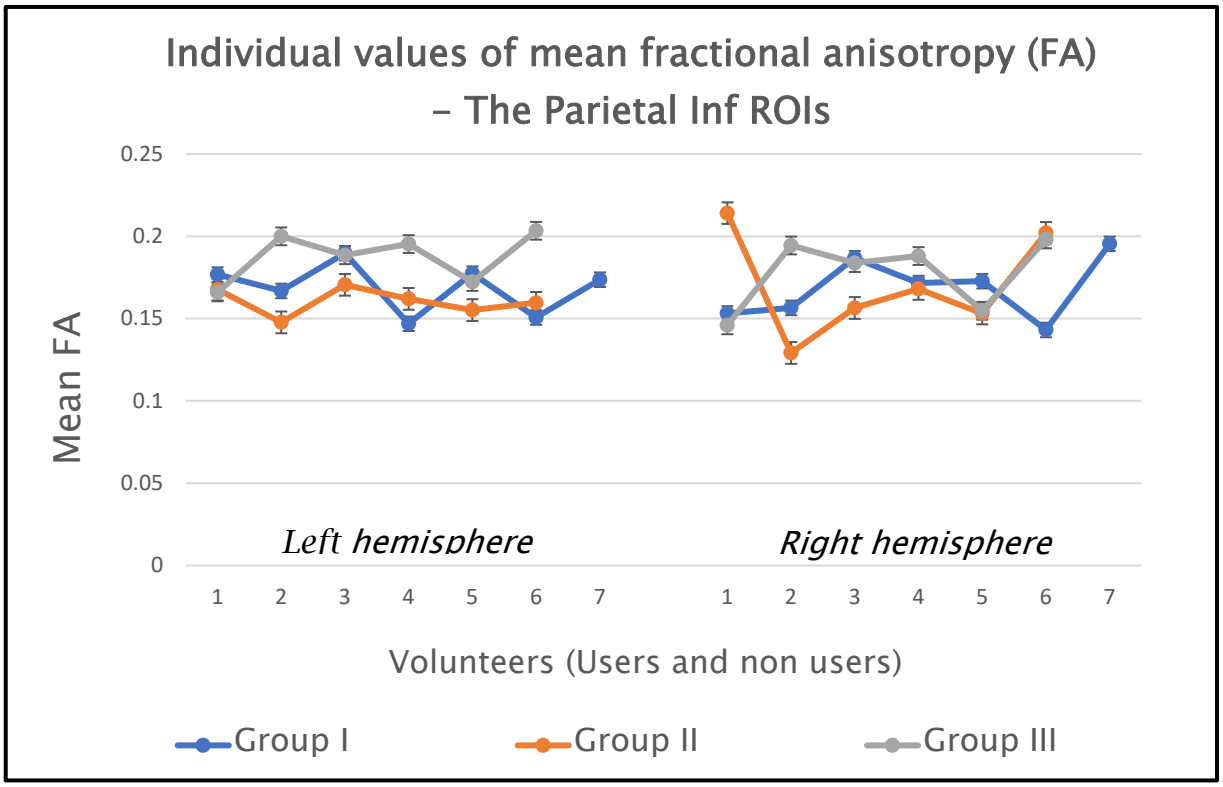

Figure 87: Individual values of mean fractional anisotropy (FA) in both hemispheres' Parietal Inf ROIs. This figure depicts the FA values of all the participants belonging to each of the three groups (Heavy and light users and healthy controls).

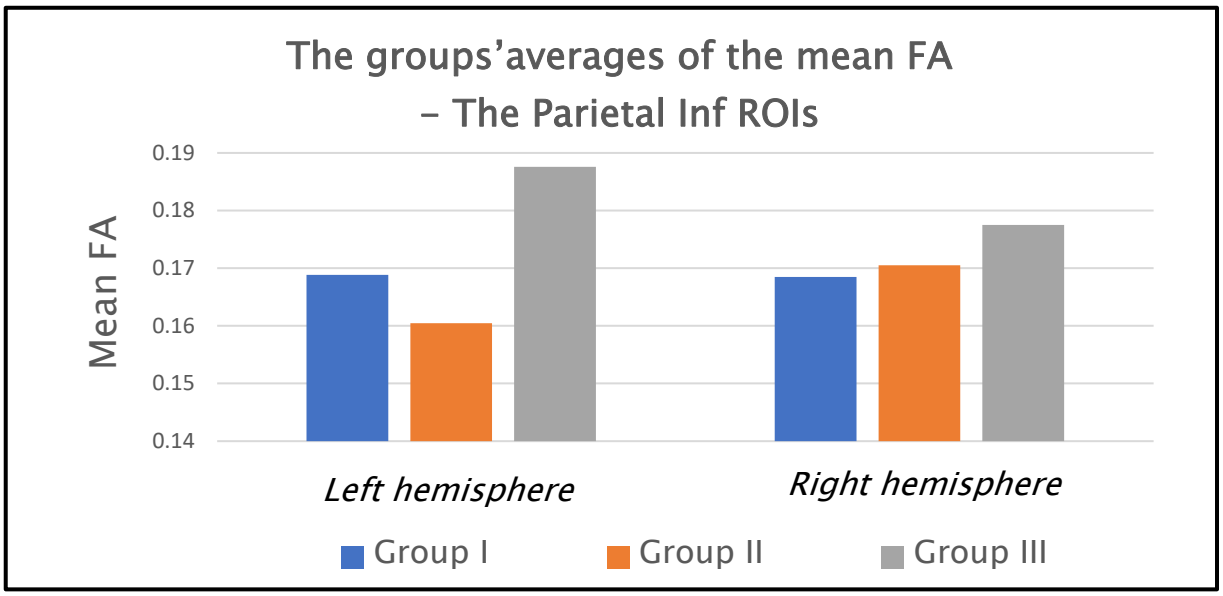

Figure 88: The mean fractional anisotropy (FA) averages of each group in the Parietal Inf ROIs in the left and the right hemispheres.

Table 31: The mean fractional anisotropy (FA) averages and standard deviations (SD) values for the groups studied in the Parietal Inf ROIs, along with intergroup comparisons.

	Left Hemisphere	Right Hemisphere
Heavy users' group (G. I)	(0,168±0,0153)	(0,168±0,0187)
Light users' group (G. II)	(0,1604±0,00832)	(0,1704±0,0319)
Non-users' group (G.III)	(0,187±0,0152)	(0,177±0,0217)
Intergroup comparison	G.III > G. I > G. II	G.III > G. II ≈ G. I

➢ **Precuneus**

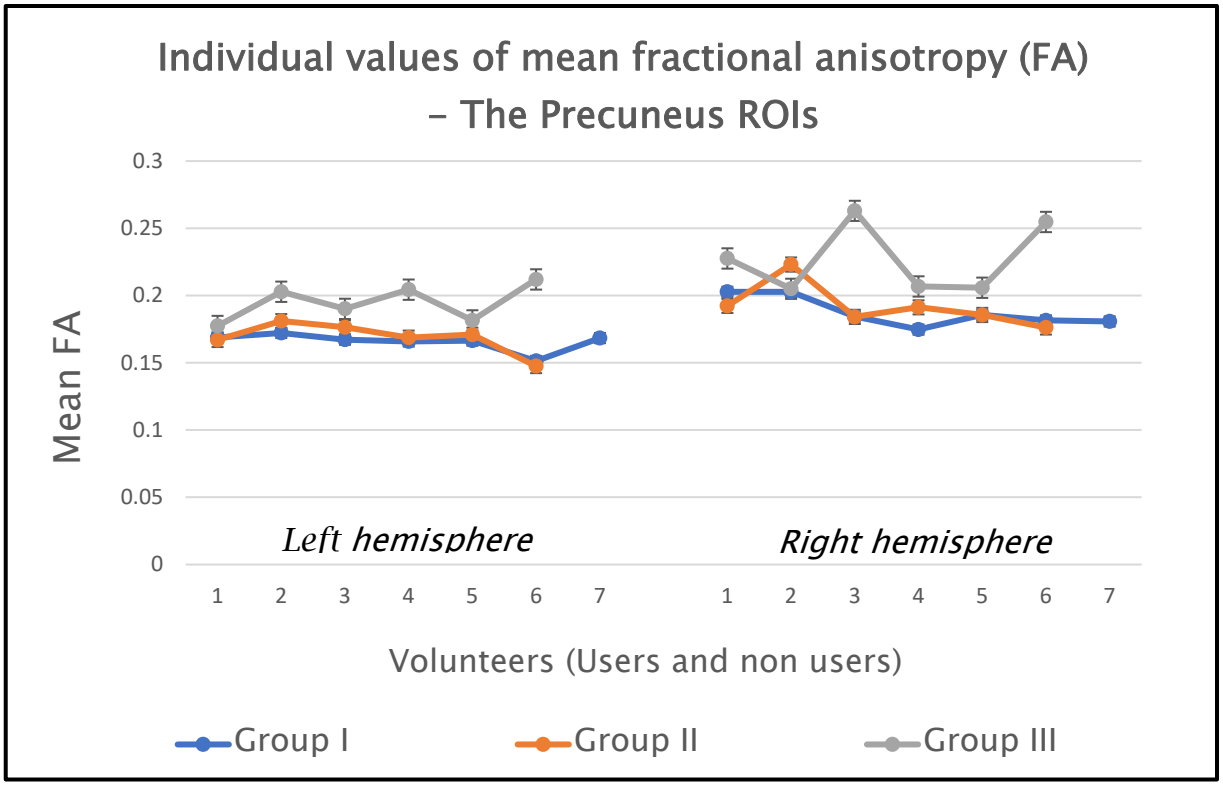

Figure 89: Individual values of mean fractional anisotropy (FA) in both hemispheres' Precuneus ROIs. This figure depicts the FA values of all the participants belonging to each of the three groups (Heavy and light users and healthy controls).

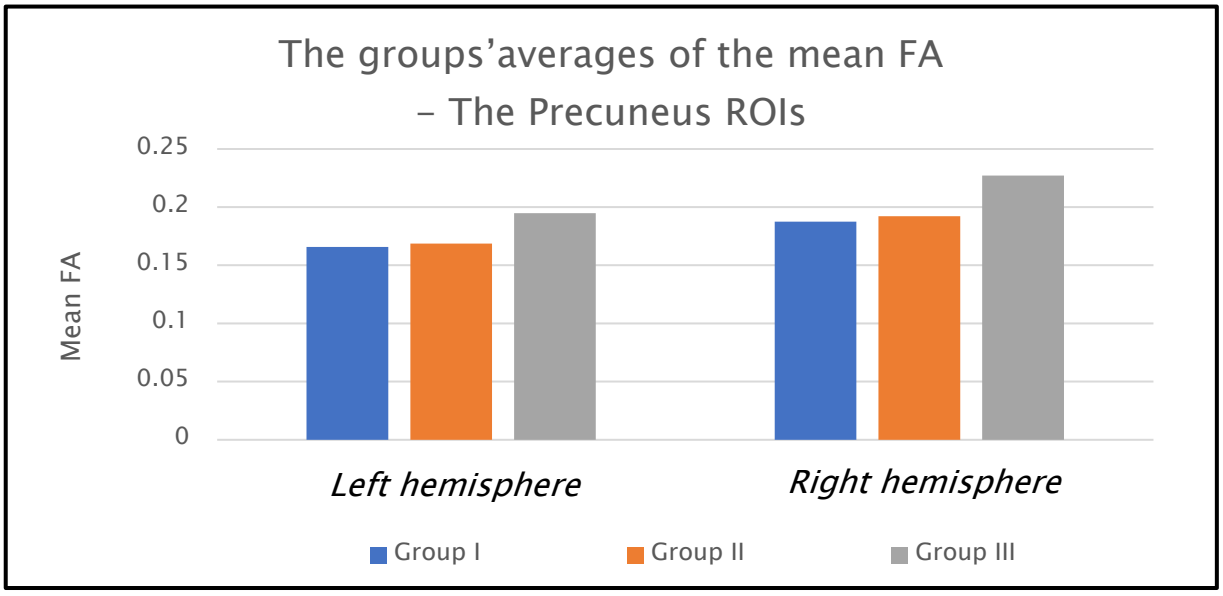

Figure 90: The mean fractional anisotropy (FA) averages of each group in the Precuneus ROIs in the left and the right hemispheres.

Table 32: The mean fractional anisotropy (FA) averages and standard deviations (SD) values for the groups studied in the Precuneus ROIs, along with intergroup comparisons.

	Left Hemisphere	Right Hemisphere
Heavy users' group (G. I)	(0,165±0,00668)	(0,187±0,011002)
Light users' group (G. II)	(0,168±0,0115)	(0,192±0,0162)
Non-users' group (G.III)	(0,194±0,0137)	(0,227±0,026107)
Intergroup comparison	G.III > G. II ≈ G. I	G.III > G. II > G. I

➢ **Temporal sup**

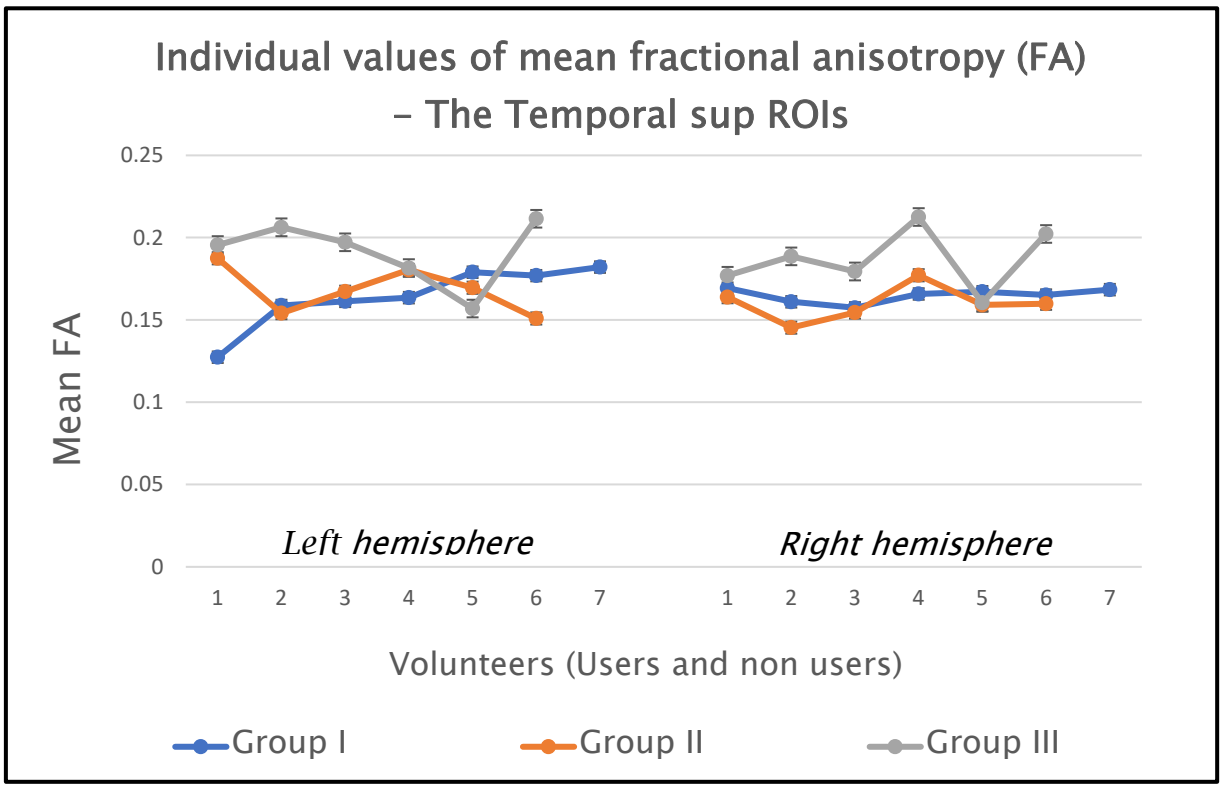

Figure 91: Individual values of mean fractional anisotropy (FA) in both hemispheres' Temporal Sup ROIs. This figure depicts the FA values of all the participants belonging to each of the three groups (Heavy and light users and healthy controls).

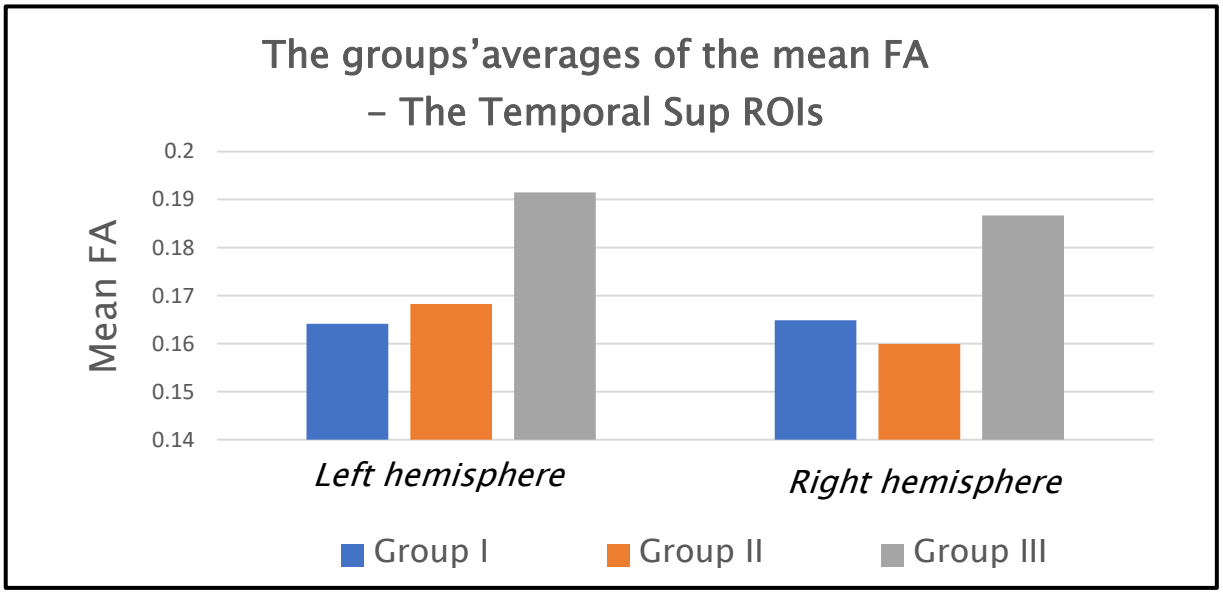

Figure 92: The mean fractional anisotropy (FA) averages of each group in the temporal Sup ROIs in the left and the right hemispheres.

Table 33: The mean fractional anisotropy (FA) averages and standard deviations (SD) values for the groups studied in the temporal Sup ROIs, along with intergroup comparisons.

	Left Hemisphere	Right Hemisphere
Heavy users' group (G. I)	(0,164±0,0186)	(0,164±0,00426)
Light users' group (G. II)	(0,168±0,0142)	(0,159±0,01054)
Non-users' group (G.III)	(0,191±0,0198)	(0,186±0,0187)
Intergroup comparison	G.III > G. II ≈ G. I	G.III > G. I > G. II

➢ Temporal Pole Sup

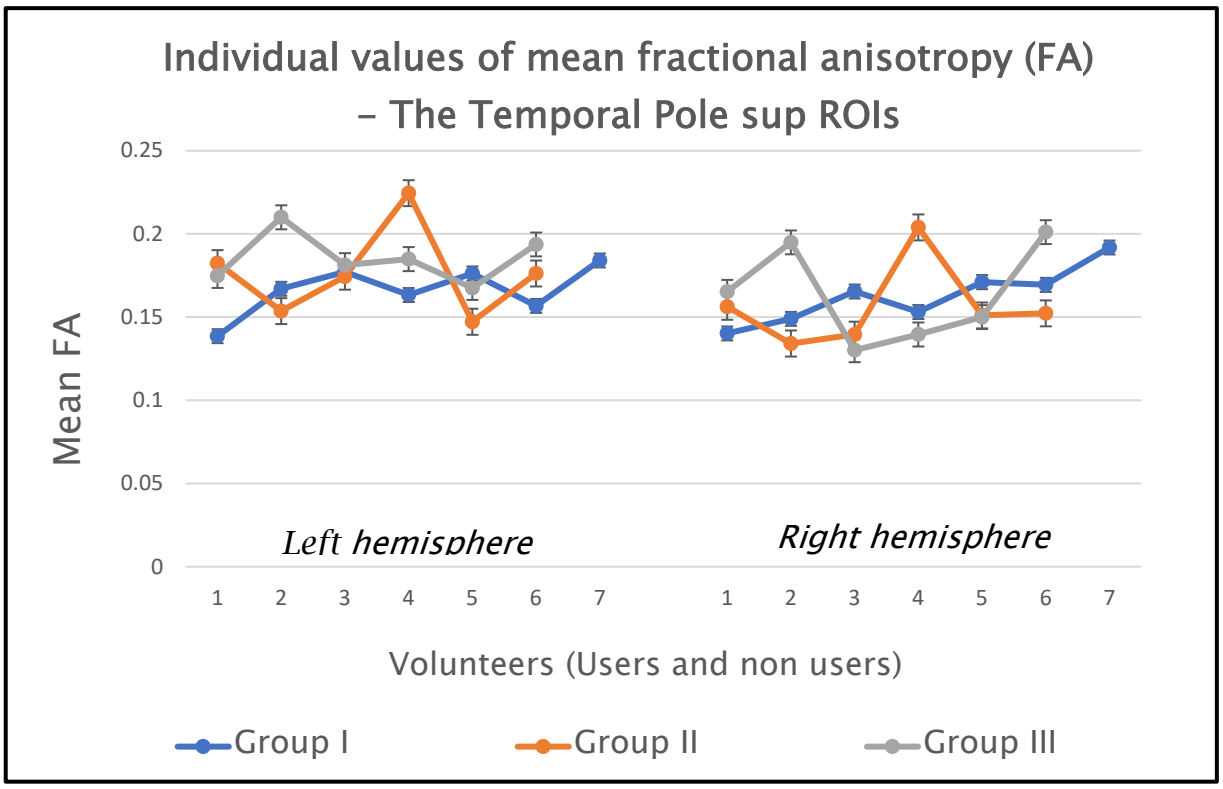

Figure 93: Individual values of mean fractional anisotropy (FA) in both hemispheres' Temporal Pole sup ROIs. This figure depicts the FA values of all the participants belonging to each of the three groups (Heavy and light users and healthy controls).

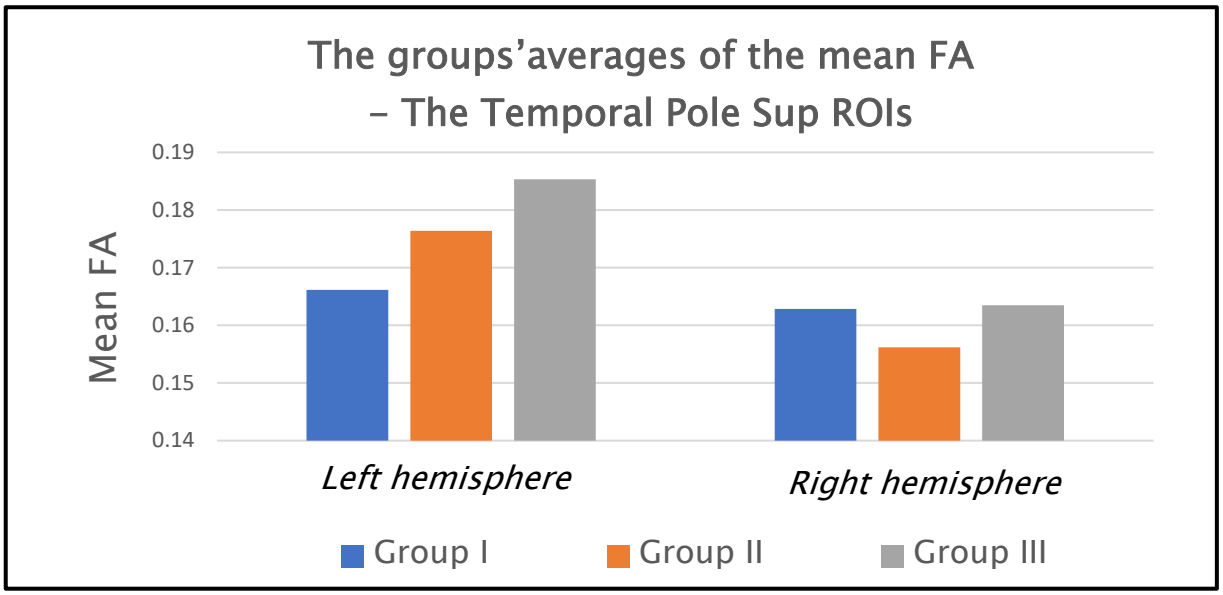

Figure 94: The mean fractional anisotropy (FA) averages of each group in the temporal Pole sup ROIs in the left and the right hemispheres.

Table 34: The mean fractional anisotropy (FA) averages and standard deviations (SD) values for the groups studied in the temporal Pole Sup ROIs, along with intergroup comparisons.

	Left Hemisphere	Right Hemisphere
Heavy users' group (G. I)	(0,166±0,0152)	(0,162±0,0171)
Light users' group (G. II)	(0,176±0,0273)	(0,156±0,0248)
Non-users' group (G.III)	(0,185±0,0149)	(0,163±0,0292)
Intergroup comparison	G.III > G. II > G. I	G.III ≈ G. I > G. II

➢ **Heschl**

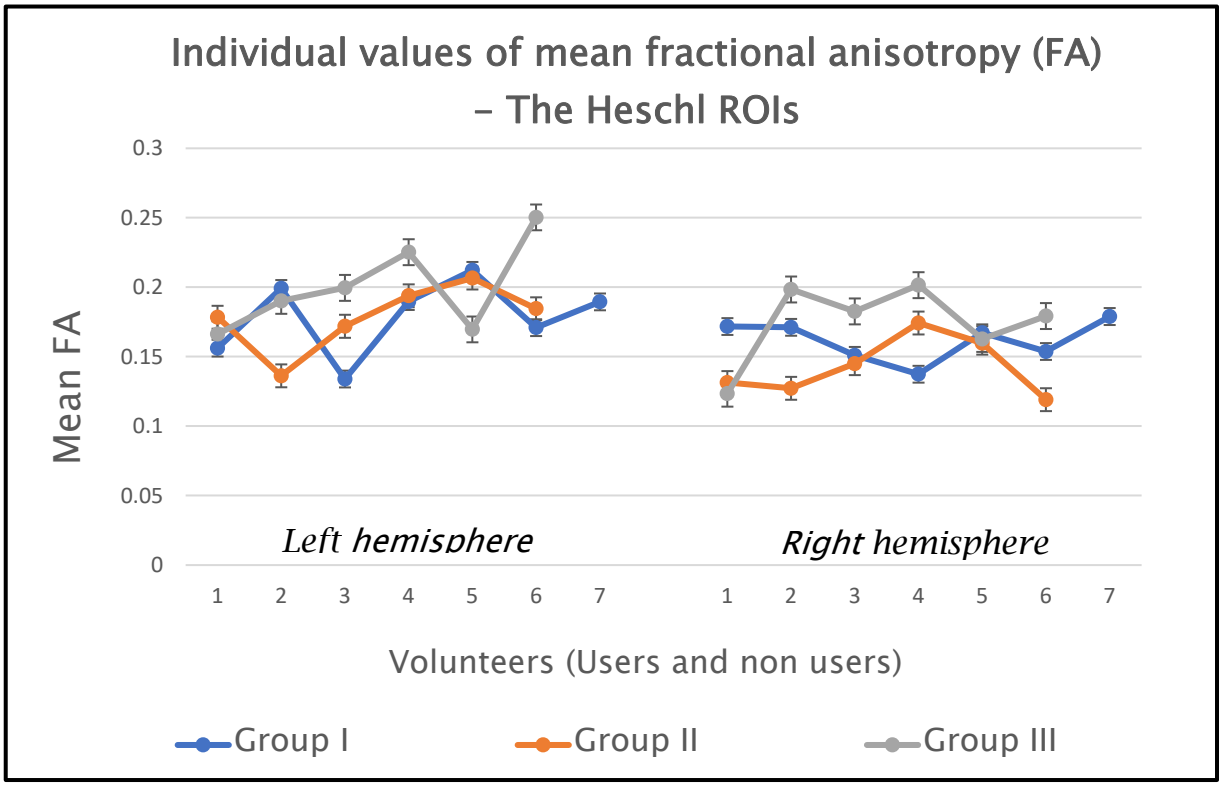

Figure 95: Individual values of mean fractional anisotropy (FA) in both hemispheres' Heschl ROIs. This figure depicts the FA values of all the participants belonging to each of the three groups (Heavy and light users and healthy controls).

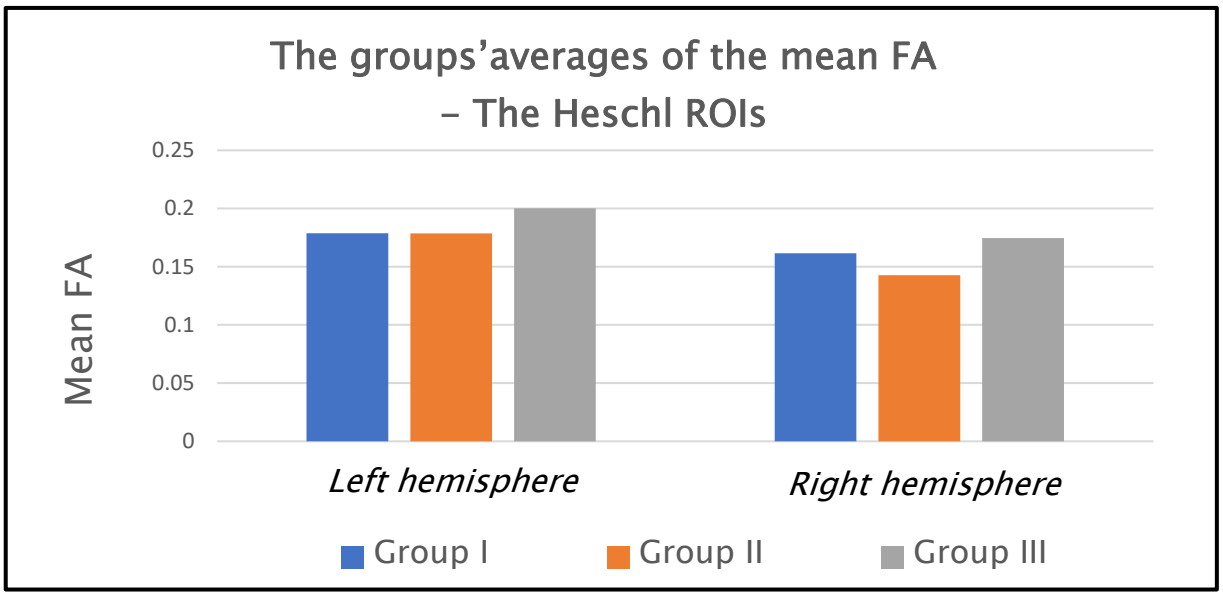

Figure 96: The mean fractional anisotropy (FA) averages of each group in the Heschl ROIs in the left and the right hemispheres.

Table 35: The mean fractional anisotropy (FA) averages and standard deviations (SD) values for the groups studied in the Heschl ROIs, along with intergroup comparisons.

	Left Hemisphere	Right Hemisphere
Heavy users' group (G. I)	(0,178±0,0269)	(0,161±0,0146)
Light users' group (G. II)	(0,178±0,02407)	(0,142±0,02103)
Non-users' group (G.III)	(0,20014±0,0326)	(0,174±0,0287)
Intergroup comparison	G.III > G. II ≈ G. I	G.III > G. I > G. II

➢ Temporal Mid

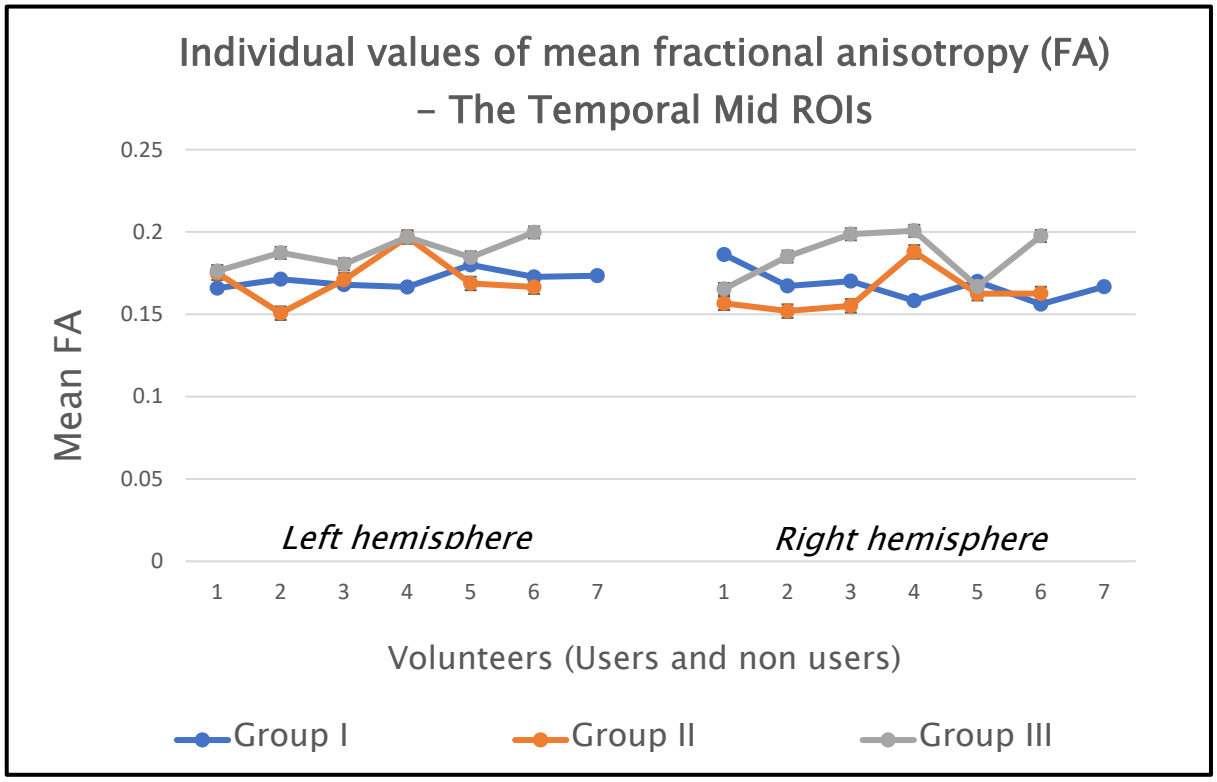

Figure 97: Individual values of mean fractional anisotropy (FA) in both hemispheres' Temporal Mid ROIs. This figure depicts the FA values of all the participants belonging to each of the three groups (Heavy and light users and healthy controls).

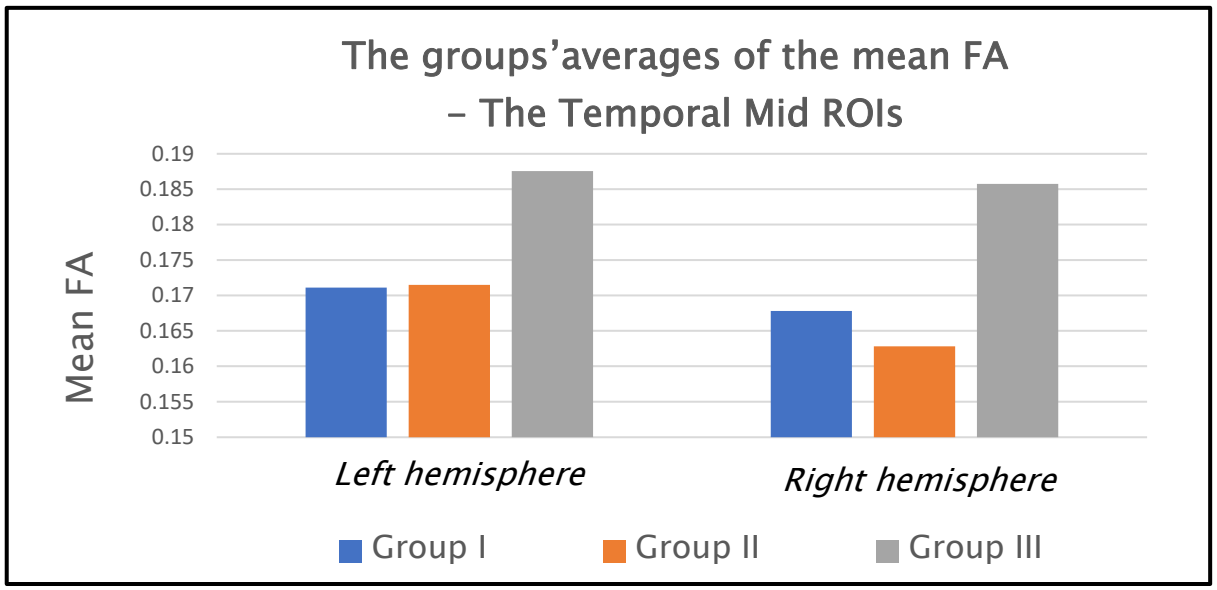

Figure 98: The mean fractional anisotropy (FA) averages of each group in the Temporal Mid ROIs in the left and the right hemispheres.

Table 36: The mean fractional anisotropy (FA) averages and standard deviations (SD) values for the groups studied in the Temporal Mid ROIs, along with intergroup comparisons.

	Left Hemisphere	Right Hemisphere
Heavy users' group (G. I)	(0,171±0,00491)	(0,167±0,00984)
Light users' group (G. II)	(0,171±0,0149)	(0,162±0,0129)
Non-users' group (G.III)	(0,187±0,009205)	(0,185±0,0161)
Intergroup comparison	G.III > G. II ≈ G. I	G.III > G. I > G. II

➢ **Temporal Pole Mid**

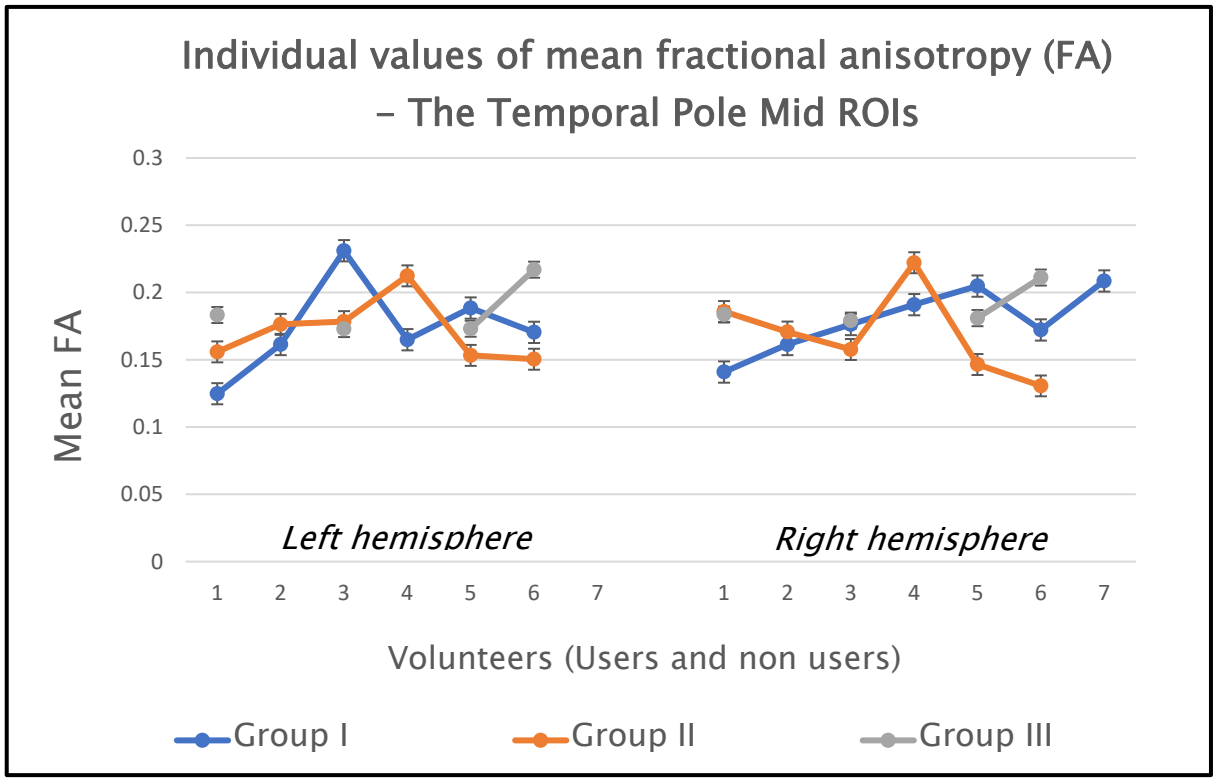

Figure 99: Individual values of mean fractional anisotropy (FA) in both hemispheres' Temporal Pole Mid ROIs. This figure depicts the FA values of all the participants belonging to each of the three groups (Heavy and light users and healthy controls).

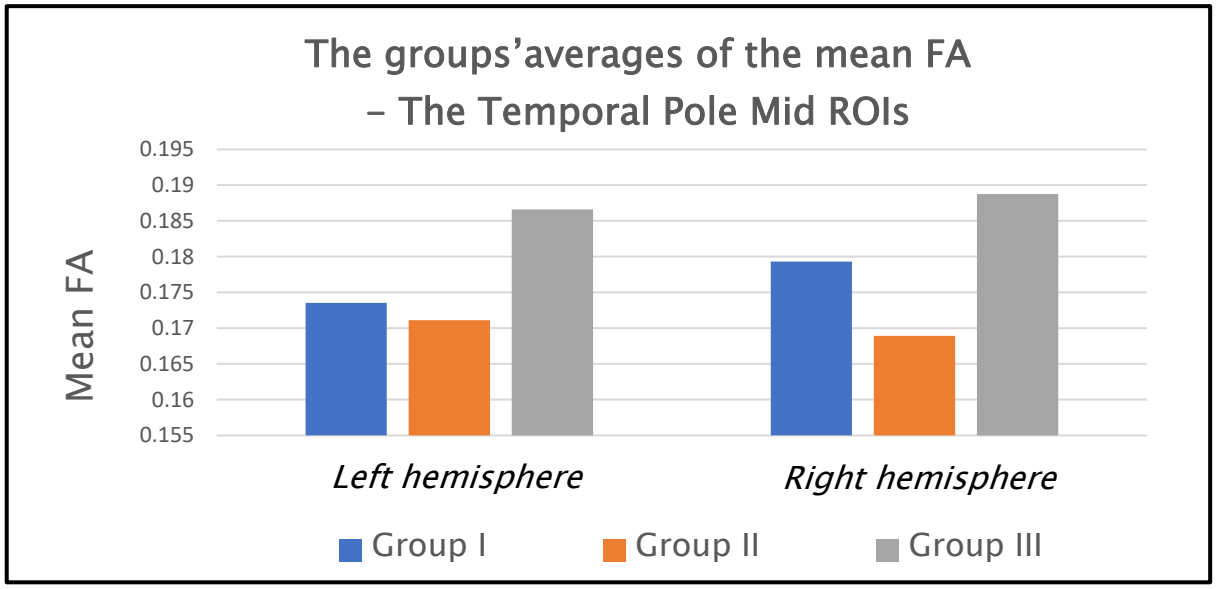

Figure 100: The mean fractional anisotropy (FA) averages of each group in the Temporal Pole Mid ROIs in the left and the right hemispheres.

Table 37: The mean fractional anisotropy (FA) averages and standard deviations (SD) values for the groups studied in the Temporal Pole Mid ROIs, along with intergroup comparisons.

	Left Hemisphere	Right Hemisphere
Heavy users' group (G. I)	(0,173±0,03503)	(0,179±0,0241)
Light users' group (G. II)	(0,171±0,0235)	(0,168±0,0323)
Non-users' group (G.III)	(0,186±0,02084)	(0,188±0,01505)
Intergroup comparison	G.III > G. I ≈ G. II	G.III > G. I > G. II

➢ Temporal Inf

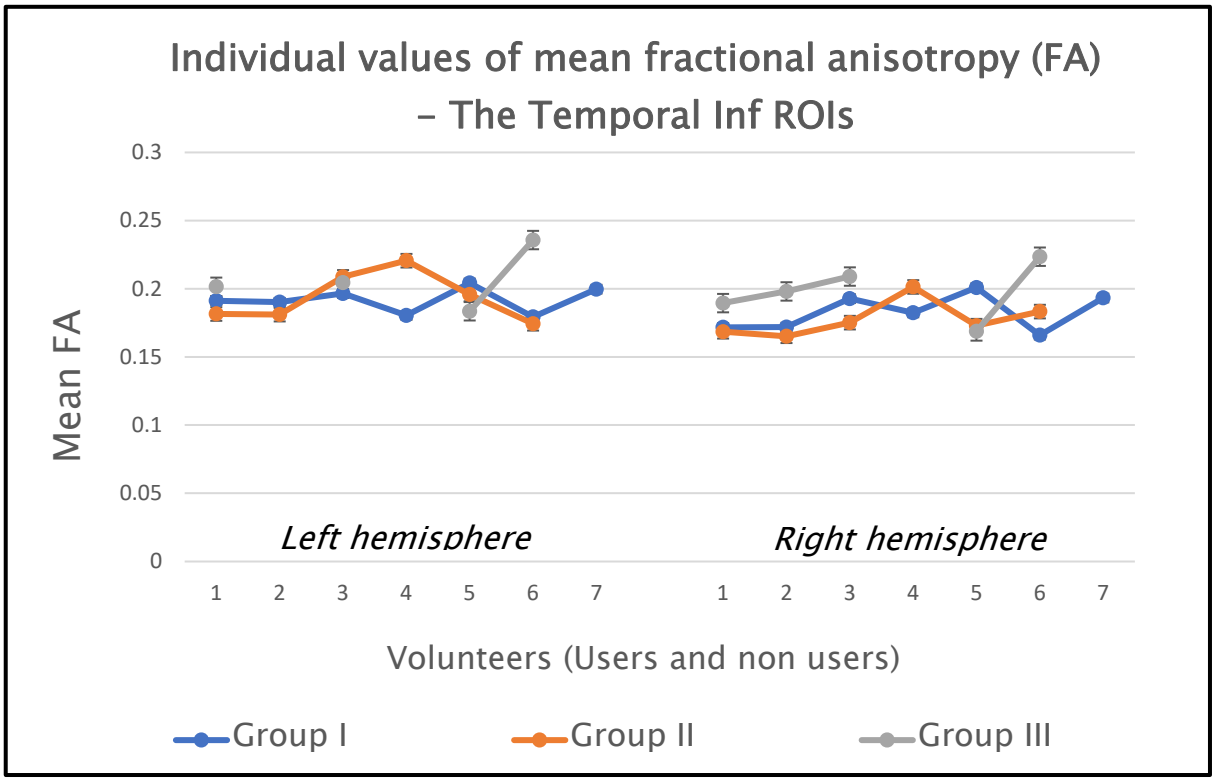

Figure 101: Individual values of mean fractional anisotropy (FA) in both hemispheres' Temporal Inf ROIs. This figure depicts the FA values of all the participants belonging to each of the three groups (Heavy and light users and healthy controls).

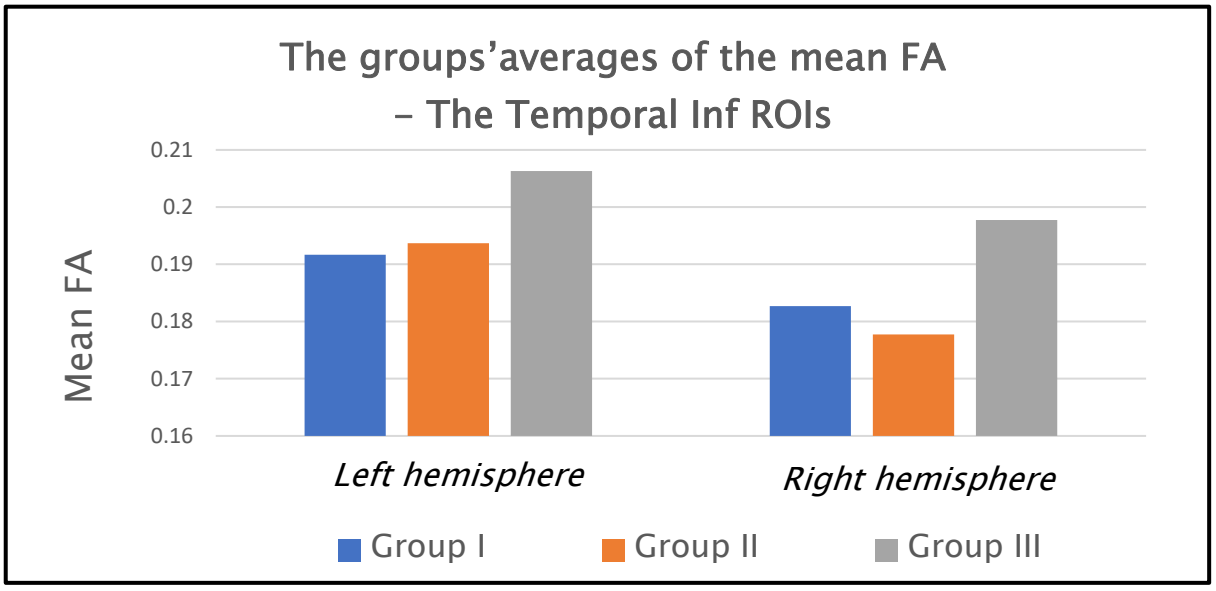

Figure 102: The mean fractional anisotropy (FA) averages of each group in the Temporal Inf ROIs in the left and the right hemispheres.

Table 38: The mean fractional anisotropy (FA) averages and standard deviations (SD) values for the groups studied in the Temporal Inf ROIs, along with intergroup comparisons.

	Left Hemisphere	Right Hemisphere
Heavy users' group (G. I)	(0,191±0,00937)	(0,182±0,0132)
Light users' group (G. II)	(0,193±0,0181)	(0,177±0,0131)
Non-users' group (G.III)	(0,2063±0,0216)	(0,197±0,02061)
Intergroup comparison	G.III > G. II ≈ G. I	G.III > G. I > G. II

➢ **Fusiform**

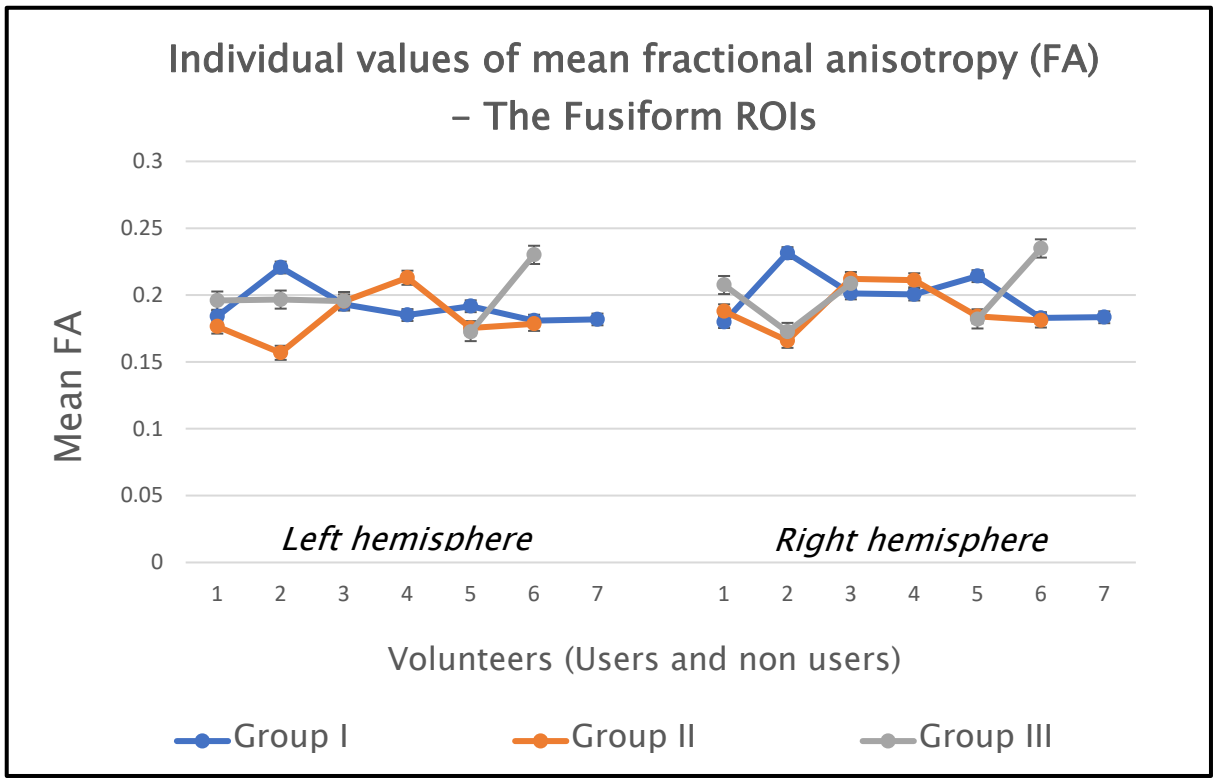

Figure 103: Individual values of mean fractional anisotropy (FA) in both hemispheres' Fusiform ROIs. This figure depicts the FA values of all the participants belonging to each of the three groups (Heavy and light users and healthy controls).

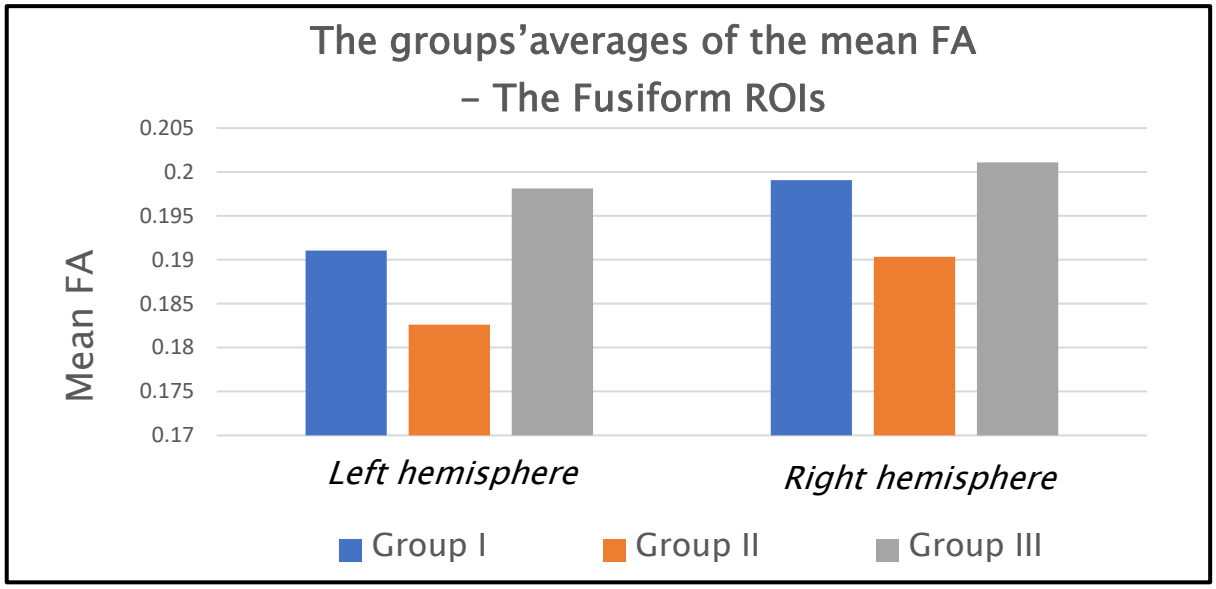

Figure 104: The mean fractional anisotropy (FA) averages of each group in the Fusiform ROIs in the left and the right hemispheres.

Table 39: The mean fractional anisotropy (FA) averages and standard deviations (SD) values for the groups studied in the Fusiform ROIs, along with intergroup comparisons.

	Left Hemisphere	Right Hemisphere
Heavy users' group (G. I)	(0,191±0,0138)	(0,199±0,0189)
Light users' group (G. II)	(0,182±0,0192)	(0,1903±0,01808)
Non-users' group (G.III)	(0,198±0,02062)	(0,20108±0,0246)
Intergroup comparison	G.III > G. I > G. II	G.III ≈ G. I > G. II

➢ Cingulum Ant

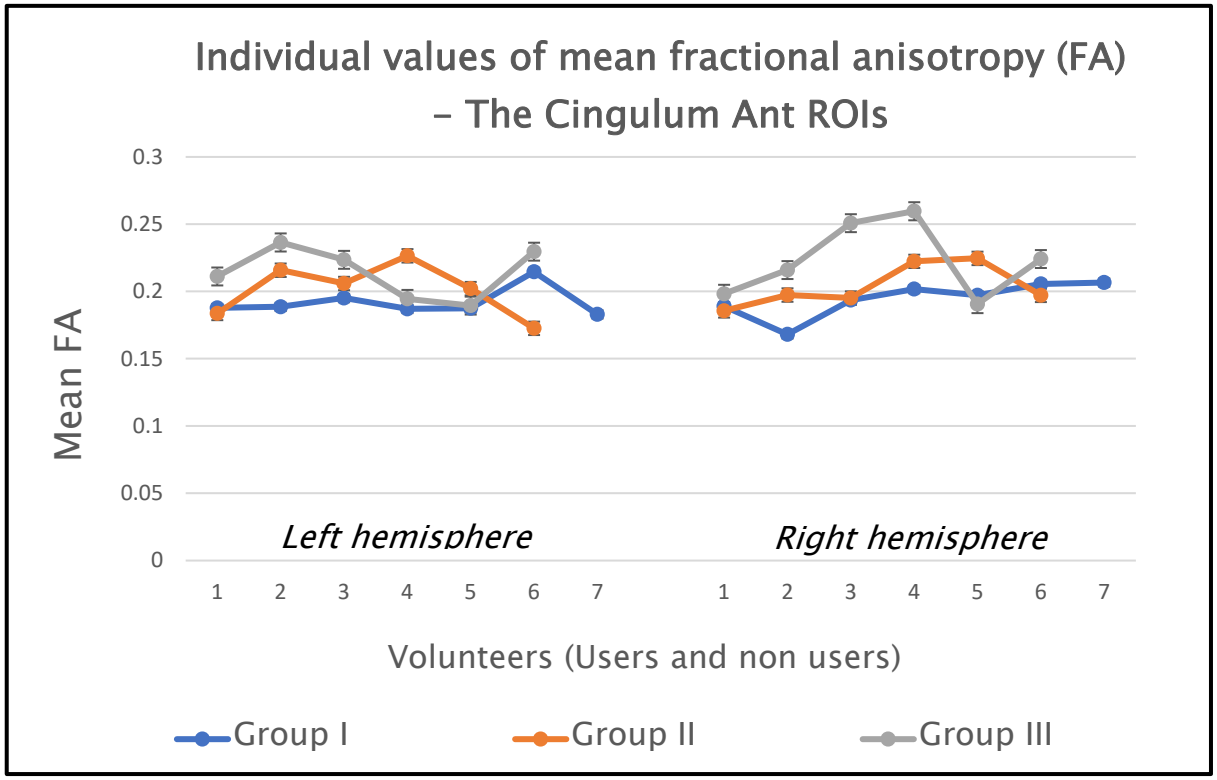

Figure 105: Individual values of mean fractional anisotropy (FA) in both hemispheres' Cingulum Ant ROIs. This figure depicts the FA values of all the participants belonging to each of the three groups (Heavy and light users and healthy controls).

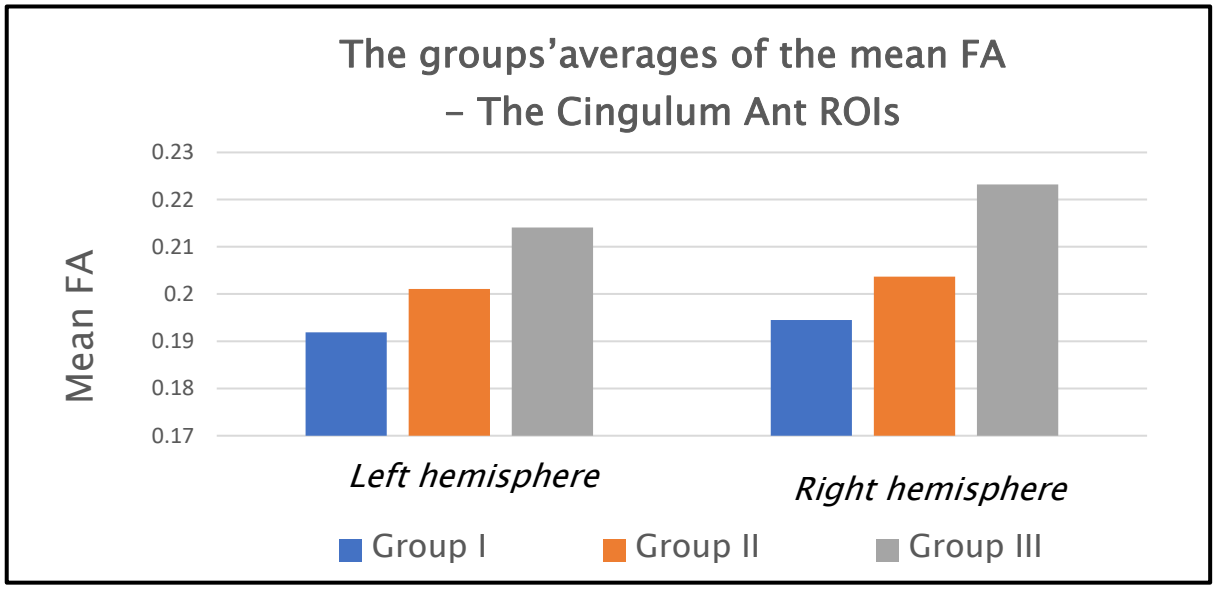

Figure 105: The mean fractional anisotropy (FA) averages of each group in the Cingulum Ant ROIs in the left and the right hemispheres.

Table 40: The mean fractional anisotropy (FA) averages and standard deviations (SD) values for the groups studied in the Cingulum Ant ROIs, along with intergroup comparisons.

	Left Hemisphere	Right Hemisphere
Heavy users' group (G. I)	(0,191±0,01061)	(0,194±0,0132)
Light users' group (G. II)	(0,20107±0,020011)	(0,2036±0,0159)
Non-users' group (G.III)	(0,214±0,0191)	(0,223±0,0276)
Intergroup comparison	G.III > G. II > G. I	G.III > G. II > G. I

➢ **Cingulum Mid**

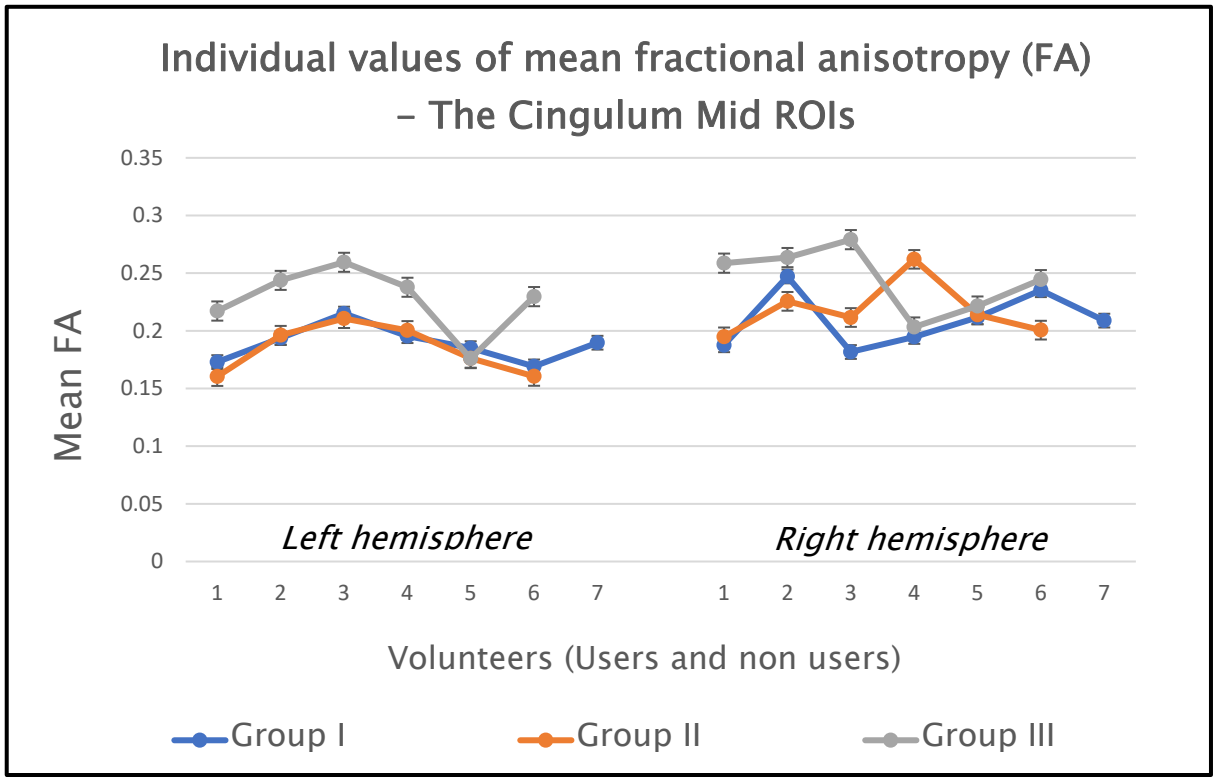

Figure 106: Individual values of mean fractional anisotropy (FA) in both hemispheres' Cingulum Mid ROIs. This figure depicts the FA values of all the participants belonging to each of the three groups (Heavy and light users and healthy controls).

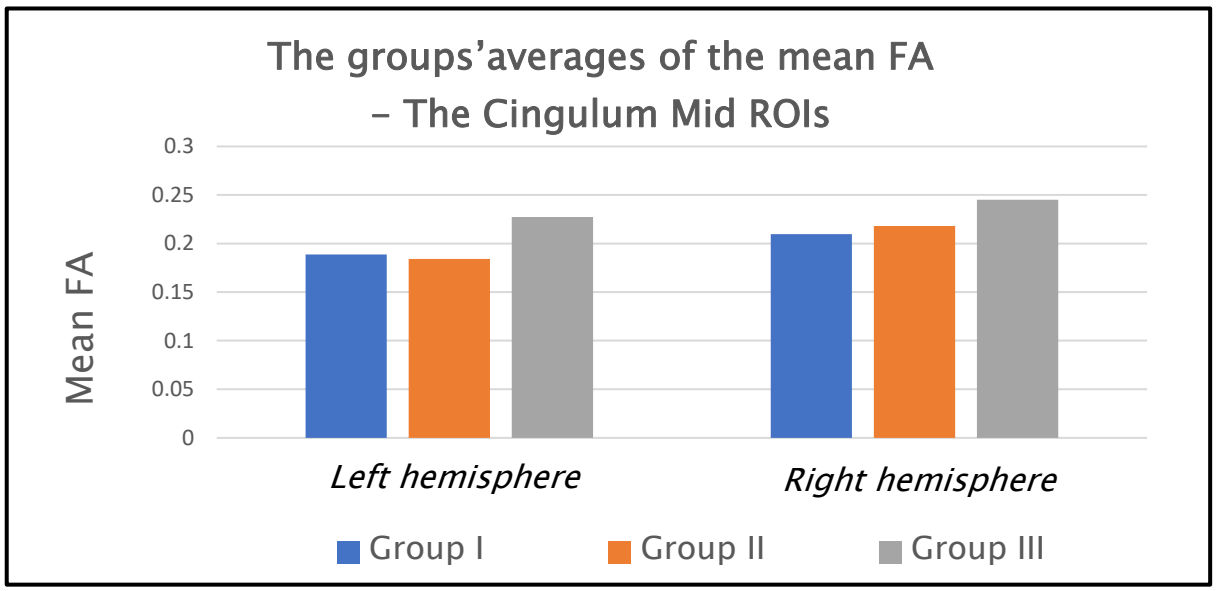

Figure 107: The mean fractional anisotropy (FA) averages of each group in the Cingulum Mid ROIs in the left and the right hemispheres.

Table 41: The mean fractional anisotropy (FA) averages and standard deviations (SD) values for the groups studied in the Cingulum Mid ROIs, along with intergroup comparisons.

	Left Hemisphere	Right Hemisphere
Heavy users' group (G. I)	(0,188±0,0153)	(0,2095±0,0243)
Light users' group (G. II)	(0,184±0,0214)	(0,218±0,02405)
Non-users' group (G.III)	(0,227±0,0288)	(0,245±0,0282)
Intergroup comparison	G.III > G. II ≈ G. I	G.III > G. II > G. I

➢ Cingulum Post

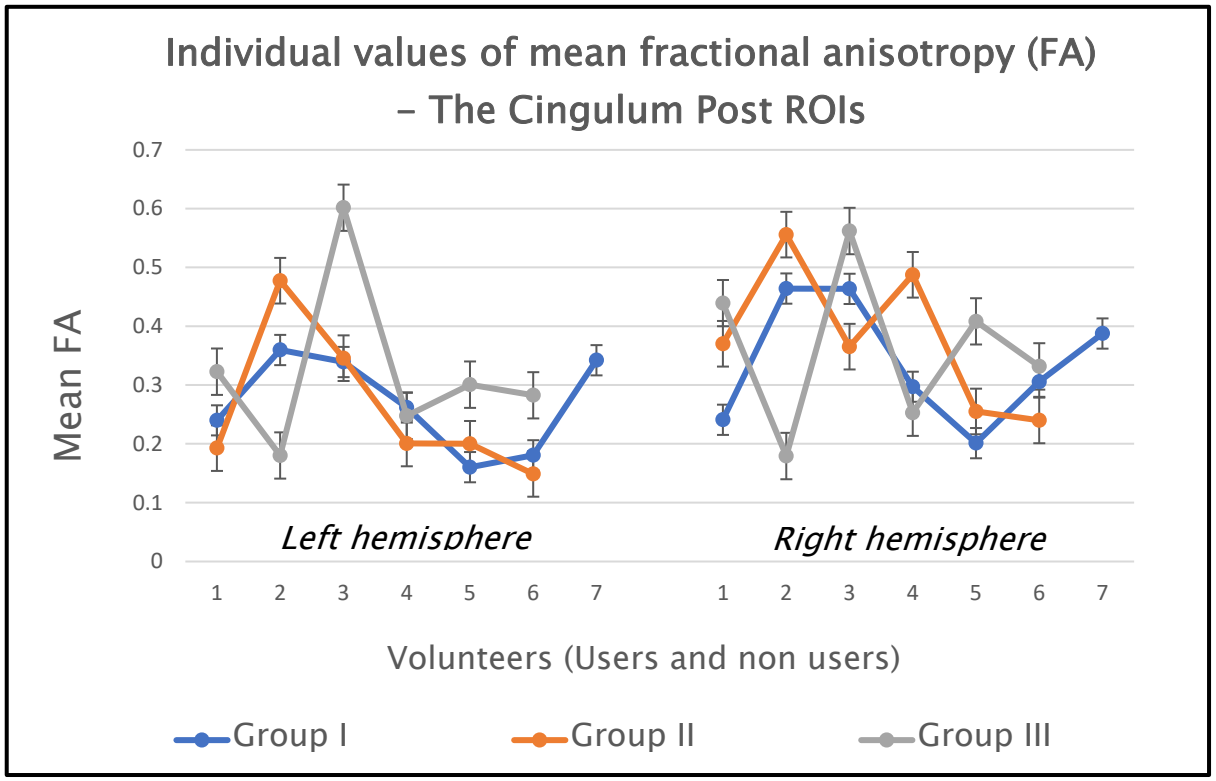

Figure 108: Individual values of mean fractional anisotropy (FA) in both hemispheres' Cingulum Post ROIs. This figure depicts the FA values of all the participants belonging to each of the three groups (Heavy and light users and healthy controls).

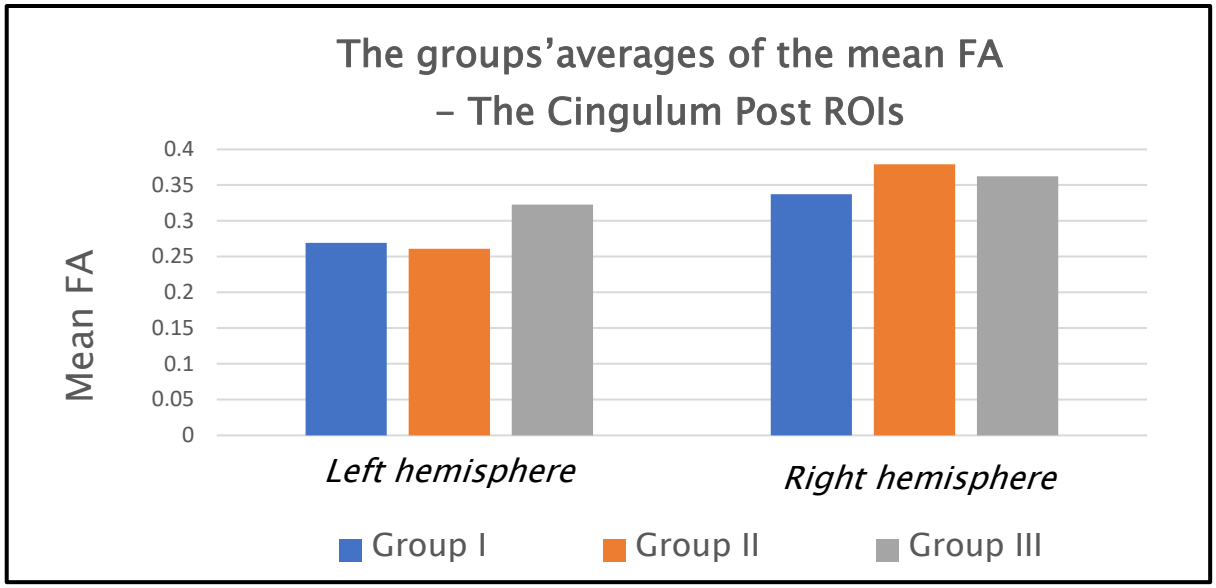

Figure 109: The mean fractional anisotropy (FA) averages of each group in the Cingulum Post ROIs in the left and the right hemispheres.

Table 42: The mean fractional anisotropy (FA) averages and standard deviations (SD) values for the groups studied in the Cingulum Post ROIs, along with intergroup comparisons.

	Left Hemisphere	Right Hemisphere
Heavy users' group (G. I)	(0,269±0,08066)	(0,337±0,10404)
Light users' group (G. II)	(0,2609±0,125)	(0,378±0,124)
Non-users' group (G.III)	(0,322±0,145)	(0,362±0,137)
Intergroup comparison	G.III > G.I > G. II	G. II ≈ G.III > G. I

➢ **ParaHippocampal**

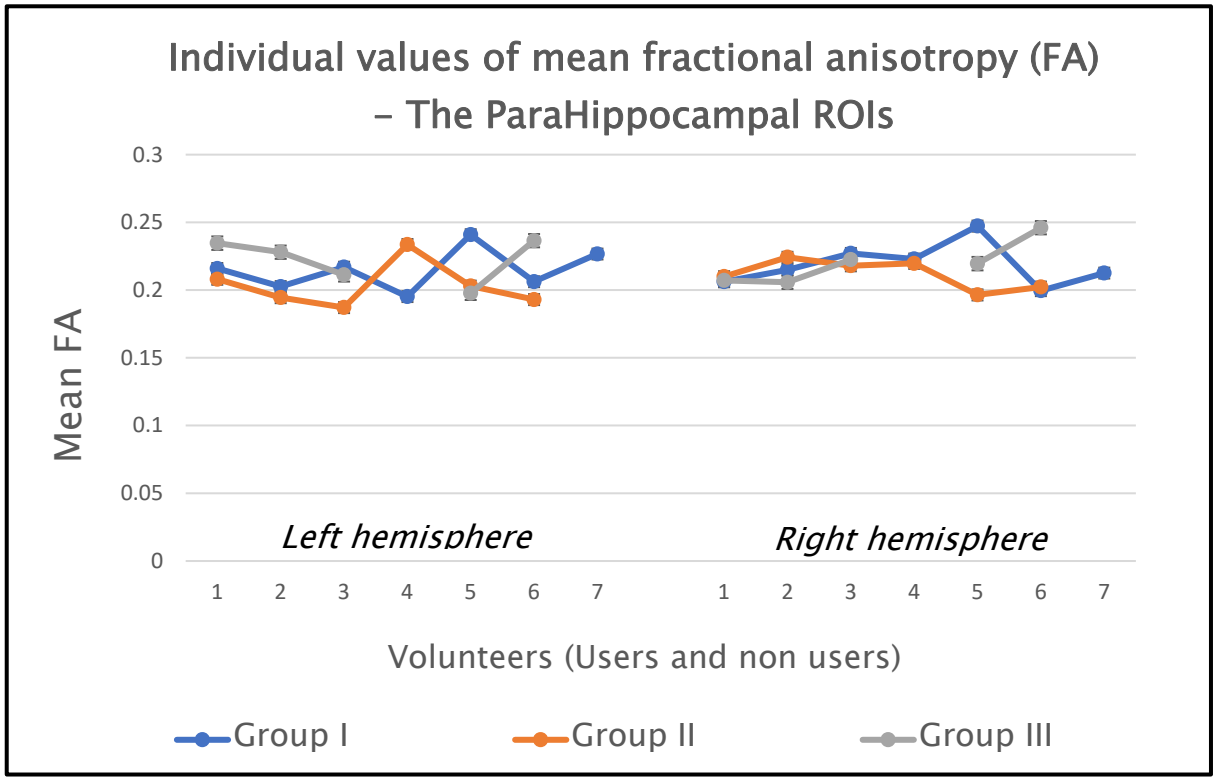

Figure 110: Individual values of mean fractional anisotropy (FA) in both hemispheres' ParaHippocampal ROIs. This figure depicts the FA values of all the participants belonging to each of the three groups (Heavy and light users and healthy controls).

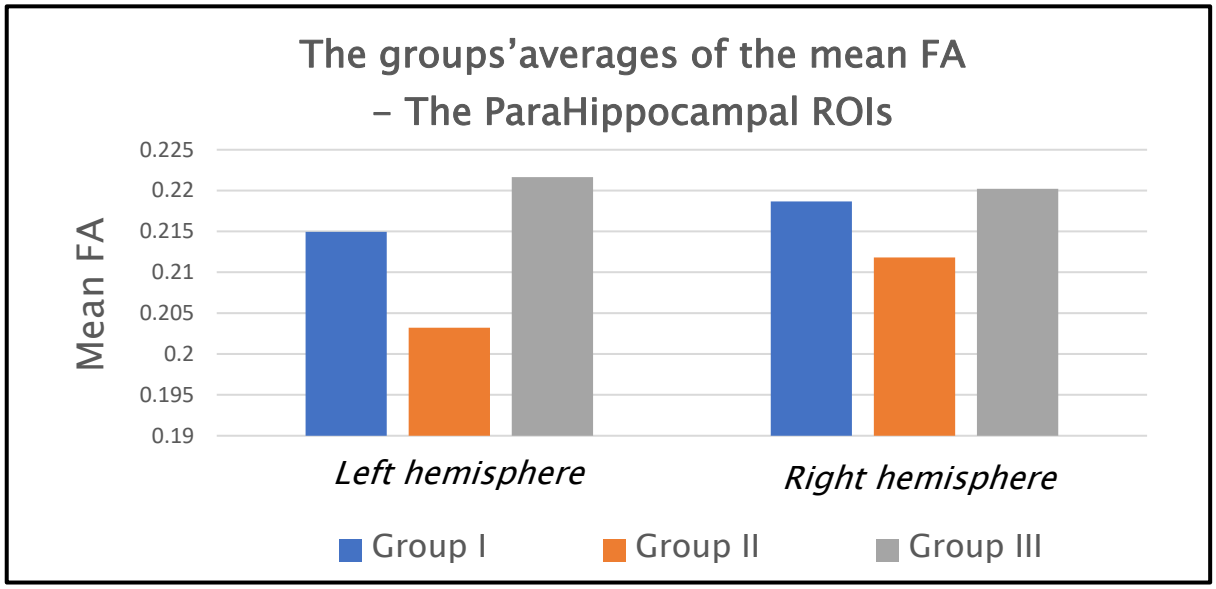

Figure 111: The mean fractional anisotropy (FA) averages of each group in the ParaHippocampal ROIs in the left and the right hemispheres.

Table 43: The mean fractional anisotropy (FA) averages and standard deviations (SD) values for the groups studied in the ParaHippocampal ROIs, along with intergroup comparisons.

	Left Hemisphere	Right Hemisphere
Heavy users' group (G. I)	(0,214±0,0154)	(0,218±0,0157)
Light users' group (G. II)	(0,2032±0,0166)	(0,211±0,01082)
Non-users' group (G.III)	(0,221±0,0166)	(0,2202±0,0162)
Intergroup comparison	G.III > G.I > G. II	G.III ≈ G. I > G. II

➢ Hippocampus

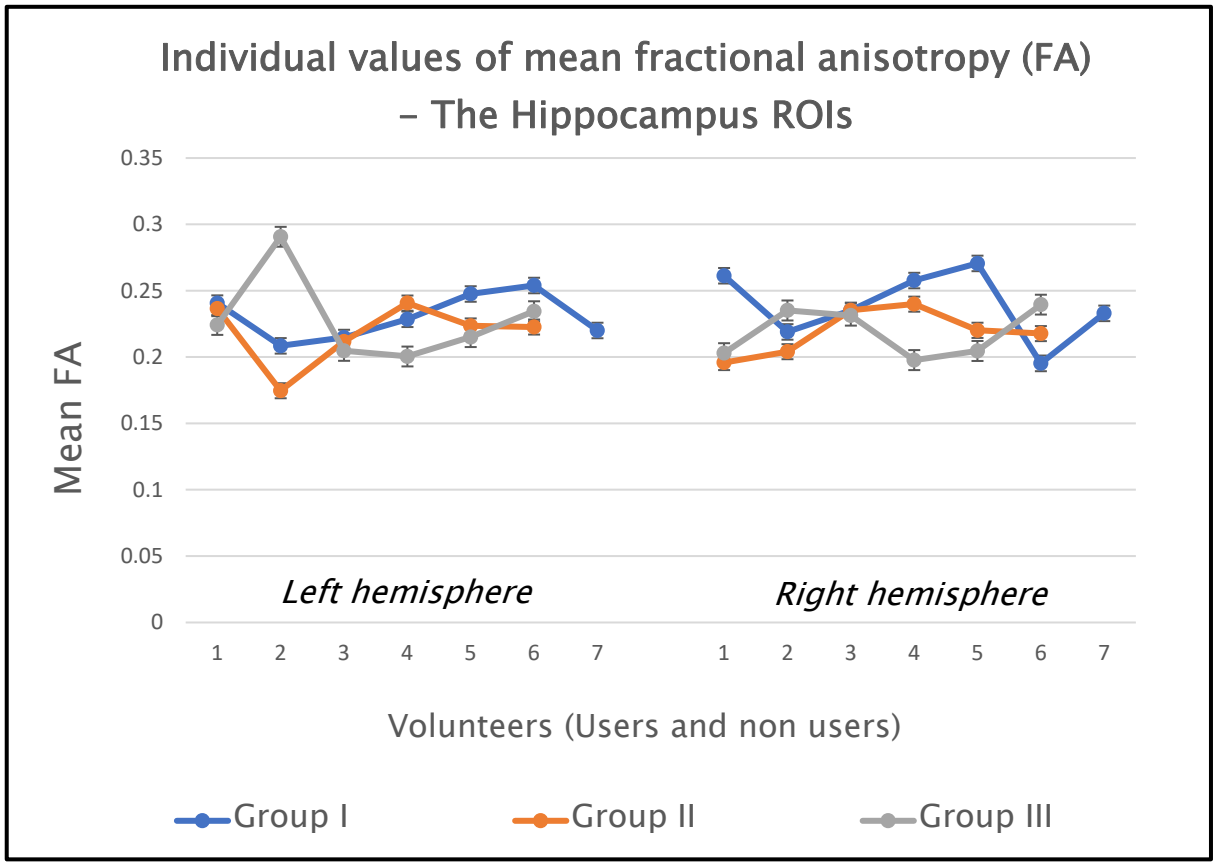

Figure 112: Individual values of mean fractional anisotropy (FA) in both hemispheres' Hippocampus ROIs. This figure depicts the FA values of all the participants belonging to each of the three groups (Heavy and light users and healthy controls).

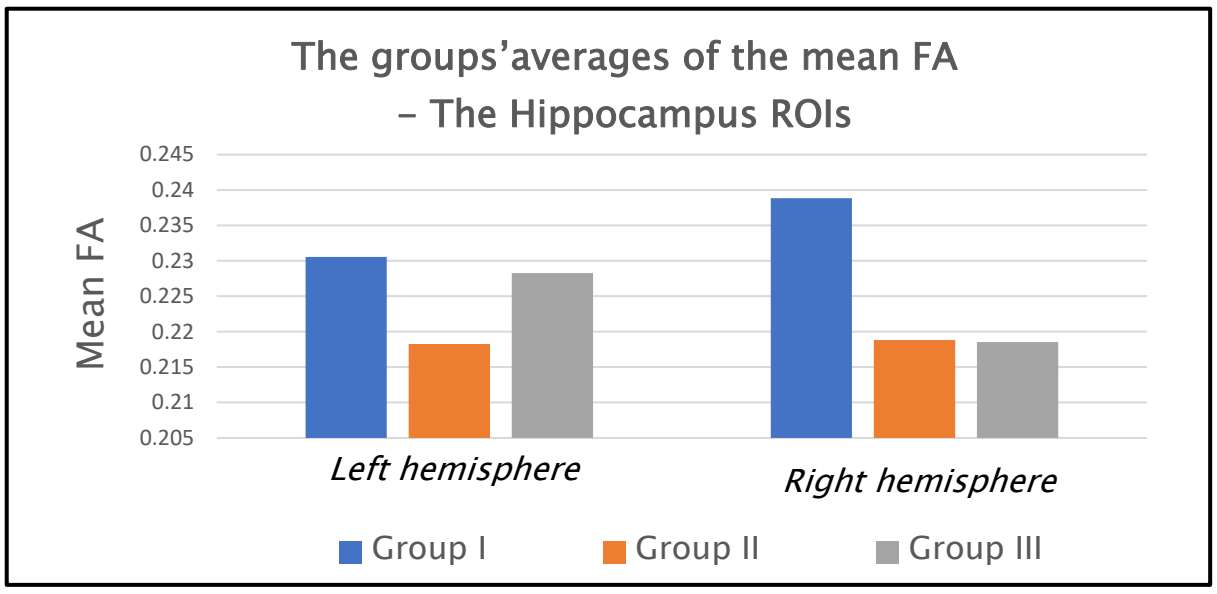

Figure 113: The mean fractional anisotropy (FA) averages of each group in the Hippocampus ROIs in the left and the right hemispheres.

Table 44: The mean fractional anisotropy (FA) averages and standard deviations (SD) values for the groups studied in the Hippocampus ROIs, along with intergroup comparisons.

	Left Hemisphere	Right Hemisphere
Heavy users' group (G. I)	(0,2305±0,0173)	(0,238±0,0264)
Light users' group (G. II)	(0,218±0,0237)	(0,218±0,01709)
Non-users' group (G.III)	(0,228±0,03302)	(0,218±0,0187)
Intergroup comparison	G. I ≈ G.III > G. II	G. I > G.III ≈ G. II

➢ **Insula**

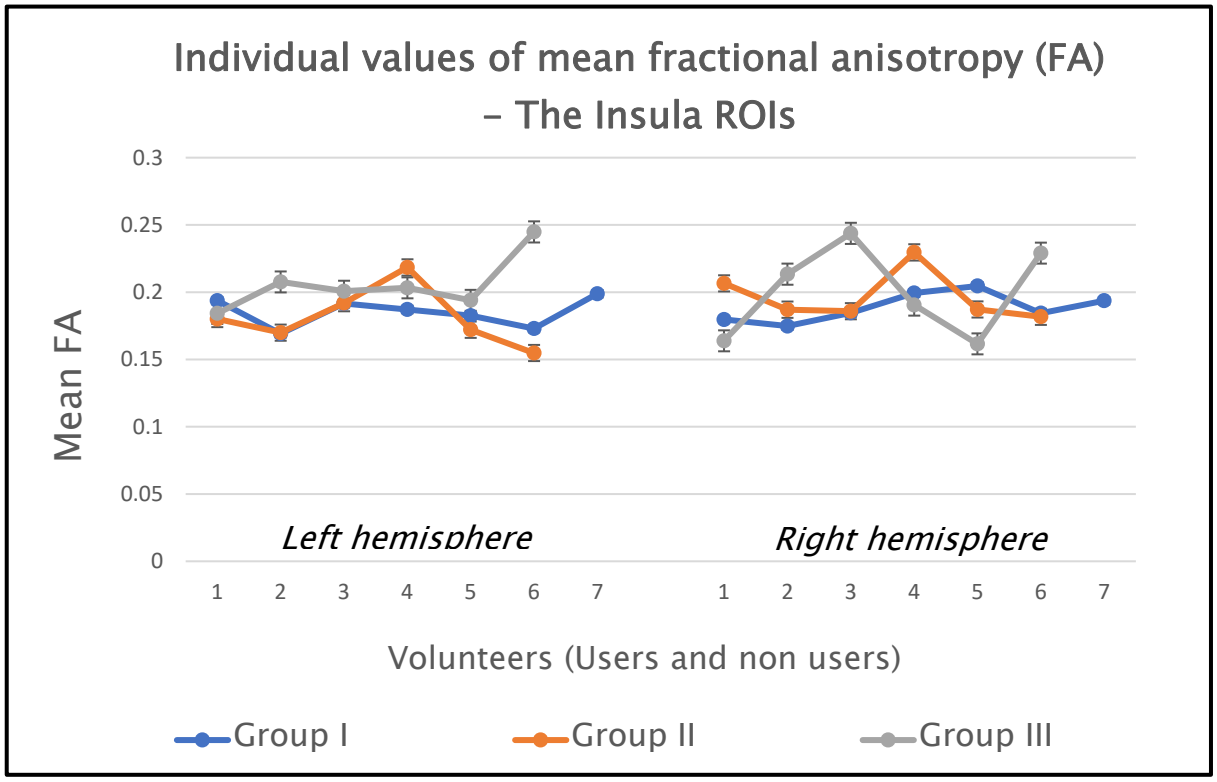

Figure 114: Individual values of mean fractional anisotropy (FA) in both hemispheres' Insula ROIs. This figure depicts the FA values of all the participants belonging to each of the three groups (Heavy and light users and healthy controls).

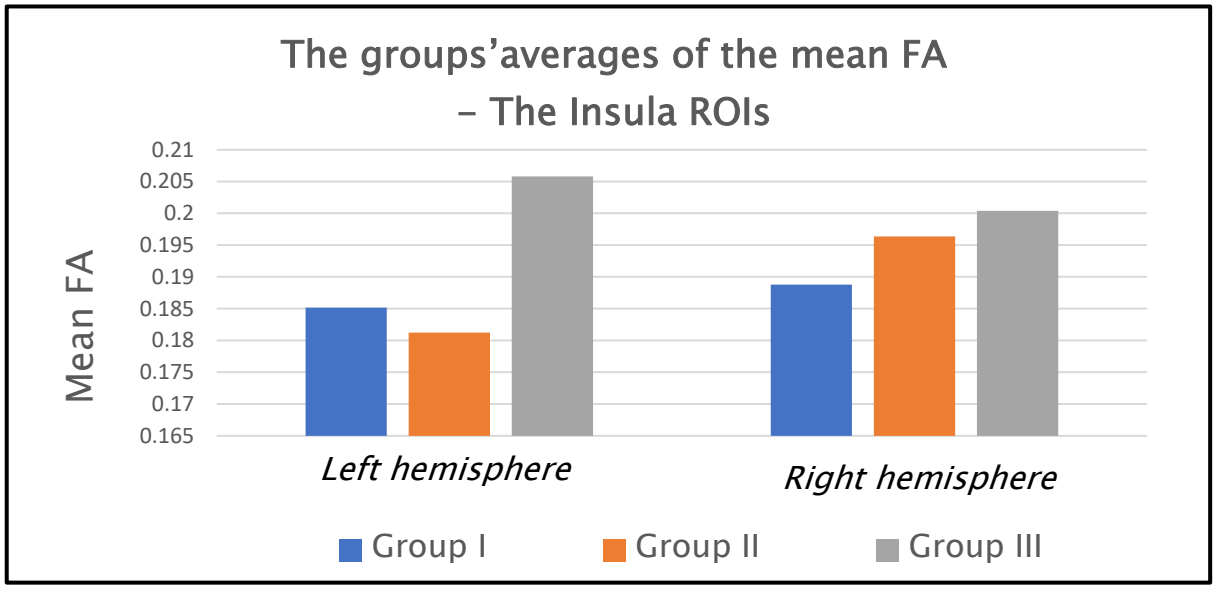

Figure 115: The mean fractional anisotropy (FA) averages of each group in the Insula ROIs in the left and the right hemispheres.

Table 45: The mean fractional anisotropy (FA) averages and standard deviations (SD) values for the groups studied in the Insula ROIs, along with intergroup comparisons.

	Left Hemisphere	Right Hemisphere
Heavy users' group (G. I)	(0,185±0,01094)	(0,188±0,01082)
Light users' group (G. II)	(0,181±0,0219)	(0,196±0,0184)
Non-users' group (G.III)	(0,2057±0,02079)	(0,20037±0,03407)
Intergroup comparison	G.III > G.I ≈ G. II	G.III ≈ G. II > G. I

➢ Amygdala

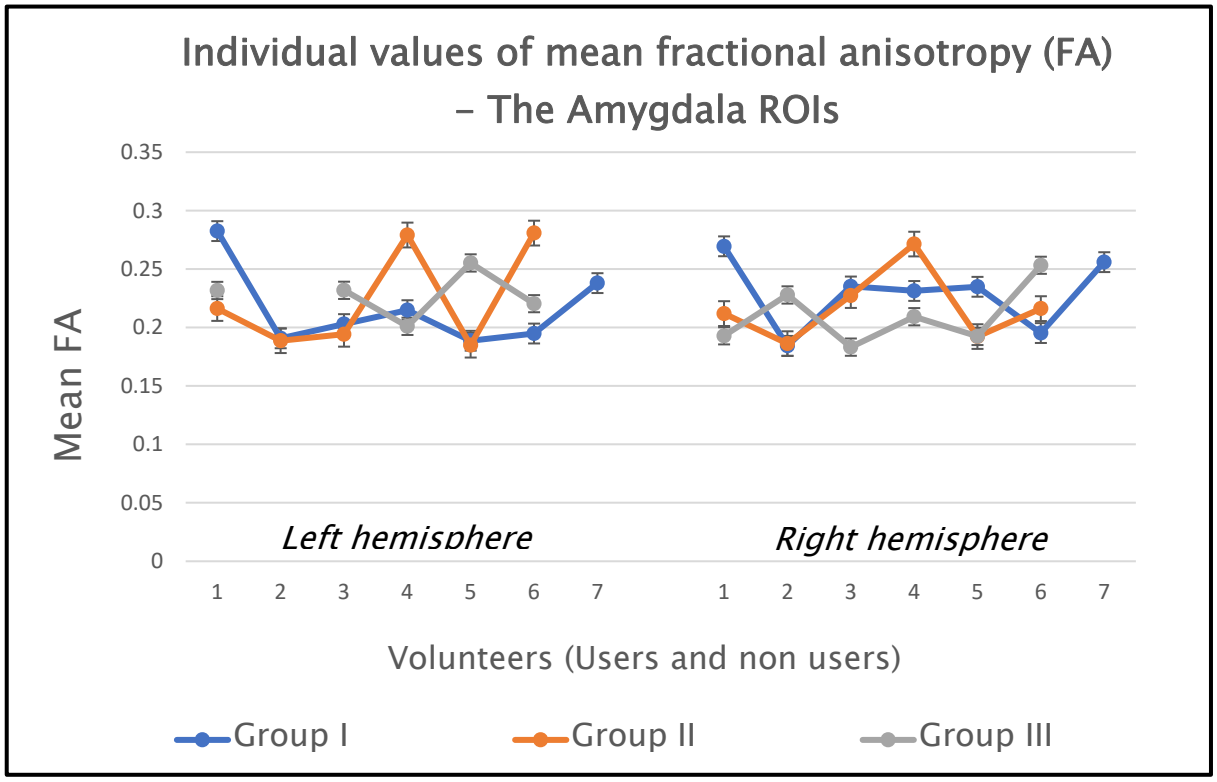

Figure 116: Individual values of mean fractional anisotropy (FA) in both hemispheres' Amygdala ROIs. This figure depicts the FA values of all the participants belonging to each of the three groups (Heavy and light users and healthy controls).

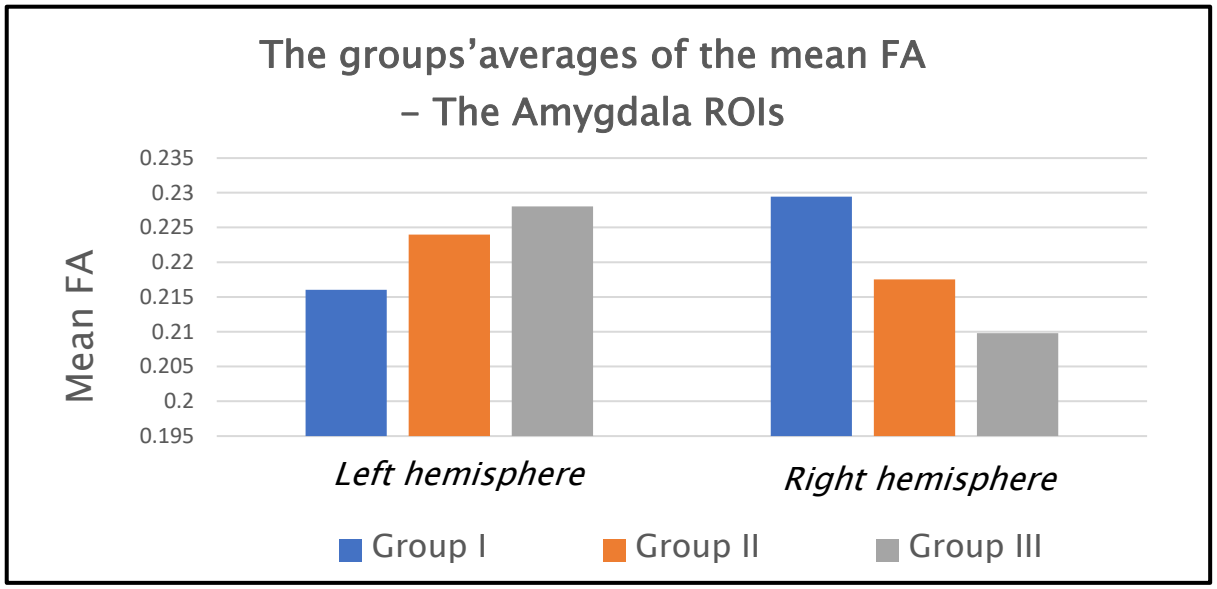

Figure 117: The mean fractional anisotropy (FA) averages of each group in the Amygdala ROIs in the left and the right hemispheres.

Table 45: The mean fractional anisotropy (FA) averages and standard deviations (SD) values for the groups studied in the Amygdala ROIs, along with intergroup comparisons.

	Left Hemisphere	Right Hemisphere
Heavy users' group (G. I)	(0,216±0,0339)	(0,229±0,03049)
Light users' group (G. II)	(0,223±0,0447)	(0,217±0,030506)
Non-users' group (G.III)	(0,228±0,0197)	(0,2097±0,0264)
Intergroup comparison	G.III ≈ G.I > G. II	G. I > G. II > G.III

➢ **Thalamus**

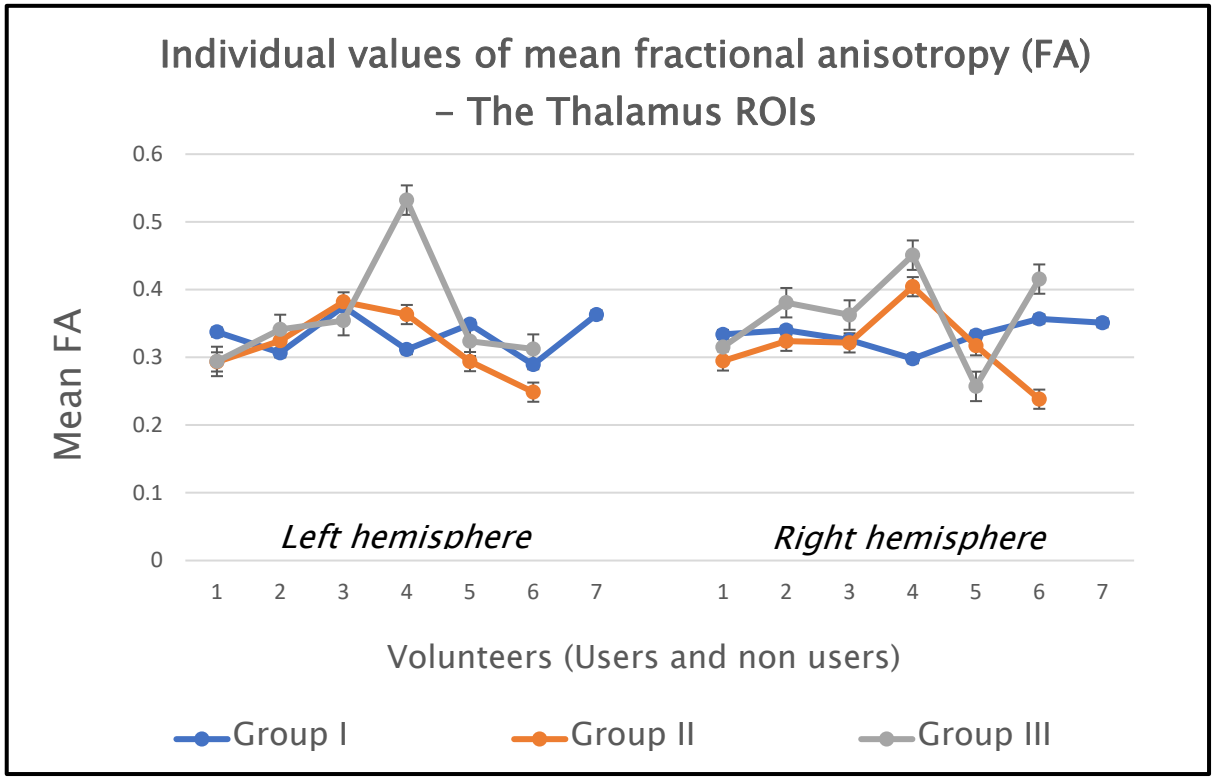

Figure 118: Individual values of mean fractional anisotropy (FA) in both hemispheres' Thalamus ROIs. This figure depicts the FA values of all the participants belonging to each of the three groups (Heavy and light users and healthy controls).

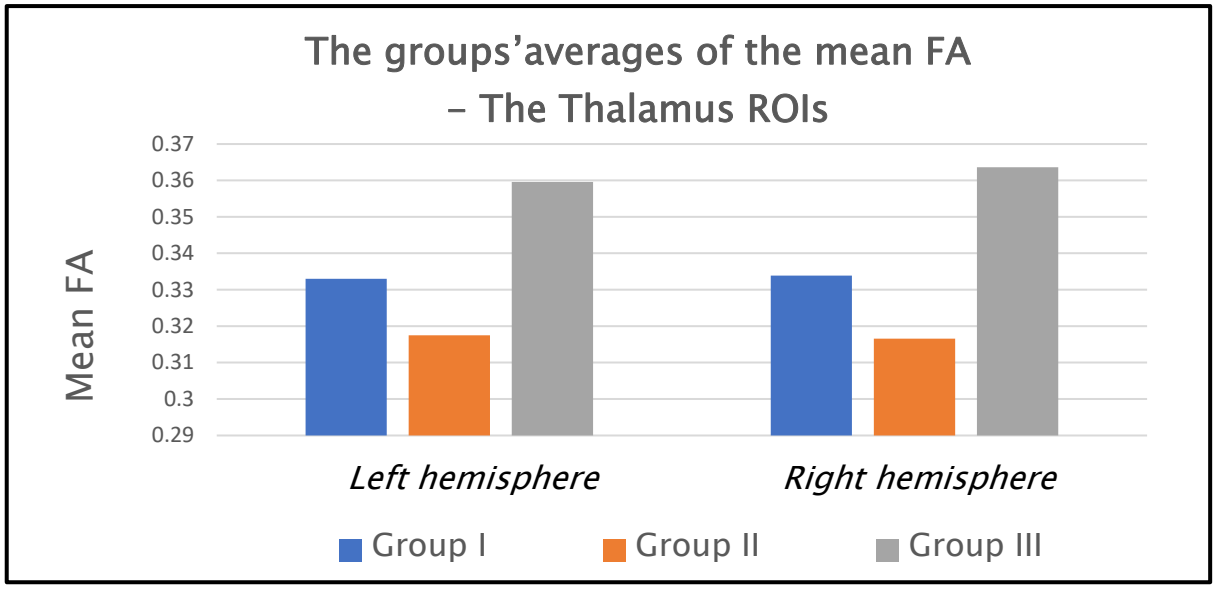

Figure 119: The mean fractional anisotropy (FA) averages of each group in the Thalamus ROIs in the left and the right hemispheres.

Table 46: The mean fractional anisotropy (FA) averages and standard deviations (SD) values for the groups studied in the Thalamus ROIs, along with intergroup comparisons.

	Left Hemisphere	Right Hemisphere
Heavy users' group (G. I)	(0,333±0,0316)	(0,333±0,0192)
Light users' group (G. II)	(0,317±0,0493)	(0,316±0,0536)
Non-users' group (G.III)	(0,359±0,0871)	(0,363±0,0697)
Intergroup comparison	G.III > G.I > G. II	G.III ≈ G. I > G. II

➢ Caudate

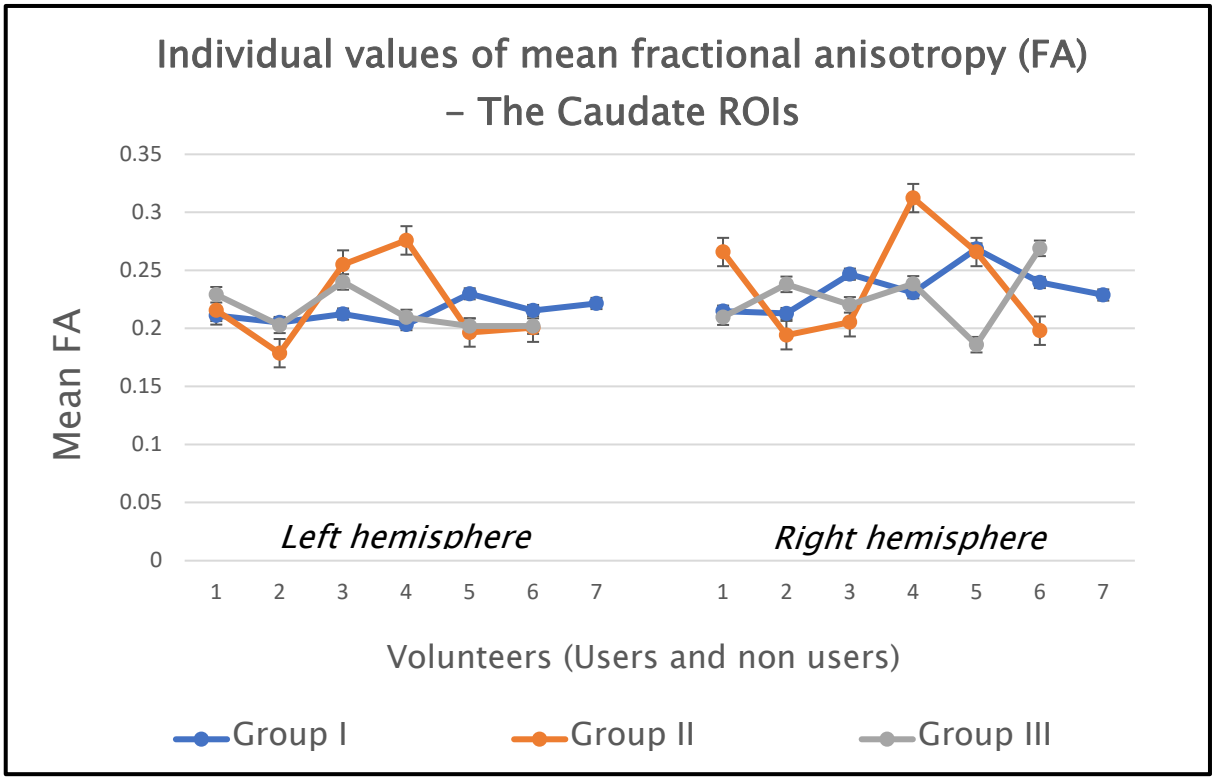

Figure 120: Individual values of mean fractional anisotropy (FA) in both hemispheres' Caudate ROIs. This figure depicts the FA values of all the participants belonging to each of the three groups (Heavy and light users and healthy controls).

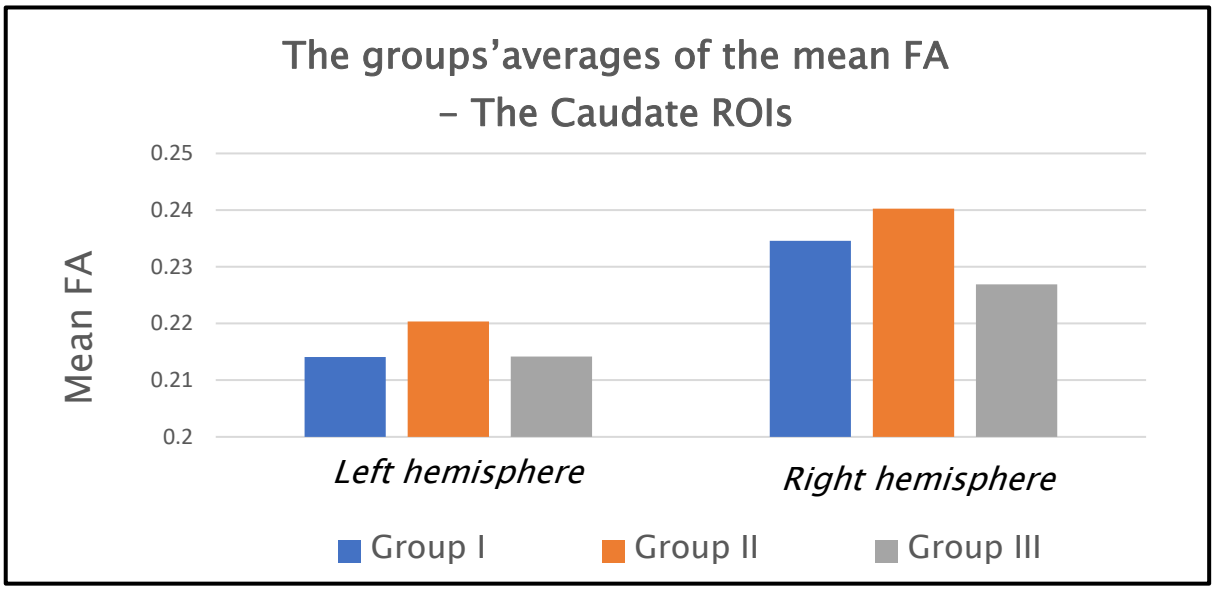

Figure 121: The mean fractional anisotropy (FA) averages of each group in the Caudate ROIs in the left and the right hemispheres.

Table 47: The mean fractional anisotropy (FA) averages and standard deviations (SD) values for the groups studied in the Caudate ROIs, along with intergroup comparisons.

	Left Hemisphere	Right Hemisphere
Heavy users' group (G. I)	(0,214±0,00926)	(0,234±0,0192)
Light users' group (G. II)	(0,2203±0,0374)	(0,2402±0,0482)
Non-users' group (G.III)	(0,214±0,0163)	(0,226±0,0284)
Intergroup comparison	G. II > G.III ≈ G. I	G. II > G. I > G.III

➢ **Putamen**

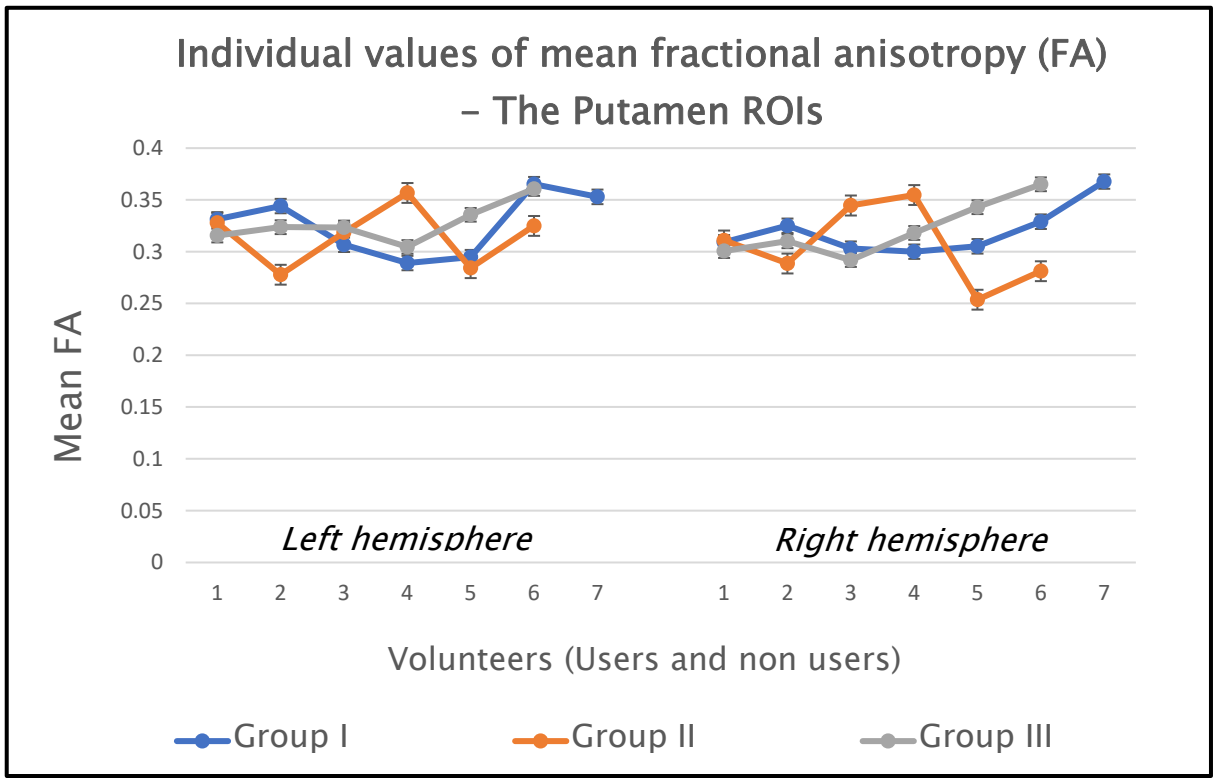

Figure 122: Individual values of mean fractional anisotropy (FA) in both hemispheres' Putamen ROIs. This figure depicts the FA values of all the participants belonging to each of the three groups (Heavy and light users and healthy controls).

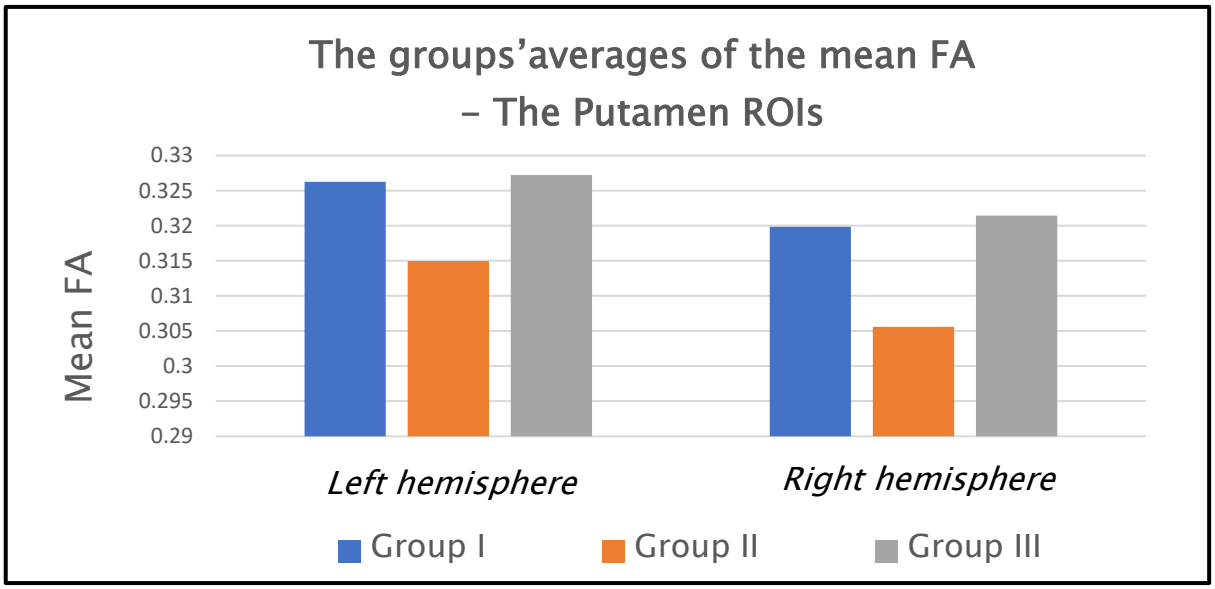

Figure 123: The mean fractional anisotropy (FA) averages of each group in the Putamen ROIs in the left and the right hemispheres.

Table 48: The mean fractional anisotropy (FA) averages and standard deviations (SD) values for the groups studied in the Putamen ROIs, along with intergroup comparisons.

	Left Hemisphere	Right Hemisphere
Heavy users' group (G. I)	(0,326±0,0298)	(0,319±0,0238)
Light users' group (G. II)	(0,314±0,0295)	(0,3055±0,0388)
Non-users' group (G.III)	(0,327±0,0192)	(0,321±0,0276)
Intergroup comparison	G.III ≈ G. I > G. II	G.III ≈ G. I > G. II

➢ **Pallidum**

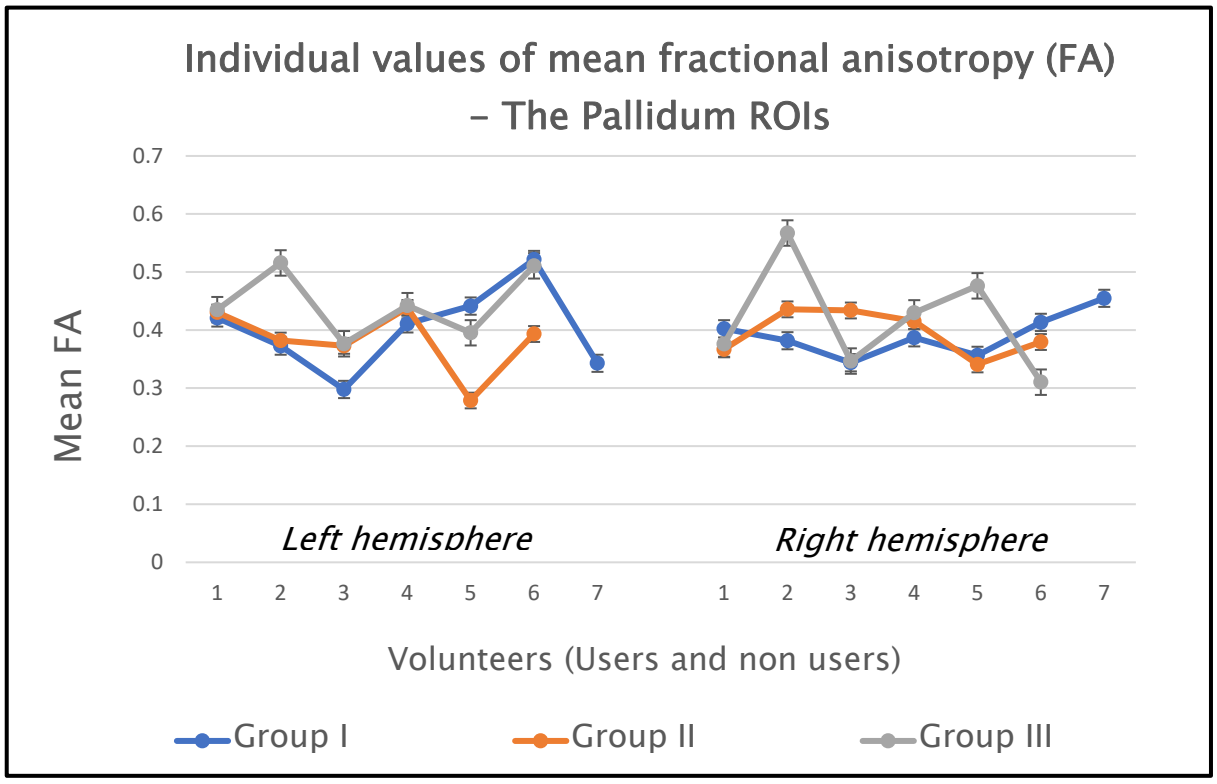

Figure 124: Individual values of mean fractional anisotropy (FA) in both hemispheres' Pallidum ROIs. This figure depicts the FA values of all the participants belonging to each of the three groups (Heavy and light users and healthy controls).

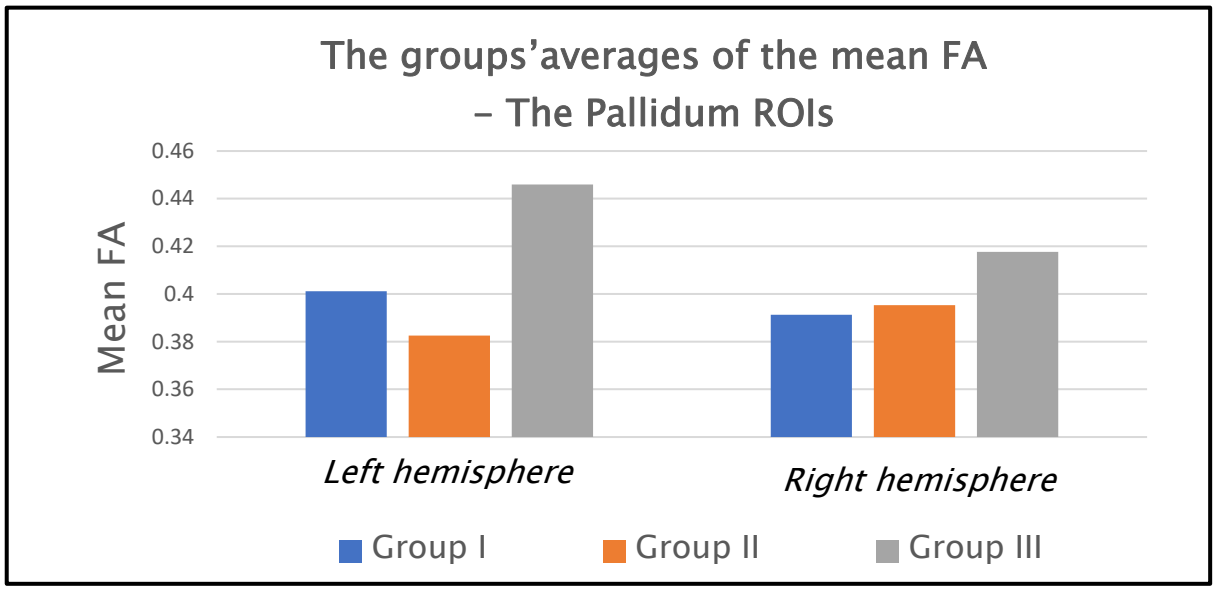

Figure 125: The mean fractional anisotropy (FA) averages of each group in the Pallidum ROIs in the left and the right hemispheres.

Table 49: The mean fractional anisotropy (FA) averages and standard deviations (SD) values for the groups studied in the Pallidum ROIs, along with intergroup comparisons.

	Left Hemisphere	Right Hemisphere
Heavy users' group (G. I)	(0,40109±0,0724)	(0,391±0,03701)
Light users' group (G. II)	(0,382±0,0572)	(0,395±0,0388)
Non-users' group (G.III)	(0,4458±0,0575)	(0,417±0,09407)
Intergroup comparison	G.III > G. I > G. II	G.III > G. II > G. I

➢ **Nucleus Accumbens**

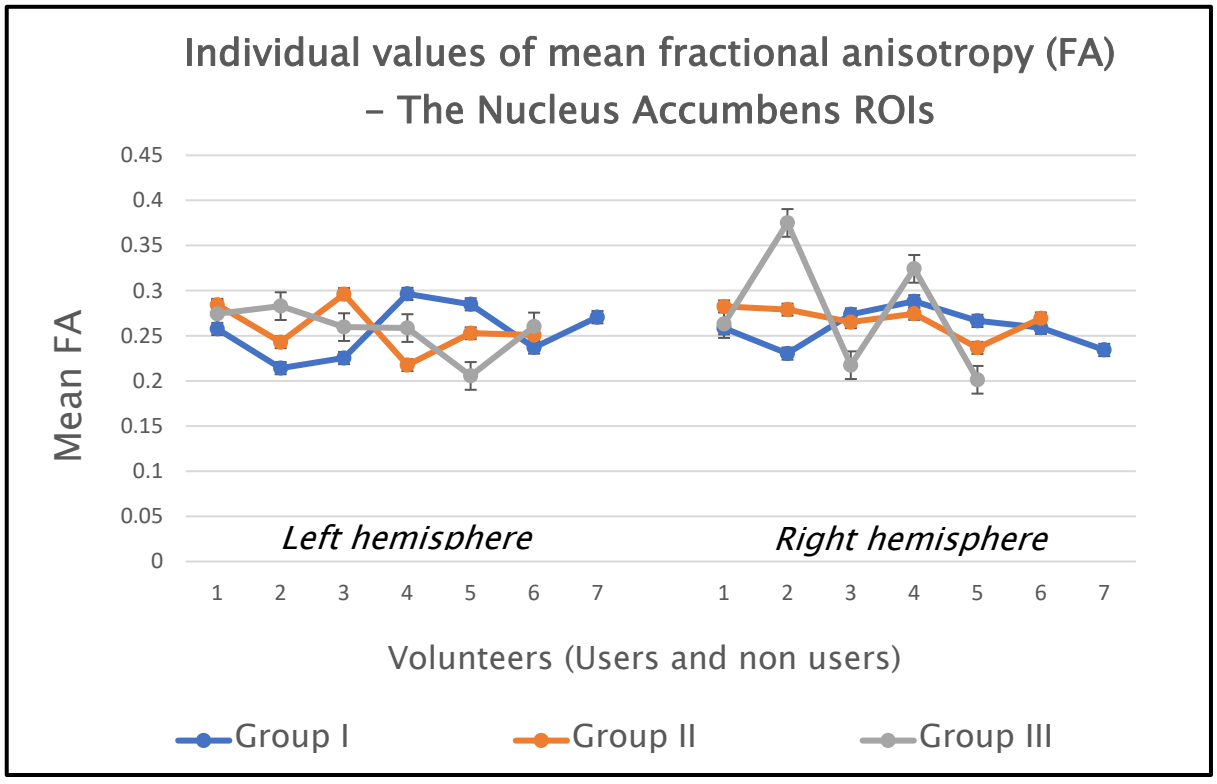

Figure 126: Individual values of mean fractional anisotropy (FA) in both hemispheres' Nucleus Accumbens ROIs. This figure depicts the FA values of all the participants belonging to each of the three groups (Heavy and light users and healthy controls).

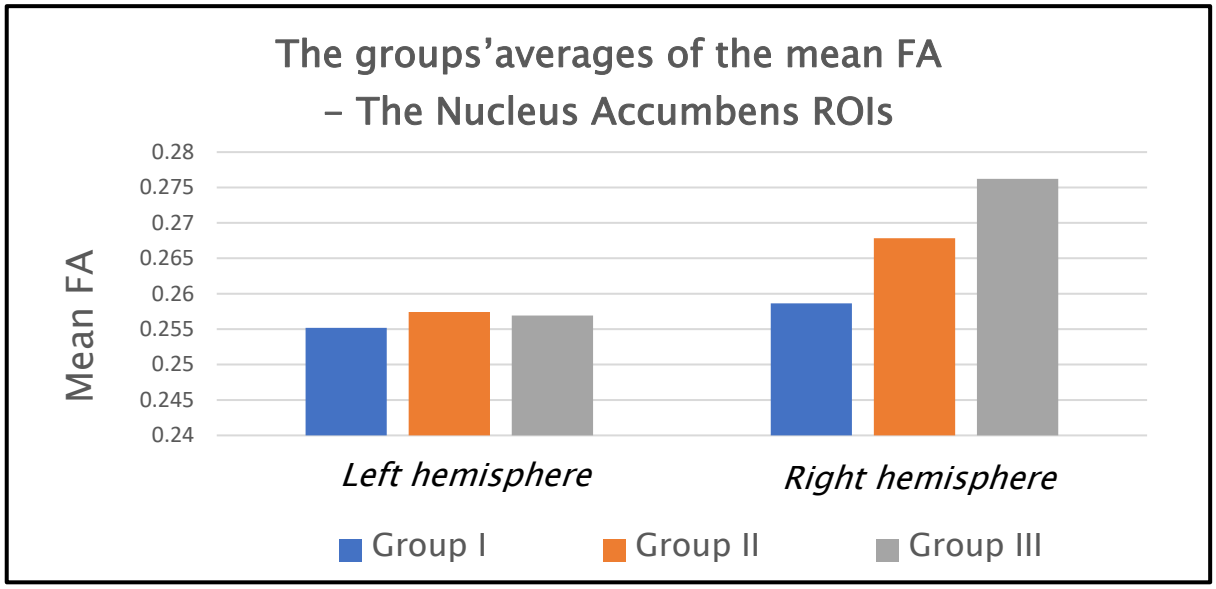

Figure 127: The mean fractional anisotropy (FA) averages of each group in the Nucleus Accumbens ROIs in the left and the right hemispheres.

Table 50: The mean fractional anisotropy (FA) averages and standard deviations (SD) values for the groups studied in the Nucleus Accumbens ROIs, along with intergroup comparisons.

	Left Hemisphere	Right Hemisphere
Heavy users' group (G. I)	(0,255±0,03087)	(0,258±0,02062)
Light users' group (G. II)	(0,257±0,0285)	(0,267±0,0165)
Non-users' group (G.III)	(0,256±0,0269)	(0,276±0,0729)
Intergroup comparison	G.III ≈ G. I ≈ G. II	G.III > G. II > G. I

2. Mean diffusivity (MD) quantitative results

a. Summary of all the quantitative findings

Table 51: Descriptive results of the overall quantitative comparisons of mean diffusivity marker in the ROIs.

Intergroup comparison	Regions	Comments
G.III ≈ G. I ≈ G. II	-Frontal Med Orb. Right -Frontal Sup Orb. Left -Frontal Mid. Left & Right -Frontal Inf Tri. Left -Postcentral. Left -Parietal Sup. Right -SupraMarginal. Left -Parietal Inf. Left -Precuneus. Left -Temporal Pole Sup. Right -Temporal Mid. Left -Temporal Inf. Right -Fusiform. Left -Cingulum ANT. Left -Cingulum Mid. Left -ParaHippocampal. Left -Hippocampus. Right -Insula. Left -Thalamus. Left -Putamen. Left & Right -Pallidum. Left & Right	This intergroup comparison arrangement was objective: * At 24 regions out of 72 (bilaterally), which represents 33.33% of the total of the regions studied. * In terms of laterality, two-third of the regions belong to the left hemisphere. * The regions with this type of intergroup comparison belong to thep following: -Cerebral cortex -Limbic system -Diencephalon (Thalamus) -Basal ganglia
G.III > G. II ≈ G. I	-Frontal Sup Orb. Right -Frontal Mid Orb. Right -Olfactory. Left -Frontal Inf Oper. Right -SupraMarginal. Right -Angular. Left & Right -Temporal Pole Mid. Right -Cingulum Mid. Right -Cingulum Post. Right -Thalamus. Right	This intergroup comparison arrangement was objective: * At 12 regions out of 72 (bilaterally), which represents 16.66% of the total of the regions studied. * In terms of laterality, two-third of the regions belong to the right hemisphere.

	-Nucleus Accumbens. Left	*The regions with this type of intergroup comparison belong to the: -Cerebral cortex -Limbic system -Diencephalon (Thalamus) -Basal ganglia
G.III > G. I > G. II	-Frontal Sup. Right -Frontal Inf Tri. Right -Temporal Sup. Right -Temporal Mid. Right -Fusiform. Right -Cingulum ANT. Right -Insula. Right -Caudate. Right	This intergroup comparison arrangement was objective in 11% of the regions studied. This intergroup comparison shows up exclusively in the right hemisphere in terms of laterality. The regions with this type of intergroup comparison belong to the: -Cerebral cortex -Limbic system -Basal ganglia
G. I > G.III ≈ G. II	-Frontal Inf Orb. Right -Frontal Sup Medial. Left -Temporal Sup. Left -Temporal Pole Sup. Left -Heschl. Left -Temporal Inf. Left -Hippocampus. Left -Amygdala. Left	This intergroup comparison arrangement was objective in 11% of the regions studied. This intergroup comparison shows up almost only in the left hemisphere (Except one region, which is the Frontal Inf Orb) The regions with this type of intergroup comparison belong to the cerebral cortex and the limbic system
G.III ≈ G. I > G. II	-Frontal Sup. Left -Postcentral. Right -Heschl. Right -Amygdala. Right -Nucleus Accumbens. Right	This comparison arrangement between the three groups was found in only five regions. Except for one region, all the five areas belong to the right hemisphere.

		The areas are divided under the cerebral cortex and the limbic system.
G.III >G. II > G. I	-Olfactory. Right -Parietal Inf. Right -ParaHippocampal. Right	Only three regions show this type of intergroup comparison. All three regions belong to the right hemisphere.
G. I > G. II > G.III	-Frontal Inf Oper. Left -Parietal Sup. Left -Temporal Pole Mid. Left	Only three regions show this type of intergroup comparison. All three regions belong to the cerebral cortex of the left hemeisphere.
G. II ≈ G. I > G.III	-Frontal Med Orb. Left -Frontal Inf Orb. Left -Frontal Sup Medial. Right	Only three regions show this type of intergroup comparison. All three regions belong to the cerebral cortex.
G. II ≈ G.III > G. I	-Rectus. Right -Precuneus. Right	The remaining four categories of intergroup comparisons account for less than 8.5% of the total. Regions belong to the: -Cerebral cortex -Limbic system -Basal ganglia The regions are almost equally distributed between the left and the right hemispheres.
G. II > G.III ≈ G. I	-Frontal Mid Orb. Left -Cingulum Post. Left	
G. I > G.III > G. II	-Caudate. Left	
G. II > G. I > G.III	-Rectus. Left	

b. The quantitative findings in each region of interest

In the same way as we did for fractional anisotropy, in each region of interest and for both hemispheres, we present our mean diffusivity (MD) findings by two separated figures. The first figure depicts the mean diffusivity values of individuals in each group using a line chart.

In the line charts:

- Each participant is denoted numerically.

-The mean diffusivity is sorted in graph individual (X, Y) points and lines in heavy cannabis users (Group I), light cannabis users (Group II), and non-users (Group III). In the “X” horizontal line, we have the nominative numbers of voluntary participants, and in the “Y” vertical line, we have mean diffusivity values.

We compared the groups’ MD averages between the three groups in the second figure. Following that, a table containing every group’s MD averages and standard deviations (SD) will be presented for a more specific summary.

➢ Frontal Med Orb:

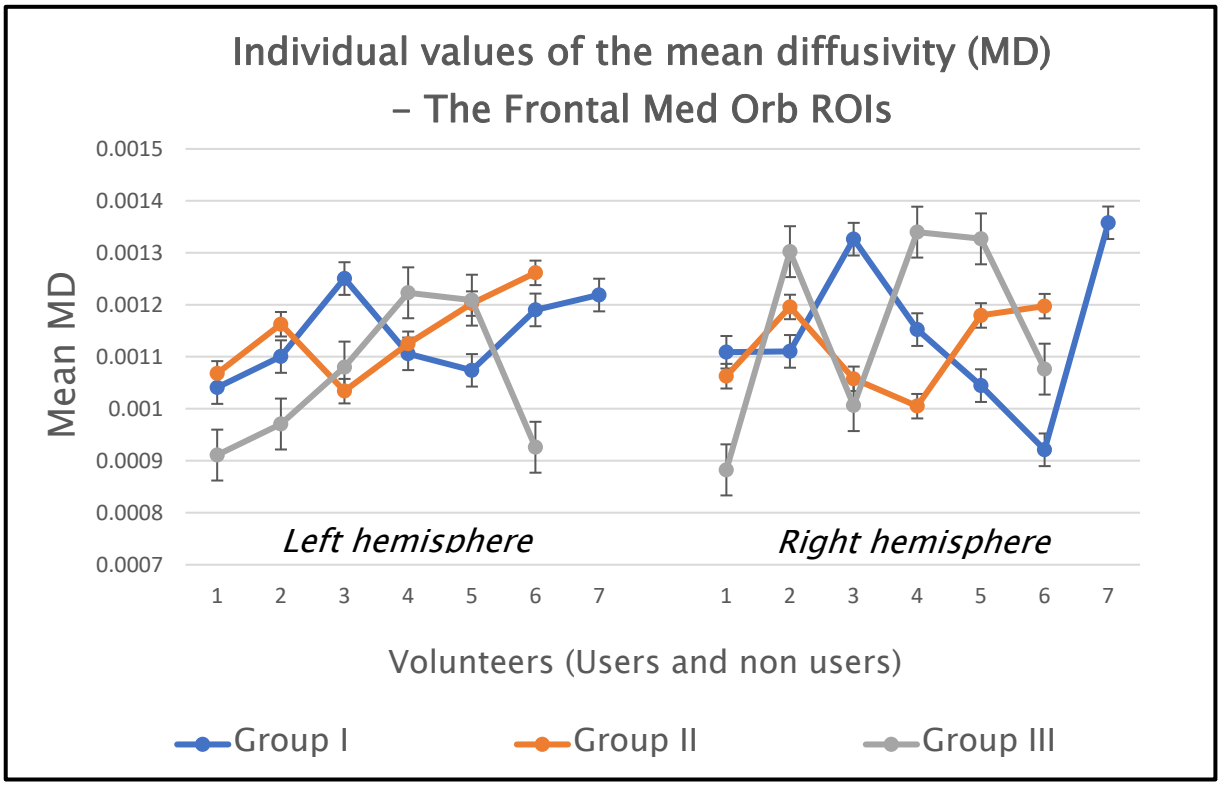

Figure 128: Individual values of mean diffusivity (MD) in both hemispheres' Frontal Med Orb ROIs. This figure depicts the MD values of all the participants belonging to each of the three groups (Heavy and light users and healthy controls).

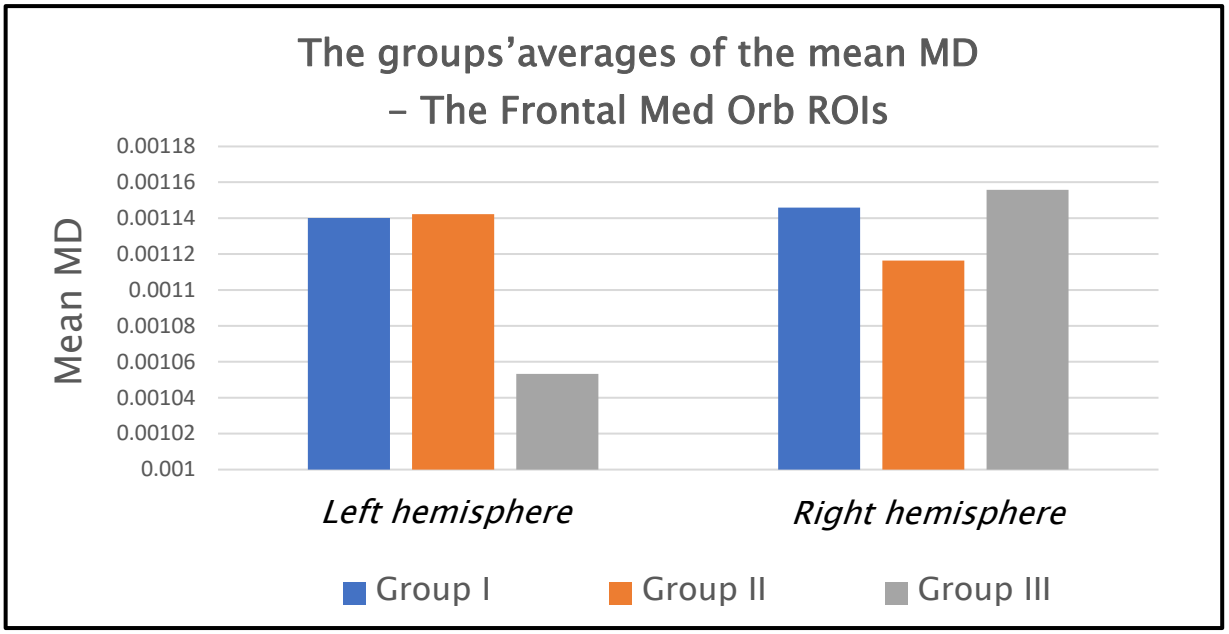

Figure 129: The mean diffusivity (MD) averages of each group in the Frontal Med Orb ROIs in the left and the right hemispheres.

Table 52: The mean diffusivity (MD) averages and standard deviations (SD) values for the groups studied in the Frontal Med Orb ROIs, along with intergroup comparisons.

	Left Hemisphere	Right Hemisphere
Heavy users' group (G. I)	(0,00114±0,0000794)	(0,00114±0,000153)
Light users' group (G. II)	(0,00114±0,0000845)	(0,00111±0,0000843)
Non-users' group (G.III)	(0,001053±0,000139)	(0,00115±0,000193)
Intergroup comparison	G. II ≈ G. I > G.III	G.III ≈ G. I ≈ G. II

➢ **Frontal Sup Orb:**

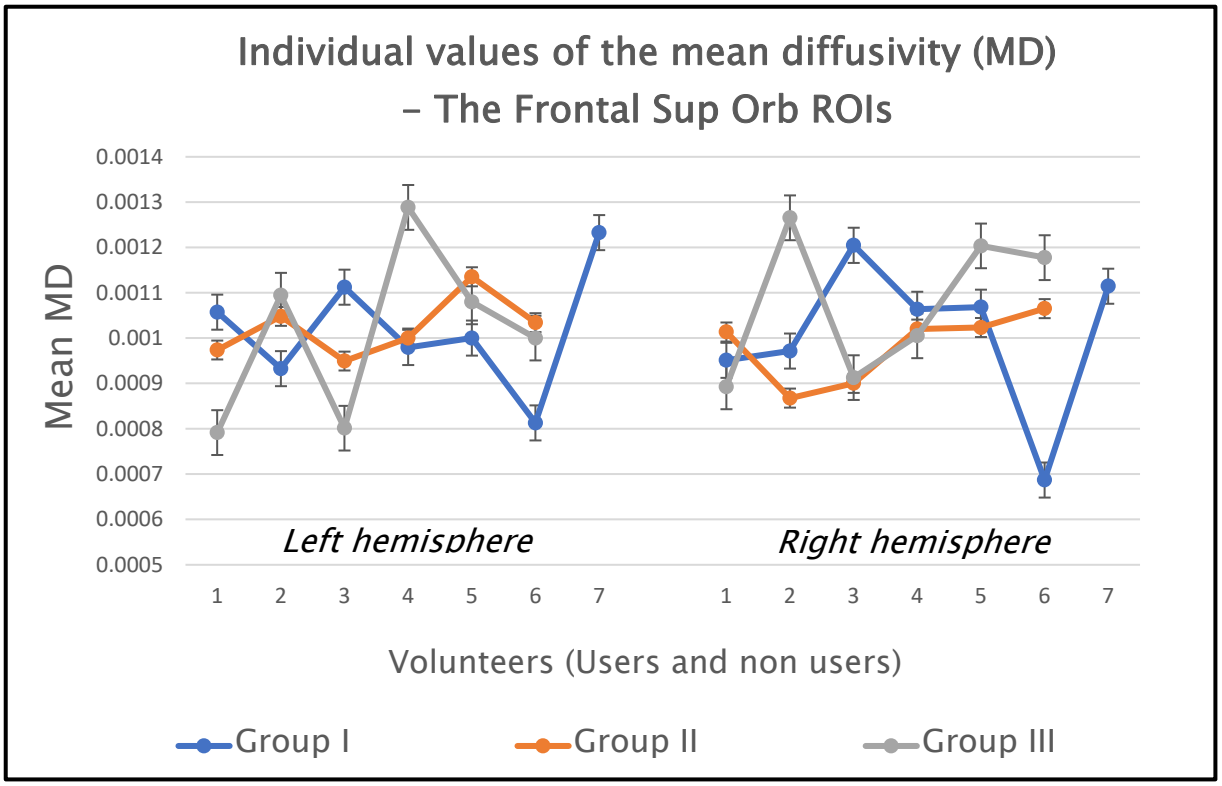

Figure 130: Individual values of mean diffusivity (MD) in both hemispheres' Frontal sup Orb ROIs. This figure depicts the MD values of all the participants belonging to each of the three groups (Heavy and light users and healthy controls).

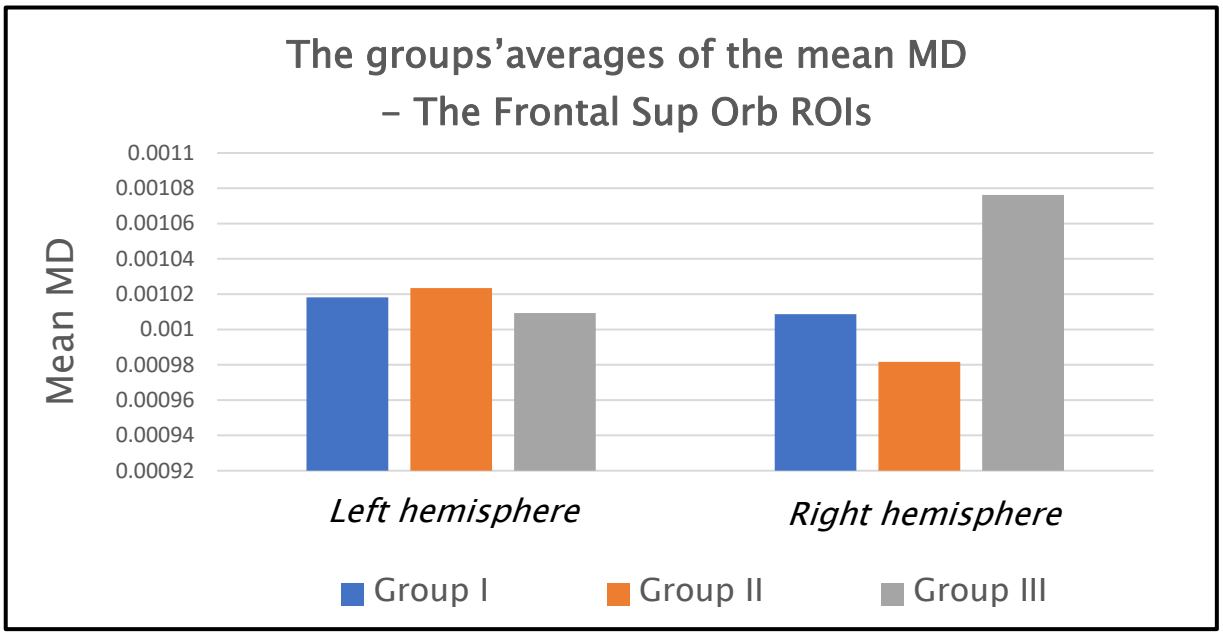

Figure 140: The mean diffusivity (MD) averages of each group in the Frontal Sup Orb ROIs in the left and the right hemispheres.

Table 53: The mean diffusivity (MD) averages and standard deviations (SD) values for the groups studied in the Frontal Sup Orb ROIs, along with intergroup comparisons.

	Left Hemisphere	Right Hemisphere
Heavy users' group (G. I)	(0,001018±0,000134)	(0,0010086±0,000165)
Light users' group (G. II)	(0,001023±0,0000659)	(0,000981±0,0000785)
Non-users' group (G.III)	(0,0010092±0,0001902)	(0,001076±0,000159)
Intergroup comparison	G. II ≈ G. I ≈ G.III	G.III > G. I ≈ G. II

➢ **Frontal Mid Orb:**

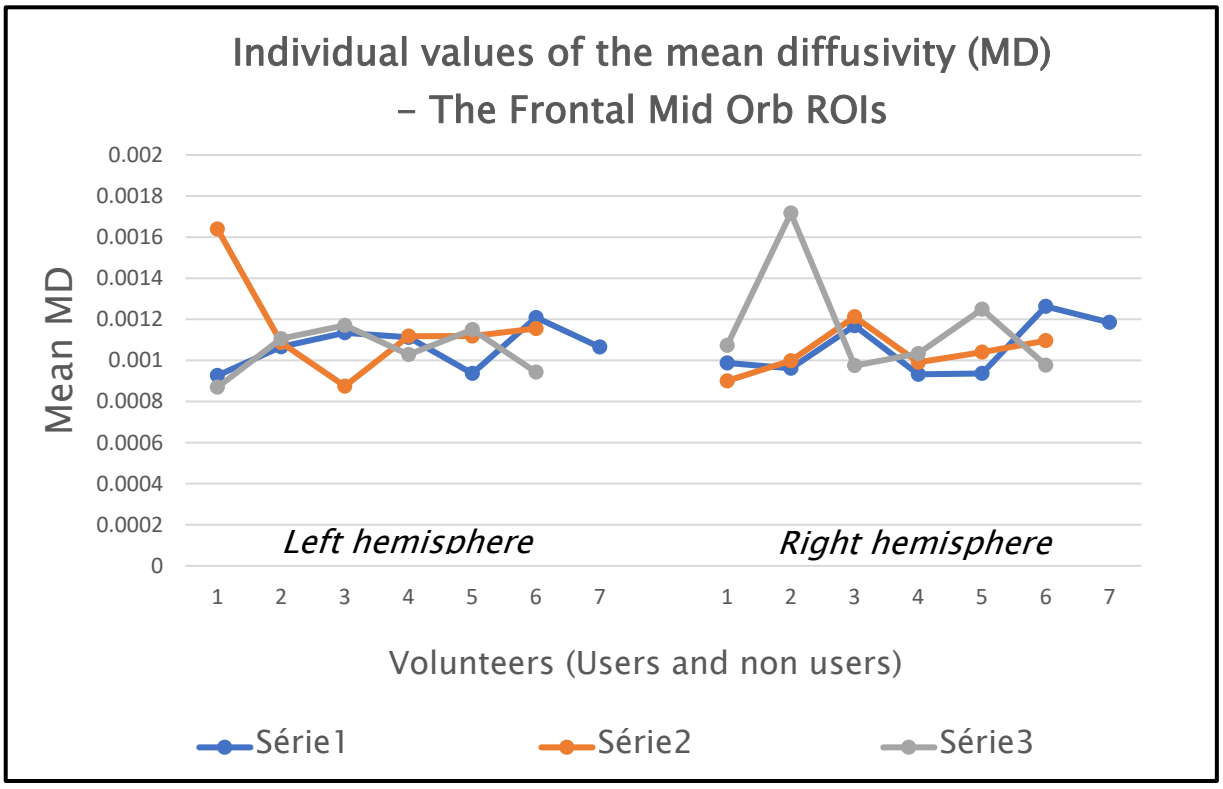

Figure 141: Individual values of mean diffusivity (MD) in both hemispheres' Frontal Mid Orb ROIs. This figure depicts the MD values of all the participants belonging to each of the three groups (Heavy and light users and healthy controls).

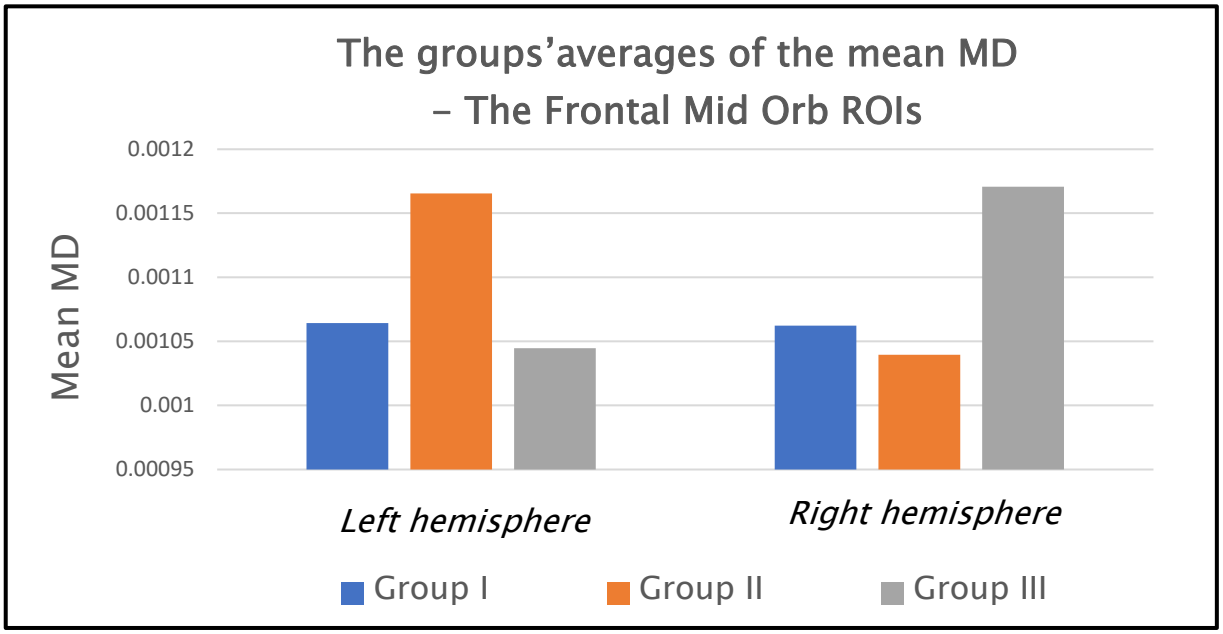

Figure 142: The mean diffusivity (MD) averages of each group in the Frontal Mid Orb ROIs in the left and the right hemispheres.

Table 54: The mean diffusivity (MD) averages and standard deviations (SD) values for the groups studied in the Frontal Mid Orb ROIs, along with intergroup comparisons.

	Left Hemisphere	Right Hemisphere
Heavy users' group (G. I)	(0,001064±0,0001027)	(0,001062±0,000138)
Light users' group (G. II)	(0,00116±0,000252)	(0,001039±0,0001063)
Non-users' group (G.III)	(0,001044±0,00012004)	(0,00117±0,000286)
Intergroup comparison	G. II > G. I ≈ G.III	G.III > G. I ≈ G. II

➢ **Frontal Inf Orb:**

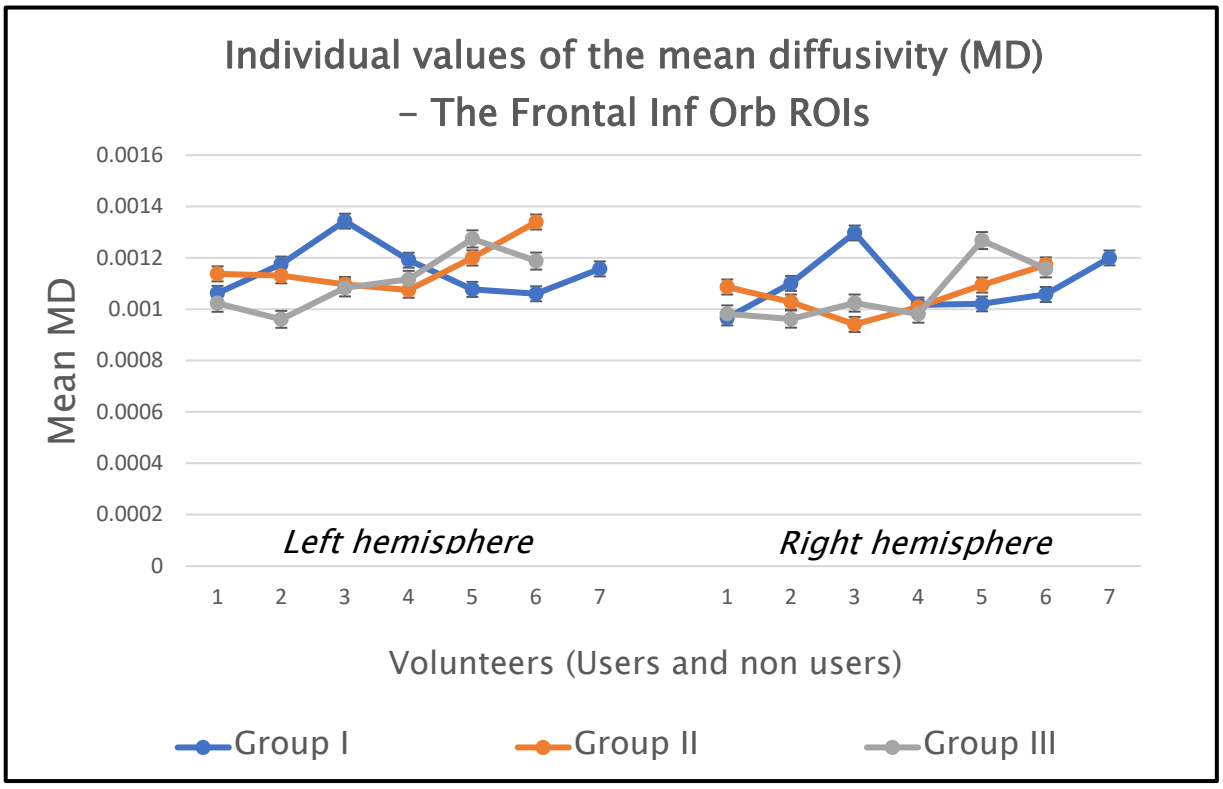

Figure 143: Individual values of mean diffusivity (MD) in both hemispheres' Frontal Inf Orb ROIs. This figure depicts the MD values of all the participants belonging to each of the three groups (Heavy and light users and healthy controls).

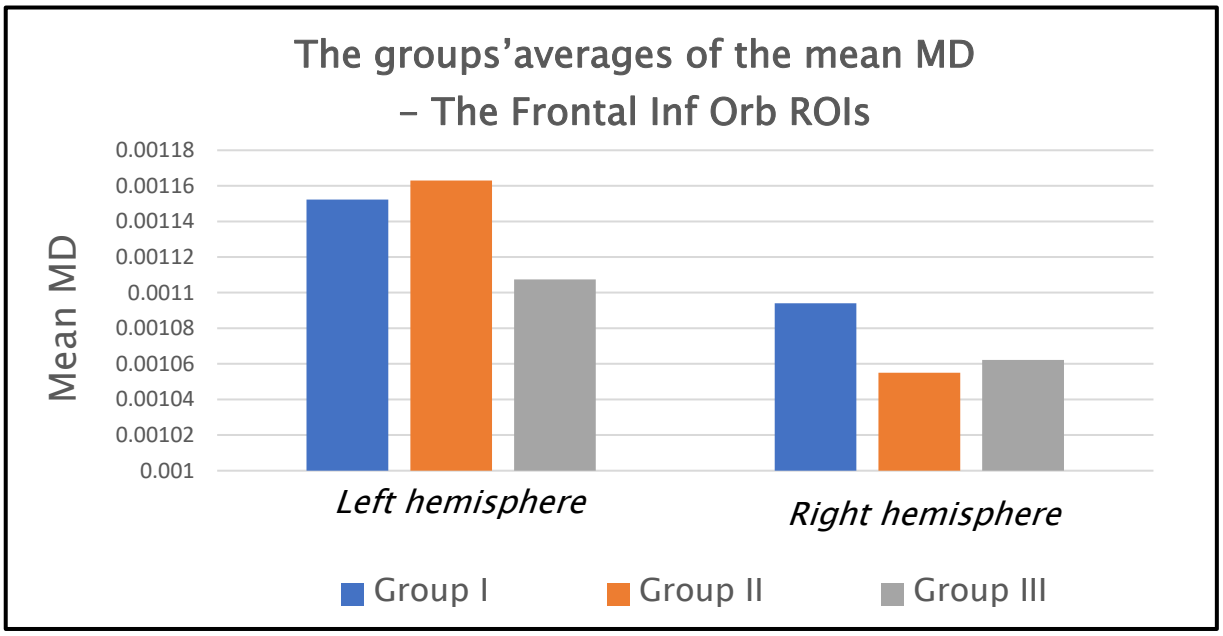

Figure 144: The mean diffusivity (MD) averages of each group in the Frontal Inf Orb ROIs in the left and the right hemispheres.

Table 55: The mean diffusivity (MD) averages and standard deviations (SD) values for the groups studied in the Frontal Inf Orb ROIs, along with intergroup comparisons.

	Left Hemisphere	Right Hemisphere
Heavy users' group (G. I)	(0,00115±0,00010063)	(0,001094±0,000116)
Light users' group (G. II)	(0,00116±0,0000965)	(0,001055±0,00008026)
Non-users' group (G.III)	(0,001107±0,000112)	(0,001062±0,000123)
Intergroup comparison	G. II ≈ G. I > G.III	G. I > G.III ≈ G. II

➢ **Rectus:**

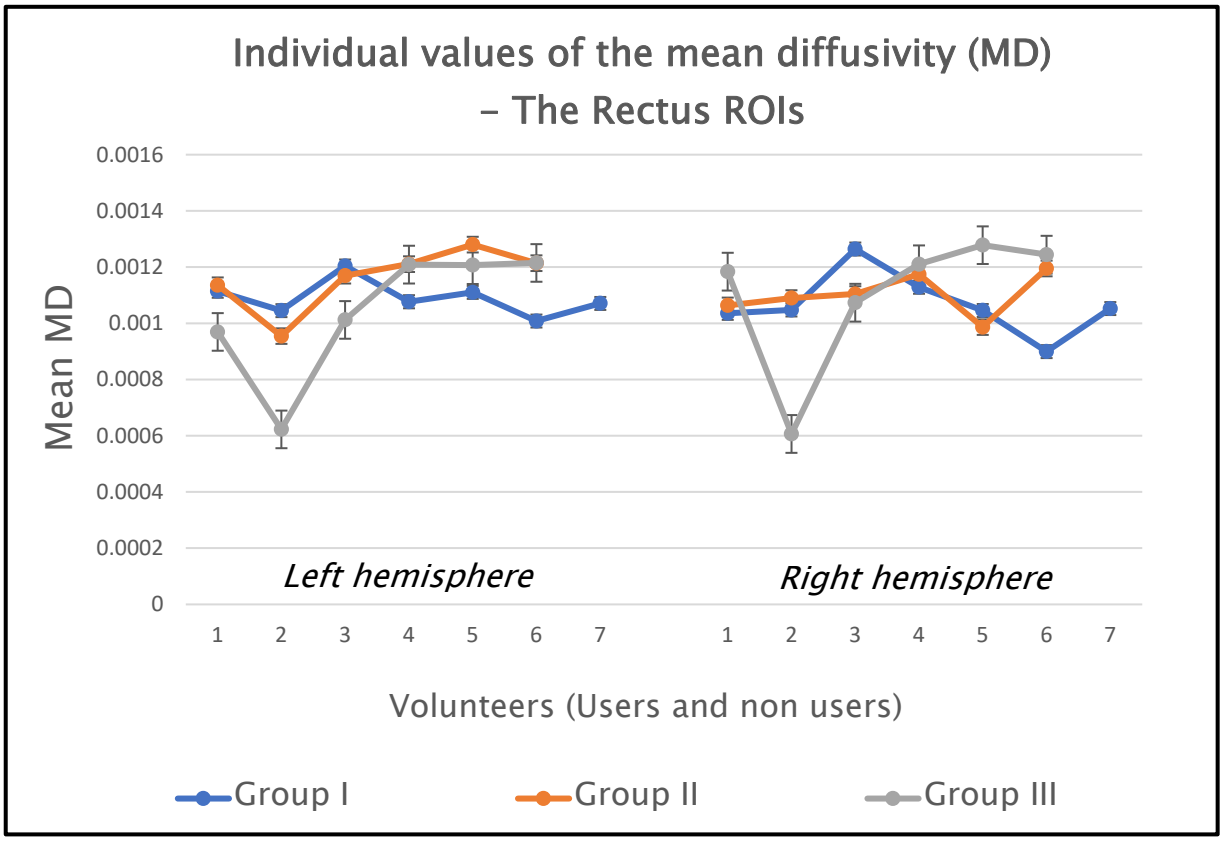

Figure 145: Individual values of mean diffusivity (MD) in both hemispheres' Rectus ROIs. This figure depicts the MD values of all the participants belonging to each of the three groups (Heavy and light users and healthy controls).

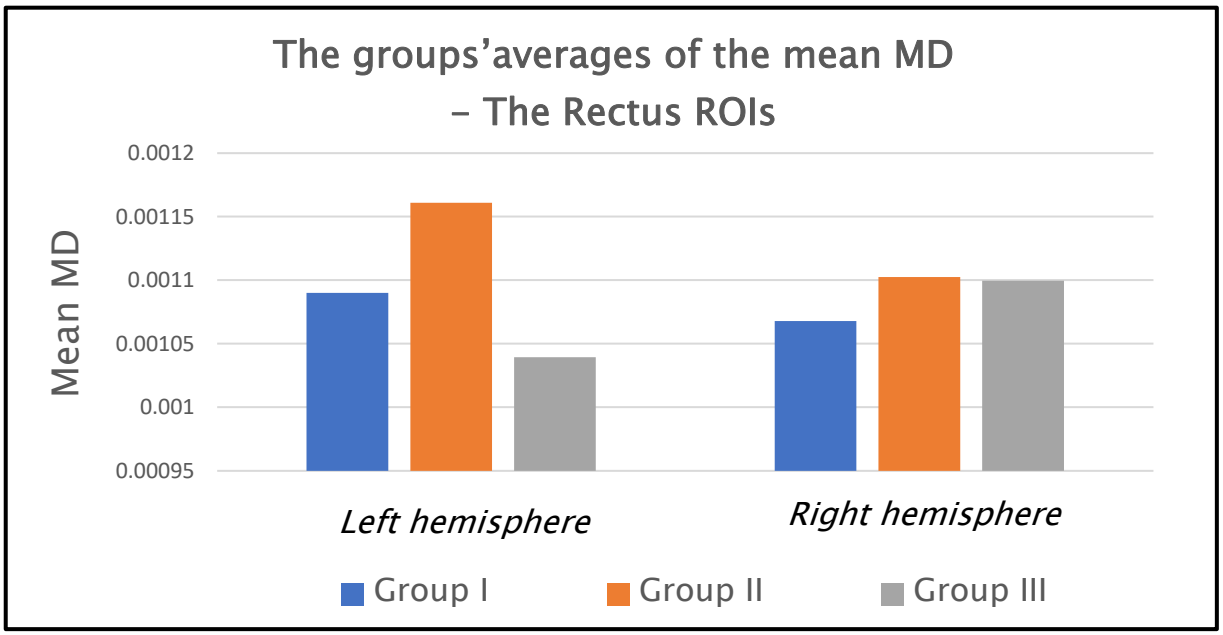

Figure 146: The mean diffusivity (MD) averages of each group in the Rectus ROIs in the left and the right hemispheres.

Table 56: The mean diffusivity (MD) averages and standard deviations (SD) values for the groups studied in the Rectus ROIs, along with intergroup comparisons.

	Left Hemisphere	Right Hemisphere
Heavy users' group (G. I)	(0,001090001±0,0000621)	(0,001067±0,0001101)
Light users' group (G. II)	(0,00116±0,000112)	(0,001102±0,00007603)
Non-users' group (G.III)	(0,001039±0,000231)	(0,001099±0,000251)
Intergroup comparison	G. II > G. I > G.III	G. II ≈ G.III > G. I

➢ **Olfactory:**

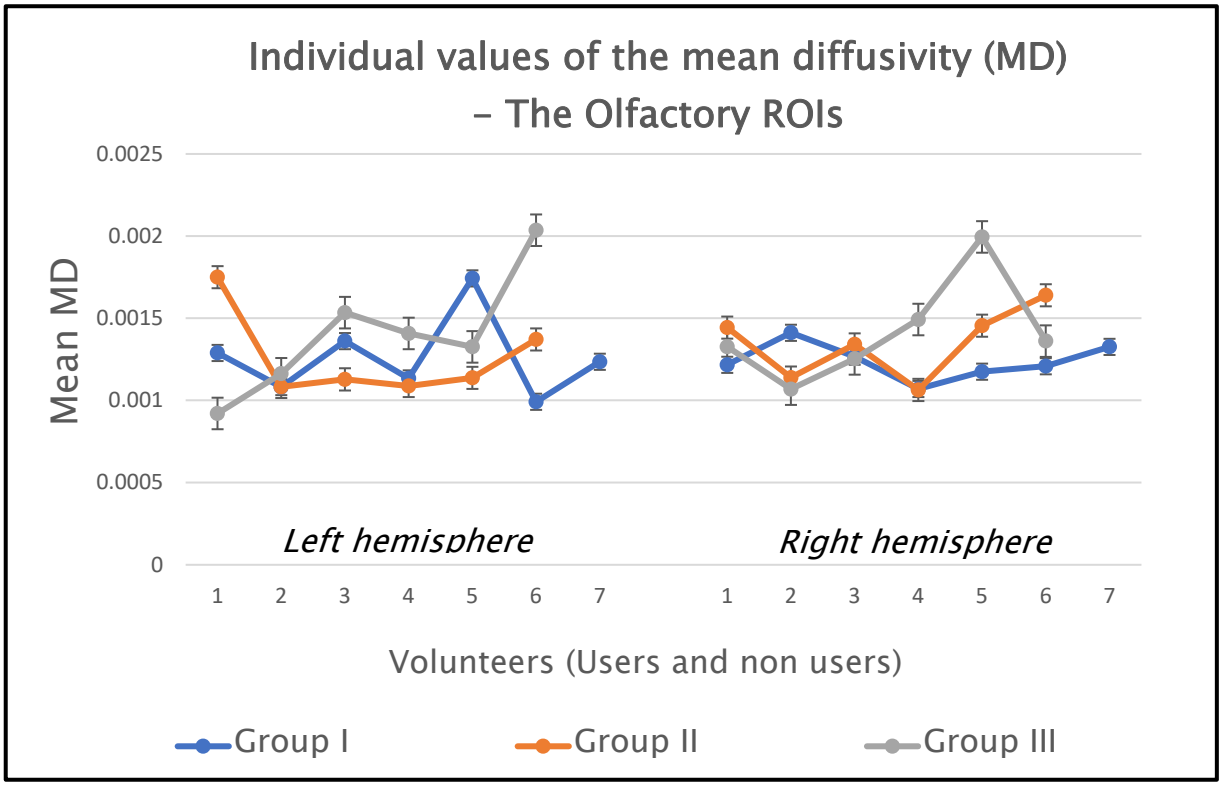

Figure 147: Individual values of mean diffusivity (MD) in both hemispheres' Olfactory ROIs. This figure depicts the MD values of all the participants belonging to each of the three groups (Heavy and light users and healthy controls).

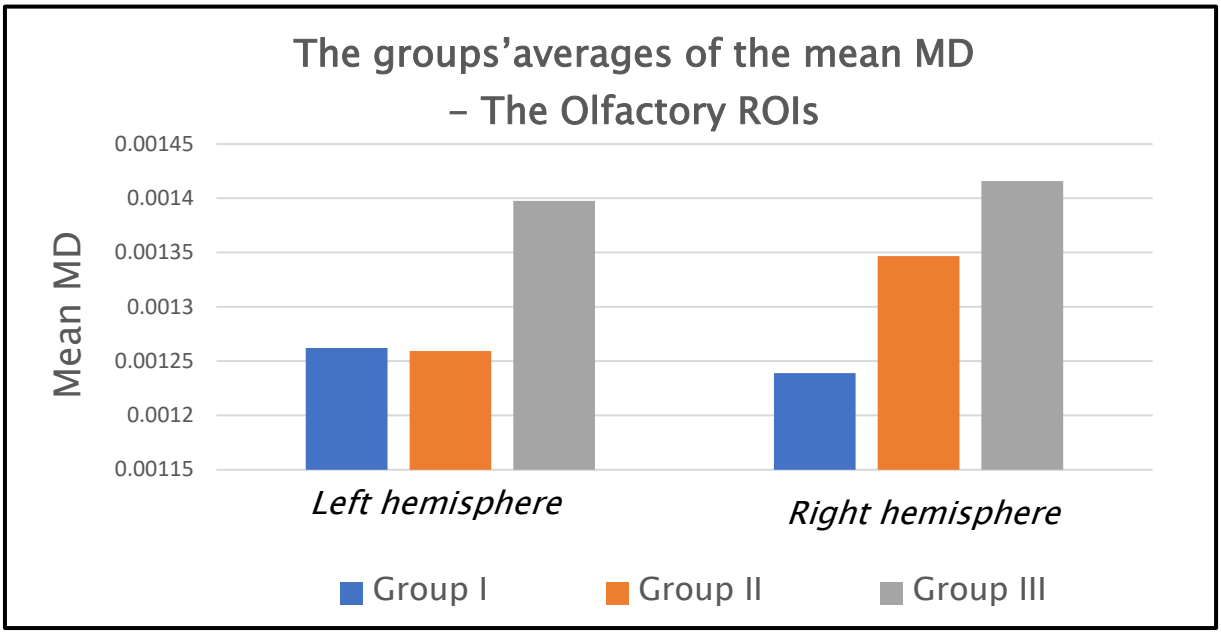

Figure 148: The mean diffusivity (MD) averages of each group in the Olfactory ROIs in the left and the right hemispheres.

Table 57: The mean diffusivity (MD) averages and standard deviations (SD) values for the groups studied in the Olfactory ROIs, along with intergroup comparisons.

	Left Hemisphere	Right Hemisphere
Heavy users' group (G. I)	(0,00126±0,000246)	(0,00123±1,2087)
Light users' group (G. II)	(0,00125±0,000263)	(0,00134±0,000214)
Non-users' group (G.III)	(0,00139±0,000377)	(0,00141±0,000315)
Intergroup comparison	G.III > G. II ≈ G. I	G.III >G. II > G. I

➢ **Frontal Sup Medial:**

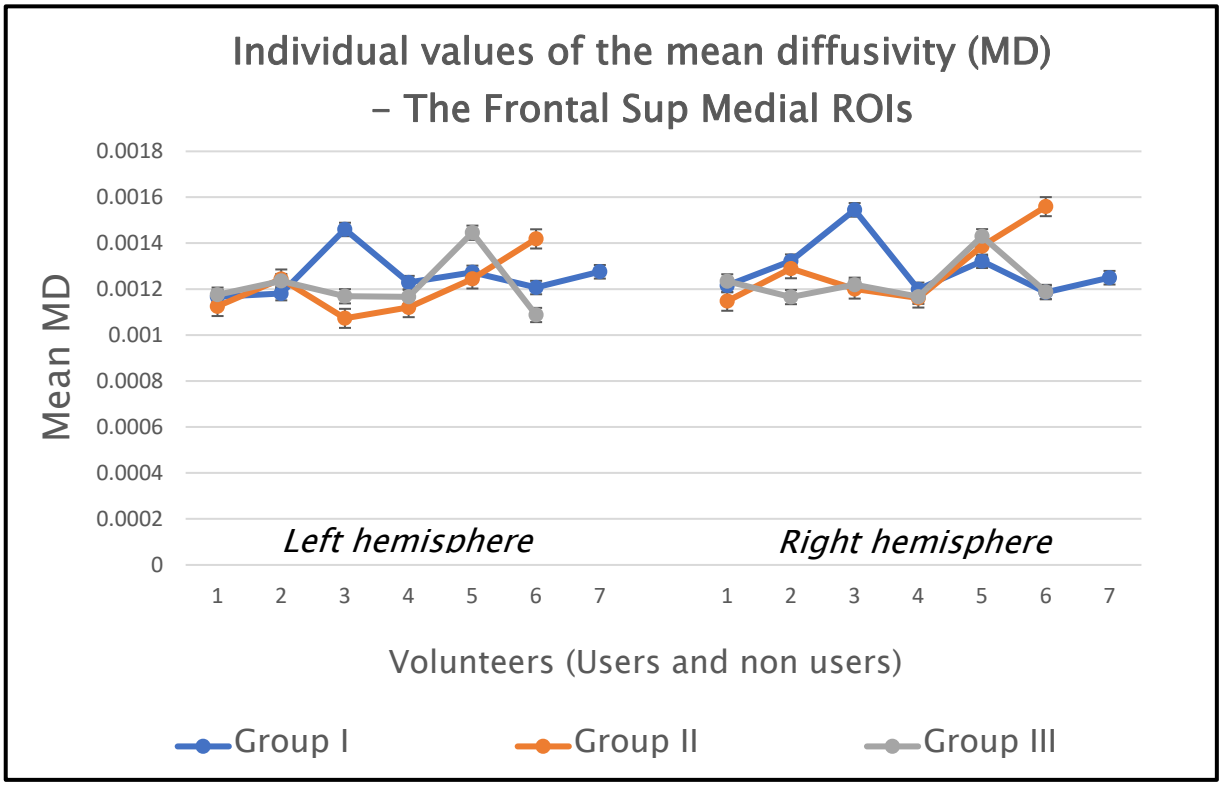

Figure 149: Individual values of mean diffusivity (MD) in both hemispheres' Frontal Sup Medial ROIs. This figure depicts the MD values of all the participants belonging to each of the three groups (Heavy and light users and healthy controls).

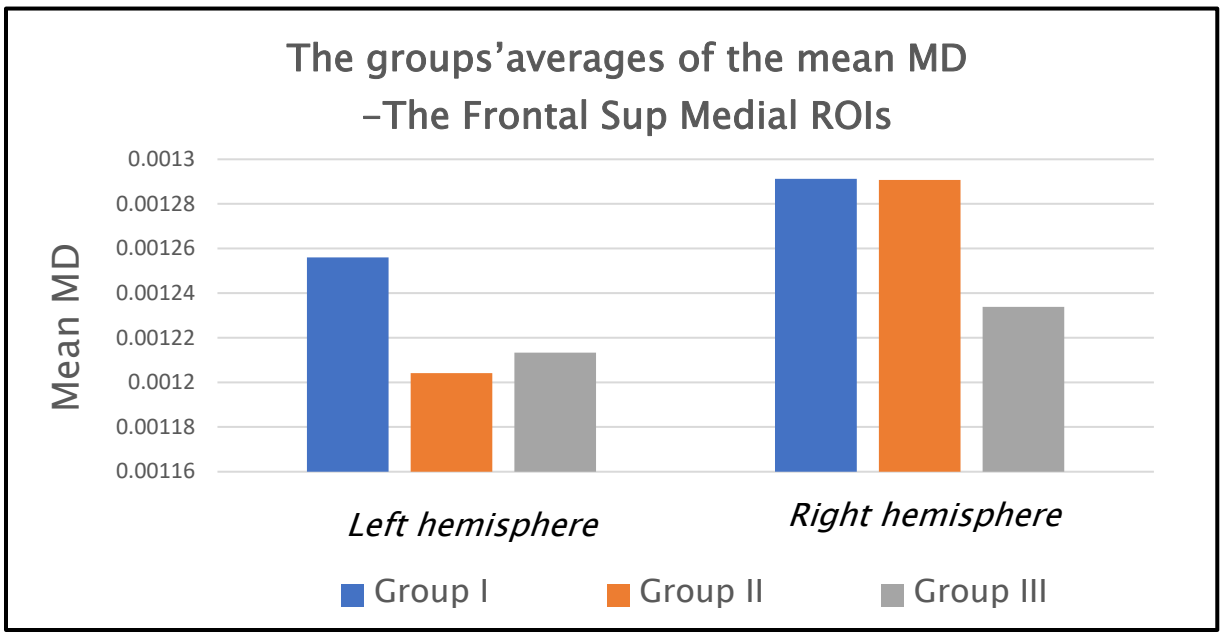

Figure 150: The mean diffusivity (MD) averages of each group in the Frontal Sup Medial ROIs in the left and the right hemispheres.

Table 58: The mean diffusivity (MD) averages and standard deviations (SD) values for the groups studied in the Frontal Sup Medial ROIs, along with intergroup comparisons.

	Left Hemisphere	Right Hemisphere
Heavy users' group (G. I)	(0,00125±0,0000992)	(0,00129±0,000124)
Light users' group (G. II)	(0,001204±0,000126)	(0,00129±0,000159)
Non-users' group (G.III)	(0,00121±0,000123)	(0,00123±0,0000999)
Intergroup comparison	G. I > G.III ≈ G. II	G. II ≈ G. I > G.III

➢ **Frontal Sup**

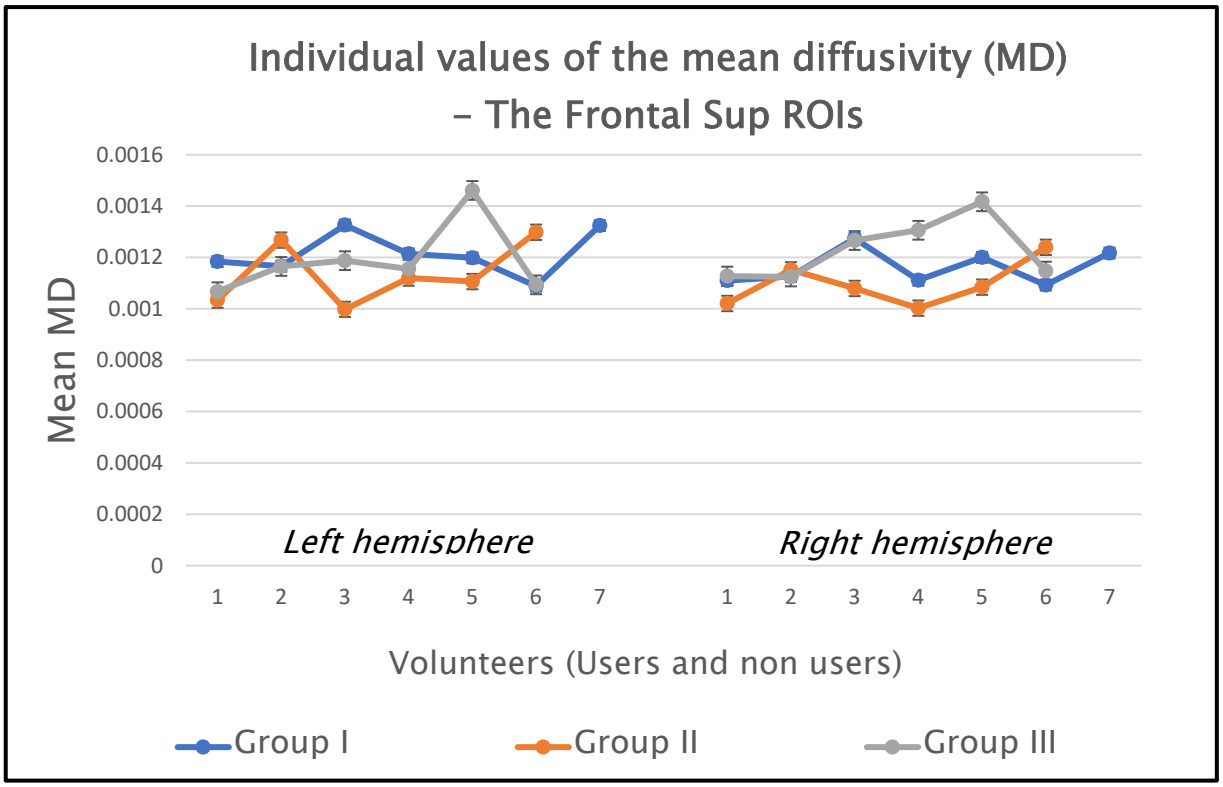

Figure 151: Individual values of mean diffusivity (MD) in both hemispheres' Frontal Sup ROIs. This figure depicts the MD values of all the participants belonging to each of the three groups (Heavy and light users and healthy controls).

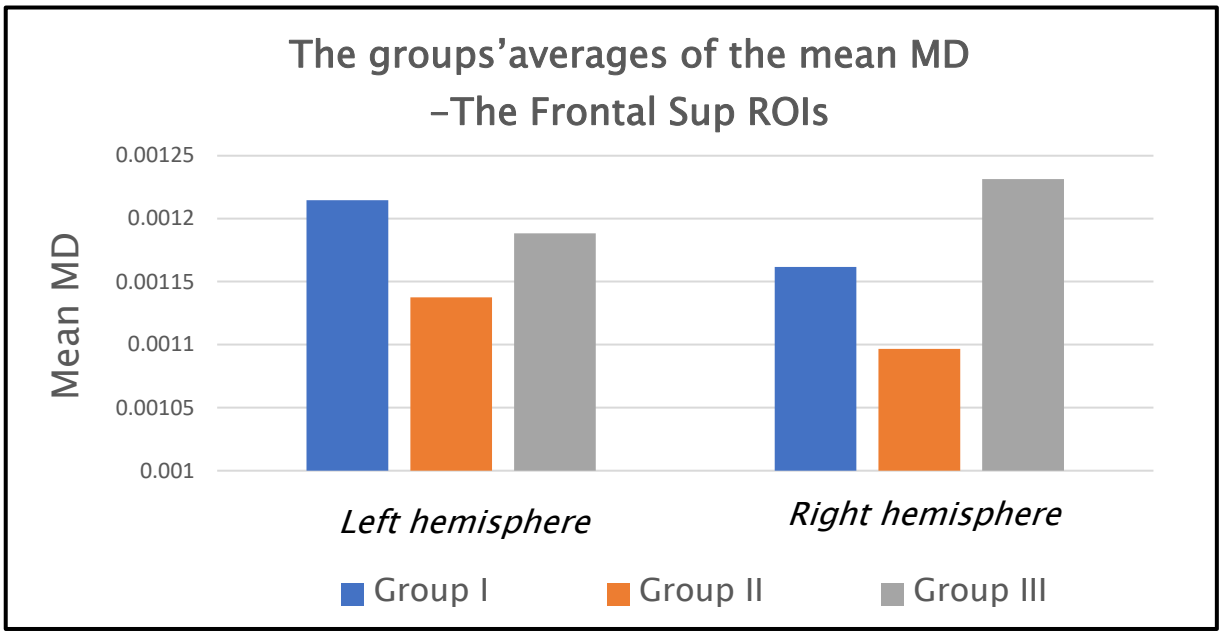

Figure 152: The mean diffusivity (MD) averages of each group in the Frontal Sup ROIs in the left and the right hemispheres.

Table 59: The mean diffusivity (MD) averages and standard deviations (SD) values for the groups studied in the Frontal Sup ROIs, along with intergroup comparisons.

	Left Hemisphere	Right Hemisphere
Heavy users' group (G. I)	(0,00121±0,0000854)	(0,00116±0,0000689)
Light users' group (G. II)	(0,00113±0,000121)	(0,001096±0,0000877)
Non-users' group (G.III)	(0,00118±0,000141)	(0,00123±0,000118)
Intergroup comparison	G.III ≈ G. I > G. II	G.III > G. I > G. II

➢ Frontal Mid

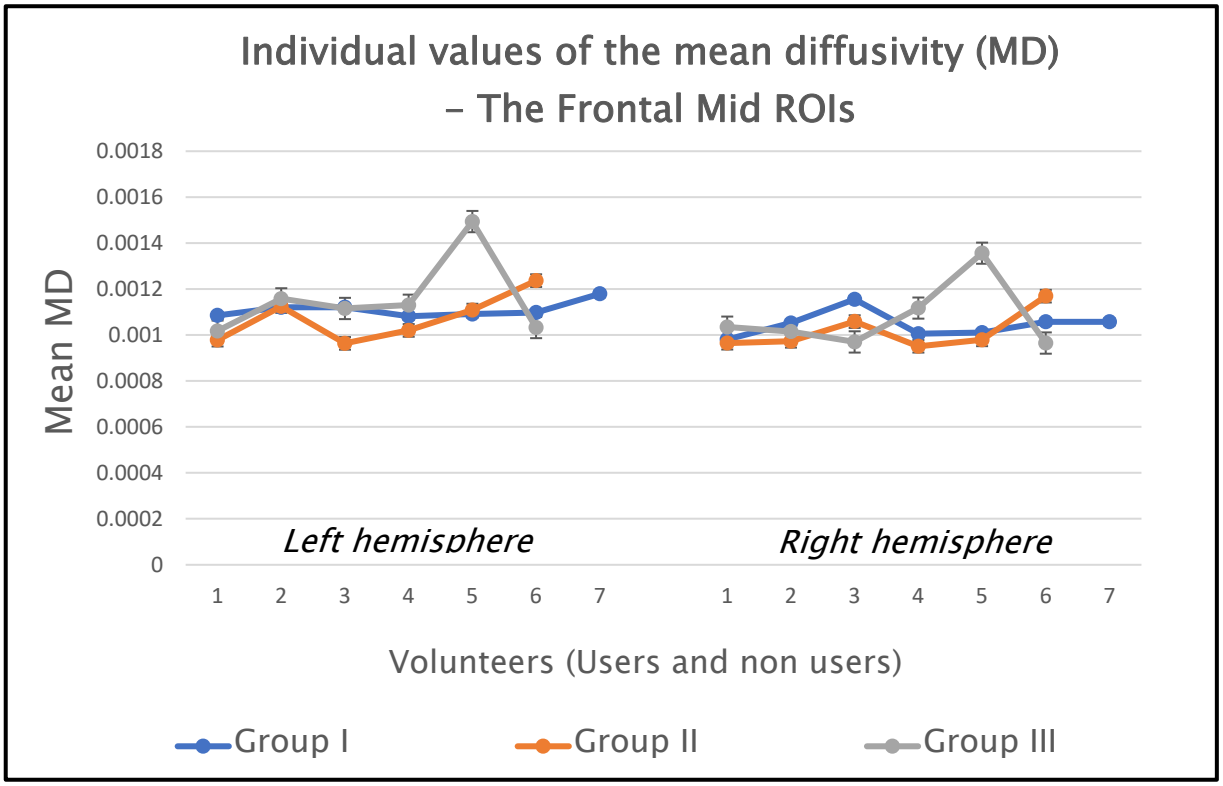

Figure 153: Individual values of mean diffusivity (MD) in both hemispheres' Frontal Mid ROIs. This figure depicts the MD values of all the participants belonging to each of the three groups (Heavy and light users and healthy controls).

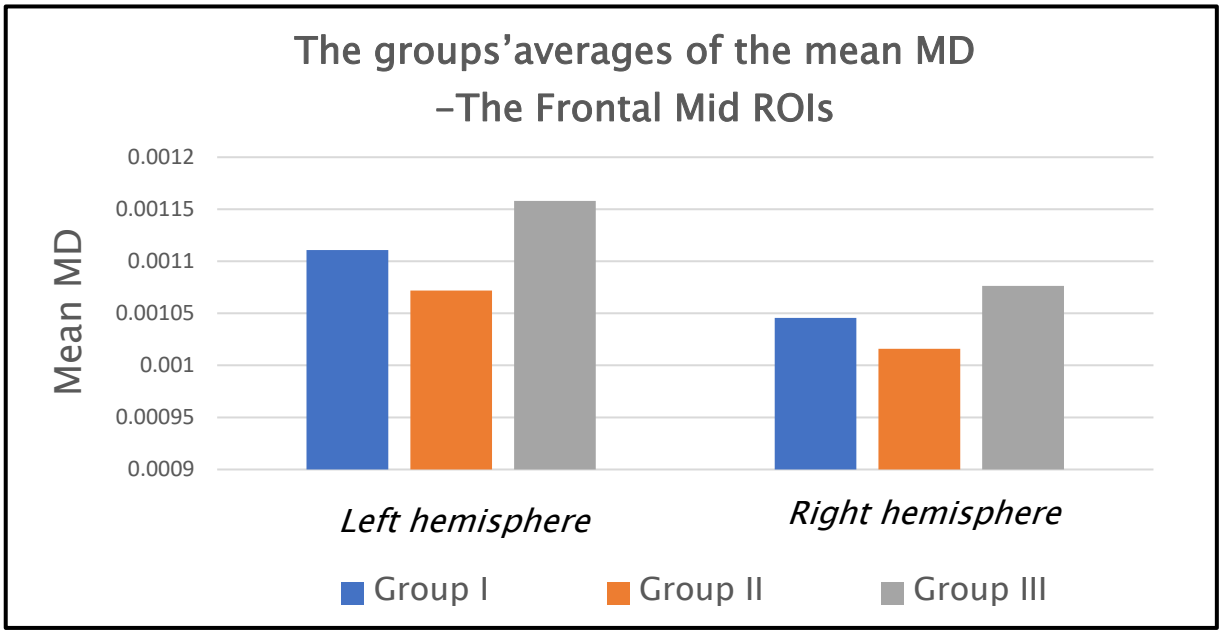

Figure 154: The mean diffusivity (MD) averages of each group in the Frontal Mid ROIs in the left and the right hemispheres.

Table 60: The mean diffusivity (MD) averages and standard deviations (SD) values for the groups studied in the Frontal Mid ROIs, along with intergroup comparisons.

	Left Hemisphere	Right Hemisphere
Heavy users' group (G. I)	(0,00111±0,000034)	(0,001045±0,0000568)
Light users' group (G. II)	(0,001071±0,0001043)	(0,001015±0,0000842)
Non-users' group (G.III)	(0,00115±0,000173)	(0,001076±0,000147)
Intergroup comparison	G.III ≈ G. I ≈ G. II	G.III ≈ G. I ≈ G. II

➢ **Frontal Inf Oper**

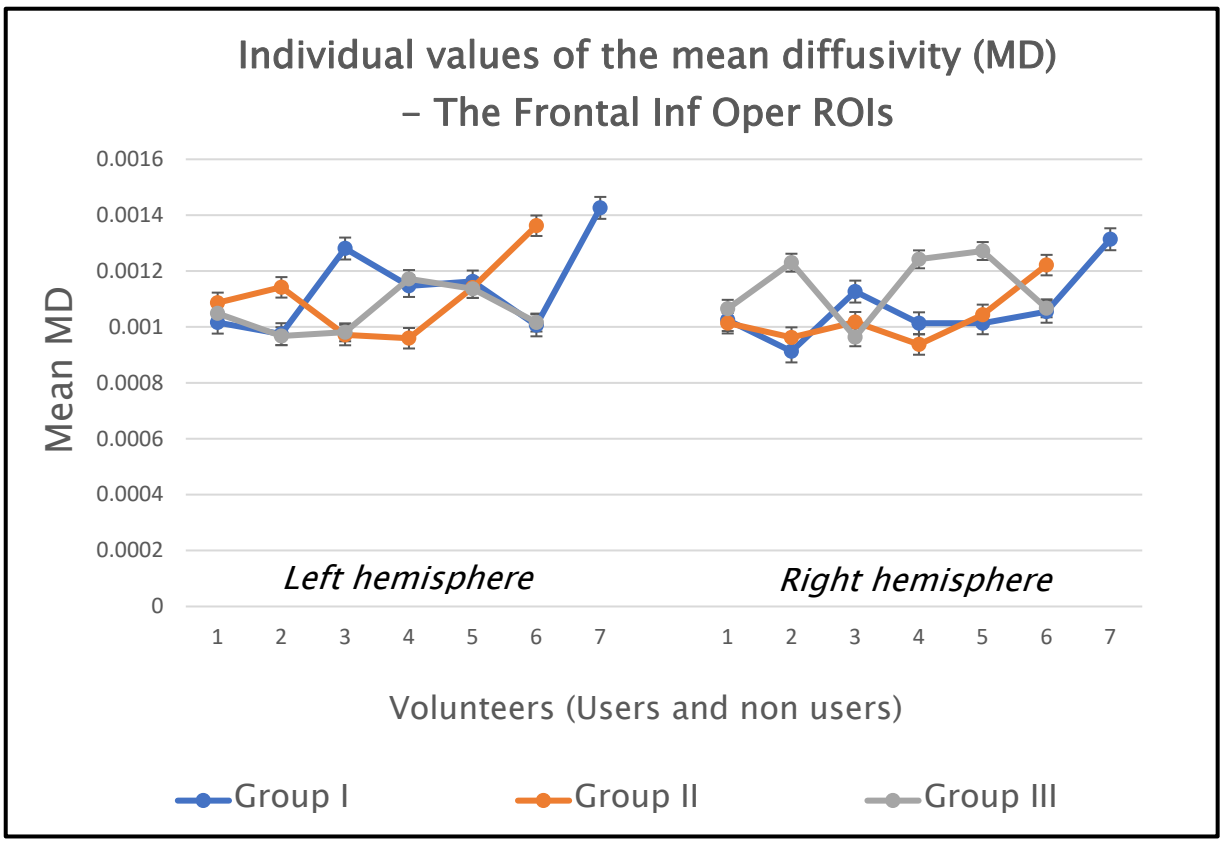

Figure155: Individual values of mean diffusivity (MD) in both hemispheres' Frontal Inf Oper ROIs. This figure depicts the MD values of all the participants belonging to each of the three groups (Heavy and light users and healthy controls).

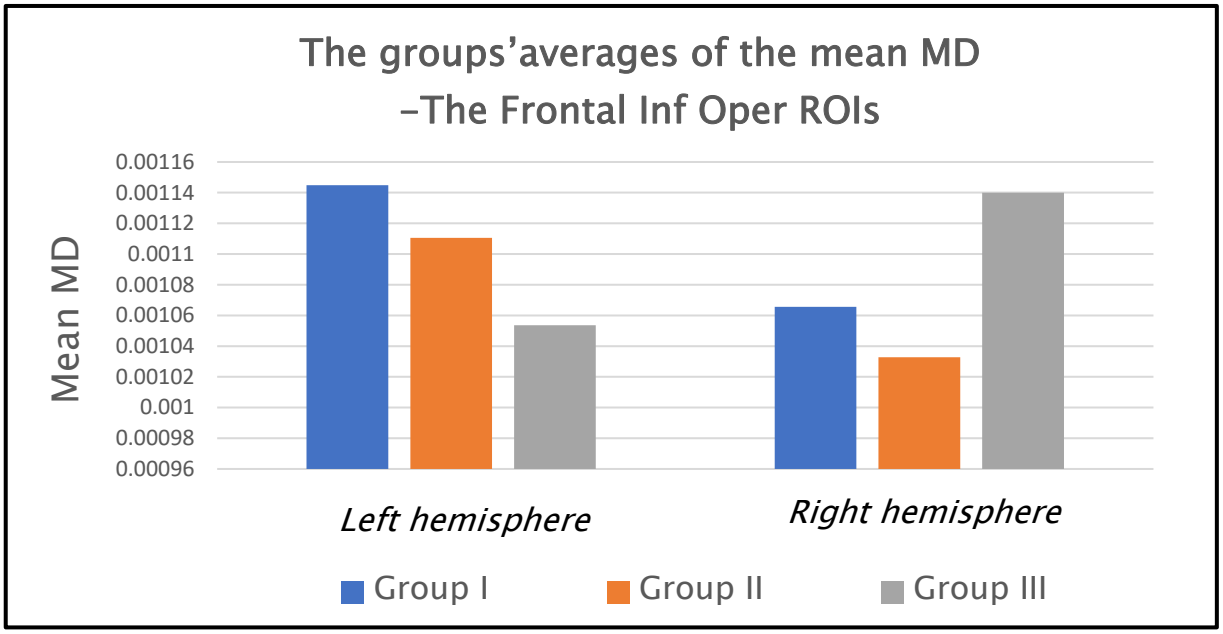

Figure 156: The mean diffusivity (MD) averages of each group in the Frontal Inf Oper ROIs in the left and the right hemispheres.

Table 61: The mean diffusivity (MD) averages and standard deviations (SD) values for the groups studied in the Frontal Inf Oper ROIs, along with intergroup comparisons.

	Left Hemisphere	Right Hemisphere
Heavy users' group (G. I)	(0,00114±0,000164)	(0,001065±0,000126)
Light users' group (G. II)	(0,00111±0,000147)	(0,001032±0,00010041)
Non-users' group (G.III)	(0,001053±0,0000836)	(0,00113±0,000125)
Intergroup comparison	G. I > G. II > G.III	G.III > G. II ≈ G. I

➢ Frontal Inf Tri

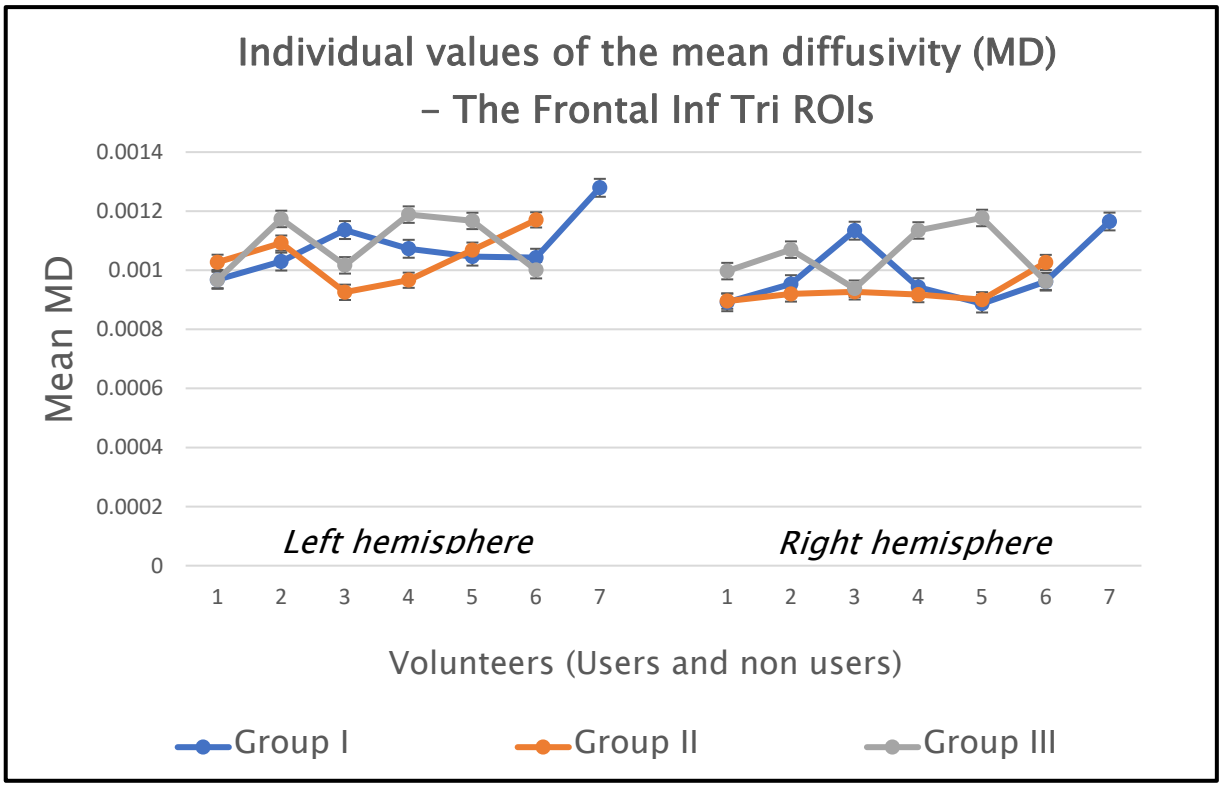

Figure 157: Individual values of mean diffusivity (MD) in both hemispheres' Frontal Inf Tri ROIs. This figure depicts the MD values of all the participants belonging to each of the three groups (Heavy and light users and healthy controls).

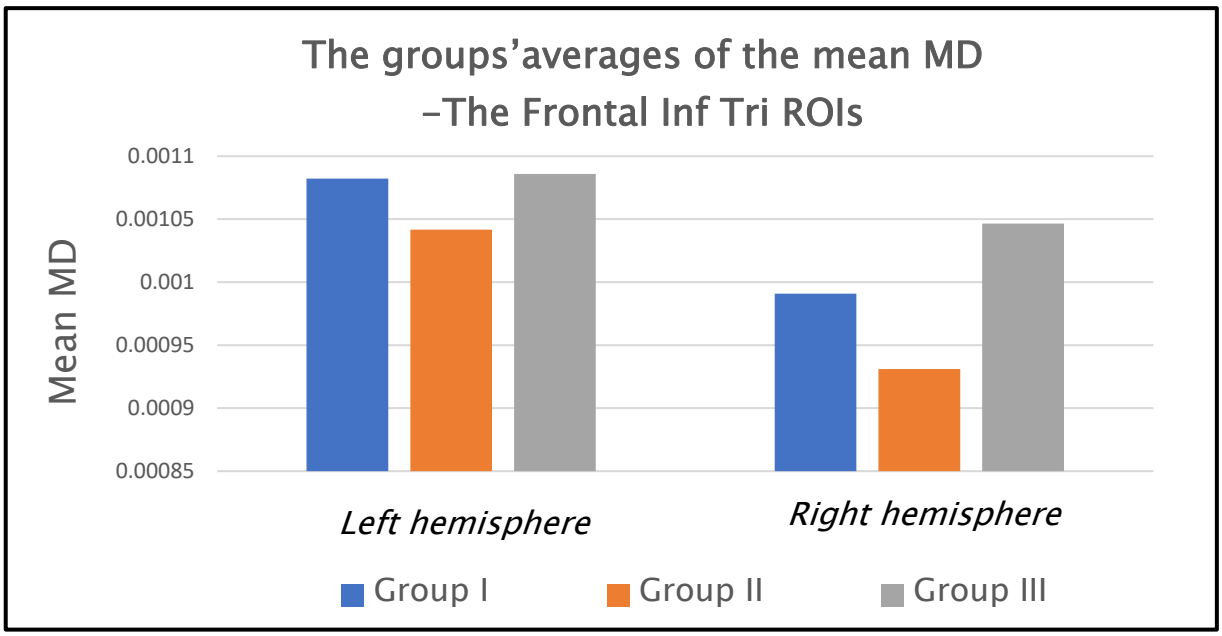

Figure 158: The mean diffusivity (MD) averages of each group in the Frontal Inf Tri ROIs in the left and the right hemispheres.

Table 62: The mean diffusivity (MD) averages and standard deviations (SD) values for the groups studied in the Frontal Inf Tri ROIs, along with intergroup comparisons.

	Left Hemisphere	Right Hemisphere
Heavy users' group (G. I)	(0,001082±0,00010043)	(0,0009908±0,000112)
Light users' group (G. II)	(0,001041±0,0000885)	(0,000931±0,0000482)
Non-users' group (G.III)	(0,001085±0,00010094)	(0,001046±0,0000968)
Intergroup comparison	G.III ≈ G. I ≈ G. II	G.III > G. I > G. II

➢ **Postcentral**

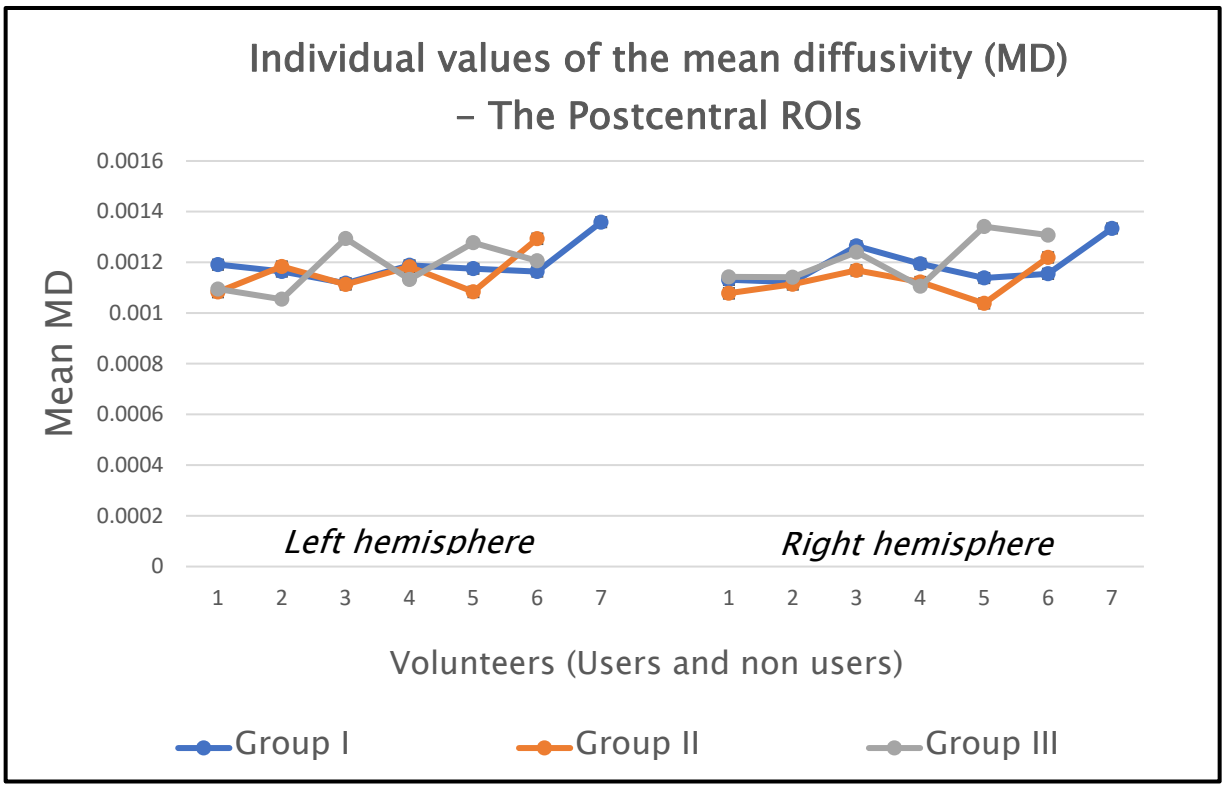

Figure 159: Individual values of mean diffusivity (MD) in both hemispheres' Postcentral ROIs. This figure depicts the MD values of all the participants belonging to each of the three groups (Heavy and light users and healthy controls).

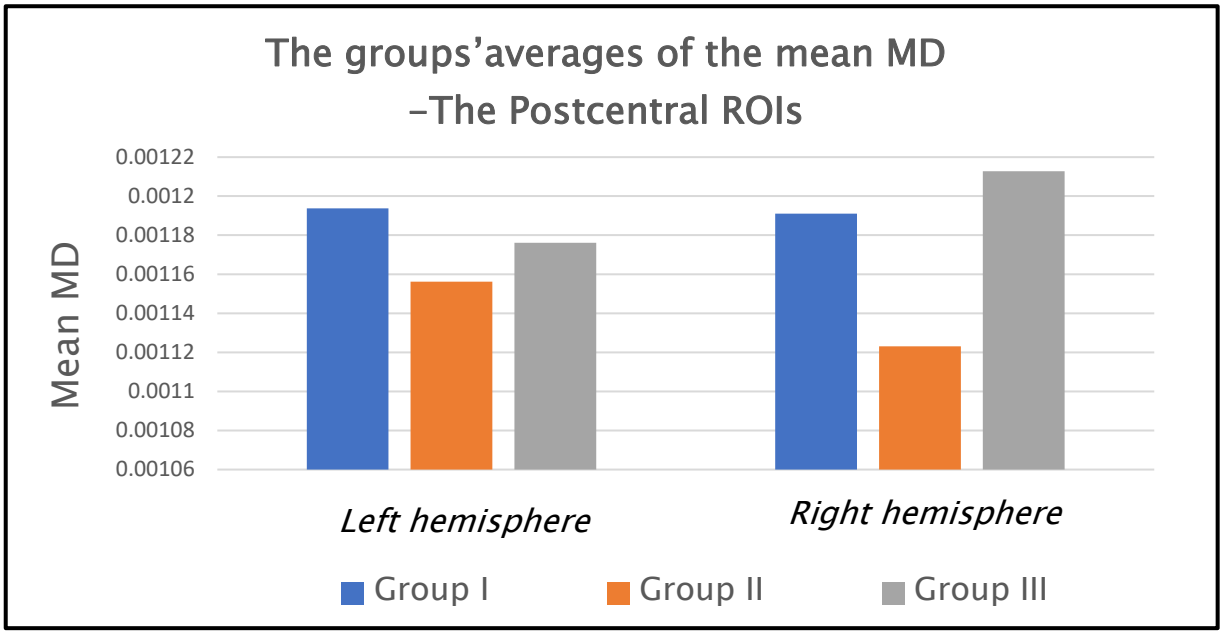

Figure 160: The mean diffusivity (MD) averages of each group in the Postcentral ROIs in the left and the right hemispheres.

Table 63: The mean diffusivity (MD) averages and standard deviations (SD) values for the groups studied in the Postcentral ROIs, along with intergroup comparisons.

	Left Hemisphere	Right Hemisphere
Heavy users' group (G. I)	(0,00119±0,0000765)	(0,00119±0,0000799)
Light users' group (G. II)	(0,00115±0,00008085)	(0,00112±0,0000643)
Non-users' group (G.III)	(0,00117±0,0000984)	(0,00121±0,0000976)
Intergroup comparison	G.III ≈ G. I ≈ G. II	G.III ≈ G. I > G. II

➢ Parietal Sup

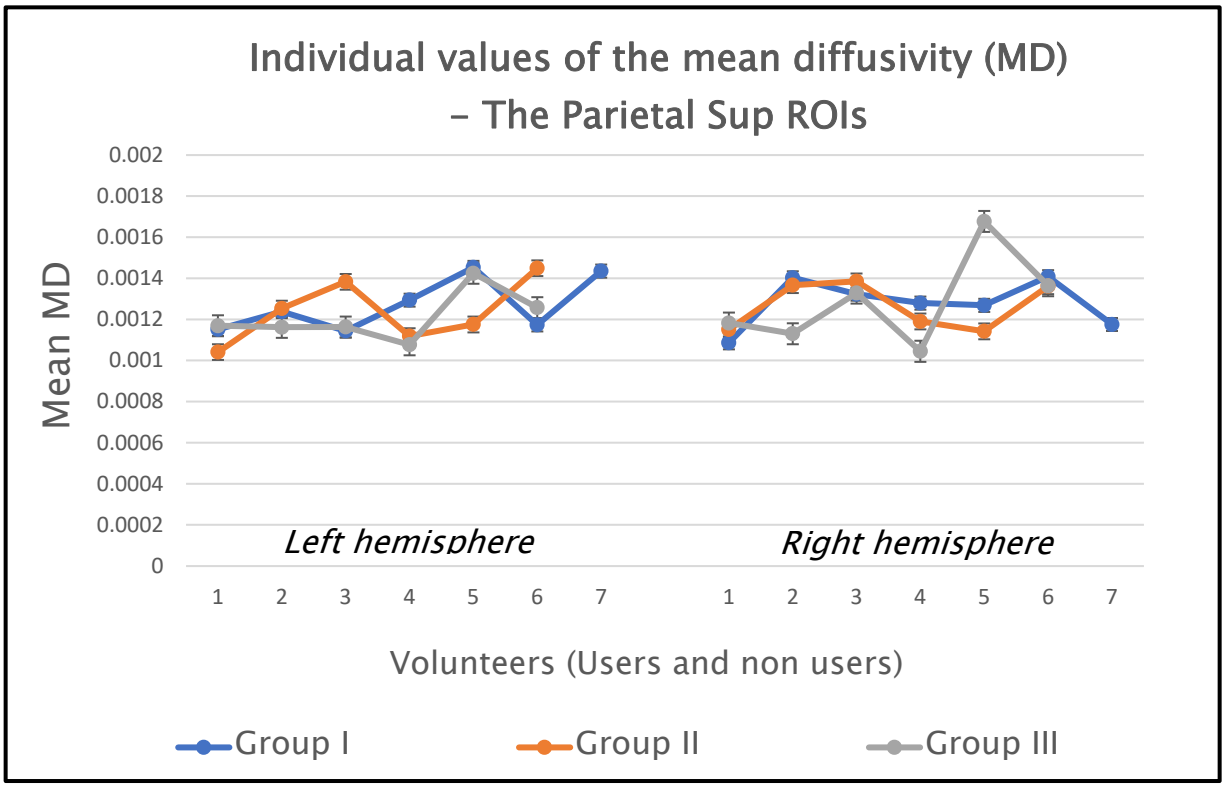

Figure 161: Individual values of mean diffusivity (MD) in both hemispheres' Parietal Sup ROIs. This figure depicts the MD values of all the participants belonging to each of the three groups (Heavy and light users and healthy controls).

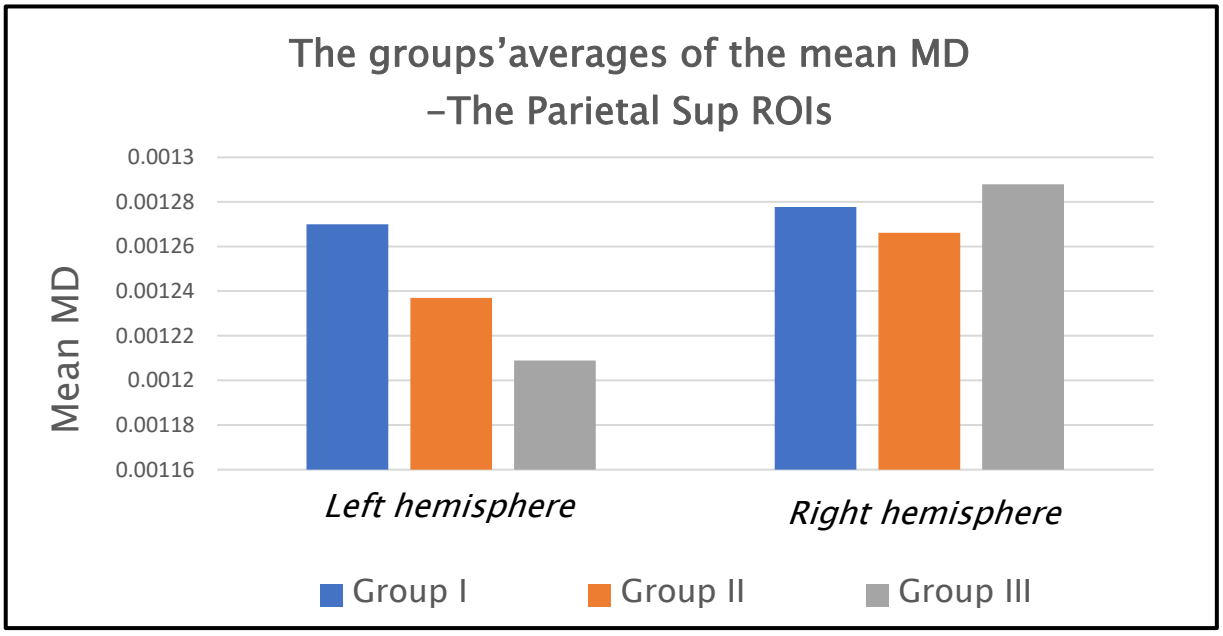

Figure 162: The mean diffusivity (MD) averages of each group in the Parietal Sup ROIs in the left and the right hemispheres.

Table 64: The mean diffusivity (MD) averages and standard deviations (SD) values for the groups studied in the Parietal Sup ROIs, along with intergroup comparisons.

	Left Hemisphere	Right Hemisphere
Heavy users' group (G. I)	(0,00126±0,0001303)	(0,001277±0,000116)
Light users' group (G. II)	(0,00123±0,000156)	(0,00126±0,0001165)
Non-users' group (G.III)	(0,001208±0,0001202)	(0,00128±0,000225)
Intergroup comparison	G. I > G. II > G.III	G.III ≈ G. I ≈ G. II

➢ **SupraMarginal**

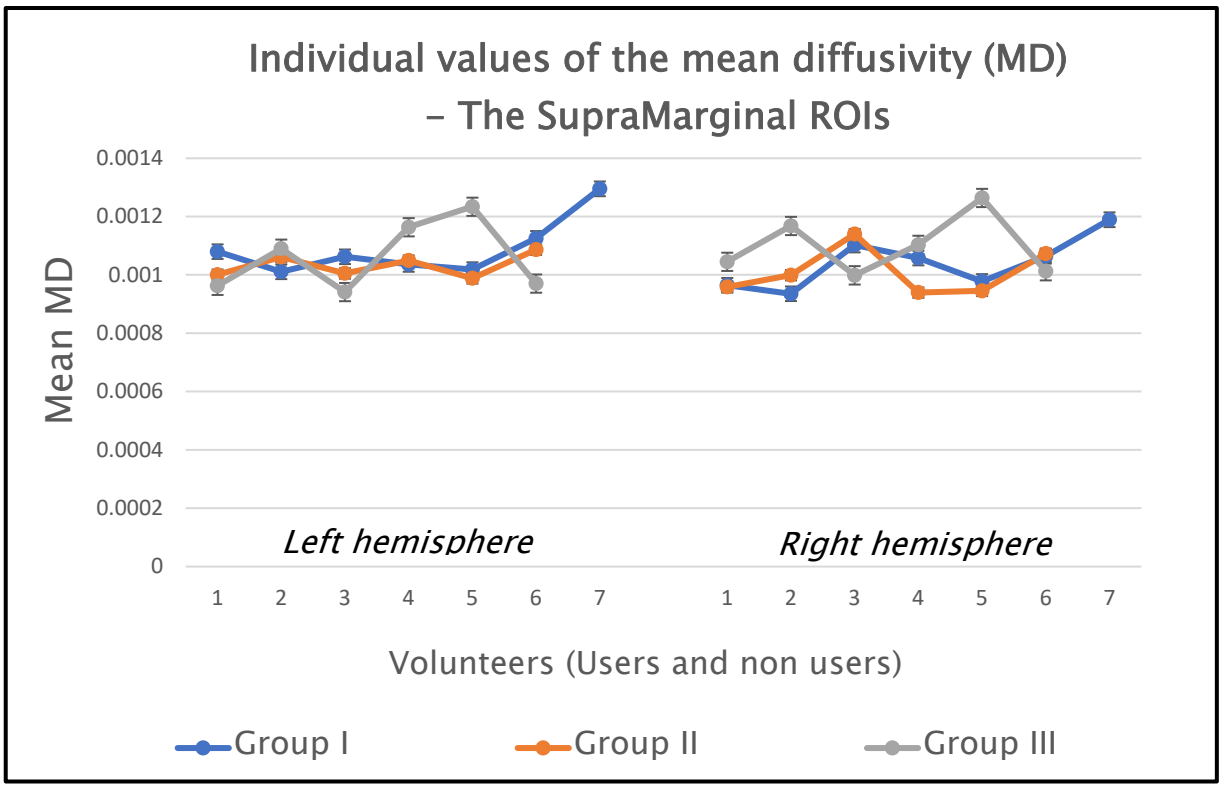

Figure 163: Individual values of mean diffusivity (MD) in both hemispheres' SupraMarginal ROIs. This figure depicts the MD values of all the participants belonging to each of the three groups (Heavy and light users and healthy controls).

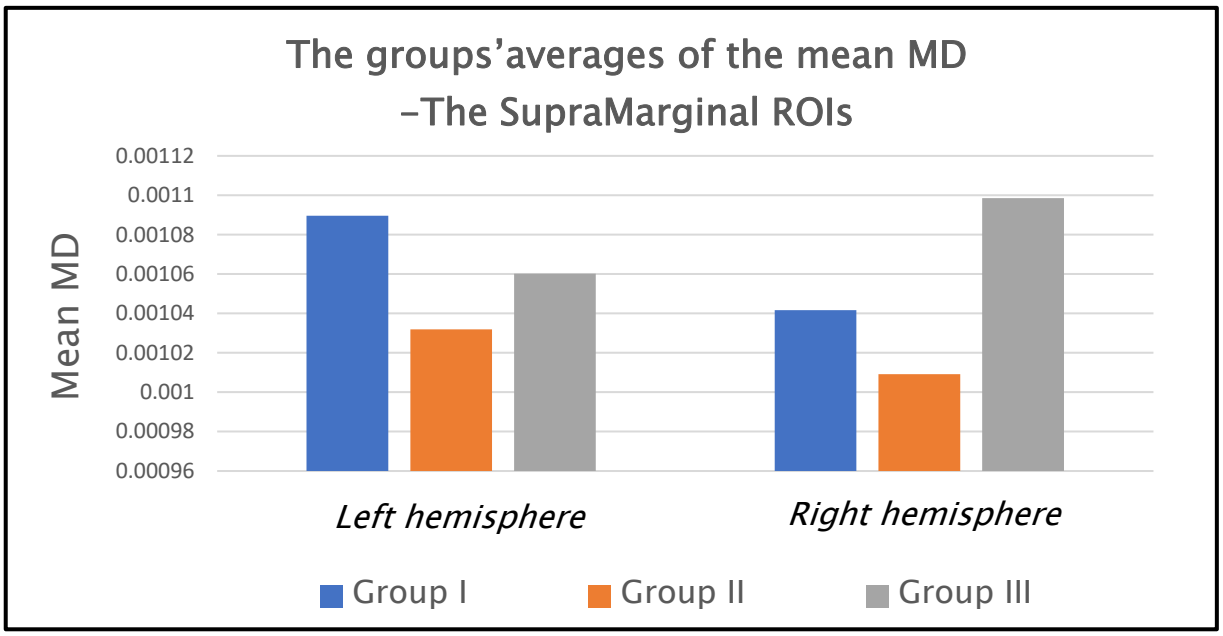

Figure 164: The mean diffusivity (MD) averages of each group in the SupraMarginal ROIs in the left and the right hemispheres.

Table 65: The mean diffusivity (MD) averages and standard deviations (SD) values for the groups studied in the SupraMarginal ROIs, along with intergroup comparisons.

	Left Hemisphere	Right Hemisphere
Heavy users' group (G. I)	(0,001089±0,0000987)	(0,001041±0,00008903)
Light users' group (G. II)	(0,001031±0,0000393)	(0,0010091±0,00008086)
Non-users' group (G.III)	(0,0010601±0,000121)	(0,001098±0,0001024)
Intergroup comparison	G. I ≈ G. II ≈ G.III	G.III > G. I ≈ G. II

➢ Angular

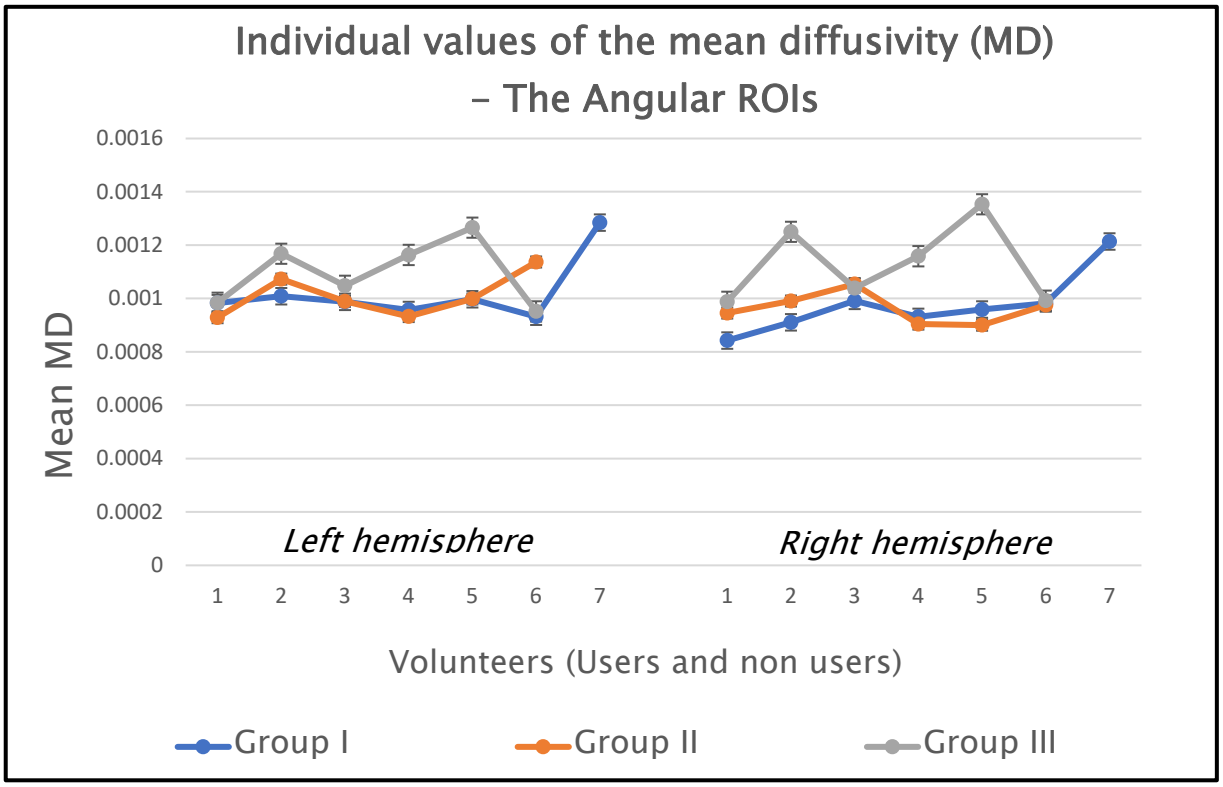

Figure 165: Individual values of mean diffusivity (MD) in both hemispheres' Angular ROIs. This figure depicts the MD values of all the participants belonging to each of the three groups (Heavy and light users and healthy controls).

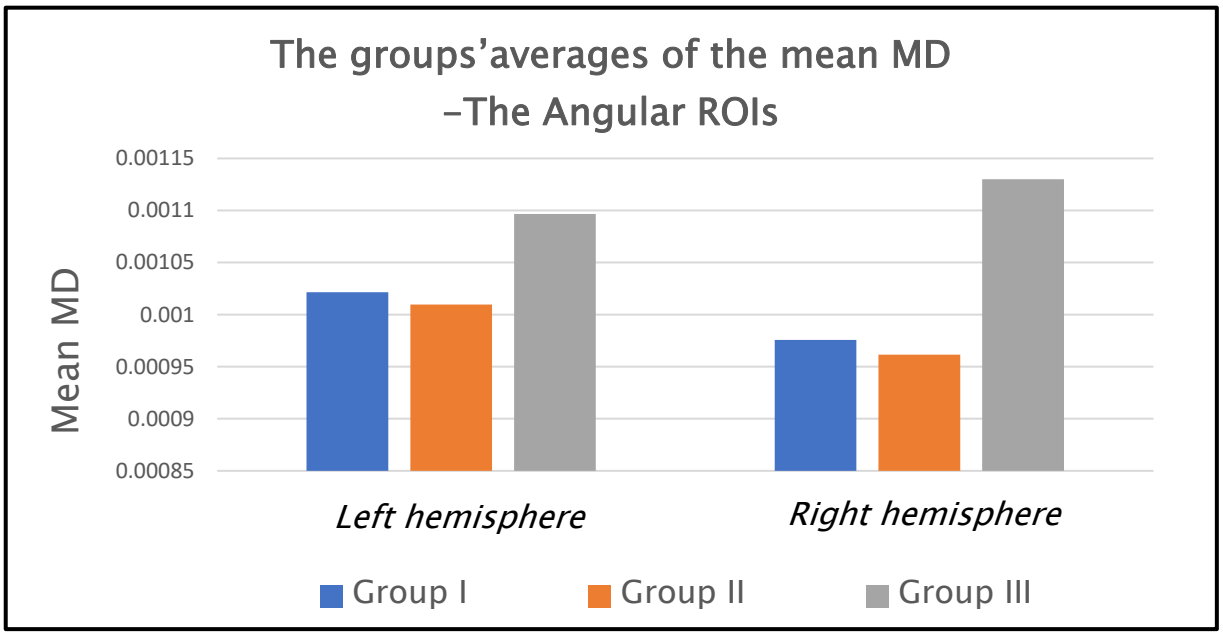

Figure 166: The mean diffusivity (MD) averages of each group in the Angular ROIs in the left and the right hemispheres.

Table 66: The mean diffusivity (MD) averages and standard deviations (SD) values for the groups studied in the Angular ROIs, along with intergroup comparisons.

	Left Hemisphere	Right Hemisphere
Heavy users' group (G. I)	(0,001021±0,000118)	(0,000975±0,000116)
Light users' group (G. II)	((0,0010096±0,0000815)	(0,000961±0,00005806)
Non-users' group (G.III)	(0,001096±0,000121)	(0,00113±0,0001501)
Intergroup comparison	G.III > G. I ≈ G. II	G.III > G. I ≈ G. II

➢ **Parietal Inf**

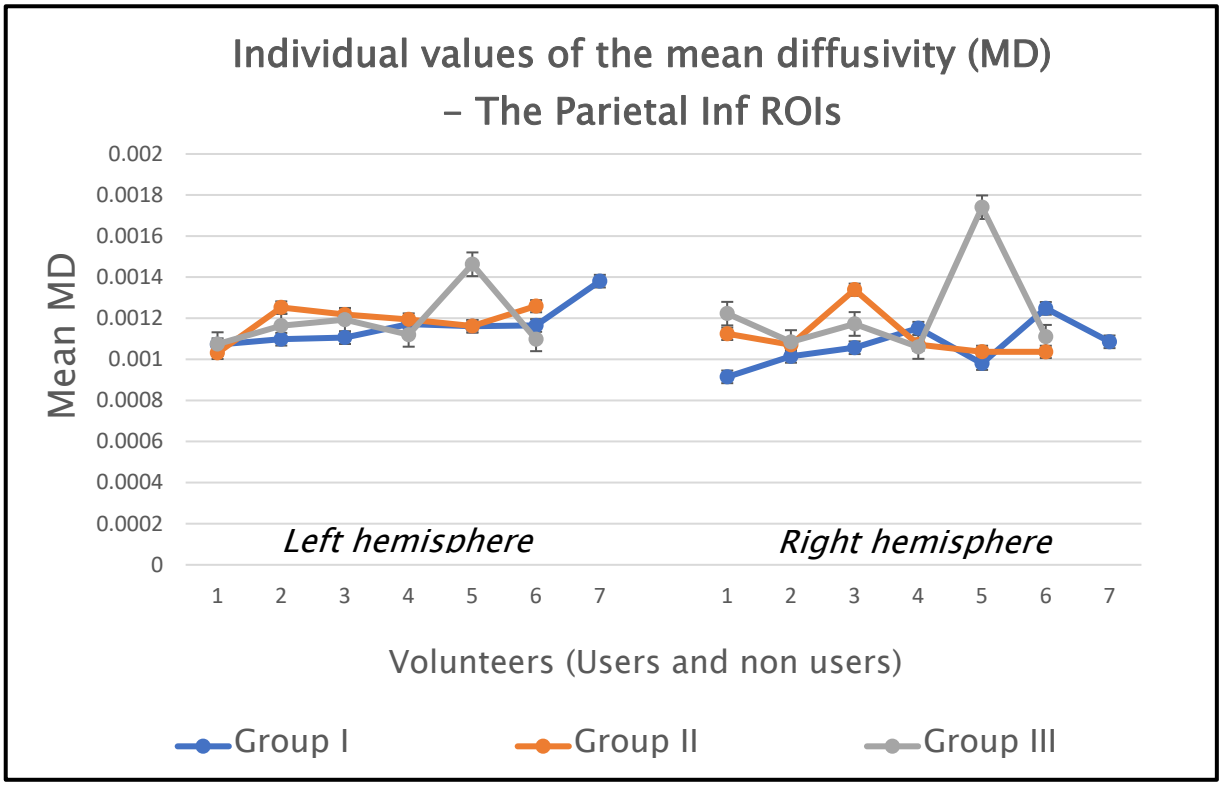

Figure 167: Individual values of mean diffusivity (MD) in both hemispheres' Parietal Inf ROIs. This figure depicts the MD values of all the participants belonging to each of the three groups (Heavy and light users and healthy controls).

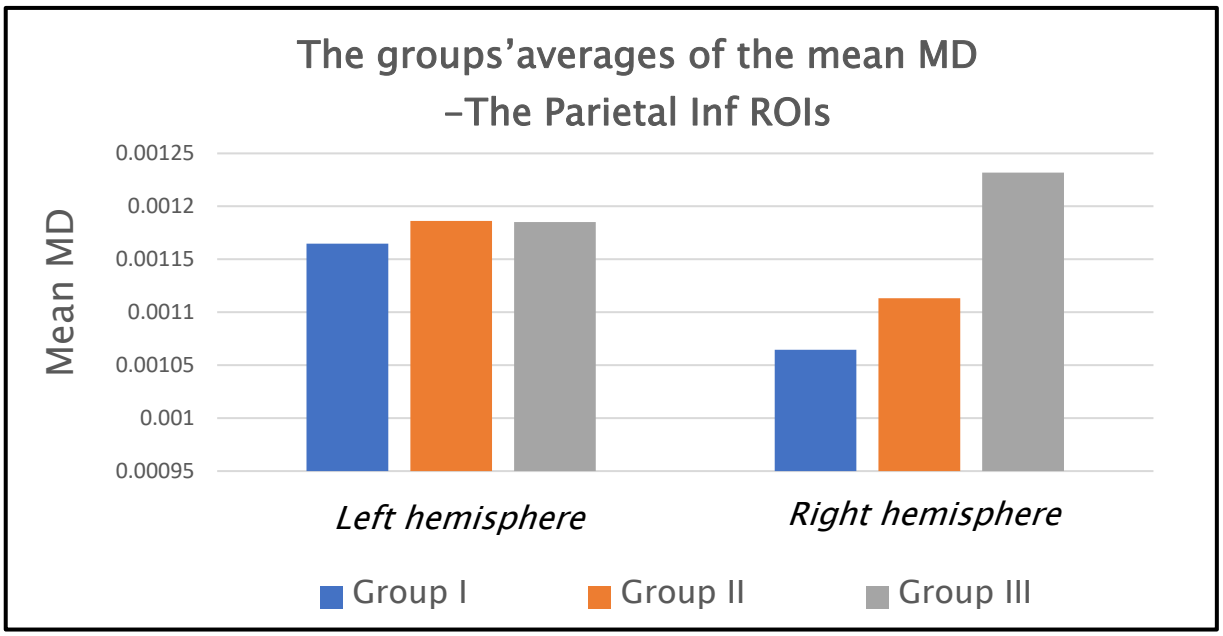

Figure 168: The mean diffusivity (MD) averages of each group in the Parietal Inf ROIs in the left and the right hemispheres.

Table 67: The mean diffusivity (MD) averages and standard deviations (SD) values for the groups studied in the Parietal Inf ROIs, along with intergroup comparisons.

	Left Hemisphere	Right Hemisphere
Heavy users' group (G. I)	(0,00116±0,0001026)	(0,001064±0,000111)
Light users' group (G. II)	(0,00118±0,0000839)	(0,00111±0,000115)
Non-users' group (G.III)	(0,00118±0,000142)	(0,00123±0,000256)
Intergroup comparison	G. I ≈ G. II ≈ G.III	G.III > G. II > G. I

➢ **Precuneus**

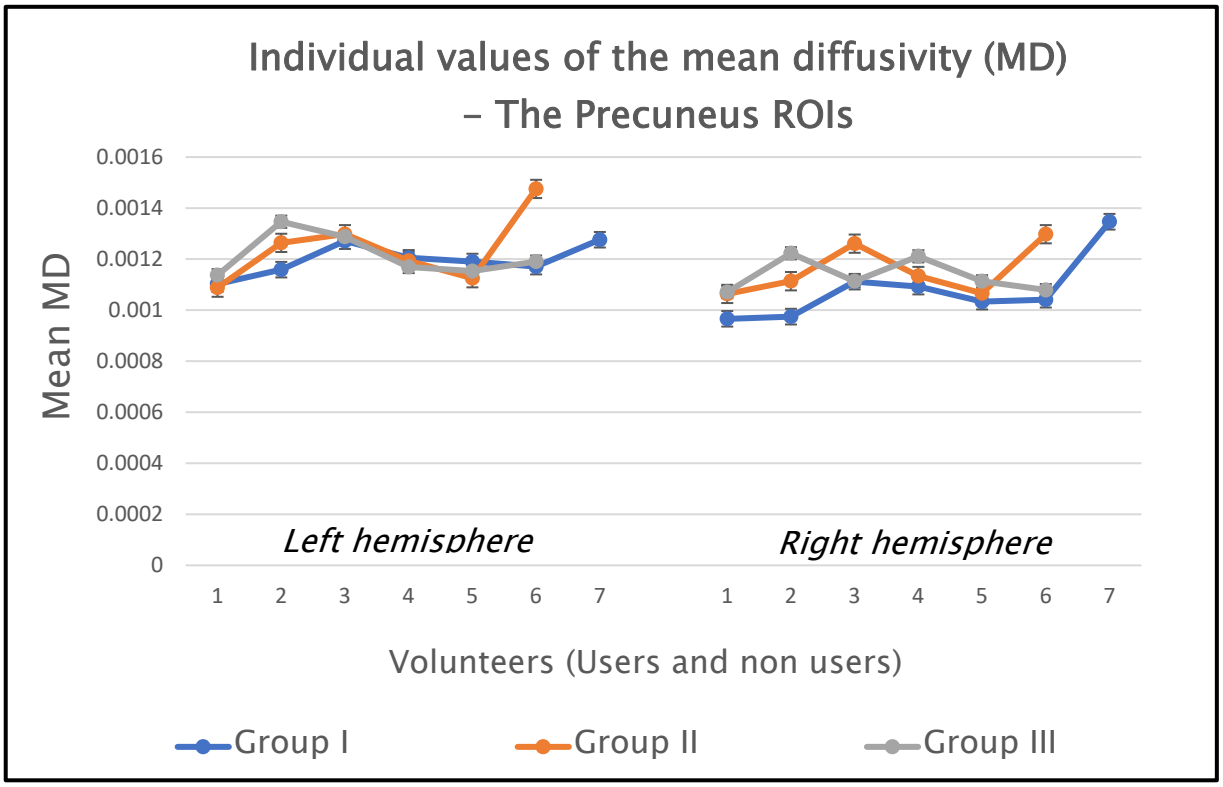

Figure 169: Individual values of mean diffusivity (MD) in both hemispheres' Precuneus ROIs. This figure depicts the MD values of all the participants belonging to each of the three groups (Heavy and light users and healthy controls).

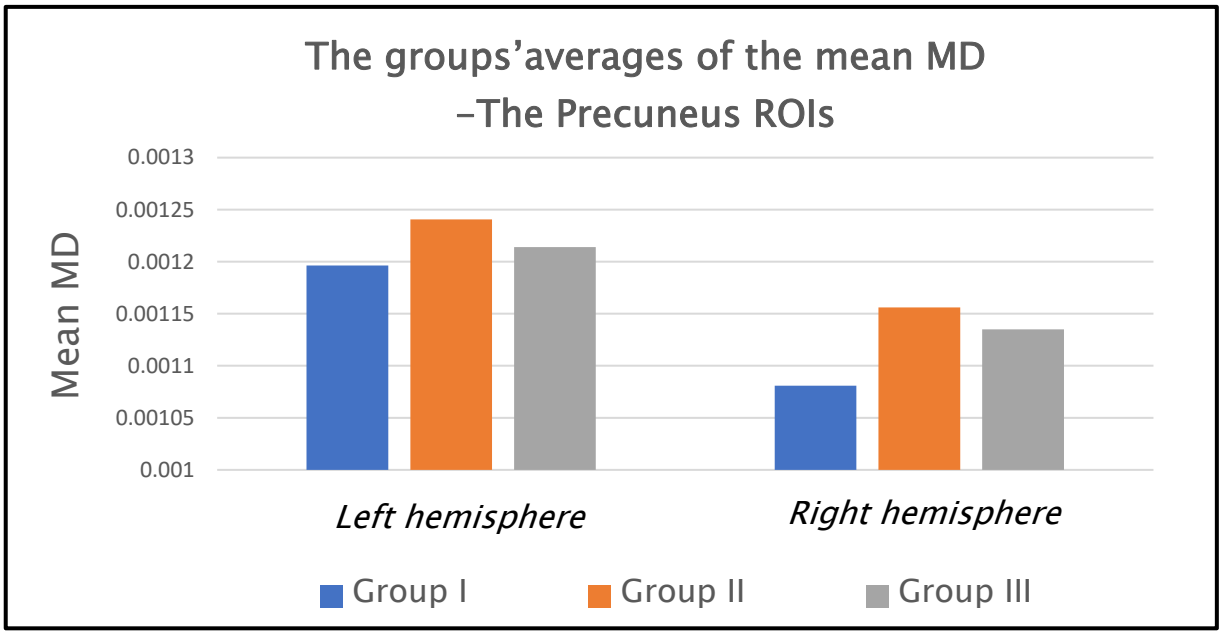

Figure 170: The mean diffusivity (MD) averages of each group in the Precuneus ROIs in the left and the right hemispheres.

Table 68: The mean diffusivity (MD) averages and standard deviations (SD) values for the groups studied in the Precuneus ROIs, along with intergroup comparisons.

	Left Hemisphere	Right Hemisphere
Heavy users' group (G. I)	(0,00119±0,0000617)	(0,0010808±0,000129)
Light users' group (G. II)	(0,00124±0,0001398)	(0,00115±0,0000999)
Non-users' group (G.III)	(0,00121±0,0000838)	(0,00113±0,0000659)
Intergroup comparison	G. I ≈ G. II ≈ G.III	G.III ≈ G. II > G. I

➢ **Temporal Sup**

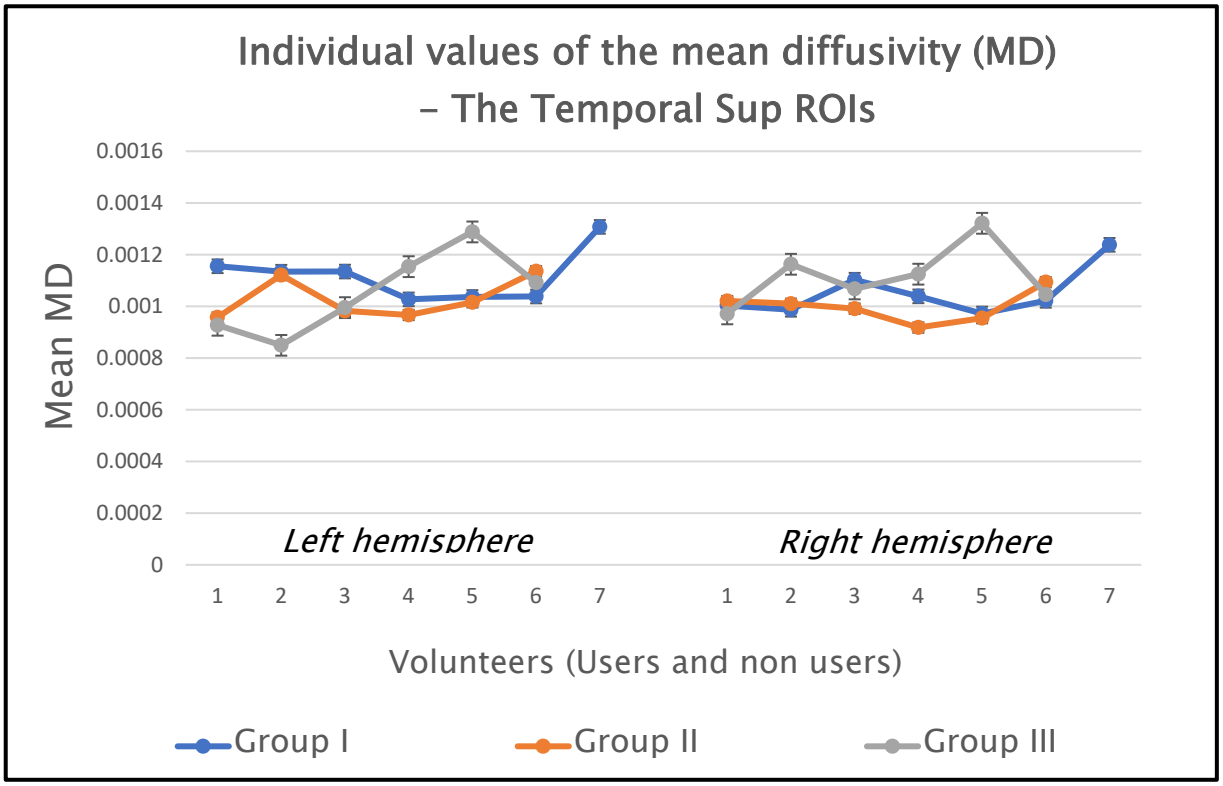

Figure 171: Individual values of mean diffusivity (MD) in both hemispheres' Temporal Sup ROIs. This figure depicts the MD values of all the participants belonging to each of the three groups (Heavy and light users and healthy controls).

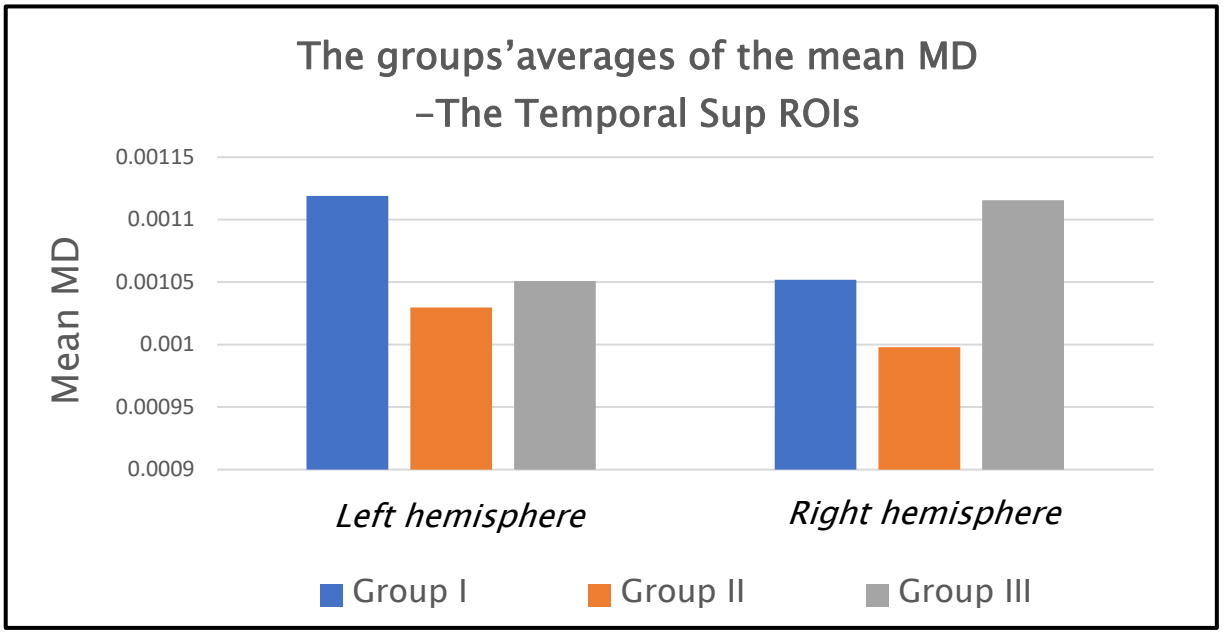

Figure 172: The mean diffusivity (MD) averages of each group in the Temporal Sup ROIs in the left and the right hemispheres.

Table 69: The mean diffusivity (MD) averages and standard deviations (SD) values for the groups studied in the Temporal Sup ROIs, along with intergroup comparisons.

	Left Hemisphere	Right Hemisphere
Heavy users' group (G. I)	(0,00111±0,0000992)	(0,001051±0,0000925)
Light users' group (G. II)	(0,001029±0,0000791)	(0,000997±0,00006027)
Non-users' group (G.III)	(0,0010508±0,000159)	(0,00111±0,0001207)
Intergroup comparison	G. I > G. II ≈ G.III	G.III > G. I > G. II

➢ Temporal Pole Sup

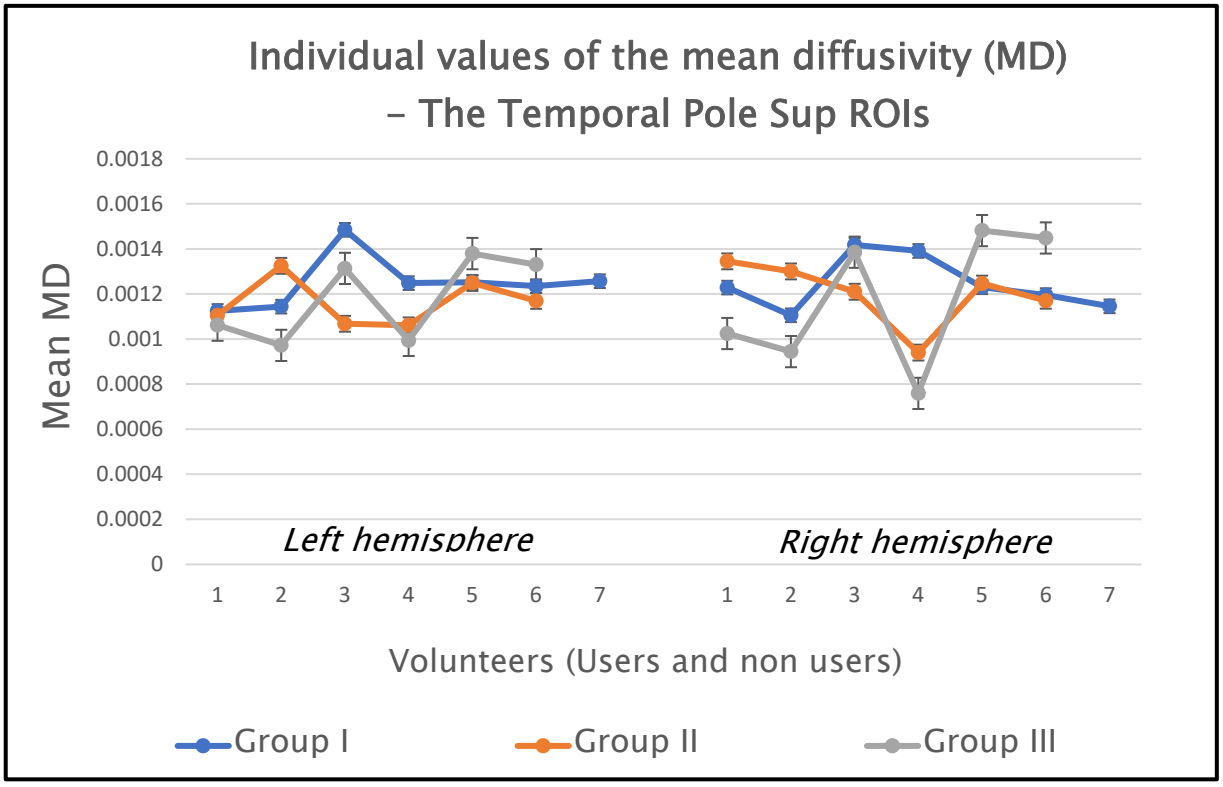

Figure 173: Individual values of mean diffusivity (MD) in both hemispheres' Temporal Pole Sup ROIs. This figure depicts the MD values of all the participants belonging to each of the three groups (Heavy and light users and healthy controls).

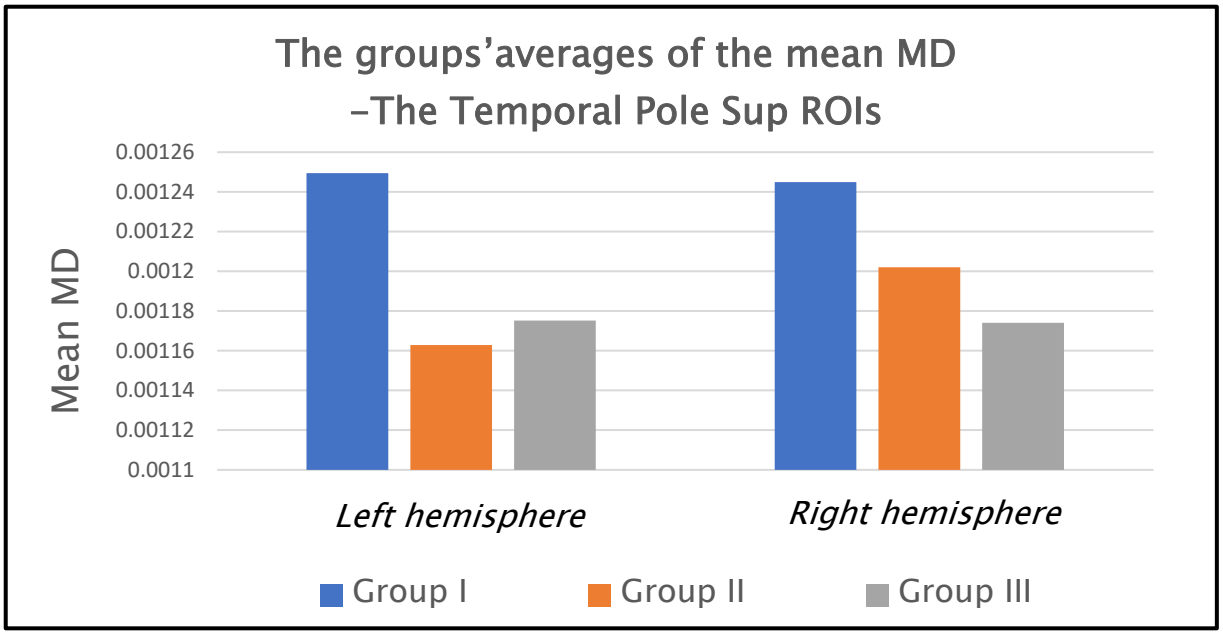

Figure 174: The mean diffusivity (MD) averages of each group in the Temporal Pole Sup ROIs in the left and the right hemispheres.

Table 70: The mean diffusivity (MD) averages and standard deviations (SD) values for the groups studied in the Temporal Pole Sup ROIs, along with intergroup comparisons.

	Left Hemisphere	Right Hemisphere
Heavy users' group (G. I)	(0,00124±0,000117)	(0,00124±0,0001179)
Light users' group (G. II)	(0,00116±0,0001063)	(0,001202±0,000142)
Non-users' group (G.III)	(0,00117±0,000185)	(0,00117±0,0003038)
Intergroup comparison	G. I > G. II ≈ G.III	G.III ≈ G. I ≈ G. II

➢ Heschl

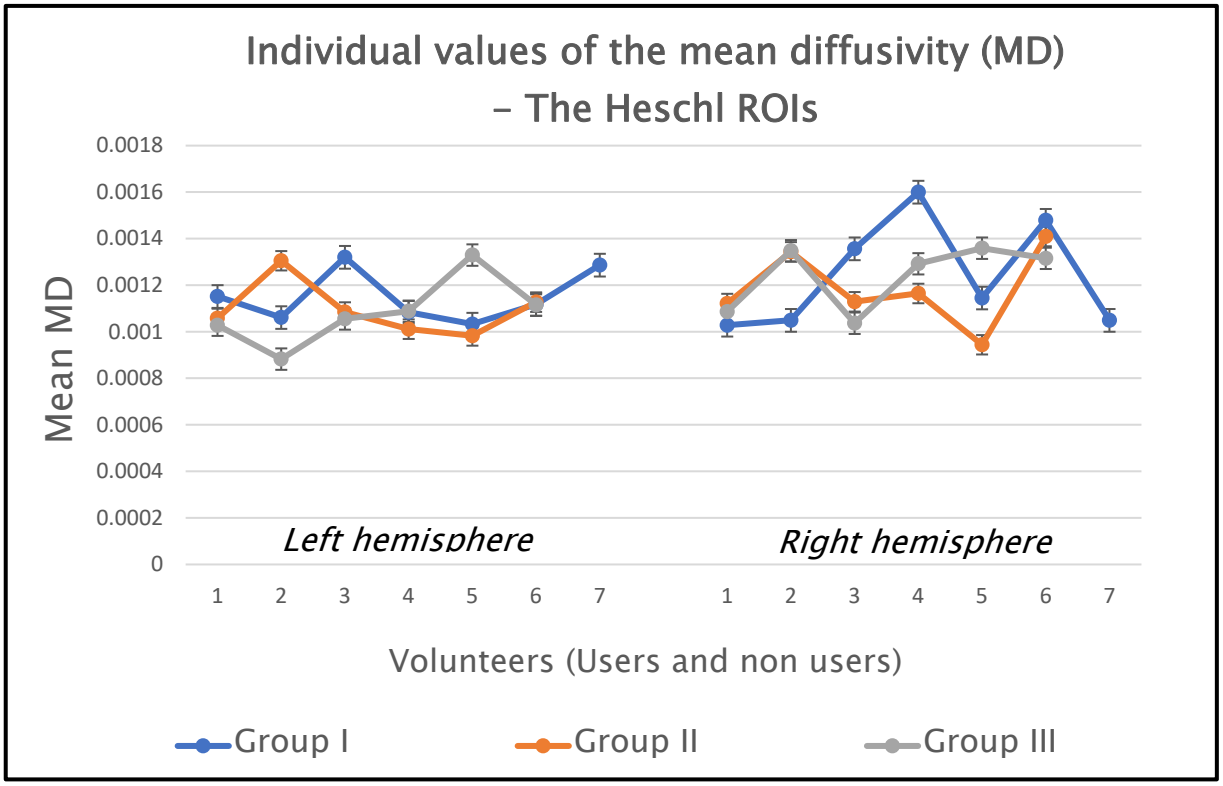

Figure 175: Individual values of mean diffusivity (MD) in both hemispheres' Heschl ROIs. This figure depicts the MD values of all the participants belonging to each of the three groups (Heavy and light users and healthy controls).

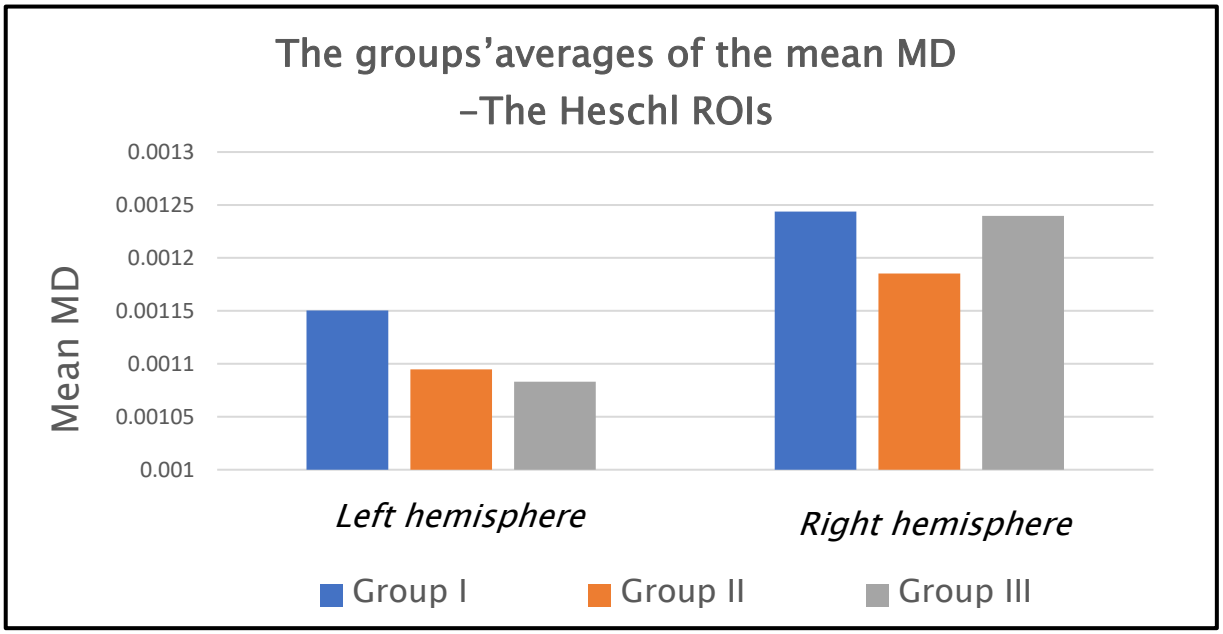

Figure 176: The mean diffusivity (MD) averages of each group in the Heschl ROIs in the left and the right hemispheres.

Table 71: The mean diffusivity (MD) averages and standard deviations (SD) values for the groups studied in the Heschl ROIs, along with intergroup comparisons.

	Left Hemisphere	Right Hemisphere
Heavy users' group (G. I)	(0,00115±0,000111)	(0,00124±0,000233)
Light users' group (G. II)	(0,001094±0,000115)	(0,00118±0,000167)
Non-users' group (G.III)	(0,001083±0,000145)	(0,00123±0,0001408)
Intergroup comparison	G. I > G. II ≈ G.III	G.III ≈ G. I > G. II

➢ Temporal Mid

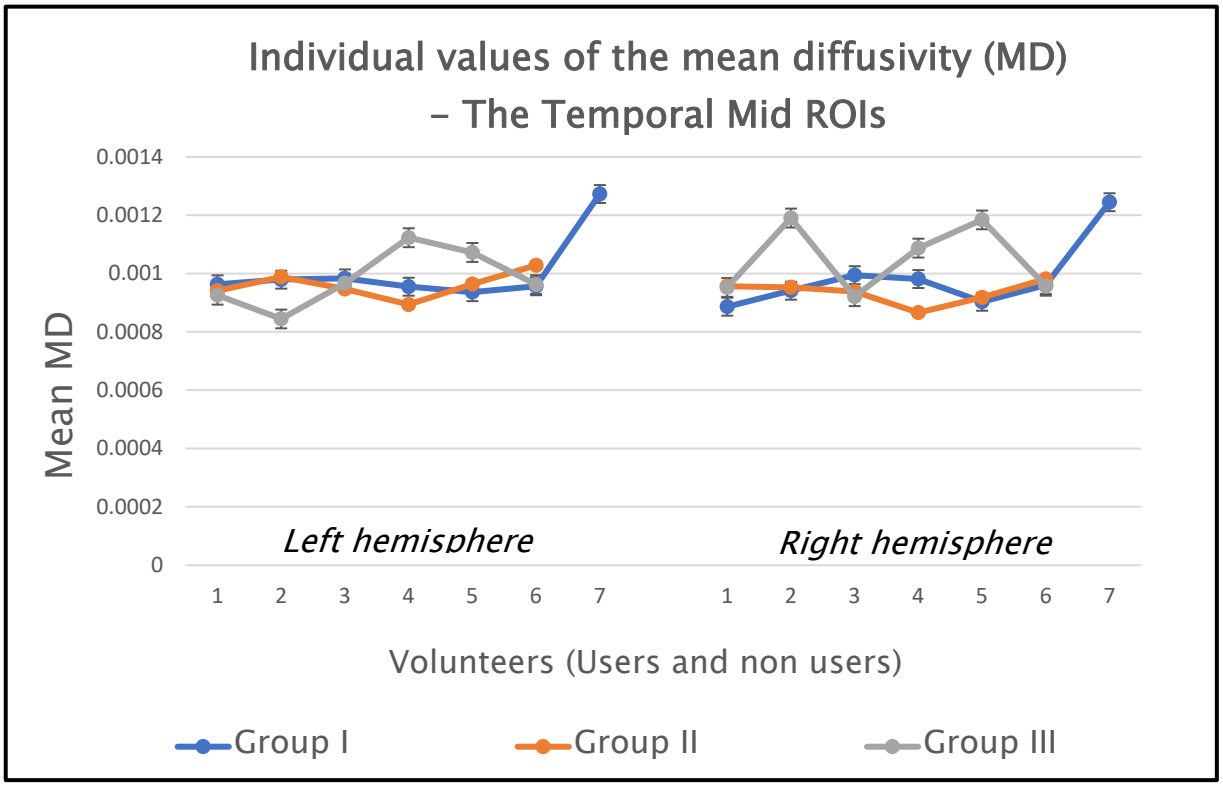

Figure 177: Individual values of mean diffusivity (MD) in both hemispheres' Temporal Mid ROIs. This figure depicts the MD values of all the participants belonging to each of the three groups (Heavy and light users and healthy controls).

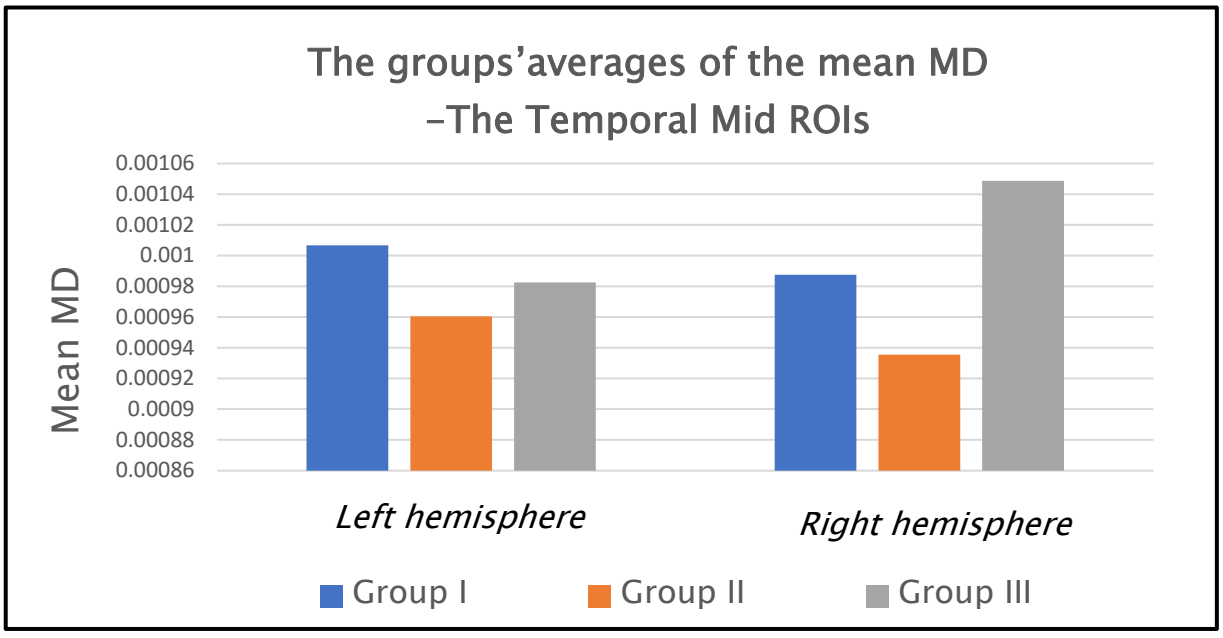

Figure 178: The mean diffusivity (MD) averages of each group in the Temporal Mid ROIs in the left and the right hemispheres.

Table 72: The mean diffusivity (MD) averages and standard deviations (SD) values for the groups studied in the temporal Mid ROIs, along with intergroup comparisons.

	Left Hemisphere	Right Hemisphere
Heavy users' group (G. I)	(0,0010067±0,000118)	(0,000987±0,00012003)
Light users' group (G. II)	(0,0009603±0,0000455)	(0,000935±0,0000399)
Non-users' group (G.III)	(0.0009824±0,00010079)	(0,001048±0,000121)
Intergroup comparison	G. I ≈ G. II ≈ G.III	G.III > G. I > G. II

➢ **Temporal Pole Mid**

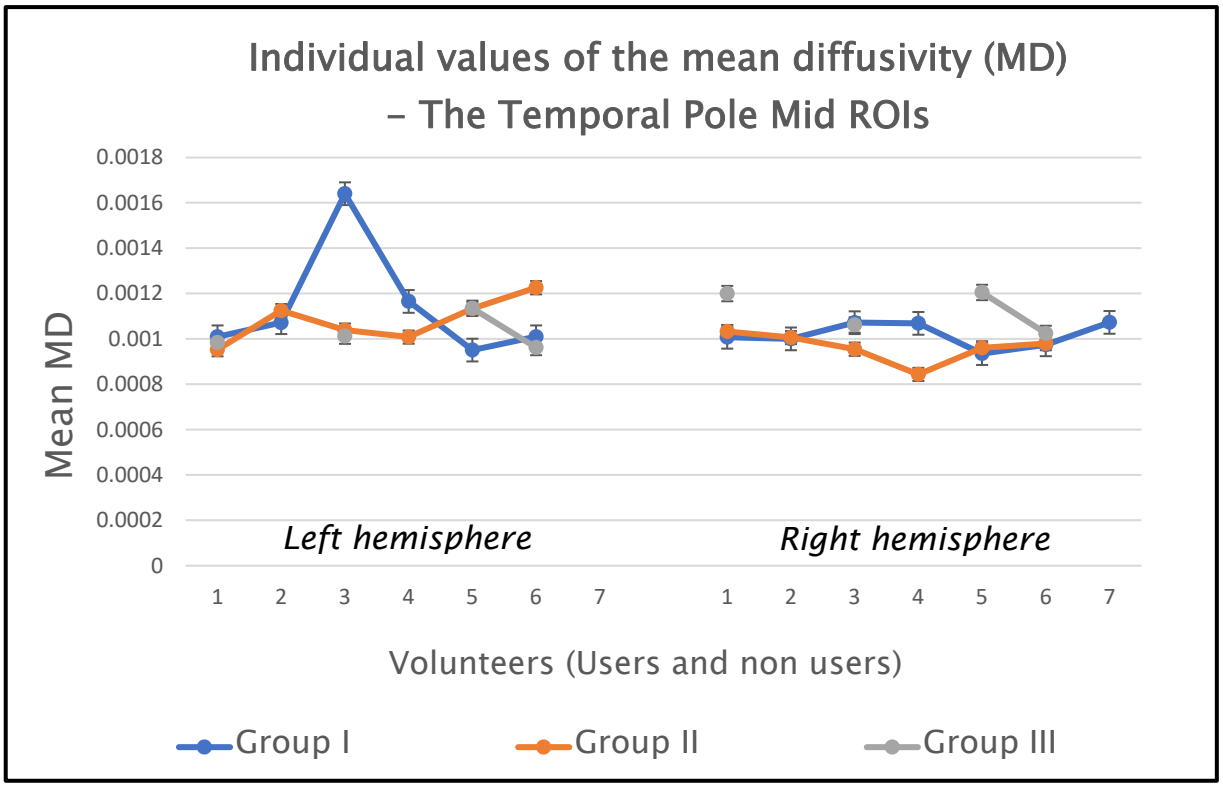

Figure 179: Individual values of mean diffusivity (MD) in both hemispheres' Temporal Pole Mid ROIs. This figure depicts the MD values of all the participants belonging to each of the three groups (Heavy and light users and healthy controls).

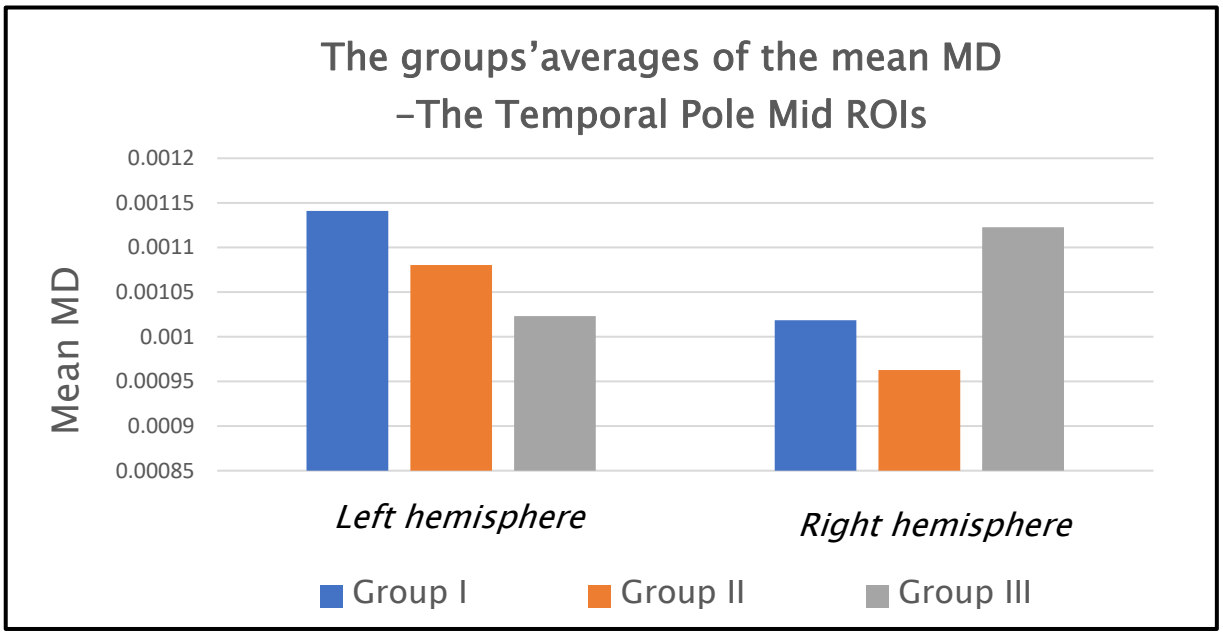

Figure 180: The mean diffusivity (MD) averages of each group in the Temporal Pole Mid ROIs in the left and the right hemispheres.

Table 73: The mean diffusivity (MD) averages and standard deviations (SD) values for the groups studied in the Temporal Pole Mid ROIs, along with intergroup comparisons.

	Left Hemisphere	Right Hemisphere
Heavy users' group (G. I)	(0,00114±0,000255)	(0,001018±0,0000542)
Light users' group (G. II)	(0,0010804±0,0000991)	(0,000962±0,0000651)
Non-users' group (G.III)	(0,001023±0,0000772)	(0,00112±0,0000932)
Intergroup comparison	G. I > G. II > G.III	G.III > G. I ≈ G. II

➢ Temporal Inf

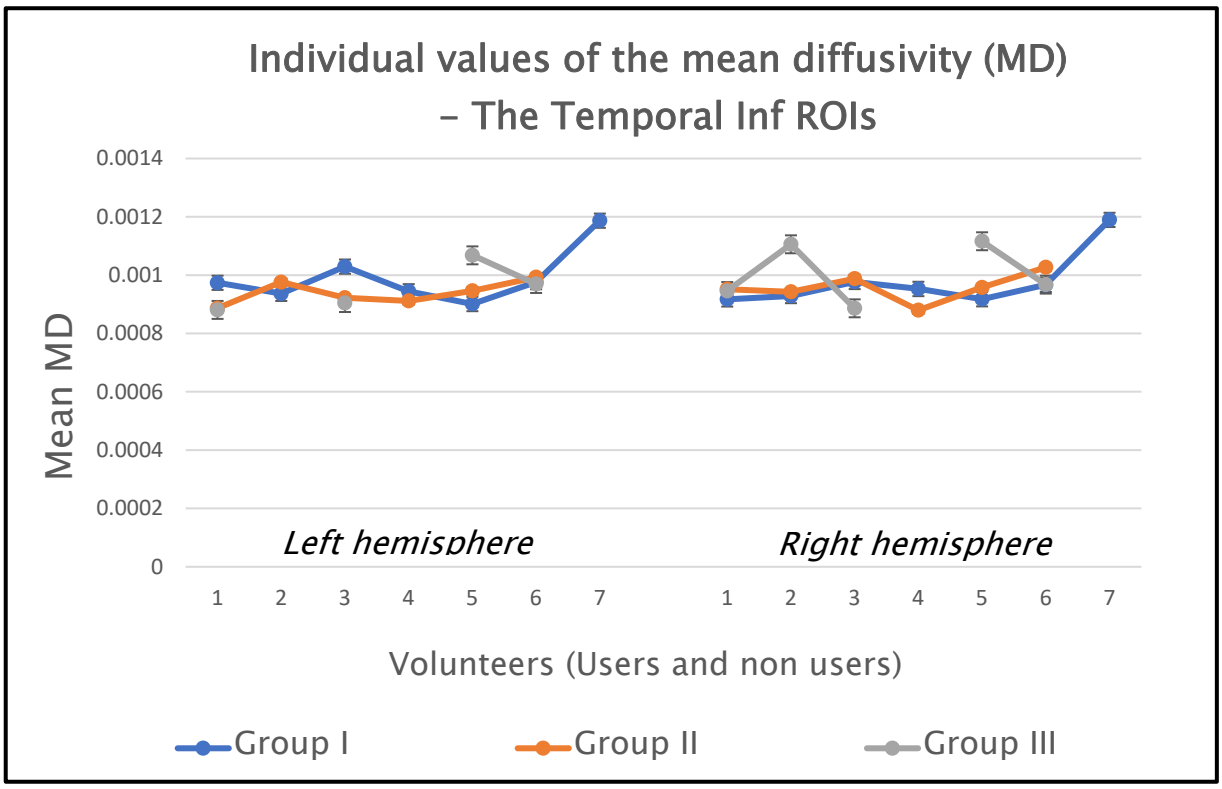

Figure 181: Individual values of mean diffusivity (MD) in both hemispheres' Temporal Inf ROIs. This figure depicts the MD values of all the participants belonging to each of the three groups (Heavy and light users and healthy controls).

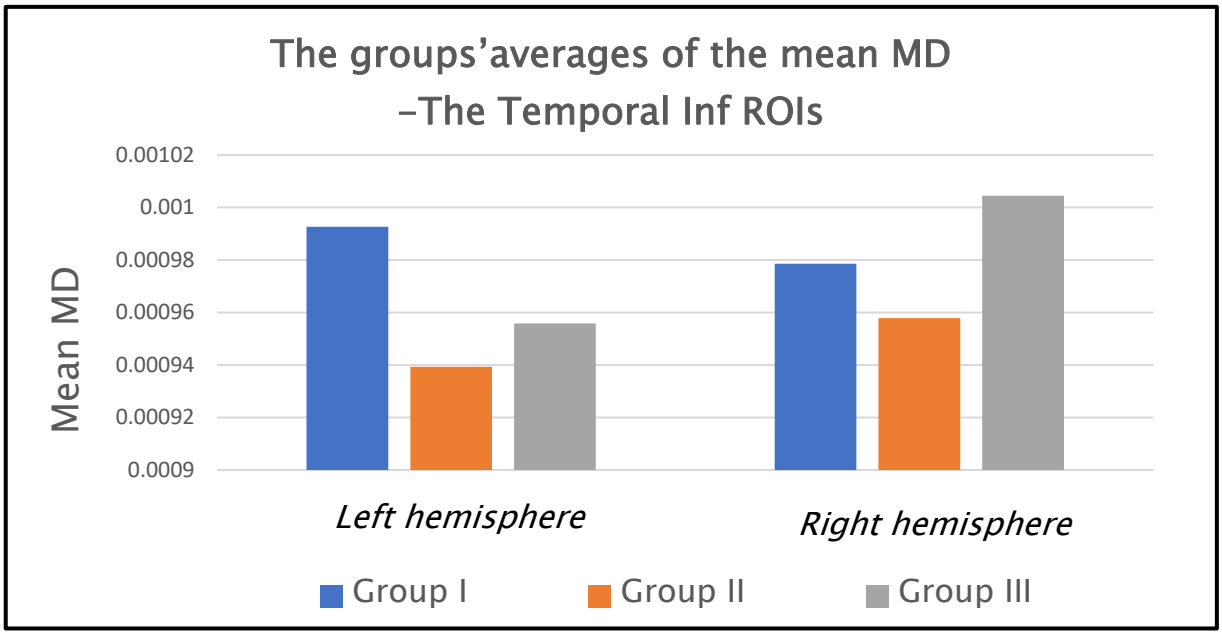

Figure 182: The mean diffusivity (MD) averages of each group in the Temporal Inf ROIs in the left and the right hemispheres.

Table 74: The mean diffusivity (MD) averages and standard deviations (SD) values for the groups studied in the Temporal Inf ROIs, along with intergroup comparisons.

	Left Hemisphere	Right Hemisphere
Heavy users' group (G. I)	(0,000992±0,0000944)	(0,000978±0,00009607)
Light users' group (G. II)	(0,000939±0,00004022)	(0,000957±0,00004903)
Non-users' group (G.III)	(0,000955±0,0000838)	(0,0010044±0,0001019)
Intergroup comparison	G. I > G. II ≈ G.III	G.III ≈ G. I ≈ G. II

➢ **Fusiform**

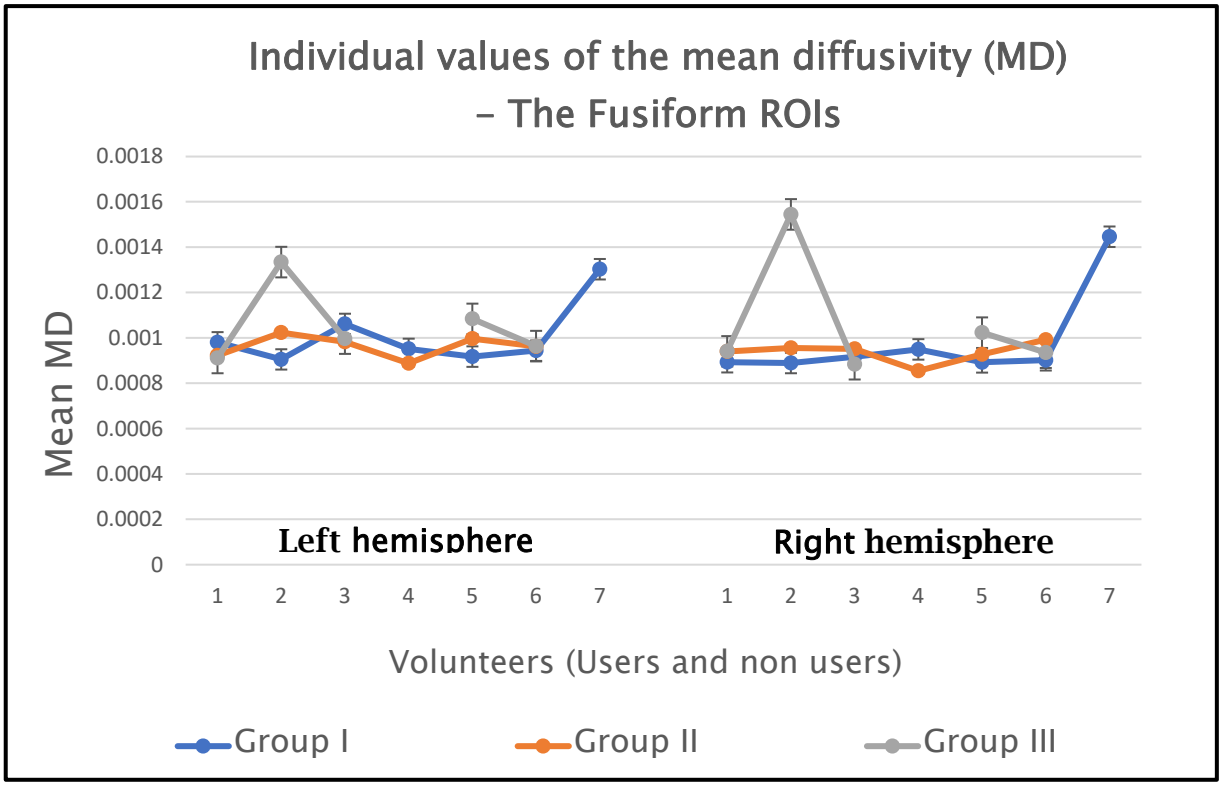

Figure 183: Individual values of mean diffusivity (MD) in both hemispheres' Fusiform ROIs. This figure depicts the MD values of all the participants belonging to each of the three groups (Heavy and light users and healthy controls).

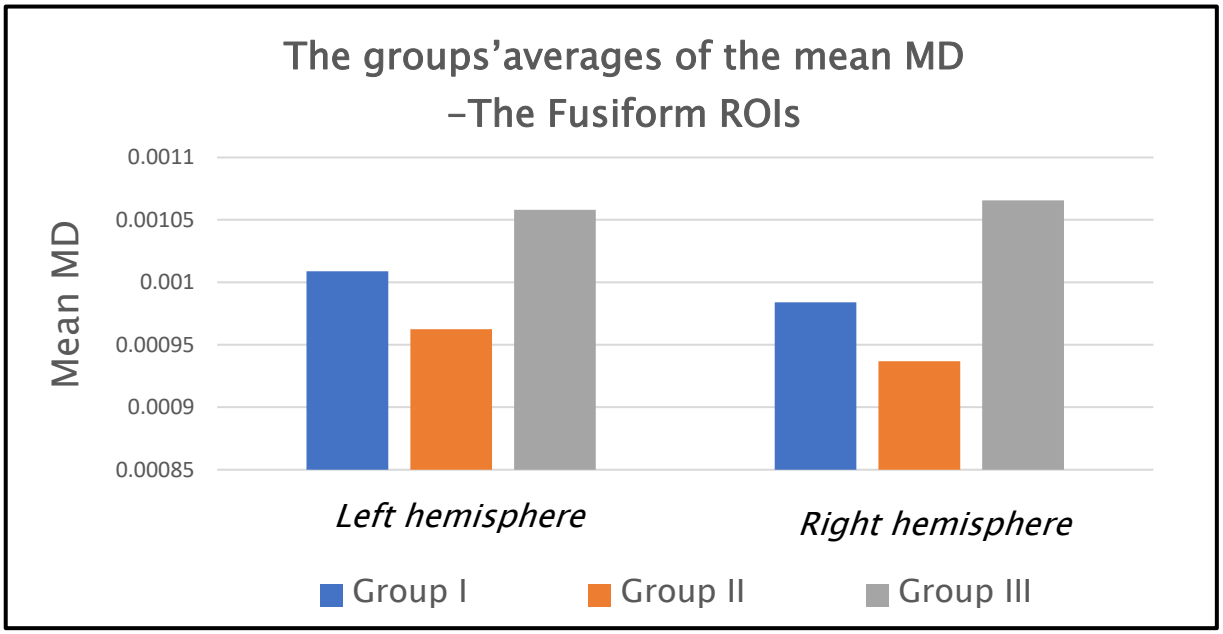

Figure 184: The mean diffusivity (MD) averages of each group in the Fusiform ROIs in the left and the right hemispheres.

Table 75: The mean diffusivity (MD) averages and standard deviations (SD) values for the groups studied in the Fusiform ROIs, along with intergroup comparisons.

	Left Hemisphere	Right Hemisphere
Heavy users' group (G. I)	(0,0010088±0,000139)	(0,000983±0,0002049)
Light users' group (G. II)	(0,000962±0,0000499)	(0,000936±0,0000455)
Non-users' group (G.III)	(0,001058±0,000166)	(0,001065±0,000272)
Intergroup comparison	G. I ≈ G. II ≈ G.III	G.III > G. I > G. II

➢ Cingulum Ant

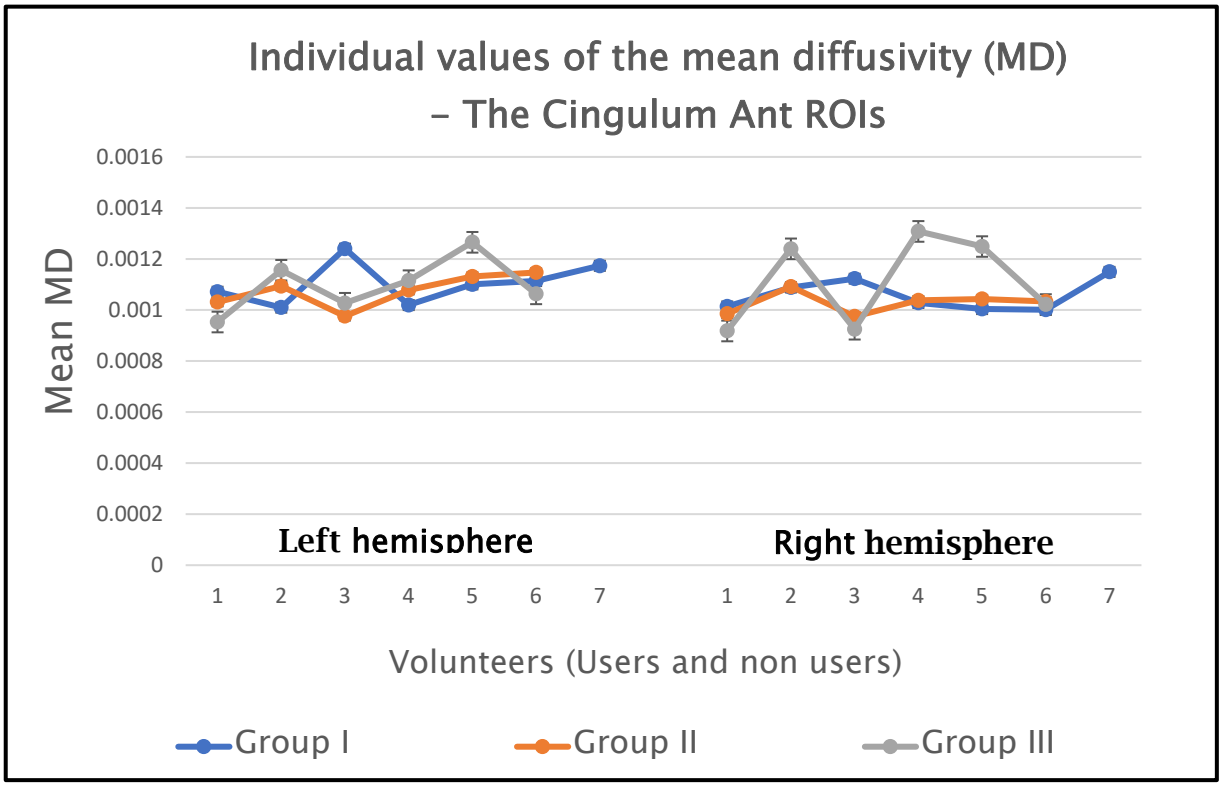

Figure 185: Individual values of mean diffusivity (MD) in both hemispheres' Cingulum Ant ROIs. This figure depicts the MD values of all the participants belonging to each of the three groups (Heavy and light users and healthy controls).

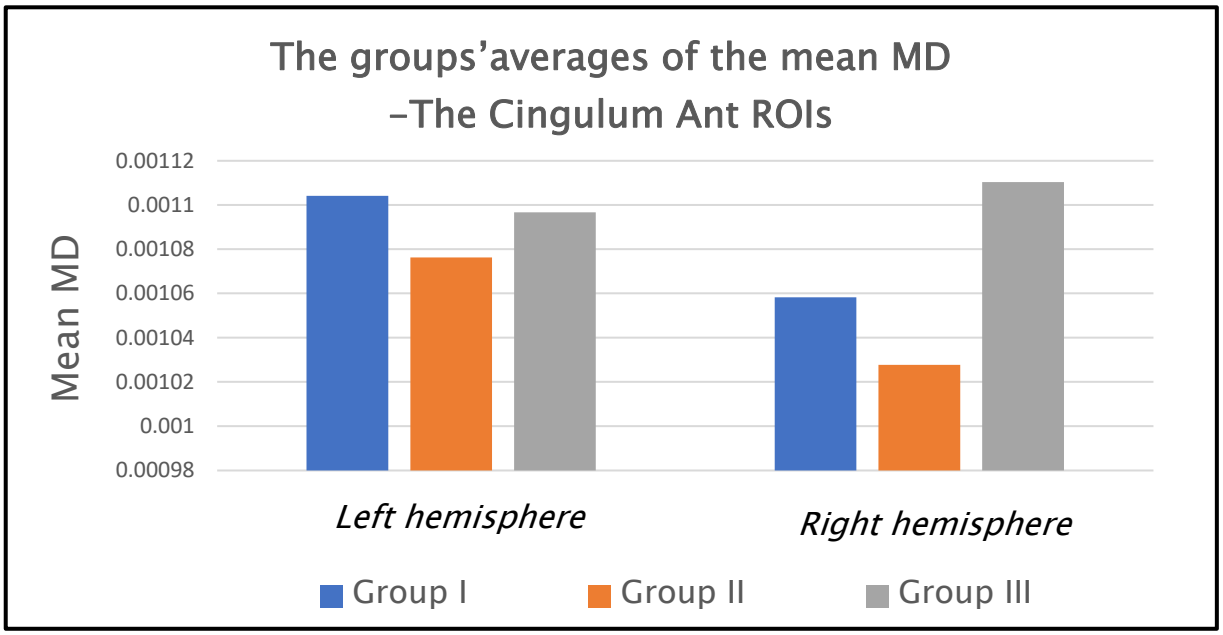

Figure 186: The mean diffusivity (MD) averages of each group in the Cingulum Ant ROIs in the left and the right hemispheres.

Table 76: The mean diffusivity (MD) averages and standard deviations (SD) values for the groups studied in the Cingulum Ant ROIs, along with intergroup comparisons.

	Left Hemisphere	Right Hemisphere
Heavy users' group (G. I)	(0,001104±0,0000822)	(0,001058±0,0000612)
Light users' group (G. II)	(0,001076±0,0000639)	(0,001027±0,0000424)
Non-users' group (G.III)	(0,001096±0,0001086)	(0,00111±0,000175)
Intergroup comparison	G. I ≈ G. II ≈ G.III	G.III > G. I > G. II

➢ **Cingulum Mid**

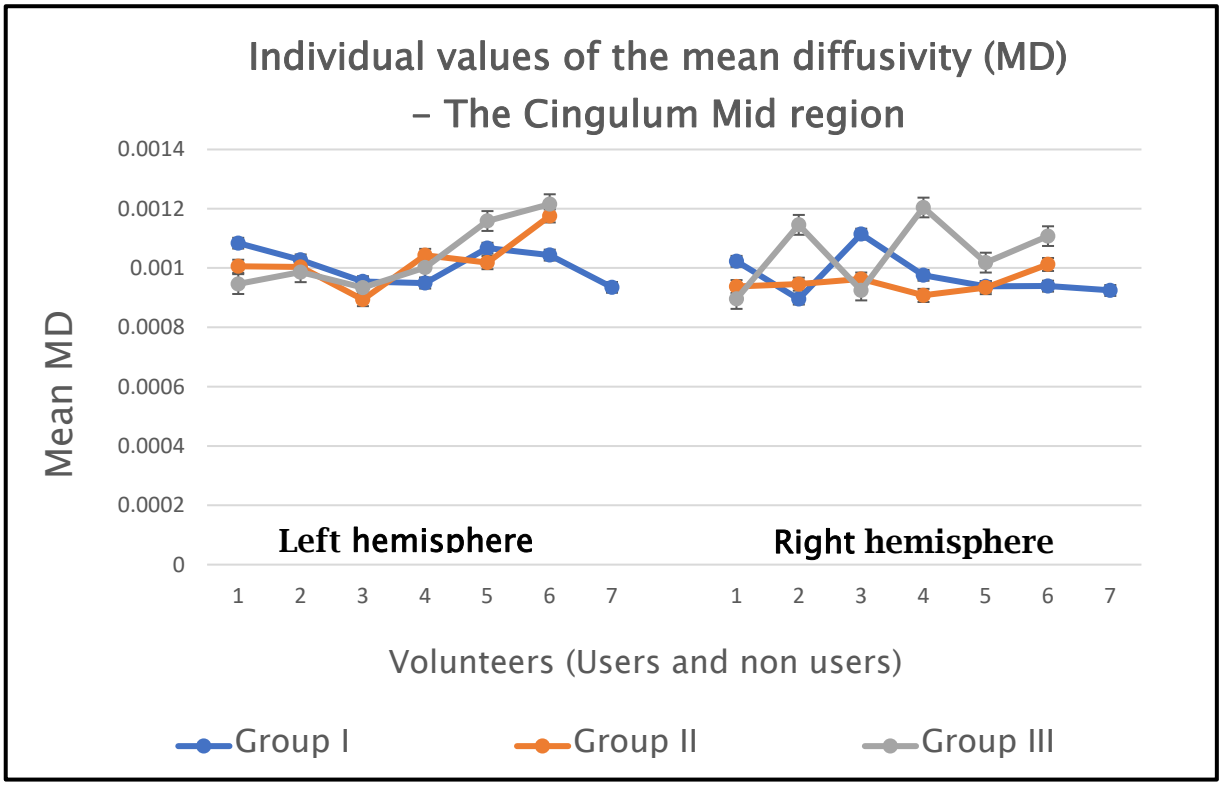

Figure 187: Individual values of mean diffusivity (MD) in both hemispheres' Cingulum Mid ROIs. This figure depicts the MD values of all the participants belonging to each of the three groups (Heavy and light users and healthy controls).

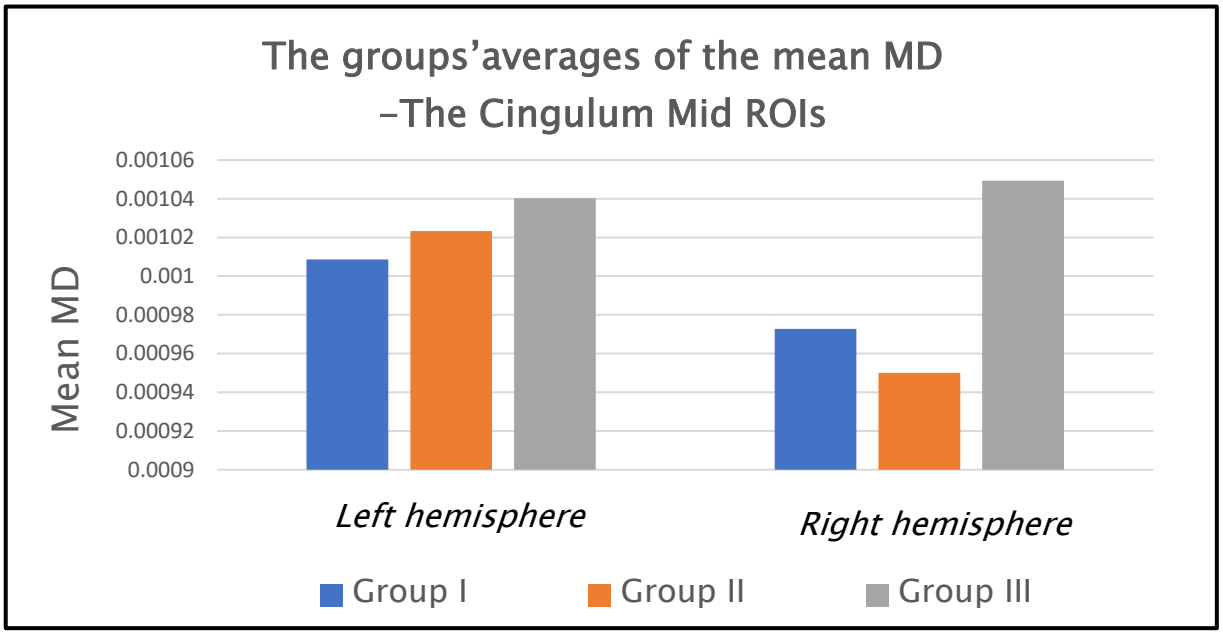

Figure 188: The mean diffusivity (MD) averages of each group in the Cingulum Mid ROIs in the left and the right hemispheres.

Table 77: The mean diffusivity (MD) averages and standard deviations (SD) values for the groups studied in the Cingulum Mid ROIs, along with intergroup comparisons.

	Left Hemisphere	Right Hemisphere
Heavy users' group (G. I)	(0,0010085±0,0000612)	(0,000972±0,0000743)
Light users' group (G. II)	(0,001023±0,00009069)	(0,000949±0,0000353)
Non-users' group (G.III)	(0,0010401±0,000117)	(0,001049±0,000123)
Intergroup comparison	G. I ≈ G. II ≈ G.III	G.III > G. I ≈ G. II

➢ Cingulum Post

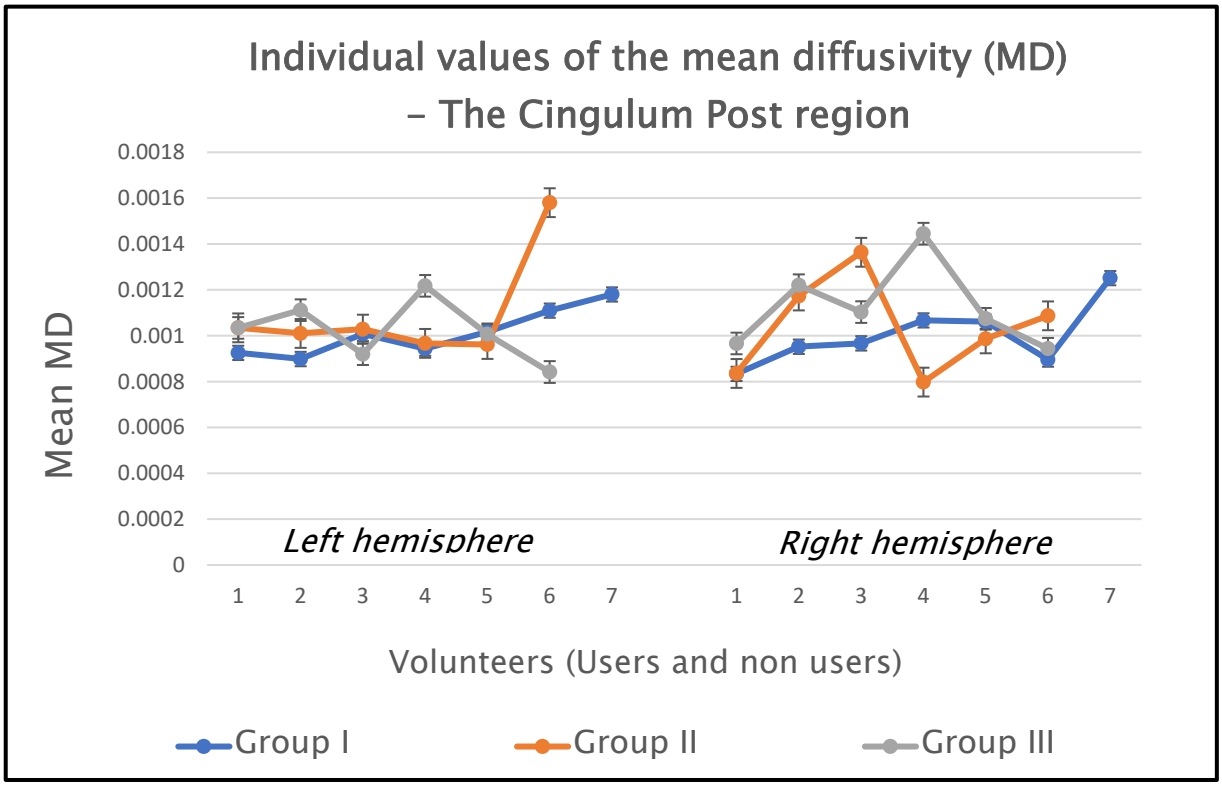

Figure 189: Individual values of mean diffusivity (MD) in both hemispheres' Cingulum Post ROIs. This figure depicts the MD values of all the participants belonging to each of the three groups (Heavy and light users and healthy controls).

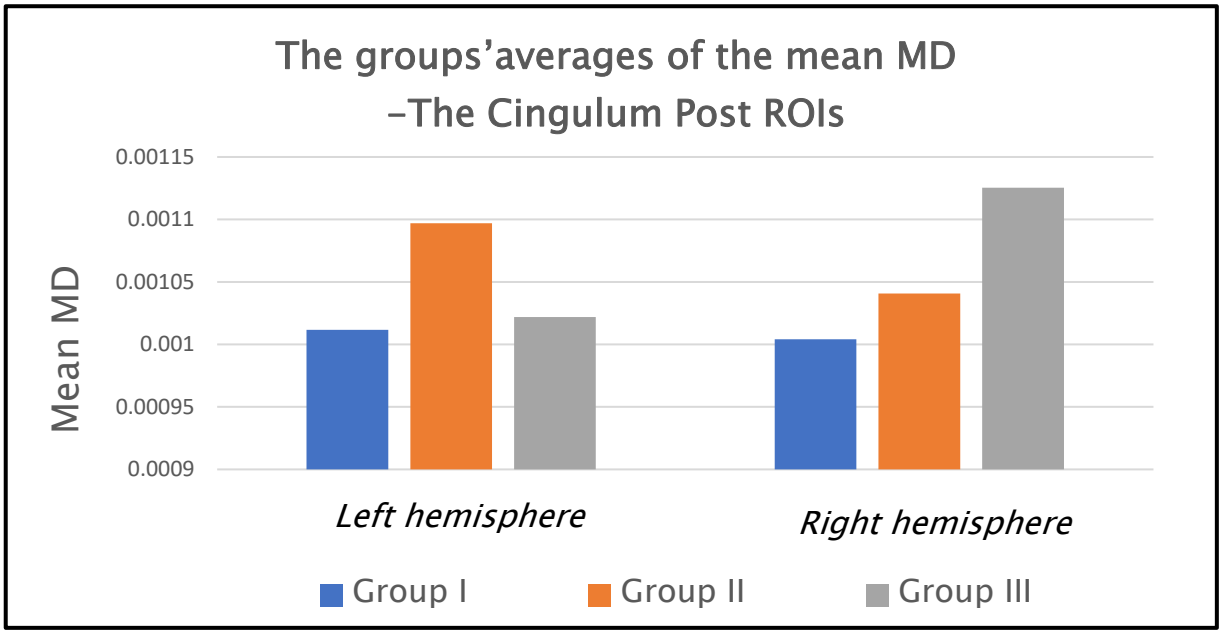

Figure 190: The mean diffusivity (MD) averages of each group in the Cingulum Post ROIs in the left and the right hemispheres.

Table 78: The mean diffusivity (MD) averages and standard deviations (SD) values for the groups studied in the Cingulum Post ROIs, along with intergroup comparisons.

	Left Hemisphere	Right Hemisphere
Heavy users' group (G. I)	(0,001011±0,0001024)	(0,00100409±0,000137)
Light users' group (G. II)	(0,001096±0,000238)	(0,0010407±0,000213)
Non-users' group (G.III)	(0,001021±0,000133)	(0,00112±0,000185)
Intergroup comparison	G. II > G. I ≈ G.III	G.III > G. I ≈ G. II

➢ **ParaHippocampal**

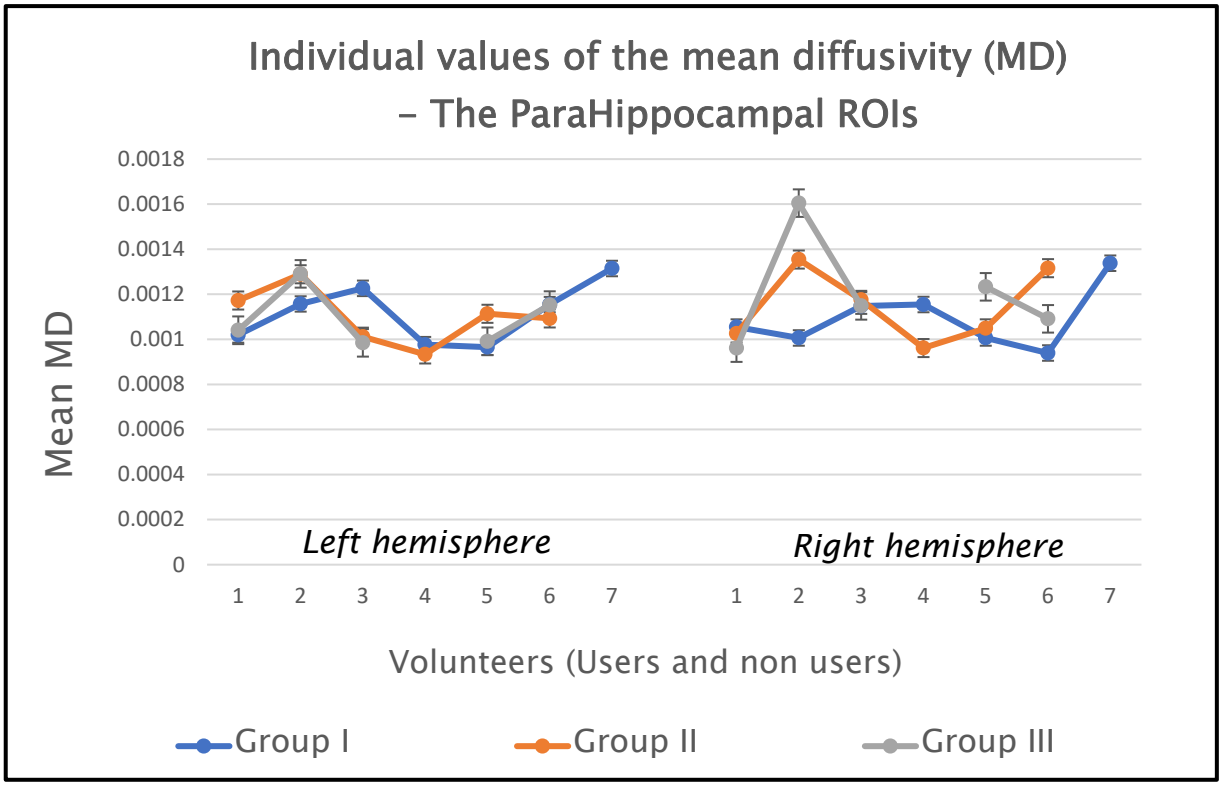

Figure 191: Individual values of mean diffusivity (MD) in both hemispheres' ParaHippocampal ROIs. This figure depicts the MD values of all the participants belonging to each of the three groups (Heavy and light users and healthy controls).

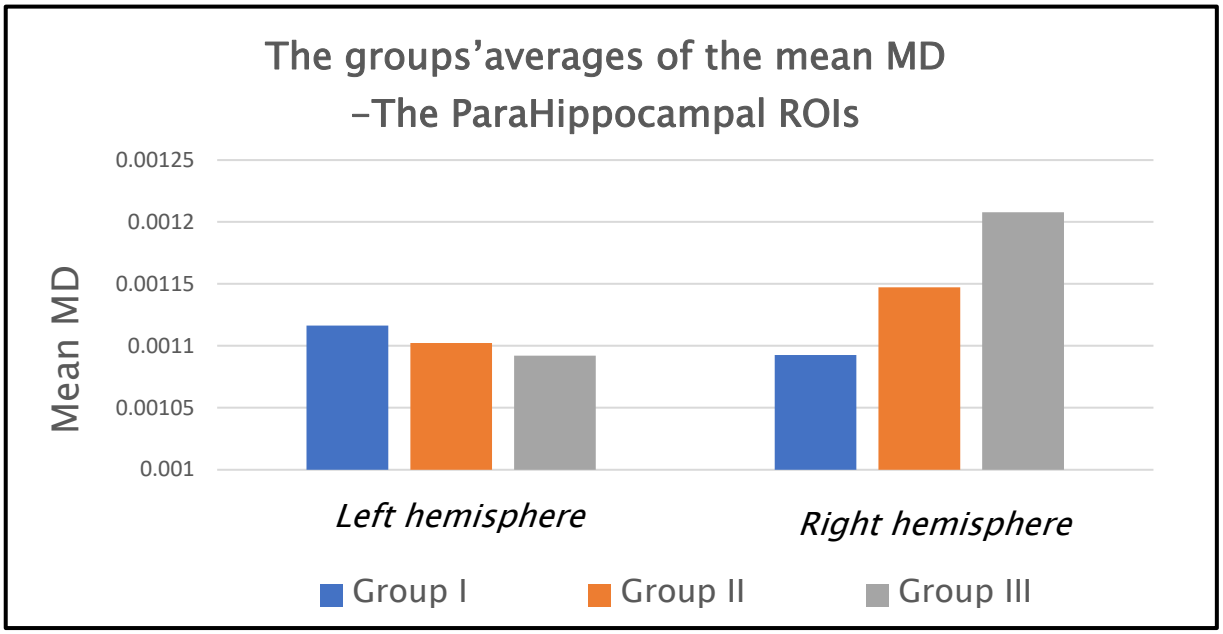

Figure 192: The mean diffusivity (MD) averages of each group in the ParaHippocampal ROIs in the left and the right hemispheres.

Table 79: The mean diffusivity (MD) averages and standard deviations (SD) values for the groups studied in the ParaHippocampal ROIs, along with intergroup comparisons.

	Left Hemisphere	Right Hemisphere
Heavy users' group (G. I)	(0,00111±0,000133)	(0,001092±0,000133)
Light users' group (G. II)	(0,001102±0,000123)	(0,00114±0,000161)
Non-users' group (G.III)	(0,001091±0,000129)	(0,001207±0,000242)
Intergroup comparison	G. II ≈ G. I ≈ G.III	G.III > G. II > G. I

➢ Hippocampus

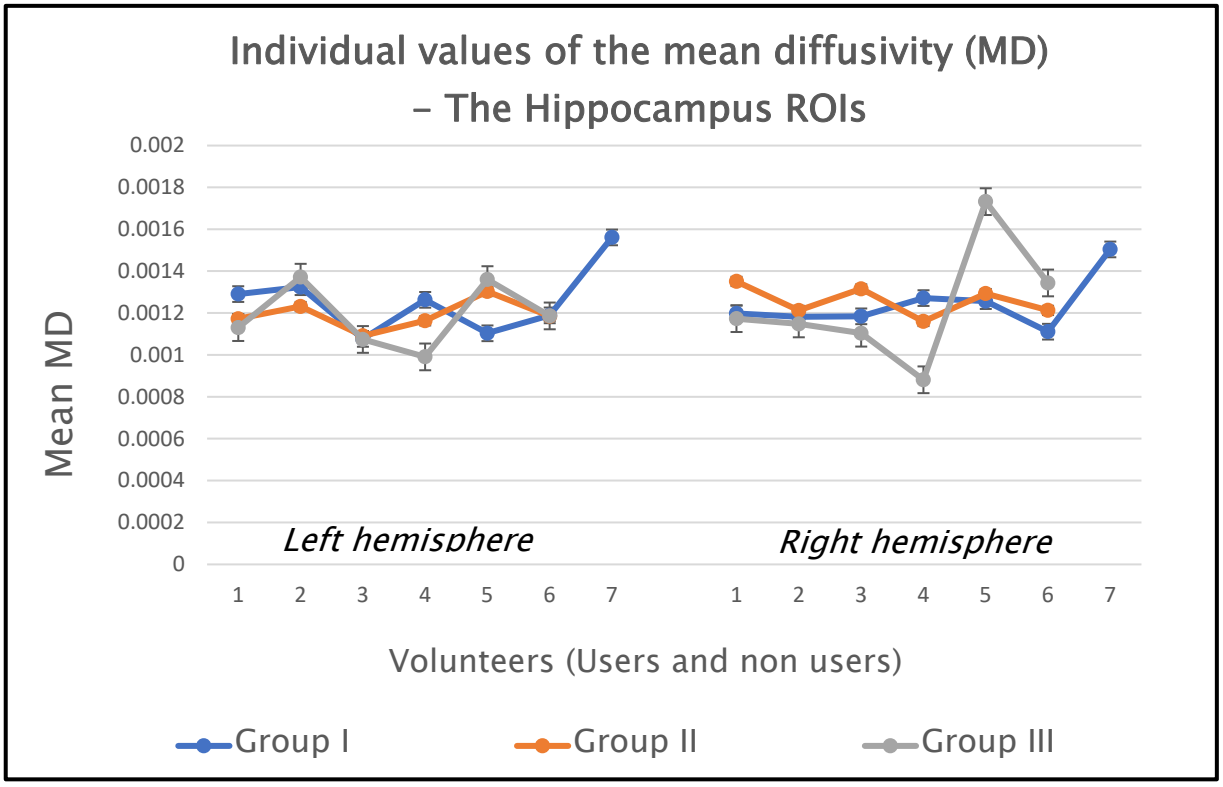

Figure 193: Individual values of mean diffusivity (MD) in both hemispheres' Hippocampus ROIs. This figure depicts the MD values of all the participants belonging to each of the three groups (Heavy and light users and healthy controls).

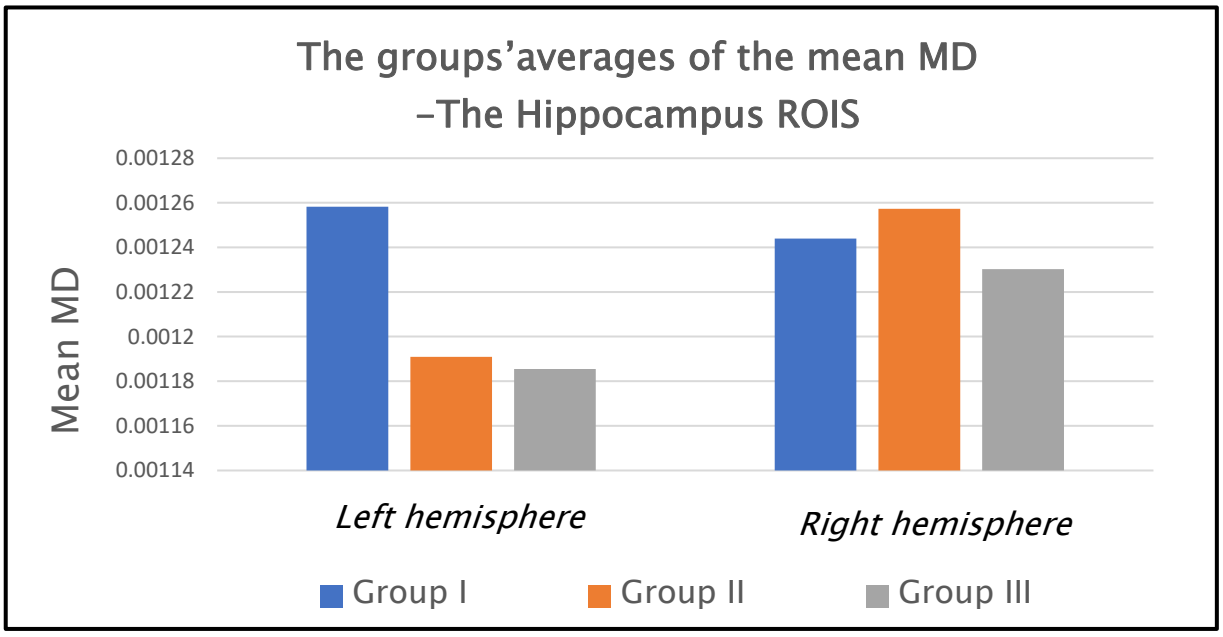

Figure 194: The mean diffusivity (MD) averages of each group in the Hippocampus ROIs in the left and the right hemispheres.

Table 80: The mean diffusivity (MD) averages and standard deviations (SD) values for the groups studied in the Hippocampus ROIs, along with intergroup comparisons.

	Left Hemisphere	Right Hemisphere
Heavy users' group (G. I)	(0,00125±0,000162)	(0,00124±0,000126)
Light users' group (G. II)	(0,00119±0,00007099)	(0,00125±0,0000732)
Non-users' group (G.III)	(0,001185±0,00015)	(0,00123±0,000287)
Intergroup comparison	G. I > G.III ≈ G. II	G. II ≈ G. I ≈ G.III

➢ **Insula**

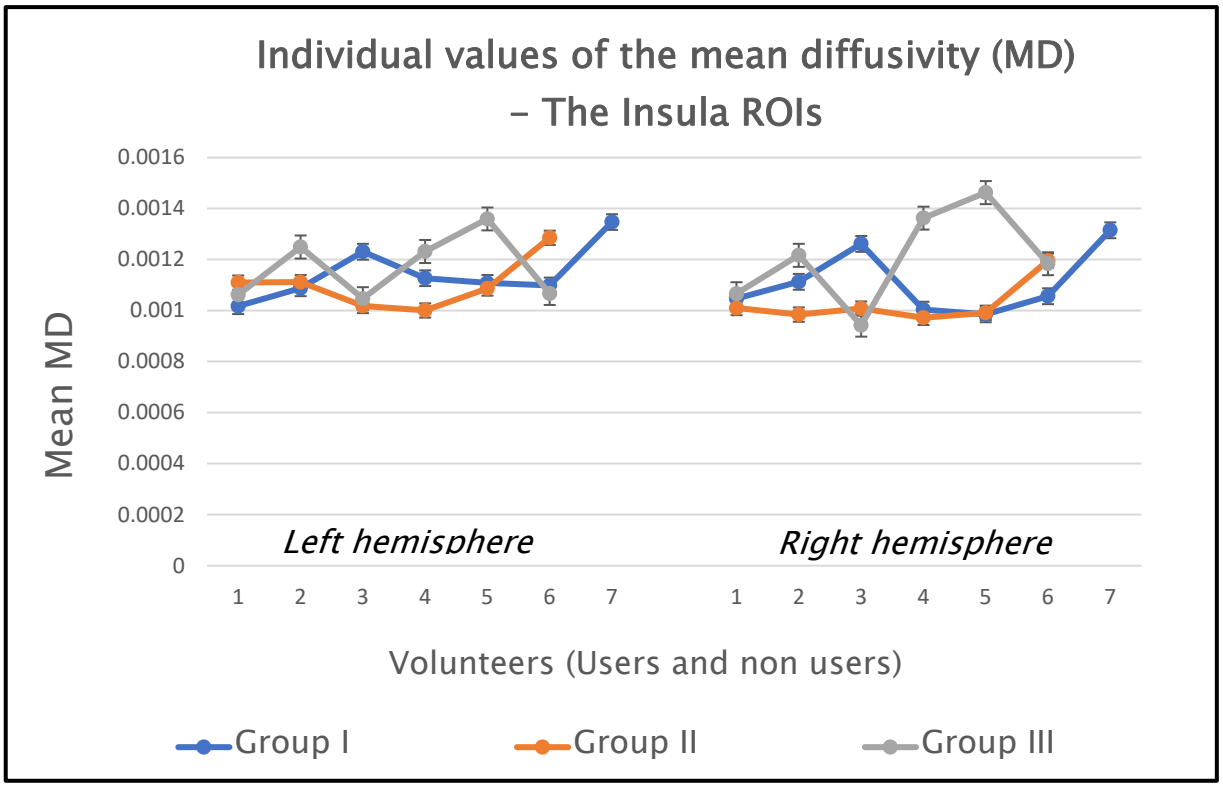

Figure 195: Individual values of mean diffusivity (MD) in both hemispheres' Insula ROIs. This figure depicts the MD values of all the participants belonging to each of the three groups (Heavy and light users and healthy controls).

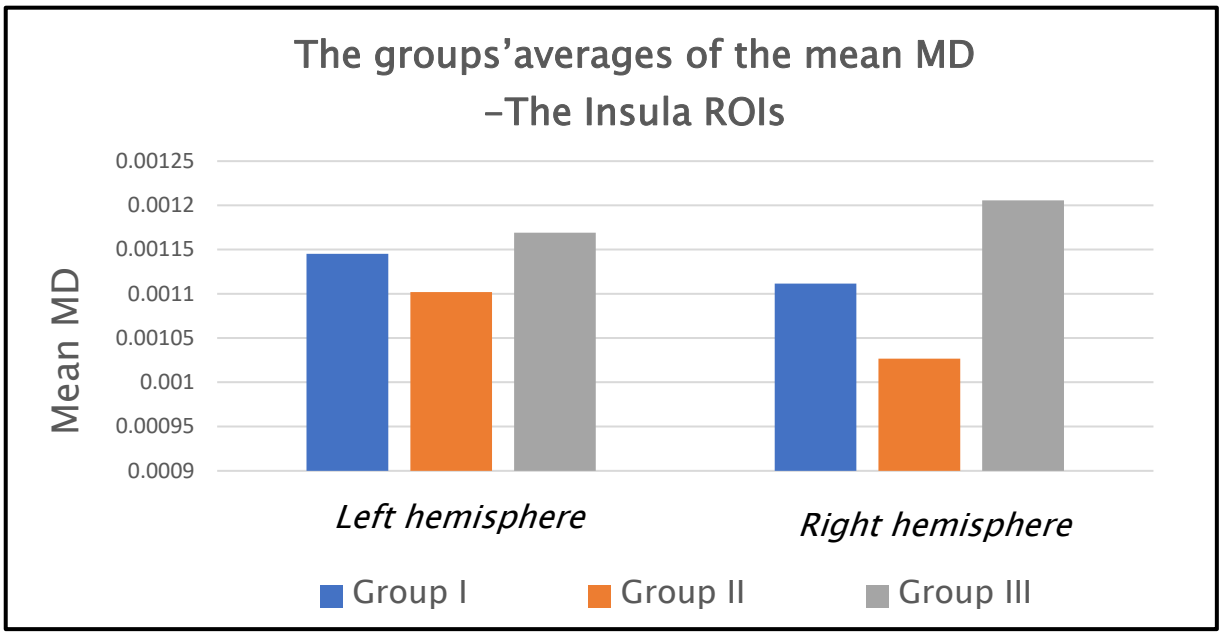

Figure 196: The mean diffusivity (MD) averages of each group in the Insula ROIs in the left and the right hemispheres.

Table 81: The mean diffusivity (MD) averages and standard deviations (SD) values for the groups studied in the Insula ROIs, along with intergroup comparisons.

	Left Hemisphere	Right Hemisphere
Heavy users' group (G. I)	(0,001145±0,0001092)	(0,00111±0,000128)
Light users' group (G. II)	(0,001101±0,0001012)	(0,001026±0,0000838)
Non-users' group (G.III)	(0,00116±0,000129)	(0,001205±0,000189)
Intergroup comparison	G. II ≈ G. I ≈ G.III	G.III > G. I > G. II

➢ Amygdala

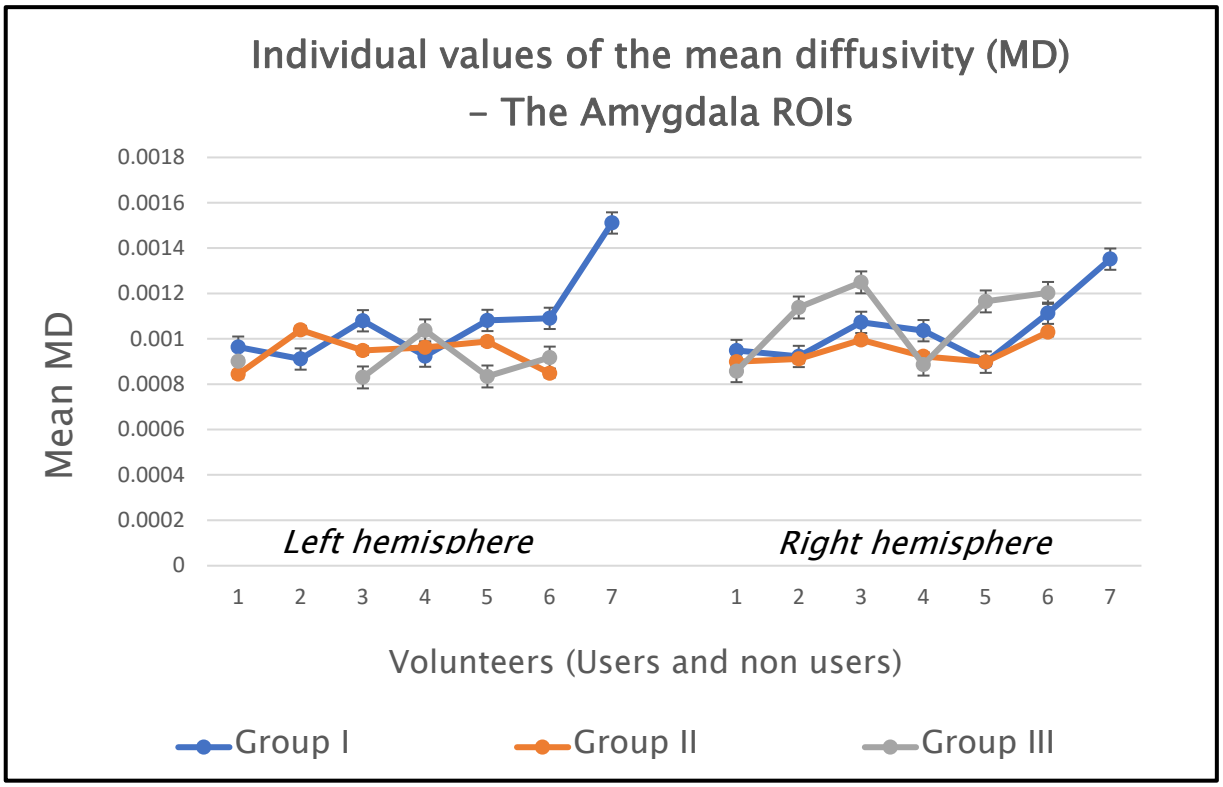

Figure 197: Individual values of mean diffusivity (MD) in both hemispheres' Amygdala ROIs. This figure depicts the MD values of all the participants belonging to each of the three groups (Heavy and light users and healthy controls).

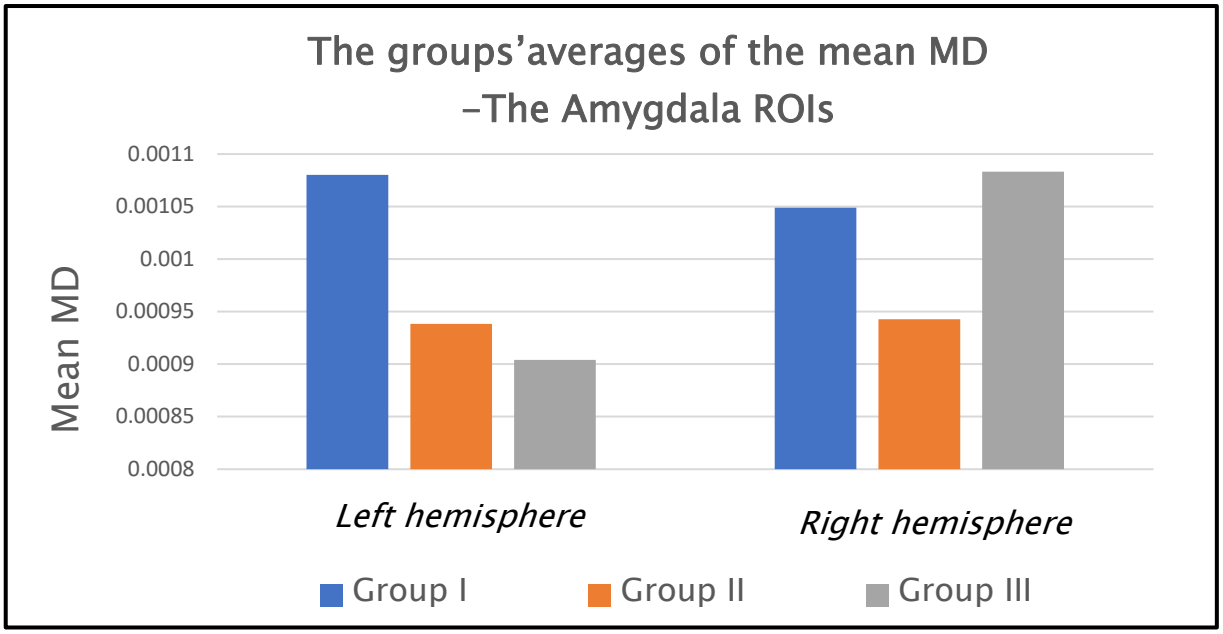

Figure 198: The mean diffusivity (MD) averages of each group in the Amygdala ROIs in the left and the right hemispheres.

Table 82: The mean diffusivity (MD) averages and standard deviations (SD) values for the groups studied in the Amygdala ROIs, along with intergroup comparisons.

	Left Hemisphere	Right Hemisphere
Heavy users' group (G. I)	(0,0010802±0,0002051)	(0,001048±0,000155)
Light users' group (G. II)	(0,000938±0,0000777)	(0,000942±0,0000557)
Non-users' group (G.III)	(0,0009039±0,0000841)	(0,001083±0,000168)
Intergroup comparison	G. I > G.III ≈ G. II	G.III ≈ G. I > G. II

➢ **Thalamus**

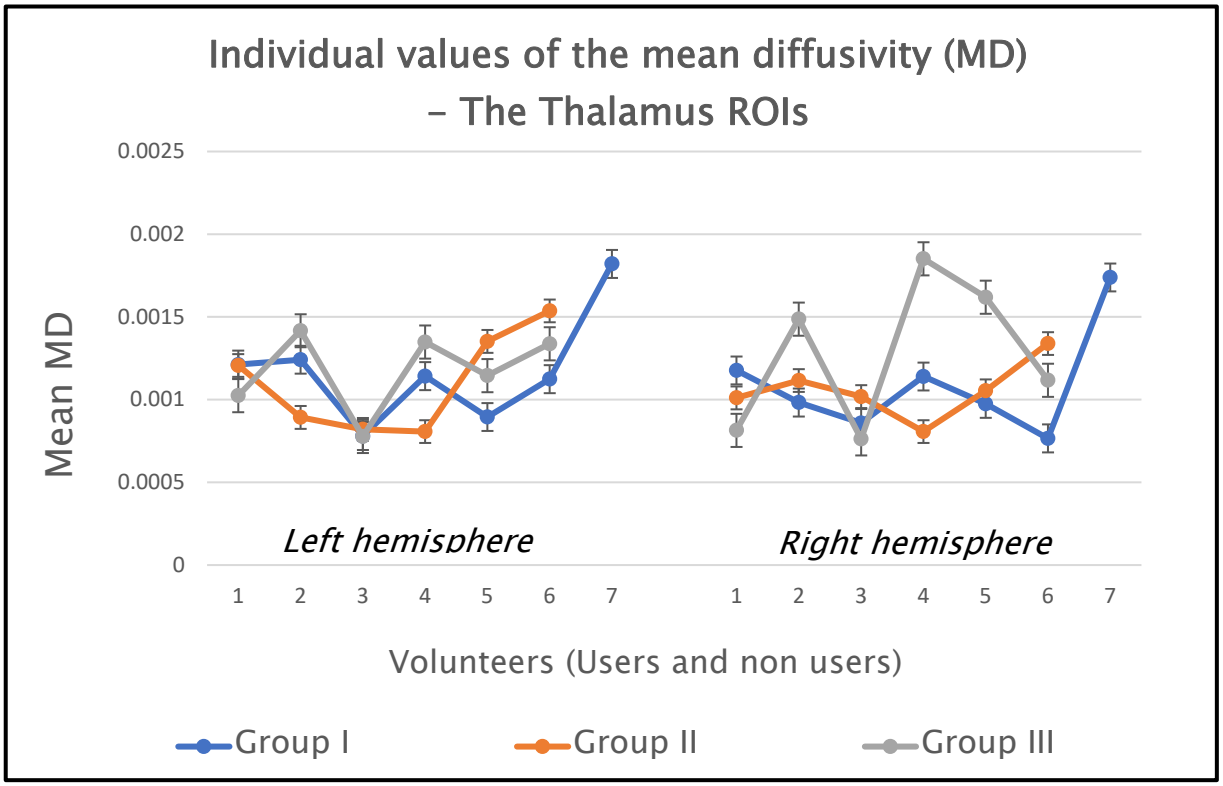

Figure 199: Individual values of mean diffusivity (MD) in both hemispheres' Thalamus ROIs. This figure depicts the MD values of all the participants belonging to each of the three groups (Heavy and light users and healthy controls).

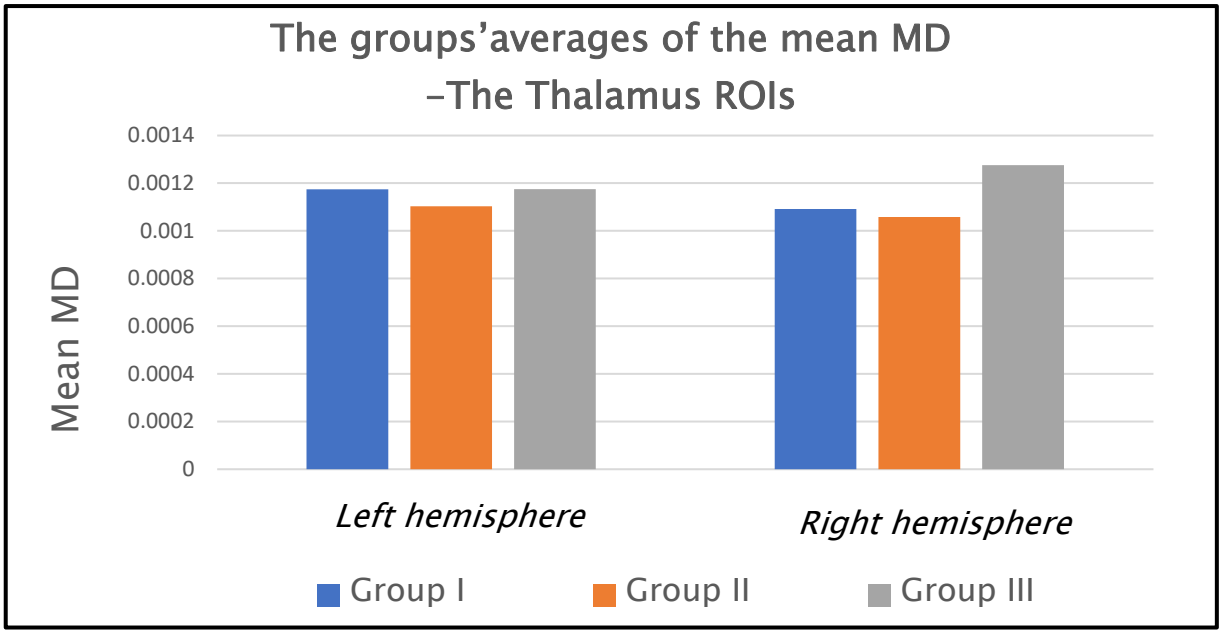

Figure 200: The mean diffusivity (MD) averages of each group in the Thalamus ROIs in the left and the right hemispheres.

Table 83: The mean diffusivity (MD) averages and standard deviations (SD) values for the groups studied in the Thalamus ROIs, along with intergroup comparisons.

	Left Hemisphere	Right Hemisphere
Heavy users' group (G. I)	(0,00117±0,000331)	(0,001091±0,000319)
Light users' group (G. II)	(0,001102±0,0003073)	(0,001057±0,000172)
Non-users' group (G.III)	(0,00117±0,000243)	(0,00127±0,000446)
Intergroup comparison	G. II ≈ G. I ≈ G.III	G.III > G. I ≈ G. II

➢ Caudate

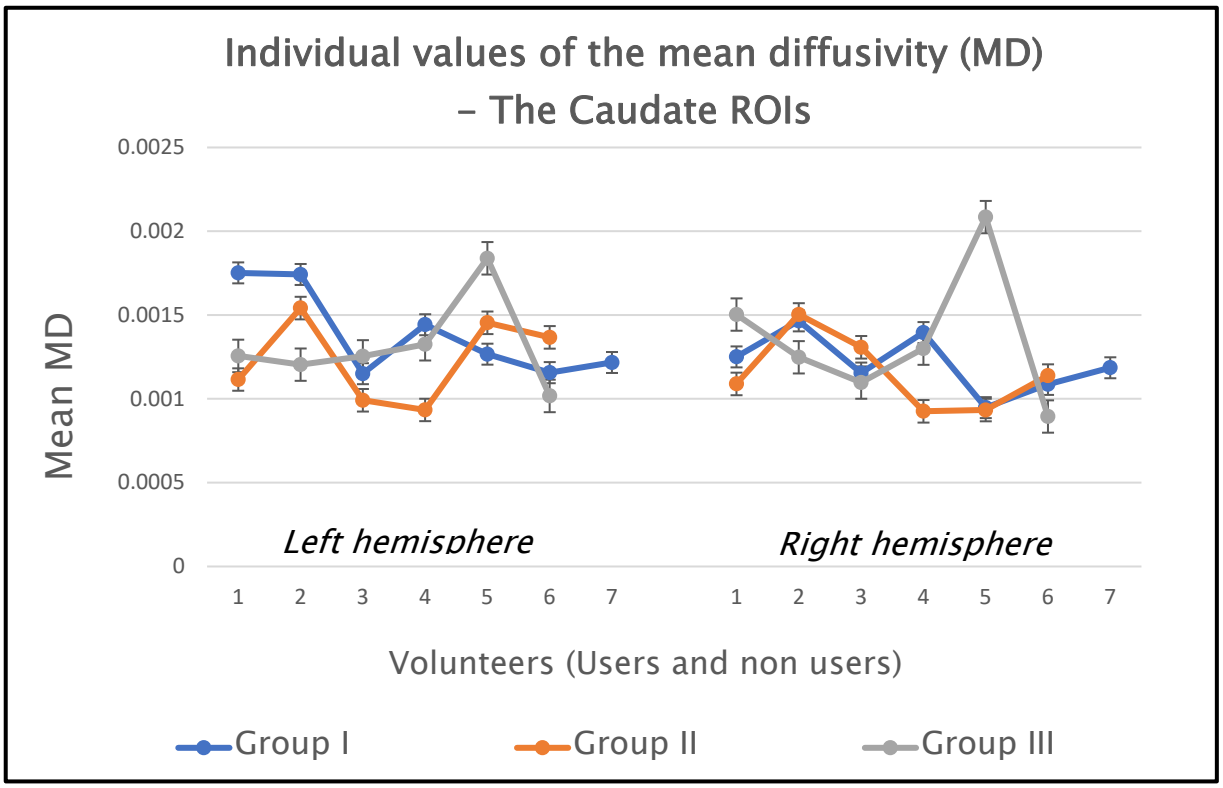

Figure 201: Individual values of mean diffusivity (MD) in both hemispheres' Caudate ROIs. This figure depicts the MD values of all the participants belonging to each of the three groups (Heavy and light users and healthy controls).

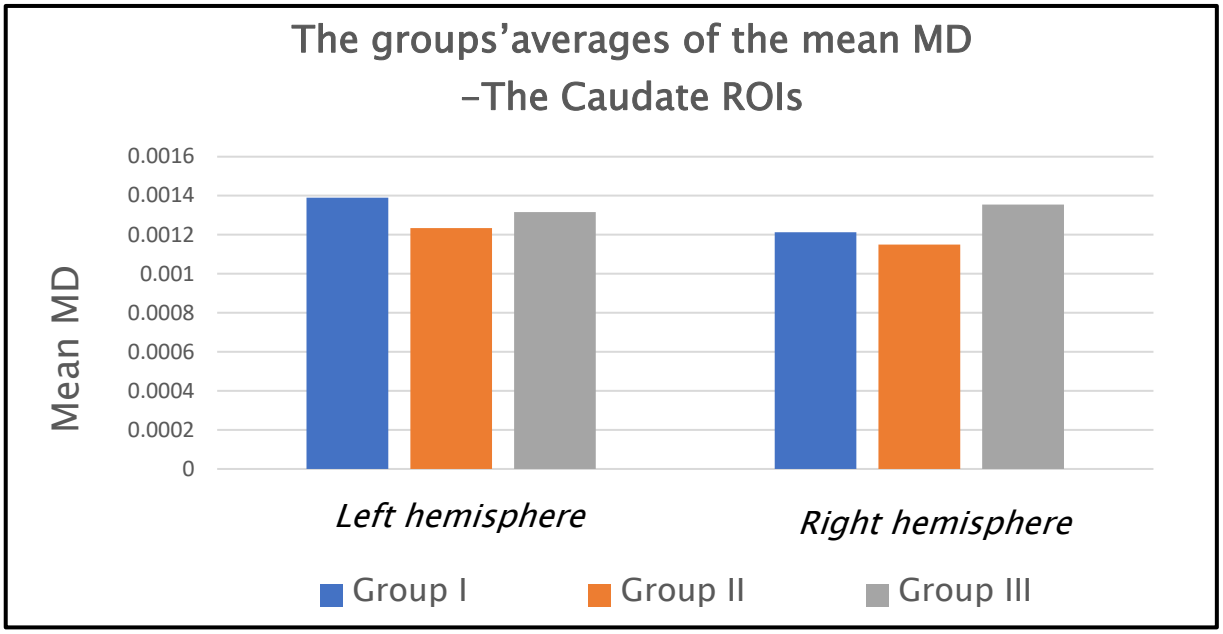

Figure 202: The mean diffusivity (MD) averages of each group in the Caudate ROIs in the left and the right hemispheres.

Table 84: The mean diffusivity (MD) averages and standard deviations (SD) values for the groups studied in the Caudate ROIs, along with intergroup comparisons.

	Left Hemisphere	Right Hemisphere
Heavy users' group (G. I)	(0,00138±0,000263)	(0,00121±0,000177)
Light users' group (G. II)	(0,00123±0,000254)	(0,00114±0,000223)
Non-users' group (G.III)	(0,00131±0,000276)	(0,00135±0,000411)
Intergroup comparison	G. I > G.III > G. II	G.III > G. I > G. II

➢ **Putamen**

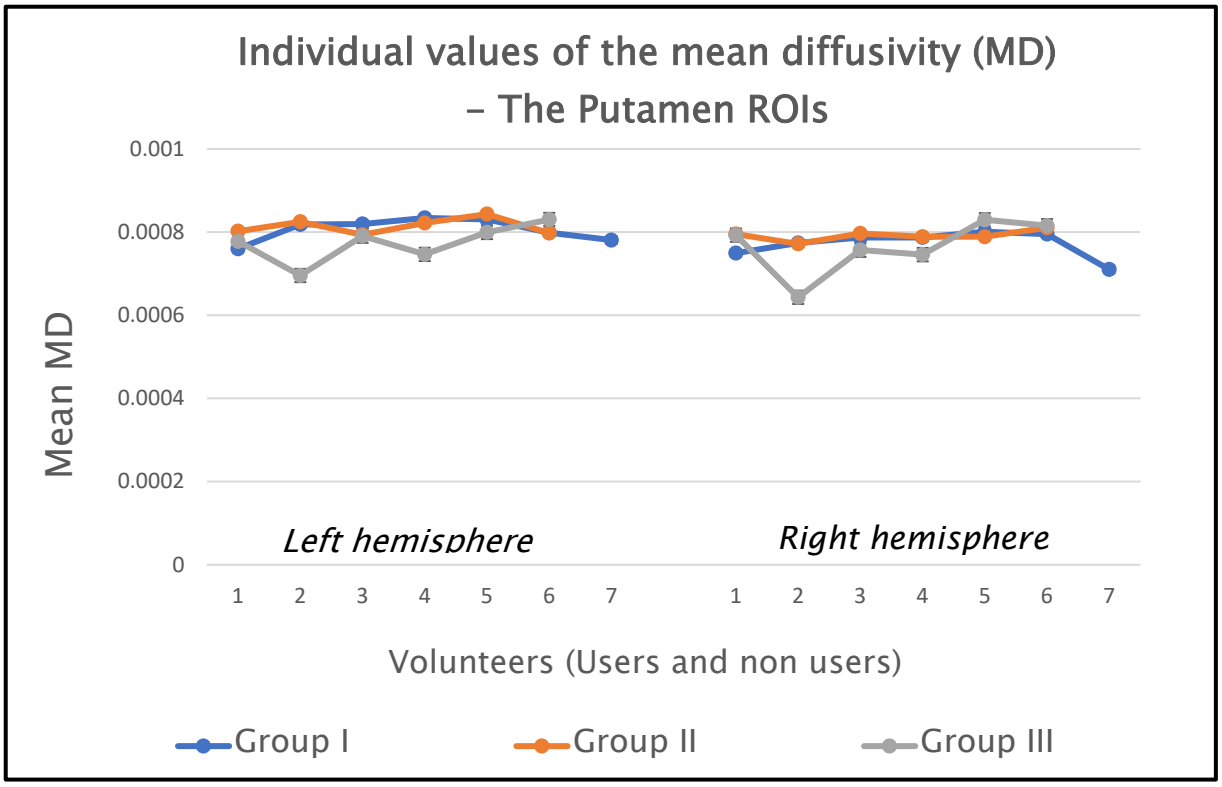

Figure 204: Individual values of mean diffusivity (MD) in both hemispheres' Putamen ROIs. This figure depicts the MD values of all the participants belonging to each of the three groups (Heavy and light users and healthy controls).

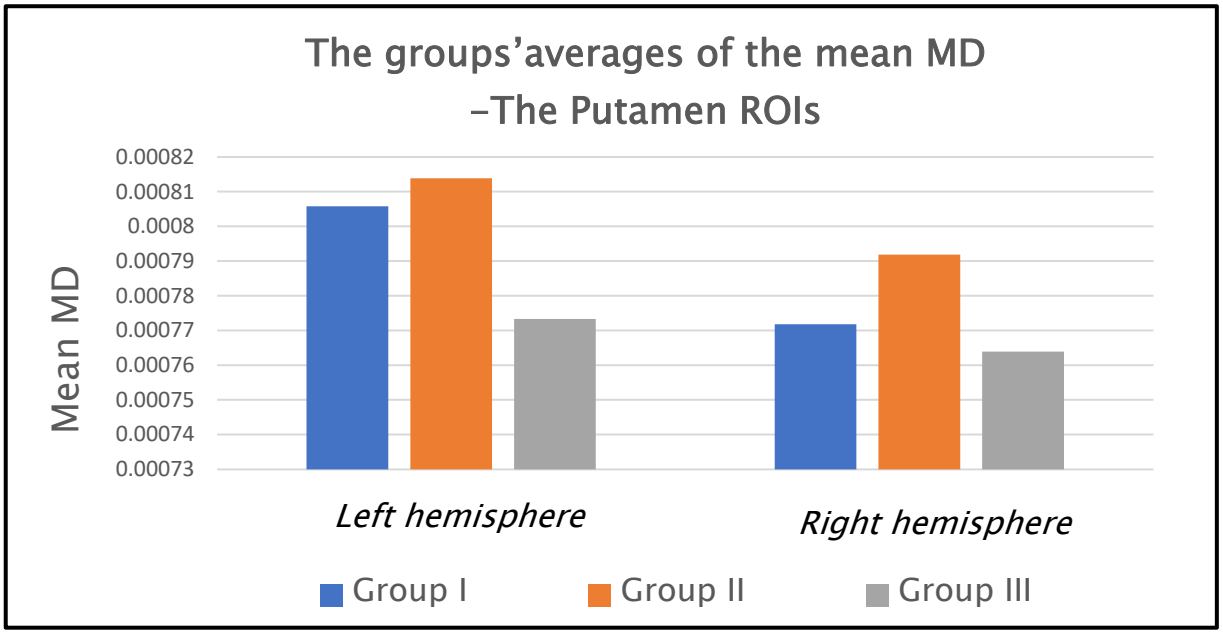

Figure 205: The mean diffusivity (MD) averages of each group in the Putamen ROIs in the left and the right hemispheres.

Table 85: The mean diffusivity (MD) averages and standard deviations (SD) values for the groups studied in the Putamen ROIs, along with intergroup comparisons

	Left Hemisphere	Right Hemisphere
Heavy users' group (G. I)	(0,0008057±0,0000274)	(0,000771±0,00003203)
Light users' group (G. II)	(0,000813±0,0000193)	(0,000791±0,0000126)
Non-users' group (G.III)	(0,000773±0,0000469)	(0,000763±0,0000673)
Intergroup comparison	G. I ≈ G.III ≈ G. II	G.III ≈ G. I ≈ G. II

➢ Pallidum

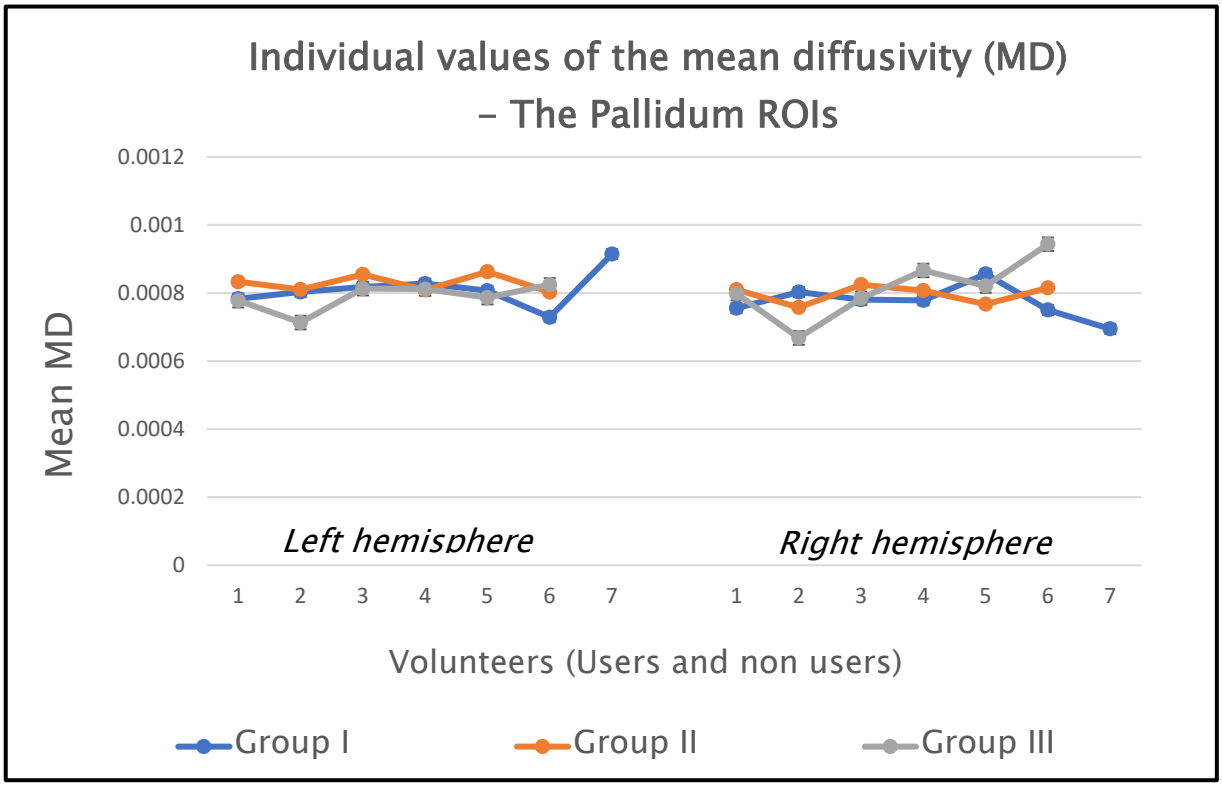

Figure 206: Individual values of mean diffusivity (MD) in both hemispheres' Pallidum ROIs. This figure depicts the MD values of all the participants belonging to each of the three groups (Heavy and light users and healthy controls).

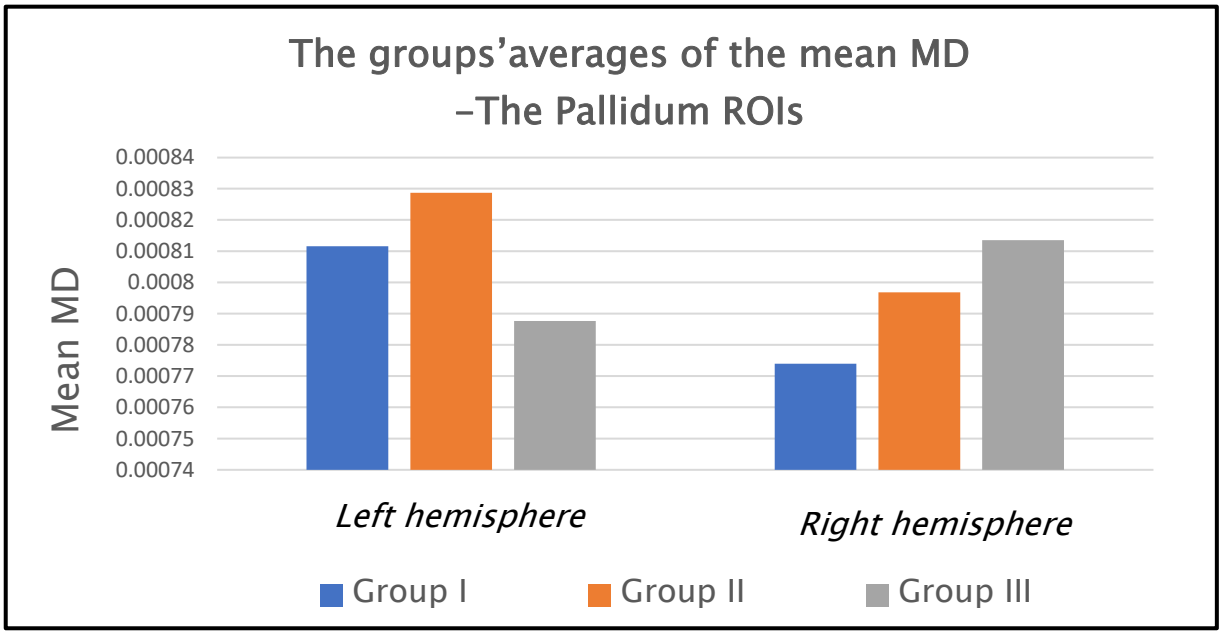

Figure 207: The mean diffusivity (MD) averages of each group in the Pallidum ROIs in the left and the right hemispheres.

Table 86: The mean diffusivity (MD) averages and standard deviations (SD) values for the groups studied in the Pallidum ROIs, along with intergroup comparisons.

	Left Hemisphere	Right Hemisphere
Heavy users' group (G. I)	(0,000811±0,0000557)	(0,000773±0,0000496)
Light users' group (G. II)	(0,000828±0,0000255)	(0,000796±0,0000274)
Non-users' group (G.III)	(0,000787±0,00004045)	(0,000813±0,0000915)
Intergroup comparison	G. I ≈ G.III ≈ G. II	G. I ≈ G.III ≈ G. II

➢ **Nucleus Accumbens**

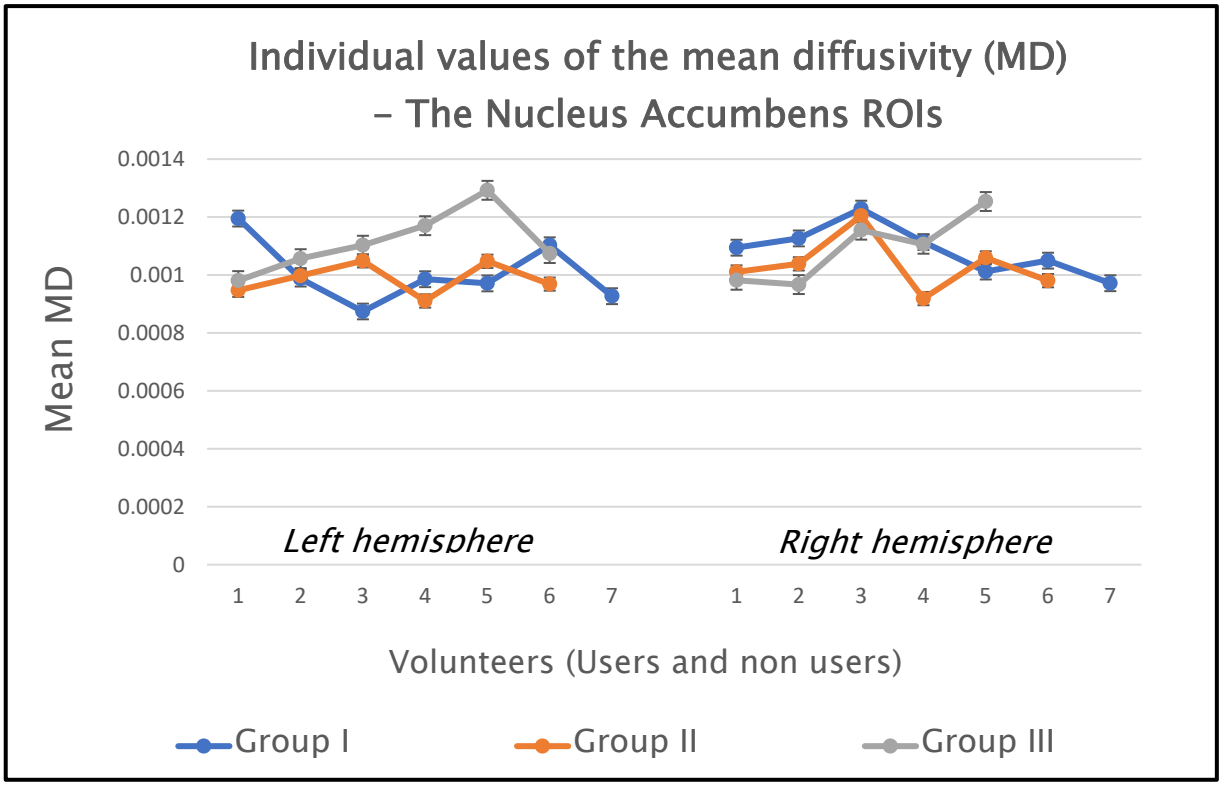

Figure 208: Individual values of mean diffusivity (MD) in both hemispheres' Nucleus Accumbens ROIs. This figure depicts the MD values of all the participants belonging to each of the three groups (Heavy and light users and healthy controls).

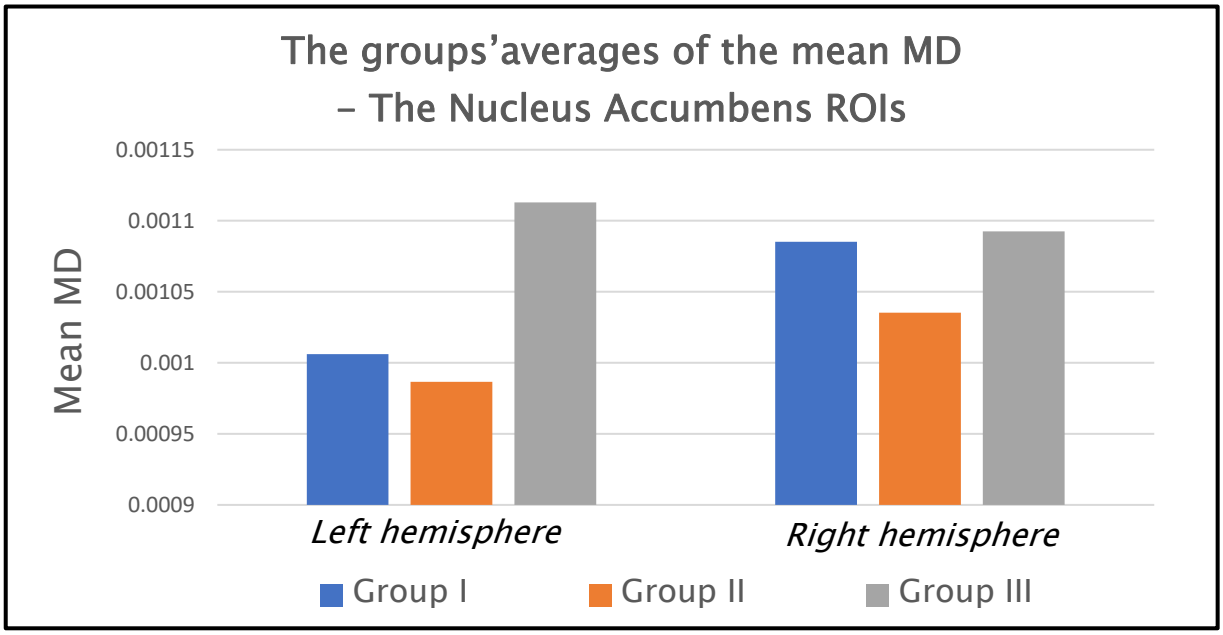

Figure 209: The mean diffusivity (MD) averages of each group in the Nucleus Accumbens ROIs in the left and the right hemispheres.

Table 87: The mean diffusivity (MD) averages and standard deviations (SD) values for the groups studied in the Nucleus Accumbens ROIs, along with intergroup comparisons.

	Left Hemisphere	Right Hemisphere
Heavy users' group (G. I)	(0,0010061±0,0001084)	(0,001085±0,0000844)
Light users' group (G. II)	(0,000986±0,0000554)	(0,001035±0,0000963)
Non-users' group (G.III)	(0,00111±0,0001075)	(0,001092±0,0001204)
Intergroup comparison	G.III > G. I ≈ G. II	G. I ≈ G.III > G. II

II. Analytical results

As we have mentioned in the statistical analysis part (Materials and methods section), ANOVA was conducted in the quantitative analysis to evaluate the levels of significant difference between pairs of users (heavy, light) and non-users groups.

Our analytical results, for FA and MD, will be presented in two parts:

- A summary of all analysis of Variance (ANOVA) findings.
- The analytical findings in each region of interest and between each of the groups studied

1. Fractional anisotropy (FA) analysis of Variance (ANOVA) results

a. Summary of all the analytical findings

For Fractional anisotropy (FA), in the 72 regions examined, 432 analyses of variance were conducted (between the three groups and in both hemispheres).

The analysis of Variance (ANOVA) results revealed 34 statistically significant results (a p-value <0.05), which is equivalent to 8% of the total conducted the analysis.

Table 88 summarizes the region with the corresponding groups compared where the statistical analysis is significant.

Table 88: A table containing regions of interest revealing statistically significant results of fractional anisotropy within the three groups (heavy and light users and control group).

Regions of interest	Groups compared
Left Rectus	Heavy users Vs. Light users
Left Frontal Sup	Heavy users Vs. Non-users Light users Vs. Non-users
Left Frontal Inf Tri	Heavy users Vs. Non-users Light users Vs. Non-users
Left Postcentral	Heavy users Vs. Non-users Light users Vs. Non-users
Left Parietal Sup	Heavy users Vs. Non-users
Right Parietal Sup	Heavy users Vs. Non-users
Left SupraMarginal	Heavy users Vs. Non-users Light users Vs. Non-users
Right SupraMarginal	Heavy users Vs. Non-users
Left Angular	Heavy users Vs. Non-users
Left Parietal Inf	Heavy users Vs. Non-users Light users Vs. Non-users
Left Precuneus	Heavy users Vs. Non-users Light users Vs. Non-users
Right Precuneus	Heavy users Vs. Non-users Light users Vs. Non-users
Left Temporal Sup	Heavy users Vs. Non-users Light users Vs. Non-users
Right Temporal Sup	Heavy users Vs. Non-users Light users Vs. Non-users
Left Temporal Pole Sup	Heavy users Vs. Non-users
Left Temporal Mid	Heavy users Vs. Non-users Light users Vs. Non-users
Right Temporal Mid	Heavy users Vs. Non-users Light users Vs. Non-users
Left Cingulum Ant	Heavy users Vs. Non-users
Right Cingulum Ant	Heavy users Vs. Non-users
Left Cingulum Mid	Heavy users Vs. Non-users Light users Vs. Non-users
Right Cingulum Mid	Heavy users Vs. Non-users
Left Insula	Heavy users Vs. Non-users

b. The analytical findings in each region of interest and between each of the groups studied

We present our mean fractional anisotropy (FA) statistical analysis findings by two tables for each region of interest and in both hemispheres. The first table represents statistical results in the left regions and the second in the right regions.

- **Frontal Med Orb**

Table 89: The statistical analysis results of the mean fractional anisotropy in the region of interest analysis technique in groups of heavy cannabis users, light users, and non-users, in **the left Frontal Med Orb region**.

	Mean fractional anisotropy of ROI analysis P-Value -Frontal Med Orb region of the left hemisphere-		
	Heavy users (Group I)	Light users (Group II)	Non-users (Group III)
Heavy users (Group I)	○	**	**
Light users (Group II)	0.966	○	**
Non users (Group III)	0.220	0.226	○

With a P-value lower than 0.05, the ANOVA analysis revealed no significant differences. The table shows that the mean fractional anisotropy values of different groups in the left Frontal Med Orb region were not significantly different in the same anatomical area.

Table 90: The statistical analysis results of the Mean fractional anisotropy in the region of interest technique of analysis in groups of heavy cannabis users, light users, and non-users, in **the right Frontal Med Orb region.**

	Mean fractional anisotropy of ROI analysis P-Value -Frontal Med Orb region of the right hemisphere-		
	Heavy users (Group I)	Light users (Group II)	Non-users (Group III)
Heavy users (Group I)	○	**	**
Light users (Group II)	0.905	○	**
Non users (Group III)	0.435	0.401	○

With a P-value lower than 0.05, the ANOVA analysis revealed no significant differences. The table indicates that the mean fractional anisotropy values of different groups in the right Frontal Med Orb region were not significantly different in the same anatomical area.

- **Frontal Sup Orb**

Table 91: The statistical analysis results of the mean fractional anisotropy in the region of interest analysis technique in groups of heavy cannabis users, light users, and non-users, in the **left Frontal Sup Orb region.**

	Mean fractional anisotropy of ROI analysis P-Value – Frontal Sup Orb region of the left hemisphere –		
	Heavy users (Group I)	Light users (Group II)	Non-users (Group III)
Heavy users (Group I)	○	**	**
Light users (Group II)	0.890	○	**
Non users (Group III)	0.297	0.388	○

With a P-value lower than 0.05, the ANOVA analysis revealed no significant differences. The table shows that the mean fractional anisotropy values of different groups in the left Frontal Sup Orb region were not significantly different in the same anatomical area.

Table 92. The statistical analysis results of the mean fractional anisotropy in the region of interest analysis technique in groups of heavy cannabis users, light users, and non-users, in **the right Frontal Sup Orb region.**

	Mean fractional anisotropy of ROI analysis P-Value Frontal Sup Orb region of the right hemisphere		
	Heavy users (Group I)	Light users (Group II)	Non-users (Group III)
Heavy users (Group I)	○	**	**
Light users (Group II)	0.476	○	**
Non users (Group III)	0.586	0.743	○

With a P-value lower than 0.05, the ANOVA analysis revealed no significant differences. The table reveals that the mean fractional anisotropy values of different groups in the right Frontal Sup Orb region were not significantly different in the same anatomical area.

➢ **Frontal Mid Orb**

Table 93: The statistical analysis results of the mean fractional anisotropy in the region of interest analysis technique in groups of heavy cannabis users, light users, and non-users, in **the left Frontal Mid Orb region.**

	Mean fractional anisotropy of ROI analysis P-Value – Frontal Mid Orb region of the left hemisphere –		
	Heavy users (Group I)	**Light users (Group II)**	**Non-users (Group III)**
Heavy users (Group I)	○	**	**
Light users (Group II)	0.474	○	**
Non users (Group III)	0.257	0.102	○

With a P-value lower than 0.05, the ANOVA analysis revealed no significant differences. The table reveals that the mean fractional anisotropy values of different groups in the left Frontal Mid Orb region were not significantly different in the same anatomical area.

Table 94: The statistical analysis results of the mean fractional anisotropy in the region of interest analysis technique in groups of heavy cannabis users, light users, and non-users, in **the right Frontal Mid Orb region.**

	Mean fractional anisotropy of ROI analysis P-Value – Frontal Mid Orb region of the right hemisphere –		
	Heavy users (Group I)	**Light users (Group II)**	**Non-users (Group III)**
Heavy users (Group I)	○	**	**
Light users (Group II)	0.851	○	**
Non users (Group III)	0.288	0.290	○

With a P-value lower than 0.05, the ANOVA analysis revealed no significant differences. The table reveals that the mean fractional anisotropy values, of different groups, in the right Frontal Mid Orb region were not significantly different in the same anatomical area.

➢ **Frontal Inf Orb**

Table 95: The statistical analysis results of the mean fractional anisotropy in the region of interest analysis technique in groups of heavy cannabis users, light users, and non-users, in the **left Frontal Inf Orb region.**

	Mean fractional anisotropy of ROI analysis P-Value – Frontal Inf Orb region of the left hemisphere –		
	Heavy users (Group I)	**Light users (Group II)**	**Non-users (Group III)**
Heavy users (Group I)	○	**	**
Light users (Group II)	0.732	○	**
Non users (Group III)	0.200	0.274	○

With a P-value lower than 0.05, the ANOVA analysis revealed no significant differences. The table reveals that the mean fractional anisotropy values of different groups in the left Frontal Inf Orb region were not significantly different in the same anatomical area.

Table 96: The statistical analysis results of the Mean fractional anisotropy in the region of interest technique of analysis in groups of heavy cannabis users, light users, and non-users, in **the right Frontal Inf Orb region.**

	Mean fractional anisotropy of ROI analysis P-Value – Frontal Inf Orb region of the right hemisphere –		
	Heavy users (Group I)	**Light users (Group II)**	**Non-users (Group III)**
Heavy users (Group I)	○	**	**
Light users (Group II)	0.781	○	**
Non users (Group III)	0.246	0.307	○

With a P-value lower than 0.05, the ANOVA analysis revealed no significant differences. The table shows that the mean fractional anisotropy values, of different groups, in the right Frontal Inf Orb region were not significantly different in the same anatomical area.

➢ **Rectus**

Table 97: The statistical analysis results of the mean fractional anisotropy in the region of interest technique of analysis in groups of heavy cannabis users, light users, and non-users, in the **left Rectus region.**

	Mean fractional anisotropy of ROI analysis P-Value – Rectus region of the left hemisphere –		
	Heavy users (Group I)	Light users (Group II)	Non-users (Group III)
Heavy users (Group I)	○	**	**
Light users (Group II)	0.037	○	**
Non users (Group III)	0.118	0.386	○

With a P-value lower than 0.05, the ANOVA analysis revealed a significant difference between heavy and light users' groups and no significant differences between the other groups. The table reveals that in the same anatomical area, the mean fractional anisotropy values of different groups in the left Rectus region were significantly different among one from three comparisons realized.

Table 98: The statistical analysis results of the mean fractional anisotropy in the region of interest technique of analysis in groups of heavy cannabis users, light users, and non-users, in **the right Rectus region.**

	Mean fractional anisotropy of ROI analysis P-Value – Rectus region of the right hemisphere –		
	Heavy users (Group I)	Light users (Group II)	Non-users (Group III)
Heavy users (Group I)	○	**	**
Light users (Group II)	0.327	○	**
Non users (Group III)	0.231	0.795	○

With a P-value lower than 0.05, the ANOVA analysis revealed no significant differences. The table reveals that the mean fractional anisotropy values of different groups in the right Rectus region were not significantly different in the same anatomical area.

➢ Olfactory

Table 99: The statistical analysis results of the mean fractional anisotropy in the region of interest analysis technique in groups of heavy cannabis users, light users, and non-users, in the **left Olfactory region.**

	Mean fractional anisotropy of ROI analysis P-Value – Olfactory region of the left hemisphere –		
	Heavy users (Group I)	Light users (Group II)	Non-users (Group III)
Heavy users (Group I)	○	**	**
Light users (Group II)	0.756	○	**
Non users (Group III)	0.184	0.156	○

With a P-value lower than 0.05, the ANOVA analysis revealed no significant differences. The table reveals that the mean fractional anisotropy values in the left Olfactory region for the three groups were not significantly different in the same anatomical area.

Table 100: The statistical analysis results of the mean fractional anisotropy in the region of interest technique of analysis in groups of heavy cannabis users, light users, and non-users, in **the right Olfactory region.**

	Mean fractional anisotropy of ROI analysis P-Value – Olfactory region of the right hemisphere –		
	Heavy users (Group I)	Light users (Group II)	Non-users (Group III)
Heavy users (Group I)	○	**	**
Light users (Group II)	0.367	○	**
Non users (Group III)	0.166	0.638	○

With a P-value lower than 0.05, the ANOVA analysis revealed no significant differences. The table reveals that groups' mean fractional anisotropy values in the right Olfactory region were not significantly different in the same anatomical area.

➢ **Frontal Sup Medial**

Table 101: The statistical analysis results of the mean fractional anisotropy in the region of interest analysis technique in groups of heavy cannabis users, light users, and non-users, in the **left Frontal Sup Medial region.**

	Mean fractional anisotropy of ROI analysis P-Value Frontal Sup Medial region of the left hemisphere		
	Heavy users (Group I)	Light users (Group II)	Non-users (Group III)
Heavy users (Group I)	○	**	**
Light users (Group II)	0.930	○	**
Non users (Group III)	0.141	0.306	○

With a P-value lower than 0.05, the ANOVA analysis revealed no significant differences. The table reveals that the mean fractional anisotropy values of different groups in the left Frontal Sup Medial region were not significantly different in the same anatomical area.

Table 102: The statistical analysis results of the mean fractional anisotropy in the region of interest analysis technique in groups of heavy cannabis users, light users, and non-users, in **the right Frontal Sup Medial region.**

	Mean fractional anisotropy of ROI analysis P-Value Frontal Sup Medial region of the right hemisphere		
	Heavy users (Group I)	Light users (Group II)	Non-users (Group III)
Heavy users (Group I)	○	**	**
Light users (Group II)	0.925	○	**
Non users (Group III)	0.262	0.222	○

With a P-value lower than 0.05, the ANOVA analysis revealed no significant differences. The table reveals that the mean fractional anisotropy values of different groups in the right Frontal Sup Medial region were not significantly different in the same anatomical area.

➢ **Frontal Sup**

Table 103: The statistical analysis results of the mean fractional anisotropy in the region of interest analysis technique in groups of heavy cannabis users, light users, and non-users, in the **left Frontal Sup region.**

	Mean fractional anisotropy of ROI analysis P-Value Frontal Sup region of the left hemisphere		
	Heavy users (Group I)	Light users (Group II)	Non-users (Group III)
Heavy users (Group I)	○	**	**
Light users (Group II)	0.451	○	**
Non users (Group III)	0.011	0.024	○

With a P-value lower than 0.05, the ANOVA analysis revealed significant differences between heavy users and non-users groups and between light users and non-users groups, but no significant difference between heavy and light users' groups. The table reveals that in the same anatomical area, the mean fractional anisotropy values of different groups in the left Frontal Sup region were significantly different among two from three comparisons realized.

Table 104: The statistical analysis results of the Mean fractional anisotropy in the region of interest technique of analysis in groups of heavy cannabis users, light users, and non-users, in the **left Frontal Sup region.**

	Mean fractional anisotropy of ROI analysis P-Value Frontal Sup region of the right hemisphere		
	Heavy users (Group I)	Light users (Group II)	Non-users (Group III)
Heavy users (Group I)	○	**	**
Light users (Group II)	0.629	○	**
Non users (Group III)	0.439	0.344	○

With a P-value lower than 0.05, the ANOVA analysis revealed no significant differences. The table reveals that the mean fractional anisotropy values of different groups in the right Frontal Sup region were not significantly different in the same anatomical area.

➢ **Frontal Mid**

Table 105: The statistical analysis results of the mean fractional anisotropy in the region of interest analysis technique in groups of heavy cannabis users, light users, and non-users, in the **left Frontal Mid region.**

	Mean fractional anisotropy of ROI analysis P-Value Frontal Mid region of the left hemisphere		
	Heavy users (Group I)	Light users (Group II)	Non-users (Group III)
Heavy users (Group I)	○	**	**
Light users (Group II)	0.920	○	**
Non users (Group III)	0.202	0.146	○

With a P-value lower than 0.05, the ANOVA analysis revealed no significant differences. The table reveals that the mean fractional anisotropy values of different groups in the left Frontal Mid region were not significantly different in the same anatomical area.

Table 106: The statistical analysis results of the mean fractional anisotropy in the region of interest analysis technique in groups of heavy cannabis users, light users, and non-users, in **the right Frontal Mid region.**

	Mean fractional anisotropy of ROI analysis P-Value Frontal Mid region of the right hemisphere		
	Heavy users (Group I)	Light users (Group II)	Non-users (Group III)
Heavy users (Group I)	○	**	**
Light users (Group II)	0.626	○	**
Non users (Group III)	0.130	0.132	○

With a P-value lower than 0.05, the ANOVA analysis revealed no significant differences. The table reveals that the mean fractional anisotropy values of different groups in the right Frontal Mid region were not significantly different in the same anatomical area.

➢ **Frontal Inf Oper**

Table 107: The results of statistical analysis of the mean fractional anisotropy in the region of interest technique of analysis in groups of heavy cannabis users, light users, and non-users, in the **left Frontal Inf Oper region.**

	Mean fractional anisotropy of ROI analysis P-Value Frontal Inf Oper region of the left hemisphere		
	Heavy users (Group I)	Light users (Group II)	Non-users (Group III)
Heavy users (Group I)	○	**	**
Light users (Group II)	0.300	○	**
Non users (Group III)	0.308	0.060	○

With a P-value lower than 0.05, the ANOVA analysis revealed no significant differences. The table reveals that the mean fractional anisotropy values of different groups in the left Frontal Inf Oper region were not significantly different in the same anatomical area.

Table 108: The statistical analysis results of the mean fractional anisotropy in the region of interest technique of analysis in groups of heavy cannabis users, light users, and non-users, in **the right Frontal Inf Oper region.**

	Mean fractional anisotropy of ROI analysis P-Value Frontal Inf Oper region of the right hemisphere		
	Heavy users (Group I)	Light users (Group II)	Non-users (Group III)
Heavy users (Group I)	○	**	**
Light users (Group II)	0.117	○	**
Non users (Group III)	0.706	0.064	○

With a P-value lower than 0.05, the ANOVA analysis revealed no significant differences. The table reveals that the mean fractional anisotropy values, of different groups, in the right Frontal Inf Oper region were not significantly different in the same anatomical area.

➢ **Frontal Inf Tri**

Table 109: The statistical analysis results of the mean fractional anisotropy in the region of interest analysis technique in groups of heavy cannabis users, light users, and non-users, in the **left Frontal Inf Tri region.**

	Mean fractional anisotropy of ROI analysis P-Value Frontal Inf Tri region of the left hemisphere		
	Heavy users (Group I)	Light users (Group II)	Non-users (Group III)
Heavy users (Group I)	○	**	**
Light users (Group II)	0.702	○	**
Non users (Group III)	0.003	0.023	○

With a P-value lower than 0.05, the ANOVA analysis revealed significant differences between heavy users and non-users groups and between light users and non-users groups, but no significant difference between heavy and light users' groups. The table reveals that in the same anatomical area, the mean fractional anisotropy values of different groups in the left Frontal Inf Tri region were significantly different among two from three comparisons realized.

Table 110: The statistical analysis results of the mean fractional anisotropy in the region of interest technique of analysis in groups of heavy cannabis users, light users, and non-users, in **the right Frontal Inf Tri region.**

	Mean fractional anisotropy of ROI analysis P-Value Frontal Inf Tri region of the right hemisphere		
	Heavy users (Group I)	Light users (Group II)	Non-users (Group III)
Heavy users (Group I)	○	**	**
Light users (Group II)	0.859	○	**
Non users (Group III)	0.410	0.365	○

With a P-value lower than 0.05, the ANOVA analysis revealed no significant differences. The table reveals that the mean fractional anisotropy values of different groups in the right Frontal Inf Tri region were not significantly different in the same anatomical area.

➢ **Postcentral**

Table 111: The results of statistical analysis of the mean fractional anisotropy in the region of interest technique of analysis in groups of heavy cannabis users, light users, and non-users, in the **left Postcentral region.**

	Mean fractional anisotropy of ROI analysis P-Value Postcentral region of the left hemisphere		
	Heavy users (Group I)	Light users (Group II)	Non-users (Group III)
Heavy users (Group I)	○	**	**
Light users (Group II)	0,951	○	**
Non users (Group III)	0,018	0,014	○

With a P-value lower than 0.05, the ANOVA analysis revealed significant differences between heavy users and non-users groups and between light users and non-users groups, but no significant difference between heavy and light users' groups. The table reveals that in the same anatomical area, the mean fractional anisotropy values of different groups in the left Postcentral region were significantly different among two from three comparisons realized.

Table 112: The statistical analysis results of the mean fractional anisotropy in the region of interest technique of analysis in groups of heavy cannabis users, light users, and non-users, in **the right Postcentral region**.

	Mean fractional anisotropy of ROI analysis P-Value Postcentral region of the right hemisphere		
	Heavy users (Group I)	Light users (Group II)	Non-users (Group III)
Heavy users (Group I)	○	**	**
Light users (Group II)	0,693	○	**
Non users (Group III)	0,068	0,155	○

With a P-value lower than 0.05, the ANOVA analysis revealed no significant differences. The table reveals that the mean fractional anisotropy values of different groups in the right Postcentral region were not significantly different in the same anatomical area.

➢ **Parietal Sup**

Table 113: The statistical analysis results of the mean fractional anisotropy in the region of interest analysis technique in groups of heavy cannabis users, light users, and non-users, in the **left Parietal Sup region.**

	Mean fractional anisotropy of ROI analysis P-Value Parietal Sup region of the left hemisphere		
	Heavy users (Group I)	**Light users (Group II)**	**Non-users (Group III)**
Heavy users (Group I)	○	**	**
Light users (Group II)	0,087	○	**
Non users (Group III)	**0,004**	0,175	○

With a P-value lower than 0.05, the ANOVA analysis revealed significant differences between heavy users and non-users groups, but no significant difference between heavy and light users' groups and between light users and non-users groups. The table reveals that in the same anatomical area, the mean fractional anisotropy values of different groups in the left Parietal Sup region were significantly different among one from three comparisons realized.

Table 114: The statistical analysis results of the Mean fractional anisotropy in the region of interest technique of analysis in groups of heavy cannabis users, light users, and non-users, in **the right Parietal Sup region.**

	Mean fractional anisotropy of ROI analysis P-Value Parietal Sup region of the right hemisphere		
	Heavy users (Group I)	**Light users (Group II)**	**Non-users (Group III)**
Heavy users (Group I)	○	**	**
Light users (Group II)	0,760	○	**
Non users (Group III)	**0,037**	0,119	○

With a P-value lower than 0.05, the ANOVA analysis revealed significant differences between heavy users and non-users groups, but no significant difference between heavy and light users' groups and between light users and non-users groups. The table reveals that in the same anatomical area, the mean fractional anisotropy values of different groups in the right Frontal Parietal Sup region were significantly different among one from three comparisons realized.

➢ SupraMarginal

Table 115: The statistical analysis results of the mean fractional anisotropy in the region of interest analysis technique in groups of heavy cannabis users, light users, and non-users, in the **left SupraMarginal region.**

	Mean fractional anisotropy of ROI analysis P-Value SupraMarginal region of the left hemisphere		
	Heavy users (Group I)	Light users (Group II)	Non-users (Group III)
Heavy users (Group I)	○	**	**
Light users (Group II)	0,835	○	**
Non users (Group III)	0,008	0,002	○

With a P-value lower than 0.05, the ANOVA analysis revealed significant differences between heavy users and non-users groups and between light users and non-users groups, but no significant difference between heavy and light users' groups. The table reveals that in the same anatomical area, the mean fractional anisotropy values of different groups in the left SupraMarginal region were significantly different among two from three comparisons realized.

Table 116: The statistical analysis results of the Mean fractional anisotropy in the region of interest technique of analysis in groups of heavy cannabis users, light users, and non-users, in **the right SupMarginal region.**

	Mean fractional anisotropy of ROI analysis P-Value SupraMarginal region of the right hemisphere		
	Heavy users (Group I)	Light users (Group II)	Non-users (Group III)
Heavy users (Group I)	○	**	**
Light users (Group II)	0,911	○	**
Non users (Group III)	0,035	0,055	○

With a P-value lower than 0.05, the ANOVA analysis revealed significant differences between heavy users and non-users groups, but no significant difference between heavy and light users' groups and between light users and non-users groups. The table reveals that in the same anatomical area, the mean fractional anisotropy values of different groups in the right SupraMarginal region were significantly different among one from three comparisons realized.

➢ **Angular**

Table 117: The statistical analysis results of the mean fractional anisotropy in the region of interest analysis technique in groups of heavy cannabis users, light users, and non-users, in **the left Angular region.**

	Mean fractional anisotropy of ROI analysis P-Value Angular region of the left hemisphere		
	Heavy users (Group I)	Light users (Group II)	Non-users (Group III)
Heavy users (Group I)	○	**	**
Light users (Group II)	0,221	○	**
Non users (Group III)	0,017	0,540	○

With a P-value lower than 0.05, the ANOVA analysis revealed significant differences between heavy users and non-users groups, but no significant difference between heavy and light users' groups and between light users and non-users groups. The table reveals that in the same anatomical area, the mean fractional anisotropy values of different groups in the left Angular region were significantly different among one from three comparisons realized.

Table 118: The statistical analysis results of the Mean fractional anisotropy in the region of interest technique of analysis in groups of heavy cannabis users, light users, and non-users, in **the right Angular region.**

	Mean fractional anisotropy of ROI analysis P-Value Angular region of the right hemisphere		
	Heavy users (Group I)	Light users (Group II)	Non-users (Group III)
Heavy users (Group I)	○	**	**
Light users (Group II)	0,480	○	**
Non users (Group III)	0,220	0,297	○

With a P-value lower than 0.05, the ANOVA analysis revealed no significant differences. The table reveals that groups' mean fractional anisotropy values in the right Angular region were not significantly different in the same anatomical area.

➢ **Parietal Inf**

Table 119:The statistical analysis results of the mean fractional anisotropy in the region of interest analysis technique in groups of heavy cannabis users, light users, and non-users, in the **left Parietal Inf region.**

	Mean fractional anisotropy of ROI analysis P-Value Parietal Inf region of the left hemisphere		
	Heavy users (Group I)	Light users (Group II)	Non-users (Group III)
Heavy users (Group I)	○	**	**
Light users (Group II)	0,25	○	**
Non users (Group III)	0,049	0,003	○

With a P-value lower than 0.05, the ANOVA analysis revealed significant differences between heavy users and non-users groups and between light users and non-users groups, but no significant difference between heavy and light users groups. The table reveals that in the same anatomical area, the mean fractional anisotropy values of different groups in the left Parietal Inf region were significantly different among two from three comparisons realized.

Table 120: The results of statistical analysis of the mean fractional anisotropy in the region of interest technique of analysis in groups of heavy cannabis users, light users, and non-users, in **the right Parietal Inf region**

	Mean fractional anisotropy of ROI analysis P-Value Parietal Inf region of the right hemisphere		
	Heavy users (Group I)	Light users (Group II)	Non-users (Group III)
Heavy users (Group I)	○	**	**
Light users (Group II)	0,889	○	**
Non users (Group III)	0,438	0,666	○

With a P-value lower than 0.05, the ANOVA analysis revealed no significant differences. The table reveals that different groups' mean fractional anisotropy values in the right Parietal Inf region were not significantly different in the same anatomical area.

➢ **Precuneus**

Table 121: The statistical analysis results of the mean fractional anisotropy in the region of interest analysis technique in groups of heavy cannabis users, light users, and non-users, in the **left Precuneus region.**

	Mean fractional anisotropy of ROI analysis P-Value Precuneus region of the left hemisphere		
	Heavy users (Group I)	Light users (Group II)	Non-users (Group III)
Heavy users (Group I)	○	**	**
Light users (Group II)	0,586	○	**
Non users (Group III)	0,0005	0,005	○

With a P-value lower than 0.05, the ANOVA analysis revealed significant differences between heavy users and non-users groups and between light users and non-users groups, but no significant difference between heavy and light users' groups. The table reveals that in the same anatomical area, the mean fractional anisotropy values of different groups in the left Precuneus region were significantly different among two from three comparisons realized.

Table 122: The statistical analysis results of the mean fractional anisotropy in the region of interest analysis technique in groups of heavy cannabis users, light users, and non-users, in the **right Precuneus region.**

	Mean fractional anisotropy of ROI analysis P-Value Precuneus region of the right hemisphere		
	Heavy users (Group I)	Light users (Group II)	Non-users (Group III)
Heavy users (Group I)	○	**	**
Light users (Group II)	0,557	○	**
Non users (Group III)	0,003	0,019	○

With a P-value lower than 0.05, the ANOVA analysis revealed significant differences between heavy users and non-users groups and between light users and non-users groups, but no significant difference between heavy and light users' groups. The table reveals that in the same anatomical area, the mean fractional anisotropy values of different groups in the right Precuneus region were significantly different among two from three comparisons realized.

➢ **Temporal Sup**

Table 123: The statistical analysis results of the mean fractional anisotropy in the region of interest analysis technique in groups of heavy cannabis users, light users, and non-users, in the **left Temporal Sup region**.

	Mean fractional anisotropy of ROI analysis P-Value Temporal Sup region of the left hemisphere		
	Heavy users (Group I)	Light users (Group II)	Non-users (Group III)
Heavy users (Group I)	○	**	**
Light users (Group II)	0,627	○	**
Non users (Group III)	0,02	0,042	○

With a P-value lower than 0.05, the ANOVA analysis revealed significant differences between heavy users and non-users groups and between light users and non-users groups, but no significant difference between heavy and light users' groups. The table reveals that in the same anatomical area, the mean fractional anisotropy values of different groups in the left Temporal Sup region were significantly different among two from three comparisons realized.

Table 124: The statistical analysis results of the mean fractional anisotropy in the region of interest technique of analysis in groups of heavy cannabis users, light users, and non-users, in the **right Temporal Sup region**.

	Mean fractional anisotropy of ROI analysis P-Value Temporal Sup region of the right hemisphere		
	Heavy users (Group I)	Light users (Group II)	Non-users (Group III)
Heavy users (Group I)	○	**	**
Light users (Group II)	0,278	○	**
Non users (Group III)	0,011	0,012	○

With a P-value lower than 0.05, the ANOVA analysis revealed significant differences between heavy users and non-users groups and between light users and non-users groups, but no significant difference between heavy and light users' groups. The table reveals that in the same anatomical area, the mean fractional anisotropy values of different groups in the right Temporal Sup region were significantly different among two from three comparisons realized.

➢ **Temporal Pole Sup**

Table 125: The statistical analysis results of the mean fractional anisotropy in the region of interest analysis technique in groups of heavy cannabis users, light users, and non-users, in **the left Temporal Pole Sup region.**

	Mean fractional anisotropy of ROI analysis P-Value Temporal Pole Sup region of the left hemisphere		
	Heavy users (Group I)	Light users (Group II)	Non-users (Group III)
Heavy users (Group I)	○	**	**
Light users (Group II)	0,411	○	**
Non users (Group III)	0,043	0,497	○

With a P-value lower than 0.05, the ANOVA analysis revealed significant differences between heavy users and non-users groups, but no significant difference between heavy and light users' groups and between light users and non-users groups. The table reveals that in the same anatomical area, the mean fractional anisotropy values of different groups in the left Temporal Pole Sup region were significantly different among one group from three comparisons realized.

Table 126: The statistical analysis results of the mean fractional anisotropy in the region of interest technique of analysis in groups of heavy cannabis users, light users, and non-users, in **the right Temporal Pole Sup region.**

	Mean fractional anisotropy of ROI analysis P-Value Temporal Pole Sup region of the right hemisphere		
	Heavy users (Group I)	Light users (Group II)	Non-users (Group III)
Heavy users (Group I)	○	**	**
Light users (Group II)	0,578	○	**
Non users (Group III)	0,961	0,650	○

With a P-value lower than 0.05, the ANOVA analysis revealed no significant differences. The table reveals that the mean fractional anisotropy values of different groups in the right Temporal Pole Sup region were not significantly different in the same anatomical area.

➢ Heschl

Table 127: The statistical analysis results of the mean fractional anisotropy in the region of interest analysis technique in groups of heavy cannabis users, light users, and non-users, in the **left Heschl region.**

	Mean fractional anisotropy of ROI analysis P-Value Heschl region of the left hemisphere		
	Heavy users (Group I)	Light users (Group II)	Non-users (Group III)
Heavy users (Group I)	○	**	**
Light users (Group II)	0.989	○	**
Non users (Group III)	0.221	0.221	○

With a P-value lower than 0.05, the ANOVA analysis revealed no significant differences. The table reveals that the mean fractional anisotropy values of different groups in the left Heschl region were not significantly different in the same anatomical area.

Table 128: The statistical analysis results of the mean fractional anisotropy in the region of interest technique of analysis in groups of heavy cannabis users, light users, and non-users, in **the right Heschl region.**

	Mean fractional anisotropy of ROI analysis P-Value Heschl region of the right hemisphere		
	Heavy users (Group I)	Light users (Group II)	Non-users (Group III)
Heavy users (Group I)	○	**	**
Light users (Group II)	0.084	○	**
Non users (Group III)	0.312	0.053	○

With a P-value lower than 0.05, the ANOVA analysis revealed no significant differences. The table reveals that the mean fractional anisotropy values of different groups in the right Heschl region were not significantly different in the same anatomical area.

➢ **Temporal Mid**

Table 129: The statistical analysis results of the mean fractional anisotropy in the region of interest technique of analysis in groups of heavy cannabis users, light users, and non-users, in the **left Temporal Mid region.**

	Mean fractional anisotropy of ROI analysis P-Value Temporal Mid region of the left hemisphere		
	Heavy users (Group I)	Light users (Group II)	Non-users (Group III)
Heavy users (Group I)	○	**	**
Light users (Group II)	0,949	○	**
Non users (Group III)	0,001	0,049	○

With a P-value lower than 0.05, the ANOVA analysis revealed significant differences between heavy users and non-users groups and between light users and non-users groups, but no significant difference between heavy and light users' groups. The table reveals that in the same anatomical area, the mean fractional anisotropy values of different groups in the left Temporal Mid region were significantly different among two from three comparisons realized.

Table 130: The statistical analysis results of the mean fractional anisotropy in the region of interest analysis technique in groups of heavy cannabis users, light users, and non-users, in the **right Temporal Mid region.**

	Mean fractional anisotropy of ROI analysis P-Value Temporal Mid region of the right hemisphere		
	Heavy users (Group I)	Light users (Group II)	Non-users (Group III)
Heavy users (Group I)	○	**	**
Light users (Group II)	0,446	○	**
Non users (Group III)	0,034	0,021	○

With a P-value lower than 0.05, the ANOVA analysis revealed significant differences between heavy users and non-users groups and between light users and non-users groups, but no significant difference between heavy and light users' groups. The table reveals that in the same anatomical area, the mean fractional anisotropy values of different groups in the right Temporal Mid region were significantly different among two from three comparisons realized.

➢ **Temporal Pole Mid**

Table 131: The statistical analysis results of the mean fractional anisotropy in the region of interest analysis technique in groups of heavy cannabis users, light users, and non-users, in the **left Temporal Pole Mid region**.

	Mean fractional anisotropy of ROI analysis P-Value Temporal Pole Mid region of the left hemisphere		
	Heavy users (Group I)	Light users (Group II)	Non-users (Group III)
Heavy users (Group I)	○	**	**
Light users (Group II)	0.891	○	**
Non users (Group III)	0.525	0.318	○

With a P-value lower than 0.05, the ANOVA analysis revealed no significant differences. The table reveals that the mean fractional anisotropy values of different groups in the left Temporal Pole Mid region were not significantly different in the same anatomical area.

Table 132: The statistical analysis results of the mean fractional anisotropy in the region of interest analysis technique in groups of heavy cannabis users, light users, and non-users, in **the right Temporal Pole Mid region**.

	Mean fractional anisotropy of ROI analysis P-Value Temporal Pole Mid region of the right hemisphere		
	Heavy users (Group I)	Light users (Group II)	Non-users (Group III)
Heavy users (Group I)	○	**	**
Light users (Group II)	0.520	○	**
Non users (Group III)	0.502	0.290	○

With a P-value lower than 0.05, the ANOVA analysis revealed no significant differences. The table reveals that the mean fractional anisotropy values of different groups in the right Temporal Pole Mid region were not significantly different in the same anatomical area.

➢ **Temporal Inf**

Table 133: The statistical analysis results of the mean fractional anisotropy in the region of interest technique of analysis in groups of heavy cannabis users, light users, and non-users, in the **left Temporal Inf region.**

	Mean fractional anisotropy of ROI analysis P-Value Temporal Inf region of the left hemisphere		
	Heavy users (Group I)	Light users (Group II)	Non-users (Group III)
Heavy users (Group I)	○	**	**
Light users (Group II)	0.800	○	**
Non users (Group III)	0.145	0.345	○

With a P-value lower than 0.05, the ANOVA analysis revealed no significant differences. The table reveals that the mean fractional anisotropy values of different groups in the left Temporal Inf region were not significantly different in the same anatomical area.

Table 134: The statistical analysis results of the mean fractional anisotropy in the region of interest technique of analysis in groups of heavy cannabis users, light users, and non-users, in **the right Temporal Inf region.**

	Mean fractional anisotropy of ROI analysis P-Value Temporal Inf region of the right hemisphere		
	Heavy users (Group I)	Light users (Group II)	Non-users (Group III)
Heavy users (Group I)	○	**	**
Light users (Group II)	0.515	○	**
Non users (Group III)	0.152	0.081	○

With a P-value lower than 0.05, the ANOVA analysis revealed no significant differences. The table reveals that the mean fractional anisotropy values of different groups in the right Temporal Inf region were not significantly different in the same anatomical area.

➢ **Fusiform**

Table 135: The statistical analysis results of the mean fractional anisotropy in the region of interest technique of analysis in groups of heavy cannabis users, light users, and non-users, in the **left Fusiform region.**

	Mean fractional anisotropy of ROI analysis P-Value Fusiform region of the left hemisphere		
	Heavy users (Group I)	Light users (Group II)	Non-users (Group III)
Heavy users (Group I)	○	**	**
Light users (Group II)	0.379	○	**
Non users (Group III)	0.490	0.229	○

With a P-value lower than 0.05, the ANOVA analysis revealed no significant differences. The table reveals that the mean fractional anisotropy values of different groups in the left Fusiform region were not significantly different in the same anatomical area.

Table 136: The statistical analysis results of the mean fractional anisotropy in the region of interest technique of analysis in groups of heavy cannabis users, light users, and non-users, in **the right Fusiform region.**

	Mean fractional anisotropy of ROI analysis P-Value Fusiform region of the right hemisphere		
	Heavy users (Group I)	Light users (Group II)	Non-users (Group III)
Heavy users (Group I)	○	**	**
Light users (Group II)	0.416	○	**
Non users (Group III)	0.875	0.425	○

With a P-value lower than 0.05, the ANOVA analysis revealed no significant differences. The table reveals that the mean fractional anisotropy values of different groups in the right Fusiform region were not significantly different in the same anatomical area.

➢ **Cingulum Ant**

Table 137: The statistical analysis results of the mean fractional anisotropy in the region of interest analysis technique in groups of heavy cannabis users, light users, and non-users in the **left Cingulum Ant region.**

	Mean fractional anisotropy of ROI analysis P-Value Cingulum Ant region of the left hemisphere		
	Heavy users (Group I)	Light users (Group II)	Non-users (Group III)
Heavy users (Group I)	○	**	**
Light users (Group II)	0,312	○	**
Non users (Group III)	0,022	0,276	○

With a P-value lower than 0.05, the ANOVA analysis revealed significant differences between heavy users and non-users groups, but no significant difference between heavy and light users' groups and between light users and non-users groups. The table reveals that in the same anatomical area, the mean fractional anisotropy values of different groups in the left Cingulum Ant region were significantly different among one from three comparisons realized.

Table 138: The statistical analysis results of the mean fractional anisotropy in the region of interest analysis technique in groups of heavy cannabis users, light users, and non-users in **the right Cingulum Ant region.**

	Mean fractional anisotropy of ROI analysis P-Value Cingulum Ant region of the right hemisphere		
	Heavy users (Group I)	Light users (Group II)	Non-users (Group III)
Heavy users (Group I)	○	**	**
Light users (Group II)	0,279	○	**
Non users (Group III)	0,032	0,165	○

With a P-value lower than 0.05, the ANOVA analysis revealed significant differences between heavy users and non-users groups, but no significant difference between heavy and light users' groups and between light users and non-users groups. The table reveals that in the same anatomical area, the mean fractional anisotropy values of different groups in the right Cingulum Ant region were significantly different among one from three comparisons realized.

➢ **Cingulum Mid**

Table 139: The statistical analysis results of the mean fractional anisotropy in the region of interest analysis technique in groups of heavy cannabis users, light users, and non-users, in the **left Cingulum Mid region.**

	Mean fractional anisotropy of ROI analysis P-Value Cingulum Mid region of the left hemisphere		
	Heavy users (Group I)	Light users (Group II)	Non-users (Group III)
Heavy users (Group I)	○	**	**
Light users (Group II)	0,658	○	**
Non users (Group III)	0,010	0,014	○

With a P-value lower than 0.05, the ANOVA analysis revealed significant differences between heavy users and non-users groups and between light users and non-users groups, but no significant difference between heavy and light users' groups. The table reveals that in the same anatomical area, the mean fractional anisotropy values of different groups in the left Cingulum Mid region were significantly different among two from three comparisons realized.

Table 140: The statistical analysis results of the mean fractional anisotropy in the region of interest analysis technique in groups of heavy cannabis users, light users, and non-users, in **the right Cingulum Mid region.**

	Mean fractional anisotropy of ROI analysis P-Value Cingulum Mid region of the right hemisphere		
	Heavy users (Group I)	Light users (Group II)	Non-users (Group III)
Heavy users (Group I)	○	**	**
Light users (Group II)	0,538	○	**
Non users (Group III)	0,032	0,104	○

With a P-value lower than 0.05, the ANOVA analysis revealed significant differences between heavy users and non-users groups, but no significant difference between heavy and light users' groups and between light users and non-users groups. The table reveals that in the same anatomical area, the mean fractional anisotropy values of different groups in the right Cingulum Mid region were significantly different among one from three comparisons realized.

➢ **Cingulum Post**

Table 141: The statistical analysis results of the mean fractional anisotropy in the region of interest analysis technique in groups of heavy cannabis users, light users, and non-users in the **left Cingulum Post region**.

	Mean fractional anisotropy of ROI analysis P-Value Cingulum Post region of the left hemisphere		
	Heavy users (Group I)	**Light users (Group II)**	**Non-users (Group III)**
Heavy users (Group I)	○	**	**
Light users (Group II)	0.889	○	**
Non users (Group III)	0.420	0.450	○

With a P-value lower than 0.05, the ANOVA analysis revealed no significant differences. The table reveals that groups' mean fractional anisotropy values in the left Cingulum Post region were not significantly different in the same anatomical area.

Table 142: The statistical analysis results of the mean fractional anisotropy in the region of interest analysis technique in groups of heavy cannabis users, light users, and non-users in **the right Cingulum Post region.**

	Mean fractional anisotropy of ROI analysis P-Value Cingulum Post region of the right hemisphere		
	Heavy users (Group I)	**Light users (Group II)**	**Non-users (Group III)**
Heavy users (Group I)	○	**	**
Light users (Group II)	0.524	○	**
Non users (Group III)	0.715	0.830	○

With a P-value lower than 0.05, the ANOVA analysis revealed no significant differences. The table reveals that groups' mean fractional anisotropy values in the right Cingulum Post region were not significantly different in the same anatomical area.

- **ParaHippocampal**

Table 143: The statistical analysis results of the mean fractional anisotropy in the region of interest technique of analysis in groups of heavy cannabis users, light users, and non-users, in the **left ParaHippocampal region.**

	Mean fractional anisotropy of ROI analysis P-Value ParaHippocampal region of the left hemisphere		
	Heavy users (Group I)	Light users (Group II)	Non-users (Group III)
Heavy users (Group I)	○	**	**
Light users (Group II)	0.214	○	**
Non users (Group III)	0.490	0.101	○

With a P-value lower than 0.05, the ANOVA analysis revealed no significant differences. The table reveals that the mean fractional anisotropy values of different groups in the left ParaHippocampal region were not significantly different in the same anatomical area.

Table 144: The statistical analysis results of the mean fractional anisotropy in the region of interest technique of analysis in groups of heavy cannabis users, light users, and non-users, in **the right ParaHippocampal region.**

	Mean fractional anisotropy of ROI analysis P-Value ParaHippocampal region of the right hemisphere		
	Heavy users (Group I)	Light users (Group II)	Non-users (Group III)
Heavy users (Group I)	○	**	**
Light users (Group II)	0.387	○	**
Non users (Group III)	0.872	0.330	○

With a P-value lower than 0.05, the ANOVA analysis revealed no significant differences. The table reveals that the mean fractional anisotropy values of different groups in the right ParaHippocampal region were not significantly different in the same anatomical area.

➢ **Hippocampus**

Table 145: The statistical analysis results of the mean fractional anisotropy in the region of interest technique of analysis in groups of heavy cannabis users, light users, and non-users, in the **left Hippocampus region.**

	Mean fractional anisotropy of ROI analysis P-Value Hippocampus region of the left hemisphere		
	Heavy users (Group I)	**Light users (Group II)**	**Non-users (Group III)**
Heavy users (Group I)	○	**	**
Light users (Group II)	0.304	○	**
Non users (Group III)	0.875	0.560	○

With a P-value lower than 0.05, the ANOVA analysis revealed no significant differences. The table reveals that the mean fractional anisotropy values of different groups in the left Hippocampus region were not significantly different in the same anatomical area.

Table 146: The statistical analysis results of the mean fractional anisotropy in the region of interest technique of analysis in groups of heavy cannabis users, light users, and non-users, in **the right Hippocampus region.**

	Mean fractional anisotropy of ROI analysis P-Value Hippocampus region of the right hemisphere		
	Heavy users (Group I)	**Light users (Group II)**	**Non-users (Group III)**
Heavy users (Group I)	○	**	**
Light users (Group II)	0.141	○	**
Non users (Group III)	0.145	0.978	○

With a P-value lower than 0.05, the ANOVA analysis revealed no significant differences. The table reveals that the mean fractional anisotropy values of different groups in the right Hippocampus region were not significantly different in the same anatomical area.

➢ **Insula**

Table 147: The results of statistical analysis of the mean fractional anisotropy in the region of interest technique of analysis in groups of heavy cannabis users, light users, and non-users, in the **left Insula region.**

	Mean fractional anisotropy of ROI analysis P-Value Insula region of the left hemisphere		
	Heavy users (Group I)	Light users (Group II)	Non-users (Group III)
Heavy users (Group I)	○	**	**
Light users (Group II)	0,684	○	**
Non users (Group III)	0,042	0,074	○

With a P-value lower than 0.05, the ANOVA analysis revealed significant differences between heavy users and non-users groups, but no significant difference between heavy and light users' groups and between light users and non-users groups. The table reveals that in the same anatomical area, the mean fractional anisotropy values of different groups in the left Insula region were significantly different among one from three comparisons realized.

Table 148: The statistical analysis results of the mean fractional anisotropy in the region of interest technique of analysis in groups of heavy cannabis users, light users, and non-users, in **the right Insula region.**

	Mean fractional anisotropy of ROI analysis P-Value Insula region of the right hemisphere		
	Heavy users (Group I)	Light users (Group II)	Non-users (Group III)
Heavy users (Group I)	○	**	**
Light users (Group II)	0.376	○	**
Non users (Group III)	0.409	0.804	○

With a P-value lower than 0.05, the ANOVA analysis revealed no significant differences. The table reveals that the mean fractional anisotropy values of different groups in the right Insula region were not significantly different in the same anatomical area.

➢ **Amygdala:**

Table 148: The statistical analysis results of the mean fractional anisotropy in the region of interest technique of analysis in groups of heavy cannabis users, light users, and non-users, in the **left Amygdala region.**

	Mean fractional anisotropy of ROI analysis P-Value Amygdala region of the left hemisphere		
	Heavy users (Group I)	Light users (Group II)	Non-users (Group III)
Heavy users (Group I)	○	**	**
Light users (Group II)	0.723	○	**
Non users (Group III)	0.497	0.855	○

With a P-value lower than 0.05, the ANOVA analysis revealed no significant differences. The table reveals that the mean fractional anisotropy values of different groups in the left Amygdala region were not significantly different in the same anatomical area.

Table 149: The results of statistical analysis of the mean fractional anisotropy in the region of interest technique of analysis in groups of heavy cannabis users, light users, and non-users, in **the right Amygdala region.**

	Mean fractional anisotropy of ROI analysis P-Value Amygdala region of the right hemisphere		
	Heavy users (Group I)	Light users (Group II)	Non-users (Group III)
Heavy users (Group I)	○	**	**
Light users (Group II)	0.497	○	**
Non users (Group III)	0.244	0.649	○

With a P-value lower than 0.05, the ANOVA analysis revealed no significant differences. The table reveals that in the same anatomical area, the mean fractional anisotropy values of different groups in the right Amygdala region were not significantly different.

➢ **Thalamus**

Table 150: The statistical analysis results of the mean fractional anisotropy in the region of interest technique of analysis in groups of heavy cannabis users, light users, and non-users, in the **left Thalamus region.**

	Mean fractional anisotropy of ROI analysis P-Value Thalamus region of the left hemisphere		
	Heavy users (Group I)	Light users (Group II)	Non-users (Group III)
Heavy users (Group I)	○	**	**
Light users (Group II)	0.506	○	**
Non users (Group III)	0.466	0.327	○

With a P-value lower than 0.05, the ANOVA analysis revealed no significant differences. The table reveals that in the same anatomical area, the mean fractional anisotropy values of different groups in the left Thalamus region were not significantly different.

Table 151: The statistical analysis results of the mean fractional anisotropy in the region of interest technique of analysis in groups of heavy cannabis users, light users, and non-users, in **the right Thalamus region.**

	Mean fractional anisotropy of ROI analysis P-Value Thalamus region of the right hemisphere		
	Heavy users (Group I)	Light users (Group II)	Non-users (Group III)
Heavy users (Group I)	○	**	**
Light users (Group II)	0.440	○	**
Non users (Group III)	0.299	0.219	○

With a P-value lower than 0.05, the ANOVA analysis revealed no significant differences. The table reveals that in the same anatomical area, the mean fractional anisotropy values of different groups in the right Thalamus region were not significantly different.

➢ **Caudate**

Table 152: The statistical analysis results of the mean fractional anisotropy in the region of interest technique of analysis in groups of heavy cannabis users, light users, and non-users, in the **left Caudate region.**

	Mean fractional anisotropy of ROI analysis P-Value Caudate region of the left hemisphere		
	Heavy users (Group I)	Light users (Group II)	Non-users (Group III)
Heavy users (Group I)	○	**	**
Light users (Group II)	0.674	○	**
Non users (Group III)	0.989	0.718	○

With a P-value lower than 0.05, the ANOVA analysis revealed no significant differences. The table reveals that in the same anatomical area, the mean fractional anisotropy values of different groups in the left Caudate region were not significantly different.

Table 153: The statistical analysis results of the mean fractional anisotropy in the region of interest technique of analysis in groups of heavy cannabis users, light users, and non-users, in **the right Caudate region.**

	Mean fractional anisotropy of ROI analysis P-Value Caudate region of the right hemisphere		
	Heavy users (Group I)	Light users (Group II)	Non-users (Group III)
Heavy users (Group I)	○	**	**
Light users (Group II)	0.779	○	**
Non users (Group III)	0.574	0.571	○

With a P-value lower than 0.05, the ANOVA analysis revealed no significant differences. The table reveals that in the same anatomical area, the mean fractional anisotropy values of different groups in the right Caudate region were not significantly different.

➢ **Putamen:**

Table 154: The statistical analysis results of the mean fractional anisotropy in the region of interest technique of analysis in groups of heavy cannabis users, light users, and non-users, in the **left Putamen region.**

	Mean fractional anisotropy of ROI analysis P-Value Putamen region of the left hemisphere		
	Heavy users (Group I)	Light users (Group II)	Non-users (Group III)
Heavy users (Group I)	○	**	**
Light users (Group II)	0.508	○	**
Non users (Group III)	0.947	0.414	○

With a P-value lower than 0.05, the ANOVA analysis revealed no significant differences. The table reveals that in the same anatomical area, the mean fractional anisotropy values of different groups in the left Putamen region were not significantly different.

Table 155: The statistical analysis results of the mean fractional anisotropy in the region of interest technique of analysis in groups of heavy cannabis users, light users, and non-users, in **the right Putamen region.**

	Mean fractional anisotropy of ROI analysis P-Value Putamen region of the right hemisphere		
	Heavy users (Group I)	Light users (Group II)	Non-users (Group III)
Heavy users (Group I)	○	**	**
Light users (Group II)	0.433	○	**
Non users (Group III)	0.913	0.434	○

With a P-value lower than 0.05, the ANOVA analysis revealed no significant differences. The table reveals that in the same anatomical area, the mean fractional anisotropy values of different groups in the right Putamen region were not significantly different.

➢ **Pallidum**

Table 156: The statistical analysis results of the mean fractional anisotropy in the region of interest analysis technique in groups of heavy cannabis users, light users, and non-users, in the **left Pallidum region.**

	Mean fractional anisotropy of ROI analysis P-Value Pallidum region of the left hemisphere		
	Heavy users (Group I)	Light users (Group II)	Non-users (Group III)
Heavy users (Group I)	○	**	**
Light users (Group II)	0.623	○	**
Non users (Group III)	0.248	0.085	○

With a P-value lower than 0.05, the ANOVA analysis revealed no significant differences. The table reveals that in the same anatomical area, the mean fractional anisotropy values of different groups in the left Pallidum region were not significantly different.

Table 157: The statistical analysis results of the mean fractional anisotropy in the region of interest technique of analysis in groups of heavy cannabis users, light users, and non-users, in **the right Pallidum region.**

	Mean fractional anisotropy of ROI analysis P-Value Pallidum region of the right hemisphere		
	Heavy users (Group I)	Light users (Group II)	Non-users (Group III)
Heavy users (Group I)	○	**	**
Light users (Group II)	0.850	○	**
Non users (Group III)	0.506	0.602	○

With a P-value lower than 0.05, the ANOVA analysis revealed no significant differences. The table reveals that in the same anatomical area, the mean fractional anisotropy values of different groups in the right Pallidum region were not significantly different.

➢ **Nucleus Accumbens**

Table 158: The results of statistical analysis of the mean fractional anisotropy in the region of interest technique of analysis in groups of heavy cannabis users, light users, and non-users, in the **left Nucleus Accumbens region.**

	Mean fractional anisotropy of ROI analysis P-Value Nucleus Accumbens region of the left hemisphere		
	Heavy users (Group I)	Light users (Group II)	Non-users (Group III)
Heavy users (Group I)	○	**	**
Light users (Group II)	0.894	○	**
Non users (Group III)	0.916	0.975	○

With a P-value lower than 0.05, the ANOVA analysis revealed no significant differences. The table reveals that in the same anatomical area, the mean fractional anisotropy values of different groups in the left Nucleus Accumbens region were not significantly different.

Table 159: The statistical analysis results of the mean fractional anisotropy in the region of interest analysis technique in groups of heavy cannabis users, light users, and non-users, in **the right Nucleus Accumbens region.**

	Mean fractional anisotropy of ROI analysis P-Value Nucleus Accumbens region of the right hemisphere		
	Heavy users (Group I)	Light users (Group II)	Non-users (Group III)
Heavy users (Group I)	○	**	**
Light users (Group II)	0.399	○	**
Non users (Group III)	0.552	0.788	○

With a P-value lower than 0.05, the ANOVA analysis revealed no significant differences. The table reveals that in the same anatomical area, the mean fractional anisotropy values of different groups in the right Nucleus Accumbens region were not significantly different.

2. Mean diffusivity (MD) analysis of Variance (ANOVA) results

a. Summary of all the analytical findings

For mean diffusivity (MD), in the 72 regions examined, 432 analyses of variance were conducted (between the three groups and in both hemispheres).

The analysis of Variance (ANOVA) results revealed only 5 statistically significant results (with p-value <0.05), which is equivalent to only 1.15 % of the total conducted the analysis.

Table 160 summarizes the region with the corresponding groups compared where the statistical analysis is significant.

Table 160: A table containing regions of interest revealing statistically significant results of mean diffusivity within the three groups (heavy and light users and control group).

Regions of interest	Groups compared
Right Frontal Sup	Light users Vs. Non-users
Right Frontal Inf Tri	Light users Vs. Non-users
Right Angular	Light users Vs. Non-users
Left Temporal Pole Mid	Heavy users Vs. Non-users Light users Vs. Non-users
Right Nucleus Accumbens	Light users Vs. Non-users

b. The analytical findings in each region of interest and between each of the groups studied

We present the mean diffusivity (MD) statistical analysis findings by two tables for each region of interest and in both hemispheres. The first table represents statistical results in the left regions and the second in the right regions.

➢ **Frontal Med Orb**

Table 161: The statistical analysis results of the mean diffusivity in the region of interest technique of analysis in groups of heavy cannabis users, light users, and non-users, in **the left Frontal Med Orb region.**

	Mean diffusivity of ROI analysis P-Value -Frontal Med Orb region of the left hemisphere-		
	Heavy users (Group I)	**Light users (Group II)**	**Non-users (Group III)**
Heavy users (Group I)	○	**	**
Light users (Group II)	0.963	○	**
Non users (Group III)	0.186	0.210	○

With a P-value lower than 0.05, the ANOVA analysis revealed no significant differences. The table reveals that in the same anatomical area, the mean diffusivity values of different groups in the left Frontal Med Orb region were not significantly different.

Table 162: The statistical analysis results of the mean Apparent Diffusion Coefficient in the region of interest technique of analysis in groups of heavy cannabis users, light users, and non-users, in **the right Frontal Med Orb region.**

	Mean diffusivity of ROI analysis P-Value -Frontal Med Orb region of the right hemisphere-		
	Heavy users (Group I)	**Light users (Group II)**	**Non-users (Group III)**
Heavy users (Group I)	○	**	**
Light users (Group II)	0.682	○	**
Non users (Group III)	0.920	0.658	○

With a P-value lower than 0.05, the ANOVA analysis revealed no significant differences. The table reveals that mean diffusivity values of different groups in the right Frontal Med Orb region were not significantly different in the same anatomical area.

➢ **Frontal Sup Orb**

Table 163: The statistical analysis results of the mean diffusivity in the region of interest technique of analysis in groups of heavy cannabis users, light users, and non-users, in **the left Frontal Sup Orb region.**

	Mean diffusivity of ROI analysis P-Value – Frontal Sup Orb region of the left hemisphere –		
	Heavy users (Group I)	**Light users (Group II)**	**Non-users (Group III)**
Heavy users (Group I)	○	**	**
Light users (Group II)	0.932	○	**
Non users (Group III)	0.923	0.866	○

With a P-value lower than 0.05, the ANOVA analysis revealed no significant differences. The table reveals that in the same anatomical area, the mean diffusivity values of different groups in the left Frontal Sup Orb region were not significantly different.

Table 164: The statistical analysis results of the mean diffusivity in the region of interest analysis technique in groups of heavy cannabis users, light users, and non-users, in the right Frontal Sup Orb region.

	Mean diffusivity of ROI analysis P-Value Frontal Sup Orb region of the right hemisphere		
	Heavy users (Group I)	**Light users (Group II)**	**Non-users (Group III)**
Heavy users (Group I)	○	**	**
Light users (Group II)	0.722	○	**
Non users (Group III)	0.472	0.222	○

With a P-value lower than 0.05, the ANOVA analysis revealed no significant differences. The table reveals that in the same anatomical area, the mean diffusivity values of different groups in the right Frontal Sup Orb region were not significantly different.

➢ **Frontal Mid Orb**

Table 165: The statistical analysis results of the mean diffusivity in the region of interest technique of analysis in groups of heavy cannabis users, light users, and non-users, in the **left Frontal Mid Orb region.**

	Mean diffusivity ROI analysis P-Value – Frontal Mid Orb region of the left hemisphere –		
	Heavy users (Group I)	Light users (Group II)	Non-users (Group III)
Heavy users (Group I)	○	**	**
Light users (Group II)	0.350	○	**
Non users (Group III)	0.756	0.315	○

With a P-value lower than 0.05, the ANOVA analysis revealed no significant differences. The table reveals that in the same anatomical area, the mean diffusivity values of different groups in the left Frontal Mid Orb region were not significantly different.

Table 166: The statistical analysis results of the mean diffusivity in the region of interest analysis technique in groups of heavy cannabis users, light users, and non-users, in **the right Frontal Mid Orb region.**

	Mean diffusivity of ROI analysis P-Value – Frontal Mid Orb region of the right hemisphere –		
	Heavy users (Group I)	Light users (Group II)	Non-users (Group III)
Heavy users (Group I)	○	**	**
Light users (Group II)	0.750	○	**
Non users (Group III)	0.391	0.317	○

With a P-value lower than 0.05, the ANOVA analysis revealed no significant differences. The table reveals that in the same anatomical area, the mean diffusivity values of different groups in the right Frontal Mid Orb region were not significantly different.

➢ **Frontal Inf Orb**

Table 167: The results of statistical analysis of the mean diffusivity in the region of interest technique of analysis in groups of heavy cannabis users, light users, and non-users, in the **left Frontal Inf Orb region.**

	Mean diffusivity of ROI analysis P-Value – Frontal Inf Orb region of the left hemisphere –		
	Heavy users (Group I)	Light users (Group II)	Non-users (Group III)
Heavy users (Group I)	○	**	**
Light users (Group II)	0.849	○	**
Non users (Group III)	0.463	0.380	○

With a P-value lower than 0.05, the ANOVA analysis revealed no significant differences. The table reveals that in the same anatomical area, the mean diffusivity values of different groups in the left Frontal Inf Orb region were not significantly different.

Table 168: The statistical analysis results of the mean diffusivity in the region of interest technique of analysis in groups of heavy cannabis users, light users, and non-users, in **the right Frontal Inf Orb region.**

	Mean diffusivity of ROI analysis P-Value – Frontal Inf Orb region of the right hemisphere –		
	Heavy users (Group I)	Light users (Group II)	Non-users (Group III)
Heavy users (Group I)	○	**	**
Light users (Group II)	0.504	○	**
Non users (Group III)	0.641	0.907	○

With a P-value lower than 0.05, the ANOVA analysis revealed no significant differences. The table reveals that in the same anatomical area, the mean diffusivity values of different groups in the right Frontal Inf Orb region were not significantly different.

➢ **Rectus**

Table 169: The statistical analysis results of the mean diffusivity in the region of interest analysis technique in groups of heavy cannabis users, light users, and non-users, in the **left Rectus region.**

	Mean diffusivity of ROI analysis P-Value – Rectus region of the left hemisphere –		
	Heavy users (Group I)	**Light users (Group II)**	**Non-users (Group III)**
Heavy users (Group I)	○	**	**
Light users (Group II)	0.177	○	**
Non users (Group III)	0.586	0.273	○

With a P-value lower than 0.05, the ANOVA analysis revealed no significant differences. The table reveals that in the same anatomical area, the mean diffusivity values of different groups in the left Rectus region were not significantly different.

Table 170: The statistical analysis results of the Mean fractional anisotropy in the region of interest technique of analysis in groups of heavy cannabis users, light users, and non-users, in **the right Rectus region.**

	Mean diffusivity of ROI analysis P-Value – Rectus region of the right hemisphere –		
	Heavy users (Group I)	**Light users (Group II)**	**Non-users (Group III)**
Heavy users (Group I)	○	**	**
Light users (Group II)	0.530	○	**
Non users (Group III)	0.767	0.979	○

With a P-value lower than 0.05, the ANOVA analysis revealed no significant differences. The table reveals that in the same anatomical area, the mean diffusivity values of different groups in the right Rectus region were not significantly different.

➢ Olfactory

Table 171: The statistical analysis results of the mean diffusivity in the region of interest analysis technique in groups of heavy cannabis users, light users, and non-users, in the **left Olfactory region.**

	Mean diffusivity of ROI analysis P-Value – Olfactory region of the left hemisphere –		
	Heavy users (Group I)	Light users (Group II)	Non-users (Group III)
Heavy users (Group I)	○	**	**
Light users (Group II)	0.984	○	**
Non users (Group III)	0.452	0.478	○

With a P-value lower than 0.05, the ANOVA analysis revealed no significant differences. The table reveals that in the same anatomical area, the mean diffusivity values of different groups in the left Olfactory region were not significantly different.

Table 172: The statistical analysis results of the mean diffusivity in the region of interest analysis technique in groups of heavy cannabis users, light users, and non-users, in **the right Olfactory region.**

	Mean diffusivity of ROI analysis P-Value – Olfactory region of the right hemisphere –		
	Heavy users (Group I)	Light users (Group II)	Non-users (Group III)
Heavy users (Group I)	○	**	**
Light users (Group II)	0.267	○	**
Non users (Group III)	0.190	0.666	○

With a P-value lower than 0.05, the ANOVA analysis revealed no significant differences. The table reveals that in the same anatomical area, the mean diffusivity values of different groups in the right Olfactory region were not significantly different.

➢ **Frontal Sup Medial**

Table 173: The statistical analysis results of the mean diffusivity in the region of interest technique of analysis in groups of heavy cannabis users, light users, and non-users, in the **left Frontal Sup Medial region.**

	Mean diffusivity of ROI analysis P-Value Frontal Sup Medial region of the left hemisphere		
	Heavy users (Group I)	Light users (Group II)	Non-users (Group III)
Heavy users (Group I)	○	**	**
Light users (Group II)	0.424	○	**
Non users (Group III)	0.503	0.901	○

With a P-value lower than 0.05, the ANOVA analysis revealed no significant differences. The table reveals that in the same anatomical area, the mean diffusivity values of different groups in the left Frontal Sup Medial region were not significantly different.

Table 174: The statistical analysis results of the mean diffusivity in the region of interest technique of analysis in groups of heavy cannabis users, light users, and non-users, in **the right Frontal Sup Medial region.**

	Mean diffusivity of ROI analysis P-Value Frontal Sup Medial region of the right hemisphere		
	Heavy users (Group I)	Light users (Group II)	Non-users (Group III)
Heavy users (Group I)	○	**	**
Light users (Group II)	0.995	○	**
Non users (Group III)	0.385	0.475	○

With a P-value lower than 0.05, the ANOVA analysis revealed no significant differences. The table reveals that in the same anatomical area, the mean diffusivity values of different groups in the right Frontal Sup Medial region were not significantly different.

➢ **Frontal Sup**

Table 175: The statistical analysis results of the mean diffusivity in the region of interest technique of analysis in groups of heavy cannabis users, light users, and non-users, in the **left Frontal Sup region.**

	Mean diffusivity of ROI analysis P-Value Frontal Sup region of the left hemisphere		
	Heavy users (Group I)	**Light users (Group II)**	**Non-users (Group III)**
Heavy users (Group I)	○	**	**
Light users (Group II)	0.208	○	**
Non users (Group III)	0.686	0.520	○

With a P-value lower than 0.05, the ANOVA analysis revealed no significant differences. The table reveals that in the same anatomical area, the mean diffusivity values of different groups in the left Frontal Sup region were not significantly different.

Table 176: The statistical analysis results of the mean diffusivity in the region of interest technique of analysis in groups of heavy cannabis users, light users, and non-users, in **the right Frontal Sup region.**

	Mean diffusivity of ROI analysis P-Value Frontal Sup region of the right hemisphere		
	Heavy users (Group I)	**Light users (Group II)**	**Non-users (Group III)**
Heavy users (Group I)	○	**	**
Light users (Group II)	0.162	○	**
Non users (Group III)	0.213	**0.049**	○

With a P-value lower than 0.05, the ANOVA analysis revealed significant differences between light users and non-users groups, but no significant difference between heavy and light users' groups and between heavy users and non-users groups. The table reveals that in the same anatomical area, the mean diffusivity values of different groups in the right Frontal Sup region were significantly different among one from three comparisons realized.

➢ **Frontal Mid**

Table 177: The statistical analysis results of the mean diffusivity in the region of interest analysis technique in groups of heavy cannabis users, light users, and non-users, in the **left Frontal Mid region.**

	Mean diffusivity of ROI analysis P-Value Frontal Mid region of the left hemisphere		
	Heavy users (Group I)	Light users (Group II)	Non-users (Group III)
Heavy users (Group I)	○	**	**
Light users (Group II)	0.368	○	**
Non users (Group III)	0.494	0.322	○

With a P-value lower than 0.05, the ANOVA analysis revealed no significant differences. The table reveals that in the same anatomical area, the mean diffusivity values of different groups in the left Frontal Mid region were not significantly different.

Table 178. The statistical analysis results of the mean diffusivity in the region of interest technique of analysis in groups of heavy cannabis users, light users, and non-users, in **the right Frontal Mid region.**

	Mean diffusivity of ROI analysis P-Value Frontal Mid region of the right hemisphere		
	Heavy users (Group I)	Light users (Group II)	Non-users (Group III)
Heavy users (Group I)	○	**	**
Light users (Group II)	0.465	○	**
Non users (Group III)	0.618	0.403	○

With a P-value lower than 0.05, the ANOVA analysis revealed no significant differences. The table reveals that in the same anatomical area, the mean diffusivity values of different groups in the right Frontal Mid region were not significantly different.

➢ Frontal Inf Oper

Table 179: The statistical analysis results of the mean diffusivity in the region of interest technique of analysis in groups of heavy cannabis users, light users, and non-users, in the **left Frontal Inf Oper region.**

	Mean diffusivity of ROI analysis P-Value Frontal Inf Oper region of the left hemisphere		
	Heavy users (Group I)	Light users (Group II)	Non-users (Group III)
Heavy users (Group I)	○	**	**
Light users (Group II)	0.702	○	**
Non users (Group III)	0.247	0.429	○

With a P-value lower than 0.05, the ANOVA analysis revealed no significant differences. The table reveals that in the same anatomical area, the mean diffusivity values of different groups in the left Frontal Inf Oper region were not significantly different.

Table 180: The statistical analysis results of the mean diffusivity in the region of interest analysis technique in groups of heavy cannabis users, light users, and non-users, in **the right Frontal Inf Oper region.**

	Mean diffusivity of ROI analysis P-Value Frontal Inf Oper region of the right hemisphere		
	Heavy users (Group I)	Light users (Group II)	Non-users (Group III)
Heavy users (Group I)	○	**	**
Light users (Group II)	0.618	○	**
Non users (Group III)	0.311	0.132	○

With a P-value lower than 0.05, the ANOVA analysis revealed no significant differences. The table reveals that in the same anatomical area, the mean diffusivity values of different groups in the right Frontal Inf Oper region were not significantly different.

➢ **Frontal Inf Tri**

Table 181: The statistical analysis results of the mean diffusivity in the region of interest analysis technique in groups of heavy cannabis users, light users, and non-users, in the **left Frontal Inf Tri region.**

	Mean diffusivity of ROI analysis P-Value Frontal Inf Tri region of the left hemisphere		
	Heavy users (Group I)	Light users (Group II)	Non-users (Group III)
Heavy users (Group I)	○	**	**
Light users (Group II)	0.460	○	**
Non users (Group III)	0.949	0.439	○

With a P-value lower than 0.05, the ANOVA analysis revealed no significant differences. The table reveals that in the same anatomical area, the mean diffusivity values of different groups in the left Frontal Inf Tri region were not significantly different.

Table 182: The statistical analysis results of the mean diffusivity in the region of interest analysis technique in groups of heavy cannabis users, light users, and non-users, in **the right Frontal Inf Tri region.**

	Mean diffusivity of ROI analysis P-Value Frontal Inf Tri region of the right hemisphere		
	Heavy users (Group I)	Light users (Group II)	Non-users (Group III)
Heavy users (Group I)	○	**	**
Light users (Group II)	0.254	○	**
Non users (Group III)	0.364	0.025	○

With a P-value lower than 0.05, the ANOVA analysis revealed significant differences between light users and non-users groups, but no significant difference between heavy and light users' groups and between heavy users and non-users groups. The table reveals that in the same anatomical area, the mean diffusivity values of different groups in the right Frontal Inf Tri region were significantly different among one from three comparisons realized.

➢ **Postcentral**

Table 183: The statistical analysis results of the mean diffusivity in the region of interest analysis technique in groups of heavy cannabis users, light users, and non-users, in the **left Postcentral region.**

	Mean diffusivity ROI analysis P-Value Postcentral region of the left hemisphere		
	Heavy users (Group I)	Light users (Group II)	Non-users (Group III)
Heavy users (Group I)	○	**	**
Light users (Group II)	0,408	○	**
Non users (Group III)	0,723	0,709	○

With a P-value lower than 0.05, the ANOVA analysis revealed no significant differences. The table reveals that in the same anatomical area, the mean diffusivity values of different groups in the **left Postcentral region** were not significantly different.

Table 184: The statistical analysis results of the mean diffusivity in the region of interest analysis technique in groups of heavy cannabis users, light users, and non-users, in **the right Postcentral region.**

	Mean diffusivity of ROI analysis P-Value Postcentral region of the right hemisphere		
	Heavy users (Group I)	Light users (Group II)	Non-users (Group III)
Heavy users (Group I)	○	**	**
Light users (Group II)	0,123	○	**
Non users (Group III)	0,666	0,089	○

With a P-value lower than 0.05, the ANOVA analysis revealed no significant differences. The table reveals that in the same anatomical area, the mean diffusivity values of different groups in the right Postcentral region were not significantly different.

➢ **Parietal Sup**

Table 185: The statistical analysis results of the mean diffusivity in the region of interest analysis technique in groups of heavy cannabis users, light users, and non-users, in the **left Parietal Sup region.**

	Mean diffusivity of ROI analysis P-Value Parietal Sup region of the left hemisphere		
	Heavy users (Group I)	Light users (Group II)	Non-users (Group III)
Heavy users (Group I)	○	**	**
Light users (Group II)	0,686	○	**
Non users (Group III)	0,401	0,734	○

With a P-value lower than 0.05, the ANOVA analysis revealed no significant differences. The table reveals that in the same anatomical area, the mean diffusivity values of different groups in the left Parietal Sup region were not significantly different.

Table 186: The statistical analysis results of the mean diffusivity in the region of interest analysis technique in groups of heavy cannabis users, light users, and non-users, in **the right Parietal Sup region.**

	Mean diffusivity of ROI analysis P-Value Parietal Sup region of the right hemisphere		
	Heavy users (Group I)	Light users (Group II)	Non-users (Group III)
Heavy users (Group I)	○	**	**
Light users (Group II)	0,862	○	**
Non users (Group III)	0,918	0,837	○

With a P-value lower than 0.05, the ANOVA analysis revealed no significant differences. The table reveals that in the same anatomical area, the mean diffusivity values of different groups in the right Parietal Sup region were not significantly different.

➢ SupraMarginal

Table 187: The statistical analysis results of the mean diffusivity in the region of interest analysis technique in groups of heavy cannabis users, light users, and non-users, in the **left SupraMarginal region.**

	Mean diffusivity of ROI analysis P-Value SupraMarginal region of the left hemisphere		
	Heavy users (Group I)	Light users (Group II)	Non-users (Group III)
Heavy users (Group I)	○	**	**
Light users (Group II)	0,208	○	**
Non users (Group III)	0,638	0,598	○

With a P-value lower than 0.05, the ANOVA analysis revealed no significant differences. The table reveals that in the same anatomical area, the mean diffusivity values of different groups in the left SupraMarginal region were not significantly different.

Table 188: The statistical analysis results of the mean diffusivity in the region of interest analysis technique in groups of heavy cannabis users, light users, and non-users, in **the right SupraMarginal region.**

	Mean diffusivity of ROI analysis P-Value SupraMarginal region of the right hemisphere		
	Heavy users (Group I)	Light users (Group II)	Non-users (Group III)
Heavy users (Group I)	○	**	**
Light users (Group II)	0,508	○	**
Non users (Group III)	0,306	0,124	○

With a P-value lower than 0.05, the ANOVA analysis revealed no significant differences. The table reveals that in the same anatomical area, the mean diffusivity values of different groups in the right SupraMarginal region were not significantly different.

➢ **Angular**

Table 189: The statistical analysis results of the mean diffusivity in the region of interest analysis technique in groups of heavy cannabis users, light users, and non-users, in the **left Angular region.**

	Mean diffusivity of ROI analysis P-Value Angular region of the left hemisphere		
	Heavy users (Group I)	Light users (Group II)	Non-users (Group III)
Heavy users (Group I)	○	**	**
Light users (Group II)	0,842	○	**
Non users (Group III)	0,284	0,176	○

With a P-value lower than 0.05, the ANOVA analysis revealed no significant differences. The table reveals that in the same anatomical area, the mean diffusivity values of different groups in the left Angular region were not significantly different.

Table 190: The statistical analysis results of the mean diffusivity in the region of interest analysis technique in groups of heavy cannabis users, light users, and non-users, in **the right Angular region.**

	Mean diffusivity of ROI analysis P-Value Angular region of the right hemisphere		
	Heavy users (Group I)	Light users (Group II)	Non-users (Group III)
Heavy users (Group I)	○	**	**
Light users (Group II)	0,793	○	**
Non users (Group III)	0,060	0,028	○

With a P-value lower than 0.05, the ANOVA analysis revealed significant differences between light users and non-users groups, but no significant difference between heavy and light users' groups and between heavy users and non-users groups. The table reveals that in the same anatomical area, the mean diffusivity values of different groups in the right Angular region were significantly different among one from three comparisons realized.

➢ **Parietal Inf**

Table 191. The statistical analysis results of the mean diffusivity in the region of interest technique of analysis in groups of heavy cannabis users, light users, and non-users, in the **left Parietal Inf region.**

	Mean diffusivity of ROI analysis P-Value Parietal Inf region of the left hemisphere		
	Heavy users (Group I)	Light users (Group II)	Non-users (Group III)
Heavy users (Group I)	○	**	**
Light users (Group II)	0,691	○	**
Non users (Group III)	0,769	0,988	○

With a P-value lower than 0.05, the ANOVA analysis revealed no significant differences. The table reveals that in the same anatomical area, the mean diffusivity values of different groups in the left Parietal Inf region were not significantly different.

Table 192: The statistical analysis results of the mean diffusivity in the region of interest analysis technique in groups of heavy cannabis users, light users, and non-users, in **the right Parietal Inf region.**

	Mean diffusivity of ROI analysis P-Value Parietal Inf region of the right hemisphere		
	Heavy users (Group I)	Light users (Group II)	Non-users (Group III)
Heavy users (Group I)	○	**	**
Light users (Group II)	0,454	○	**
Non users (Group III)	0,144	0,325	○

With a P-value lower than 0.05, the ANOVA analysis revealed no significant differences. The table reveals that in the same anatomical area, the mean diffusivity values of different groups in the right Parietal Inf region were not significantly different.

➢ **Precuneus**

Table 193: The statistical analysis results of the mean diffusivity in the region of interest technique of analysis in groups of heavy cannabis users, light users, and non-users, in the **left Precuneus region.**

	Mean diffusivity of ROI analysis P-Value Precuneus region of the left hemisphere		
	Heavy users (Group I)	Light users (Group II)	Non-users (Group III)
Heavy users (Group I)	○	**	**
Light users (Group II)	0,463	○	**
Non users (Group III)	0,670	0,697	○

With a P-value lower than 0.05, the ANOVA analysis revealed no significant differences. The table reveals that in the same anatomical area, the mean diffusivity values of different groups in the left Precuneus region were not significantly different.

Table 194: The statistical analysis results of the mean diffusivity in the region of interest technique of analysis in groups of heavy cannabis users, light users, and non-users, in **the right Precuneus region.**

	Mean diffusivity of ROI analysis P-Value Precuneus region of the right hemisphere		
	Heavy users (Group I)	Light users (Group II)	Non-users (Group III)
Heavy users (Group I)	○	**	**
Light users (Group II)	0,272	○	**
Non users (Group III)	0,374	0,677	○

With a P-value lower than 0.05, the ANOVA analysis revealed no significant differences. The table reveals that in the same anatomical area, the mean diffusivity values of different groups in the right Precuneus region were not significantly different.

➢ Temporal Sup

Table 195: The statistical analysis results of the mean diffusivity in the region of interest technique analysis in groups of heavy cannabis users, light users, and non-users, in the **left Temporal Sup region.**

	Mean diffusivity of ROI analysis P-Value Temporal Sup region of the left hemisphere		
	Heavy users (Group I)	Light users (Group II)	Non-users (Group III)
Heavy users (Group I)	○	**	**
Light users (Group II)	0,104	○	**
Non users (Group III)	0,367	0,777	○

With a P-value lower than 0.05, the ANOVA analysis revealed no significant differences. The table reveals that in the same anatomical area, the mean diffusivity values of different groups in the left Temporal Sup region were not significantly different.

Table 196: The statistical analysis results of the mean diffusivity in the region of interest technique of analysis in groups of heavy cannabis users, light users, and non-users, in **the right Temporal Sup region.**

	Mean diffusivity of ROI analysis P-Value Temporal Sup region of the right hemisphere		
	Heavy users (Group I)	Light users (Group II)	Non-users (Group III)
Heavy users (Group I)	○	**	**
Light users (Group II)	0,248	○	**
Non users (Group III)	0,304	0,058	○

With a P-value lower than 0.05, the ANOVA analysis revealed no significant differences. The table reveals that in the same anatomical area, the mean diffusivity values of different groups in the right Temporal Sup region were not significantly different.

➢ **Temporal Pole Sup**

Table 197: The statistical analysis results of the mean diffusivity in the region of interest analysis technique in groups of heavy cannabis users, light users, and non-users, in the **left Temporal Pole Sup region.**

	Mean diffusivity of ROI analysis P-Value Temporal Pole Sup region of the left hemisphere		
	Heavy users (Group I)	Light users (Group II)	Non-users (Group III)
Heavy users (Group I)	○	**	**
Light users (Group II)	0,193	○	**
Non users (Group III)	0,398	0,890	○

With a P-value lower than 0.05, the ANOVA analysis revealed no significant differences. The table reveals that in the same anatomical area, the mean diffusivity values of different groups in the left Temporal Pole Sup region were not significantly different.

Table 198: The statistical analysis results of the mean diffusivity in the region of interest analysis technique in groups of heavy cannabis users, light users, and non-users, in **the right Temporal Pole Sup region.**

	Mean diffusivity of ROI analysis P-Value Temporal Pole Sup region of the right hemisphere		
	Heavy users (Group I)	Light users (Group II)	Non-users (Group III)
Heavy users (Group I)	○	**	**
Light users (Group II)	0,565	○	**
Non users (Group III)	0,578	0,842	○

With a P-value lower than 0.05, the ANOVA analysis revealed no significant differences. The table reveals that in the same anatomical area, the mean diffusivity values of different groups in the right Temporal Pole Sup region were not significantly different.

➢ Heschl

Table 199: The statistical analysis results of the mean diffusivity in the region of interest technique of analysis in groups of heavy cannabis users, light users, and non-users, in the **left Heschl region.**

	Mean diffusivity of ROI analysis P-Value Heschl region of the left hemisphere		
	Heavy users (Group I)	Light users (Group II)	Non-users (Group III)
Heavy users (Group I)	○	**	**
Light users (Group II)	0.396	○	**
Non users (Group III)	0.365	0.880	○

With a P-value lower than 0.05, the ANOVA analysis revealed no significant differences. The table indicates that in the same anatomical area, the mean diffusivity values of different groups in the left Heschl region were not significantly different.

Table 200: The statistical analysis results of the mean diffusivity in the region of interest analysis technique in groups of heavy cannabis users, light users, and non-users in **the right Heschl region.**

	Mean diffusivity of ROI analysis P-Value Heschl region of the right hemisphere		
	Heavy users (Group I)	Light users (Group II)	Non-users (Group III)
Heavy users (Group I)	○	**	**
Light users (Group II)	0.620	○	**
Non users (Group III)	0.970	0.556	○

With a P-value lower than 0.05, the ANOVA analysis revealed no significant differences. The table reveals that in the same anatomical area, the mean diffusivity values of different groups in the right Heschl region were not significantly different.

- **Temporal Mid**

Table 201: The statistical analysis results of the mean diffusivity in the region of interest technique of analysis in groups of heavy cannabis users, light users, and non-users, in the **left Temporal Mid region.**

	Mean diffusivity of ROI analysis P-Value Temporal Mid region of the left hemisphere		
	Heavy users (Group I)	Light users (Group II)	Non-users (Group III)
Heavy users (Group I)	○	**	**
Light users (Group II)	0.388	○	**
Non users (Group III)	0.701	0.635	○

With a P-value lower than 0.05, the ANOVA analysis revealed no significant differences. The table reveals that in the same anatomical area, the mean diffusivity values of different groups in the left Temporal Mid region were not significantly different.

Table 202: The statistical analysis results of the mean diffusivity in the region of interest analysis technique in groups of heavy cannabis users, light users, and non-users, in **the right Temporal Mid region.**

	Mean diffusivity of ROI analysis P-Value Temporal Mid region of the right hemisphere		
	Heavy users (Group I)	Light users (Group II)	Non-users (Group III)
Heavy users (Group I)	○	**	**
Light users (Group II)	0.334	○	**
Non users (Group III)	0.382	0.055	○

With a P-value lower than 0.05, the ANOVA analysis revealed no significant differences. The table reveals that in the same anatomical area, the mean diffusivity values of different groups in the right Temporal Mid region were not significantly different.

➢ **Temporal Pole Mid**

Table 203 : The statistical analysis results of the mean diffusivity t in the region of interest technique of analysis in groups of heavy cannabis users, light users, and non-users, in the **left Temporal Pole Mid region.**

	Mean diffusivity of ROI analysis P-Value Temporal Pole Mid region of the left hemisphere		
	Heavy users (Group I)	Light users (Group II)	Non-users (Group III)
Heavy users (Group I)	○	**	**
Light users (Group II)	0.599	○	**
Non users (Group III)	0.403	0.361	○

With a P-value lower than 0.05, the ANOVA analysis revealed no significant differences. The table reveals that in the same anatomical area, the mean diffusivity values of different groups in the left Temporal Pole Mid region were not significantly different.

Table 204: The statistical analysis results of the mean diffusivity in the region of interest technique of analysis in groups of heavy cannabis users, light users, and non-users, in **the right Temporal Pole Mid region.**

	Mean diffusivity of ROI analysis P-Value Temporal Pole Mid region of the right hemisphere		
	Heavy users (Group I)	Light users (Group II)	Non-users (Group III)
Heavy users (Group I)	○	**	**
Light users (Group II)	0.120	○	**
Non users (Group III)	0.040	0.012	○

With a P-value lower than 0.05, the ANOVA analysis revealed significant differences between heavy users and non-users groups and between light users and non-users groups, but no significant difference between heavy and light users' groups. The table reveals that in the same anatomical area, the mean diffusivity values of different groups in the right Temporal Pole Mid region were significantly different among two groups from three comparisons realized.

➢ **Temporal Inf**

Table 205: The statistical analysis results of the mean diffusivity in the region of interest technique of analysis in groups of heavy cannabis users, light users, and non-users, in **the left Temporal Inf region.**

	Mean diffusivity of ROI analysis P-Value Temporal Inf region of the left hemisphere		
	Heavy users (Group I)	**Light users (Group II)**	**Non-users (Group III)**
Heavy users (Group I)	○	**	**
Light users (Group II)	0.226	○	**
Non users (Group III)	0.535	0.682	○

With a P-value lower than 0.05, the ANOVA analysis revealed no significant differences. The table shows that in the same anatomical area, the mean diffusivity values of different groups in the left Temporal Inf region were not significantly different.

Table 206: The statistical analysis results of the mean diffusivity in the region of interest technique of analysis in groups of heavy cannabis users, light users, and non-users, in **the right Temporal Inf region.**

	Mean diffusivity of ROI analysis P-Value Temporal Inf region of the right hemisphere		
	Heavy users (Group I)	**Light users (Group II)**	**Non-users (Group III)**
Heavy users (Group I)	○	**	**
Light users (Group II)	0.643	○	**
Non users (Group III)	0.662	0.344	○

With a P-value lower than 0.05, the ANOVA analysis revealed no significant differences. The table reveals that in the same anatomical area, the mean diffusivity values of different groups in the right Temporal Inf region were not significantly different.

➢ **Fusiform**

Table 207: The statistical analysis results of the mean diffusivity in the region of interest technique of analysis in groups of heavy cannabis users, light users, and non-users, in the **left Fusiform region.**

	Mean diffusivity of ROI analysis P-Value Fusiform region of the left hemisphere		
	Heavy users (Group I)	Light users (Group II)	Non-users (Group III)
Heavy users (Group I)	○	**	**
Light users (Group II)	0.457	○	**
Non users (Group III)	0.589	0.211	○

With a P-value lower than 0.05, the ANOVA analysis revealed no significant differences. The table reveals that in the same anatomical area, the mean diffusivity values of different groups in the left Fusiform region were not significantly different.

Table 208: The statistical analysis results of the mean diffusivity in the region of interest analysis technique in groups of heavy cannabis users, light users, and non-users, in **the right Fusiform region.**

	Mean diffusivity of ROI analysis P-Value Fusiform region of the right hemisphere		
	Heavy users (Group I)	Light users (Group II)	Non-users (Group III)
Heavy users (Group I)	○	**	**
Light users (Group II)	0.594	○	**
Non users (Group III)	0.565	0.279	○

With a P-value lower than 0.05, the ANOVA analysis revealed no significant differences. The table reveals that in the same anatomical area, the mean diffusivity values of different groups in the right Fusiform region were not significantly different.

➢ Cingulum Ant

Table 209: The statistical analysis results of the mean diffusivity in the region of interest analysis technique in groups of heavy cannabis users, light users, and non-users, in the **left Cingulum Ant region.**

	Mean diffusivity of ROI analysis P-Value Cingulum Ant region of the left hemisphere		
	Heavy users (Group I)	Light users (Group II)	Non-users (Group III)
Heavy users (Group I)	○	**	**
Light users (Group II)	0.514	○	**
Non users (Group III)	0.890	0.699	○

With a P-value lower than 0.05, the ANOVA analysis revealed no significant differences. The table reveals that in the same anatomical area, the mean diffusivity values of different groups in the left Cingulum Ant region were not significantly different.

Table 210: The statistical analysis results of the mean diffusivity in the region of interest technique of analysis in groups of heavy cannabis users, light users, and non-users, in **the right Cingulum Ant region.**

	Mean diffusivity of ROI analysis P-Value Cingulum Ant region of the right hemisphere		
	Heavy users (Group I)	Light users (Group II)	Non-users (Group III)
Heavy users (Group I)	○	**	**
Light users (Group II)	0.327	○	**
Non users (Group III)	0.475	0.288	○

With a P-value lower than 0.05, the ANOVA analysis revealed no significant differences. The table reveals that in the same anatomical area, the mean diffusivity values of different groups in the right Cingulum Ant region were not significantly different.

➢ **Cingulum Mid**

Table 211: The statistical analysis results of the mean diffusivity in the region of interest analysis technique in groups of heavy cannabis users, light users, and non-users, in the **left Cingulum Mid region.**

	Mean diffusivity of ROI analysis P-Value Cingulum Mid region of the left hemisphere		
	Heavy users (Group I)	Light users (Group II)	Non-users (Group III)
Heavy users (Group I)	○	**	**
Light users (Group II)	0.735	○	**
Non users (Group III)	0.546	0.785	○

With a P-value lower than 0.05, the ANOVA analysis revealed no significant differences. The table reveals that in the same anatomical area, the mean diffusivity values of different groups in the left Cingulum Mid region were not significantly different.

Table 212: The statistical analysis results of the mean diffusivity in the region of interest analysis technique in groups of heavy cannabis users, light users, and non-users, in **the right Cingulum Mid region.**

	Mean diffusivity of ROI analysis P-Value Cingulum Mid region of the right hemisphere		
	Heavy users (Group I)	Light users (Group II)	Non-users (Group III)
Heavy users (Group I)	○	**	**
Light users (Group II)	0.509	○	**
Non users (Group III)	0.196	0.088	○

With a P-value lower than 0.05, the ANOVA analysis revealed no significant differences. The table reveals that in the same anatomical area, the mean diffusivity values of different groups in the right Cingulum Mid region were not significantly different.

➢ **Cingulum Post**

Table 213. The statistical analysis results of the mean diffusivity in the region of interest technique of analysis in groups of heavy cannabis users, light users, and non-users, in the **left Cingulum Post region.**

	Mean diffusivity of ROI analysis P-Value Cingulum Post region of the left hemisphere		
	Heavy users (Group I)	Light users (Group II)	Non-users (Group III)
Heavy users (Group I)	○	**	**
Light users (Group II)	0.406	○	**
Non users (Group III)	0.878	0.517	○

With a P-value lower than 0.05, the ANOVA analysis revealed no significant differences. The table reveals that in the same anatomical area, the mean diffusivity values of different groups in the left Cingulum Post region were not significantly different.

Table 214: The statistical analysis results of the mean diffusivity in the region of interest technique of analysis in groups of heavy cannabis users, light users, and non-users, in **the right Cingulum Post region.**

	Mean diffusivity of ROI analysis P-Value Cingulum Post region of the right hemisphere		
	Heavy users (Group I)	Light users (Group II)	Non-users (Group III)
Heavy users (Group I)	○	**	**
Light users (Group II)	0.715	○	**
Non users (Group III)	0.203	0.480	○

With a P-value lower than 0.05, the ANOVA analysis revealed no significant differences. The table reveals that in the same anatomical area, the mean diffusivity values of different groups in the right Cingulum Post region were not significantly different.

➢ ParaHippocampal

Table 215: The statistical analysis results of the mean diffusivity in the region of interest technique of analysis in groups of heavy cannabis users, light users, and non-users, in the **left ParaHippocampal region.**

	Mean diffusivity of ROI analysis P-Value ParaHippocampal region of the left hemisphere		
	Heavy users (Group I)	Light users (Group II)	Non-users (Group III)
Heavy users (Group I)	○	**	**
Light users (Group II)	0.847	○	**
Non users (Group III)	0.758	0.897	○

With a P-value lower than 0.05, the ANOVA analysis revealed no significant differences. The table reveals that in the same anatomical area, the mean diffusivity values of different groups in the left ParaHippocampal region were not significantly different.

Table 216: The statistical analysis results of the mean diffusivity in the region of interest technique of analysis in groups of heavy cannabis users, light users, and non-users, in **the right ParaHippocampal region.**

	Mean diffusivity of ROI analysis P-Value ParaHippocampal region of the right hemisphere		
	Heavy users (Group I)	Light users (Group II)	Non-users (Group III)
Heavy users (Group I)	○	**	**
Light users (Group II)	0.518	○	**
Non users (Group III)	0.312	0.631	○

With a P-value lower than 0.05, the ANOVA analysis revealed no significant differences. The table reveals that in the same anatomical area, the mean diffusivity values of different groups in the right ParaHippocampal region were not significantly different.

➢ **Hippocampus**

Table 217: The statistical analysis results of the mean diffusivity in the region of interest technique of analysis in groups of heavy cannabis users, light users, and non-users, in **the left Hippocampus region.**

	Mean diffusivity of ROI analysis P-Value Hippocampus region of the left hemisphere		
	Heavy users (Group I)	Light users (Group II)	Non-users (Group III)
Heavy users (Group I)	○	**	**
Light users (Group II)	0.369	○	**
Non users (Group III)	0.427	0.939	○

With a P-value lower than 0.05, the ANOVA analysis revealed no significant differences. The table reveals that in the same anatomical area, the mean diffusivity values of different groups in the left Hippocampus region were not significantly different.

Table 218. The statistical analysis results of the mean diffusivity in the region of interest technique of analysis in groups of heavy cannabis users, light users, and non-users, in **the right Hippocampus region.**

	Mean diffusivity of ROI analysis P-Value Hippocampus region of the right hemisphere		
	Heavy users (Group I)	Light users (Group II)	Non-users (Group III)
Heavy users (Group I)	○	**	**
Light users (Group II)	0.825	○	**
Non users (Group III)	0.910	0.827	○

With a P-value lower than 0.05, the ANOVA analysis revealed no significant differences. The table reveals that in the same anatomical area, the mean diffusivity values of different groups in the right Hippocampus region were not significantly different.

➢ **Insula**

Table 219: The statistical analysis results of the mean diffusivity in the region of interest technique of analysis in groups of heavy cannabis users, light users, and non-users, in the **left Insula region.**

	Mean diffusivity of ROI analysis P-Value Insula region of the left hemisphere		
	Heavy users (Group I)	Light users (Group II)	Non-users (Group III)
Heavy users (Group I)	○	**	**
Light users (Group II)	0,478	○	**
Non users (Group III)	0,723	0,339	○

With a P-value lower than 0.05, the ANOVA analysis revealed no significant differences. The table reveals that in the same anatomical area, the mean diffusivity values of different groups in the left Insula region were not significantly different.

Table 220: The statistical analysis results of the mean diffusivity in the region of interest technique of analysis in groups of heavy cannabis users, light users, and non-users, in **the right Insula region.**

	Mean diffusivity of ROI analysis P-Value Insula region of the right hemisphere		
	Heavy users (Group I)	Light users (Group II)	Non-users (Group III)
Heavy users (Group I)	○	**	**
Light users (Group II)	0.194	○	**
Non users (Group III)	0.310	0.060	○

With a P-value lower than 0.05, the ANOVA analysis revealed no significant differences. The table reveals that in the same anatomical area, the mean diffusivity values of different groups in the right Insula region were not significantly different.

➢ **Amygdala**

Table 221: The statistical analysis results of the mean diffusivity in the region of interest technique of analysis in groups of heavy cannabis users, light users, and non-users, in the **left Amygdala region.**

	Mean diffusivity ROI analysis P-Value Amygdala region of the left hemisphere		
	Heavy users (Group I)	**Light users (Group II)**	**Non-users (Group III)**
Heavy users (Group I)	○	**	**
Light users (Group II)	0.139	○	**
Non users (Group III)	0.102	0.499	○

With a P-value lower than 0.05, the ANOVA analysis revealed no significant differences. The table reveals that in the same anatomical area, the mean diffusivity values of different groups in the left Amygdala region were not significantly different.

Table 222. The statistical analysis results of the mean diffusivity in the region of interest technique of analysis in groups of heavy cannabis users, light users, and non-users, in **the right Amygdala region.**

	Mean diffusivity of ROI analysis P-Value Amygdala region of the right hemisphere		
	Heavy users (Group I)	**Light users (Group II)**	**Non-users (Group III)**
Heavy users (Group I)	○	**	**
Light users (Group II)	0.142	○	**
Non users (Group III)	0.710	0.080	○

With a P-value lower than 0.05, the ANOVA analysis revealed no significant differences. The table reveals that in the same anatomical area, the mean diffusivity values of different groups in the right Amygdala region were not significantly different.

➢ **Thalamus**

Table 223: The statistical analysis results of the mean diffusivity in the region of interest technique of analysis in groups of heavy cannabis users, light users, and non-users, in the **left Thalamus region.**

	Mean diffusivity of ROI analysis P-Value Thalamus region of the left hemisphere		
	Heavy users (Group I)	**Light users (Group II)**	**Non-users (Group III)**
Heavy users (Group I)	○	**	**
Light users (Group II)	0.698	○	**
Non users (Group III)	0.994	0.661	○

With a P-value lower than 0.05, the ANOVA analysis revealed no significant differences. The table reveals that in the same anatomical area, the mean diffusivity values of different groups in the left Thalamus region were not significantly different.

Table 224. The statistical analysis results of the mean diffusivity in the region of interest technique of analysis in groups of heavy cannabis users, light users, and non-users, in **the right Thalamus region.**

	Mean diffusivity of ROI analysis P-Value Thalamus region of the right hemisphere		
	Heavy users (Group I)	**Light users (Group II)**	**Non-users (Group III)**
Heavy users (Group I)	○	**	**
Light users (Group II)	0.822	○	**
Non users (Group III)	0.404	0.290	○

With a P-value lower than 0.05, the ANOVA analysis revealed no significant differences. The table reveals that in the same anatomical area, the mean diffusivity values of different groups in **the right Thalamus region** were not significantly different.

➢ **Caudate**

Table 225. The results of statistical analysis of the mean diffusivity in the region of interest technique of analysis in groups of heavy cannabis users, light users, and non-users, in the **left Caudate region.**

	Mean diffusivity of ROI analysis P-Value Caudate region of the left hemisphere		
	Heavy users (Group I)	Light users (Group II)	Non-users (Group III)
Heavy users (Group I)	○	**	**
Light users (Group II)	0.303	○	**
Non users (Group III)	0.632	0.604	○

With a P-value lower than 0.05, the ANOVA analysis revealed no significant differences. The table reveals that in the same anatomical area, the mean diffusivity values of different groups in the left Caudate region were not significantly different.

Table 226. The statistical analysis results of the mean diffusivity in the region of interest technique of analysis in groups of heavy cannabis users, light users, and non-users, in **the right Caudate region.**

	Mean diffusivity Coefficient of ROI analysis P-Value Caudate region of the right hemisphere		
	Heavy users (Group I)	Light users (Group II)	Non-users (Group III)
Heavy users (Group I)	○	**	**
Light users (Group II)	0.584	○	**
Non users (Group III)	0.421	0.308	○

With a P-value lower than 0.05, the ANOVA analysis revealed no significant differences. The table reveals that in the same anatomical area, the mean diffusivity values of different groups in the right Caudate region were not significantly different.

➢ **Putamen**

Table 228: The statistical analysis results of the mean diffusivity in the region of interest technique of analysis in groups of heavy cannabis users, light users, and non-users, in the **left Putamen region.**

	Mean diffusivity of ROI analysis P-Value Putamen region of the left hemisphere		
	Heavy users (Group I)	Light users (Group II)	Non-users (Group III)
Heavy users (Group I)	○	**	**
Light users (Group II)	0.559	○	**
Non users (Group III)	0.148	0.078	○

With a P-value lower than 0.05, the ANOVA analysis revealed no significant differences. The table reveals that in the same anatomical area, the mean diffusivity values of different groups in the left Putamen region were not significantly different.

Table 229: The statistical analysis results of the mean diffusivity in the region of interest analysis technique in groups of heavy cannabis users, light users, and non-users, in **the right Putamen region.**

	Mean diffusivity of ROI analysis P-Value Putamen region of the right hemisphere		
	Heavy users (Group I)	Light users (Group II)	Non-users (Group III)
Heavy users (Group I)	○	**	**
Light users (Group II)	0.179	○	**
Non users (Group III)	0.787	0.341	○

With a P-value lower than 0.05, the ANOVA analysis revealed no significant differences. The table reveals that in the same anatomical area, the mean diffusivity values of different groups in the right Putamen region were not significantly different.

➢ **Pallidum**

Table 230: The statistical analysis results of the mean diffusivity in the region of interest technique of analysis in groups of heavy cannabis users, light users, and non-users, in the **left Pallidum region.**

	Mean diffusivity Coefficient of ROI analysis P-Value Pallidum region of the left hemisphere		
	Heavy users (Group I)	Light users (Group II)	Non-users (Group III)
Heavy users (Group I)	○	**	**
Light users (Group II)	0.540	○	**
Non users (Group III)	0.402	0.062	○

With a P-value lower than 0.05, the ANOVA analysis revealed no significant differences. The table reveals that in the same anatomical area, the mean diffusivity values of different groups in the left Pallidum region were not significantly different.

Table 231: The statistical analysis results of the mean diffusivity in the region of interest analysis technique in groups of heavy cannabis users, light users, and non-users, in **the right Pallidum region.**

	Mean diffusivity of ROI analysis P-Value Pallidum region of the right hemisphere		
	Heavy users (Group I)	Light users (Group II)	Non-users (Group III)
Heavy users (Group I)	○	**	**
Light users (Group II)	0.338	○	**
Non users (Group III)	0.343	0.678	○

With a P-value lower than 0.05, the ANOVA analysis revealed no significant differences. The table reveals that in the same anatomical area, the mean diffusivity values of different groups in the right Pallidum region were not significantly different.

➢ **Nucleus Accumbens**

Table 232: The statistical analysis results of the mean diffusivity in the region of interest analysis technique in groups of heavy cannabis users, light users, and non-users in **the left Nucleus Accumbens region.**

	Mean diffusivity of ROI analysis P-Value Nucleus Accumbens region of the left hemisphere		
	Heavy users (Group I)	**Light users (Group II)**	**Non-users (Group III)**
Heavy users (Group I)	○	**	**
Light users (Group II)	0.699	○	**
Non users (Group III)	0.103	0.028	○

With a P-value lower than 0.05, the ANOVA analysis revealed significant differences between light users and non-users groups, but no significant difference between heavy and light users' groups and between heavy users and non-users groups. The table reveals that in the same anatomical area, the mean diffusivity values of different groups in the left Nucleus Accumbens region were significantly different among one group from three comparisons realized.

Table 233: The statistical analysis results of the mean diffusivity in the region of interest technique of analysis in groups of heavy cannabis users, light users, and non-users, in **the right Nucleus Accumbens region.**

	Mean diffusivity of ROI analysis P-Value Nucleus Accumbens region of the right hemisphere		
	Heavy users (Group I)	**Light users (Group II)**	**Non-users (Group III)**
Heavy users (Group I)	○	**	**
Light users (Group II)	0.340	○	**
Non users (Group III)	0.903	0.403	○

With a P-value lower than 0.05, the ANOVA analysis revealed no significant differences. The table reveals that in the same anatomical area, the mean diffusivity values of different groups in the right Nucleus Accumbens region were not significantly different.

Chapter IV: Diffusion tensor imaging results in white matter (Tractography)

I. Descriptive statistics

For FA and MD, in a first part, we will report our descriptive results of the overall quantitative comparisons of the diffusion markers of white matter's region in tables containing a column indicating the type of noted comparison, another column with corresponding regions, and the third column of commentary for each comparison type. We mentioned that the data is displayed in the tables to assist in understanding the results of white matter integrity of cannabis users' bran compared to healthy controls on a global scale.

Secondly, in the pages following the tables, with graphical curves, we will present compared FA and MD, each separately, by region of interest, and in each hemisphere individual by individual between the three groups. Using column graph, we also compared in the same way in each region of interest of each hemisphere the averages of FA and MD between the three groups.

Finally, with a table, we summarise for each region related white matter the averages and standard deviations (SD) values for the groups studied, along with intergroup comparisons.

1. Fractional anisotropy (FA) quantitative results

a. Summary of all the quantitative findings

Table 243: Tractography descriptive results of the overall quantitative comparisons of fractional anisotropy diffusion marker.

Intergroup comparison of Tractography Results.	Regions	Comments
G.III >G. II > G. I	-Frontal Med Orb. Left -Frontal Sup Orb. Left -Frontal Sup Medial. Right -Frontal Sup. Left & Right -Frontal Mid. Left -Frontal Inf Oper. Left -SupraMarginal. Left -Temporal Mid. Right -Temporal Inf. Right -Cingulum Ant. Right -Cingulum Mid. Left -Hippocampus. Left -Caudate. Left -Putamen. Left -Pallidum. Left	From a total of 70 regions, 16 regions' white matter tract revealed this comparison arrangement. 11 of the areas belong to the left hemisphere. They belong to: -Cerebral cortex -Limbic system -Basal ganglia
G.III > G. II ≈ G. I	-Frontal Med Orb. Right -Frontal Sup Orb. Right -Rectus. Right -Frontal Sup Medial. Left -Frontal Inf Oper. Right -Temporal Sup. Left & Right -Temporal Pole Sup. Right -Temporal Mid. Left -Temporal Pole Mid. Left -Fusiform. Right	From a total of 70 regions, 15 regions' white matter tract revealed this comparison arrangement. 9 of the areas belong to the right hemisphere. They belong to:

	-Cingulum Ant. Left -Cingulum Post. Right -Insula. Right -Amygdala. Left	-Cerebral cortex -Limbic system
G.III > G. I > G. II	-Frontal Mid Orb. Left -Frontal Inf Orb. Left & Right -Frontal Inf Tri. Left -Heschl. Left & Right -Temporal Inf. Left -Cingulum Post. Left -ParaHippocampal. Left	9 regions' white matter tract revealed this comparison arrangement. They belong mostly to the left hemisphere. They belong to: -Cerebral cortex -Limbic system
G. II ≈ G.III > G. I	-Rectus. Left -Frontal Mid. Right -Postcentral. Right -Angular. Left -Precuneus. Left & Right -Cingulum Mid. Right -Hippocampus. Right -Putamen. Right	9 regions' white matter tract revealed this comparison arrangement. They belong mostly to the right hemisphere. They belong to the cerebral cortex and the limbic system
G. II > G.III > G. I	-Olfactory. Left -Parietal Sup. Left & Right -Temporal Pole Mid. Right -ParaHippocampal. Right -Thalamus. Left -Pallidum. Right	7 regions' white matter tract revealed this comparison arrangement. 4 of the regions belong mostly to the right hemisphere and distributed

		among the cerebral cortex, limbic system diencephalon and basal ganglia.
G.III ≈ G. I > G. II	-Olfactory. Right -Temporal Pole Sup. Left -Fusiform. Left -Insula. Left -Caudate. Right	The remaining three categories of intergroup comparisons account for less than 20% of the total. Regions belong to the: -Cerebral cortex -Limbic system -Diencephalon -Basal ganglia
G. II > G.III ≈ G. I	-Frontal Mid Orb. Right -Postcentral. Left -Parietal Inf. Right -Amygdala. Right -Thalamus. Right	
G.III ≈ G. I ≈ G. II	-Frontal Inf Tri. Right -SupraMarginal. Right -Angular. Right -Parietal Inf. Left	

a. The quantitative findings of the white matter related to each region of interest

For each WM tracts related to a region and in both hemispheres, we present our mean fractional anisotropy (FA) findings by two separated figures. The first figure depicts the mean FA values of individuals in each group using a line chart.

In the line charts:

- Each participant is denoted numerically.

-The mean fractional anisotropy is sorted in graph individual (X, Y) points and lines in heavy cannabis users (Group I), light cannabis users (Group II), and non-users (Group III). In the "X" horizontal line, we have the nominative numbers of voluntary participants, and in the "Y" vertical line, we have mean fractional anisotropy values.

In the second figure, we compared the groups' FA averages between the three groups. A table containing every group's FA averages and standard deviations (SD) will be presented as a synthesis.

➢ Frontal Med Orb

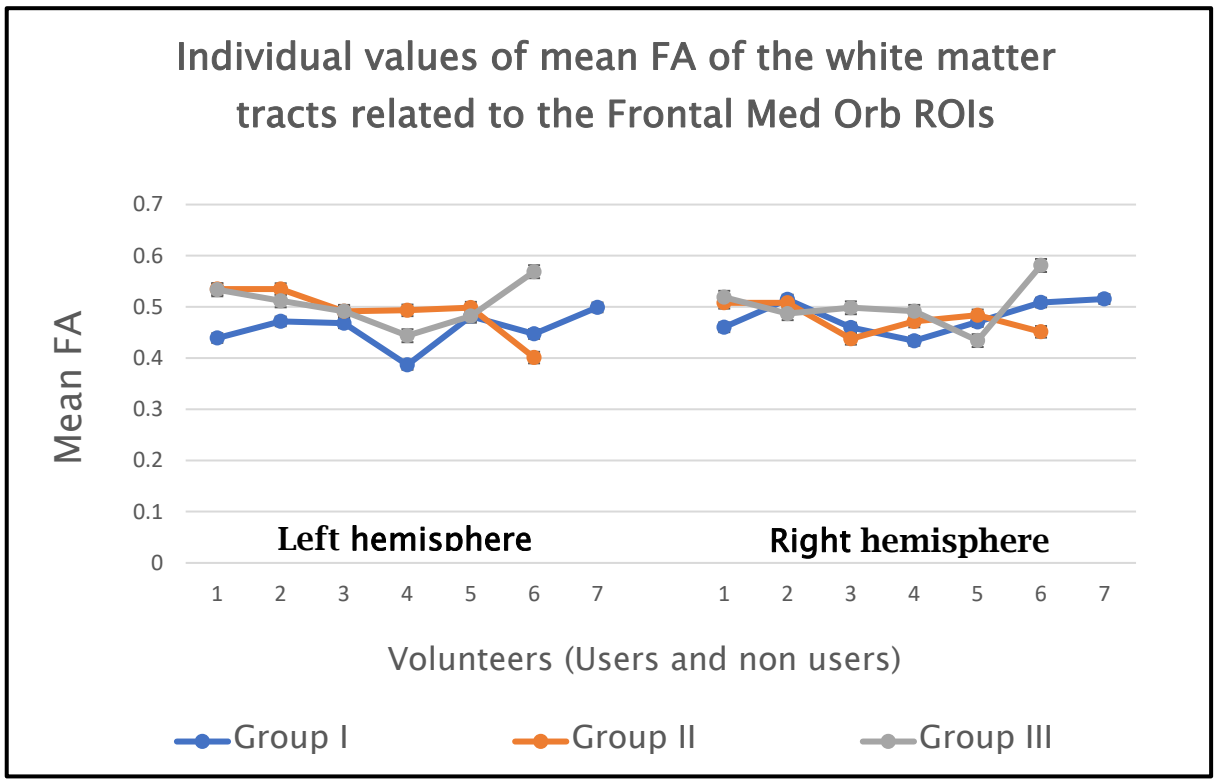

Figure 210: Individual values of mean fractional anisotropy (FA) in both hemispheres' white matter tracts related to the Frontal Med Orb ROIs. This figure depicts the FA values of all the participants belonging to each of the three groups (Heavy and light users and healthy controls).

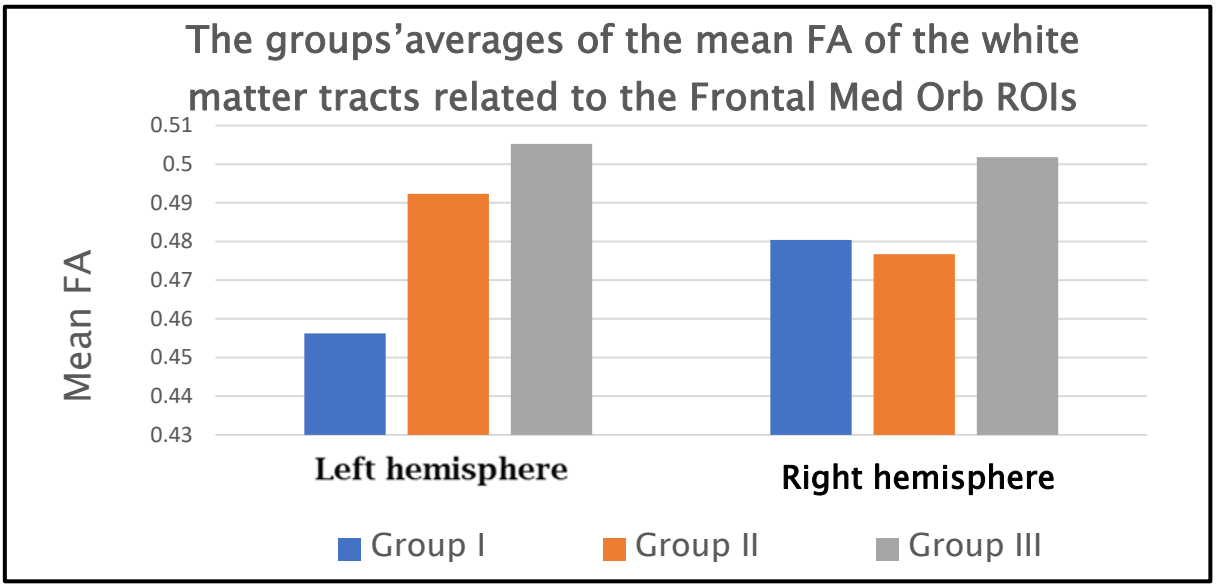

Figure: 211 The mean fractional anisotropy (FA) averages of each group of the white matter tracts related to the Frontal Med Orb ROIs in the left and the right hemispheres.

Table 244: The mean fractional anisotropy (FA) averages and standard deviations (SD) values for the groups studied of the white matter tracts related to the Frontal Med Orb ROIs, along with intergroup comparisons.

	Left Hemisphere	Right Hemisphere
Heavy users' group (G. I)	(0,456±0,0366)	(0,4803±0,0324)
Light users' group (G. II)	(0,492±0,0489)	(0,4767±0,029)
Non-users' group (G.III)	(0,5052±0,0433)	(0,5017±0,0479)
Intergroup comparison	G.III > G. II > G. I	G.III > G. I ≈ G. II

➢ **Frontal Sup Orb**

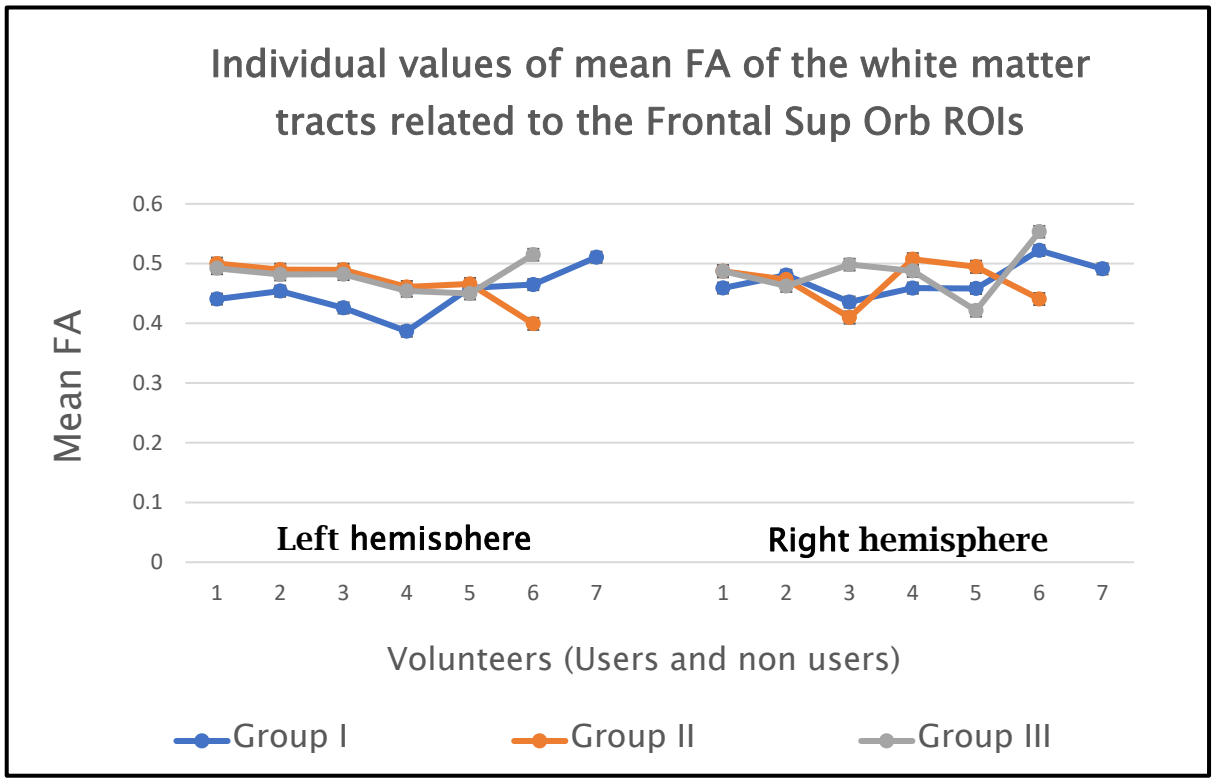

Figure 212: Individual values of mean fractional anisotropy (FA) in both hemispheres' white matter tracts related to the Frontal Sups Orb ROIs. This figure depicts the FA values of all the participants belonging to each of the three groups (Heavy and light users and healthy controls).

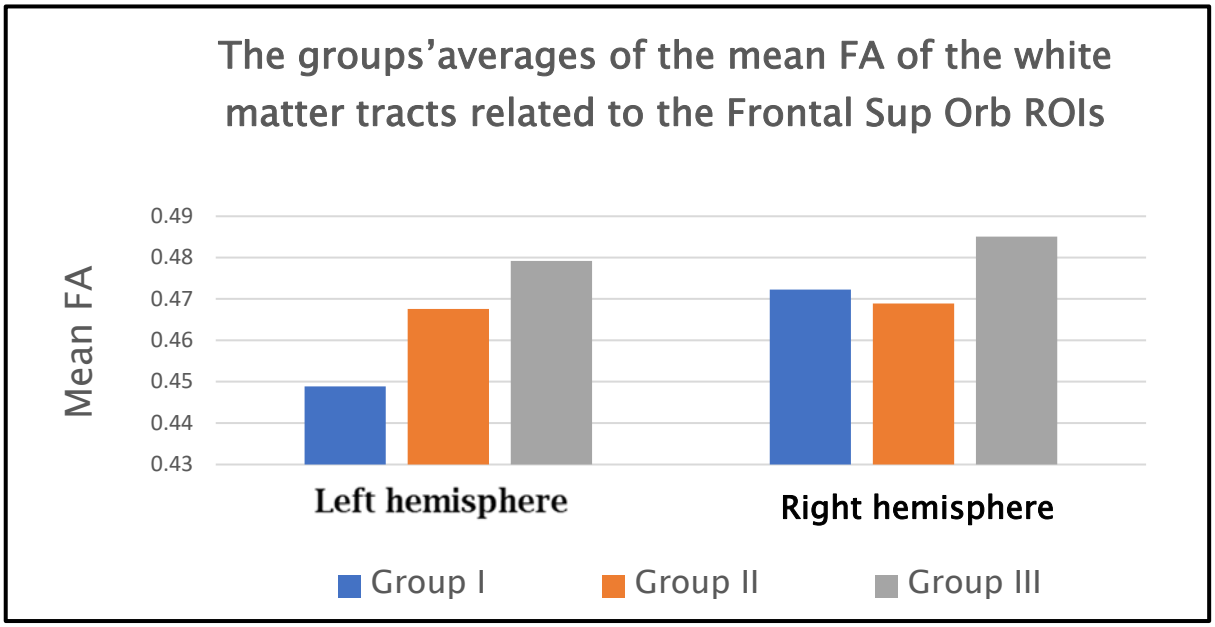

Figure 213: The mean fractional anisotropy (FA) averages of each group of the white matter tracts related to the Frontal Sup Orb ROIs in the left and the right hemispheres.

Table 245: The mean fractional anisotropy (FA) averages and standard deviations (SD) values for the groups studied of the white matter tracts related to the Frontal Sup Orb ROIs, along with intergroup comparisons.

	Left Hemisphere	Right Hemisphere
Heavy users' group (G. I)	(0,448±0,038)	(0,472±0,028)
Light users' group (G. II)	(0,467±0,0367)	(0,468±0,0368)
Non-users' group (G.III)	(0,479±0,0242)	(0,485±0,0434)
Intergroup comparison	G.III > G. II > G. I	G.III > G. I ≈ G. II

➢ Frontal Mid Orb:

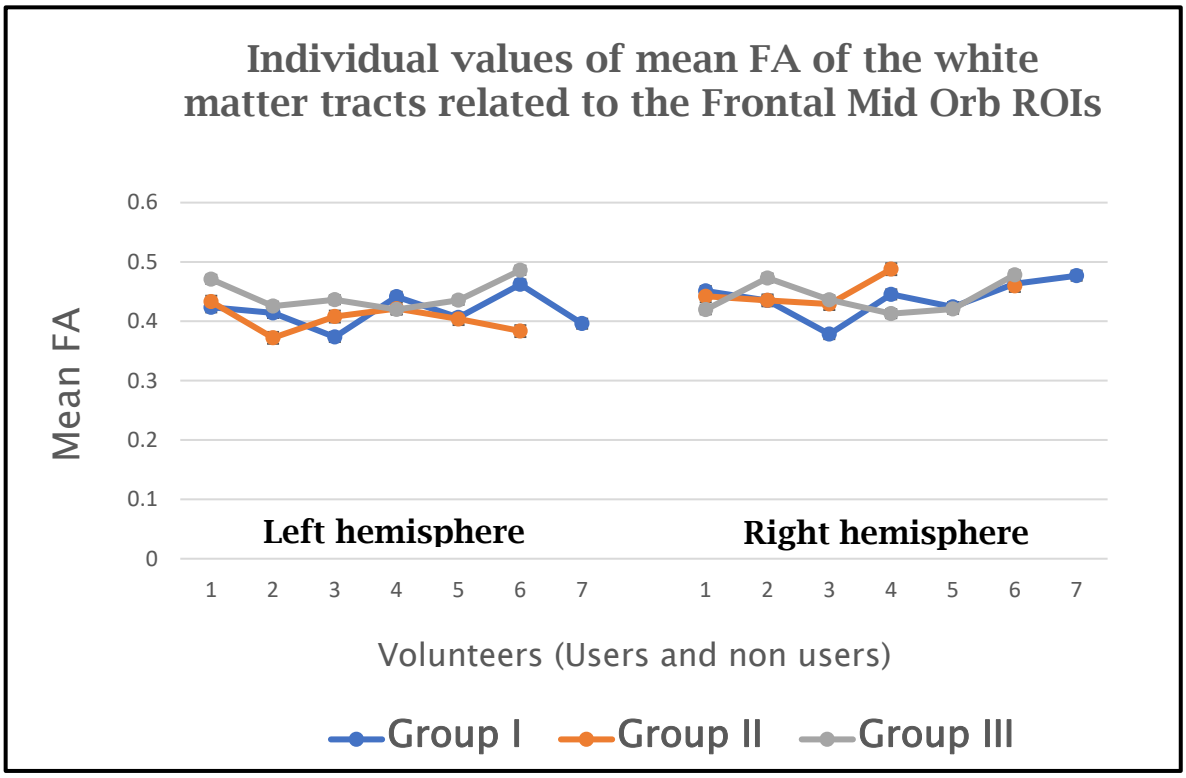

Figure 214: Individual values of mean fractional anisotropy (FA) in both hemispheres' white matter tracts related to the Frontal Mid Orb ROIs. This figure depicts the FA values of all the participants belonging to each of the three groups (Heavy and light users and healthy controls).

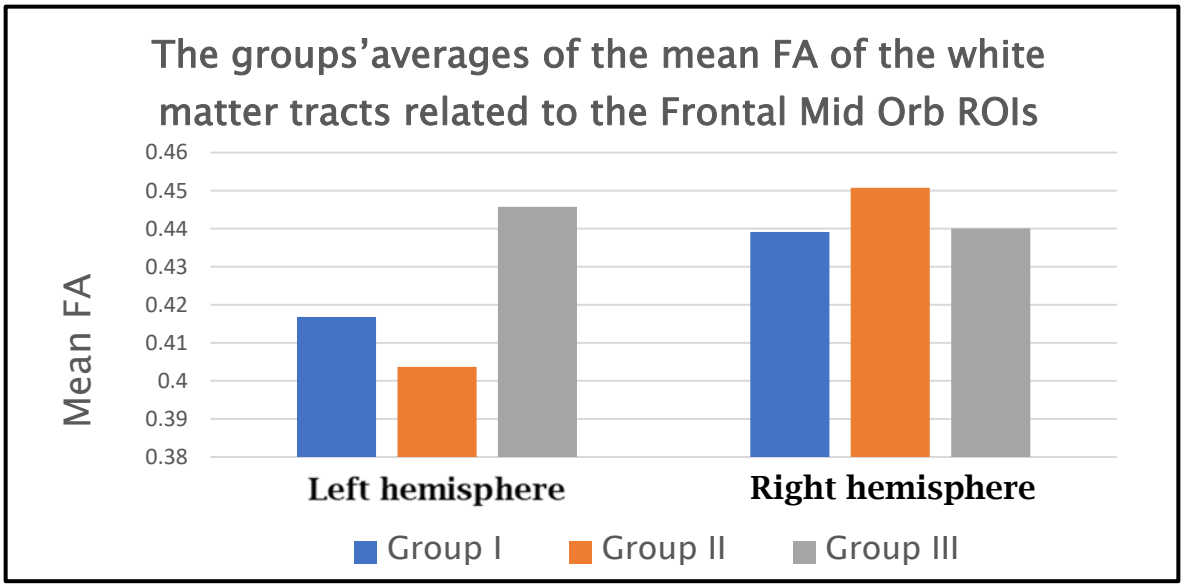

Figure 215: The mean fractional anisotropy (FA) averages of each group of the white matter tracts related to the Frontal Mid Orb ROIs in the left and the right hemispheres.

Table 246: The mean fractional anisotropy (FA) averages and standard deviations (SD) values for the groups studied of the white matter tracts related to the Frontal Mid Orb ROIs, along with intergroup comparisons.

	Left Hemisphere	Right Hemisphere
Heavy users' group (G. I)	(0,4167±0,0008)	(0,439±0,0319)
Light users' group (G. II)	(0,4036±0,0227)	(0,4507±0,0236)
Non-users' group (G.III)	(0,4457±0,0265)	(0,44006±0,0285)
Intergroup comparison	G.III > G. I > G. II	G. II > G.III ≈ G. I

➢ Frontal Inf Orb

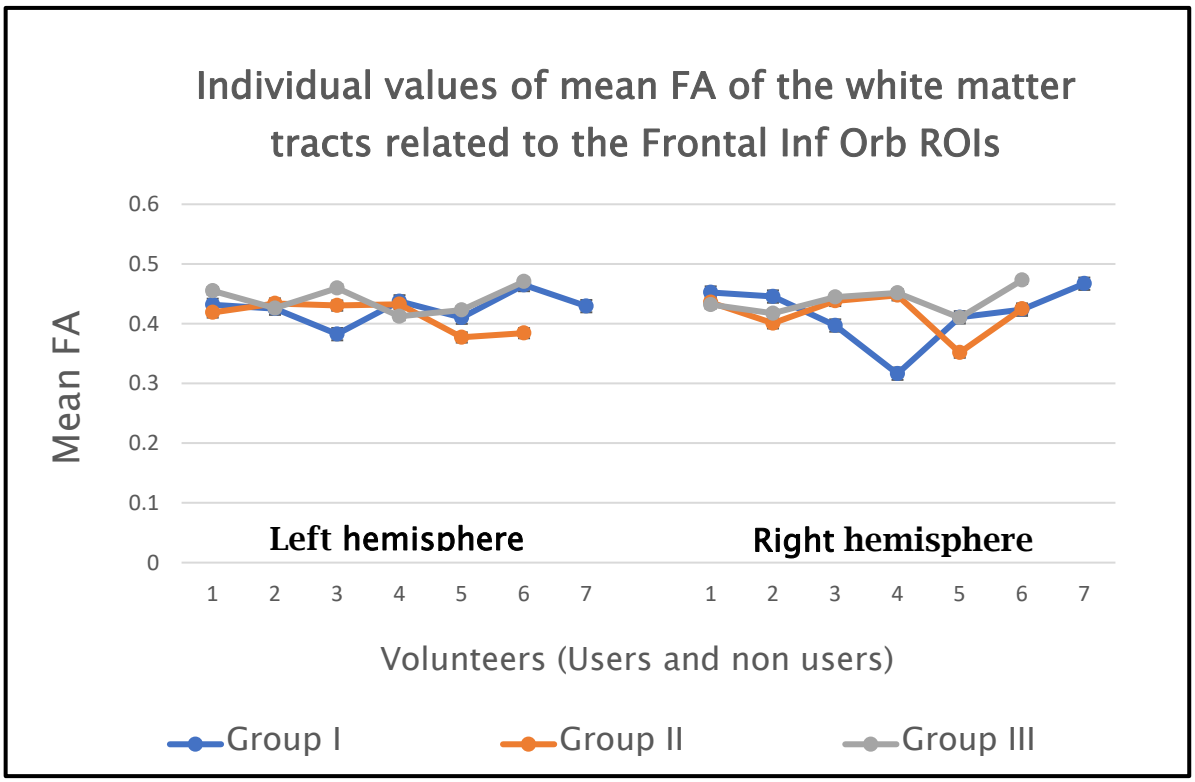

Figure 216: Individual values of mean fractional anisotropy (FA) in both hemispheres' white matter tracts related to the Frontal Inf Orb ROIs. This figure depicts the FA values of all the participants belonging to each of the three groups (Heavy and light users and healthy controls).

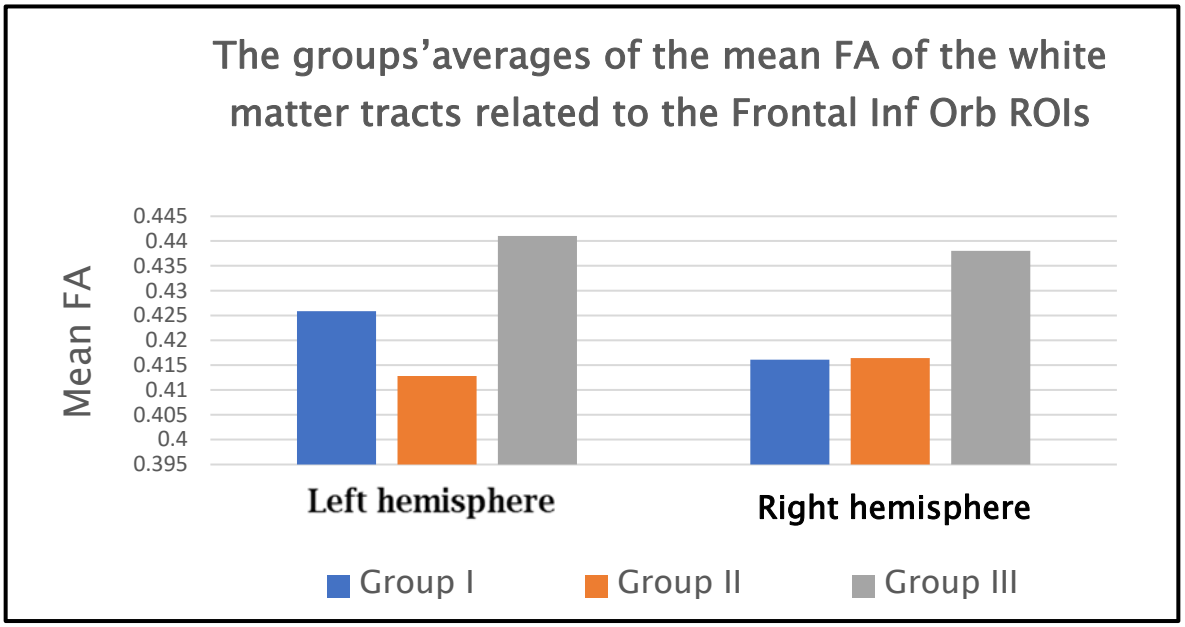

Figure 217: The mean fractional anisotropy (FA) averages of each group of the white matter tracts related to the Frontal Inf Orb ROIs in the left and the right hemispheres.

Table 247: The mean fractional anisotropy (FA) averages and standard deviations (SD) values for the groups studied of the white matter tracts related to the Frontal Inf Orb ROIs, along with intergroup comparisons.

	Left Hemisphere	Right Hemisphere
Heavy users' group (G. I)	(0,425± 0,0252)	(0,416±0,05029)
Light users' group (G. II)	(0,412±0,0255)	(0,416±0,0355)
Non-users' group (G.III)	(0,441±0,0236)	(0,438±0,0232)
Intergroup comparison	G.III > G. I > G. II	G.III > G. I > G. II

➢ Rectus

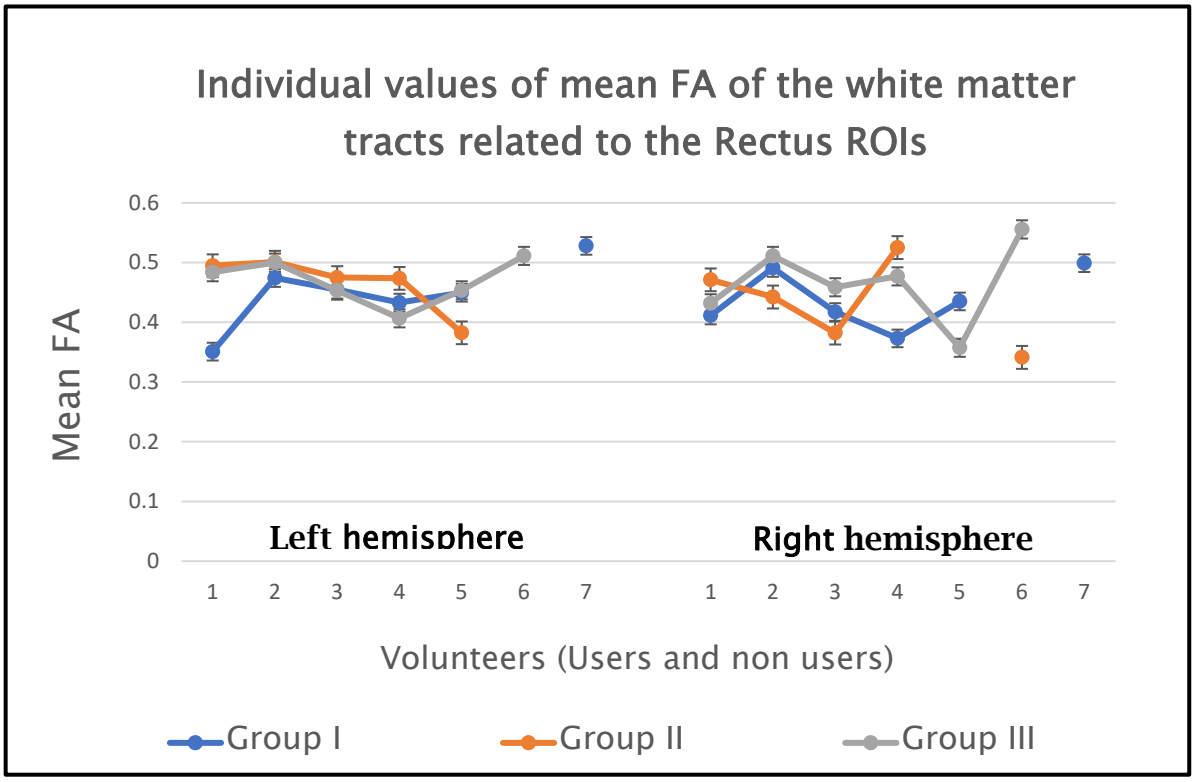

Figure 218: Individual values of mean fractional anisotropy (FA) in both hemispheres' white matter tracts related to the Rectus ROIs. This figure depicts the FA values of all the participants belonging to each of the three groups (Heavy and light users and healthy controls).

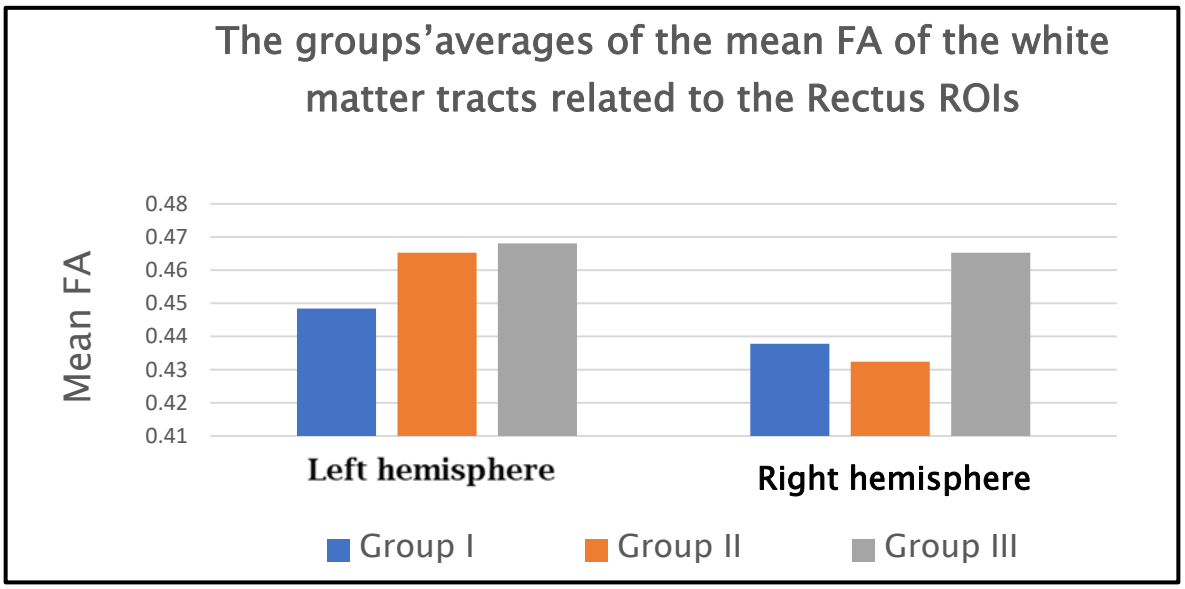

Figure 219: The mean fractional anisotropy (FA) averages of each group of the white matter tracts related to the Rectus ROIs in the left and the right hemispheres.

Table 248: The mean fractional anisotropy (FA) averages and standard deviations (SD) values for the groups studied of the white matter tracts related to the Rectus ROIs, along with intergroup comparisons.

	Left Hemisphere	Right Hemisphere
Heavy users' group (G. I)	(0,448±0,0579)	(0,4378±0,0487)
Light users' group (G. II)	(0,465±0,0478)	(0,4324±0,0724)
Non-users' group (G.III)	(0,468±0,038)	(0,4652±0,068)
Intergroup comparison	G. II ≈ G.III > G. I	G.III > G. II ≈ G. I

➢ **Olfactory**

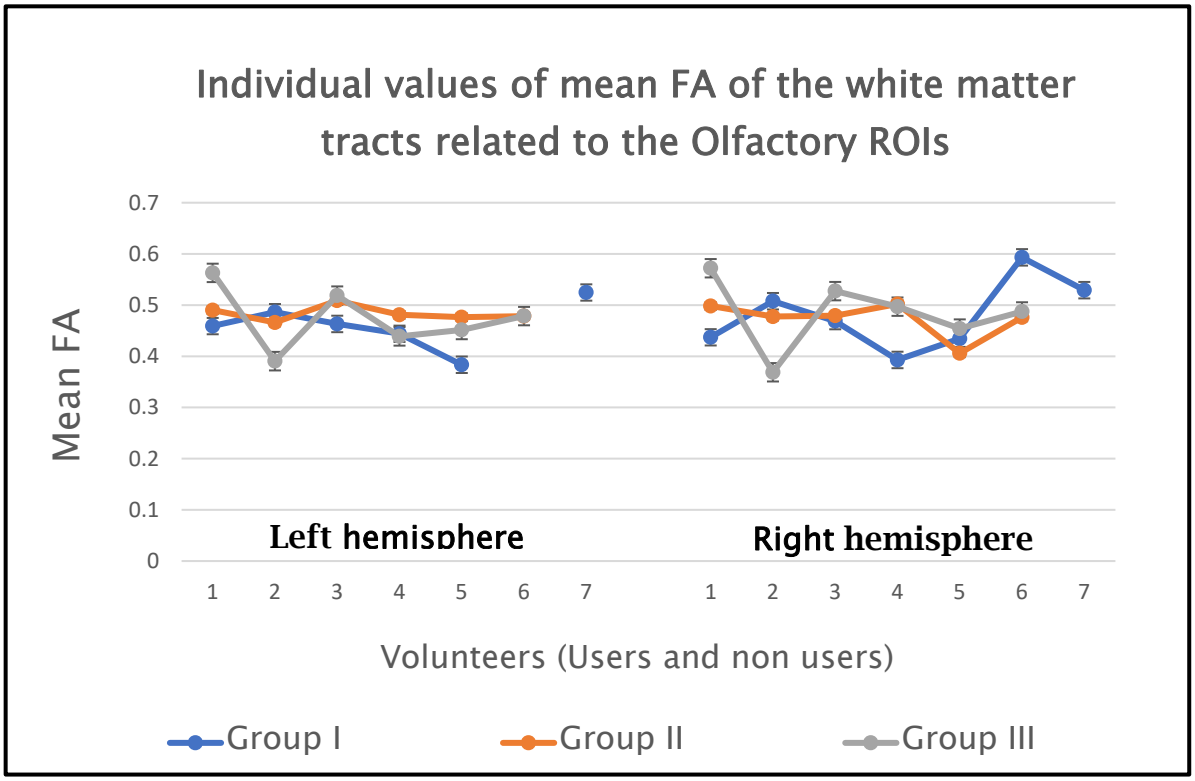

Figure 220: Individual values of mean fractional anisotropy (FA) in both hemispheres' white matter tracts related to the Olfactory ROIs. This figure depicts the FA values of all the participants belonging to each of the three groups (Heavy and light users and healthy controls).

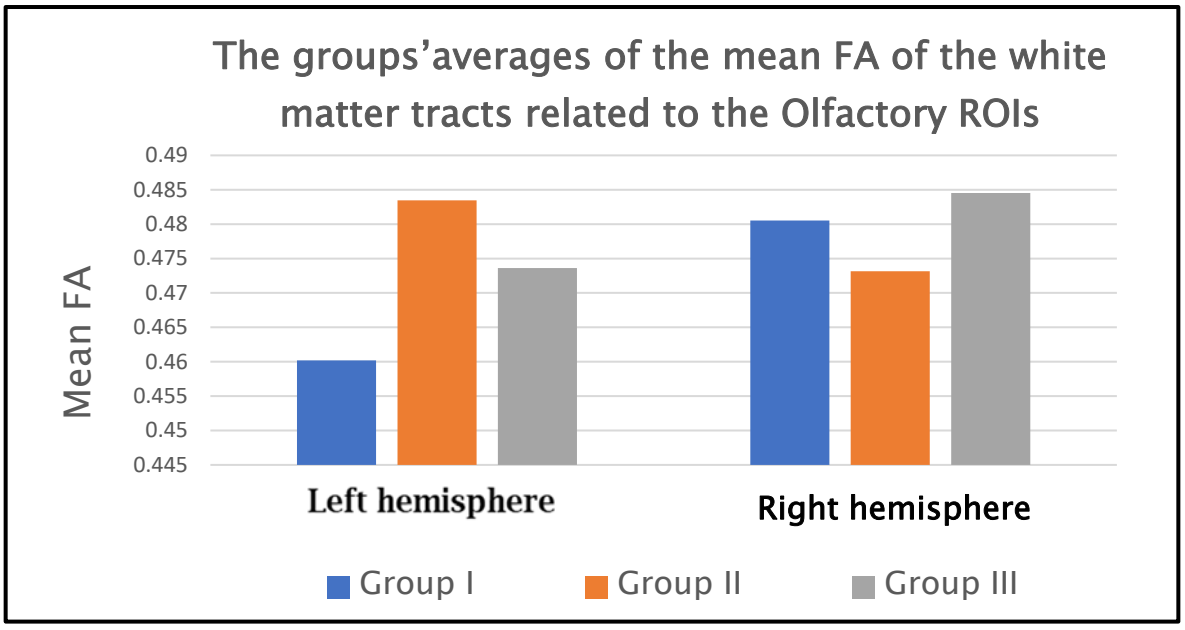

Figure 221: The mean fractional anisotropy (FA) averages of each group of the white matter tracts related to the Olfactory ROIs in the left and the right hemispheres.

Table 249: The mean fractional anisotropy (FA) averages and standard deviations (SD) values for the groups studied of the white matter tracts related to the Olfactory ROIs, along with intergroup comparisons.

	Left Hemisphere	Right Hemisphere
Heavy users' group (G. I)	(0,4602±0,0469)	(0,4805±0,0678)
Light users' group (G. II)	(0,4834±0,0147)	(0,4731±0,0347)
Non-users' group (G.III)	(0,4736±0,0610)	(0,4845±0,0692)
Intergroup comparison	G. II > G.III > G. I	G.III ≈ G. I > G. II

➢ Frontal Sup Medial

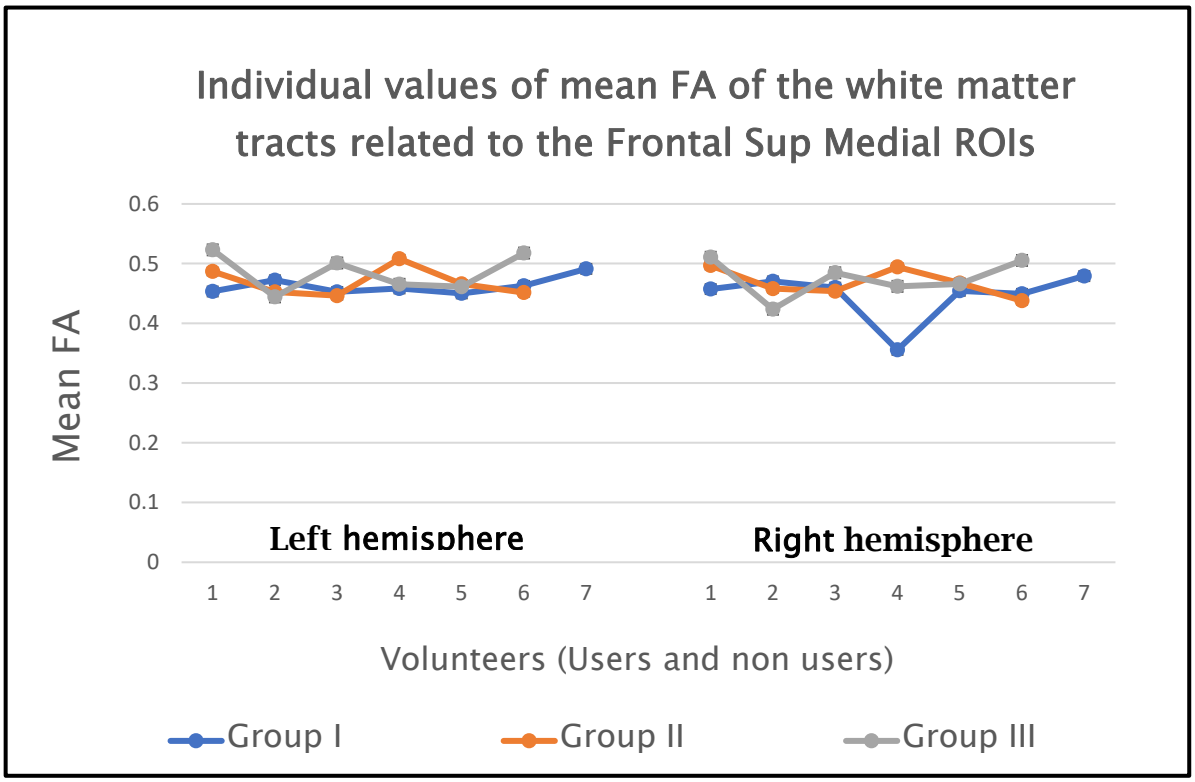

Figure 222: Individual values of mean fractional anisotropy (FA) in both hemispheres' white matter tracts related to the Frontal Sup Medial ROIs. This figure depicts the FA values of all the participants belonging to each of the three groups (Heavy and light users and healthy controls).

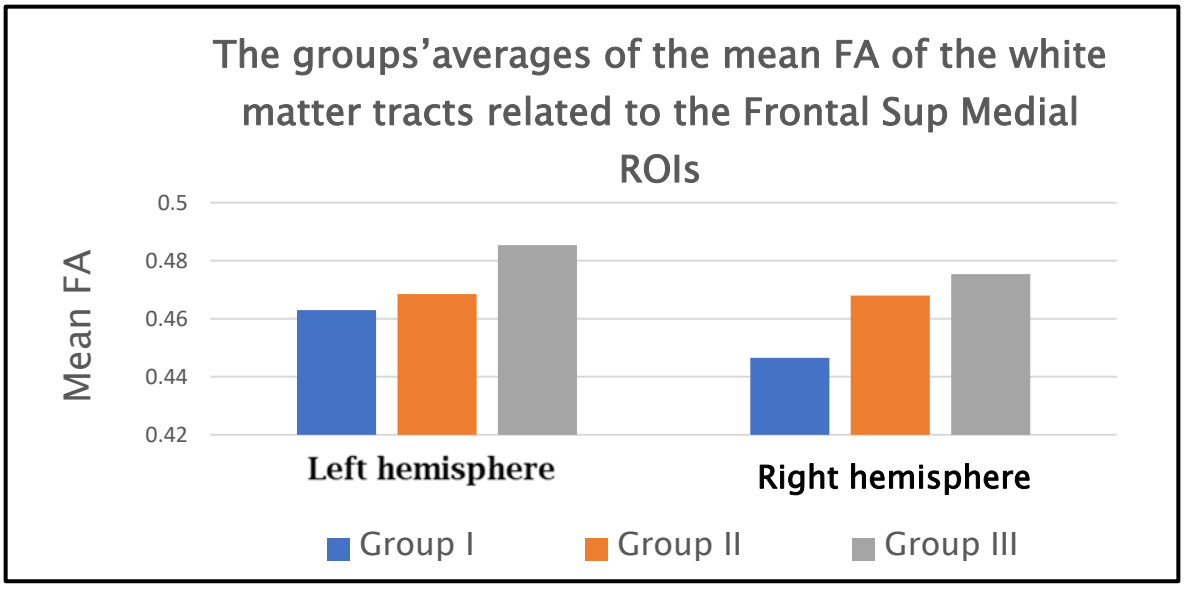

Figure 223: The mean fractional anisotropy (FA) averages of each group of the white matter tracts related to the Frontal Sup Medial ROIs in the left and the right hemispheres.

Table 250: The mean fractional anisotropy (FA) averages and standard deviations (SD) values for the groups studied of the white matter tracts related to the Frontal Sup Medial ROIs, along with intergroup comparisons.

	Left Hemisphere	Right Hemisphere
Heavy users' group (G. I)	(0,4629±0,0145)	(0,4465±0,0413)
Light users' group (G. II)	(0,4684±0,0242)	(0,4679±0,0233)
Non-users' group (G.III)	(0,4853±0,0328)	(0,4753±0,0321)
Intergroup comparison	G.III > G. I ≈ G. II	G.III > G. II > G. I

➢ **Frontal Sup**

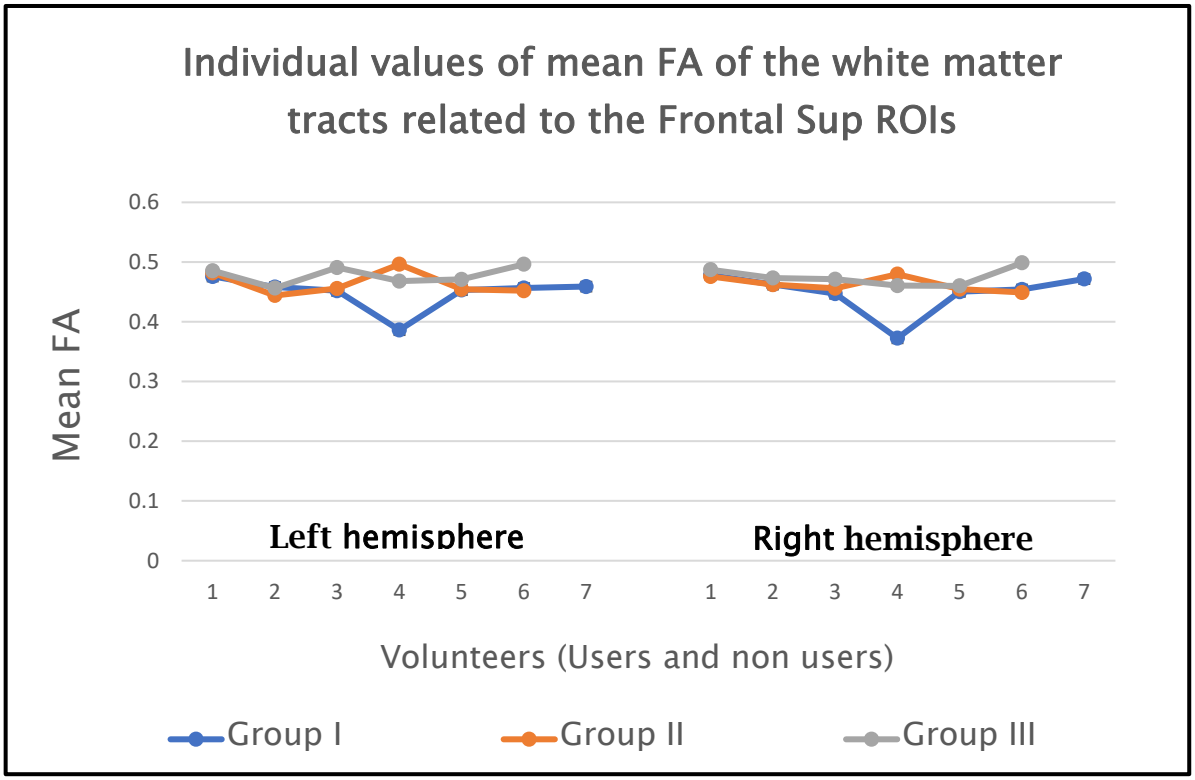

Figure 224: Individual values of mean fractional anisotropy (FA) in both hemispheres' white matter tracts related to the Frontal Sup ROIs. This figure depicts the FA values of all the participants belonging to each of the three groups (Heavy and light users and healthy controls).

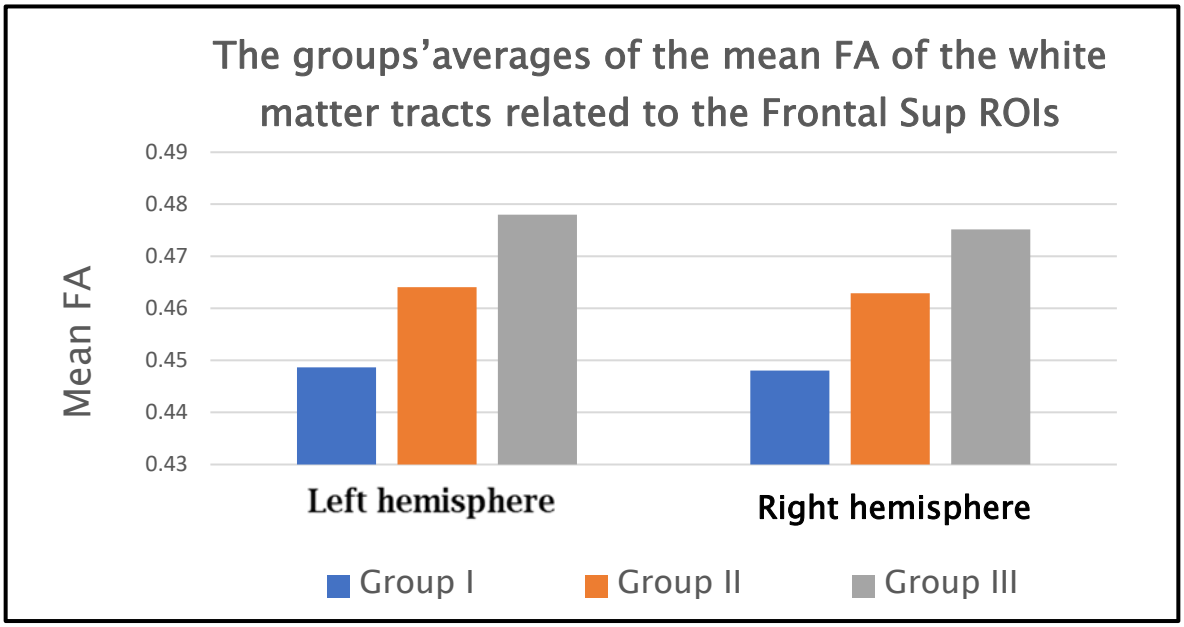

Figure 225: The mean fractional anisotropy (FA) averages of each group of the white matter tracts related to the Frontal Sup ROIs in the left and the right hemispheres.

Table 251: The mean fractional anisotropy (FA) averages and standard deviations (SD) values for the groups studied of the white matter tracts related to the Frontal Sup ROIs, along with intergroup comparisons.

	Left Hemisphere	Right Hemisphere
Heavy users' group (G. I)	(0,4486±0,0286)	(0,448±0,0351)
Light users' group (G. II)	(0,46405±0,0203)	(0,4628±0,0123)
Non-users' group (G.III)	(0,4779±0,0152)	(0,47514±0,0152)
Intergroup comparison	G.III > G. II > G. I	G.III > G. II > G. I

➢ **Frontal Mid**

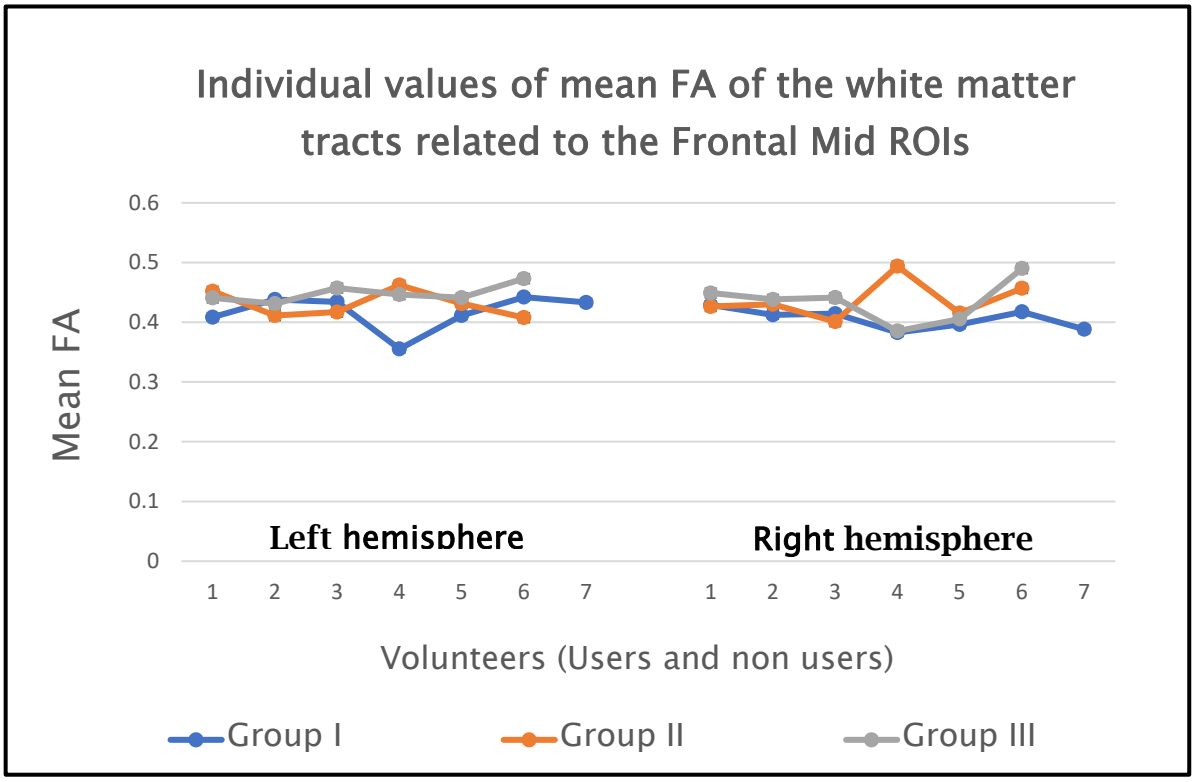

Figure 226: Individual values of mean fractional anisotropy (FA) in both hemispheres' white matter tracts related to the Frontal Mid ROIs. This figure depicts the FA values of all the participants belonging to each of the three groups (Heavy and light users and healthy controls).

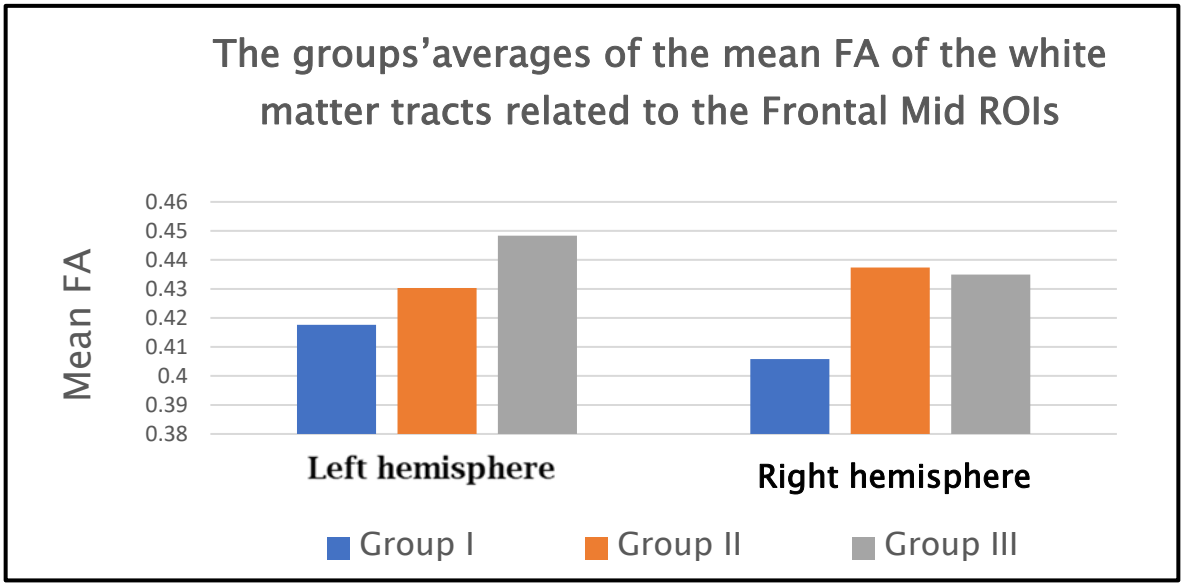

Figure 227: The mean fractional anisotropy (FA) averages of each group of the white matter tracts related to the Frontal Mid ROIs in the left and the right hemispheres.

Table 252: The mean fractional anisotropy (FA) averages and standard deviations (SD) values for the groups studied of the white matter tracts related to the Frontal Mid ROIs, along with intergroup comparisons.

	Left Hemisphere	Right Hemisphere
Heavy users' group (G. I)	(0,41759±0,0303)	(0,4058±0,0168)
Light users' group (G. II)	(0,4303±0,0225)	(0,43736±0,0333)
Non-users' group (G.III)	(0,448±0,0148)	(0,4349±0,0363)
Intergroup comparison	G.III > G. II > G. I	G. II ≈ G.III > G. I

➢ **Frontal Inf Oper**

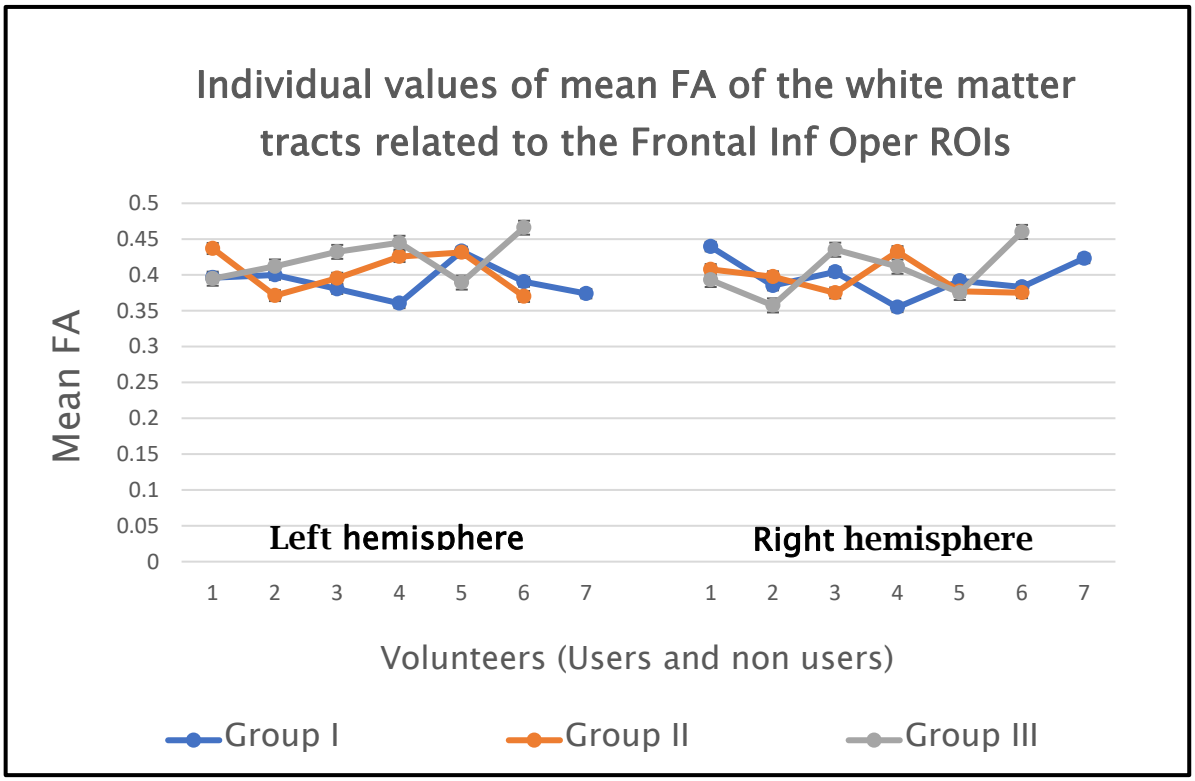

Figure 228: Individual values of mean fractional anisotropy (FA) in both hemispheres' white matter tracts related to the Frontal Inf Oper ROIs. This figure depicts the FA values of all the participants belonging to each of the three groups (Heavy and light users and healthy controls).

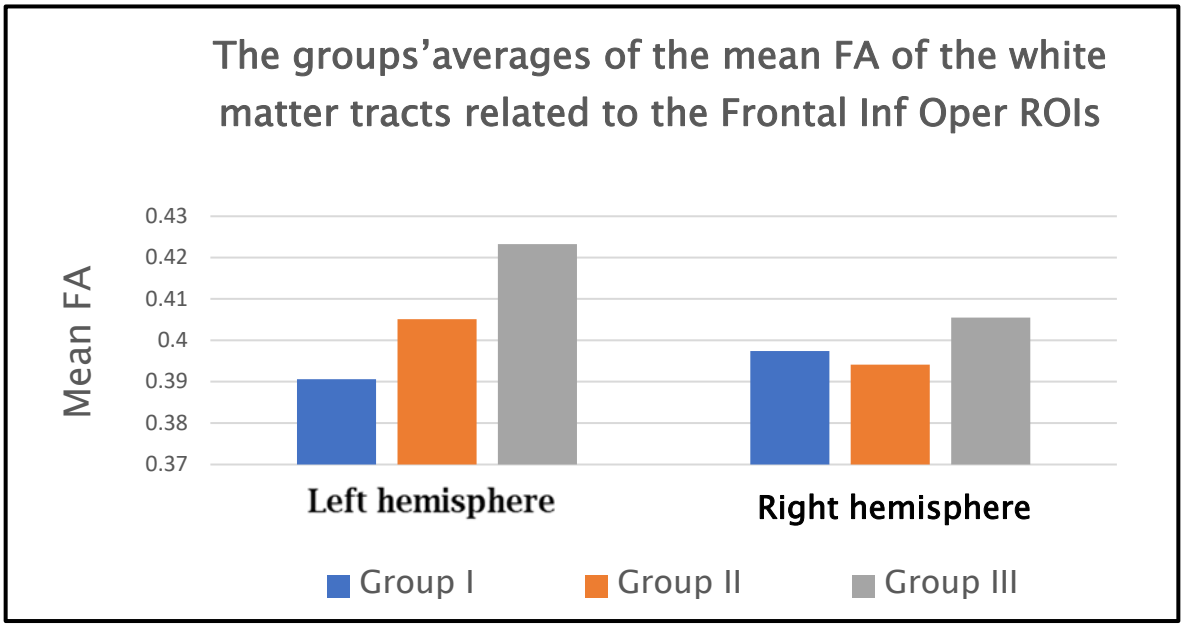

Figure 229: The mean fractional anisotropy (FA) averages of each group of the white matter tracts related to the Frontal Inf Oper ROIs in the left and the right hemispheres.

Table 253: The mean fractional anisotropy (FA) averages and standard deviations (SD) values for the groups studied of the white matter tracts related to the Frontal Inf Oper ROIs, along with intergroup comparisons.

	Left Hemisphere	Right Hemisphere
Heavy users' group (G. I)	(0,39058±0,0231)	(0,397379±0,0279)
Light users' group (G. II)	(0,40508±0,03036)	(0,3941±0,023)
Non-users' group (G.III)	(0,4232±0,0298)	(0,40547±0,038)
Intergroup comparison	G.III > G. II > G. I	G.III > G. II ≈ G. I

➢ Frontal Inf Tri

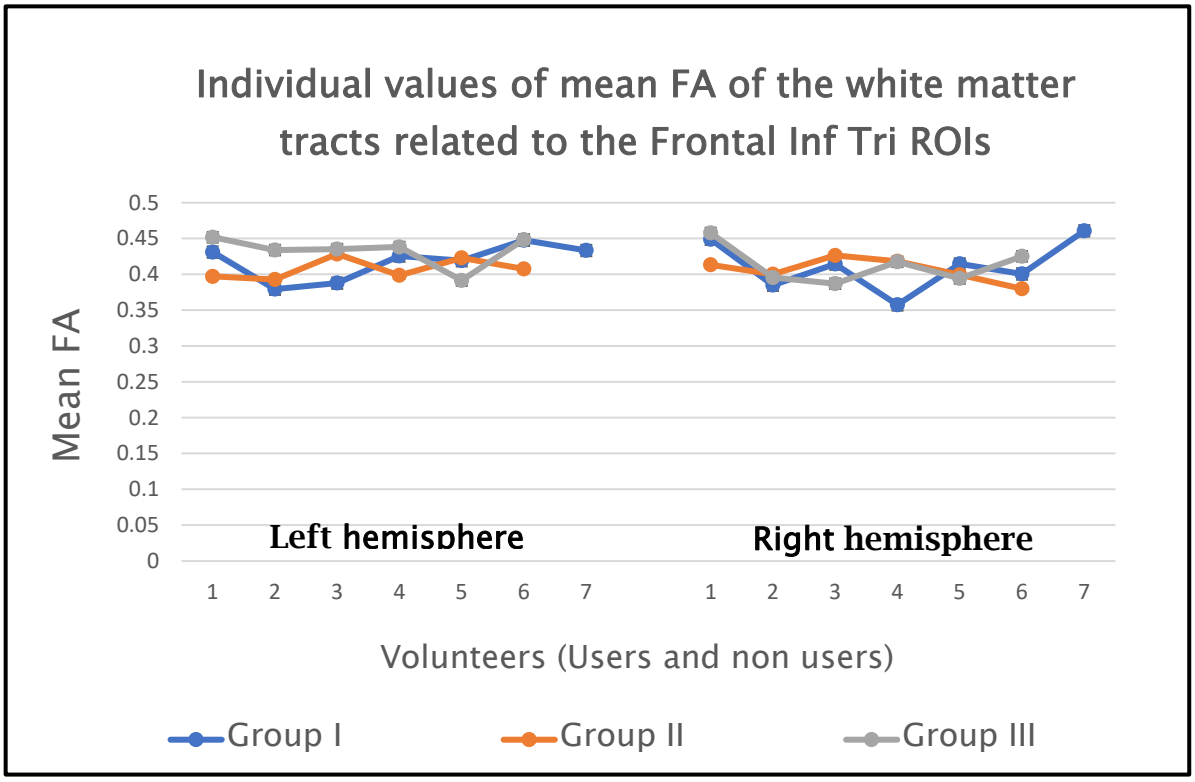

Figure 230: Individual values of mean fractional anisotropy (FA) in both hemispheres' white matter tracts related to the Frontal Inf Tri ROIs. This figure depicts the FA values of all the participants belonging to each of the three groups (Heavy and light users and healthy controls).

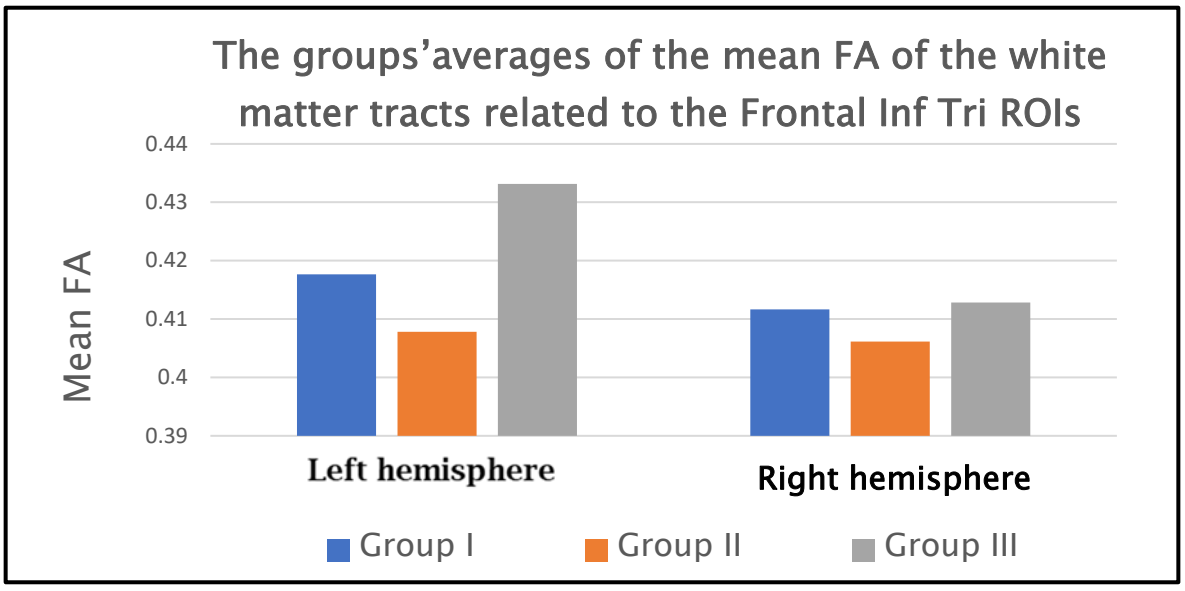

Figure 231: The mean fractional anisotropy (FA) averages of each group of the white matter tracts related to the Frontal Inf Tri ROIs in the left and the right hemispheres.

Table 254: The mean fractional anisotropy (FA) averages and standard deviations (SD) values for the groups studied of the white matter tracts related to the Frontal Inf Tri ROIs, along with intergroup comparisons.

	Left Hemisphere	Right Hemisphere
Heavy users' group (G. I)	(0,417±0,025)	(0,4116±0,0355)
Light users' group (G. II)	(0,4078±0,0147)	(0,406±0,0166)
Non-users' group (G.III)	(0,433±0,0216)	(0,4128±0,02646)
Intergroup comparison	G.III > G. I > G. II	G.III ≈ G. I ≈ G. I

➢ **Postcentral**

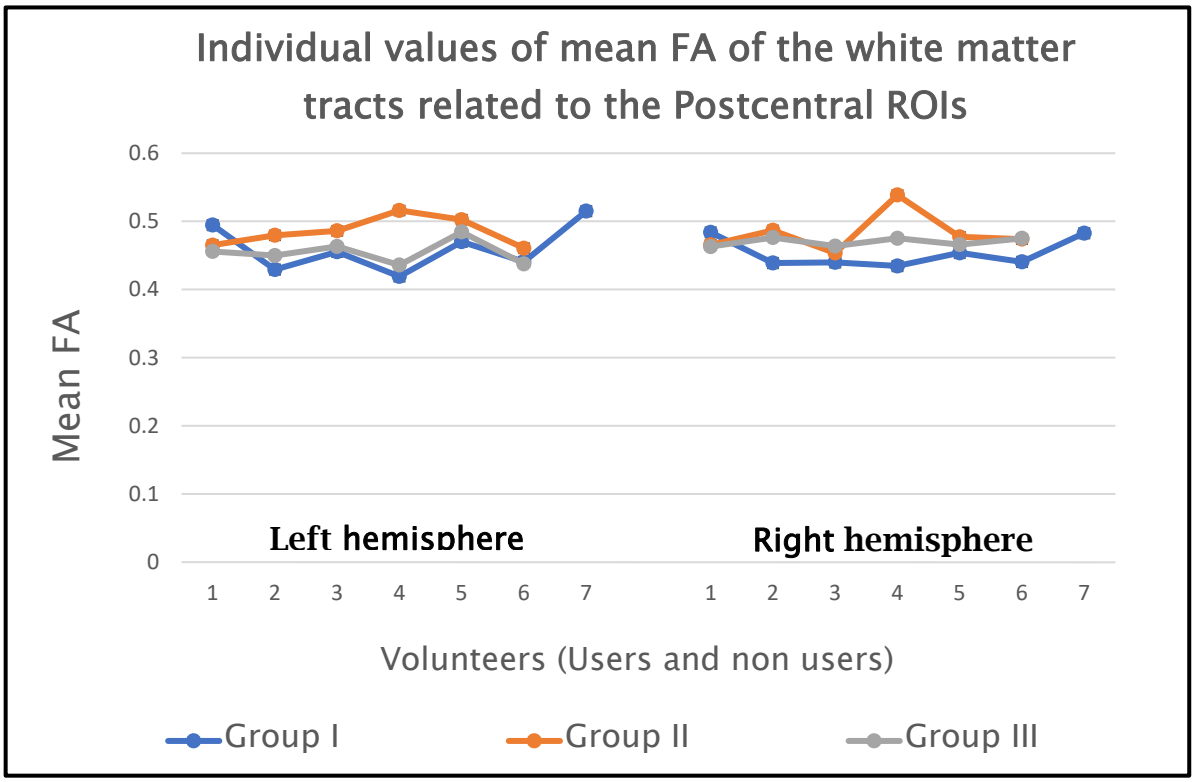

Figure 232: Individual values of mean fractional anisotropy (FA) in both hemispheres' white matter tracts related to the Postcentral ROIs. This figure depicts the FA values of all the participants belonging to each of the three groups (Heavy and light users and healthy controls).

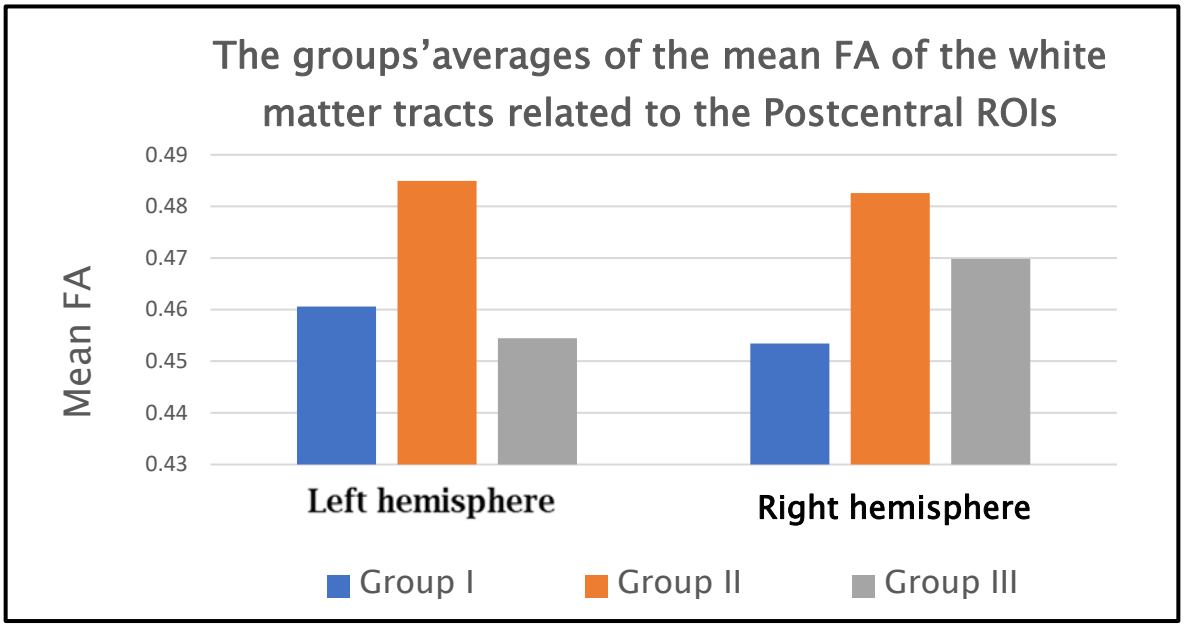

Figure 233: The mean fractional anisotropy (FA) averages of each group of the white matter tracts related to the Postcentral ROIs in the left and the right hemispheres.

Table 255: The mean fractional anisotropy (FA) averages and standard deviations (SD) values for the groups studied of the white matter tracts related to the Postcentral ROIs, along with intergroup comparisons.

	Left Hemisphere	Right Hemisphere
Heavy users' group (G. I)	(0,4605±0,0349)	(0,4534±0,0212)
Light users' group (G. II)	(0,4849±0,02136)	(0,4825±0,0296)
Non-users' group (G.III)	(0,4544±0,01805)	(0,4698±0,00628)
Intergroup comparison	G. II > G.III ≈ G. I	G. II ≈ G.III > G. I

➢ Parietal Sup

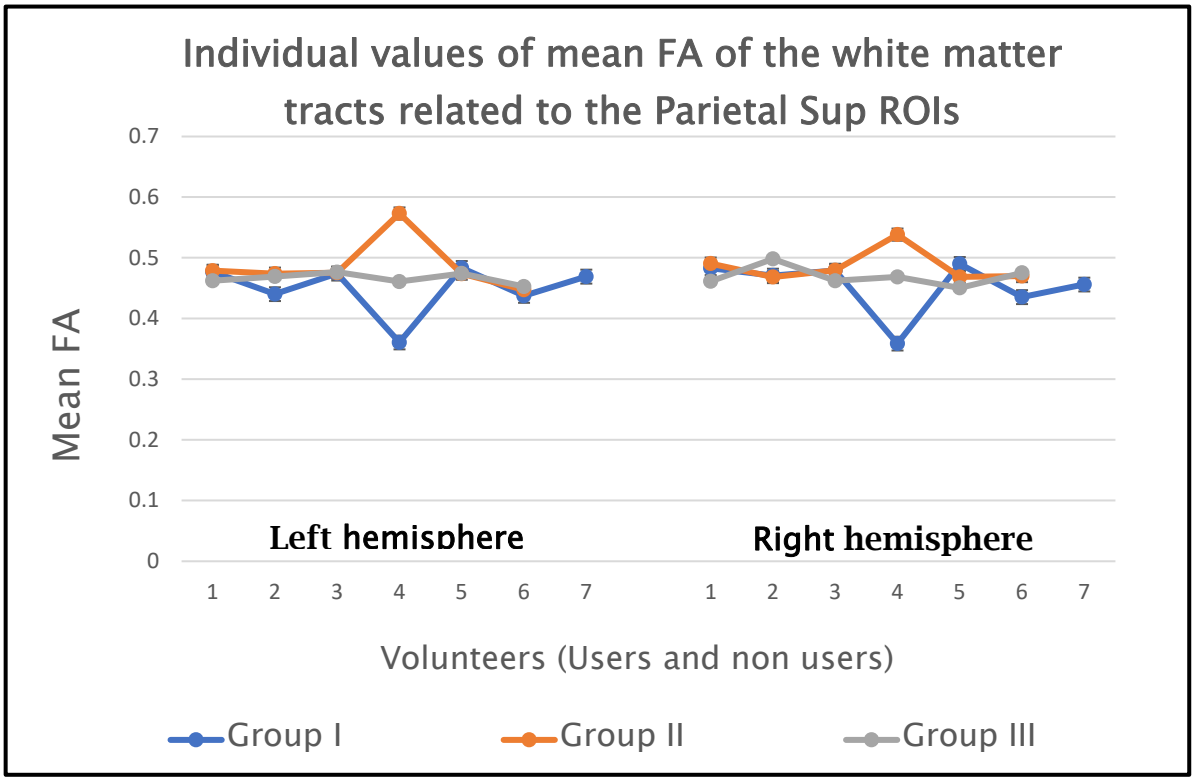

Figure 234: Individual values of mean fractional anisotropy (FA) in both hemispheres' white matter tracts related to the Parietal Sup ROIs. This figure depicts the FA values of all the participants belonging to each of the three groups (Heavy and light users and healthy controls).

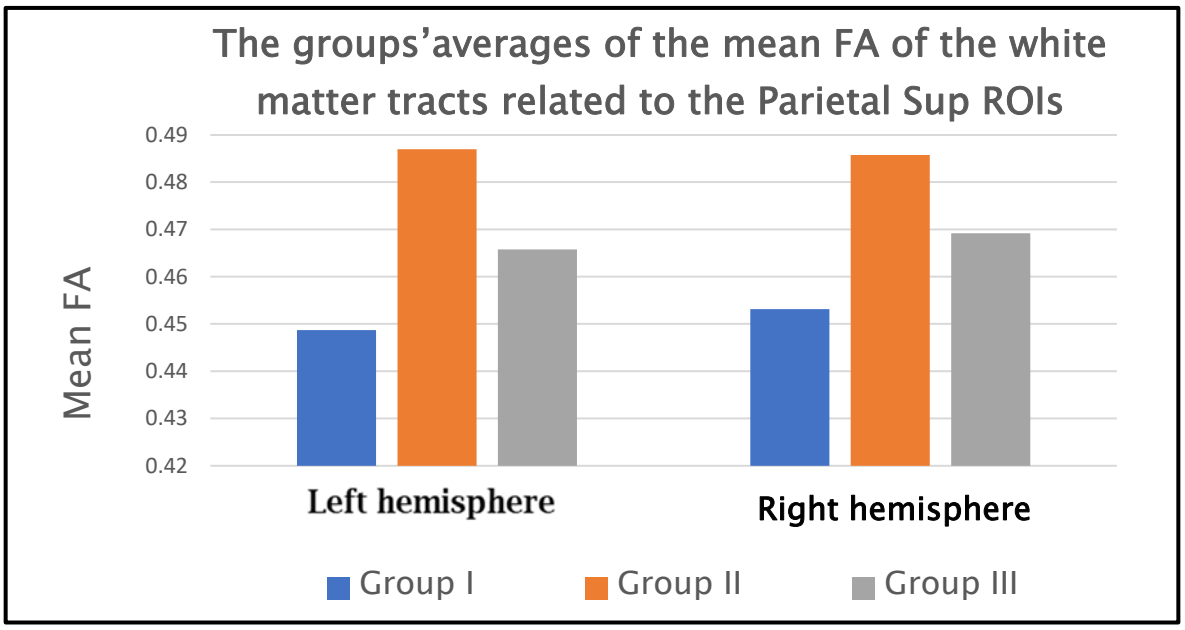

Figure 235: The mean fractional anisotropy (FA) averages of each group of the white matter tracts related to the Parietal Sup ROIs in the left and the right hemispheres.

Table 256: The mean fractional anisotropy (FA) averages and standard deviations (SD) values for the groups studied of the white matter tracts related to the Parietal Sup ROIs, along with intergroup comparisons.

	Left Hemisphere	Right Hemisphere
Heavy users' group (G. I)	(0,44868±0,0428)	(0,45314±0,0455)
Light users' group (G. II)	(0,4869±0,0436)	(0,485±0,027)
Non-users' group (G.III)	(0,4657±0,00897)	(0,469±0,0164)
Intergroup comparison	G. II > G.III > G. I	G. II > G.III > G. I

➢ **SupraMarginal**

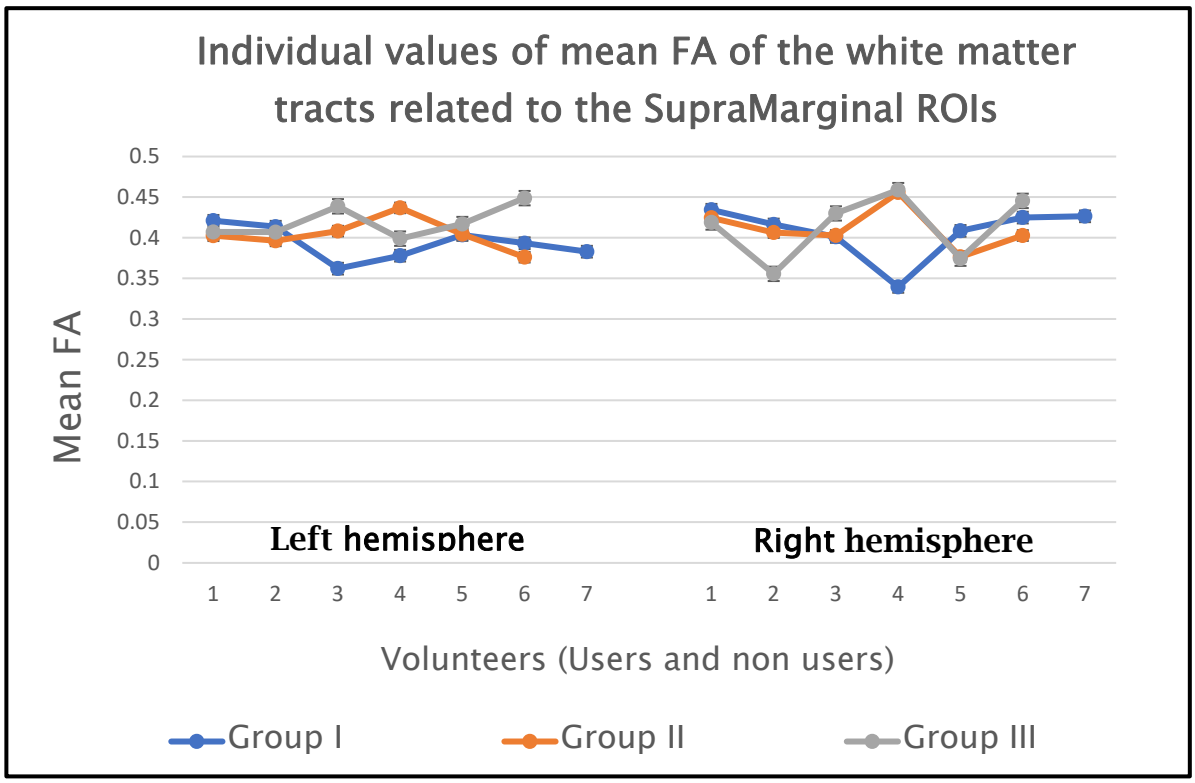

Figure 236: Individual values of mean fractional anisotropy (FA) in both hemispheres' white matter tracts related to the SupraMarginal ROIs. This figure depicts the FA values of all the participants belonging to each of the three groups (Heavy and light users and healthy controls).

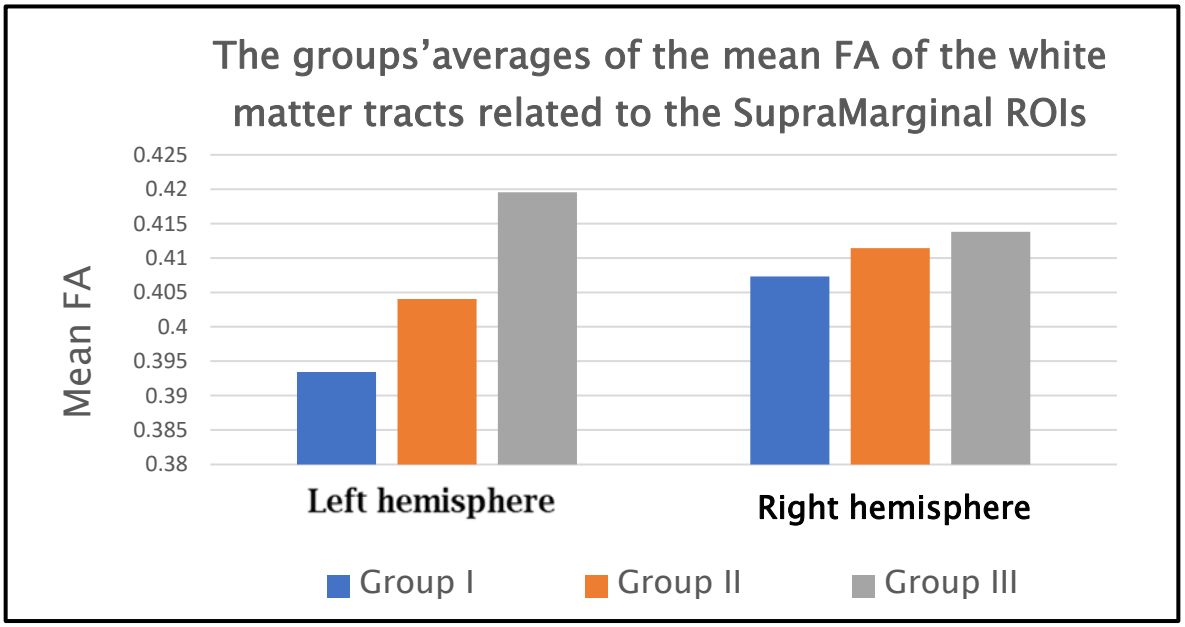

Figure 237: The mean fractional anisotropy (FA) averages of each group of the white matter tracts related to the SupraMarginal ROIs in the left and the right hemispheres.

Table 257: The mean fractional anisotropy (FA) averages and standard deviations (SD) values for the groups studied of the white matter tracts related to the SupraMarginal ROIs, along with intergroup comparisons.

	Left Hemisphere	Right Hemisphere
Heavy users' group (G. I)	(0,393±0,0208)	(0,4073± 0,0319)
Light users' group (G. II)	(0,404±0,0196)	(0,4114± 0,0265)
Non-users' group (G.III)	(0,4195±0,0198)	(0,41379± 0,04058)
Intergroup comparison	G.III > G. II > G. I	G.III ≈ G. I ≈ G. II

➢ Angular

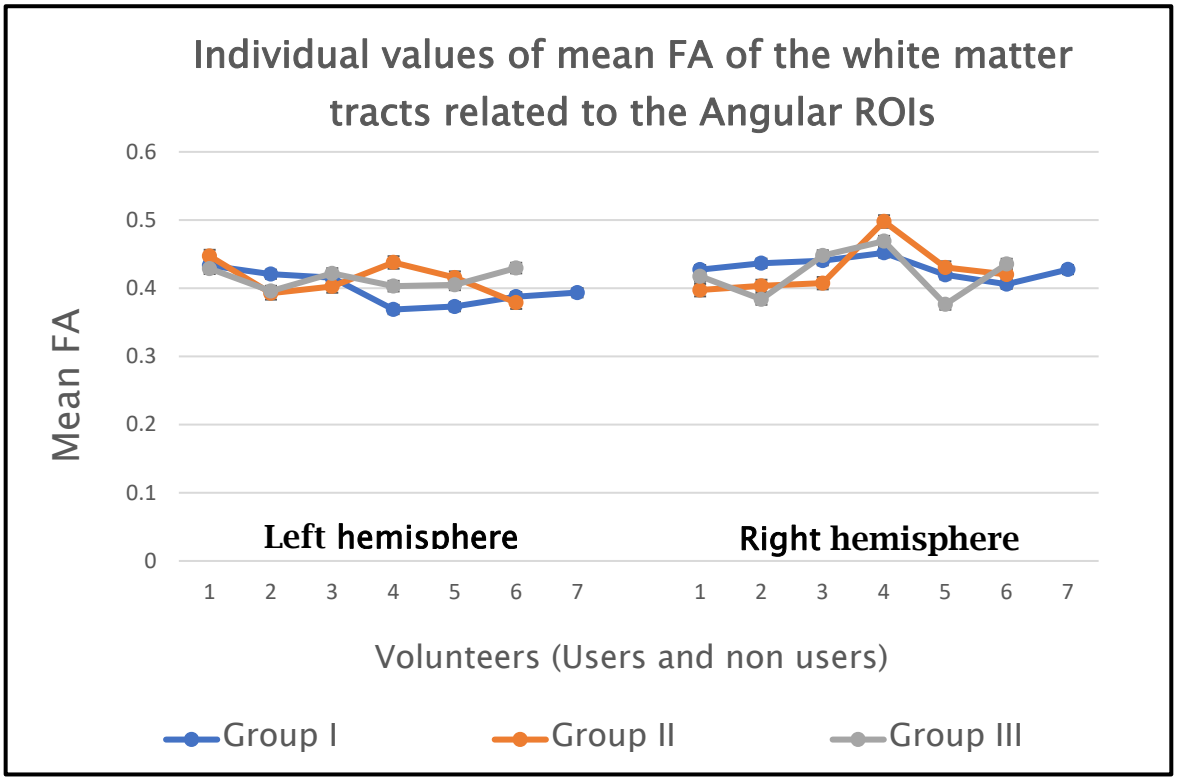

Figure 238: Individual values of mean fractional anisotropy (FA) in both hemispheres' white matter tracts related to the Angular ROIs. This figure depicts the FA values of all the participants belonging to each of the three groups (Heavy and light users and healthy controls).

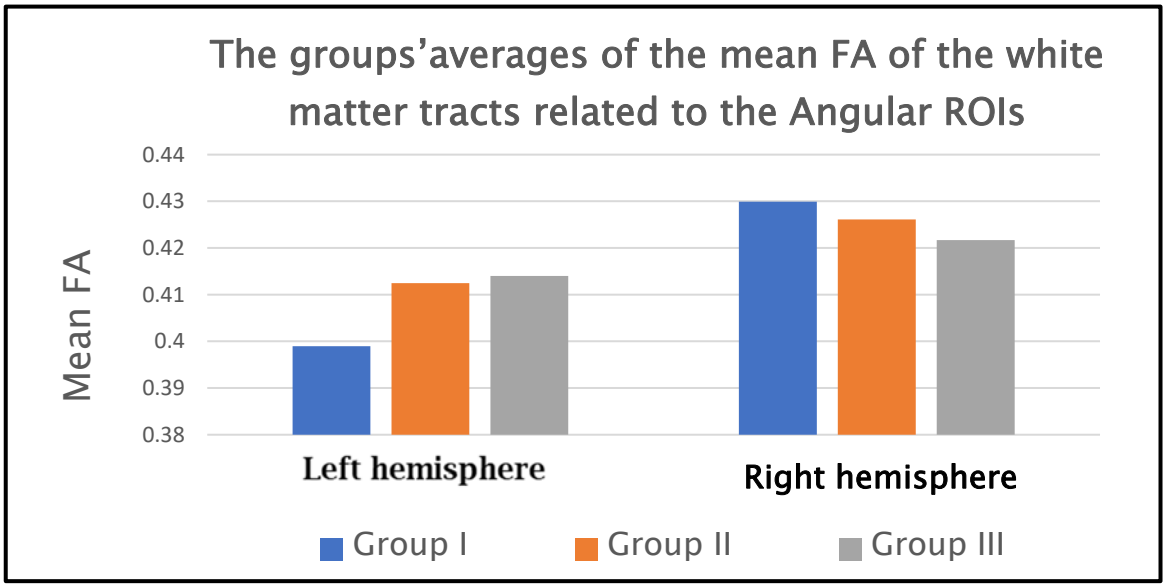

Figure 239: The mean fractional anisotropy (FA) averages of each group of the white matter tracts related to the Angular ROIs in the left and the right hemispheres.

Table 258: The mean fractional anisotropy (FA) averages and standard deviations (SD) values for the groups studied of the white matter tracts related to the Angular ROIs, along with intergroup comparisons.

	Left Hemisphere	Right Hemisphere
Heavy users' group (G. I)	(0,3989±0,0247)	(0,4299±0,0149)
Light users' group (G. II)	(0,41247±0,02636)	(0,4261±0,03719)
Non-users' group (G.III)	(0,41398±0,0145)	(0,42167±0,03649)
Intergroup comparison	G.III ≈ G. II > G. I	G.III ≈ G. I ≈ G. II

➢ **Parietal Inf**

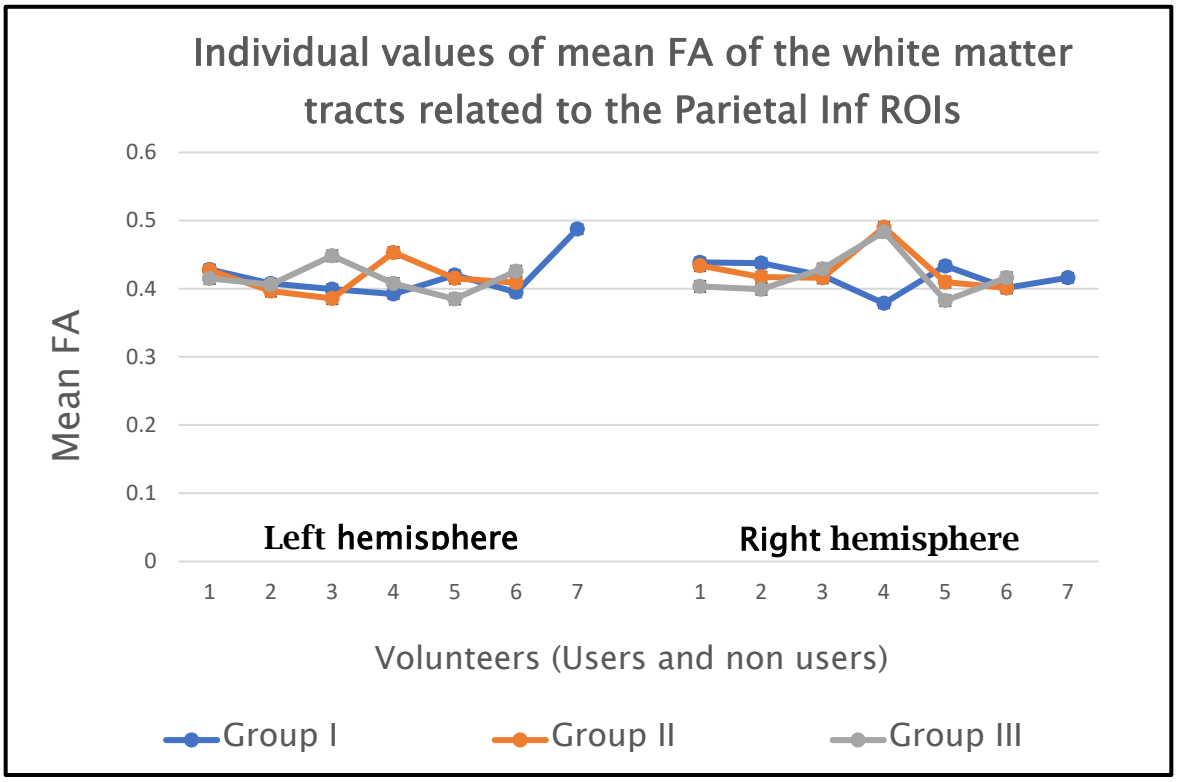

Figure 240: Individual values of mean fractional anisotropy (FA) in both hemispheres' white matter tracts related to the Parietal Inf ROIs. This figure depicts the FA values of all the participants belonging to each of the three groups (Heavy and light users and healthy controls).

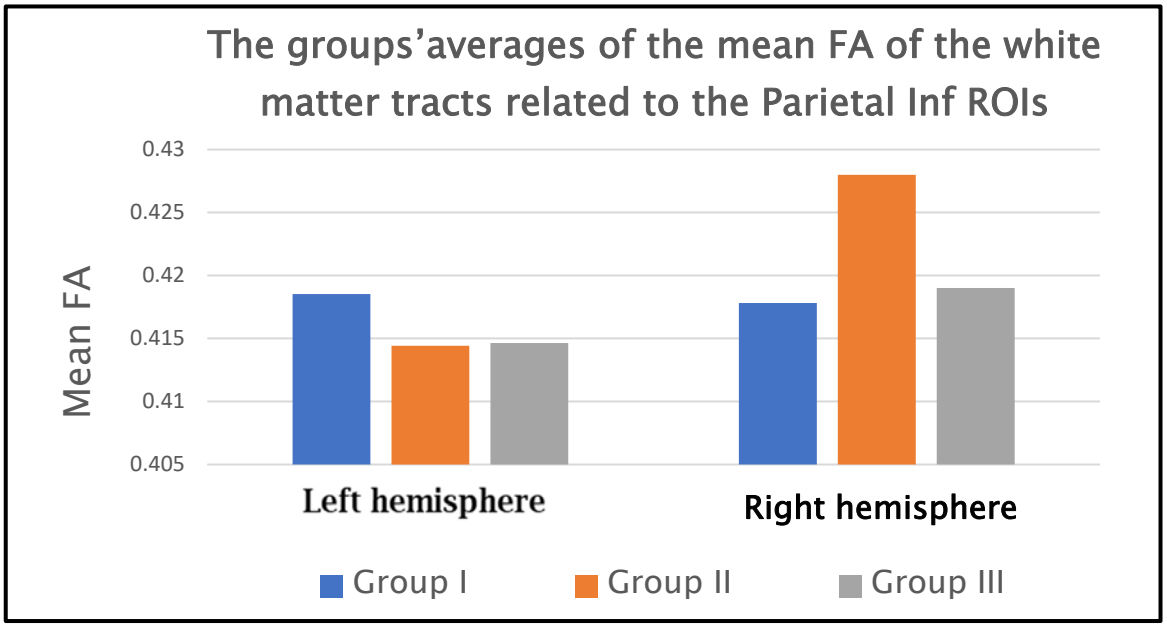

Figure 241: The mean fractional anisotropy (FA) averages of each group of the white matter tracts related to the Parietal Inf ROIs in the left and the right hemispheres.

Table 259: The mean fractional anisotropy (FA) averages and standard deviations (SD) values for the groups studied of the white matter tracts related to the Parietal Inf ROIs, along with intergroup comparisons.

	Left Hemisphere	Right Hemisphere
Heavy users' group (G. I)	(0,4185±0,033169)	(0,4178±0,02187)
Light users' group (G. II)	(0,4144±0,02384)	(0,42799±0,03226)
Non-users' group (G.III)	(0,4146±0,021248)	(0,419±0,0353)
Intergroup comparison	G.III ≈ G. I ≈ G. II	G. II > G.III ≈ G. I

➢ **Precuneus**

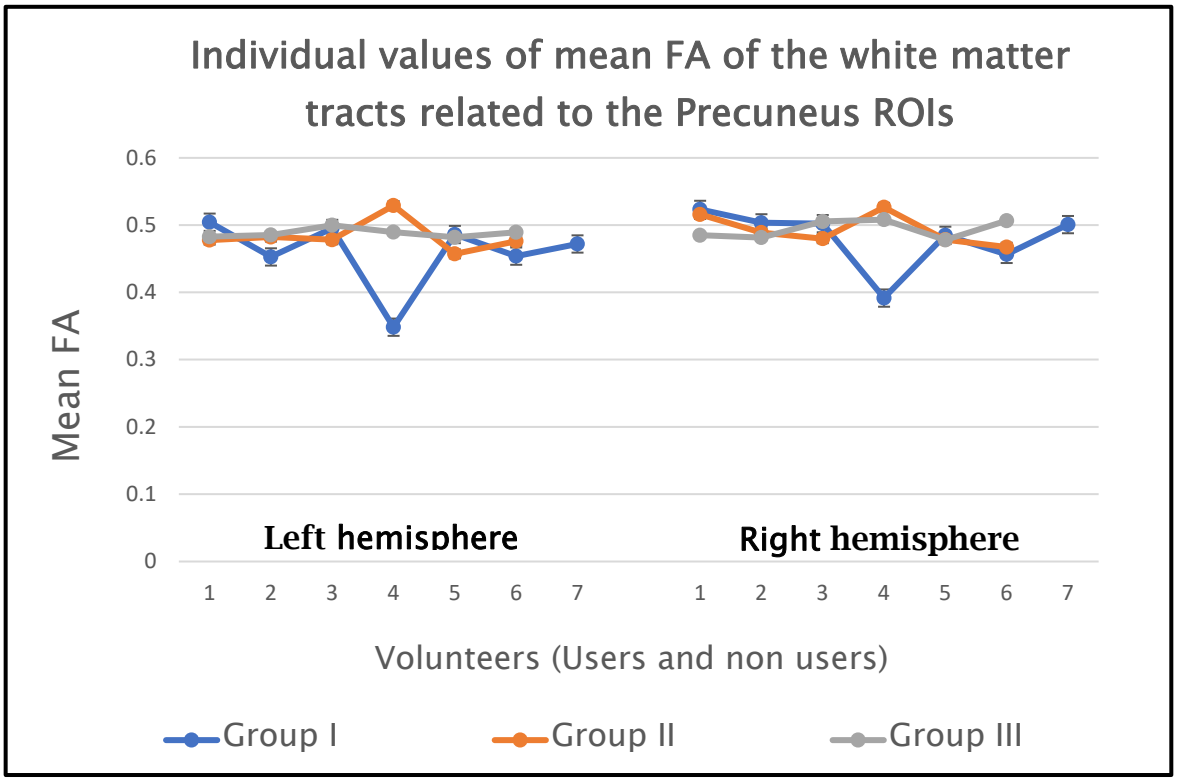

Figure 242: Individual values of mean fractional anisotropy (FA) in both hemispheres' white matter tracts related to the Precuneus ROIs. This figure depicts the FA values of all the participants belonging to each of the three groups (Heavy and light users and healthy controls).

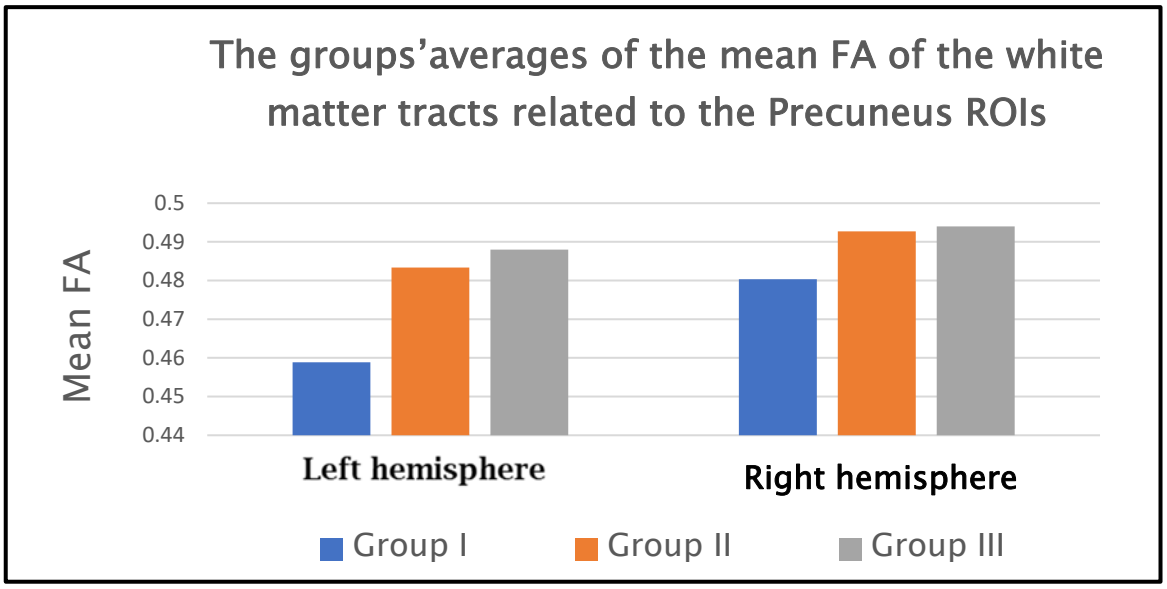

Figure 243: The mean fractional anisotropy (FA) averages of each group of the white matter tracts related to the Precuneus ROIs in the left and the right hemispheres.

Table 260: The mean fractional anisotropy (FA) averages and standard deviations (SD) values for the groups studied of the white matter tracts related to the Parietal Inf ROIs, along with intergroup comparisons.

	Left Hemisphere	Right Hemisphere
Heavy users' group (G. I)	(0,4588±0,0525)	(0,48033±0,04422)
Light users' group (G. II)	(0,4833±0,024)	(0,49268±0,02326)
Non-users' group (G.III)	(0,4879±0,0065)	(0,49398±0,01400)
Intergroup comparison	G.III ≈ G. II > G. I	G. II ≈ G.III > G. I

➢ **Temporal Sup**

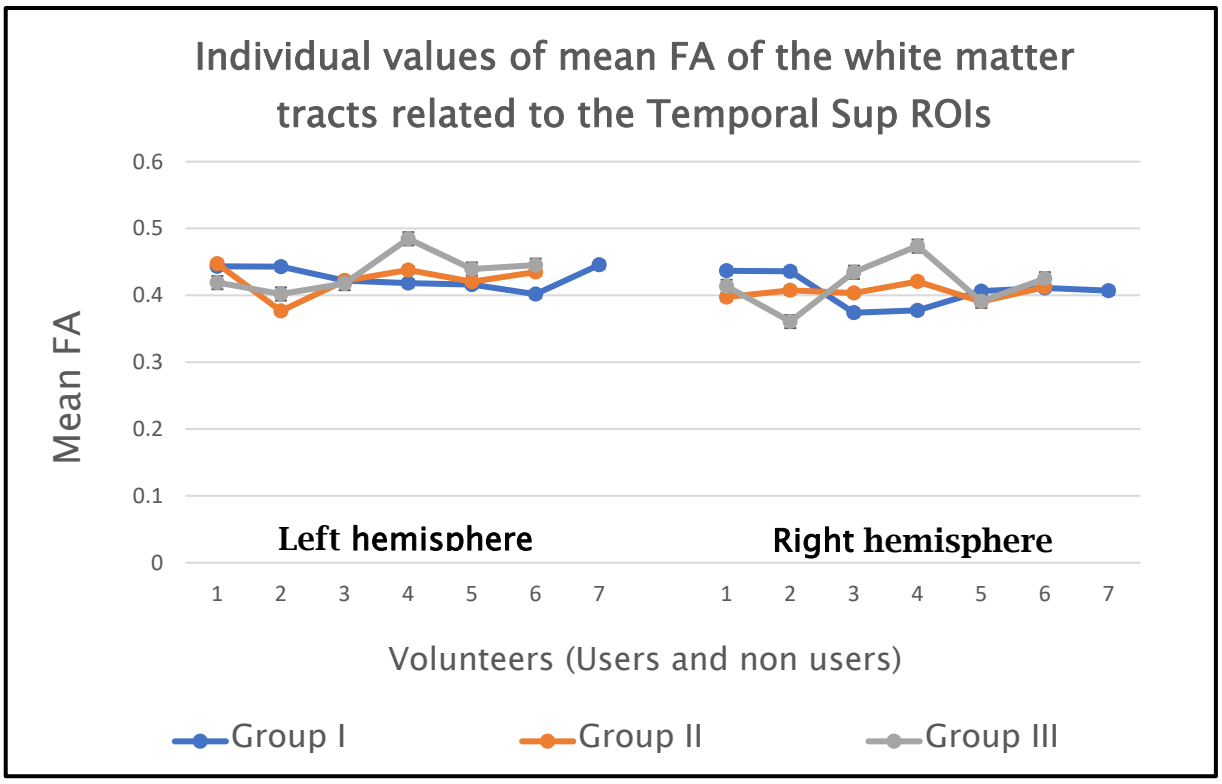

Figure 244: Individual values of mean fractional anisotropy (FA) in both hemispheres' white matter tracts related to the Temporal Sup ROIs. This figure depicts the FA values of all the participants belonging to each of the three groups (Heavy and light users and healthy controls).

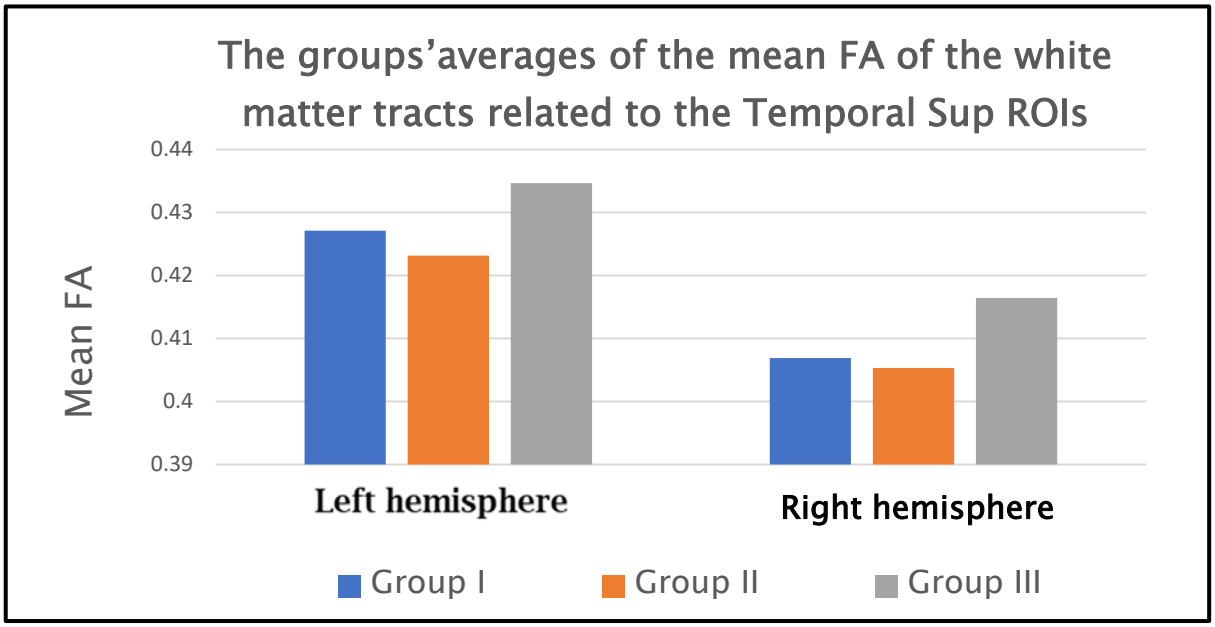

Figure 245: The mean fractional anisotropy (FA) averages of each group of the white matter tracts related to the Temporal Sup ROIs in the left and the right hemispheres.

Table 261: The mean fractional anisotropy (FA) averages and standard deviations (SD) values for the groups studied of the white matter tracts related to the Parietal Inf ROIs, along with intergroup comparisons.

	Left Hemisphere	Right Hemisphere
Heavy users' group (G. I)	(0,4271±0,0169)	(0,4068±0,02477)
Light users' group (G. II)	(0,423138±0,0249)	(0,4053±0,010728)
Non-users' group (G.III)	(0,4346±0,0291)	(0,4164±0,03857)
Intergroup comparison	G.III > G. II ≈ G. I	G.III > G. II ≈ G. I

➢ Temporal Pole Sup

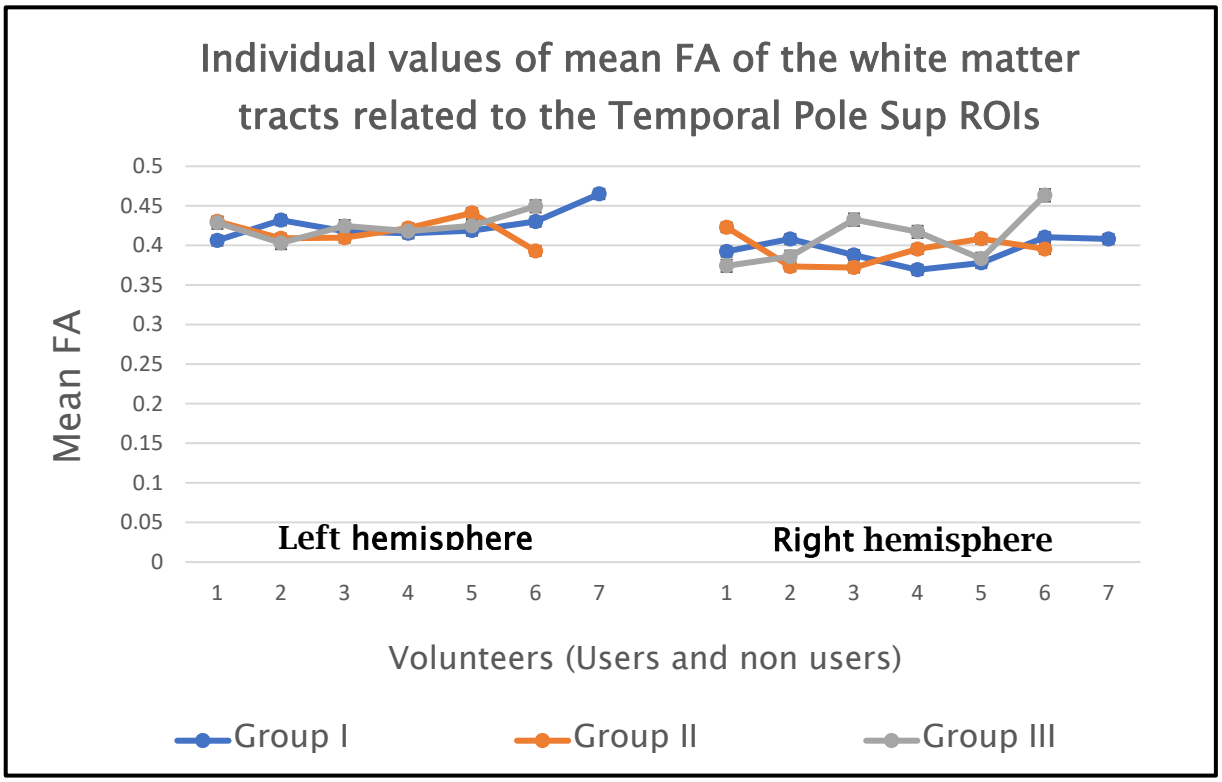

Figure 246: Individual values of mean fractional anisotropy (FA) in both hemispheres' white matter tracts related to the Temporal Pole Sup ROIs. This figure depicts the FA values of all the participants belonging to each of the three groups (Heavy and light users and healthy controls).

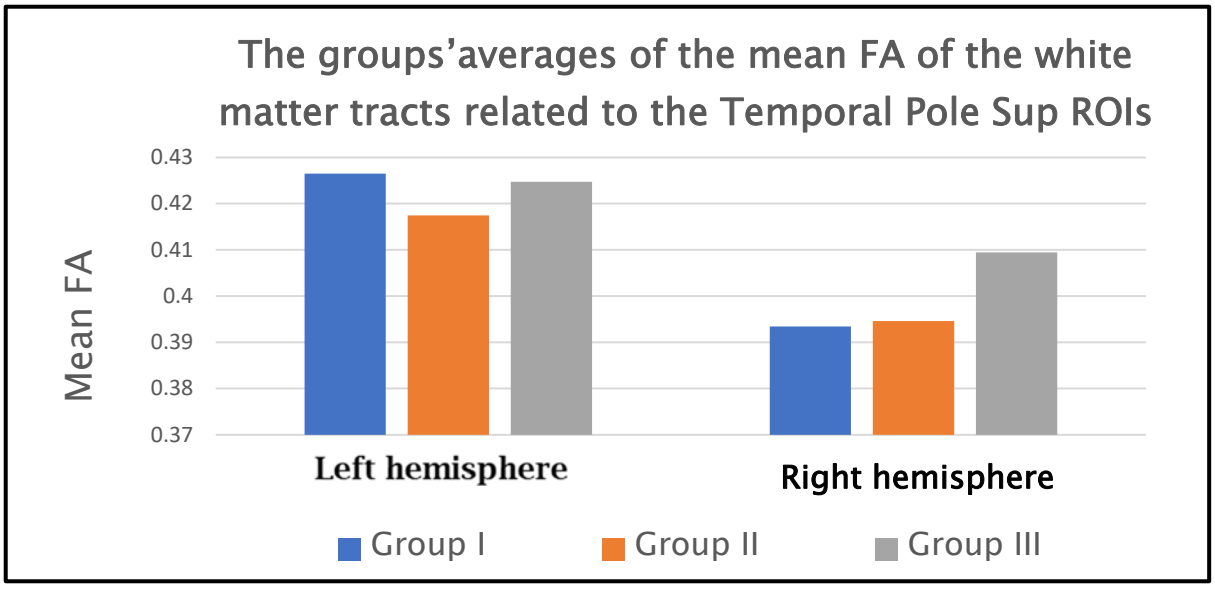

Figure 247: The mean fractional anisotropy (FA) averages of each group of the white matter tracts related to the Temporal Pole Sup ROIs in the left and the right hemispheres.

Table 262: The mean fractional anisotropy (FA) averages and standard deviations (SD) values for the groups studied of the white matter tracts related to the Temporal Pole Sup ROIs, along with intergroup comparisons.

	Left Hemisphere	Right Hemisphere
Heavy users' group (G. I)	(0,4264±0,01917)	(0,3934±0,01619)
Light users' group (G. II)	(0,4174±0,01714)	(0,39457±0,0197)
Non-users' group (G.III)	(0,42472±0,01511)	(0,4094±0,0346)
Intergroup comparison	G.III ≈ G. I > G. II	G.III > G. II ≈ G. I

➢ **Heschl**

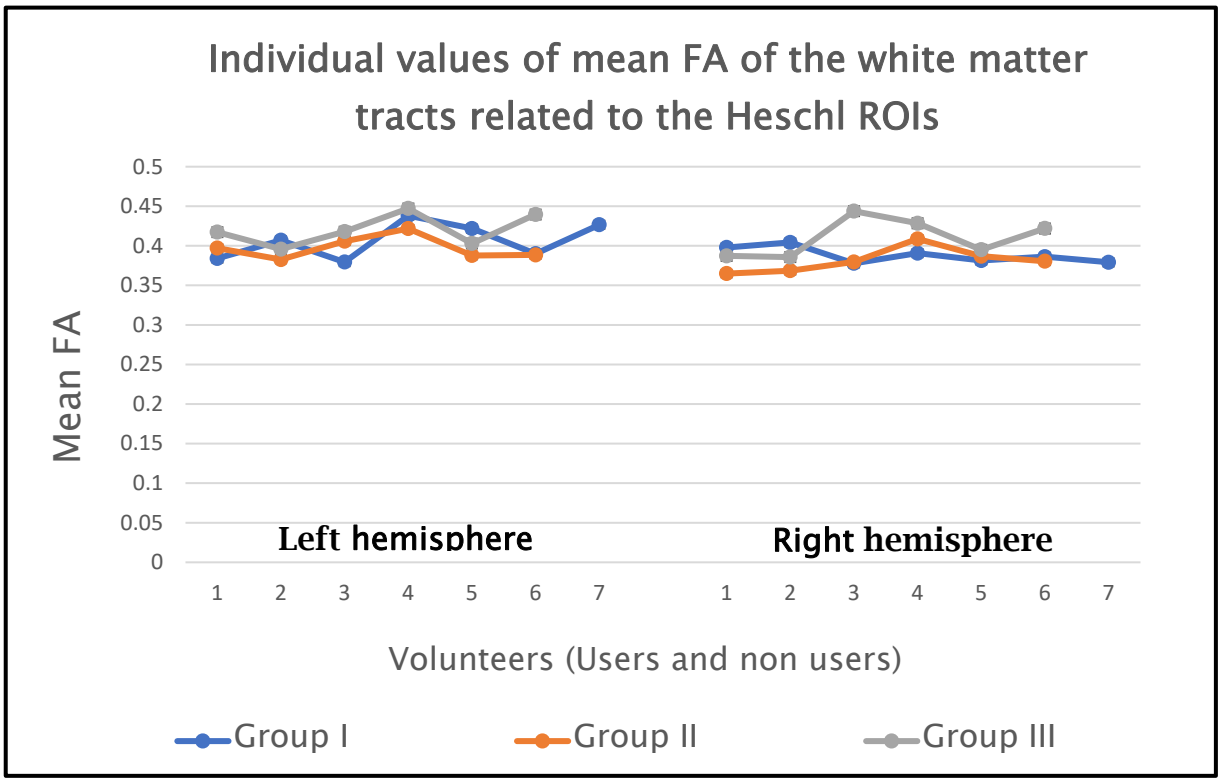

Figure 248: Individual values of mean fractional anisotropy (FA) in both hemispheres' white matter tracts related to the Heschl ROIs. This figure depicts the FA values of all the participants belonging to each of the three groups (Heavy and light users and healthy controls).

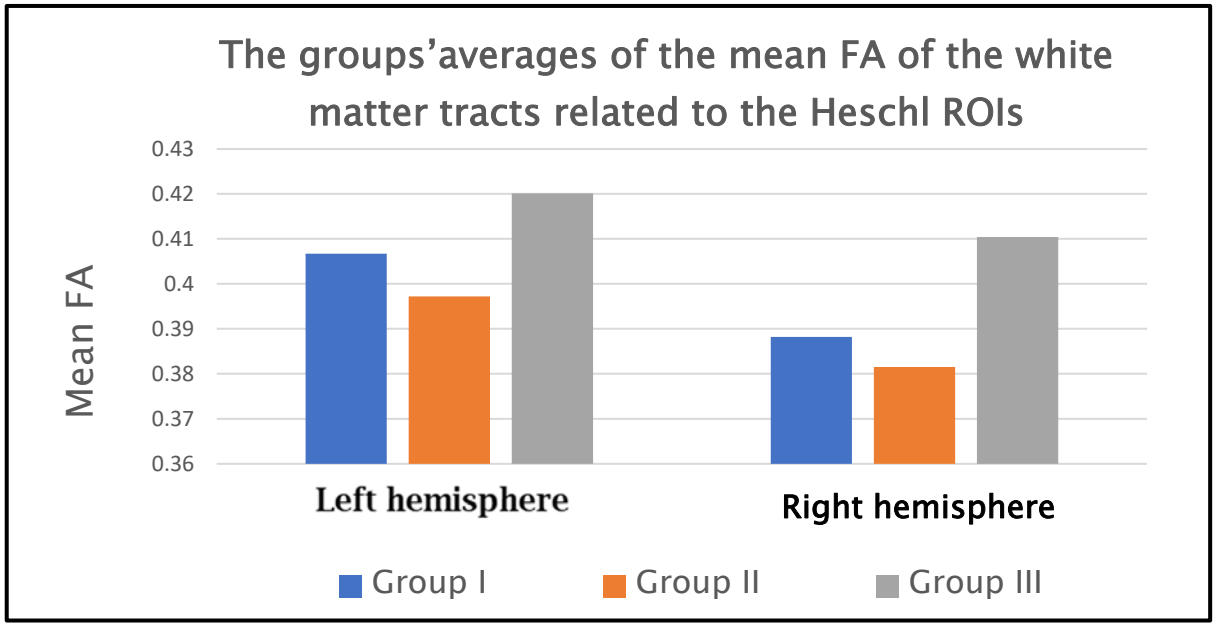

Figure 249: The mean fractional anisotropy (FA) averages of each group of the white matter tracts related to the Heschl ROIs in the left and the right hemispheres.

Table 263: The mean fractional anisotropy (FA) averages and standard deviations (SD) values for the groups studied of the white matter tracts related to the Heschl ROIs, along with intergroup comparisons.

	Left Hemisphere	Right Hemisphere
Heavy users' group (G. I)	(0,40669±0,0229)	(0,388193±0,00996)
Light users' group (G. II)	(0,397±0,0145)	(0,38149±0,0156138)
Non-users' group (G.III)	(0,42009±0,02011)	(0,41038±0,0243)
Intergroup comparison	G.III > G. I > G. II	G.III > G. I > G. II

➢ Temporal Mid

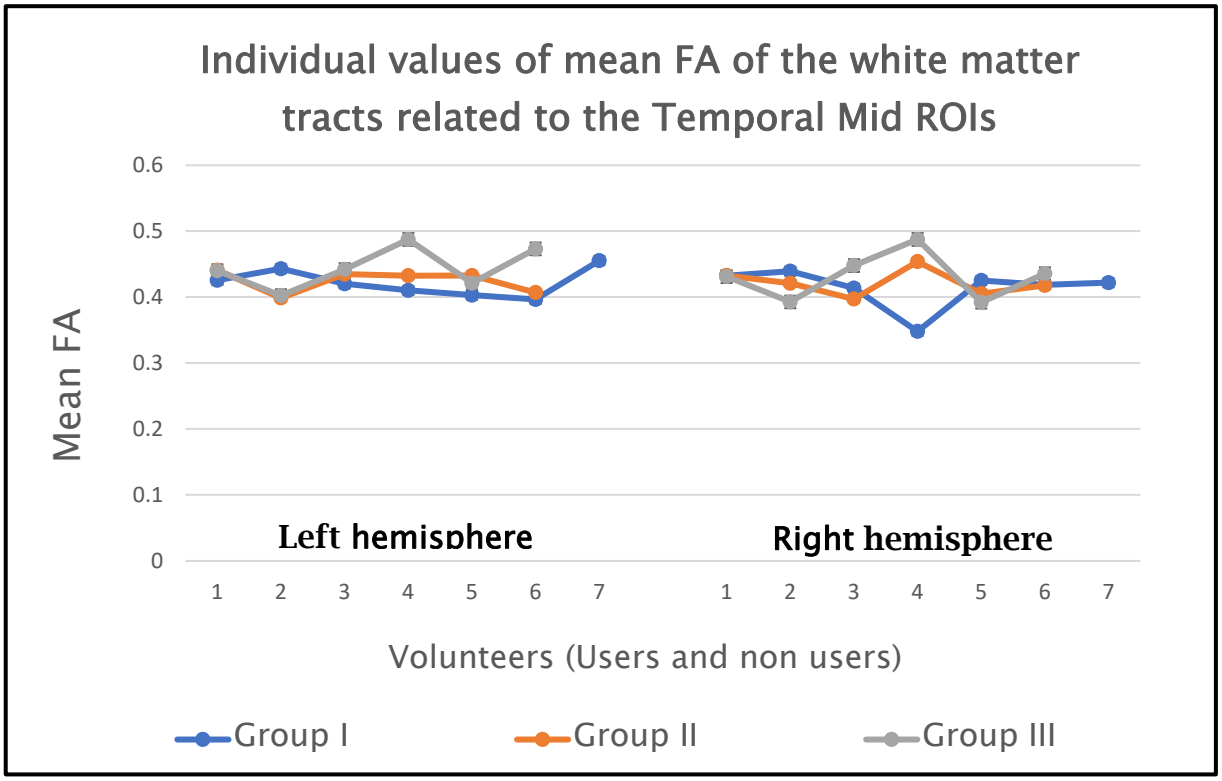

Figure 250: Individual values of mean fractional anisotropy (FA) in both hemispheres' white matter tracts related to the Temporal Mid ROIs. This figure depicts the FA values of all the participants belonging to each of the three groups (Heavy and light users and healthy controls).

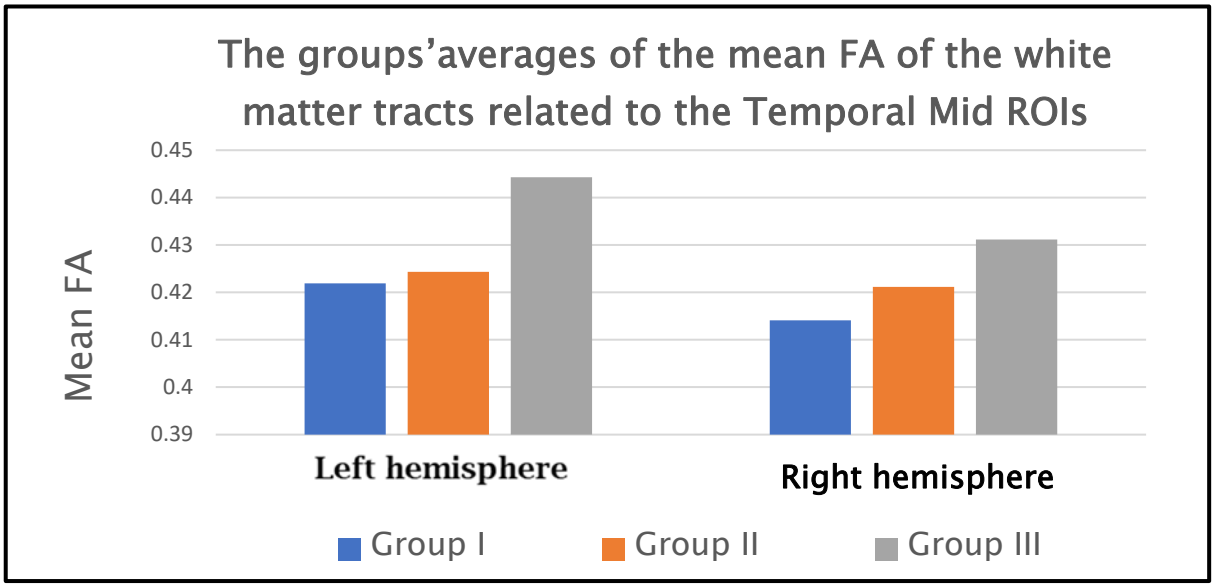

Figure 251: The mean fractional anisotropy (FA) averages of each group of the white matter tracts related to the Temporal Mid ROIs in the left and the right hemispheres.

Table 264: The mean fractional anisotropy (FA) averages and standard deviations (SD) values for the groups studied of the white matter tracts related to the Temporal Mid ROIs, along with intergroup comparisons.

	Left Hemisphere	Right Hemisphere
Heavy users' group (G. I)	(0,42187±0,021307)	(0,4141±0,03035)
Light users' group (G. II)	(0,424326±0,017164)	(0,42116±0,020188)
Non-users' group (G.III)	(0,44429±0,031648)	(0,43113±0,03595)
Intergroup comparison	G.III > G. I ≈ G. II	G.III > G. II > G. I

➢ **Temporal Pole Mid**

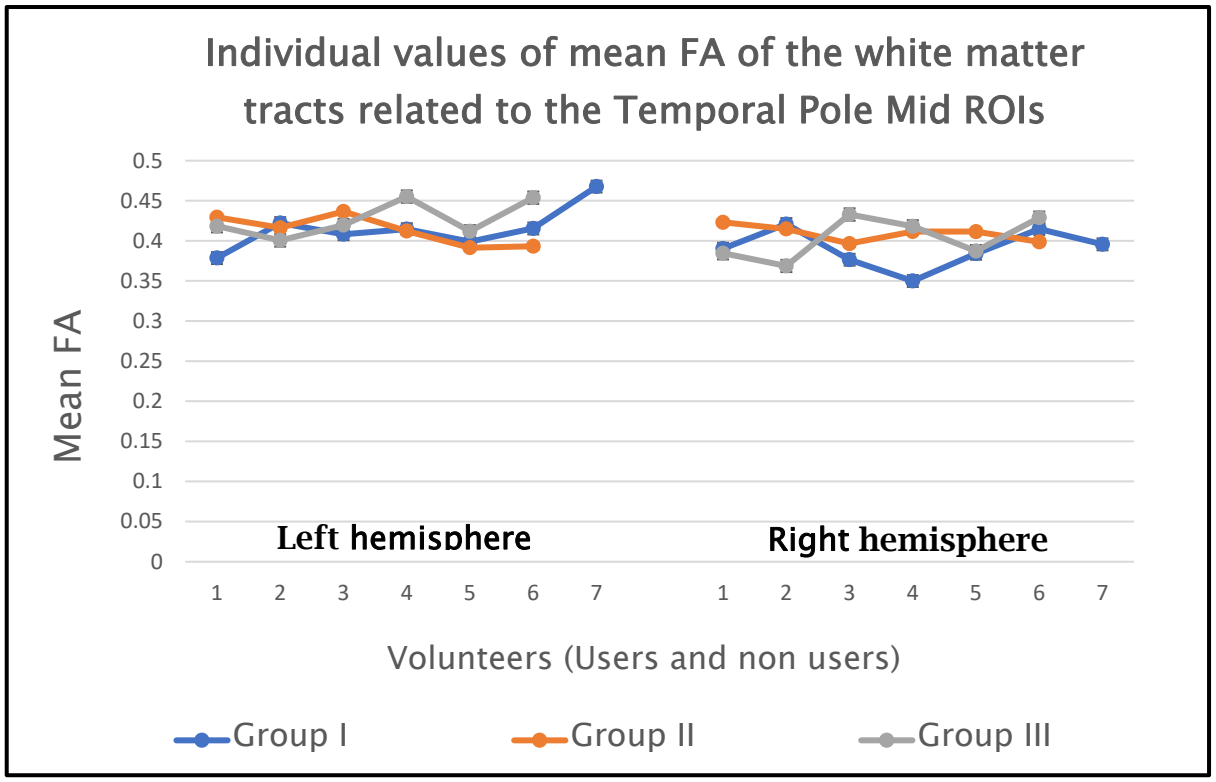

Figure 252: Individual values of mean fractional anisotropy (FA) in both hemispheres' white matter tracts related to the Temporal Pole Mid ROIs. This figure depicts the FA values of all the participants belonging to each of the three groups (Heavy and light users and healthy controls).

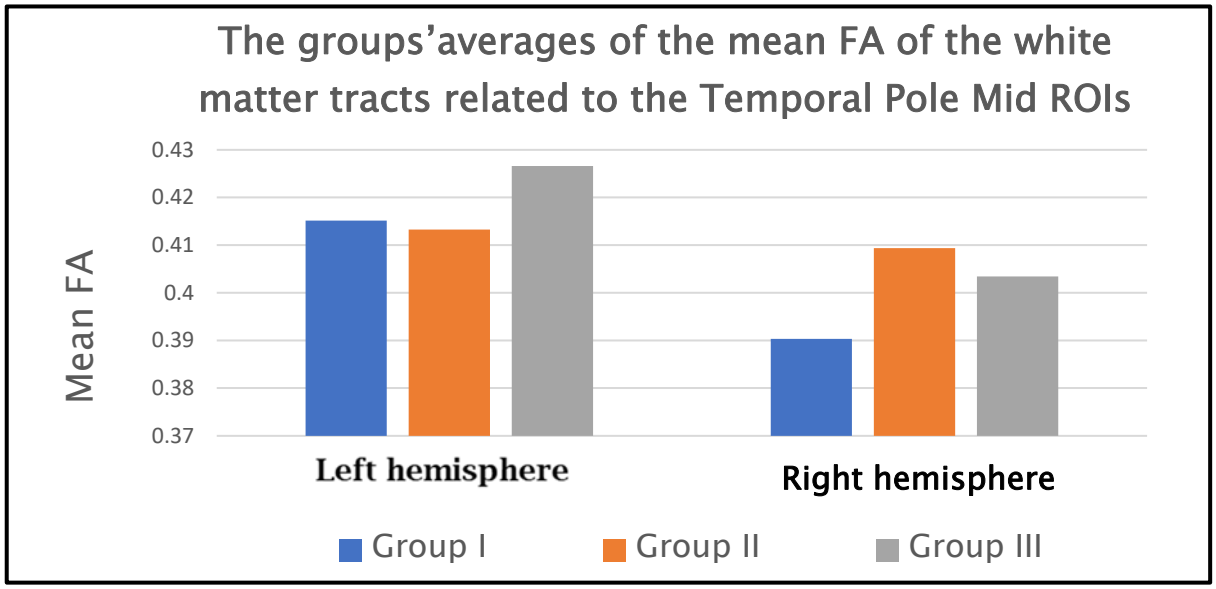

Figure 253: The mean fractional anisotropy (FA) averages of each group of the white matter tracts related to the Temporal Pole Mid ROIs in the left and the right hemispheres.

Table 265: The mean fractional anisotropy (FA) averages and standard deviations (SD) values for the groups studied of the white matter tracts related to the Temporal Pole Mid ROIs, along with intergroup comparisons.

	Left Hemisphere	Right Hemisphere
Heavy users' group (G. I)	(0,415±0,027)	(0,39032±0,02386)
Light users' group (G. II)	(0,4132±0,01838)	(0,4093±0,01006)
Non-users' group (G.III)	(0,42656±0,02266)	(0,4034±0,02666)
Intergroup comparison	G.III > G. I ≈ G. II	G. II > G.III > G. I

➢ Temporal Inf

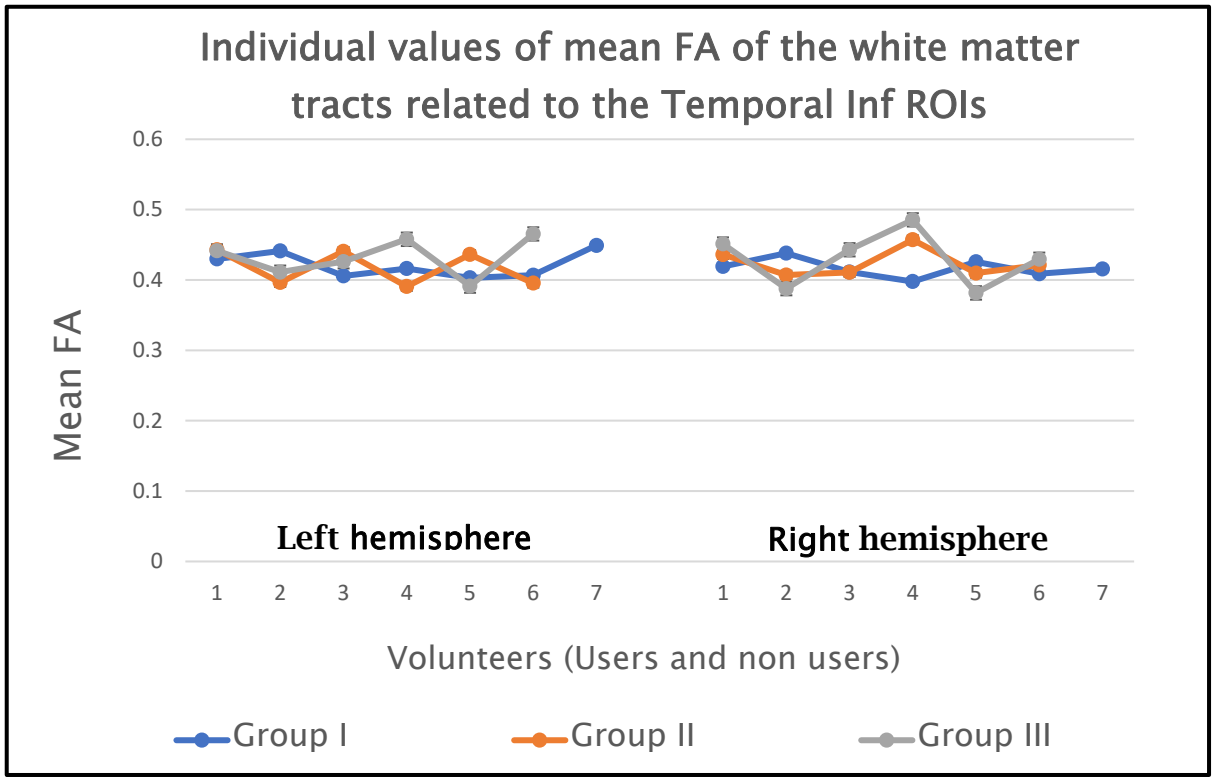

Figure 254: Individual values of mean fractional anisotropy (FA) in both hemispheres' white matter tracts related to the Temporal Inf ROIs. This figure depicts the FA values of all the participants belonging to each of the three groups (Heavy and light users and healthy controls).

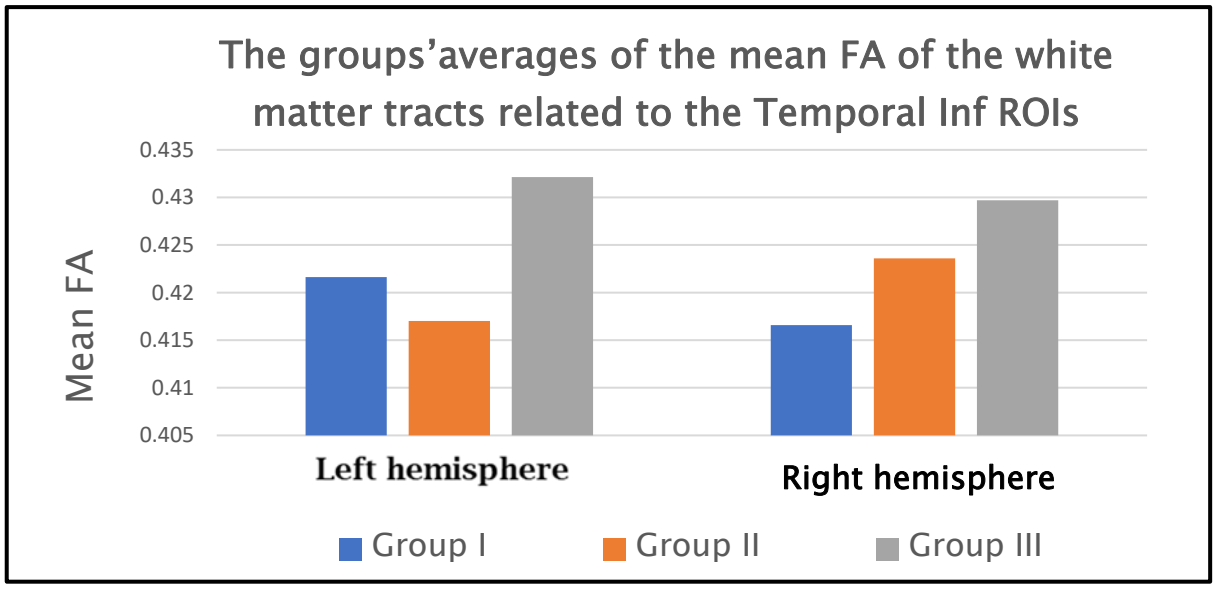

Figure 256: The mean fractional anisotropy (FA) averages of each group of the white matter tracts related to the Temporal Inf Sup ROIs in the left and the right hemispheres.

Table 266: The mean fractional anisotropy (FA) averages and standard deviations (SD) values for the groups studied of the white matter tracts related to the Temporal Inf ROIs, along with intergroup comparisons.

	Left Hemisphere	Right Hemisphere
Heavy users' group (G. I)	(0,4216±0,01849)	(0,4165±0,01287)
Light users' group (G. II)	(0,417±0,025146)	(0,42359±0,0196)
Non-users' group (G.III)	(0,43214±0,02828)	(0,42969±0,0395)
Intergroup comparison	G.III > G. I > G. II	G.III > G. II > G. I

➢ **Fusiform**

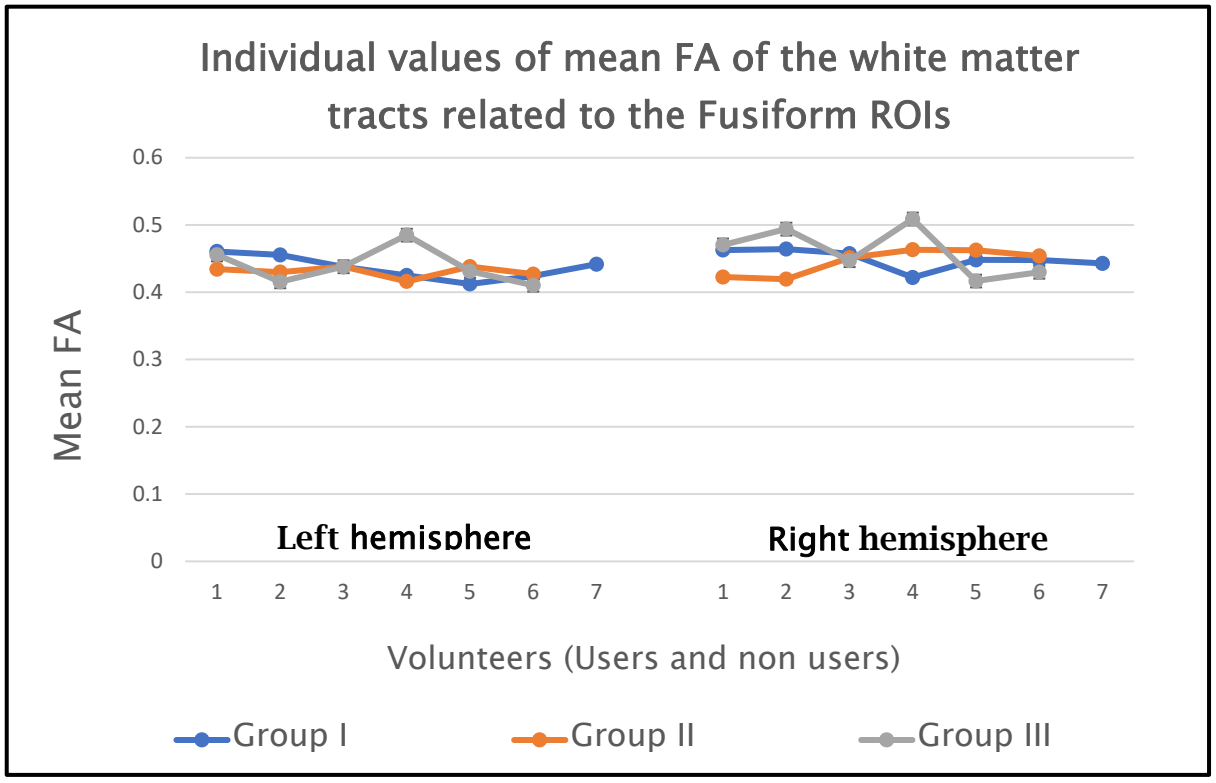

Figure 257: Individual values of mean fractional anisotropy (FA) in both hemispheres' white matter tracts related to the Fusiform ROIs. This figure depicts the FA values of all the participants belonging to each of the three groups (Heavy and light users and healthy controls).

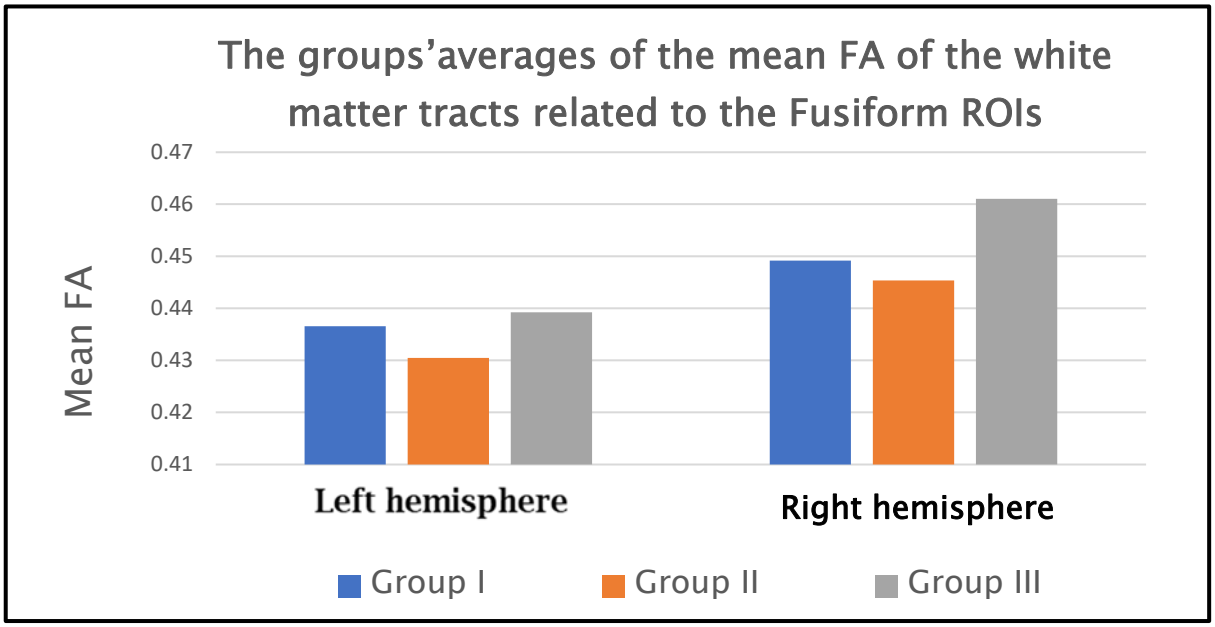

Figure 258: The mean fractional anisotropy (FA) averages of each group of the white matter tracts related to the Fusiform ROIs in the left and the right hemispheres.

Table 267: The mean fractional anisotropy (FA) averages and standard deviations (SD) values for the groups studied of the white matter tracts related to the Fusiform ROIs, along with intergroup comparisons.

	Left Hemisphere	Right Hemisphere
Heavy users' group (G. I)	(0,4365±0,0175)	(0,44917±0,01449)
Light users' group (G. II)	(0,43046±0,0083)	(0,4453±0,0195)
Non-users' group (G.III)	(0,4392±0,0276)	(0,461±0,0363)
Intergroup comparison	G.III ≈ G. I > G. II	G.III > G. II ≈ G. I

➢ Cingulum Ant

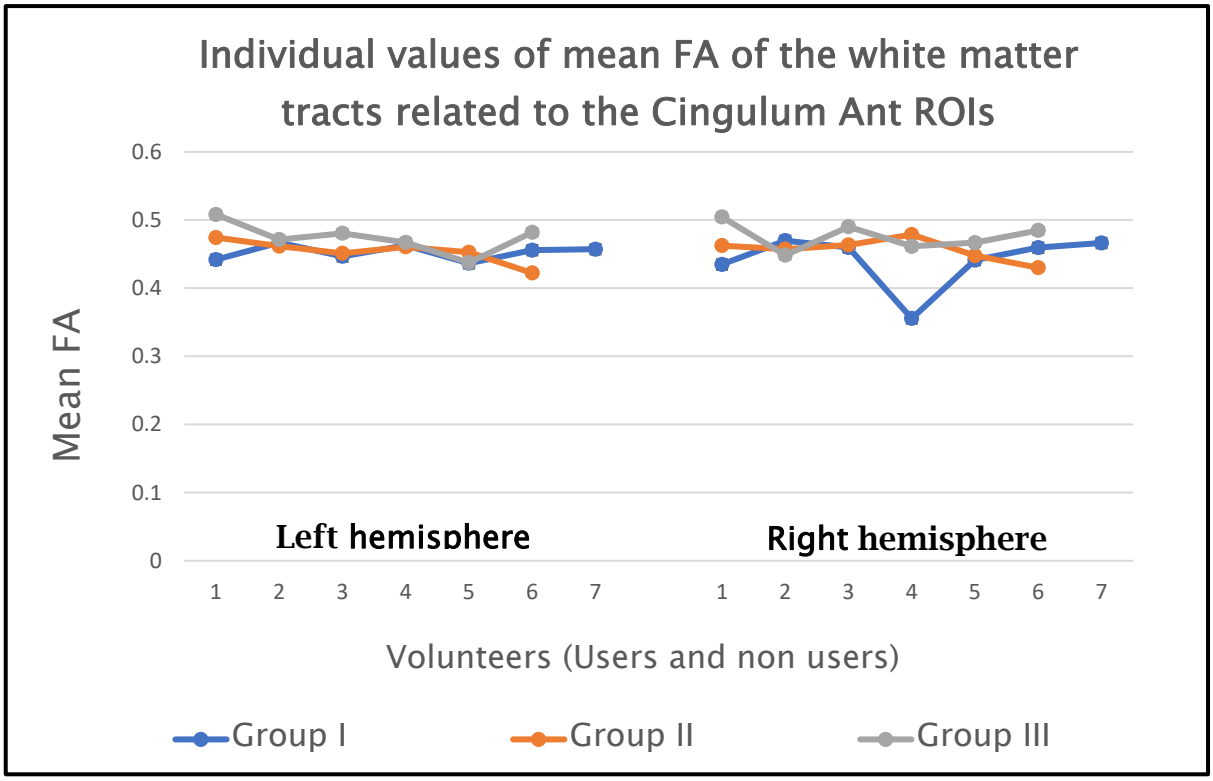

Figure 259: Individual values of mean fractional anisotropy (FA) in both hemispheres' white matter tracts related to the Cingulum Ant ROIs. This figure depicts the FA values of all the participants belonging to each of the three groups (Heavy and light users and healthy controls).

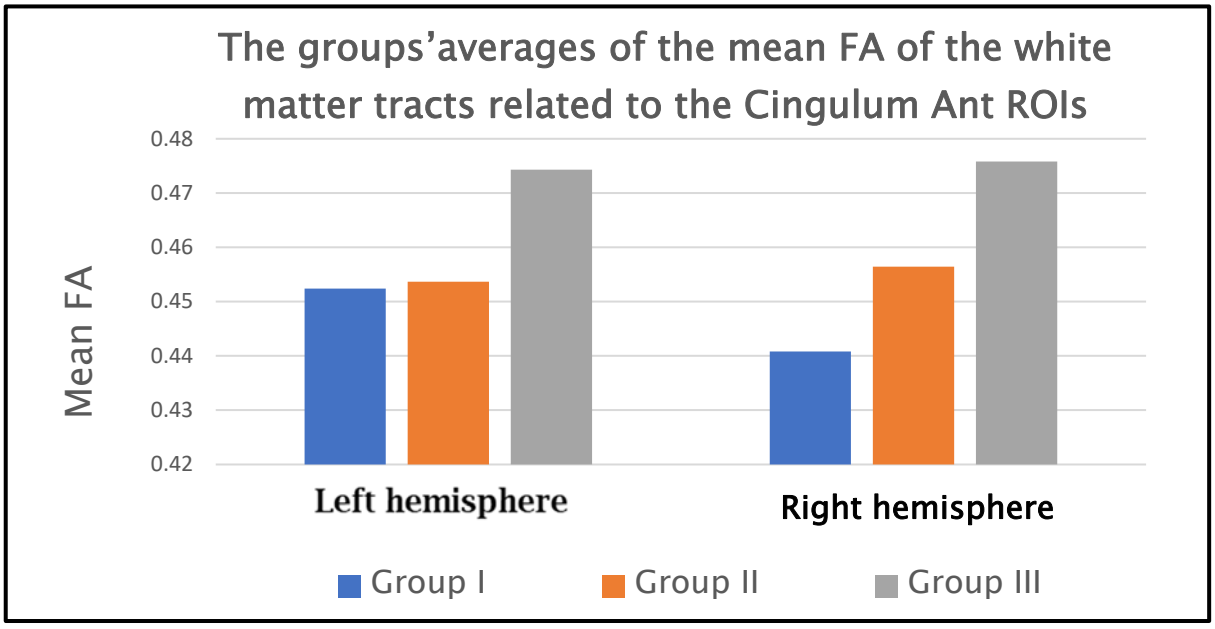

Figure 260: The mean fractional anisotropy (FA) averages of each group of the white matter tracts related to the Cingulum Ant ROIs in the left and the right hemispheres.

Table 268: The mean fractional anisotropy (FA) averages and standard deviations (SD) values for the groups studied of the white matter tracts related to the Cingulum Ant ROIs, along with intergroup comparisons.

	Left Hemisphere	Right Hemisphere
Heavy users' group (G. I)	(0,45238±0,011136)	(0,44079±0,0397)
Light users' group (G. II)	(0,4536±0,0174)	(0,4564±0,01644)
Non-users' group (G.III)	(0,4743±0,023)	(0,4758±0,020746)
Intergroup comparison	G.III > G. II ≈ G. I	G.III > G. II > G. I

➢ **Cingulum Mid**

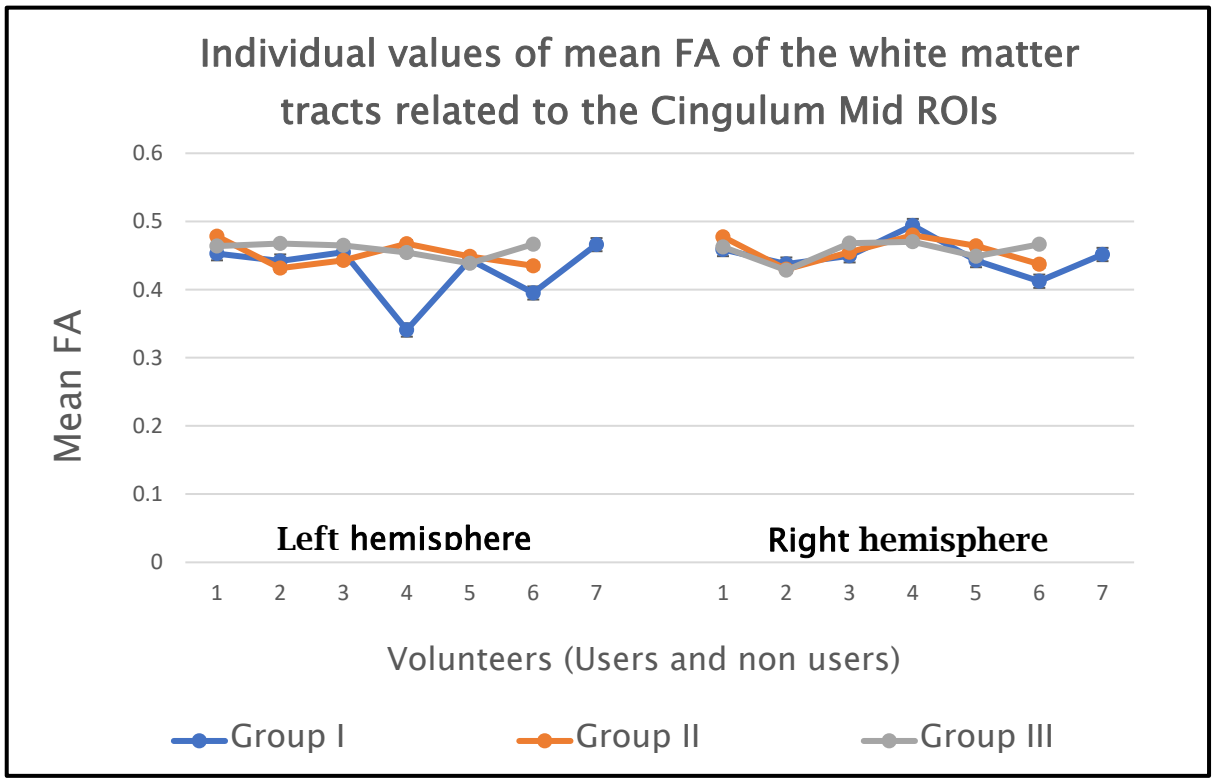

Figure 261: Individual values of mean fractional anisotropy (FA) in both hemispheres' white matter tracts related to the Cingulum Mid ROIs. This figure depicts the FA values of all the participants belonging to each of the three groups (Heavy and light users and healthy controls).

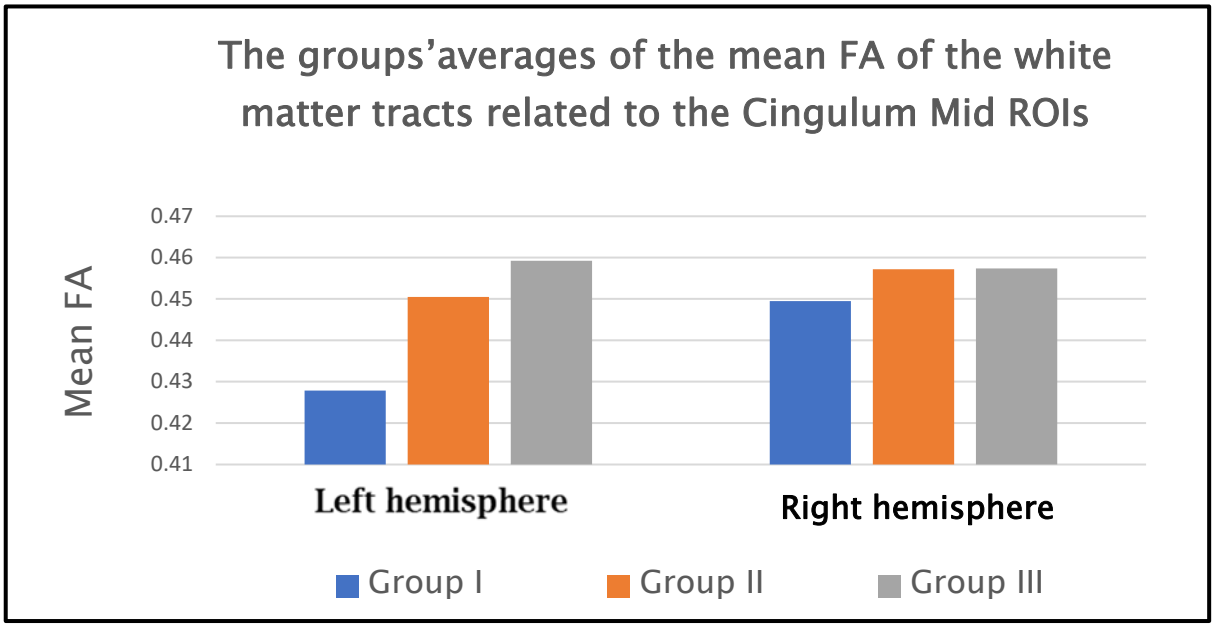

Figure 262: The mean fractional anisotropy (FA) averages of each group of the white matter tracts related to the Cingulum Mid ROIs in the left and the right hemispheres.

Table 269: The mean fractional anisotropy (FA) averages and standard deviations (SD) values for the groups studied of the white matter tracts related to the Cingulum Mid ROIs, along with intergroup comparisons.

	Left Hemisphere	Right Hemisphere
Heavy users' group (G. I)	(0,4278±0,044546)	(0,449±0,0246)
Light users' group (G. II)	(0,45046±0,0185)	(0,457178±0,02058)
Non-users' group (G.III)	(0,4592±0,01124)	(0,45737±0,01609)
Intergroup comparison	G.III > G. II > G. I	G.III ≈ G. II > G. I

➢ Cingulum Post

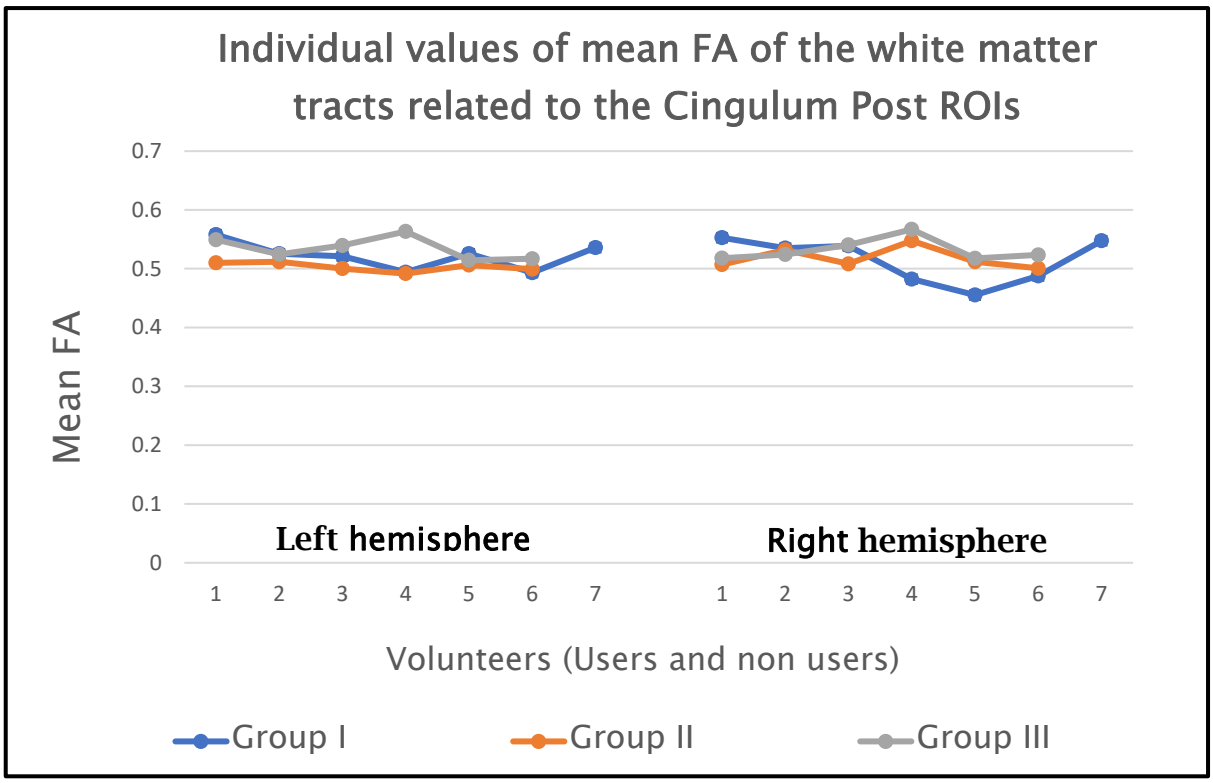

Figure 263: Individual values of mean fractional anisotropy (FA) in both hemispheres' white matter tracts related to the Cingulum Post ROIs. This figure depicts the FA values of all the participants belonging to each of the three groups (Heavy and light users and healthy controls).

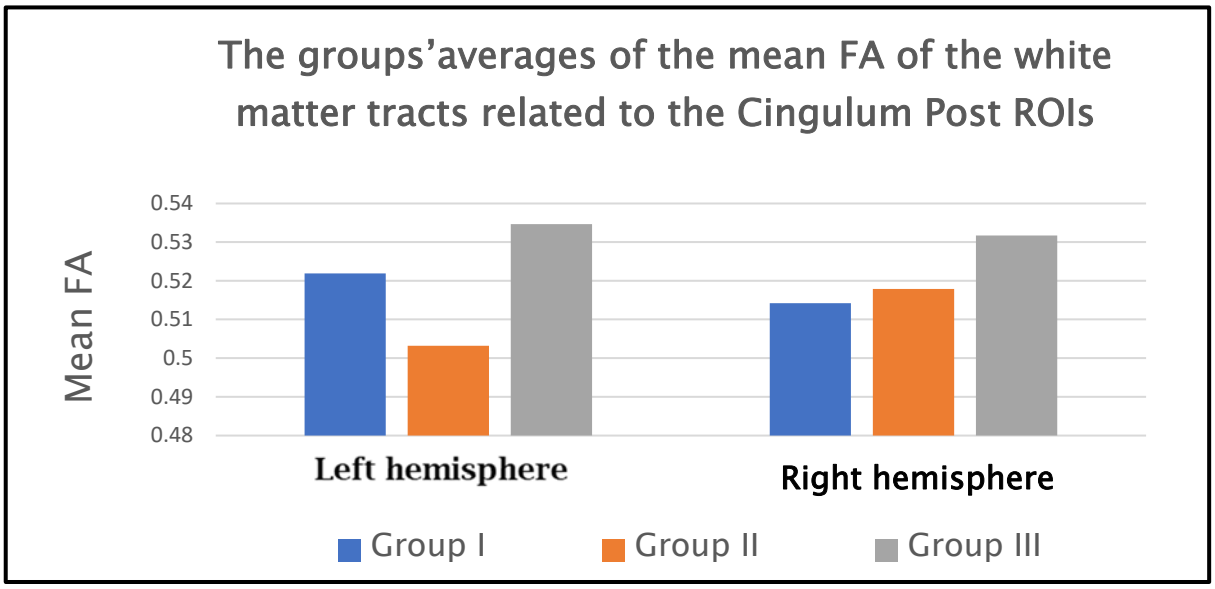

Figure 264: The mean fractional anisotropy (FA) averages of each group of the white matter tracts related to the Cingulum Post ROIs in the left and the right hemispheres.

Table 270: The mean fractional anisotropy (FA) averages and standard deviations (SD) values for the groups studied of the white matter tracts related to the Cingulum Post ROIs, along with intergroup comparisons.

	Left Hemisphere	Right Hemisphere
Heavy users' group (G. I)	(0,52188±0,0227)	(0,5142±0,0383)
Light users' group (G. II)	(0,5031±0,00749)	(0,5178±0,018068)
Non-users' group (G.III)	(0,5346±0,01946)	(0,5317±0,01913)
Intergroup comparison	G.III > G. I > G. II	G.III > G. II ≈ G. I

➢ **ParaHippocampal**

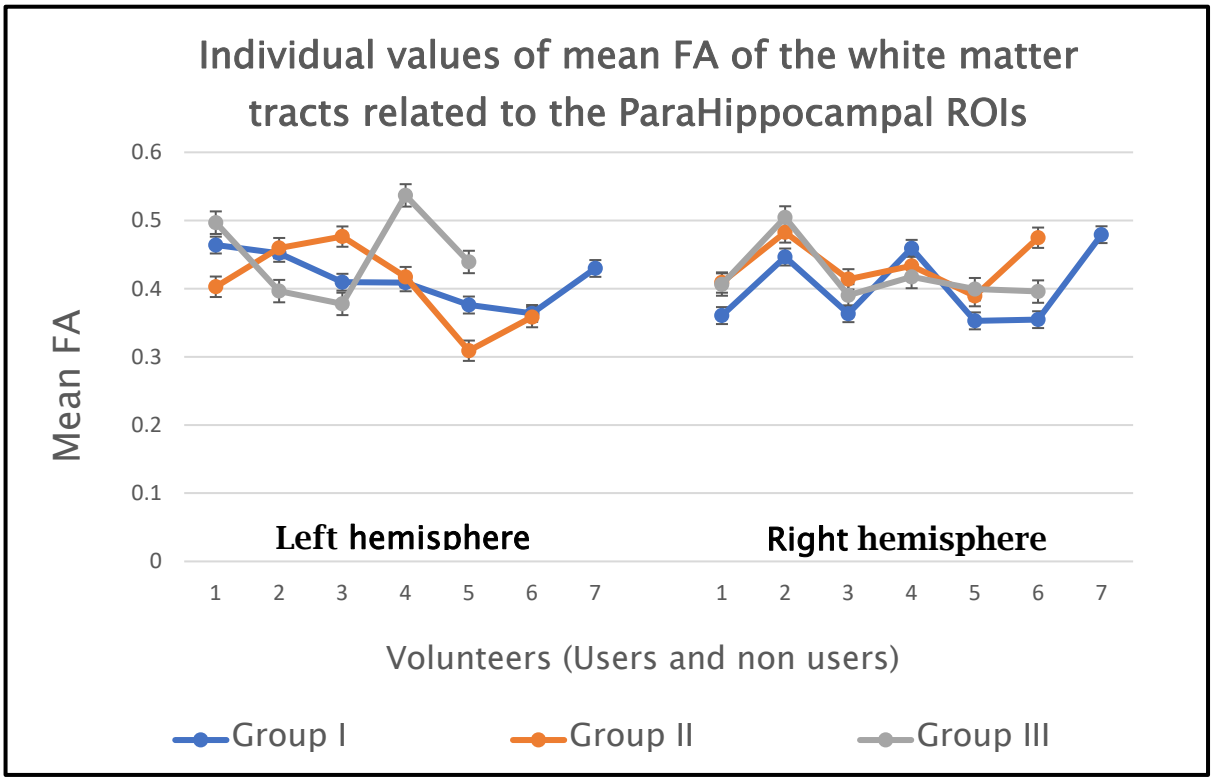

Figure 265: Individual values of mean fractional anisotropy (FA) in both hemispheres' white matter tracts related to the ParaHippocampal ROIs. This figure depicts the FA values of all the participants belonging to each of the three groups (Heavy and light users and healthy controls).

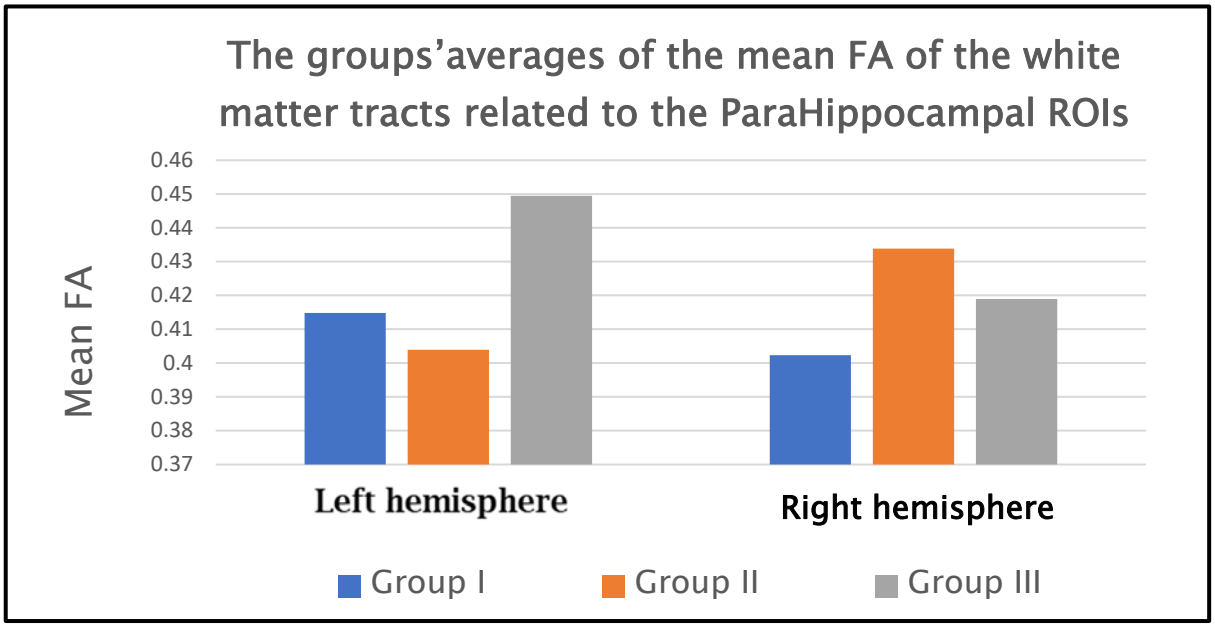

Figure 266: The mean fractional anisotropy (FA) averages of each group of the white matter tracts related to the ParaHippocampal ROIs in the left and the right hemispheres.

Table 271: The mean fractional anisotropy (FA) averages and standard deviations (SD) values for the groups studied of the white matter tracts related to the ParaHippocampal ROIs, along with intergroup comparisons.

	Left Hemisphere	Right Hemisphere
Heavy users' group (G. I)	(0,414±0,0369)	(0,4023±0,0564)
Light users' group (G. II)	(0,4039±0,0626)	(0,433±0,0375)
Non-users' group (G.III)	(0,449±0,06706)	(0,418±0,0429)
Intergroup comparison	G.III > G. I > G. II	G. II > G.III > G. I

➢ Hippocampus

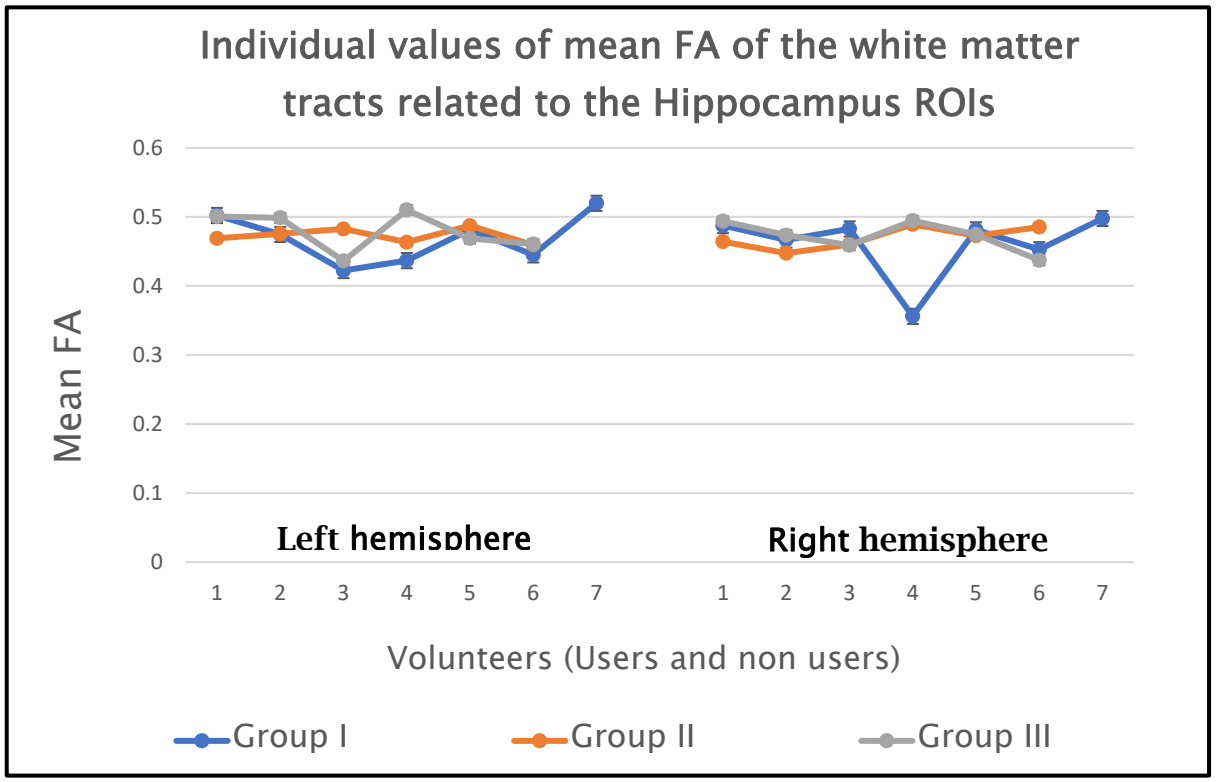

Figure 267: Individual values of mean fractional anisotropy (FA) in both hemispheres' white matter tracts related to the Hippocampus ROIs. This figure depicts the FA values of all the participants belonging to each of the three groups (Heavy and light users and healthy controls).

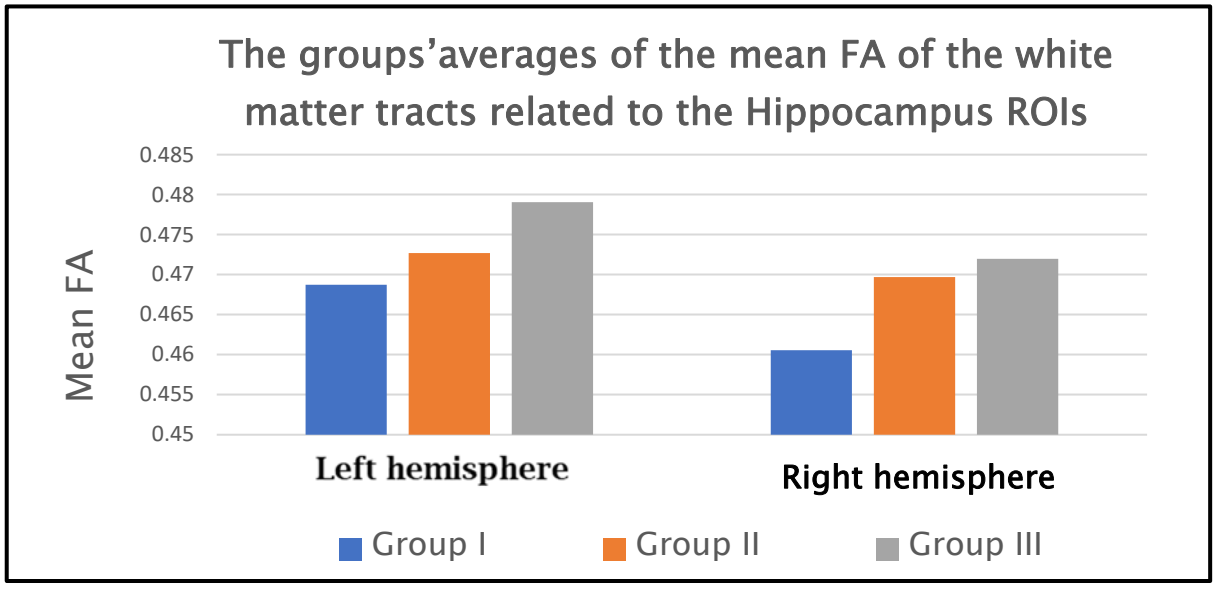

Figure 268: The mean fractional anisotropy (FA) averages of each group of the white matter tracts related to the Hippocampus ROIs in the left and the right hemispheres.

Table 272: The mean fractional anisotropy (FA) averages and standard deviations (SD) values for the groups studied of the white matter tracts related to the Hippocampus ROIs, along with intergroup comparisons.

	Left Hemisphere	Right Hemisphere
Heavy users' group (G. I)	(0,468±0,0357)	(0,4605±0,0483)
Light users' group (G. II)	(0,472±0,01094)	(0,469±0,0158)
Non-users' group (G.III)	(0,479±0,0286)	(0,471±0,0217)
Intergroup comparison	G.III > G. II > G. I	G.III ≈ G. II > G. I

➢ **Insula**

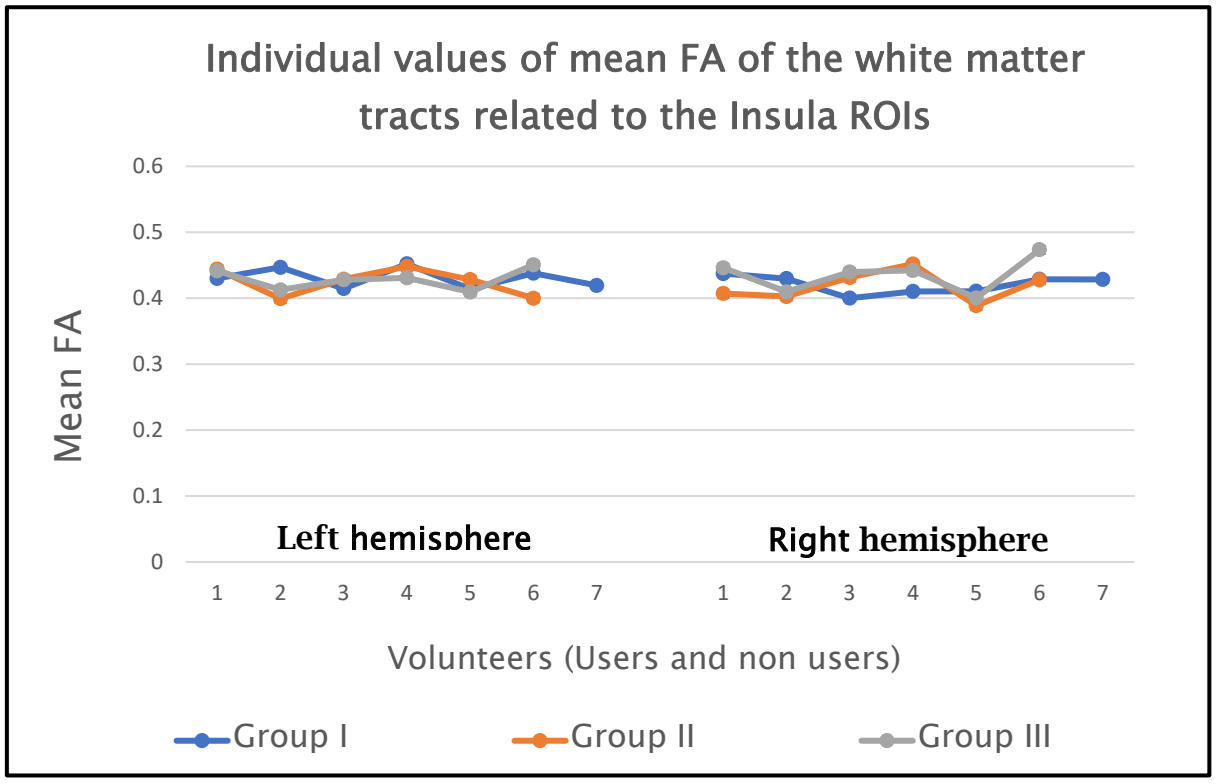

Figure 269: Individual values of mean fractional anisotropy (FA) in both hemispheres' white matter tracts related to the insula ROIs. This figure depicts the FA values of all the participants belonging to each of the three groups (Heavy and light users and healthy controls).

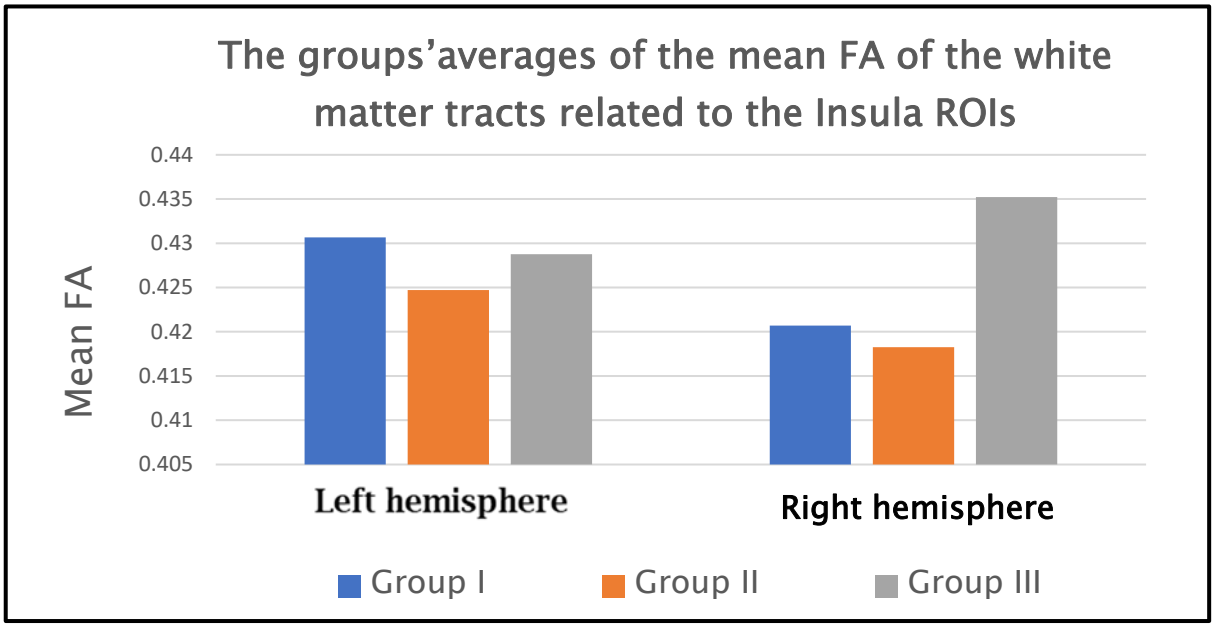

Figure 270: The mean fractional anisotropy (FA) averages of each group of the white matter tracts related to the Insula ROIs in the left and the right hemispheres.

Table 273: The mean fractional anisotropy (FA) averages and standard deviations (SD) values for the groups studied of the white matter tracts related to the Insula ROIs, along with intergroup comparisons.

	Left Hemisphere	Right Hemisphere
Heavy users' group (G. I)	(0,4306±0,0154)	(0,4206±0,0136)
Light users' group (G. II)	(0,424±0,02099)	(0,418±0,02302)
Non-users' group (G.III)	(0,428±0,01602)	(0,435±0,0265)
Intergroup comparison	G.III ≈ G. I > G. II	G.III > G. II ≈ G. I

➢ Amygdala

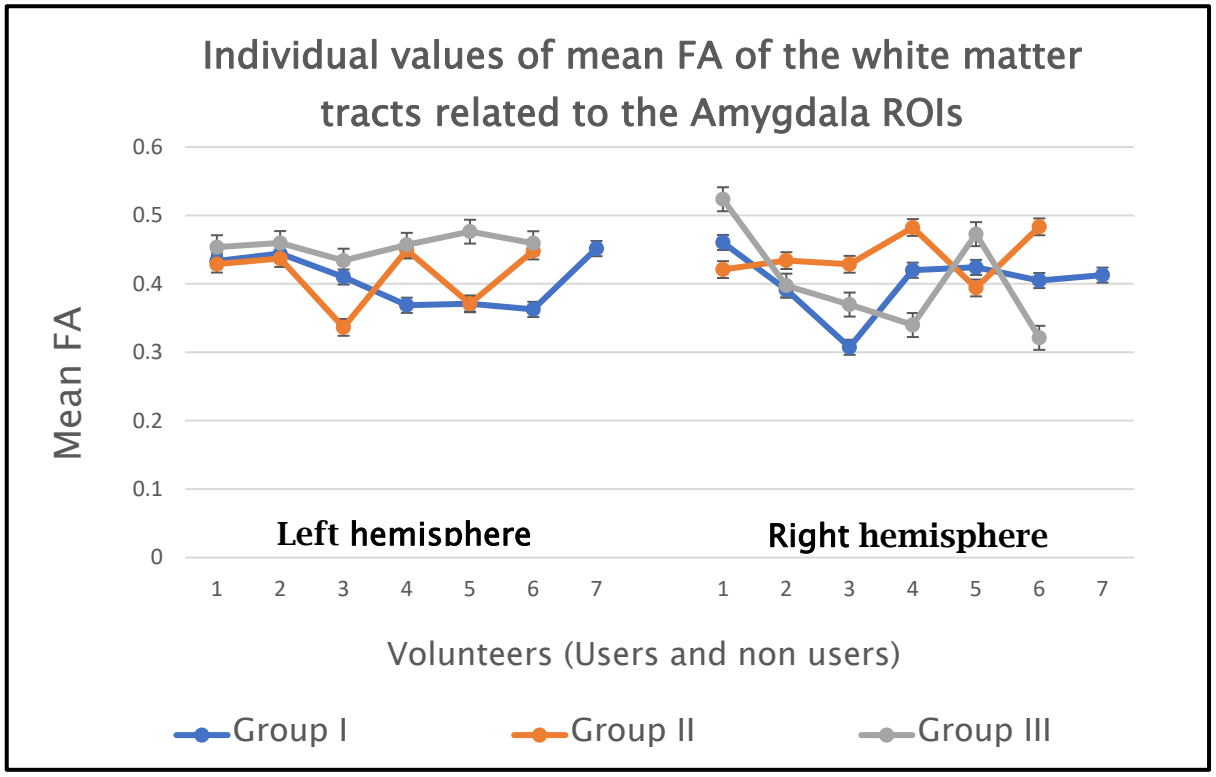

Figure 271: Individual values of mean fractional anisotropy (FA) in both hemispheres' white matter tracts related to the Amygdala ROIs. This figure depicts the FA values of all the participants belonging to each of the three groups (Heavy and light users and healthy controls).

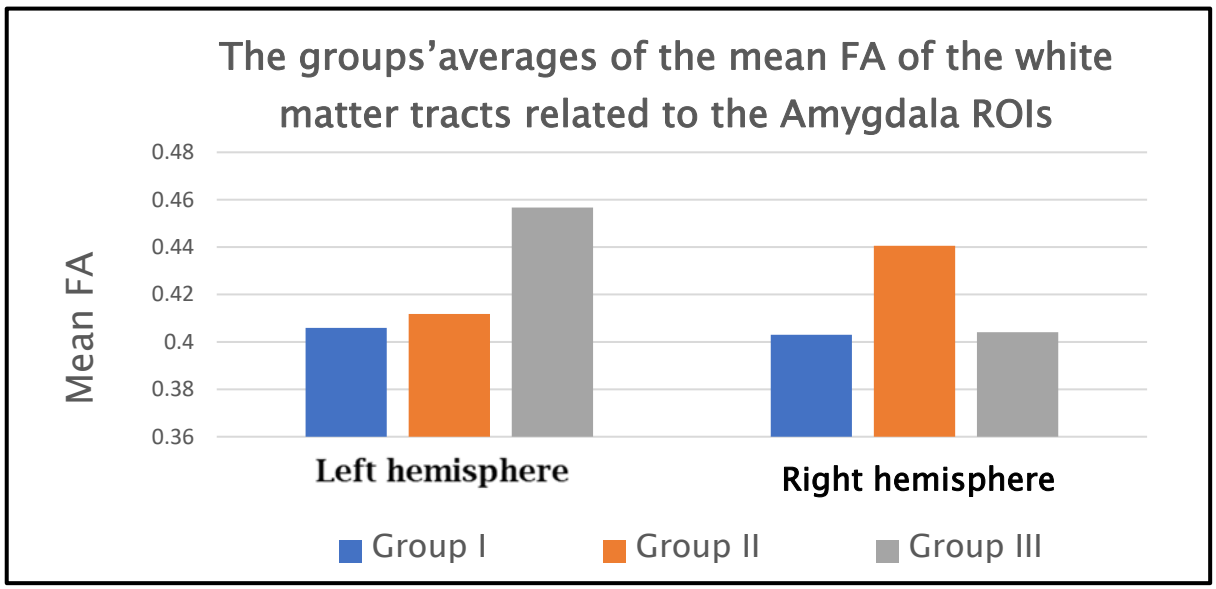

Figure 272: The mean fractional anisotropy (FA) averages of each group of the white matter tracts related to the Amygdala ROIs in the left and the right hemispheres.

Table 274: The mean fractional anisotropy (FA) averages and standard deviations (SD) values for the groups studied of the white matter tracts related to the Amygdala ROIs, along with intergroup comparisons.

	Left Hemisphere	Right Hemisphere
Heavy users' group (G. I)	(0,4059±0,0383)	(0,403009±0,0473)
Light users' group (G. II)	(0,411±0,0468)	(0,4405±0,0355)
Non-users' group (G.III)	(0,456±0,0136)	(0,4041±0,07907)
Intergroup comparison	G.III > G. I ≈ G. II	G. II > G.III ≈ G. I

➢ **Thalamus**

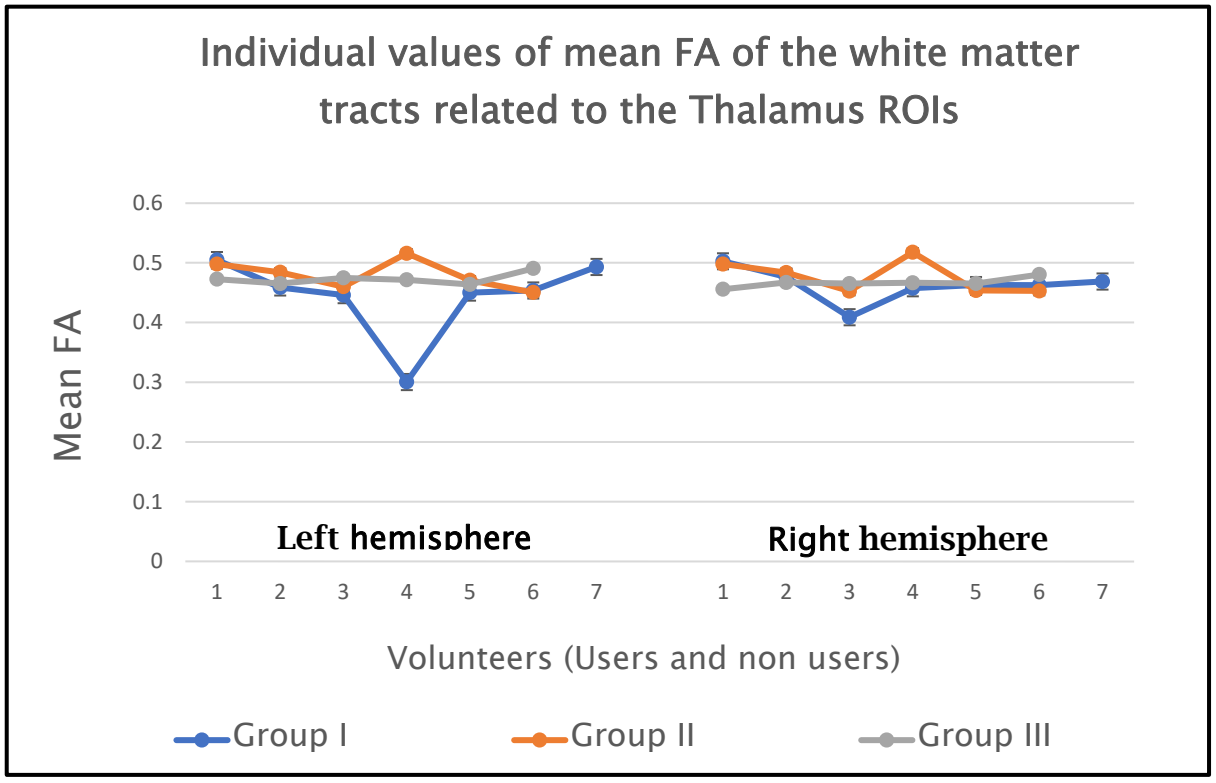

Figure 273: Individual values of mean fractional anisotropy (FA) in both hemispheres' white matter tracts related to the Thalamus ROIs. This figure depicts the FA values of all the participants belonging to each of the three groups (Heavy and light users and healthy controls).

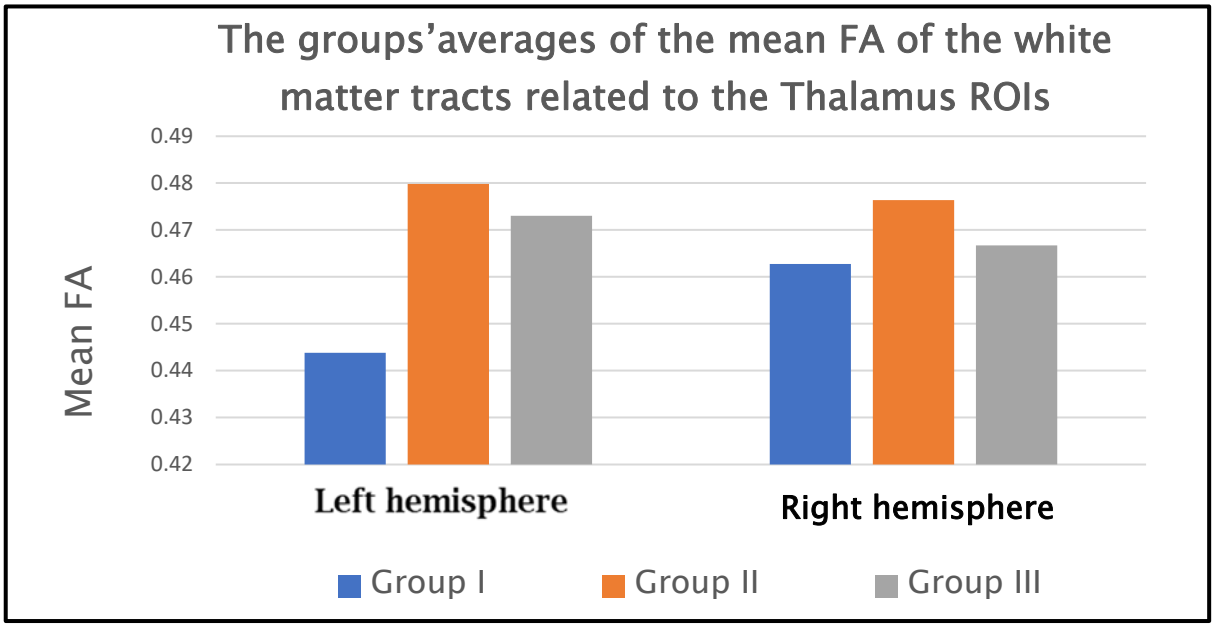

Figure 274: The mean fractional anisotropy (FA) averages of each group of the white matter tracts related to the Thalamus ROIs in the left and the right hemispheres.

Table 275: The mean fractional anisotropy (FA) averages and standard deviations (SD) values for the groups studied of the white matter tracts related to the Thalamus ROIs, along with intergroup comparisons.

	Left Hemisphere	Right Hemisphere
Heavy users' group (G. I)	(0,443±0,0671)	(0,462±0,02806)
Light users' group (G. II)	(0,479±0,0243)	(0,476±0,0277)
Non-users' group (G.III)	(0,473±0,00959)	(0,466±0,00788)
Intergroup comparison	G. II > G.III > G. I	G. II > G.III ≈ G. I

➢ Caudate

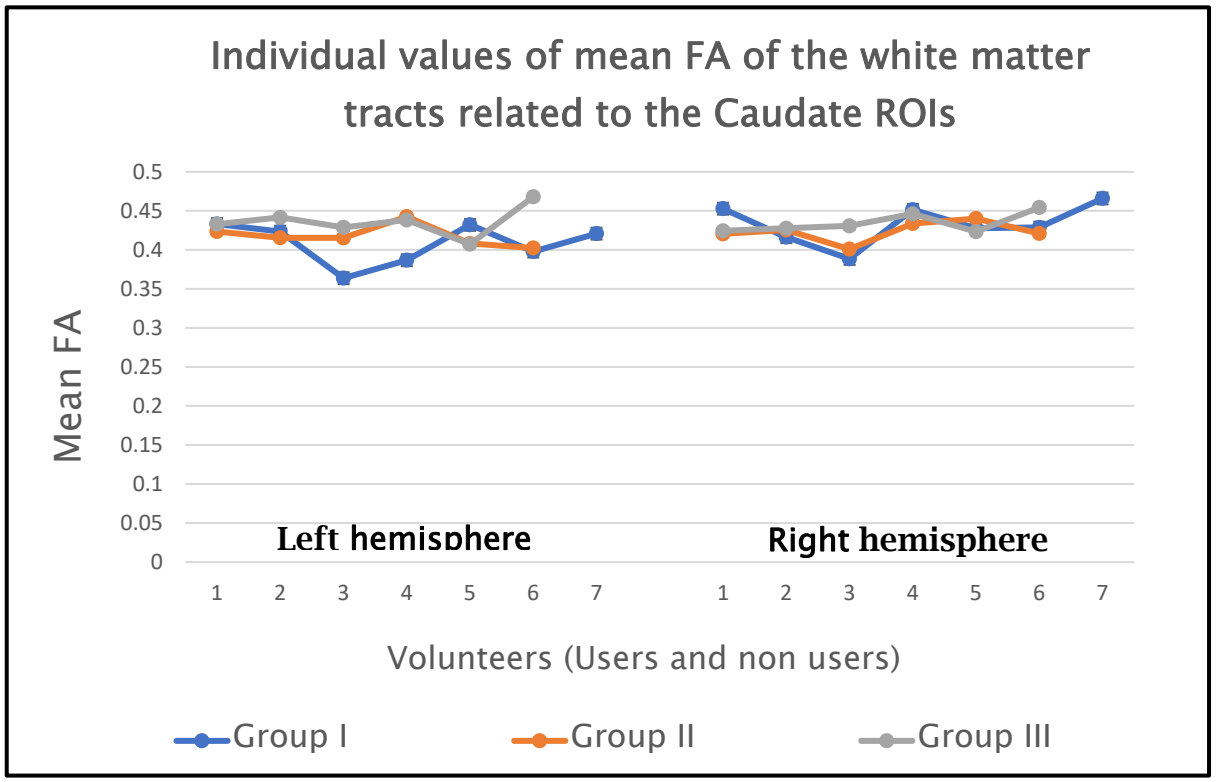

Figure 275: Individual values of mean fractional anisotropy (FA) in both hemispheres' white matter tracts related to the Caudate ROIs. This figure depicts the FA values of all the participants belonging to each of the three groups (Heavy and light users and healthy controls).

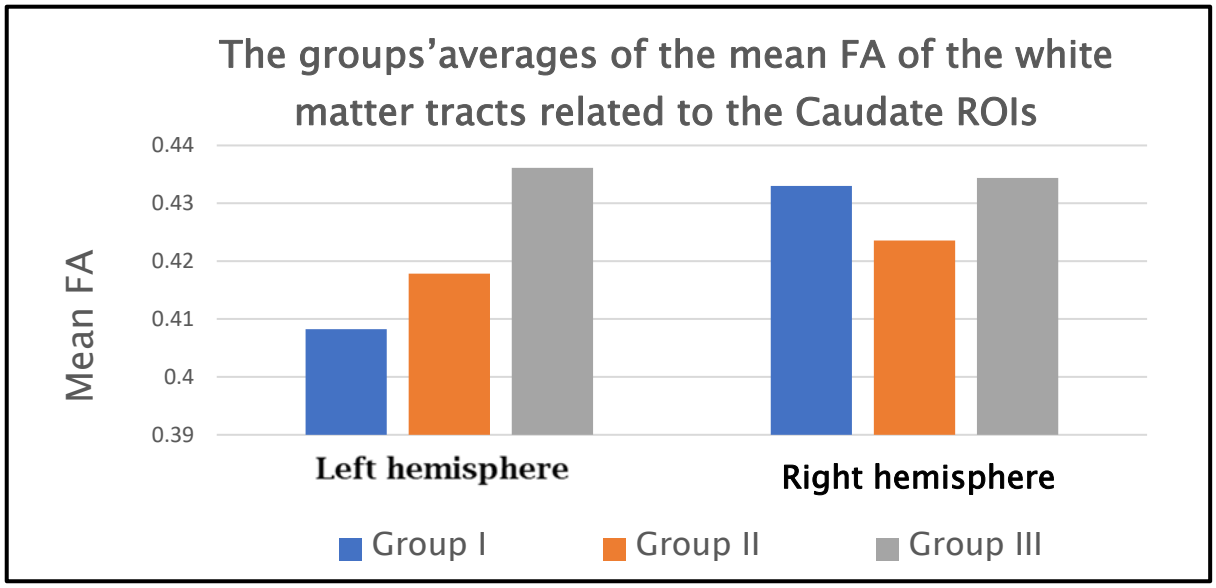

Figure 276: The mean fractional anisotropy (FA) averages of each group of the white matter tracts related to the Caudate ROIs in the left and the right hemispheres.

Table 276: The mean fractional anisotropy (FA) averages and standard deviations (SD) values for the groups studied of the white matter tracts related to the Caudate ROIs, along with intergroup comparisons.

	Left Hemisphere	Right Hemisphere
Heavy users' group (G. I)	(0,4082±0,0262)	(0,432±0,0262)
Light users' group (G. II)	(0,417±0,01404)	(0,423±0,0134)
Non-users' group (G.III)	(0,436±0,0197)	(0,434±0,0127)
Intergroup comparison	G.III > G. II > G. I	G.III ≈ G. I > G. II

➢ **Putamen**

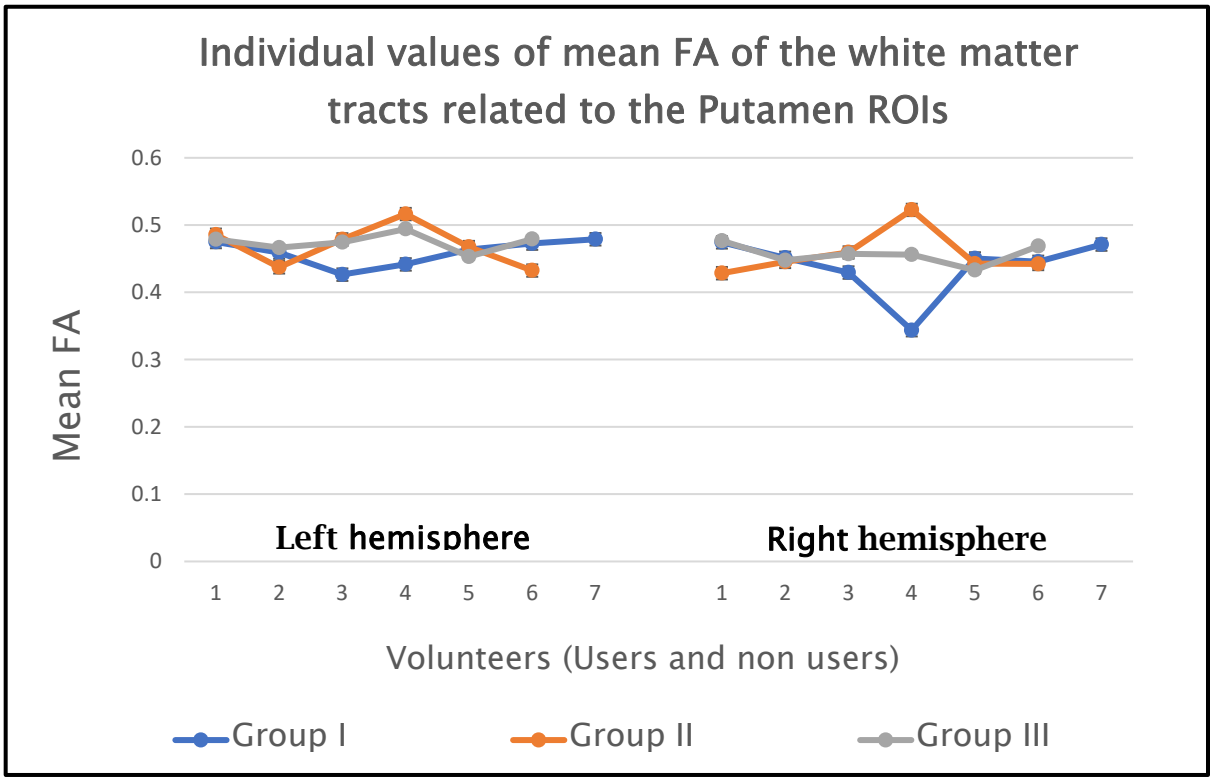

Figure 277: Individual values of mean fractional anisotropy (FA) in both hemispheres' white matter tracts related to the Putamen ROIs. This figure depicts the FA values of all the participants belonging to each of the three groups (Heavy and light users and healthy controls).

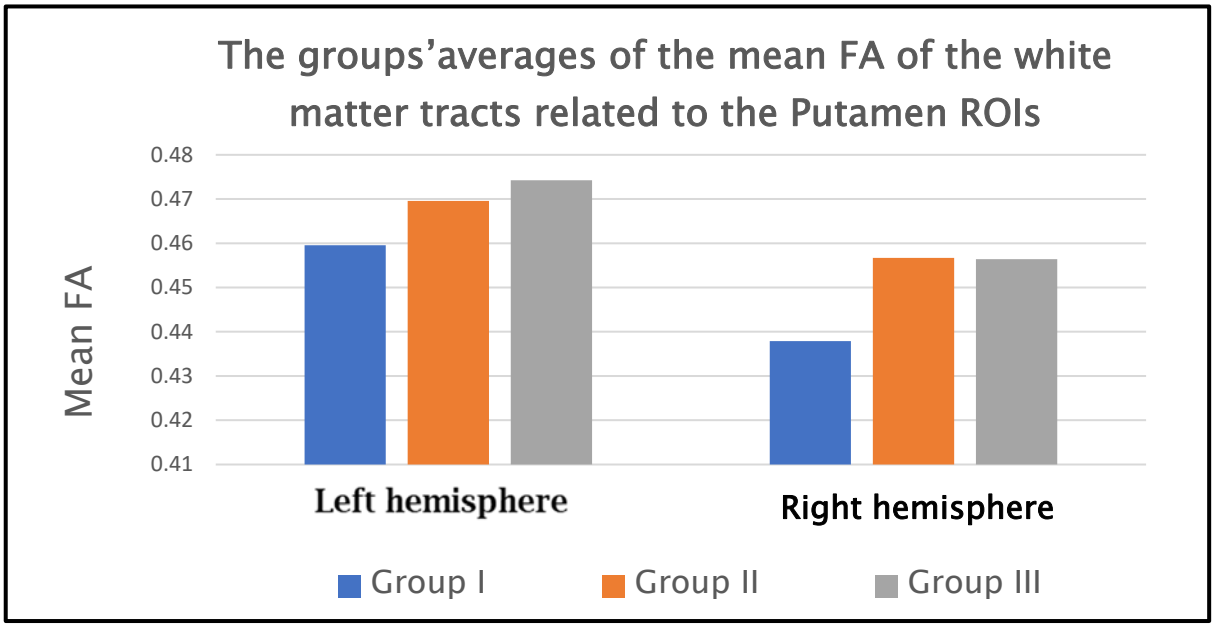

Figure 278: The mean fractional anisotropy (FA) averages of each group of the white matter tracts related to the Putamen ROIs in the left and the right hemispheres.

Table 277: The mean fractional anisotropy (FA) averages and standard deviations (SD) values for the groups studied of the white matter tracts related to the Putamen ROIs, along with intergroup comparisons.

	Left Hemisphere	Right Hemisphere
Heavy users' group (G. I)	(0,459±0,0192)	(0,437±0,0442)
Light users' group (G. II)	(0,469±0,0314)	(0,456±0,0337)
Non-users' group (G.III)	(0,474±0,0138)	(0,456±0,0153)
Intergroup comparison	G.III > G. II > G. I	G.III ≈ G. II > G. I

➢ **Pallidum**

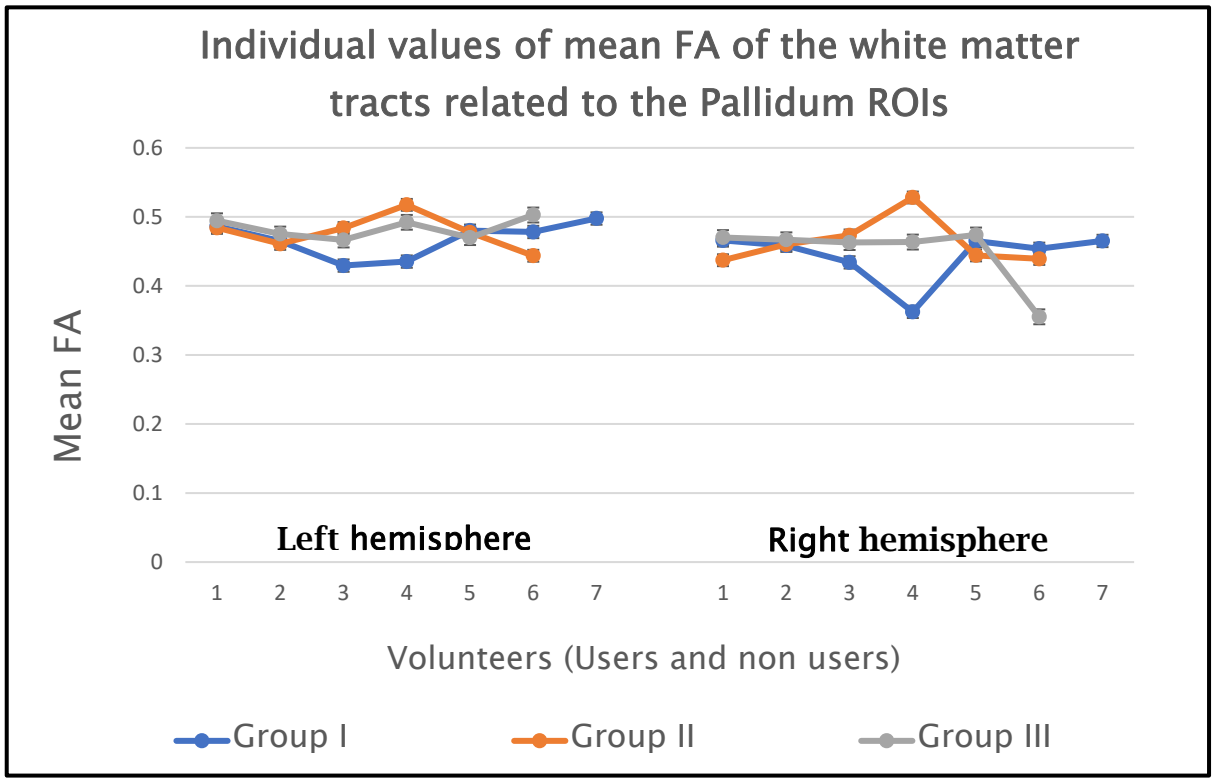

Figure 279: Individual values of mean fractional anisotropy (FA) in both hemispheres' white matter tracts related to the Pallidum ROIs. This figure depicts the FA values of all the participants belonging to each of the three groups (Heavy and light users and healthy controls).

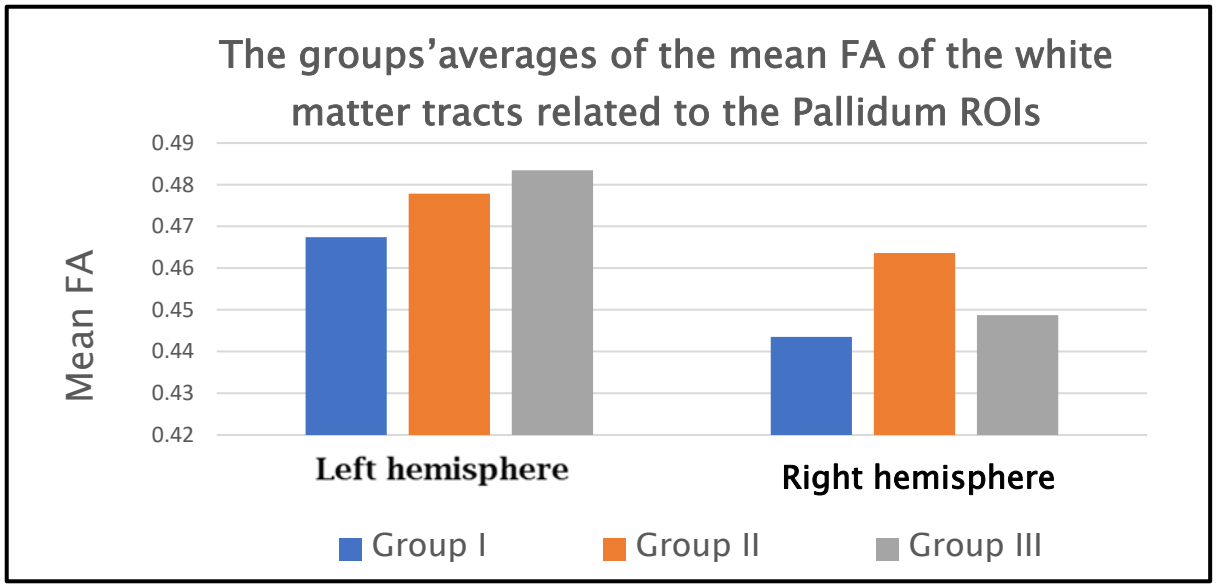

Figure 280: The mean fractional anisotropy (FA) averages of each group of the white matter tracts related to the Pallidum ROIs in the left and the right hemispheres.

Table 278: The mean fractional anisotropy (FA) averages and standard deviations (SD) values for the groups studied of the white matter tracts related to the Pallidum ROIs, along with intergroup comparisons.

	Left Hemisphere	Right Hemisphere
Heavy users' group (G. I)	(0,467±0,0259)	(0,443±0,0374)
Light users' group (G. II)	(0,477±0,0248)	(0,463±0,0344)
Non-users' group (G.III)	(0,483±0,0148)	(0,448±0,0459)
Intergroup comparison	G.III > G. II > G. I	G. II > G.III > G. I

2. Mean diffusivity (MD) quantitative results

a. Summary of all the quantitative findings

Table 279: Tractography descriptive results of the overall quantitative comparisons of mean diffusivity diffusion marker.

Intergroup comparison of Tractography Results.	Regions	Comments
G.III ≈ G. I ≈ G. II	-Olfactory. Left -Frontal Sup. Right -Frontal Mid. Right -Frontal Inf Oper. Right -Frontal Inf Tri. Right -Postcentral. Right -Parietal Sup. Right -SupraMarginal. Right -Precuneus. Right -Temporal Pole Sup. Right -Temporal Mid. Right -Temporal Pole Mid. Right -Temporal Inf. Right -Fusiform. Right -Cingulum Mid. Left & Right -Cingulum Post. Left & Right -ParaHippocampal. Left & Right -Insula. Right -Caudate. Right	A comparison objectified in 31.4 percent of our findings, equivalent to 22 areas, mostly in the right hemisphere and with an extensive distribution on most systems and brain areas.
G. I ≈ G. II > G.III	-Frontal Med Orb. Left -Frontal Sup Orb. Left -Frontal Sup Medial. Left -Frontal Sup. Left -Frontal Mid. Left -Frontal Inf Oper. Left -Frontal Inf Tri. Left -Postcentral. Left -Temporal Pole Sup. Left -Heschl. Left	With 16 areas, this is the second most prevalent comparison arrangement. The most intriguing thing about this comparison is that it is only marked on the left

	-Temporal Pole Mid. Left -Cingulum Ant. Left -Insula. Left -Amygdala. Left -Putamen. Left -Pallidum. Left	hemisphere. In addition, this sort of comparison is found in the tracts of one or more ROIs belonging to each of the cerebral cortex, limbic system, and basal ganglia.
G. I > G. II ≈ G.III	-Parietal Sup. Left -Angular. Left & Right -Parietal Inf. Left -Precuneus. Left -Temporal Sup. Left -Temporal Mid. Left -Fusiform. Left -Thalamus. Left -Caudate. Left -Putamen. Right	Comparison arrangement objective: * At 11 regions out of 70 (bilaterally), which represents 15.71% of the total of the regions studied. * In terms of laterality, regions belong mostly to the left hemisphere. * Regions belong to the following: -Cerebral cortex -Diencephalon(Thalamus) -Basal ganglia
G. II > G. I > G.III	-Frontal Med Orb. Right -Frontal Sup Orb. Right -Frontal Mid Orb. Left -Frontal Inf Orb. Left -Rectus. Left -Frontal Sup Medial. Right	Comparison arrangement objective: * At six regions, which represents 8.57% of the regions studied. *The six regions belong equally to the left and right hemispheres and only the cerebral cortex.
G.III > G. II ≈ G. I	-Parietal Inf. Right -Temporal Sup. Right -Heschl. Right -Thalamus. Right -Pallidum. Right	Comparison arrangement objective in only five regions and the right hemisphere.

G. II ≈ G.III > G. I	-Frontal Inf Orb. Right -Hippocampus. Right -Amygdala. Right
G. II > G.III > G. I	-Frontal Mid Orb. Right -Rectus. Right -Hippocampus. Left
G. II > G.III ≈ G. I	-Olfactory. Right -Cingulum Ant. Right
G. I > G. II > G.III	-SupraMarginal. Left -Temporal Inf. Left

The remaining four categories of intergroup comparisons account for 14.26% of the total.

Regions belong mostly to the right hemisphere and to:

-Cerebral cortex

-Limbic system

b. The quantitative findings of the white matter related to each region of interest

In the same way as we did for the previous results, in each region of interest's white matter and for both hemispheres, we present our mean diffusivity (MD) findings by two separated figures. The first figure depicts the mean diffusivity values of individuals in each group using a line chart.

In the line charts:

- Each participant is denoted numerically.

-The mean diffusivity is sorted in graph individual (X, Y) points and lines in heavy cannabis users (Group I), light cannabis users (Group II), and non-users (Group III). In the "X" horizontal line, we have the nominative numbers of voluntary participants, and in the "Y" vertical line, we have mean diffusivity values.

We compared the groups' MD averages between the three groups in the second figure. Following that, a table containing every group's MD averages and standard deviations (SD) will be presented for a synthesis.

➢ Frontal Med Orb

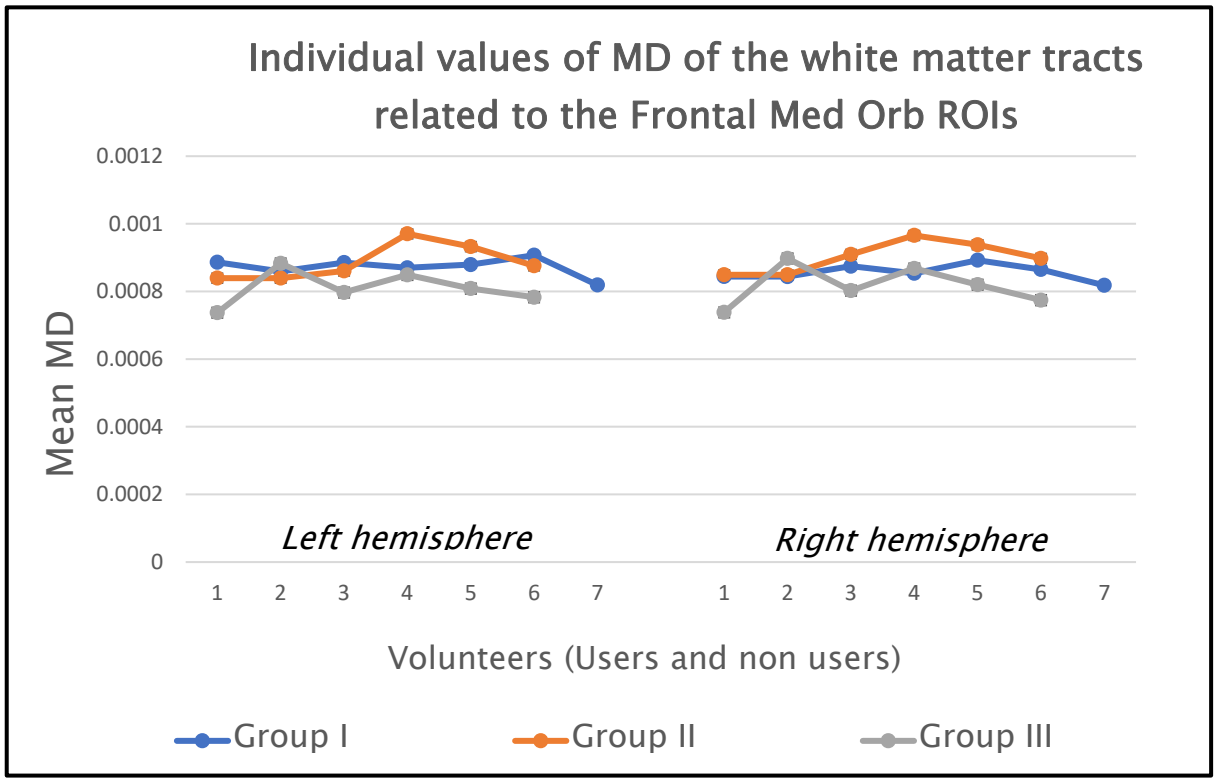

Figure 281: Individual values of mean diffusivity (MD) in both hemispheres' white matter tracts related to the Frontal Med Orb ROIs. This figure depicts the MD values of all the participants belonging to each of the three groups (Heavy and light users and healthy controls).

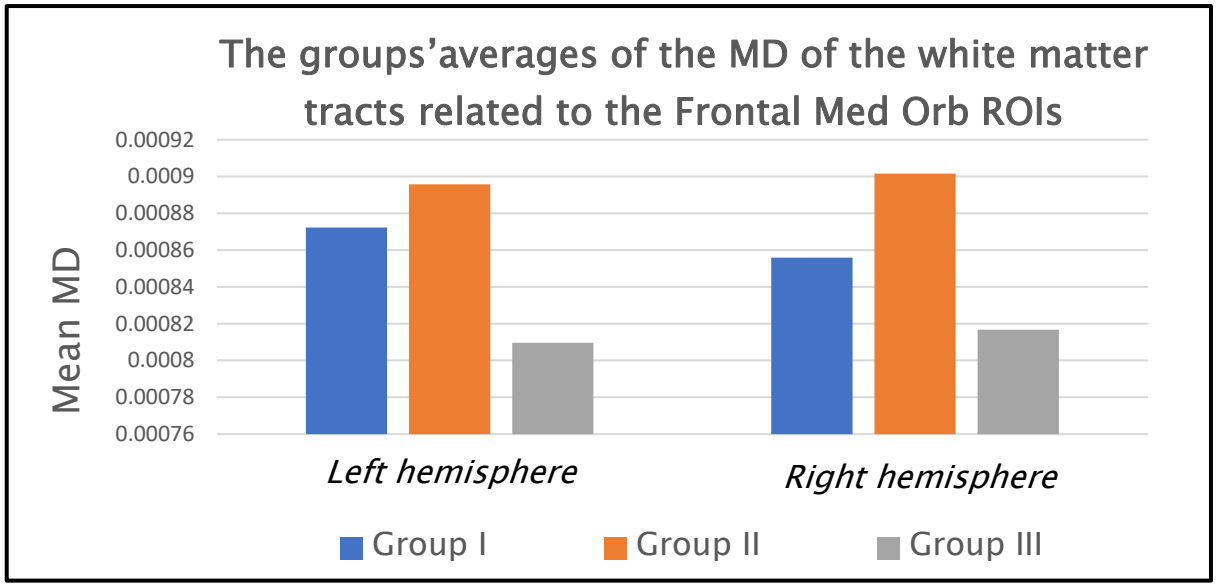

Figure 282: The mean diffusivity (MD) averages of each group of the white matter tracts related to the Frontal Med Orb ROIs in the left and the right hemispheres.

Table 280: The mean diffusivity (MD) averages and standard deviations (SD) values for the groups studied of the white matter tracts related to the Frontal Med Orb ROIs, along with intergroup comparisons.

	Left Hemisphere	Right Hemisphere
Heavy users' group (G. I)	(0,0008722±0,0000277)	(0,0008558±0,0000240)
Light users' group (G. II)	(0,0008863±0,0000535)	(0,0009015±0,0000468)
Non-users' group (G.III)	(0,0008095±0,0000510)	(0,0008167±0,0000588)
Intergroup comparison	G. I ≈ G. II > G.III	G. II > G. I > G.III

➢ **Frontal Sup Orb**

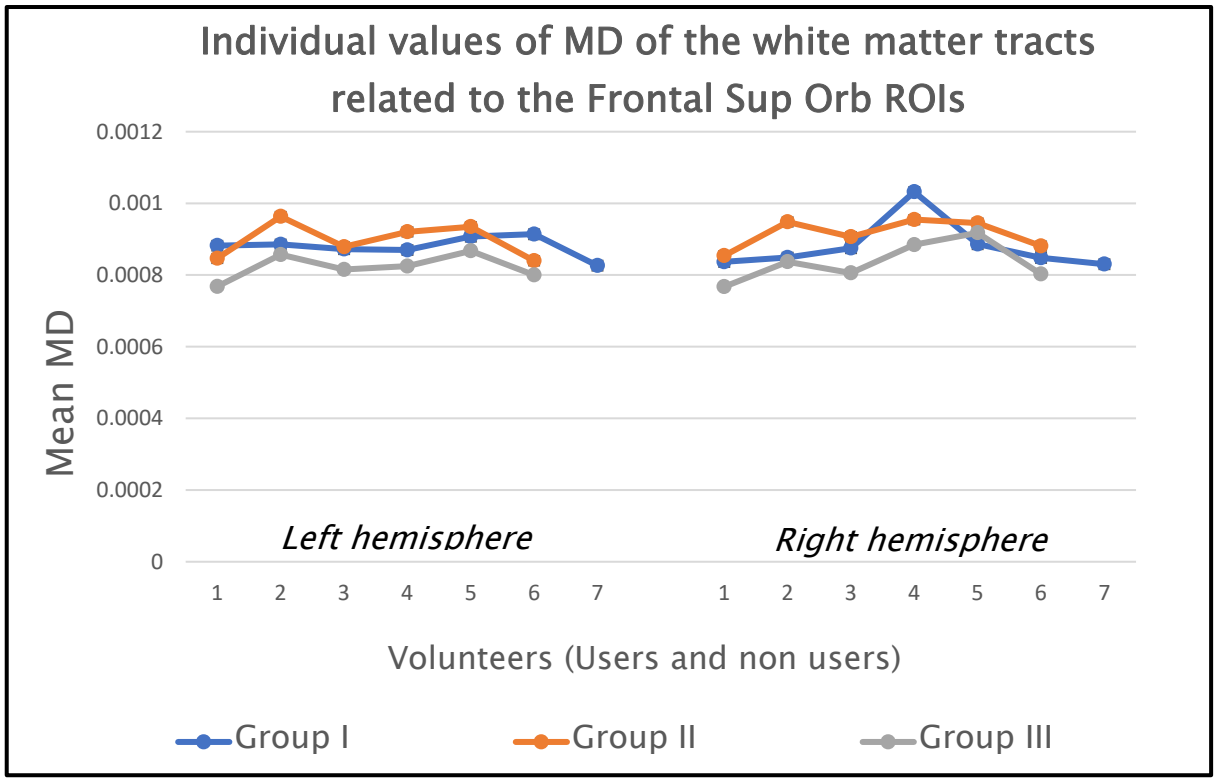

Figure 283: Individual values of mean diffusivity (MD) in both hemispheres' white matter tracts related to the Frontal Sup Orb ROIs. This figure depicts the MD values of all the participants belonging to each of the three groups (Heavy and light users and healthy controls).

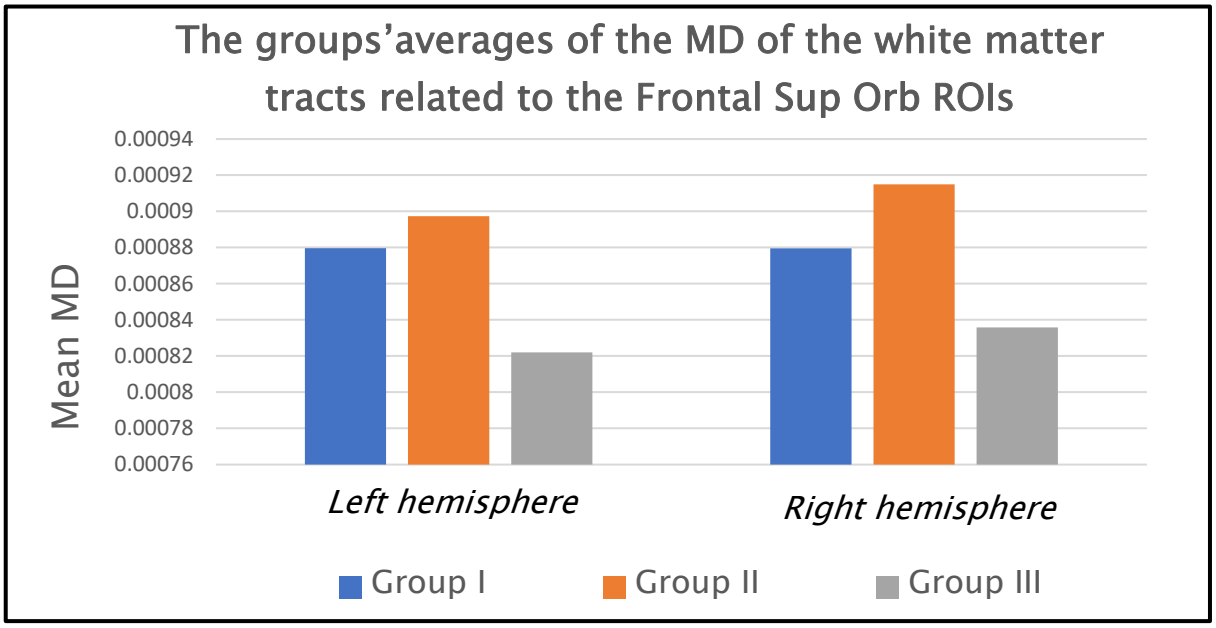

Figure 284: The mean diffusivity (MD) averages of each group of the white matter tracts related to the Frontal Sup Orb ROIs in the left and the right hemispheres.

Table 281: The mean diffusivity (MD) averages and standard deviations (SD) values for the groups studied of the white matter tracts related to the Frontal Sup Orb ROIs, along with intergroup comparisons.

	Left Hemisphere	Right Hemisphere
Heavy users' group (G. I)	(0,0008795±0,00002875)	(0,0008795±0,00007017)
Light users' group (G. II)	(0,0008973±0,00005011)	(0,0009148±0,00004132)
Non-users' group (G.III)	(0,0008219±0,00003665)	(0,0008357±0,00005618)
Intergroup comparison	G. I ≈ G. II > G.III	G. II > G. I > G.III

➢ Frontal Mid Orb

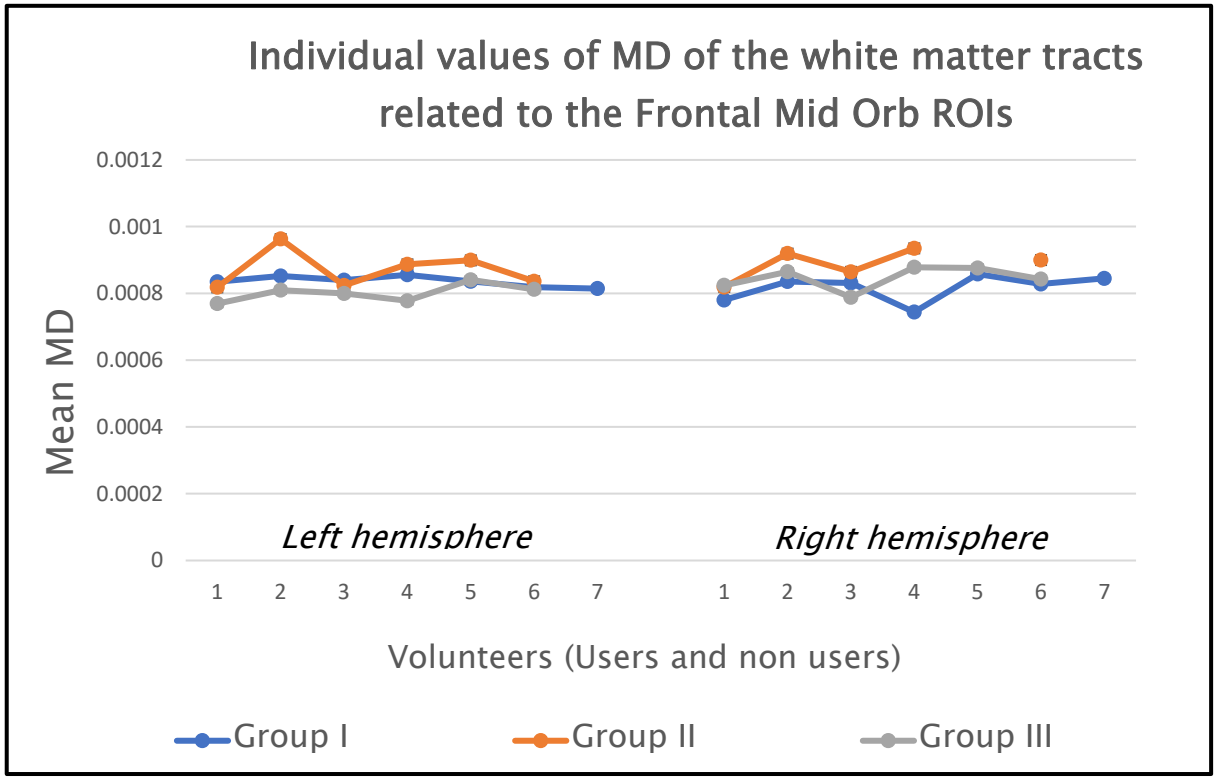

Figure 285: Individual values of mean diffusivity (MD) in both hemispheres' white matter tracts related to the Frontal Mid Orb ROIs. This figure depicts the MD values of all the participants belonging to each of the three groups (Heavy and light users and healthy controls).

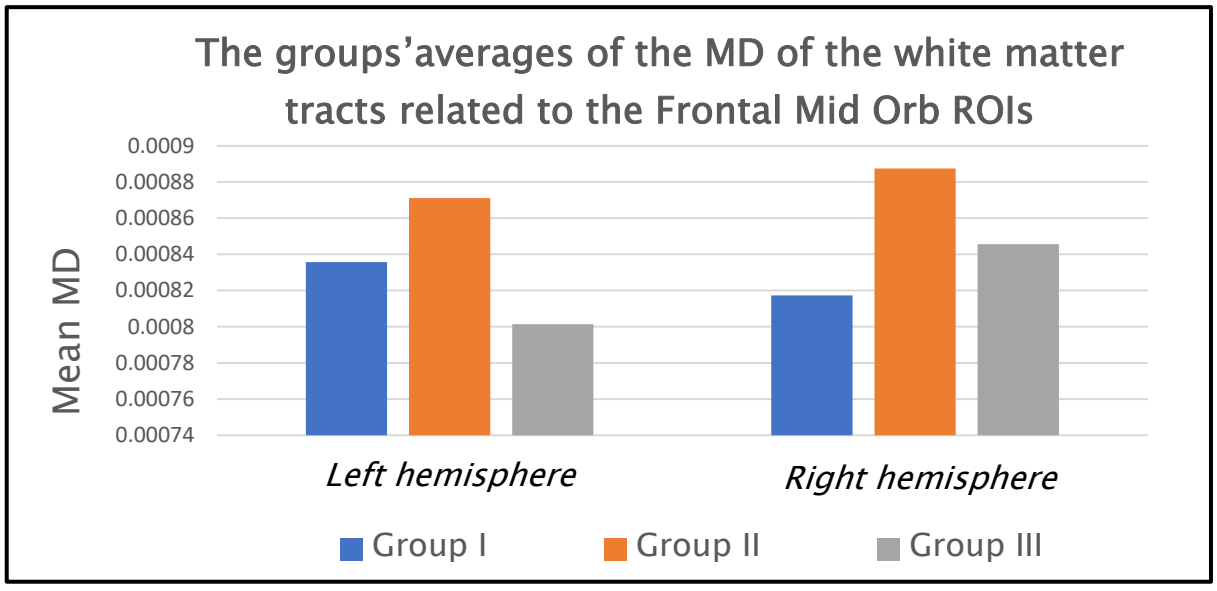

Figure 286: The mean diffusivity (MD) averages of each group of the white matter tracts related to the Frontal Mid Orb ROIs in the left and the right hemispheres.

Table 282: The mean diffusivity (MD) averages and standard deviations (SD) values for the groups studied of the white matter tracts related to the Frontal Mid Orb ROIs, along with intergroup comparisons.

	Left Hemisphere	Right Hemisphere
Heavy users' group (G. I)	(0,0008357±0,00001545)	(0,00081733±0,00004042)
Light users' group (G. II)	(0,0008711±0,00005609)	(0,0008874±0,00004653)
Non-users' group (G.III)	(0,0008013±0,00002568)	(0,0008455±0,000035003)
Intergroup comparison	G. II > G. I > G.III	G. II > G.III > G. I

➢ **Frontal Inf Orb**

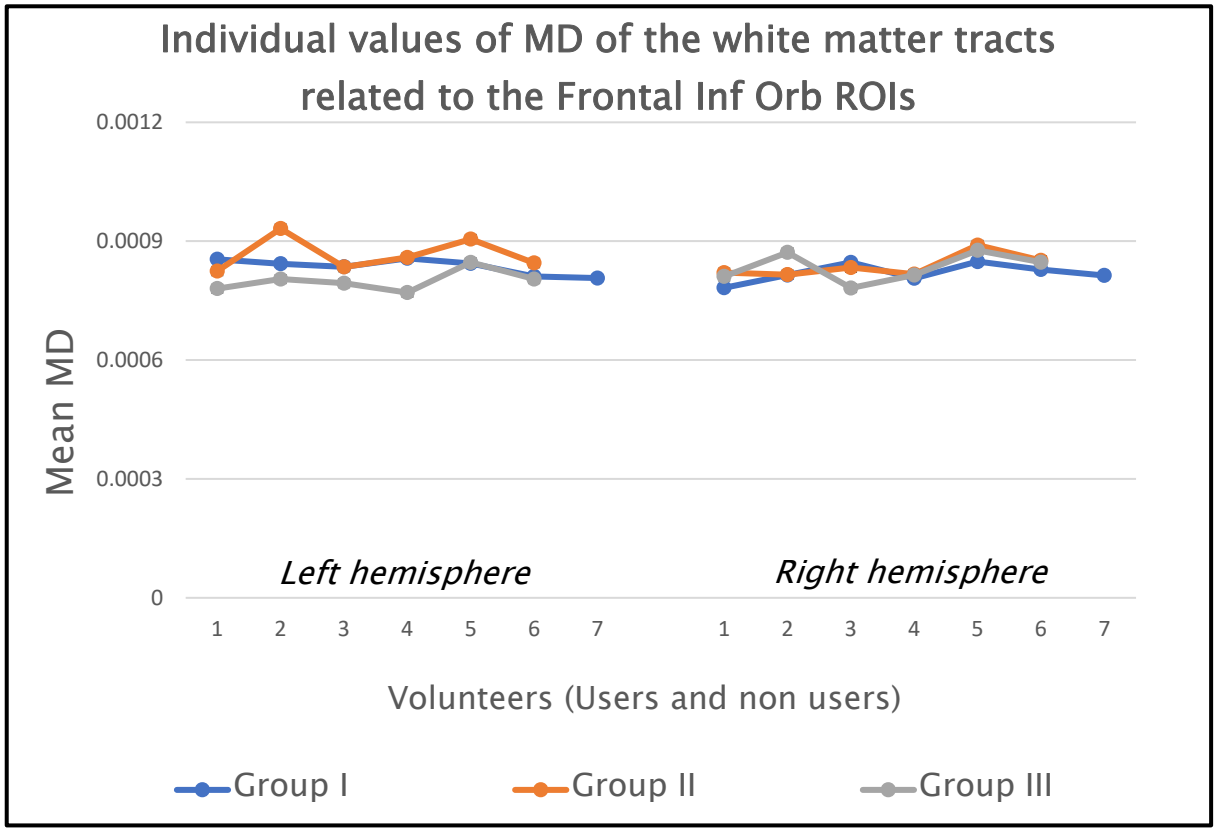

Figure 287: Individual values of mean diffusivity (MD) in both hemispheres' white matter tracts related to the Frontal Inf Orb ROIs. This figure depicts the MD values of all the participants belonging to each of the three groups (Heavy and light users and healthy controls).

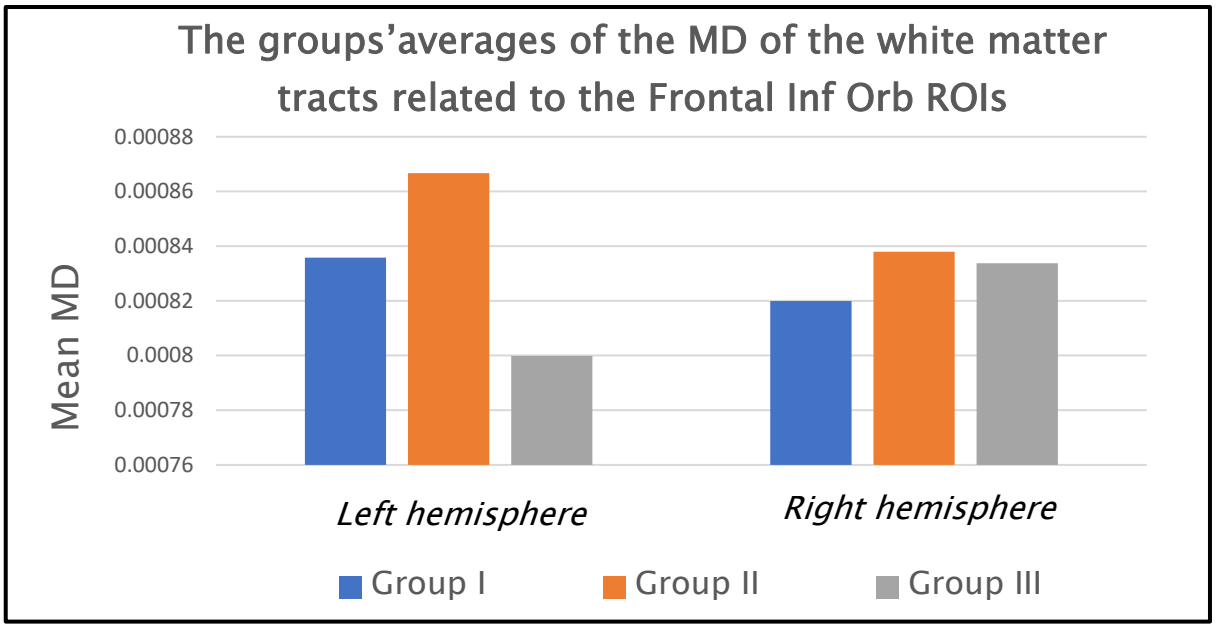

Figure 288: The mean diffusivity (MD) averages of each group of the white matter tracts related to the Frontal Inf Orb ROIs in the left and the right hemispheres.

Table 283: The mean diffusivity (MD) averages and standard deviations (SD) values for the groups studied of the white matter tracts related to the Frontal Inf Orb ROIs, along with intergroup comparisons.

	Left Hemisphere	Right Hemisphere
Heavy users' group (G. I)	(0,0008357±0,00001973)	(0,0008195±0,00002326)
Light users' group (G. II)	(0,0008666±0,00004252)	(0,0008379±0,00002887)
Non-users' group (G.III)	(0.0007998±0,00002646)	(0,0008337±0,00003759)
Intergroup comparison	G. II > G. I > G.III	G. II ≈ G.III > G. I

➢ Rectus

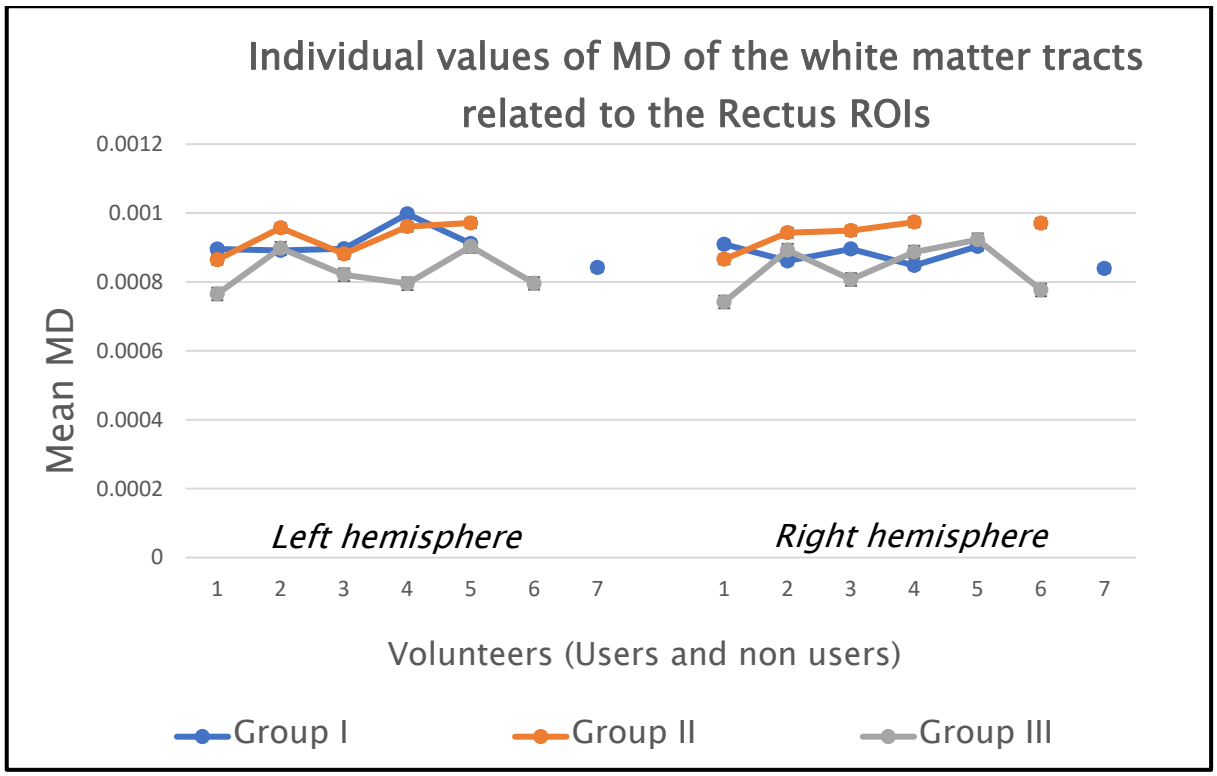

Figure 289: Individual values of mean diffusivity (MD) in both hemispheres' white matter tracts related to the Rectus ROIs. This figure depicts the MD values of all the participants belonging to each of the three groups (Heavy and light users and healthy controls).

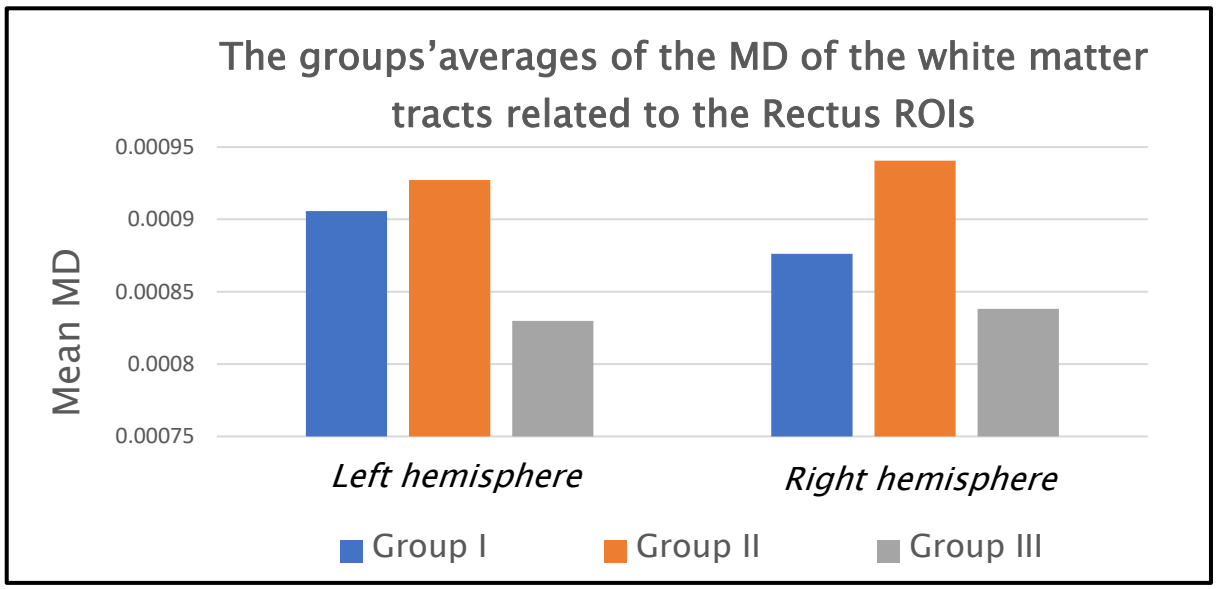

Figure 290: The mean diffusivity (MD) averages of each group of the white matter tracts related to the Rectus ROIs in the left and the right hemispheres.

Table 284: The mean diffusivity (MD) averages and standard deviations (SD) values for the groups studied of the white matter tracts related to the Rectus ROIs, along with intergroup comparisons.

	Left Hemisphere	Right Hemisphere
Heavy users' group (G. I)	(0,0009057±0,0000508)	(0,0008761±0,00003)
Light users' group (G. II)	(0,0009271±0,000049)	(0,0009405±0,00004376)
Non-users' group (G.III)	(0,0008297±0,000057)	(0,0008381±0,0000727)
Intergroup comparison	G. II > G. I > G.III	G. II > G.III > G. I

➢ Olfactory

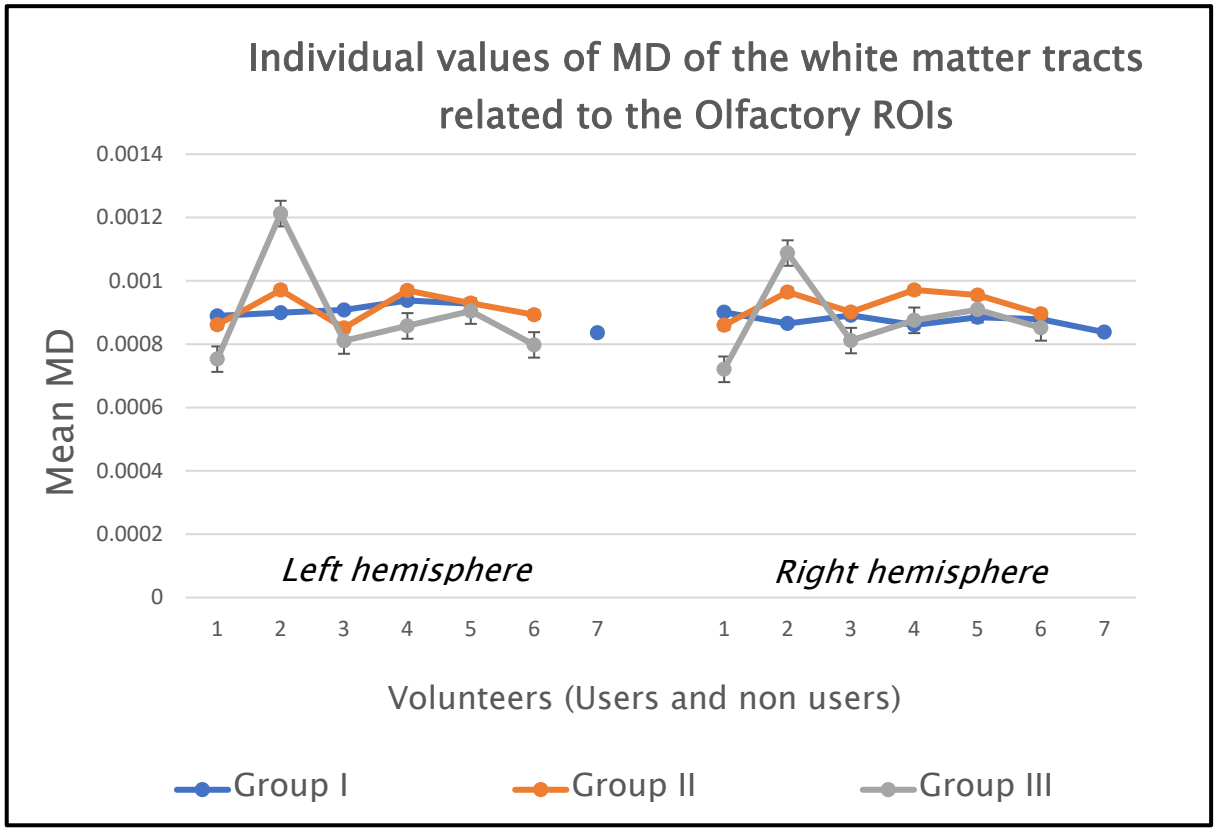

Figure 291: Individual values of mean diffusivity (MD) in both hemispheres' white matter tracts related to the Olfactory ROIs. This figure depicts the MD values of all the participants belonging to each of the three groups (Heavy and light users and healthy controls).

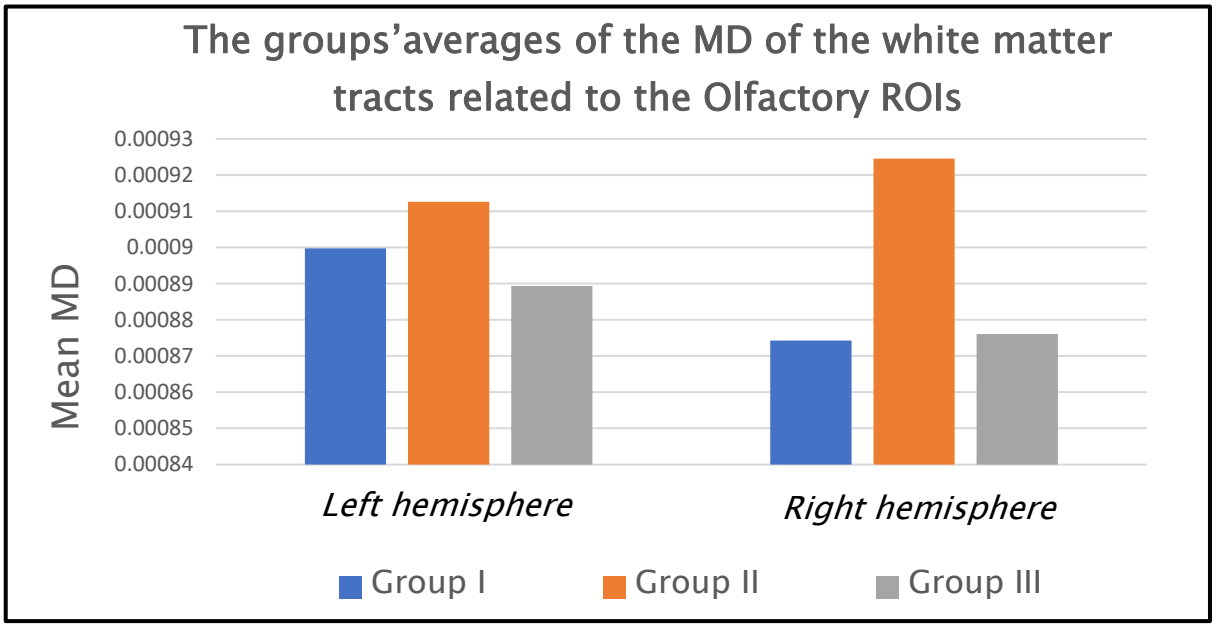

Figure 292: The mean diffusivity (MD) averages of each group of the white matter tracts related to the Olfactory ROIs in the left and the right hemispheres.

Table 285: The mean diffusivity (MD) averages and standard deviations (SD) values for the groups studied of the white matter tracts related to the Olfactory ROIs, along with intergroup comparisons.

	Left Hemisphere	Right Hemisphere
Heavy users' group (G. I)	(0,0008997±0,00003592)	(0,000874±0,00002115)
Light users' group (G. II)	(0,0009126±0,00005243)	(0,000924±0,00004527)
Non-users' group (G.III)	(0,0008893±0,0001666)	(0,000876±0,0001223)
Intergroup comparison	G. II ≈ G. I ≈ G.III	G. II > G.III ≈ G. I

➢ Frontal Sup Medial

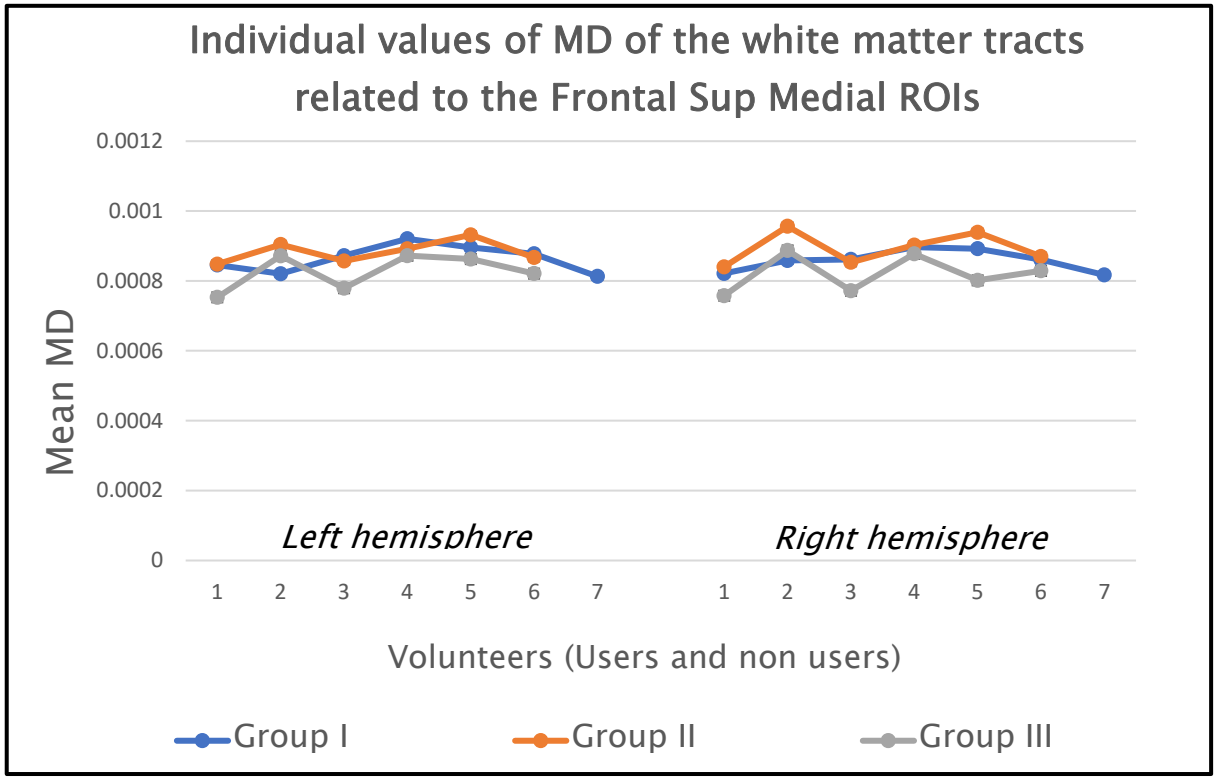

Figure 293: Individual values of mean diffusivity (MD) in both hemispheres' white matter tracts related to the Frontal Sup Medial Orb ROIs. This figure depicts the MD values of all the participants belonging to each of the three groups (Heavy and light users and healthy controls).

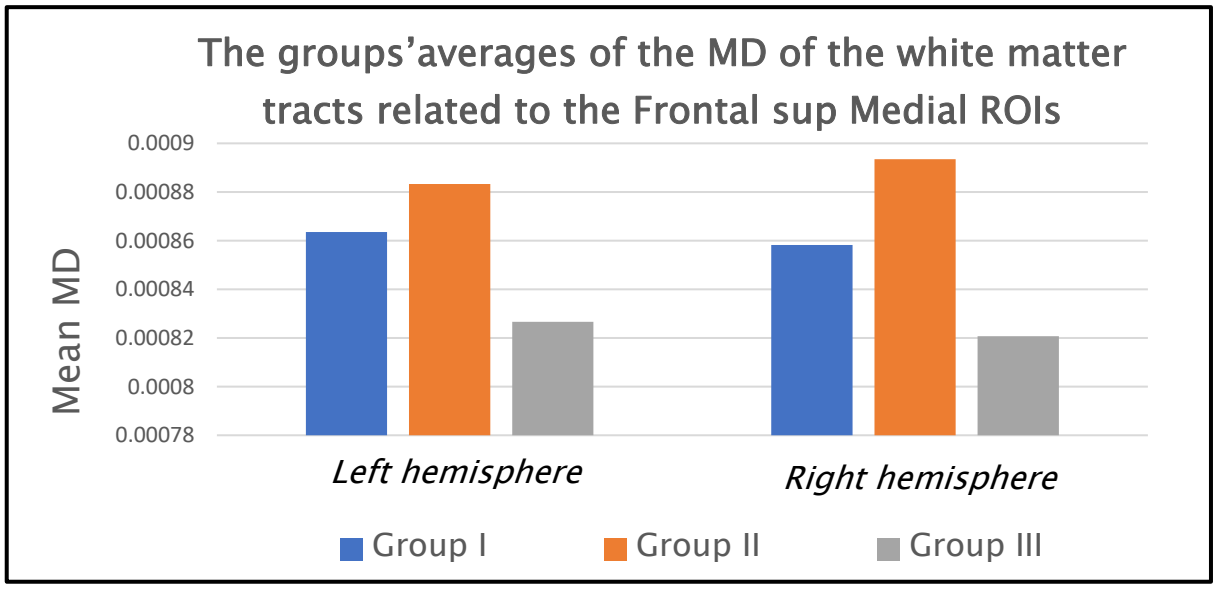

Figure 294: The mean diffusivity (MD) averages of each group of the white matter tracts related to the Frontal Sup Medial ROIs in the left and the right hemispheres.

Table 286: The mean diffusivity (MD) averages and standard deviations (SD) values for the groups studied of the white matter tracts related to the Frontal Sup Medial ROIs, along with intergroup comparisons.

	Left Hemisphere	Right Hemisphere
Heavy users' group (G. I)	(0,0008635±0,00003943)	(0,0008581±0,00003079)
Light users' group (G. II)	(0,0008832±0,00003183)	(0,0008934±0,00004713)
Non-users' group (G.III)	(0,0008266±0,00005118)	(0,0008207±0,00005368)
Intergroup comparison	G. II ≈ G. I > G.III	G. II > G. I > G.III

➢ **Frontal Sup**

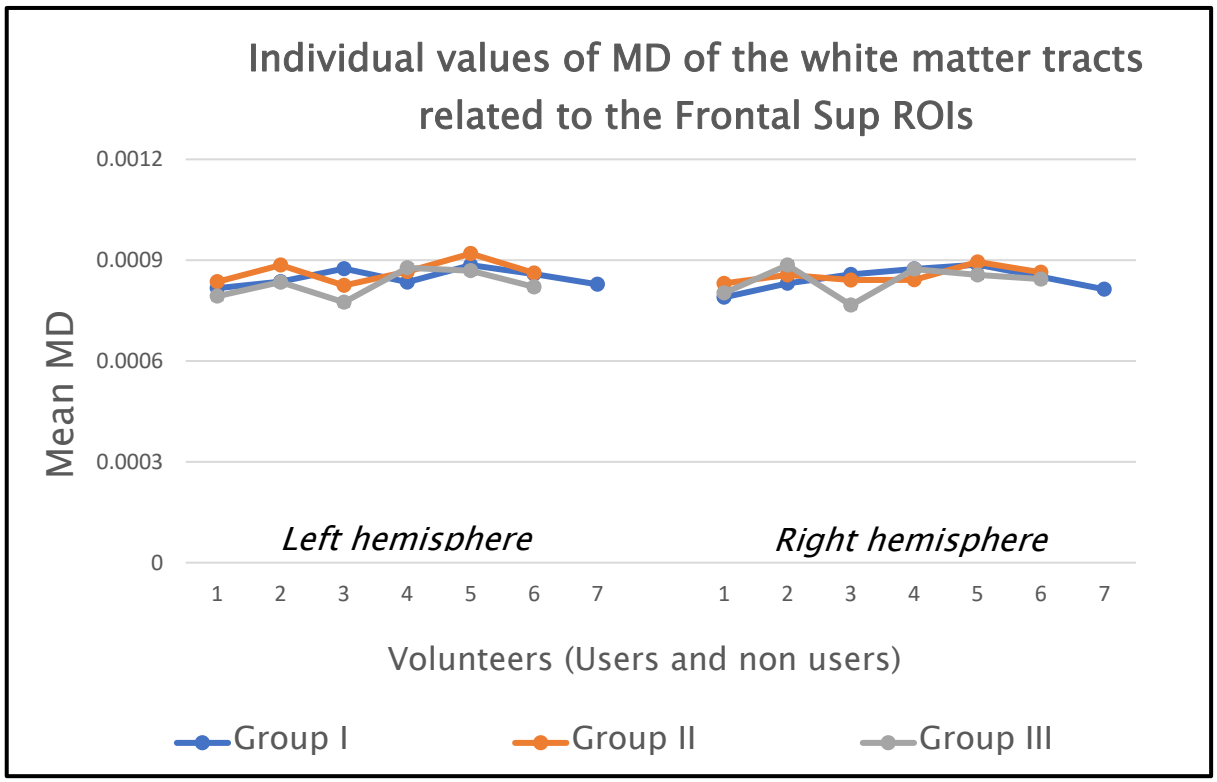

Figure 295: Individual values of mean diffusivity (MD) in both hemispheres' white matter tracts related to the Frontal Sup ROIs. This figure depicts the MD values of all the participants belonging to each of the three groups (Heavy and light users and healthy controls).

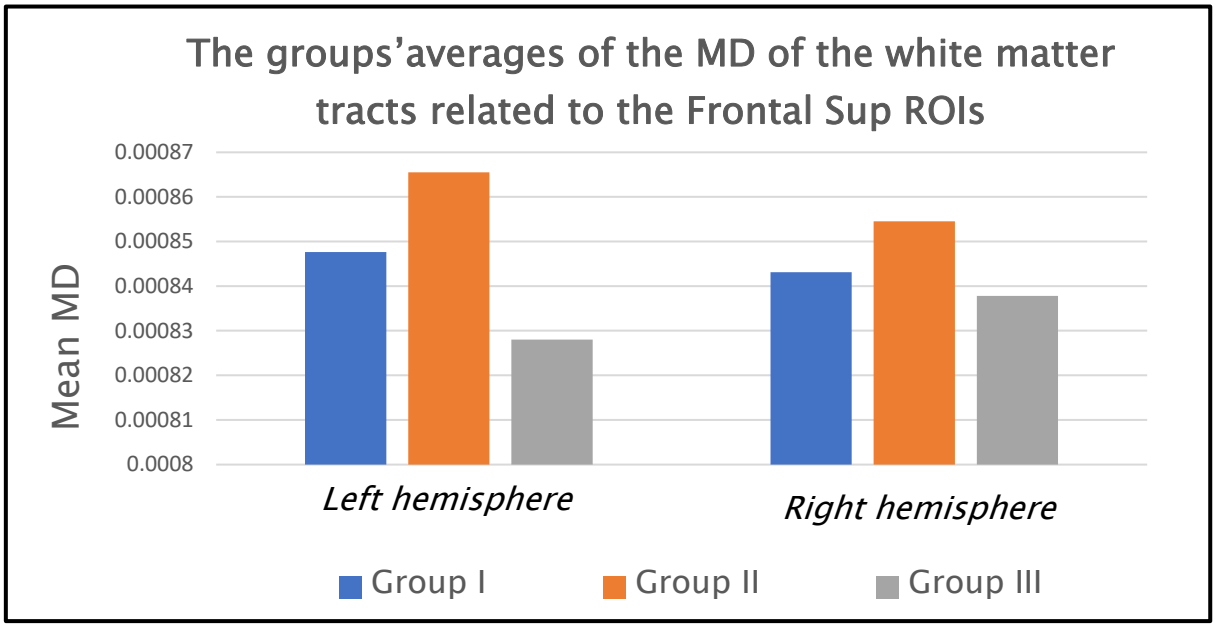

Figure 296: The mean diffusivity (MD) averages of each group of the white matter tracts related to the Frontal Sup ROIs in the left and the right hemispheres.

Table 287: The mean diffusivity (MD) averages and standard deviations (SD) values for the groups studied of the white matter tracts related to the Frontal Sup ROIs, along with intergroup comparisons.

	Left Hemisphere	Right Hemisphere
Heavy users' group (G. I)	(0,000847±0,0000254)	(0,000843±0,0000341)
Light users' group (G. II)	(0,000865±0,0000341)	(0,000854±0,0000228)
Non-users' group (G.III)	(0,000828±0,0000406)	(0,000837±0,0000453)
Intergroup comparison	G. II ≈ G. I > G.III	G. II ≈ G. I ≈ G.III

➢ Frontal Mid

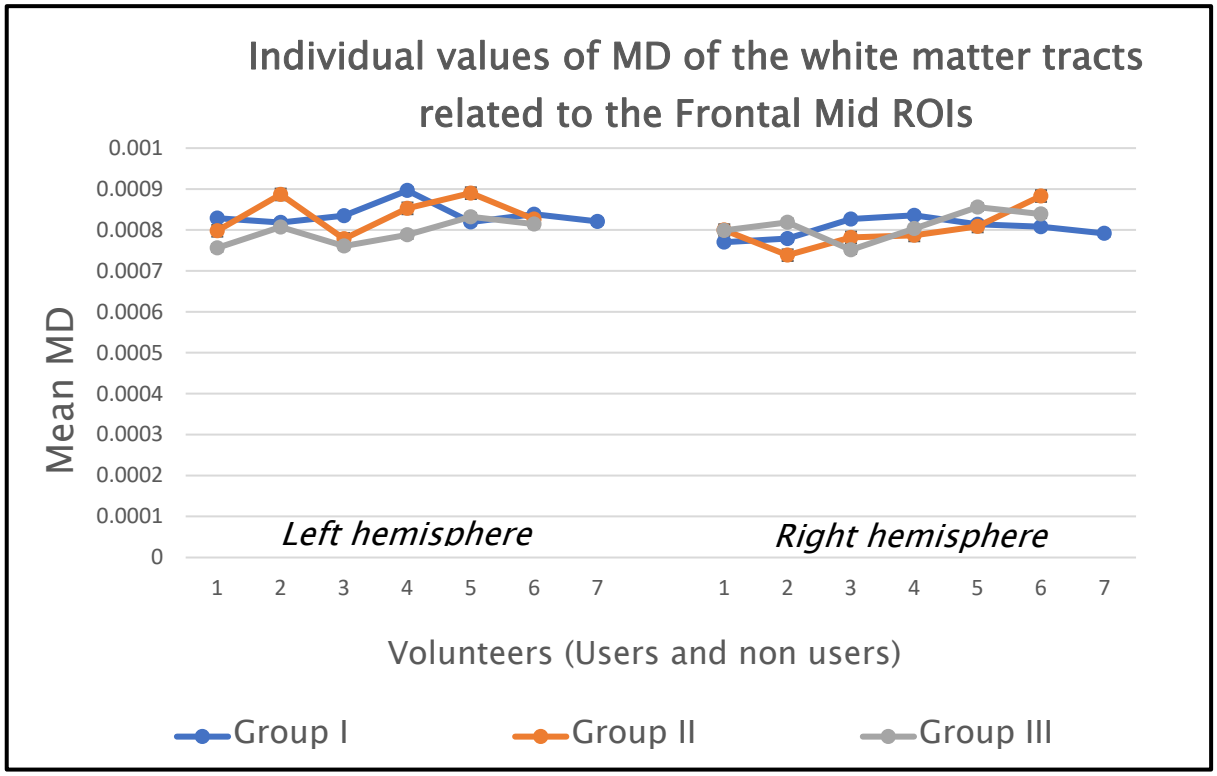

Figure 297: Individual values of mean diffusivity (MD) in both hemispheres' white matter tracts related to the Frontal Mid ROIs. This figure depicts the MD values of all the participants belonging to each of the three groups (Heavy and light users and healthy controls).

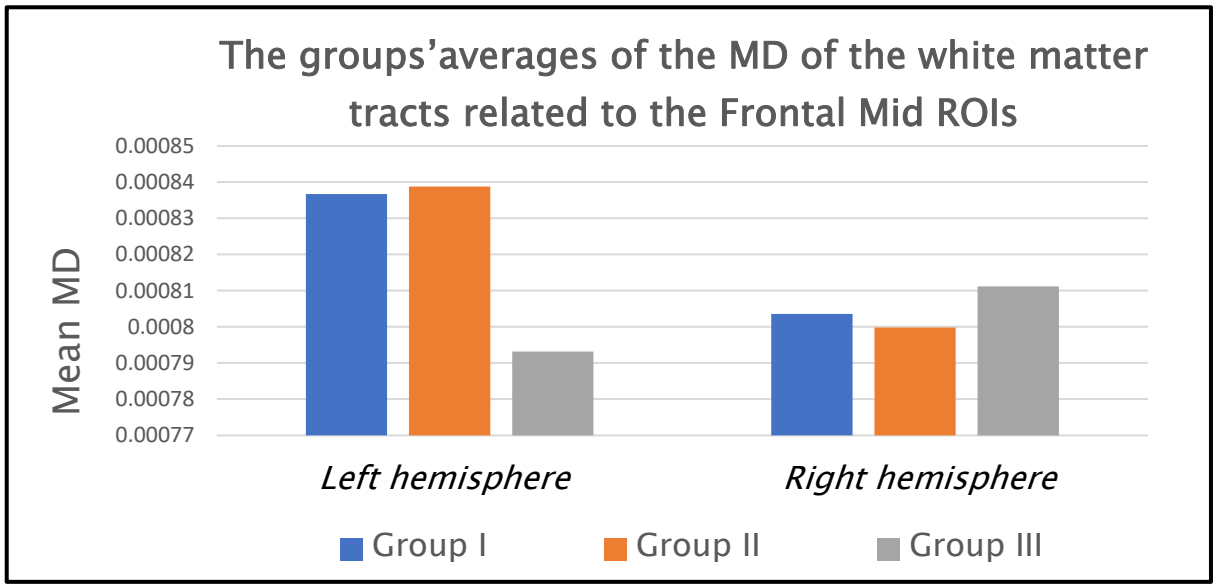

Figure 298: The mean diffusivity (MD) averages of each group of the white matter tracts related to the Frontal Mid ROIs in the left and the right hemispheres.

Table 288: The mean diffusivity (MD) averages and standard deviations (SD) values for the groups studied of the white matter tracts related to the Frontal Mid ROIs, along with intergroup comparisons.

	Left Hemisphere	Right Hemisphere
Heavy users' group (G. I)	(0,000836±0,00002749)	(0,000803±0,00002429)
Light users' group (G. II)	(0,000838±0,00004605)	(0,000799±0,0000474)
Non-users' group (G.III)	(0,000793±0,0000303)	(0,000811±0,0000363)
Intergroup comparison	G. II ≈ G. I > G.III	G. II ≈ G. I ≈ G.III

➢ **Frontal Inf Oper**

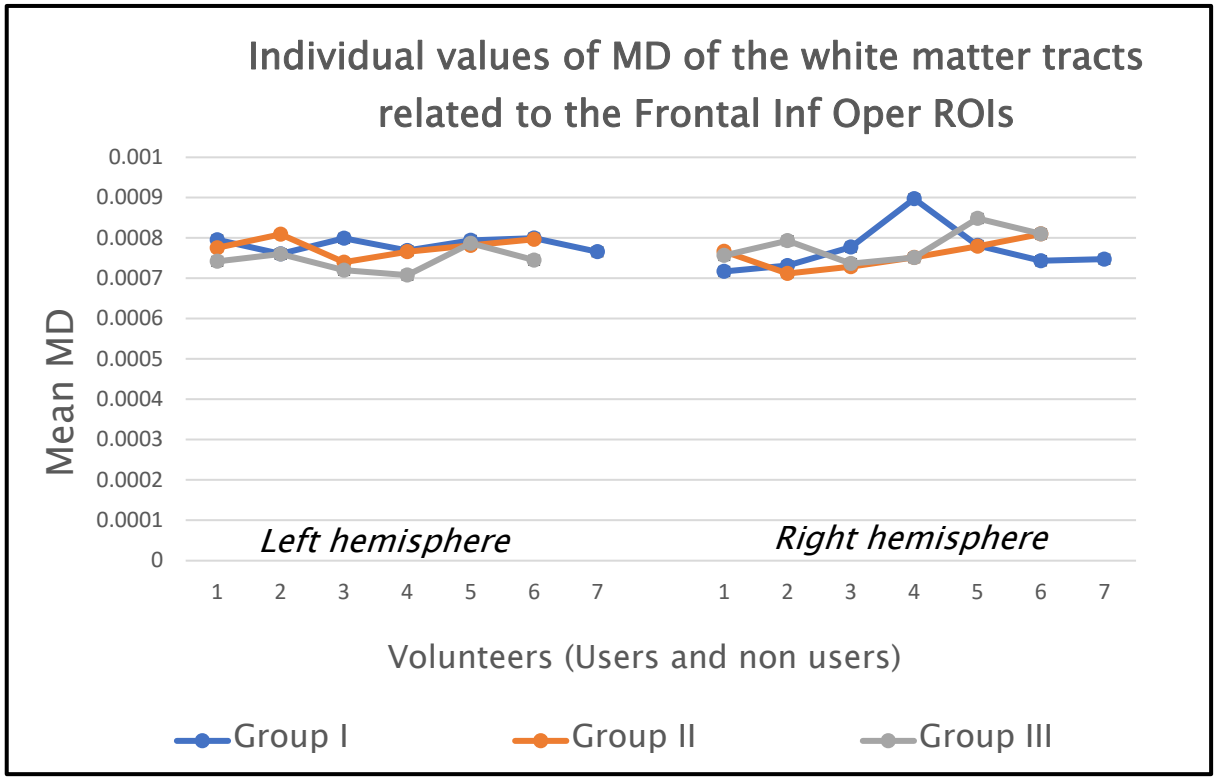

Figure 299: Individual values of mean diffusivity (MD) in both hemispheres' white matter tracts related to the Frontal Inf Oper ROIs. This figure depicts the MD values of all the participants belonging to each of the three groups (Heavy and light users and healthy controls).

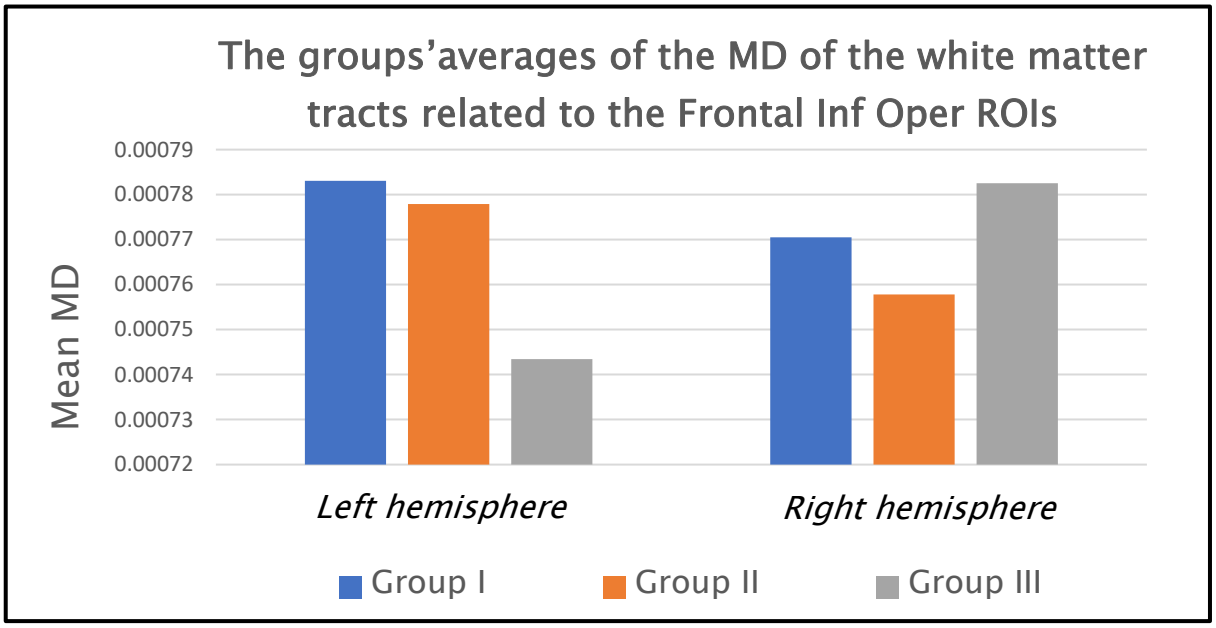

Figure 300: The mean diffusivity (MD) averages of each group of the white matter tracts related to the Frontal Inf Oper ROIs in the left and the right hemispheres.

Table 289: The mean diffusivity (MD) averages and standard deviations (SD) values for the groups studied of the white matter tracts related to the Frontal Inf Oper ROIs, along with intergroup comparisons.

	Left Hemisphere	Right Hemisphere
Heavy users' group (G. I)	(0,000783±0,0000174)	(0,000770±0,0000603)
Light users' group (G. II)	(0,000777±0,0000242)	(0,000757±0,0000353)
Non-users' group (G.III)	(0,000743±0,0000281)	(0,000783±0,0000424)
Intergroup comparison	G. II ≈ G. I > G.III	G. II ≈ G. I ≈ G.III

➢ Frontal Inf Tri

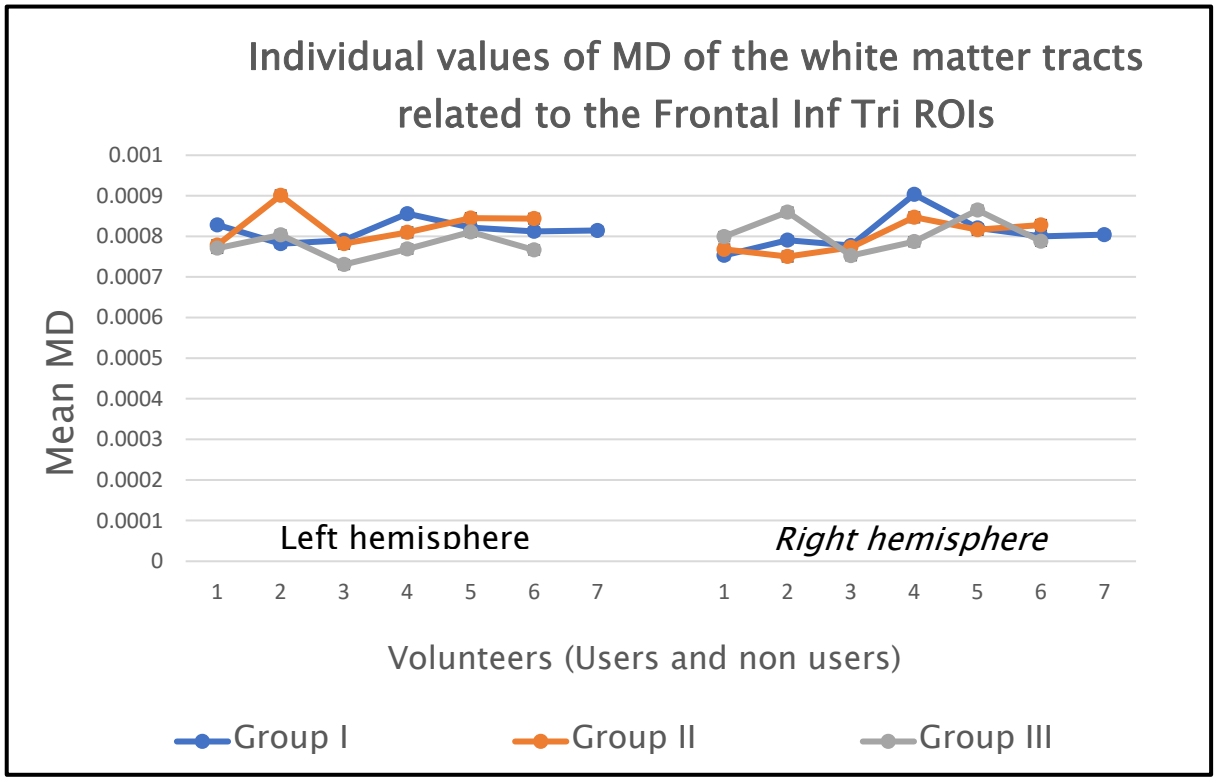

Figure 301: Individual values of mean diffusivity (MD) in both hemispheres' white matter tracts related to the Frontal Inf Tri ROIs. This figure depicts the MD values of all the participants belonging to each of the three groups (Heavy and light users and healthy controls).

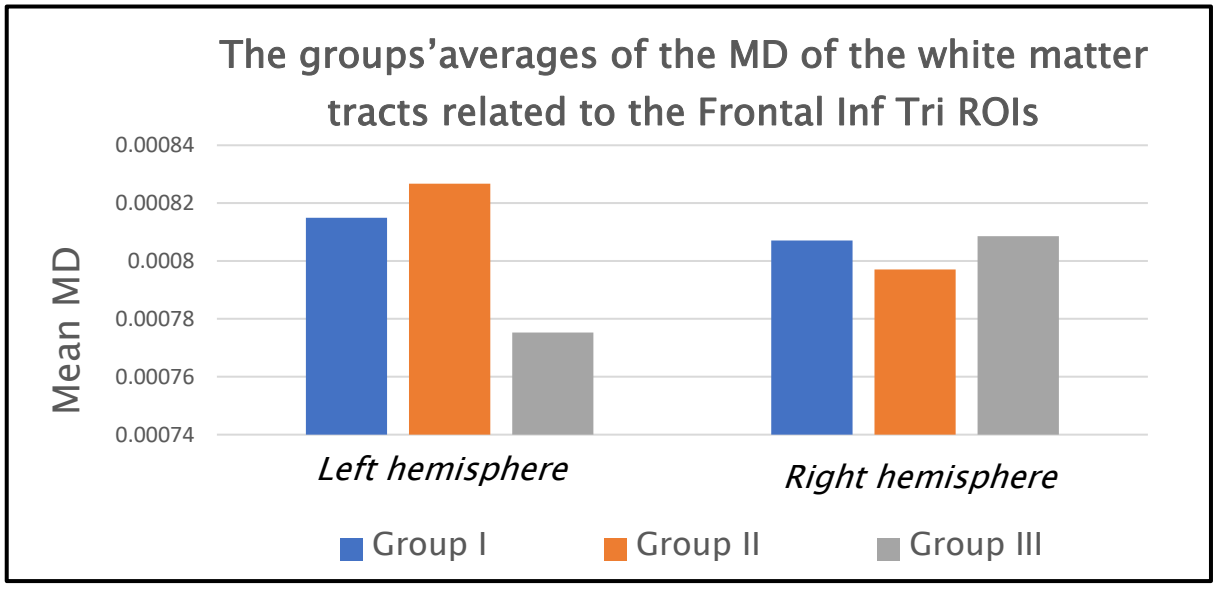

Figure 302: The mean diffusivity (MD) averages of each group of the white matter tracts related to the Frontal Inf Tri ROIs in the left and the right hemispheres.

Table 290: The mean diffusivity (MD) averages and standard deviations (SD) values for the groups studied of the white matter tracts related to the Frontal Inf Tri ROIs, along with intergroup comparisons.

	Left Hemisphere	Right Hemisphere
Heavy users' group (G. I)	(0,0008149±0,0000244)	(0,000807±0,0000475)
Light users' group (G. II)	(0,000827±0,000046)	(0,000797±0,0000386)
Non-users' group (G.III)	(0,000775±0,0000289)	(0,000808±0,0000445)
Intergroup comparison	G. II ≈ G. I > G.III	G. II ≈ G. I ≈ G.III

➢ **Postcentral**

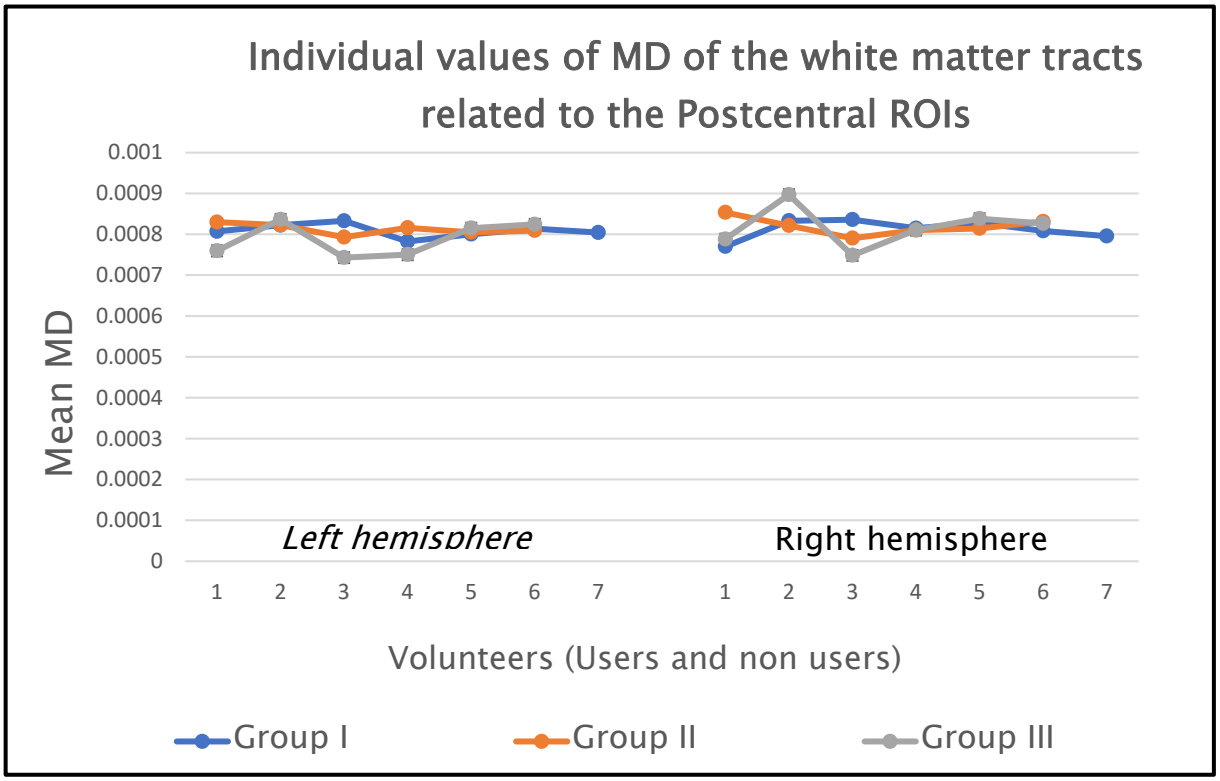

Figure 303: Individual values of mean diffusivity (MD) in both hemispheres' white matter tracts related to the Postcentral ROIs. This figure depicts the MD values of all the participants belonging to each of the three groups (Heavy and light users and healthy controls).

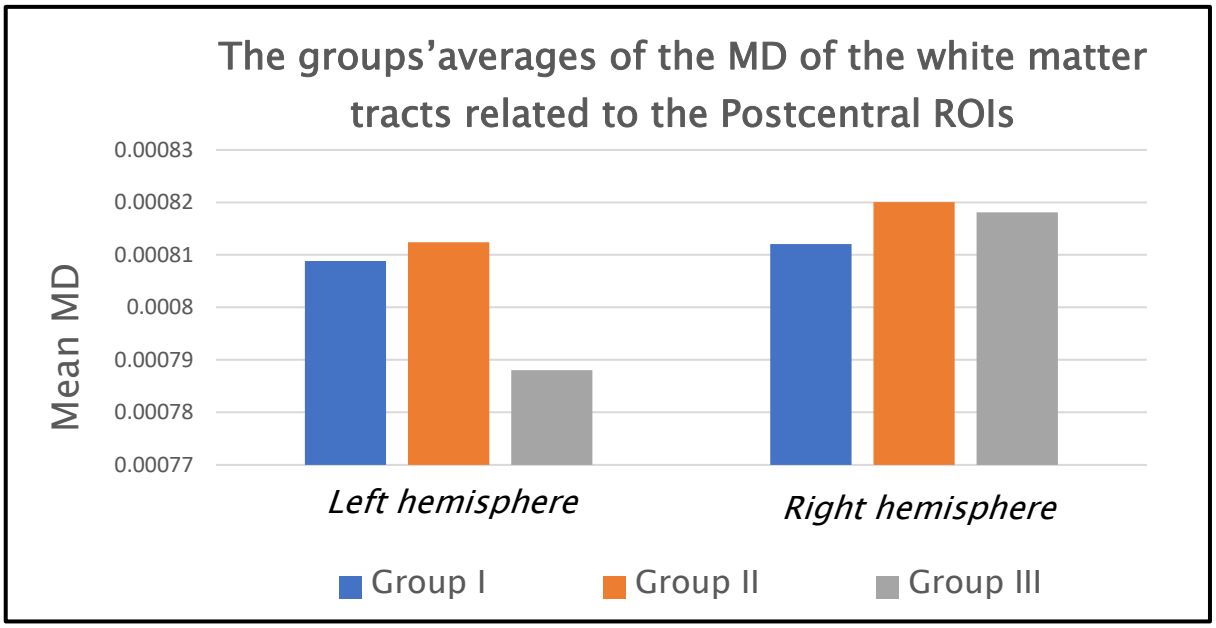

Figure 304: The mean diffusivity (MD) averages of each group of the white matter tracts related to the Postcentral ROIs in the left and the right hemispheres.

Table 291: The mean diffusivity (MD) averages and standard deviations (SD) values for the groups studied of the white matter tracts related to the Postcentral ROIs, along with intergroup comparisons.

	Left Hemisphere	Right Hemisphere
Heavy users' group (G. I)	(0,000808±0,0000162)	(0,000812±0,0000234)
Light users' group (G. II)	(0,000812±0,0000131)	(0,000820±0,0000212)
Non-users' group (G.III)	(0,000788±0,0000415)	(0,000818±0,0000500)
Intergroup comparison	G. II ≈ G. I > G.III	G. II ≈ G. I ≈ G.III

➢ Parietal Sup

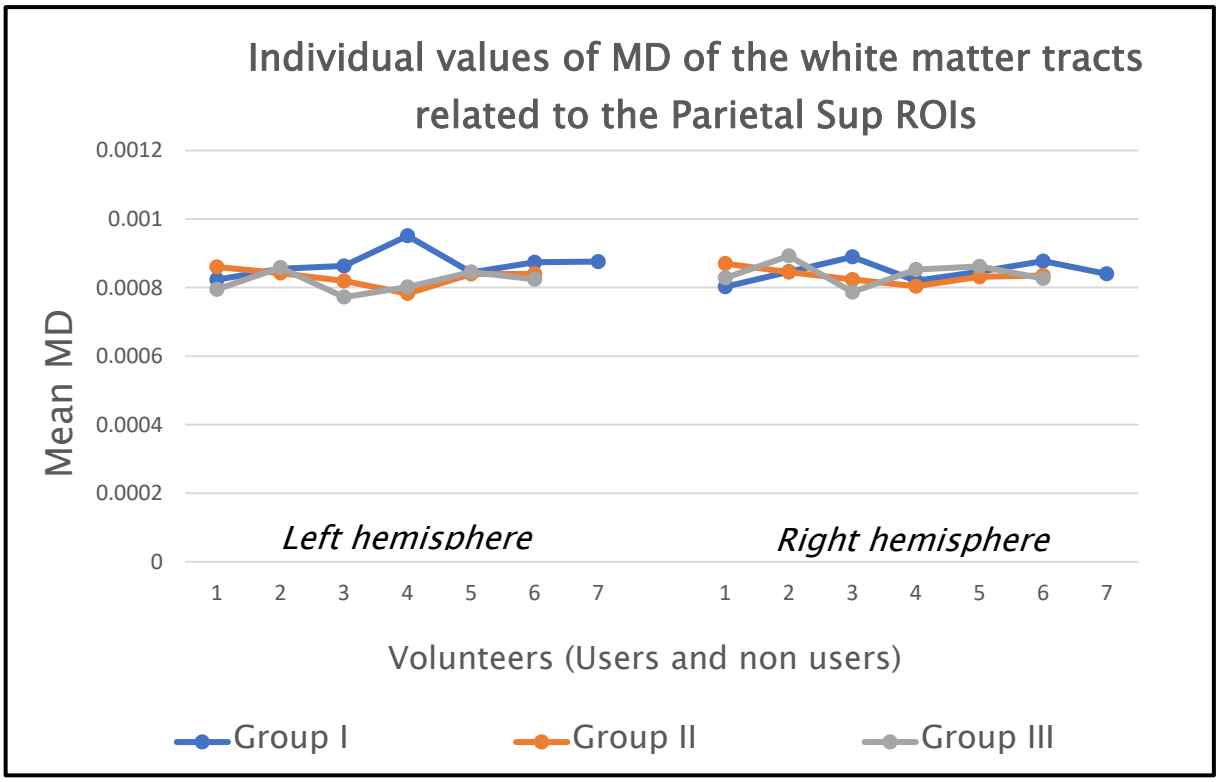

Figure 305: Individual values of mean diffusivity (MD) in both hemispheres' white matter tracts related to the Parietal Sup ROIs. This figure depicts the MD values of all the participants belonging to each of the three groups (Heavy and light users and healthy controls).

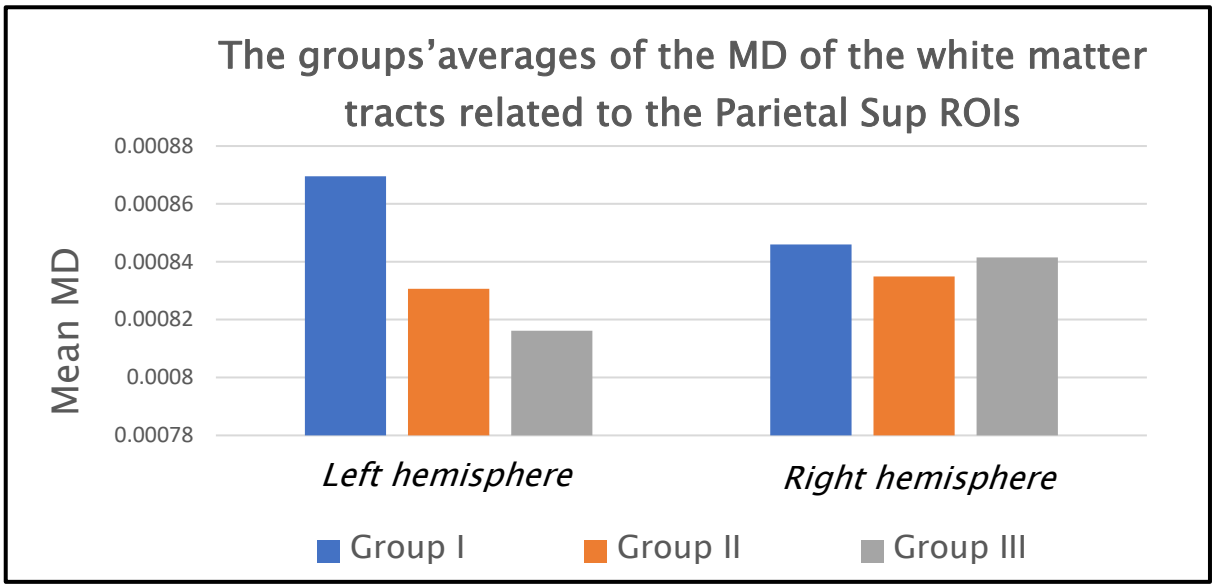

Figure 306: The mean diffusivity (MD) averages of each group of the white matter tracts related to the Parietal Sup ROIs in the left and the right hemispheres.

Table 292: The mean diffusivity (MD) averages and standard deviations (SD) values for the groups studied of the white matter tracts related to the Parietal Sup ROIs, along with intergroup comparisons.

	Left Hemisphere	Right Hemisphere
Heavy users' group (G. I)	(0,000869±0,0000404)	(0,000845±0,0000302)
Light users' group (G. II)	(0,000830±0,0000269)	(0,000834±0,0000221)
Non-users' group (G.III)	(0,000816±0,0000324)	(0,000841±0,0000360)
Intergroup comparison	G. I > G. II ≈ G.III	G. II ≈ G. I ≈ G.III

➢ **SupraMarginal**

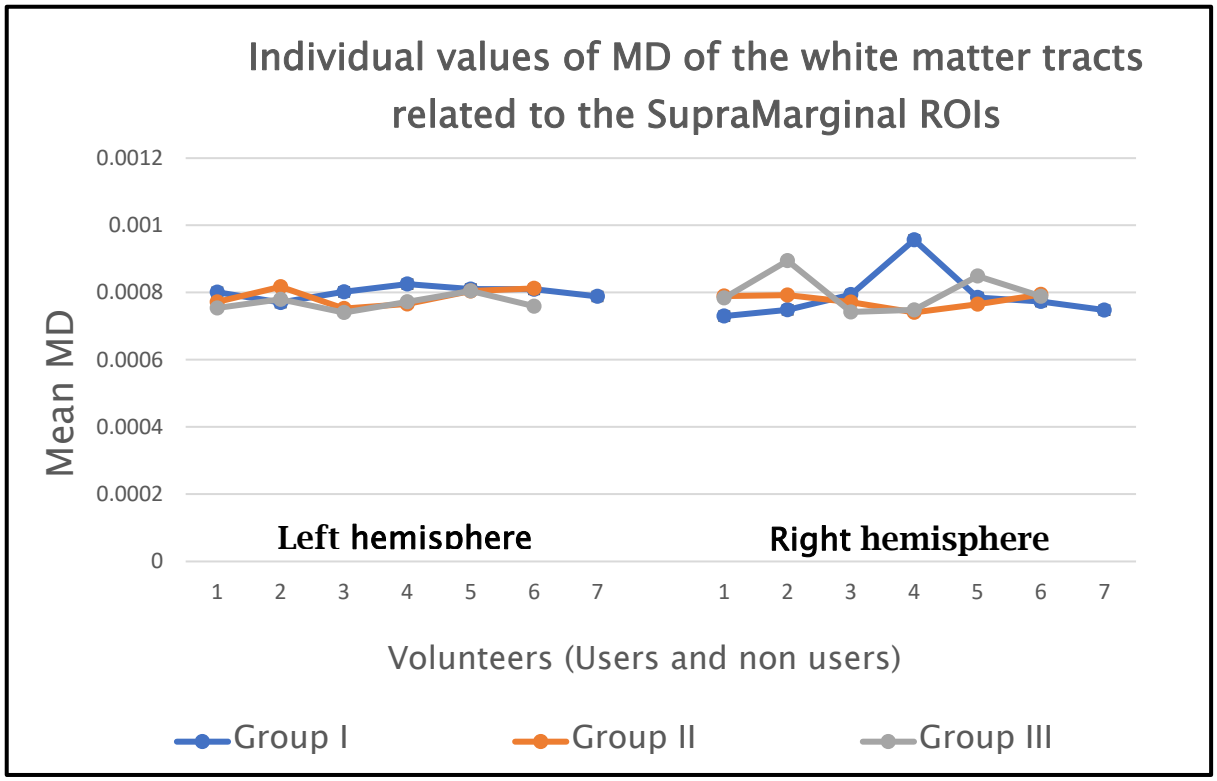

Figure 307: Individual values of mean diffusivity (MD) in both hemispheres' white matter tracts related to the SupraMarginal ROIs. This figure depicts the MD values of all the participants belonging to each of the three groups (Heavy and light users and healthy controls).

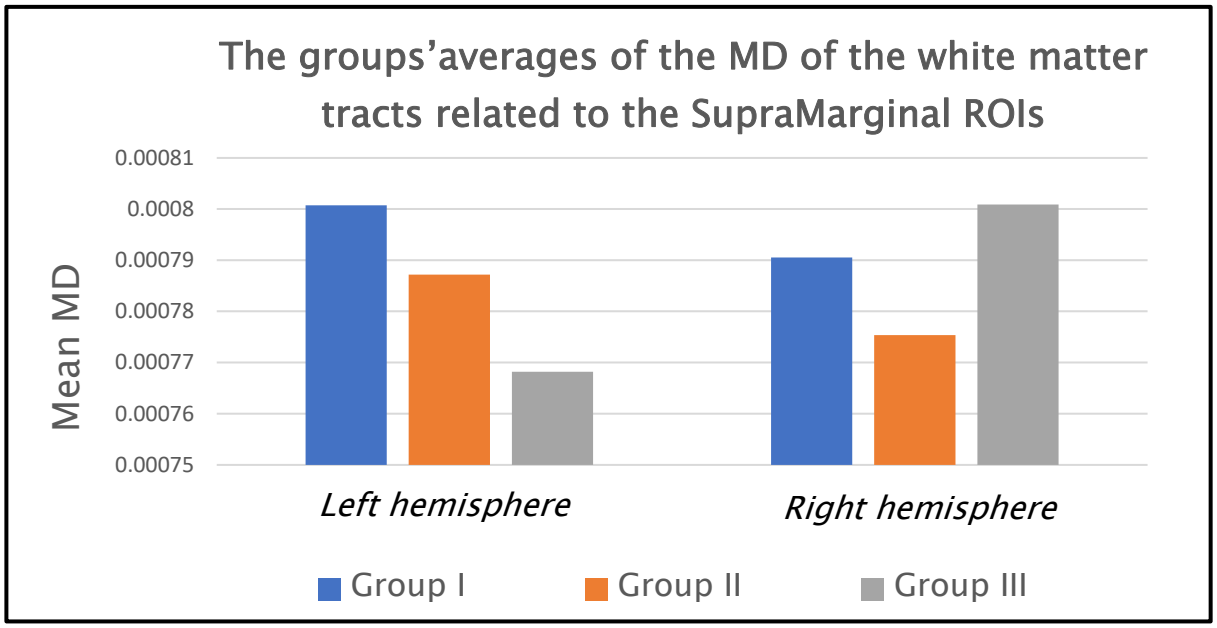

Figure 308: The mean diffusivity (MD) averages of each group of the white matter tracts related to the SupraMarginal ROIs in the left and the right hemispheres.

Table 293: The mean diffusivity (MD) averages and standard deviations (SD) values for the groups studied of the white matter tracts related to the SupraMarginal ROIs, along with intergroup comparisons.

	Left Hemisphere	Right Hemisphere
Heavy users' group (G. I)	(0,0008007±0,0000175)	(0,000790± 0,0000766)
Light users' group (G. II)	(0,000787± 0,0000273)	(0,000775± 0,0000206)
Non-users' group (G.III)	(0,000768± 0,0000224)	(0,0008008± 0,0000597)
Intergroup comparison	G. I > G. II > G.III	G. II ≈ G. I ≈ G.III

➢ Angular

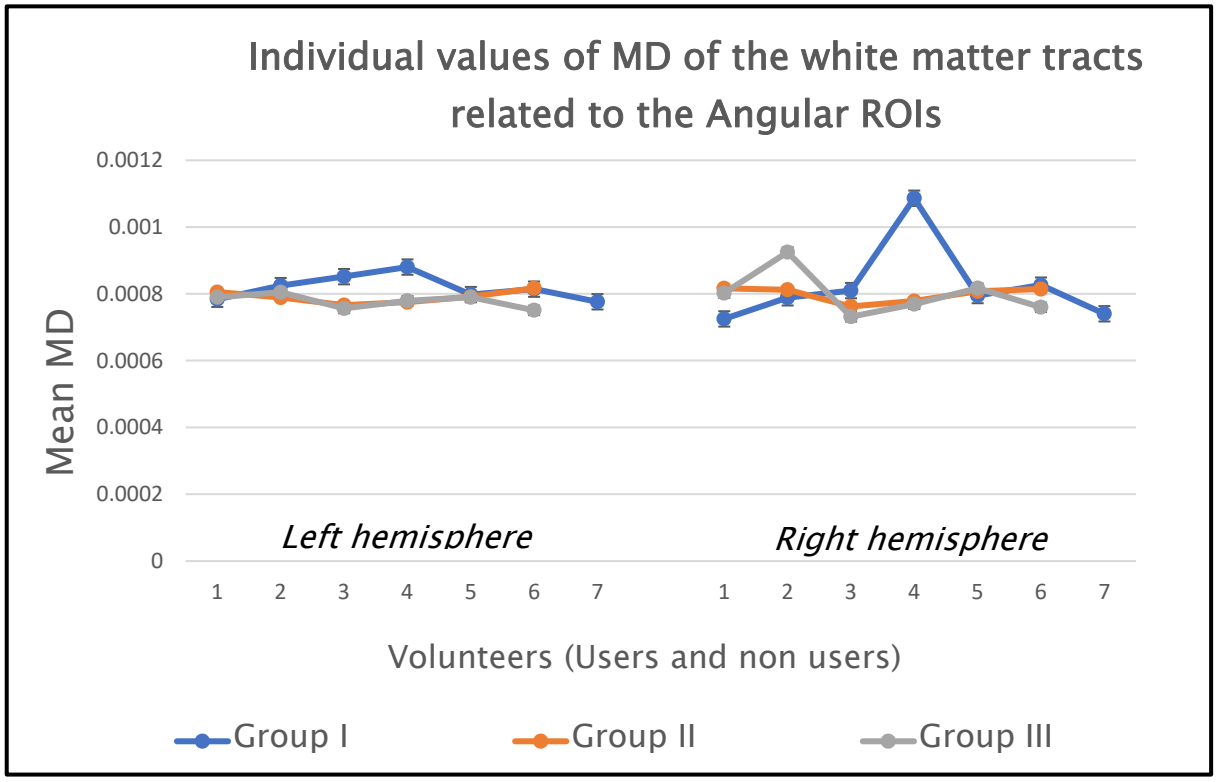

Figure 309: Individual values of mean diffusivity (MD) in both hemispheres' white matter tracts related to the Angular ROIs. This figure depicts the MD values of all the participants belonging to each of the three groups (Heavy and light users and healthy controls).

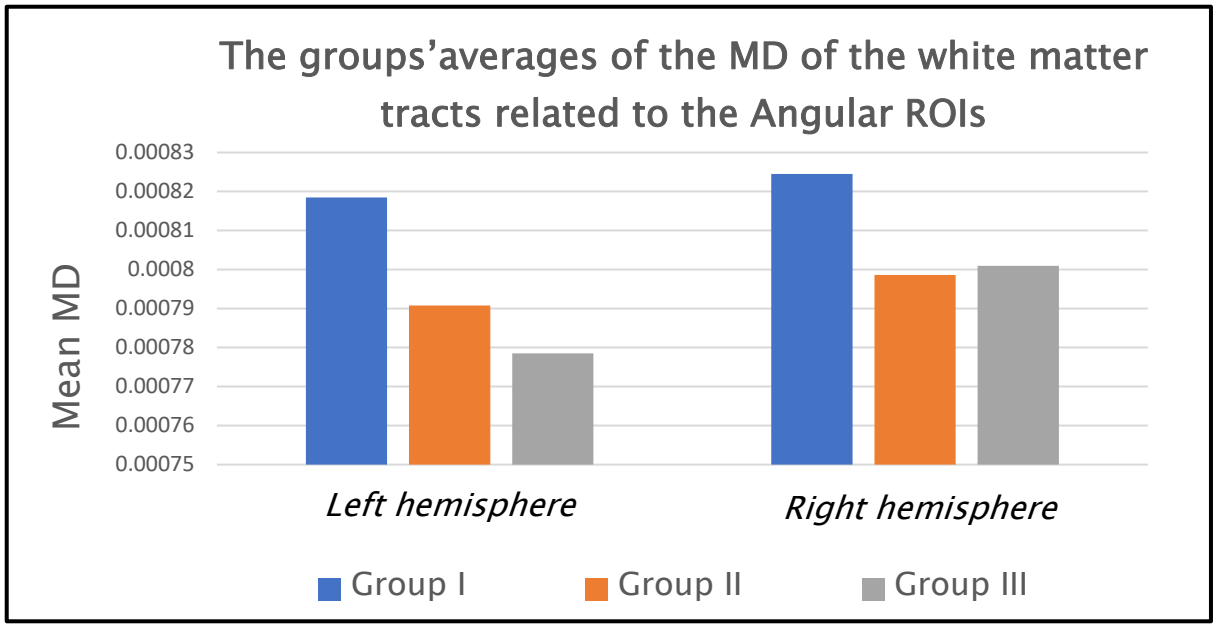

Figure 310: The mean diffusivity (MD) averages of each group of the white matter tracts related to the Angular ROIs in the left and the right hemispheres.

Table 294: The mean diffusivity (MD) averages and standard deviations (SD) values for the groups studied of the white matter tracts related to the Angular ROIs, along with intergroup comparisons.

	Left Hemisphere	Right Hemisphere
Heavy users' group (G. I)	(0,000818±0,0000373)	(0,000824±0,000121)
Light users' group (G. II)	(0,000790±0,0000188)	(0,000798±0,00002267)
Non-users' group (G.III)	(0,000778±0,0000209)	(0,0008009±0,00006800)
Intergroup comparison	G. I > G. II ≈ G.III	G. I > G. II ≈ G.III

➢ **Parietal Inf**

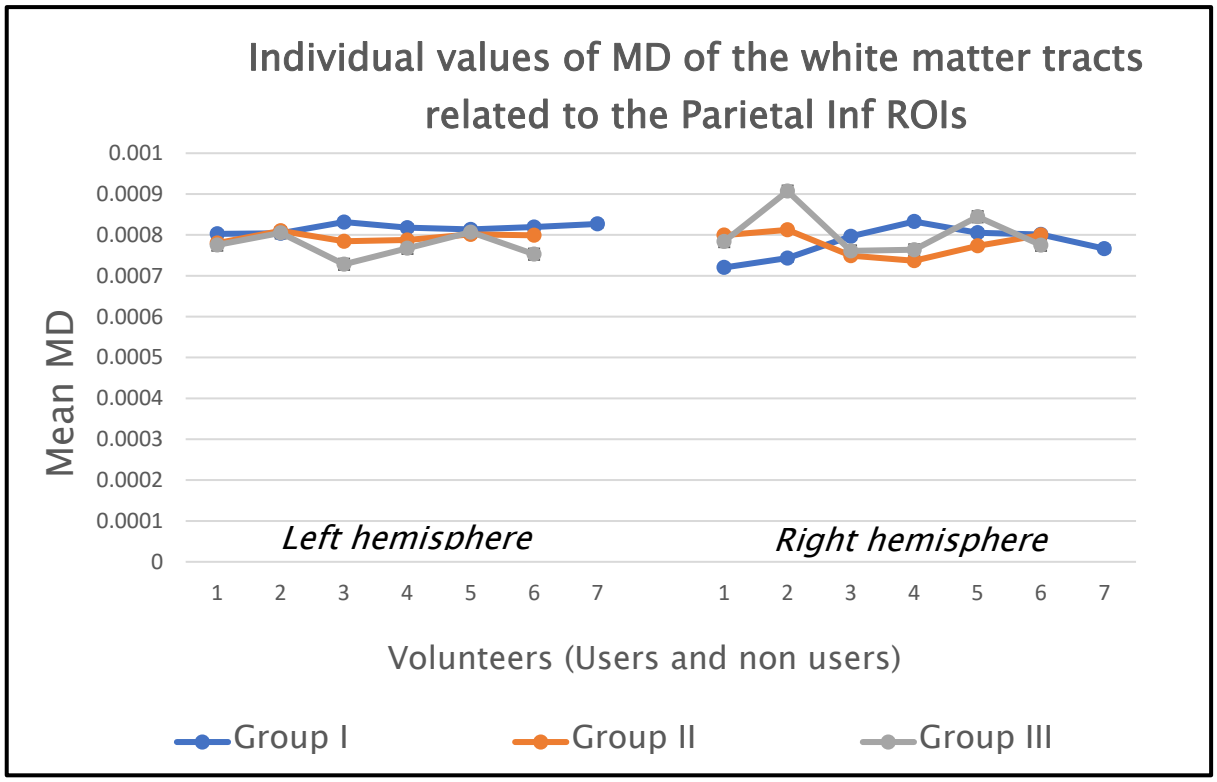

Figure 311: Individual values of mean diffusivity (MD) in both hemispheres' white matter tracts related to the Parietal Inf ROIs. This figure depicts the MD values of all the participants belonging to each of the three groups (Heavy and light users and healthy controls).

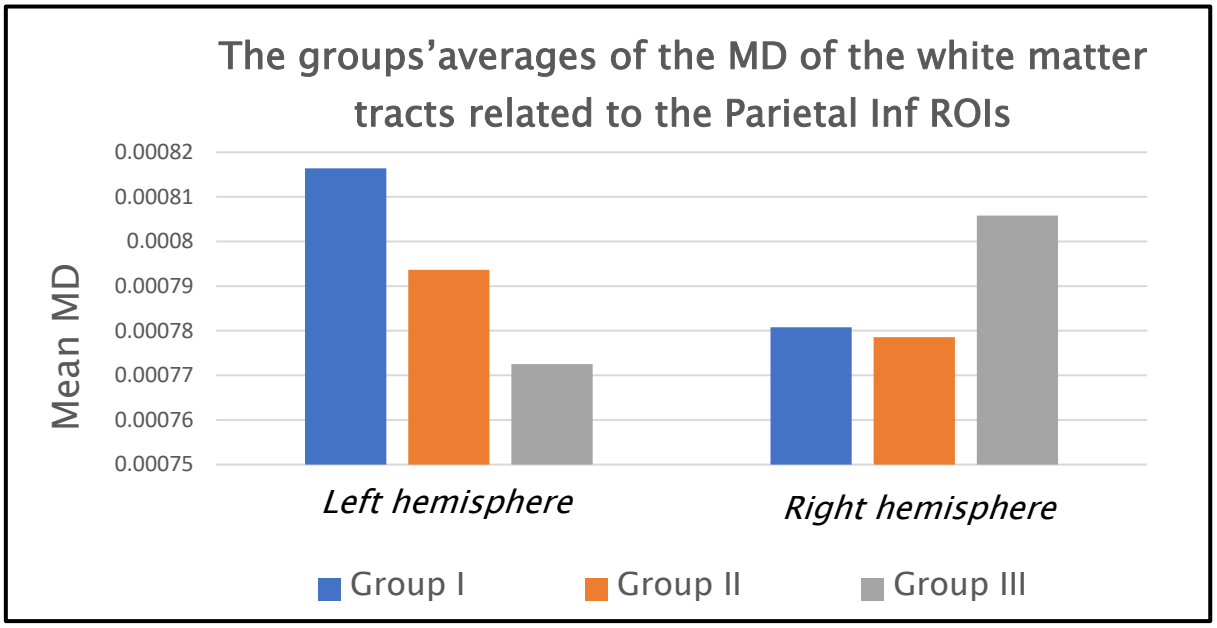

Figure 312: The mean diffusivity (MD) averages of each group of the white matter tracts related to the Parietal Inf ROIs in the left and the right hemispheres.

Table 295: The mean diffusivity (MD) averages and standard deviations (SD) values for the groups studied of the white matter tracts related to the Parietal Inf ROIs, along with intergroup comparisons.

	Left Hemisphere	Right Hemisphere
Heavy users' group (G. I)	(0,000816±0,00001076)	(0,0007807±0,00003925)
Light users' group (G. II)	(0,000793±0,00001156)	(0,000778±0,00003057)
Non-users' group (G.III)	(0,000772±0,00003036)	(0,000805±0,00005834)
Intergroup comparison	G. I > G. II ≈ G.III	G.III > G. II ≈ G. I

➢ **Precuneus**

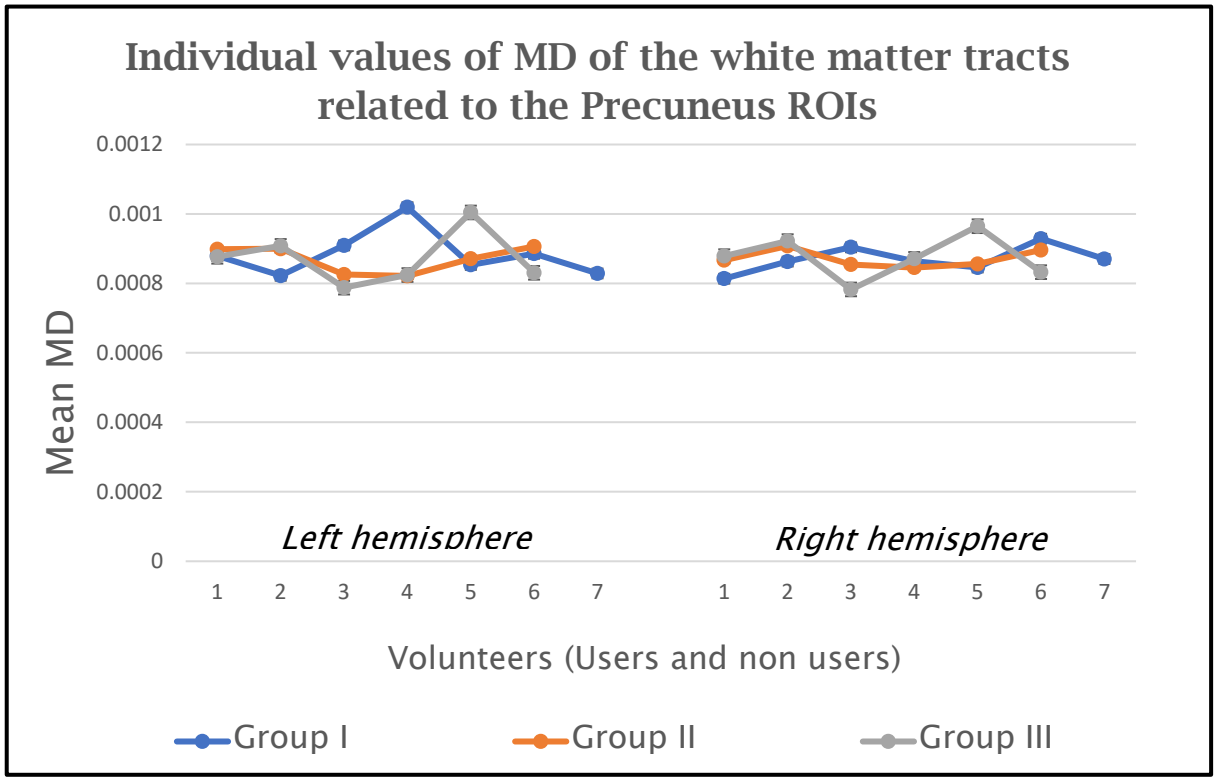

Figure 313: Individual values of mean diffusivity (MD) in both hemispheres' white matter tracts related to the Precuneus ROIs. This figure depicts the MD values of all the participants belonging to each of the three groups (Heavy and light users and healthy controls).

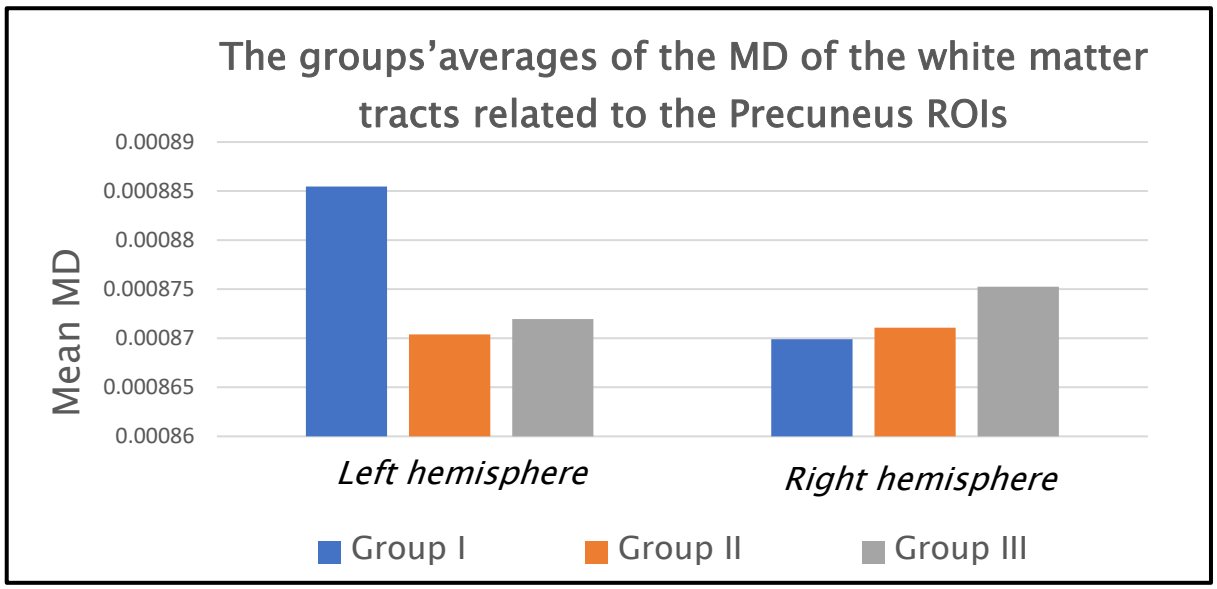

Figure 314: The mean diffusivity (MD) averages of each group of the white matter tracts related to the Precuneus ROIs in the left and the right hemispheres.

Table 296: The mean diffusivity (MD) averages and standard deviations (SD) values for the groups studied of the white matter tracts related to the Precuneus ROIs, along with intergroup comparisons.

	Left Hemisphere	Right Hemisphere
Heavy users' group (G. I)	(0,000885±0,0000668)	(0,000869±0,0000375)
Light users' group (G. II)	(0,0008703±0,0000382)	(0,000871±0,0000251)
Non-users' group (G.III)	(0,0008719±0,0000774)	(0,000875±0,0000642)
Intergroup comparison	G. I > G. II ≈ G.III	G.III ≈ G. II ≈ G. I

➢ **Temporal Sup**

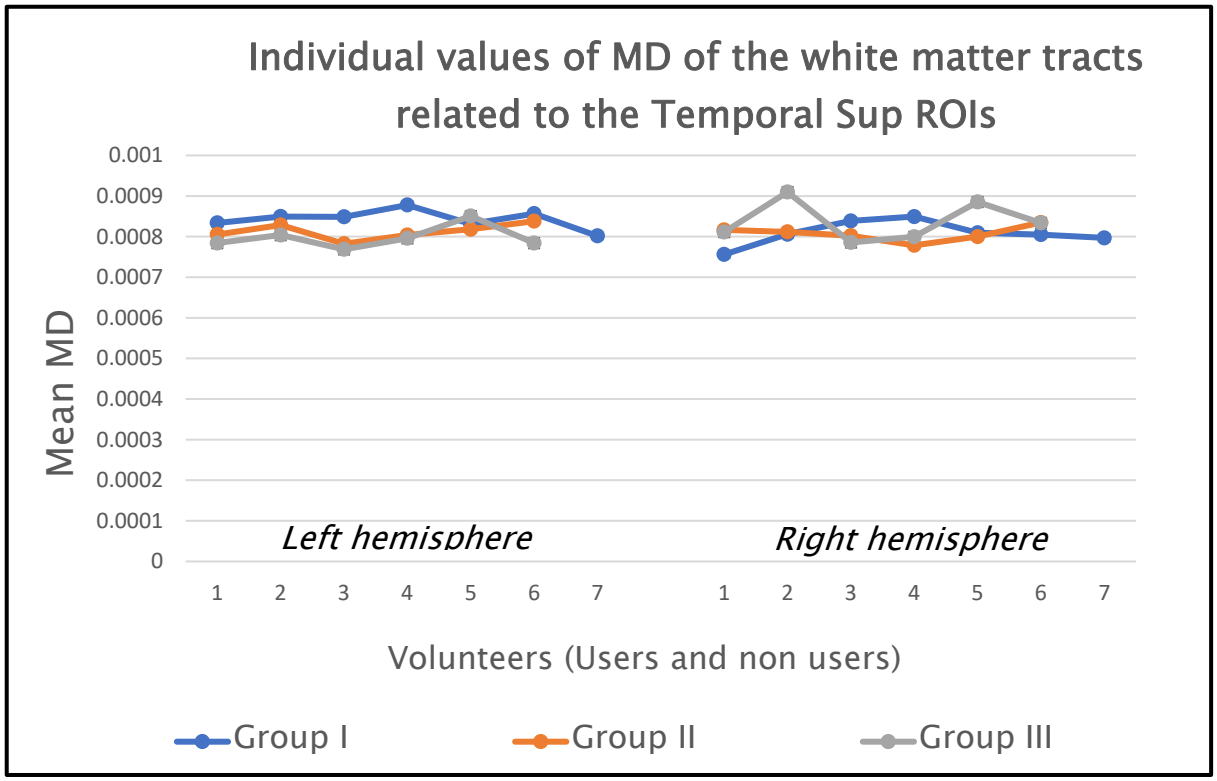

Figure 315: Individual values of mean diffusivity (MD) in both hemispheres' white matter tracts related to the Temporal Sup ROIs. This figure depicts the MD values of all the participants belonging to each of the three groups (Heavy and light users and healthy controls).

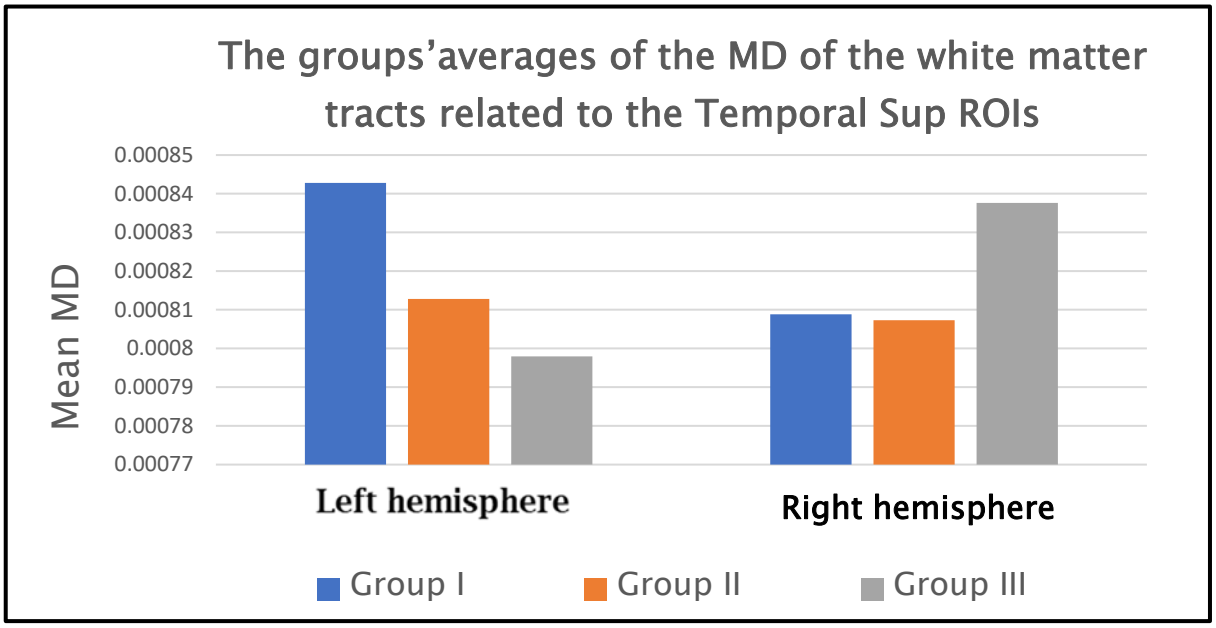

Figure 316: The mean diffusivity (MD) averages of each group of the white matter tracts related to the Temporal Sup ROIs in the left and the right hemispheres.

Table 297: The mean diffusivity (MD) averages and standard deviations (SD) values for the groups studied of the white matter tracts related to the Temporal Sup ROIs, along with intergroup comparisons.

	Left Hemisphere	Right Hemisphere
Heavy users' group (G. I)	(0,000842±0,0000238)	(0,000808±0,00003019)
Light users' group (G. II)	(0,000812±0,0000198)	(0,000807±0,00001875)
Non-users' group (G.III)	(0,000797±0,0000284)	(0,0008376±0,0000497)
Intergroup comparison	G. I > G. II ≈ G.III	G.III > G. II ≈ G. I

➢ Temporal Pole Sup

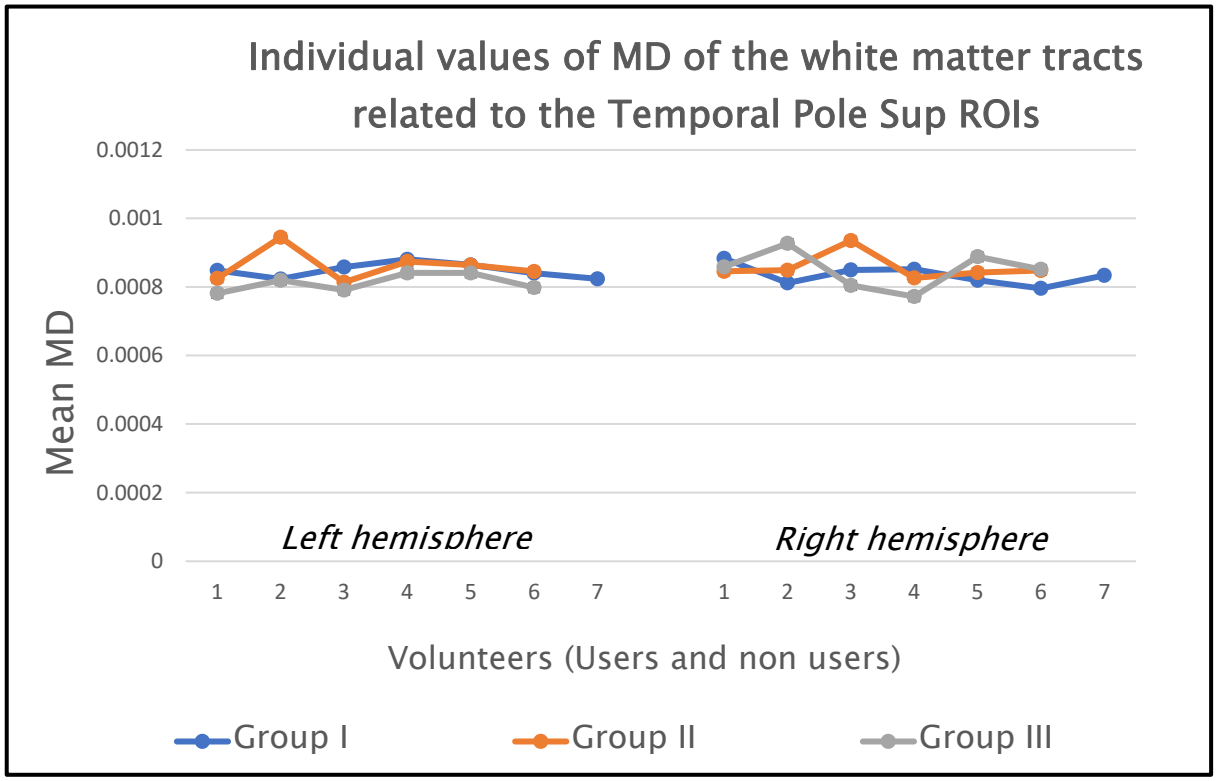

Figure 317: Individual values of mean diffusivity (MD) in both hemispheres' white matter tracts related to the Temporal Pole Sup ROIs. This figure depicts the MD values of all the participants belonging to each of the three groups (Heavy and light users and healthy controls).

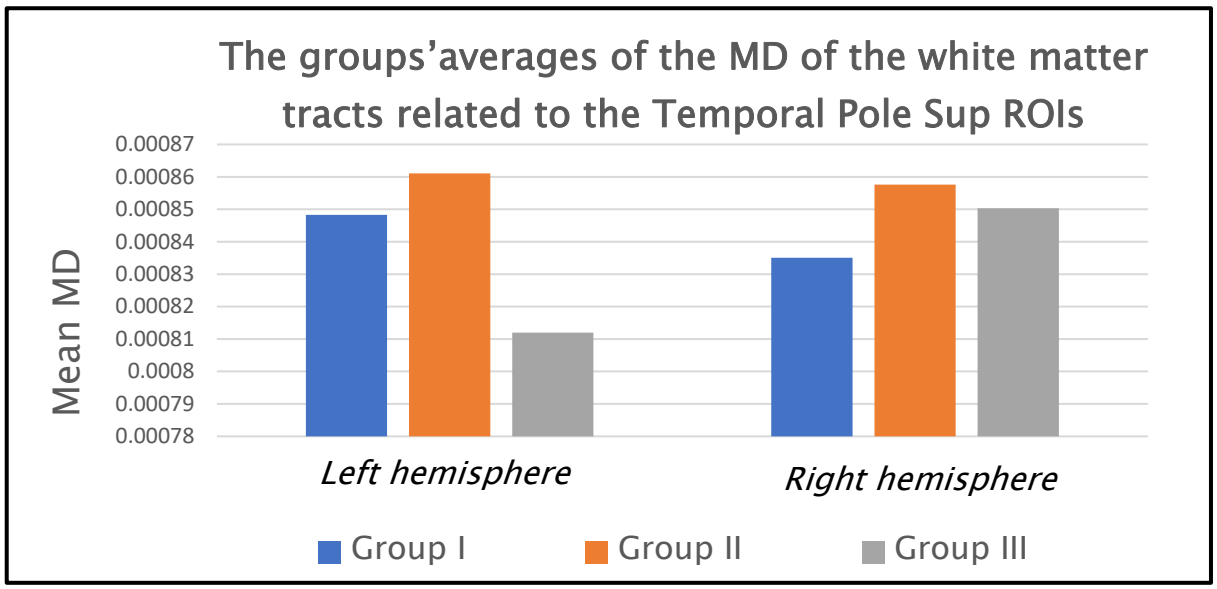

Figure 318: The mean diffusivity (MD) averages of each group of the white matter tracts related to the Temporal Pole Sup ROIs in the left and the right hemispheres.

Table 298: The mean diffusivity (MD) averages and standard deviations (SD) values for the groups studied of the white matter tracts related to the Temporal Pole Sup ROIs, along with intergroup comparisons.

	Left Hemisphere	Right Hemisphere
Heavy users' group (G. I)	(0,000848±0,0000211)	(0,000835±0,0000292)
Light users' group (G. II)	(0,000861±0,0000469)	(0,000857±0,0000388)
Non-users' group (G.III)	(0,000811±0,0000256)	(0,000850±0,00005588)
Intergroup comparison	G. I ≈ G. II > G.III	G.III ≈ G. II ≈ G. I

➢ **Heschl**

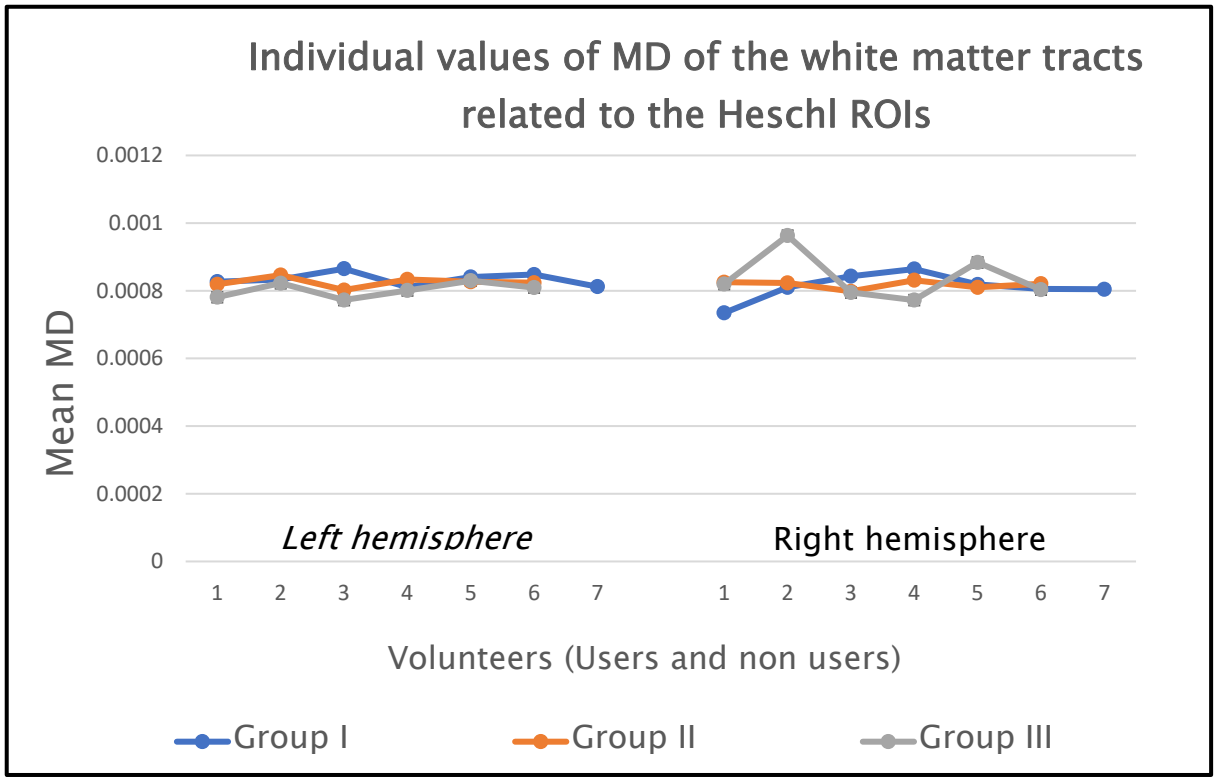

Figure 319: Individual values of mean diffusivity (MD) in both hemispheres' white matter tracts related to the Heschl ROIs. This figure depicts the MD values of all the participants belonging to each of the three groups (Heavy and light users and healthy controls).

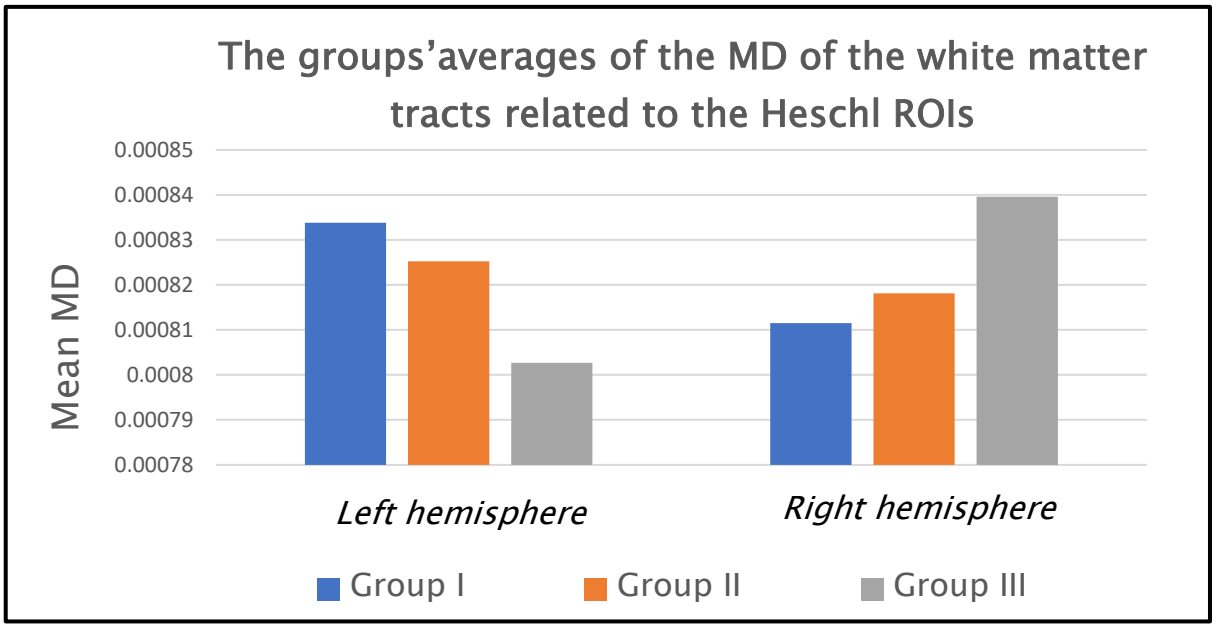

Figure 320: The mean diffusivity (MD) averages of each group of the white matter tracts related to the Heschl ROIs in the left and the right hemispheres.

Table 299: The mean diffusivity (MD) averages and standard deviations (SD) values for the groups studied of the white matter tracts related to the Heschl ROIs, along with intergroup comparisons.

	Left Hemisphere	Right Hemisphere
Heavy users' group (G. I)	(0,000833±0,0000195)	(0,000811±0,0000404)
Light users' group (G. II)	(0,000825±0,0000148)	(0,000818±0,00001187)
Non-users' group (G.III)	(0,0008026±0,0000224)	(0,000839±0,0000713)
Intergroup comparison	G. I ≈ G. II > G.III	G.III > G. II ≈ G. I

➢ Temporal Mid

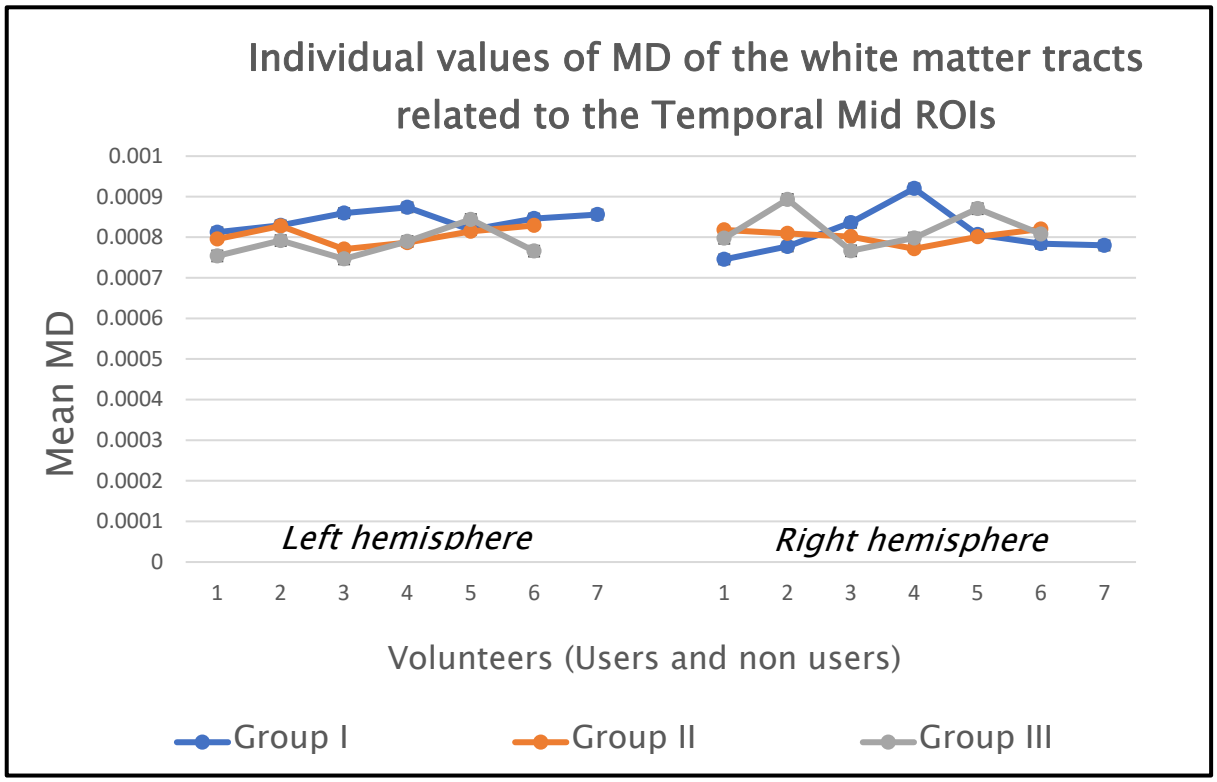

Figure 321: Individual values of mean diffusivity (MD) in both hemispheres' white matter tracts related to the Temporal Mid ROIs. This figure depicts the MD values of all the participants belonging to each of the three groups (Heavy and light users and healthy controls).

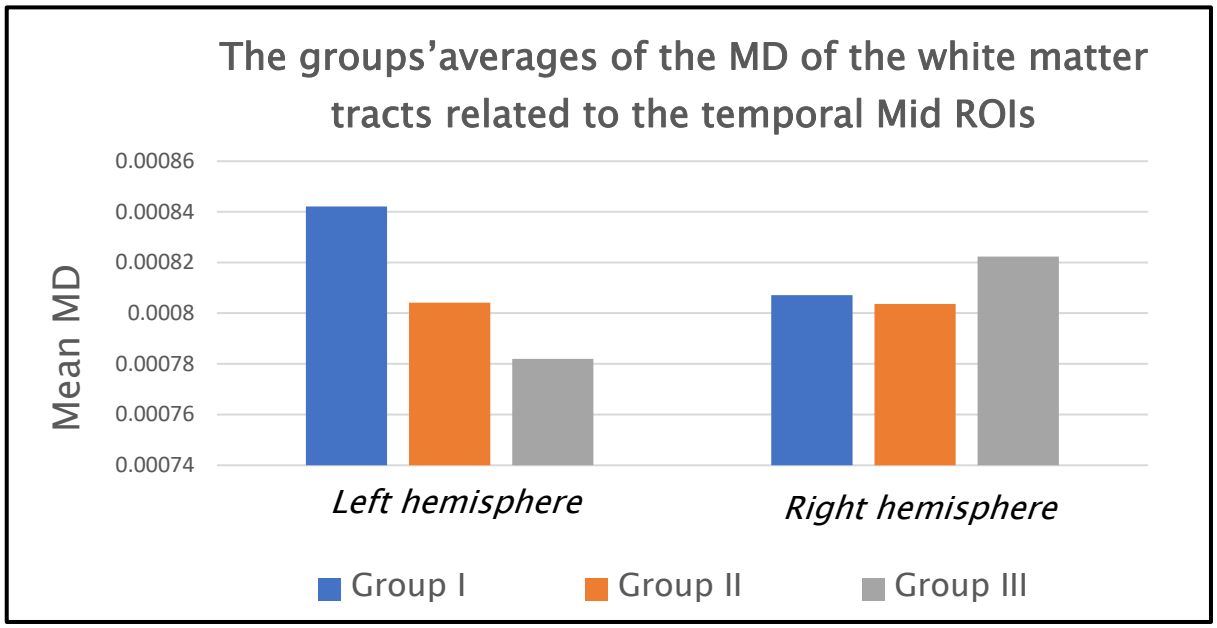

Figure 322: The mean diffusivity (MD) averages of each group of the white matter tracts related to the Temporal Mid ROIs in the left and the right hemispheres.

Table 300: The mean diffusivity (MD) averages and standard deviations (SD) values for the groups studied of the white matter tracts related to the Temporal Mid ROIs, along with intergroup comparisons.

	Left Hemisphere	Right Hemisphere
Heavy users' group (G. I)	(0,000842±0,0000228)	(0,000807±0,0000571)
Light users' group (G. II)	(0,000804±0,0000235)	(0,000803±0,0000176)
Non-users' group (G.III)	(0,000781±0,0000353)	(0,000822±0,0000486)
Intergroup comparison	G. I > G. II ≈ G.III	G.III ≈ G. II ≈ G. I

➢ **Temporal Pole Mid**

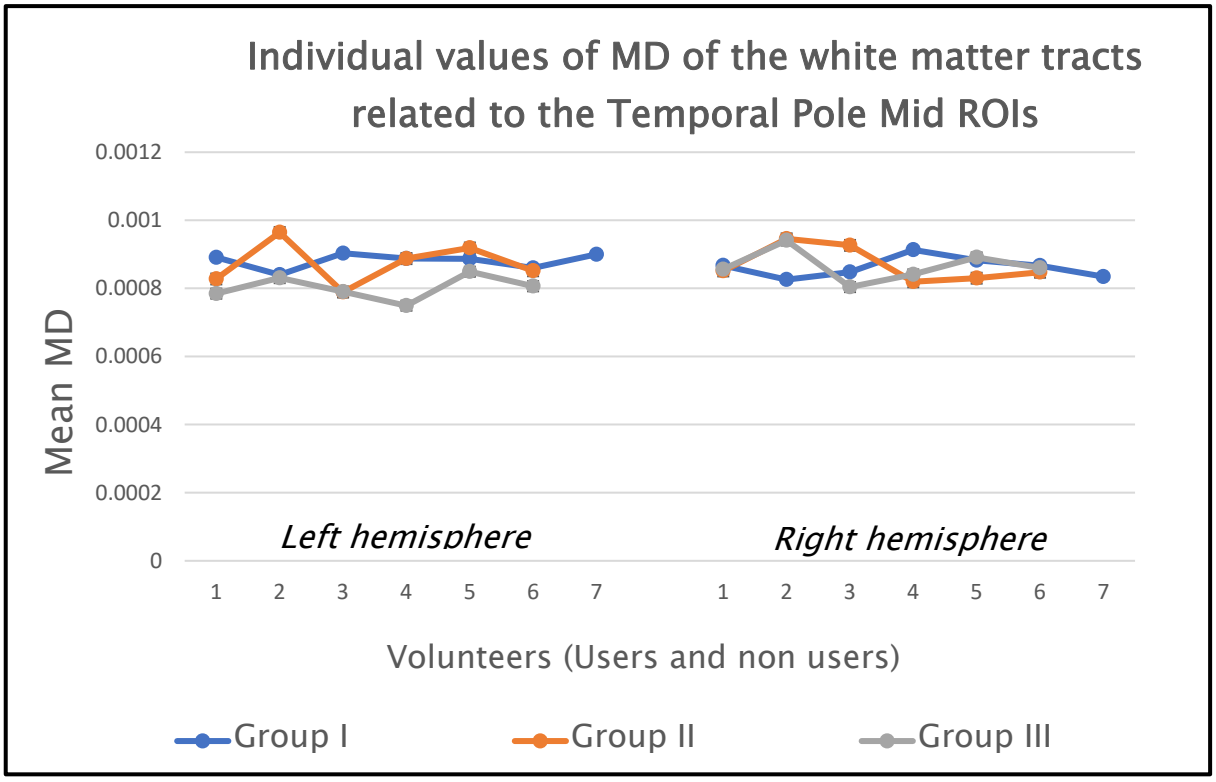

Figure 323: Individual values of mean diffusivity (MD) in both hemispheres' white matter tracts related to the Temporal Pole Mid ROIs. This figure depicts the MD values of all the participants belonging to each of the three groups (Heavy and light users and healthy controls).

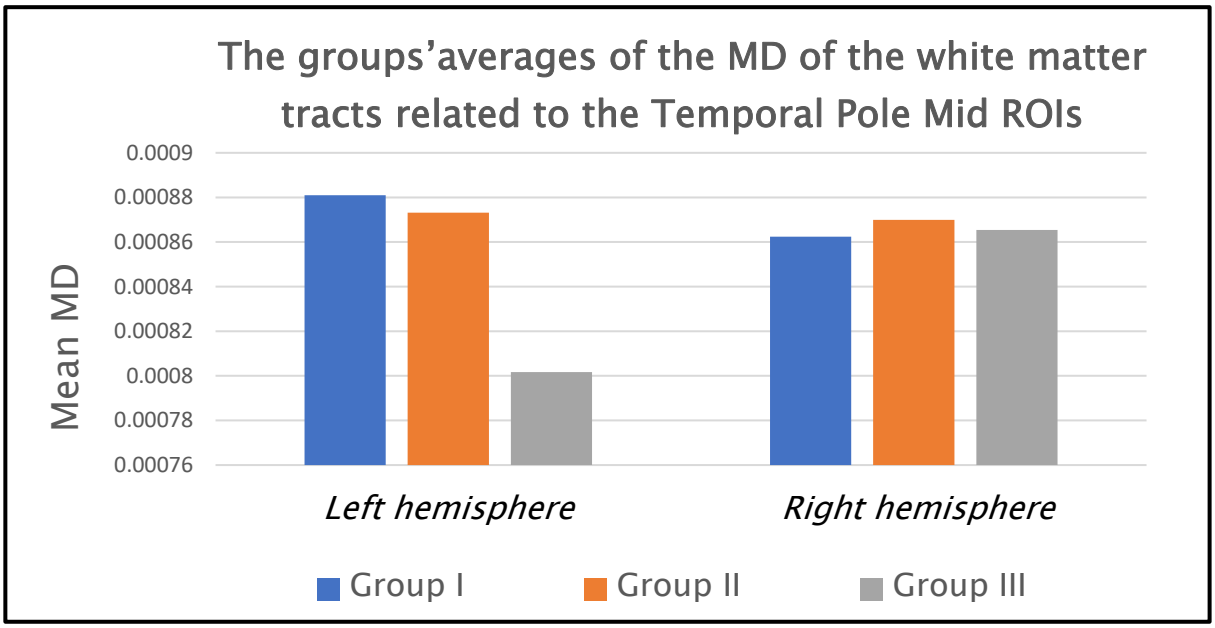

Figure 324: The mean diffusivity (MD) averages of each group of the white matter tracts related to the Temporal Pole Mid ROIs in the left and the right hemispheres.

Table 301: The mean diffusivity (MD) averages and standard deviations (SD) values for the groups studied of the white matter tracts related to the Temporal Pole Mid ROIs, along with intergroup comparisons.

	Left Hemisphere	Right Hemisphere
Heavy users' group (G. I)	(0,000880±0,0000229)	(0,000862±0,0000298)
Light users' group (G. II)	(0,000873±0,0000636)	(0,000869±0,0000527)
Non-users' group (G.III)	(0,000801±0,0000353)	(0,000865±0,0000465)
Intergroup comparison	G. I ≈ G. II > G.III	G.III ≈ G. II ≈ G. I

➢ Temporal Inf

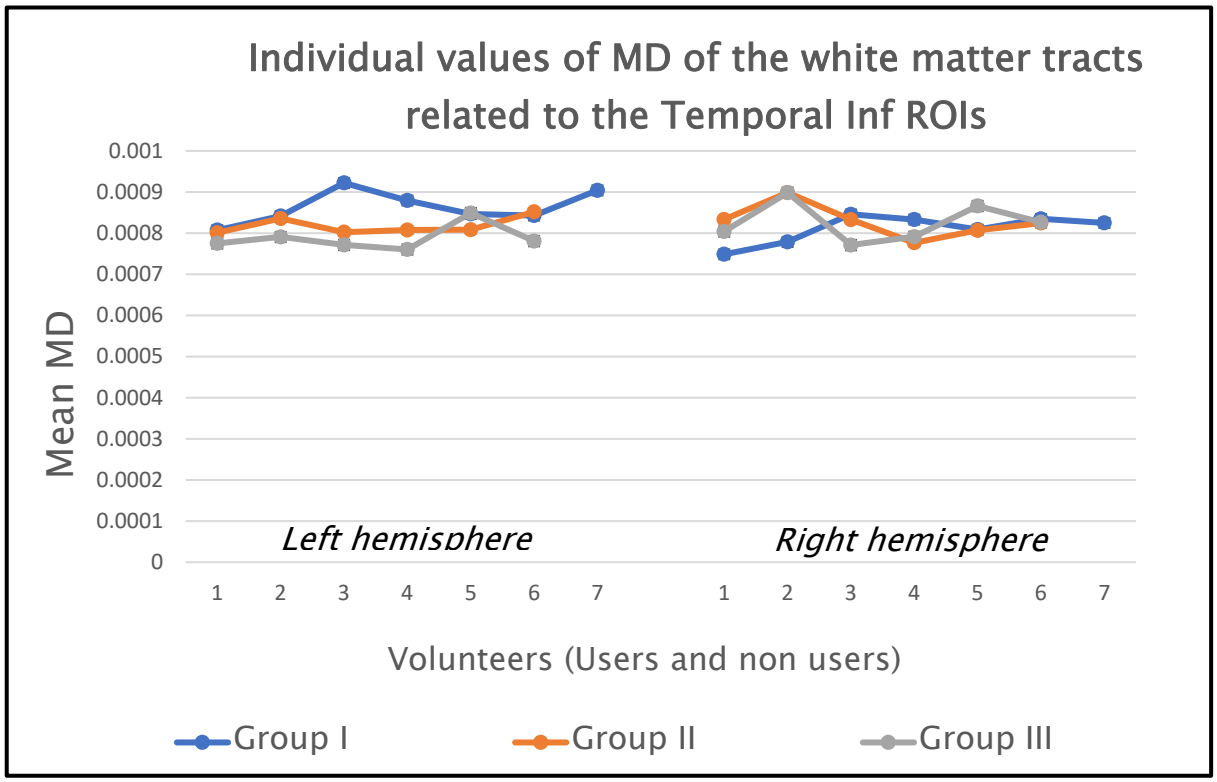

Figure 325: Individual values of mean diffusivity (MD) in both hemispheres' white matter tracts related to the Temporal Inf ROIs. This figure depicts the MD values of all the participants belonging to each of the three groups (Heavy and light users and healthy controls).

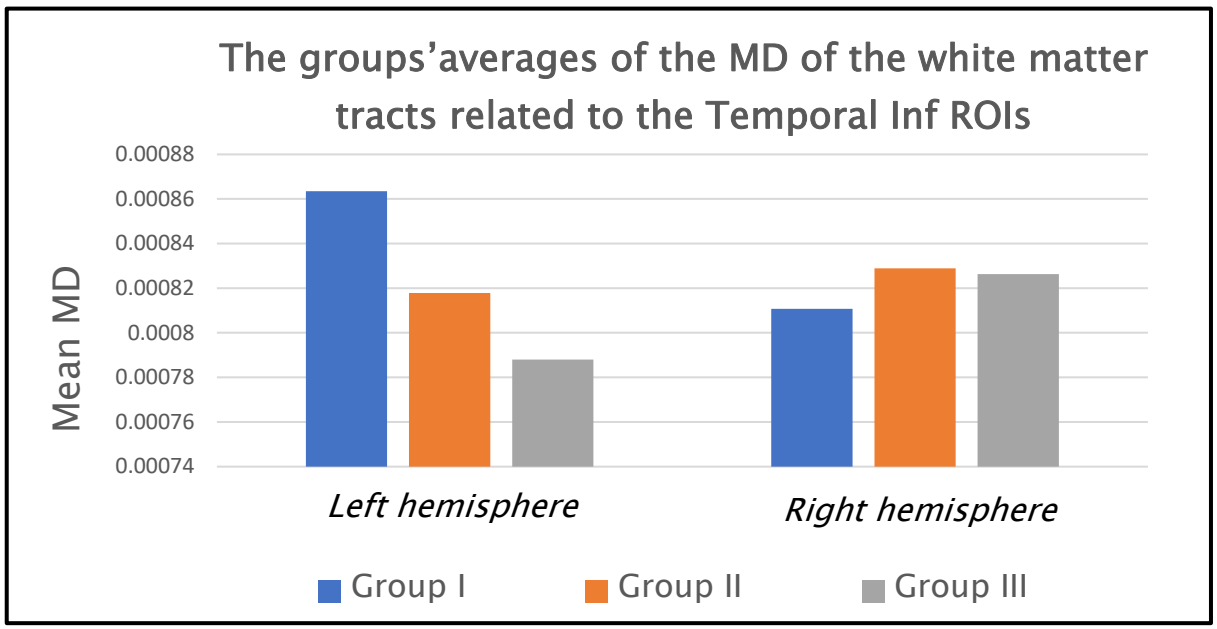

Figure 326: The mean diffusivity (MD) averages of each group of the white matter tracts related to the Temporal Inf ROIs in the left and the right hemispheres.

Table 302: The mean diffusivity (MD) averages and standard deviations (SD) values for the groups studied of the white matter tracts related to the Temporal Inf ROIs, along with intergroup comparisons.

	Left Hemisphere	Right Hemisphere
Heavy users' group (G. I)	(0,000863±0,0000401)	(0,000810±0,0000350)
Light users' group (G. II)	(0,000817±0,0000208)	(0,000828±0,0000403)
Non-users' group (G.III)	(0,000787±0,0000315)	(0,000826±0,0000481)
Intergroup comparison	G. I > G. II > G.III	G.III ≈ G. II ≈ G. I

➢ **Fusiform:**

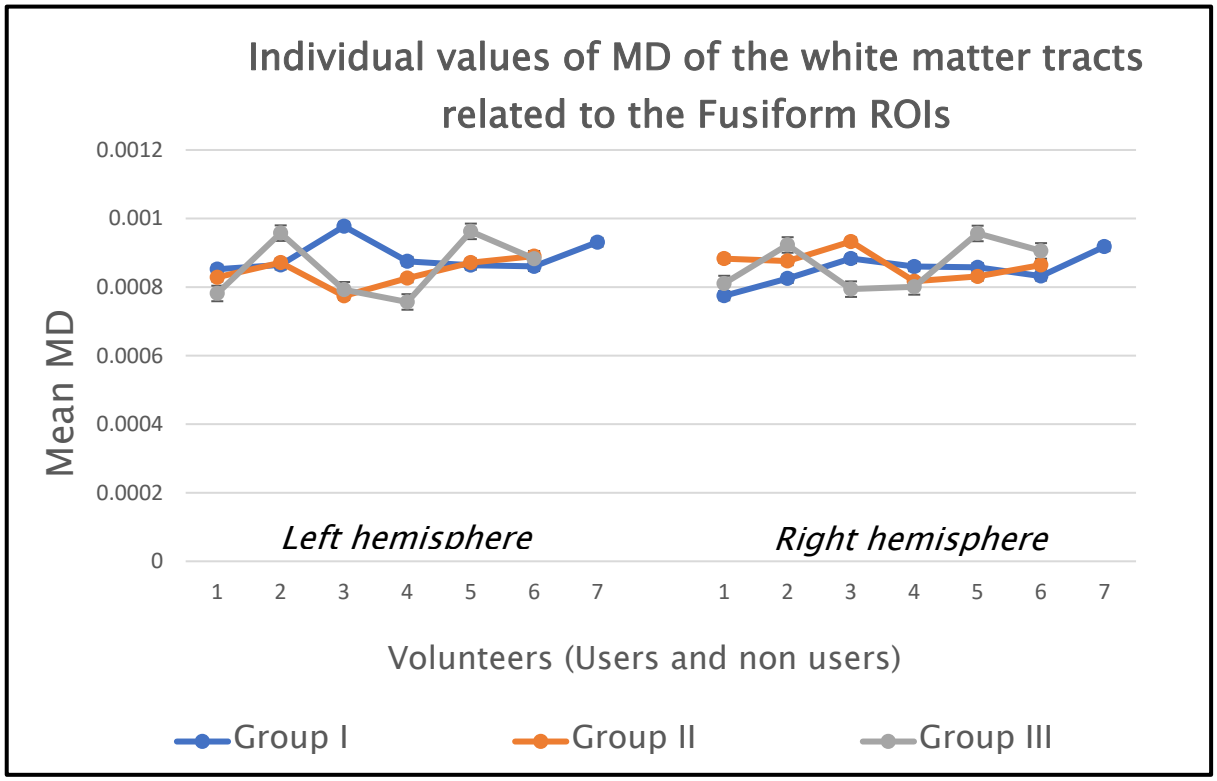

Figure 327: Individual values of mean diffusivity (MD) in both hemispheres' white matter tracts related to the Fusiform ROIs. This figure depicts the MD values of all the participants belonging to each of the three groups (Heavy and light users and healthy controls).

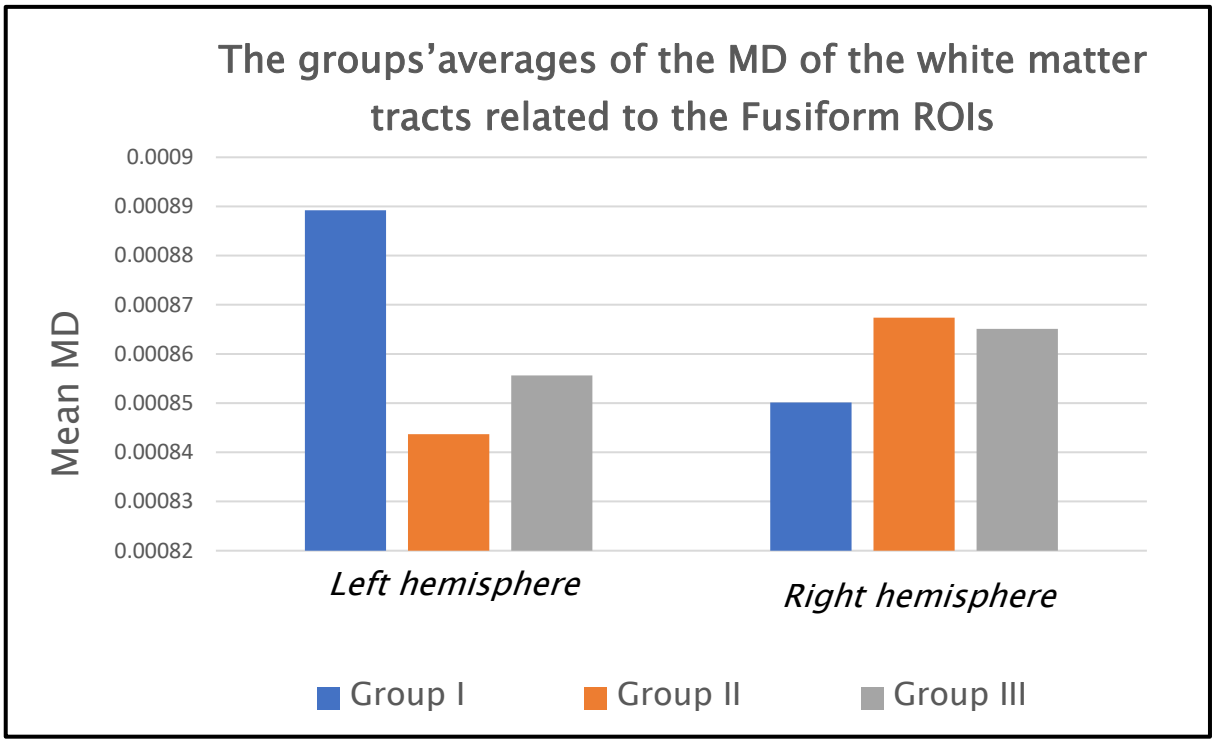

Figure 328: The mean diffusivity (MD) averages of each group of the white matter tracts related to the Fusiform ROIs in the left and the right hemispheres.

Table 303: The mean diffusivity (MD) averages and standard deviations (SD) values for the groups studied of the white matter tracts related to the Fusiform ROIs, along with intergroup comparisons.

	Left Hemisphere	Right Hemisphere
Heavy users' group (G. I)	(0,000889±0,0000469)	(0,000850±0,0000455)
Light users' group (G. II)	(0,000843±0,0000424)	(0,000867±0,0000412)
Non-users' group (G.III)	(0,000855±0,0000915)	(0,000865±0,0000714)
Intergroup comparison	G. I > G. II ≈ G.III	G.III ≈ G. II ≈ G. I

➢ Cingulum Ant

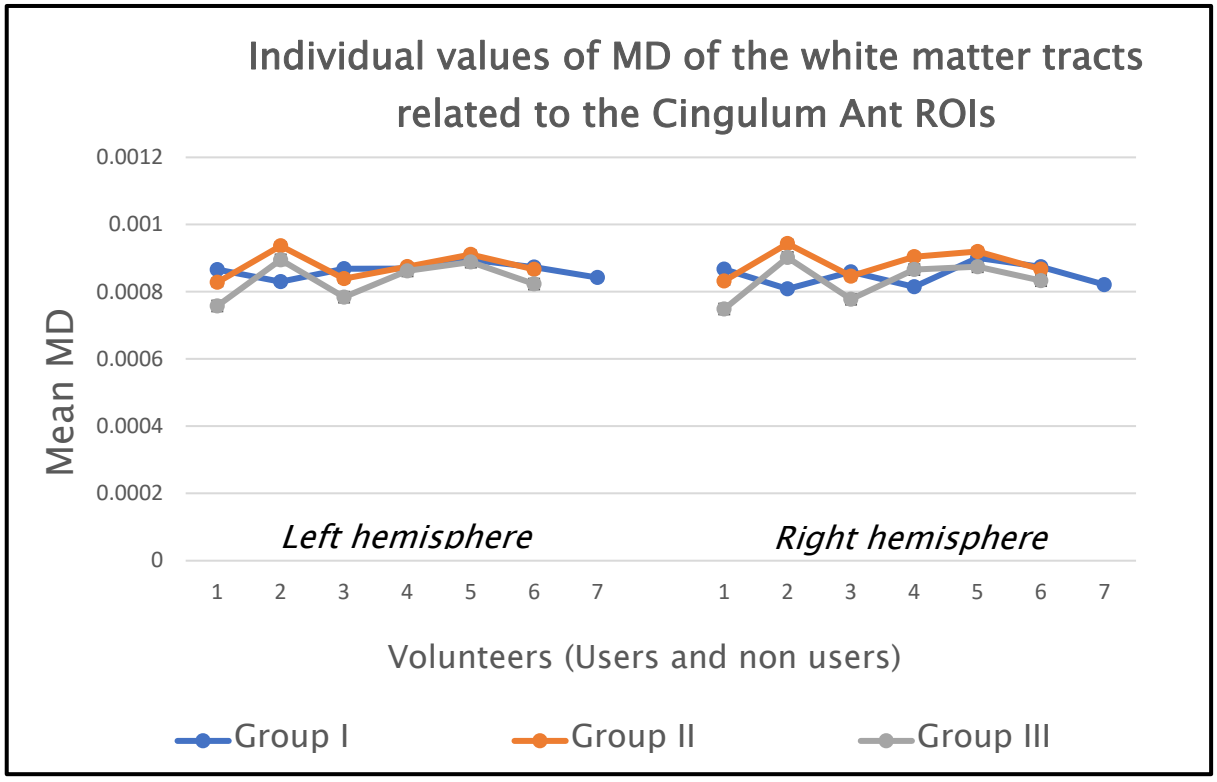

Figure 329: Individual values of mean diffusivity (MD) in both hemispheres' white matter tracts related to the Cingulum Ant ROIs. This figure depicts the MD values of all the participants belonging to each of the three groups (Heavy and light users and healthy controls).

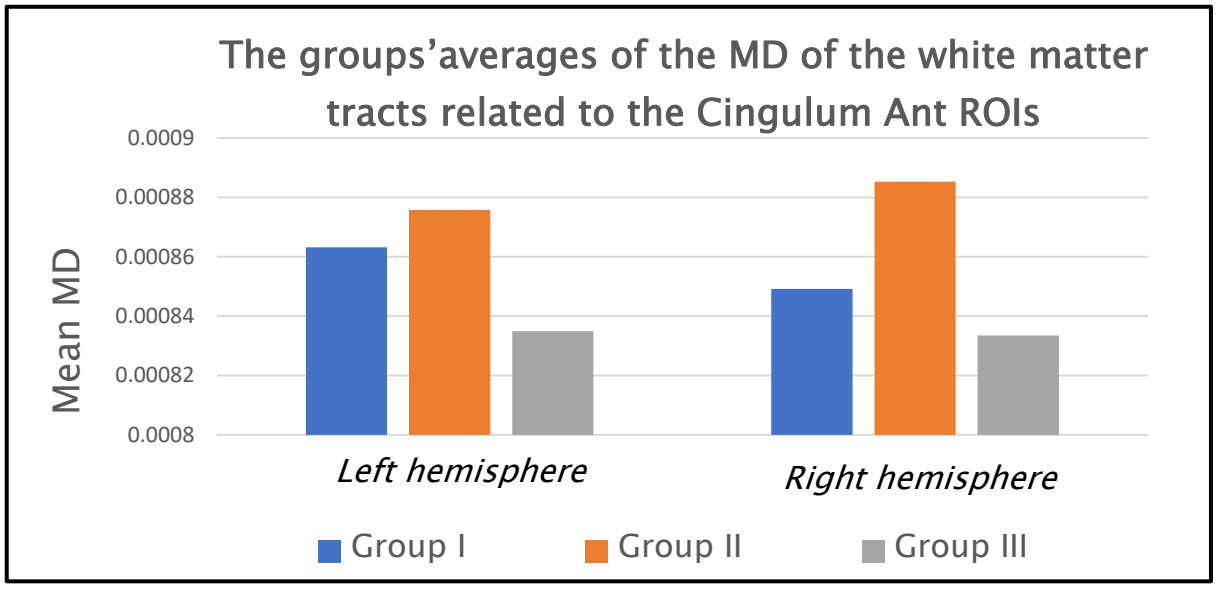

Figure 330: The mean diffusivity (MD) averages of each group of the white matter tracts related to the Cingulum Ant ROIs in the left and the right hemispheres.

Table 304: The mean diffusivity (MD) averages and standard deviations (SD) values for the groups studied of the white matter tracts related to the Cingulum Ant ROIs, along with intergroup comparisons.

	Left Hemisphere	Right Hemisphere
Heavy users' group (G. I)	(0,000863±0,0000212)	(0,000849±0,0000349)
Light users' group (G. II)	(0,000875±0,0000415)	(0,000885±0,0000437)
Non-users' group (G.III)	(0,000834±0,0000563)	(0,000833±0,0000595)
Intergroup comparison	G. I ≈ G. II > G.III	G. II > G. I ≈ G.III

➢ **Cingulum Mid**

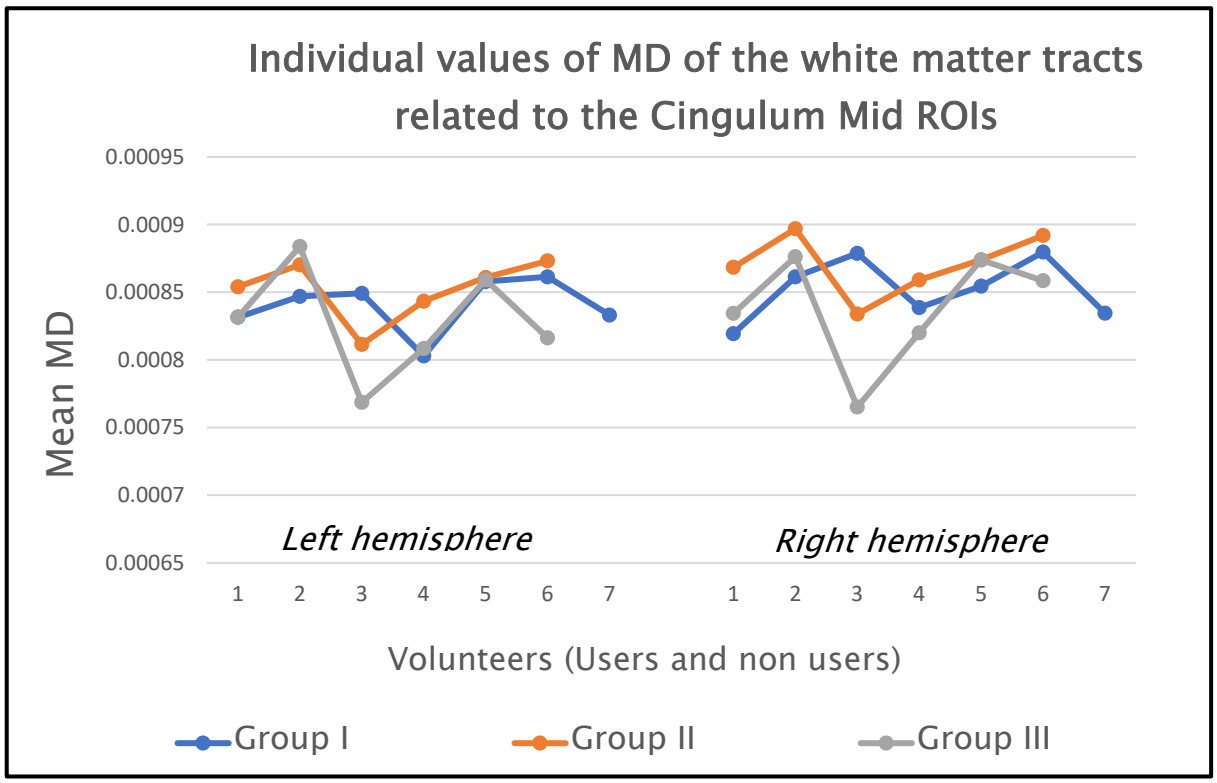

Figure 331: Individual values of mean diffusivity (MD) in both hemispheres' white matter tracts related to the Cingulum Mid ROIs. This figure depicts the MD values of all the participants belonging to each of the three groups (Heavy and light users and healthy controls).

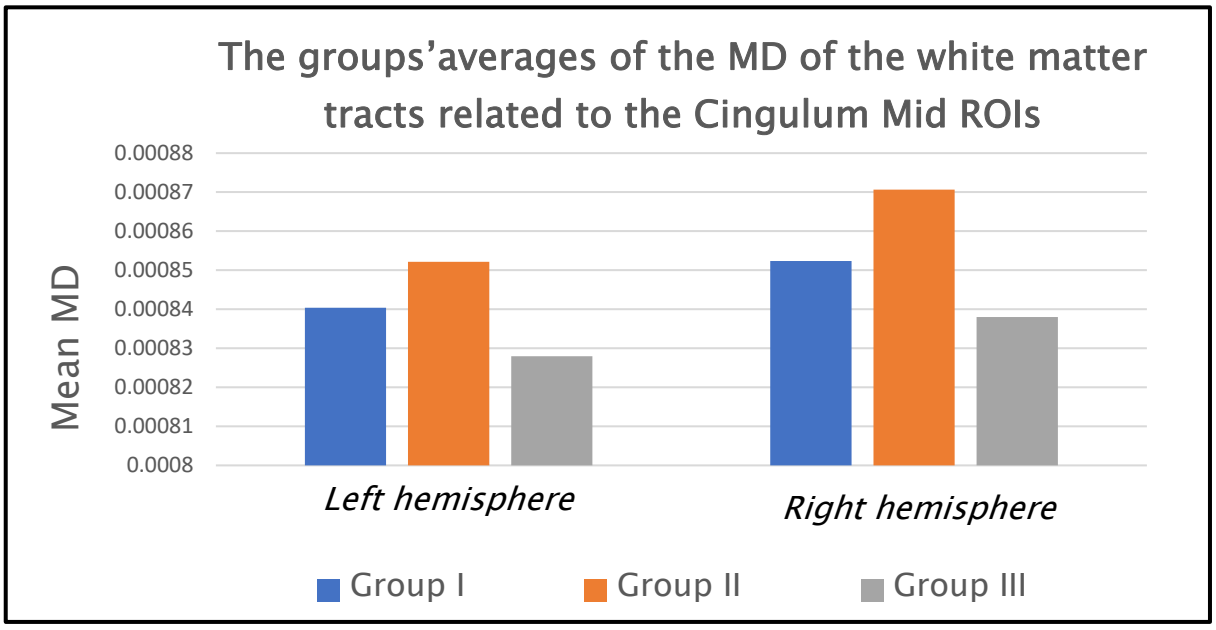

Figure 332: The mean diffusivity (MD) averages of each group of the white matter tracts related to the Cingulum Mid ROIs in the left and the right hemispheres.

Table 305: The mean diffusivity (MD) averages and standard deviations (SD) values for the groups studied of the white matter tracts related to the Cingulum Mid ROIs, along with intergroup comparisons.

	Left Hemisphere	Right Hemisphere
Heavy users' group (G. I)	(0,000840±0,0000200)	(0,000852±0,0000228)
Light users' group (G. II)	(0,000852±0,0000227)	(0,000870±0,0000229)
Non-users' group (G.III)	(0,000827±0,0000403)	(0,000837±0,0000419)
Intergroup comparison	G. I ≈ G. II ≈ G.III	G. II ≈ G. I ≈ G.III

➢ Cingulum Post

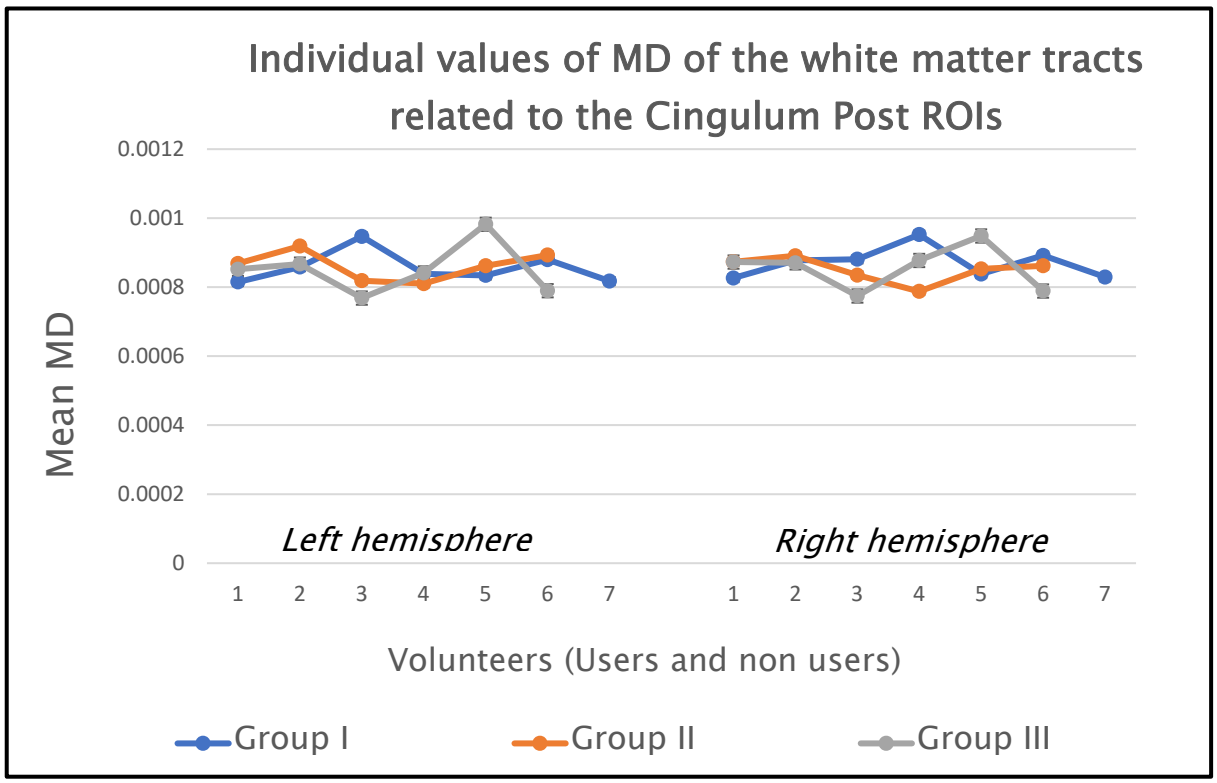

Figure 333: Individual values of mean diffusivity (MD) in both hemispheres' white matter tracts related to the Cingulum Post ROIs. This figure depicts the MD values of all the participants belonging to each of the three groups (Heavy and light users and healthy controls).

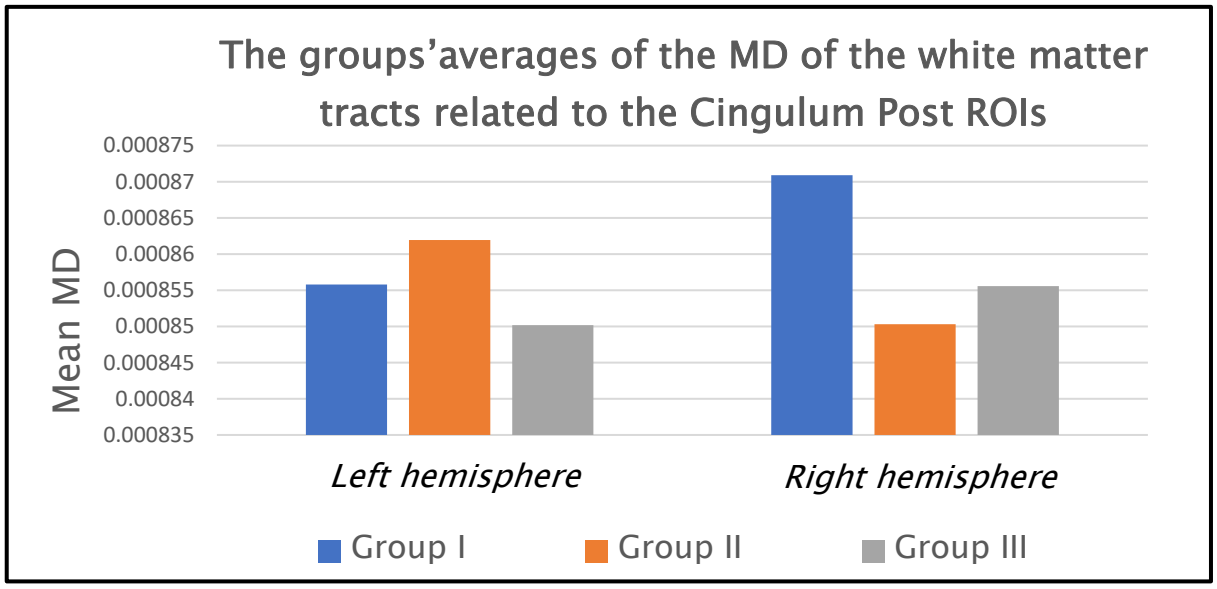

Figure 334: The mean diffusivity (MD) averages of each group of the white matter tracts related to the Cingulum Post ROIs in the left and the right hemispheres.

Table 306: The mean diffusivity (MD) averages and standard deviations (SD) values for the groups studied of the white matter tracts related to the Cingulum Post ROIs, along with intergroup comparisons.

	Left Hemisphere	Right Hemisphere
Heavy users' group (G. I)	(0,000855±0,0000461)	(0,000870±0,0000448)
Light users' group (G. II)	(0,000861±0,0000419)	(0,000850±0,0000359)
Non-users' group (G.III)	(0,000850±0,0000751)	(0,000855±0,0000642)
Intergroup comparison	G. I ≈ G. II ≈ G.III	G. II ≈ G. I ≈ G.III

➢ ParaHippocampal

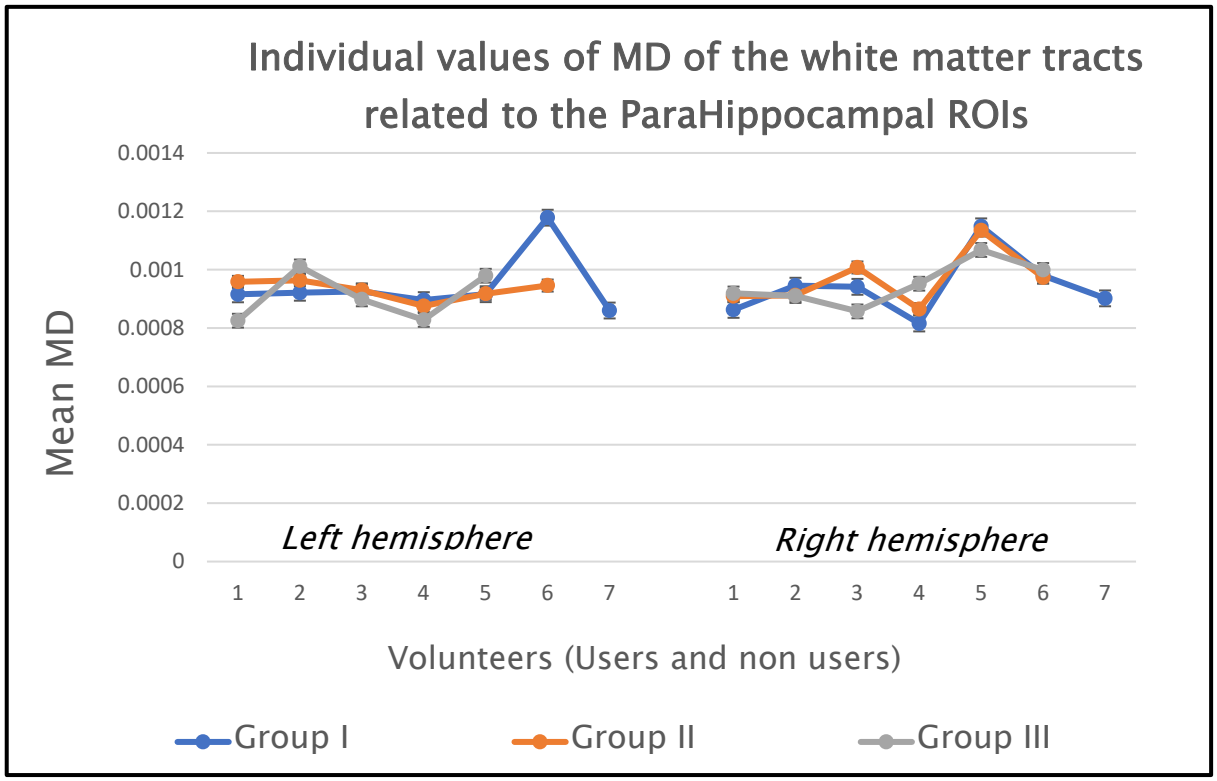

Figure 335: Individual values of mean diffusivity (MD) in both hemispheres' white matter tracts related to the ParaHippocampal ROIs. This figure depicts the MD values of all the participants belonging to each of the three groups (Heavy and light users and healthy controls).

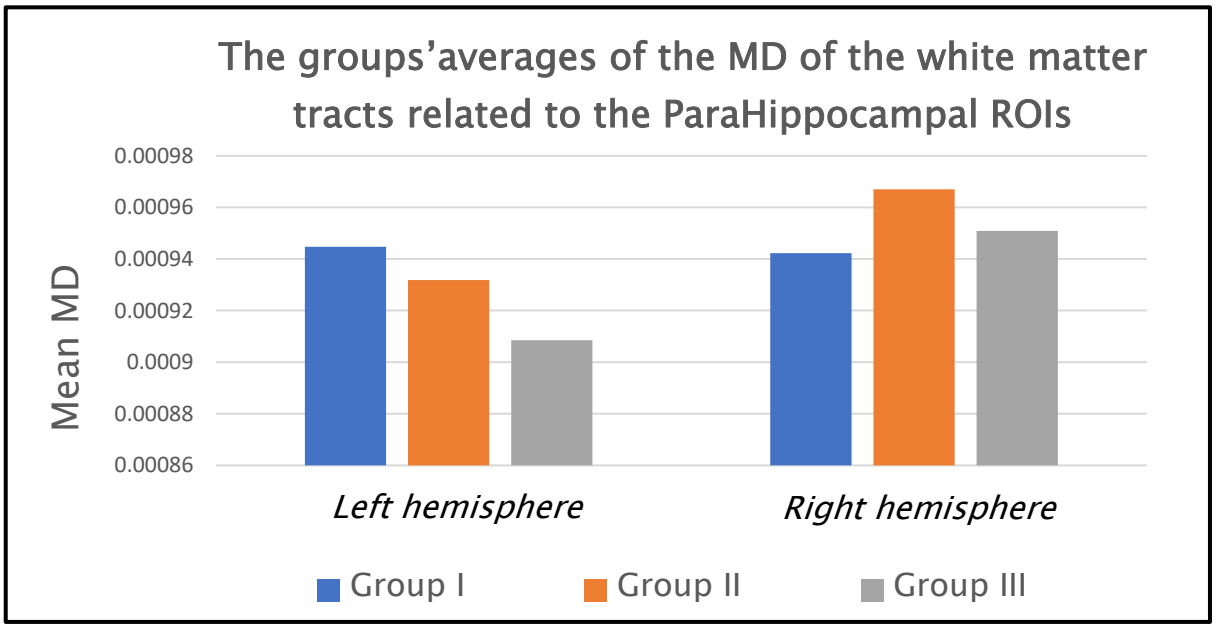

Figure 336: The mean diffusivity (MD) averages of each group of the white matter tracts related to the ParaHippocampal ROIs in the left and the right hemispheres.

Table 307: The mean diffusivity (MD) averages and standard deviations (SD) values for the groups studied of the white matter tracts related to the ParaHippocampal ROIs, along with intergroup comparisons.

	Left Hemisphere	Right Hemisphere
Heavy users' group (G. I)	(0,000944±0,0001054)	(0,000942±0,0001064)
Light users' group (G. II)	(0,000931±0,0000325)	(0,000967±0,0000964)
Non-users' group (G.III)	(0,000908±0,0000851)	(0,000950±0,0000741)
Intergroup comparison	G. I ≈ G. II ≈ G.III	G. II ≈ G. I ≈ G.III

➢ Hippocampus

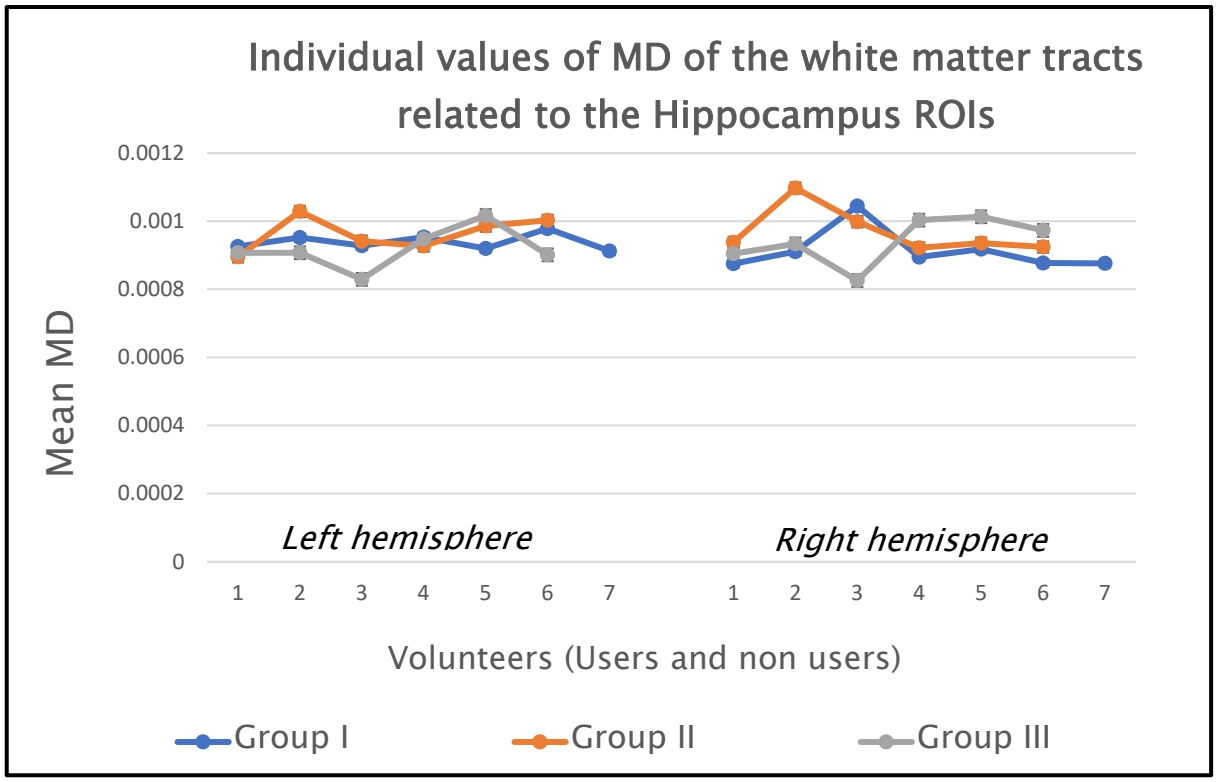

Figure 337: Individual values of mean diffusivity (MD) in both hemispheres' white matter tracts related to the Hippocampus ROIs. This figure depicts the MD values of all the participants belonging to each of the three groups (Heavy and light users and healthy controls).

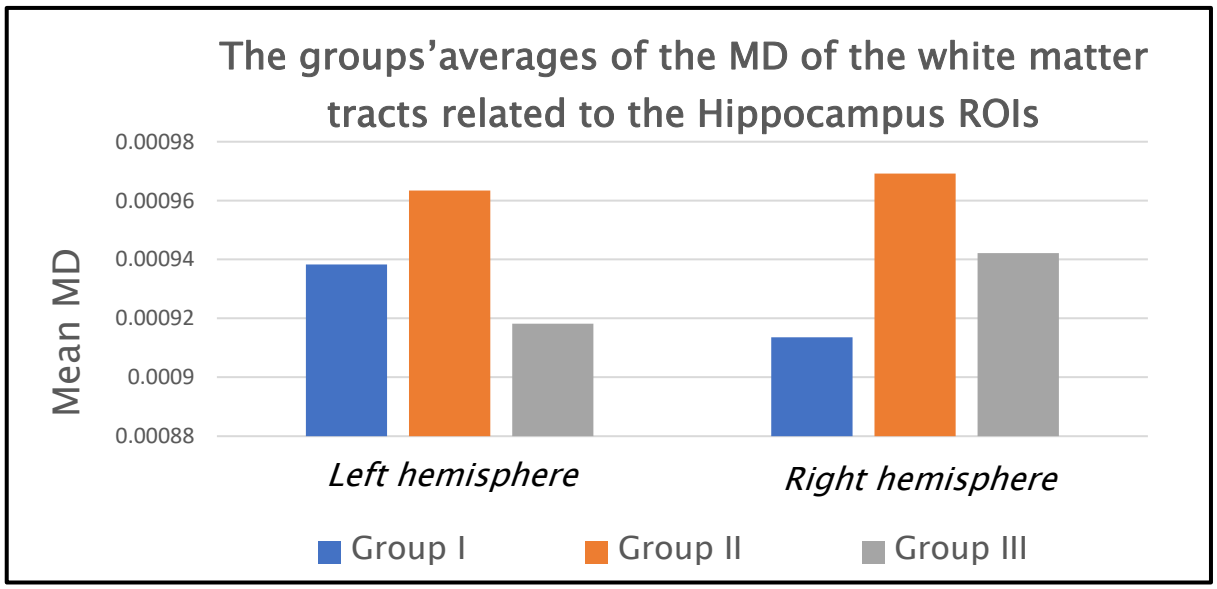

Figure 338: The mean diffusivity (MD) averages of each group of the white matter tracts related to the Hippocampus ROIs in the left and the right hemispheres.

Table 308: The mean diffusivity (MD) averages and standard deviations (SD) values for the groups studied of the white matter tracts related to the Hippocampus ROIs, along with intergroup comparisons.

	Left Hemisphere	Right Hemisphere
Heavy users' group (G. I)	(0,000913±0,000060057)	(0,000938±0,0000233)
Light users' group (G. II)	(0,000969±0,0000688)	(0,000963±0,00005045)
Non-users' group (G.III)	(0,000942±0,00007029)	(0,000918±0,0000617)
Intergroup comparison	G. II > G.III > G. I	G. II ≈ G.III > G. I

➢ **Insula**

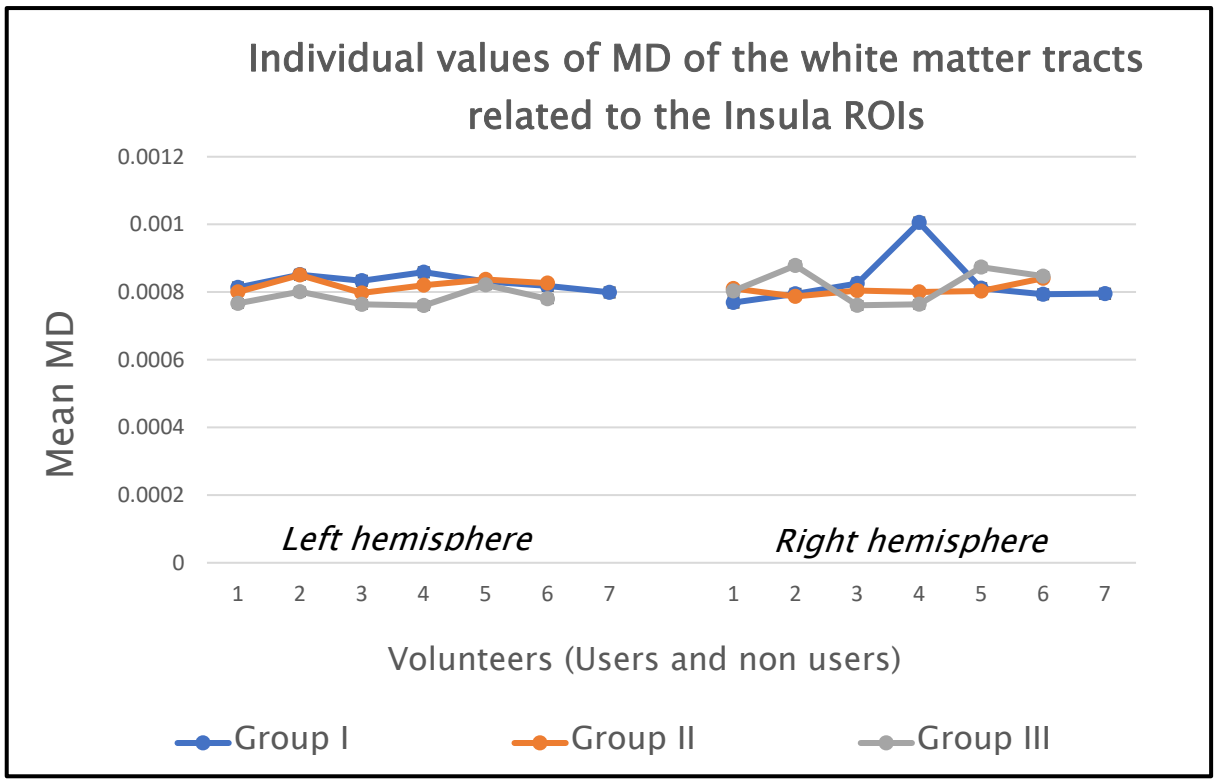

Figure 339: Individual values of mean diffusivity (MD) in both hemispheres' white matter tracts related to the Insula ROIs. This figure depicts the MD values of all the participants belonging to each of the three groups (Heavy and light users and healthy controls).

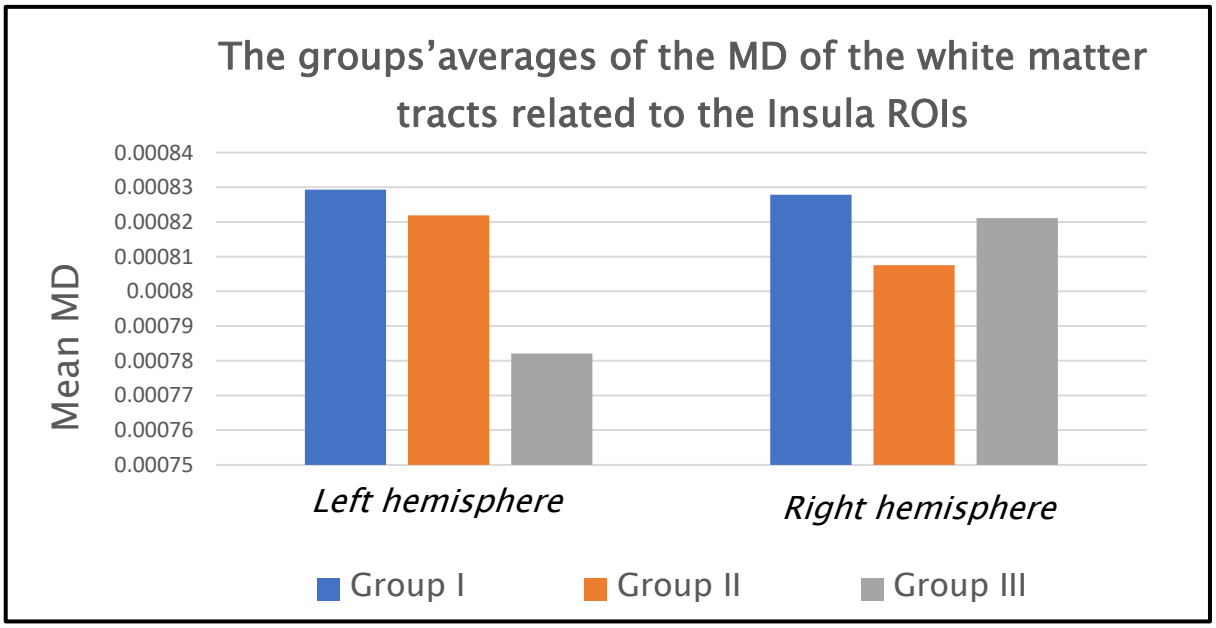

Figure 340: The mean diffusivity (MD) averages of each group of the white matter tracts related to the Insula ROIs in the left and the right hemispheres.

Table 309: The mean diffusivity (MD) averages and standard deviations (SD) values for the groups studied of the white matter tracts related to the Insula ROIs, along with intergroup comparisons.

	Left Hemisphere	Right Hemisphere
Heavy users' group (G. I)	(0,000821±0,00002103)	(0,000827±0,00008034)
Light users' group (G. II)	(0,000821±0,00002072)	(0,0008075±0,0000179)
Non-users' group (G.III)	(0,000782±0,0000242)	(0,000821±0,0000528)
Intergroup comparison	G. II ≈ G. I > G.III	G. II ≈ G.III ≈ G. I

➢ Amygdala

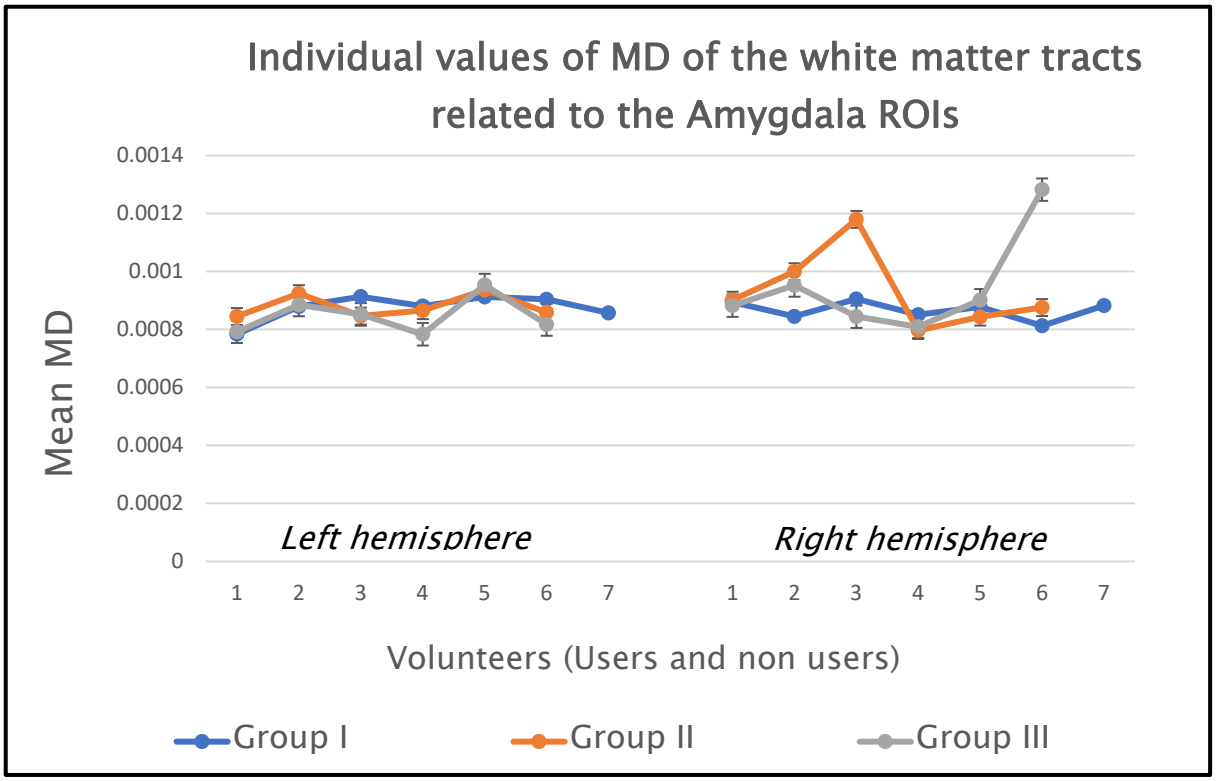

Figure 341: Individual values of mean diffusivity (MD) in both hemispheres' white matter tracts related to the Amygdala ROIs. This figure depicts the MD values of all the participants belonging to each of the three groups (Heavy and light users and healthy controls).

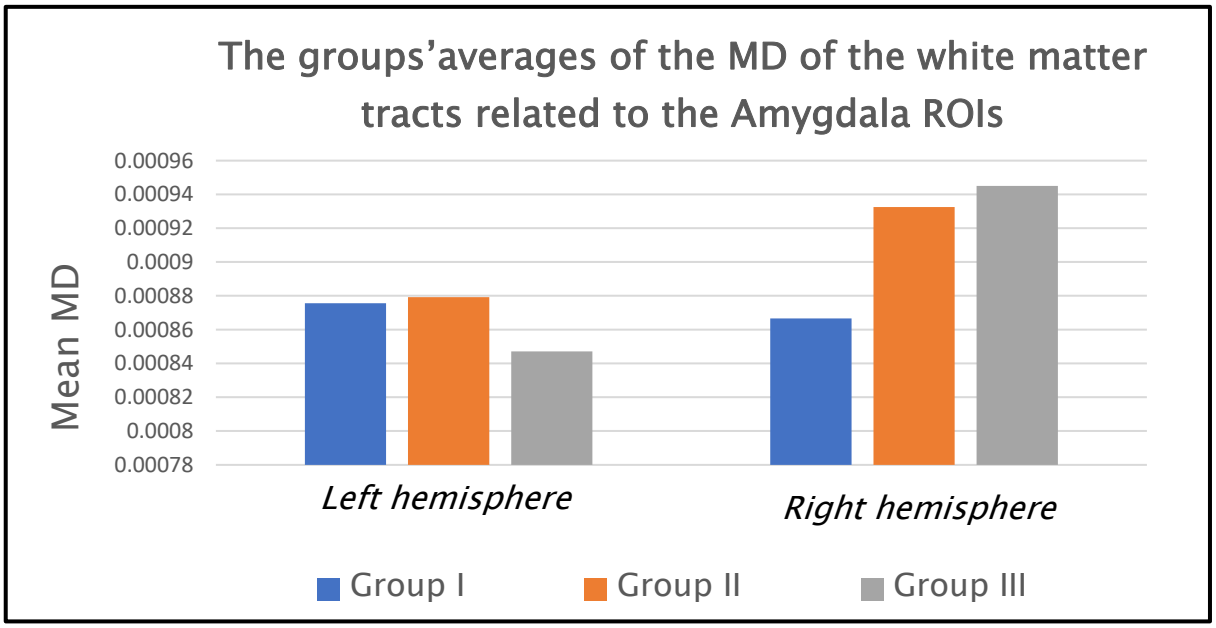

Figure 342: The mean diffusivity (MD) averages of each group of the white matter tracts related to the Amygdala ROIs in the left and the right hemispheres.

Table 310: The mean diffusivity (MD) averages and standard deviations (SD) values for the groups studied of the white matter tracts related to the Amygdala ROIs, along with intergroup comparisons.

	Left Hemisphere	Right Hemisphere
Heavy users' group (G. I)	(0,000875±0,0000453)	(0,000866±0,0000321)
Light users' group (G. II)	(0,000879±0,00004022)	(0,000932±0,000138)
Non-users' group (G.III)	(0,000847±0,0000642)	(0,000945±0,000172)
Intergroup comparison	G. II ≈ G. I > G.III	G. II ≈ G.III > G. I

➢ **Thalamus**

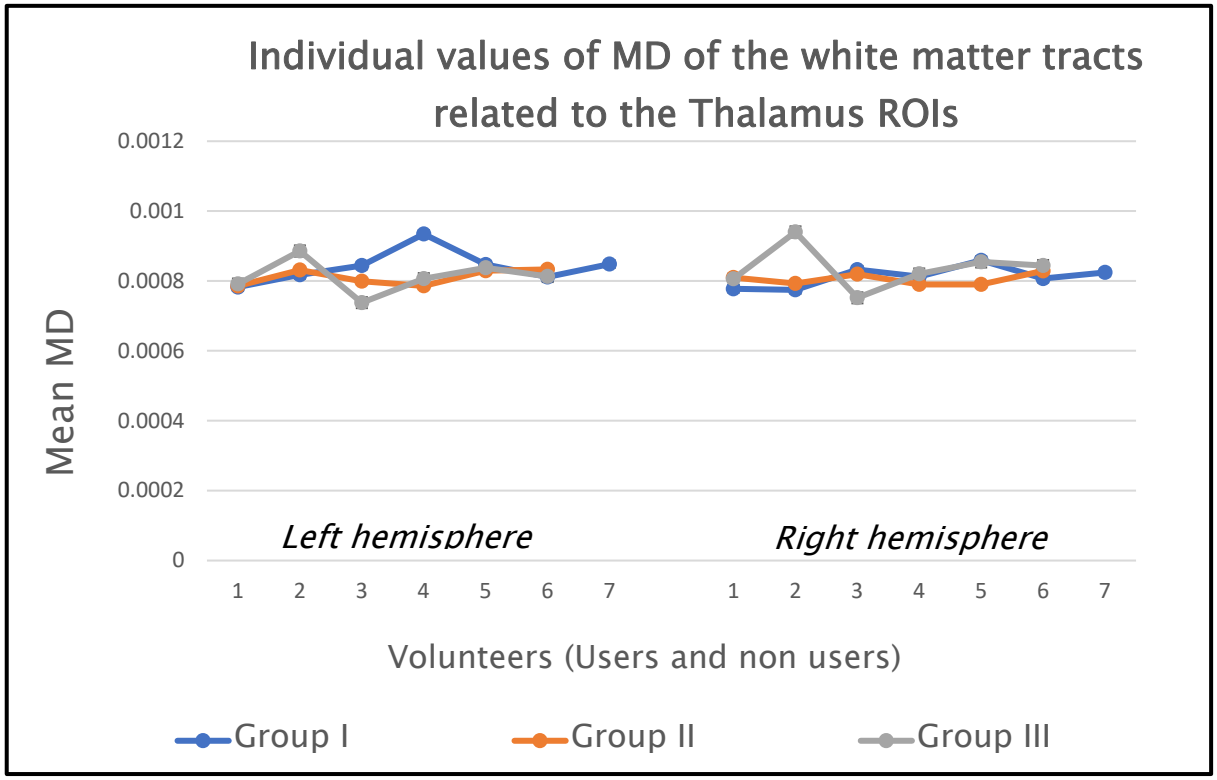

Figure 343: Individual values of mean diffusivity (MD) in both hemispheres' white matter tracts related to the Thalamus ROIs. This figure depicts the MD values of all the participants belonging to each of the three groups (Heavy and light users and healthy controls).

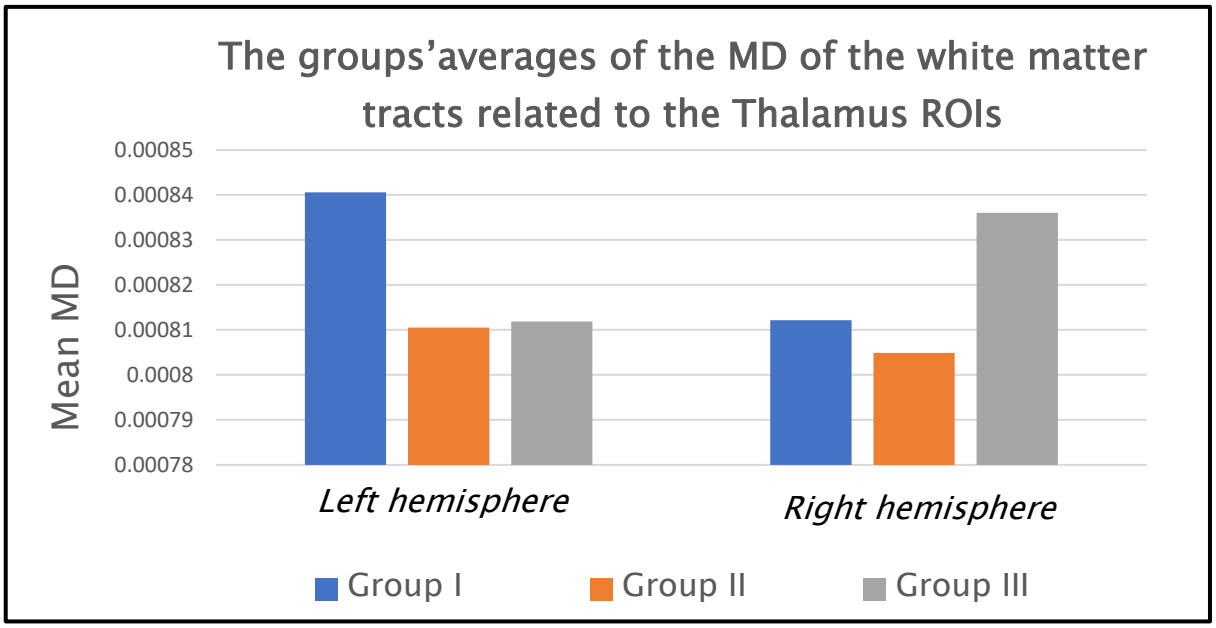

Figure 344: The mean diffusivity (MD) averages of each group of the white matter tracts related to the Thalamus ROIs in the left and the right hemispheres.

Table 311: The mean diffusivity (MD) averages and standard deviations (SD) values for the groups studied of the white matter tracts related to the thalamus ROIs, along with intergroup comparisons.

	Left Hemisphere	Right Hemisphere
Heavy users' group (G. I)	(0,0008405±0,0000477)	(0,0008121±0,0000299)
Light users' group (G. II)	(0,0008105±0,0000229)	(0,0008048±0,0000167)
Non-users' group (G.III)	(0,000811±0,00004904)	(0,000835±0,0000624)
Intergroup comparison	G. I > G. II ≈ G.III	G.III > G. II ≈ G. I

➢ Caudate

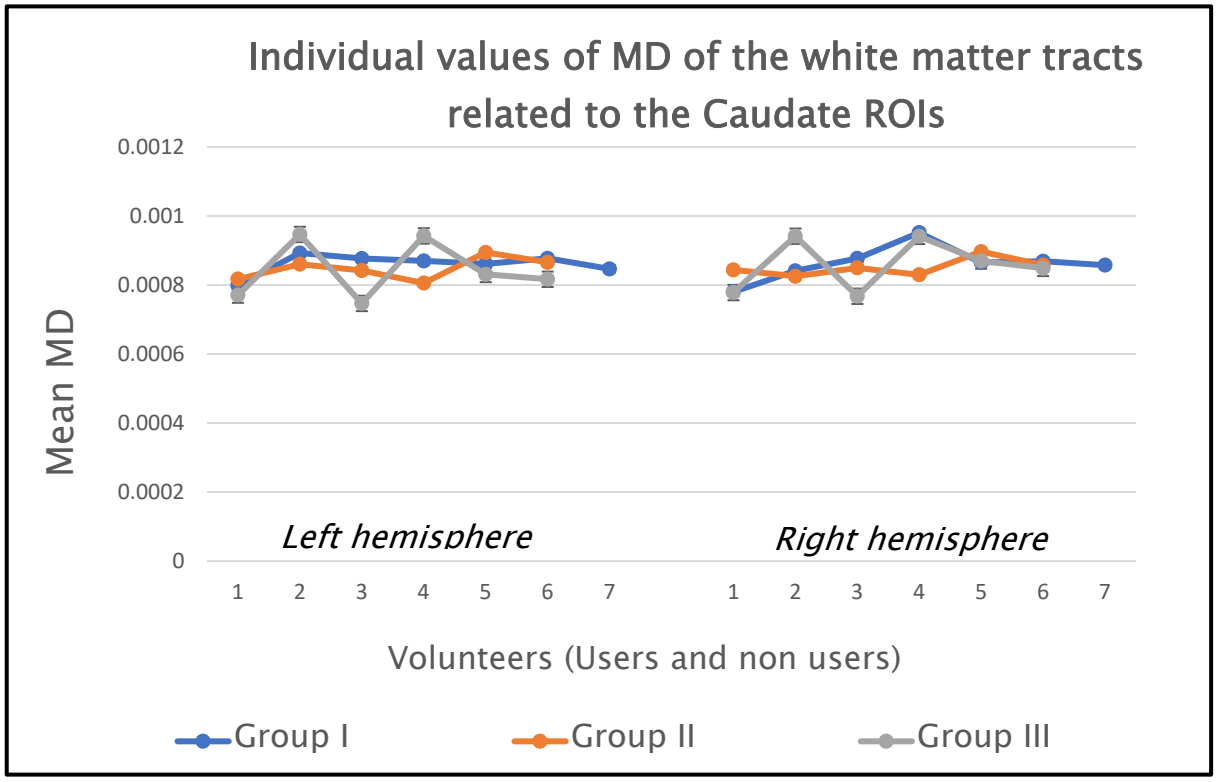

Figure 345: Individual values of mean diffusivity (MD) in both hemispheres' white matter tracts related to the Caudate ROIs. This figure depicts the MD values of all the participants belonging to each of the three groups (Heavy and light users and healthy controls).

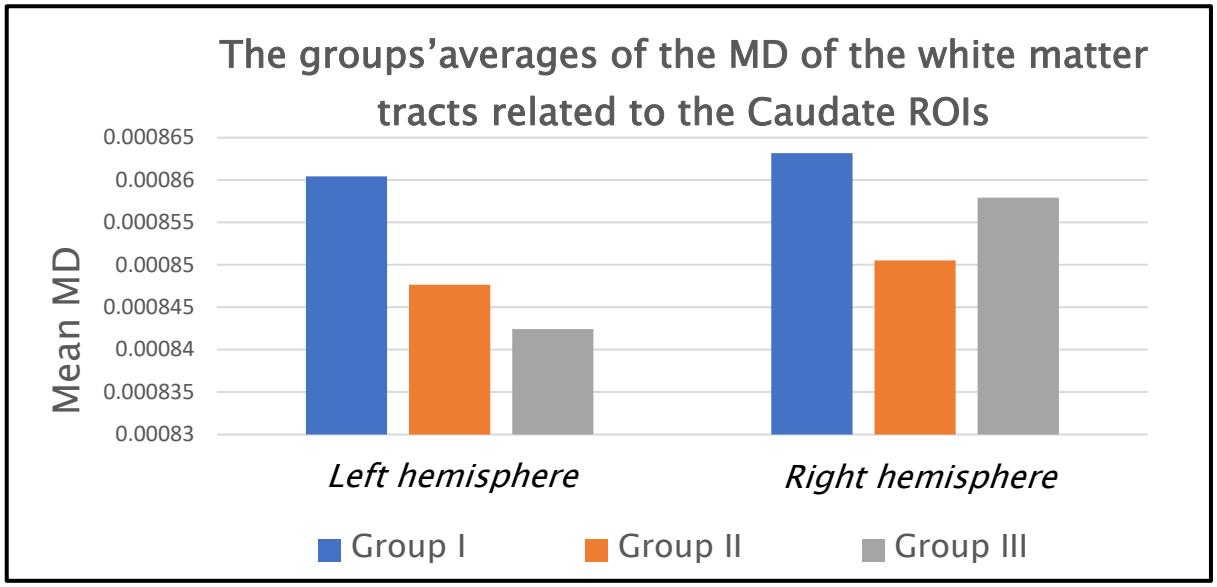

Figure 346: The mean diffusivity (MD) averages of each group of the white matter tracts related to the Caudate ROIs in the left and the right hemispheres.

Table 312: The mean diffusivity (MD) averages and standard deviations (SD) values for the groups studied of the white matter tracts related to the Caudate ROIs, along with intergroup comparisons.

	Left Hemisphere	Right Hemisphere
Heavy users' group (G. I)	(0,0008604±0,00003072)	(0,000863±0,00005079)
Light users' group (G. II)	(0,000847±0,0000328)	(0,0008505±0,0000257)
Non-users' group (G.III)	(0,000842±0,0000847)	(0,000857±0,0000756)
Intergroup comparison	G. I > G. II ≈ G.III	G.III ≈ G. II ≈ G. I

➢ **Putamen**

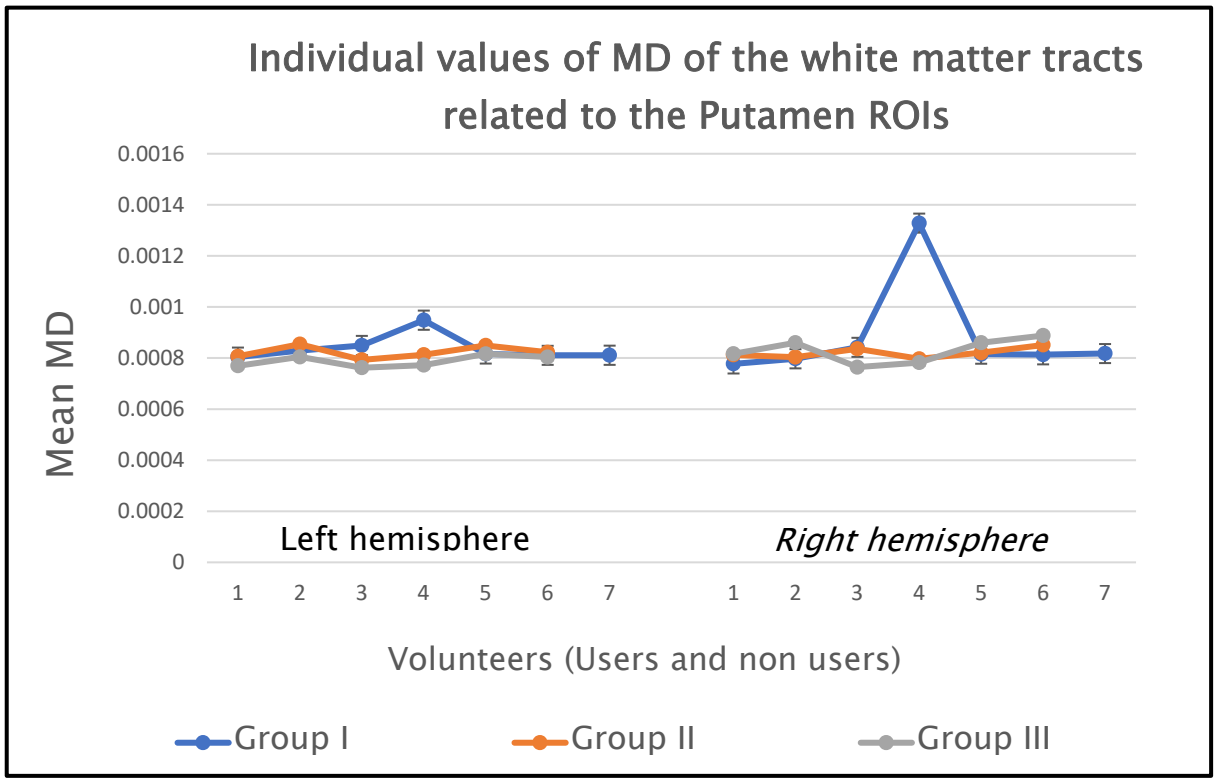

Figure 347: Individual values of mean diffusivity (MD) in both hemispheres' white matter tracts related to the Putamen ROIs. This figure depicts the MD values of all the participants belonging to each of the three groups (Heavy and light users and healthy controls).

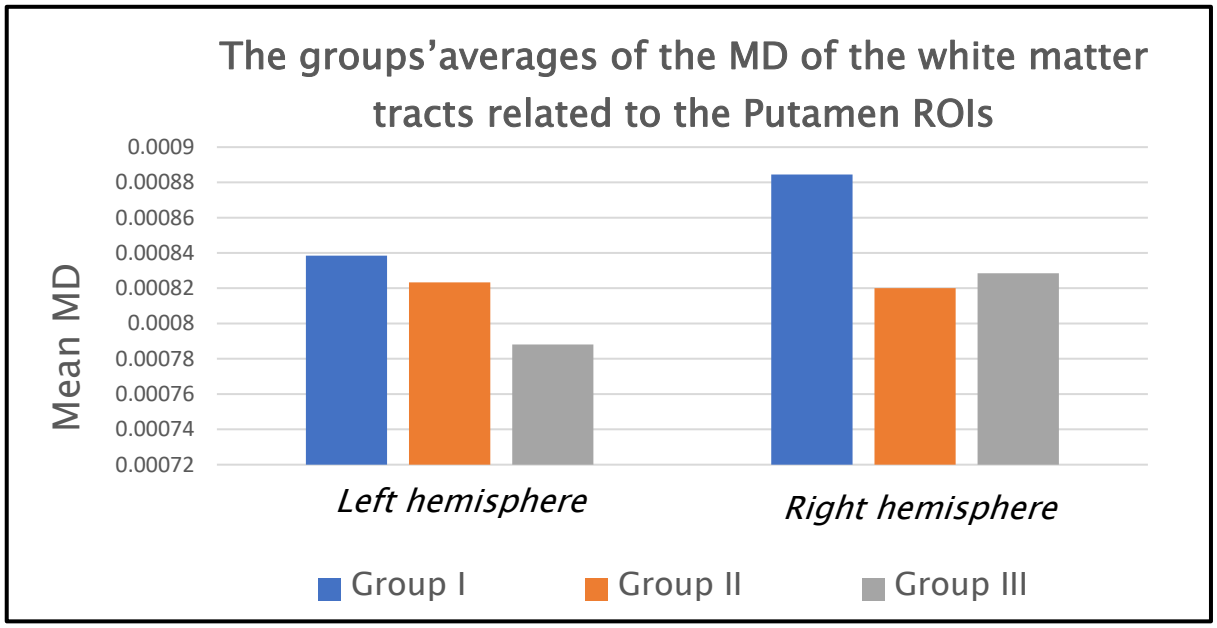

Figure 348: The mean diffusivity (MD) averages of each group of the white matter tracts related to the Putamen ROIs in the left and the right hemispheres.

Table 313: The mean diffusivity (MD) averages and standard deviations (SD) values for the groups studied of the white matter tracts related to the Putamen ROIs, along with intergroup comparisons.

	Left Hemisphere	Right Hemisphere
Heavy users' group (G. I)	(0,000838±0,0000242)	(0,000884±0,000196)
Light users' group (G. II)	(0,000823±0,0000242)	(0,00082001±0,0000204)
Non-users' group (G.III)	(0,000788±0,0000227)	(0,000828±0,0000488)
Intergroup comparison	G. I ≈ G. II > G.III	G. I > G. II ≈ G.III

➢ **Pallidum**

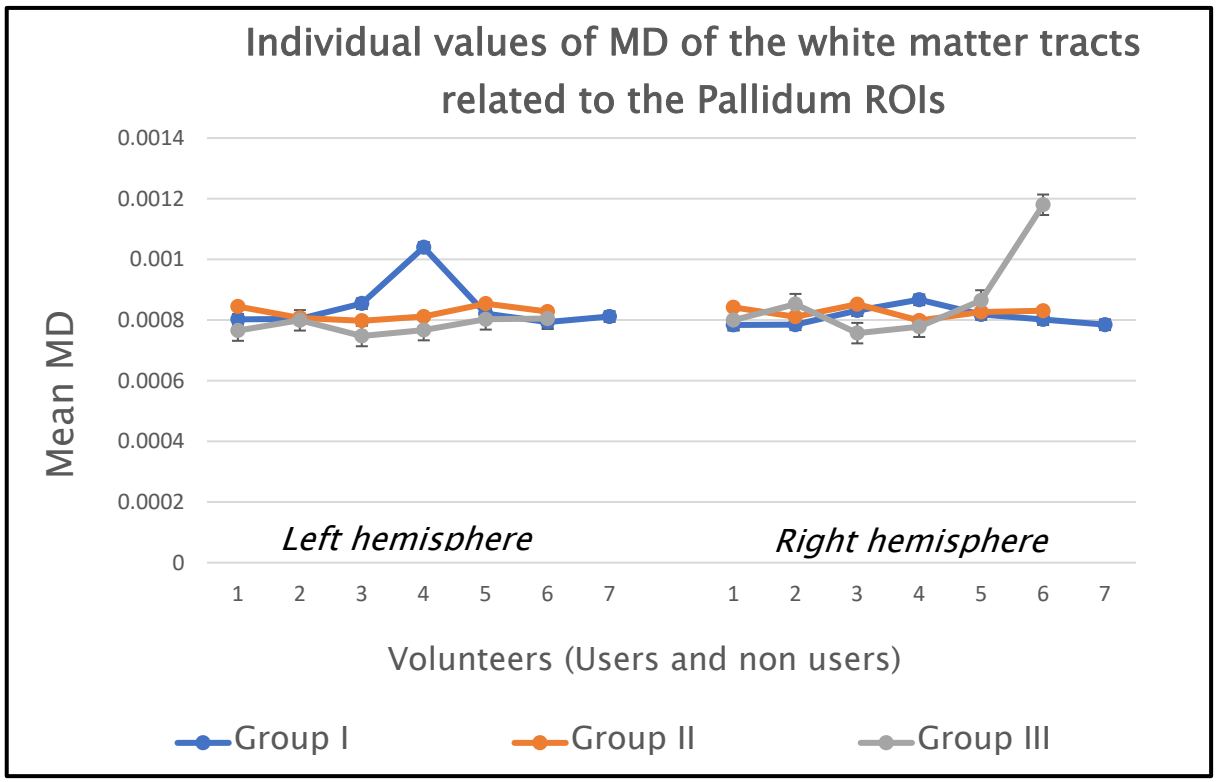

Figure 349: Individual values of mean diffusivity (MD) in both hemispheres' white matter tracts related to the Pallidum ROIs. This figure depicts the MD values of all the participants belonging to each of the three groups (Heavy and light users and healthy controls).

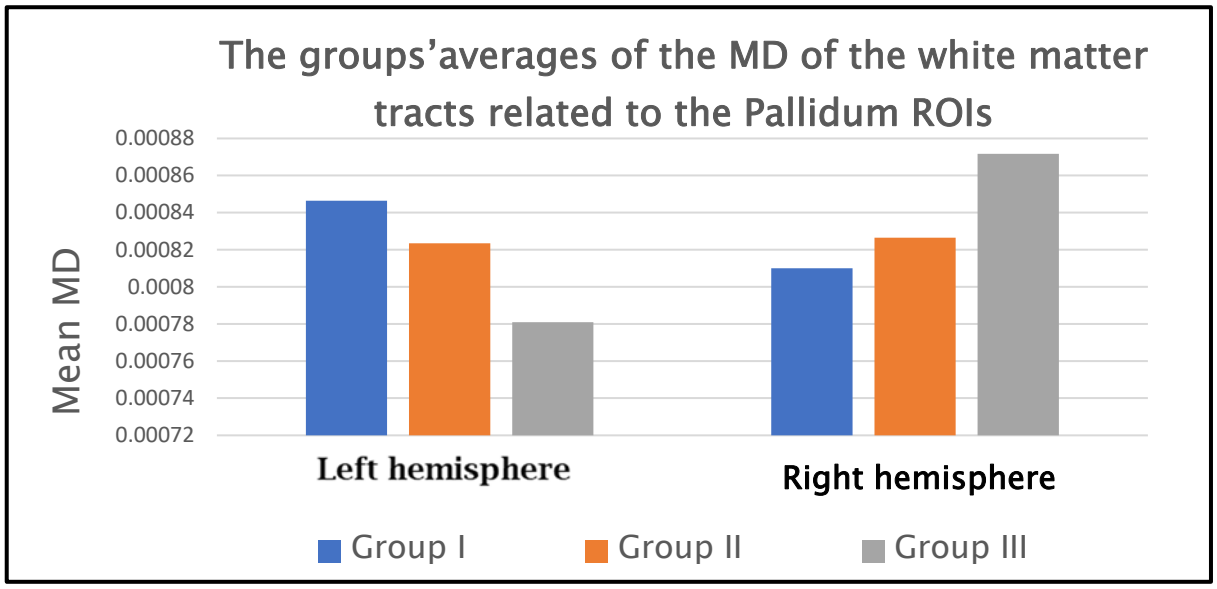

Figure 350: The mean diffusivity (MD) averages of each group of the white matter tracts related to the Pallidum ROIs in the left and the right hemispheres.

Table 314: The mean diffusivity (MD) averages and standard deviations (SD) values for the groups studied of the white matter tracts related to the Pallidum ROIs, along with intergroup comparisons.

	Left Hemisphere	Right Hemisphere
Heavy users' group (G. I)	(0,000846±0,0000874)	(0,0008099±0,00003109)
Light users' group (G. II)	(0,000823±0,0000222)	(0,000826±0,0000198)
Non-users' group (G.III)	(0,0007809±0,0000241)	(0,000871±0,000156)
Intergroup comparison	G. I ≈ G. II > G.III	G.III > G. I ≈ G. II

II. Analytical results

ANOVA was conducted in the quantitative results to evaluate the levels of significant difference between pairs of users (heavy, light) and non-users groups.

Our analytical results, for FA and MD, will be presented in two parts:

- A summary of all analysis of Variance (ANOVA) findings.
- The analytical findings in each region of interest and between each of the groups studied

1. Fractional anisotropy (FA) analysis of Variance (ANOVA) results

a. Summary of all the analytical findings

For Fractional anisotropy (FA), in the 70 regions examined, 420 analyses of variance were conducted (between the three groups and in both hemispheres).

The analysis of Variance (ANOVA) results revealed 16 statistically significant results (a p-value <0.05), which is equivalent to 4% of the total conducted the analysis.

Table 315 summarizes the region with the corresponding groups compared where the statistical analysis is significant.

Table 315: A table containing regions of interest revealing statistically significant results of white matter's fractional anisotropy within the three groups (heavy and light users and control group).

The ROIs in which the WM tracts examined are located.	Groups compared
Left Frontal Med Orb	Heavy users Vs. Non-users
Left Frontal Mid Orb	Light users Vs. Non-users
Left Frontal Sup	Heavy users Vs. Non-users
Left Frontal Mid	Heavy users Vs. Non-users
Right Frontal Mid	Heavy users Vs. Light users
Left Frontal Inf Oper	Heavy users Vs. Non-users
Left Frontal Inf Tri	Light users Vs. Non-users
Left Postcentral	Light users Vs. Non-users
Left SupraMarginal	Heavy users Vs. Non-users
Left Heschl	Light users Vs. Non-users
Right Heschl	Heavy users Vs. Non-users Light users Vs. Non-users
Left Cingulum Ant	Heavy users Vs. Non-users
Left Cingulum Post	Light users Vs. Non-users
Left Amygdala	Heavy users Vs. Non-users Light users Vs. Non-users

b. The analytical findings in the white matter of each region of interest and between each of the groups studied

We present our mean fractional anisotropy (FA) statistical analysis findings by two tables for each region of interest and in both hemispheres. The first table represents statistical results in the left regions and the second in the right regions.

➢ **Frontal Med Orb**

Table 316: The statistical analysis results of the mean fractional anisotropy in tractography analysis technique in groups of heavy cannabis users, light users, and non-users in the **left Frontal Med Orb region.**

	Mean fractional anisotropy of tractography analysis P-Value. -Frontal Med Orb region of the left hemisphere-		
	Heavy users (Group I)	**Light users (Group II)**	**Non-users (Group III)**
Heavy users (Group I)	○	**	**
Light users (Group II)	0.156	○	**
Non users (Group III)	**0.049**	0.638	○

With a P-value lower than 0.05, the ANOVA analysis revealed significant differences between heavy users and non-users groups, but no significant difference between heavy and light users' groups and between light users and non-users groups. The table reveals that in the same anatomical area, the mean fractional anisotropy values of different groups in the left Frontal Med Orb region were significantly different among one from three comparisons realized.

Table 317: The statistical analysis results of the mean fractional anisotropy in tractography analysis technique in groups of heavy cannabis users, light users, and non-users in the **right Frontal Med Orb region.**

	Mean fractional anisotropy of tractography analysis P-Value. -Frontal Med Orb region of the right hemisphere-		
	Heavy users (Group I)	**Light users (Group II)**	**Non-users (Group III)**
Heavy users (Group I)	○	**	**
Light users (Group II)	0.834	○	**
Non users (Group III)	0.359	0.298	○

With a P-value lower than 0.05, the ANOVA analysis revealed no significant differences. The table reveals that in the same anatomical area, the mean fractional anisotropy values of different groups in the right Frontal Med Orb region were not significantly different.

➢ Frontal Sup Orb

Table 318: The statistical analysis results of the mean fractional anisotropy in tractography analysis technique in groups of heavy cannabis users, light users, and non-users in the **left Frontal Sup Orb region.**

	Mean fractional anisotropy of tractography analysis P-Value. – Frontal Sup Orb region of the left hemisphere –		
	Heavy users (Group I)	Light users (Group II)	Non-users (Group III)
Heavy users (Group I)	○	**	**
Light users (Group II)	0.387	○	**
Non users (Group III)	0.121	0.532	○

With a P-value lower than 0.05, the ANOVA analysis revealed no significant differences. The table reveals that in the same anatomical area, the mean fractional anisotropy values of different groups in the left Frontal Sup Orb region were not significantly different.

Table 319: The statistical analysis results of the mean fractional anisotropy in tractography analysis technique in groups of heavy cannabis users, light users, and non-users in the **right Frontal Sup Orb region.**

	Mean fractional anisotropy of tractography analysis P-Value. Frontal Sup Orb region of the right hemisphere		
	Heavy users (Group I)	Light users (Group II)	Non-users (Group III)
Heavy users (Group I)	○	**	**
Light users (Group II)	0.854	○	**
Non users (Group III)	0.535	0.502	○

With a P-value lower than 0.05, the ANOVA analysis revealed no significant differences. The table reveals that in the same anatomical area, the mean fractional anisotropy values of different groups in the right Frontal Sup Orb region were not significantly different.

➢ **Frontal Mid Orb**

Table 320: The statistical analysis results of the mean fractional anisotropy in tractography analysis technique in groups of heavy cannabis users, light users, and non-users in the **left Frontal Mid Orb region.**

	Mean fractional anisotropy of tractography analysis P-Value. – Frontal Mid Orb region of the left hemisphere –		
	Heavy users (Group I)	**Light users (Group II)**	**Non-users (Group III)**
Heavy users (Group I)	○	**	**
Light users (Group II)	0.392	○	**
Non users (Group III)	0.090	0.014	○

With a P-value lower than 0.05, the ANOVA analysis revealed a significant difference between light users and non-users groups and no significant differences between the other groups. The table reveals that in the same anatomical area, the mean fractional anisotropy values of different groups in the left Frontal Mid Orb region were significantly different among one from three comparisons realized.

Table 321: The statistical analysis results of the mean fractional anisotropy in tractography analysis technique in groups of heavy cannabis users, light users, and non-users in the **right Frontal Mid Orb region.**

	Mean fractional anisotropy of tractography analysis P-Value. – Frontal Mid Orb region of the right hemisphere –		
	Heavy users (Group I)	**Light users (Group II)**	**Non-users (Group III)**
Heavy users (Group I)	○	**	**
Light users (Group II)	0.509	○	**
Non users (Group III)	0.819	0.522	○

With a P-value lower than 0.05, the ANOVA analysis revealed no significant differences. The table reveals that in the same anatomical area, the mean fractional anisotropy values of different groups in the right Frontal Mid Orb region were not significantly different.

➢ Frontal Inf Orb

Table 322: The statistical analysis results of the mean fractional anisotropy in tractography analysis technique in groups of heavy cannabis users, light users, and non-users in the **left Frontal Inf Orb region.**

	Mean fractional anisotropy of tractography analysis P-Value. – Frontal Inf Orb region of the left hemisphere –		
	Heavy users (Group I)	**Light users (Group II)**	**Non-users (Group III)**
Heavy users (Group I)	○	**	**
Light users (Group II)	0.375	○	**
Non users (Group III)	0.291	0.075	○

With a P-value lower than 0.05, the ANOVA analysis revealed no significant differences. The table reveals that in the same anatomical area, the mean fractional anisotropy values of different groups in the left Frontal Inf Orb region were not significantly different.

Table 323 The statistical analysis results of the mean fractional anisotropy in tractography analysis technique in groups of heavy cannabis users, light users, and non-users in the **right Frontal Inf Orb region.**

	Mean fractional anisotropy of tractography analysis P-Value. – Frontal Inf Orb region of the right hemisphere –		
	Heavy users (Group I)	**Light users (Group II)**	**Non-users (Group III)**
Heavy users (Group I)	○	**	**
Light users (Group II)	0.989	○	**
Non users (Group III)	0.348	0.240	○

With a P-value lower than 0.05, the ANOVA analysis revealed no significant differences. The table reveals that in the same anatomical area, the mean fractional anisotropy values of different groups in the right Frontal Inf Orb region were not significantly different.

➢ **Rectus**

Table 324: The statistical analysis results of the mean fractional anisotropy in tractography analysis technique in groups of heavy cannabis users, light users, and non-users in the **left Rectus region.**

	Mean fractional anisotropy of tractography analysis P-Value. – Rectus region of the left hemisphere –		
	Heavy users (Group I)	**Light users (Group II)**	**Non-users (Group III)**
Heavy users (Group I)	○	**	**
Light users (Group II)	0.615	○	**
Non users (Group III)	0.503	0.916	○

With a P-value lower than 0.05, the ANOVA analysis revealed no significant differences. The table reveals that in the same anatomical area, the mean fractional anisotropy values of different groups in **the left Rectus region** were not significantly different.

Table 325: The statistical analysis results of the mean fractional anisotropy in tractography analysis technique in groups of heavy cannabis users, light users, and non-users in the **right Rectus region.**

	Mean fractional anisotropy of tractography analysis P-Value. – Rectus region of the right hemisphere –		
	Heavy users (Group I)	**Light users (Group II)**	**Non-users (Group III)**
Heavy users (Group I)	○	**	**
Light users (Group II)	0.885	○	**
Non users (Group III)	0.440	0.458	○

With a P-value lower than 0.05, the ANOVA analysis revealed no significant differences. The table reveals that in the same anatomical area, the mean fractional anisotropy values of different groups in the right Rectus region were not significantly different.

➢ Olfactory

Table 326: The statistical analysis results of the mean fractional anisotropy in tractography analysis technique in groups of heavy cannabis users, light users, and non-users in the **left Olfactory region.**

	Mean fractional anisotropy of tractography analysis P-Value. – Olfactory region of the left hemisphere –		
	Heavy users (Group I)	Light users (Group II)	Non-users (Group III)
Heavy users (Group I)	○	**	**
Light users (Group II)	0.273	○	**
Non users (Group III)	0.678	0.708	○

With a P-value lower than 0.05, the ANOVA analysis revealed no significant differences. The table reveals that in the same anatomical area, the mean fractional anisotropy values of different groups in the left Olfactory region were not significantly different.

Table 327: The statistical analysis results of the mean fractional anisotropy in tractography analysis technique in groups of heavy cannabis users, light users, and non-users in the **right Olfactory region.**

	Mean fractional anisotropy of tractography analysis P-Value. – Olfactory region of the right hemisphere –		
	Heavy users (Group I)	Light users (Group II)	Non-users (Group III)
Heavy users (Group I)	○	**	**
Light users (Group II)	0.815	○	**
Non users (Group III)	0.918	0.726	○

With a P-value lower than 0.05, the ANOVA analysis revealed no significant differences. The table reveals that in the same anatomical area, the mean fractional anisotropy values of different groups in the right Olfactory region were not significantly different.

- **Frontal Sup Medial**

Table 328: The statistical analysis results of the mean fractional anisotropy in tractography analysis technique in groups of heavy cannabis users, light users, and non-users in the **left Frontal Sup Medial region.**

	Mean fractional anisotropy of tractography analysis P-Value. -Frontal Sup Medial region of the left hemisphere-		
	Heavy users (Group I)	**Light users (Group II)**	**Non-users (Group III)**
Heavy users (Group I)	○	**	**
Light users (Group II)	0.622	○	**
Non users (Group III)	0.129	0.334	○

With a P-value lower than 0.05, the ANOVA analysis revealed no significant differences. The table reveals that in the same anatomical area, the mean fractional anisotropy values of different groups in the left Frontal Sup Medial region were not significantly different.

Table 329: The statistical analysis results of the mean fractional anisotropy in tractography analysis technique in groups of heavy cannabis users, light users, and non-users in the **right Frontal Sup Medial region.**

	Mean fractional anisotropy of tractography analysis P-Value. -Frontal Sup Medial region of the right hemisphere-		
	Heavy users (Group I)	**Light users (Group II)**	**Non-users (Group III)**
Heavy users (Group I)	○	**	**
Light users (Group II)	0.285	○	**
Non users (Group III)	0.194	0.659	○

With a P-value lower than 0.05, the ANOVA analysis revealed no significant differences. The table reveals that in the same anatomical area, the mean fractional anisotropy values of different groups in the right Frontal Sup Medial region were not significantly different.

➢ **Frontal Sup**

Table 330: The statistical analysis results of the mean fractional anisotropy in tractography analysis technique in groups of heavy cannabis users, light users, and non-users in the **left Frontal Sup region.**

	Mean fractional anisotropy of tractography analysis P-Value. -Frontal Sup region of the left hemisphere-		
	Heavy users (Group I)	**Light users (Group II)**	**Non-users (Group III)**
Heavy users (Group I)	○	**	**
Light users (Group II)	0.295	○	**
Non users (Group III)	**0.046**	0.209	○

With a P-value lower than 0.05, the ANOVA analysis revealed significant differences between heavy users and non-users groups, but no significant difference between heavy and light users' groups and between light users and non-users groups. The table reveals that in the same anatomical area, the mean fractional anisotropy values of different groups in the left Frontal Sup region were significantly different among one from three comparisons realized.

Table 331: The statistical analysis results of the mean fractional anisotropy in tractography analysis technique in groups of heavy cannabis users, light users, and non-users in the **right Frontal Sup region.**

	Mean fractional anisotropy of tractography analysis P-Value. -Frontal Sup region of the right hemisphere-		
	Heavy users (Group I)	**Light users (Group II)**	**Non-users (Group III)**
Heavy users (Group I)	○	**	**
Light users (Group II)	0.347	○	**
Non users (Group III)	0.108	0.156	○

With a P-value lower than 0.05, the ANOVA analysis revealed no significant differences. The table reveals that in the same anatomical area, the mean fractional anisotropy values of different groups in the right Frontal Sup region were not significantly different.

➢ **Frontal Mid**

Table 332: The statistical analysis results of the mean fractional anisotropy in tractography analysis technique in groups of heavy cannabis users, light users, and non-users in the **left Frontal Mid region.**

	Mean fractional anisotropy of tractography analysis P-Value. -Frontal Mid region of the left hemisphere-		
	Heavy users (Group I)	Light users (Group II)	Non-users (Group III)
Heavy users (Group I)	○	**	**
Light users (Group II)	0.416	○	**
Non users (Group III)	0.045	0.131	○

With a P-value lower than 0.05, the ANOVA analysis revealed significant differences between heavy users and non-users groups, but no significant difference between heavy and light users' groups and between light users and non-users groups. The table reveals that in the same anatomical area, the mean fractional anisotropy values of different groups in the left Frontal Mid region were significantly different among one from three comparisons realized.

Table 333: The statistical analysis results of the mean fractional anisotropy in tractography analysis technique in groups of heavy cannabis users, light users, and non-users in the **right Frontal Mid region.**

	Mean fractional anisotropy of tractography analysis P-Value. -Frontal Mid region of the right hemisphere-		
	Heavy users (Group I)	Light users (Group II)	Non-users (Group III)
Heavy users (Group I)	○	**	**
Light users (Group II)	0.049	○	**
Non users (Group III)	0.083	0.906	○

With a P-value lower than 0.05, the ANOVA analysis revealed significant differences between heavy users and light users' groups, but no significant difference between heavy and non-users groups and between light users and non-users groups. The table reveals that in the same anatomical area, the mean fractional anisotropy values of different groups in the right Frontal Mid region were significantly different among one from three comparisons realized.

➢ **Frontal Inf Oper**

Table 334: The statistical analysis results of the mean fractional anisotropy in tractography analysis technique in groups of heavy cannabis users, light users, and non-users in the **left Frontal Inf Oper region.**

	Mean fractional anisotropy of tractography analysis P-Value. -Frontal Inf Oper region of the left hemisphere-		
	Heavy users (Group I)	**Light users (Group II)**	**Non-users (Group III)**
Heavy users (Group I)	○	**	**
Light users (Group II)	0.349	○	**
Non users (Group III)	0.048	0.321	○

With a P-value lower than 0.05, the ANOVA analysis revealed significant differences between heavy users and non-users groups, but no significant difference between heavy and light users' groups and between light users and non-users groups. The table reveals that in the same anatomical area, the mean fractional anisotropy values of different groups in the left Frontal Inf Oper region were significantly different among one from three comparisons realized.

Table 335: The statistical analysis results of the mean fractional anisotropy in tractography analysis technique in groups of heavy cannabis users, light users, and non-users in the **right Frontal Inf Oper region.**

	Mean fractional anisotropy of tractography analysis P-Value. -Frontal Inf Oper region of the right hemisphere-		
	Heavy users (Group I)	**Light users (Group II)**	**Non-users (Group III)**
Heavy users (Group I)	○	**	**
Light users (Group II)	0.824	○	**
Non users (Group III)	0.667	0.547	○

With a P-value lower than 0.05, the ANOVA analysis revealed no significant differences. The table reveals that in the same anatomical area, the mean fractional anisotropy values of different groups in the right Frontal Inf Oper region were not significantly different.

➢ **Frontal Inf Tri**

Table 336: The statistical analysis results of the mean fractional anisotropy in tractography analysis technique in groups of heavy cannabis users, light users, and non-users in the **Frontal Inf Tri region.**

	Mean fractional anisotropy of tractography analysis P-Value. -Frontal Inf Tri region of the left hemisphere-		
	Heavy users (Group I)	**Light users (Group II)**	**Non-users (Group III)**
Heavy users (Group I)	○	**	**
Light users (Group II)	0.417	○	**
Non users (Group III)	0.261	**0.039**	○

With a P-value lower than 0.05, the ANOVA analysis revealed a significant difference between light users and non-users groups and no significant differences between the other groups. The table reveals that in the same anatomical area, the mean fractional anisotropy values of different groups in the left Frontal Inf Tri region were significantly different among one from three comparisons realized.

Table 337: The statistical analysis results of the mean fractional anisotropy in tractography analysis technique in groups of heavy cannabis users, light users, and non-users in the **right Frontal Inf Tri region.**

	Mean fractional anisotropy of tractography analysis P-Value -Frontal Inf Tri region of the right hemisphere-		
	Heavy users (Group I)	**Light users (Group II)**	**Non-users (Group III)**
Heavy users (Group I)	○	**	**
Light users (Group II)	0.736	○	**
Non users (Group III)	0.946	0.611	○

With a P-value lower than 0.05, the ANOVA analysis revealed no significant differences. The table reveals that in the same anatomical area, the mean fractional anisotropy values of different groups in the right Frontal Inf Tri region were not significantly different.

➢ **Postcentral**

Table 338: The statistical analysis results of the mean fractional anisotropy in tractography analysis technique in groups of heavy cannabis users, light users, and non-users in the **left Postcentral region.**

	Mean fractional anisotropy of tractography analysis P-Value. -Postcentral region of the left hemisphere-		
	Heavy users (Group I)	Light users (Group II)	Non-users (Group III)
Heavy users (Group I)	○	**	**
Light users (Group II)	0,166	○	**
Non users (Group III)	0,705	0,023	○

With a P-value lower than 0.05, the ANOVA analysis revealed a significant difference between light users and non-users groups and no significant differences between the other groups. The table reveals that in the same anatomical area, the mean fractional anisotropy values of different groups in the left Postcentral region were significantly different among one from three comparisons realized.

Table 339: The statistical analysis results of the mean fractional anisotropy in tractography analysis technique in groups of heavy cannabis users, light users, and non-users in the **right Postcentral region.**

	Mean fractional anisotropy of tractography analysis P-Value. -Postcentral region of the right hemisphere-		
	Heavy users (Group I)	Light users (Group II)	Non-users (Group III)
Heavy users (Group I)	○	**	**
Light users (Group II)	0,063	○	**
Non users (Group III)	0,096	0,326	○

With a P-value lower than 0.05, the ANOVA analysis revealed no significant differences. The table reveals that in the same anatomical area, the mean fractional anisotropy values of different groups in the right Postcentral region were not significantly different.

.

➢ **Parietal Sup**

Table 340: The statistical analysis results of the mean fractional anisotropy in tractography analysis technique in groups of heavy cannabis users, light users, and non-users in the **left Parietal Sup region.**

	Mean fractional anisotropy of tractography analysis P-Value. -Parietal Sup region of the left hemisphere-		
	Heavy users (Group I)	**Light users (Group II)**	**Non-users (Group III)**
Heavy users (Group I)	○	**	**
Light users (Group II)	0,139	○	**
Non users (Group III)	0,360	0,271	○

With a P-value lower than 0.05, the ANOVA analysis revealed no significant differences. The table reveals that in the same anatomical area, the mean fractional anisotropy values of different groups in the left Parietal Sup region were not significantly different.

Table 341: The statistical analysis results of the mean fractional anisotropy in tractography analysis technique in groups of heavy cannabis users, light users, and non-users in the **right Parietal Sup region.**

	Mean fractional anisotropy of tractography analysis P-Value. -Parietal Sup region of the right hemisphere-		
	Heavy users (Group I)	**Light users (Group II)**	**Non-users (Group III)**
Heavy users (Group I)	○	**	**
Light users (Group II)	0,154	○	**
Non users (Group III)	0,433	0,228	○

With a P-value lower than 0.05, the ANOVA analysis revealed no significant differences. The table reveals that in the same anatomical area, the mean fractional anisotropy values of different groups in the right Parietal Sup region were not significantly different.

➢ SupraMarginal

Table 342: The statistical analysis results of the mean fractional anisotropy in tractography analysis technique in groups of heavy cannabis users, light users, and non-users in the **left SupraMarginal region.**

	Mean fractional anisotropy of tractography analysis P-Value. -SupraMarginal region of the left hemisphere-		
	Heavy users (Group I)	Light users (Group II)	Non-users (Group III)
Heavy users (Group I)	○	**	**
Light users (Group II)	0,368	○	**
Non users (Group III)	0,041	0,203	○

With a P-value lower than 0.05, the ANOVA analysis revealed significant differences between heavy users and non-users groups, but no significant difference between heavy and light users' groups and between light users and non-users groups. The table reveals that in the same anatomical area, the mean fractional anisotropy values of different groups in the left SupraMarginal region were significantly different among one group from three comparisons realized.

Table 343: The statistical analysis results of the mean fractional anisotropy in tractography analysis technique in groups of heavy cannabis users, light users, and non-users in the **right SupraMarginal region.**

	Mean fractional anisotropy of tractography analysis P-Value. -SupraMarginal region of the right hemisphere-		
	Heavy users (Group I)	Light users (Group II)	Non-users (Group III)
Heavy users (Group I)	○	**	**
Light users (Group II)	0,807	○	**
Non users (Group III)	0,753	0,907	○

With a P-value lower than 0.05, the ANOVA analysis revealed no significant differences. The table reveals that in the same anatomical area, the mean fractional anisotropy values of different groups in the right SupraMarginal region were not significantly different.

➢ **Angular**

Table 344: The statistical analysis results of the mean fractional anisotropy in tractography analysis technique in groups of heavy cannabis users, light users, and non-users in the **left Angular region.**

	Mean fractional anisotropy of tractography analysis P-Value. -Angular region of the left hemisphere-		
	Heavy users (Group I)	**Light users (Group II)**	**Non-users (Group III)**
Heavy users (Group I)	○	**	**
Light users (Group II)	0,360	○	**
Non users (Group III)	0,218	0,904	○

With a P-value lower than 0.05, the ANOVA analysis revealed no significant differences. The table reveals that in the same anatomical area, the mean fractional anisotropy values of different groups in the left Angular region were not significantly different.

Table 345: The statistical analysis results of the mean fractional anisotropy in tractography analysis technique in groups of heavy cannabis users, light users, and non-users in the **right Angular region.**

	Mean fractional anisotropy of tractography analysis P-Value. -Angular region of the right hemisphere-		
	Heavy users (Group I)	**Light users (Group II)**	**Non-users (Group III)**
Heavy users (Group I)	○	**	**
Light users (Group II)	0,806	○	**
Non users (Group III)	0,593	0,839	○

With a P-value lower than 0.05, the ANOVA analysis revealed no significant differences. The table reveals that in the same anatomical area, the mean fractional anisotropy values of different groups in the right Angular region were not significantly different.

➢ **Parietal Inf**

Table 346: The statistical analysis results of the mean fractional anisotropy in tractography analysis technique in groups of heavy cannabis users, light users, and non-users in the **left Parietal Inf region.**

	Mean fractional anisotropy of tractography analysis P-Value -Parietal Inf region of the left hemisphere-		
	Heavy users (Group I)	Light users (Group II)	Non-users (Group III)
Heavy users (Group I)	○	**	**
Light users (Group II)	0,806	○	**
Non users (Group III)	0,810	0,987	○

With a P-value lower than 0.05, the ANOVA analysis revealed no significant differences. The table reveals that in the same anatomical area, the mean fractional anisotropy values of different groups in the left Parietal Inf region were not significantly different.

Table 347: The statistical analysis results of the mean fractional anisotropy in tractography analysis technique in groups of heavy cannabis users, light users, and non-users in the **right Parietal Inf region.**

	Mean fractional anisotropy of tractography analysis P-Value. -Parietal Inf region of the right hemisphere-		
	Heavy users (Group I)	Light users (Group II)	Non-users (Group III)
Heavy users (Group I)	○	**	**
Light users (Group II)	0,513	○	**
Non users (Group III)	0,941	0,655	○

With a P-value lower than 0.05, the ANOVA analysis revealed no significant differences. The table reveals that in the same anatomical area, the mean fractional anisotropy values of different groups in the right Parietal Inf region were not significantly different.

➢ **Precuneus**

Table 348: The statistical analysis results of the mean fractional anisotropy in tractography analysis technique in groups of heavy cannabis users, light users, and non-users in the **left Precuneus region.**

	Mean fractional anisotropy of tractography analysis P-Value. -Precuneus region of the left hemisphere-		
	Heavy users (Group I)	**Light users (Group II)**	**Non-users (Group III)**
Heavy users (Group I)	○	**	**
Light users (Group II)	0,317	○	**
Non users (Group III)	0,207	0,657	○

With a P-value lower than 0.05, the ANOVA analysis revealed no significant differences. The table reveals that in the same anatomical area, the mean fractional anisotropy values of different groups in the left Precuneus region were not significantly different.

Table 349: The statistical analysis results of the mean fractional anisotropy in tractography analysis technique in groups of heavy cannabis users, light users, and non-users in the **right Precuneus region.**

	Mean fractional anisotropy of tractography analysis P-Value. -Precuneus region of the right hemisphere-		
	Heavy users (Group I)	**Light users (Group II)**	**Non-users (Group III)**
Heavy users (Group I)	○	**	**
Light users (Group II)	0,552	○	**
Non users (Group III)	0,485	0,908	○

With a P-value lower than 0.05, the ANOVA analysis revealed no significant differences. The table reveals that in the same anatomical area, the mean fractional anisotropy values of different groups in the right Precuneus region were not significantly different.

➢ Temporal Sup

Table 350: The statistical analysis results of the mean fractional anisotropy in tractography analysis technique in groups of heavy cannabis users, light users, and non-users in the **left Temporal Sup region.**

	Mean fractional anisotropy of tractography analysis P-Value. -Temporal Sup region of the left hemisphere-		
	Heavy users (Group I)	Light users (Group II)	Non-users (Group III)
Heavy users (Group I)	○	**	**
Light users (Group II)	0,740	○	**
Non users (Group III)	0,571	0,478	○

With a P-value lower than 0.05, the ANOVA analysis revealed no significant differences. The table reveals that in the same anatomical area, the mean fractional anisotropy values of different groups in the left Temporal Sup region were not significantly different.

Table 351: The statistical analysis results of the mean fractional anisotropy in tractography analysis technique in groups of heavy cannabis users, light users, and non-users in the **right Precuneus region.**

	Mean fractional anisotropy of tractography analysis P-Value. -Temporal Sup region of the right hemisphere-		
	Heavy users (Group I)	Light users (Group II)	Non-users (Group III)
Heavy users (Group I)	○	**	**
Light users (Group II)	0,888	○	**
Non users (Group III)	0,600	0,511	○

With a P-value lower than 0.05, the ANOVA analysis revealed no significant differences. The table reveals that in the same anatomical area, the mean fractional anisotropy values of different groups in the right Precuneus region were not significantly different.

➢ Temporal Pole Sup

Table 352: The statistical analysis results of the mean fractional anisotropy in tractography analysis technique in groups of heavy cannabis users, light users, and non-users in the **left Temporal Pole Sup region.**

	Mean fractional anisotropy of tractography analysis P-Value. -Temporal Pole Sup region of the left hemisphere-		
	Heavy users (Group I)	**Light users (Group II)**	**Non-users (Group III)**
Heavy users (Group I)	○	**	**
Light users (Group II)	0,392	○	**
Non users (Group III)	0,859	0,452	○

With a P-value lower than 0.05, the ANOVA analysis revealed no significant differences. The table reveals that in the same anatomical area, the mean fractional anisotropy values of different groups in the left Temporal Pole Sup region were not significantly different.

Table 353: The statistical analysis results of the mean fractional anisotropy in tractography analysis technique in groups of heavy cannabis users, light users, and non-users in the **right Temporal Pole Sup region.**

	Mean fractional anisotropy of tractography analysis P-Value. -Temporal Pole Sup region of the right hemisphere-		
	Heavy users (Group I)	**Light users (Group II)**	**Non-users (Group III)**
Heavy users (Group I)	○	**	**
Light users (Group II)	0,908	○	**
Non users (Group III)	0,295	0,382	○

With a P-value lower than 0.05, the ANOVA analysis revealed no significant differences. The table reveals that in the same anatomical area, the mean fractional anisotropy values of different groups in the right Temporal Pole Sup region were not significantly different.

➢ **Heschl**

Table 354: The statistical analysis results of the mean fractional anisotropy in tractography analysis technique in groups of heavy cannabis users, light users, and non-users in the **left Heschl region.**

	Mean fractional anisotropy of tractography analysis P-Value. -Heschl region of the left hemisphere-		
	Heavy users (Group I)	Light users (Group II)	Non-users (Group III)
Heavy users (Group I)	○	**	**
Light users (Group II)	0.402	○	**
Non users (Group III)	0.290	0.047	○

With a P-value lower than 0.05, the ANOVA analysis revealed a significant difference between light users and non-users groups and no significant differences between the other groups. The table reveals that in the same anatomical area, the mean fractional anisotropy values of different groups in the left Heschl region were significantly different among one from three comparisons realized.

Table 355: The statistical analysis results of the mean fractional anisotropy in tractography analysis technique in groups of heavy cannabis users, light users, and non-users in the **right Heschl region.**

	Mean fractional anisotropy of tractography analysis P-Value. -Heschl region of the right hemisphere-		
	Heavy users (Group I)	Light users (Group II)	Non-users (Group III)
Heavy users (Group I)	○	**	**
Light users (Group II)	0.368	○	**
Non users (Group III)	0.048	0.034	○

With a P-value lower than 0.05, the ANOVA analysis revealed significant differences between heavy users and non-users groups and between light users and non-users groups, but no significant difference between heavy and light users' groups. The table reveals that in the same anatomical area, the mean fractional anisotropy values of different groups in the right Heschl region were significantly different among two from three comparisons realized.

- **Temporal Mid**

Table 356: The statistical analysis results of the mean fractional anisotropy in tractography analysis technique in groups of heavy cannabis users, light users, and non-users in the **left Temporal Mid region.**

	Mean fractional anisotropy of tractography analysis P-Value. -Temporal Mid region of the left hemisphere-		
	Heavy users (Group I)	**Light users (Group II)**	**Non-users (Group III)**
Heavy users (Group I)	○	**	**
Light users (Group II)	0,825	○	**
Non users (Group III)	0,156	0,204	○

With a P-value lower than 0.05, the ANOVA analysis revealed no significant differences. The table reveals that in the same anatomical area, the mean fractional anisotropy values of different groups in the left Temporal Mid region were not significantly different.

Table 357: The statistical analysis results of the mean fractional anisotropy in tractography analysis technique in groups of heavy cannabis users, light users, and non-users in the right Temporal Mid region.

	Mean fractional anisotropy of tractography analysis P-Value. -Temporal Mid region of the right hemisphere-		
	Heavy users (Group I)	**Light users (Group II)**	**Non-users (Group III)**
Heavy users (Group I)	○	**	**
Light users (Group II)	0,638	○	**
Non users (Group III)	0,373	0,566	○

With a P-value lower than 0.05, the ANOVA analysis revealed no significant differences. The table reveals that in the same anatomical area, the mean fractional anisotropy values of different groups in the right Temporal Mid region were not significantly different.

- **Temporal Pole Mid**

Table 358: The statistical analysis results of the mean fractional anisotropy in tractography analysis technique in groups of heavy cannabis users, light users, and non-users in the **left Temporal Pole Mid region.**

	Mean fractional anisotropy of tractography analysis P-Value. -Temporal Pole Mid region of the left hemisphere-		
	Heavy users (Group I)	**Light users (Group II)**	**Non-users (Group III)**
Heavy users (Group I)	○	**	**
Light users (Group II)	0.888	○	**
Non users (Group III)	0.433	0.289	○

With a P-value lower than 0.05, the ANOVA analysis revealed no significant differences. The table reveals that in the same anatomical area, the mean fractional anisotropy values of different groups in the left Temporal Pole Mid region were not significantly different.

Table 359: The statistical analysis results of the mean fractional anisotropy in tractography analysis technique in groups of heavy cannabis users, light users, and non-users in the **right Temporal Pole Mid region.**

	Mean fractional anisotropy of tractography analysis P-Value. -Temporal Pole Mid region of the right hemisphere-		
	Heavy users (Group I)	**Light users (Group II)**	**Non-users (Group III)**
Heavy users (Group I)	○	**	**
Light users (Group II)	0.097	○	**
Non users (Group III)	0.370	0.620	○

With a P-value lower than 0.05, the ANOVA analysis revealed no significant differences. The table reveals that in the same anatomical area, the mean fractional anisotropy values of different groups in the right Temporal Pole Mid region were not significantly different.

- **Temporal Inf**

Table 360: The statistical analysis results of the mean fractional anisotropy in tractography analysis technique in groups of heavy cannabis users, light users, and non-users in the **left Temporal Inf region.**

	Mean fractional anisotropy of tractography analysis P-Value. -Temporal Inf region of the left hemisphere-		
	Heavy users (Group I)	**Light users (Group II)**	**Non-users (Group III)**
Heavy users (Group I)	○	**	**
Light users (Group II)	0.710	○	**
Non users (Group III)	0.437	0.350	○

With a P-value lower than 0.05, the ANOVA analysis revealed no significant differences. The table reveals that in the same anatomical area, the mean fractional anisotropy values of different groups in the left Temporal Inf region were not significantly different.

Table 361: The statistical analysis results of the mean fractional anisotropy in tractography analysis technique in groups of heavy cannabis users, light users, and non-users in the **right Temporal Inf region.**

	Mean fractional anisotropy of tractography analysis P-Value. -Temporal Inf region of the right hemisphere-		
	Heavy users (Group I)	**Light users (Group II)**	**Non-users (Group III)**
Heavy users (Group I)	○	**	**
Light users (Group II)	0.454	○	**
Non users (Group III)	0.422	0.742	○

With a P-value lower than 0.05, the ANOVA analysis revealed no significant differences. The table reveals that in the same anatomical area, the mean fractional anisotropy values of different groups in the right Temporal Inf region were not significantly different.

➢ **Fusiform**

Table 362: The statistical analysis results of the mean fractional anisotropy in tractography analysis technique in groups of heavy cannabis users, light users, and non-users in the **left Fusiform region.**

	Mean fractional anisotropy of tractography analysis P-Value. -Fusiform region of the left hemisphere-		
	Heavy users (Group I)	**Light users (Group II)**	**Non-users (Group III)**
Heavy users (Group I)	○	**	**
Light users (Group II)	0.453	○	**
Non users (Group III)	0.836	0.474	○

With a P-value lower than 0.05, the ANOVA analysis revealed no significant differences. The table reveals that in the same anatomical area, the mean fractional anisotropy values of different groups in the left Fusiform region were not significantly different.

Table 363: The statistical analysis results of the mean fractional anisotropy in tractography analysis technique in groups of heavy cannabis users, light users, and non-users in the **right Fusiform region.**

	Mean fractional anisotropy of tractography analysis P-Value -Fusiform region of the right hemisphere-		
	Heavy users (Group I)	**Light users (Group II)**	**Non-users (Group III)**
Heavy users (Group I)	○	**	**
Light users (Group II)	0.693	○	**
Non users (Group III)	0.442	0.373	○

With a P-value lower than 0.05, the ANOVA analysis revealed no significant differences. The table reveals that in the same anatomical area, the mean fractional anisotropy values of different groups in the right Fusiform region were not significantly different.

➢ **Cingulum Ant**

Table 364: The statistical analysis results of the mean fractional anisotropy in tractography analysis technique in groups of heavy cannabis users, light users, and non-users in the **left Cingulum Ant region.**

	Mean fractional anisotropy of tractography analysis P-Value. -Cingulum Ant region of the left hemisphere-		
	Heavy users (Group I)	**Light users (Group II)**	**Non-users (Group III)**
Heavy users (Group I)	○	**	**
Light users (Group II)	0,877	○	**
Non users (Group III)	**0,046**	0,110	○

With a P-value lower than 0.05, the ANOVA analysis revealed significant differences between heavy users and non-users groups, but no significant difference between heavy and light users' groups and between light users and non-users groups. The table reveals that in the same anatomical area, the mean fractional anisotropy values of different groups in the left Cingulum Ant region were significantly different among one group from three comparisons realized.

Table 365: The statistical analysis results of the mean fractional anisotropy in tractography analysis technique in groups of heavy cannabis users, light users, and non-users in the **right Cingulum Ant region.**

	Mean fractional anisotropy of tractography analysis P-Value. -Cingulum Ant region of the right hemisphere-		
	Heavy users (Group I)	**Light users (Group II)**	**Non-users (Group III)**
Heavy users (Group I)	○	**	**
Light users (Group II)	0,390	○	**
Non users (Group III)	0,079	0,103	○

With a P-value lower than 0.05, the ANOVA analysis revealed no significant differences. The table reveals that in the same anatomical area, the mean fractional anisotropy values of different groups in the right Cingulum Ant region were not significantly different.

➢ Cingulum Mid

Table 366: The statistical analysis results of the mean fractional anisotropy in tractography analysis technique in groups of heavy cannabis users, light users, and non-users in the **left Cingulum Mid region.**

	Mean fractional anisotropy of tractography analysis P-Value. -Cingulum Mid region of the left hemisphere-		
	Heavy users (Group I)	**Light users (Group II)**	**Non-users (Group III)**
Heavy users (Group I)	○	**	**
Light users (Group II)	0.272	○	**
Non users (Group III)	0.123	0.345	○

With a P-value lower than 0.05, the ANOVA analysis revealed no significant differences. The table reveals that in the same anatomical area, the mean fractional anisotropy values of different groups in the left Cingulum Mid region were not significantly different.

Table 367: The statistical analysis results of the mean fractional anisotropy in tractography analysis technique in groups of heavy cannabis users, light users, and non-users in the **right Cingulum Mid region.**

	Mean fractional anisotropy of tractography analysis P-Value. -Cingulum Mid region of the right hemisphere-		
	Heavy users (Group I)	**Light users (Group II)**	**Non-users (Group III)**
Heavy users (Group I)	○	**	**
Light users (Group II)	0.557	○	**
Non users (Group III)	0.516	0.985	○

With a P-value lower than 0.05, the ANOVA analysis revealed no significant differences. The table reveals that in the same anatomical area, the mean fractional anisotropy values of different groups in the right Cingulum Mid region were not significantly different.

➢ **Cingulum Post**

Table 368: The statistical analysis results of the mean fractional anisotropy in tractography analysis technique in groups of heavy cannabis users, light users, and non-users in the **left Cingulum Post region.**

	Mean fractional anisotropy of tractography analysis P-Value. -Cingulum Post region of the left hemisphere-		
	Heavy users (Group I)	**Light users (Group II)**	**Non-users (Group III)**
Heavy users (Group I)	○	**	**
Light users (Group II)	0.081	○	**
Non users (Group III)	0.305	**0.004**	○

With a P-value lower than 0.05, the ANOVA analysis revealed a significant difference between light users and non-users groups and no significant differences between the other groups. The table reveals that in the same anatomical area, the mean fractional anisotropy values of different groups in the left Cingulum Post region were significantly different among one from three comparisons realized.

Table 369: The statistical analysis results of the mean fractional anisotropy in tractography analysis technique in groups of heavy cannabis users, light users, and non-users in the **right Cingulum Post region.**

	Mean fractional anisotropy of tractography analysis P-Value. -Cingulum Post region of the right hemisphere-		
	Heavy users (Group I)	**Light users (Group II)**	**Non-users (Group III)**
Heavy users (Group I)	○	**	**
Light users (Group II)	0.834	○	**
Non users (Group III)	0.333	0.226	○

With a P-value lower than 0.05, the ANOVA analysis revealed no significant differences. The table reveals that in the same anatomical area, the mean fractional anisotropy values of different groups in the right Cingulum Post region were not significantly different.

- **ParaHippocampal**

Table 370: The statistical analysis results of the mean fractional anisotropy in tractography analysis technique in groups of heavy cannabis users, light users, and non-users in the **left ParaHippocampal region.**

	Mean fractional anisotropy of tractography analysis P-Value. -ParaHippocampal region of the left hemisphere-		
	Heavy users (Group I)	**Light users (Group II)**	**Non-users (Group III)**
Heavy users (Group I)	○	**	**
Light users (Group II)	0.704	○	**
Non users (Group III)	0.274	0.274	○

With a P-value lower than 0.05, the ANOVA analysis revealed no significant differences. The table reveals that in the same anatomical area, the mean fractional anisotropy values of different groups in the left ParaHippocampal region were not significantly different.

Table 371: The statistical analysis results of the mean fractional anisotropy in tractography analysis technique in groups of heavy cannabis users, light users, and non-users in the **right ParaHippocampal region.**

	Mean fractional anisotropy of tractography analysis P-Value. -ParaHippocampal region of the right hemisphere-		
	Heavy users (Group I)	**Light users (Group II)**	**Non-users (Group III)**
Heavy users (Group I)	○	**	**
Light users (Group II)	0.270	○	**
Non users (Group III)	0.568	0.535	○

With a P-value lower than 0.05, the ANOVA analysis revealed no significant differences. The table reveals that in the same anatomical area, the mean fractional anisotropy values of different groups in the right ParaHippocampal region were not significantly different.

➢ Hippocampus

Table 372: The statistical analysis results of the mean fractional anisotropy in tractography analysis technique in groups of heavy cannabis users, light users, and non-users in the **left Hippocampus region.**

	Mean fractional anisotropy of tractography analysis P-Value. -Hippocampus region of the left hemisphere-		
	Heavy users (Group I)	**Light users (Group II)**	**Non-users (Group III)**
Heavy users (Group I)	○	**	**
Light users (Group II)	0.799	○	**
Non users (Group III)	0.582	0.622	○

With a P-value lower than 0.05, the ANOVA analysis revealed no significant differences. The table reveals that in the same anatomical area, the mean fractional anisotropy values of different groups in the left Hippocampus region were not significantly different.

Table 373: The statistical analysis results of the mean fractional anisotropy in tractography analysis technique in groups of heavy cannabis users, light users, and non-users in the **right Hippocampus region.**

	Mean fractional anisotropy of tractography analysis P-Value. -Hippocampus region of the right hemisphere-		
	Heavy users (Group I)	**Light users (Group II)**	**Non-users (Group III)**
Heavy users (Group I)	○	**	**
Light users (Group II)	0.667	○	**
Non users (Group III)	0.605	0.840	○

With a P-value lower than 0.05, the ANOVA analysis revealed no significant differences. The table reveals that in the same anatomical area, the mean fractional anisotropy values of different groups in the right Hippocampus region were not significantly different.

➢ Insula

Table 374: The statistical analysis results of the mean fractional anisotropy in tractography analysis technique in groups of heavy cannabis users, light users, and non-users in the **left Insula region.**

	Mean fractional anisotropy of tractography analysis P-Value. -Insula region of the left hemisphere-		
	Heavy users (Group I)	**Light users (Group II)**	**Non-users (Group III)**
Heavy users (Group I)	○	**	**
Light users (Group II)	0,568	○	**
Non users (Group III)	0,832	0,714	○

With a P-value lower than 0.05, the ANOVA analysis revealed no significant differences. The table reveals that in the same anatomical area, the mean fractional anisotropy values of different groups in the left Insula region were not significantly different.

Table 375. The statistical analysis results of the mean fractional anisotropy in tractography analysis technique in groups of heavy cannabis users, light users, and non-users in the **right Insula region.**

	Mean fractional anisotropy of tractography analysis P-Value. -Insula region of the right hemisphere-		
	Heavy users (Group I)	**Light users (Group II)**	**Non-users (Group III)**
Heavy users (Group I)	○	**	**
Light users (Group II)	0.815	○	**
Non users (Group III)	0.230	0.264	○

With a P-value lower than 0.05, the ANOVA analysis revealed no significant differences. The table reveals that in the same anatomical area, the mean fractional anisotropy values of different groups in the right Insula region were not significantly different.

➢ **Amygdala**

Table 376: The statistical analysis results of the mean fractional anisotropy in tractography analysis technique in groups of heavy cannabis users, light users, and non-users in the **left Amygdala region.**

	Mean fractional anisotropy of tractography analysis P-Value. -Amygdala region of the left hemisphere-		
	Heavy users (Group I)	**Light users (Group II)**	**Non-users (Group III)**
Heavy users (Group I)	○	**	**
Light users (Group II)	0.809	○	**
Non users (Group III)	**0.010**	**0.047**	○

With a P-value lower than 0.05, the ANOVA analysis revealed significant differences between heavy users and non-users groups and between light users and non-users groups, but no significant difference between heavy and light users' groups. The table reveals that in the same anatomical area, the mean fractional anisotropy values of different groups in the left Amygdala region were significantly different among two from three comparisons realized.

Table 377: The statistical analysis results of the mean fractional anisotropy in tractography analysis technique in groups of heavy cannabis users, light users, and non-users in the **right Amygdala region.**

	Mean fractional anisotropy of tractography analysis P-Value. -Amygdala region of the right hemisphere-		
	Heavy users (Group I)	**Light users (Group II)**	**Non-users (Group III)**
Heavy users (Group I)	○	**	**
Light users (Group II)	0.139	○	**
Non users (Group III)	0.975	0.327	○

With a P-value lower than 0.05, the ANOVA analysis revealed no significant differences. The table reveals that in the same anatomical area, the mean fractional anisotropy values of different groups in the right Amygdala region were not significantly different.

➢ **Thalamus**

Table 378: The statistical analysis results of the mean fractional anisotropy in tractography analysis technique in groups of heavy cannabis users, light users, and non-users in the **left Thalamus region.**

	Mean fractional anisotropy of tractography analysis P-Value. -Thalamus region of the left hemisphere-		
	Heavy users (Group I)	**Light users (Group II)**	**Non-users (Group III)**
Heavy users (Group I)	○	**	**
Light users (Group II)	0.241	○	**
Non users (Group III)	0.316	0.540	○

With a P-value lower than 0.05, the ANOVA analysis revealed no significant differences. The table reveals that in the same anatomical area, the mean fractional anisotropy values of different groups in the left Thalamus region were not significantly different.

Table 379: The statistical analysis results of the mean fractional anisotropy in tractography analysis technique in groups of heavy cannabis users, light users, and non-users in the **right Thalamus region.**

	Mean fractional anisotropy of tractography analysis P-Value. -Thalamus region of the right hemisphere-		
	Heavy users (Group I)	**Light users (Group II)**	**Non-users (Group III)**
Heavy users (Group I)	○	**	**
Light users (Group II)	0.398	○	**
Non users (Group III)	0.745	0.430	○

With a P-value lower than 0.05, the ANOVA analysis revealed no significant differences. The table reveals that in the same anatomical area, the mean fractional anisotropy values of different groups in the right Thalamus region were not significantly different.

➢ Caudate

Table 380: The statistical analysis results of the mean fractional anisotropy in tractography analysis technique in groups of heavy cannabis users, light users, and non-users in the **left Caudate region.**

	Mean fractional anisotropy of tractography analysis P-Value. -Caudate region of the left hemisphere-		
	Heavy users (Group I)	**Light users (Group II)**	**Non-users (Group III)**
Heavy users (Group I)	○	**	**
Light users (Group II)	0.440	○	**
Non users (Group III)	0.056	0.094	○

With a P-value lower than 0.05, the ANOVA analysis revealed no significant differences. The table reveals that in the same anatomical area, the mean fractional anisotropy values of different groups in the left Caudate region were not significantly different.

Table 381: The statistical analysis results of the mean fractional anisotropy in tractography analysis technique in groups of heavy cannabis users, light users, and non-users in the **right Caudate region.**

	Mean fractional anisotropy of tractography analysis P-Value. -Caudate region of the right hemisphere-		
	Heavy users (Group I)	**Light users (Group II)**	**Non-users (Group III)**
Heavy users (Group I)	○	**	**
Light users (Group II)	0.444	○	**
Non users (Group III)	0.909	0.183	○

With a P-value lower than 0.05, the ANOVA analysis revealed no significant differences. The table reveals that in the same anatomical area, the mean fractional anisotropy values of different groups in the right Caudate region were not significantly different.

➢ **Putamen**

Table 382: The statistical analysis results of the mean fractional anisotropy in tractography analysis technique in groups of heavy cannabis users, light users, and non-users in the **left Putamen region.**

	Mean fractional anisotropy of tractography analysis P-Value. -Putamen region of the left hemisphere-		
	Heavy users (Group I)	**Light users (Group II)**	**Non-users (Group III)**
Heavy users (Group I)	○	**	**
Light users (Group II)	0.493	○	**
Non users (Group III)	0.147	0.747	○

With a P-value lower than 0.05, the ANOVA analysis revealed no significant differences. The table reveals that in the same anatomical area, the mean fractional anisotropy values of different groups in the left Putamen region were not significantly different.

Table 383: The statistical analysis results of the mean fractional anisotropy in tractography analysis technique in groups of heavy cannabis users, light users, and non-users in the **right Putamen region.**

	Mean fractional anisotropy of tractography analysis P-Value. -Putamen region of the right hemisphere-		
	Heavy users (Group I)	**Light users (Group II)**	**Non-users (Group III)**
Heavy users (Group I)	○	**	**
Light users (Group II)	0.413	○	**
Non users (Group III)	0.351	0.985	○

With a P-value lower than 0.05, the ANOVA analysis revealed no significant differences. The table reveals that in the same anatomical area, the mean fractional anisotropy values of different groups in the right Putamen region were not significantly different.

➢ **Pallidum**

Table 384: The statistical analysis results of the mean fractional anisotropy in tractography analysis technique in groups of heavy cannabis users, light users, and non-users in the **left Pallidum region.**

	Mean fractional anisotropy of tractography analysis P-Value. -Pallidum region of the left hemisphere-		
	Heavy users (Group I)	**Light users (Group II)**	**Non-users (Group III)**
Heavy users (Group I)	○	**	**
Light users (Group II)	0.475	○	**
Non users (Group III)	0.209	0.646	○

With a P-value lower than 0.05, the ANOVA analysis revealed no significant differences. The table reveals that in the same anatomical area, the mean fractional anisotropy values of different groups in the left Pallidum region were not significantly different.

Table 385: The statistical analysis results of the mean fractional anisotropy in tractography analysis technique in groups of heavy cannabis users, light users, and non-users in the **right Pallidum region.**

	Mean fractional anisotropy of tractography analysis P-Value. -Pallidum region of the right hemisphere-		
	Heavy users (Group I)	**Light users (Group II)**	**Non-users (Group III)**
Heavy users (Group I)	○	**	**
Light users (Group II)	0.337	○	**
Non users (Group III)	0.824	0.539	○

With a P-value lower than 0.05, the ANOVA analysis revealed no significant differences. The table reveals that in the same anatomical area, the mean fractional anisotropy values of different groups in the right Pallidum region were not significantly different.

2. Mean diffusivity (MD) analysis of Variance (ANOVA) results

a. Summary of all the analytical findings

For mean diffusivity (MD), in the 70 regions examined, 420 analyses of variance were conducted (between the three groups and in both hemispheres).

The analysis of Variance (ANOVA) results revealed 45 statistically significant results (with p-value <0.05), which is equivalent to 10.7 % of the total conducted analysis.

Table 386 summarizes the regions with the corresponding groups compared where the statistical analysis is significant.

Table 386: A table containing regions of interest revealing statistically significant results of white matter mean diffusivity within the three groups (heavy and light users and control group).

The ROIs in which the WM tracts examined are located.	Groups compared
Left Frontal Med Orb	Heavy users Vs. Non-users Light users Vs. Non-users
Right Frontal Med Orb	Heavy users Vs. Light users Light users Vs. Non-users
Left Frontal Sup Orb	Heavy users Vs. Non-users Light users Vs. Non-users
Right Frontal Sup Orb	Light users Vs. Non-users
Left Frontal Mid Orb	Heavy users Vs. Non-users Light users Vs. Non-users
Right Frontal Mid Orb	Heavy users Vs. Light users
Left Frontal Inf Orb	Heavy users Vs. Non-users Light users Vs. Non-users
Left Rectus	Heavy users Vs. Non-users Light users Vs. Non-users
Right Rectus	Heavy users Vs. Light users Light users Vs. Non-users
Right Olfactory	Heavy users Vs. Light users
Left Frontal Sup Medial	Light users Vs. Non-users

Right Frontal Sup Medial	Light users Vs. Non-users
Left Frontal Mid	Heavy users Vs. Non-users
Left Frontal Inf Oper	Heavy users Vs. Non-users Light users Vs. Non-users
Left Frontal Inf Tri	Heavy users Vs. Non-users Light users Vs. Non-users
Left Parietal Sup	Heavy users Vs. Non-users
Left SupraMarginal	Heavy users Vs. Non-users
Left Angular	Heavy users Vs. Non-users
Left Parietal Inf	Heavy users Vs. Light users Heavy users Vs. Non-users
Left Temporal Sup	Heavy users Vs. Light users Heavy users Vs. Non-users
Left Temporal Pole Sup	Heavy users Vs. Non-users Light users Vs. Non-users
Left Heschl	Heavy users Vs. Non-users
Left Temporal Mid	Heavy users Vs. Light users Heavy users Vs. Non-users
Left Temporal Pole Mid	Heavy users Vs. Non-users Light users Vs. Non-users
Left Temporal Inf	Heavy users Vs. Light users Heavy users Vs. Non-users
Left Insula	Heavy users Vs. Non-users Light users Vs. Non-users
Left Putamen	Heavy users Vs. Non-users Light users Vs. Non-users
Left Pallidum	Light users Vs. Non-users

b. The analytical findings of the white matter related to each region of interest and between each of the groups studied

We present the mean diffusivity (MD) statistical analysis findings by two tables for each region of interest and in both hemispheres. The first table represents statistical results in the left regions and the second in the right regions.

➢ Frontal Med Orb

Table 387: The statistical analysis results of the mean diffusivity in tractography analysis technique in groups of heavy cannabis users, light users, and non-users in the left Frontal Med Orb region.

	Mean diffusivity of tractography analysis P-Value. -Frontal Med Orb region of the left hemisphere-		
	Heavy users (Group I)	Light users (Group II)	Non-users (Group III)
Heavy users (Group I)	○	**	**
Light users (Group II)	0.553	○	**
Non users (Group III)	0.016	0.029	○

With a P-value lower than 0.05, the ANOVA analysis revealed significant differences between heavy users and non-users groups and between light users and non-users groups, but no significant difference between heavy and light users' groups. The table reveals that in the same anatomical area, the mean diffusivity values of different groups in the left Frontal Med Orb region were significantly different among two from three comparisons realized.

Table 388: The statistical analysis results of the mean diffusivity in tractography analysis technique in groups of heavy cannabis users, light users, and non-users in the right Frontal Med Orb region.

	Mean diffusivity of tractography analysis P-Value. -Frontal Med Orb region of the right hemisphere-		
	Heavy users (Group I)	Light users (Group II)	Non-users (Group III)
Heavy users (Group I)	○	**	**
Light users (Group II)	0.044	○	**
Non users (Group III)	0.253	0.020	○

With a P-value lower than 0.05, the ANOVA analysis revealed significant differences between heavy users and light users' groups and between light users and non-users groups, but no significant difference between heavy and non-users groups. The table reveals that in the same anatomical area, the mean diffusivity values of different groups in the right Frontal Med Orb region were significantly different among two from three comparisons realized.

➢ Frontal Sup Orb

Table 389: The statistical analysis results of the mean diffusivity in tractography analysis technique in groups of heavy cannabis users, light users, and non-users in the left Frontal Sup Orb region.

	Mean diffusivity of tractography analysis P-Value. -Frontal Sup Orb region of the left hemisphere -		
	Heavy users (Group I)	Light users (Group II)	Non-users (Group III)
Heavy users (Group I)	○	**	**
Light users (Group II)	0.440	○	**
Non users (Group III)	0.008	0.013	○

With a P-value lower than 0.05, the ANOVA analysis revealed significant differences between heavy users and non-users groups and between light users and non-users groups, but no significant difference between heavy and light users' groups. The table reveals that in the same anatomical area, the mean diffusivity values of different groups in the left Frontal Sup Orb region were significantly different among two from three comparisons realized.

Table 390: The statistical analysis results of the mean diffusivity in tractography analysis technique in groups of heavy cannabis users, light users, and non-users in the right Frontal Sup Orb region.

	Mean diffusivity of tractography analysis P-Value. -Frontal Sup Orb region of the right hemisphere-		
	Heavy users (Group I)	Light users (Group II)	Non-users (Group III)
Heavy users (Group I)	○	**	**
Light users (Group II)	0.303	○	**
Non users (Group III)	0.246	0.019	○

With a P-value lower than 0.05, the ANOVA analysis revealed significant differences between light users and non-users groups, but no significant difference between heavy and light users' groups and between heavy users and non-users groups. The table reveals that in the same anatomical area, the mean diffusivity values of different groups in the right Frontal Sup Orb region were significantly different among one from three comparisons realized.

➢ **Frontal Mid Orb**

Table 391: The statistical analysis results of the mean diffusivity in tractography analysis technique in groups of heavy cannabis users, light users, and non-users in the left Frontal Mid Orb region.

	Mean Apparent Diffusion Coefficient of tractography analysis P-Value. -Frontal Mid Orb region of the left hemisphere-		
	Heavy users (Group I)	Light users (Group II)	Non-users (Group III)
Heavy users (Group I)	○	**	**
Light users (Group II)	0.135	○	**
Non users (Group III)	0.012	0.019	○

With a P-value lower than 0.05, the ANOVA analysis revealed significant differences between heavy users and non-users groups and between light users and non-users groups, but no significant difference between heavy and light users' groups. The table reveals that in the same anatomical area, the mean diffusivity values of different groups in the left Frontal Mid Orb region were significantly different among two from three comparisons realized.

Table 392: The statistical analysis results of the mean diffusivity in tractography analysis technique in groups of heavy cannabis users, light users, and non-users in the right Frontal Mid Orb region.

	Mean Apparent Diffusion Coefficient of tractography analysis P-Value. -Frontal Mid Orb region of the right hemisphere -		
	Heavy users (Group I)	Light users (Group II)	Non-users (Group III)
Heavy users (Group I)	○	**	**
Light users (Group II)	0.019	○	**
Non users (Group III)	0.209	0.122	○

With a P-value lower than 0.05, the ANOVA analysis revealed significant differences between heavy users and light users' groups, but no significant difference between heavy and non-users groups and between light users and non-users groups. The table reveals that in the same anatomical area, the mean diffusivity values of different groups in the right Frontal Mid Orb region were significantly different among one from three comparisons realized.

➢ Frontal Inf Orb

Table 393: The statistical analysis results of the mean diffusivity in tractography analysis technique in groups of heavy cannabis users, light users, and non-users in the Frontal Inf Orb region.

	Mean diffusivity of tractography analysis P-Value. -Frontal Inf Orb region of the left hemisphere-		
	Heavy users (Group I)	Light users (Group II)	Non-users (Group III)
Heavy users (Group I)	○	**	**
Light users (Group II)	0.111	○	**
Non users (Group III)	0.017	0.008	○

With a P-value lower than 0.05, the ANOVA analysis revealed significant differences between heavy users and non-users groups and between light users and non-users groups, but no significant difference between heavy and light users' groups. The table reveals that in the same anatomical area, the mean diffusivity values of different groups in the left Frontal inf Orb region were significantly different among two from three comparisons realized.

Table 394: The statistical analysis results of the mean diffusivity in tractography analysis technique in groups of heavy cannabis users, light users, and non-users in the right Frontal Inf Orb region.

	Mean Apparent Diffusion Coefficient of tractography analysis P-Value. -Frontal Inf Orb region of the right hemisphere-		
	Heavy users (Group I)	Light users (Group II)	Non-users (Group III)
Heavy users (Group I)	○	**	**
Light users (Group II)	0.238	○	**
Non users (Group III)	0.435	0.830	○

With a P-value lower than 0.05, the ANOVA analysis revealed no significant differences. The table reveals that in the same anatomical area, the mean diffusivity values of different groups in the right Frontal Inf Orb region were not significantly different.

➢ **Rectus**

Table 395: The statistical analysis results of the mean diffusivity in tractography analysis technique in groups of heavy cannabis users, light users, and non-users in the left Rectus region.

	Mean diffusivity of tractography analysis P-Value. -Rectus region of the left hemisphere-		
	Heavy users (Group I)	Light users (Group II)	Non-users (Group III)
Heavy users (Group I)	○	**	**
Light users (Group II)	0.500	○	**
Non users (Group III)	0.036	0.015	○

With a P-value lower than 0.05, the ANOVA analysis revealed significant differences between heavy users and non-users groups and between light users and non-users groups, but no significant difference between heavy and light users' groups. The table reveals that in the same anatomical area, the mean diffusivity values of different groups in the left Rectus region were significantly different among two from three comparisons realized.

Table 396: The statistical analysis results of the mean diffusivity in tractography analysis technique in groups of heavy cannabis users, light users, and non-users in the right Rectus region.

	Mean diffusivity of tractography analysis P-Value. -Rectus region of the right hemisphere-		
	Heavy users (Group I)	Light users (Group II)	Non-users (Group III)
Heavy users (Group I)	○	**	**
Light users (Group II)	0.018	○	**
Non users (Group III)	0.264	0.022	○

With a P-value lower than 0.05, the ANOVA analysis revealed significant differences between heavy users and light users' groups and between light users and non-users groups, but no significant difference between heavy and non-users groups. The table reveals that in the same anatomical area, the mean diffusivity values of different groups in the right Frontal Med Orb region were significantly different among two from three comparisons realized.

➢ Olfactory

Table 397: The statistical analysis results of the mean diffusivity in tractography analysis technique in groups of heavy cannabis users, light users, and non-users in the left Olfactory region.

	Mean diffusivity of tractography analysis P-Value. -Olfactory region of the left hemisphere-		
	Heavy users (Group I)	Light users (Group II)	Non-users (Group III)
Heavy users (Group I)	○	**	**
Light users (Group II)	0.629	○	**
Non users (Group III)	0.884	0.750	○

With a P-value lower than 0.05, the ANOVA analysis revealed no significant differences. The table reveals that in the same anatomical area, the mean diffusivity values of different groups in the left Olfactory region were not significantly different.

Table 398: The statistical analysis results of the mean diffusivity in tractography analysis technique in groups of heavy cannabis users, light users, and non-users in the right Olfactory region.

	Mean diffusivity of tractography analysis P-Value. -Olfactory region of the right hemisphere-		
	Heavy users (Group I)	Light users (Group II)	Non-users (Group III)
Heavy users (Group I)	○	**	**
Light users (Group II)	0.023	○	**
Non users (Group III)	0.969	0.383	○

With a P-value lower than 0.05, the ANOVA analysis revealed significant differences between heavy users and light users' groups, but no significant difference between heavy and non-users groups and between light users and non-users groups. The table reveals that in the same anatomical area, the mean diffusivity values of different groups in the right Olfactory region were significantly different among one group from three comparisons realized.

➢ **Frontal Sup Medial**

Table 399: The statistical analysis results of the mean diffusivity in tractography analysis technique in groups of heavy cannabis users, light users, and non-users in the left Frontal Sup Medial region.

	Mean diffusivity of tractography analysis P-Value. -Frontal Sup Medial region of the left hemisphere-		
	Heavy users (Group I)	Light users (Group II)	Non-users (Group III)
Heavy users (Group I)	○	**	**
Light users (Group II)	0.347	○	**
Non users (Group III)	0.170	0.044	○

With a P-value lower than 0.05, the ANOVA analysis revealed significant differences between light users and non-users groups, but no significant difference between heavy and light users' groups and between heavy users and non-users groups. The table reveals that in the same anatomical area, the mean diffusivity values of different groups in the left Frontal Sup Medial region were significantly different among one from three comparisons realized.

Table 400: The statistical analysis results of the mean diffusivity in tractography analysis technique in groups of heavy cannabis users, light users, and non-users in the right Frontal Sup Medial region.

	Mean diffusivity of tractography analysis P-Value. -Frontal Sup Medial region of the right hemisphere-		
	Heavy users (Group I)	Light users (Group II)	Non-users (Group III)
Heavy users (Group I)	○	**	**
Light users (Group II)	0.133	○	**
Non users (Group III)	0.244	0.031	○

With a P-value lower than 0.05, the ANOVA analysis revealed significant differences between light users and non-users groups, but no significant difference between heavy and light users' groups and between heavy users and non-users groups. The table reveals that in the same anatomical area, the mean diffusivity values of different groups in the right Frontal Sup Medial region were significantly different among one from three comparisons realized.

➢ Frontal Sup

Table 401: The statistical analysis results of the mean diffusivity in tractography analysis technique in groups of heavy cannabis users, light users, and non-users in the left Frontal Sup region.

	Mean diffusivity of tractography analysis P-Value. -Frontal Sup region of the left hemisphere-		
	Heavy users (Group I)	Light users (Group II)	Non-users (Group III)
Heavy users (Group I)	○	**	**
Light users (Group II)	0.302	○	**
Non users (Group III)	0.310	0.114	○

With a P-value lower than 0.05, the ANOVA analysis revealed no significant differences. The table reveals that in the same anatomical area, the mean diffusivity values of different groups in the left Frontal Sup region were not significantly different.

Table 402: The statistical analysis results of the mean diffusivity in tractography analysis technique in groups of heavy cannabis users, light users, and non-users in the right Frontal Sup region.

	Mean diffusivity of tractography analysis P-Value. -Frontal Sup region of the right hemisphere-		
	Heavy users (Group I)	Light users (Group II)	Non-users (Group III)
Heavy users (Group I)	○	**	**
Light users (Group II)	0.501	○	**
Non users (Group III)	0.814	0.438	○

With a P-value lower than 0.05, the ANOVA analysis revealed no significant differences. The table reveals that in the same anatomical area, the mean diffusivity values of different groups in the right Frontal Sup region were not significantly different.

➢ **Frontal Mid**

Table 403: The statistical analysis results of the mean diffusivity in tractography analysis technique in groups of heavy cannabis users, light users, and non-users in the left Frontal Mid region.

	Mean diffusivity of tractography analysis P-Value. -Frontal Mid region of the left hemisphere-		
	Heavy users (Group I)	Light users (Group II)	Non-users (Group III)
Heavy users (Group I)	○	**	**
Light users (Group II)	0.920	○	**
Non users (Group III)	0.020	0.070	○

With a P-value lower than 0.05, the ANOVA analysis revealed significant differences between heavy users and non-users groups, but no significant difference between light and non-users groups and between heavy users and light users groups. The table reveals that in the same anatomical area, the mean diffusivity values of different groups in the left Frontal Mid region were significantly different among one from three comparisons realized.

Table 404: The statistical analysis results of the mean diffusivity in tractography analysis technique in groups of heavy cannabis users, light users, and non-users in the right Frontal Mid region.

	Mean diffusivity of tractography analysis P-Value. -Frontal Mid region of the right hemisphere-		
	Heavy users (Group I)	Light users (Group II)	Non-users (Group III)
Heavy users (Group I)	○	**	**
Light users (Group II)	0.857	○	**
Non users (Group III)	0.660	0.650	○

With a P-value lower than 0.05, the ANOVA analysis revealed no significant differences. The table reveals that in the same anatomical area, the mean diffusivity values of different groups in the right Frontal Mid region were not significantly different.

➢ Frontal Inf Oper

Table 405: The statistical analysis results of the mean diffusivity in tractography analysis technique in groups of heavy cannabis users, light users, and non-users in the left Frontal Inf Oper region.

	Mean diffusivity of tractography analysis P-Value. -Frontal Inf Oper region of the left hemisphere-		
	Heavy users (Group I)	Light users (Group II)	Non-users (Group III)
Heavy users (Group I)	○	**	**
Light users (Group II)	0.663	○	**
Non users (Group III)	0.009	0.046	○

With a P-value lower than 0.05, the ANOVA analysis revealed significant differences between heavy users and non-users groups and between light users and non-users groups, but no significant difference between heavy and light users' groups. The table reveals that in the same anatomical area, the mean diffusivity values of different groups in the left Frontal Inf Oper region were significantly different among two from three comparisons realized.

Table 406: The statistical analysis results of the mean diffusivity in tractography analysis technique in groups of heavy cannabis users, light users, and non-users in the right Frontal Inf Oper region.

	Mean diffusivity of tractography analysis P-Value. -Frontal Inf Oper region of the right hemisphere-		
	Heavy users (Group I)	Light users (Group II)	Non-users (Group III)
Heavy users (Group I)	○	**	**
Light users (Group II)	0.660	○	**
Non users (Group III)	0.691	0.298	○

With a P-value lower than 0.05, the ANOVA analysis revealed no significant differences. The table reveals that in the same anatomical area, the mean diffusivity values of different groups in the right Frontal Inf Oper region were not significantly different.

➢ **Frontal Inf Tri**

Table 407: The statistical analysis results of the mean diffusivity in tractography analysis technique in groups of heavy cannabis users, light users, and non-users in the left Frontal Inf Tri region.

	Mean diffusivity of tractography analysis P-Value. -Frontal Inf Tri region of the left hemisphere-		
	Heavy users (Group I)	Light users (Group II)	Non-users (Group III)
Heavy users (Group I)	o	**	**
Light users (Group II)	0.629	o	**
Non users (Group III)	0.021	0.043	o

With a P-value lower than 0.05, the ANOVA analysis revealed significant differences between heavy users and non-users groups and between light users and non-users groups, but no significant difference between heavy and light users' groups. The table reveals that in the same anatomical area, the mean diffusivity values of different groups in the left Frontal Inf Tri region were significantly different among two from three comparisons realized.

Table 408: The statistical analysis results of the mean diffusivity in tractography analysis technique in groups of heavy cannabis users, light users, and non-users in the right Frontal Inf Tri region.

	Mean diffusivity of tractography analysis P-Value. -Frontal Inf Tri region of the right hemisphere-		
	Heavy users (Group I)	Light users (Group II)	Non-users (Group III)
Heavy users (Group I)	o	**	**
Light users (Group II)	0.688	o	**
Non users (Group III)	0.954	0.642	o

With a P-value lower than 0.05, the ANOVA analysis revealed no significant differences. The table reveals that in the same anatomical area, the mean diffusivity values of different groups in the right Frontal Inf Tri region were not significantly different.

➢ **Postcentral**

Table 409: The statistical analysis results of the mean diffusivity in tractography analysis technique in groups of heavy cannabis users, light users, and non-users in the left Postcentral region.

	Mean diffusivity of tractography analysis P-Value. -Postcentral region of the left hemisphere-		
	Heavy users (Group I)	Light users (Group II)	Non-users (Group III)
Heavy users (Group I)	○	**	**
Light users (Group II)	0,676	○	**
Non users (Group III)	0,245	0,200	○

With a P-value lower than 0.05, the ANOVA analysis revealed no significant differences. The table reveals that in the same anatomical area, the mean diffusivity values of different groups in the left Postcentral region were not significantly different.

Table 410: The statistical analysis results of the mean diffusivity in tractography analysis technique in groups of heavy cannabis users, light users, and non-users in the right Postcentral region.

	Mean diffusivity of tractography analysis P-Value. -Postcentral region of the right hemisphere-		
	Heavy users (Group I)	Light users (Group II)	Non-users (Group III)
Heavy users (Group I)	○	**	**
Light users (Group II)	0,536	○	**
Non users (Group III)	0,779	0,932	○

With a P-value lower than 0.05, the ANOVA analysis revealed no significant differences. The table reveals that in the same anatomical area, the mean diffusivity values of different groups in the right Postcentral region were not significantly different.

➢ **Parietal Sup**

Table 411: The statistical analysis results of the mean diffusivity in tractography analysis technique in groups of heavy cannabis users, light users, and non-users in the left Parietal Sup region.

	Mean diffusivity of tractography analysis P-Value. -Parietal Sup region of the left hemisphere-		
	Heavy users (Group I)	Light users (Group II)	Non-users (Group III)
Heavy users (Group I)	○	**	**
Light users (Group II)	0,071	○	**
Non users (Group III)	0,025	0,419	○

With a P-value lower than 0.05, the ANOVA analysis revealed significant differences between heavy users and non-users groups, but no significant difference between heavy and light users' groups and between light users and non-users groups. The table reveals that in the same anatomical area, the mean diffusivity values of different groups in the left Parietal Sup region were significantly different among one group from three comparisons realized.

Table 412: The statistical analysis results of the mean diffusivity in tractography analysis technique in groups of heavy cannabis users, light users, and non-users in the right Parietal Sup region.

	Mean diffusivity of tractography analysis P-Value. -Parietal Sup region of the right hemisphere-		
	Heavy users (Group I)	Light users (Group II)	Non-users (Group III)
Heavy users (Group I)	○	**	**
Light users (Group II)	0,476	○	**
Non users (Group III)	0,812	0,712	○

With a P-value lower than 0.05, the ANOVA analysis revealed no significant differences. The table reveals that in the same anatomical area, the mean diffusivity values of different groups in the right Parietal Sup region were not significantly different.

- SupraMarginal

Table 413: The statistical analysis results of the mean diffusivity in tractography analysis technique in groups of heavy cannabis users, light users, and non-users in the left SupraMarginal region.

	Mean diffusivity of tractography analysis P-Value. -SupraMarginal region of the left hemisphere-		
	Heavy users (Group I)	Light users (Group II)	Non-users (Group III)
Heavy users (Group I)	○	**	**
Light users (Group II)	0,302	○	**
Non users (Group III)	0,013	0,217	○

With a P-value lower than 0.05, the ANOVA analysis revealed significant differences between heavy users and non-users groups, but no significant difference between heavy and light users' groups and between light users and non-users groups. The table reveals that in the same anatomical area, the mean diffusivity values of different groups in the left SupraMarginal region were significantly different among one group from three comparisons realized.

Table 414: The statistical analysis results of the mean diffusivity in tractography analysis technique in groups of heavy cannabis users, light users, and non-users in the right SupraMarginal region.

	Mean diffusivity tractography analysis P-Value. -SupraMarginal region of the right hemisphere-		
	Heavy users (Group I)	Light users (Group II)	Non-users (Group III)
Heavy users (Group I)	○	**	**
Light users (Group II)	0,649	○	**
Non users (Group III)	0,793	0,345	○

With a P-value lower than 0.05, the ANOVA analysis revealed no significant differences. The table reveals that in the same anatomical area, the mean diffusivity values of different groups in the right SupraMarginal region were not significantly different.

➢ Angular

Table 415: The statistical analysis results of the mean diffusivity in tractography analysis technique in groups of heavy cannabis users, light users, and non-users in the left Angular region.

	Mean diffusivity of tractography analysis P-Value. -Angular region of the left hemisphere-		
	Heavy users (Group I)	Light users (Group II)	Non-users (Group III)
Heavy users (Group I)	○	**	**
Light users (Group II)	0,129	○	**
Non users (Group III)	0,040	0,311	○

With a P-value lower than 0.05, the ANOVA analysis revealed significant differences between heavy users and non-users groups, but no significant difference between heavy and light users' groups and between light users and non-users groups. The table reveals that in the same anatomical area, the mean diffusivity values of different groups in the left Angular region were significantly different among one group from three comparisons realized.

Table 416: The statistical analysis results of the mean diffusivity in tractography analysis technique in groups of heavy cannabis users, light users, and non-users in the right Angular region.

	Mean diffusivity of tractography analysis P-Value. -Angular region of the right hemisphere-		
	Heavy users (Group I)	Light users (Group II)	Non-users (Group III)
Heavy users (Group I)	○	**	**
Light users (Group II)	0,618	○	**
Non users (Group III)	0,827	0,938	○

With a P-value lower than 0.05, the ANOVA analysis revealed no significant differences. The table reveals that in the same anatomical area, the mean diffusivity values of different groups in the right Angular region were not significantly different.

➢ **Parietal Inf**

Table 417: The statistical analysis results of the mean diffusivity in tractography analysis technique in groups of heavy cannabis users, light users, and non-users in the left Parietal Inf region.

	Mean diffusivity of tractography analysis P-Value. -Parietal Inf region of the left hemisphere-		
	Heavy users (Group I)	Light users (Group II)	Non-users (Group III)
Heavy users (Group I)	○	**	**
Light users (Group II)	0,003	○	**
Non users (Group III)	0,004	0,142	○

With a P-value lower than 0.05, the ANOVA analysis revealed significant differences between heavy users and non-users groups and between heavy users and light users' groups, but no significant difference between light and non-users groups. The table reveals that in the same anatomical area, the mean diffusivity values of different groups in the left Parietal Inf region were significantly different among two from three comparisons realized.

Table 418: The statistical analysis results of the mean diffusivity in tractography analysis technique in groups of heavy cannabis users, light users, and non-users in the right Parietal Inf region.

	Mean diffusivity of tractography analysis P-Value. -Parietal Inf region of the right hemisphere-		
	Heavy users (Group I)	Light users (Group II)	Non-users (Group III)
Heavy users (Group I)	○	**	**
Light users (Group II)	0,912	○	**
Non users (Group III)	0,376	0,334	○

With a P-value lower than 0.05, the ANOVA analysis revealed no significant differences. The table reveals that in the same anatomical area, the mean diffusivity values of different groups in the right Parietal Inf region were not significantly different.

➢ **Precuneus**

Table 419: The statistical analysis results of the mean diffusivity in tractography analysis technique in groups of heavy cannabis users, light users, and non-users in the left Precuneus region.

	Mean diffusivity of tractography analysis P-Value. -Precuneus region of the left hemisphere-		
	Heavy users (Group I)	Light users (Group II)	Non-users (Group III)
Heavy users (Group I)	○	**	**
Light users (Group II)	0,636	○	**
Non users (Group III)	0,741	0,965	○

With a P-value lower than 0.05, the ANOVA analysis revealed no significant differences. The table reveals that in the same anatomical area, the mean diffusivity values of different groups in the left Precuneus region were not significantly different.

Table 420: The statistical analysis results of the mean diffusivity in tractography analysis technique in groups of heavy cannabis users, light users, and non-users in the right Precuneus region.

	Mean diffusivity of tractography analysis P-Value. -Precuneus region of the right hemisphere-		
	Heavy users (Group I)	Light users (Group II)	Non-users (Group III)
Heavy users (Group I)	○	**	**
Light users (Group II)	0,949	○	**
Non users (Group III)	0,854	0,885	○

With a P-value lower than 0.05, the ANOVA analysis revealed no significant differences. The table reveals that in the same anatomical area, the mean diffusivity values of different groups in the right Precuneus region were not significantly different.

➢ Temporal Sup

Table 421: The statistical analysis results of the mean diffusivity in tractography analysis technique in groups of heavy cannabis users, light users, and non-users in the left Temporal Sup region.

	Mean diffusivity of tractography analysis P-Value. -Temporal Sup region of the left hemisphere-		
	Heavy users (Group I)	Light users (Group II)	Non-users (Group III)
Heavy users (Group I)	○	**	**
Light users (Group II)	0,032	○	**
Non users (Group III)	0,010	0,319	○

With a P-value lower than 0.05, the ANOVA analysis revealed significant differences between heavy users and non-users groups and between heavy users and light users' groups, but no significant difference between light and non-users groups. The table reveals that in the same anatomical area, the mean diffusivity values of different groups in the left Temporal Sup region were significantly different among two from three comparisons realized.

Table 422: The statistical analysis results of the mean diffusivity in tractography analysis technique in groups of heavy cannabis users, light users, and non-users in the right Temporal Sup region.

	Mean diffusivity of tractography analysis P-Value. -Temporal Sup region of the right hemisphere-		
	Heavy users (Group I)	Light users (Group II)	Non-users (Group III)
Heavy users (Group I)	○	**	**
Light users (Group II)	0,917	○	**
Non users (Group III)	0,225	0,192	○

With a P-value lower than 0.05, the ANOVA analysis revealed no significant differences. The table reveals that in the same anatomical area, the mean diffusivity values of different groups in the right Temporal Sup region were not significantly different.

➢ Temporal Pole Sup

Table 423: The statistical analysis results of the mean diffusivity in tractography analysis technique in groups of heavy cannabis users, light users, and non-users in the left Temporal Pole Sup region.

	Mean diffusivity of tractography analysis P-Value. -Temporal Pole Sup region of the left hemisphere-		
	Heavy users (Group I)	Light users (Group II)	Non-users (Group III)
Heavy users (Group I)	○	**	**
Light users (Group II)	0,528	○	**
Non users (Group III)	0,017	0,048	○

With a P-value lower than 0.05, the ANOVA analysis revealed significant differences between heavy users and non-users groups and between light users and non-users groups, but no significant difference between heavy and light users' groups. The table reveals that in the same anatomical area, the mean diffusivity values of different groups in the left Temporal Pole Sup region were significantly different among two from three comparisons realized.

Table 424: The statistical analysis results of the mean diffusivity in tractography analysis technique in groups of heavy cannabis users, light users, and non-users in the right Temporal Pole Sup region.

	Mean diffusivity of tractography analysis P-Value. -Temporal Pole Sup region of the right hemisphere-		
	Heavy users (Group I)	Light users (Group II)	Non-users (Group III)
Heavy users (Group I)	○	**	**
Light users (Group II)	0,257	○	**
Non users (Group III)	0,540	0,797	○

With a P-value lower than 0.05, the ANOVA analysis revealed no significant differences. The table reveals that in the same anatomical area, the mean diffusivity values of different groups in the right Temporal Pole Sup region were not significantly different.

➢ Heschl

Table 425: The statistical analysis results of the mean diffusivity in tractography analysis technique in groups of heavy cannabis users, light users, and non-users in the left Heschl region.

	Mean diffusivity of tractography analysis P-Value. -Heschl region of the left hemisphere-		
	Heavy users (Group I)	Light users (Group II)	Non-users (Group III)
Heavy users (Group I)	○	**	**
Light users (Group II)	0.399	○	**
Non users (Group III)	0.022	0.067	○

With a P-value lower than 0.05, the ANOVA analysis revealed significant differences between heavy users and non-users groups, but no significant difference between heavy and light users' groups and between light users and non-users groups. The table reveals that in the same anatomical area, the mean diffusivity values of different groups in the left Heschl region were significantly different among one group from three comparisons realized.

Table 426: The statistical analysis results of the mean diffusivity in tractography analysis technique in groups of heavy cannabis users, light users, and non-users in the right Heschl region.

	Mean diffusivity of tractography analysis P-Value. -Heschl region of the right hemisphere-		
	Heavy users (Group I)	Light users (Group II)	Non-users (Group III)
Heavy users (Group I)	○	**	**
Light users (Group II)	0.708	○	**
Non users (Group III)	0.391	0.483	○

With a P-value lower than 0.05, the ANOVA analysis revealed no significant differences. The table reveals that in the same anatomical area, the mean diffusivity values of different groups in the right Heschl region were not significantly different.

➢ **Temporal Mid**

Table 427: The statistical analysis results of the mean diffusivity in tractography analysis technique in groups of heavy cannabis users, light users, and non-users in the left Temporal Mid region.

	Mean diffusivity of tractography analysis P-Value. -Temporal Mid region of the left hemisphere-		
	Heavy users (Group I)	Light users (Group II)	Non-users (Group III)
Heavy users (Group I)	○	**	**
Light users (Group II)	0.013	○	**
Non users (Group III)	0.003	0.230	○

With a P-value lower than 0.05, the ANOVA analysis revealed significant differences between heavy users and non-users groups and between heavy users and light users' groups, but no significant difference between light and non-users groups. The table reveals that in the same anatomical area, the mean diffusivity values of different groups in the left Temporal Mid region were significantly different among two from three comparisons realized.

Table 428: The statistical analysis results of the mean diffusivity in tractography analysis technique in groups of heavy cannabis users, light users, and non-users in the right Temporal Mid region.

	Mean Apparent Diffusion diffusivity. -Temporal Mid region of the right hemisphere-		
	Heavy users (Group I)	Light users (Group II)	Non-users (Group III)
Heavy users (Group I)	○	**	**
Light users (Group II)	0.888	○	**
Non users (Group III)	0.618	0.396	○

With a P-value lower than 0.05, the ANOVA analysis revealed no significant differences. The table reveals that in the same anatomical area, the mean diffusivity values of different groups in the right Temporal Mid region were not significantly different.

➢ **Temporal Pole Mid**

Table 429: The statistical analysis results of the mean diffusivity in tractography analysis technique in groups of heavy cannabis users, light users, and non-users in the left Temporal Pole Mid region.

	Mean diffusivity of tractography analysis P-Value. -Temporal Pole Mid region of the left hemisphere-		
	Heavy users (Group I)	Light users (Group II)	Non-users (Group III)
Heavy users (Group I)	○	**	**
Light users (Group II)	0.766	○	**
Non users (Group III)	0.0005	0.037	○

With a P-value lower than 0.05, the ANOVA analysis revealed significant differences between heavy users and non-users groups and between light users and non-users groups, but no significant difference between heavy and light users' groups. The table reveals that in the same anatomical area, the mean diffusivity values of different groups in the left Temporal Pole Mid region were significantly different among two from three comparisons realized.

Table 430: The statistical analysis results of the mean diffusivity in tractography analysis technique in groups of heavy cannabis users, light users, and non-users in the right Temporal Pole Mid region.

	Mean diffusivity of tractography analysis P-Value. -Temporal Pole Mid region of the right hemisphere-		
	Heavy users (Group I)	Light users (Group II)	Non-users (Group III)
Heavy users (Group I)	○	**	**
Light users (Group II)	0.752	○	**
Non users (Group III)	0.942	0.878	○

With a P-value lower than 0.05, the ANOVA analysis revealed no significant differences. The table reveals that in the same anatomical area, the mean diffusivity values of different groups in the right Temporal Pole Mid region were not significantly different.

➢ Temporal Inf

Table 431: The statistical analysis results of the mean diffusivity in tractography analysis technique in groups of heavy cannabis users, light users, and non-users in the left Temporal Inf region.

	Mean diffusivity of tractography analysis P-Value. -Temporal Inf region of the left hemisphere-		
	Heavy users (Group I)	Light users (Group II)	Non-users (Group III)
Heavy users (Group I)	○	**	**
Light users (Group II)	0.029	○	**
Non users (Group III)	0.003	0.081	○

With a P-value lower than 0.05, the ANOVA analysis revealed significant differences between heavy users and non-users groups and between heavy users and light users' groups, but no significant difference between light and non-users groups. The table reveals that in the same anatomical area, the mean diffusivity values of different groups in the left Temporal Inf region were significantly different among two from three comparisons realized.

Table 432: The statistical analysis results of the mean diffusivity in tractography analysis technique in groups of heavy cannabis users, light users, and non-users in the right Temporal Inf region.

	Mean diffusivity of tractography analysis P-Value. -Temporal Inf region of the right hemisphere-		
	Heavy users (Group I)	Light users (Group II)	Non-users (Group III)
Heavy users (Group I)	○	**	**
Light users (Group II)	0.404	○	**
Non users (Group III)	0.513	0.923	○

With a P-value lower than 0.05, the ANOVA analysis revealed no significant differences. The table reveals that in the same anatomical area, the mean diffusivity values of different groups in the right Temporal Inf region were not significantly different.

➢ Fusiform

Table 433: The statistical analysis results of the mean diffusivity in tractography analysis technique in groups of heavy cannabis users, light users, and non-users in the left Fusiform region.

	Mean diffusivity of tractography analysis P-Value. -Fusiform region of the left hemisphere-		
	Heavy users (Group I)	Light users (Group II)	Non-users (Group III)
Heavy users (Group I)	○	**	**
Light users (Group II)	0.096	○	**
Non users (Group III)	0.411	0.777	○

With a P-value lower than 0.05, the ANOVA analysis revealed no significant differences. The table reveals that in the same anatomical area, the mean diffusivity values of different groups in the left Fusiform region were not significantly different.

Table 434: The statistical analysis results of the mean diffusivity in tractography analysis technique in groups of heavy cannabis users, light users, and non-users in the right Fusiform region.

	Mean diffusivity tractography analysis P-Value. -Fusiform region of the right hemisphere-		
	Heavy users (Group I)	Light users (Group II)	Non-users (Group III)
Heavy users (Group I)	○	**	**
Light users (Group II)	0.492	○	**
Non users (Group III)	0.655	0.947	○

With a P-value lower than 0.05, the ANOVA analysis revealed no significant differences. The table reveals that in the same anatomical area, the mean diffusivity values of different groups in the right Fusiform region were not significantly different.

➢ Cingulum Ant

Table 435: The statistical analysis results of the mean diffusivity in tractography analysis technique in groups of heavy cannabis users, light users, and non-users in the left Cingulum Ant region.

	Mean diffusivity of tractography analysis P-Value. -Cingulum Ant region of the left hemisphere-		
	Heavy users (Group I)	Light users (Group II)	Non-users (Group III)
Heavy users (Group I)	○	**	**
Light users (Group II)	0.497	○	**
Non users (Group III)	0.242	0.184	○

With a P-value lower than 0.05, the ANOVA analysis revealed no significant differences. The table reveals that in the same anatomical area, the mean diffusivity values of different groups in the left Cingulum Ant region were not significantly different.

Table 436: The statistical analysis results of the mean diffusivity in tractography analysis technique in groups of heavy cannabis users, light users, and non-users in the right Cingulum Ant region.

	Mean diffusivity of tractography analysis P-Value. -Cingulum Ant region of the right hemisphere-		
	Heavy users (Group I)	Light users (Group II)	Non-users (Group III)
Heavy users (Group I)	○	**	**
Light users (Group II)	0.126	○	**
Non users (Group III)	0.566	0.312	○

With a P-value lower than 0.05, the ANOVA analysis revealed no significant differences. The table reveals that in the same anatomical area, the mean diffusivity values of different groups in the right Cingulum Ant region were not significantly different.

➢ Cingulum Mid

Table 437: The statistical analysis results of the mean diffusivity in tractography analysis technique in groups of heavy cannabis users, light users, and non-users in the left Cingulum Mid region.

	Mean diffusivity of tractography analysis P-Value. -Cingulum Mid region of the left hemisphere-		
	Heavy users (Group I)	Light users (Group II)	Non-users (Group III)
Heavy users (Group I)	○	**	**
Light users (Group II)	0.341	○	**
Non users (Group III)	0.485	0.229	○

With a P-value lower than 0.05, the ANOVA analysis revealed no significant differences. The table reveals that in the same anatomical area, the mean diffusivity values of different groups in the left Cingulum Mid region were not significantly different.

Table 438: The statistical analysis results of the mean diffusivity in tractography analysis technique in groups of heavy cannabis users, light users, and non-users in the right Cingulum Mid region.

	Mean diffusivity of tractography analysis P-Value. -Cingulum Mid region of the right hemisphere-		
	Heavy users (Group I)	Light users (Group II)	Non-users (Group III)
Heavy users (Group I)	○	**	**
Light users (Group II)	0.178	○	**
Non users (Group III)	0.449	0.125	○

With a P-value lower than 0.05, the ANOVA analysis revealed no significant differences. The table reveals that in the same anatomical area, the mean diffusivity values of different groups in the right Cingulum Mid region were not significantly different.

➢ Cingulum Post

Table 439: The statistical analysis results of the mean diffusivity in tractography analysis technique in groups of heavy cannabis users, light users, and non-users in the left Cingulum Post region.

	Mean diffusivity of tractography analysis P-Value. -Cingulum Post region of the left hemisphere-		
	Heavy users (Group I)	Light users (Group II)	Non-users (Group III)
Heavy users (Group I)	○	**	**
Light users (Group II)	0.807	○	**
Non users (Group III)	0.871	0.744	○

With a P-value lower than 0.05, the ANOVA analysis revealed no significant differences. The table reveals that in the same anatomical area, the mean diffusivity values of different groups in the left Cingulum Post region were not significantly different.

Table 440: The statistical analysis results of the mean diffusivity in tractography analysis technique in groups of heavy cannabis users, light users, and non-users in the right Cingulum Post region.

	Mean diffusivity of tractography analysis P-Value. -Cingulum Post region of the right hemisphere-		
	Heavy users (Group I)	Light users (Group II)	Non-users (Group III)
Heavy users (Group I)	○	**	**
Light users (Group II)	0.386	○	**
Non users (Group III)	0.623	0.864	○

With a P-value lower than 0.05, the ANOVA analysis revealed no significant differences. The table reveals that in the same anatomical area, the mean diffusivity values of different groups in the right Cingulum Post region were not significantly different.

- ParaHippocampal

Table 441: The statistical analysis results of the mean diffusivity in tractography analysis technique in groups of heavy cannabis users, light users, and non-users in the left ParaHippocampal region.

	Mean diffusivity of tractography analysis P-Value. -ParaHippocampal region of the left hemisphere-		
	Heavy users (Group I)	Light users (Group II)	Non-users (Group III)
Heavy users (Group I)	○	**	**
Light users (Group II)	0.779	○	**
Non users (Group III)	0.540	0.547	○

With a P-value lower than 0.05, the ANOVA analysis revealed no significant differences. The table reveals that in the same anatomical area, the mean diffusivity values of different groups in the left ParaHippocampal region were not significantly different.

Table 442: The statistical analysis results of the mean diffusivity in tractography analysis technique in groups of heavy cannabis users, light users, and non-users in the right ParaHippocampal region.

	Mean diffusivity of tractography analysis P-Value. -ParaHippocampal region of the right hemisphere-		
	Heavy users (Group I)	Light users (Group II)	Non-users (Group III)
Heavy users (Group I)	○	**	**
Light users (Group II)	0.671	○	**
Non users (Group III)	0.871	0.751	○

With a P-value lower than 0.05, the ANOVA analysis revealed no significant differences. The table reveals that in the same anatomical area, the mean diffusivity values of different groups in the right ParaHippocampal region were not significantly different.

➢ Hippocampus

Table 443: The statistical analysis results of the mean diffusivity in tractography analysis technique in groups of heavy cannabis users, light users, and non-users in the left Hippocampus region.

	Mean diffusivity of tractography analysis P-Value Hippocampus region of the left hemisphere		
	Heavy users (Group I)	Light users (Group II)	Non-users (Group III)
Heavy users (Group I)	○	**	**
Light users (Group II)	0.369	○	**
Non users (Group III)	0.427	0.939	○

With a P-value lower than 0.05, the ANOVA analysis revealed no significant differences. The table reveals that in the same anatomical area, the mean diffusivity values of different groups in the left Hippocampus region were not significantly different.

Table 444: The statistical analysis results of the mean diffusivity in tractography analysis technique in groups of heavy cannabis users, light users, and non-users in the right Hippocampus region.

	Mean diffusivity of tractography analysis P-Value Hippocampus region of the right hemisphere		
	Heavy users (Group I)	Light users (Group II)	Non-users (Group III)
Heavy users (Group I)	○	**	**
Light users (Group II)	0.825	○	**
Non users (Group III)	0.910	0.827	○

With a P-value lower than 0.05, the ANOVA analysis revealed no significant differences. The table reveals that in the same anatomical area, the mean diffusivity values of different groups in the right Hippocampus region were not significantly different.

➢ Insula

Table 445: The statistical analysis results of the mean diffusivity in tractography analysis technique in groups of heavy cannabis users, light users, and non-users in the left Insula region.

	Mean diffusivity of tractography analysis P-Value. -Insula region of the left hemisphere-		
	Heavy users (Group I)	Light users (Group II)	Non-users (Group III)
Heavy users (Group I)	○	**	**
Light users (Group II)	0,535	○	**
Non users (Group III)	0,003	0,012	○

With a P-value lower than 0.05, the ANOVA analysis revealed significant differences between heavy users and non-users groups and between light users and non-users groups, but no significant difference between heavy and light users' groups. The table reveals that in the same anatomical area, the mean diffusivity values of different groups in the left Insula region were significantly different among two from three comparisons realized.

Table 446: The statistical analysis results of the mean diffusivity in tractography analysis technique in groups of heavy cannabis users, light users, and non-users in the right Insula region.

	Mean diffusivity of tractography analysis P-Value. -Insula region of the right hemisphere-		
	Heavy users (Group I)	Light users (Group II)	Non-users (Group III)
Heavy users (Group I)	○	**	**
Light users (Group II)	0.559	○	**
Non users (Group III)	0.864	0.564	○

With a P-value lower than 0.05, the ANOVA analysis revealed no significant differences. The table reveals that in the same anatomical area, the mean diffusivity values of different groups in the right Insula region were not significantly different.

- **Amygdala**

Table 447: The statistical analysis results of the mean diffusivity in tractography analysis technique in groups of heavy cannabis users, light users, and non-users in the left Amygdala region.

	Mean diffusivity of tractography analysis P-Value. -Amygdala region of the left hemisphere-		
	Heavy users (Group I)	Light users (Group II)	Non-users (Group III)
Heavy users (Group I)	○	**	**
Light users (Group II)	0.883	○	**
Non users (Group III)	0.370	0.324	○

With a P-value lower than 0.05, the ANOVA analysis revealed no significant differences. The table reveals that in the same anatomical area, the mean diffusivity values of different groups in the left Amygdala region were not significantly different.

Table 448: The statistical analysis results of the mean diffusivity in tractography analysis technique in groups of heavy cannabis users, light users, and non-users in the right Amygdala region.

	Mean diffusivity of tractography analysis P-Value. -Amygdala region of the right hemisphere-		
	Heavy users (Group I)	Light users (Group II)	Non-users (Group III)
Heavy users (Group I)	○	**	**
Light users (Group II)	0.245	○	**
Non users (Group III)	0.259	0.892	○

With a P-value lower than 0.05, the ANOVA analysis revealed no significant differences. The table reveals that in the same anatomical area, the mean diffusivity values of different groups in the right Amygdala region were not significantly different.

- **Thalamus**

Table 449: The statistical analysis results of the mean diffusivity in tractography analysis technique in groups of heavy cannabis users, light users, and non-users in the left Thalamus region.

	Mean diffusivity of tractography analysis P-Value. -Thalamus region of the left hemisphere-		
	Heavy users (Group I)	Light users (Group II)	Non-users (Group III)
Heavy users (Group I)	○	**	**
Light users (Group II)	0.188	○	**
Non users (Group III)	0.308	0.953	○

With a P-value lower than 0.05, the ANOVA analysis revealed no significant differences. The table reveals that in the same anatomical area, the mean diffusivity values of different groups in the left Thalamus region were not significantly different.

Table 450: The statistical analysis results of the mean diffusivity in tractography analysis technique in groups of heavy cannabis users, light users, and non-users in the right Thalamus region.

	Mean diffusivity of tractography analysis P-Value. -Thalamus region of the right hemisphere-		
	Heavy users (Group I)	Light users (Group II)	Non-users (Group III)
Heavy users (Group I)	○	**	**
Light users (Group II)	0.610	○	**
Non users (Group III)	0.300	0.265	○

With a P-value lower than 0.05, the ANOVA analysis revealed no significant differences. The table reveals that in the same anatomical area, the mean diffusivity values of different groups in **the right Thalamus region** were not significantly different.

- Caudate

Table 451: The statistical analysis results of the mean diffusivity in tractography analysis technique in groups of heavy cannabis users, light users, and non-users in the left Caudate region.

	Mean diffusivity of tractography analysis P-Value. -Caudate region of the left hemisphere-		
	Heavy users (Group I)	Light users (Group II)	Non-users (Group III)
Heavy users (Group I)	○	**	**
Light users (Group II)	0.483	○	**
Non users (Group III)	0.609	0.890	○

With a P-value lower than 0.05, the ANOVA analysis revealed no significant differences. The table reveals that in the same anatomical area, the mean diffusivity values of different groups in the left Caudate region were not significantly different.

Table 452: The statistical analysis results of the mean diffusivity in tractography analysis technique in groups of heavy cannabis users, light users, and non-users in the right Caudate region.

	Mean diffusivity of tractography analysis P-Value. -Caudate region of the right hemisphere-		
	Heavy users (Group I)	Light users (Group II)	Non-users (Group III)
Heavy users (Group I)	○	**	**
Light users (Group II)	0.593	○	**
Non users (Group III)	0.884	0.825	○

With a P-value lower than 0.05, the ANOVA analysis revealed no significant differences. The table reveals that in the same anatomical area, the mean diffusivity values of different groups in the right Caudate region were not significantly different.

➢ **Putamen**

Table 453: The statistical analysis results of the mean diffusivity in tractography analysis technique in groups of heavy cannabis users, light users, and non-users in the left Putamen region.

	Mean diffusivity of tractography analysis P-Value. -Putamen region of the left hemisphere-		
	Heavy users (Group I)	Light users (Group II)	Non-users (Group III)
Heavy users (Group I)	○	**	**
Light users (Group II)	0.520	○	**
Non users (Group III)	0.047	0.026	○

With a P-value lower than 0.05, the ANOVA analysis revealed significant differences between heavy users and non-users groups and between light users and non-users groups, but no significant difference between heavy and light users' groups. The table reveals that in the same anatomical area, the mean diffusivity values of different groups in the left Putamen region were significantly different among two from three comparisons realized.

Table 454: The statistical analysis results of the mean diffusivity in tractography analysis technique in groups of heavy cannabis users, light users, and non-users in the right Putamen region.

	Mean diffusivity of tractography analysis P-Value. -Putamen region of the right hemisphere-		
	Heavy users (Group I)	Light users (Group II)	Non-users (Group III)
Heavy users (Group I)	○	**	**
Light users (Group II)	0.444	○	**
Non users (Group III)	0.513	0.702	○

With a P-value lower than 0.05, the ANOVA analysis revealed no significant differences. The table reveals that in the same anatomical area, the mean diffusivity values of different groups in the right Putamen region were not significantly different.

➢ **Pallidum**

Table 455: The results of statistical analysis of the mean diffusivity in the region of interest technique of analysis in groups of heavy cannabis users, light users, and non-users, in the left Pallidum region.

	Mean diffusivity of tractography analysis P-Value. -Pallidum region of the left hemisphere-		
	Heavy users (Group I)	Light users (Group II)	Non-users (Group III)
Heavy users (Group I)	○	**	**
Light users (Group II)	0.546	○	**
Non users (Group III)	0.104	0.009	○

With a P-value lower than 0.05, the ANOVA analysis revealed significant differences between light users and non-users groups, but no significant difference between heavy and light users' groups and between heavy users and non-users groups. The table reveals that in the same anatomical area, the mean diffusivity values of different groups in the left Pallidum region were significantly different among one group from three comparisons realized.

Table 456: The results of statistical analysis of the mean diffusivity te mean diffusivity in the region of interest technique of analysis in groups of heavy cannabis users, light users, and non-users, in the right Pallidum region.

	Mean diffusivity of tractography analysis P-Value. -Pallidum region of the right hemisphere-		
	Heavy users (Group I)	Light users (Group II)	Non-users (Group III)
Heavy users (Group I)	○	**	**
Light users (Group II)	0.288	○	**
Non users (Group III)	0.326	0.498	○

With a P-value lower than 0.05, the ANOVA analysis revealed no significant differences. The table reveals that in the same anatomical area, the mean diffusivity values of different groups in the right Pallidum region were not significantly different.

Chapter V: Correlations results between clinical, psychological features outcomes and tractography findings

In this part, we expose the results of statistical correlations between the clinical (Psychometric tests: CUDIT-R, BIS-11, and PSS) and tractography findings (diffusion markers: FA and MD) in 17 regions.

The Pearson correlation was used to determine the association between these two functional and structural indicators.

The FA and MD values of the tracts in each selected region were associated with the individual test values for each participant in the three groups.

Our results will be displayed in two sections. The first section for the overall results (with and without statistical significance) using a table containing the correlation coefficient for each calculated correlation, the r squared and the two-tailed p-value, and the interpretation of the significance

In the second section, using graphs, we present the statistically significant correlations (p-value <0.05).

I. The overall results of the correlations

With the three psychometric tests and over the white matter of 17 regions studied and through the two diffusion markers (FA and MD), we realized 204 correlations calculations.

Our findings reveal that FA correlates negatively with the CUD, impulsivity, and perceived stress (91,17% over the 104 correlations of the FA with the three tested). The mean diffusivity correlates positively with the three tests in 75,5% of the conducted calculations. Statistically significant correlations (p-value$<$0.05), represent 20% of the total 204 realized calculations. All are negative correlations with the total scores of CUDIT-R, BIS-11, and PSS for fractional anisotropy and positive correlations for mean diffusivity.

Table 457: Results of white matter's FA and MD correlations in several regions with CUDIT-R, BIS-11 and PSS scores.

		CUDIT-R		BIS		PSS	
		Left	Right	Left	Right	Left	Right
Frontal Med Orb	FA	Pearson r: r: -0.4657 R squared: 0.2169 P value: 0.0445 Significant: Yes	Pearson r: r: -0.2225 R squared: 0.0495 P value: 0.3599 Significant: NO	Pearson r: r: -0.4800 R squared: 0.2304 P value: 0.0375 Significant: YES	Pearson r: r: -0.2185 R squared: 0.04775 P value: 0.3688 Significant: NO	Pearson r: r: -0,4904 R squared: 0,2405 P value: 0,0330 Significant: YES	Pearson r: r: -0,4294 R squared: 0,1844 P value: 0,0665 Significant: NO
	MD	Pearson r: r: 0.3768 R squared: 0.1420 P value: 0.1118 Significant: NO	Pearson r: r: 0.1919 R squared: 0.03684 P value: 0.4312 Significant: NO	Pearson r: r: 0.2455 R squared: 0.06028 P value: 0.3110 Significant: NO	Pearson r: r: 0.07438 R squared: 0.005533 P value: 0.7622 Significant: NO	Pearson r: r: 0,4037 R squared: 0,1630 P value: 0,0865 Significant: NO	Pearson r: r:0,3303 R squared: 0,1091 P value: 0,1673 Significant: NO
Frontal Sup Orb	FA	Pearson r: r: -0.3615 R squared: 0.1306 P value: 0.1284 Significant: NO	Pearson r: r: -0.1149 R squared: 0.01320 P value: 0.6396 Significant: NO	Pearson r: r: -0.4080 R squared: 0.1664 P value: 0.0829 Significant: NO	Pearson r: r: -0.07939 R squared: 0.006302 P value: 0.7466 Significant: NO	Pearson r: r: -0,5118 R squared: 0,2620 P value: 0,0251 Significant: YES	Pearson r: r: -0,4163 R squared: 0,1733 P value: 0,0762 Significant: NO

	MD	Pearson r: r: 0.4108 R squared: 0.1688 P value: 0.0806 Significant: NO	Pearson r: r:0.2984 R squared: 0.08904 P value: 0.2146 Significant: NO	Pearson r: r: 0.3762 R squared: 0.1415 P value: 0.1124 Significant: YES	Pearson r: r: 0.4329 R squared: 0.1874 P value: 0.0641 Significant: YES	Pearson r: r: 0,3640 R squared: 0,2558 P value: 0,1255 Significant: YES	Pearson r: r: 0,4302 R squared: 0,1851 P value: 0,0660 Significant: NO
Frontal Mid Orb	FA	Pearson r: r: -0.2926 R squared: 0.08564 P value: 0.2240 Significant: NO	Pearson r: r: -0.005130 R squared: 2.632e-005 P value: 0.9839 Significant: NO	Pearson r: r: -0.1873 R squared: 0.03510 P value: 0.4425 Significant: NO	Pearson r: r: -0.07679 R squared: 0.005897 P value: 0.7620 Significant: NO	Pearson r: r: -0,5655 R squared: 0,3197 P value: 0,0116 Significant: YES	Pearson r: r: -0,2031 R squared: 0,04123 P value: 0,4190 Significant: NO
	MD	Pearson r: r: 0.2393 R squared: 0.05726 P value: 0.3238 Significant: NO	Pearson r: r:-0.3228 R squared: 0.1042 P value: 0.1914 Significant: NO	Pearson r: r: 0.2840 R squared: 0.08065 P value: 0.2387 Significant: NO	Pearson r: r: -0.2900 R squared: 0.084409 P value: 0.2431 Significant: NO	Pearson r: r: 0,4330 R squared: 0,1875 P value: 0,0640 Significant: NO	Pearson r: r: -0,1997 R squared: 0,03986 P value: 0,4270 Significant: NO

Frontal Inf Orb	FA	Pearson r: r: -0.1230 R squared: 0.01514 P value: 0.6158 Significant: NO	Pearson r: r:-0.2982 R squared: 0.08895 P value: 0.2149 Significant: NO	Pearson r: r: 0.02865 R squared: 0.0008210 P value: 0.9073 Significant: NO	Pearson r: r: -0.3167 R squared: 0.1003 P value: 0.1865 Significant: NO	Pearson r: r: -0,4586 R squared: 0,2104 P value: 0,0483 Significant: YES	Pearson r: r: -0,3731 R squared: 0,1392 P value: 0,1156 Significant: NO
	MD	Pearson r: r: 0.2745 R squared: 0.07535 P value: 0.2554 Significant: NO	Pearson r: r: -0.1961 R squared: 0.03846 P value: 0.4210 Significant: NO	Pearson r: r: 0.2650 R squared: 0.07021 P value: 0.2730 Significant: NO	Pearson r: r: -0.3247 R squared: 0.1055 P value: 0.1749 Significant: NO	Pearson r: r: 0,3805 R squared: 0,1448 P value: 0,1081 Significant: NO	Pearson r: r: -0,05550 R squared: 0,003080 P value: 0,8215 Significant: NO
Frontal Sup Medial	FA	Pearson r: r: -0.3401 R squared: 0.1157 P value: 0.1542 Significant: NO	Pearson r: r: -0.4497 R squared: 0.2023 P value: 0.0534 Significant: NO	Pearson r: r: -0.3032 R squared: 0.09194 P value: 0.2070 Significant: NO	Pearson r: r: -0.5269 R squared: 0.2776 P value: 0.0205 Significant: YES	Pearson r: r: -0,4811 R squared: 0,2314 P value: 0,0370 Significant: YES	Pearson r: r: -0,4806 R squared: 0,2309 P value: 0,0373 Significant: YES

	MD	Pearson r: r: 0.3177 R squared: 0.1009 P value: 0.1850 Significant: NO	Pearson r: r: 0.2643 R squared: 0.06984 P value: 0.2743 Significant: NO	Pearson r: r: 0.3326 R squared: 0.1106 P value: 0.1642 Significant: NO	Pearson r: r:0.3035 R squared: 0.09208 P value: 0.2066 Significant: NO	Pearson r: r:0,3449 R squared: 0,1190 P value: 0,1481 Significant: NO	Pearson r: r:0,3276 R squared: 0,1073 P value: 0,1709 Significant: NO
Frontal Sup	FA	Pearson r: r: -0.5931 R squared: 0.3518 P value: 0.0074 Significant: YES	Pearson r: r: -0.5405 R squared: 0.2921 P value: 0.0169 Significant: YES	Pearson r: r: -0.6023 R squared: 0.3627 P value: 0.0064 Significant: YES	Pearson r: r: -0.5769 R squared: 0.3328 P value: 0.0097 Significant: YES	Pearson r: r: -0,6048 R squared: 0,3658 P value: 0,0061 Significant: YES	Pearson r: r: -0,5457 R squared: 0,2978 P value: 0,0157 Significant: YES
	MD	Pearson r: r: 0.1886 R squared: 0.03557 P value: 0.4394 Significant: NO	Pearson r: r: 0.1145 R squared: 0.01310 P value: 0.6408 Significant: NO	Pearson r: r: 0.1647 R squared: 0.02713 P value: 0.5004 Significant: NO	Pearson r: r:0.1305 R squared: 0.01702 P value: 0.5945 Significant: NO	Pearson r: r: 0,2567 R squared: 0,06588 P value: 0,2888 Significant: NO	Pearson r: r: 0,2184 R squared: 0,04771 P value: 0,3690 Significant: NO

Frontal Mid	FA	Pearson r: r: -0.5613 R squared: 0.3151 P value: 0.0124 Significant: YES	Pearson r: r: -0.4911 R squared: 0.2411 P value: 0.0328 Significant: YES	Pearson r: r: -0.5777 R squared: 0.3337 P value: 0.0096 Significant: YES	Pearson r: r: -0.5236 R squared: 0.2742 P value: 0.0214 Significant: YES	Pearson r: r: -0,6187 R squared: 0,3828 P value: 0,0047 Significant: YES	Pearson r: r: -0,4790 R squared: 0,2294 P value: 0,0380 Significant: YES
	MD	Pearson r: r: 0.4539 R squared: 0.2060 P value: 0.0509 Significant: NO	Pearson r: r: -0.05239 R squared: 0.002745 P value: 0.8313 Significant: NO	Pearson r: r:0.4790 R squared: 0.2295 P value: 0.0380 Significant: YES	Pearson r: r: -0.1830 R squared: 0.03350 P value: 0.4533 Significant: NO	Pearson r: r: 0,4116 R squared: 0,1694 P value: 0,0800 Significant: NO	Pearson r: r: 0,01321 R squared: 0,0001746 P value: 0,9572 Significant: NO
Cingulum Ant	FA	Pearson r: r:-0.4075 R squared: 0.1660 P value: 0.0833 Significant: NO	Pearson r: r: -0.5333 R squared: 0.2844 P value: 0.0187 Significant: YES	Pearson r: r: -0.2467 R squared: 0.06088 P value: 0.3085 Significant: NO	Pearson r: r:-0.5547 R squared: 0.3077 P value: 0.0137 Significant: YES	Pearson r: r: -0,4779 R squared: 0,2284 P value: 0,0385 Significant: YES	Pearson r: r: -0,5369 R squared: 0,2882 P value: 0,0178 Significant: YES

	MD	Pearson r: r:0.2633 R squared: 0.06932 P value: 0.2761 Significant: NO	Pearson r: r: 0.07057 R squared: 0.004980 P value: 0.7740 Significant: NO	Pearson r: r: 0.3098 R squared: 0.09600 P value: 0.1967 Significant: NO	Pearson r: r: 0.08484 R squared: 0.007198 P value: 0.7298 Significant: NO	Pearson r: r: 0,2805 R squared: 0,07869 P value: 0,2447 Significant: NO	Pearson r: r: 0,09653 R squared: 0,009317 P value: 0,6942 Significant: NO
Cingulum Mid	FA	Pearson r: r: -0.5265 R squared: 0.2772 P value: 0.0206 Significant: YES	Pearson r: r: -0.1434 R squared: 0.02055 P value: 0.5582 Significant: NO	Pearson r: r: -0.5953 R squared: 0.3543 P value: 0.0072 Significant: YES	Pearson r: r: 0.03236 R squared: 0.001047 P value: 0.8954 Significant: NO	Pearson r: r: -0,3605 R squared: 0,1299 P value: 0,1295 Significant: NO	Pearson r: r: -0,01309 R squared: 0,0001713 P value: 0,9576 Significant: NO
	MD	Pearson r: r: 0.07605 R squared: 0.005783 P value: 0.7570 Significant: NO	Pearson r: r: 0.08168 R squared: 0.006672 P value: 0.7396 Significant: NO	Pearson r: r: -0.1586 R squared: 0.02515 P value: 0.5167 Significant: NO	Pearson r: r:-0.1273 R squared: 0.01620 P value: 0.6036 Significant: NO	Pearson r: r: 0,02974 R squared: 0,0008843 P value: 0,9038 Significant: NO	Pearson r: r:0,03884 R squared: 0,001508 P value: 0,8746 Significant: NO

Cingulum Post	FA	Pearson r: r: -0.1791 R squared: 0.03209 P value: 0.4631 Significant: NO	Pearson r: r: -0.3491 R squared: 0.1219 P value: 0.1429 Significant: NO	Pearson r: r: 0.06394 R squared: 0.004088 P value: 0.7948 Significant: NO	Pearson r: r: 0.09823 R squared: 0.009648 P value: 0.6891 Significant: NO	Pearson r: r: -0,04713 R squared: 0,002222 P value: 0,8480 Significant: NO	Pearson r: r: -0,1472 R squared: 0,02166 P value: 0,5477 Significant: NO
	MD	Pearson r: r: -0.02758 R squared: 0.0007606 P value: 0.9108 Significant: NO	Pearson r: r: 0.1760 R squared: 0.3097 P value: 0.4711 Significant: NO	Pearson r: r: -0.09336 R squared: 0.008716 P value: 0.7038 Significant: NO	Pearson r: r: 0.2501 R squared: 0.06256 P value: 0.3017 Significant: NO	Pearson r: r: 0,02308 R squared: 0,0005329 P value: 0,9253 Significant: NO	Pearson r: r: 0,1351 R squared: 0,01824 P value: 0,5814 Significant: NO
ParaHippocampal	FA	Pearson r: r: -0.2111 R squared: 0.04458 P value: 0.4003 Significant: NO	Pearson r: r: -0.1257 R squared: 0.01579 P value: 0.6083 Significant: NO	Pearson r: r: 0.1333 R squared: 0.01777 P value: 0.5980 Significant: NO	Pearson r: r:-0.01220 R squared: 0.0001487 P value: 0.9605 Significant: NO	Pearson r: r: -0,1187 R squared: 0,01409 P value: 0,6390 Significant: NO	Pearson r: r: -0,04078 R squared: 0,001663 P value: 0,8684 Significant: NO

	MD	Pearson r: r: 0.1240 R squared: 0.01537 P value: 0.6241 Significant: NO	Pearson r: r: -0.01334 R squared: 0.0001779 P value: 0.9568 Significant: NO	Pearson r: r: -0.1179 R squared: 0.01391 P value: 0.6412 Significant: NO	Pearson r: r: -0.1266 R squared: 0.01603 P value: 0.6055 Significant: NO	Pearson r: r: -0,2071 R squared: 0,04288 P value: 0,4097 Significant: NO	Pearson r: r: 0,09192 R squared: 0,008449 P value: 0,7082 Significant: NO
Hippocampus	FA	Pearson r: r: -0.1266 R squared: 0.01603 P value: 0.6056 Significant: NO	Pearson r: r: -0.2481 R squared: 0.06155 P value: 0.3058 Significant: NO	Pearson r: r: -0.01762 R squared: 0.0003106 P value: 0.9429 Significant: NO	Pearson r: r: -0.3737 R squared: 0.1396 P value: 0.1150 Significant: NO	Pearson r: r: -0,05228 R squared: 0,002733 P value: 0,8317 Significant: NO	Pearson r: r: -0,1352 R squared: 0,01828 P value: 0,5811 Significant: NO
	MD	Pearson r: r: 0.1204 R squared: 0.01450 P value: 0.6234 Significant: NO	Pearson r: r: -0.2448 R squared: 0.05993 P value: 0.3124 Significant: NO	Pearson r: r: 0.1650 R squared: 0.02722 P value: 0.4997 Significant: NO	Pearson r: r: -0.1049 R squared: 0.01101 P value: 0.6691 Significant: NO	Pearson r: r: 0,1481 R squared: 0,02195 P value: 0,5450 Significant: NO	Pearson r: r: -0,04035 R squared: 0,001628 P value: 0,8697 Significant: NO

Insula	FA	Pearson r: r: 0.05478 R squared: 0.003001 P value: 0.8237 Significant: NO	Pearson r: r: -0.2481 R squared: 0.06155 P value: 0.3058 Significant: NO	Pearson r: r: 0.1162 R squared: 0.01350 P value: 0.6357 Significant: NO	Pearson r: r: -0.1169 R squared: 0.01367 P value: 0.6336 Significant: NO	Pearson r: r: -0,07315 R squared: 0,005351 P value: 0,7660 Significant: NO	Pearson r: r: -0,3330 R squared: 0,1109 P value: 0,1636 Significant: NO
	MD	Pearson r: r: 0.6214 R squared: 0.3862 P value: 0.0045 Significant: YES	Pearson r: r: 0.1771 R squared: 0.03136 P value: 0.4683 Significant: NO	Pearson r: r: 0.5339 R squared: 0.2850 P value: 0.0185 Significant: YES	Pearson r: r: 0.2381 R squared: 0.05669 P value: 0.3263 Significant: NO	Pearson r: r: 0,6377 R squared: 0,4066 P value: 0,0033 Significant: YES	Pearson r: r:0,2003 R squared: 0,04011 P value: 0,4110 Significant: NO
Amygdala	FA	Pearson r: r: -0.5222 R squared: 0.2727 P value: 0.0218 Significant: YES	Pearson r: r: -0.04411 R squared: 0.001946 P value: 0.8577 Significant: NO	Pearson r: r: -0.2924 R squared: 0.08549 P value: 0.2245 Significant: NO	Pearson r: r: -0.1066 R squared: 0.01137 P value: 0.6640 Significant: NO	Pearson r: r: -0,4541 R squared: 0,2062 P value: 0,0508 Significant: NO	Pearson r: r: -0,1295 R squared: 0,01677 P value: 0,5973 Significant: NO

	MD	Pearson r: r: 0.2625 R squared: 0.06893 P value: 0.2775 Significant: NO	Pearson r: r: -0.2708 R squared: 0.07332 P value: 0.2622 Significant: NO	Pearson r: r: 0.1537 R squared: 0.02362 P value: 0.5299 Significant: NO	Pearson r: r: -0.2661 R squared: 0.07084 P value: 0.2707 Significant: NO	Pearson r: r: 0,2365 R squared: 0,05593 P value: 0,3296 Significant: NO	Pearson r: r: -0,1503 R squared: 0,02258 P value: 0,5392 Significant: NO
Caudate	FA	Pearson r: r: -0.4519 R squared: 0.2042 P value: 0.0521 Significant: NO	Pearson r: r: 0.1157 R squared: 0.01338 P value: 0.6372 Significant: NO	Pearson r: r: -0.2267 R squared: 0.05141 P value: 0.3506 Significant: NO	Pearson r: r: 0.3150 R squared: 0.09921 P value: 0.1890 Significant: NO	Pearson r: r: -0.4710 R squared: 0.2219 P value: 0.0418 Significant: YES	Pearson r: r: -0.08176 R squared: 0.006685 P value: 0.7393 Significant: NO
	MD	Pearson r: r: 0.1749 R squared: 0.03058 P value: 0.4740 Significant: NO	Pearson r: r: 0.1462 R squared: 0.02137 P value: 0.5504 Significant: NO	Pearson r: r: 0.2346 R squared: 0.05502 P value: 0.3337 Significant: NO	Pearson r: r: 0.2356 R squared: 0.05552 P value: 0.3315 Significant: NO	Pearson r: r: 0.2954 R squared: 0.08724 P value: 0.2196 Significant: NO	Pearson r: r: 0.2128 R squared: 0.04530 P value: 0.3816 Significant: NO

Putamen	FA	Pearson r: r: -0.2809 R squared: 0.07893 P value: 0.2440 Significant: NO	Pearson r: r: -0.3063 R squared: 0.09385 P value: 0.2021 Significant: NO	Pearson r: r: -0.2074 R squared: 0.04301 P value: 0.3942 Significant: NO	Pearson r: r: -0.3233 R squared: 0.1046 P value: 0.1769 Significant: NO	Pearson r: r: -0.4241 R squared: 0.1798 P value: 0.0704 Significant: NO	Pearson r: r: -0.2971 R squared: 0.09928 P value: 0.2167 Significant: NO
	MD	Pearson r: r: 0.5591 R squared: 0.3126 P value: 0.0128 Significant: YES	Pearson r: r: 0.3322 R squared: 0.1103 P value: 0.1647 Significant: NO	Pearson r: r: 0.5667 R squared: 0.3211 P value: 0.0114 Significant: YES	Pearson r: r: 0.4349 R squared: 0.1891 P value: 0.0628 Significant: NO	Pearson r: r: 0.5647 R squared: 0.3189 P value: 0.0118 Significant: YES	Pearson r: r: 0.3078 R squared: 0.09476 P value: 0.1998 Significant: NO
Pallidum	FA	Pearson r: r: -0.2837 R squared: 0.08049 P value: 0.2392 Significant: NO	Pearson r: r: -0.1279 R squared: 0.01635 P value: 0.6019 Significant: NO	Pearson r: r: -0.2231 R squared: 0.04977 P value: 0.3586 Significant: NO	Pearson r: r: -0.1357 R squared: 0.01841 P value: 0.5796 Significant: NO	Pearson r: r: -0.4397 R squared: 0.1934 P value: 0.0596 Significant: NO	Pearson r: r: -0.1104 R squared: 0.01219 P value: 0.6528 Significant: NO

	MD	Pearson r: r: 0.5050 R squared: 0.2550 P value: 0.0274 Significant: YES	Pearson r: r: -0.2460 R squared: 0.06051 P value: 0.3100 Significant: NO	Pearson r: r: 0.4729 R squared: 0.2236 P value: 0.0409 Significant: YES	Pearson r: r: -0.2112 R squared: 0.04462 P value: 0.3853 Significant: NO	Pearson r: r: 0.4999 R squared: 0.2499 P value: 0.0293 Significant: YES	Pearson r: r: -0.2224 R squared: 0.04948 P value: 0.3600 Significant: NO

II. Statistically significant findings

Over the 204 realized correlations, we found 39 significant statistical correlations that we present in scatterplots and figures.

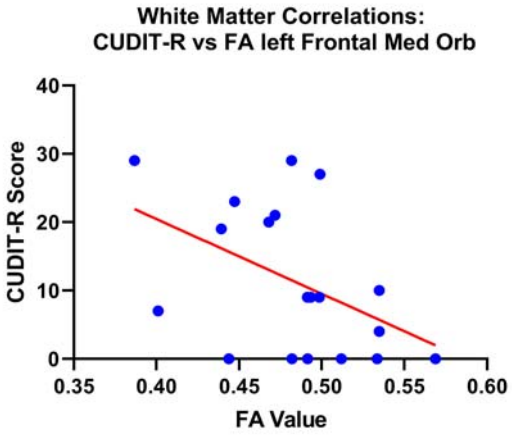
White Matter Correlations:
CUDIT-R vs FA left Frontal Med Orb
CUDIT-R Score
FA Value
0
10
20
30
40
0.35
0.40
0.45
0.50
0.55
0.60

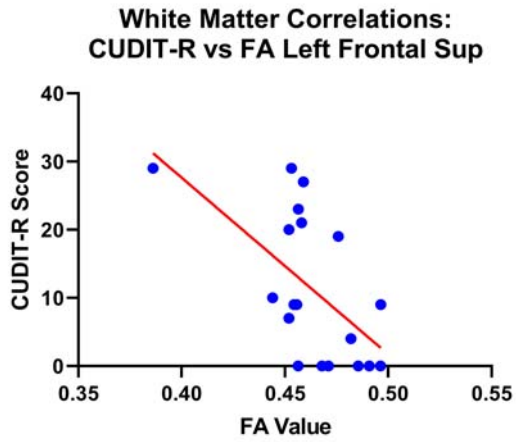
White Matter Correlations:
CUDIT-R vs FA Left Frontal Sup
CUDIT-R Score
FA Value
0
10
20
30
40
0.35
0.40
0.45
0.50
0.55

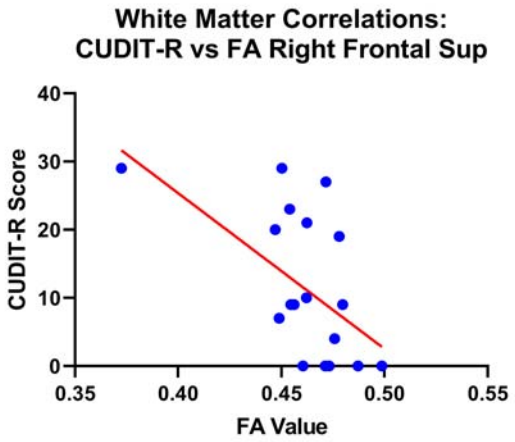
White Matter Correlations:
CUDIT-R vs FA Right Frontal Sup
CUDIT-R Score
FA Value
0
10
20
30
40
0.35
0.40
0.45
0.50
0.55

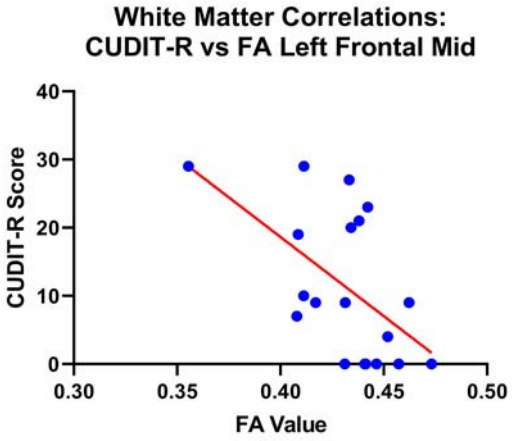
White Matter Correlations:
CUDIT-R vs FA Left Frontal Mid
CUDIT-R Score
FA Value
0
10
20
30
40
0.30
0.35
0.40
0.45
0.50

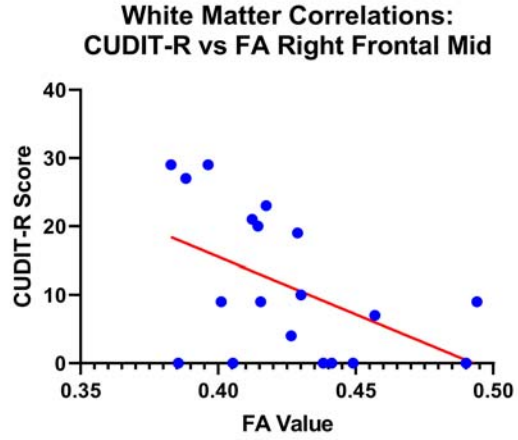
White Matter Correlations:
CUDIT-R vs FA Right Frontal Mid
CUDIT-R Score
FA Value
0
10
20
30
40
0.35
0.40
0.45
0.50

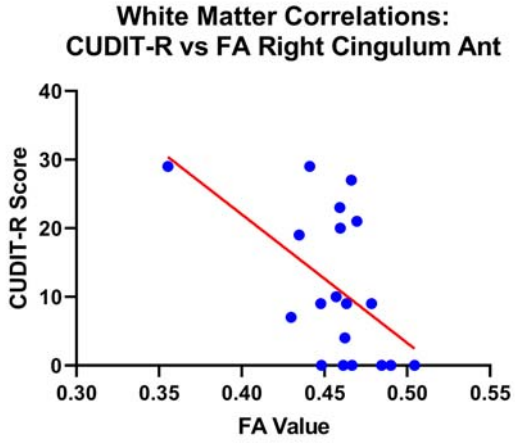
White Matter Correlations:
CUDIT-R vs FA Right Cingulum Ant
CUDIT-R Score
FA Value
0
10
20
30
40
0.30
0.35
0.40
0.45
0.50
0.55

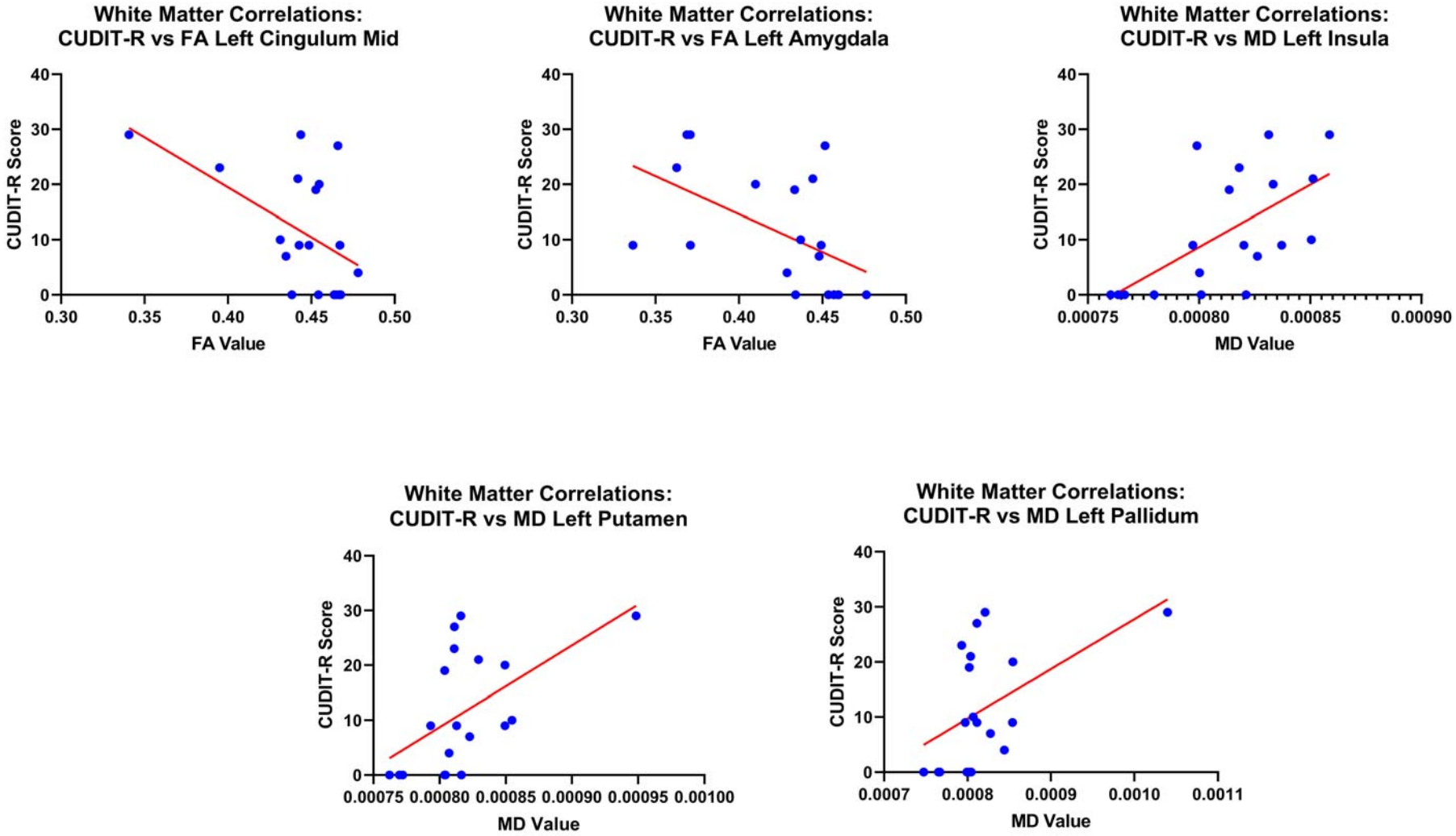

Figure 351: Correlation scatterplots for cannabis use disorder and white matter in regions with statistically significant analysis. CUDIT-R=The Cannabis Use Disorder Identification Test-Revised – FA= Fractional anisotropy – MD= Mean diffusivity

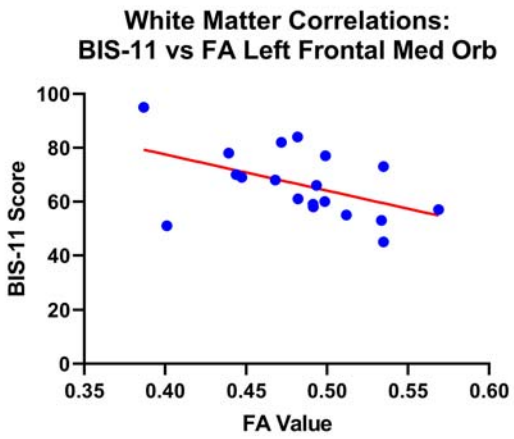
White Matter Correlations:
BIS-11 vs FA Left Frontal Med Orb
BIS-11 Score
FA Value
0
20
40
60
80
100
0.35
0.40
0.45
0.50
0.55
0.60

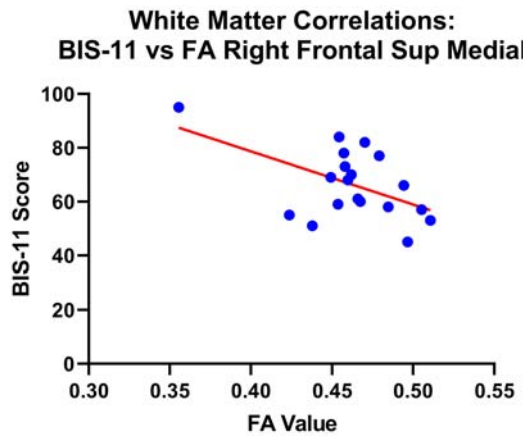
White Matter Correlations:
BIS-11 vs FA Right Frontal Sup Medial
BIS-11 Score
FA Value
0
20
40
60
80
100
0.30
0.35
0.40
0.45
0.50
0.55

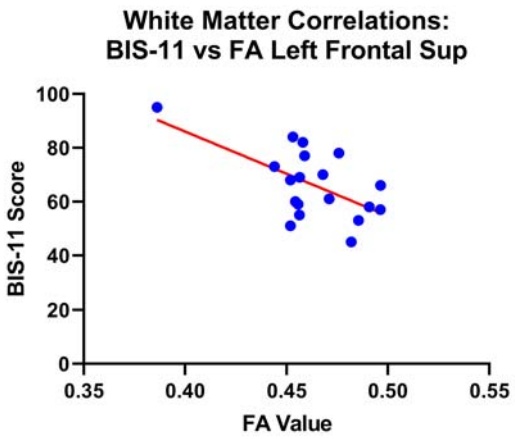
White Matter Correlations:
BIS-11 vs FA Left Frontal Sup
BIS-11 Score
FA Value
0
20
40
60
80
100
0.35
0.40
0.45
0.50
0.55

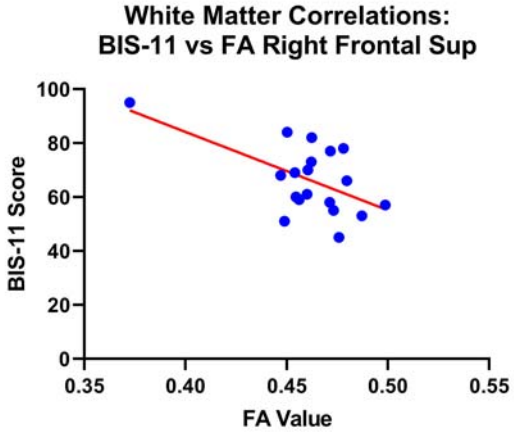
White Matter Correlations:
BIS-11 vs FA Right Frontal Sup
BIS-11 Score
FA Value
0
20
40
60
80
100
0.35
0.40
0.45
0.50
0.55

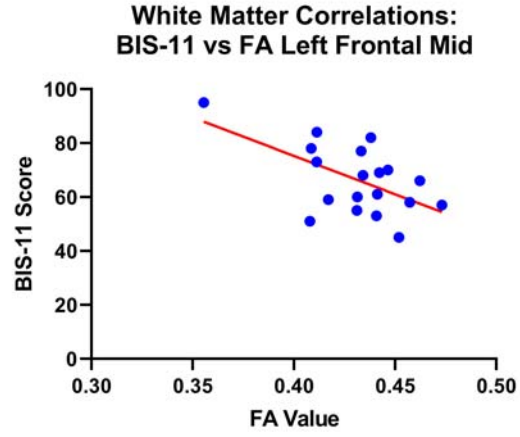
White Matter Correlations:
BIS-11 vs FA Left Frontal Mid
BIS-11 Score
FA Value
0
20
40
60
80
100
0.30
0.35
0.40
0.45
0.50

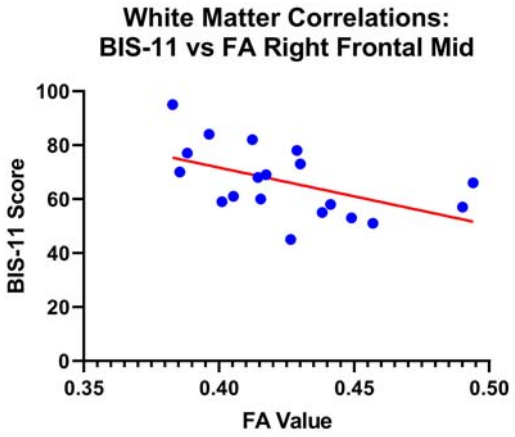
White Matter Correlations:
BIS-11 vs FA Right Frontal Mid
BIS-11 Score
FA Value
0
20
40
60
80
100
0.35
0.40
0.45
0.50

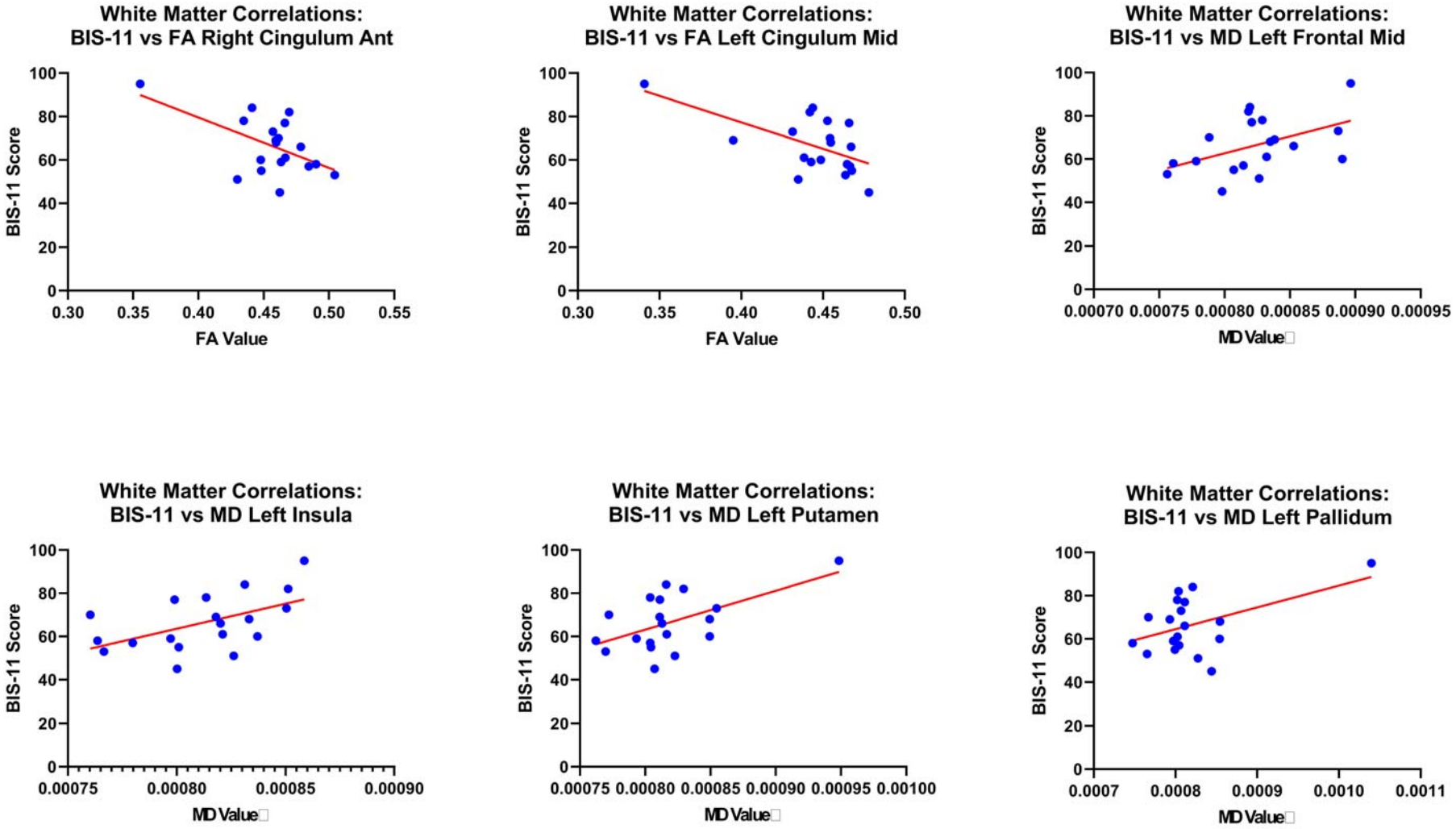

Figure 352: Correlation scatterplots for impulsivity and white matter in regions with statistically significant analysis.

BIS-11=The Barratt Impulsiveness Scale-11 – FA= Fractional anisotropy – MD= Mean diffusivity

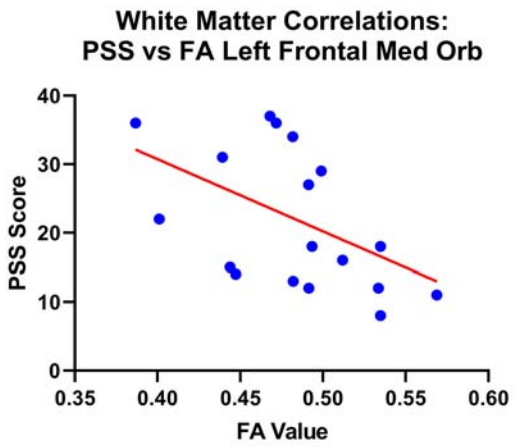
White Matter Correlations:
PSS vs FA Left Frontal Med Orb
PSS Score
FA Value
0
10
20
30
40
0.35
0.40
0.45
0.50
0.55
0.60

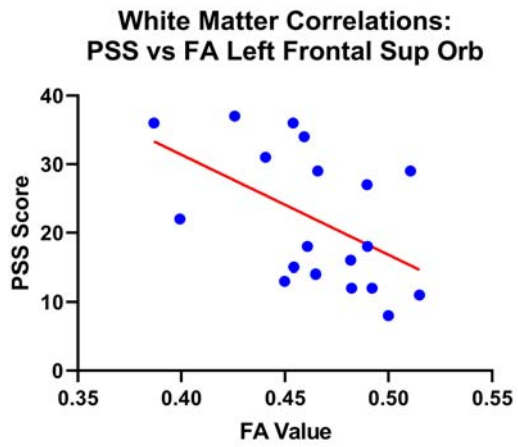
White Matter Correlations:
PSS vs FA Left Frontal Sup Orb
PSS Score
FA Value
0
10
20
30
40
0.35
0.40
0.45
0.50
0.55

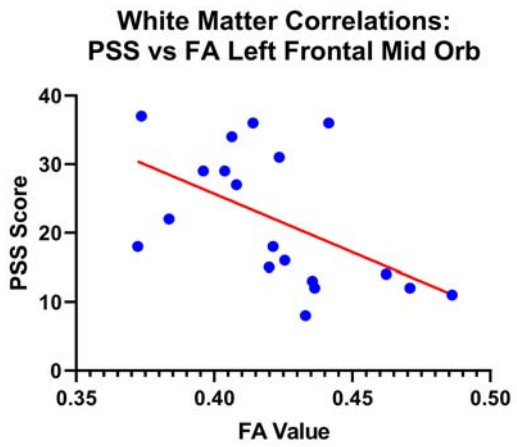
White Matter Correlations:
PSS vs FA Left Frontal Mid Orb
PSS Score
FA Value
0
10
20
30
40
0.35
0.40
0.45
0.50

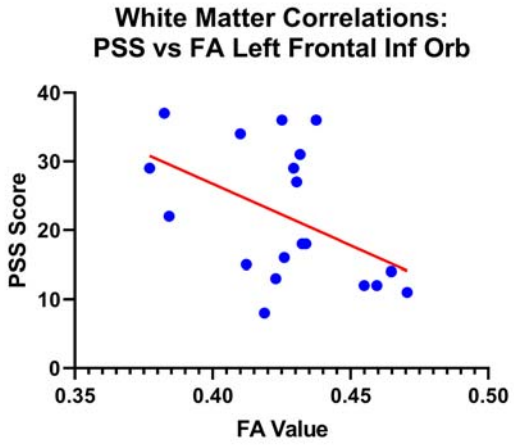
White Matter Correlations:
PSS vs FA Left Frontal Inf Orb
PSS Score
FA Value
0
10
20
30
40
0.35
0.40
0.45
0.50

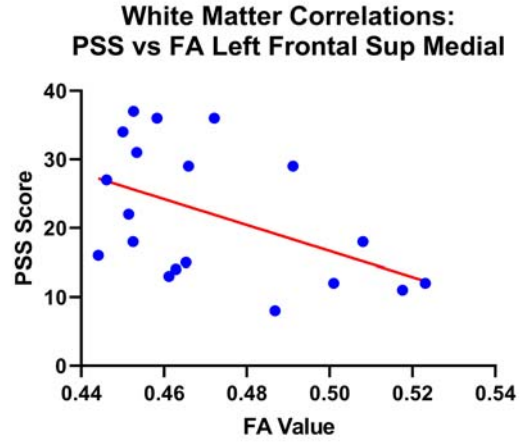
White Matter Correlations:
PSS vs FA Left Frontal Sup Medial
PSS Score
FA Value
0
10
20
30
40
0.44
0.46
0.48
0.50
0.52
0.54

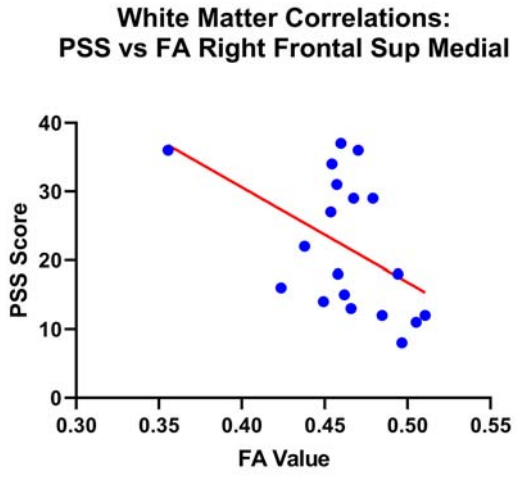
White Matter Correlations:
PSS vs FA Right Frontal Sup Medial
PSS Score
FA Value
0
10
20
30
40
0.30
0.35
0.40
0.45
0.50
0.55

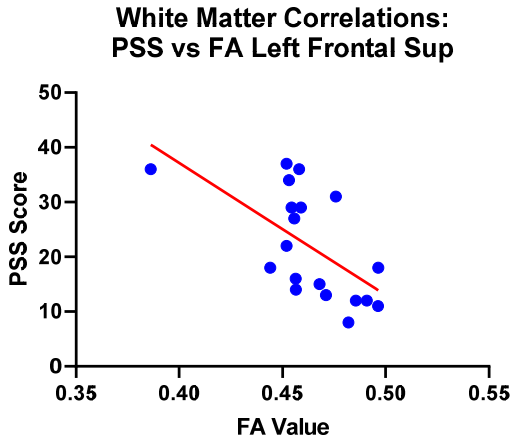
White Matter Correlations:
PSS vs FA Left Frontal Sup
PSS Score
FA Value
0
10
20
30
40
50
0.35
0.40
0.45
0.50
0.55

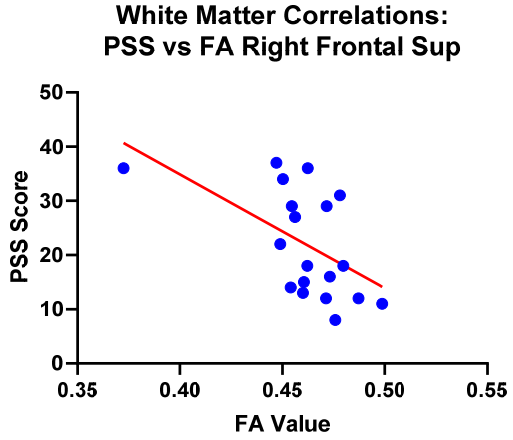
White Matter Correlations:
PSS vs FA Right Frontal Sup
PSS Score
FA Value
0
10
20
30
40
50
0.35
0.40
0.45
0.50
0.55

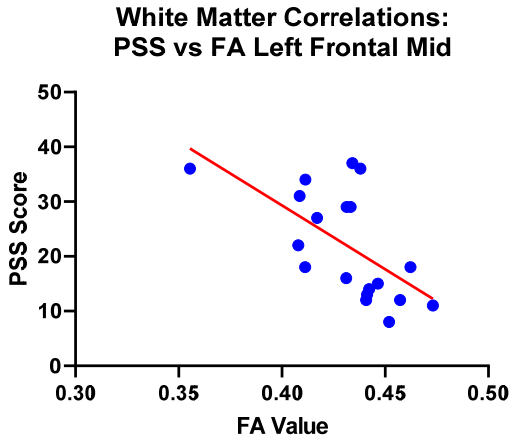
White Matter Correlations:
PSS vs FA Left Frontal Mid
PSS Score
FA Value
0
10
20
30
40
50
0.30
0.35
0.40
0.45
0.50

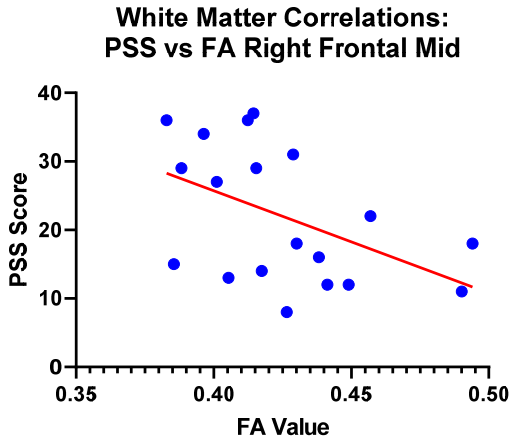
White Matter Correlations:
PSS vs FA Right Frontal Mid
PSS Score
FA Value
0
10
20
30
40
0.35
0.40
0.45
0.50

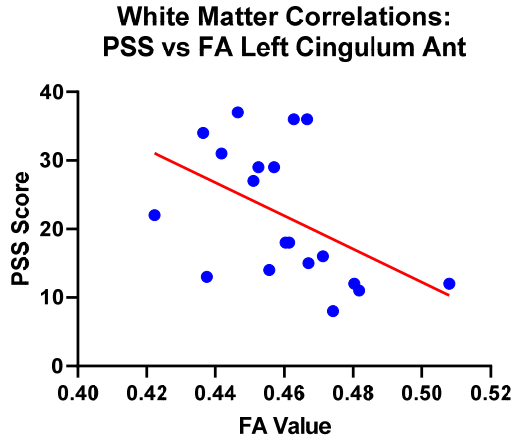
White Matter Correlations:
PSS vs FA Left Cingulum Ant
PSS Score
FA Value
0
10
20
30
40
0.40
0.42
0.44
0.46
0.48
0.50
0.52

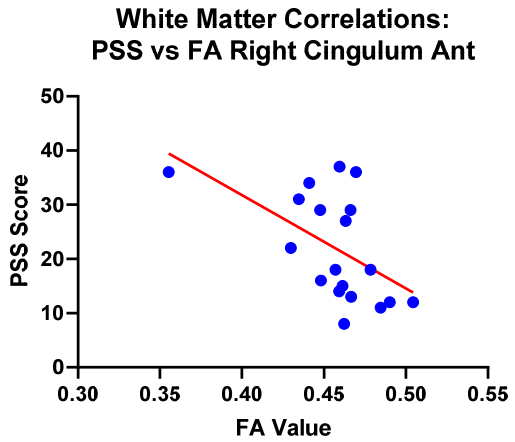
White Matter Correlations:
PSS vs FA Right Cingulum Ant
PSS Score
FA Value
0
10
20
30
40
50
0.30
0.35
0.40
0.45
0.50
0.55

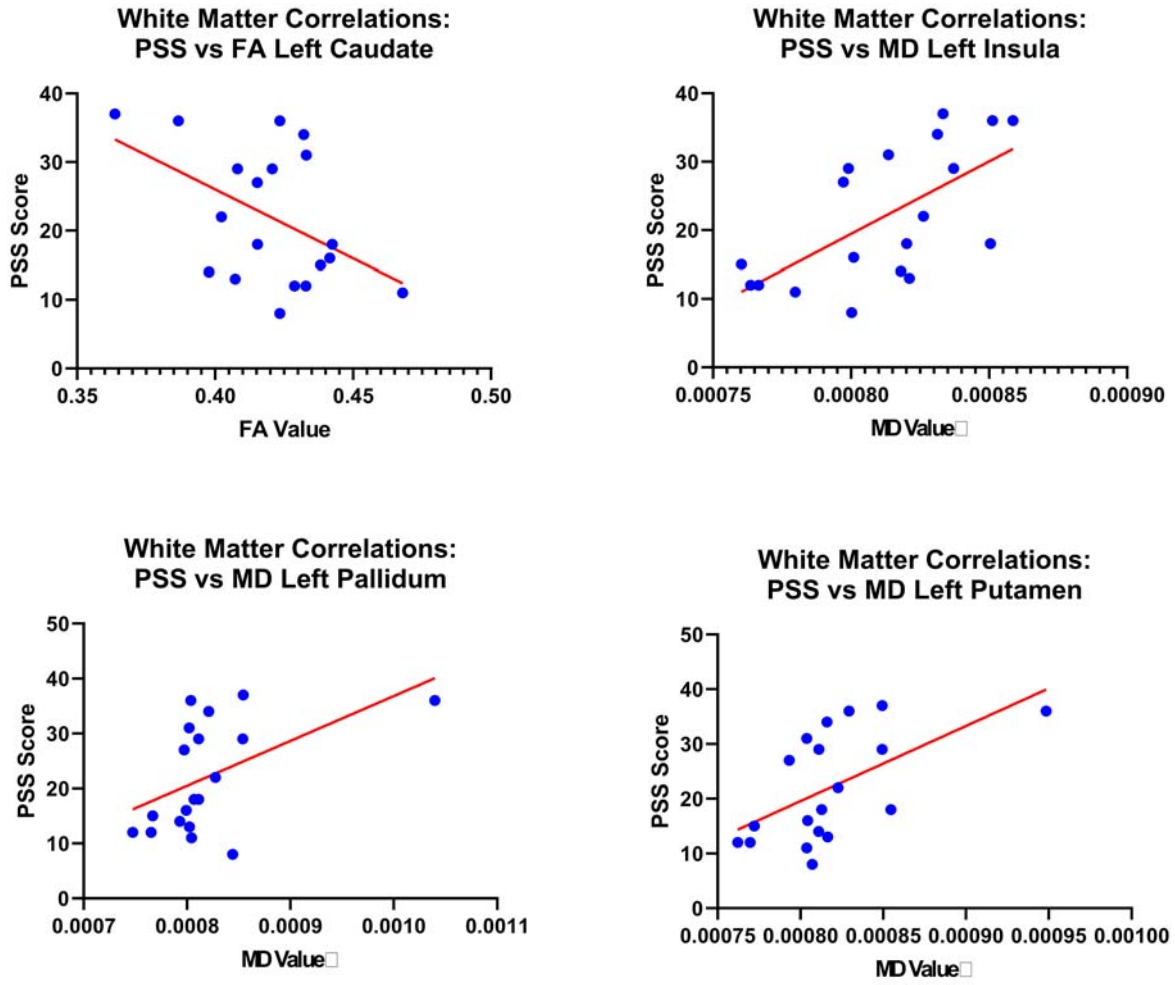

Figure 353: Correlation scatterplots for stress and white matter in regions with statistically significant analysis.

PSS= Perceived Stress Scale – FA= Fractional anisotropy – MD= Mean diffusivity

Discussions

Chapter I: Discussion of cannabis use disorder and psychological functioning assessment.

I. Cannabis use disorder: The Cannabis Use Disorder Identification Test-Revised (CUDIT-R)

The severity of cannabis usage and associated difficulties was evaluated in our research using the 8-item Cannabis Use Identification Test-Revised (CUDIT-R)[323].

The Cannabis Use Identification Test-Revised (CUDIT-R) is a self-report screening test comprised of eight items that assess consumption, cannabis-related problems, dependency, and psychological characteristics. Scores may vary from 0 to 32. A total score of 8 or more indicates "hazardous cannabis usage," while a total score of 13 or above indicates "probable cannabis use disorder."

Findings from the CUDIT-R results in our sample showed that all the heavy cannabis users score above 19, which mean that all of them have a probable cannabis use disorder, in the other hand, four-light users have a probable "hazardous cannabis usage," and two of them scores under 8. Concerning averages, they were widely widened between the two groups of users, and scores of the two groups showed a statistical significant with a p=value of **4.9274 E-06** between the two groups.

Given that the healthy controls had never smoked cannabis, they all got a score of 0 on the CUDIT-R total score. In terms of statistical analysis, the ANOVA revealed a very significant difference between healthy controls and heavy cannabis users (p-value =**3.0823 E-08**) as well as between healthy controls and light users (p-value =**4.3755 E-06**).

These findings are critical for our research since they demonstrate that the distribution we created on the two groups (heavy and light) was mainly significant for the cannabis use disorder as well.

The ROC curve was used to statistically determine and compare the screening test's performance (CUDIT-R) in establishing a distinction between the two groups (heavy and light consumers) based on the criteria of cannabis use disorder.

The results reported in Figure 48 below shows that the test has high sensitivity and specificity since the curve is located at the top and left and has the highest effectiveness with AUC =1 and P <0.0027. With results reported in Figure 48, we have to strengthen the fact that by studying the impact of cannabis use on brain functioning and structure, we are not only examining the impact of chronic cannabis use, but we are also examining the role of CUD in this process (since we have two groups one with CUD and another with "hazardous cannabis usage,").

Returning to the literature works with a similar objective to ours (study of brain structure in cannabis users), and those who used the CUDIT or CUDIT-R to assess cannabis use disorders in their volunteers revealed scores and averages of CUDIT significantly lower than our heavy cannabis users and approaching or exceeding our light cannabis users by a slight margin.

Janna Cousijn and colleagues (2021)[324] compared the whole-brain white matter microstructure between daily cannabis users and matched controls using diffusion tensor imaging (DTI). They concluded that there was no difference in white matter microstructure between cannabis users and controls and that it did not correlate with the degree of dependency or duration of use. However, the CUDIT-R scores for cannabis users in this study were very low (average (SD) 13.7 (4.3)) compared to the heavy cannabis users in our study (average (SD) 24 (4.28)).

Another study conducted by the same author Janna Cousijn and colleagues (2011)[325] in heavy cannabis users (Cannabis use lifetime (joints= 1579.5) with a score of CUDIT (average (SD) 12.4 (5.7)), this study on grey matter alterations associated with cannabis use conclude that the distinct patterns of structural changes linked with varying degrees of cannabis use indicate that changes in brain structure are associated with particular features of cannabis use and dependence. And that was just what we attempted to demonstrate in our study too by correlating consumption parameters (duration of use, age of onset, and level of consumption) with various psychometric tests, including the CUDIT-R, as well as psychometric results, including the CUDIT-R, with DTI results that reflect the brain structure of cannabis users.

II. Impulsivity trait: Barratt Impulsiveness Scale (BIS-11)

In general, impulsivity is a wide concept that encompasses various aspects, including an inability to defer pleasure, sensation-seeking, risk-taking, and insensitivity to long-term repercussions[326]. However, this description remains extremely broad and nonspecific, and to date, there is no unified and universally accepted psychological definition for impulsivity[327].

First, we should know that there is a difference between impulsivity as a trait and impulsivity as a state.

Trait impulsivity, almost always evaluated through self-report personality tests, is determined by internal perceptions of behaviors. While the impulsive trait is consistent throughout time, the impulsive state is characterized by varying impulsivity levels. Impulsivity as the state is regarded as both a standard characteristic of behavior and a pathological component of several diagnosable mental illnesses[327].

In the current study, we assess trait impulsivity using the Barratt Impulsiveness Scale[328]. The BIS-11 is a thirty-item questionnaire that assesses impulsivity in three dimensions: attentional/cognitive, motor, and non-planning.

It is frequently stated that a defining feature of substance use disorders is an inability to suppress the impulse to use drugs despite significant negative consequences, and there is a considerable prevalence of co-occurring impulse control and substance use problems[329] [327].

In this regard, to determine this association in our cannabis users, we correlated the degree of cannabis abuse and dependence (as measured by the CUDIT-R) and weekly cannabis use (joins per week) with the BIS-11 total scores. In addition, correlations between the test and factors related to cannabis use (age of onset, duration of use since the first time, and degree of consumption) were conducted.

In the current research, heavy cannabis users expressed more trait impulsivity than light cannabis users (ANOVA's p-value=0.00332) and healthy controls (ANOVA's p-value = 0.000882), as indicated by higher BIS-11 total scores.

These findings suggest that heavy cannabis use may affect the reward or/and decision-making circuits resulting in various behavioral changes, including increased impulsivity. Ultimately, we will test these hypotheses by correlating clinical outcomes to DTI findings.

The average of total BIS-11 scores in light cannabis users was equal to healthy controls, with a p-value=1, and that can be interpreted, by two hypotheses, as :

-Light consumption of cannabis does not affect the impulsivity trait in consumers

-With a low impulsivity trait, individuals have a lower risk of consuming high doses of cannabis.

Cannabis users are often reported to be more impulsive and have higher scores on the BIS-11 test. Gruber SA. and his colleagues (2011) [330] reported higher BIS scores for all domains and statistical significance for the total BIS score. The same study reported an equal average (59) for total BIS in the control group to our healthy control group and light users group, and a cannabis users group with a lower (69.8) average to our heavy cannabis users group average (79). Dougherty et al. (2013)[331] also found that current cannabis users had higher BIS scores.

Delibas et al. (2018)[332] revealed an interesting finding involving chronic marijuana use: Former cannabis users exhibited greater impulsivity, indicating that these gains were not due to current usage. This finding aligns with our results since all of the cannabis users in our study are chronic users. Another recent research conducted by O'Donnell BF. (2021) [326] and colleagues to assess decision-making in chronic cannabis users revealed that cannabis users expressed higher impulsivity on the Barratt Impulsiveness Scale scores than non-users.

III. Perceived stress: Perceived Stress Scale (PSS)

Perceived stress refers to an individual's emotions or perceptions about the amount of stress they are experiencing at any given moment or during a given period. Perceived stress is characterized by feelings about the unpredictability and uncontrollability of the individual's life, the frequency with which the individual needs to deal with unpleasant problems, the amount of change occurring in the individual's life, and confidence in the individual's ability to cope with problems or challenges[333].

As reported in our thesis's bibliographic and theoretical part, chronic relapsing of addiction appears to be associated with underlying neurophysiological abnormalities in the stress functions circuit[27].

Given the difficulty of studying all forms of stress in a single research and the importance of perceived stress among cannabis users, we assessed this aspect by performing the PSS test on all participants.

To evaluate the perceived stress levels in our volunteers and study it adequately and profoundly by comparing stress levels between groups and correlating stress to other cannabis-related components, our volunteers (cannabis users and healthy controls) completed the Perceived Stress Scale (PSS)[233]. This measure assesses chronic life stress. It was developed to measure the extent to which current life status was appraised as stressful.

In the 19 volunteers studied, spread over the three groups, heavy cannabis users showed very high scores (31) compared to light users and healthy controls. This elevation was statistically significant, ANOVA'S p-value = 0.032 when heavy cannabis users group compared to the scores of light users group and ANOVA'S p-value = 0.00026 when the scores of heavy cannabis users group are compared to scores of the healthy users' group.

Additionally, light users scored higher than healthy control groups (with an average of 20.33 compared to 13 among healthy groups). This increase was also statistically significant, with a p-value of 0.048 for ANOVA.

In 2016 Vujanovic AA and all[334], with a study that had the purpose of examining a novel attentional bias task in adults with cannabis use disorders, conducted among 12 cannabis users, reported that the cannabis use disorders group showed significantly greater perceived stress. Despite this elevation, the scores among cannabis users in this study exhibited lower scores than our heavy and light cannabis users.

In our work, too, we did correlate levels of the perceived stress to cannabis use disorder through the results of the CUDIT-R test. We will discuss these results and other correlations in more detail later in the "Discussion" section.

In this context, Spradlin and Cuttler (2019) [335] found that perceived stress was significantly associated with experiencing more cannabis-use-related problems among college students. The study also suggested that these individuals may be using cannabis to cope with their perceived stress. Further, the same research found that early life stress was linked with increased frequency of cannabis use and that both early life and chronic stress were associated with more problematic cannabis use.

These disclosures were also examined in our sample by correlating scores of the PSS test to the age of onset, duration of use, and degree of consumption (joints smoked per week) in addition to their correlations to the CUDIT-R test.

Another pertinent study by Jessica M. Cavalli and Anita Cservenka (2021)[336], examined the role of negative affect, discovered that having more stressful life events and greater emotion dysregulation was associated with experiencing more severe problematic cannabis use.

These results emphasize the critical importance of evaluating both emotion dysregulation and stress and comparing various dimensions of stress in connection to cannabis usage outcomes.

IV. Discussion of the correlations between psychometric tests and factors associated with cannabis use

The severity and degree of cannabis-induced neuropathological alterations are said to vary depending on the **dosage**, frequency, and **duration of exposure**, as well as the **age of onset**, with adolescence being a particularly susceptible phase[322].

To test this hypothesis, we correlated these three parameters with the outcomes of psychometric tests (CUDIT-R, BIS-11, PSS) in our sample of volunteers. Figure 354 schematize the conducted correlations.

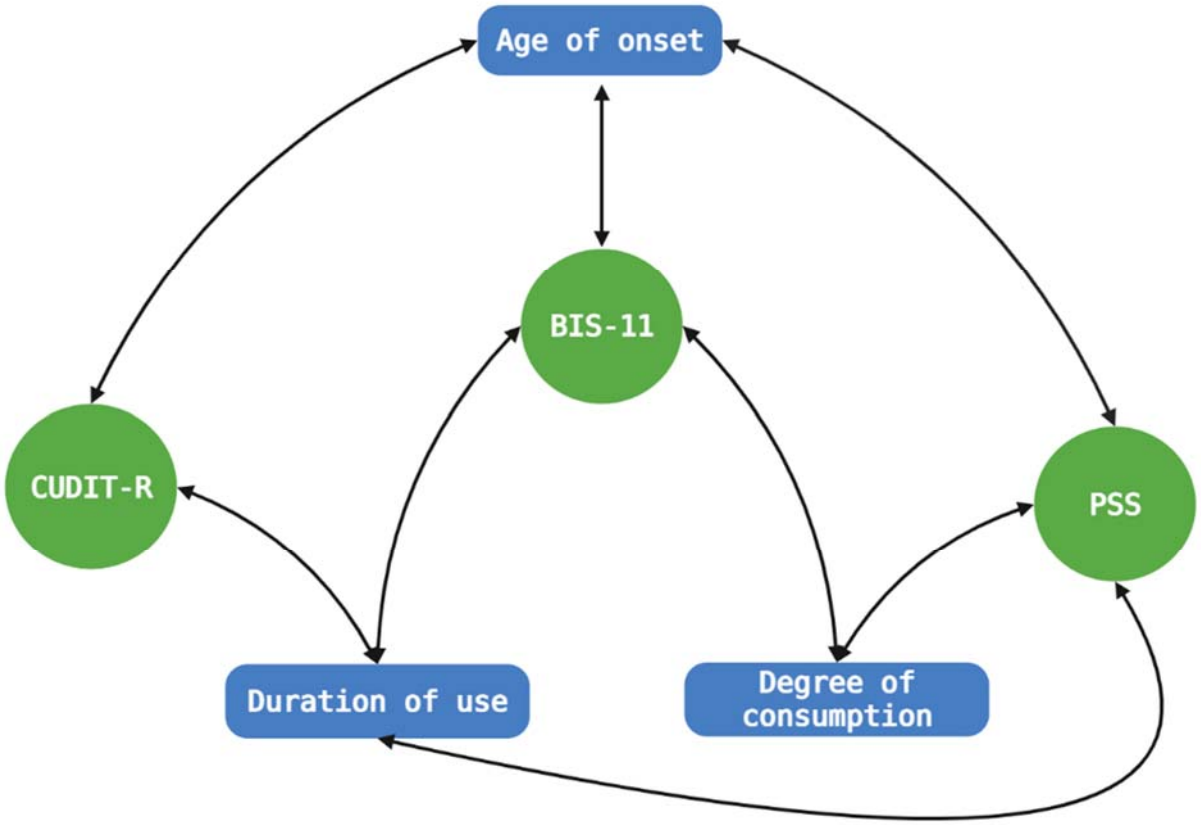

Figure 354: Schematization of the conducted correlations between the clinical features and some profiles of consumptions

- Age of onset

Age of onset cannabis use reflects how early a person started using cannabis. Cannabis usage at a younger age and greater exposure to cannabis were often linked with increased cannabis-induced alterations[337].

Given the endocannabinoid system's well-established role in neurodevelopment[338], it is unsurprising that initiation of cannabis use at critical developmental stages such as adolescence has been found to affect the amount and severity of cannabis effects on brain structure and function[339].

In this respect, we opted to correlate this factor related to cannabis consumption with the following:

-CUDIT-R scores: To determine the effect of an early onset on the severity of a cannabis use disorder. Assuming that the age of onset is a fixed constant associated with the consumer, any correlation established will simply be explained by: Age of onset has an effect on CUD, or that age of onset and CUD are both influenced by another factor.

-BIS-11: This correlation is pertinent since an early age of onset may be at a later date the cause of high levels of impulsivity, or high levels of impulsivity in young ages may be a factor of cannabis usage at a very early age.

-PSS: To examine the impact of age of onset on stress, and given that the test assesses perceived stress in a specific instant, we may deduce that, if a correlation exists, it will be as follows: Age of onset affects perceived stress; the converse is not accurate.

Our results revealed a negative correlation between the three tests and the age of onset. CUDIT-R and BIS-11 correlate with a statistical significance; respective p-values were **0.0066** and **0.0146.**

CUDIT-R and the age of onset correlation prove that, in our sample of cannabis users, the age of onset influence the severity of the cannabis use disorder. This influence is pretty strong in our sample since we have an **r=-0.7095 and r^2= 0.4325**, then **43.25%** of the CUDIT-R variance in our sample can be explained by the variation of the age of onset.

This correlation confirms the hypotheses that initiating cannabis use at an early age the risk of developing CUD and the rate of progression to CUD.

The literature also supports our results; Le Strat et al.[340] revealed an inverse correlation between the age at which cannabis usage began and the likelihood of developing cannabis dependency in a cross-sectional sample of 8068 individuals. Swift and colleagues reported similar findings in a sample of 1520 adolescents aged 14.9–17.4 years; heavy, chronic, and early-onset cannabis use significantly predict cannabis issues.

Millar, Seán R. et al.[341] in a more recent study that analyzed data of 12 139 individuals, aged 15 years and over, reported that among people who report past cannabis use, it is those with a more precocious pattern of early use of cannabis who are more likely to report ongoing, heavy and problematic cannabis use.

Regarding impulsivity, the correlation conducted between BIS-11 scores and ages of onset showed a strong negative correlation **r= -0.7095.** As CUDIT-R correlation, influence is also pretty strong **r^2= 0.5034,** which means that **50.34%** of the variation in impulsivity levels can be explained by the variation of the age of onset and vice versa.

Given this association, the critical issue is: Is impulsivity a risk factor for cannabis use or a consequence?

This question has been very well studied in a recent review by Linda Rineharta et al. (2021)[327]. They highlighted that impulsivity is associated with the age of onset and has been consistently identified as a risk factor for cannabis use and cannabis-related disorders. Additionally, they reported that impulsivity might be a risk factor or a consequence of chronic cannabis use. To overcome this matter, longitudinal research, including psychometric testing and correlations with consumption parameters throughout the study, may provide a significant amount of insight and understanding.

Perceived stress (measured through PSS test) was also negatively correlated to the age of onset **($r=-0.4282$, $r^2= 0.1833$).** However, this variation was not proven to be statistically significant **(p-value=0.144)**. This lack of statistical significance is probably due to the relatively small size of our samples. To make a firm conclusion, we will need to larger our data.

According to Scott M. Hyman et al.[342], stressful life events may predispose to early-onset cannabis use, higher coping-related use, and a higher probability of developing cannabis addiction. To support this conclusion, a longitudinal, functional, and structural study of consumers who have recently begun using cannabis and people at risk of using cannabis will be highly beneficial and answer several questions about the stress caused or induced by cannabis.

- **Duration of use in years and degree of consumption**

Correlations conducted in duration of use in years with CUDIT-R, BIS-11, and PSS show significant positive associations between these three tests and the duration of use. Regarding the heaviness of consumption, we decided to correlate it with only BIS-11 and PSS. Scores of CUDIT-R were not correlated because one of the questions of the CUDIT-R is 'How often do you use cannabis?' and it is going to be inaccurate correlating CUDIT-R to joints smoked per week.

The level of cannabis use disorder measured through CUDIT-R reveals a high positive significant correlation, **r=0.7952, r^2=0.6324, and p=0.0012**. It means that the chronicity of cannabis consumption may impact the reward circuit and be manifest in a high level of cannabis use disorder

Impulsivity trait is also positively correlated with chronicity of use (evaluate it through the duration of cannabis use in years). Pearson's correlation reveals an **r= 0.7096, r^2= 0.5036, and p=0.0066**. As chronicity, BIS-11 correlate strongly, significantly and positively with degree of consumption: : **r= 0.7776, r^2= 0.6047**, and **p=0.0018**.

Here we also face the question: is the high trait impulsivity responsible for the heavy or/and chronic cannabis consumption, or does the chronic or/and cannabis consumption induces high trait impulsivity? To further elucidate the association between impulsivity and cannabis use, a longitudinal study is needed with the pinpoint accuracy of factors associated with consumption or previous to the onset of consumption in a highly codified manner.

Like cannabis use disorder and impulsivity trait, chronic and prolonged consumption has also correlated with perceived stress (PSS). The correlation was positive and with : **r= 0.5619, r^2= 0.3157, and p=0.0457.**

Perceived stress correlate positively with degree of consumption **r= 0.5310, r^2= 0.2819,** but not statistically significant **p=0.0619**.

Our findings regarding perceived stress in cannabis users integrated what Scott M. Hyman et al.[342] reported about stress in cannabis users. A recent review by Jason Patel and Raman Marwaha (2021) revealed that a substantial percentage of cannabis users use it for stress management or relaxation[343]. This suggests that the positive correlation observed in our results may also be explained in this respect. However, we need to increase data to come to a more consistent conclusion.

In our literature searching, we attempted to find studies that previously correlated the degree of chronicity and consumption analytically with cannabis use disorder, trait impulsivity and perceived stress, however no previous study has conducted such correlations.

Chapter II: Discussion of diffusion tensor imaging results in grey matter (ROI).

To our knowledge, this is the first study to reveal results about FA and MD diffusion markers of cannabis users' brains (Heavy and light users) compared to healthy controls.

FA and MD values of 36 anatomical regions in each hemisphere (a total of 72 regions) were calculated for 19 subjects (13 cannabis users and six matched controls), and quantitative comparisons between groups revealed different types of comparisons. We determined the significance of these quantitative differences using the analytical method "ANOVA" for all the 72 regions.

I. Fractional anisotropy

For FA, 11 different comparisons were observed. However, only three comparisons accounted for 73% of the results. Those three intergroup comparisons are:

-Non-users' group > Light users' group ≈ Heavy users' group,

-Non-users' group > Heavy users' group > Light users' group

-Non-users' group > Light users' group > Heavy users' group

We can notice from these results that FA's value is reduced in cannabis users compared to the non-consuming subjects in 73 percent of our results, which is equivalent to 53 anatomical regions. From these 53 anatomical regions, analytical findings showed 21 anatomical areas where there are significant differences between heavy cannabis users, light cannabis users, and controls.

To these 21 regions, an additional exceptional region is included, with an FA average that is higher in heavy users than in healthy controls or light users (Heavy users' group > Non-users group > Light users' group), with a statistical difference between heavy and light cannabis smokers. Table 458 summarizes these findings in those regions with different significant comparisons.

Table 458:The descriptive and analytical results of fractional anisotropy in regions of interest that revealed significant differences, as well as the functional anatomical regions that correspond to them

Functional Anatomical areas	Regions Of interest	The significant differences	The quantitative intergroup comparisons
Orbital surface of the frontal lobe	Left Rectus	L Vs H	G. I > G.III > G. II
Prefrontal cortex	Left Frontal Sup	L Vs C | H Vs C	G.III > G. I > G. II
Broca's area	Left Frontal Inf Tri	L Vs C | H Vs C	G.III > G. II ≈ G. I
Parietal Lobe	Left Postcentral	L Vs C | H Vs C	G.III > G. II ≈ G. I
	Left Parietal Sup	H Vs C	G.III >G. II > G. I
	Right Parietal Sup	H Vs C	G.III > G. II ≈ G. I
	Left SupraMarginal	L Vs C | H Vs C	G.III > G. II ≈ G. I
	Right SupraMarginal	H Vs C	G.III > G. II ≈ G. I
	Left Angular	H Vs C	G.III > G. II ≈ G. I
	Left Parietal Inf	L Vs C | H Vs C	G.III > G. I > G. II
	Left Precuneus	L Vs C | H Vs C	G.III > G. II ≈ G. I
	Right Precuneus	L Vs C | H Vs C	G.III >G. II > G. I
Temporal Lobe	Left Temporal Sup	L Vs C | H Vs C	G.III > G. II ≈ G. I
	Right Temporal Sup	L Vs C | H Vs C	G.III > G. I > G. II
	Left Temporal Pole Sup	H Vs C	G.III >G. II > G. I
	Left Temporal Mid	L Vs C | H Vs C	G.III > G. II ≈ G. I
	Right Temporal Mid	L Vs C | H Vs C	G.III > G. I > G. II
Limbic System	Left Cingulum ANT	H Vs C	G.III >G. II > G. I
	Right Cingulum ANT	H Vs C	G.III >G. II > G. I
	Left Cingulum Mid	L Vs C | H Vs C	G.III > G. II ≈ G. I
	Right Cingulum Mid	H Vs C	G.III >G. II > G. I
	Left Insula	H Vs C	G.III > G. II ≈ G. I

From table 458, where we presented statistical analysis and quantitative intergroup comparisons findings, we can conclude that FA is decreased in cannabis users' groups compared to healthy non-users' groups.

From the same findings, we can also come to the conclusion that there was generally equality of averages between heavy users and lights users groups (in 12 regions), and even in the ten other locations where there were differences between the two categories of users (heavy and light), these differences were statistically insignificant.

We found out also, in the following regions, that when FA is significantly decreased in light cannabis users, there is always a significant decrease in heavy users compared to healthy non-users:

-Left Frontal Sup
-Left Frontal Inf Tri
-Left Postcentral
-Left SupraMarginal
-Left Parietal Inf
-Left Precuneus
-Right Precuneus
-Left Temporal Sup
-Right Temporal Sup
-Left Temporal Mid
-Right Temporal Mid
-Left Cingulum Mid

The significant decrease in FA values in heavy cannabis users is not always associated with a significant decrease of FA values in light users in these regions:

-Left Parietal Sup
-Right Parietal Sup
-Right SupraMarginal
-Left Angular
-Left Insula
-Left Temporal Pole Sup
-Left Cingulum ANT
-Right Cingulum ANT
-Right Cingulum Mid

From these results, we can come out with two main general conclusions:

-Chronic consumption of cannabis, whether light or heavy, reduces fractional anisotropy in the cerebral cortex's gray matter.

- Heavy chronic cannabis use reduces the fractional anisotropy in more regions of the cerebral cortex than light consumption.

II. Mean diffusivity

Twelve different intergroup comparisons were observed, and for the MD also only four intergroup comparisons have emerged, 72% of the results, this corresponds to 49 anatomical areas. Those four intergroup comparisons are:

- Non-users group ≈ Heavy users' group ≈ Light users' group
- Non-users group > Light users' group ≈ Heavy users' group
- Non-users group > Heavy users' group > Light users' group
- Heavy users' group, > Non-users group ≈ Light users' group

From these 49 anatomical regions, analytical findings showed only five anatomical regions where there are significant differences between heavy cannabis users, light cannabis users, and controls.

Table 459 summarizes these findings in those regions with different significant comparisons.

Table 459: The descriptive and analytical results of Mean Apparent Diffusion in regions of interest that revealed significant differences, as well as the functional anatomical regions that correspond to them

Functional Anatomical areas	Regions Of interest	The significant differences	The quantitative intergroup comparisons
Prefrontal cortex	Right Frontal Sup	L Vs C	G.III > G. I > G. II
Broca's area	Left Frontal Inf Tri	L Vs. C	G.III > G. I > G. II
Parietal Lobe	Right Angular	L Vs. C	G.III > G. II ≈ G. I
Temporal Lobe	Right Temporal Pole Mid	L Vs. C | H Vs C	G.III > G. II ≈ G. I
Limbic System	Left Nucleus Accumbens	L Vs. C	G.III > G. II ≈ G. I

. From our statistical and quantitative intergroup comparisons findings presented above, we can conclude that:

-MD is decreased in cannabis users' groups compared to the healthy non-users group.

-In three regions, from a total of five, the MD is decreased in both heavy and light users without any descriptive or statistical difference between those groups.

For the right Frontal Sup and Frontal Inf Tri regions, there was a difference between the two groups of users but not statistically significant.

We found that also that the statistically significant differences were present between light and control groups in right Frontal Sup, right Frontal Inf Tri, right Angular, left Nucleus Accumbens in contrast to the results reported for fractional anisotropy where this difference has never been significant without being associated with a significant difference between heavy and control as well.

In the region "Right Temporal Pole Mid," there are significant differences in MD averages between heavy and light users, as well as between heavy users and controls.

We can assume two main general conclusions from our MD value findings:

-Chronic light consumption of cannabis decreases MD in the gray matter of consumers in the following regions:

*Right Frontal Sup

*Right Frontal Inf Tri

*Right Angular

*Left Nucleus Accumbens

-The chronic consumption of cannabis, whether moderate or heavy, decreases the MD in consumers compared to healthy non-users in the Right Temporal Pole Mid region.

III. Discussion of FA and MD

Results of the mean apparent diffusion coefficient and especially fractional anisotropy in the gray matter indicate that the gray matter of chronic cannabis users, whether it in light or heavy users, has an altered microstructure in several brain regions.

Before addressing microstructural changes, it is necessary to know that the cerebral cortex is a thin layer of nerve tissue surrounding the brain's subcortical white and deep grey matter. The histological approach of a human brain slice reveals six layers of alternating white and grey matter, although the number of layers varies according to the cortex type[344].

Therefore, non-neuronal components like vasculature and glial cells will influence MRI findings as well. Glia is thought to outnumber neurons about 6:1 in human grey matter, with the ratio changing in various brain areas[345].

Given that MRI averages all cellular components and that glial cells in general and astrocytes, in particular, constitute the majority of cells in the brain, it is fair to expect that changes in diffusion MRI may be significantly influenced by glial morphology[346].

The problem then becomes which abnormal microstructural alterations are detectable using cortical FA and MD. DTI is sensitive to the intrinsic features of water diffusion in tissue and gives information on the microstructural qualities of the tissue based on diffusivity, expressed as MD, and coherence, represented as FA, of highly organized tissue.

In contrast to white matter, gray matter has a mixed composition of neurons, axons, and neuroglia. It may be challenging to determine the precise pathogenic alterations associated with FA decrease simply because the white matter has a more precise physical definition of FA. Furthermore, the interpretation of DTI diffusivity parameters in GM remains a point of contention.

However, FA generally refers to the directional coherence of water diffusion in the brain, which reflects axonal or dendritic projections. On the other hand, MD represents the degree of tissue density and indicates the rotationally invariant magnitude of water diffusion within brain tissue. Whereas decreased FA in brain tissue can be attributed to decreased axonal number, increased MD indicates decreased tissue density [347]. Furthermore, increased FA and decreased MD in the brain have been linked to glial activation and axonal swelling.

According to our findings, the difference between consumers groups and healthy control individuals was only seen in the cortex, not in the basal ganglia, diencephalon (Thalamus), telencephalon (Hippocampus), or amygdala. Regarding our fractional anisotropy results, there is a decrease in FA values of cannabis users compared to controls in regions with significant differences.

The brain lesions caused by THC may explain this reduction in FA in these brain areas. These pathogenic lesions include the following[168 169 170 171]:

-Shrinkage of neuronal cell nuclei and bodies,

-Decrease synapse number,

-Decrease in pyramidal cell density.

All of these lesions may increase the intercellular space of the cortex, which logically results in a reduction in FA.

Concerning MD, the cortical areas that showed significant changes between consumers and healthy controls are distinct from those that exhibited significant differences in FA findings and are limited to only five regions, three in the right hemispheres.

Furthermore, what distinguishes these findings is that the differences are mostly between light consumers and controls, except for a difference between heavy consumers and controls at the “Right Temporal Pole Mid” area.

Given the reduction in MD and the fact that the above-stated lesions, caused by the THC, are instead responsible for a rise in MD, which is somewhat contradictory, three different hypotheses may be suggested to take account of this decrease in MD:

-A hypothesis related to a limitation of our research design is the age difference between light users and controls (light: 21-28 Vs. Control 28-48), which is somewhat more important than the age difference between heavy users and controls (Heavy: 20-38 Vs. Control 28-48). While this difference of age is tolerable, it may answer the disparity between the two groups. This suggested hypothesis is founded on the findings in the literature. Brain water content declines with maturation, and components such as the cell and axonal membranes are densely packed during the maturation process, thereby limiting the mobility of the water molecule, consequently reducing diffusivity and the MD of the relevant region[219].

Following this, another study named "Age-related Apparent Diffusion Coefficient Changes in the Normal Brain" reported that brain ADC was shown to exhibit age-related variations throughout four different stages of life, with age-associated exponential decays for the maturation and development phases, a constant term for maturity, and a linear rise with age for senescence[348].

-The second hypothesis is that, because decreased MD values indicated increased diffusion restriction due to biological barriers, this MD decrease could be due to an increase in axonal density, which has been observed in the majority of regions studied previously (amygdala, PFC, parietal cortex, and striatum) in previous studies of cannabis users' brain axonal density[24].

- A third hypothesis can be advocated since new studies in animal models indicate that THC can stimulate neurogenesis, restore memory, and protect against neurodegenerative processes and cognitive decline in Alzheimer's disease. Physically, this neurogenesis will manifest itself as an increase in neuronal density and a decrease in extracellular diffusion, resulting in a reduction in MD.

Recent reviews on imaging evidence of brain impacts linked with regular cannabis use highlight that various studies on the brain anatomy have revealed inconsistent findings[34964350]. According to the most recent of these three reviews[350], approximately half of structural imaging investigations conducted so far have not shown significant differences in the brains of cannabis users and healthy controls.

Therefore, our study aims to contribute to the scientific revolution regarding cannabis's impact on brain structure. As previously mentioned, our research revealed no statistically significant difference in the following anatomical regions:

-Orbitofrontal Cortex
-The inferior temporal gyrus.
-The occipitotemporal gyrus (Fusiform).
-The posterior cingulum.
-ParaHippocamapal region
-Hippocampus
-Amygdala
-Thalamus
-Caudate
-Putamen
-Pallidum

On the other hand, we have found in the following regions that there are significant differences between users and healthy controls:

-Prefrontal cortex -including broca's area-
-The parietal lobe
-The temporal lobe
-The postcentral gyrus.
-The superior parietal lobule.
-The inferior parietal lobule.
-The precuneus.
-The superior temporal gyrus.
-The middle temporal gyrus.
-The anterior and middle cingulum lobe
-The insula

Given that our work on the gray matter is the first of its type to use diffusion analysis over a total ROI, we will compare our findings to those of previous studies that investigated the brain structures of cannabis users using a variety of structural neuroimaging methods. The reviewed studies are presented in table 460.

Table 460: Summary of the reviewed DTI analysis results of previous studies on grey matter in cannabis users.

Reviews	Regions	Techniques	Results
Chye. Y. 2020[350]	Orbitofrontal cortex	Volume	Reduced volume in cannabis users relative to non-users.
	Prefrontal Cortex	Volume	No difference.
	Hippocampus	Volume	Reduced volume in cannabis users relative to non-users
	Amygdala	Volume	No significant net effect
	Striatum	Volume	No significant net effect: Alternately reduced or increased striatal subregion volumes in cannabis users.
	Anterior cingulate cortex	Volume	No difference
Bloomfield MAP. 2019[64]	Orbitofrontal cortex	sMRI - Volume[351]	-No difference between CB users (including CB dependent and and CB non dependent) and healthy controls. -CB dependent exhibit smaller volume than CB non dependent in the medial and the lateral OFC. -Reduced volume in the CB dependent was associated with higher monthly cannabis dosage.
		sMRI - VBM[352] -DTI study -	-Cannabis users had significantly less bilateral orbitofrontal gyri volume.
	Parietal Lobe	sMRI - VBM[353]	-Lower white matter density in the left parietal lobe.

		sMRI – VBM[354].	-Reduced volume in regular users compared to non-users.
	Fusifrom	sMRI – VBM [353]	-Cannabis users compared to healthy control have higher density in the left fusiform gyrus.
	Hippocampus	sMRI[355]	-Past history of cannabis use disorder may be associated with notable diffrences in hippocampal morphology and episodic memory impairments among adults with and without schizophrenia.
	ParaHippocamapal	sMRI – VBM [353]	-Cannabis user compared to healthy control have lower density in the right parahippocampal gyrus. -Cannabis users compared to healthy control have higher density in the left parahippocamapal.
Lorenzetti. V. 2019[349]	Orbitofrontal cortex	sMRI-Volume[356]	-Smaller medial orbitofrontal lobule mOFC.
	Prefrontal Cortex	sMRI-Volume[357] (Adolescent)	-Decrease right moPFC volume of cannabis users compared to controls.
		sMRI-Volume & Thikness[358] (Adolecence and early adulthood)	-In the right frontal lobe: Cannabis users showed bilaterally decrease concavity of the sulci and thinner sulci.
		sMRI-Volume[359]	-No difference between cannabis users and controls in PFC volume.
	Parietal Lobe	sMRI-Volume[356]	-Smaller inferior parietal volumes.
	Anterior	sMRI – VBM [325].	-No variation in gray matter volume.

	cingulate cortex	sMRI – VBM [360]	-No variation in gray matter volume between cannabis users and healthy control.
		sMRI -Volume[361]	-No alteration in the anterior cingulate cortice in very heavy cannabis users compared to healthy control.
	Hippocampus	sMRI – Volume[362]	-Reduced volume of hippocampus in heavy cannabis compared to healthy controls.
	Amygdala	sMRI[363] .	-Reduced volumes of the amygdala in heavy and long term cannabis users.
		sMRI[364].	-No significant differences in the amygdala volume of heavy cannabis users compared to controls.
		sMRI – VBM [325].	- Within the group of heavy cannabis users, grey matter volume in the amygdala correlated negatively with the amount of cannabis use or dependence.
		sMRI – Volume[362]	-Reduced volume of amygdala in heavy cannabis compared to healthy controls.
		sMRI – VBM [365].	-No differences found between daily users and non-users on volume or shape in the amygdala.
		sMRI – VBM and volumetric analysis[366].	-No cortical differences nor smaller volume in the amygdala region of cannabis users compared to healthy control.
	Thalamus	sMRI – VBM [353].	-Greater gray matter density in the right thalamus of cannabis users compared to healthy controls.

	Caudate	sMRI – Volume[351]	-No significant diffrences between healthy controls and cannabis users.
		sMRI – Voxel-based morphometry and volumetric analysis[366].	-Cannabis users showed significantly larger volume than healthy controls of the caudate.
	Putamen	sMRI[367]	-In comparison to healthy controls cannabis dependent participants have a smaller putamenal volume.
		sMRI – VBM [366].	-Cannabis users showed significantly larger volume than healthy controls of the putamen.
	Pallidum	sMRI – VBM and volumetric analysis[366].	-Larger gray matter volume in the pallidum of cannabis users compared to healthy controls.
	Nucleus Accumbens	sMRI – VBM[365].	-No differences found between daily users and non-users on volume or shape in the nucleus accumbens.
		sMRI – Voxel-based morphometry and volumetric analysis[366].	Larger gray matter volume in the nucleus accumbens of cannabis users compared to healthy controls.
Lorenzetti. V. 2016[24]	Parietal Lobe	sMRI – VBM for gray matter density[368]	-High gray matter density in: *Precuneus *Postcentral gyrus

			of cannabis users compared to healthy controls.
	Temporal Lobe	sMRI – VBM for gray matter density[368]	-Lower gray matter density in: *Temporal pole *Superio temporal gyrus. of cannabis users compared to healthy controls.
		sMRI – VBM [369]	-Gray matter volume reduction in cannabis user compared to healthy control in the medial temporal cortex and temporal pole.
	ParaHippocampal	sMRI – VBM [369]	-Gray matter volume reduction in cannabis user compared to healthy control in the parahippocampal gyrus.
	Insular lobe	sMRI – VBM [369]	-Gray matter volume reduction in cannabis user compared to healthy control in the insular lobe.
		sMRI – VBM for gray matter density[368]	-High gray matter density in insula region of cannabis users compared to healthy controls.
		sMRI – Volume[370]	-Compared to non-users cannabis users have decreased cortical thickness in the bilateral insula.
Other studies			
	Temporal Lobe	sMRI – Volume	

Lynn E DeLisi, 2006[371]	Hippocampus and amygdala complex	-DTI study-	-Any significant change in the cannabis users compared with controls.
Ashtari.M[364]	Hippocampus Amygdala	sMRI - Volume	-Smaller volume of the right and left hippocampus of cannabis users. -Smaller right hippocampus volume was correlated a higher amount of cannabis use. -No significant diffrences in the amygdala compared to controls.

Most studies on the impact of cannabis use on the brain structure evaluated the grey matter thickness or the volume, and VBM is among the most commonly used techniques. In this respect, the findings of our research cannot be compared or contrasted with those of other investigations. Since then, no study has employed a similar approach to ours to examine the brain structure of cannabis users.

The VBM is a technique developed in the 1990s by Wright and colleagues[372] for extracting grey matter "density" throughout the whole brain (the relative amount of grey matter but not the cell packing density). The technique is built on the assumption that each MRI voxel includes a combination of three tissue types: grey matter, white matter, and cerebrospinal fluid (CSF). It comprises a series of image processing procedures, including grey matter voxel extraction from T1-weighted images and registration to a standard brain template for subject comparison. Therefore, the voxel-based morphometry technique allows us to estimate the grey matter density in a specific area. In contrast to DTI, this method can only reveal information about the macrostructure of grey matter and overlooks the other components of grey matter.

Considering that, following our research, a VBM study with the same volunteers is envisaged to determine whether or not changes in FA and MD are related to the density of the regions on grey matter neurons. Additionally, by comparing the findings of the two investigations, we can see if differences in FA and MD correspond to variances in grey matter cellular density.

As a result, we will know whether high or light cannabis use changes or impacts axonal, neuroglial, or grey matter neurons.

Chapter III: Discussion of diffusion tensor imaging results in white matter (Tractography).

To assess the structural quality of the cerebral connectivity and the connecting links between the elements of the cerebral circuits, we extracted the fibres originating from, going to, and passing through each region of interest. We then analyzed the variations in the values of the diffusion markers (FA and MD) relating to these bundles to assess the structural quality of the connection links. As a recap, we employed and used graph theory to accomplish this.

White matter is made up of neuronal tracts (axons) that serve as a network connection between brain areas[373]. These tracts are maintained by glial cells, which play a critical role in a variety of fundamental activities, depending on their types [373] [374] [375]:

-Astrocytes serve as a bridge between the circulatory system and adjacent neurons. They are responsible for maintaining the equilibrium of ions and transmitters, as well as metabolism and neural function.

-Oligodendrocytes: produce the myelin sheath and control signal transmission speed, timing, and synchronization.

-Microglial cells are part of the brain's innate immune system and play a role in synaptogenesis and removing some synapses.

THC may have a meaningful impact on the white matter since these glial cells can express functional cannabinoid receptors involved in the endocannabinoid system, therefore influencing neuronal plasticity and indirectly affecting the white matter of the brain[375].

An increasing number of researchers are using diffusion-weighted imaging and diffusion tensor imaging to study cannabis use and cannabis use disorder's impact on the brain.

Several studies and meta-analyses indicate a relationship between substance abuse and white matter microstructure. However, for cannabis use or abuse, the association with white matter integrity is less clear. Moreover, differences in FA and MD values of users compared to non-users differ between studies. One of the possible explanations is that certain findings were limited to the most significant white matter pathways. As a response, we used the graph model to study all white matter associated with a region, as well as a broad range of anatomical locations in both hemispheres.

We were also able to overcome two additional major obstacles that faced researchers[376]:

-Polydrug: Polydrug usage complicates the interpretation of data relating certain drugs to specific white matter differences. In this regard, the selection of our volunteers was based on the fact that our cannabis users are not known to use other drugs and are not even to known to be alcoholic drinkers; only occasional alcohol use is permitted as long as it does not exceed three drinks (glasses) per week, including all types of wine and beer.

-Comorbidity: Most diffusion imaging studies ignore control of mental diseases from their selection criteria, even though some mental illnesses, such as depression, occur at a higher rate in the general population, particularly among drug users. Because of the known association of these diseases with white matter and the difficulty of establishing a satisfying conclusion in their involvement, all cannabis users and non-users were screened for any potential mental comorbidities using the Mini International Neuropsychiatric Interview (MINI).

Since the structural and functional correlation would have a higher sensitivity and be a stronger indicator of abnormalities than those based only on imaging modalities, and since the functional implications of structural alterations in cannabis users is still not determined, we opted to do a statistical correlation of the clinical (Psychometric tests: CUDIT-R, BIS-11 and PSS) and imaging findings (diffusion markers: FA and MD) in several regions.

To do this, we realized an extensive correlation (17 regions, which represents 24.2% of the regions studied) on the regions linked to cognitive functions, reported in the literature, altered among cannabis users.

Table 461 reminds the regions and functions with which they are linked that we have investigated.

Table 461: Regions and functions with which they are linked that we have investigated in correlation analyses.

Reward	-Medial Orbitofrontal cortex & Frontal Med Orb & Frontal Sup Orb -Cingulum ANT -Cingulum Mid -Amygdala -Putamen -Pallidum
Decision making	-Medial Orbitofrontal cortex: Frontal Med Orb & Frontal Sup Orb -PFC -Cingulum Post -Amygdala
Personality trait	-PFC
Learning	-Lateral orbitofrontal cortex: Frontal Mid Orb & Frontal Inf Orb -Hippocampus -Amygdala -Caudate -Putamen
Emotion regulation	-Lateral orbitofrontal cortex: Frontal Mid Orb & Frontal Inf Orb -Cingulate ANT -Parahippocampal -Hippocampus -Insula -Amygdala
Memory	-Hippocampus -Insula -caudate
Prospective memory	-PFC
Speech & Language	-PFC -Insula -Putamen

I. Fractional anisotropy

For FA, eight different comparisons were observed. However, half of them (4) comparisons accounted for 70.5% of the results. Those four intergroup comparisons are:

-Non-users group > Light users' group ≈ Heavy users' group:

Approximately 21,5% of the global intergroup comparisons reveal this variant of comparison.

-Non-users group > Light users' group > Heavy users' group:

Approximately 23% of the global intergroup comparisons reveal this variant of comparison.

-Non-users group > Heavy users' group > Light users' group:

Approximately 13% of the global intergroup comparisons reveal this variant of comparison.

-Non-users group ≈ Light users' group > Heavy users' group:

Approximately 13% of the global intergroup comparisons reveal this variant of comparison.

These data show clearly that FA's value is reduced compared to the non-consuming subject in 70.5 percent of our results, equivalent to 49 anatomical regions. Furthermore, from these 49 anatomical regions, analytical findings showed 14 anatomical areas where there are significant differences between heavy cannabis users, light cannabis users, and controls.

Table 462 summarizes these findings in those regions with different significant comparisons.

Table 462: The quantitative and analytical results of fractional anisotropy in fibers related to each region of interest, revealing significant differences, as well as the functional and structural anatomical regions that correspond to them.

Functional Anatomical areas	The Anatomic Structure	Regions Of interest	The significant differences	The quantitative intergroup comparisons
Orbitofrontal cortex	Medial Orbitofrontal cortex	Left Frontal Med Orb	H Vs C	G.III > G. II > G. I
	Lateral orbitofrontal cortex	Left Frontal Mid Orb	L Vs C	G.III > G. I > G. II
Prefrontal cortex	Dorsomedial prefrontal cortex	Left Frontal Sup	H Vs. C	G.III > G. II > G. I
	Dorsolateral prefrontal cortex	Left frontal mid	H Vs C	G.III > G. II > G. I
		Right frontal mid	L Vs H	G. II ≈ G.III > G. I
Broca's area	Ventrolateral prefrontal cortex	Left frontal inf Oper	H Vs C	G.III > G. II > G. I
		Left Frontal Inf Tri	L Vs C	G.III > G. I > G. II
Parietal Lobe	Postcentral gyrus	Left Postcentral	L Vs C	G. II > G.III ≈ G. I
	Inferior parietal lobule	Left SupraMarginal	H Vs C	G.III > G. II > G. I
Temporal Lobe	Superior temporal gyrus	Left Heschl	L Vs C	G.III > G. I > G. II
		Right Heschl	L Vs C | H Vs C	G.III > G. I > G. II
Limbic Sytsem	Cingulate Gyrus	Left Cingulum ANT	H Vs C	G.III > G. II ≈ G. I
		Left cingulum Post	H Vs C	G.III > G. I > G. II
	Amygdala	Left amygdala	L Vs C | H Vs C	G.III > G. I ≈ G. II

We may derive from table 462 that:

-In the 14 regions (20% of the regions studied) with significant differences between groups, averages of FA were reduced in cannabis users compared to healthy controls in 12 regions.

-The two other regions, the Right frontal mid and the Left Postcentral, show:

*For the right Frontal Mid region light user's group have a higher average than heavy and controls groups, with a significant difference between light and heavy users' groups.

*Concerning the left Postcentral region light users group has a higher average than healthy control and heavy users' groups. The significant difference was between light and heavy users' groups.

-Only two regions, right Heschl and left amygdala, showed significant differences between the two groups of cannabis users and the healthy control group (heavy Vs control & light Vs control).

-Significant difference between **heavy and healthy** control was the meanly observed significant difference in our results (**9 regions**). Following the regions:

*Left Frontal Med Orb	*Left frontal inf Oper	*Left Cingulum ANT
*Left Frontal Sup	*Left SupraMarginal	*Left cingulum Post
*Left frontal mid	*Right Heschl	*Left amygdala

- Significant difference between **light and healthy controls** was the second most observed significant difference, with **six regions** that are:

*Left Frontal Mid Orb	*Left Heschl
*Left Frontal Inf Tri	*Right Heschl
*Left Postcentral	*Left amygdala

-From all the 16 significant differences reported in our results, only one was within the **cannabis users** groups (heavy Vs light). This one was in the right Frontal Mid region.

- Finally, we can also relate that, based on the functional anatomy division that we have been considering from the start of our work and in our ATLAS, except for basal ganglia, each Groupement of regions studied (OFC, PFC, Parietal, Temporal, Limbic system) showed a region or more with significant differences between some of the three compared groups.

We may conclude from all of these observations and findings that:

-Heavy and light consumption of cannabis affects the anisotropy of white matter by decreasing it compared to healthy controls in several brain areas.

-With the white matter of 9 regions that have lower FA in heavy cannabis users' group compared to the healthy control group and white matter of 6 regions with significant difference between light users and healthy control group (1 region, Left Postcentral, with a higher average of FA value and five regions with a lower average of FA value), we may assume that heavy cannabis usage has a greater impact on users' brain areas than moderate use.

-Since, in the right Frontal Mid region, the light users group and healthy control group have almost the same average of FA value, and there is a significant difference within users groups, we can assume that heavy use of cannabis affects the structure of white matter of this region and that light usage does not affect bundle related to this area.

II. Mean diffusivity

For MD, nine different comparisons were observed. One of those comparisons, equality within the three groups, represents 31.5% equivalent to 22 regions. The significant differences were observed in six different combinations of intergroup comparisons:

-G. I > G. II > G.III: Two regions with significant differences demonstrate this variation of group difference.

-G. I > G. II ≈ G.III: Five regions with significant differences demonstrate this variation of group difference.

-G. I ≈ G. II > G.III: Twelve regions with significant differences demonstrate this variation of group difference.

-G. II > G. I > G.III: Six regions with significant differences demonstrate this variation of group difference.

-G. II > G.III ≈ G. I: One region with significant differences demonstrates this variation of group difference.

-G. II > G.III > G. I: Two regions with significant differences demonstrate this variation of group difference.

Forty percent of the regions studied show significant differences between the groups. Furthermore, in 20 regions, cannabis users groups had a higher average of MD than the healthy control group.

In the other eight regions:

- Five regions have a higher MD average in the heavy cannabis users' group than in the light users and healthy control groups, which have a nearly identical MD average.

- In two regions, the average MD was higher in the light cannabis users group than in the healthy control group, and the average MD was lower in the heavy cannabis user group than in the healthy control group.

-The remaining region has a higher average of MD in light user groups than in heavy user groups or in the control group, which have an approximately equal average.

Table 463 summarises these findings in those regions with different significant comparisons.

Table 463: The quantitative and analytical results of Mean Apparent Diffusion coefficient in the white matter related to each region of interest that revealed significant differences, as well as the functional and structural anatomical regions that correspond to them

Functional Anatomical areas	The Anatomic Structure	Regions Of interest	The significant differences	The quantitative intergroup comparisons
Orbitofrontal cortex	Medial Orbitofrontal cortex	Left Frontal Med Orb	L Vs C | H Vs C	G. I ≈ G. II > G.III
		Right Frontal Med Orb	H Vs L | L Vs C	G. II > G. I > G.III
		Left Frontal Sup Orb	L Vs C | H Vs C	G. I ≈ G. II > G.III
		Right Frontal Sup Orb	L Vs C	G. II > G. I > G.III
	Lateral orbitofrontal cortex	Left Frontal Mid Orb	L Vs C | H Vs C	G. II > G. I > G.III
		Right Frontal Mid Orb	H Vs L	G. II > G.III > G. I
		Left Frontal Inf Orb	L Vs C | H Vs C	G. II > G. I > G.III
Orbital surface of the frontal lobe	Gyrus rectus	Left Rectus	L Vs C | H Vs C	G. II > G. I > G.III
		Right Rectus	H Vs L | L Vs C	G. II > G.III > G. I
	The piriform (Or primary olfactory)	Right Olfactory	H Vs L	G. II > G.III ≈ G. I
Prefrontal cortex	Ventromedial prefrontal cortex	Left Frontal Sup Medial	L Vs C	G. II ≈ G. I > G.III
		Right Frontal Sup Medial	L Vs C	G. II > G. I > G.III
	Dorsolateral prefrontal cortex	Left frontal mid	H Vs C	G. II ≈ G. I > G.III
Broca's area	Ventrolateral prefrontal cortex	Left frontal inf Oper	L Vs C | H Vs C	G. II ≈ G. I > G.III
		Left Frontal Inf Tri	L Vs C | H Vs C	G. II ≈ G. I > G.III

Parietal Lobe	The superior parietal Lobule	Left Parietal Sup	H Vs C	G. I > G. II ≈ G.III
	Inferior parietal lobule	Left SupraMarginal	H Vs C	G. I > G. II > G.III
	Left Angular	H Vs C	G. I > G. II ≈ G.III	
	Left Parietal Inf	H Vs L | H Vs C	G. I > G. II ≈ G.III	
Temporal Lobe	Superior temporal gyrus	Left Temporal Sup	H Vs L | H Vs C	G. I > G. II ≈ G.III
		Left Temporal Pole Sup	L Vs C | H Vs C	G. I ≈ G. II > G.III
		Left Heschl	H Vs C	G. I ≈ G. II > G.III
	The middle temporal gyrus	Left Temporal Mid	H Vs L | H Vs C	G. I > G. II ≈ G.III
		Left Temporal Pole Mid	L Vs C | H Vs C	G. I ≈ G. II > G.III
	The inferior temporal gyrus	Left Temporal Inf	H Vs L | H Vs C	G. I > G. II > G.III
Limbic System	Insula	Left Insula	L Vs C | H Vs C	G. II ≈ G. I > G.III
The Basal Ganglia	Putamen	Left Putamen	L Vs C | H Vs C	G. I ≈ G. II > G.III
	Pallidum	Left Pallidum	L Vs C	G. I ≈ G. II > G.III

We may infer that from the table above, where we presented statistical analysis and quantitative descriptive findings:

-In the 28 regions (40% of the regions studied), we found 46 significant differences between groups:

*20 statistical significance between heavy and control groups.

*18 statistical significance between light and control groups.

*8 statistical significance between heavy and light groups.

The statistical results support what was observed in the descriptive findings: the variations in MD are mostly between cannabis users and controls.

Finally, we can mention that consistent with the functional anatomy divisions we have used throughout our work and in our ATLAS, each Groupement of regions studied (OFC, PFC, Parietal, Temporal, Limbic system, and basal ganglia) revealed at least one region with significant differences between two of the three compared groups.

III. Discussion of white matter's fractional anisotropy, mean diffusivity, and the correlations with the clinical and psychological evaluations by anatomical regions

We can assume from all of these observations and findings regarding fractional a nisotropy and apparent diffusion:

-Heavy and light consumption of cannabis affects the diffusivity and anisotropy of white matter by decreasing the fractional anisotropy and increasing mean apparent diffusion compared to healthy controls in several brain areas.

- Taking into account:

*The nine regions with a lower FA value in heavy cannabis users compared to the healthy control group and six regions having a significant difference between light users and the healthy control group (1 region, Left Postcentral, having a higher average FA value and five regions having a lower average FA value).

*The statistical significance, concerning MD, between user groups and healthy control.

We can perceive that heavy and light cannabis usage has, to a certain degree, the same effect on FA and MD of with matter of users' brain.

Ultimately, we can presume that chronic cannabis usage, eighter heavy or light, affects white matter microstructure, with an impact overstated a bit more in heavy cannabis users.

These microstructural changes indicated by a decrease in FA and an increase in MD may be linked to[231]:

- Degenerative axonal processes and a reduction in neuronal density.

-Demyelination.

We will discuss the FA and MD results, statistically significant, and the correlations (clinical findings with DTI data) based on the anatomical division (OFC, PFC, Parietal,

Temporal, Limbic system, and basal ganglia) to consolidate our discussion and compare our findings to previous studies.

➢ Orbitofrontal cortex:

The white matter related to the medial region of the OFC, compared to healthy controls heavy cannabis users demonstrate a low fractional anisotropy in **Frontal Med Orb (left)** and higher MD in **Frontal Med Orb (Left and Right) and Frontal Sup Orb (Left)**.

On the other hand, light cannabis users show a high MD in **Frontal Med Orb and Frontal Sup Orb (Left and Right) compared to healthy controls.** No significant differences were found within cannabis users (H Vs. L).

Concerning the white matter of the lateral part of the OFC, we identified low fractional anisotropy in heavy cannabis users in **Frontal Mid Orb (Left)** compared to the healthy control. Heavy users also show higher MD than healthy controls in Frontal Mid Orb and Frontal Inf Orb (Left) regions.

Addressing the light users, differences are reported with healthy controls in the Frontal Mid Orb and Frontal Inf Orb, with a high MD in cannabis users. On this side of the OFC, we report a difference within cannabis users also with a higher MD in light users in the Frontal Mid Orb (Right).

Significantly, our findings posit that chronic cannabis use is associated with alterations of a cluster parts of OFC.

As we have mentioned before in out Atlas section the OFC is highly interconnected with several brain areas: PFC, the nucleus of the mediodorsal thalamus, nucleus accumbens, hippocampus, temporal lobe, insula and amygdala[247]. In certain aspects, owing to this connectivity, some functions such as anticipation of rewards, decision-making, associative learning, and part in emotion regulation are strongly related to the OFC[249]. And it is for this reason that it is crucial to explore the structure of OFC

in chronic cannabis users, since these functions have repeatedly been demonstrated to be impaired in the latter.

The relevance of studying this region's connectivity is also related to the fact that the chronic relapsing nature of addiction appears to be associated with underlying neurophysiological abnormalities in the reward, stress, and executive function circuits[27].

Additionally, we conducted correlation analyses to understand the relation between these structural alterations and behavior state by correlating psychometric test scores with FA and MD values.

Concerning the association of CUDIT-R, BIS-11, and PSS scores to FA and MD results of the medial orbitofrontal cortex, all tests scores were negatively correlated with FA values and positively correlated with MD values.

Regarding statistically significant correlations:

-The **fractional anisotropy** values of the **left Fontal Med Orb** part correlate with statistical significance with the three tests:

*__CUDIT-R__: r=-0.4657, r^2=0.2169, and p-value=0.0445

*__BIS-11__: r=-0.4800, r^2=0.2304, and p-value=0.0375

*__PSS__: r=-0.4904, r^2=0.2405, and p-value=0.0330

-**Fractional anisotropy** values of **left Frontal Sup Orb** and **PSS** test correlate with statistical significance also with PSS test: r=-0.5118, r^2=0.2620, and p-value=0.0351.

Correlation analysis findings in the lateral orbitofrontal cortex show a negative association between values of fractional anisotropy and PSS scores, in the **left** hemisphere's **Frontal Mid Orb** and **Frontal Inf Orb** and a positive association between MD values of the **left Frontal Inf Orb** and PSS scores:

*The Frontal Mid Orb, FA and PSS correlation:

r=-0.5655, r^2=0.3197, and p-value=0.0116.

*The Frontal Inf Orb, FA and PSS correlation:

r=-0.4586, r^2=0.2104, and p-value=0.0483.

This result reaffirms the critical role described in the literature for this region in reward and addiction associated with the cannabis use disorder and trait impulsivity levels), decision-making (association with the trait impulsivity levels), and emotional processes (association with the perceived stress levels).

Additionally, our findings demonstrate that the clinical manifestations of cannabis use and dependence in our volunteers are highly associated with microstructural changes revealed by diffusion markers (FA and MD).

Our findings are consistent with those of a previous study of white matter microstructure in marijuana smokers. Filbey 2014 et al.[352] found high fractional anisotropy (FA) (increased structural connectivity) in tracts innervating the OFC (forceps minor) with regular use but decreased following long-term heavy use, implying that chronic drug use affects structural connectivity.

Filbey (2014) also reported high functional connectivity in the orbitofrontal cortex (OFC) network of marijuana users. Along with these results, Zimmermann et al. (2018)[377] found alterations in mOFC neural activity and mOFC-dorsal striatal connectivity in response to negative stimuli and in the absence of task difficulty using task-based and resting-state fMRI. Positive content processing and behavioral markers of emotion perception, on the other hand, were shown to remain intact.

The functional outcomes from these two studies reinforce the results of our correlation between behavior and structural connectivity, which revealed a strong negative correlation among FA in mOFC and the scores of CUDIT-R, BIS-11, and PSS, as well as a correlation, slightly less significant, between the PSS and FA and MD of lateral OFC, a region known for its involvement in emotional regulation[249].

➢ Orbital surface of the frontal lobe

Two gyri compose this region: the gyrus rectus and olfactory gyrus. Fractional anisotropy results of cannabis users and healthy controls don't show any significant differences between the three groups.

Regarding mean diffusivity, light cannabis smokers have an elevated MD than heavy smokers and healthy controls with significant differences between light users and healthy controls in the **gyrus rectus** (left and right) and higher MD with statistical significance with heavy users in the **gyrus rectus (left) and the right olfactory region.**

Heavy smokers volunteers, on the other hand, in addition to the differences with light smokers, have an MD significantly greater than healthy controls in the **gyrus rectus (left)**.

Since we considered the gyrus rectus as part of medial OFC in our ATLAS, and as reported in literature also, we can add our results for this region to the mOFC results. This supports the results of our work and the literature on mOFC in cannabis users.

Along with the olfactory system, the piriform gyrus is densely concentrated in CB1 receptors[378]. CB1 receptors have been identified mostly at GABAergic synapses in the anterior PC (aPC), where they influence inhibitory transmission and plasticity[378 379]. CB1 receptors in the aPC specifically regulate olfactory memory retrieval associated with pleasantly motivated behaviors[380]. In addition to the thalamus and hypothalamus, the piriform gyrus is closely connected to limbic structures (hippocampus and amygdala) [254]. Functions, connectivity of the region, and the high density of CB1 receptors point to the necessity of investigating the white matter structure of this brain area in cannabis smokers.

The PC is a brain region that is also capable of producing epileptiform activity[381]. Furthermore, Lazarini-Lopes W et al (2021)[382]. revealed that CBD reduced prolonged

neuronal hyperactivity in an animal model of epilepsy by reducing FosB immunostaining in the forebrain (basolateral amygdala nucleus and piriform cortex) [382]. In conditions such as drug addiction, Parkinson's disease, depression, and antidepressant therapy, FosB is a critical transcription factor in long-term adaptative changes[383].

However, in another animal study carried by Lazenka MF et al.(2017) [384], they discovered that a history of repetitive THC administration primes THC-mediated FosB expression in the NAc and PFC.

Regarding our work, we report an increase among MD in light smokers compared to healthy controls and heavy users, but only a statistically significant difference between light and heavy smokers. Dose-dependent structural changes in this region may explain these findings.

Together with those from the literature, our findings demonstrate how this area is intricately related to the cannabinoid component (THC and CBD).

Therefore, to study the impact of cannabis use on the white matter at this brain structure, further, well-conducted structural and functional neuroimaging studies are required, with monitoring of the concentration of cannabis smoked in dosages of THC and CBD.

➢ The prefrontal cortex

The dorsolateral, dorsomedial, ventromedial, and orbitofrontal cortical divisions are the essential functional divisions[267]. Previously we discussed the results of our work in the orbitofrontal part; we will now continue our discussion of the outcomes in the remaining parts.

The white matter related to the Ventromedial prefrontal gyrus (Frontal Sup Medial) revealed only significant differences between light smokers and healthy controls in mean diffusivity, with high levels of MD in light cannabis users compared to healthy controls in Frontal Sup Medial (Left and right).

For the white matter of the dorsomedial prefrontal cortex (Frontal Sup), heavy users exhibit low fractional anisotropy (in the left hemisphere) compared to healthy controls.

On the other hand, tracts associated with the dorsolateral prefrontal gyrus (frontal mid) show a high fractional anisotropy in heavy users compared to healthy controls in the left hemisphere and a difference between light and heavy smokers in the right hemisphere with a lower FA in heavy users.

These findings demonstrate the prefrontal region tissues' significant vulnerability to cannabis usage at both levels of intake that we supposed: heavy and light, manifested by both diffusion markers (FA and MD).

Our findings of decreased FA and increased MD in several areas of the prefrontal cortex show clues that cannabis has a detrimental effect on the integrity of the frontal white matter, not just in heavy users, but also in light users.

Our findings also provide an extension for previous studies in cannabis users, which noted altered FA and/or altered MD in the prefrontal region's parts. Arnone D et al.(2008) [385] reported an MD significantly increased in marijuana users relative to controls in the corpus callosum region where white matter passes between the

prefrontal lobes. Three years later, Gruber SA et al. (2011)[330] had reinforced these findings by reporting significant reductions in the left frontal FA in marijuana smokers relative to non-smoking controls.

A more recent study by Becker et al. (2015)[386] found that young adults with adolescent-onset marijuana use showed reduced longitudinal development of FA in key frontal white matter tracts.

The findings in our study and the overwhelming majority of research carried on this region, however, are in disagreement with the work of DeLisi et al. (2006)[371]. The apparent diffusion coefficient (ADC) for adolescent cannabis users was significantly lower relative to non-cannabis users in the left middle frontal gyrus. The fractional anisotropy (FA) was significantly higher in cannabis users in the left superior frontal gyrus. DeLisi and colleagues, on the other hand, did not provide precise data on characteristics associated with the onset, dose, and frequency of drug usage.

Additionally, none of the ten cannabis users examined were current frequent users. They also employed only six gradient directions and one b = 0 images in their DTI methodology as well. Moreover, since the number of directions chosen during acquisition impacts the estimation of fractional anisotropy[214], their investigations seem to be not very sensitive to structural variations.

The prefrontal cortex plays an important role in psychological regulation during adolescence[131]. Its interaction with other functionally specialized brain regions via white matter tracts is critical for integrative some major brain functions (Prospective memory[260], speech, and language[261], Personality[264], Decision making[265 266]). Those functions are reported to be significantly impacted by chronic cannabis usage[26].

To evaluate the relation between some of the psychological aspects and the structural variations in this region, we correlated CUDIT-R, BIS-11, and PSS scores with the diffusions markers FA and MD.

Our findings revealed a strong association between the behavioral aspect evaluated in our volunteers and the structural variation (predominantly fractional anisotropy) in the prefrontal region.

A negative association between the fractional anisotropy values of the right Frontal Sup Medial and the BIS-11 scores was found r=-0.5269, r^2=0.2776, and p-value=0.0205 and between the fractional anisotropy values of the Frontal Sup Medial (left and right) and the PSS:

* The Left side: r=-0.4811, r^2=0.2314, and p-value=0.0370.

* The right side: r=-0.4806, r^2=0.2309, and p-value=0.0373.

The fractional anisotropy in the Frontal Sup part (Left and Right) also correlated negatively and with the three tests: CUDIT-R, BIS-11, and PSS.

CUDIT-R:

*Left: r=-0.5931, r^2=0.3518, and p-value=0.0074.

*Right: r=-0.5405, r^2=0.2921, and p-value=0.0169.

BIS-11:

*Left: r=-0.6023, r^2=0.3627, and p-value=0.0064.

*Right: r=-0.5769, r^2=0.3328, and p-value=0.0097.

PSS:

*Left: r=-0.6048, r^2=0.3658, and p-value=0.0061.

*Right: r=-0.5457, r^2=0.2978, and p-value=0.0157.

The same findings as the Frontal Sup Part (Left and Right) are reported in the Frontal Mid (Left and right) with a correlation of the mean diffusivity, also, with the left Frontal Mid with BIS-11 scores.

CUDIT-R:

*Left: r=-0.5613, r^2=0.3151, and p-value=0.0124.

*Right: r=-0.4911, r^2=0.2411, and p-value=0.0328.

BIS-11:

FA in the Left: r=-0.5777, r^2=0.3337, and p-value=0.0096.

FA in the Right: r=-0.5236, r^2=0.2742, and p-value=0.0214.

MD in the left: r=0.4790, r^2=0.2295, and p-value=0.0380.

PSS:

*Left: r=-0.6187, r^2=0.3828, and p-value=0.0047.

*Right: r=-0.4790, r^2=0.2294, and p-value=0.0380.

Prior to our study, research that correlated psychometric results with DTI data in the prefrontal region demonstrated strong evidence that structural variation in this region is strongly related to cognitive and behavioral state.

Clark DB et al. (2012)[387] used the Behavior Rating Inventory of Executive Function to assess psychological dysregulation and diffusion tensor imaging to assess white matter structure (FA, RD, AD). The statistical analysis of those data indicated that, in addition to the considerable prefrontal and parietal WM disarray, white matter disorganization was highly correlated with psychological instability and cannabis-related symptoms.

Concerning the impulsivity trait, a work consisting of two studies that may be considered as a reference in its category has reported contradictory findings, but which contribute significantly to our knowledge of variations in FA values (depending on the protocol used) and impulsivity levels in relation to cannabis usage.

First, Gruber et al. (2011)[330] revealed frontal white matter changes among marijuana smokers, as well as a positive association between BIS scores and frontal FA. However, in the second study, Gruber et al. (2013)[388] reported that Marijuana smokers had reduced FA, which is consistent with prior research; but, when it came

to the association between BIS scores and FA, they found that greater impulsivity levels were associated with lower FA.

The association between BIS and FA was identified in the early onset smokers but not in the late-onset smokers. This finding also corroborates our findings of the correlation between age of onset and BIS levels, which were shown to be highly inversely associated. Concerning the reasoning for the divergence between the two studies in the correlation findings, the initial study used a limited DTI technique, collecting data from just six directions and only a subgroup of participants (N = 10). study In comparison, the second investigation used a complete DTI collection method (48 directions), and a considerably larger sample size (N = 25), all of which lends credibility to the second conclusion.

➢ The Broca's area

Our findings in this region, involved in speech production, revealed remarkable differences (in only the left hemisphere) between heavy, light cannabis users and healthy controls.

In the Frontal Inf Oper area, differences in the fractional anisotropy between heavy smokers and healthy controls were identified, as were differences in the mean diffusivity between light smokers and healthy controls and between heavy users and healthy controls.

The Frontal Inf Tri area results differ from the Frontal Inf Oper area results only in terms of FA, since here differences between light smokers (not heavy users) and healthy controls are identified; however, the MD results are identical to those found in the Frontal Inf Oper area.

The Broca's area is associated with the coordination of information translation across large-scale cortical networks involved in spoken word creation and the creation of a suitable articulatory code to be applied by the motor cortex[261].

Verbal learning and memory have been reported to be impaired in chronic cannabis users[26]. A study comparing the speech of individuals with a history of recreational cannabis use to non-drug-using healthy controls discovered slight changes in speech timing, vocal control, and voice quality between individuals with a history of predominantly low-to-moderate cannabis use and matched controls[389].

Returning to the DTI research, Ashtari M etal.[390] investigated the white matter integrity in young adult cannabis users compared to matched healthy control subjects, and tractography findings in the arcuate areas revealed reduced FA and increased MD.

These results join and reinforce our findings since the arcuate fasciculus is the main bundle that composes the Broca's area. It is the pathway that communicates this later to the Wernicke's area in the temporal lobe[273].

➢ The parietal cortex

The parietal lobe is a region with strong connections to the cortical[271272 274275276] and subcortical regions; its functions vary according to subregion, but it is known to be involved in the initial cortical processing of tactile and proprioceptive information, as well as higher-order tasks such as motor planning and as a secondary somatosensory that generates a high-order input (Sensorimotor planing, learning, language, spatial recognition, and stereognosis)[265].

Our findings in this region revealed high impairment in heavy cannabis smokers compared to healthy controls and even to light consumers (in one subregion). All the structural alterations and variations were identified within the left hemisphere. For the fractional anisotropy, heavy users show low FA in the left Supramarginal part compared to healthy controls.

Heavy users also revealed higher mean diffusivity than healthy controls in the left Parietal Sup, SupraMarginal, angular and Parietal Inf regions. This reveals that heavy consumption alters the posterior structure of the parietal lobe, the area with the most corticocortical connectivity. In addition to the differences between heavy consumers and healthy controls, heavy users have higher MD than light consumers in the left parietal Inf area (part of the parietal cortex above the supramarginalis gyrus and between the supramarginal and angular gyri that does not belong to the supramarginal and angular cortex).

The other difference detected in the light consumers' group is a difference with healthy controls for the FA in the left postcentral region, an area implicated in the initial cortical processing of tactile and proprioceptive information[265].

The current findings of our study are largely consistent with those reported in the previous researches that examined parietal white matter. Orr et al. (2016)[391], in one of the few longitudinal studies of chronic cannabis use, found that earlier age of onset use was associated with decreased FA in long-range tracts, including the Superior Longitudinal Fasciculus and Inferior Longitudinal Fasciculus. Acknowledging that, the superior longitudinal fascicule comprises three separate segments and connects all the posterior parietal cortex's components to the frontal cortex[271].

Moreover, Becker et al. (2015)[386], over the course of two years, found that young adults with adolescent-onset of marijuana use showed reduced longitudinal development of FA in key frontal, central, and parietal white matter tracts.

A recent study, conducted by Manza P et al. (2020)[392], reinforced these results of white matter (related to the parietal cortex) anisotropy disruptions.

Manza P et al. (2020)[392] demonstrated that cannabis-dependent individuals had lower fractional anisotropy than controls in white matter bundles innervating the parietal cortex, particularly precuneus[392].

➢ The temporal cortex

In addition to the high connectivity of the temporal lobe that we have previously detailed in our Atlas, it is reported that chronic cannabis use decreases the availability of CB1R in this cortical region[152]. That altered medial temporal lobe morphology[355]and function[393] is associated with Episodic memory dysfunction in cannabis use, including increased risk of false memories. These findings, among other aspects, illustrate the strong interest in studying the white matter of this anatomical region in cannabis users.

In our study, fractional anisotropy results revealed lower FA for the light users than healthy controls in the Heschl area (left and right) and a lower FA in heavy consumers in the right Heschl.

Mean diffusivity was higher sensible to variations; higher MD was found in heavy and light users compared to the control group in several subregions and lobule and exclusively on the left hemisphere.

Heavy cannabis users have a higher MD than the control group in the Temporal Sup, Temporal Pole Sup, Heschl, Temporal Mid, Temporal Pole Mid and the Temporal Inf regions. In two regions, in addition to the significant differences between heavy smokers and healthy controls also light users revealed a higher MD than controls; these regions are as follows:

-Temporal Pole Sup

-Temporal Pole Mid.

Significant variation in the temporal lobe outcomes was also seen within cannabis users (heavy and light groups); these variations were observed in the left hemisphere as well and at the following regions:

-The Temporal Sup -The Temporal Mid -The Temporal Inf

Returning to the literature, a DTI research conducted by Ashtari et al. (2009)[394] that used voxel-wise and tractography techniques to examine the connectivity of this area in marijuana users reported reduced FA and increased trace in frontotemporal regions relative to non-marijuana smoking control subjects. It is worth noting, nevertheless, that a subgroup of marijuana smokers in this study meet the diagnostic criteria for alcohol misuse, which, while improbable, may have influenced the findings; yet, as previously stated, we excluded cannabis smokers who are alcohol users from our study design.

As for the frontal and parietal lobes, Becker et al. (2015)[386] found that young adults with adolescent-onset of marijuana use showed reduced longitudinal development of FA in key temporal white matter tracts as well.

In our Atlas, we have previously indicated that the corticocortical connection of the temporal lobe is ensured by the superior longitudinal fasciculus, uncinate fasciculus, and inferior longitudinal fasciculus.

These three pathways are critical for the temporal lobe's functioning; the superior longitudinal fasciculus is claimed to be engaged in executive processing[395396], uncinate fasciculus connects temporal regions with the orbitofrontal cortex, which facilitates the integration of affective memory associations into decision processes[397] and the inferior longitudinal fasciculus, connecting the occipital region to the temporal lobe, plays a crucial role in visual guiding of cognition[398].

A recent DTI study, done by Cousijn J et al. [324], evaluated the relationship between cannabis use, dependence severity, and white matter microstructure hypothesis that lower FA in the uncinate fasciculus and inferior longitudinal fasciculus plays a role in the biassed cognitions in response to (visual) cannabis cues towards cannabis use that are often observed in heavy cannabis users.

Although some studies, Ashtari et al. (2009) [390] and Becker et al. (2015)[386], have demonstrated a reduction in temporal lobe's tracts FA, our research has shown variances in MD. Given the wealth of differences results obtained for the MD and our investigation's lack of sensitivity to changes in FA, and given that the number of directions chosen during acquisition affects the estimation of fractional anisotropy[214], the lack of results in FA may be due to the acquisition protocol used in our study. Therefore, more investigations with a well-conducted MRI acquisition protocol and controlled drug co-use are required to study the implications and processes behind the current findings.

➢ The limbic system

The structures that have been hypothesized to belong to the limbic system in our work and for which we could explore related white matter are: Cingulum Ant, Cingulum Mid, Cingulum Post, ParaHippocampal, Hippocampus, Insula, Amygdala. These structures are shown to be highly concentrated in cannabinoid receptors[139]. Furthermore, through the network of the limbic system, they contribute to different cognitive functions, including spatial memory, learning, motivation, emotional and social processing[290], which are highly vulnerable to chronic cannabis use and abuse[26 27 154].

As evidence, studying the brain structures of cannabis users cannot be sufficient without investigating the limbic system network.

In our clinical sections, we evaluated and discussed three clinical and psychological parameters (reward processing, impulsivity, and perceived stress) that are intrinsically linked to the limbic network and altered in cannabis users. Therefore to enhance our work and further one of our objectives, investigating the functional implications of structural abnormalities, we correlated all DTI findings in structures studied of the limbic system to all the outcomes of the three psychometric tests.

The structural investigations, through tractography, revealed restricted findings, in the left hemisphere only, to anterior and posterior cingulate, amygdala and insula The fractional anisotropy in the left Cingulum Ant and the left Cingulum Post of heavy cannabis smokers were significantly lower than controls. The white matter related to the amygdala of cannabis users (heavy and light groups) is also lower than controls.

Regarding the mean diffusivity, heavy and light users' left insula showed a higher MD than healthy controls.

We found rich and numerous significant correlations between clinical and DTI findings in the previous three regions (only) with significant differences between groups.

CUDIT-R correlations:

-*With fractional anisotropy values of white matter related to:*

*The right cingulum Ant: r=-0.5333, r^2=0.2844, and p-value=0.0187.

*The left cingulum Mid: r=-0.5265, r^2=0.2772, and p-value=0.0206.

*The left Amygdala: r=-0.5222, r^2=0.2727, and p-value=0.0218.

-With mean diffusivity values of white matter related to:

*The left Insula: r=0.6214, r^2=0.3862, and p-value=0.0045.

BIS-11 correlations:

-With fractional anisotropy values of white matter related to:

*The right cingulum Ant: r=-0.5547, r^2=0.3077, and p-value=0.0137.

*The left cingulum Mid: r=-0.5953, r^2=0.3543, and p-value=0.0072.

*The left Amygdala: r=-0.5222, r^2=0.2727, and p-value=0.0218.

-With mean diffusivity values of white matter related to:

*The left Insula: r=0.5339, r^2=0.2850, and p-value=0.0185.

PSS correlations:

-With fractional anisotropy values of white matter related to:

*The left cingulum Ant: r=-0.4779, r^2=0.2284, and p-value=0.0385.

*The right cingulum Ant: r=-0.5369, r^2=0.2882, and p-value=0.0178.

-With mean diffusivity values of white matter related to:

*The left Insula: r=0.6377, r^2=0.4066, and p-value=0.0033.

❖ Cingulum region

One of the few studies that applied the graph theory to diffusion tensor imaging and tractography, just as we did, Kim D-J et al. (2011)[399], found that cannabis users had less efficiently integrated global structural networks alongside altered local connectivity in the cingulate. Furthermore, schizotypal and impulsive personality traits were correlated to global network efficiency across all participants.

In the cingulum region, another more recent study, Jakabek D et al. (2016)[400], reported lower FA in several brain regions of cannabis users and a higher axial diffusivity association with duration of cannabis use in the cingulum angular bundle. On the contrary, they reported that younger users showed predominantly reduced axial diffusivity. Their findings imply that exogenous cannabis affects normal brain maturation, with effects varying according to the neurodevelopmental stage.

Our correlations findings may provide further evidence for functional impairment in the reward, executive function, and emotional circuits to be associated with structural alterations of cingulum white matter in cannabis smokers.

In terms of correlations between psychometric and DTI results in limbic structures, our work is so far the first of its kind. However, the functioning of the reward, executive, stress, and emotional circuits in chronic cannabis users has been widely explored.

An fMRI study examined whether cannabis use sensitizes and disrupts the mesocorticolimbic reward processes in chronic cannabis users using a hedonic cue-reactivity task. The cingulate gyrus (along with the orbitofrontal cortex (OFC), striatum, and ventral tegmental area (VTA)) regions along the mesocorticolimbic reward pathway showed a greater BOLD response to cannabis cues[401].

Regarding impulsivity, a study that used the Stroop and Go/No-go tasks, which is excellent for measuring impulsiveness, revealed impaired response inhibition in cannabis users compared to non-users associated with anterior cingulate hypoactivation[402][403].

On the other hand, during negative emotional stimuli, some studies have found decreases in BLOD response within the cingulate (in addition to the frontal cortex and the amygdala) in adult heavy and regular cannabis users[404] [405].

❖ Amygdala

The main tracts connecting the amygdala to the other brain structures are fibres constituting the cingulum (which linked it to the cingulate cortex) and the uncinate fasciculus, a crucial pathway of the limbic system that connects the amygdala structure to the OFC.

Our considerable concomitant white matter results related to the orbitofrontal cortex, cingulum, and amygdala highlight the important influence of cannabis usage on this network.

Previous DTI research of white matter in younger cannabis users has generally found significant impairment results in the uncinate tract of cannabis users. Shollenbarger et al. (2015) [406] reported significant results with lower FA and increased MD in uncinate fasciculus of cannabis users. While most studies do not correlate the functional and psychometric findings with the DTI data, Shollenbarger et al. (2015)[406] reported differences in depressive symptoms correlating with FA in the left uncinate fasciculus.

Furthermore, in Jakabek D et al. (2016) [400] work on white matter tract integrity in regular cannabis users with evaluating the effects of cannabis use and age, they reported higher Radial Diffusivity (RD) of the right angular bundle (tract belonging to the cingulum) and right uncinate fasciculus tracts in younger users compared to non-using controls. Acknowledging that the elevation of RD can be interpreted as demyelination or axonal density decreasing or axonal degeneration.

Moreover, as we previously reviewed, Cousijn J et al. (2021) [324] reported that earlier onset of weekly cannabis use was related to lower FA in the right uncinate fasciculus, and this despite the lack of group differences which is the inclusion of sporadic cannabis users rather than cannabis naïve individuals in the control group.

Regarding functional and emotional findings alongside the literature studies that we previously reviewed, our correlations (left amygdala white matter FA with CUDIT-R and BIS-11 scores) find their scientific strengthening with a functional study that showed hypoconnectivity between the amygdala and DLPFC within active users and orbitofrontal-striatal and amygdalar hyperconnectivity following 28 days of abstinence[377].

❖ Insula

The insula is one of the main structures of the limbic system that belong to "Yakovlev's circuit"[293]. Through different networks, the insula is known to be implicated in several functions related to our research interest: emotion, empathy, pain, language, speech, memory, and work memory are all functions related to this area[299 300 301].

Our findings, which reveal an increase in MD of white matter in cannabis users in this region, demonstrate and confirm the influence of heavy and light consumption on WM in the insula.

Our work is the first to apply graph theoretical tractography to exclusively elucidate the precise impact of cannabis use on insular WM tracts, which may help add knowledge about the neurobiology of cannabis and THC addiction.

Nevertheless, the functional activity and connectivity related to the insula have previously been studied. In Pujol et al. (2014)[407] study, the activity of the posterior cingulate cortex and the insula were shown to be anticorrelated. These connectivity characteristics were linked with a decrease in anxiety ratings, indicating a modification in affect state due to alterations in brain function with cannabis addiction. It was also suggested that cannabis might enhance visceral sensations via insula activation to modify affect status[407 27]. In addition, one study, Filbey et al. (2016)[401], found substantial positive relationships between cue-induced self-rated craving for cannabis and BOLD responses in the mesocorticolimbic system and the insula in cannabis users. Furthermore, these findings support the addictive concept of cannabis as insula activation may serve as a biomarker to potentially predict relapse [401 27].

❖ Hippocampus and ParaHippocampal formation.

In terms of the hippocampus and parahippocampal white matter findings, descriptive FA results revealed that heavy and light users in the left hippocampus and parahippocampal had lower averages than controls. On the other hand, heavy users had lower hippocampus values than light users and non-using controls on the right side, while light users had greater FA in the right parahippocampal than healthy controls and heavy users.

Regarding the MD results, white matte results of all three groups in the parahippocampal were roughly equal in both hemispheres.

Concerning the hippocampus, heavy users had a lower MD than the other three groups, indicating a stronger white matter structure in both hemispheres.

Also, our correlations statistical analysis did show any significant correlation with the three psychometric tests (CUDIT-R, BIS-11, and PSS).

As for all brain regions and white matter tracts, only a few DTI studies and neuroimaging studies have investigated structural impairments of hippocampus WM in cannabis users, and so far, no DTI study on parahippocampal white matter in cannabis smokers.

Yücel et al. (2010) [408] Zalesky et al. (2012)[409] are the two principal DTI studies that reported WM results in the hippocampus.

Yücel et al. (2010)[408] stated that inhalant users had lower FA in white matter surrounding the hippocampus in the left and right hemispheres relative to controls.

Zalesky et al.(2012)[409] found impaired axonal connectivity in the right fimbria of the hippocampus. Radial and axial diffusivity in these pathways was associated with the age of cannabis onset.

The contradiction of our findings with Yücel et al. (2010)[408] and Zalesky et al. (2012)[409] works can be addressed and elucidated from several technical, demographic, chemical, and neuropathological points of view.

Firstly the lack of significance may be due to the restricted number of participants compared to Zalesky et al. (2012)[409] study (59 cannabis users Vs 33 matched controls).

Our protocol of MRI data acquisition is another parameter that may be impacted our findings. Since the number of directions chosen during acquisition impacts the estimation of fractional anisotropy and thus, MD and FA values vary with the used field strength with an increased number of direction, and field strengthening increase the sensitivity to the variations of diffusion markers[410214]. The two studies can be considered more efficient in this regard since they used a higher field than our (3T vs 1.5T) and higher directions.

On the other hand, alcohol consumption reinforces and values our findings and analysis since our participants are known to be not alcoholic consumers. There was considerable alcohol co-consumption with cannabis in both of the studies mentioned above, which can have a major effect on the hippocampus structure as alcohol significantly impacts it[411].

➢ Basal Ganglia

The analysis of connecting fibres related to Caudate, Putamen, and Pallidum nuclei indicated limited results regarding FA and MD.

Variations in fractional anisotropy (FA) at the left hemisphere showed heavy users group with lower FA values than light users, who had lower FA values than the control group, but without any statistical significance between the three groups. However, FA values and differences of fibres associated with these three regions on the right side were unspecific and highly variable.

On the other hand, the MD results revealed three statistical significance between groups. In the left putamen, significance was detected between light smokers and controls and between heavy smokers and controls with an MD higher in cannabis users than the healthy controls. Moreover, in the left pallidum, light users significantly differ from healthy controls with a higher MD in cannabis users than controls.

Even that CB1 receptors are densely expressed in areas associated with reward processing and conditioning, including the ventral pallidum, caudate putamen[116159], almost any previous DTI study on cannabis users' brain connectivity did extract and report results of diffusion markers of WM tracts related to these regions.

The Conveying information from the internal, self-generated activity is functionally transmitted to basal ganglia from the frontal lobe via segregated frontal-subcortical circuits, and to further modulate purposeful behaviours according to the context; basal ganglia receive additional influence from the sensory system.

For this purpose, Blanco-Hinojo L et al. (2017)[412] used resting-state fMRI to investigate the effects of cannabis on basal ganglia functional connectivity in early-onset chronic cannabis users. They hypothesized that cannabis use would affect functional connectivity between the basal ganglia and both internal (frontal cortex) and external (sensory cortices) sources of impacts. Their outcomes had shown that frontal and sensory inputs to the basal ganglia are attenuated after chronic exposure to cannabis.

This impact was in line with the predicted behavioural effects of chronic cannabis use, including decreased reactivity to internal and external motivating signals.

As we have frequently mentioned, significant impairments in the emotional and motivational domains have been identified in cannabis users. As we demonstrated in our study, this broad profile of behavioural changes is compatible with an effect of cannabis on brain structures critical to the integration of multiple-source information.

Furthermore, the basal ganglia network may be seen as multifaceted loops and circuits of reentering, wherein the motor and associative, which are primarily engaged in the control of movement, behaviour and emotions[306].

By correlating FA and MD results to behavioural states (psychometric test findings), we demonstrate that structural changes are compatible with behavioural and functional conditions in our participants.

Positive statistically significant correlations were present with results of MD in the three tests in the left pallidum and putamen. In addition, FA caudate results also showed a significant negative correlation with PSS results.

CUDIT-R:

With the *MD* of *left Putamen WM*:

r=0.5591, r^2=0.3126, and p value=0.0128.

With the *MD* of *left Pallidum WM*:

r=0.5050, r^2=0.2550, and p value=0.0274.

BIS-11:

With the *MD* of l*eft Putamen WM*:

r=0.5667, r^2=0.3211, and p value=0.0114.

With the *MD* of *left Pallidum WM*:

r=0.4729, r^2=0.2236, and p value=0.0409.

PSS:

With the *FA* of *the left caudate WM*:

r=-0.4710, r^2=0.2219, and p value=0.0418.

With the *MD* of *left Putamen WM*:

r=0.5647, r^2=0.3189, and p value=0.0118.

With the *MD* of *left Pallidum WM*:

r=0.4999, r^2=0.2499, and p value=0.0293.

Table 464: Summary of the reviewed DTI analysis results of previous studies on white matter in cannabis users, accompanied by clinical and psychometric correlations.

First Author and publication year	Cannabis users (SD)		Non-cannabis users (SD)		Cannabis use (SD)				DTI findings		Correlations to clinical findings
	N	Age	N	Age M ± SD	Age of onset	Duration in years	Lifetime joints or cons	Weekly joints or cons	FA	MD	
Orbitofrontal											
Filbey 2014 et al.[352]	Cannabis users (CU): 48 Exclusively cannabis users (ECU): 27	(CU): 28.3 (8.3) (ECU): 28.1 (8.9)	62	30.0 (7.4)	(CU): 18.1 (3.4) (ECU): 18.7 (2.9)	-	-	(CU): 11.1 (1.4) (ECU): 11.2(1.4)	↓↑	Ns	-
Prefrontal											
Arnone D et al.(2008) [385]	9	25 (2.96)	11	23.36 (2.94)	15.27 (2.84)	8.91(3.52)	-	44.18 (29.43)	↓	Ns	-
Becker et al. (2015)[386]	23	19.45 (0.66)	23	19.19 (2.31)	15.35 (1.16)	>1year	-	Past 12 months: 3032.55 (2395.31)	↓	Ns	-

Gruber SA et al. (2011)[330]	15	25 (8.7)	15	25.2 (8.4)	14.9 (2.5)	10.1 (9.7)		25.5 (27.8)	↓	Ns	-Impulsivity (BIS) to the frontal region.
Delisi LE et al., (2006)[371]	10	21.1 (2.9)	10	23.0 (4.4)	-	-	-	-	↑	↓	-
Clark DB et al. (2012)[387]	19	16.8 (1.2)	9	16.2 (1.0)	-	-	-	--	↓	Ns	- Psychological dysregulation through (BRIEF-SR).
Gruber SA et al. (2013)[388]	25	23.16 (5.87)	18	23.11 (3.51)	**Early MJ:** 14.46 (0.69) **Late MJ:** 17.93 (2.13)	**Early MJ:** 8.82 (5.67) **Late MJ:** 5.14 (4.42)	-	**Early MJ:** 18.76 (9.38) **Late MJ:** 15.51 (7.19)	↓	↑	-Impulsivity (BIS) to the frontal.
Broca's region											
Ashtari M etal. (2009)[390]	14	19.3 (0.8)	14	18.5 (1.4)	13.1 (1.6)	5.3 (2.1)	-	40.6 (18.2)	↓	↑	-
Parietal Cortex											
Orr et al. (2016)[391]	466	22-35	393	22-35	> 50% of users first use:	-	Range from 1-5/ lifetime to	-	↓	Ns	-

					15-20 years		>1000/ lifetime				
Becker et al. (2015)[386]	23	19.45 (0.66)	23	19.19 (2.31)	15.35 (1.16)	>1year	-	Past 12 months: 3032.55 (2395.31)	↓	Ns	-
Manza P et al. (2020)[392]	89	28.6 (3.5)	89	28.6 (3.9)	-	-	-	-	↓	Ns	-
Temporal Cortex											
Ashtari M etal. (2009)[390]	14	19.3 (0.8)	14	18.5 (1.4)	13.1 (1.6)	5.3 (2.1)	-	40.6 (18.2)	↓	↑	-
Becker et al. (2015)[386]	23	19.45 (0.66)	23	19.19 (2.31)	15.35 (1.16)	>1year	-	Past 12 months: 3032.55 (2395.31)	↓	Ns	-
Cousijn J et al. [324]	39	21.5 (2.3)	28	21.4 (2.0)	15.33 (1.9)	4.1 (2.2)	-	4.7 (1.7) days of consumption during the week	↓	Ns	-

Limbic system											
Cingulate											
Kim D-J et al. (2011)[399]	12	19.33 (0.98)	13	21.62 (3.84)	16.00 (2.37)	3.36 (2.50)	-	5.00 (1.71) a week before	↓	↑	-Schizotypal and impulsive personality traits
Jakabek D et al. (2016)[400]	56	32.3 (10.8)	20	30.0 (10.6)	**First cannabis use** : 15.1 (2.3) **Regular cannabis use :** 16.3 (2.6)	15.5 (9.7)		Cones/month : 460.7 (350.1)	↓	–	-
Amygdala											
Shollenbarger et al. (2015) [406]	33	21.21 [18-25]	34	21.12 [18-25]	17.9 [10-24]	-	-	Past year cannabis use: 548.36 [26-3895]	↓	↑	Depressive symptoms (Beck Depression Inventory Total-2)

Jakabek D et al. (2016) [400]	56	32.3 (10.8)	20	30.0 (10.6)	**First cannabis use** : 15.1 (2.3) **Regular cannabis use :** 16.3 (2.6)	15.5 (9.7)		Cones/month : 460.7 (350.1)	Radial diffusivity instead of FA and MD: ↑		-
Cousijn J et al.(2021) [324]	39	21.5 (2.3)	28	21.4 (2.0)	15.33 (1.9)	4.1 (2.2)	-	4.7 (1.7) days of consumption during the week	↓	Ns	-
Hippocampus											
Yücel et al. (2010)[408]	Inhalant: 11 Cannabis use: 11	Inhalant: 18.2 (1.6) Cannabis use: 19.4 (1.9)	8	19.7 (2.7)	Inhalant: 15.2 (1.8) Cannabis use: 15.0 (1.6)	-		Inhalant-per day-: (No. of grams in a typical day) 0.8 (0.5) Cannabis use per day: (No. of cans in a typical day) 1.61 (1.3)	↓	Ns	-

Zalesky et al. (2012)[409]	59	33.4 (10.9)	33	31.5 (12.0)	16.7 (3.3)	15.6 (9.5)	25922 (25838)	Joints per months: 147 (142)	↓	Ns	-
Our Work											
Our team	**Heavy users:** 7 **Light users:** 6	**Heavy users:** 28.5 (6.62) **Light users:** 26.5 (2.58)	6	32 (14.14)	**Heavy users:** 17.42 (2.69) **Light users:** 20.58 (1.02)	**Heavy users:** 11 (6.37) **Light users:** 2.83 (2.84)	**Heavy users:** 64257.14 (49946.13) **Light users:** 258.93 (274.76)	**Heavy users:** 108.85 (49.18) **Light users:** 3.91 (2.87)	↓	↑	- **Cannabis use disorder:** CUDIT-R **-Impulsivity trait:** BIS)11 **-Perceived stress:** PSS

General conclusion and perspectives

This study aims to evaluate the major brain structures and functions among cannabis users. This work is intriguing in its framework and content. Firstly, our work encompasses both clinical and radiological disciplines and has used enormous quantitative, qualitative, and statistical analysis tools. Secondly, it revealed captivating outcomes on functionality, structural alterations, and the correlation between the two of them.

Our clinical findings join what was previously reported and concord with the literature. In this regard, we demonstrated the high levels of cannabis use disorder (CUD) in chronic heavy users compared to chronic light users. Furthermore, we also report the negative association between the levels of CUD and the age of onset and the positive association between the duration of use and CUD.

Moreover, the impulsivity trait evaluation shows considerable differences between the chronic heavy cannabis users and the chronic light cannabis users and the healthy control group. We highlight additionally fascinating associations since the BIS-11 scores correlate negatively with the age of onset and positively with duration of use and usage levels.

Finally, measuring how stressful consumers and non-consumers perceive their lives demonstrates the relation between consumption and stress levels since there was a remarkably high level of PSS in heavy users than light users and light users than healthy non-users. There was also a positive association with the duration of use for the perceived stress.

The impact of cannabis on reward, executive function, emotion, and stress circuits that we discovered in our clinical section was supported in the second, third, and fourth parts of our work done by the DTI assessment and the statistical correlations.

The evaluation of grey matter integrity in chronic heavy and light cannabis consumers revealed intriguing results through the two diffusion parameters: FA and MD. However, FA findings were more noticeable and pertinent.

All over the regions examined, fractional anisotropy values were reduced in cannabis users compared to the non-consuming subjects in 74 per cent (equivalent to 53 regions) of the investigated brain regions, and the significant statistical differences in FA between consumers groups and healthy control individuals were only seen in the cortex, not in the basal ganglia, diencephalon (Thalamus), telencephalon (Hippocampus), or amygdala. The FA reduction may reflect a decrease in axonal density or myelination. However, in contrast to white matter, grey matter has a mixed composition of neurons, axons, and neuroglia, and It is more challenging to determine the precise pathogenic alterations associated with this decrease in FA. Therefore, pathological and post-mortem studies are needed to be confronted with DTI findings.

In the third part of our work on assessing white matter integrity, where we tried to take the much profit of DTI and its added value in making it possible to segment and reach microstructural properties and alterations of white matter, we came out with enormous results and revelations.

According to our findings, FA's value of white matter of cannabis users is reduced compared to the non-consuming subject in 70.5 per cent of our results, equivalent to 49 anatomical regions. Furthermore, from these 49 anatomical regions, analytical findings showed 14 anatomical areas where there are significant differences between heavy cannabis users, light cannabis users, and controls.

Regarding mean diffusivity, white matter MD's values of cannabis users were increased compared to healthy controls in 48.5% of the region studied, equivalent to 34 anatomical regions. Analytical findings revealed that in 20 regions, cannabis users groups had a higher average of MD than the healthy control group.

From all tractography work and outcomes regarding fractional anisotropy and mean diffusivity, we found that chronic heavy and light consumption of cannabis in our population affects the diffusivity and anisotropy of white matter by decreasing the fractional anisotropy and increasing mean apparent diffusion compared to healthy controls in several brain areas. These diffusivity manifestations conventionally reflect degenerative axonal processes and reduced neuronal density or demyelination[231].

In terms of determining the impact of the two levels of consumption (heavy and light) on white matter, we come out that chronic heavy and light cannabis usage has the same effect on FA and MD, consequently on the microstructural changes.

Finally, in the fourth part of our work on statistical correlations of the clinical and DTI findings in the white matter of several brain regions, we were able to link structural changes to functional consequences and vice versa. FA correlates negatively with the CUD, impulsivity, and perceived stress (91,17% over the 104 correlations of the FA with the three tested). The mean diffusivity correlates positively with the three tests in 75,5% of the conducted calculations. Statistically significant correlations (p-value$<$0.05), represent 20% of the total 204 realized calculations. All are negative correlations with the total scores of CUDIT-R, BIS-11, and PSS for fractional anisotropy and positive correlations for mean diffusivity.

Based on CUDIT-R correlations with FA and MD results (statistically significant) in the overall correlated regions, several regions showed associations with cannabis use disorder. We identified associations with the left medial part of the OFC, the left and right dorsomedial and dorsolateral parts of the PFC, and with the limbic system through the right anterior and the left middle parts of the cingulate gyrus, the left insula, the left amygdala, and the left putamen and pallidum.

Concerning impulsivity, we identified associations with the left medial part of the OFC, the right ventromedial PFC and the left and right dorsomedial and dorsolateral parts of the PFC and with the limbic system through the right anterior and the left middle parts of the cingulate gyrus, the left insula, and the left putamen and pallidum.

Finally, it was found that perceived stress was associated with anatomical locations of the left regions of the medial and lateral parts of the OFC, all the regions of the PFC, and also with the limbic system through the left and right anterior part of the cingulate gyrus, the left insula, the left caudate, putamen, and pallidum.

There are some limitations of the current study that should be taken into account. First, regarding diffusion imaging acquisition, in our study, we used a DTI protocol with 25 directions and a 1.5 Tesla MRI system, however currently 3T scanners are more recommended to 1.5T scanners, and a higher number of directions increase the relevance and the sensitivity of the DTI analysis, in particular the calculation of the FA, and especially for tractography. Second, statistically, the number of participants and groups available to us may have compromised the statistical significance of some results in some regions and/or some tracts. Third, the average age of the controls sample is a little elevated, especially when compared to the light consumers' group. Therefore, following studies with more efficiently age-matching is needed.

As perspectives and recommendations for the following projects and research, it would be interesting to consider longitudinal studies to determine the causal association between cannabis use or abuse and grey and white matter. This will also assist determine if the reason and to what extent cannabis-affected brain tissues may regenerate and recover following drug cessation and whether this change interacts with other life indices. Furthermore, even if there is a homogeneous method of cannabis use in our study since all of our participants live in the same district and from the same environment and report smoking joints made from Moroccan cannabis

resin, objective measures are required throughout the study to avoid the lack of sensitivity of self-assessments filled out by consumers. Additionally, regarding the grey matter, since the voxel-based morphometry technique allows us to estimate the grey matter density in a specific area, following our research, a VBM study with the same volunteers will be beneficial to determine whether or not changes identified in FA and MD are related to the density of the regions on grey matter neurons.

We also advocate that pathological and post-mortem studies should be considered in future projects to confront histological to DTI findings. This will be tremendously useful not only for investigating the effects of cannabis usage but also for assessing the DTI's sensitivity and specificity in detecting neurodegenerative alterations.

Our Work In Numbers

As part of our work:

-We created and elucidated: • 15 Atlas with 73 anatomical plates.

• 3 plates containing 6 images of ROIs nodes and Tractograms.

•7 plates of the quality assessment.

-We evaluated 11 characteristics of the profile of cannabis consumption.

-Over the 19 participants, we collected clinical and psychological data in 57 forms for three psychometric tests.

-We Extracted and analyzed 1368 anatomical regions and white matter related to 1330 regions.

As outcomes, we:

-Came out to 57 clinical findings (test scores) over the 19 volunteers.

-Calculated 2738 FA and MD values in ROI analysis.

-Calculated 2660 FA and MD values in tractography analysis.

-Illustrated our clinical and DTI findings in 290 graphs and 429 tables.

-Did 861 ANOVA analysis.

-Did 212 correlation calculation.

-Illustrated our correlation findings in 48 graphs.

And more…

Abstracts

Abstract

According to the "World Drug Report 2020," cannabis is the most used drug worldwide. Δ-9-tetrahydrocannabinol (THC) is the major psychoactive substance in cannabis[3]. It was revealed that cannabis potency had increased worldwide lately[4] and especially Moroccan cannabis resin. Studies on acute and chronic effects of cannabis showed that cannabis use is involved in the impairments of a broad range of cognitive functions[26]. Several neuroimaging studies revealed the long-term effects of chronic cannabis use on the integrity of several different brain systems[27]. So far, there is no complete study of the grey and white matters connectivity alterations induced by chronic-heavy and light-chronic cannabis use. Therefore, the fundamental purpose of our work is to evaluate the major brain structures and functions among Moroccan cannabis users, including the impact and contribution of two different levels of cannabis use on grey and white matter integrity and many brain functions. Furthermore, we studied the correlation between some consumption profiles and functional findings and functional and structural outcomes.

Our work is a cross-sectional study conducted on Moroccan cannabis users; they were compared to healthy non-users controls. The subjects were recruited in the Addiction centre, Department of Psychiatry, University Hospital of Fez; Fez, Morocco. They gave written consent to participate to the clinical and MRI study conducted by Clinical Neuroscience Laboratory, Faculty of Medicine and Pharmacy of Fez; University of Fez in collaboration with the Addiction centre affiliated to the Psychiatry Department, and Radiology and Clinical Imaging Department, University Hospital of Fez. All participants underwent the same Diffusion Tensor MRI protocol and the same series of psychometric tests. Participants were divided into three groups: Chronic heavy cannabis users, chronic light cannabis users and healthy non-users control.

Firstly, we evaluated the impact of chronic and heavy cannabis use on brain functions that are part of the reward, cognition, and emotional regulation circuits. Secondly, using DTI and ROI, we extracted 36 regions of interest for each hemisphere. Over 19 participants, the integrity of anatomical structures was assessed using quantitative fractional anisotropy (FA) and mean diffusivity (MD). Thirdly we extracted tracts related to 35 regions of interest for each hemisphere, of 19 cannabis users. Afterwards; we calculated the diffusion characteristics using FA and MD in associated networks studied. Finally, we calculated the correlation between the clinical aspects on the one hand, including Psychometric tests such as CUDIT-R, BIS-11, and PSS to DTI findings on the other hand including FA and MD in the tracts related to the involved brain regions. All descriptive and statistical outcomes (Psychometric, ROI, and tractography) of the three groups were compared. The significant difference between pairs of users of heavy, light and non-users groups were reported.

Our work exposed outcomes on functional and structural alterations. We demonstrated the high levels of cannabis use disorder (CUD) in chronic heavy users, considerable differences in impulsivity levels between the three groups and an association between consumption and stress. Correlation of consumption profiles and the levels of CUD, impulsivity and perceived stress showed a negative association between the levels of CUD and the onset age. Age of onset was associated negatively with impulsivity levels. Positive association was demonstrated between impulsivity and the use duration and usage levels, while stress was shown that the duration of use impacts stress levels and vice versa.

The evaluation of grey matter integrity in chronic heavy and light cannabis consumers revealed intriguing results through two diffusion parameters: FA and MD. However, FA findings were more noticeable and pertinent. All over the regions examined, fractional anisotropy values were reduced in cannabis users compared to

the non-consuming subjects in 74 per cent (equivalent to 53 regions) of the investigated brain regions, and the significant statistical differences in FA between consumers groups and healthy control individuals were only seen in the cortex.

In the third part of our work we assessed white matter integrity; we yielded tremendous results and revelations. From all tractography work and outcomes regarding fractional anisotropy and mean diffusivity, we found that chronic heavy and light consumption of cannabis in our population affects the diffusivity and anisotropy of white matter by decreasing the fractional anisotropy and increasing mean apparent diffusion compared to healthy controls in several brain areas. We concluded that chronic heavy and light cannabis usage has the same effect on FA and MD, consequently on the microstructural changes.

Finally, in the fourth part of our work we achieved statistical correlations between the clinical and DTI findings in the white matter of several brain regions, we showed direct correlation between structural changes and functional impact and vice versa. FA correlates negatively with the CUD, impulsivity, and perceived stress. The mean diffusivity correlates positively with the three tests in 75,5% of the conducted calculations. Statistically significant correlations ($p\text{-value} < 0.05$), represent 20% of the total 204 realized calculations. All are negative correlations with the total scores of CUDIT-R, BIS-11, and PSS for fractional anisotropy and positive correlations for mean diffusivity.

This research project is unique and is the first of its kind in the world on several dimensions (ROI for an entire anatomical region, correlations done for the first time, etc.). Indeed, further investigations, prospective and longitudinal studies are recommended with more effective monitoring of several indices and factors related to consumption, and this should be accompanied by a parallel pathological and/or post-mortem studies.

Résumé

Selon le « World Drug Report 2020 », le cannabis est la drogue la plus consommée dans le monde. Le Δ-9-tétrahydrocannabinol (THC) est la principale substance psychoactive du cannabis. Il a été révélé que l'intensité et la sévérité du cannabis avait augmenté dans le monde ces derniers temps et en particulier la résine de cannabis marocaine. Des études sur les effets aigus et chroniques du cannabis ont montré que la consommation de cannabis est impliquée dans les déficiences d'un large éventail de fonctions cognitives. Plusieurs études de neuroimagerie ont révélé les effets à long terme de la consommation chronique de cannabis sur l'intégrité de plusieurs systèmes cérébraux différents. Jusqu'à présent, il n'y a pas d'étude complète des altérations de la connectivité des matières grises et blanches induites par la consommation chronique-forte et légère-chronique de cannabis. Par conséquent, l'objectif fondamental de notre travail est d'évaluer les principales structures et fonctions cérébrales chez les consommateurs marocains de cannabis, y compris l'impact et la contribution de deux niveaux différents de consommation de cannabis sur l'intégrité de la matière grise et blanche et de nombreuses fonctions cérébrales. De plus, nous avons étudié la corrélation entre certains profils de consommation et les résultats fonctionnels et les résultats fonctionnels et structurels.

Notre travail est une étude transversale menée sur des consommateurs marocains de cannabis ; ils ont été comparés à des témoins sains non-utilisateurs. Les sujets ont été recrutés au Centre d'addictologie, Service de psychiatrie, CHU de Fès ; Fès, Maroc. Ils ont donné leur consentement écrit pour participer à l'étude clinique et IRM menée par le Laboratoire de Neuroscience Clinique, Faculté de Médecine et de Pharmacie de Fès ; Université de Fès en collaboration avec le Centre de l'addictologie rattaché au service de psychiatrie, et le service de radiologie et d'imagerie clinique, CHU de Fès. Tous les participants ont subi le même protocole d IRM du tenseur de diffusion et la même série de tests psychométriques. Les participants ont été divisés en trois groupes : les consommateurs forts chroniques de cannabis, les consommateurs chroniques légers de cannabis et les non-consommateurs en bonne santé. Premièrement, nous avons évalué l'impact de la consommation chronique et

intensive de cannabis sur les fonctions cérébrales qui font partie des circuits de récompense, de cognition et de régulation émotionnelle.

Deuxièmement, en utilisant le DTI et le ROI, nous avons extrait 36 régions d'intérêt pour chaque hémisphère. Sur 19 participants, l'intégrité des structures anatomiques a été évaluée en utilisant l'anisotropie fractionnelle (FA) et la diffusion moyenne (MD). Troisièmement, nous avons extrait des tracts liés à 35 régions d'intérêt pour chaque hémisphère, de 19 consommateurs de cannabis. Après ; nous avons calculé les caractéristiques de diffusion en utilisant FA et MD dans les réseaux associés étudiés. Enfin, nous avons calculé la corrélation entre les aspects cliniques d'une part, y compris les tests psychométriques tels que CUDIT-R, BIS-11 et PSS aux résultats DTI d'autre part, y compris FA et MD dans les voies liées aux régions cérébrales impliquées dans ces fonctions. Tous les résultats descriptifs et statistiques (psychométriques, région d'intérêt (ROI) et tractographie) des trois groupes ont été comparés. La différence significative entre les paires d'utilisateurs des groupes lourds, légers et non-utilisateurs a été signalée.

Notre travail a exposé les résultats sur les altérations fonctionnelles et structurelles. Nous avons démontré les niveaux élevés de troubles liés à l'usage de cannabis (CUD) chez les consommateurs forts chroniques, des différences considérables dans les niveaux d'impulsivité entre les trois groupes et une association entre la consommation et le stress. La corrélation des profils de consommation et des niveaux de CUD, d'impulsivité et de stress perçu a montré une association négative entre les niveaux de CUD et l'âge d'apparition. L'âge d'apparition était associé négativement aux niveaux d'impulsivité. Une association positive a été démontrée entre l'impulsivité et la durée d'utilisation et les niveaux d'utilisation, tandis que le stress a été montré que la durée d'utilisation avait un impact sur les niveaux de stress et vice versa.

L'évaluation de l'intégrité de la matière grise chez les consommateurs chroniques de cannabis lourd et léger a révélé des résultats intrigants à travers deux paramètres de diffusion: FA et MD. Cependant, les résultats de l'AF étaient plus visibles et pertinents. Dans toutes les régions examinées, les valeurs d'anisotropie fractionnaire ont été réduites chez les

consommateurs de cannabis par rapport aux sujets non-consommateurs dans 74% (équivalent à 53 régions) des régions cérébrales étudiées, et les différences statistiques significatives de FA entre les groupes de consommateurs et les témoins sains les individus n'ont été observés que dans le cortex.

Dans la troisième partie de notre travail, nous avons évalué l'intégrité de la substance blanche; nous avons donné des résultats et des révélations exceptionnelles. À partir de tous les travaux de tractographie et des résultats concernant l'anisotropie fractionnelle et la diffusivité moyenne, nous avons constaté que la consommation chronique lourde et légère de cannabis dans notre population affecte la diffusivité et l'anisotropie de la substance blanche en diminuant l'anisotropie fractionnelle et en augmentant la diffusion apparente moyenne par rapport aux témoins sains dans plusieurs zones cérébrales. Nous avons conclu que la consommation chronique lourde et légère de cannabis a le même effet sur FA et MD, par conséquent sur les changements microstructuraux.

Enfin, dans la quatrième partie de notre travail, nous avons réalisé des corrélations statistiques entre les résultats cliniques et DTI dans la substance blanche de plusieurs régions du cerveau, nous avons montré une corrélation directe entre les changements structurels et l'impact fonctionnel et vice versa. L'AF est en corrélation négative avec le CUD, l'impulsivité et le stress perçu. La diffusivité moyenne est corrélée positivement avec les trois tests dans 75,5% des calculs effectués. Les corrélations statistiquement significatives (valeur $p < 0,05$) représentent 20 % du total des 204 calculs réalisés. Tous sont des corrélations négatives avec les scores totaux de CUDIT-R, BIS-11 et PSS pour l'anisotropie fractionnaire et des corrélations positives pour la diffusion moyenne.

Ce projet de recherche est unique et est le premier du genre au monde sur plusieurs dimensions (ROI pour une région anatomique entière, certaines corrélations faites pour la première fois, etc.). En effet, des investigations complémentaires, des études prospectives et longitudinales sont recommandées avec un suivi plus efficace de plusieurs indices et facteurs liés à la consommation, et cela devrait s'accompagner d'une étude pathologique et/ou post-mortem parallèle.

ملخص

وفقًا لـ "تقرير المخدرات العالمي 2020" ، يعتبر القنب الهندي أكثر المخدرات استخدامًا في جميع أنحاء العالم. 9-Δ-رباعي هيدروكانابينول (THC) هو المادة النفسانية التأثير الرئيسية في القنب. تم الكشف عن زيادة فاعلية القنب في جميع أنحاء العالم في الآونة الأخيرة وخاصة القنب المغربي. أظهرت الدراسات التي أجريت على الآثار الحادة والمزمنة للقنب أن استخدامه له دور في إعاقات مجموعة واسعة من الوظائف الإدراكية. كشفت العديد من دراسات التصوير العصبي عن الآثار طويلة المدى لاستخدام القنب المزمن على سلامة العديد من أنظمة الدماغ المختلفة. حتى الآن ، لا توجد دراسة كاملة لتغييرات اتصال المواد الرمادية والبيضاء الناجمة عن تعاطي الحشيش المزمن الثقيل والمزمن الخفيف. لذلك ، فإن الغرض الأساسي من عملنا هو تقييم هياكل ووظائف الدماغ الرئيسية بين مستخدمي القنب المغربي ، بما في ذلك تأثير ومساهمة مستويين مختلفين من استخدام القنب على سلامة المادة الرمادية والبيضاء والعديد من وظائف الدماغ. علاوة على ذلك ، قمنا بدراسة الارتباط بين بعض ملفات تعريف الاستهلاك والنتائج الوظيفية والنتائج الوظيفية والهيكلية.

عملنا عبارة عن دراسة مستعرضة أجريت على متعاطي القنب المغربي. تم مقارنتهم مع غير المستخدمين الأصحاء. تم اختيار المستهلكين في مركز الإدمان بقسم الطب النفسي بالمستشفى الجامعي بفاس. فاس ، المغرب. أعطوا موافقة خطية للمشاركة في الدراسة السريرية ودراسة التصوير بالرنين المغناطيسي التي أجراها مختبر علم الأعصاب السريري ، كلية الطب والصيدلة بفاس ؛ جامعة فاس بالتعاون مع مركز الإدمان التابع لقسم الطب النفسي وقسم الأشعة والتصوير السريري بالمستشفى الجامعي بفاس. خضع جميع المشاركين لنفس بروتوكول موترالتصوير الموزن بمعامل الانتشار Diffusion Tensor Imging ونفس سلسلة الاختبارات السيكومترية. تم تقسيم المشاركين إلى ثلاث مجموعات: متعاطو الحشيش المزمن الثقيل ، ومتعاطو القنب الخفيف المزمن ، والمجموعة الأصحاء من غير المستخدمين. أولاً ، قمنا بتقييم تأثير استخدام الحشيش المزمن والثقيل على وظائف المخ التي تعد جزءًا من دوائر المكافأة والإدراك والتنظيم العاطفي. ثانيًا ، باستخدام DTI و ROI ، استخرجنا 36 منطقة لكل نصف دماغ. عند 19 مشاركًا ، تم تقييم سلامة الهياكل التشريحية باستخدام التباين الجزئي (FA) والمتوسط (MD). ثالثًا ، استخرجنا ألياف المسالك مرتبطة بـ 35 منطقة ذات أهمية لكل نصف دماغ ، من 19 مستخدمًا للقنب. عقب ذلك مباشرة؛ قمنا بحساب خصائص الانتشار باستخدام FA و MD في الشبكات المرتبطة التي تمت دراستها. أخيرًا ، قمنا بحساب الارتباط بين الجوانب السريرية من ناحية ، بما في ذلك الاختبارات السيكومترية مثل CUDIT-R و BIS-11 و PSS إلى نتائج DTI من ناحية أخرى بما في ذلك FA و MD في المسالك المتعلقة بمناطق الدماغ المعنية . تمت مقارنة جميع النتائج الوصفية والإحصائية للمجموعات الثلاث. تم الإبلاغ عن فرق كبير بين أزواج المستخدمين من المجموعات الثقيلة والخفيفة وغير المستخدمين.

كشف عملنا نتائج على التعديلات الوظيفية والهيكلية. أظهرنا المستويات العالية لاضطراب تعاطي الحشيش (CUD) لدى المستخدمين الثقيل المزمن ، وفروقًا كبيرة في مستويات الاندفاع بين المجموعات الثلاث وعلاقة بين

الاستهلاك والضغط العصبي. أظهر ارتباط ملفات تعريف الاستهلاك ومستويات CUD والاندفاع والضغط العصبي ارتباطًا سلبيًا بين مستويات CUD وعمر البداية. ارتبط عمر البداية سلبًا بمستويات الاندفاع. تم إثبات الارتباط الإيجابي بين الاندفاع ومدة الاستخدام ومستويات الاستخدام ، بينما تم إثبات أن مدة الاستخدام تؤثر على مستويات التوتر والعكس صحيح.

كشف تقييم سلامة المادة الرمادية في مستهلكي الحشيش المزمن الثقيل والخفيف عن نتائج مثيرة للاهتمام من خلال معلمتين للنشر: FA و MD. و كانت نتائج FA أكثر وضوحًا وذات صلة. في جميع المناطق التي تم فحصها ، تم تخفيض قيم التباين الجزئي في مستخدمي القنب مقارنة بالأفراد غير المستهلكة في 74 في المائة (ما يعادل 53 منطقة) من مناطق الدماغ التي تم فحصها ، والاختلافات الإحصائية الهامة في FA بين مجموعات المستهلكين و الأصحاء ، تم رؤية الاختلافات الإحصائية فقط في قشرة الدماغ.

في الجزء الثالث من عملنا قمنا بتقييم سلامة المادة البيضاء. لقد حققنا نتائج هائلة. من جميع النتائج المتعلقة بالتباين الجزئي والانتشار المتوسط ، وجدنا أن الاستهلاك الثقيل والخفيف المزمن للقنب في مجتمعنا يؤثر على انتشار وتباين المادة البيضاء عن طريق تقليل التباين الجزئي وزيادة الانتشار مقارنة بالضوابط الصحية في العديد من مناطق الدماغ. خلصنا إلى أن استخدام الحشيش المزمن الثقيل والخفيف له نفس التأثير على FA و MD ، وبالتالي على التغيرات الهيكلية المجهرية.

أخيرًا ، في الجزء الرابع من عملنا ، حققنا ارتباطات إحصائية بين النتائج السريرية ونتائج DTI في المادة البيضاء للعديد من مناطق الدماغ ، وأظهرنا ارتباطًا مباشرًا بين التغييرات الهيكلية والتأثير الوظيفي والعكس صحيح. يرتبط FA بشكل سلبي مع CUD والاندفاع والضغط العصبي. يرتبط متوسط الانتشار إيجابياً بالاختبارات الثلاثة في 75.5٪ من الحسابات التي تم إجراؤها. تمثل الارتباطات ذات الدلالة الإحصائية (القيمة الاحتمالية <0.05) 20٪ من إجمالي 204 حسابات محققة. كلها ارتباطات سلبية مع مجموع درجات CUDIT-R و BIS-11 و PSS للتباين الجزئي والارتباطات الإيجابية لمتوسط الانتشار.

هذا المشروع البحثي فريد من نوعه وهو الأول من نوعه في العالم من عدة أبعاد (عزل و دراسة لمنطقة تشريحية كاملة ، الارتباطات التي تم إجراؤها لأول مرة ، وما إلى ذلك). في الواقع ، يوصى بإجراء مزيد من التحقيقات والدراسات المستقبلية والطولية مع مراقبة أكثر فعالية للعديد من المؤشرات والعوامل المتعلقة بالاستهلاك ، ويجب أن يكون هذا مصحوبًا بدراسات مرضية و / أو دراسات تشريحية.

Bibliographical references

1. United Nations Office on Drugs and Crime. *World Drug Report 2020: Drug Use and Health Consequences*.; 2020. https://www.unodc.org/doc/wdr2016/WORLD_DRUG_REPORT_2016_web.pdf
2. Toufiq PJ, Omari F El, Sabir M. *Rapport Annuel de 2014 de l'Observatoire National Des Drogues et Addictions.*; 2014. https://omda.ma/index.php/fr/rapports
3. Wachtel S, ElSohly M, Ross S, Ambre J, De Wit H. Comparison of the subjective effects of Δ9-tetrahydrocannabinol and marijuana in humans. *Psychopharmacology (Berl)*. 2002;161(4):331-339. doi:10.1007/s00213-002-1033-2
4. Freeman TP, Groshkova T, Cunningham A, Sedefov R, Griffiths P, Lynskey MT. Increasing potency and price of cannabis in Europe, 2006-16. *Addiction*. 2019;114(6):1015-1023. doi:10.1111/add.14525
5. Chandra S, Radwan MM, Majumdar CG, Church JC, Freeman TP, ElSohly MA. New trends in cannabis potency in USA and Europe during the last decade (2008-2017). *Eur Arch Psychiatry Clin Neurosci*. 2019;269(1):5-15. doi:10.1007/s00406-019-00983-5
6. Cadet-Taïrou A, Gandilhon M, Martinez M, Néfau T. Substances psychoactives en France : tendances récentes (2014-2015). *Tendances*. Published online 2015.
7. Stambouli H, El Bouri A, Bouayoun T. Évolution de la teneur en δ9-THC dans les saisies de résines de cannabis au Maroc de 2005 à 2014. *Toxicol Anal Clin*. 2016;28(2):146-152. doi:10.1016/j.toxac.2015.11.001
8. Cadet-Taïrou A, Gandilhon M, Martinez M, Néfau T. Substances illicites ou détournées : les tendances récentes (2013-2014). *Tend OFDT*. Published online 2014:1-6.
9. Howlett AC, Barth F, Bonner TI, et al. International Union of Pharmacology. XXVII. Classification of cannabinoid receptors. *Pharmacol Rev*. 2002;54(2):161-202. doi:10.1124/pr.54.2.161
10. Di Marzo V, Piscitelli F. The Endocannabinoid System and its Modulation by Phytocannabinoids. *Neurotherapeutics*. 2015;12(4):692-698. doi:10.1007/s13311-015-0374-6
11. Glass M, Dragunow M, Faull RLM. Cannabinoid receptors in the human brain: A detailed anatomical and quantitative autoradiographic study in the fetal, neonatal and adult human brain. *Neuroscience*. 1997;77(2):299-318. doi:10.1016/S0306-4522(96)00428-9
12. Wang X, Dow-Edwards D, Keller E, Hurd YL. Preferential limbic expression of the cannabinoid receptor mRNA in the human fetal brain. *Neuroscience*. 2003;118(3):681-694. doi:10.1016/S0306-4522(03)00020-4
13. Mechoulam R, Parker LA. The endocannabinoid system and the brain. *Annu Rev Psychol*. 2013;64(July 2012):21-47. doi:10.1146/annurev-psych-113011-143739
14. Ashton J, Friberg D, Darlington C, letters PS-N, 2006 undefined. Expression of the cannabinoid CB2 receptor in the rat cerebellum: an immunohistochemical study. *Elsevier*. Accessed April 12, 2021. https://www.sciencedirect.com/science/article/pii/S0304394005013200
15. Onaivi E, Ishiguro H, Gong J, … SP-A of the N, 2008 undefined. Functional expression of brain neuronal CB2 cannabinoid receptors are involved in the effects of drugs of abuse and in depression. *ncbi.nlm.nih.gov*. Accessed April 12, 2021. https://www.ncbi.nlm.nih.gov/pmc/articles/PMC3922202/
16. Van Sickle MD, Duncan M, Kingsley PJ, et al. Neuroscience: Identification and functional characterization of brainstem cannabinoid CB2 receptors. *Science (80-)*. 2005;310(5746):329-332. doi:10.1126/science.1115740
17. Núñez E, Benito C, Pazos MR, et al. Cannabinoid CB2 receptors are expressed by perivascular microglial cells in the human brain: An Immunohistochemical Study. *Synapse*. 2004;53(4):208-

213. doi:10.1002/syn.20050
18. Stella N. Cannabinoid signaling in glial cells. *Glia*. 2004;48(4):267-277. doi:10.1002/glia.20084
19. Zhang HY, Gao M, Liu QR, et al. Cannabinoid CB2 receptors modulate midbrain dopamine neuronal activity and dopamine-related behavior in mice. *Proc Natl Acad Sci U S A*. 2014;111(46):E5007-E5015. doi:10.1073/pnas.1413210111
20. Monnet-Tschudi F, Hazekamp A, Perret N, et al. Delta-9-tetrahydrocannabinol accumulation, metabolism and cell-type-specific adverse effects in aggregating brain cell cultures. *Toxicol Appl Pharmacol*. 2008;228(1):8-16. doi:10.1016/j.taap.2007.11.007
21. Burston JJ, Wiley JL, Craig AA, Selley DE, Sim-Selley LJ. Regional enhancement of cannabinoid CB1 receptor desensitization in female adolescent rats following repeated Δ9-tetrahydrocannabinol exposure. *Br J Pharmacol*. 2010;161(1):103-112. doi:10.1111/j.1476-5381.2010.00870.x
22. Martin BR, Sim-Selley LJ, Selley DE. Signaling pathways involved in the development of cannabinoid tolerance. *Trends Pharmacol Sci*. 2004;25(6):325-330. doi:10.1016/j.tips.2004.04.005
23. Breivogel CS, Childers SR, Deadwyler SA, Hampson RE, Vogt LJ, Sim-Selley LJ. Chronic Δ9-tetrahydrocannabinol treatment produces a time-dependent loss of cannabinoid receptors and cannabinoid receptor-activated G proteins in rat brain. *J Neurochem*. 1999;73(6):2447-2459. doi:10.1046/j.1471-4159.1999.0732447.x
24. Lorenzetti V, Solowij N, Yücel M. The role of cannabinoids in neuroanatomic alterations in cannabis users. *Biol Psychiatry*. Published online 2016. doi:10.1016/j.biopsych.2015.11.013
25. Seeley WW, Crawford RK, Zhou J, Miller BL, Greicius MD. Neurodegenerative Diseases Target Large-Scale Human Brain Networks. *Neuron*. 2009;62(1):42-52. doi:10.1016/j.neuron.2009.03.024
26. Broyd SJ, Van Hell HH, Beale C, Yücel M, Solowij N. Acute and chronic effects of cannabinoids on human cognition - A systematic review. *Biol Psychiatry*. 2016;79(7):557-567. doi:10.1016/j.biopsych.2015.12.002
27. Zehra A, Burns J, Liu CK, et al. Cannabis Addiction and the Brain: a Review. *Focus (Madison)*. 2019;17(2):169-182. doi:10.1176/appi.focus.17204
28. Russo EB. History of cannabis and its preparations in saga, science, and sobriquet. *Chem Biodivers*. 2007;4(8):1614-1648. doi:10.1002/cbdv.200790144
29. Pisanti S, Bifulco M. Medical Cannabis: A plurimillennial history of an evergreen. *J Cell Physiol*. Published online 2019. doi:10.1002/jcp.27725
30. Li HL. An archaeological and historical account of cannabis in China. *Econ Bot*. Published online 1973. doi:10.1007/BF02862859
31. Cherney JH, Small E. Industrial hemp in North America: Production, politics and potential. *Agronomy*. Published online 2016. doi:10.3390/agronomy6040058
32. Zuardi AW. History of cannabis as a medicine: A review. *Rev Bras Psiquiatr*. 2006;28(2):153-157. doi:10.1590/S1516-44462006000200015
33. Small E. Evolution and Classification of Cannabis sativa (Marijuana , Hemp) in Relation to Human Utilization. Published online 2015:189-294. doi:10.1007/s12229-015-9157-3
34. Groom Q. R.C. Clarke & M.D. Merlin (2013) – Cannabis: Evolution and Ethnobotany. *Plant Ecol Evol*. Published online 2014. doi:10.5091/plecevo.2014.933
35. Tamuda JB-H, 2013 undefined. L'historie du chanvre au Maghreb. *dialnet.unirioja.es*. Accessed January 9, 2021. https://dialnet.unirioja.es/servlet/articulo?codigo=6007950

36. Bellakhdar J. Les voies suivies par le chanvre dans sa conquête du Maghreb. *Hesperis Tamuda*. 2017;(52):117-150.
37. Labrousse A, Romero L. Rapport sur la situation du cannabis dans le Rif marocain. Published online 2001.
38. Chouvy P-A. Production de cannabis et de haschich au Maroc: contexte et enjeux. *L'esp Polit Rev en ligne géographie Polit géopolitique*. 2008;(4):1-15. doi:10.4000/espacepolitique.59
39. Chouvy P. Du kif au haschich _ évolution de l'industrie du cannabis au Maroc. Published online 2018:308-321.
40. Erosion-Bulletin AL-R, 1995 undefined. Démographie, système de production et dégradation des sols dans la région nord du Maroc. *documentation.ird.fr*. Accessed January 9, 2021. https://www.documentation.ird.fr/hor/fdi:42431
41. Méditerranée GF-, 1979 undefined. L'évolution d'une paysannerie montagnarde: les Jbalas Sud-Rifains. *persee.fr*. Accessed January 9, 2021. https://www.persee.fr/doc/medit_0025-8296_1979_num_35_1_1901?hc_location=ufi
42. Benabud A. PSYCHO-PATHOLOGICAL ASPECTS OF THE CANNABIS SITUATION IN MOROCCO-STATISTICAL DATA FOR 1956. *Bull Narcotics ,*. 1957;9(4):1-16. Accessed January 9, 2021. https://scholar.google.com/scholar?cluster=9771336026965207548&hl=fr&as_sdt=2005&sciodt=0,5#d=gs_cit&u=%2Fscholar%3Fq%3Dinfo%3A_Ok8hFjCmocJ%3Ascholar.google.com%2F%26output%3Dcite%26scirp%3D0%26scfhb%3D1%26hl%3Dfr
43. Bellakhdar J. Hommes et plantes au Maghreb: éléments pour une méthode en ethnobotanique. Published online 2008. Accessed January 9, 2021. https://books.google.com/books?hl=fr&lr=&id=-y0Gf5FTjroC&oi=fnd&pg=PA9&dq=BELLAKHDAR+J.,+Hommes+et+plantes+au+Maghreb.+Éléments+pour+une+méthode+en+ethnobotanique,+Metz,+Plurimondes,+2008,+386+pages.&ots=e-3ISA8tzR&sig=Cp51q9x4ydJFUeeazvciDzMck98
44. Clarke RC. *HASHISH!* .; 1998. Accessed January 9, 2021. http://www.onlinepot.org/hash/DownloadedFromFoundOnMedicalMarijuanaWebsite10000PagesOnlinePotwww.onlinepot.org-96531frn.pdf
45. Chandra S, Lata H, ElSohly MA. *Cannabis Sativa L. - Botany and Biotechnology*.; 2017. doi:10.1007/978-3-319-54564-6
46. Evans W. *Trease and Evans Pharmacognosy 16th Edition*.; 2009.
47. McPartland JM. Cannabis Systematics at the Levels of Family, Genus, and Species. *Cannabis Cannabinoid Res*. Published online 2018. doi:10.1089/can.2018.0039
48. Riboulet-zemouli K. ' Cannabis ' ontologies I : Conceptual issues with Cannabis and cannabinoids terminology. Published online 2020. doi:10.1177/2050324520945797
49. McPartland JM, Guy GW. The evolution of Cannabis and coevolution with the cannabinoid receptor - a hypothesis. In: *The Medicinal Uses of Cannabis and Cannabinoids*. ; 2004.
50. Chandra S, Lata H, ElSohly MA, Walker LA, Potter D. Cannabis cultivation: Methodological issues for obtaining medical-grade product. *Epilepsy Behav*. Published online 2017. doi:10.1016/j.yebeh.2016.11.029
51. El Alaoui MA, Melloul M, Alaoui Amine S, et al. Extraction of High Quality DNA from Seized Moroccan Cannabis Resin (Hashish). *PLoS One*. 2013;8(10):1-6. doi:10.1371/journal.pone.0074714
52. Jin D, Dai K, Xie Z, Chen J. Secondary Metabolites Profiled in Cannabis Inflorescences, Leaves, Stem Barks, and Roots for Medicinal Purposes. *Sci Rep*. Published online 2020. doi:10.1038/s41598-020-60172-6

53. Chouvy PA, Macfarlane J. Agricultural innovations in Morocco's cannabis industry. *Int J Drug Policy*. 2018;58(April):85-91. doi:10.1016/j.drugpo.2018.04.013
54. United Nations Office on Drugs and Crime. *World Drug Report 2009*.; 2009.
55. Chouvy PA, Afsahi K. Hashish revival in Morocco. *Int J Drug Policy*. 2014;25(3):416-423. doi:10.1016/j.drugpo.2014.01.001
56. Maroc RDU, Ministre LEP, Pour A, et al. Enquête sur le cannabis 2004. Published online 2005.
57. Ladha KS, Ajrawat P, Yang Y, Clarke H. Understanding the Medical Chemistry of the Cannabis Plant is Critical to Guiding Real World Clinical Evidence. *Molecules*. 2020;25(18):1-13. doi:10.3390/molecules25184042
58. ElSohly MA, Radwan MM, Gul W, Chandra S, Galal A. Phytochemistry of Cannabis sativa L. *Prog Chem Org Nat Prod*. Published online 2017. doi:10.1007/978-3-319-45541-9_1
59. Lumír L, Ondřej O, Hanuš H, et al. Phytocannabinoids: a unified critical inventory. *Nat Prod Rep*. 2016;33:1347-1448. doi:10.1039/c6np00074f
60. Flores-Sanchez IJ, Verpoorte R. Secondary metabolism in cannabis. *Phytochem Rev*. 2008;7(3):615-639. doi:10.1007/s11101-008-9094-4
61. Press DP-A in hemp research. FP, 1999 undefined. The phytochemistry of Cannabis: Its ecological and evolutionary implications. *books.google.com*. Accessed February 2, 2021. https://books.google.com/books?hl=fr&lr=&id=6U1ZDwAAQBAJ&oi=fnd&pg=PA21&dq=The+phytochemistry+of+Cannabis:+Its+ecological+and+evolutionary+implications&ots=XWaoVDor8U&sig=_XmB0oj5EHrVLLVm7cB6HsR3ia0
62. Radwan MM, Wanas AS, Chandra S, ElSohly MA. *Natural Cannabinoids of Cannabis and Methods of Analysis*.; 2017. doi:10.1007/978-3-319-54564-6_7
63. Gaoni Y, Mechoulam R. Isolation, Structure, and Partial Synthesis of an Active Constituent of Hashish. *J Am Chem Soc*. 1964;86(8):1646-1647. doi:10.1021/ja01062a046
64. Bloomfield MAP, Hindocha C, Green SF, et al. The neuropsychopharmacology of cannabis: A review of human imaging studies. *Pharmacol Ther*. 2019;195:132-161. doi:10.1016/j.pharmthera.2018.10.006
65. Bloomfield MAP, Ashok AH, Volkow ND, Howes OD. The effects of δ9-tetrahydrocannabinol on the dopamine system. *Nature*. 2016;539(7629):369-377. doi:10.1038/nature20153
66. Pertwee RG. The diverse CB1 and CB2 receptor pharmacology of three plant cannabinoids: Δ9-tetrahydrocannabinol, cannabidiol and Δ9-tetrahydrocannabivarin. *Br J Pharmacol*. 2008;153(2):199-215. doi:10.1038/sj.bjp.0707442
67. Devinsky O, Cilio MR, Cross H, et al. Cannabidiol: Pharmacology and potential therapeutic role in epilepsy and other neuropsychiatric disorders. *Epilepsia*. Published online 2014. doi:10.1111/epi.12631
68. Mechoulam R, Tetrahedron YS-, 1963 undefined. Hashish—I: the structure of cannabidiol. *Elsevier*. Accessed April 13, 2021. https://www.sciencedirect.com/science/article/pii/004040206385022X
69. Wakeford AGP, Wetzell BB, Pomfrey RL, et al. The effects of cannabidiol (CBD) on Δ9-tetrahydrocannabinol (thc) self-administration in male and female Long-Evans rats. *Exp Clin Psychopharmacol*. 2017;25(4):242-248. doi:10.1037/pha0000135
70. Pertwee RG. The diverse CB 1 and CB 2 receptor pharmacology of three plant cannabinoids: Δ 9-tetrahydrocannabinol, cannabidiol and Δ 9-tetrahydrocannabivarin. *Br J Pharmacol*. 2008;153(2):199-215. doi:10.1038/sj.bjp.0707442
71. Gonçalves ECD, Baldasso GM, Bicca MA, Paes RS, Capasso R, Dutra RC. molecules Terpenoids, Cannabimimetic Ligands, beyond the Cannabis Plant. doi:10.3390/molecules25071567

72. Russo EB. Taming THC: Potential cannabis synergy and phytocannabinoid-terpenoid entourage effects. *Br J Pharmacol*. 2011;163(7):1344-1364. doi:10.1111/j.1476-5381.2011.01238.x
73. Volkow ND, Baler RD, Compton WM, Weiss SRB. Adverse Health Effects of Marijuana Use. *N Engl J Med*. 2014;370(23):2219-2227. doi:10.1056/nejmra1402309
74. Jerrold S. Meyer, Linda F. Quenzer. Marijuana and the Cannabinoids. In: *Psychopharmacology Drugs, the Brain, and Behavior Third Edition*. Third Edit. Oxford University Press; 2019:467-499.
75. Devane WA, Dysarz Iii FA, Johnson MR, Melvin LS, Howlett AC. Determination and Characterization of a Cannabinoid Receptor in Rat Brain. *Mol Pharmacol*. 1988;(34):605-613.
76. Kelly BF, Nappe TM. *Cannabinoid Toxicity*. StatPearls Publishing; 2019. Accessed April 15, 2021. http://www.ncbi.nlm.nih.gov/pubmed/29489164
77. Straiker AJ, Maguire G, Mackie K et al. Localization of cannabinoid CB1 receptors in the human anterior eye and retina. *Invest Ophthalmol Vis Sci*. 1999;40:2442-2448. Accessed April 11, 2021. https://arvojournals.org/article.aspx?articleid=2162341
78. Mackie K. Cannabinoid receptors: Where they are and what they do. In: *Journal of Neuroendocrinology*. Vol 20. ; 2008:10-14. doi:10.1111/j.1365-2826.2008.01671.x
79. Djeungoue-Petga MA, Hebert-Chatelain E. Linking Mitochondria and Synaptic Transmission: The CB1 Receptor. *BioEssays*. 2017;39(12). doi:10.1002/bies.201700126
80. Romero J, Garcia-Palomero E, Berrendero F, et al. Atypical location of cannabinoid receptors in white matter areas during rat brain development. *Synapse*. 1997;26(3):317-323. doi:10.1002/(SICI)1098-2396(199707)26:3<317::AID-SYN12>3.0.CO;2-S
81. Bilkei-Gorzo A. The endocannabinoid system in normal and pathological brain ageing. *Philos Trans R Soc B Biol Sci*. 2012;367(1607):3326-3341. doi:10.1098/rstb.2011.0388
82. Maccarrone M, Bab I, Bíró T, Cabral G, … SD-T in, 2015 undefined. Endocannabinoid signaling at the periphery: 50 years after THC. *Elsevier*. Accessed April 12, 2021. https://www.sciencedirect.com/science/article/pii/S0165614715000346
83. Howlett AC, Abood ME. CB1 and CB2 Receptor Pharmacology. In: *Advances in Pharmacology*. Vol 80. Academic Press Inc.; 2017:169-206. doi:10.1016/bs.apha.2017.03.007
84. Pacher P, Mechoulam R. Is lipid signaling through cannabinoid 2 receptors part of a protective system? *Prog Lipid Res*. 2011;50(2):193-211. doi:10.1016/j.plipres.2011.01.001
85. Devane WA, Hanuš L, Breuer A, et al. Isolation and structure of a brain constituent that binds to the cannabinoid receptor. *Science (80-)*. 1992;258(5090):1946-1949. doi:10.1126/science.1470919
86. Mechoulam R, Ben-Shabat S, Hanus L, et al. Identification of an endogenous 2-monoglyceride, present in canine gut, that binds to cannabinoid receptors. *Biochem Pharmacol*. 1995;50(1):83-90. doi:10.1016/0006-2952(95)00109-D
87. Sugiura T, Kondo S, Sukagawa A, et al. 2-arachidonoylglycerol: A possible endogenous cannabinoid receptor ligand in brain. *Biochem Biophys Res Commun*. 1995;215(1):89-97. doi:10.1006/bbrc.1995.2437
88. Hanus L, Abu-Lafi S, Fride E, et al. 2-Arachidonyl glyceryl ether, an endogenous agonist of the cannabinoid CB1 receptor. *Proc Natl Acad Sci U S A*. 2001;98(7):3662-3665. doi:10.1073/pnas.061029898
89. BISOGNO T, MELCK D, BOBROV MY, et al. N-acyl-dopamines: novel synthetic CB1 cannabinoid-receptor ligands and inhibitors of anandamide inactivation with cannabimimetic activity in vitro and in vivo. *Biochem J*. 2000;351(3):817-824. doi:10.1042/bj3510817
90. Porter A, Sauer J, Knierman M, … GB-… of P and, 2002 undefined. Characterization of a novel

endocannabinoid, virodhamine, with antagonist activity at the CB1 receptor. *ASPET*. Accessed April 13, 2021. https://jpet.aspetjournals.org/content/301/3/1020.short

91. Blankman JL, Cravatt BF. Chemical probes of endocannabinoid metabolism. *Pharmacol Rev*. 2013;65(2):849-871. doi:10.1124/pr.112.006387
92. Fu J, Bottegoni G, Sasso O, et al. A catalytically silent FAAH-1 variant drives anandamide transport in neurons. *Nat Neurosci*. 2012;15(1):64-69. doi:10.1038/nn.2986
93. Gaetani S, Dipasquale P, Romano A, et al. Chapter 5 The Endocannabinoid System as A Target for Novel Anxiolytic and Antidepressant Drugs. *Int Rev Neurobiol*. 2009;85:57-72. doi:10.1016/S0074-7742(09)85005-8
94. Shu-Jung Hu S, Mackie K. Distribution of the endocannabinoid system in the central nervous system. In: *Handbook of Experimental Pharmacology*. Vol 231. Springer New York LLC; 2015:59-93. doi:10.1007/978-3-319-20825-1_3
95. Cristino L, Imperatore R, Di Marzo V. Techniques for the Cellular and Subcellular Localization of Endocannabinoid Receptors and Enzymes in the Mammalian Brain. In: *Methods in Enzymology*. Vol 593. Academic Press Inc.; 2017:61-98. doi:10.1016/bs.mie.2017.05.003
96. Ohno-Shosaku T, Maejima T, Kano M. Endogenous cannabinoids mediate retrograde signals from depolarized postsynaptic neurons to presynaptic terminals. *Neuron*. 2001;29(3):729-738. doi:10.1016/S0896-6273(01)00247-1
97. Maejima T, Hashimoto K, Yoshida T, Aiba A, Kano M. Presynaptic inhibition caused by retrograde signal from metabotropic glutamate to cannabinoid receptors. *Neuron*. 2001;31(3):463-475. doi:10.1016/S0896-6273(01)00375-0
98. Kreitzer AC, Regehr WG. Retrograde inhibition of presynaptic calcium influx by endogenous cannabinoids at excitatory synapses onto Purkinje cells. *Neuron*. 2001;29(3):717-727. doi:10.1016/S0896-6273(01)00246-X
99. Wilson RI, Nicoll RA. Endogenous cannabinoids mediate retrograde signalling at hippocampal synapses. *Nature*. 2001;410(6828):588-592. doi:10.1038/35069076
100. Katona I, Tamás &, Freund F. Endocannabinoid signaling as a synaptic circuit breaker in neurological disease. *nature.com*. Published online 2008. doi:10.1038/nm.f.1869
101. Mátyás F, Urbán GM, Watanabe M, et al. Identification of the sites of 2-arachidonoylglycerol synthesis and action imply retrograde endocannabinoid signaling at both GABAergic and glutamatergic synapses in the ventral tegmental area. *Neuropharmacology*. 2008;54(1):95-107. doi:10.1016/j.neuropharm.2007.05.028
102. Kano M, Ohno-Shosaku T, Hashimotodani Y, Uchigashima M, Watanabe M. Endocannabinoid-mediated control of synaptic transmission. *Physiol Rev*. 2009;89(1):309-380. doi:10.1152/physrev.00019.2008
103. Koch M, Varela L, Kim JG, et al. Hypothalamic POMC neurons promote cannabinoid-induced feeding. *Nature*. 2015;519(7541):45-50. doi:10.1038/nature14260
104. Morello G, Imperatore R, Palomba L, et al. Orexin-A represses satiety-inducing POMC neurons and contributes to obesity via stimulation of endocannabinoid signaling. *Proc Natl Acad Sci U S A*. 2016;113(17):4759-4764. doi:10.1073/pnas.1521304113
105. Jager G, Witkamp RF. The endocannabinoid system and appetite: Relevance for food reward. *Nutr Res Rev*. 2014;27(1):172-185. doi:10.1017/S0954422414000080
106. Soria-Gomez E, Bellocchio L, Marsicano G. New insights on food intake control by olfactory processes: The emerging role of the endocannabinoid system. *Mol Cell Endocrinol*. 2014;397(1-2):59-66. doi:10.1016/j.mce.2014.09.023
107. Hebert-Chatelain E, Desprez T, Serrat R, Nature LB-, 2016 undefined. A cannabinoid link

between mitochondria and memory. *nature.com*. Accessed April 15, 2021. https://www.nature.com/articles/nature20127

108. Bénard G, Massa F, Puente N, et al. Mitochondrial CB1 receptors regulate neuronal energy metabolism. *nature.com*. Published online 2012. doi:10.1038/nn.3053
109. McLaughlin RJ, Gobbi G. Cannabinoids and emotionality: A neuroanatomical perspective. *Neuroscience*. 2012;204:134–144. doi:10.1016/j.neuroscience.2011.07.052
110. Bosier B, Bellocchio L, Metna-Laurent M, et al. Astroglial CB1 cannabinoid receptors regulate leptin signaling in mouse brain astrocytes. *Mol Metab*. 2013;2(4):393–404. doi:10.1016/j.molmet.2013.08.001
111. Robin LM, Oliveira da Cruz JF, Langlais VC, et al. Astroglial CB1 Receptors Determine Synaptic D-Serine Availability to Enable Recognition Memory. *Neuron*. 2018;98(5):935–944.e5. doi:10.1016/j.neuron.2018.04.034
112. Prenderville JA, Kelly ÁM, Downer EJ. The role of cannabinoids in adult neurogenesis Commissioning Editor: Steve Alexander. *Wiley Online Libr*. 2015;172(16):3950–3963. doi:10.1111/bph.13186
113. Cristino L, Bisogno T, Di Marzo V. Cannabinoids and the expanded endocannabinoid system in neurological disorders. *Nat Rev Neurol*. 2020;16(1):9–29. doi:10.1038/s41582-019-0284-z
114. Aymerich M, Aso E, Abellanas M, … RT-B, 2018 undefined. Cannabinoid pharmacology/therapeutics in chronic degenerative disorders affecting the central nervous system. *Elsevier*. Accessed April 15, 2021. https://www.sciencedirect.com/science/article/pii/S000629521830337X
115. Stempel A, Stumpf A, Zhang H, Neuron TÖ-, 2016 undefined. Cannabinoid type 2 receptors mediate a cell type-specific plasticity in the hippocampus. *Elsevier*. Accessed April 15, 2021. https://www.sciencedirect.com/science/article/pii/S0896627316300253
116. Parsons LH, Hurd YL. Endocannabinoid signalling in reward and addiction. *Nat Rev Neurosci*. 2015;16(10):579–594. doi:10.1038/nrn4004
117. Koob GF, Volkow ND. Neurocircuitry of addiction. *Neuropsychopharmacology*. 2010;35(1):217–238. doi:10.1038/npp.2009.110
118. Herkenham M, Lynn AB, Johnson MR, Melvin LS, De Costa BR, Rice KC. Characterization and localization of cannabinoid receptors in rat brain: A quantitative in vitro autoradiographic study. *J Neurosci*. 1991;11(2):563–583. doi:10.1523/jneurosci.11-02-00563.1991
119. Sidhpura N, Parsons LH. Endocannabinoid-mediated synaptic plasticity and addiction-related behavior. *Neuropharmacology*. 2011;61(7):1070–1087. doi:10.1016/j.neuropharm.2011.05.034
120. Panagis G, Mackey B, Vlachou S. Cannabinoid Regulation of Brain Reward Processing with an Emphasis on the Role of CB1 Receptors: A Step Back into the Future. *Front Psychiatry*. 2014;5:92. doi:10.3389/fpsyt.2014.00092
121. Salamone JD, Correa M, Mingote SM, Weber SM. Beyond the reward hypothesis: Alternative functions of nucleus accumbens dopamine. *Curr Opin Pharmacol*. 2005;5(1):34–41. doi:10.1016/j.coph.2004.09.004
122. Carlezon WA, Thomas MJ. Biological substrates of reward and aversion: A nucleus accumbens activity hypothesis. *Neuropharmacology*. 2009;56(SUPPL. 1):122–132. doi:10.1016/j.neuropharm.2008.06.075
123. Lupica CR, Riegel AC, Hoffman AF. Marijuana and cannabinoid regulation of brain reward circuits. *Br J Pharmacol*. 2004;143(2):227–234. doi:10.1038/sj.bjp.0705931
124. Chye Y, Kirkham R, Lorenzetti V, McTavish E, Solowij N, Yücel M. Cannabis, Cannabinoids, and

Brain Morphology: A Review of the Evidence. *Biol Psychiatry Cogn Neurosci Neuroimaging*. Published online 2020:1-9. doi:10.1016/j.bpsc.2020.07.009

125. DOWNER EJ, CAMPBELL VA. Phytocannabinoids, CNS cells and development: A dead issue? *Drug Alcohol Rev*. 2009;29(1):91-98. doi:10.1111/j.1465-3362.2009.00102.x
126. Smith AM, Fried PA, Hogan MJ, Cameron I. Effects of prenatal marijuana on visuospatial working memory: An fMRI study in young adults. *Neurotoxicol Teratol*. 2006;28(2):286-295. doi:10.1016/j.ntt.2005.12.008
127. Smith AM, Mioduszewski O, Hatchard T, Byron-Alhassan A, Fall C, Fried PA. Prenatal marijuana exposure impacts executive functioning into young adulthood: An fMRI study. *Neurotoxicol Teratol*. 2016;58:53-59. doi:10.1016/j.ntt.2016.05.010
128. Choudhury S, Blakemore S-J, Charman T. Social cognitive development during adolescence. *Soc Cogn Affect Neurosci*. 2006;1(3):165-174. doi:10.1093/scan/nsl024
129. Lebel C, Beaulieu C. Longitudinal development of human brain wiring continues from childhood into adulthood. *J Neurosci*. 2011;31(30):10937-10947. doi:10.1523/JNEUROSCI.5302-10.2011
130. Baumrind D. A developmental perspective on adolescent risk taking in contemporary America. *New Dir Child Adolesc Dev*. 1987;1987(37):93-125. doi:10.1002/cd.23219873706
131. Spear LP. The adolescent brain and age-related behavioral manifestations. *Neurosci Biobehav Rev*. 2000;24(4):417-463. doi:10.1016/S0149-7634(00)00014-2
132. Brenhouse HC, Andersen SL. Developmental trajectories during adolescence in males and females: A cross-species understanding of underlying brain changes. *Neurosci Biobehav Rev*. 2011;35(8):1687-1703. doi:10.1016/j.neubiorev.2011.04.013
133. Dow-Edwards D, Silva L. Endocannabinoids in brain plasticity: Cortical maturation, HPA axis function and behavior. *Brain Res*. 2017;1654:157-164. doi:10.1016/j.brainres.2016.08.037
134. Chye Y, Christensen E, Yücel M. Cannabis Use in Adolescence: A Review of Neuroimaging Findings. *J Dual Diagn*. 2020;16(1):83-105. doi:10.1080/15504263.2019.1636171
135. Iversen L. *The Science of Marijuana*. Oxford University Press. ; 2001.
136. GREEN B, KAVANAGH D, YOUNG R. Being stoned: a review of self-reported cannabis effects. *Drug Alcohol Rev*. 2003;22(4):453-460. doi:10.1080/09595230310001613976
137. Sewell RA, Ranganathan M, D'Souza DC. Cannabinoids and psychosis. *Int Rev Psychiatry*. 2009;21(2 SPEC. ISS.):152-162. doi:10.1080/09540260902782802
138. Böcker KBE, Hunault CC, Gerritsen J, Kruidenier M, Mensinga TT, Kenemans JL. Cannabinoid modulations of resting state EEG theta power and working memory are correlated in humans. *J Cogn Neurosci*. 2010;22(9):1906-1916. doi:10.1162/jocn.2009.21355
139. Bloomfield MAP, Hindocha C, Green SF, et al. The neuropsychopharmacology of cannabis: A review of human imaging studies. *Pharmacol Ther*. 2019;195:132-161. doi:10.1016/j.pharmthera.2018.10.006
140. Hindocha C, Freeman TP, Schafer G, et al. Acute effects of delta-9-tetrahydrocannabinol, cannabidiol and their combination on facial emotion recognition: A randomised, double-blind, placebo-controlled study in cannabis users. *Eur Neuropsychopharmacol*. 2015;25(3):325-334. doi:10.1016/j.euroneuro.2014.11.014
141. Gorka SM, Phan KL, Lyons M, Mori S, Angstadt M, Rabinak CA. Cannabinoid Modulation of Frontolimbic Activation and Connectivity during Volitional Regulation of Negative Affect. *Neuropsychopharmacology*. 2016;41(7):1888-1896. doi:10.1038/npp.2015.359
142. Volkow ND, Baler RD, Compton WM, Weiss SRB. Adverse Health Effects of Marijuana Use. *N Engl J Med*. 2014;370(23):2219-2227. doi:10.1056/NEJMra1402309

143. Copeland J, Swift W. Cannabis use disorder: Epidemiology and management. *Int Rev Psychiatry*. 2009;21(2 SPEC. ISS.):96–103. doi:10.1080/09540260902782745
144. Panlilio L, Goldberg S, Justinova Z. Cannabinoid abuse and addiction: Clinical and preclinical findings. *Clin Pharmacol Ther*. 2015;97(6):616–627. doi:10.1002/cpt.118
145. Karila L, Roux P, Rolland B, et al. Acute and Long-Term Effects of Cannabis Use: A Review. *Curr Pharm Des*. 2014;20:4112–4118. www.dsm5.org,
146. Davis JP, Smith DC, Morphew JW, Lei X, Zhang S. Cannabis withdrawal, posttreatment abstinence, and days to first cannabis use among emerging adults in substance use treatment: A prospective study. *J Drug Issues*. 2016;46(1):64–83. doi:10.1177/0022042615616431
147. Volkow ND, Wang GJ, Telang F, et al. Decreased dopamine brain reactivity in marijuana abusers is associated with negative emotionality and addiction severity. *Proc Natl Acad Sci U S A*. 2014;111(30):E3149–E3156. doi:10.1073/pnas.1411228111
148. Koob GF, Volkow ND. Neurobiology of addiction: a neurocircuitry analysis. *The Lancet Psychiatry*. 2016;3(8):760–773. doi:10.1016/S2215-0366(16)00104-8
149. González S, Cebeira M, Fernández-Ruiz J. Cannabinoid tolerance and dependence: A review of studies in laboratory animals. In: *Pharmacology Biochemistry and Behavior*. Vol 81. Elsevier Inc.; 2005:300–318. doi:10.1016/j.pbb.2005.01.028
150. PANAGIS, George, VLACHOU, Styliani, NOMIKOS, Gorge G . Behavioral pharmacology of cannabinoids with a focus on preclinical models for studying reinforcing and dependence-producing properties. *Curr Drug Abuse Rev*. 2008;1(3):350–374.
151. Hirvonen J, Goodwin RS, Li CT, et al. Reversible and regionally selective downregulation of brain cannabinoid CB 1 receptors in chronic daily cannabis smokers. *Mol Psychiatry*. 2012;17(6):642–649. doi:10.1038/mp.2011.82
152. Ceccarini J, Kuepper R, Kemels D, Van Os J, Henquet C, Van Laere K. [18 F]MK-9470 PET measurement of cannabinoid CB 1 receptor availability in chronic cannabis users. *Wiley Online Libr*. 2013;20(2):357–367. doi:10.1111/adb.12116
153. D'Souza DC, Cortes-Briones JA, Ranganathan M, et al. Rapid Changes in Cannabinoid 1 Receptor Availability in Cannabis-Dependent Male Subjects after Abstinence from Cannabis. *Biol Psychiatry Cogn Neurosci Neuroimaging*. 2016;1(1):60–67. doi:10.1016/j.bpsc.2015.09.008
154. Linda A. Parker. Cannabinoids and Emotional Regulation. In: *CANNABINOIDS and the BRAIN*. The MIT Press; Reprint edition; 2017:35–54.
155. Ramírez BG, Blázquez C, Gómez Del Pulgar T, Guzmán M, De Ceballos ML. Prevention of Alzheimer's disease pathology by cannabinoids: Neuroprotection mediated by blockade of microglial activation. *J Neurosci*. 2005;25(8):1904–1913. doi:10.1523/JNEUROSCI.4540-04.2005
156. Bilkei-Gorzo A, Albayram O, Draffehn A, medicine KM-N, 2017 undefined. A chronic low dose of Δ9-tetrahydrocannabinol (THC) restores cognitive function in old mice. *Nat Med* . 2017;23:782. doi:10.1038/nm.4311
157. Calabrese EJ, Rubio-Casillas A. Biphasic effects of THC in memory and cognition. *Eur J Clin Invest*. 2018;48(5):e12920. doi:10.1111/eci.12920
158. Burggren AC, Shirazi A, Ginder N, London ED. Cannabis effects on brain structure, function, and cognition: considerations for medical uses of cannabis and its derivatives. *Am J Drug Alcohol Abuse*. 2019;45(6):563–579. doi:10.1080/00952990.2019.1634086
159. Volkow ND, Hampson AJ, Baler RD. Don't Worry, Be Happy: Endocannabinoids and Cannabis at the Intersection of Stress and Reward. *Annu Rev Pharmacol Toxicol*. 2017;57(June 2016):285–

308. doi:10.1146/annurev-pharmtox-010716-104615
160. Colizzi M, McGuire P, Pertwee RG, Bhattacharyya S. Effect of cannabis on glutamate signalling in the brain: A systematic review of human and animal evidence. *Neurosci Biobehav Rev*. 2016;64. doi:10.1016/j.neubiorev.2016.03.010
161. Scherma M, Dessì C, Muntoni AL, et al. Adolescent Δ9-Tetrahydrocannabinol Exposure Alters WIN55,212-2 Self-Administration in Adult Rats. *Neuropsychopharmacology*. 2016;41(5). doi:10.1038/npp.2015.295
162. Jasinska AJ, Stein EA, Kaiser J, Naumer MJ, Yalachkov Y. Factors modulating neural reactivity to drug cues in addiction: A survey of human neuroimaging studies. *Neurosci Biobehav Rev*. 2014;38. doi:10.1016/j.neubiorev.2013.10.013
163. Curran HV, Freeman TP, Mokrysz C, Lewis DA, Morgan CJA, Parsons LH. Keep off the grass? Cannabis, cognition and addiction. *Nat Rev Neurosci*. 2016;17(5):293-306. doi:10.1038/nrn.2016.28
164. Somaini L, Manfredini M, Amore M, et al. Psychobiological responses to unpleasant emotions in cannabis users. *Eur Arch Psychiatry Clin Neurosci*. 2012;262(1). doi:10.1007/s00406-011-0223-5
165. Cuttler C, Spradlin A, Nusbaum AT, Whitney P, Hinson JM, McLaughlin RJ. Blunted stress reactivity in chronic cannabis users. *Psychopharmacology (Berl)*. 2017;234(15). doi:10.1007/s00213-017-4648-z
166. Caballero A, Tseng KY. Association of Cannabis Use during Adolescence, Prefrontal CB1 Receptor Signaling, and Schizophrenia. *Front Pharmacol*. 2012;3. doi:10.3389/fphar.2012.00101
167. Renard J, Vitalis T, Rame M, et al. Chronic cannabinoid exposure during adolescence leads to long-term structural and functional changes in the prefrontal cortex. *Eur Neuropsychopharmacol*. 2016;26(1). doi:10.1016/j.euroneuro.2015.11.005
168. Heath RG, Fitzjarrell AT, Fontana CJ, Garey RE. Cannabis sativa: Effects on brain function and ultrastructure in rhesus monkeys. *Biol Psychiatry*. 1980;15(5):657-690.
169. Scallet AC, Uemura E, Andrews A, et al. Morphometric studies of the rat hippocampus following chronic delta-9-tetrahydrocannabinol (THC). *Brain Res*. 1987;436(1):193-198. doi:10.1016/0006-8993(87)91576-9
170. Scallet AC. Neurotoxicology of cannabis and THC: A review of chronic exposure studies in animals. *Pharmacol Biochem Behav*. 1991;40(3):671-676. doi:10.1016/0091-3057(91)90380-K
171. Lawston J, Borella A, Robinson JK, Whitaker-Azmitia PM. Changes in hippocampal morphology following chronic treatment with the synthetic cannabinoid WIN 55,212-2. *Brain Res*. 2000;877(2):407-410. doi:10.1016/S0006-8993(00)02739-6
172. Niederschlags P. Concerns diffusion and concentration gradient. *Ann Phys*. 1851;170(1):59-86. doi:https://doi.org/10.1002/andp.18551700105
173. Einstein A. Einstain diffusion paper. Published online 1905:322(8).
174. Einstein A. Investigations O N the Theory .of ,the Brownian Movement R. F Ü R T H Translated By. *Dover, New York*. Published online 1956.
175. Fourier J baron de. Théorie analytique de la chaleur. Published online 1822. Accessed February 20, 2021. https://books.google.com/books?hl=fr&lr=&id=lj1RAAAAcAAJ&oi=fnd&pg=PA1&dq=Joseph+Fourier,+Théorie+analytique+de+la+chaleur,+1822&ots=KsiwOetVqf&sig=1eW5qQa7PKV9tmlhOKotsJPOVtI

176. Brown R. XXVII. A brief account of microscopical observations made in the months of June, July and August 1827, on the particles contained in the pollen of plants; and on the general existence of active molecules in organic and inorganic bodies . *Philos Mag*. Published online 1828. doi:10.1080/14786442808674769
177. Kastler B. Magnétisme nucléaire. In: *Comprendre L'IRM*. Elsevier; 2011:1-4. doi:10.1016/b978-2-294-71044-5.00001-4
178. Kastler B. Le phénomène de résonance magnétique. In: *Comprendre L'IRM*. Elsevier; 2011:5-17. doi:10.1016/b978-2-294-71044-5.00002-6
179. Meder JF, Frédy D. Imagerie en tenseur de diffusion et système nerveux central Pour quelles applications cliniques ? *J Radiol*. 2004;85(3):287-296. doi:https://doi.org/10.1016/S0221-0363(04)97580-4
180. Basser PJ, Özarslan E. Introduction to diffusion MR. In: *Diffusion MRI*. Elsevier Inc.; 2009:2-10. doi:10.1016/B978-0-12-374709-9.00001-8
181. Rowe M, Siow B, Alexander DC, Ferizi U, Richardson S. Concepts of diffusion in MRI. In: *Diffusion Tensor Imaging: A Practical Handbook*. Springer New York; 2016:23-35. doi:10.1007/978-1-4939-3118-7_3
182. Vetter D, Kastler B, Patay Z. Imagerie de diffusion, de perfusion et IRM fonctionnelle. In: *Comprendre L'IRM*. Elsevier; 2011:307-326. doi:10.1016/b978-2-294-71044-5.00016-6
183. Hahn EL. Spin echoes. *Phys Rev*. 1950;80(4):580-594. doi:10.1103/PhysRev.80.580
184. Carr HY, Purcell EM. Effects of diffusion on free precession in nuclear magnetic resonance experiments. *Phys Rev*. 1954;94(3):630-638. doi:10.1103/PhysRev.94.630
185. Stejskal EO, Tanner JE. Spin Diffusion Measurements: Spin Echoes in the Presence of a Time Dependent Field Gradient. *Cit J Chem Phys*. 1965;42(1):288. doi:10.1063/1.1695690
186. BIHAN D LE, BRETON E. Imagerie de diffusion in vivo par résonance magnétique nucléaire. *Comptes rendus l'Académie des Sci Série 2, Mécanique, Phys Chim Sci l'univers, Sci la Terre*. 1985;301(15).
187. Emsell L, Van Hecke W, Tournier JD. *Introduction to Diffusion Tensor Imaging*.; 2016. doi:10.1007/978-1-4939-3118-7_2
188. Mori S. Practical aspects of diffusion tensor imaging. In: *Introduction to Diffusion Tensor Imaging*. Elsevier; 2007:49-67. doi:10.1016/b978-044452828-5/50020-x
189. Stejskal EO, Tanner JE. Spin diffusion measurements: Spin echoes in the presence of a time-dependent field gradient. *J Chem Phys*. 1965;42(1):288-292. doi:10.1063/1.1695690
190. Luypaert R, Boujraf S, Sourbron S, Osteaux M. Diffusion and perfusion MRI: basic physics. 2001;38:19-27.
191. Boujraf S, Luypaert R, Eisendrath H, Osteaux M. Echo planar magnetic resonance imaging of anisotropic diffusion in asparagus stems. *Magn Reson Mater Physics, Biol Med*. 2001;13(2):82-90. doi:10.1016/S1352-8661(01)00132-6
192. Dhollander T. From diffusion to the diffusion tensor. In: *Diffusion Tensor Imaging: A Practical Handbook*. Springer New York; 2016:37-63. doi:10.1007/978-1-4939-3118-7_4
193. Mori S. Practical aspects of diffusion tensor imaging. *Introd to Diffus Tensor Imaging*. Published online 2007:49-67. doi:10.1016/b978-044452828-5/50020-x
194. Basser PJ, Mattiello J, Lebihan D. Estimation of the Effective Self-Diffusion Tensor from the NMR Spin Echo. *J Magn Reson Ser B*. 1994;103(3):247-254. doi:10.1006/jmrb.1994.1037
195. Pierpaoli C, Basser PJ. Toward a quantitative assessment of diffusion anisotropy. *Magn Reson Med*. 1996;36(6):893-906. doi:10.1002/mrm.1910360612
196. Moseley ME, Cohen Y, Kucharczyk J, et al. Diffusion-weighted MR imaging of anisotropic water

diffusion in cat central nervous system. *Radiology*. 1990;176(2):439-445. doi:10.1148/radiology.176.2.2367658

197. Le Bihan D. Molecular diffusion nuclear magnetic resonance imaging. *Magn Reson Q*. 1991;7(1):1-30. Accessed March 22, 2021. https://europepmc.org/article/med/2043461
198. Basser PJ, Mattiello J, LeBihan D. MR diffusion tensor spectroscopy and imaging. *Biophys J*. 1994;66(1):259-267. doi:10.1016/S0006-3495(94)80775-1
199. Basser PJ, Pierpaoli C. Microstructural and physiological features of tissues elucidated by quantitative-diffusion-tensor MRI. *J Magn Reson*. 2011;213(2):560-570. doi:10.1016/j.jmr.2011.09.022
200. Moseley ME, Cohen Y, Mintorovitch J, et al. Early detection of regional cerebral ischemia in cats: Comparison of diffusion- and T2-weighted MRI and spectroscopy. *Magn Reson Med*. 1990;14(2):330-346. doi:10.1002/mrm.1910140218
201. Sotak CH. The role of diffusion tensor imaging in the evaluation of ischemic brain - A review. *NMR Biomed*. 2002;15(7-8):561-569. doi:10.1002/nbm.786
202. Jones DK. Gaussian Modeling of the Diffusion Signal. In: *Diffusion MRI: From Quantitative Measurement to In Vivo Neuroanatomy: Second Edition*. Elsevier Inc.; 2013:87-104. doi:10.1016/B978-0-12-396460-1.00005-6
203. Boujraf S, Luypaert R, Shabana W, De Meirleir L, Sourbron S, Osteaux M. Study of pediatric brain development using magnetic resonance imaging of anisotropic diffusion. *Magn Reson Imaging*. 2002;20(4):327-336. doi:10.1016/S0730-725X(02)00501-5
204. William Rowan Hamilton B. *ON SOME EXTENSIONS OF QUATERNIONS*. Vol viii.; 1854. Accessed April 7, 2021. http://www.math.unam.mx/EMIS/classics/Hamilton/ExtQuat.pdf
205. Ricci-Curbastro G. Le calcul différentiel absolu. Bulletin des sciences mathématiques. *Bull des Sci mathématiques*. 1892;16:167-189.
206. Ricci MMG, Levi-Civita T. Méthodes de calcul différentiel absolu et leurs applications. *Math Ann*. 1900;54(1-2):125-201. doi:10.1007/BF01454201
207. Boujraf S, Luypaert R, Osteaux M. b matrix errors in echo planar diffusion tensor imaging. *J Appl Clin Med Phys*. 2001;2(3):178-183. doi:10.1120/jacmp.v2i3.2612
208. Arfken G. Tensor Analysis. . In: *Mathematical Methods for Physicists* . 3rd edn. Orlando, FL: Academic Press; 1985:118-167.
209. Boujraf S. Diffusion tensor magnetic resonance imaging strategies for color mapping of human brain anatomy. *J Med Signals Sens*. 2018;8(2):73-80. doi:10.4103/2228-7477.232082
210. Van Hecke W, Emsell L. Strategies and challenges in DTI analysis. In: *Diffusion Tensor Imaging: A Practical Handbook*. Springer New York; 2016:153-173. doi:10.1007/978-1-4939-3118-7_8
211. Armitage PA, Bastin ME. Utilizing the diffusion-to-noise ratio to optimize magnetic resonance diffusion tensor acquisition strategies for improving measurements of diffusion anisotropy. *Magn Reson Med*. 2001;45(6):1056-1065. doi:10.1002/mrm.1140
212. Jones DK, Horsfield MA, Simmons A. Optimal strategies for measuring diffusion in anisotropic systems by magnetic resonance imaging. *Magn Reson Med*. 1999;42(3). doi:10.1002/(SICI)1522-2594(199909)42:3<515::AID-MRM14>3.0.CO;2-Q
213. Alexander DC, Barker GJ. Optimal imaging parameters for fiber-orientation estimation in diffusion MRI. *Neuroimage*. 2005;27(2). doi:10.1016/j.neuroimage.2005.04.008
214. Tournier JD, Mori S, Leemans A. Diffusion tensor imaging and beyond. *Magn Reson Med*. 2011;65(6):1532-1556. doi:10.1002/mrm.22924
215. Basser PJ, Pierpaoli C. A simplified method to measure the diffusion tensor from seven MR

images. *Magn Reson Med*. 1998;39(6). doi:10.1002/mrm.1910390610
216. Jones DK. The effect of gradient sampling schemes on measures derived from diffusion tensor MRI: A Monte Carlo study. *Magn Reson Med*. 2004;51(4). doi:10.1002/mrm.20033
217. Papadakis NG, Xing D, Houston GC, et al. A study of rotationally invariant and symmetric indices of diffusion anisotropy. *Magn Reson Imaging*. 1999;17(6). doi:10.1016/S0730-725X(99)00029-6
218. Skare S, Hedehus M, Moseley ME, Li T-Q. Condition Number as a Measure of Noise Performance of Diffusion Tensor Data Acquisition Schemes with MRI. *J Magn Reson*. 2000;147(2). doi:10.1006/jmre.2000.2209
219. Curran KM, Emsell L, Leemans A. Quantitative DTI measures. In: *Diffusion Tensor Imaging: A Practical Handbook*. Springer New York; 2016:65-87. doi:10.1007/978-1-4939-3118-7_5
220. Song S-K, Sun S-W, Ramsbottom MJ, Chang C, Russell J, Cross AH. Dysmyelination Revealed through MRI as Increased Radial (but Unchanged Axial) Diffusion of Water. *Neuroimage*. 2002;17(3). doi:10.1006/nimg.2002.1267
221. Concha L. A macroscopic view of microstructure: Using diffusion-weighted images to infer damage, repair, and plasticity of white matter. *Neuroscience*. 2014;276. doi:10.1016/j.neuroscience.2013.09.004
222. Wheeler-Kingshott CAM, Cercignani M. About "axial" and "radial" diffusivities. *Magn Reson Med*. 2009;61(5). doi:10.1002/mrm.21965
223. Hüppi PS, Dubois J. Diffusion tensor imaging of brain development. *Semin Fetal Neonatal Med*. 2006;11(6). doi:10.1016/j.siny.2006.07.006
224. Werring DJ, Clark CA, Barker GJ, Thompson AJ, Miller DH. Diffusion tensor imaging of lesions and normal-appearing white matter in multiple sclerosis. *Neurology*. 1999;52(8). doi:10.1212/WNL.52.8.1626
225. Horsfield MA, Jones DK. Applications of diffusion-weighted and diffusion tensor MRI to white matter diseases - a review. *NMR Biomed*. 2002;15(7-8). doi:10.1002/nbm.787
226. Cascio CJ, Gerig G, Piven J. Diffusion tensor imaging: Application to the study of the developing brain. *J Am Acad Child Adolesc Psychiatry*. 2007;46(2):213-223. doi:10.1097/01.chi.0000246064.93200.e8
227. Wozniak JR, Lim KO. Advances in white matter imaging: A review of in vivo magnetic resonance methodologies and their applicability to the study of development and aging. *Neurosci Biobehav Rev*. 2006;30(6). doi:10.1016/j.neubiorev.2006.06.003
228. Nagy Z, Westerberg H, Klingberg T. Maturation of White Matter is Associated with the Development of Cognitive Functions during Childhood. *J Cogn Neurosci*. 2004;16(7). doi:10.1162/0898929041920441
229. Schmithorst VJ, Wilkes M, Dardzinski BJ, Holland SK. Cognitive functions correlate with white matter architecture in a normal pediatric population: A diffusion tensor HRI study. *Hum Brain Mapp*. 2005;26(2):139-147. doi:10.1002/hbm.20149
230. Mabbott DJ, Noseworthy M, Bouffet E, Laughlin S, Rockel C. White matter growth as a mechanism of cognitive development in children. *Neuroimage*. 2006;33(3). doi:10.1016/j.neuroimage.2006.07.024
231. Alexander AL, Hurley SA, Samsonov AA, et al. Characterization of Cerebral White Matter Properties Using Quantitative Magnetic Resonance Imaging Stains. *Brain Connect*. 2011;1(6). doi:10.1089/brain.2011.0071
232. Adamson SJ, Sellman JD. A prototype screening instrument for cannabis use disorder: The Cannabis Use Disorders Identification Test (CUDIT) in an alcohol-dependent clinical sample.

Drug Alcohol Rev. 2003;22(3):309-315. doi:10.1080/0959523031000154454
233. Cohen S, Kamarck T, Mermelstein R. A global measure of perceived stress. *J Health Soc Behav*. 1983;24(4):385-396. doi:10.2307/2136404
234. Leemans A, Jeurissen B, Sijbers J, DK. J. *"ExploreDTI: A Graphical Toolbox for Processing, Analyzing, and Visualizing Diffusion MR Data". : A Graphical Toolbox for Processing.*; 2009.
235. Medixant. RadiAnt DICOM Viewer [Software] Version 2020.2. Jul 19, 2020. https://www.radiantviewer.com.
236. Leemans A, Jones DK. The B-matrix must be rotated when correcting for subject motion in DTI data. *Magn Reson Med*. 2009;61(6):1336-1349. doi:10.1002/mrm.21890
237. Froeling M, Pullens P, Leemans A. DTI analysis methods: Region of interest analysis. In: *Diffusion Tensor Imaging: A Practical Handbook*. Springer New York; 2016:175-182. doi:10.1007/978-1-4939-3118-7_9
238. Soares JM, Marques P, Alves V, Sousa N. A hitchhiker's guide to diffusion tensor imaging. *Front Neurosci*. 2013;7(7 MAR):31. doi:10.3389/fnins.2013.00031
239. Tzourio-Mazoyer N, Landeau B, Papathanassiou D, et al. Automated anatomical labeling of activations in SPM using a macroscopic anatomical parcellation of the MNI MRI single-subject brain. *Neuroimage*. 2002;15(1):273-289. doi:10.1006/nimg.2001.0978
240. Hagmann P, Cammoun L, Gigandet X, et al. Mapping the Structural Core of Human Cerebral Cortex. *PLoS Biol*. 2008;6(7). doi:10.1371/journal.pbio.0060159
241. Bassett DS, Brown JA, Deshpande V, Carlson JM, Grafton ST. Conserved and variable architecture of human white matter connectivity. *Neuroimage*. 2011;54(2). doi:10.1016/j.neuroimage.2010.09.006
242. Reijmer YD, Leemans A, Caeyenberghs K, Heringa SM, Koek HL, Biessels GJ. Disruption of cerebral networks and cognitive impairment in Alzheimer disease. *Neurology*. 2013;80(15). doi:10.1212/WNL.0b013e31828c2ee5
243. Basser PJ, Pajevic S, Pierpaoli C, Duda J, Aldroubi A. In vivo fiber tractography using DT-MRI data. *Magn Reson Med*. 2000;44(4). doi:10.1002/1522-2594(200010)44:4<625::AID-MRM17>3.0.CO;2-O
244. Euler Leonhard. Solutio problematis ad geometriam situs pertinentis. *Comment Acad Sci Petropolitanae*. Published online 1741:128-140.
245. Zhang Y, Vakhtin AA, Jennings JS, et al. Diffusion tensor tractography of brainstem fibers and its application in pain. *PLoS One*. 2020;15(2). doi:10.1371/journal.pone.0213952
246. Rolls ET, Cheng W, Feng J. The orbitofrontal cortex: reward, emotion and depression. *Brain Commun*. 2020;2(2). doi:10.1093/braincomms/fcaa196
247. Rudebeck PH, Rich EL. Orbitofrontal cortex. *Curr Biol*. 2018;28(18):R1083-R1088. doi:10.1016/j.cub.2018.07.018
248. Kringelbach ML, Rolls ET. The functional neuroanatomy of the human orbitofrontal cortex: Evidence from neuroimaging and neuropsychology. *Prog Neurobiol*. 2004;72(5):341-372. doi:10.1016/j.pneurobio.2004.03.006
249. Fettes P, Schulze L, Downar J. Cortico-Striatal-Thalamic Loop Circuits of the Orbitofrontal Cortex: Promising Therapeutic Targets in Psychiatric Illness. *Front Syst Neurosci*. 2017;0:25. doi:10.3389/FNSYS.2017.00025
250. Du J, Rolls ET, Cheng W, et al. Functional connectivity of the orbitofrontal cortex, anterior cingulate cortex, and inferior frontal gyrus in humans. *Cortex*. 2020;123:185-199. doi:10.1016/j.cortex.2019.10.012
251. Heather Hsu CC, Rolls ET, Huang CC, et al. Connections of the Human Orbitofrontal Cortex and

Inferior Frontal Gyrus. *Cereb Cortex*. 2020;30(11):5830-5843. doi:10.1093/cercor/bhaa160
252. JEAN TAMRAZ, Youssef Comair. Brain Cortical Mantle and White Matter Core. In: *Atlas of Regional Anatomy of the Brain Using MRI*. Springer-Verlag Berlin Heidelberg; 2006:51-116. doi:10.1007/3-540-30672-2_3
253. Ruberte J, Navarro M, Carretero A, König HE, Puelles L. Nervous System. In: *Morphological Mouse Phenotyping: Anatomy, Histology and Imaging*. Elsevier Inc.; 2017:377-474. doi:10.1016/B978-0-12-812972-2.50013-1
254. Todd Vanderah, Gould D. The Chemical Senses of Taste and Smell. In: *Nolte's The Human Brain 7th Edition*. 7th ed. Elsevier; 2015:329-347.
255. Doty RL. Sense of smell. In: *The Curated Reference Collection in Neuroscience and Biobehavioral Psychology*. Elsevier Science Ltd.; 2016:366-372. doi:10.1016/B978-0-12-809324-5.06559-7
256. Watanabe M. *The Prefrontal Cortex as an Executive, Emotional, and Social Brain*.; 2017. doi:10.1007/978-4-431-56508-6
257. Kamigaki T. Prefrontal circuit organization for executive control. *Neurosci Res*. 2019;140:23-36. doi:10.1016/j.neures.2018.08.017
258. Watanabe M. Emotional and motivational functions of the Prefrontal Cortex. *Brain and Nerve*. 2016;68(11):1291-1299. doi:10.11477/mf.1416200593
259. Forbes CE, Grafman J. The role of the human prefrontal cortex in social cognition and moral judgment *. *Annu Rev Neurosci*. 2010;33:299-324. doi:10.1146/annurev-neuro-060909-153230
260. Neulinger K, Oram J, Tinson H, O'Gorman J, Shum DHK. Prospective memory and frontal lobe function. *Neuropsychol Dev Cogn B Aging Neuropsychol Cogn*. 2016;23(2):171-183. doi:10.1080/13825585.2015.1069252
261. Flinker A, Korzeniewska A, Shestyuk AY, et al. Redefining the role of broca's area in speech. *Proc Natl Acad Sci U S A*. 2015;112(9):2871-2875. doi:10.1073/pnas.1414491112
262. Harlow JM. Passage of an iron rod through the head. *Bost Med Surg J*. 1848;39(20):0-1.
263. Harlow JM. History of Psychiatry History of Psychiatry Recovery from the passage of an iron bar through the head. *journals.sagepub.com*. 1993;4(14):274-281. doi:10.1177/0957154X9300401407
264. Barrash J, Stuss DT, Aksan N, et al. "Frontal lobe syndrome"? Subtypes of acquired personality disturbances in patients with focal brain damage. *Cortex*. 2018;106:65-80. doi:10.1016/j.cortex.2018.05.007
265. Jawabri KH, Sharma S. *Physiology, Cerebral Cortex Functions*. StatPearls Publishing; 2019. Accessed June 11, 2021. http://www.ncbi.nlm.nih.gov/pubmed/30860731
266. Collins A, Koechlin E. Reasoning, learning, and creativity: Frontal lobe function and human decision-making. *PLoS Biol*. 2012;10(3):e1001293. doi:10.1371/journal.pbio.1001293
267. Marie Carlén. What constitutes the prefrontal cortex? *Science (80-)*. 2017;482(October):478-482. http://science.sciencemag.org/
268. Fuster JM. Anatomy of the Prefrontal Cortex. In: *The Prefrontal Cortex*. Elsevier; 2015:9-62. doi:10.1016/b978-0-12-407815-4.00002-7
269. Vanderah TW, Gould. DJ. Gross Anatomy and General Organization of the Central Nervous System. In: *NOLTE'S the HUMAN BRAIN An Introduction to Its Functional Anatomy*. 7th editio. Elsevier; 2015:62-89.
270. Cavanna AE, Trimble MR. The precuneus: a review of its functional anatomy and behavioural correlates. *Brain*. 2006;129(3). doi:10.1093/brain/awl004

271. Caspers S, Zilles K. Microarchitecture and connectivity of the parietal lobe. In: ; 2018. doi:10.1016/B978-0-444-63622-5.00003-6
272. Forkel SJ, Thiebaut de Schotten M, Kawadler JM, Dell'Acqua F, Danek A, Catani M. The anatomy of fronto-occipital connections from early blunt dissections to contemporary tractography. *Cortex*. 2014;56:73-84. doi:10.1016/J.CORTEX.2012.09.005
273. Catani M, Thiebaut de Schotten M. A diffusion tensor imaging tractography atlas for virtual in vivo dissections. *Cortex*. Published online 2008. doi:10.1016/j.cortex.2008.05.004
274. Catani M, Jones DK, ffytche DH. Perisylvian language networks of the human brain. *Ann Neurol*. 2005;57(1):8-16. doi:10.1002/ANA.20319
275. Makris N, Papadimitriou GM, Kaiser JR, Sorg S, Kennedy DN, Pandya DN. Delineation of the Middle Longitudinal Fascicle in Humans: A Quantitative, In Vivo, DT-MRI Study. *Cereb Cortex*. 2009;19(4):777-785. doi:10.1093/CERCOR/BHN124
276. Maldonado IL, Champfleur NM de, Velut S, Destrieux C, Zemmoura I, Duffau H. Evidence of a middle longitudinal fasciculus in the human brain from fiber dissection. *J Anat*. 2013;223(1):38-45. doi:10.1111/JOA.12055
277. neurology MG-A in, 2003 undefined. Subcortical projections of the parietal lobes. *europepmc.org*. Accessed November 5, 2021. https://europepmc.org/article/med/12894400
278. Behrens TEJ, Johansen-Berg H, Woolrich MW, et al. Non-invasive mapping of connections between human thalamus and cortex using diffusion imaging. *Nat Neurosci 2003 67*. 2003;6(7):750-757. doi:10.1038/nn1075
279. Traynor C, Heckemann RA, Hammers A, et al. Reproducibility of thalamic segmentation based on probabilistic tractography. *Neuroimage*. 2010;52(1). doi:10.1016/j.neuroimage.2010.04.024
280. Mai JK, Paxinos G, Voss T. *Atlas of the Human Brain*. 3rd Editio. ELSEVIER; 2008. https://www.elsevier.com/books/atlas-of-the-human-brain/mai/978-0-12-802800-1
281. Kiernan JA. Anatomy of the Temporal Lobe. *Epilepsy Res Treat*. 2012;2012:1-12. doi:10.1155/2012/176157
282. Javed K, Lui F. Neuroanatomy, Cerebral Cortex. *StatPearls*. Published online August 10, 2020. Accessed June 23, 2021. http://www.ncbi.nlm.nih.gov/pubmed/30725932
283. Binder JR. Current Controversies on Wernicke's Area and its Role in Language. *Curr Neurol Neurosci Rep*. 2017;17(8). doi:10.1007/s11910-017-0764-8
284. Weiner KS, Zilles K. The anatomical and functional specialization of the fusiform gyrus. *Neuropsychologia*. 2016;83:48-62. doi:10.1016/j.neuropsychologia.2015.06.033
285. Gage NM, Baars BJ. The Brain. In: *Fundamentals of Cognitive Neuroscience*. Elsevier; 2018:17-52. doi:10.1016/B978-0-12-803813-0.00002-7
286. Ramos-Fresnedo A, Segura-Duran I, Chaichana KL, Pillai JJ. Supratentorial white matter tracts. In: *Comprehensive Overview of Modern Surgical Approaches to Intrinsic Brain Tumors*. Elsevier; 2019:23-35. doi:10.1016/B978-0-12-811783-5.00002-1
287. Papagno C, Miracapillo C, Casarotti A, et al. What is the role of the uncinate fasciculus? Surgical removal and proper name retrieval. *Brain*. 2010;134(2):405-414. doi:10.1093/brain/awq283
288. Mesulam M. Behavioural neuroanatomy: large-scale networks, association cortex, frontal syndromes, the limbic system, and the hemispheric specializations. In: *Principles of Behavioural and Cognitive Neurology.* Oxford University Press; 2nd edition; 2000:1-120.
289. RajMohan V, Mohandas E. The limbic system. *Indian J Psychiatry*. 2007;49(2):139. doi:10.4103/0019-5545.33264
290. Torrico TJ, Abdijadid S. Neuroanatomy, Limbic System. *StatPearls*. Published online July 31,

2020. Accessed June 14, 2021. http://www.ncbi.nlm.nih.gov/pubmed/30860726
291. Broca PP. Anatomie comparée des circonvolutions cérébrales: Le grand lobe limbique et la scissure limbique dans la série des mammifères. *Rev D'Anthropol*. 1878;1:385-498.
292. Papez JW. A proposed mechanism of emotion. *Arch Neurol Psychiatry*. 1937;38(4):725-743. doi:10.1001/archneurpsyc.1937.02260220069003
293. YAKOVLEV PI. Motility, behavior and the brain; stereodynamic organization and neural coordinates of behavior. *J Nerv Ment Dis*. 1948;107(4):313-335. doi:10.1097/00005053-194810740-00001
294. MacLean PD. Some psychiatric implications of physiological studies on frontotemporal portion of limbic system (Visceral brain). *Electroencephalogr Clin Neurophysiol*. 1952;4(4):407-418. doi:10.1016/0013-4694(52)90073-4
295. Stevens FL, Hurley RA, Taber KH. Anterior Cingulate Cortex: Unique Role in Cognition and Emotion. *J Neuropsychiatry Clin Neurosci*. 2011;23(2). doi:10.1176/jnp.23.2.jnp121
296. Rolls ET. The cingulate cortex and limbic systems for emotion, action, and memory. *Brain Struct Funct*. 2019;224(9):3001-3018. doi:10.1007/S00429-019-01945-2
297. Lew CH, Semendeferi K. Evolutionary Specializations of the Human Limbic System. *Evol Nerv Syst Second Ed*. 2017;4-4:277-291. doi:10.1016/B978-0-12-804042-3.00115-9
298. Dhikav V, Anand K. Hippocampus in health and disease: An overview. *Ann Indian Acad Neurol*. 2012;15(4). doi:10.4103/0972-2327.104323
299. Wang X, Gu X, Fan J, et al. Recovery of empathetic function following resection of insular gliomas. *J Neurooncol*. 2014;117(2). doi:10.1007/s11060-014-1380-y
300. Shu L, Wang Y. HIGHLIGHTS IN BASIC AUTONOMIC NEUROSCIENCE: INSULAR CORTEX INJURY LEADS TO CARDIOVASCULAR DYSFUNCTION. *Auton Neurosci*. 2014;185. doi:10.1016/j.autneu.2014.07.001
301. Ibañez A, Gleichgerrcht E, Manes F. Clinical effects of insular damage in humans. *Brain Struct Funct*. 2010;214(5-6). doi:10.1007/s00429-010-0256-y
302. Pessoa L. Emotion and cognition and the amygdala: From "what is it?" to "what's to be done?" *Neuropsychologia*. 2010;48(12). doi:10.1016/j.neuropsychologia.2010.06.038
303. Schmahmann JD. Vascular Syndromes of the Thalamus. *Stroke*. 2003;34(9). doi:10.1161/01.STR.0000087786.38997.9E
304. Catani M, Dell'Acqua F, Thiebaut de Schotten M. A revised limbic system model for memory, emotion and behaviour. *Neurosci Biobehav Rev*. 2013;37(8):1724-1737. doi:10.1016/j.neubiorev.2013.07.001
305. Mega MS, Cummings JL, Salloway S, Malloy P. The limbic system: An anatomic, phylogenetic, and clinical perspective. *J Neuropsychiatry Clin Neurosci*. 1997;9(3):315-330. doi:10.1176/jnp.9.3.315
306. Lanciego JL, Luquin N, Obeso JA. Functional neuroanatomy of the basal ganglia. *Cold Spring Harb Perspect Med*. 2012;2(12). doi:10.1101/cshperspect.a009621
307. Florio TM, Scarnati E, Rosa I, et al. The Basal Ganglia: More than just a switching device. *CNS Neurosci Ther*. 2018;24(8):677-684. doi:10.1111/cns.12987
308. Riva D, Taddei M, Bulgheroni S. The neuropsychology of basal ganglia. *Eur J Paediatr Neurol*. 2018;22(2):321-326. doi:10.1016/j.ejpn.2018.01.009
309. Graff-Radford J, Williams L, Jones DT, Benarroch EE. Caudate nucleus as a component of networks controlling behavior. *Neurology*. 2017;89(21):2192-2197. doi:10.1212/WNL.0000000000004680
310. Driscoll ME, Bollu PC, Tadi P. Neuroanatomy, Nucleus Caudate. *StatPearls*. Published online July

31, 2020. Accessed July 28, 2021. https://www.ncbi.nlm.nih.gov/books/NBK557407/
311. Ghandili M, Munakomi S. Neuroanatomy, Putamen. *StatPearls*. Published online February 8, 2021. Accessed July 28, 2021. https://www.ncbi.nlm.nih.gov/books/NBK542170/
312. Cardinal RN, Parkinson JA, Hall J, Everitt BJ. Emotion and motivation: the role of the amygdala, ventral striatum, and prefrontal cortex. *Neurosci Biobehav Rev*. 2002;26(3). doi:10.1016/S0149-7634(02)00007-6
313. McCullough LD, Sokolowski JD, Salamone JD. A neurochemical and behavioral investigation of the involvement of nucleus accumbens dopamine in instrumental avoidance. *Neuroscience*. 1993;52(4). doi:10.1016/0306-4522(93)90538-Q
314. Yun IA. The Ventral Tegmental Area Is Required for the Behavioral and Nucleus Accumbens Neuronal Firing Responses to Incentive Cues. *J Neurosci*. 2004;24(12). doi:10.1523/JNEUROSCI.5282-03.2004
315. Basar K, Sesia T, Groenewegen H, Steinbusch HWM, Visser-Vandewalle V, Temel Y. Nucleus accumbens and impulsivity. *Prog Neurobiol*. 2010;92(4). doi:10.1016/j.pneurobio.2010.08.007
316. Salgado S, Kaplitt MG. The Nucleus Accumbens: A Comprehensive Review. *Stereotact Funct Neurosurg*. 2015;93(2). doi:10.1159/000368279
317. Wager TD, Davidson ML, Hughes BL, Lindquist MA, Ochsner KN. Prefrontal-Subcortical Pathways Mediating Successful Emotion Regulation. *Neuron*. 2008;59(6). doi:10.1016/j.neuron.2008.09.006
318. Javed N, Cascella M. Neuroanatomy, Globus Pallidus. *StatPearls*. Published online July 31, 2020. Accessed July 28, 2021. https://www.ncbi.nlm.nih.gov/books/NBK557755/
319. Smith KS, Tindell AJ, Aldridge JW, Berridge KC. Ventral pallidum roles in reward and motivation. *Behav Brain Res*. 2009;196(2). doi:10.1016/j.bbr.2008.09.038
320. Alexander GE, DeLong MR, Strick PL. Parallel organization of functionally segregated circuits linking basal ganglia and cortex. *Annu Rev Neurosci*. 1986;VOL. 9:357-381. doi:10.1146/annurev.ne.09.030186.002041
321. Middleton FA, Strick PL. Anatomical evidence for cerebellar and basal ganglia involvement in higher cognitive function. *Science (80-)*. 1994;266(5184):458-461. doi:10.1126/science.7939688
322. Mandelbaum DE, de la Monte SM. Adverse Structural and Functional Effects of Marijuana on the Brain: Evidence Reviewed. *Pediatr Neurol*. 2017;66:12-20. doi:10.1016/j.pediatrneurol.2016.09.004
323. Adamson SJ, Kay-Lambkin FJ, Baker AL, et al. An improved brief measure of cannabis misuse: The Cannabis Use Disorders Identification Test-Revised (CUDIT-R). *Drug Alcohol Depend*. 2010;110(1-2):137-143. doi:10.1016/J.DRUGALCDEP.2010.02.017
324. J C, YJ T, LS van V, AM K. The relation between cannabis use, dependence severity and white matter microstructure: A diffusion tensor imaging study. *Addict Biol*. Published online 2021. doi:10.1111/ADB.13081
325. Cousijn J, Wiers RW, Ridderinkhof KR, Van den Brink W, Veltman DJ, Goudriaan AE. Grey matter alterations associated with cannabis use: Results of a VBM study in heavy cannabis users and healthy controls. *Neuroimage*. Published online 2012. doi:10.1016/j.neuroimage.2011.09.046
326. O'Donnell BF, Skosnik PD, Hetrick WP, Fridberg DJ. Decision Making and Impulsivity in Young Adult Cannabis Users. *Front Psychol*. 2021;0:2594. doi:10.3389/FPSYG.2021.679904
327. Rinehart L, Spencer S. Which came first: Cannabis use or deficits in impulse control? *Prog Neuro-Psychopharmacology Biol Psychiatry*. 2021;106:110066.

doi:10.1016/J.PNPBP.2020.110066

328. Patton JH, Stanford MS, Barratt ES. Factor structure of the barratt impulsiveness scale. *J Clin Psychol*. 1995;51(6):768-774. doi:10.1002/1097-4679(199511)51:6<768::AID-JCLP2270510607>3.0.CO;2-1
329. Fontenelle LF, Oostermeijer S, Harrison BJ, Pantelis C, Yücel M. Obsessive-Compulsive Disorder, Impulse Control Disorders and Drug Addiction. *Drugs 2011 717*. 2012;71(7):827-840. doi:10.2165/11591790-000000000-00000
330. Gruber SA, Silveri MM, Dahlgren MK, Yurgelun-Todd D. Why So Impulsive? White Matter Alterations Are Associated With Impulsivity in Chronic Marijuana Smokers. *Exp Clin Psychopharmacol*. 2011;19(3):231-242. doi:10.1037/a0023034
331. Dougherty DM, Mathias CW, Dawes MA, et al. Impulsivity, attention, memory, and decision-making among adolescent marijuana users. *Psychopharmacol 2012 2262*. 2012;226(2):307-319. doi:10.1007/S00213-012-2908-5
332. DH D, HS A, E E, N Z, Ş G. Impulsivity, Sensation Seeking, and Decision-Making in Long-Term Abstinent Cannabis Dependent Patients. *Noro Psikiyatr Ars*. 2018;55(4):315-319. doi:10.5152/NPA.2017.19304
333. Phillips AC. Perceived Stress. *Encycl Behav Med*. Published online 2013:1453-1454. doi:10.1007/978-1-4419-1005-9_479
334. Vujanovic AA, Wardle MC, Liu S, Dias NR, Lane SD. Attentional bias in adults with cannabis use disorders. *http://dx.doi.org/101080/105508872015111635 4*. 2016;35(2):144-153. doi:10.1080/10550887.2015.1116354
335. Spradlin A, Cuttler C. Problems Associated with Using Cannabis to Cope with Stress. Published online 2019. doi:10.26828/cannabis.2019.01.003
336. Cavalli JM, Cservenka A. Emotion Dysregulation Moderates the Association Between Stress and Problematic Cannabis Use. *Front Psychiatry*. 2021;0:1537. doi:10.3389/FPSYT.2020.597789
337. Blithikioti C, Miquel L, Batalla A, et al. Cerebellar alterations in cannabis users: A systematic review. *Addict Biol*. 2019;24(6):1121-1137. doi:10.1111/adb.12714
338. Lu H-C, Mackie K. An Introduction to the Endogenous Cannabinoid System. *Biol Psychiatry*. 2016;79(7):516-525. doi:10.1016/J.BIOPSYCH.2015.07.028
339. Ganesh S, Vidya KL, Rashid AA, Singh J, D'Souza DC. Revisiting the Consequences of Adolescent Cannabinoid Exposure Through the Lens of the Endocannabinoid System. *Curr Addict Reports 2018 54*. 2018;5(4):418-427. doi:10.1007/S40429-018-0233-8
340. Le Strat Y, Dubertret C, Le Foll B. Impact of age at onset of cannabis use on cannabis dependence and driving under the influence in the United States. *Accid Anal Prev*. 2015;76. doi:10.1016/j.aap.2014.12.015
341. Millar SR, Mongan D, Smyth BP, Perry IJ, Galvin B. Relationships between age at first substance use and persistence of cannabis use and cannabis use disorder. *BMC Public Health*. 2021;21(1). doi:10.1186/s12889-021-11023-0
342. Hyman SM, Sinha R. Stress-related factors in cannabis use and misuse: Implications for prevention and treatment. *J Subst Abuse Treat*. 2009;36(4). doi:10.1016/j.jsat.2008.08.005
343. Patel J, Marwaha R. Cannabis Use Disorder. *Clin Handb Adolesc Addict*. Published online July 12, 2021:202-212. Accessed October 20, 2021. https://www.ncbi.nlm.nih.gov/books/NBK538131/
344. D'Arceuil H, de Crespigny A. Diffusion Imaging in Gray Matter. *Diffus MRI*. Published online February 7, 2013:647-660. doi:10.1093/MED/9780195369779.003.0039
345. Zatorre RJ, Fields RD, Johansen-Berg H. Plasticity in Gray and White: Neuroimaging changes in

brain structure during learning. *Nat Neurosci*. 2012;15(4):528. doi:10.1038/NN.3045
346. Blumenfeld-Katzir T, Pasternak O, Dagan M, Assaf Y. Diffusion MRI of Structural Brain Plasticity Induced by a Learning and Memory Task. *PLoS One*. 2011;6(6). doi:10.1371/JOURNAL.PONE.0020678
347. Alexander AL, Lee JE, Lazar M, Field AS. Diffusion Tensor Imaging of the Brain. *Neurotherapeutics*. 2007;4(3):316-329. doi:10.1016/J.NURT.2007.05.011
348. M W, O S, A O, S K, H J. Age-related apparent diffusion coefficient changes in the normal brain. *Radiology*. 2013;266(2):575-582. doi:10.1148/RADIOL.12112420
349. Lorenzetti V, Chye Y, Silva P, Solowij N, Roberts CA. Does regular cannabis use affect neuroanatomy? An updated systematic review and meta-analysis of structural neuroimaging studies. *Eur Arch Psychiatry Clin Neurosci*. 2019;269(1). doi:10.1007/s00406-019-00979-1
350. Chye Y, Kirkham R, Lorenzetti V, McTavish E, Solowij N, Yücel M. Cannabis, Cannabinoids, and Brain Morphology: A Review of the Evidence. *Biol Psychiatry Cogn Neurosci Neuroimaging*. Published online 2020:1-9. doi:10.1016/j.bpsc.2020.07.009
351. Chye Y, Solowij N, Suo C, et al. Orbitofrontal and caudate volumes in cannabis users: a multi-site mega-analysis comparing dependent versus non-dependent users. *Psychopharmacology (Berl)*. 2017;234(13). doi:10.1007/s00213-017-4606-9
352. Filbey FM, Aslan S, Calhoun VD, et al. Long-term effects of marijuana use on the brain. *Proc Natl Acad Sci U S A*. 2014;111(47):16913-16918. doi:10.1073/pnas.1415297111
353. Matochik JA, Eldreth DA, Cadet JL, Bolla KI. Altered brain tissue composition in heavy marijuana users. *Drug Alcohol Depend*. 2005;77(1):23-30. doi:10.1016/J.DRUGALCDEP.2004.06.011
354. Hill SY, Sharma V, Jones BL. Lifetime use of cannabis from longitudinal assessments, cannabinoid receptor (CNR1) variation, and reduced volume of the right anterior cingulate. *Psychiatry Res Neuroimaging*. 2016;255:24-34. doi:10.1016/J.PSCYCHRESNS.2016.05.009
355. Smith MJ, Cobia DJ, Reilly JL, et al. Cannabis-related episodic memory deficits and hippocampal morphological differences in healthy individuals and schizophrenia subjects. *Hippocampus*. 2015;25(9). doi:10.1002/hipo.22427
356. Price JS, McQueeny T, Shollenbarger S, Browning EL, Wieser J, Lisdahl KM. Effects of marijuana use on prefrontal and parietal volumes and cognition in emerging adults. *Psychopharmacol 2015 23216*. 2015;232(16):2939-2950. doi:10.1007/S00213-015-3931-0
357. JC C, M L-L, DA Y-T. Altered frontal cortical volume and decision making in adolescent cannabis users. *Front Psychol*. 2010;1(DEC). doi:10.3389/FPSYG.2010.00225
358. Mata I, Perez-Iglesias R, Roiz-Santiañez R, et al. Gyrification brain abnormalities associated with adolescence and early-adulthood cannabis use. *Brain Res*. 2010;1317:297-304. doi:10.1016/J.BRAINRES.2009.12.069
359. Medina KL, McQueeny T, Nagel BJ, Hanson KL, Yang TT, Tapert SF. IMAGING STUDY: Prefrontal cortex morphometry in abstinent adolescent marijuana users: subtle gender effects. *Addict Biol*. 2009;14(4):457-468. doi:10.1111/J.1369-1600.2009.00166.X
360. Batalla A, Soriano-Mas C, López-Solà M, et al. Modulation of brain structure by catechol-O-methyltransferase Val158Met polymorphism in chronic cannabis users. *Addict Biol*. 2014;19(4):722-732. doi:10.1111/ADB.12027
361. Lorenzetti V, Solowij N, Whittle S, et al. Gross morphological brain changes with chronic, heavy cannabis use. *Br J Psychiatry*. 2015;206(1). doi:10.1192/bjp.bp.114.151407
362. Schacht JP, Hutchison KE, Filbey FM. Associations between Cannabinoid Receptor-1 (CNR1) Variation and Hippocampus and Amygdala Volumes in Heavy Cannabis Users. *Neuropsychopharmacol 2012 3711*. 2012;37(11):2368-2376. doi:10.1038/npp.2012.92

363. Yücel M, Solowij N, Respondek C, et al. Regional brain abnormalities associated with long-term heavy cannabis use. *Arch Gen Psychiatry*. Published online 2008. doi:10.1001/archpsyc.65.6.694
364. Ashtari M, Avants B, Cyckowski L, et al. Medial temporal structures and memory functions in adolescents with heavy cannabis use. *J Psychiatr Res*. 2011;45(8):1055-1066. doi:10.1016/J.JPSYCHIRES.2011.01.004
365. Weiland BJ, Thayer RE, Depue BE, Sabbineni A, Bryan AD, Hutchison KE. Daily Marijuana Use Is Not Associated with Brain Morphometric Measures in Adolescents or Adults. *J Neurosci*. 2015;35(4):1505-1512. doi:10.1523/JNEUROSCI.2946-14.2015
366. Moreno-Alcázar A, Gonzalvo B, Canales-Rodríguez EJ, et al. Larger Gray Matter Volume in the Basal Ganglia of Heavy Cannabis Users Detected by Voxel-Based Morphometry and Subcortical Volumetric Analysis. *Front Psychiatry*. 2018;0(MAY):175. doi:10.3389/FPSYT.2018.00175
367. SW Y, EE D, H K, PD W, KM C, MN P. Pretreatment measures of brain structure and reward-processing brain function in cannabis dependence: an exploratory study of relationships with abstinence during behavioral treatment. *Drug Alcohol Depend*. 2014;140:33-41. doi:10.1016/J.DRUGALCDEP.2014.03.031
368. Gilman JM, Kuster JK, Lee S, et al. Cannabis Use Is Quantitatively Associated with Nucleus Accumbens and Amygdala Abnormalities in Young Adult Recreational Users. *J Neurosci*. 2014;34(16):5529-5538. doi:10.1523/JNEUROSCI.4745-13.2014
369. Battistella G, Fornari E, Annoni JM, et al. Long-term effects of cannabis on brain structure. *Neuropsychopharmacology*. Published online 2014. doi:10.1038/npp.2014.67
370. Lopez-Larson MP, Bogorodzki P, Rogowska J, et al. Altered prefrontal and insular cortical thickness in adolescent marijuana users. *Behav Brain Res*. 2011;220(1):164-172. doi:10.1016/J.BBR.2011.02.001
371. Delisi LE, Bertisch HC, Szulc KU, et al. A preliminary DTI study showing no brain structural change associated with adolescent cannabis use. *Harm Reduct J*. Published online 2006. doi:10.1186/1477-7517-3-17
372. Wright IC, McGuire PK, Poline JB, et al. A Voxel-Based Method for the Statistical Analysis of Gray and White Matter Density Applied to Schizophrenia. *Neuroimage*. 1995;2(4):244-252. doi:10.1006/NIMG.1995.1032
373. Matute C, Ransom BR. Roles of White Matter in Central Nervous System Pathophysiologies. *ASN Neuro*. 2012;4(2). doi:10.1042/AN20110060
374. Ishibashi T, Dakin KA, Stevens B, et al. Astrocytes Promote Myelination in Response to Electrical Impulses. *Neuron*. 2006;49(6). doi:10.1016/j.neuron.2006.02.006
375. Scheller A, Kirchhoff F. Endocannabinoids and Heterogeneity of Glial Cells in Brain Function. *Front Integr Neurosci*. 2016;10. doi:10.3389/fnint.2016.00024
376. WH H, IM H, IR O. Substance abuse and white matter: Findings, limitations, and future of diffusion tensor imaging research. *Drug Alcohol Depend*. 2019;197. doi:10.1016/J.DRUGALCDEP.2019.02.005
377. Zimmermann K, Yao S, Heinz M, et al. Altered orbitofrontal activity and dorsal striatal connectivity during emotion processing in dependent marijuana users after 28 days of abstinence. *Psychopharmacology (Berl)*. 2018;235(3). doi:10.1007/s00213-017-4803-6
378. Terral G, Busquets-Garcia A, Varilh M, et al. CB1 Receptors in the Anterior Piriform Cortex Control Odor Preference Memory. *Curr Biol*. 2019;29(15). doi:10.1016/j.cub.2019.06.041
379. Terral G, Varilh M, Cannich A, Massa F, Ferreira G, Marsicano G. Synaptic Functions of Type-1 Cannabinoid Receptors in Inhibitory Circuits of the Anterior Piriform Cortex. *Neuroscience*.

2020;433. doi:10.1016/j.neuroscience.2020.03.002
380. Terral G, Marsicano G, Grandes P, Soria-Gómez E. Cannabinoid Control of Olfactory Processes: The Where Matters. *Genes (Basel)*. 2020;11(4). doi:10.3390/genes11040431
381. Piredda S, Gale K. A crucial epileptogenic site in the deep prepiriform cortex. *Nature*. 1985;317(6038). doi:10.1038/317623a0
382. Lazarini-Lopes W, Do Val-da Silva RA, da Silva-Júnior RMP, et al. Chronic cannabidiol (CBD) administration induces anticonvulsant and antiepileptogenic effects in a genetic model of epilepsy. *Epilepsy Behav*. 2021;119. doi:10.1016/j.yebeh.2021.107962
383. McClung CA, Ulery PG, Perrotti LI, Zachariou V, Berton O, Nestler EJ. ΔFosB: a molecular switch for long-term adaptation in the brain. *Mol Brain Res*. 2004;132(2). doi:10.1016/j.molbrainres.2004.05.014
384. Lazenka MF, Kang M, De DD, Selley DE, Sim-Selley LJ. Δ9-Tetrahydrocannabinol Experience Influences ΔFosB and Downstream Gene Expression in Prefrontal Cortex. *Cannabis Cannabinoid Res*. 2017;2(1). doi:10.1089/can.2017.0022
385. Arnone D, Barrick TR, Chengappa S, Mackay CE, Clark CA, Abou-Saleh MT. Corpus callosum damage in heavy marijuana use: Preliminary evidence from diffusion tensor tractography and tract-based spatial statistics. *Neuroimage*. Published online 2008. doi:10.1016/j.neuroimage.2008.02.064
386. Becker MP, Collins PF, Lim KO, Muetzel RL, Luciana M. Longitudinal changes in white matter microstructure after heavy cannabis use. *Dev Cogn Neurosci*. 2015;16:23-35. doi:10.1016/j.dcn.2015.10.004
387. Clark DB, Chung T, Thatcher DL, Pajtek S, Long EC. Psychological dysregulation, white matter disorganization and substance use disorders in adolescence. *Addiction*. 2012;107(1):206-214. doi:10.1111/J.1360-0443.2011.03566.X
388. Gruber SA, Dahlgren MK, Sagar KA, Gönenç A, Lukas SE. Worth the wait: Effects of age of onset of marijuana use on white matter and impulsivity. *Psychopharmacology (Berl)*. 2014;231(8):1455-1465. doi:10.1007/s00213-013-3326-z
389. Vogel AP, Pearson-Dennett V, Magee M, et al. Adults with a history of recreational cannabis use have altered speech production. *Drug Alcohol Depend*. 2021;227:108963. doi:10.1016/J.DRUGALCDEP.2021.108963
390. Ashtari M, Cervellione K, Cottone J, Ardekani BA, Kumra S. Diffusion abnormalities in adolescents and young adults with a history of heavy cannabis use. *J Psychiatr Res*. Published online 2009. doi:10.1016/j.jpsychires.2008.12.002
391. Orr JM, Paschall CJ, Banich MT. Recreational marijuana use impacts white matter integrity and subcortical (but not cortical) morphometry. *NeuroImage Clin*. 2016;12. doi:10.1016/j.nicl.2016.06.006
392. Manza P, Yuan K, Shokri-Kojori E, Tomasi D, Volkow ND. Brain structural changes in cannabis dependence: association with MAGL. *Mol Psychiatry*. 2020;25(12). doi:10.1038/s41380-019-0577-z
393. Riba J, Valle M, Sampedro F, et al. Telling true from false: cannabis users show increased susceptibility to false memories. *Mol Psychiatry*. 2015;20(6). doi:10.1038/mp.2015.36
394. Ashtari M, Cervellione K, Cottone J, Ardekani BA, Kumra S. Diffusion abnormalities in adolescents and young adults with a history of heavy cannabis use. *J Psychiatr Res*. 2009;43(3):189-204. doi:10.1016/j.jpsychires.2008.12.002
395. Depue BE, Orr JM, Smolker HR, Naaz F, Banich MT. The Organization of Right Prefrontal Networks Reveals Common Mechanisms of Inhibitory Regulation Across Cognitive, Emotional,

and Motor Processes. *Cereb Cortex*. 2016;26(4). doi:10.1093/cercor/bhu324

396. Smolker HR, Depue BE, Reineberg AE, Orr JM, Banich MT. Individual differences in regional prefrontal gray matter morphometry and fractional anisotropy are associated with different constructs of executive function. *Brain Struct Funct*. 2015;220(3). doi:10.1007/s00429-014-0723-y
397. Von Der Heide RJ, Skipper LM, Klobusicky E, Olson IR. Dissecting the uncinate fasciculus: disorders, controversies and a hypothesis. *Brain*. 2013;136(6). doi:10.1093/brain/awt094
398. Herbet G, Zemmoura I, Duffau H. Functional Anatomy of the Inferior Longitudinal Fasciculus: From Historical Reports to Current Hypotheses. *Front Neuroanat*. 2018;12. doi:10.3389/fnana.2018.00077
399. Kim D-J, Skosnik PD, Cheng H, et al. Structural Network Topology Revealed by White Matter Tractography in Cannabis Users: A Graph Theoretical Analysis. *Brain Connect*. 2011;1(6). doi:10.1089/brain.2011.0053
400. Jakabek D, Yücel M, Lorenzetti V, Solowij N. An MRI study of white matter tract integrity in regular cannabis users: effects of cannabis use and age. *Psychopharmacology (Berl)*. 2016;233(19-20):3627-3637. doi:10.1007/s00213-016-4398-3
401. Filbey FM, Dunlop J, Ketcherside A, et al. fMRI study of neural sensitization to hedonic stimuli in long-term, daily cannabis users. *Hum Brain Mapp*. 2016;37(10):3431-3443. doi:10.1002/HBM.23250
402. Gruber SA, Yurgelun-Todd DA. Neuroimaging of marijuana smokers during inhibitory processing: a pilot investigation. *Cogn Brain Res*. 2005;23(1). doi:10.1016/j.cogbrainres.2005.02.016
403. Hester R, Nestor L, Garavan H. Impaired Error Awareness and Anterior Cingulate Cortex Hypoactivity in Chronic Cannabis Users. *Neuropsychopharmacology*. 2009;34(11). doi:10.1038/npp.2009.67
404. Gruber SA, Rogowska J, Yurgelun-Todd DA. Altered affective response in marijuana smokers: An FMRI study. *Drug Alcohol Depend*. 2009;105(1-2). doi:10.1016/j.drugalcdep.2009.06.019
405. Zimmermann K, Walz C, Derckx RT, et al. Emotion regulation deficits in regular marijuana users. *Hum Brain Mapp*. 2017;38(8). doi:10.1002/hbm.23671
406. Shollenbarger SG, Price J, Wieser J, Lisdahl K. Poorer frontolimbic white matter integrity is associated with chronic cannabis use, FAAH genotype, and increased depressive and apathy symptoms in adolescents and young adults. *NeuroImage Clin*. 2015;8:117-125. doi:10.1016/j.nicl.2015.03.024
407. Pujol J, Blanco-Hinojo L, Batalla A, et al. Functional connectivity alterations in brain networks relevant to self-awareness in chronic cannabis users. *J Psychiatr Res*. 2014;51(1):68-78. doi:10.1016/J.JPSYCHIRES.2013.12.008
408. Yücel M. White-matter abnormalities in adolescents with long-term inhalant and cannabis use: a diffusion magnetic resonance imaging study. *J Psychiatry Neurosci*. 2010;35(6). doi:10.1503/jpn.090177
409. Zalesky A, Solowij N, Yücel M, et al. Effect of long-term cannabis use on axonal fibre connectivity. *Brain*. Published online 2012. doi:10.1093/brain/aws136
410. Huisman TAGM, Loenneker T, Barta G, et al. Quantitative diffusion tensor MR imaging of the brain: Field strength related variance of apparent diffusion coefficient (ADC) and fractional anisotropy (FA) scalars. *Eur Radiol*. 2006;16(8):1651-1658. doi:10.1007/s00330-006-0175-8
411. Kim Y-T, Shim J-H, Kim S, Baek H-M. Diffusion Tensor Imaging Analysis of Subcortical Gray Matter in Patients with Alcohol Dependence. *Appl Magn Reson*. 2021;52(1).

doi:10.1007/s00723-020-01272-4

412. Blanco-Hinojo L, Pujol J, Harrison BJ, et al. Attenuated frontal and sensory inputs to the basal ganglia in cannabis users. *Addict Biol*. 2017;22(4):1036-1047. doi:10.1111/ADB.12370
413. Linda A. Parker. *Cannabinoids and the Brain*. The MIT Press; 2017.
414. Zou S, Kumar U. Cannabinoid receptors and the endocannabinoid system: Signaling and function in the central nervous system. *Int J Mol Sci*. Published online 2018. doi:10.3390/ijms19030833
415. Passingham RE, Wise SP. Introduction. In: *The Neurobiology of the Prefrontal Cortex*. Oxford University Press; 2015:1-25. doi:10.1093/acprof:osobl/9780199552917.003.0001
416. Fan L, Li H, Zhuo J, et al. The human brainnetome atlas: a new brain atlas based on connectional architecture. *academic.oup.com*. Accessed June 8, 2021. https://academic.oup.com/cercor/article-abstract/26/8/3508/2429104
417. Wise SP. Forward frontal fields: phylogeny and fundamental function. *Trends Neurosci*. 2008;31(12):599-608. doi:10.1016/j.tins.2008.08.008

جامعة سيدي محمد بن عبد الله - فاس
UNIVERSITÉ SIDI MOHAMED BEN ABDELLAH DE FES
كلية الطب والصيدلة وطب الأسنان
FACULTÉ DE MÉDECINE, DE PHARMACIE ET DE MÉDECINE DENTAIRE

سنة 2021 أطروحة رقم :21/ 338

دراسة الاتصال الدماغي لمستخدمي القتّب المزمن والثقيل: تقييم بواسطة موترالتصوير الموزن بمعامل الانتشار و بواسطة الخاصيات السريرية.

الأطروحة

قدمت ونوقشت علانية يوم 2021/12/31

من طرف

السيد بنمسعود محمود
المزداد في 1995/08/06 بفاس

لنيل شهادة الدكتوراه في الطب

الكلمات الأساسية :

ألياف المسالك – ROI – الأطلس – THC– الاتصال الدماغي الهيكلي
–الاندفاعية – الارتباطات – اضطراب تعاطي الحشيش – الشبكات الدماغية

اللجنة

السيد رموز اسماعيل..... أستاذ في علم الأمراض النفسية	الرئيس
السيد بجراف سعيد ..... أستاذ في علم الفيزياء الأحيائية و تقنيات التصوير بالرنين المغناطيسي الإكلينيكية	المشرف
السيد علوان رشيد..... أستاذ في علم الأمراض النفسية	*أعضاء*
السيد المعروفي مصطفى ..... أستاذ في الطب الاشعاعي	
السيد بنزكموت محمد ..... أستاذ في جراحة الدماغ والأعصاب	
السيد العلمي بدر الدين ..... أستاذ في علم الفيزياء الأحيائية	
السيد بوت أمين ..... أستاذ مساعد في علم الأمراض النفسية	عضو مشارك